

Supporting information for

**Hydrogen Bonding Phase-Transfer Catalysis with Ionic Reactants:
Enantioselective Synthesis of γ -Fluoroamines**

Giulia Roagna,^{§,†} David M. H. Ascough,^{§,†} Francesco Ibba,[†] Anna Chiara Vicini,[†] Alberto Fontana,[‡] Kirsten E. Christensen,[†] Aldo Peschiulli,^{||} Daniel Oehlrich,^{||} Antonio Misale,[‡] Andrés A. Trabanco,[‡] Robert S. Paton,^{†,f} Gabriele Pupo,^{†*} and Véronique Gouverneur^{†*}

[†] *University of Oxford, Chemistry Research Laboratory, 12 Mansfield Road, Oxford, OX1 3TA, UK*

[‡] *Janssen Cilag Research and Development, Calle Jarama 75A, Toledo 45007, Spain*

^{||} *Discovery Sciences Medicinal Chemistry, Janssen Research & Development, Janssen Pharmaceutica N.V., Turnhoutseweg 30, Beerse B-2340, Belgium*

^f *Department of Chemistry, Colorado State University, Fort Collins, CO 80523, USA*

[§] These authors contributed equally to this work.

* To whom correspondence should be addressed: gabriele.pupo@chem.ox.ac.uk and veronique.gouverneur@chem.ox.ac.uk.

Table of Contents

General Information	3
Catalysts Synthesis and Characterization	4
Optimization of Reaction Conditions	4
HB-PTC/Homogeneous Conditions Comparison.....	8
Effect of Water	9
Counteranion effect	9
Non-linear Effect Studies	10
Anion Binding Studies	11
Fluorination under Chiral Anion Phase Transfer (CAPT).....	16
General Procedure for the Asymmetric Nucleophilic Fluorination of Azetidinium Ions.....	17
Substrates Synthesis and Characterization	18
Substrates Synthesis	18
General Procedures.....	18
Characterization of Substrate Precursors.....	20
Stereochemical Assignment of Substrates.....	40
Characterization of Substrates	40
Product Characterization	55
Additional Unsuccessful Substrates	73
Determination of the Absolute Configuration (Single Crystal X-ray Diffraction Studies).....	74
Computational Studies.....	77
Level of Theory	77
Azetidinium Substrate Reactivity	79
CsF Phase-Transfer	98
Enantioselective Fluorination of cis-Azet _{Bzh,Me}	100
Enantioselective Fluorination of trans-Azet _{Bzh,Me}	111
Summary of Computational Work	115
Tabulated Thermochemical Data.....	116
Copies of NMR Spectra.....	135
Copies of HPLC traces	346
References	383

General Information

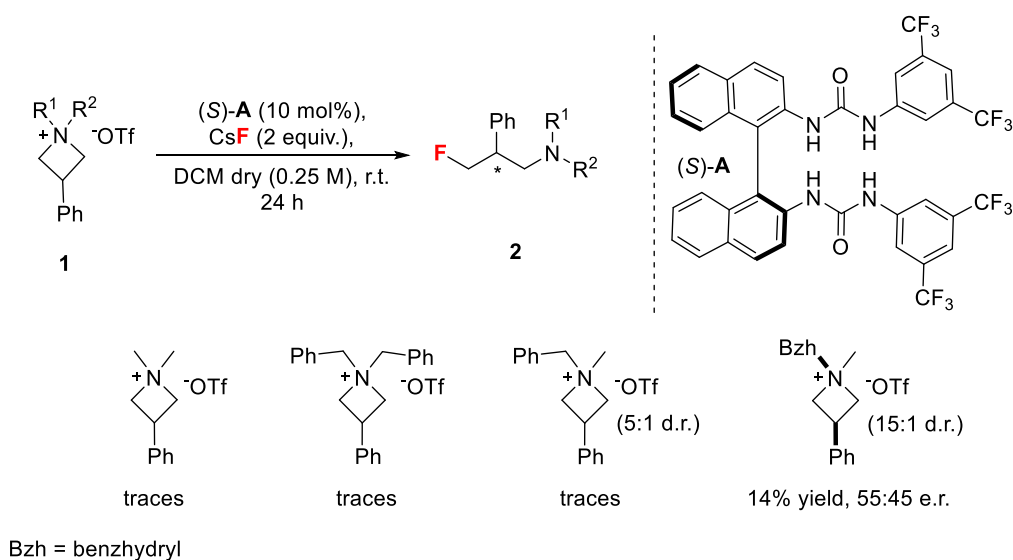
Unless otherwise stated, all reagents were purchased from commercial suppliers (Sigma-Aldrich, Alfa Aesar, Fluorochem, Apollo Scientific and CombiBlock) and used without further purification. Unless otherwise stated, solvents were used without prior drying/degassing. Reactions requiring anhydrous conditions are clearly stated and were conducted after flame-drying of the appropriate reaction vessel (round-bottom two-neck flasks, Schlenks or microwave vials) and under an inert atmosphere of N₂. Dry solvents were purchased from commercial suppliers. The dry 1,2-dichloroethane (DCE) employed in the fluorination was purchased from Sigma-Aldrich (99.8%, anhydrous). CsF (99.9% trace metal basis from Sigma-Aldrich) was ground prior to the reaction and used without pre-drying. KF (99.9% trace metal basis from Alfa Aesar) was used as provided by the supplier (fine powder) and used without pre-drying. Reactions were monitored by thin layer chromatography (TLC) on silica gel pre-coated aluminium sheets (Merck Kieselgel 60 F₂₅₄ plates). Visualization was accomplished by irradiation with UV light at 254 nm, and/or phosphomolybdic acid (PMA) stain, and/or cerium ammonium molybdate (CAM) stain, and/or permanganate stain. Flash column chromatography (FCC) was performed on Merck silica gel (60, particle size 0.040-0.063 mm). Optical rotations were measured on an Autopol L 2000 (Schmidt-Haensch) or a Rudolf Autopol V plus at 589 nm, 25 °C. Data are reported as: $[\alpha]_D^{25}$, concentration (c in g/100 mL), and solvent. The absolute configuration was determined by X-ray analysis of compounds (*S*)-**2ma**·HCl and (*R*)-**3ab**. The configuration of the other products was assigned by analogy. All NMR spectra were recorded on Bruker AVIIIHD 400, AVIIIHD 500 or VII 500. ¹H and ¹³C NMR spectral data are reported as chemical shifts (δ) in parts per million (ppm) relative to the solvent peak using the Bruker internal referencing procedure (edlock). ¹⁹F NMR spectra are referenced relative to CFCI₃. Data are reported as follows: chemical shift, multiplicity (s = singlet, d = doublet, t = triplet, q = quartet, pent = pentet, sept = septet, br = broad, m = multiplet), coupling constants (Hz) and integration. NMR spectra were processed with MestReNova 11.0 or Topsin 3.5. High resolution mass spectra (HRMS, *m/z*) were recorded on a Thermo Exactive mass spectrometer equipped with Waters Acquity liquid chromatography system using the heated electrospray (HESI-II) probe for positive electrospray ionization (ESI⁺). Infrared spectra were recorded as the neat compound or in solution using a Bruker tensor 27 FT-IR spectrometer. Absorptions are reported in wavenumber (cm⁻¹). Melting points of solids were measured on a Griffin apparatus and are uncorrected. The enantiomeric ratios were determined by HPLC analysis on a Shimadzu *i*-Prominence LC-2030 (PDA detector) or SFC analysis on an Agilent Aurora SFC-1260 Infinity system (DAD detector) or a Waters SFC UPC2 (PDA and QDa MS detector), employing a chiral stationary phase column specified in the individual experiment by comparing the samples with the appropriate racemic mixtures.

Catalysts Synthesis and Characterization

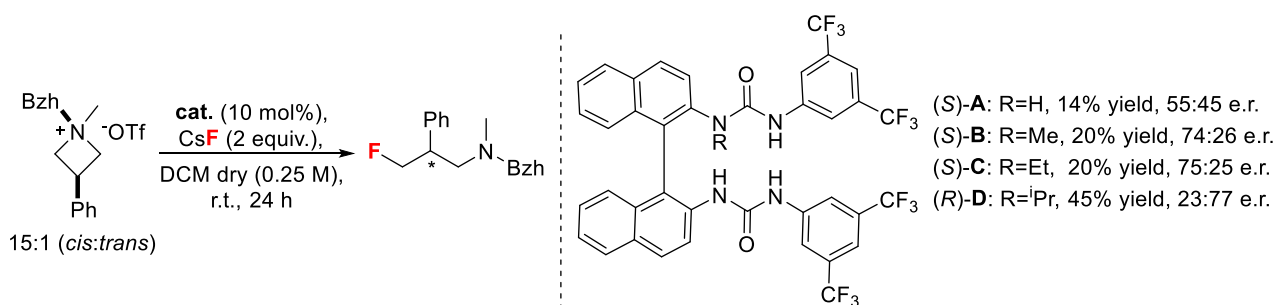
Catalyst **A–D** were prepared according to literature procedures and their analytical data were in agreement with the literature values.¹

Optimization of Reaction Conditions

General reaction conditions: 0.05 mmol of **1**, CsF and the organocatalyst were stirred in the appropriate solvent at 900 rpm at r.t. Yields determined by ¹⁹F NMR using 4-fluoroanisole as internal standard; e.r. = enantiomeric ratio, determined by HPLC using a chiral stationary phase.

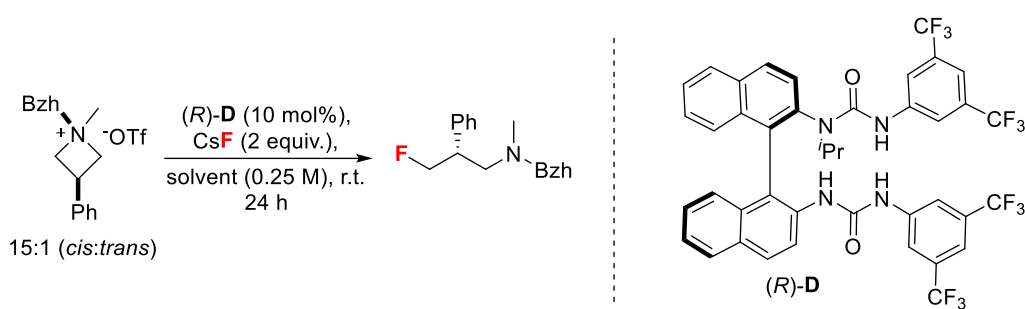


Scheme S1: Preliminary N-protecting groups screening



Scheme S2: Catalyst Screening

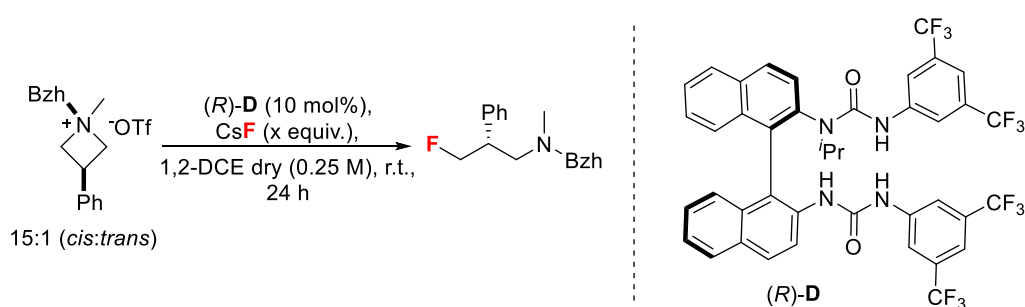
Table S1: Solvent Screening (using catalyst (R)-D)



Entry	Solvent	NMR Yield	e.r.	Background reactivity ^[1]
1	CH ₂ Cl ₂ (dry)	45%	77:23	6%
2	CH ₂ Cl ₂	34%	76:24	6%
3	CHCl ₃	56%	67:33	33%
4 ^[2]	1,2-DCE (dry)	55%	81:19	8%
5 ^[3]	1,2-DCE (dry)	51%	81:19	--
6	1,2-DCE	37%	81:19	8%
7	Toluene	51%	79:21	4%
8	1,2-DFB	47%	79:21	12%
9	α,α,α -trifluorotoluene (dry)	69%	78:22	0%
10	Fluorobenzene	63%	76.5:23.5	0%
11	CH ₃ CN	4%	61.5:38.5	traces
12	EtOAc	9%	77.5:22.5	0%

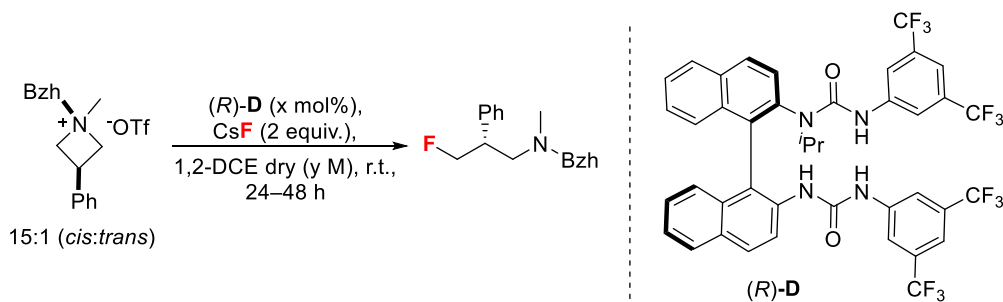
^[1] Background reactivity = ¹⁹F-NMR yield of the corresponding reaction in the absence of catalyst. ^[2] Under otherwise identical reaction conditions, when KF (5 equiv.) was employed instead of CsF (2 equiv.), only traces of product were obtained; ^[3] CsF was dried for 3d at 190 °C prior to usage. 1,2-DFB = 1,2-difluorobenzene; 1,2-DCE = 1,2-dichloroethane.

Table S2: Nucleophile Equivalents Screening (using catalyst (R)-D)



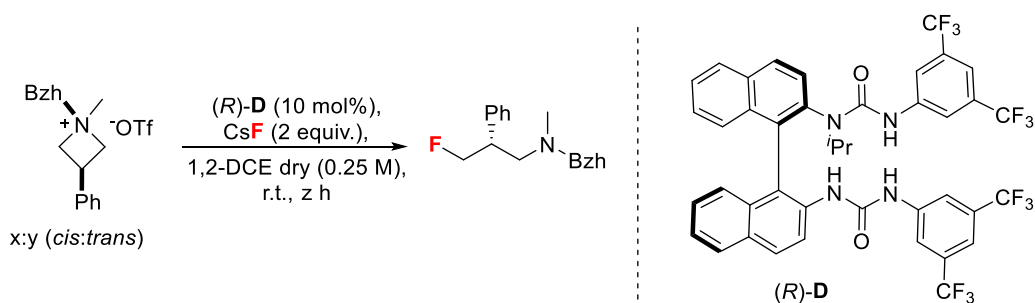
CsF equiv.	NMR Yield	e.r.
1.2	28%	82:18
2	55%	80.5:19.5
3	69%	70:30
5	68%	70:30

Table S3: Concentration and Catalyst Loading Screening (using catalyst (*R*)-**D**)

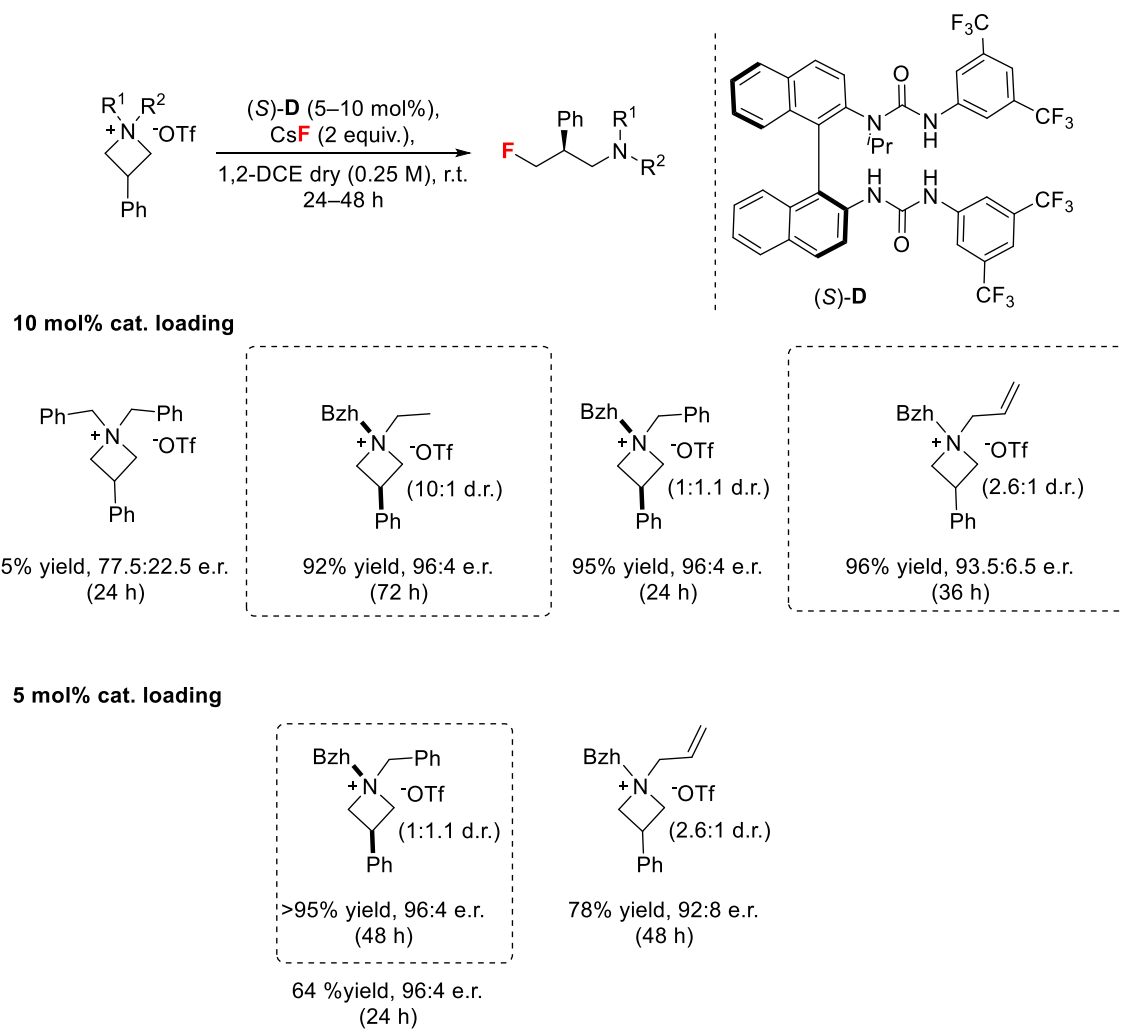


Molarity [M]	Cat. Loading	Time	NMR Yield	e.r.
0.1	10 mol%	24 h	50%	80:20
0.25	10 mol%	24 h	55%	80.5:19.5
0.5	10 mol%	24 h	34%	81.5:18.5
0.25	10 mol%	48 h	93%	80:20
0.25	5 mol%	48 h	46%	79.5:20.5

Table S4: Reaction Time and Diastereomeric Ratio of Substrate (using catalyst (*R*)-**D**)

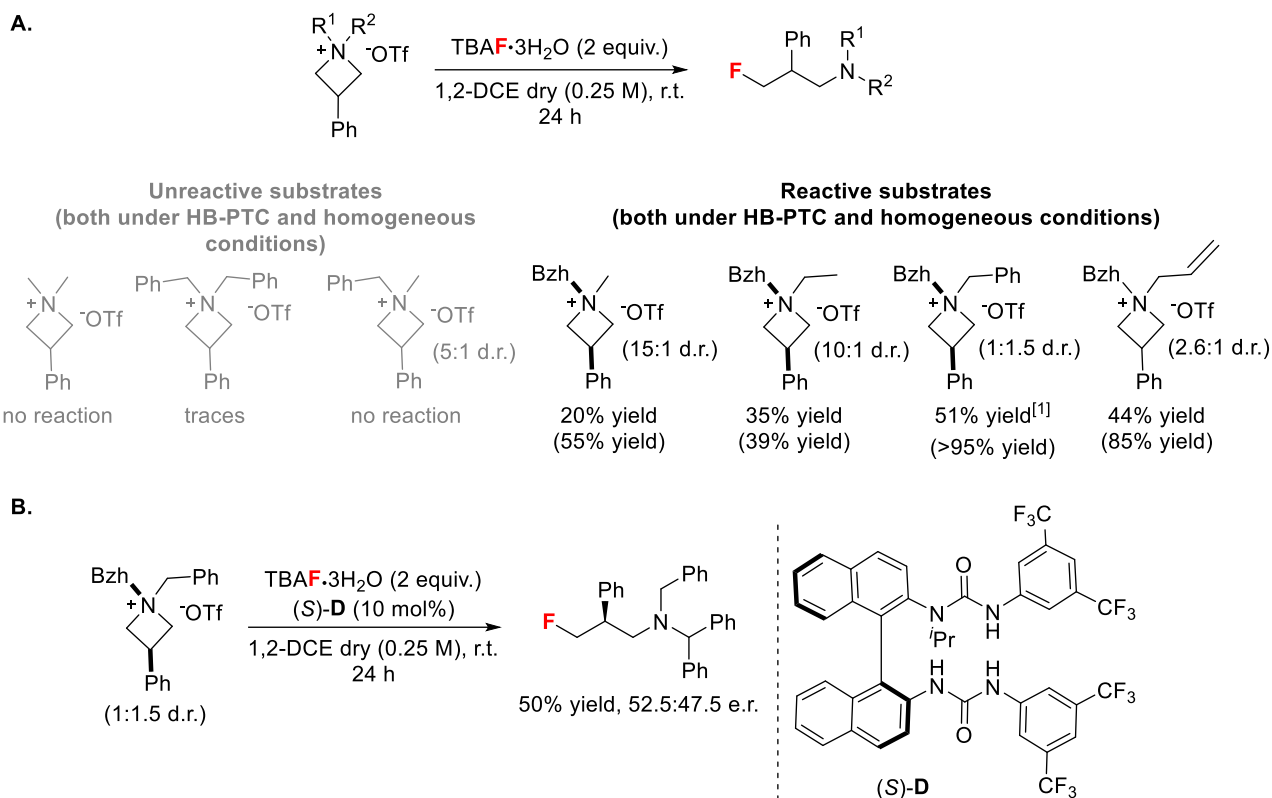


Diastereomeric ratio of substrate	Time	NMR Yield	e.r.
15:1	24 h	55%	80.5:19.5
15:1	48 h	93%	80:20
15:1	72 h	> 95%	80.5:19.5
>99:1 (<i>cis</i>)	24 h	57%	80.5:19.5
>99:1 (<i>cis</i>)	72 h	> 95%	80.5:19.5
>1:99 (<i>trans</i>)	24 h	35%	80:20
>1:99 (<i>trans</i>)	72 h	53%	81.5:19.5

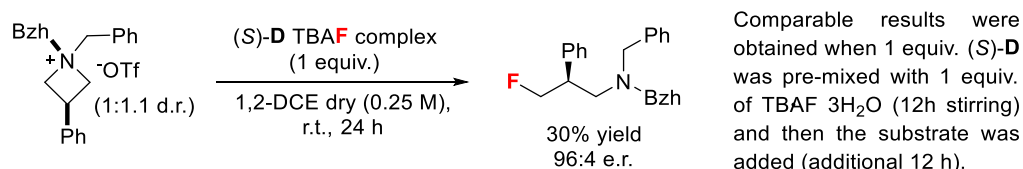


Scheme S3: Final *N*-protecting groups screening and determination of the optimized conditions for the substrate scope using catalyst (*S*)-**D**. Reaction times are optimized to achieve full conversion.

HB-PTC/Homogeneous Conditions Comparison



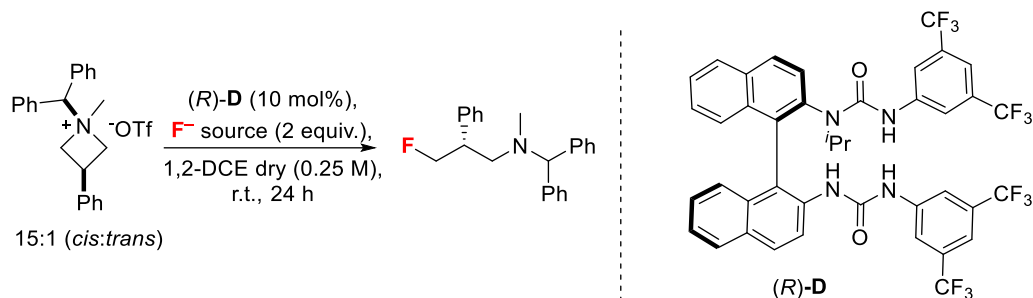
Scheme S4: A) Comparison between HB-PTC and homogeneous reaction conditions. In parenthesis, the yield obtained under the optimized HB-PTC conditions using 10 mol% of (*S*)-**D** and 2 equiv. of CsF (24 h); B) Fluorination under homogeneous conditions with the addition of 10 mol% of (*S*)-**D**.



Scheme S5: Asymmetric reaction using stoichiometric amounts of (*S*)-**D**·TBAF complex.

Effect of Water

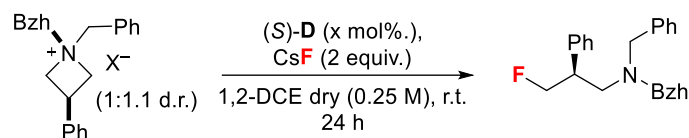
Table S5: Effect of water on reactivity and enantioselectivity.



Entry	F ⁻ source	H ₂ O added (equiv.)	Catalyst	Yield	e.r.	Background reactivity
1	CsF	//	(R)-D	55%	80.5:19.5	8%
2	CsF	1 equiv.	(R)-D	40%	81:19	0%
3	CsF	5 equiv.	(R)-D	2%	82:18	0%
4	TBAF·3H ₂ O	//	//	51%	//	//
5	TBAF·3H ₂ O	1 equiv.	//	32%	//	//
6	TBAF·3H ₂ O	5 equiv.	//	16%	//	//

Counteranion effect

Table S6: Effect of the counteranion on reactivity and enantioselectivity.



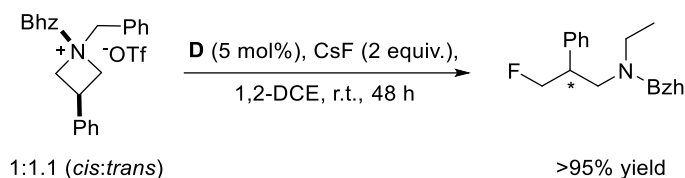
Entry	X ⁻	Cat. loading	Yield	e.r.	Background reactivity
1	OTf	5 mol%	64%	96:4	17%
2 ^a	OTf	10 mol%	> 95%	96:4	17%
3	BF ₄	5 mol%	> 95%	85:15	95% ^b
4	BF ₄	10 mol%	> 95%	90:10	95% ^b
5	BF ₄	20 mol%	> 95%	95:5	95% ^b
6	PF ₆	5 mol%	31%	96:4	9%

^a 48h reaction; ^b In the absence of CsF no product was obtained. Background reactivity due to the tetrafluoroborate anion itself as a fluoride source is therefore absent.

Non-linear Effect Studies

The non-linear effect study was conducted with (*R*) and (*S*) mixtures of catalyst **D** by employing the previously described protocol for reaction optimization (see detailed conditions in scheme below). Under these conditions (1,2-DCE as solvent, r.t.), (*S*)-**3d** affords the product in 92% ee (96:4 e.r.).

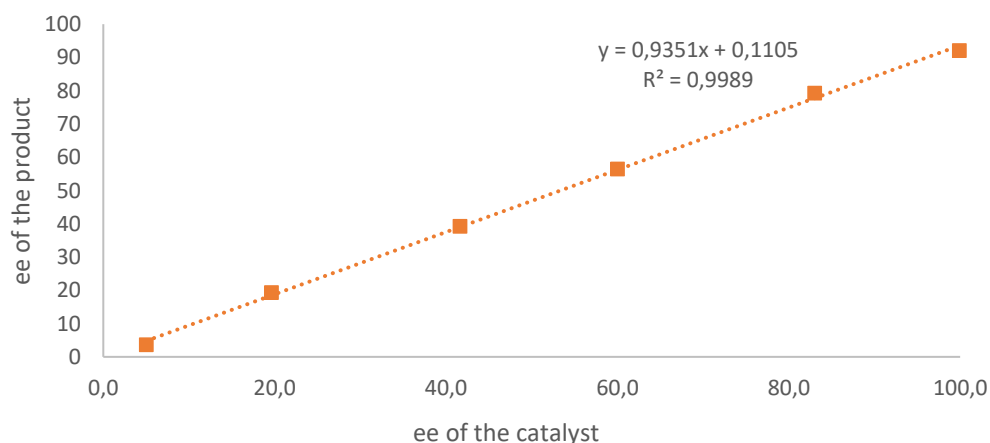
Table S7. Non-linear effect study



Entry	ee of catalyst ^[1]	ee of product ^[2]
1	5.0	3.6
2	19.6	19.3
3	41.6	39.2
4	60.0	56.4
5	83.0	79.2
6	99.9	92.0

^[1] (*R*)-**D** and (*S*)-**D** were premixed in a ratio between 50:50 and 0:100, respectively. The precise ee of the catalyst was determined by HPLC analysis using a chiral stationary phase at 254 nm (DAICEL CHIRALPAK[®] IG, 96:4 Heptane:EtOH, 1mL/min).

^[2] The ee of the product was determined by HPLC analysis using a chiral stationary phase at 254 nm (DAICEL CHIRALCEL[®] OJ-H, 95:5 Heptane:EtOH, 1mL/min).



Conclusion: No non-linear effect was observed. The computed transition state model (see computational analysis section) involving only one molecule of the urea catalyst is thus consistent with the experimental data.

Anion Binding Studies

A stock solution of urea (*S*)-**D** (2 mM) in CH₂Cl₂:CD₂Cl₂ (3:2) was prepared in a volumetric flask. A *ca.* 80 mM solution of the appropriate tetrabutylammonium salt (OTf⁻, BF₄⁻ or PF₆⁻) was then prepared by accurately weighting the solid and dissolving it in the previously prepared urea solution using a volumetric flask. An aliquot of 0.5 mL of stock solution was transferred into an NMR tube to which increasing amounts of TBA salt (1 – 200 μL) were added using a microsyringe. After every addition a ¹H NMR spectrum was acquired, using a dedicated pulse sequence to suppress the CH₂Cl₂ resonance at 5.37 ppm (perfect echo excitation sculpting sequence).² The chemical shift variation of three diagnostic aromatic protons was monitored and plotted against the concentration of added anion. The association constants were determined from the experimental data by non-linear curve fitting using Bindfit (<http://supramolecular.org>)³ and expressed as an averaged value of three replicated experiments. Different binding model were evaluated, 1:1 resulting in the one giving consistently better fit. For every experiment a representative example of data analysis (in each case, only replica **I** is shown) is reported below. The full data set are made available open access on <http://supramolecular.org>.

Tetrabutylammonium trifluoromethanesulfonate (TBAOTf)

Table S8: Input data for the titration of (*S*)-**D** with TBAOTf (variation of three distinct protons in replica **I**).

(<i>S</i>)- D concentration [M]	TBAOTf concentration [M]	Equivalents	$\delta^1\text{H-(A)}$ [ppm]	$\delta^1\text{H-(B)}$ [ppm]	$\delta^1\text{H-(C)}$ [ppm]
0.0019	0.0000	0.00	8.178	7.879	6.943
0.0019	0.0002	0.09	8.181	7.876	6.933
0.0019	0.0003	0.17	8.183	7.874	6.926
0.0019	0.0005	0.26	8.185	7.871	6.918
0.0019	0.0008	0.43	8.189	7.867	6.906
0.0019	0.0012	0.60	8.192	7.863	6.896
0.0019	0.0015	0.76	8.195	7.859	6.887
0.0019	0.0018	0.93	8.198	7.857	6.879
0.0019	0.0023	1.18	8.201	7.853	6.869
0.0019	0.0032	1.66	8.206	7.848	6.854
0.0019	0.0048	2.45	8.212	7.842	6.836
0.0019	0.0077	3.93	8.218	7.835	6.818
0.0019	0.0140	7.21	8.224	7.830	6.800
0.0019	0.0195	9.98	8.225	7.827	6.794

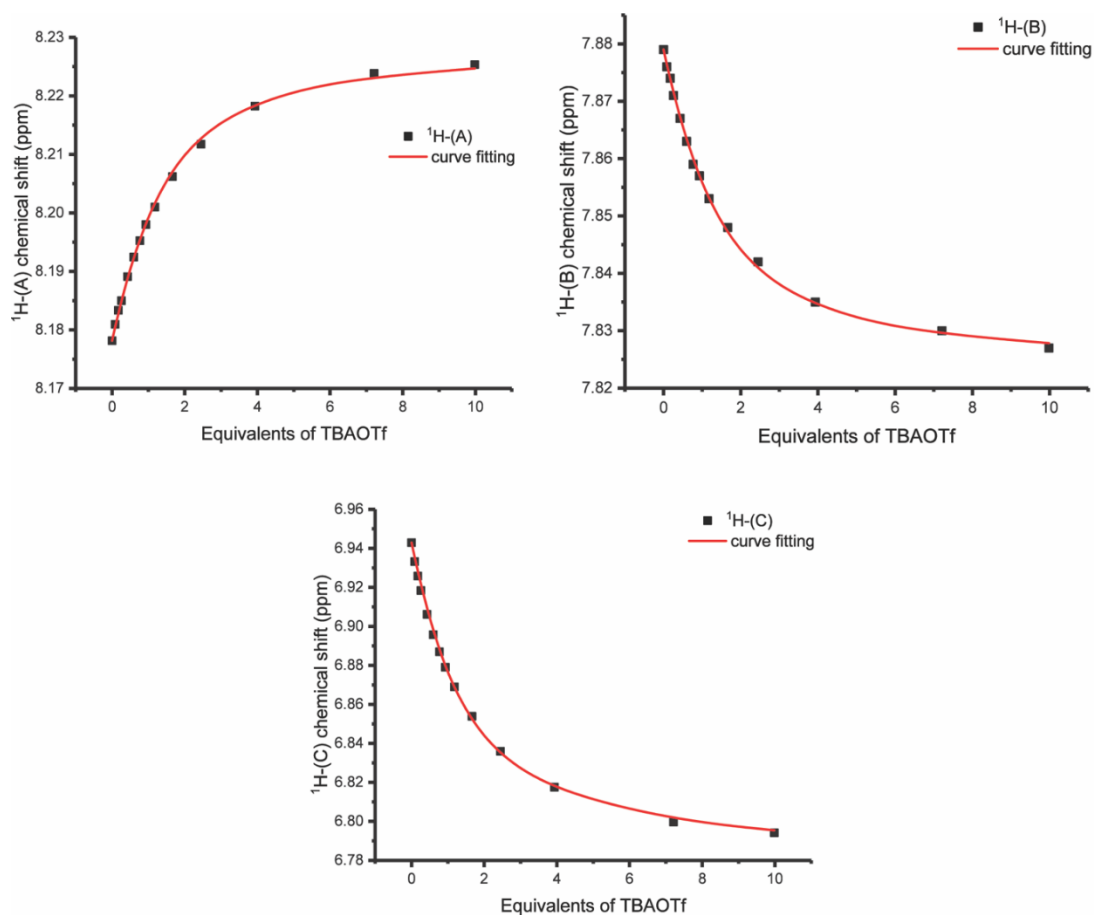


Figure S1: Titration profiles of diagnostic protons in replica I, experimental data point and curve fitting.

Table S9: Calculated association constant, K_a (1:1), and fit quality parameters of each single experiment.

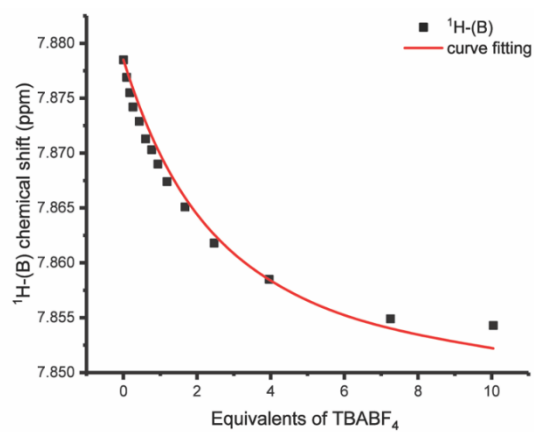
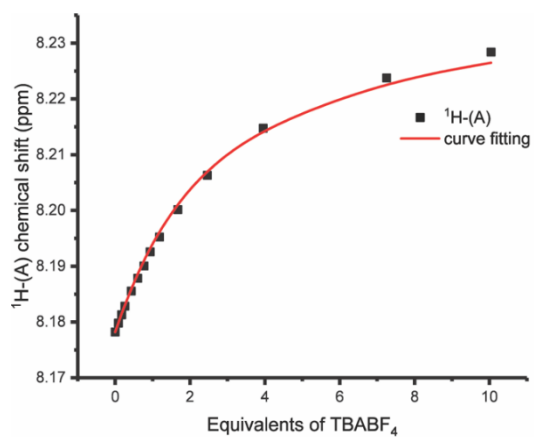
	K_a (1:1) [M^{-1}]	Residual sum of squares	Cov_{fit}
Replica I	617	6.9469×10^{-5}	7.0739×10^{-4}
Replica II	545	6.0937×10^{-5}	7.0157×10^{-4}
Replica III	528	6.9531×10^{-5}	7.5339×10^{-4}

Table S10: Calculated association constant, K_a (1:1), and relative binding free energy (averaged value of three replicated experiments).

K_a (1:1) [M^{-1}]	ΔG [kJ/mol]
560 ± 47	-15.7 ± 0.20

Table S11: Input data for the titration of (S)-**D** with TBABF₄ (variation of three distinct protons in replica I).

(S)- D concentration [M]	TBABF ₄ concentration [M]	Equivalents	$\delta^1\text{H}-(\text{A})$ [ppm]	$\delta^1\text{H}-(\text{B})$ [ppm]	$\delta^1\text{H}-(\text{C})$ [ppm]
0.0020	0.0000	0.00	8.178	7.879	6.942
0.0020	0.0002	0.09	8.180	7.877	6.937
0.0020	0.0003	0.17	8.181	7.876	6.934
0.0020	0.0005	0.26	8.183	7.874	6.931
0.0020	0.0009	0.43	8.186	7.873	6.925
0.0020	0.0012	0.60	8.188	7.871	6.920
0.0020	0.0015	0.77	8.190	7.870	6.916
0.0020	0.0019	0.94	8.193	7.869	6.912
0.0020	0.0024	1.19	8.195	7.867	6.907
0.0020	0.0033	1.67	8.200	7.865	6.899
0.0020	0.0049	2.46	8.206	7.862	6.888
0.0020	0.0079	3.96	8.215	7.859	6.874
0.0020	0.0145	7.25	8.224	7.855	6.856
0.0020	0.0200	10.04	8.228	7.854	6.848



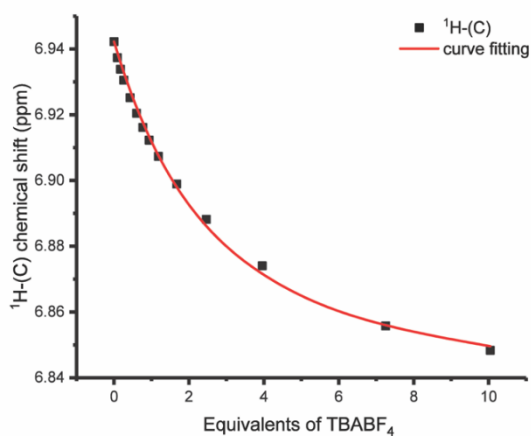


Figure S2: Titration profiles of diagnostic protons in replica I, experimental data point and curve fitting.

Table S12: Calculated association constant, $K_{a(1:1)}$, and fit quality parameters for each single experiment.

	$K_{a(1:1)}$ [M^{-1}]	Residual sum of squares	Cov_{fit}
Replica I	254	6.8255×10^{-5}	1.55384×10^{-3}
Replica II	248	3.9894×10^{-5}	1.12533×10^{-3}
Replica III	287	1.4294×10^{-4}	3.32541×10^{-3}

Table S13: Calculated association constant, $K_{a(1:1)}$, and relative binding free energy (averaged value of three replicated experiments).

$K_{a(1:1)}$ [M^{-1}]	ΔG [kJ/mol]
260 ± 20	-13.8 ± 0.19

Table S14: Input data for the titration of (S)-D with TBAPF₆ (variation of three distinct protons in replica I).

(S)-D concentration [M]	TBAPF ₆ concentration [M]	Equivalents	$\delta^1\text{H-(A)}$ [ppm]	$\delta^1\text{H-(B)}$ [ppm]	$\delta^1\text{H-(C)}$ [ppm]
0.0019	0.0000	0.00	8.178	7.879	6.942
0.0019	0.0002	0.09	8.179	7.878	6.941
0.0019	0.0005	0.28	8.179	7.878	6.941
0.0019	0.0017	0.92	8.180	7.877	6.938
0.0019	0.0026	1.36	8.181	7.876	6.937
0.0019	0.0058	3.06	8.183	7.874	6.932
0.0019	0.0116	6.10	8.186	7.871	6.925
0.0019	0.0178	9.36	8.188	7.868	6.920
0.0019	0.0230	12.13	8.190	7.866	6.915
0.0019	0.0276	14.52	8.191	7.864	6.911
0.0019	0.0329	17.36	8.193	7.862	6.904

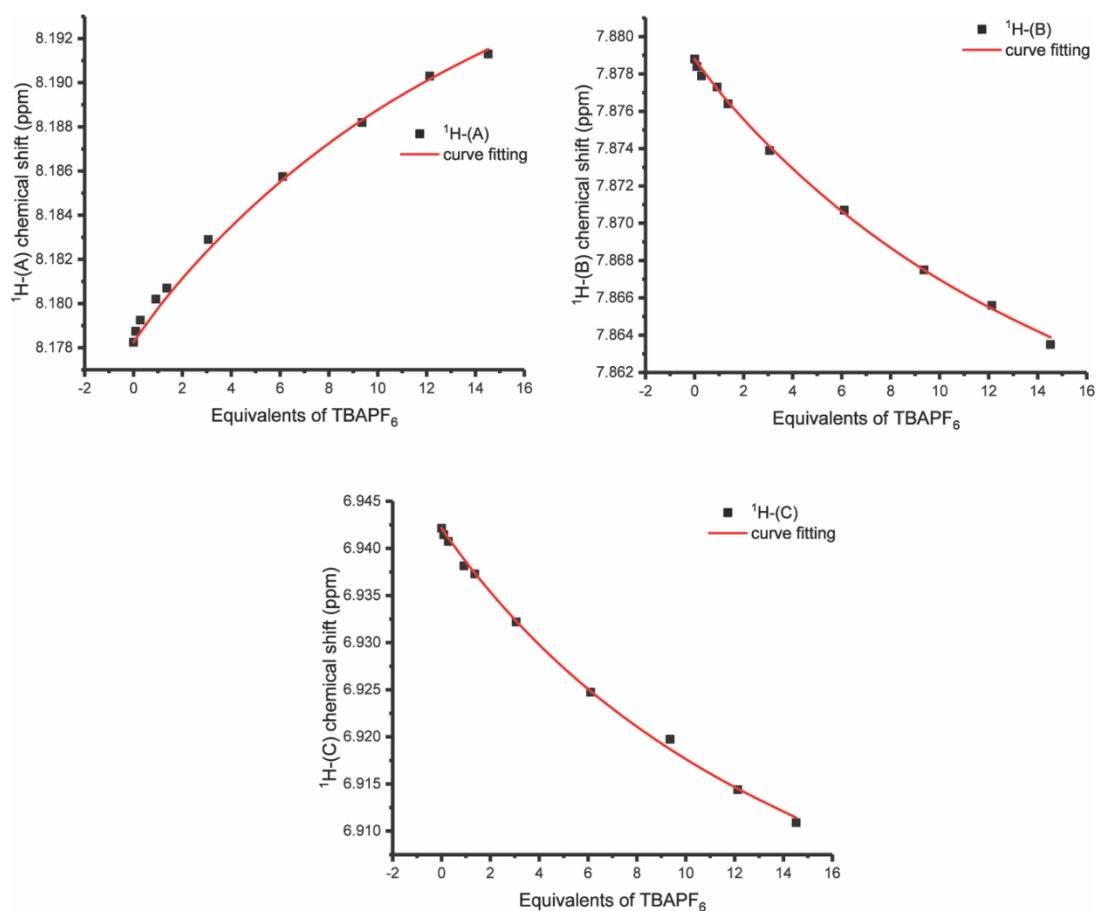


Figure S3: Titration profiles of diagnostic protons in replica I, experimental data point and curve fitting.

Table S15 Calculated association constant, $K_{a(1:1)}$, and fit quality parameters for each single experiment.

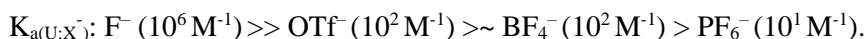
	$K_{a(1:1)}$ [M^{-1}]	Residual sum of squares	Cov_{fit}
Replica I	30	3.8713×10^{-6}	1.16848×10^{-3}
Replica II	32	5.8417×10^{-6}	1.73996×10^{-3}
Replica III	30	6.0144×10^{-6}	2.13053×10^{-3}

Table S16: Calculated association constant, $K_{a(1:1)}$, and relative binding free energy (averaged value of three replicated experiments).

$K_{a(1:1)}$ [M^{-1}]	ΔG [kJ/mol]
31 ± 1.2	-8.51 ± 0.096

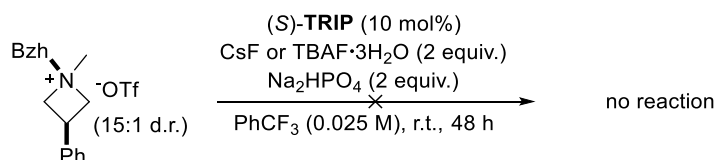
Conclusion

The binding affinity of (S)-D towards three different anions, encountered as counter ions in the desymmetrization of aziridinium salts (OTf⁻, BF₄⁻ and PF₆⁻), were evaluated to assess whether these counterions could be involved in competitive binding interactions to F⁻ ($K_{a(U:F^-)}$ was previously measured by UV-Vis titrations).¹ The experimental data shows the following trend:



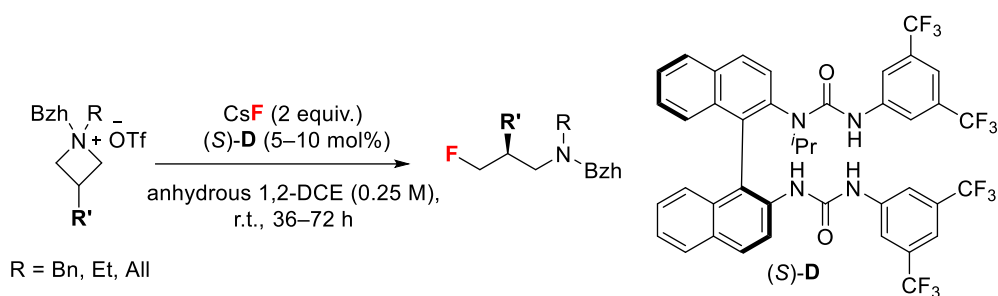
This shows that hydrogen bonding to fluoride is at least four order of magnitude higher than the hydrogen bonding interactions with the other studied anions. These findings combined with the reactivity/enantioselectivity data of the three salts (Table S6) suggest that an anion binding/ion pairing catalysis mechanism⁴ is unlikely.

Fluorination under Chiral Anion Phase Transfer (CAPT)



Scheme S6: Fluorination under CAPT conditions (Sun *et al.*),⁵ no product formation was observed.

General Procedure for the Asymmetric Nucleophilic Fluorination of Azetidinium Ions



In a screw-capped vial equipped with a magnetic stirring bar were added CsF (2 equiv., 0.2 mmol), organocatalyst (S)-D (5–10 mol%) and the substrate (1 equiv., 0.1 mmol). Anhydrous 1,2-DCE (0.25M, 0.4 mL) was added, the vial was sealed and the reaction mixture was stirred at 900 rpm at r.t. for the indicated time. The crude mixture was then directly purified by flash column chromatography (FCC).

For reaction optimization was filtered through a small plug of silica, evaporated to dryness and the crude mixture was analyzed by ^1H and ^{19}F NMR (4-fluoroanisole as internal standard) to determine the yield; an aliquot of the reaction mixture was purified by preparative TLC and analyzed by HPLC (chiral stationary phase) to determine the e.r.

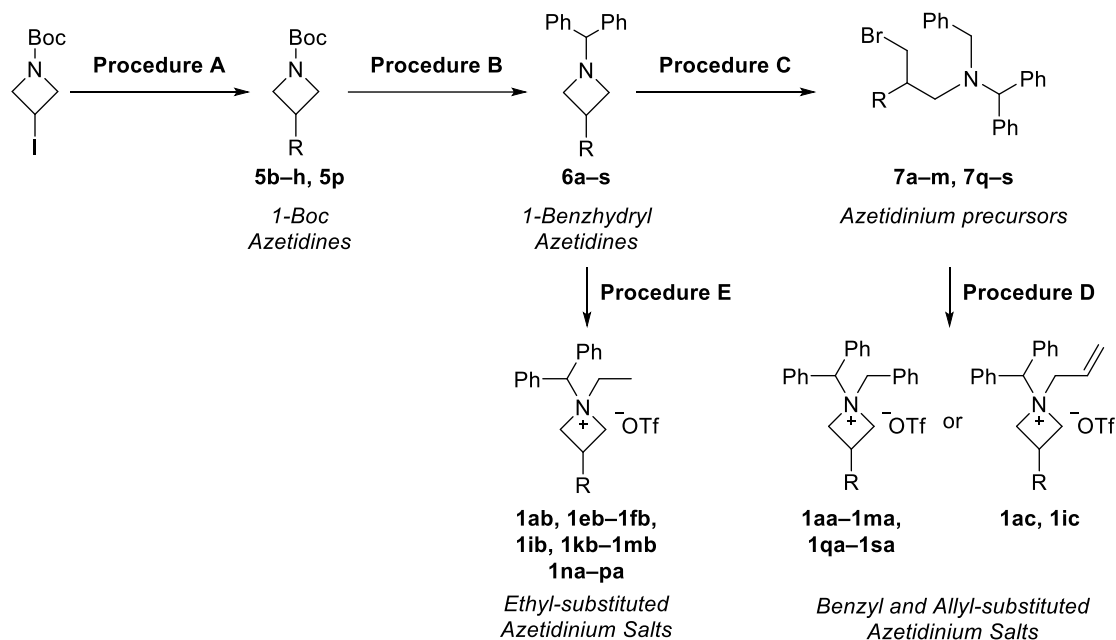
Note: CsF (99.9% trace metal basis from Sigma-Aldrich) was ground prior to the reaction and used without pre-drying.

Racemate synthesis: The racemic reference products for HPLC analysis were obtained using stoichiometric amounts of TBAF·3H₂O in THF (0.25 M, r.t., 12h). Alternatively, the substrate was reacted with CsF (2 equiv.) in 1,2-DCE (0.25 M) at 60 °C for 6 h.

Substrates Synthesis and Characterization

Substrates Synthesis

Substrate precursors **5** and **6** (1-Boc and 1-benzhydryl azetidines) were commercially available and used without further purification or synthesized according to the following route:



General Procedures

Azetidines (5, 6) and Brominated Precursors (7)

General Procedure A: Synthesis of 1-Boc Azetidines (5)

The appropriate boronic acid (2 equiv.), NiI₂ (6 mol%) and *trans*-2-aminocyclohexanol hydrochloride (6 mol%) were weighed into a microwave vial and placed under an inert atmosphere. Commercially available 1-Boc-3-iodoazetidine (1 equiv.) and dry isopropanol (2 mL/mmol) were then added, followed by NaHMDS (1M in THF, 2 equiv.) at r.t. The mixture was heated at 80 °C for 30 min under microwave irradiation. After cooling to r.t., the mixture was diluted with EtOH (0.25 mmol/mL) and filtered through a celite plug. The filter cake was rinsed with EtOH and the filtrate was concentrated *in vacuo*. The crude mixture was purified by flash column chromatography (Heptane:EtOAc as eluent) to afford the desired 1-Boc-azetidine.

General procedure B: Synthesis of 1-benzhydryl Azetidines (6)

The appropriate 1-Boc-azetidine (1 equiv.) was dissolved in CH₂Cl₂ (10 mL/mmol) and TFA (5.8 mL/mmol) was slowly added at 0 °C. The reaction was stirred at r.t. for 12 h, the solvent was removed *in vacuo* and the obtained oil was washed twice with pentane to obtain the desired azetidinium·TFA salt. The salt was then dissolved in dry CH₃CN (1 M) before DIPEA (5 equiv.) was added dropwise. Bromodiphenylmethane (1 equiv.) was then added and the reaction mixture was stirred at 100 °C for 2 h. The reaction mixture was then concentrated *in vacuo* and the residual slurry was purified by flash column chromatography (Heptane:EtOAc as eluent) to afford the desired 1-benzhydryl azetidines.

General procedure C: Synthesis of brominated azetidinium precursors (7)

Under a flow of N₂, an oven-dried flask was charged with 1-benzhydryl-azetidine and dry CH₃CN (1.0 mL/mmol). Benzyl or allyl bromide (1.6 equiv.) were added and the mixture was stirred at 60 °C for 12 h. The solvent was removed under vacuum and the crude mixture was purified by flash column chromatography (Hexane:EtOAc) to afford the desired azetidinium precursor.

Azetidinium substrates (1)

General procedure D: Synthesis of 1-Benzyl and 1-Allyl Azetidinium·TFA Salts*

Under a N₂ atmosphere, to an oven-dried flask charged with AgOTf (1 equiv.), a solution of 1-benzhydryl-1-benzyl-3-bromo-propan-1-amine (1 equiv.) in dry CH₂Cl₂ (10 mL/mmol) was added. The reaction mixture was stirred at r.t. for 12 h in the dark. The mixture was then filtered through celite and the filtrate was evaporated under reduced pressure. The resulting powder was washed with cold Et₂O to afford the desired azetidinium salt.

* The tetrafluoroborate and hexafluorophosphate salts (Table S6) were prepared according to the same procedure by employing AgBF₄ and AgPF₆ respectively instead of AgOTf.

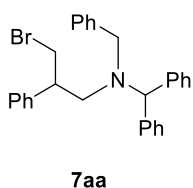
General procedure E: Synthesis of 1-Methyl and 1-Ethyl Azetidinium Salts

To a solution of 1-benzhydryl-azetidine in dry CH₂Cl₂ (2 M) at 0 °C, methyl or ethyl triflate (1.5 equiv.) were added dropwise and the reaction was stirred overnight at r.t. The solvent was then evaporated, the white precipitate was washed with Et₂O and filtered. The solid was further washed with cold Et₂O to afford the desired compound.

Characterization of Substrate Precursors

Azetidines, Brominated Precursors and Intermediates

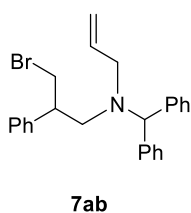
1-benzhydryl-1-benzyl-3-bromo-2-phenylpropan-1-amine (7aa)



Prepared according to a slightly modified version of general procedure C. Under a flow of N_2 , an oven-dried flask was charged with commercially available 1-benzhydryl-3-phenylazetidine (8.48 mmol, 2.52 g) in dry CH_3CN (1 M, 8.4 mL). Benzyl bromide (0.95 equiv., 8.06 mmol, 0.95 mL) was added and the mixture was stirred at 60 °C for 12 h. The

crude mixture was purified by flash column chromatography (Pentane:EtOAc = 100:0 to 98:2, gradient) to afford the desired product in 85% yield (7.21 mmol, 3.36 g) as a colorless oil. 1H NMR (400 MHz, $CDCl_3$) δ ppm: 7.42 – 7.20 (m, 18H), 7.01 – 6.91 (m, 2H), 4.96 (s, 1H), 3.76 (dd, J = 10.0, 5.6 Hz, 1H), 3.65 (s, 2H), 3.34 (dd, J = 10.0, 8.6 Hz, 1H), 3.19 – 3.07 (m, 1H), 2.89 (dd, J = 13.3, 7.6 Hz, 1H), 2.75 (dd, J = 13.3, 7.2 Hz, 1H); ^{13}C NMR (101 MHz, $CDCl_3$) δ ppm: 141.58, 140.72, 140.51, 139.40, 129.51, 129.22, 129.11, 128.52, 128.44, 128.40, 128.31, 128.04, 127.34, 127.17, 127.15, 69.67, 55.77, 55.72, 46.96, 36.58. IR (thin layer film) ν (cm^{-1}) = 3027, 2834, 1601, 1493, 1452, 1265, 1122, 1076, 1029, 920, 741, 697. HRMS (ESI⁺) m/z $C_{29}H_{29}BrN^+$ [M+H]⁺: calculated 470.1483, found 470.1487. Spectroscopic data were in agreement with the ones previously reported in literature.⁵

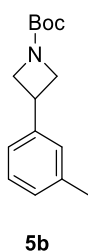
1-benzhydryl-1-(3-bromo-2-phenylpropyl)prop-2-en-1-amine (7ab)



Prepared according to general procedure C using commercially available 1-benzhydryl-3-phenylazetidine (6.68 mmol, 2.0 g) and allyl bromide (11.13 mmol, 0.96 mL). The crude mixture was purified by flash column chromatography (Heptane 100%) to afford the desired product in 75% yield (5.00 mmol, 2.10 g) as a colorless oil. 1H NMR (500 MHz, $CDCl_3$) δ ppm: 7.33 – 7.27 (m, 6H), 7.26 (dt, J = 2.8, 1.4 Hz, 1H), 7.25 – 7.17 (m, 6H),

7.08 – 7.02 (m, 2H), 5.83 (ddt, J = 17.0, 10.2, 6.6 Hz, 1H), 5.12 (ddt, J = 10.2, 2.2, 1.2 Hz, 1H), 5.05 (dq, J = 17.1, 1.5 Hz, 1H), 4.86 (s, 1H), 3.86 (dd, J = 10.0, 5.4 Hz, 1H), 3.50 (dd, J = 10.0, 8.6 Hz, 1H), 3.25 – 3.15 (m, 2H), 3.13 – 3.05 (m, 1H), 2.85 (dd, J = 13.4, 8.3 Hz, 1H), 2.69 (dd, J = 13.3, 6.7 Hz, 1H); ^{13}C NMR (126 MHz, $CDCl_3$) δ ppm: 141.74, 141.63, 141.61, 135.36, 128.92, 128.84, 128.51, 128.44, 128.41, 128.02, 127.21, 127.17, 127.15, 118.01, 70.69, 55.48, 53.96, 46.92, 36.69. IR (thin layer film) ν (cm^{-1}) = 3062, 3027, 2980, 1600, 1493, 1452, 1249, 1155, 1078, 1030, 996, 922, 759, 699, 611. HRMS (ESI⁺) m/z $C_{25}H_{27}BrN^+$ [M+H]⁺: calculated 420.1321, found 420.1325.

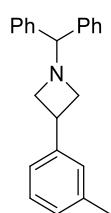
tert-butyl 3-(m-tolyl)azetidine-1-carboxylate (5b)



Prepared according to general procedure A using commercially available 1-Boc-3-iodoazetidine (7.56 mmol, 2.14 g) and 3-methylphenylboronic acid (15.1 mmol, 2.06 g). The crude mixture was purified by flash column chromatography (Heptane:EtOAc = 100:0 to 90:10, gradient) to give the desired product in 57% yield (4.34 mmol, 1.07 g) as a colorless oil. 1H NMR (500 MHz, $CDCl_3$) δ ppm: 7.24 (t, J = 7.6 Hz, 1H), 7.15 – 7.04 (m, 3H), 4.31 (t, J = 8.6 Hz, 2H), 4.03 – 3.94 (m, 2H),

3.70 (tt, $J = 8.7, 6.0$ Hz, 1H), 2.36 (s, 3H), 1.47 (s, 9H); $^{13}\text{C NMR}$ (126 MHz, CDCl_3) δ ppm: 156.45, 142.23, 138.40, 128.61, 127.70, 127.48, 123.81, 79.49, 56.74, 33.44, 28.45, 21.43. **IR** (thin layer film) ν (cm^{-1}) = 2973, 2883, 1702, 1609, 1479, 1392, 1366, 1296, 1255, 1163, 1133, 863, 781, 702. **HRMS** (ESI^+) m/z $\text{C}_{15}\text{H}_{22}\text{NO}_2^+$ $[\text{M}+\text{H}]^+$: calculated 248.1645, found 248.1646.

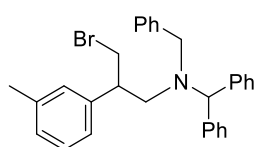
1-benzhydryl-3-(m-tolylphenyl)azetidene (6b)



6b

Prepared according to general procedure B using 1-Boc-3-(m-tolylphenyl)azetidene **5b** (4.04 mmol, 1.00 g). The crude mixture was purified by flash column chromatography (Heptane:EtOAc = 100:0 to 85:15, gradient) to give the desired product in 65% yield (2.63 mmol, 0.82 g) as a colorless oil. $^1\text{H NMR}$ (500 MHz, CDCl_3) δ ppm: 7.56 – 7.50 (m, 4H), 7.35 (dd, $J = 8.4, 6.9$ Hz, 4H), 7.29 – 7.24 (m, 3H), 7.20 – 7.13 (m, 2H), 7.10 (d, $J = 7.5$ Hz, 1H), 4.48 (s, 1H), 3.81 – 3.69 (m, 3H), 3.27 – 3.19 (m, 2H), 2.41 (s, 3H); $^{13}\text{C NMR}$ (126 MHz, CDCl_3) δ ppm: 143.06, 142.35, 138.05, 128.56, 128.44, 127.84, 127.67, 127.20, 127.14, 124.00, 78.42, 60.73, 34.86, 21.57. **IR** (thin layer film) ν (cm^{-1}) = 3025, 2945, 2826, 1607, 1490, 1452, 1346, 1275, 1204, 1147, 1075, 1029, 927, 778, 742, 698, 639, 621, 611. **HRMS** (ESI^+) m/z $\text{C}_{23}\text{H}_{24}\text{N}^+$ $[\text{M}+\text{H}]^+$: calculated 314.1903, found 314.1902. Spectroscopic data were in agreement with the ones previously reported in literature.⁶

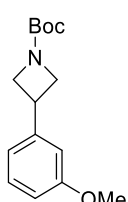
1-benzhydryl-1-benzyl-3-bromo-2-(m-tolyl)propan-1-amine (7ba)



7ba

Prepared according to general procedure C using 1-benzhydryl-3-(m-tolyl)azetidene **6b** (1.28 mmol, 0.40 g) and benzyl bromide (2.04 mmol, 0.24 mL). The crude mixture was purified by flash column chromatography (Pentane:EtOAc = 100:0 to 98:2, gradient) to afford the desired product in 46% yield (0.58 mmol, 0.28 g) as a colorless oil. $^1\text{H NMR}$ (500 MHz, CDCl_3) δ ppm: 7.38 (d, $J = 4.4$ Hz, 4H), 7.34 – 7.22 (m, 11H), 7.22 – 7.16 (m, 1H), 7.12 – 7.08 (m, 1H), 6.81 – 6.77 (m, 1H), 6.75 (d, $J = 1.9$ Hz, 1H), 4.97 (s, 1H), 3.73 (dd, $J = 10.0, 5.9$ Hz, 1H), 3.70 – 3.61 (m, 2H), 3.35 (dd, $J = 10.0, 8.5$ Hz, 1H), 3.13 (qd, $J = 7.5, 5.8$ Hz, 1H), 2.89 (dd, $J = 13.3, 7.3$ Hz, 1H), 2.74 (dd, $J = 13.3, 7.4$ Hz, 1H), 2.33 (s, 3H); $^{13}\text{C NMR}$ (126 MHz, CDCl_3) δ ppm: 141.51, 140.81, 140.41, 139.49, 138.02, 129.58, 129.22, 129.07, 128.77, 128.41, 128.40, 128.38, 128.27, 127.97, 127.33, 127.12, 127.11, 125.14, 69.51, 55.67, 55.65, 46.90, 36.56, 21.63. **IR** (thin layer film) ν (cm^{-1}) = 3026, 2921, 2838, 1604, 1493, 1451, 1247, 1076, 1029, 970, 910, 784, 763, 743, 700. **HRMS** (ESI^+) m/z $\text{C}_{30}\text{H}_{31}\text{BrN}^+$ $[\text{M}+\text{H}]^+$: calculated 484.1634, found 484.1634.

tert-butyl 3-(3-methoxyphenyl)azetidene-1-carboxylate (5c)

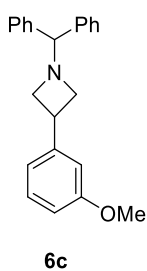


5c

Prepared according to general procedure procedure A using commercially available 1-Boc-3-iodoazetidene (7.50 mmol, 2.12 g) and 3-methoxyphenylboronic acid (15.0 mmol, 2.28 g). The crude mixture was purified by flash column chromatography (Heptane:EtOAc = 100:0 to 90:10, gradient) to give the desired product in 69% yield (5.20 mmol, 1.97 g) as a colorless oil. $^1\text{H NMR}$ (400 MHz, CDCl_3) δ ppm: 7.26 (t, $J = 7.9$ Hz, 1H), 6.92 – 6.87 (m, 1H), 6.86 – 6.83

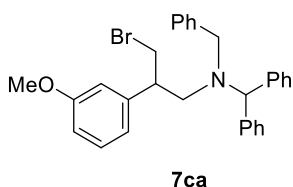
(m, 1H), 6.82 – 6.77 (m, 1H), 4.35 – 4.25 (m, 2H), 4.01 – 3.94 (m, 2H), 3.81 (s, 3H), 3.70 (tt, $J = 8.7, 6.0$ Hz, 1H), 1.47 (s, 9H); $^{13}\text{C NMR}$ (126 MHz, CDCl_3) δ ppm: 160.03, 156.51, 143.99, 129.85, 119.18, 112.70, 112.27, 79.62, 56.53, 55.35, 33.63, 28.53. **IR** (thin layer film) ν (cm^{-1}) = 2971, 2884, 1698, 1603, 1586, 1481, 1456, 1390, 1366, 1293, 1254, 1158, 1130, 1041, 980, 918, 863, 774, 697. **HRMS** (ESI^+) m/z $\text{C}_{15}\text{H}_{22}\text{NO}_3^+$ $[\text{M}+\text{H}]^+$: calculated 264.1594, found 264.1595. Spectroscopic data were in agreement with the ones previously reported in literature.^{6, 7}

1-benzhydryl-3-(3-methoxyphenyl)azetidine (6c)



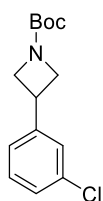
Prepared according to general procedure B using 1-Boc-3-(3-methoxyphenyl)azetidine **5c** (4.44 mmol, 1.17 g). The crude mixture was purified by flash column chromatography (Heptane:EtOAc = 100:0 to 85:15, gradient) to give the desired product in 45% yield (2.03 mmol, 0.67 g) as a colorless oil. $^1\text{H NMR}$ (500 MHz, CDCl_3) δ ppm: 7.45 (dd, $J = 8.2, 1.4$ Hz, 4H), 7.29 (dd, $J = 8.3, 6.9$ Hz, 4H), 7.24 (t, $J = 7.9$ Hz, 1H), 7.22 – 7.17 (m, 2H), 6.92 – 6.85 (m, 2H), 6.80 – 6.74 (m, 1H), 4.40 (s, 1H), 3.81 (s, 3H), 3.73 – 3.61 (m, 3H), 3.19 – 3.12 (m, 2H); $^{13}\text{C NMR}$ (126 MHz, CDCl_3) δ ppm: 159.83, 144.97, 142.35, 129.52, 128.59, 127.66, 127.23, 119.46, 112.99, 111.54, 78.39, 60.66, 55.33, 34.96; **IR** (thin layer film) ν (cm^{-1}) = 3026, 2942, 2832.34, 1601, 1583, 1489, 1451, 1434, 1290, 1267, 1207, 1158, 1076, 1046, 927, 868, 778, 744, 697, 638. **HRMS** (ESI^+) m/z $\text{C}_{23}\text{H}_{24}\text{NO}^+$ $[\text{M}+\text{H}]^+$: calculated 330.1852, found 330.1851. Spectroscopic data were in agreement with the ones previously reported in literature.⁶

1-benzhydryl-1-benzyl-3-bromo-2-(3-methoxyphenyl)propan-1-amine (7ca)



Prepared according to general procedure C using 1-benzhydryl-3-(3-methoxyphenyl)azetidine **6c** (1.21 mmol, 0.40 g) and benzyl bromide (1.94 mmol, 0.23 mL). The crude mixture was purified by flash column chromatography (Pentane:EtOAc = 100:0 to 98:2, gradient) to afford the desired product in 83% yield (1.00 mmol, 0.50 g) as a colorless oil. $^1\text{H NMR}$ (500 MHz, CDCl_3) δ ppm: 7.40 – 7.35 (m, 4H), 7.34 – 7.24 (m, 11H), 7.24 – 7.19 (m, 1H), 6.82 (dd, $J = 8.0, 2.6$ Hz, 1H), 6.60 – 6.55 (m, 1H), 6.48 (t, $J = 2.1$ Hz, 1H), 4.96 (s, 1H), 3.76 (s, 4H), 3.65 (d, $J = 1.7$ Hz, 2H), 3.32 (dd, $J = 10.0, 8.6$ Hz, 1H), 3.09 (qd, $J = 7.4, 5.4$ Hz, 1H), 2.89 (dd, $J = 13.4, 7.5$ Hz, 1H), 2.75 (dd, $J = 13.3, 7.1$ Hz, 1H); $^{13}\text{C NMR}$ (126 MHz, CDCl_3) δ ppm: 159.68, 143.28, 140.77, 140.57, 139.43, 129.51, 129.49, 129.22, 129.10, 128.44, 128.41, 128.32, 127.35, 127.18, 127.17, 120.41, 113.80, 112.44, 69.77, 55.84, 55.80, 55.25, 47.10, 36.39. **IR** (thin layer film) ν (cm^{-1}) = 3027, 2934, 2834, 1600, 1492, 1453, 1262, 1156, 1047, 970, 873, 764, 744, 699, 616. **HRMS** (ESI^+) m/z $\text{C}_{30}\text{H}_{31}\text{BrNO}^+$ $[\text{M}+\text{H}]^+$: calculated 500.1583, found 500.1581.

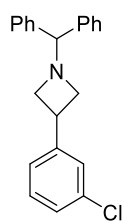
tert-butyl 3-(3-chlorophenyl)azetidine-1-carboxylate (**5d**)



5d

Prepared according to general procedure A using commercially available 1-Boc-3-iodoazetidine (15.1 mmol, 4.28 g) and 3-chlorophenylboronic acid (30.3 mmol, 4.73 g). The crude mixture was purified by flash column chromatography (Heptane:EtOAc = 100:0 to 90:10, gradient) to give the desired product in 71% yield (10.7 mmol, 2.86 g) as a colorless oil. **¹H NMR** (400 MHz, CDCl₃) δ ppm: 7.32 – 7.27 (m, 2H), 7.25 – 7.15 (m, 2H), 4.37 – 4.28 (m, 2H), 3.99 – 3.89 (m, 2H), 3.69 (tt, J = 8.8, 5.9 Hz, 1H), 1.47 (s, 9H); **¹³C NMR** (101 MHz, CDCl₃) δ ppm: 156.48, 144.46, 134.75, 130.14, 127.31, 127.17, 125.09, 79.85, 56.50, 33.36, 28.55. **IR** (thin layer film) ν (cm⁻¹) = 2974, 2885, 1698, 1599, 1573, 1479, 1390, 1366, 1296, 1255, 1129, 1082, 999, 977, 913, 860, 775, 693. **HRMS** (ESI⁺) m/z C₁₄H₁₉ClNO₂⁺ [M+H]⁺: calculated 268.1099, found 268.1099. Spectroscopic data were in agreement with the ones previously reported in literature.⁸

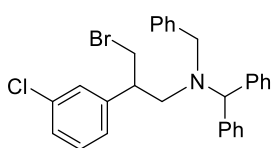
1-benzhydryl-3-(*m*-chlorophenyl)azetidine (**6d**)



6d

Prepared according to general procedure B using 1-Boc-3-(*m*-chlorophenyl)azetidine **5d** (2.05 mmol, 0.55 g). The crude mixture was purified by flash column chromatography (Heptane:EtOAc = 100:0 to 85:15, gradient) to give the desired product in 40% yield (0.75 mmol, 0.25 g) as a colorless oil. **¹H NMR** (500 MHz, CDCl₃) δ ppm: 7.53 – 7.39 (m, 4H), 7.32 – 7.27 (m, 5H), 7.25 – 7.17 (m, 5H), 4.40 (s, 1H), 3.72 – 3.57 (m, 3H), 3.18 – 3.08 (m, 2H); **¹³C NMR** (126 MHz, CDCl₃) δ ppm: 145.40, 142.19, 134.38, 129.81, 128.63, 127.64, 127.33, 127.30, 126.62, 125.33, 78.36, 60.53, 34.70. **IR** (thin layer film) ν (cm⁻¹) = 3026, 2953, 2828, 2360, 1598, 1571, 1489, 1452, 1432, 1347, 1275, 1198, 1153, 1078, 1029, 1000, 927, 876, 782, 745, 702, 694, 637, 621, 611. **HRMS** (ESI⁺) m/z C₂₂H₂₁ClN⁺ [M+H]⁺: calculated 334.1357, found 334.1356.

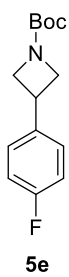
1-benzhydryl-1-benzyl-3-bromo-2-(3-chlorophenyl)propan-1-amine (**7da**)



7da

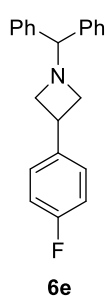
Prepared according to a slightly modified version of general procedure C. Under a flow of N₂, an oven-dried flask was charged with 1-benzhydryl-3-(3-chlorophenyl)azetidine **6d** (5.72 mmol, 1.91 g) in dry CH₃CN (0.8 M, 7.0 mL). Benzyl bromide (1.2 equiv., 6.87 mmol, 0.82 mL) was added and the mixture was stirred at 60 °C for 12 h. The crude mixture was purified by flash column chromatography (Pentane:EtOAc = 100:0 to 98:2, gradient) to afford the desired product in 89% yield (5.09 mmol, 2.62 g) as a colorless oil. **¹H NMR** (400 MHz, CDCl₃) δ ppm: 7.45 – 7.18 (m, 17H), 6.91 (t, J = 1.9 Hz, 1H), 6.87 – 6.80 (m, 1H), 4.94 (s, 1H), 3.72 – 3.58 (m, 3H), 3.28 (dd, J = 10.1, 8.4 Hz, 1H), 3.14 – 3.03 (m, 1H), 2.88 (dd, J = 13.4, 7.0 Hz, 1H), 2.75 (dd, J = 13.3, 7.7 Hz, 1H); **¹³C NMR** (101 MHz, CDCl₃) δ ppm: 143.66, 140.85, 140.23, 139.21, 134.32, 129.72, 129.55, 129.08, 129.06, 128.51, 128.47, 128.39, 128.15, 127.46, 127.38, 127.30, 127.25, 126.44, 69.98, 55.95, 55.61, 46.80, 35.84. **IR** (thin layer film) ν (cm⁻¹) = 3060, 3027, 2924, 2842, 1598, 1573, 1493, 1452, 1246, 1079, 1029, 809, 784, 763, 744, 699, 623. **HRMS** (ESI⁺) m/z C₂₉H₂₈BrClN⁺ [M+H]⁺: calculated 504.1088, found 504.1087.

tert-butyl 3-(4-fluorophenyl)azetidine-1-carboxylate (5e)



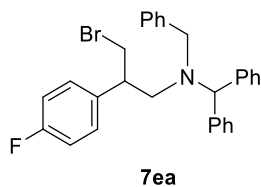
Prepared according to general procedure procedure A using 4-fluorophenylboronic acid (30.3 mmol, 4.24 g). The crude mixture was purified by flash column chromatography (Heptane:EtOAc = 100:0 to 90:10, gradient) to give the desired product in 84% yield (12.6 mmol, 3.18 g) as a colorless oil. **¹H NMR** (500 MHz, CDCl₃) δ ppm: 7.31 – 7.24 (m, 2H), 7.07 – 6.99 (m, 2H), 4.38 – 4.29 (m, 2H), 3.97 – 3.89 (m, 2H), 3.71 (tt, *J* = 8.7, 6.0 Hz, 1H), 1.47 (s, 9H); **¹³C NMR** (126 MHz, CDCl₃) δ ppm: 161.93 (d, *J* = 245.4 Hz), 156.51, 138.13 (d, *J* = 3.1 Hz), 128.42 (d, *J* = 8.0 Hz), 115.66 (d, *J* = 21.5 Hz), 79.74, 56.65, 33.01, 28.54; **¹⁹F NMR** (377 MHz, CDCl₃) δ ppm: -115.78 (tt, *J* = 8.8, 5.4 Hz, 1F). **IR** (thin layer film) ν (cm⁻¹) = 3658, 3492, 2980, 2927, 2344, 2116, 1983, 1703, 1607, 1513, 1457, 1392, 1228, 1158, 1138, 953, 832, 774, 705, 640, 621. **HRMS** (ESI⁺) *m/z* C₁₄H₁₈FNNaO₂⁺ [M+Na]⁺: calculated 274.1214, found 274.1215. Spectroscopic data were in agreement with the ones previously reported in literature.⁷

1-benzhydryl-3-(4-fluorophenyl)azetidine (6e)



Prepared according to general procedure procedure B using 1-Boc-3-(4-fluorophenyl)azetidine **5e** (12.3 mmol, 3.1 g). The crude mixture was purified by flash column chromatography (Heptane:EtOAc = 100:0 to 85:15, gradient) to give the desired product in 39% yield (4.8 mmol, 1.50 g) as a colorless oil. **¹H NMR** (500 MHz, CDCl₃) δ ppm: 7.49 – 7.44 (m, 4H), 7.34 – 7.27 (m, 6H), 7.23 – 7.18 (m, 2H), 7.05 – 6.98 (m, 2H), 4.42 (s, 1H), 3.71 – 3.61 (m, 3H), 3.18 – 3.09 (m, 2H); **¹³C NMR** (126 MHz, CDCl₃) δ ppm: 161.62 (d, *J* = 244.4 Hz), 142.23, 138.97 (d, *J* = 3.2 Hz), 128.61, 128.54 (d, *J* = 8.0 Hz), 127.63, 127.27, 115.27 (d, *J* = 21.3 Hz), 78.37, 60.91, 34.35; **¹⁹F NMR** {¹H} (470 MHz, CDCl₃) δ ppm: -116.85 (s, 1F). **IR** (thin layer film) ν (cm⁻¹) = 3027, 2947, 2827, 1600, 1510, 1491, 1452, 1223, 1157, 1098, 1076, 1029, 924, 830, 743, 702. **HRMS** (ESI⁺) *m/z* C₂₂H₂₁FN⁺ [M+H]⁺: calculated 318.1653, found 318.1652. Spectroscopic data were in agreement with the ones previously reported in literature.⁶

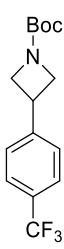
1-benzhydryl-1-benzyl-3-bromo-2-(3-fluorophenyl)propan-1-amine (7ea)



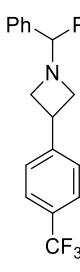
Prepared according to a slightly modified version of general procedure C. Under a flow of N₂, an oven-dried flask was charged with 1-benzhydryl-3-(3-fluorophenyl)azetidine **6e** (2.52 mmol, 0.80 g) in dry CH₃CN (1 M, 2.5 mL). Benzyl bromide (0.95 equiv., 42.39 mmol, 0.28 mL) was added and the mixture was stirred at 60 °C for 12 h. The crude mixture was purified by flash column chromatography (Pentane:EtOAc = 100:0 to 98:2, gradient) to afford the desired product in 89% yield (2.24 mmol, 1.09 g) as a colorless oil. **¹H NMR** (400 MHz, CDCl₃) δ ppm: 7.53 – 7.33 (m, 15H), 7.15 – 7.06 (m, 2H), 7.01 (ddd, *J* = 8.7, 5.3, 2.6 Hz, 2H), 5.08 (s, 1H), 3.88 – 3.79 (m, 1H), 3.77 (d, *J* = 5.6 Hz, 2H), 3.40 (dd, *J* = 10.1, 8.5 Hz, 1H), 3.27 – 3.15 (m, 1H), 3.00 (dd, *J* = 13.3, 7.3 Hz, 1H), 2.85 (dd, *J* = 13.3, 7.4 Hz, 1H); **¹³C NMR** (101 MHz, CDCl₃) δ ppm: 161.99 (d, *J* = 245.1 Hz), 140.80, 140.35, 139.31, 137.26 (d, *J* = 3.2 Hz), 129.52, 129.46 (d, *J* = 7.9 Hz), 129.14, 129.11, 128.47, 128.44, 128.36, 127.42, 127.25, 127.23, 115.31 (d, *J* = 21.2 Hz), 69.88,

55.93, 55.75, 46.22, 36.55; ^{19}F NMR (377 MHz, CDCl_3) δ ppm: -115.63 (tt, $J = 8.7, 5.3$ Hz, 1F). IR (thin layer film) ν (cm^{-1}) = 3027, 2833, 1603, 1509, 1493, 1451, 1225, 1159, 1123, 1076, 1028, 968, 919, 830, 764, 738, 698, 627. HRMS (ESI $^+$) m/z $\text{C}_{29}\text{H}_{28}\text{BrFN}^+$ $[\text{M}+\text{H}]^+$: calculated 488.1384, found. 488.1385.

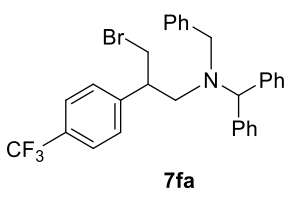
tert-butyl 3-(4-(trifluoromethyl)azetidine-1-carboxylate (5f)

 Prepared according to general procedure A using commercially available 1-Boc-3-iodoazetidine (15.1 mmol, 4.28 g) and 4-(trifluoromethylphenylboronic acid (30.3 mmol, 5.75 g). The crude mixture was purified by flash column chromatography (Heptane:EtOAc = 100:0 to 90:10, gradient) to give the desired product in 69% yield (10.5 mmol, 3.16 g) as a colorless oil. ^1H NMR (500 MHz, CDCl_3) δ ppm: 7.61 (d, $J = 8.0$ Hz, 2H), 7.43 (d, $J = 8.1$ Hz, 2H), 4.36 (m, $J = 8.7$ Hz, 2H), 3.97 (m, 2H), 3.78 (tt, $J = 8.8, 5.9$ Hz, 1H), 1.47 (s, 9H); ^{13}C NMR (126 MHz, CDCl_3) δ ppm: 156.47, 146.45, 129.48 (q, $J = 32.5$ Hz), 127.30, 125.84 (q, $J = 3.8$ Hz), 124.24 (q, $J = 271.9$ Hz), 79.93, 56.55, 33.45, 28.53; ^{19}F NMR (470 MHz, CDCl_3) δ -62.51 (s, 3F). IR (thin layer film) ν (cm^{-1}) = 2976, 1702, 1620, 1393, 1367, 1326, 1256, 1164, 1125, 1069, 1017, 909, 836, 774. HRMS (ESI $^+$) m/z $\text{C}_{15}\text{H}_{19}\text{F}_3\text{NO}_2^+$ $[\text{M}+\text{H}]^+$: calculated 302.1362, found 302.1363. Spectroscopic data were in agreement with the ones previously reported in literature.⁷

1-benzhydryl-3-(4-(trifluoromethyl)phenyl)azetidine (6f)

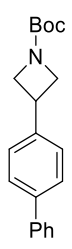
 Prepared according to general procedure B using 1-Boc-3-(4-(trifluoromethyl)phenyl) azetidine **5f** (10.5 mmol, 3.16 g). The crude mixture was purified by flash column chromatography (Heptane:EtOAc = 100:0 to 90:10, gradient) to give the desired product in 45% yield (6.68 mmol, 1.36 g) as a colorless oil. ^1H NMR (500 MHz, CDCl_3) δ ppm: 7.58 (d, $J = 8.1$ Hz, 2H), 7.48 – 7.42 (m, 6H), 7.33 – 7.26 (m, 4H), 7.24 – 7.17 (m, 2H), 4.41 (s, 1H), 3.75 – 3.68 (m, 1H), 3.68 – 3.61 (m, 2H), 3.20 – 3.14 (m, 2H); ^{13}C NMR { ^1H , ^{19}F } (126 MHz, CDCl_3) δ ppm: 147.49, 142.12, 128.75, 128.65, 127.60, 127.43, 127.33, 125.50, 124.42, 78.30, 60.43, 34.78; ^{19}F NMR (470 MHz, CDCl_3) δ ppm: -62.48 (s, 3F). IR (thin layer film) ν (cm^{-1}) = 2954, 2830, 1619, 1491, 1453, 1326, 1164, 1121, 1069, 1018, 835, 744, 704, 641. HRMS (ESI $^+$) m/z $\text{C}_{23}\text{H}_{21}\text{F}_3\text{N}^+$ $[\text{M}+\text{H}]^+$: calculated 368.1621, found 368.1620.

1-benzhydryl-1-benzyl-3-bromo-2-(4-(trifluoromethyl)phenyl)propan-1-amine (7fa)

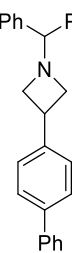
 Prepared according to a slightly modified version of general procedure C. Under a flow of N_2 , an oven-dried flask was charged with 1-benzhydryl-3-(4-(trifluoromethyl) phenyl)azetidine **6f** (2.18 mmol, 0.80 g) in dry CH_3CN (1 M, 2.1 mL). Benzyl bromide (0.95 equiv., 2.07 mmol, 0.25 mL) was added and the mixture was stirred at 60 $^\circ\text{C}$ for 12 h. The crude mixture was purified by flash column chromatography (Pentane:Et $_2$ O = 100:0 to 98:2, gradient) to afford the desired product in 87% yield (1.90 mmol, 1.02 g) as a colorless oil. ^1H NMR (400 MHz, CDCl_3) δ ppm: 7.41 (d, $J = 8.0$ Hz, 2H), 7.33 – 7.07 (m, 15H), 6.90 (d, $J = 8.0$ Hz, 2H), 4.83 (s, 1H), 3.64 – 3.53 (m, 2H), 3.50 (d, $J = 13.7$ Hz, 1H), 3.18 (dd, $J = 10.1, 8.6$ Hz, 1H), 3.08 – 2.96 (m, 1H), 2.79 (dd, $J = 13.4, 7.1$ Hz, 1H), 2.66 (dd, $J = 13.4, 7.4$ Hz,

1H); ^{13}C NMR (^1H , ^{19}F) (126 MHz, CDCl_3) [overlapping signals] δ ppm: 145.70, 140.79, 140.19, 139.14, 130.22, 129.52, 129.38, 129.11, 129.05, 128.51, 128.40, 127.51, 127.34, 127.30, 125.42, 124.35, 70.09, 56.12, 55.77, 46.92, 35.65; ^{19}F NMR (377 MHz, CDCl_3) δ ppm: -62.38. **IR** (thin layer film) ν (cm^{-1}) = 3028, 1619, 1494, 1452, 1325, 1165, 1123, 1069, 1018, 836, 764, 745, 700. **HRMS** (ESI^+) m/z $\text{C}_{30}\text{H}_{28}\text{BrF}_3\text{N}^+$ $[\text{M}+\text{H}]^+$: calculated 538.1352, found. 538.1350.

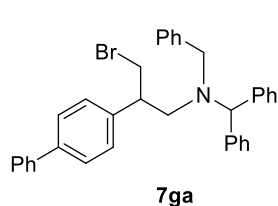
tert-butyl 3-([1,1'-biphenyl]-4-yl)azetidine-1-carboxylate (**5g**)

 Prepared according to general procedure A using commercially available 1-Boc-3-iodoazetidine (7.57 mmol, 2.14 g) and [1,1'-biphenyl]-4-ylboronic acid (15.1 mmol, 3.00 g). The crude mixture was purified by flash column chromatography (Heptane:EtOAc = 100:0 to 90:10, gradient) to give the desired product in 77% yield (5.82 mmol, 1.80 g) as a colorless oil. ^1H NMR (500 MHz, CDCl_3) δ ppm: 7.62 – 7.57 (m, 4H), 7.45 (dd, J = 8.4, 7.0 Hz, 2H), 7.42 – 7.38 (m, 2H), 7.38 – 7.33 (m, 1H), 4.43 – 4.31 (m, 2H), 4.10 – 3.99 (m, 2H), 3.78 (tt, J = 8.8, 6.0 Hz, 1H), 1.49 (s, 9H); ^{13}C NMR (126 MHz, CDCl_3) δ ppm: 156.54, 141.43, 140.82, 140.08, 128.91, 127.55, 127.43, 127.34, 127.15, 79.66, 56.95, 33.35, 28.56. **IR** (thin layer film) ν (cm^{-1}) = 2972, 2884, 1697, 1485, 1391, 1366, 1296, 1254, 1130, 1008, 966, 909, 834, 764, 730, 698. **HRMS** (ESI^+) m/z $\text{C}_{20}\text{H}_{24}\text{NO}_2^+$ $[\text{M}+\text{H}]^+$: calculated 310.1802, found 310.1802.

1-benzhydryl-3-([1,1'-biphenyl]-4-yl)azetidine (**6g**)

 Prepared according to general procedure B using 1-Boc-3-([1,1'-biphenyl]-4-yl)phenylazetidine **5g** (4.95 mmol, 1.53 g). The crude mixture was purified by flash column chromatography (Heptane:EtOAc = 100:0 to 85:15, gradient) to give the desired product in 46% yield (2.28 mmol, 0.85 g) as a colorless oil. ^1H NMR (500 MHz, CDCl_3) δ ppm: 7.63 – 7.54 (m, 4H), 7.51 – 7.47 (m, 4H), 7.47 – 7.42 (m, 2H), 7.40 (d, J = 2.1 Hz, 2H), 7.38 – 7.33 (m, 1H), 7.33 – 7.28 (m, 4H), 7.24 – 7.18 (m, 2H), 4.44 (s, 1H), 3.80 – 3.71 (m, 1H), 3.71 – 3.66 (m, 2H), 3.24 – 3.18 (m, 2H); ^{13}C NMR (126 MHz, CDCl_3) [overlapping signals] δ ppm: 142.35 (br), 141.10, 139.44, 128.89, 128.60, 127.68, 127.54, 127.29, 127.25, 127.16, 78.42, 60.81, 34.72. **IR** (thin layer film) ν (cm^{-1}) = 3658, 2980, 2889, 1462, 1383, 1252, 1152, 1073, 955, 816. **HRMS** (ESI^+) m/z $\text{C}_{28}\text{H}_{26}\text{N}^+$ $[\text{M}+\text{H}]^+$: calculated 376.2060, found 376.2059. Spectroscopic data were in agreement with the ones previously reported in literature.⁶

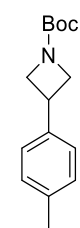
2-([1,1'-biphenyl]-4-yl)-1-benzhydryl-1-benzyl-3-bromopropan-1-amine (**7ga**)



Prepared according to a slightly modified version of general procedure C. Under a flow of N_2 , an oven-dried flask was charged with 1-benzhydryl-3-([1,1'-biphenyl]-4-yl)azetidine **6g** (2.13 mmol, 0.80 g) in dry CH_3CN (1 M, 2.5 mL). Benzyl bromide (1.2 equiv., 2.56 mmol, 0.30 mL) was added and the mixture was stirred at 60 °C for 12 h. The crude mixture was purified by flash column chromatography (Pentane 100%) to afford the desired product in 43% yield (0.92 mmol, 0.50 g) as a colorless oil. ^1H NMR (400 MHz, CDCl_3) δ ppm: 7.56 – 7.49 (m, 2H), 7.49 – 7.10 (m, 20H), 6.96 – 6.89 (m, 2H), 4.89 (s, 1H), 3.68 (dd, J =

10.0, 5.7 Hz, 1H), 3.57 (d, $J = 3.1$ Hz, 2H), 3.28 (dd, $J = 10.1, 8.5$ Hz, 1H), 3.13 – 3.02 (m, 1H), 2.83 (dd, $J = 13.3, 7.3$ Hz, 1H), 2.69 (dd, $J = 13.3, 7.3$ Hz, 1H); ^{13}C NMR (101 MHz, CDCl_3) [overlapping signals] δ ppm: 141.05, 140.83, 140.72, 140.45, 140.04, 139.43, 129.57, 129.21, 129.13, 128.92, 128.46, 128.43, 128.33, 127.39, 127.35, 127.23, 127.20, 127.18, 69.75, 55.86, 55.82, 46.69, 36.47. **IR** (thin layer film) ν (cm^{-1}) = 3059, 3027, 2922, 2837, 1600, 1487, 1451, 1247, 1122, 1075, 1029, 1008, 918, 834, 764, 743, 699, 653. **HRMS** (ESI⁺) m/z $\text{C}_{35}\text{H}_{33}\text{BrN}^+$ [M+H]⁺: calculated 546.1791, found 546.1790.

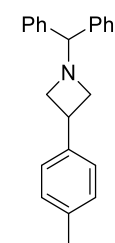
tert-butyl 3-(*p*-tolyl)azetidine-1-carboxylate (5h)



5h

Prepared according to general procedure A using commercially available 1-Boc-3-iodoazetidine (3.75 mmol, 1.06 g) and 4-methylphenylboronic acid (7.50 mmol, 1.02 g). The crude mixture was purified by flash column chromatography (Heptane:EtOAc = 100:0 to 90:10, gradient) to give the desired product in 75% yield (2.81 mmol, 0.66 g) as a colorless oil. ^1H NMR (500 MHz, CDCl_3) δ ppm: 7.23 – 7.18 (m, 2H), 7.18 – 7.13 (m, 2H), 4.31 (t, $J = 8.7$ Hz, 2H), 3.95 (dd, $J = 8.6, 6.1$ Hz, 2H), 3.74 – 3.65 (m, 1H), 2.34 (s, 3H), 1.47 (s, 9H); ^{13}C NMR (126 MHz, CDCl_3) δ ppm: 156.58, 139.39, 136.73, 129.51, 126.80, 79.59, 56.73, 33.32, 28.58, 21.18. **IR** (thin layer film) ν (cm^{-1}) = 2980, 2885, 1701, 1517, 1479, 1456, 1392, 1366, 1296, 1252, 1161, 1132, 966, 909, 860, 813, 773. **HRMS** (ESI⁺) m/z $\text{C}_{15}\text{H}_{23}\text{NNaO}_2^+$ [M+Na]⁺: calculated 270.1465, found 270.1466. Spectroscopic data were in agreement with the ones previously reported in literature.⁷

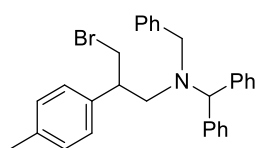
1-benzhydryl-3-(4-methylphenyl)azetidine (6h)



6h

Prepared according to general procedure B using 1-Boc-3-(4-methylphenyl)azetidine **5h** (5.43 mmol, 1.34 g). The crude mixture was purified by flash column chromatography (Heptane:EtOAc = 100:0 to 85:15, gradient) to give the desired product in 58% yield (3.2 mmol, 0.99 g) as a colorless oil. ^1H NMR (500 MHz, CDCl_3) δ ppm: 7.49 – 7.44 (m, 4H), 7.33 – 7.27 (m, 4H), 7.25 – 7.18 (m, 4H), 7.14 (d, $J = 8.0$ Hz, 2H), 4.42 (s, 1H), 3.74 – 3.62 (m, 3H), 3.19 – 3.11 (m, 2H), 2.35 (s, 3H); ^{13}C NMR (126 MHz, CDCl_3) δ ppm: 142.41, 140.18, 135.97, 129.20, 128.57, 127.67, 127.20, 126.98, 78.42, 60.92, 34.66, 21.16. **IR** (thin layer film) ν (cm^{-1}) = 3025, 2922, 2826, 1599, 1515, 1490, 1452, 1344, 1309, 1273, 1197, 1151, 1113, 1076, 1029, 924, 811, 742, 702, 6218, 611. **HRMS** (ESI⁺) m/z $\text{C}_{23}\text{H}_{24}\text{N}^+$ [M+H]⁺: calculated 314.1903, found 314.1903. Spectroscopic data were in agreement with the ones previously reported in literature.⁶

1-benzhydryl-1-benzyl-3-bromo-2-(4-methylphenyl)propan-1-amine (7ha)

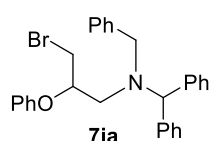


7ha

Prepared according to a slightly modified version of general procedure C. Under a flow of N_2 , an oven-dried flask was charged with 1-benzhydryl-3-(4-methylphenyl)azetidine **6h** (1.82 mmol, 0.57 g) in dry CH_3CN (1 M, 1.8 mL). Benzyl bromide (1.2 equiv., 2.18 mmol, 0.26 mL) was added and the mixture was stirred at 60 °C for 12 h. The crude mixture was purified by flash column chromatography (Pentane 100%) to afford

the desired product in 67% yield (1.21 mmol, 0.59 g) as a colorless oil. **¹H NMR** (400 MHz, CDCl₃) δ ppm: 7.44 – 7.22 (m, 15H), 7.11 (d, *J* = 7.8 Hz, 2H), 6.90 – 6.83 (m, 2H), 4.97 (s, 1H), 3.79 (dd, *J* = 10.0, 5.5 Hz, 1H), 3.73 – 3.59 (m, 2H), 3.33 (dd, *J* = 10.0, 8.8 Hz, 1H), 3.16 – 3.04 (m, 1H), 2.88 (dd, *J* = 13.3, 7.9 Hz, 1H), 2.73 (dd, *J* = 13.3, 6.9 Hz, 1H), 2.37 (s, 3H); **¹³C NMR** (101 MHz, CDCl₃) [overlapping signals] δ ppm: 140.69, 140.64, 139.45, 138.51, 136.72, 129.46, 129.29, 129.24, 129.11, 128.44, 128.39, 128.30, 127.86, 127.31, 127.16, 69.67, 55.85, 55.79, 46.57, 36.83, 21.27. **IR** (thin layer film) ν (cm⁻¹) = 3026, 2919, 2850, 1738, 1635, 1600, 1514, 1493, 1452, 1371, 1244, 1121, 1076, 1028, 918, 812, 763, 743, 700. **HRMS** (ESI⁺) *m/z* C₃₀H₃₁BrN⁺ [M+H]⁺: calculated 484.1634, found 484.1635.

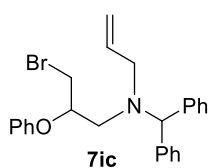
1-benzhydryl-1-benzyl-3-bromo-2-phenoxypropan-1-amine (7ia)



Prepared according to a slightly modified version of general procedure C. Under a flow of N₂, an oven-dried flask was charged with commercially available 1-benzhydryl-3-phenoxyazetidene (4.75 mmol, 1.5 g) in dry CH₃CN (5.8 mL). Benzyl bromide (1.2 equiv., 5.71 mmol, 0.68 mL) was added and the mixture was stirred at 60 °C for 12 h.

The residue was purified by flash column chromatography (Pentane:EtOAc = 98:2) to afford the desired product in quantitative yield (4.75 mmol, 1.94 g) as a colorless oil. **¹H NMR** (400 MHz, CDCl₃) δ ppm: 7.50 – 7.21 (m, 17H), 7.02 – 6.93 (m, 1H), 6.77 – 6.69 (m, 2H), 5.03 (s, 1H), 4.37 – 4.27 (m, 1H), 3.84 – 3.70 (m, 2H), 3.52 (dd, *J* = 10.8, 5.0 Hz, 1H), 3.36 (dd, *J* = 10.7, 5.2 Hz, 1H), 2.98 (dd, *J* = 6.0, 1.1 Hz, 2H); **¹³C NMR** (101 MHz, CDCl₃) δ ppm: 157.63, 141.34, 140.91, 139.50, 129.69, 129.38, 129.15, 129.11, 128.57, 128.53, 128.51, 127.43, 127.35, 127.31, 121.58, 116.19, 76.80, 71.15, 56.92, 53.55, 33.29. **IR** (thin layer film) ν (cm⁻¹) = 3027, 2835, 1598, 1492, 1452, 1237, 1172, 1077, 1029, 921, 745, 698. **HRMS** (ESI⁺) *m/z* C₂₉H₂₉BrNO⁺ [M+H]⁺: calculated 486.1427, found 486.1426.

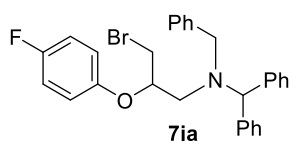
1-benzhydryl-1-(3-bromo-2-phenoxypropyl)prop-2-en-1-amine (7ic)



Prepared according to a slightly modified version of general procedure C. Under a flow of N₂, an oven-dried flask was charged with commercially available 1-benzhydryl-3-phenoxyazetidene (2.53 mmol, 0.8 g) in CH₃CN (2.3 mL). Benzyl bromide (1.2 equiv., 2.28 mmol, 0.20 mL) was added and the mixture was stirred at 60 °C for 12 h. The residue

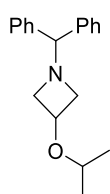
was purified by flash column chromatography (Pentane:Et₂O = 98.5:1.5) to afford the desired product in 62% yield (0.79 g, 1.57 mmol) as colorless oil. **¹H NMR** (400 MHz, CDCl₃) δ ppm: 7.32 – 7.10 (m, 12H), 6.88 (tt, *J* = 7.3, 1.1 Hz, 1H), 6.75 – 6.67 (m, 2H), 5.84 (ddt, *J* = 16.8, 10.2, 6.5 Hz, 1H), 5.11 – 4.97 (m, 2H), 4.87 (s, 1H), 4.40 – 4.30 (m, 1H), 3.59 (dd, *J* = 10.7, 4.8 Hz, 1H), 3.44 (dd, *J* = 10.7, 5.4 Hz, 1H), 3.20 – 3.10 (m, 2H), 2.84 (d, *J* = 6.2 Hz, 2H); **¹³C NMR** (101 MHz, CDCl₃) δ ppm: 157.82, 141.87, 141.67, 135.38, 129.69, 129.03, 128.75, 128.54, 128.53, 127.37, 127.24, 121.63, 118.26, 116.36, 77.48, 71.50, 55.37, 52.95, 33.53. **IR** (thin layer film) ν (cm⁻¹) = 3061, 3027, 2834, 1598, 1587, 1492, 1452, 1418, 1336, 1289, 1237, 1171, 1077, 1029, 995, 922, 823, 750, 704, 610. **HRMS** (ESI⁺): *m/z* C₂₅H₂₇BrNO⁺ [M+H]⁺: calculated 436.1271, found 436.1270.

1-benzhydryl-1-benzyl-3-bromo-2-(4-fluorophenoxy)propan-1-amine (7ja)



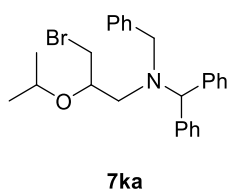
Prepared according to general procedure C using commercially available 1-benzhydryl-3-(4-fluorophenoxy)azetidine (0.60 mmol, 0.20 g) and benzyl bromide (0.96 mmol, 0.11 mL). The residue was purified by flash column chromatography (Heptane:EtOAc = 95:5) to afford the desired product in 62% yield (0.19 g, 0.38 mmol) as colorless oil. **¹H NMR** (400 MHz, CDCl₃) δ ppm: 7.44 – 7.26 (m, 15H), 6.95 – 6.84 (m, 2H), 6.66 – 6.56 (m, 2H), 4.98 (s, 1H), 4.16 – 4.06 (m, 1H), 3.79 – 3.66 (m, 2H), 3.50 (dd, J = 10.8, 4.6 Hz, 1H), 3.30 (dd, J = 10.8, 5.5 Hz, 1H), 2.99 – 2.85 (m, 2H); **¹³C NMR** (101 MHz, CDCl₃) δ ppm: 157.80 (d, J = 239.4 Hz), 153.76, 141.30, 140.89, 139.42, 129.36, 129.16, 129.07, 128.60, 128.57, 128.56, 127.49, 127.42, 127.37, 117.68 (d, J = 7.9 Hz), 116.02 (d, J = 23.0 Hz), 78.06, 71.41, 57.14, 53.72, 33.40; **¹⁹F NMR** (470 MHz, CDCl₃) δ ppm: -78.22. **IR** (thin layer film) ν (cm⁻¹) = 3065, 1498, 1459, 1257, 1224, 1155, 1030, 902, 851, 754, 700, 638. **HRMS** (ESI⁺): m/z C₂₉H₂₈BrFNO⁺ [M+H]⁺: calculated 504.1333, found 504.1332.

1-benzhydryl-3-isopropoxyazetidine (6k)



Prepared according to a slightly modified version of general procedure B. To a solution of commercially available 3-isopropoxyazetidine hydrochloride (10.02 mmol, 1.52 g) in dry CH₃CN (9.2 mL), DIPEA (2.7 equiv., 27.32 mmol, 4.7 mL) and bromodiphenylmethane (0.9 equiv., 9.10 mmol, 2.25 g) were subsequently added. The reaction mixture was stirred at 100 °C for 2 h after which it was concentrated *in vacuo*. The crude mixture was purified by flash column chromatography (Heptane:EtOAc = 100:0 to 85:15, gradient) to give the desired product in 98% yield (8.88 mmol, 2.6 g) as a colorless oil. **¹H NMR** (400 MHz, CDCl₃) δ ppm: 7.45 – 7.37 (m, 4H), 7.32 – 7.22 (m, 4H), 7.22 – 7.13 (m, 2H), 4.37 (s, 1H), 4.25 – 4.11 (m, 1H), 3.63 – 3.49 (m, 3H), 2.97 – 2.80 (m, 2H), 1.11 (d, J = 6.1 Hz, 6H); **¹³C NMR** (101 MHz, CDCl₃) δ ppm: 142.38, 128.54, 127.63, 127.21, 78.68, 71.32, 66.35, 62.25, 22.67. **IR** (thin layer film) ν (cm⁻¹) = 3061, 3027, 2972, 2833, 1599, 1491, 1452, 1379, 1334, 1273, 1195, 1174, 1143, 1074, 1029, 1000, 970, 938, 834, 745, 703, 637, 612. **HRMS** (ESI⁺) m/z C₁₉H₂₄NO⁺ [M+H]⁺: calculated 282.1852, found 282.1852.

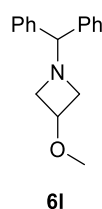
1-benzhydryl-1-benzyl-3-bromo-2-isopropoxypropan-1-amine (7ka)



Prepared according to general procedure C using 1-benzhydryl-3-isopropoxyazetidine **6k** (3.01 mmol, 0.85 g) and benzyl bromide (4.83 mmol, 0.57 mL). The crude mixture was purified by flash column chromatography (Pentane:EtOAc = 100:0 to 95:5, gradient) to afford the desired product in 89% yield (2.67 mmol, 1.36 g) as a colorless oil. **¹H NMR** (500 MHz, CDCl₃) δ ppm: 7.58 – 7.14 (m, 15H), 4.97 (s, 1H), 3.68 (d, J = 2.1 Hz, 2H), 3.57 – 3.43 (m, 2H), 3.42 – 3.29 (m, 1H), 3.16 (dd, J = 10.5, 6.2 Hz, 1H), 2.71 (dd, J = 13.7, 7.5 Hz, 1H), 2.62 (dd, J = 13.8, 5.4 Hz, 1H), 1.04 (dd, J = 13.9, 6.1 Hz, 6H); **¹³C NMR** (126 MHz, CDCl₃) [overlapping signals] δ ppm: 141.04, 140.95, 139.58, 129.37, 129.28, 129.11, 128.52, 128.43, 128.40, 127.31, 127.27, 75.95, 71.27, 70.81, 56.98, 54.77, 35.63, 22.91, 22.67. **IR** (thin layer film) ν (cm⁻¹) = 3027, 2970, 2927, 1600, 1493, 1452,

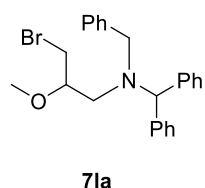
1379, 1332, 1247, 1120, 1047, 1029, 970, 922, 763, 743, 699, 667, 621. **HRMS** (ESI⁺) m/z C₂₆H₃₁BrNO⁺ [M+H]⁺: calculated 452.1584, found 452.1581.

1-benzhydryl-3-methoxyazetidine (**6l**)



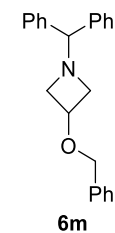
Prepared according to a slightly modified version of general procedure B. To a solution of commercially available 3-methoxyazetidine hydrochloride (10.02 mmol, 1.24 g) in dry acetonitrile (9.2 mL), DIPEA (2.7 equiv., 27.32 mmol, 4.7 mL) and bromodiphenylmethane (0.9 equiv., 9.10 mmol, 2.25 g) were subsequently added. The reaction mixture was stirred at 100 °C for 2 h after which it was concentrated *in vacuo*. The crude mixture was purified by flash column chromatography (Heptane:EtOAc = 100:0 to 85:15, gradient) to give the desired product in 98% yield (8.88 mmol, 2.25 g) as a colorless oil. **¹H NMR** (400 MHz, CDCl₃) δ ppm: 7.53 – 7.43 (m, 4H), 7.37 – 7.29 (m, 4H), 7.28 – 7.21 (m, 2H), 4.42 (s, 1H), 4.11 (m, 1H), 3.60 – 3.52 (m, 2H), 3.29 (s, 3H), 3.02 – 2.94 (m, 2H); **¹³C NMR** (101 MHz, CDCl₃) δ ppm: 142.27, 128.56, 127.60, 127.26, 78.66, 69.49, 60.63, 56.01. **IR** (thin layer film) ν (cm⁻¹) = 3027, 2936, 2829, 1599, 1491, 1452, 1368, 1307, 1276, 1222, 1177, 1155, 1120, 1075, 1029, 1012, 822, 745, 703, 634. **HRMS** (ESI⁺) m/z C₁₇H₂₀NO⁺ [M+H]⁺: calculated 254.1539, found 254.1544. Spectroscopic data were in agreement with the ones previously reported in literature.⁵

1-benzhydryl-1-benzyl-3-bromo-2-methoxypropan-1-amine (**7la**)



Prepared according to general procedure C using 1-benzhydryl-3-(methoxy)azetidine **6l** (3.01 mmol, 0.76 g) and benzyl bromide (5.01 mmol, 0.6 mL). The crude mixture was purified by flash column chromatography (Heptane:EtOAc = 100:0 to 95:5, gradient) to afford the desired product in 99% yield (3.00 mmol, 1.27 g) as a colorless oil. **¹H NMR** (400 MHz, CDCl₃) δ ppm: 7.37 – 7.26 (m, 9H), 7.26 – 7.13 (m, 6H), 4.91 (s, 1H), 3.68 – 3.55 (m, 2H), 3.43 – 3.34 (m, 1H), 3.22 – 3.10 (m, 5H), 2.69 – 2.59 (m, 2H); **¹³C NMR** (101 MHz, CDCl₃) δ ppm: 141.05, 140.86, 139.60, 129.33, 129.29, 129.08, 128.51, 128.44, 128.42, 127.31, 127.29, 127.25, 79.99, 70.62, 57.90, 56.65, 53.24, 34.35. **IR** (thin layer film) ν (cm⁻¹) = 3060, 3027, 2929, 2826, 1600, 1493, 1452, 1094, 1029, 977, 763, 744, 699, 670. **HRMS** (ESI⁺) m/z C₂₄H₂₇BrNO⁺ [M+H]⁺: calculated 424.1271, found 424.1269.

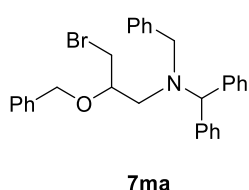
1-benzhydryl-3-(benzyloxy)azetidine (**6m**)



In a round-bottom flask under a flow of N₂, NaH 60 wt% in mineral oil (15.0 mmol, 0.60 g) was added to a solution of commercially available 1-benzhydrylazetidin-3-ol (10.0 mmol, 2.40 g) in THF (20 mL) at 0 °C. The mixture was stirred at r.t. for 30 min before benzyl bromide (13.0 mmol, 1.52 mL) was added dropwise. The reaction mixture was stirred at 60 °C for 18 h and then allowed to cool to r.t. A saturated aqueous NH₄Cl solution (20 mL) was then added. The layers were separated, and the aqueous layer was extracted with EtOAc (2 x 50 mL). The combined organic layers were washed with brine (20 mL), dried over Na₂SO₄, and concentrated under reduced pressure. The crude mixture

was purified by flash column chromatography (Heptane:EtOAc = 100:0 to 90:10, gradient) to give the desired compound in 90% yield (9.1 mmol, 3.0 g) as a colorless oil. **¹H NMR** (500 MHz, CDCl₃) δ ppm: 7.41 – 7.36 (m, 4H), 7.34 – 7.22 (m, 9H), 7.21 – 7.14 (m, 2H), 4.40 (s, 2H), 4.36 (s, 1H), 4.23 (m, 1H), 3.49 (dd, *J* = 6.2, 2.0 Hz, 2H), 2.94 (dd, *J* = 6.2, 2.0 Hz, 2H); **¹³C NMR** (126 MHz, CDCl₃) δ ppm: 142.20, 137.74, 128.46, 128.44, 127.95, 127.84, 127.48, 127.12, 78.51, 70.96, 67.65, 60.94. **IR** (thin layer film) ν (cm⁻¹) = 3027, 2942, 2833, 1599, 1492, 1452, 1354, 1308, 1274, 1207, 1172, 1112, 1074, 1027, 912, 821, 742, 696, 636, 621, 611. **HRMS** (ESI⁺) *m/z* C₂₃H₂₄NO⁺ [M+H]⁺: calculated 330.1858, found 330.1862. Spectroscopic data were in agreement with the ones previously reported in literature.⁹

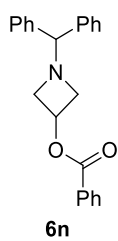
1-benzhydryl-1-benzyl-2-(benzyloxy)-3-bromopropan-1-amine (7ma)



Prepared according to general procedure C using 1-benzhydryl-3-(benzyloxy)azetidine **6m** (3.01 mmol, 0.99 g) and benzyl bromide (4.82 mmol, 0.6 mL). The crude mixture was purified by flash column chromatography (Heptane:EtOAc = 100:0 to 95:5, gradient) to afford the desired product in 99% (3.00 mmol, 1.50 g) as a colorless oil.

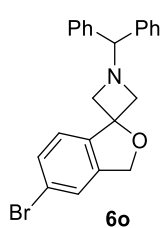
¹H NMR (400 MHz, CDCl₃) δ ppm: 7.33 – 7.12 (m, 20H), 4.88 (s, 1H), 4.43 (d, *J* = 11.4 Hz, 1H), 4.34 (d, *J* = 11.4 Hz, 1H), 3.59 (s, 2H), 3.48 – 3.38 (m, 2H), 3.26 – 3.16 (m, 1H), 2.68 (d, *J* = 6.0 Hz, 2H); **¹³C NMR** (101 MHz, CDCl₃) [overlapping signals] δ ppm: 140.98, 140.89, 139.48, 138.16, 129.33, 129.27, 129.09, 128.51, 128.42, 128.10, 127.90, 127.31, 127.27, 127.24, 77.75, 72.42, 70.58, 56.60, 53.84, 34.70. **IR** (thin layer film) ν (cm⁻¹) = 3061, 3028, 2842, 1600, 1493, 1453, 1339, 1062, 1028, 921, 764, 742, 698. **HRMS** (ESI⁺) *m/z* C₃₀H₃₁BrNO⁺ [M+H]⁺: calculated 500.1581, found 500.1583.

1-benzhydrylazetid-3-yl benzoate (6n)



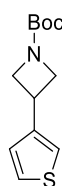
Benzoic anhydride (13.8 mmol, 3.12 g) was added to a pre-stirred mixture of 1-benzhydrylazetid-3-ol (9.19 mmol, 2.20 g) and N,N-dimethylaminopyridine (18.4 mmol, 2.25 g) in CH₂Cl₂ (48 mL), and the resulting mixture was stirred for 12 h. An aqueous NaHCO₃ solution (8 wt%, 50 mL) was added and the reaction was stirred for a further 30 min. The phases were separated, and the aqueous layer extracted with CH₂Cl₂ (50 mL). The combined organic layers were concentrated and purified by flash column chromatography (Heptane:EtOAc = 100:0 to 90:10, gradient) to afford the desired compound in 99% yield (9.19 mmol, 3.16 g) as yellow oil. **¹H NMR** (500 MHz, CDCl₃) δ ppm: 8.09 – 8.04 (m, 2H), 7.61 – 7.54 (m, 1H), 7.49 – 7.42 (m, 6H), 7.34 – 7.25 (m, 4H), 7.25 – 7.18 (m, 2H), 5.33 (m, 1H), 4.45 (s, 1H), 3.78 – 3.72 (m, 2H), 3.22 – 3.16 (m, 2H); **¹³C NMR** (126 MHz, CDCl₃) δ ppm: 166.07, 142.01, 133.25, 129.91, 129.77, 128.62, 128.50, 127.55, 127.36, 78.46, 64.40, 60.37. **IR** (thin layer film) ν (cm⁻¹) = 3061, 3027, 2963, 2837, 1718, 1601, 1585, 1490, 1451, 1344, 1314, 1268, 1208, 1171, 1115, 1070, 1025, 925, 847, 827, 745, 703, 666, 634, 621, 611. **HRMS** (ESI⁺) *m/z* C₂₃H₂₂NO₂⁺ [M+H]⁺: calculated 344.1650, found 344.1649.

1-benzhydryl-5'-bromo-3'H-spiro[azetidine-3,1'-isobenzofuran] (6o)



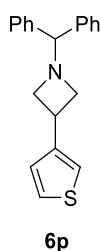
Prepared according to general procedure B using commercially available 1-Boc-5'-bromo-3'H-spiro[azetidine-3,1'-isobenzofuran] (1.393 mmol, 0.47 g) The crude mixture was purified by flash column chromatography (Heptane:EtOAc = 100:0 to 85:15, gradient) to give the desired product in 62% yield (0.86 mmol, 0.35 g) as a white solid. **¹H NMR** (400 MHz, CDCl₃) δ ppm: 7.75 (d, *J* = 8.0 Hz, 1H), 7.53 (m, 1H), 7.50 – 7.44 (m, 4H), 7.33 – 7.26 (m, 5H), 7.21 – 7.14 (m, 2H), 5.04 (d, *J* = 1.0 Hz, 2H), 4.43 (s, 1H), 3.51 – 3.43 (m, 2H), 3.43 – 3.35 (m, 2H); **¹³C NMR** (101 MHz, CDCl₃) δ ppm: 142.51, 142.40, 140.91, 131.37, 128.61, 127.55, 127.31, 123.93, 122.63, 121.84, 82.64, 78.20, 72.25, 67.53. **IR** (thin layer film) ν (cm⁻¹) = 3049, 3026, 2947, 2830, 1600, 1492, 1472, 1452, 1414, 1350, 1313, 1271, 1249, 1208, 1194, 1175, 1154, 1074, 1027, 1006, 857, 821, 743, 703, 672, 641, 614. **HRMS** (ESI⁺) *m/z* C₂₃H₂₁BrNO⁺ [M+H]⁺: calculated 406.0801, found 406.0800. **MP** 148 – 150 °C.

tert-butyl 3-(thiophen-3-yl)azetidine-1-carboxylate (5p)



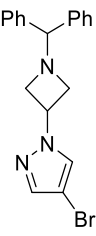
To a pre-formed solution of (1-(tert-butoxycarbonyl)azetidin-3-yl)zinc(II) iodide¹⁰ in THF (0.3 M, 28.6 mL), 3-bromothiophene (4.29 mmol, 0.70 g), bis(dibenzylideneacetone) palladium (5 mol%, 0.22 mmol, 123 mg) and XPhos (10 mol%, 0.43 mmol, 205 mg) were added. The mixture was stirred at 50 °C for 2 h. After cooling the mixture to r.t., the solvent was evaporated *in vacuo* and the crude product was purified by flash column chromatography (Heptane:EtOAc = 100:0 to 90:10, gradient) to afford the desired compound in 64% yield (2.75 mmol, 0.66 g) as a colorless oil. **¹H NMR** (400 MHz, CDCl₃) δ ppm: 7.33 (dd, *J* = 4.7, 3.2 Hz, 1H), 7.11 – 7.05 (m, 2H), 4.34 – 4.25 (m, 2H), 3.99 – 3.89 (m, 2H), 3.86 – 3.74 (m, 1H), 1.46 (s, 9H); **¹³C NMR** (101 MHz, CDCl₃) δ ppm: 156.56, 143.25, 126.68, 126.42, 120.73, 79.68, 56.56, 29.36, 28.56. **IR** (thin layer film) ν (cm⁻¹) = 2973, 2884, 1698, 1479, 1456, 1390, 1366, 1294, 1253, 1161, 1131, 929, 849, 774, 647. **HRMS** (ESI⁺) *m/z* C₁₂H₁₈NO₂S⁺ [M+H]⁺: calculated 240.1053, found 240.1054.

1-benzhydryl-3-(thiophen-3-yl)azetidine (6p)



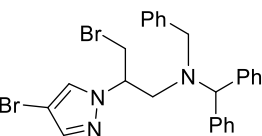
Prepared according to a slightly modified version of general procedure B. To a solution of *tert*-butyl 3-(thiophen-3-yl)azetidine-1-carboxylate **5p** (4.18 mmol, 0.74 g) in dry CH₃CN (3.8 mL), DIPEA (3.6 equiv., 15.21 mmol, 2.6 mL) and bromodiphenylmethane (0.9 equiv., 3.80 mmol, 0.94 g) were subsequently added. The crude mixture was purified by flash column chromatography (Heptane:EtOAc = 100:0 to 85:15, gradient) to give the desired product in 80% yield (3.35 mmol, 0.93 g) as a colorless oil. **¹H NMR** (400 MHz, CDCl₃) δ ppm: 7.48 – 7.43 (m, 4H), 7.33 – 7.24 (m, 5H), 7.22 – 7.16 (m, 2H), 7.10 (dd, *J* = 5.0, 1.3 Hz, 1H), 7.05 – 7.01 (m, 1H), 4.40 (s, 1H), 3.72 (p, *J* = 7.2 Hz, 1H), 3.66 – 3.57 (m, 2H), 3.16 – 3.08 (m, 2H); **¹³C NMR** (101 MHz, CDCl₃) δ ppm: 144.33, 142.32, 128.58, 127.65, 127.23, 127.18, 125.85, 120.12, 78.43, 61.03, 30.79. **IR** (thin layer film) ν (cm⁻¹) = 3025, 2948, 2825, 1598, 1490, 1451, 1076, 1029, 822, 778, 742, 702, 643, 610. **HRMS** (ESI⁺) *m/z* C₂₀H₂₀NS⁺ [M+H]⁺: calculated 306.1311, found 306.1310.

1-(1-benzhydrylazetididin-3-yl)-4-bromo-1H-pyrazole (6q)


6q

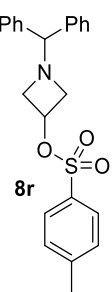
Prepared according to general procedure B using commercially available 1-(1-Boc-azetididin-3-yl)-4-bromo-1H-pyrazole (3.32 mmol, 1.00 g). The crude mixture was purified by flash column chromatography (Heptane:EtOAc = 100:0 to 80:20, gradient) to afford the desired product in 29% yield (0.87 mmol, 0.32 g) as a colorless oil. **¹H NMR** (500 MHz, CDCl₃) δ ppm: 7.65 (s, 1H), 7.49 (s, 1H), 7.46 – 7.40 (m, 4H), 7.28 (dd, *J* = 8.4, 6.9 Hz, 5H), 7.24 – 7.16 (m, 2H), 4.95 – 4.86 (m, 1H), 4.50 (s, 1H), 3.69 – 3.62 (m, 2H), 3.47 – 3.41 (m, 2H); **¹³C NMR** (126 MHz, CDCl₃) δ ppm: 141.71, 140.14, 128.72, 128.55, 127.54, 127.49, 93.48, 77.95, 60.21, 51.89. **IR** (thin layer film) ν (cm⁻¹) = 3026, 2960, 2848, 1598, 1491, 1451, 1383, 1310, 1263, 1206 1180, 1149, 1076, 1029, 1004, 952, 843, 804, 744, 704, 644, 613. **HRMS** (ESI⁺) *m/z* C₁₉H₁₉BrN₃⁺ [M+H]⁺: calculated 368.0757, found 368.0761.

1-benzhydryl-1-benzyl-3-bromo-2-(4-bromo-1H-pyrazol-1-yl)propan-1-amine (7qa)


7qa

Prepared according to a slightly modified version of general procedure C. Under a flow of N₂, an oven-dried flask was charged with 1-benzhydryl-3-(4-bromo-1H-pyrazol-1-yl)azetididine **6q** (0.92 mmol, 0.34 g) in dry CH₃CN (1 M, 0.9 mL). Benzyl bromide (0.98 equiv., 0.90 mmol, 0.11 mL) was added and the mixture was stirred at 60 °C for 12 h. The crude mixture was purified by flash column chromatography (Heptane:EtOAc = 100:0 to 98:2, gradient) to afford the desired product in 96% yield (0.88 mmol, 0.48 g) as a colorless oil. **¹H NMR** (500 MHz, CDCl₃) δ ppm: 7.43 (s, 1H), 7.40 – 7.22 (m, 15H), 7.09 (s, 1H), 4.83 (s, 1H), 4.03 – 3.94 (m, 1H), 3.62 (s, 2H), 3.53 (dd, *J* = 10.7, 4.4 Hz, 1H), 3.41 (dd, *J* = 10.7, 8.8 Hz, 1H), 3.11 – 2.98 (m, 2H); **¹³C NMR** (126 MHz, CDCl₃) [overlapping signals] δ ppm: 140.79, 140.51, 140.45, 138.96, 130.24, 129.32, 129.12, 128.92, 128.72, 128.66, 128.62, 127.63, 127.49, 92.54, 71.27, 63.73, 57.02, 55.06, 32.85. **IR** (thin layer film) ν (cm⁻¹) = 3061, 3029, 2845, 1600, 1493, 1452, 1381, 1313, 1179, 1121, 1077, 1028, 976, 952, 913, 846, 765, 745, 700, 611. **HRMS** (ESI⁺) *m/z* C₂₆H₂₆Br₂N₃⁺ [M+H]⁺: calculated 538.0488, found 538.0486.

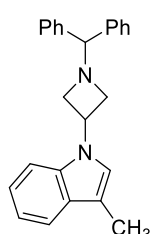
1-benzhydrylazetididin-3-yl 4-methylbenzenesulfonate (8r)


8r

In a flame-dried round bottom flask under a flow of N₂, NaH 60 wt% in mineral oil (62.7 mmol, 2.50 g) and 4-methylbenzenesulfonyl chloride (50.1 mmol, 9.55 g) were subsequently added to a solution of commercially available 1-benzhydrylazetididin-3-ol (41.8 mmol, 10.0 g) in dry THF (100 mL) at 0 °C. The reaction mixture was stirred for 12 h at r.t. After completion of the reaction (LC-MS monitoring), the reaction mixture was quenched with water (50 mL). The aqueous phase was extracted with EtOAc (2 x 250 mL). The organic phases were combined, washed with brine (200 mL), dried over Na₂SO₄, filtered and concentrated *in vacuo*. The crude mixture was purified by flash column chromatography (Heptane:EtOAc = 100:0 to 90:10, gradient) to give the desired product as a white solid in 32% yield (13.7 mmol, 5.40 g). **¹H NMR** (500 MHz, CDCl₃) δ ppm: 7.81 – 7.75 (m, 2H), 7.39 – 7.32 (m, 6H), 7.30 – 7.15 (m, 6H), 4.91 (p, *J* = 6.0 Hz, 1H), 4.35 (s, 1H), 3.52 – 3.45 (m, 2H), 3.11 – 3.04

(m, 2H), 2.45 (s, 3H); ^{13}C NMR (126 MHz, CDCl_3) δ ppm: 145.22, 141.62, 133.36, 130.07, 128.65, 128.00, 127.46, 127.43, 78.22, 68.26, 60.20, 21.80. **IR** (thin layer film) ν (cm^{-1}) = 3028, 2965, 2841, 1598, 1492, 1452, 1366, 1308, 1191, 1177, 1097, 1079, 1049, 1001, 952, 922, 864, 839, 815, 755, 705, 661. **HRMS** (ESI^+) m/z $\text{C}_{23}\text{H}_{24}\text{NO}_3\text{S}^+$ $[\text{M}+\text{H}]^+$: calculated 394.1471, found. 394.1470. **MP** 106 – 108 °C.

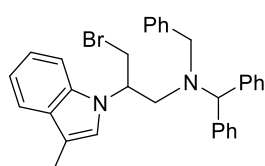
1-(1-benzhydrylazetididin-3-yl)-3-methyl-1H-indole (**6r**)



6r

In a flame-dried round bottom flask under a flow of N_2 , NaH 60 wt% in mineral oil (15.8 mmol, 0.63 g) was added portion-wise to a solution of 1-benzhydrylazetididin-3-yl 4-methylbenzenesulfonate **8r** (7.88 mmol, 3.10 g) in dry DMF (15.5 mL). The mixture was stirred for 30 min, then 3-methylindole (9.45 mmol, 1.24 g) was added. The reaction mixture was stirred for 24 h at r.t. After completion, a saturated aqueous NH_4Cl solution (20 mL) was added. The layers were separated, and the aqueous layer was extracted with EtOAc (2 x 50 mL). The combined organic layers were washed with brine (20 mL), dried over Na_2SO_4 , and concentrated under reduced pressure. The crude mixture was purified by flash column chromatography (Heptane:EtOAc = 100:0 to 95:5, gradient) to afford the desired compound in 70% yield (5.51 mmol, 1.94 g) as a colorless oil. ^1H NMR (500 MHz, CDCl_3) δ ppm: 7.55 (dt, J = 7.8, 1.0 Hz, 1H), 7.48 – 7.42 (m, 4H), 7.32 – 7.23 (m, 5H), 7.23 – 7.12 (m, 4H), 7.09 (ddd, J = 7.9, 6.9, 1.0 Hz, 1H), 5.00 (p, J = 6.8 Hz, 1H), 4.45 (s, 1H), 3.80 – 3.73 (m, 2H), 3.38 – 3.32 (m, 2H), 2.34 (d, J = 1.1 Hz, 3H); ^{13}C NMR (126 MHz, CDCl_3) δ ppm: 141.93, 136.47, 129.00, 128.71, 127.55, 127.46, 122.53, 121.72, 119.24, 119.13, 111.32, 109.36, 78.32, 60.55, 45.20, 9.84. **IR** (thin layer film) ν (cm^{-1}) = 3026, 2917, 2838, 1599, 1491, 1463, 1452, 1388, 1371, 1317, 1278, 1234, 1210, 1076, 1029, 1014, 923, 739, 703, 641, 612. **HRMS** (ESI^+) m/z $\text{C}_{25}\text{H}_{25}\text{N}_2^+$ $[\text{M}+\text{H}]^+$: calculated 353.2012, found. 353.2011.

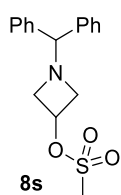
1-benzhydryl-1-benzyl-3-bromo-2-(3-methyl-1H-indol-1-yl)propan-1-amine (**7ra**)



7ra

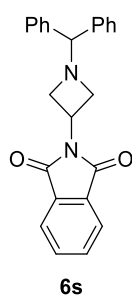
Prepared according to a slightly modified version of general procedure C. Under a flow of N_2 , an oven-dried flask was charged with 1-benzhydryl-3-(3-methyl-1H-indol-1-yl)azetididine **6r** (1.53 mmol, 0.54 g) in dry CH_3CN (1 M, 1.5 mL). Benzyl bromide (0.95 equiv., 1.45 mmol, 0.2 mL) was added and the mixture was stirred at 60 °C for 12 h. The crude mixture was purified by flash column chromatography (Heptane:EtOAc = 100:0 to 98:2, gradient) to afford the desired product in 68% yield (1.04 mmol, 0.54 g) as a colorless oil. ^1H NMR (400 MHz, CDCl_3) δ ppm: 7.56 – 7.48 (m, 1H), 7.37 – 7.26 (m, 14H), 7.14 – 7.03 (m, 2H), 6.89 – 6.80 (m, 1H), 6.51 – 6.46 (m, 1H), 4.84 (s, 1H), 4.40 – 4.29 (m, 1H), 3.74 (dd, J = 10.7, 4.9 Hz, 1H), 3.65 (d, J = 1.9 Hz, 2H), 3.35 (dd, J = 10.7, 8.4 Hz, 1H), 3.18 (dd, J = 13.9, 7.4 Hz, 1H), 2.98 (dd, J = 13.9, 6.8 Hz, 1H), 2.26 (d, J = 1.1 Hz, 3H); ^{13}C NMR (101 MHz, CDCl_3) [overlapping signals] δ ppm: 141.12, 140.90, 139.22, 129.30, 129.19, 128.96, 128.87, 128.69, 128.67, 128.58, 127.60, 127.53, 127.37, 122.05, 121.56, 119.17, 119.03, 111.41, 109.40, 71.53, 57.16, 56.19, 54.67, 34.10, 9.85. **IR** (thin layer film) ν (cm^{-1}) = 3061, 1498, 1461, 1389, 1258, 1225, 1159, 1030, 742, 706, 638. **HRMS** (ESI^+) m/z $\text{C}_{32}\text{H}_{31}\text{BrN}_2^+$ $[\text{M}+\text{H}]^+$: calculated 523.1743, found 523.1741.

1-benzhydrylazetididin-3-yl methanesulfonate (**8s**)



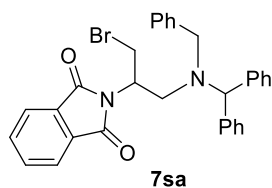
In a flame-dried round bottom flask under a flow of N₂, commercially available 1-benzhydrylazetididin-3-ol (8.36 mmol, 2.0 g) was dissolved in dry CH₂Cl₂ (20.0 mL) and a premixed solution of methanesulfonyl chloride (10.0 mmol, 1.15 g) and triethylamine (11.7 mmol, 1.64 mL) in dry CH₂Cl₂ (5.0 mL) was slowly added to it at 0 °C. The solution was stirred at r.t. for 12 h, then water (20 mL) was added and the mixture was extracted with CH₂Cl₂ (3 x 20 mL). The organic phases were combined, washed with brine (20 mL), dried over Na₂SO₄, filtered and concentrated *in vacuo* to afford the desired product in quantitative yield (8.86 mmol, 2.64 g) as a pale yellow solid. ¹H NMR (400 MHz, CDCl₃) δ ppm: 7.43 – 7.35 (m, 4H), 7.28 (tq, *J* = 8.2, 1.1 Hz, 4H), 7.23 – 7.16 (m, 2H), 5.10 (p, *J* = 5.8 Hz, 1H), 4.40 (s, 1H), 3.67 – 3.59 (m, 2H), 3.24 – 3.15 (m, 2H), 2.98 (s, 3H); ¹³C NMR (101 MHz, CDCl₃) δ ppm: 141.55, 128.71, 127.54, 127.45, 78.32, 68.11, 60.33, 38.27. IR (thin layer film) ν (cm⁻¹) = 3027, 2937, 2842, 1599, 1491, 1452, 1358, 1207, 1177, 1161, 1079, 1051, 1002, 971, 947, 924, 866, 841, 819, 749, 706, 636, 612. HRMS (ESI⁺) *m/z* C₁₇H₂₀NO₃S⁺ [M+H]⁺: calculated 318.1158, found 318.1158. MP 110 – 114 °C.

2-(1-benzhydrylazetididin-3-yl)isoindoline-1,3-dione (**6s**)



In a flame-dried round bottom flask under a flow of N₂, tributylhexadecylphosphonium bromide (0.84 mmol, 0.43 mg) and phthalimide potassium salt (10.0 mmol, 1.82 g) were added to a solution of 1-benzhydrylazetididin-3-yl methane sulfonate **8s** (8.35 mmol, 2.65 g) in toluene (45 mL). The reaction was refluxed for 24 h, cooled to r.t. and filtered. The residual solid was washed with CH₂Cl₂ and the combined filtrate was evaporated under vacuum. The crude mixture was purified by flash column chromatography (Pentane:EtOAc = 100:0 to 95:5, gradient) to afford the desired product in 65% yield (5.43 mmol, 1.99 g). ¹H NMR (400 MHz, CDCl₃) δ ppm: 7.74 (dd, *J* = 5.5, 3.0 Hz, 2H), 7.67 – 7.58 (m, 2H), 7.42 – 7.35 (m, 4H), 7.25 – 7.16 (m, 4H), 7.17 – 7.07 (m, 2H), 4.80 (p, *J* = 7.9 Hz, 1H), 4.59 (s, 1H), 3.66 – 3.52 (m, 4H); ¹³C NMR (101 MHz, CDCl₃) δ ppm: 168.34, 142.22, 134.25, 131.98, 128.59, 127.68, 127.28, 123.36, 77.90, 57.38, 39.85. IR (thin layer film) ν (cm⁻¹) = 3027, 2836, 1600, 1487, 1450, 1266, 1076, 1029, 1008, 918, 834, 764, 735, 698, 652. MP 120 – 122 °C. HRMS (ESI⁺) *m/z* C₂₄H₂₁N₂O₂⁺ [M+H]⁺: calculated 369.1598, found 369.1599. Spectroscopic data were in agreement with the ones previously reported in literature.¹¹

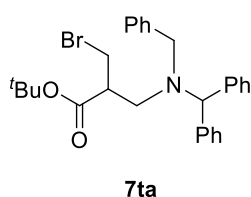
2-(1-(benzhydryl(benzyl)amino)-3-bromopropan-2-yl)isoindoline-1,3-dione (**7sa**)



Prepared according to a slightly modified version of general procedure C. Under a flow of N₂, an oven-dried flask was charged with 2-(1-benzhydrylazetididin-3-yl)isoindoline-1,3-dione **6s** (3.72 mmol, 1.37 g) in dry CH₃CN (0.77 M, 4.8 mL). Benzyl bromide (1.2 equiv., 4.46 mmol, 0.5 mL) was added and the mixture was stirred at 60 °C for 12 h. The crude mixture was purified by flash column chromatography (Heptane:EtOAc = 100:0 to 95:5, gradient) to afford the desired product in 88% yield (3.27 mmol, 1.76 g) as a colorless oil. ¹H NMR (400 MHz, CDCl₃) δ ppm: 7.82 – 7.76 (m, 2H), 7.76 – 7.71

(m, 2H), 7.40 – 7.21 (m, 9H), 7.21 – 7.08 (m, 6H), 4.93 (s, 1H), 4.67 – 4.55 (m, 1H), 3.82 – 3.71 (m, 2H), 3.54 (d, $J = 13.5$ Hz, 1H), 3.48 (dd, $J = 10.5, 5.4$ Hz, 1H), 3.23 (dd, $J = 14.0, 8.2$ Hz, 1H), 2.95 (dd, $J = 14.0, 4.4$ Hz, 1H); $^{13}\text{C NMR}$ (101 MHz, CDCl_3) δ ppm: 167.97, 140.90, 140.14, 138.83, 134.02, 132.03, 129.40, 129.24, 129.15, 128.59, 128.43, 128.31, 127.49, 127.24, 127.22, 123.47, 69.74, 55.95, 52.16, 51.09, 30.96. **IR** (thin layer film) ν (cm^{-1}) = 3027, 1773, 1711, 1494, 1452, 1378, 1083, 1029, 874, 764, 746, 720, 700. **HRMS** (ESI^+) m/z $\text{C}_{31}\text{H}_{28}\text{BrN}_2\text{O}_2^+$ $[\text{M}+\text{H}]^+$: calculated 539.1334, found 539.1328.

Tert-butyl 3-(benzhydryl(benzyl)amino)-2-(bromomethyl)propanoate (7ta)

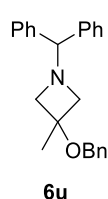


Prepared according to general procedure B using *tert*-butyl 1-benzhydrylazetidino-3-carboxylate* (2.69 mmol, 862 mg). The crude mixture was purified by flash column chromatography (Pentane:Et₂O = 100:0 to 95:5, gradient) to afford the desired product in 85% yield (2.28 mmol, 1.13 g) as a colorless oil. $^1\text{H NMR}$ (400 MHz, CDCl_3) δ ppm: 7.45 – 7.25 (m, 15H), 5.01 (s, 1H), 3.72 (d, $J = 13.9$ Hz, 1H), 3.63 (d, $J = 13.9$

Hz, 1H), 3.46 (dd, $J = 9.8, 4.3$ Hz, 1H), 3.37 (dd, $J = 9.8, 8.8$ Hz, 1H), 2.99 – 2.88 (m, 1H), 2.83 (dd, $J = 13.3, 6.3$ Hz, 1H), 2.66 (dd, $J = 13.2, 7.8$ Hz, 1H), 1.48 (s, 9H); $^{13}\text{C NMR}$ (101 MHz, CDCl_3) δ ppm: 171.71, 140.65, 140.13, 138.85, 129.41, 129.22, 129.14, 128.49, 128.44, 128.40, 127.38, 127.35, 127.31, 81.56, 69.37, 55.20, 51.73, 48.28, 31.83, 28.19. **IR** (thin layer film) ν (cm^{-1}) = 3028, 2977, 1728, 1600, 1494, 1452, 1392, 1368, 1250, 1216, 1147, 1076, 1029, 972, 910, 843, 763, 739, 700, 649, 601, 517. **HRMS** (ESI^+) m/z $\text{C}_{28}\text{H}_{33}\text{BrNO}_2^+$ $[\text{M}+\text{H}]^+$: calculated 494.1689, found 494.1688.

* Prepared by transesterification from the corresponding commercially available methyl 1-benzhydrylazetidino-3-carboxylate, according to a known procedure (5 equiv. *t*BuONa, 50 °C, 24 h; US Patent 2013 n. 0225552)

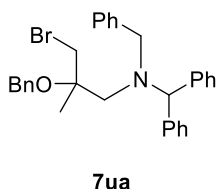
1-benzhydryl-3-(benzyloxy)-3-methylazetidino (6u)



In a flame-dried round-bottom flask under a flow of N_2 , NaH 60 wt% in mineral oil (1.2 equiv., 12.0 mmol, 0.48 g) was added portionwise to a solution of commercially available 1-benzhydryl-3-methylazetidino-3-ol (1 equiv., 9.9 mmol, 2.50 g) in THF (20 mL) at 0 °C. The mixture was stirred at r.t. for 30 min then benzyl bromide (1.3 equiv., 12.8 mmol, 1.49 mL) was added dropwise. The reaction mixture was stirred at 60 °C for 18 h and then allowed to cool to r.t. A saturated aqueous NH_4Cl solution (20 mL) was then added. The layers were separated, and the aqueous layer was extracted with EtOAc (2 x 50 mL). The combined organic layers were washed with brine (20 mL), dried over Na_2SO_4 , and concentrated under reduced pressure. The crude mixture was purified by flash column chromatography (Hexane:EtOAc = 90:10 to 80:20, gradient) to give the desired compound in 77% yield (7.6 mmol, 2.6 g) as a pale yellow solid. $^1\text{H NMR}$ (400 MHz, CDCl_3) δ ppm: 7.45 – 7.39 (m, 4H), 7.33 (d, $J = 4.4$ Hz, 4H), 7.29 – 7.23 (m, 5H), 7.20 – 7.14 (m, 2H), 4.40 (s, 1H), 4.38 (s, 2H), 3.22 – 3.15 (m, 2H), 3.08 (d, $J = 8.0$ Hz, 2H), 1.62 (s, 3H); $^{13}\text{C NMR}$ (101 MHz, CDCl_3) [overlapping signals] δ ppm: 142.66, 138.87, 128.53, 127.67,

127.64, 127.61, 127.19, 78.11, 72.39, 65.54, 64.51, 22.98. **IR** (thin layer film) ν (cm⁻¹) = 3027, 2933, 2837, 1599, 1492, 1452, 1371, 1344, 1314, 1226, 1055, 1029, 964, 883, 741, 702, 637, 622, 545, 482, 422, 409. **MP** 71 – 72 °C. **HRMS** (ESI⁺) m/z C₂₄H₂₆NO⁺ [M+H]⁺: calculated 344.2009, found 344.2003.

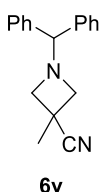
1-benzhydryl-1-benzyl-2-(benzyloxy)-3-bromo-2-methylpropan-1-amine (7ua)



Prepared according to general procedure C using 1-benzhydryl-3-(benzyloxy)-3-methylazetidide **6u** (2.91 mmol, 1.0 g) and benzyl bromide (2.85 mmol, 0.34 mL). The crude mixture was purified by flash column chromatography (Heptane:EtOAc = 100:0 to 95:5, gradient) to afford the desired product in 64% yield (1.8 mmol, 0.95 g) as a colorless oil. ¹H NMR (400 MHz, CDCl₃) δ ppm: 7.47 – 7.16 (m, 20H), 5.38 (s, 1H),

4.48 – 4.36 (m, 2H), 3.86 (d, J = 13.6 Hz, 1H), 3.62 (d, J = 13.6 Hz, 1H), 3.45 – 3.35 (m, 2H), 2.95 – 2.82 (m, 2H), 1.28 (s, 3H); ¹³C NMR (101 MHz, CDCl₃) [overlapping signals] δ ppm: 141.04, 140.02, 139.87, 138.87, 130.29, 129.70, 129.45, 128.40, 128.38, 128.16, 127.55, 127.44, 127.18, 127.11, 127.01, 78.17, 68.57, 64.35, 56.14, 55.88, 39.59, 20.86. **IR** (thin layer film) ν (cm⁻¹) = 3220, 2835, 1493, 1452, 1064, 1028, 741, 699, 542, 465, 418. **HRMS** (ESI⁺) m/z C₃₁H₃₃BrNO⁺ [M+H]⁺: calculated 514.1740, found 514.1738.

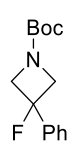
1-benzhydryl-3-methylazetidide-3-carbonitrile (6v)



A flame-dried round-bottom flask under a flow of N₂ was charged with commercially available 1-benzhydrylazetidide-3-carbonitrile (1 equiv., 20.1 mmol, 5.0 g) in dry THF (0.90 mol, 73.2 mL), and a solution of LiHMDS (1.06 M in THF, 1.1 equiv., 22.1 mmol, 22.1 mL) was added at -78 °C. While keeping the same temperature, the reaction was first stirred for 30 min, then CH₃I (1.5 equiv., 30.2 mmol, 1.88 mL) was added dropwise. After stirring for further 45 min at -78 °C, the reaction

was quenched with NH₄Cl (10 mL) and extracted with EtOAc (3 x 20 mL). The combined organic layers were dried over Na₂SO₄ and concentrated under reduced pressure. The crude mixture was purified by flash column chromatography (Hexane:EtOAc = 100:0 to 90:10, gradient) to give the desired compound in 91% yield (18.3 mmol, 4.8 g) as white solid. ¹H NMR (400 MHz, CDCl₃) δ ppm: 7.43 – 7.36 (m, 4H), 7.32 – 7.24 (m, 4H), 7.23 – 7.17 (m, 2H), 4.38 (s, 1H), 3.49 – 3.43 (m, 2H), 3.14 – 3.07 (m, 2H), 1.66 (s, 3H); ¹³C NMR (101 MHz, CDCl₃) δ ppm: 141.26, 128.75, 127.60, 127.45, 123.63, 77.40, 62.94, 26.45, 23.05. **IR** (thin layer film) ν (cm⁻¹) = 3061, 3027, 2958, 2840, 2238, 1599, 1493, 1452, 1380, 1348, 1313, 1256, 1227, 1076, 1029, 927, 863, 745, 705, 623, 599, 549. **MP** 86 – 88 °C. **HRMS** (ESI⁺) m/z C₁₈H₁₉N₂⁺ [M+H]⁺: calculated 263.1543, found 263.1545.

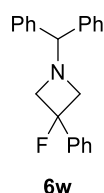
***Tert*-butyl 3-fluoro-3-phenylazetidide-1-carboxylate (**8w**)**



In a flame-dried round bottom flask, *tert*-butyl 3-oxoazetidide-1-carboxylate (1 equiv., 17.5 mmol, 3 g) was dissolved in anhydrous THF (55 mL) and the solution cooled to 0 °C. Phenylmagnesium bromide (3 M in Et₂O, 1.3 equiv., 22.75 mmol, 8 mL) was added dropwise at the same temperature.

8w The reaction was stirred for 2 h at r.t. then quenched at 0 °C by addition of aqueous NH₄Cl_(sat) (20 mL) and extracted with Et₂O (3 x 20 mL). The combined organic layers were dried over MgSO₄ and concentrated *in vacuo* to afford the crude alcohol as a pale-yellow solid. This residue was re-dissolved in anhydrous CH₂Cl₂ (120 mL) and the solution cooled to -78 °C. Deoxo-fluor[®] (2.7 M in Toluene, 1.2 equiv., 21 mmol, 8 mL) was added dropwise at -78 °C and the reaction was stirred for 20 h at r.t. The reaction was quenched at 0 °C by addition of aqueous NaHCO_{3(sat)} (15 mL) followed by aqueous NaOH (1 M, 10 mL) and extracted with Et₂O (3 x 20 mL). The combined organic layers were dried over MgSO₄ and concentrated under reduced pressure. The crude product was purified by flash column chromatography (Pentane:Et₂O = 100:0 to 94:6, gradient) to afford the desired compound as a colorless oil in 44% yield (7.7 mmol, 1.95 g). **¹H NMR** (400 MHz, CDCl₃) δ ppm: 7.50 – 7.32 (m, 5H), 4.40 (ddd, *J* = 22.4, 10.1, 1.3 Hz, 2H), 4.27 (ddd, *J* = 19.3, 10.1, 1.3 Hz, 2H), 1.48 (s, 9H); **¹³C NMR** (101 MHz, CDCl₃) δ ppm: 156.39 (d, *J* = 2.8 Hz), 139.20 (d, *J* = 23.2 Hz), 128.80, 128.73 (d, *J* = 1.7 Hz), 124.22 (d, *J* = 8.3 Hz), 91.49 (d, *J* = 206.7 Hz), 80.37, 62.69 (br), 28.48; **¹⁹F NMR** (377 MHz, CDCl₃) δ ppm: -148.75 – -149.07 (m, 1F). **IR** (thin layer film) ν (cm⁻¹) = 2978, 2885, 1705, 1475, 1450, 1390, 1365, 1290, 1253, 1163, 1115, 1045, 1020, 935, 863, 760, 698. **HRMS** (ESI⁺) *m/z* C₁₄H₁₈FN₂O₂Na⁺ [M+Na]⁺: calculated 274.1214, found 272.1215.

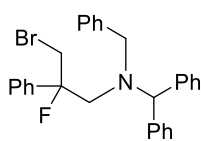
1-benzhydryl-3-fluoro-3-phenylazetidide (6w**)**



In a flame-dried round bottom flask, *tert*-butyl 3-fluoro-3-phenylazetidide-1-carboxylate **8w** (1 equiv., 6.30 mmol, 2.0 g) was dissolved in 2 mL of Et₂O. The solution was cooled to 0 °C and HCl (6 M in ⁱPrOH, 4.7 equiv., 30.0 mmol, 5 mL) was added dropwise. The reaction was stirred for 18 h at r.t. then volatiles were removed *in vacuo* to afford the azetidinium hydrochloride salt as a white solid. The compound was directly re-dissolved in dry CH₃CN (7 mL). The solution was

cooled to 0 °C and DIPEA (5 equiv., 31.5 mmol, 5.5 mL) was added dropwise. The reaction was stirred for 10 min at 0 °C then bromodiphenylmethane (1.2 equiv., 7.56 mmol, 1.9 g) was added portionwise. The solution was refluxed for 3 h then cooled to r.t. and volatiles were evaporated *in vacuo*. The crude product was purified by flash column chromatography (Pentane: Et₂O = 100:0 to 99:1, gradient) to afford the desired product as a white solid in 99% yield (6.23 mmol, 2.0 g). **¹H NMR** (400 MHz, CDCl₃) δ ppm: 7.64 (d, *J* = 7.2 Hz, 2H), 7.55 – 7.14 (m, 13H), 4.53 (s, 1H), 3.73 – 3.46 (m, 4H); **¹³C NMR** (101 MHz, CDCl₃) δ ppm: 142.06, 140.89 (d, *J* = 23.2 Hz), 128.69, 128.60, 128.22 (d, *J* = 1.0 Hz), 127.54, 127.44, 124.34 (d, *J* = 8.7 Hz), 90.93 (d, *J* = 206.5 Hz), 78.20, 65.79 (d, *J* = 22.9 Hz); **¹⁹F NMR** (377 MHz, CDCl₃) δ ppm: -157.07 – -157.45 (m, 1F). **IR** (thin layer film) ν (cm⁻¹) = 3028, 2956, 2843, 1599, 1493, 1450, 1346, 1305, 1213, 1179, 1076, 1057, 1028, 914, 858, 754, 670, 637, 622, 613, 550. **MP** 88 – 90 °C. **HRMS** (ESI⁺) *m/z* C₂₂H₂₁FN⁺ [M+H]⁺: calculated 318.1653, found 318.1653.

1-benzhydryl-1-benzyl-3-bromo-2-fluoro-2-phenylpropan-1-amine (7wa)



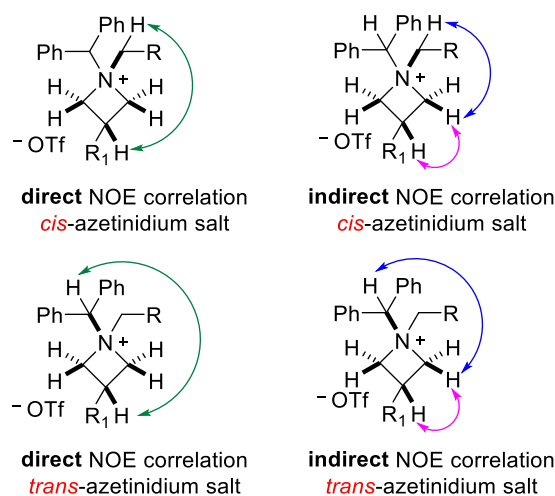
7wa

Prepared according to a slightly modified version of general procedure C. Under a flow of N₂, an oven-dried flask was charged with 1-benzhydryl-3-fluoro-3-phenylazetidene **6w** (4.70 mmol, 1.49 g) in dry CH₃CN (0.5 M, 6.5 mL). Benzyl bromide (1.6 equiv., 7.52 mmol, 0.90 mL) was added and the mixture was stirred at 60 °C for 24 h. Additional benzyl bromide (2 x 0.3 equiv.) was added after 24 h and 48 h, respectively. After 72 h,

the volatiles were evaporated *in vacuo*. The crude product was purified by flash column chromatography (Pentane:CH₂Cl₂ = 100:0 to 90:10, gradient) to afford the desired product in 68% yield (3.19 mmol, 1.56 g) as a colorless oil. **¹H NMR** (400 MHz, CDCl₃) δ ppm: 7.43 – 7.14 (m, 18H), 7.07 – 6.98 (m, 2H), 5.23 (s, 1H), 4.15 – 4.05 (m, 1H), 3.85 (d, *J* = 13.4 Hz, 1H), 3.57 (d, *J* = 13.4 Hz, 1H), 3.30 (dd, *J* = 31.9, 11.8 Hz, 1H), 3.16 (m, 1H), 3.10 (m, 1H); **¹³C NMR** (101 MHz, CDCl₃) δ ppm: 140.34, 140.24 (d, *J* = 21.2 Hz), 139.34, 138.84, 129.88, 129.72, 129.70, 128.49, 128.40, 128.36 (d, *J* = 1.9 Hz), 128.30, 128.00, 127.42, 127.39, 127.33, 124.88 (d, *J* = 10.0 Hz), 99.50 (d, *J* = 183.6 Hz), 68.50 (d, *J* = 3.5 Hz), 57.06 (d, *J* = 21.2 Hz), 55.46 (d, *J* = 3.3 Hz), 38.46 (d, *J* = 25.4 Hz); **¹⁹F NMR** (377 MHz, CDCl₃) δ ppm: -157.26 (dddd, *J* = 32.9, 26.4, 21.3, 12.5 Hz). **IR** (thin layer film) ν (cm⁻¹) = 3060, 3028, 2840, 1600, 1494, 1449, 1266, 1127, 1047, 1029, 979, 918, 836, 761, 744, 699, 603, 562. **MP** 118 – 120 °C. **HRMS** (ESI⁺) *m/z* C₂₉H₂₈BrFN⁺ [M+H]⁺: calculated 488.1384, found 488.1384.

Stereochemical Assignment of Substrates

The relative stereochemistry of the *cis* or *trans* diastereomer has been assigned by analysis of the ¹H-NOESY spectrum of the mixtures (see NMR copies section) according to the following scheme:

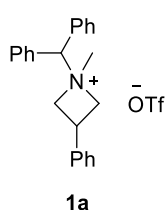


Each ¹H-NOESY spectrum indicates if direct or indirect NOE correlation was used for assignment (see NMR copies section). For substrate **1wa**, the assignment was based on ¹H-¹⁹F HOESY correlation instead.

For substrates in which the d.r. > 5:1, only the major diastereomer has been reported and characterized. For mixtures, the characterization distinguishes between H_{major} (protons of the major diastereomer), H_{minor} (protons of the minor diastereomer) and H_{major + minor} (protons of major and minor diastereomer overlapped): e.g. 2H_{major + minor} corresponds to the signal of 2H_{major} + 2H_{minor}.

Characterization of Substrates

1-benzhydryl-1-methyl-3-phenylazetidinium trifluoromethanesulfonate (1a)

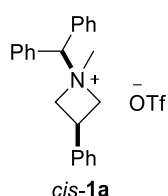


Prepared according to general procedure E using commercially available 1-benzhydryl-3-phenylazetidinium (13.40 mmol, 4.0 g) and methyl triflate (1.3 equiv., 17.37 mmol, 1.9 mL) to afford the desired product in 96% yield (12.77 mmol, 5.92 g, d.r. 15:1 *cis:trans*) as a white powder. ¹H NMR (400 MHz, CDCl₃) δ ppm: 7.67 – 7.60 (m, 4H), 7.56 – 7.44 (m, 6H), 7.18 – 7.13 (m, 1H), 7.13 – 7.07 (m, 2H), 6.53 – 6.46 (m, 2H), 6.06 (s, 1H), 4.87 (dd, *J* = 9.6, 2.2 Hz, 2H), 4.57 (dd, *J* = 8.9, 2.3 Hz, 2H), 4.42 (m, 1H), 3.54 (s, 3H); ¹⁹F NMR (377 MHz, CDCl₃) δ ppm: -78.22 (s, 3F). IR (thin layer film) ν (cm⁻¹) = 2361, 1498, 1454, 1256, 1224, 1153, 1029, 989, 896, 853, 782, 755, 730, 700, 636. HRMS (ESI⁺) *m/z* C₂₃H₂₄N⁺ [M-OTf]⁺: calculated 314.1909, found 314.1908.

cis-**1aa** and *trans*-**1aa** were separated by SFC purification (Stationary phase: Chiralpak IG 5μm 250*20mm, Mobile phase: CO₂:MeOH = 70:30 + 0.01% CF₃SO₃H). The fractions were evaporated at 25 °C and freeze dried. Alternatively, flash column chromatography (EtOAc:MeOH = 100:0 to 95:5) can also be employed. Spectroscopic data were in agreement with the ones previously reported in literature.⁸

A single recrystallization of the diastereomeric mixture (15:1 *cis:trans*) in CH₂Cl₂/Et₂O at 5 °C affords *cis*-**1a** as a single diastereomer (>50:1).

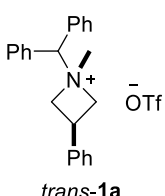
***cis*-1-benzhydryl-1-methyl-3-phenylazetidinium trifluoromethanesulfonate (*cis*-**1a**)**



¹H NMR (400 MHz, CDCl₃) δ ppm: 7.68 – 7.56 (m, 4H), 7.56 – 7.43 (m, 6H), 7.21 – 7.14 (m, 1H), 7.14 – 7.02 (m, 2H), 6.58 – 6.41 (m, 2H), 6.06 (s, 1H), 4.87 (dd, *J* = 9.6, 2.2 Hz, 2H), 4.57 (dd, *J* = 8.9, 2.3 Hz, 2H), 4.42 (m, 1H), 3.54 (s, 3H); ¹³C NMR (101 MHz, CDCl₃) δ ppm: 135.97, 132.71, 130.50, 130.38, 130.07, 129.23, 128.47, 126.87, 120.97 (q, *J* = 320.1 Hz), 78.05, 67.75, 51.21, 32.51; ¹⁹F NMR (377 MHz, CDCl₃) δ ppm: -78.23 (s, 3F). HRMS (ESI⁺)

m/z C₂₃H₂₄N⁺ [M-OTf]⁺: calculated 314.1909, found 314.1908.

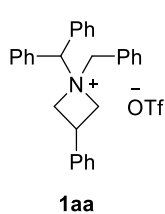
***trans*-1-benzhydryl-1-methyl-3-phenylazetidinium trifluoromethanesulfonate (*trans*-**1a**)**



¹H NMR (400 MHz, CDCl₃) δ ppm: 7.75 – 7.66 (m, 4H), 7.56 – 7.41 (m, 6H), 7.41 – 7.32 (m, 2H), 7.33 – 7.27 (m, 1H), 7.19 – 7.10 (m, 2H), 6.37 (s, 1H), 5.46 (dd, *J* = 11.7, 9.8 Hz, 2H), 4.47 – 4.31 (m, 2H), 3.62 – 3.48 (m, 1H), 3.30 (s, 3H); ¹³C NMR (101 MHz, CDCl₃) δ ppm: 137.35, 132.53, 130.47, 130.24, 130.00, 129.58, 128.31, 126.18, 120.95 (q, *J* = 320.1 Hz), 77.94, 68.98, 52.25, 30.77; ¹⁹F NMR (377 MHz, CDCl₃) δ ppm: -78.20 (s, 3F). HRMS (ESI⁺)

m/z C₂₃H₂₄N⁺ [M-OTf]⁺: calculated 314.1909, found 314.1908.

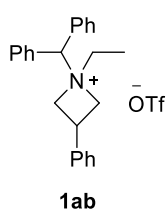
1-benzhydryl-1-benzyl-3-phenylazetidinium trifluoromethanesulfonate (1aa**)**



Prepared according to general procedure D using 1-benzhydryl-1-benzyl-3-bromo-2-phenylpropan-1-amine **7aa** (1.06 mmol, 0.50 g) to afford the desired product in 95% yield (1.00 mmol, 1.01 g, d.r. 1.5:1 *cis:trans*) as a white powder. ¹H NMR (500 MHz, CDCl₃) δ ppm: 7.86 – 7.81 (m, 4H_{minor}), 7.79 – 7.74 (m, 2H_{major}), 7.74 – 7.68 (m, 4H_{major}), 7.64 – 7.47 (m, 11H_{minor} + 9H_{major}), 7.12 – 7.04 (m, 1H_{major + minor}), 7.02 – 6.95 (m, 2H_{major + minor}), 6.48 (s, 1H_{minor}), 6.30 (s, 1H_{major}), 6.17 – 6.12 (m, 2H_{minor}), 6.12 – 6.04 (m, 2H_{major}), 5.15 – 5.07 (m, 2H_{minor}), 5.02 – 4.94 (m, 2H_{major}), 4.88 – 4.79 (m, 2H_{major + minor}), 4.76 (s, 2H_{major}), 4.61 (s, 2H_{minor}), 2.72 (p, *J* = 9.6 Hz, 1H_{major}), 2.49 (p, *J* = 9.6 Hz, 1H_{minor}); ¹³C NMR (126 MHz, CDCl₃) δ ppm: 136.01, 135.98, 134.05, 133.63, 133.21, 132.85, 131.28, 131.12, 130.80, 130.38, 130.35, 130.23, 130.19, 130.12, 129.99, 129.86, 129.05, 128.99, 128.77, 128.54, 128.32, 128.12, 126.56, 126.38, 120.99 (q, *J* = 319.9 Hz), 77.87, 77.83, 65.52, 65.44, 63.65, 63.26, 32.86, 31.89; ¹⁹F NMR (470 MHz, CDCl₃) δ ppm: -77.11 (s, 3F). IR (thin layer film) ν (cm⁻¹) = 3061, 1498, 1456, 1259, 1224, 1155, 1030, 908, 757, 725, 701, 638. HRMS (ESI⁺) *m/z* C₂₉H₂₈N⁺ [M-OTf]⁺: calculated 390.2221, found 390.2218.

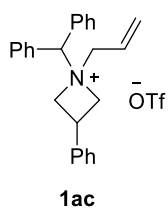
Multi-gram scale reaction (10 mmol scale, 4.70 g) and subsequent purification by flash column chromatography (CH₂Cl₂:MeOH = 100:0 to 95:5, gradient), afforded the title compound (7.5 mmol, 4.05 g, d.r. 1:1.1 *cis:trans*) as a white powder.

1-benzhydryl-1-ethyl-3-phenylazetidinium trifluoromethanesulfonate (**1ab**)



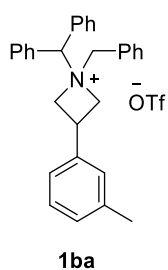
Prepared according to general procedure E using commercially available 1-benzhydryl-3-phenylazetidinium (2.67 mmol, 0.80 g) with ethyl triflate (4.01 mmol, 0.52 mL) to afford the desired product in 94% yield (2.51 mmol, 1.20 g, d.r. 8:1 *cis:trans*) as a white powder. $^1\text{H NMR}$ major (500 MHz, CDCl_3) δ ppm: 7.67 – 7.47 (m, 10H), 7.17 – 7.11 (m, 1H), 7.09 – 7.02 (m, 2H), 6.45 – 6.26 (m, 2H), 5.71 (s, 1H), 4.94 – 4.81 (m, 2H), 4.75 – 4.63 (m, 2H), 4.36 (p, $J = 9.4$ Hz, 1H), 3.94 (q, $J = 7.1$ Hz, 2H), 1.52 (t, $J = 7.1$ Hz, 3H); $^1\text{H NMR}$ minor (500 MHz, CDCl_3) δ ppm: 7.43 – 7.65 (m, 10 H), 6.99 – 7.18 (m, 3 H), 6.31 – 6.42 (m, 2 H), 5.97 (s, 1 H), 5.26 – 5.36 (m, 2 H), 4.59 – 4.66 (m, 2 H), 3.66 (q, $J = 7.22$ Hz, 2 H), 2.91 (q, $J = 9.18$ Hz, 1 H), 1.37 (t, $J = 7.1$ Hz, 3H); $^{13}\text{C NMR}$ major (126 MHz, CDCl_3) δ ppm: 136.24, 132.38, 130.59, 130.35, 130.09, 129.12, 128.29, 126.82, 121.24 (q, $J = 320.0$ Hz), 74.52, 64.80, 57.64, 32.74, 8.96; $^{19}\text{F NMR}$ (470 MHz, CDCl_3) δ ppm: -78.24 (s, 3F). **IR** (thin layer film) ν (cm^{-1}) = 3061, 1498, 1456, 1260, 1224, 1154, 1030, 781, 755, 728, 701, 637. **HRMS** (ESI^+) m/z $\text{C}_{24}\text{H}_{26}\text{N}^+$ [M-OTf] $^+$: calculated 328.2065, found 328.2061.

1-allyl-1-benzhydryl-3-phenylazetidinium trifluoromethanesulfonate (**1ac**)



Prepared according to general procedure D using 1-benzhydryl-1-allyl-3-bromo-2-phenylpropan-1-amine **7ab** (5.00 mmol, 2.1 g) to afford the desired product in 94% yield (4.70 mmol, 2.30 g, d.r. 2:1 *cis:trans*) as a white powder. $^1\text{H NMR}$ (500 MHz, CDCl_3) δ ppm: 7.75 – 7.70 (m, 4H_{minor}), 7.62 – 7.56 (m, 4H_{major}), 7.55 – 7.43 (m, 6H_{major + minor}), 7.31 (t, $J = 7.5$ Hz, 2H_{minor}), 7.24 (d, $J = 7.4$ Hz, 1H_{minor}), 7.14 (t, $J = 7.4$ Hz, 1H_{major}), 7.09 – 7.02 (m, 2H_{major + minor}), 6.39 – 6.33 (m, 2H_{major}), 6.31 – 6.19 (m, 1H_{major}), 6.04 – 5.93 (m, 2H_{minor}), 5.82 (s, 1H_{major}), 5.74 (dd, $J = 10.1, 1.0$ Hz, 1H_{major}), 5.68 (dd, $J = 16.9, 1.3$ Hz, 1H_{major}), 5.61 (d, $J = 10.2$ Hz, 1H_{minor}), 5.43 (dd, $J = 16.8, 1.2$ Hz, 1H_{minor}), 5.27 – 5.19 (m, 2H_{minor}), 4.93 – 4.86 (m, 2H_{major}), 4.80 – 4.67 (m, 2H_{major + minor}), 4.33 (d, $J = 7.3$ Hz, 2H_{major}), 4.20 (p, $J = 9.5$ Hz, 1H_{major}), 4.11 (d, $J = 7.2$ Hz, 2H_{minor}), 2.95 (p, $J = 9.4$ Hz, 1H_{minor}); $^{13}\text{C NMR}$ (126 MHz, CDCl_3) [overlapping signals] δ ppm: 136.65, 136.17, 132.80, 132.53, 130.65, 130.44, 130.39, 130.05, 130.02, 129.35, 129.16, 128.35, 128.19, 126.79, 126.34, 124.80, 121.00 (q, $J = 320.3$ Hz), 76.70, 76.53, 65.92, 64.80, 64.38, 64.35, 32.65, 31.08; $^{19}\text{F NMR}$ (470 MHz, CDCl_3) δ ppm: -78.21 (s, 3F). **IR** (thin layer film) ν (cm^{-1}) = 3062, 1604, 1498, 1455, 1256, 1224, 1153, 1029, 954, 913, 875, 842, 802, 781, 754, 735, 699, 636. **HRMS** (ESI^+) m/z $\text{C}_{25}\text{H}_{26}\text{N}^+$ [M-OTf] $^+$: calculated 340.2065, found 340.2064.

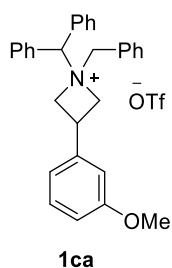
1-benzhydryl-1-benzyl-3-(*m*-tolyl)azetidinium trifluoromethanesulfonate (**1ba**)



Prepared according to general procedure D using 1-benzhydryl-1-benzyl-3-bromo-2-(*m*-tolyl)propan-1-amine **7ba** (0.58 mmol, 0.28 g) to afford the desired product in 80% yield (0.46 mmol, 257.6 mg, d.r. 2:1 *cis:trans*) as a white powder. $^1\text{H NMR}$ (500 MHz, CDCl_3) δ ppm: 7.89 – 7.42 (m, 15H_{major + minor}), 6.94 – 6.83 (m, 2H_{major + minor}), 6.47 (s, 1H_{minor}), 6.29 (s, 1H_{major}), 6.03 – 5.95 (m, 1H_{major + minor}), 5.86 (d, $J = 2.2$ Hz, 1H_{minor}), 5.82 (d, $J = 2.0$ Hz, 1H_{major}), 5.18 – 5.03 (m, 2H_{minor}), 5.03 – 4.92 (m, 2H_{major}), 4.89 – 4.78 (m, 2H_{major + minor}), 4.74

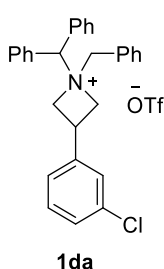
(s, 2H_{major}), 4.59 (s, 2H_{minor}), 2.64 (p, $J = 9.6$ Hz, 1H_{major}), 2.43 (p, $J = 9.7$ Hz, 1H_{minor}), 2.06 (s, 3H_{major + minor}); ¹³C NMR (126 MHz, CDCl₃) [overlapping signals] δ ppm: 138.81, 138.74, 135.88, 135.82, 134.19, 133.68, 133.28, 132.83, 131.25, 131.21, 130.86, 130.42, 130.31, 130.19, 130.10, 129.92, 129.84, 129.11, 128.91, 128.80, 128.77, 128.72, 128.63, 126.77, 126.71, 124.13, 123.89, 121.01 (q, $J = 320.0$ Hz), 77.90, 77.84, 65.44, 63.68, 63.25, 32.97, 32.00, 21.17; ¹⁹F NMR (470 MHz, CDCl₃) δ ppm: -78.00 (s, 3F). IR (thin layer film) ν (cm⁻¹) = 3057, 1609, 1497, 1456, 1259, 1224, 1156, 1030, 862, 757, 702, 638. HRMS (ESI⁺) m/z C₃₀H₃₀N⁺ [M-OTf]⁺: calculated 404.2373, found 404.2373.

1-benzhydryl-1-benzyl-3-(3-methoxyphenyl)azetidinium trifluoromethanesulfonate (1ca)



Prepared according to general procedure D using 1-benzhydryl-1-benzyl-3-bromo-2-(3-methoxyphenyl)propan-1-amine **7ca** (0.81 mmol, 0.41 g) to afford the desired product in 82% yield (0.66 mmol, 379.9 mg, d.r. 2.2:1 *cis:trans*) as a white powder. ¹H NMR (500 MHz, CDCl₃) δ ppm: 7.91 – 7.37 (m, 15H_{major + minor}), 6.87 (t, $J = 8.0$ Hz, 1H_{major + minor}), 6.63 – 6.55 (m, 1H_{major + minor}), 6.35 (s, 1H_{minor}), 6.17 (s, 1H_{major}), 5.86 (t, $J = 2.2$ Hz, 1H_{minor}), 5.81 (t, $J = 2.1$ Hz, 1H_{major}), 5.75 (dd, $J = 7.6, 1.7$ Hz, 1H_{minor}), 5.64 (dd, $J = 7.6, 1.7$ Hz, 1H_{major}), 5.16 – 5.08 (m, 2H_{minor}), 4.99 – 4.91 (m, 2H_{major}), 4.89 – 4.76 (m, 2H_{major + minor}), 4.72 (s, 2H_{major}), 4.54 (s, 2H_{minor}), 3.60 (s, 3H_{major + minor}), 2.75 (p, $J = 9.6$ Hz, 1H_{major}), 2.54 (p, $J = 9.6$ Hz, 1H_{minor}); ¹³C NMR (126 MHz, CDCl₃) [overlapping signals] δ ppm: 159.89, 159.85, 137.55, 137.39, 133.79, 133.56, 133.13, 132.79, 131.20, 131.09, 130.69, 130.34, 130.24, 130.20, 130.14, 130.06, 130.03, 129.94, 129.80, 128.70, 128.35, 121.07 (q, $J = 320.3$ Hz), 118.26, 118.15, 113.44, 113.35, 112.69, 112.26, 78.07, 77.95, 65.57, 65.41, 63.42, 63.12, 55.44, 55.41, 32.75, 31.60; ¹⁹F NMR (470 MHz, CDCl₃) δ ppm: -78.12 (s, 3F). IR (thin layer film) ν (cm⁻¹) = 1602, 1497, 1456, 1256, 1224, 1156, 1029, 859, 756, 704, 637. HRMS (ESI⁺) m/z C₃₀H₃₀NO⁺ [M-OTf]⁺: calculated 420.2322, found 420.2323.

1-benzhydryl-1-benzyl-3-(3-chlorophenyl)azetidinium trifluoromethanesulfonate (1da)

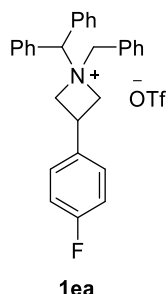


Prepared according to general procedure E using 1-benzhydryl-1-benzyl-3-bromo-2-(3-chlorophenyl)propan-1-amine **7da** (0.33 mmol, 0.16 g) to afford the desired product in 80% yield (0.26 mmol, 0.15 g, d.r. 1.8:1 *cis:trans*) as a white powder. ¹H NMR (500 MHz, CDCl₃) δ ppm: 7.88 – 7.45 (m, 15H_{major + minor}), 7.10 – 7.02 (m, 1H_{major + minor}), 6.96 – 6.89 (m, 1H_{major + minor}), 6.47 (s, 1H_{minor}), 6.24 (s, 1H_{major}), 6.14 – 6.07 (m, 1H_{major + minor}), 6.03 (t, $J = 1.9$ Hz, 1H_{minor}), 5.98 (t, $J = 1.9$ Hz, 1H_{major}), 5.19 – 5.07 (m, 2H_{minor}), 5.02 – 4.92 (m, 2H_{major}), 4.92 – 4.83 (m, 2H_{major}), 4.83 – 4.70 (m, 2H_{major + minor}), 4.57 (s, 2H_{minor}), 2.73 (p, $J = 9.6$ Hz, 1H_{major}), 2.50 (p, $J = 9.6$ Hz, 1H_{minor}); ¹³C NMR (126 MHz, CDCl₃) [overlapping signals] δ ppm: 137.97, 137.94, 134.95, 134.83, 134.01, 133.47, 132.97, 132.84, 131.65, 131.35, 130.74, 130.71, 130.39, 130.25, 130.20, 130.15, 129.98, 129.90, 128.59, 128.58, 128.33, 128.25, 126.33, 126.25, 125.29, 124.96, 121.00 (q, $J = 319.9$ Hz), 78.14, 77.94, 65.46, 63.29, 62.72, 32.39, 31.33; ¹⁹F NMR (470 MHz, CDCl₃) δ ppm: -78.13 (s, 3F). IR (thin

layer film) ν (cm⁻¹) = 3656, 2980, 2888, 1600, 1457, 1383, 1258, 1225, 1155, 1088, 1030, 954, 751, 707, 638.

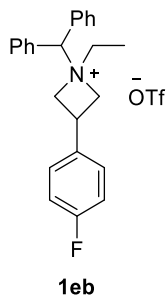
HRMS (ESI⁺) m/z C₂₉H₂₇ClN⁺ [M-OTf]⁺: calculated 424.1827, found 424.1822.

1-benzhydryl-1-benzyl-3-(4-fluorophenyl)azetidinium trifluoromethanesulfonate (1ea)



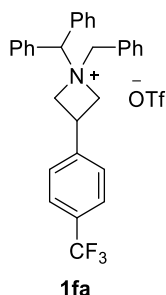
Prepared according to general procedure D using 1-benzhydryl-1-benzyl-3-bromo-2-(4-fluorophenyl)propan-1-amine **7ea** (2.04 mmol, 0.97 g) to afford the desired product in 85% yield (1.73 mmol, 0.97 g, d.r. 1.8:1 *cis:trans*) as a white powder. **¹H NMR** (400 MHz, CDCl₃) δ ppm: 8.08 – 7.28 (m, 15H_{major + minor}), 6.77 – 6.50 (m, 2H_{major + minor}), 6.36 (s, 1H_{minor}), 6.26 – 5.98 (m, 2H_{minor} + 3H_{major}), 5.22 – 5.06 (m, 2H_{minor}), 5.03 – 4.66 (m, 2H_{minor} + 6H_{major}), 4.55 (s, 2H_{minor}), 2.78 (p, $J = 9.5$ Hz, 1H_{major}), 2.52 (p, $J = 9.7$ Hz, 1H_{minor}); **¹³C NMR** (101 MHz, CDCl₃) [overlapping signals] δ ppm: 162.28 (d, $J = 247.9$ Hz), 133.98, 133.47, 133.10, 132.82, 131.95 (d, $J = 2.8$ Hz, minor), 131.87 (d, $J = 3.3$ Hz, major), 131.26, 131.07, 130.76, 130.35, 130.31, 130.21, 130.10, 129.92, 129.83, 128.58, 128.47, 128.30 (d, $J = 8.2$ Hz, major), 128.12 (d, $J = 8.1$ Hz, minor), 121.01 (q, $J = 320.1$ Hz), 115.90 (d, $J = 21.7$ Hz, major), 115.81 (d, $J = 21.6$ Hz, minor), 78.14, 77.92, 65.50, 65.42, 63.78, 63.34, 32.00, 31.00; **¹⁹F NMR** (470 MHz, CDCl₃) δ ppm: -78.14 (s, 3F), -113.23 (s, 1F, major), -113.54 (s, 1F, minor). **IR** (thin layer film) ν (cm⁻¹) = 3065, 1606, 1514, 1456, 1258, 1225, 1161, 1030, 834, 757, 706, 638. **HRMS** (ESI⁺) m/z C₂₉H₂₇FN⁺ [M-OTf]⁺: calculated 408.2122, found 408.2116.

1-benzhydryl-1-ethyl-3-(4-fluorophenyl)azetidinium trifluoromethanesulfonate (1eb)



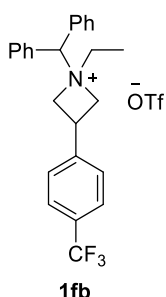
Prepared according to general procedure E using 1-benzhydryl-3-(4-fluorophenyl)azetidinium trifluoromethanesulfonate **7eb** (1.26 mmol, 0.40 g) to afford the desired product in 96% yield (1.20 mmol, 0.60 g, d.r. = 16:1 *cis:trans*) as a white powder. **¹H NMR** major (500 MHz, CDCl₃) δ ppm: 7.60 (d, $J = 6.8$ Hz, 4H), 7.53 – 7.46 (m, 6H), 6.73 – 6.67 (m, 2H), 6.32 (dd, $J = 8.3, 5.0$ Hz, 2H), 5.69 (s, 1H), 4.84 – 4.76 (m, 2H), 4.72 – 4.64 (m, 2H), 4.43 – 4.33 (m, 1H), 3.89 (q, $J = 7.1$ Hz, 2H), 1.44 (t, $J = 7.1$ Hz, 3H); **¹³C NMR** major (126 MHz, CDCl₃) δ ppm: 162.32 (d, $J = 247.8$ Hz), 132.36, 132.22 (d, $J = 3.0$ Hz), 130.59, 130.32, 130.05, 128.56 (d, $J = 8.2$ Hz), 121.01 (q, $J = 320.4$ Hz), 115.93 (d, $J = 21.7$ Hz), 74.37, 64.93, 57.63, 31.84, 8.81; **¹⁹F NMR** major (470 MHz, CDCl₃) δ ppm: -78.19 (s, 3F), -113.58 (m, 1F). **IR** (thin layer film) ν (cm⁻¹) = 3063, 1605, 1515, 1455, 1260, 1225, 1161, 1030, 931, 833, 780, 753, 725, 705, 638. **HRMS** (ESI⁺) m/z C₂₄H₂₅FN⁺ [M-OTf]⁺: calculated 346.1966, found 346.1960.

1-benzhydryl-1-benzyl-3-(4-(trifluoromethyl)phenyl)azetidinium trifluoromethanesulfonate (1fa)



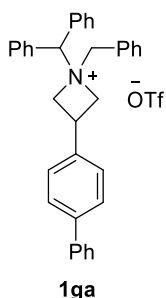
Prepared according to general procedure D using 1-benzhydryl-1-benzyl-3-bromo-2-(4-(trifluoromethyl)phenyl)propan-1-amine **7fa** (1.70 mmol, 0.92 g) to afford the desired product in 88% yield (1.50 mmol, 0.91 g, d.r. 5.3:1 *cis:trans*) as a white powder. $^1\text{H NMR}$ (500 MHz, CDCl_3) δ ppm: 7.89 – 7.84 (m, 4 H_{minor}), 7.77 (dd, $J = 7.0, 1.8$ Hz, 2 H_{major}), 7.71 (dd, $J = 7.0, 1.9$ Hz, 4 H_{major}), 7.61 – 7.36 (m, 11 H_{minor} + 9 H_{major}), 7.24 – 7.18 (m, 2 H_{major} + minor), 6.36 (d, $J = 4.2$ Hz, 2 H_{minor}), 6.34 (s, 1 H_{minor}), 6.27 (d, $J = 8.1$ Hz, 2 H_{major}), 6.16 (s, 1 H_{major}), 5.28 – 5.17 (m, 2 H_{minor}), 5.03 – 4.91 (m, 4 H_{major}), 4.87 – 4.78 (m, 2 H_{minor}), 4.74 (s, 2 H_{major}), 4.55 (s, 2 H_{minor}), 2.91 (p, $J = 9.5$ Hz, 1 H_{major}), 2.67 (p, $J = 9.4$ Hz, 1 H_{minor}); $^{13}\text{C NMR}$ [^{19}F at -62ppm] (126 MHz, CDCl_3) δ ppm: 140.26, 140.14, 133.86, 133.33, 132.96, 132.84, 131.32, 131.10, 130.71, 130.44, 130.39, 130.34, 130.22, 130.12, 129.87, 129.84, 128.42, 128.26, 126.98, 126.72, 125.86, 125.84, 125.81, 125.78, 125.71, 125.69, 124.84, 124.80, 121.03 (q, $J = 320.1$ Hz), 78.45, 78.05, 65.97, 65.53, 63.23, 62.71, 32.06, 30.87; $^{19}\text{F NMR}$ (470 MHz, CDCl_3) δ ppm: -62.81 (s, 3 F_{major}), -62.82 (s, 3 F_{minor}), -78.11 (s, 3 F). **IR** (thin layer film) ν (cm^{-1}) = 3065, 1621, 1499, 1456, 1326, 1257, 1225, 1159, 1124, 1070, 1030, 1018, 930, 902, 836, 757, 705, 638, 608. **HRMS** (ESI^+) m/z $\text{C}_{30}\text{H}_{27}\text{F}_3\text{N}^+ [\text{M-OTf}]^+$: calculated 458.2090, found 458.2087.

1-benzhydryl-1-ethyl-3-(4-(methoxy)phenyl)azetidinium trifluoromethanesulfonate (1fb)



Prepared according to general procedure E using 1-benzhydryl-3-(4-(methoxy)phenyl)azetidinium trifluoromethanesulfonate **7fb** (1.09 mmol, 0.40 g) to afford the desired product in 94% yield (1.02 mmol, 0.56 g, d.r. $\geq 20:1$ *cis:trans*) as a white powder. $^1\text{H NMR}$ major (400 MHz, CDCl_3) δ ppm: 7.67 – 7.58 (m, 4H), 7.58 – 7.47 (m, 6H), 7.28 (d, $J = 7.9$ Hz, 2H), 6.52 (d, $J = 8.0$ Hz, 2H), 5.68 (s, 1H), 4.93 – 4.83 (m, 2H), 4.82 – 4.72 (m, 2H), 4.51 (p, $J = 9.1$ Hz, 1H), 3.94 (q, $J = 7.1$ Hz, 2H), 1.46 (t, $J = 7.0$ Hz, 3H); $^{13}\text{C NMR}$ major (126 MHz, CDCl_3) [overlapping signals] δ ppm: 140.50, 132.20, 130.53, 130.35, 130.05, 127.24, 125.86, 123.80 (q, $J = 280.0$ Hz), 121.02 (q, $J = 317.2$ Hz), 74.34, 64.46, 57.78, 31.90, 8.72; $^{19}\text{F NMR}$ (470 MHz, CDCl_3) δ ppm: -62.82 (s, 3 F), -78.25 (s, 3 F). **IR** (thin layer film) ν (cm^{-1}) = 3061, 1621, 1498, 1455, 1326, 1256, 1224, 1158, 1123, 1070, 1029, 964, 931, 834, 782, 737, 705, 637, 607. **HRMS** (ESI^+) m/z $\text{C}_{25}\text{H}_{25}\text{F}_3\text{N}^+ [\text{M-OTf}]^+$: calculated 396.1933, found 396.1929.

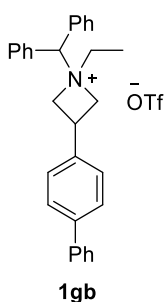
3-([1,1'-biphenyl]-4-yl)-1-benzhydryl-1-benzylazetidinium trifluoromethanesulfonate (1ga)



Prepared according to general procedure D using 1-benzhydryl-1-benzyl-3-bromo-2-([1,1'-biphenyl]-4-yl)propan-1-amine **7ga** (0.91 mmol, 0.50 g) to afford the desired product in 68% yield (0.62 mmol, 0.38 g, d.r. 1.8:1 *cis:trans*) as a white powder. $^1\text{H NMR}$ (500 MHz, CDCl_3) δ ppm: 7.85 (d, $J = 7.6$ Hz, 4 H_{minor}), 7.78 (d, $J = 6.8$ Hz, 2 H_{major}), 7.73 (d, $J = 7.0$ Hz, 4 H_{major}), 7.63 (d, $J = 6.8$ Hz, 2 H_{minor}), 7.61 – 7.28 (m, 14 H_{major} + minor), 7.19 (d, $J = 8.0$ Hz, 2 H_{major} + minor), 6.45 (s, 1 H_{minor}), 6.26 (s, 1 H_{major}), 6.22 (d, $J = 8.1$ Hz, 2 H_{minor}), 6.16 (d, $J = 8.3$ Hz, 2 H_{major}), 5.19 – 5.11 (m, 2 H_{minor}), 5.04 – 4.96 (m, 2 H_{major}), 4.92 – 4.81 (m,

2H_{major + minor}), 4.76 (s, 2H_{major}), 4.61 (s, 2H_{minor}), 2.80 (p, *J* = 9.6 Hz, 1H_{major}), 2.56 (p, *J* = 9.6 Hz, 1H_{minor}); ¹³C NMR (126 MHz, CDCl₃) [overlapping signals] δ ppm: 141.24, 140.99, 140.11, 140.06, 135.00, 134.93, 134.05, 133.60, 133.20, 132.85, 131.28, 131.10, 130.81, 130.37, 130.33, 130.24, 130.21, 130.12, 129.99, 129.86, 128.93, 128.72, 128.54, 127.78, 127.75, 127.65, 127.58, 127.05, 127.02, 126.85, 121.02 (q, *J* = 320.1 Hz), 78.00, 77.88, 65.54, 65.45, 63.70, 63.30, 32.54, 31.54; ¹⁹F NMR (376 MHz, CDCl₃) δ ppm: -78.11 (s, 3F). IR (thin layer film) ν (cm⁻¹) = 3063, 1488, 1456, 1259, 1224, 1155, 1030, 840, 765, 702, 638. HRMS (ESI⁺) *m/z* C₃₅H₃₂N⁺ [M-OTf]⁺: calculated 466.2529, found 466.2526.

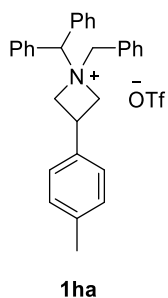
3-([1,1'-biphenyl]-4-yl)-1-benzhydryl-1-ethylazetid-1-ium trifluoromethanesulfonate (1gb)



Prepared according to general procedure E using 1-benzhydryl-3-([1,1'-biphenyl]-4-yl)phenylazetid-1-ium trifluoromethanesulfonate **7gb** (0.25 mmol, 94.0 mg) to afford the desired product in 93% yield (0.23 mmol, 138.7 mg, d.r. *cis:trans* = 8:1) as a white powder. ¹H NMR major (400 MHz, CDCl₃) δ ppm: 7.65 – 7.58 (m, 4H), 7.55 – 7.50 (m, 5H), 7.46 – 7.43 (m, 2H), 7.42 – 7.37 (m, 2H), 7.36 – 7.30 (m, 1H), 7.28 – 7.24 (m, 3H), 6.46 – 6.38 (m, 2H), 5.72 (s, 1H), 4.97 – 4.85 (m, 2H), 4.76 – 4.63 (m, 2H), 4.43 (p, *J* = 9.5 Hz, 1H), 3.96 (q, *J* = 7.0 Hz, 2H), 1.52 (t, *J* = 7.1 Hz, 3H); ¹³C NMR major (101 MHz, CDCl₃) δ ppm: 141.29, 140.18, 135.17, 132.38,

130.61, 130.44, 130.16, 128.96, 127.78, 127.76, 127.31, 127.10, 120.99 (q, *J* = 319.1 Hz), 74.70, 64.86, 57.72, 32.49, 9.04; ¹⁹F NMR major (470 MHz, CDCl₃) δ ppm: -78.19 (s, 3F). IR (thin layer film) ν (cm⁻¹) = 3063, 1488, 1456, 1259, 1224, 1155, 1030, 840, 765, 702, 638. HRMS (ESI⁺) *m/z* C₃₀H₃₀N⁺ [M-OTf]⁺: calculated 404.2373, found 404.2378.

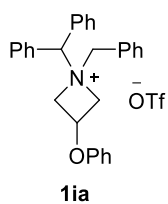
1-benzhydryl-1-benzyl-3-(4-methylphenyl)azetid-1-ium trifluoromethanesulfonate (1ha)



Prepared according to general procedure D using 1-benzhydryl-1-benzyl-3-bromo-2-(4-methylphenyl)propan-1-amine **7ha** (1.45 mmol, 0.70 g) to afford the desired product in 78% yield (1.86 mmol, 0.65 g, d.r. 2.2:1 *cis:trans*) as a white powder. ¹H NMR (400 MHz, CDCl₃) δ ppm: 7.83 (d, *J* = 7.0 Hz, 4H_{minor}), 7.75 (d, *J* = 6.8 Hz, 2H_{major}), 7.71 (d, *J* = 6.2 Hz, 4H_{major}), 7.60 (d, *J* = 6.8 Hz, 2H_{minor}), 7.58 – 7.43 (m, 9H_{major + minor}), 6.76 (d, *J* = 7.7 Hz, 2H_{major + minor}), 6.38 (s, 1H_{minor}), 6.20 (s, 1H_{major}), 6.02 (d, *J* = 7.9 Hz, 2H_{minor}), 5.96 (d, *J* = 8.0

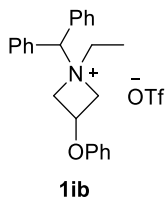
Hz, 2H_{major}), 5.13 – 5.03 (m, 2H_{minor}), 4.98 – 4.88 (m, 2H_{major}), 4.87 – 4.73 (m, 2H_{major + minor}), 4.71 (s, 2H_{major}), 4.56 (s, 2H_{minor}), 2.69 (p, *J* = 9.6 Hz, 1H_{major}), 2.45 (p, *J* = 9.6 Hz, 1H_{minor}), 2.16 (s, 3H_{major + minor}); ¹³C NMR (101 MHz, CDCl₃) [overlapping signals] δ ppm: 138.11, 137.88, 134.01, 133.62, 133.21, 133.03, 132.95, 132.80, 131.19, 131.01, 130.78, 130.29, 130.25, 130.18, 130.06, 129.93, 129.79, 129.64, 129.58, 128.73, 128.55, 126.44, 126.30, 120.95 (q, *J* = 319.7 Hz), 77.95, 77.87, 65.48, 65.38, 63.86, 63.51, 32.59, 31.66, 20.99; ¹⁹F NMR (376 MHz, CDCl₃) δ ppm: -78.09 (s, 3F). IR (thin layer film) ν (cm⁻¹) = 3063, 1488, 1456, 1259, 1224, 1155, 1030, 840, 765, 702, 638. HRMS (ESI⁺) *m/z* C₃₀H₃₀N⁺ [M-OTf]⁺: calculated 404.2373, found 404.2372.

1-benzhydryl-1-benzyl-3-phenoxyazetidinium trifluoromethanesulfonate (**1ia**)



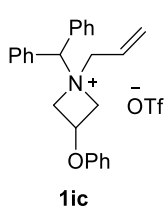
Prepared according to general procedure D using 1-benzhydryl-1-benzyl-3-bromo-2-phenoxypropan-1-amine **7ia** (2.94 mmol, 1.20 g) to afford the desired product in 65% yield (1.91 mmol, 1.06 g, d.r. 1:1.6 *cis:trans*) as a white powder. $^1\text{H NMR}$ (400 MHz, CDCl_3) δ ppm: 7.78 (dd, $J = 7.3, 1.8$ Hz, 4H_{major}), 7.75 – 7.68 (m, 2H_{minor}), 7.68 – 7.60 (m, 4H_{minor}), 7.58 – 7.39 (m, $9\text{H}_{\text{minor}} + 11\text{H}_{\text{major}}$), 7.18 – 7.08 (m, $2\text{H}_{\text{major} + \text{minor}}$), 6.90 (t, $J = 7.4$ Hz, $1\text{H}_{\text{major} + \text{minor}}$), 6.40 (s, 1H_{major}), 6.29 – 6.19 (m, $2\text{H}_{\text{major} + \text{minor}}$), 6.16 (s, 1H_{minor}), 5.31 – 5.21 (m, 2H_{major}), 5.08 – 4.98 (m, 2H_{minor}), 4.87 – 4.78 (m, 2H_{minor}), 4.76 (s, 2H_{minor}), 4.70 – 4.61 (m, 4H_{major}), 3.90 – 3.81 (m, $1\text{H}_{\text{major} + \text{minor}}$); $^{13}\text{C NMR}$ (126 MHz, CDCl_3) [overlapping signals] δ ppm: 155.00, 154.93, 133.35, 133.04, 132.99, 132.77, 131.43, 131.22, 130.48, 130.42, 130.38, 130.17, 130.10, 129.93, 129.77, 128.36, 127.94, 122.61, 121.03 (q, $J = 320.2$ Hz), 114.65, 114.60, 78.35, 65.97, 65.83, 64.18, 64.16, 62.46, 62.27; $^{19}\text{F NMR}$ (376 MHz, CDCl_3) δ ppm: -78.12 (s, 3F). **IR** (thin layer film) ν (cm^{-1}) = 3064, 1600, 1496, 1457, 1373, 1256, 1225, 1153, 1079, 1029, 859, 755, 735, 704, 636. **HRMS** (ESI⁺) m/z $\text{C}_{29}\text{H}_{28}\text{NO}^+$ [M-OTf]⁺: calculated 406.2165, found 406.2165.

1-benzhydryl-1-ethyl-3-phenoxyazetidinium trifluoromethanesulfonate (**1ib**)



Prepared according to a slightly modified general procedure E. To a solution of commercially available 1-benzhydryl-3-phenoxyazetidinium (4.76 mmol, 1.50 g), ethyl triflate (1.1 equiv., 0.68 mL, 5.23 mmol) was added dropwise and the reaction was stirred overnight at r.t. The solvent was then evaporated, the white precipitate was washed with Et_2O and filtered. The solid was further washed with cold Et_2O to afford the desired compound in 98% yield (4.65 mmol, 2.30 g, d.r. 1:50 *cis:trans*) as a white powder. $^1\text{H NMR}$ major (500 MHz, CDCl_3) δ ppm: 7.66 – 7.73 (m, 4H) 7.40 – 7.54 (m, 6H) 7.16 – 7.36 (m, 2H), 6.96 – 7.04 (m, 1H), 6.59 – 6.66 (m, 2H), 6.12 (s, 1H), 5.39 – 5.31 (m, 2H), 4.48 – 4.41 (m, 2H), 4.36 – 4.28 (m, 1H), 3.75 (q, $J = 7.2$ Hz, 2H) 1.47 (t, $J = 7.17$ Hz, 3H); $^{13}\text{C NMR}$ major (126 MHz, CDCl_3) δ ppm: 155.19, 132.13, 130.47, 130.37, 130.28, 130.04, 123.02, 120.60 (q, $J = 320.3$ Hz), 114.85, 75.71, 66.14, 63.45, 59.56, 8.92; $^{19}\text{F NMR}$ (470 MHz, CDCl_3) δ ppm: -78.16 (s, 3F). **IR** (thin layer film) ν (cm^{-1}) = 3062, 1600, 1491, 1456, 1258, 1224, 1152, 1029, 916, 754, 704, 637. **HRMS** (ESI⁺) m/z $\text{C}_{24}\text{H}_{26}\text{NO}^+$ [M-OTf]⁺: calculated 344.2014, found 344.2017.

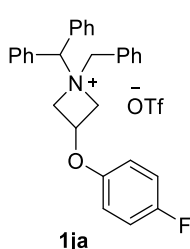
1-allyl-1-benzhydryl-3-phenoxyazetidinium trifluoromethanesulfonate **7a** (**1ic**)



Prepared according to general procedure D, 1-benzhydryl-1-allyl-3-bromo-2-phenoxypropan-1-amine **7ic** (1.55 mmol, 0.68 g) to afford the desired product in 70% yield (1.08 mmol, 0.55 g, d.r. 1:1.2 *cis:trans*) as a white powder. $^1\text{H NMR}$ (500 MHz, CDCl_3) δ ppm: 7.76 – 7.62 (m, 4H_{minor}), 7.58 – 7.38 (m, $6\text{H}_{\text{minor}} + 10\text{H}_{\text{major}}$), 7.30 – 7.20 (m, 2H_{minor}), 7.20 – 7.12 (m, 2H_{major}), 6.97 (t, $J = 7.4$ Hz, 1H_{minor}), 6.92 (t, $J = 7.4$ Hz, 1H_{major}), 6.62 (d, $J = 8.3$ Hz, 2H_{minor}), 6.47 (d, $J = 8.0$ Hz, 2H_{major}), 6.23 – 6.10 (m, 1H_{major}), 6.10 – 5.99 (m, 2H_{minor}), 5.77 – 5.58 (m, $1\text{H}_{\text{minor}} + 3\text{H}_{\text{major}}$), 5.44

(d, $J = 16.7$ Hz, $1H_{\text{minor}}$), 5.30 (dd, $J = 13.1, 6.8$ Hz, $2H_{\text{minor}}$), 5.12 (p, $J = 5.9$ Hz, $1H_{\text{major}}$), 5.03 – 4.92 (m, $2H_{\text{major}}$), 4.78 (dd, $J = 12.6, 5.5$ Hz, $2H_{\text{major}}$), 4.54 (dd, $J = 13.2, 4.2$ Hz, $2H_{\text{minor}}$), 4.33 – 4.26 (m, $1H_{\text{minor}} + 2H_{\text{major}}$), 4.22 (d, $J = 7.2$ Hz, $2H_{\text{minor}}$); $^{13}\text{C NMR}$ (101 MHz, CDCl_3) [overlapping signals] δ ppm: 155.21, 155.04, 132.21, 130.55, 130.52, 130.48, 130.36, 130.24, 130.08, 130.02, 129.96, 129.82, 124.74, 124.54, 122.94, 122.60, 120.96 (q, $J = 320.0$ Hz), 114.97, 114.86, 77.22, 77.09, 65.82, 65.71, 65.17 (br), 63.56, 62.62; $^{19}\text{F NMR}$ (376 MHz, CDCl_3) δ ppm: -78.19 (s, 3F). **IR** (thin layer film) ν (cm^{-1}) = 3063, 1589, 1492, 1455, 1425, 1376, 1257, 1225, 1153, 1079, 1029, 954, 867, 754, 704, 637. **HRMS** (ESI^+) m/z $\text{C}_{25}\text{H}_{26}\text{NO}^+$ $[\text{M-OTf}]^+$: calculated 356.2009, found 356.2004.

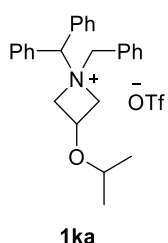
1-benzhydryl-1-benzyl-3-(4-fluorophenoxy)azetidinium trifluoromethanesulfonate (1ja)



Prepared according to general procedure D using 1-benzhydryl-1-benzyl-3-bromo-2-(4-fluorophenoxy)-1-amine **7ja** (0.19 g, 0.38 mmol) to afford the desired product in 93% yield (0.20 g, 0.35 mmol, d.r. 1:1.2 *cis:trans*) as a white powder. $^1\text{H NMR}$ (500 MHz, CDCl_3) δ ppm: 7.80 – 7.74 (m, $4H_{\text{major}}$), 7.73 – 7.65 (m, $2H_{\text{minor}}$), 7.65 – 7.59 (m, $4H_{\text{minor}}$), 7.58 – 7.43 (m, $9H_{\text{minor}} + 11H_{\text{major}}$), 6.88 – 6.78 (m, $2H_{\text{major} + \text{minor}}$), 6.40 (s, $1H_{\text{major}}$), 6.27 – 6.16 (m, $2H_{\text{major} + \text{minor}}$), 6.10 (s, $1H_{\text{minor}}$), 5.30 – 5.22 (m, $2H_{\text{major}}$), 5.09 – 5.01 (m, $2H_{\text{minor}}$),

4.85 – 4.78 (m, $4H_{\text{minor}}$), 4.68 – 4.61 (m, $4H_{\text{major}}$), 3.96 – 3.85 (m, $1H_{\text{major} + \text{minor}}$); $^{13}\text{C NMR}$ (126 MHz, CDCl_3) δ ppm: 158.25 (d, $J = 241.3$ Hz), 151.06 (d, $J = 2.3$ Hz), 151.02 (d, $J = 2.4$ Hz), 133.37, 132.99, 132.89, 132.73, 131.50, 131.31, 130.56, 130.51, 130.41, 130.39, 130.21, 130.14, 129.97, 129.83, 128.25, 127.93, 120.99 (q, $J = 320.6$ Hz), 116.47 (d, $J = 23.4$ Hz), 116.02 (d, $J = 8.0$ Hz), 115.96 (d, $J = 7.9$ Hz), 78.36, 78.10, 65.87, 65.84, 64.25, 64.23, 63.03, 62.90; $^{19}\text{F NMR}$ $\{^1\text{H}\}$ (470 MHz, CDCl_3) δ ppm: -78.15 (s, 3F), -120.98 (s, $1F_{\text{major}}$), -121.02 (s, $1F_{\text{minor}}$). **IR** (thin layer film) ν (cm^{-1}) = 3657, 2981, 2888, 1505, 1458, 1382, 1258, 1224, 1154, 1090, 1030, 953, 831, 757, 734, 706, 638. **HRMS** (ESI^+) m/z $\text{C}_{29}\text{H}_{27}\text{FNO}^+$ $[\text{M-OTf}]^+$: calculated 424.2071, found 424.2069.

1-benzhydryl-1-benzyl-3-(isopropoxy)azetidinium trifluoromethanesulfonate (1ka)

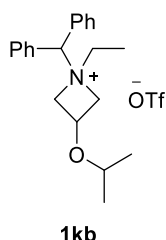


Prepared according to general procedure D, 1-benzhydryl-1-benzyl-3-bromo-2-isopropoxyamine **7ka** (1.10 mmol, 0.50 g) to afford the desired product in 90% yield (0.99 mmol, 0.52 g, d.r. 1:1.2 *cis:trans*) as a white powder. $^1\text{H NMR}$ (400 MHz, CDCl_3) δ ppm: 7.73 – 7.62 (m, $5H_{\text{major} + \text{minor}}$), 7.55 – 7.40 (m, $10H_{\text{major} + \text{minor}}$), 6.14 – 6.08 (m, $1H_{\text{major} + \text{minor}}$), 5.06 – 4.97 (m, $2H_{\text{major}}$), 4.82 – 4.72 (m, $2H_{\text{minor}}$), 4.67 – 4.57 (m, $4H_{\text{minor}} + 2H_{\text{major}}$), 4.54 – 4.45 (m, $2H_{\text{major}}$), 3.25 – 3.04 (m, $2H_{\text{major} + \text{minor}}$), 0.78 (d, $J = 6.1$ Hz,

$6H_{\text{major}}$), 0.71 (d, $J = 6.1$ Hz, $6H_{\text{minor}}$); $^{13}\text{C NMR}$ (101 MHz, CDCl_3) [overlapping signals] δ ppm: 133.30, 133.20, 133.04, 131.16, 131.10, 130.49, 130.31, 130.29, 130.06, 129.98, 129.76, 129.63, 128.61, 128.18, 121.06 (q, $J = 320.1$ Hz), 78.28, 77.45, 71.71, 71.67, 66.19, 65.87, 65.52, 65.50, 62.48, 62.45, 21.99; $^{19}\text{F NMR}$ (470 MHz, CDCl_3) δ ppm: -78.14 (s, 3F). **IR** (thin layer film) ν (cm^{-1}) = 2975, 1499, 1457, 1384, 1338, 1257,

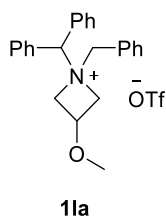
1224, 1154, 1030, 860, 757, 706, 637. **HRMS** (ESI⁺) m/z C₂₆H₃₀FNO⁺ [M-OTf]⁺: calculated 372.2322, found 372.2325.

1-benzhydryl-1-ethyl-3-isopropoxyazetid-1-ium trifluoromethanesulfonate (1kb)



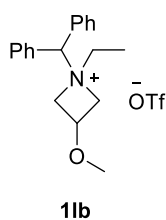
Prepared according to general procedure E, 1-benzhydryl-3-isopropoxyazetid-1-ium trifluoromethanesulfonate **7kb** (1.78 mmol, 0.50 g) to afford the desired product in 99% yield (1.75 mmol, 0.81 g, d.r. 1:1.2 *cis:trans*) as a white powder. **¹H NMR** (500 MHz, CDCl₃) δ 7.67 – 7.61 (m, 2H_{major + minor}), 7.55 – 7.40 (m, 8H_{major + minor}), 5.94 (s, 1H_{major}), 5.57 (s, 1H_{minor}), 5.15 – 5.08 (m, 2H_{major}), 4.72 – 4.65 (m, 2H_{minor}), 4.65 – 4.59 (m, 1H_{minor}), 4.59 – 4.54 (m, 2H_{minor}), 4.29 – 4.22 (m, 2H_{major}), 3.78 – 3.70 (m, 2H_{major + minor}), 3.62 – 3.55 (m, 1H_{major}), 3.51 (sept, $J = 6.1$ Hz, 1H_{major}), 3.42 (sept, $J = 6.1$ Hz, 1H_{minor}), 1.45 (t, $J = 7.2$ Hz, 3H_{major}), 1.41 (t, $J = 7.1$ Hz, 3H_{minor}), 1.05 (d, $J = 6.1$ Hz, 6H_{major}), 0.89 (d, $J = 6.1$ Hz, 6H_{minor}); **¹³C NMR** (126 MHz, CDCl₃) overlapping signals: δ 132.25, 130.39, 130.30, 130.24, 129.94, 129.91, 121.01 (q, $J = 320.4$ Hz), 75.60, 74.73, 72.61, 72.01, 67.79, 66.76, 63.39, 63.04, 59.85, 58.43, 22.27, 22.19, 9.06, 8.76; **¹⁹F NMR** (470 MHz, CDCl₃) δ -78.25 (s, 3F). **IR** (thin layer film) ν (cm⁻¹) = 2977, 1499, 1456, 1384, 1336, 1258, 1224, 1154, 1030, 932, 780, 754, 708, 637. **HRMS** (ESI⁺) m/z C₂₁H₂₈NO⁺ [M-OTf]⁺: calculated 310.2165, found 310.2173.

1-benzhydryl-1-benzyl-3-(methoxy)azetid-1-ium trifluoromethanesulfonate (1la)



Prepared according to general procedure D using 1-benzhydryl-1-benzyl-3-bromo-2-methoxy-1-amine **7la** (1.62 mmol, 0.69 g) to afford the desired product in 88% yield (1.43 mmol, 0.70 g, d.r. 1:1.3 *cis:trans*) as a white powder. **¹H NMR** (500 MHz, CDCl₃) δ ppm: 7.69 – 7.62 (m, 5H_{major + minor}), 7.55 – 7.41 (m, 10H_{major + minor}), 6.13 (s, 1H_{minor}), 6.02 (s, 1H_{major}), 5.05 – 4.96 (m, 2H_{major}), 4.83 – 4.75 (m, 2H_{minor}), 4.69 (s, 2H_{major}), 4.64 (d, $J = 5.8$ Hz, 4H_{minor}), 4.59 – 4.52 (m, 2H_{major}), 3.17 – 3.08 (m, 1H_{major}), 3.01 (p, $J = 6.6$ Hz, 1H_{minor}), 2.94 (s, 3H_{major}), 2.81 (s, 3H_{minor}); **¹³C NMR** (126 MHz, CDCl₃) [overlapping signals] δ ppm: 133.14, 133.09, 133.00, 132.93, 131.23, 130.46, 130.39, 130.35, 130.30, 130.12, 130.03, 129.82, 129.67, 128.44, 127.99, 121.05 (q, $J = 320.3$ Hz), 78.41, 66.30, 66.16, 65.84, 65.67, 64.97, 64.61, 56.73, 56.68; **¹⁹F NMR** (470 MHz, CDCl₃) δ ppm: -78.15 (s, 3F). **IR** (thin layer film) ν (cm⁻¹) = 2981, 1498, 1456, 1360, 1255, 1224, 1153, 1029, 1002, 858, 736, 701, 636. **HRMS** (ESI⁺) m/z C₂₄H₂₆NO⁺ [M-OTf]⁺: calculated 344.2009, found 344.2010.

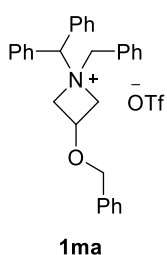
1-benzhydryl-1-ethyl-3-methoxyazetid-1-ium trifluoromethanesulfonate (1lb)



Prepared according to general procedure E using 1-benzhydryl-3-methoxyazetid-1-ium trifluoromethanesulfonate **7lb** (1.97 mmol, 0.50 g) to afford the desired product in quantitative yield (1.96 mmol, 0.85 g, d.r. 1:2.6 *cis:trans*) as a white powder. **¹H NMR** (500 MHz, CDCl₃) δ ppm: 7.65 – 7.57 (m, 3H_{major + minor}), 7.54 – 7.41 (m, 7H_{major + minor}), 5.88 (s, 1H_{major}), 5.59 (s, 1H_{minor}), 5.13 – 5.05 (m, 2H_{major}), 4.72 – 4.65 (m, 2H_{minor}), 4.61 – 4.53 (m, 2H_{minor}), 4.49 (p, $J = 6.4$ Hz, 1H_{minor}), 4.33 – 4.26 (m, 2H_{major}), 3.80 – 3.70 (m, 2H_{major + minor}), 3.58 – 3.50 (m, 1H_{major}), 3.25 (s, 3H_{major}), 3.07 (s, 3H_{minor}), 1.50

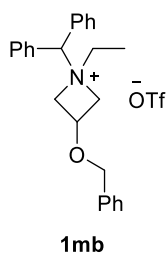
- 1.39 (m, 3H_{major + minor}); ¹³C NMR (126 MHz, CDCl₃) [overlapping signals] δ ppm: 132.22, 132.16, 130.31, 130.25, 129.91, 129.85, 124.84, 122.30, 121.02 (q, *J* = 320.3 Hz), 119.75, 117.20, 75.52, 74.46, 67.00, 66.45, 66.41, 65.77, 59.87, 58.57, 57.06, 56.88, 8.94, 8.50; ¹⁹F NMR (470 MHz, CDCl₃) δ ppm: -78.26 (s, 3F). IR (thin layer film) ν (cm⁻¹) = 2982, 1499, 1456, 1382, 1258, 1224, 1154, 1082, 1030, 935, 781, 754, 709, 637. HRMS (ESI⁺) *m/z* C₁₉H₂₄NO⁺ [M-OTf]⁺: calculated 282.1852, found 282.1860.

1-benzhydryl-1-benzyl-3-(benzyloxy)azetidinium trifluoromethanesulfonate (1ma)



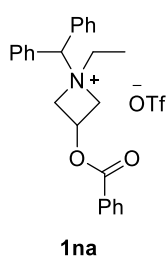
Prepared according to general procedure D using 1-benzhydryl-1-benzyl-3-bromo-2-benzyloxy-1-amine **7ma** (1.64 mmol, 0.82 g) to afford the desired product in 88% yield (1.44 mmol, 0.83 g, d.r. 1:1.3 *cis:trans*) as a white powder. ¹H NMR (500 MHz, CDCl₃) δ ppm: 7.67 – 7.56 (m, 5H_{major + minor}), 7.54 – 7.39 (m, 10H_{major + minor}), 7.32 – 7.22 (m, 3H_{major + minor}), 6.96 – 6.90 (m, 2H_{major}), 6.87 – 6.81 (m, 2H_{minor}), 6.12 (s, 1H_{minor}), 6.09 (s, 1H_{major}), 4.94 – 4.87 (m, 2H_{major}), 4.66 – 4.54 (m, 6H_{minor + 2H_{major}}), 4.53 – 4.46 (m, 2H_{major}), 4.10 (s, 2H_{major}), 4.00 (s, 2H_{minor}), 3.22 – 3.14 (m, 1H_{major}), 3.12 (p, *J* = 6.7 Hz, 1H_{minor}); ¹³C NMR (126 MHz, CDCl₃) δ ppm: 136.01, 135.99, 133.27, 133.06, 132.98, 132.94, 131.16, 130.46, 130.35, 130.31, 130.24, 130.06, 130.04, 129.74, 129.72, 128.68, 128.61, 128.54, 128.43, 128.14, 128.09, 128.07, 121.04 (q, *J* = 320.3 Hz), 78.22, 71.72, 71.68, 66.08, 65.50, 64.97, 64.64, 64.11, 64.07; ¹⁹F NMR (470 MHz, CDCl₃) δ ppm: -78.12 (s, 3F). IR (thin layer film) ν (cm⁻¹) = 3064, 1499, 1456, 1377, 1256, 1224, 1153, 1029, 991, 858, 757, 704, 637. HRMS (ESI⁺) *m/z* C₃₀H₃₀NO⁺ [M-OTf]⁺: calculated 420.2322, found 420.2323.

1-benzhydryl-3-(benzyloxy)-1-ethylazetidinium trifluoromethanesulfonate (1mb)



Prepared according to general procedure E using 1-benzhydryl-3-benzyloxyazetidinium **7mb** (3.95 mmol, 1.30 g) was reacted with ethyl triflate (0.77 mL, 5.92 mmol) to afford the desired product in 99% yield (3.94 mmol, 2.00 g, d.r. 1:5 *cis:trans*) as a white powder. ¹H NMR major (400 MHz, CDCl₃) δ ppm: 7.65 – 7.56 (m, 3H), 7.50 – 7.38 (m, 7H), 7.35 – 7.27 (m, 3H), 7.25 – 7.20 (m, 2H), 5.84 (s, 1H), 5.09 – 4.97 (m, 2H), 4.41 (s, 2H), 4.35 – 4.25 (m, 2H), 3.73 (q, *J* = 7.2 Hz, 2H), 3.69 – 3.57 (m, 1H), 1.40 (t, *J* = 7.2 Hz, 3H); ¹³C NMR major (101 MHz, CDCl₃) δ ppm: 136.06, 132.16, 130.32, 130.26, 129.95, 128.87, 128.67, 128.36, 121.06 (q, *J* = 320.3 Hz), 74.72, 72.07, 66.77, 65.03, 59.80, 8.65; ¹⁹F NMR (470 MHz, CDCl₃) δ ppm: -78.17 (s, 3F). IR (thin layer film) ν (cm⁻¹) = 1498, 1455, 1359, 1257, 1224, 1153, 1029, 932, 782, 75, 702, 637. HRMS (ESI⁺) *m/z* C₂₅H₂₈NO⁺ [M-OTf]⁺: calculated 358.2171, found 358.2178.

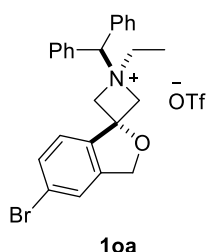
1-benzhydryl-3-(benzyloxy)-1-ethylazetidinium trifluoromethanesulfonate (1na)



Prepared according to general procedure E using 1-benzhydrylazetidinium-3-yl benzoate (2.43 mmol, 0.83 g) to afford the desired product in 95% yield (2.30 mmol, 1.27 g, d.r. 1:1.1 *cis:trans*) as a white powder. $^1\text{H NMR}$ (400 MHz, CDCl_3) δ ppm: 8.02 – 7.95 (m, $1\text{H}_{\text{major} + \text{minor}}$), 7.70 – 7.31 (m, $14\text{H}_{\text{major} + \text{minor}}$), 6.03 (s, 1H_{major}), 5.87 (s, 1H_{minor}), 5.44 (p, $J = 6.5$ Hz, 1H_{minor}), 5.40 – 5.31 (m, 2H_{major}), 5.03 – 4.97 (m, 4H_{minor}), 4.76 – 4.67 (m, 2H_{major}), 4.48 – 4.38 (m, 1H_{major}), 3.87 – 3.76 (m, $2\text{H}_{\text{major} + \text{minor}}$), 1.56 – 1.47 (m, $3\text{H}_{\text{major} + \text{minor}}$); $^{13}\text{C NMR}$

(126 MHz, CDCl_3) [overlapping signals] δ ppm: 165.61, 165.18, 134.42, 134.11, 132.29, 132.11, 130.56, 130.46, 130.33, 130.19, 130.13, 130.08, 129.92, 129.87, 128.91, 128.48, 127.81, 120.87 (q, $J = 319.8$ Hz), 75.82, 75.17, 65.72, 64.75, 61.01, 60.80, 60.49, 59.04, 9.06, 8.92; $^{19}\text{F NMR}$ (470 MHz, CDCl_3) δ ppm: -78.27 (s, 3F). **IR** (thin layer film) ν (cm^{-1}) = 3062, 1722, 1602, 1498, 1454, 1426, 1260, 1225, 1154, 1114, 1072, 1030, 934, 754, 711, 637. **HRMS** (ESI $^+$) m/z $\text{C}_{25}\text{H}_{26}\text{NO}_2^+$ [M-OTf] $^+$: calculated 372.1964, found 372.1964.

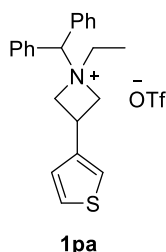
1-benzhydryl-5'-bromo-1-ethyl-3'H-spiro[azetidine-3,1'-isobenzofuran]-1-ium trifluoromethanesulfonate (1oa)



Prepared according to general procedure E using 1-benzhydryl-5'-bromo-3'H-spiro[azetidine-3,1'-isobenzofuran] (0.74 mmol, 0.30 g) to afford the desired product in 97% yield (0.72 mmol, 0.42 g, single diastereomer) as a white powder. $^1\text{H NMR}$ (400 MHz, $\text{DMSO}-d_6$) δ ppm: 7.75 (dd, $J = 6.7, 3.0$ Hz, 4H), 7.62 – 7.54 (m, 7H), 7.26 (d, $J = 8.1$ Hz, 1H), 5.96 (s, 1H), 5.15 – 5.03 (m, 5H), 4.86 (d, $J = 13.4$ Hz, 2H), 3.82 (q, $J = 7.0$ Hz, 2H), 1.32 (t, $J = 7.0$ Hz, 3H); $^{13}\text{C NMR}$ (101 MHz, $\text{DMSO}-d_6$) δ ppm: 141.80,

136.33, 132.44, 130.76, 130.69, 130.03, 129.51, 124.74, 122.46, 121.92, 120.68 (q, $J = 322.4$ Hz), 81.53, 72.08, 71.40, 71.01, 58.42, 8.06; $^{19}\text{F NMR}$ (470 MHz, CDCl_3) δ ppm: -78.32 (s, 3F). **IR** (thin layer film) ν (cm^{-1}) = 3657, 2981, 2888, 1462, 1383, 1254, 1152, 1071, 1030, 955, 817, 705, 638. **HRMS** (ESI $^+$) m/z $\text{C}_{25}\text{H}_{25}\text{BrNO}^+$ [M-OTf] $^+$: calculated 434.1119, found 434.1119.

1-benzhydryl-1-ethyl-3-(thiophen-3-yl)azetidinium trifluoromethanesulfonate (1pa)

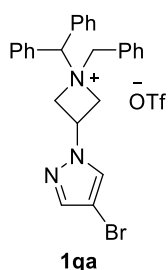


Prepared according to a slightly modified general procedure E. To a solution of, 1-benzhydryl-3-(thiophen-3-yl)azetidinium **7pa** (0.66 mmol, 0.20 g), ethyl triflate (1 equiv., 0.65 mmol, 0.08 mL) was added dropwise and the reaction was stirred overnight at r.t. The solvent was then evaporated, the white precipitate was washed with Et_2O and filtered. The solid was further washed with cold Et_2O to afford the desired compound in 95% yield (0.30 g, 0.62 mmol, d.r. 8.2:1 *cis:trans*) as a white powder. $^1\text{H NMR}$ major (500 MHz, CDCl_3) δ ppm: 7.63 – 7.55

(m, 4H), 7.55 – 7.45 (m, 6H), 7.04 (dd, $J = 5.0, 3.0$ Hz, 1H), 6.48 (dd, $J = 3.0, 1.4$ Hz, 1H), 5.92 (dd, $J = 5.1, 1.4$ Hz, 1H), 5.68 (s, 1H), 4.88 – 4.72 (m, 2H), 4.72 – 4.57 (m, 2H), 4.46 (p, $J = 9.3$ Hz, 1H), 3.87 (q, $J = 7.1$ Hz, 2H), 1.45 (t, $J = 7.1$ Hz, 3H); $^{13}\text{C NMR}$ major (126 MHz, CDCl_3) δ ppm: 136.82, 132.24, 130.43, 130.33, 129.99, 127.07, 125.13, 122.78, 120.83 (q, $J = 320.4$ Hz), 74.44, 64.86, 57.43, 28.17, 8.82; $^{19}\text{F NMR}$ (470

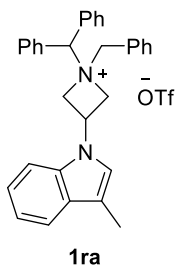
MHz, CDCl₃) δ ppm: -78.21 (s, 3F). **IR** (thin layer film) ν (cm⁻¹) = 1498, 1455, 1259, 1224, 1155, 1030, 934, 784, 753, 721, 705, 637. **HRMS** (ESI⁺) m/z C₂₂H₂₄NS⁺ [M-OTf]⁺: calculated 334.1624, found 334.1628.

2-((1-benzhydryl-3-(4-bromo-1H-pyrazol-1-yl)azetidinium-1-yl)methyl)benzen-1-ide trifluoromethanesulfonate salt (1qa)



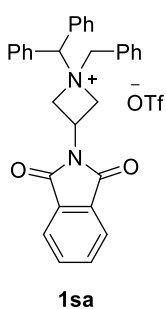
Prepared according to general procedure D using 1-benzhydryl-1-benzyl-3-bromo-2-(4-bromo-1H-pyrazol-1-yl)propan-1-amine **7qa** (0.88 mmol, 0.48 g.) to afford the desired product in 90% yield (0.79 mmol, 0.48 g, d.r. 1:2.1 *cis:trans*) as a white powder. **¹H NMR** (500 MHz, CDCl₃) δ ppm: 7.71 – 7.64 (m, 3H_{major + minor}), 7.64 – 7.42 (m, 12H_{major + minor}), 7.27 (s, 1H_{minor}), 7.08 (s, 1H_{major}), 7.04 (s, 1H_{minor}), 6.87 (s, 1H_{major}), 6.09 (s, 1H_{major}), 6.06 (s, 1H_{minor}), 5.36 – 5.23 (m, 2H_{major + minor}), 5.13 – 5.06 (m, 2H_{minor}), 5.02 – 4.95 (m, 2H_{major}), 4.90 (s, 2H_{minor}), 4.85 (s, 2H_{major}), 4.49 (p, $J = 8.2$ Hz, 1H_{major}), 4.30 (p, $J = 8.0$ Hz, 1H_{minor}); **¹³C NMR** (126 MHz, CDCl₃) δ ppm: 141.51, 141.30, 133.10, 132.92, 132.47, 132.39, 131.64, 131.48, 130.71, 130.61, 130.57, 130.40, 130.26, 130.23, 130.21, 130.14, 129.98, 129.57, 127.84, 127.55, 120.92 (q, $J = 320.1$ Hz), 94.69, 94.60, 78.16, 77.32, 65.67, 65.29, 64.34, 63.51, 48.13, 47.77; **¹⁹F NMR** (470 MHz, CDCl₃) δ ppm: -78.19 (s, 3F). **IR** (thin layer film) ν (cm⁻¹) = 3063, 1498, 1456, 1384, 1324, 1256, 1224, 1156, 1030, 989, 950, 868, 757, 703, 637, 608. **HRMS** (ESI⁺) m/z C₂₆H₂₅BrN₃⁺ [M-OTf]⁺: calculated 458.1226, found 458.1228.

1-benzhydryl-1-benzyl-3-(3-methyl-1H-indol-1-yl)azetidinium trifluoromethanesulfonate (1ra)



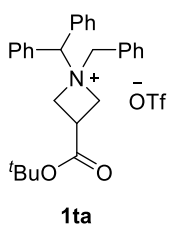
Prepared according to general procedure D using 1-benzhydryl-1-benzyl-3-bromo-2-(3-methyl-1H-indol-1-yl)propan-1-amine **7ra** (0.90 mmol, 0.46 g) to afford the desired product in 90% yield (0.81 mmol, 0.48 g, d.r. 1:1.9 *cis:trans*) as a white powder. **¹H NMR** (500 MHz, CDCl₃) δ ppm: 7.93 – 7.88 (m, 2H_{major}), 7.88 – 7.82 (m, 4H_{minor}), 7.81 – 7.75 (m, 4H_{major}), 7.75 – 7.70 (m, 2H_{minor}), 7.69 – 7.53 (m, 9H_{major + minor}), 7.36 – 7.30 (m, 1H_{major + minor}), 7.04 – 6.94 (m, 2H_{major + minor}), 6.60 (s, 1H_{minor}), 6.46 (s, 1H_{major}), 6.38 – 6.30 (m, 1H_{major + minor}), 5.27 – 5.19 (m, 2H_{minor}), 5.14 – 5.07 (m, 2H_{major}), 5.05 (s, 1H_{minor}), 5.03 – 4.96 (m, 3H_{major}), 4.96 – 4.90 (m, 2H_{minor}), 4.76 (s, 2H_{major}), 4.66 (s, 2H_{minor}), 3.90 (p, $J = 8.7$ Hz, 1H_{major}), 3.71 (p, $J = 8.8$ Hz, 1H_{minor}), 1.98 (d, $J = 1.0$ Hz, 3H_{major}), 1.97 (d, $J = 1.1$ Hz, 3H_{minor}); **¹³C NMR** (126 MHz, CDCl₃) [overlapping signals] δ ppm: 136.43, 136.36, 134.39, 133.17, 133.06, 132.82, 131.66, 131.39, 130.66, 130.62, 130.46, 130.37, 130.30, 130.10, 128.66, 128.64, 128.44, 128.40, 122.64, 122.55, 120.98 (q, $J = 320.1$ Hz), 120.16, 120.11, 119.39, 118.99, 118.75, 114.66, 114.47, 107.85, 107.75, 78.45, 78.41, 65.71, 65.49, 64.09, 63.73, 41.60, 40.98, 9.42, 9.40; **¹⁹F NMR** (470 MHz, CDCl₃) δ ppm: -78.11 (s, 3F). **IR** (thin layer film) ν (cm⁻¹) = 3062, 1498, 1461, 1390, 1258, 1225, 1159, 1030, 742, 706, 638. **HRMS** (ESI⁺) m/z C₃₂H₃₁N₂⁺ [M-OTf]⁺: calculated 443.2482, found 443.2482.

1-benzhydryl-1-benzyl-3-(1,3-dioxoisindolin-2-yl)azetidinium trifluoromethanesulfonate (1sa)



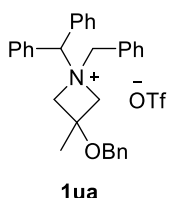
Prepared according to general procedure D using 2-(1-(benzhydryl(benzyl)amino)-3-bromopropan-2-yl)isoindoline-1,3-dione **7sa** (1.0 g, 1.85 mmol) to afford the desired product in 69% yield (0.77 g, 1.28 mmol, d.r. 1: 2.2 *cis:trans*) as a white powder. $^1\text{H NMR}$ (400 MHz, CDCl_3) δ ppm: 7.74 – 7.41 (m, 16 $\text{H}_{\text{major} + \text{minor}}$), 7.38 – 7.20 (m, 3 $\text{H}_{\text{major} + \text{minor}}$), 6.30 (s, 1 H_{major}), 5.88 (s, 1 H_{minor}), 5.56 – 5.42 (m, 2 $\text{H}_{\text{major} + \text{minor}}$), 5.28 – 5.18 (m, 2 H_{minor}), 4.99 – 4.89 (m, 2 $\text{H}_{\text{major} + \text{minor}}$), 4.71 (s, 2 H_{major}), 3.78 (p, $J = 8.3$ Hz, 1 H_{major}), 3.67 (p, $J = 8.4$ Hz, 1 H_{minor}); $^{13}\text{C NMR}$ (101 MHz, CDCl_3) δ ppm: 167.15, 166.91, 134.75, 134.73, 132.76, 132.60, 132.54, 132.50, 131.50, 131.21, 131.11, 131.02, 130.50, 130.34, 130.23, 130.07, 130.04, 129.63, 128.02, 127.74, 123.71, 123.62, 120.92 (q, $J = 320.2$ Hz), 79.51, 76.68, 67.01, 64.88, 62.55, 61.13, 38.20, 37.20; $^{19}\text{F NMR}$ (377 MHz, CDCl_3) δ ppm: -78.17 (s, 3F). **IR** (thin layer film) ν (cm^{-1}) = 3065, 1779, 1716, 1498, 1456, 1388, 1258, 1224, 1156, 1089, 1030, 876, 755, 717, 637. **HRMS** (ESI^+) m/z $\text{C}_{31}\text{H}_{27}\text{N}_2\text{O}_2^+$ [M-OTf] $^+$: calculated 459.2067, found 459.2066.

1-benzhydryl-1-benzyl-3-(tert-butoxycarbonyl)azetidinium trifluoromethanesulfonate (1ta)



Prepared according to general procedure D using *tert*-butyl 3-(benzhydryl(benzyl)amino)-2-(bromomethyl)propanoate **7ta** (1.13 g, 2.28 mmol) to afford the desired product in 61% yield (785 mg, 1.39 mmol, d.r. 1.3:1 *cis:trans*) as a white powder. $^1\text{H NMR}$ (400 MHz, CDCl_3) δ ppm: 7.81 – 7.66 (m, 5 $\text{H}_{\text{minor} + \text{major}}$), 7.60 – 7.41 (m, 10 $\text{H}_{\text{minor} + \text{major}}$), 6.31 (s, 1 H_{minor}), 6.17 (s, 1 H_{major}), 5.04 – 4.91 (m, 2 $\text{H}_{\text{minor} + \text{major}}$), 4.86 – 4.76 (m, 2 H_{minor}), 4.73 – 4.62 (m, 4 H_{major}), 4.54 (s, 2 H_{minor}), 2.37 – 2.08 (m, 1 $\text{H}_{\text{minor} + \text{major}}$), 1.16 (s, 9 H_{minor}), 1.13 (s, 9 H_{major}); $^{13}\text{C NMR}$ (101 MHz, CDCl_3) δ ppm: 167.24, 167.17, 133.49, 133.08, 132.88, 132.83, 131.28, 131.17, 130.47, 130.36, 130.20, 130.12, 130.08, 129.89, 129.82, 128.24, 127.92, 121.02 (q, $J = 320.1$ Hz), 83.37, 83.29, 77.99, 77.92, 65.57, 65.46, 58.85, 58.73, 31.19, 30.64, 27.70, 27.65; $^{19}\text{F NMR}$ (377 MHz, CDCl_3) δ ppm: (377 MHz, CDCl_3) δ ppm: -78.14 (s, 3F). **IR** (thin layer film) ν (cm^{-1}) = 2980, 1733, 1498, 1457, 1370, 1256, 1224, 1153, 1068, 1029, 843, 800, 760, 734, 705, 637, 573, 413. **HRMS** (ESI^+) m/z $\text{C}_{28}\text{H}_{32}\text{NO}_2^+$ [M-OTf] $^+$: calculated 414.2428, found 414.2426.

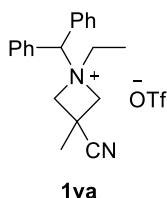
1-benzhydryl-1-benzyl-3-(benzyloxy)-3-methylazetidinium trifluoromethanesulfonate (1ua)



Prepared according to general procedure D using 1-benzhydryl-1-benzyl-2-(benzyloxy)-3-bromo-2-methylpropan-1-amine **7ua** (0.97 mmol, 0.50 g) to afford the desired product in 76% yield (0.74 mmol, 0.43 g, d.r. 1.5:1 *cis:trans*) as a white powder. $^1\text{H NMR}$ (400 MHz, CDCl_3) δ ppm: 7.71 – 7.16 (m, 18 $\text{H}_{\text{minor} + \text{major}}$), 7.13 (dd, $J = 7.5, 2.1$ Hz, 2 H_{major}), 6.82 (dd, $J = 6.5, 3.0$ Hz, 2 H_{minor}), 6.14 (s, 1 H_{minor}), 5.69 (s, 1 H_{major}), 5.02 (d, $J = 12.6$ Hz, 2 H_{minor}), 4.94 – 4.77 (m, 6 H_{major}), 4.70 (d, $J = 12.7$ Hz, 2 H_{minor}), 4.63 (s, 2 H_{minor}), 4.23 (s, 2 H_{major}), 3.86 (s, 2 H_{minor}), 0.64 (s, 3 H_{major}), 0.52 (s, 3 H_{minor}); $^{13}\text{C NMR}$ (101 MHz, CDCl_3) [overlapping signals] δ ppm: 137.09, 136.85, 133.84, 133.46, 132.81, 132.76, 131.31, 131.04, 130.55, 130.42, 130.37, 130.12, 130.07, 129.82, 129.48, 128.56,

128.49, 128.18, 127.98, 127.91, 127.73, 127.69, 127.39, 121.14 (q, $J = 319.5$ Hz), 79.36, 76.62, 70.99, 69.42, 68.60, 67.74, 67.02, 65.99, 65.84, 65.34, 19.51, 18.67; ^{19}F NMR (377 MHz, CDCl_3) δ ppm: -78.00 (s, 3F). IR (thin layer film) ν (cm^{-1}) = 2919, 1498, 1456, 1260, 1224, 1154, 1030, 907, 758, 731, 702, 638, 577, 569, 558, 539, 473, 415. HRMS (ESI⁺) m/z $\text{C}_{31}\text{H}_{32}\text{NO}^+$ [M-OTf]⁺: calculated 434.2478, found 434.2477.

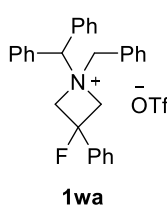
1-benzhydryl-3-cyano-1-ethyl-3-methylazetidinium trifluoromethanesulfonate (1va)



Prepared according to a slightly modified procedure E. Under a N_2 atmosphere, to an oven-dried flask charged with AgOTf (1 equiv., 0.57 mmol, 72.3 mg), a solution of 1-benzhydryl-3-methylazetidinium-3-carbonitrile **7va** (1 equiv., 0.57 mmol, 0.30 g) in dry CH_2Cl_2 (5.7 mL) was added. The reaction mixture was stirred at 40 °C for 12 h in the dark. The mixture was then filtered through celite and the filtrate was evaporated under reduced pressure. The

resulting powder was washed with cold Et_2O to afford the desired product in 50% yield (1.02 mmol, 0.16 g, d.r. > 1:50) as a white powder. ^1H NMR (400 MHz, CDCl_3) δ ppm: 7.65 – 7.58 (m, 4H), 7.57 – 7.43 (m, 6H), 5.80 (s, 1H), 4.91 (s, 4H), 3.84 (q, $J = 7.1$ Hz, 2H), 1.52 (t, $J = 7.1$ Hz, 3H), 0.79 (s, 3H); ^{13}C NMR (101 MHz, CDCl_3) δ ppm: 131.67, 130.80, 130.53, 130.20, 120.11, 120.95 (q, $J = 319.9$ Hz), 75.65, 66.36, 60.36, 25.83, 21.23, 8.86; ^{19}F NMR (377 MHz, CDCl_3) δ ppm: -78.00 (s, 3F). IR (thin layer film) ν (cm^{-1}) = 3060, 1499, 1455, 1423, 1259, 1225, 1157, 1030, 779, 754, 729, 706, 638. 574, 543. HRMS (ESI⁺) m/z $\text{C}_{20}\text{H}_{23}\text{N}_2^+$ [M-OTf]⁺: calculated 291.1856, found 291.1857.

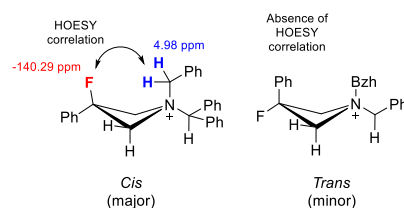
1-benzhydryl-1-benzyl-3-fluoro-3-phenylazetidinium trifluoromethanesulfonate (1wa)



Prepared according to general procedure D using 1-benzhydryl-1-benzyl-3-bromo-2-fluoro-2-phenylpropan-1-amine **7wa** (3.20 mmol, 1.56 g) to afford, following a silica plug purification ($\text{CH}_2\text{Cl}_2:\text{Et}_2\text{O} = 80:20$), the desired product in 80% yield (2.56 mmol, 1.43 g, d.r. 1:2 *cis:trans*)* as a white powder. ^1H NMR (400 MHz, CDCl_3) δ ppm: 7.84 – 7.73 (m, 4H_{minor}), 7.68 – 7.58 (m, 4H_{major}), 7.58 – 7.36 (m, 10H_{minor+major}), 7.23 – 7.03 (m, 4H_{minor+major}),

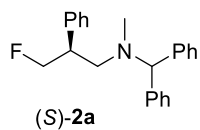
6.69 – 6.63 (m, 2H_{minor}), 6.51 – 6.47 (m, 2H_{major}), 6.46 (s, 1H_{minor}), 6.20 (s, 1H_{major}), 5.55 – 5.23 (m, 4H_{minor+major}), 4.99 (s, 2H_{major}), 4.68 (s, 2H_{minor}); ^{13}C NMR (101 MHz, CDCl_3) [overlapping signals] δ ppm: 133.54, 133.51, 133.30, 133.26, 133.07, 132.46, 131.36, 131.02, 130.57, 130.54, 130.41, 130.39, 130.17, 130.03, 129.80, 129.65, 129.44, 128.82, 128.75, (d, $J = 1.9$ Hz), 127.88, 127.29, 125.31 (d, $J = 4.0$ Hz), 124.55 (d, $J = 6.1$ Hz), 121.10 (d, $J = 320.3$ Hz), 89.26 (d, $J = 202.3$ Hz), 79.58, 77.83 (d, $J = 1.9$ Hz), 68.19 (d, $J = 30.2$ Hz), 67.17, 67.14 (d, $J = 32.3$ Hz), 66.23 (d, $J = 1.8$ Hz). ^{19}F NMR (377 MHz, CDCl_3) δ ppm: -78.16 (s, 3F), -128.22 (p, $J = 18.6$ Hz, 1F_{minor}), -140.29 (p, $J = 20.0$ Hz, 1F_{major}). IR (thin layer film) ν (cm^{-1}) = 3064, 1499, 1454, 1413, 1351, 1256, 1224, 1155, 1065, 1030, 1003, 887, 757, 699, 637, 574. HRMS (ESI⁺) m/z $\text{C}_{29}\text{H}_{27}\text{FN}^+$ [M-OTf]⁺: calculated 408.2122, found 408.2122.

* Assignment of the major diastereoisomer by ^1H - ^{19}F 1D-HOESY. A correlation between the F atom and the benzylic protons was detected in the major *cis* diastereomer but not in the minor *trans* diastereomer.



Product Characterization

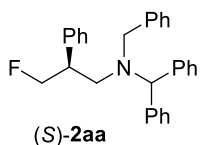
(S)-N-benzhydryl-3-fluoro-N-methyl-2-phenylpropan-1-amine (2a)



(S)-2a was prepared from **1a** (1 equiv., 0.1 mmol, 46.4 mg), according to the general procedure using 10 mol% of catalyst (S)-**D** (0.01 mmol, 8.4 mg) and stirring for 72 h.

Purification: FCC eluent = Pentane:Et₂O (90:0 to 70:30, gradient). Colorless oil, 27.5 mg, 82% yield, e.r. = 80.5:19.5. ¹H NMR (400 MHz, CDCl₃) δ ppm: 7.33 – 7.10 (m, 15H) 4.80 – 4.57 (m, 2H), 4.38 (s, 1H), 3.30 – 3.15 (m, 1H), 2.75 (dd, *J* = 12.6, 8.2 Hz, 1H), 2.53 (dddd, *J* = 12.6, 7.1, 2.3 Hz, 1H), 2.22 (s, 3H); ¹³C NMR (101 MHz, CDCl₃) δ ppm: 142.87, 142.79 140.66 (d, *J* = 3.1 Hz), 128.51, 128.50, 128.46, 128.34, 128.31, 128.22, 127.05, 127.03, 127.01, 85.5 (d, *J* = 171.1 Hz), 76.15, 57.48 (d, *J* = 6.1 Hz), 45.00 (d, *J* = 18.3 Hz), 40.62; ¹⁹F NMR (376 MHz, CDCl₃) δ ppm: -222.24 (tdd, *J* = 47.5, 21.3, 1.5 Hz, 1F). HRMS (ESI⁺) *m/z* C₂₃H₂₅FN⁺ [M+H]⁺: calculated 334.1966, found 334.1956. IR (thin layer film) ν (cm⁻¹) = 3061, 3027, 2958, 2781, 1599, 1492, 1452, 1263, 1201, 1080, 1016, 926, 760, 746, 700. [α]_D²⁵ °C = + 14.6 ° (c = 0.5, CHCl₃, e.r. = 80.5:19.5). HPLC separation DAICEL CHIRALPAK® IB-3, Heptane:PrOH = 99.75:0.25, 1 mL/min; t₁ = 4.57 min (minor), t₂ = 4.96 min (major).

(S)-N-benzhydryl-N-benzyl-3-fluoro-2-phenylpropan-1-amine (2aa)

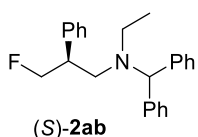


(S)-2aa was prepared from **1aa** (1 equiv., 0.1 mmol, 53.9 mg), according to the general procedure using 5 mol% of catalyst (S)-**D** (0.005 mmol, 4.2 mg) and stirring for 48 h.

Purification: FCC eluent = Pentane:Et₂O (100:0 to 90:10, gradient). Colorless oil, 40.1 mg, 98% yield, e.r. = 96:4. **Gram scale reaction using opposite enantiomer of the catalyst**

(R)-**D**: In a round-bottom flask, **1aa** (1 equiv., 1.85 mmol 1.0 g), CsF (2 equiv., 3.70 mmol, 562 mg) and 3 mol% of catalyst (R)-**D** (0.056 mmol, 46.4 mg) were stirred at r.t. in dry 1,2-DCE (0.25 M, 7.4 mL) at 900 rpm. After 72 h, the reaction mixture was directly purified by flash column chromatography. *Purification:* FCC eluent = Pentane:Et₂O (100:0 to 90:10, gradient) to elute the pure product as the (R)-enantiomer (colorless oil, 696.1 mg, 92% yield, e.r. = 96:4 e.r.); then Pentane:Et₂O (90:10 to 50:50, gradient) to recover the catalyst (46.0 mg, 99% catalyst recovery). ¹H NMR (400 MHz, CDCl₃) δ ppm: 7.40 – 7.36 (m, 4H), 7.22 – 7.22 (m, 14H), 7.07 – 7.02 (m, 2H), 5.00 (s, 1H), 4.62 (ddd, *J* = 47.6, 9.0, 5.5 Hz, 1H), 4.52 (ddd, *J* = 47.5, 9.0, 6.4 Hz, 1H), 3.69 (d, *J* = 1.0 Hz, 2H), 3.23–3.12 (m, 1H), 2.91 (dd, *J* = 13.3, 7.3 Hz, 1H), 2.75 (ddd, *J* = 13.3, 7.5, 2.1 Hz, 1H); ¹³C NMR (101 MHz, CDCl₃) [overlapping signals] δ ppm: 140.80, 140.62 (d, *J* = 3.7 Hz), 140.47, 139.56, 129.51, 129.26, 129.03, 128.54, 128.44, 128.40, 128.35, 128.25, 127.27, 127.10, 127.03, 85.70 (d, *J* = 171.4 Hz), 69.40, 55.57, 52.85 (d, *J* = 6.1 Hz), 45.14 (d, *J* = 18.4 Hz); ¹⁹F NMR (377 MHz, CDCl₃) δ ppm: -221.09 (tdd, *J* = 47.5, 21.1, 1.7 Hz). HRMS (ESI⁺) *m/z* C₂₉H₂₉FN⁺ [M+H]⁺: calculated 410.2279, found 410.2278. IR (thin layer film) ν (cm⁻¹) = 3028, 2926, 2834, 1601, 1493, 1452, 1261, 1027, 762, 743, 698. [α]_D²⁵ °C = + 10.1 ° (c = 0.3, CHCl₃, e.r. = 96:4). HPLC separation DAICEL CHIRALCEL® OJ-H, Heptane:EtOH = 95:5, 1 mL/min; t₁ = 8.83 min (minor), t₂ = 13.52 min (major).

(S)-N-benzhydryl-N-ethyl-3-fluoro-2-phenylpropan-1-amine (2ab)

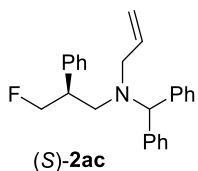


(S)-**2ab** was prepared from **1ab** (1 equiv., 0.1 mmol, 47.8 mg), according to the general procedure using 10 mol% of catalyst (S)-**D** (0.01 mmol, 8.4 mg) and stirring for 72 h.

Purification: FCC eluent = Pentane:Et₂O (100:0 to 90:10, gradient). Colorless oil, 32.3

mg, 93% yield, e.r. = 96:4. **Gram scale reaction:** In a round-bottom flask, **1ab** (1 equiv., 2.11 mmol 1.01 g), CsF (2 equiv., 4.22 mmol, 641 mg) and 10 mol% of catalyst (S)-**D** (0.21 mmol, 176 mg) were stirred at r.t. in dry 1,2-DCE (0.25M, 8.4 mL) at 900 rpm. After 72 h, the reaction mixture was directly purified by flash column chromatography. *Purification:* FCC eluent = Pentane:Et₂O (100:0 to 98.5:1.5, gradient) to elute the pure product (colorless oil, 601 mg, 82% yield, e.r. = 96:4 e.r.); then Pentane:Et₂O (90:10 to 50:50, gradient) to recover the catalyst (174 mg, 99% catalyst recovery). **¹H NMR** (500 MHz, CDCl₃) δ ppm: 7.34 – 7.15 (m, 13H), 7.13 – 7.08 (m, 2H), 4.82 (s, 1H), 4.70 (dd, J = 47.5, 5.5 Hz, 2H), 3.14 – 2.99 (m, 1H), 2.86 (dd, J = 13.5, 8.6 Hz, 1H), 2.73 – 2.52 (m, 3H), 0.96 (t, J = 7.0 Hz, 3H); **¹³C NMR** (126 MHz, CDCl₃) [overlapping signals] δ ppm: 142.38, 142.15, 140.94 (d, J = 2.8 Hz), 128.85, 128.79, 128.51, 128.33, 128.31, 127.04, 127.01, 126.94, 86.23, 85.57 (d, J = 171.2 Hz), 70.90, 52.24 (d, J = 6.4 Hz), 45.41 (d, J = 18.2 Hz), 44.40, 10.87; **¹⁹F NMR** (470 MHz, CDCl₃) δ ppm: -222.84 (tdd, J = 47.4, 23.0, 1.9 Hz). **HRMS** (ESI⁺) m/z C₂₄H₂₇FN⁺ [M+H]⁺: calculated 348.2122, found 348.2120. **IR** (thin layer film) ν (cm⁻¹) = 3026, 2966, 1493, 1452, 1028, 759, 699, 623. $[\alpha]_D^{25}$ °C = + 8.8 ° (c = 0.5, CHCl₃, e.r. = 96:4). **HPLC separation** DAICEL CHIRALCEL[®] OJ-H, Heptane:EtOH = 96:4, 1 mL/min; t_1 = 10.43 min (minor), t_2 = 12.59 min (major).

(S)-N-benzhydryl-N-(3-fluoro-2-phenylpropyl)prop-2-en-1-amine (2ac)

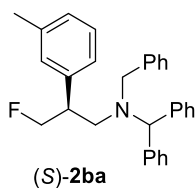


(S)-**2ac** was prepared from **1ac** (1 equiv., 0.1 mmol, 48.9 mg), according to the general procedure using 10 mol% of catalyst (S)-**D** (0.01 mmol, 8.4 mg) and stirring for 36 h.

Purification: FCC eluent = Pentane:Et₂O (100:0 to 90:10, gradient). Colorless oil, 34.5

mg, 96% yield, e.r. = 94:6. **¹H NMR** (400 MHz, CDCl₃) δ ppm: 7.34 – 7.18 (m, 13H), 7.14 – 7.10 (m, 2H), 5.92 – 5.81 (m, 1H), 5.16 – 5.04 (m, 2H), 4.90 (s, 1H), 4.78 – 4.59 (m, 2H), 3.26 – 3.08 (m, 3H), 2.88 (dd, J = 13.3, 8.4 Hz, 1H), 2.72 (dddd, J = 13.3, 7.0, 2.3 Hz, 1H); **¹³C NMR** (101 MHz, CDCl₃) [overlapping signals] δ ppm: 141.75, 141.61, 140.75 (d, J = 3.0 Hz), 135.45, 128.90, 128.84, 128.49, 128.37, 128.33, 127.12, 127.07, 126.96, 117.76, 85.57 (d, J = 171.0 Hz), 70.52, 53.89, 52.55 (d, J = 6.4 Hz), 45.09 (d, J = 18.1 Hz); **¹⁹F NMR** (376 MHz, CDCl₃) δ ppm: -222.34 (tdd, J = 47.1, 21.2, 1.7 Hz, 1F). **HRMS** (ESI⁺) m/z C₂₅H₂₇FN⁺ [M+H]⁺: calculated 360.2122, found 360.2123. **IR** (thin layer film) ν (cm⁻¹) = 3061, 3027, 2956, 2831, 1600, 1493, 1452, 1079, 1005, 922, 760, 735, 699. $[\alpha]_D^{25}$ °C = + 6.5 ° (c = 0.5, CHCl₃, e.r. = 94:6). **HPLC separation** DAICEL CHIRALCEL[®] OJ-H, Heptane:EtOH = 99.5:0.5, 1 mL/min; t_1 = 16.91 min (minor), t_2 = 22.62 min (major).

(S)-N-benzhydryl-N-benzyl-3-fluoro-2-(m-tolyl)propan-1-amine (2ba)

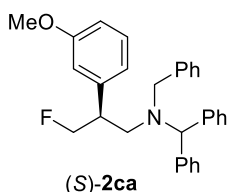


(S)-**2ba** was prepared from **1ba** (1 equiv., 0.1 mmol, 55.4 mg), according to the general procedure using 5 mol% of catalyst (S)-**D** (0.005 mmol, 4.2 mg) and stirring for 48 h.

Purification: FCC eluent = Pentane:Et₂O (100:0 to 90:10, gradient). Colorless oil, 37.2 mg, 88% yield, e.r. = 97.5:2.5. ¹H NMR (400 MHz, CDCl₃) δ ppm: 7.36 – 7.13 (m, 16H),

7.09 – 7.05 (m, 1H), 6.84 – 6.77 (m, 2H), 4.96 (s, 1H), 4.64 – 4.39 (m, 2H), 3.68 – 3.58 (m, 2H), 3.18 – 3.05 (m, 1H), 2.85 (dd, *J* = 13.3, 7.0 Hz, 1H), 2.72 (dddd, *J* = 13.2, 7.7, 1.9 Hz, 1H), 2.30 (s, 3H); ¹³C NMR (101 MHz, CDCl₃) [overlapping signals] δ ppm: 140.87, 140.46 (d, *J* = 3.8 Hz), 140.38, 139.6, 138.0, 129.56, 129.25, 129.16, 129.00, 128.41, 128.37, 128.31, 128.21, 127.80, 127.25, 127.05, 125.53, 85.78 (d, *J* = 171.4 Hz), 69.27, 55.47, 52.82 (d, *J* = 5.8 Hz), 45.03 (d, *J* = 18.1 Hz), 21.59; ¹⁹F NMR (376 MHz, CDCl₃) δ ppm: -220.64 (tdd, *J* = 47.3, 21.1, 1.4 Hz, 1F). HRMS (ESI⁺) *m/z* C₃₀H₃₁FN⁺ [M+H]⁺: calculated 424.2435, found 424.2434. IR (thin layer film) ν (cm⁻¹) = 2980, 1492, 1452, 1381, 1252, 1154, 1073, 954, 764, 743, 700; [α]_D²⁵° = + 7.7 ° (c = 0.3, CHCl₃, e.r. = 97.5:2.5). HPLC separation DAICEL CHIRALCEL® OJ-H, Heptane:ⁱPrOH = 96:4, 1 mL/min; t₁ = 6.89 min (minor), t₂ = 9.69 min (major).

(S)-N-benzhydryl-N-benzyl-3-fluoro-2-(3-methoxyphenyl)propan-1-amine (2ca)

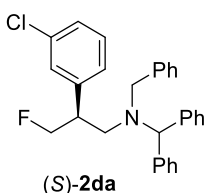


(S)-**2ca** was prepared from **1ca** (1 equiv., 0.1 mmol, 57.0 mg), according to the general procedure using 5 mol% of catalyst (S)-**D** (0.005 mmol, 4.2 mg) and stirring for 48 h.

Purification: FCC eluent = Pentane:Et₂O (100:0 to 90:10, gradient). Colorless oil, 42.2 mg, 96% yield, e.r. = 97:3. ¹H NMR (400 MHz, CDCl₃) δ ppm: 7.36 – 7.15 (m, 16 H),

6.81 – 6.76 (m, 1H), 6.61 (d, *J* = 7.6 Hz, 1H), 6.52 (t, *J* = 2.1 Hz, 1H), 4.95 (s, 1H), 4.65 – 4.38 (m, 2H), 3.72 (s, 3H), 3.64 (s, 2H), 3.15 – 3.00 (m, 1H), 2.86 (dd, *J* = 13.3, 7.2 Hz, 1H), 2.75 (dddd, *J* = 13.2, 7.4, 2.1 Hz, 1H); ¹³C NMR (101 MHz, CDCl₃) [overlapping signals] δ ppm: 159.74, 142.28 (d, *J* = 3.7 Hz), 140.84, 140.51, 139.57, 129.49, 129.24, 129.01, 128.40, 128.34, 128.25, 127.27, 127.10, 120.80, 114.08, 112.46, 85.64 (d, *J* = 171.7 Hz), 69.49, 55.62, 55.25, 52.94 (d, *J* = 6.1 Hz), 45.23 (d, *J* = 18.2 Hz); ¹⁹F NMR (376 MHz, CDCl₃) δ ppm: -220.94 (tdd, *J* = 47.3, 21.0 1.5 Hz, 1F). HRMS (ESI⁺) *m/z* C₃₀H₃₁FNO⁺ [M+H]⁺: calculated 440.2384, found 440.2382. IR (thin layer film) ν (cm⁻¹) = 3027, 2956, 2836, 1600, 1492, 1452, 1262, 1159, 1021, 764, 743, 699. [α]_D²⁵° = + 3.8 ° (c = 0.3, CHCl₃, e.r. = 97:3). HPLC separation DAICEL CHIRALCEL® OJ-H, Heptane:EtOH = 90:10, 1 mL/min; t₁ = 9.30 min (minor), t₂ = 15.39 min (major).

(S)-N-benzhydryl-N-benzyl-2-(3-chlorophenyl)-3-fluoropropan-1-amine (2da)



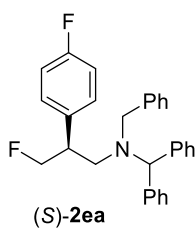
(S)-**2da** was prepared from **1da** (1 equiv., 0.1 mmol, 57.4 mg), according to the general procedure using 5 mol% of catalyst (S)-**D** (0.005 mmol, 4.2 mg) and stirring for 48 h.

Purification: FCC eluent = Pentane:Et₂O (100:0 to 90:10, gradient). Colorless oil, 40.0 mg, 90% yield, e.r. = 96:4. **For the synthesis of F-Lorcaserin (gram scale):** In a round-

bottom flask, **1da** (1 equiv., 1.74 mmol 1.0 g), CsF (2 equiv., 3.48 mmol, 521 mg) and 5 mol% of catalyst (R)-**D** (0.17 mmol, 73 mg) were stirred at r.t. in dry 1,2-DCE (0.25M, 7.0 mL) at 900 rpm. After 48 h, the reaction

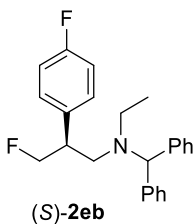
mixture was directly purified by flash column chromatography. *Purification*: FCC eluent = Pentane:Et₂O (100:0 to 90:10, gradient). Colorless oil, 749 mg, 97% yield, e.r. = 96:4 ¹H NMR (400 MHz, CDCl₃) δ ppm: 7.38 – 7.16 (m, 17H), 6.97 – 6.93 (m, 1H), 6.87 (d, *J* = 6.5 Hz, 1H), 4.93 (s, 1H), 4.61 – 4.34 (m, 2H), 3.68 (d, *J* = 14.0 Hz, 1H), 3.59 (d, *J* = 14.0 Hz, 1H), 3.14 – 2.99 (m, 1H), 2.84 (dd, *J* = 13.3, 6.8 Hz, 1H), 2.75 (dddd, *J* = 13.3, 8.0, 1.6 Hz, 1H); ¹³C NMR (101 MHz, CDCl₃) [overlapping signals] δ ppm: 142.63 (d, *J* = 3.3 Hz), 140.87, 140.13, 139.31, 134.29, 129.71, 129.52, 129.08, 128.99, 128.54, 128.46, 128.41, 128.33, 127.36, 127.22, 127.18, 126.81, 85.32 (d, *J* = 172.1 Hz), 69.68, 55.72, 52.67 (d, *J* = 6.4 Hz), 45.95 (d, *J* = 18.4 Hz); ¹⁹F NMR (376 MHz, CDCl₃) δ ppm: -221.53 (td, *J* = 47.2, 21.0 Hz, 1F). **HRMS** (ESI⁺) *m/z* C₂₉H₂₈ClFN⁺ [M+H]⁺: calculated 444.1889, found 444.1883. **IR** (thin layer film) ν (cm⁻¹) = 3060, 3026, 2923, 2838, 1597, 1573, 1493, 1451, 1080, 1028, 785, 763, 744, 698; [α]_D²⁵ °C = + 1.6 ° (c = 0.3, CHCl₃, e.r. = 96:4). **HPLC separation** DAICEL CHIRALCEL[®] OJ-H, Heptane:EtOH = 90:10, 1 mL/min; t₁ = 6.69 min (minor), t₂ = 12.75 min (major).

(S)-N-benzhydryl-N-benzyl-3-fluoro-2-(4-fluorophenyl)propan-1-amine (2ea)



(S)-2ea was prepared from 1ea (1 equiv., 0.1 mmol, 55.8 mg), according to the general procedure using 5 mol% of catalyst (S)-D (0.005 mmol, 4.2 mg) and stirring for 48 h. *Purification*: FCC eluent = Pentane:Et₂O (100:0 to 90:10, gradient). Colorless oil, 42.0 mg, 98% yield, e.r. = 94.5:5.5. ¹H NMR (400 MHz, CDCl₃) δ ppm: 7.38 – 7.19 (m, 15 H), 6.99 – 6.88 (m, 4H), 4.95 (s, 1H), 4.61 – 4.35 (m, 2H), 3.67 (d, *J* = 13.8 Hz, 1H), 3.60 (d, *J* = 13.8 Hz, 1H), 3.14 – 3.00 (m, 1H), 2.84 (dd, *J* = 13.3, 7.1 Hz, 1H), 2.75 (dddd, *J* = 13.2, 7.8, 1.7 Hz, 1H); ¹³C NMR (101 MHz, CDCl₃) [overlapping signals] δ ppm: 161.99 (d, *J* = 245.0 Hz), 140.86, 140.27, 139.45, 136.28 (m), 129.86 (d, *J* = 7.8 Hz), 129.51, 129.17, 129.02, 128.42, 128.38, 128.29, 127.34, 127.17, 115.28 (d, *J* = 21.0 Hz), 85.63 (d, *J* = 172.0 Hz), 69.58, 55.70, 52.90 (d, *J* = 6.0 Hz), 44.43 (d, *J* = 18.1 Hz); ¹⁹F NMR (376 MHz, CDCl₃) δ ppm: -116.12 – -116.26 (m, 1F), -221.61 (td, *J* = 47.7, 21.8 Hz, 1F). **HRMS** (ESI⁺) *m/z* C₂₉H₂₈F₂N⁺ [M+H]⁺: calculated 428.2184, found 428.2186. **IR** (thin layer film) ν (cm⁻¹) = 3027, 2891, 1603, 1510, 1493, 1452, 1381, 1224, 1160, 1136, 1077, 1028, 967, 832, 764, 744. [α]_D²⁵ °C = + 8.2 ° (c = 0.5, CHCl₃, e.r. = 94.5:5.5). **HPLC separation** DAICEL CHIRALPAK[®] IB-3, Heptane:PrOH = 99.75:0.25, 1 mL/min; t₁ = 5.32 min (minor), t₂ = 5.77 min (major).

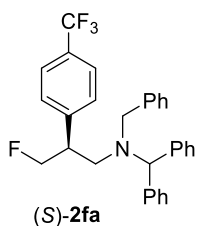
(S)-N-benzhydryl-N-ethyl-3-fluoro-2-(4-fluorophenyl)propan-1-amine (2eb)



(S)-2eb was prepared from 1eb (1 equiv., 0.1 mmol, 55.8 mg), according to the general procedure using 5 mol% of catalyst (S)-D (0.01 mmol, 8.4 mg) and stirring for 48 h. *Purification*: FCC eluent = Pentane:Et₂O (100:0 to 90:10, gradient). Colorless oil, 35.3 mg, 97% yield, e.r. = 95:5. ¹H NMR (400 MHz, CDCl₃) δ ppm: 7.33 – 7.16 (m, 10 H), 7.09 – 7.02 (m, 2H), 7.01 – 6.94 (m, 2H), 4.81 (s, 1H), 4.74 – 4.56 (m, 2H), 3.09 – 2.95 (m, 1H), 2.83 (dd, *J* = 13.4, 8.4 Hz, 1H), 2.71 – 2.51 (m, 3H); 0.96 (t, *J* = 7.0 Hz, 3H); ¹³C NMR (101 MHz, CDCl₃) [overlapping signals] δ ppm: 161.94 (d, *J* = 247.2 Hz), 142.26, 142.14, 136.62 (m), 129.74 (d, *J* = 7.9

Hz), 128.87, 128.73, 128.37, 127.12, 127.07, 115.28 (d, $J = 21.6$ Hz), 85.47 (d, $J = 170.6$ Hz), 70.96, 52.27 (d, $J = 6.0$ Hz), 44.73 (d, $J = 18.2$ Hz), 44.51, 10.86; ^{19}F NMR (376 MHz, CDCl_3) δ ppm: -116.25 – -116.36 (m, 1F), -223.39 (tdd, $J = 48.1, 23.8, 1.6$ Hz, 1F). **HRMS** (ESI⁺) m/z $\text{C}_{24}\text{H}_{26}\text{F}_2\text{N}^+$ [M+H]⁺: calculated 366.2028, found 366.2025. **IR** (thin layer film) ν (cm^{-1}) = 3026, 2970, 1603, 1510, 1492, 1452, 1375, 1225, 1160, 1080, 1015, 832, 761, 745, 706. $[\alpha]_{\text{D}}^{25}$ °C = + 3.6 ° (c = 0.4, CHCl_3 , e.r. = 95:5). **HPLC separation** DAICEL CHIRALPAK[®] IB-3, Heptane:ⁱPrOH = 99.9:0.1, 1 mL/min; $t_1 = 5.85$ min (minor), $t_2 = 6.51$ min (major).

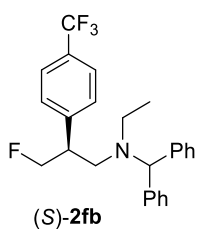
(S)-N-benzhydryl-N-benzyl-3-fluoro-2-(4-(trifluoromethyl)phenyl)propan-1-amine (2fa)



(S)-2fa was prepared from **1fa** (1 equiv., 0.1 mmol, 60.8 mg), according to the general procedure using 5 mol% of catalyst (S)-**D** (0.005 mmol, 4.2 mg) and stirring for 48 h.

Purification: FCC eluent = Pentane:Et₂O (100:0 to 90:10, gradient). Colorless oil, 47.2 mg, 99% yield, e.r. = 95:5. ^1H NMR (400 MHz, CDCl_3) δ ppm: 6.50 (d, $J = 7.9$ Hz, 2H), 7.38 – 7.20 (m, 15H), 7.07 (d, $J = 8.1$ Hz, 2H), 4.95 (s, 1H), 4.64 – 4.38 (m, 2H), 3.69 (d, $J = 13.9$ Hz, 1H), 3.60 (d, $J = 13.9$ Hz, 1H), 3.19 – 3.05 (m, 1H), 2.90 (dd, $J = 13.4, 7.1$ Hz, 1H), 2.79 (dddd, $J = 13.3, 7.8, 1.7$ Hz, 1H); ^{13}C NMR (101 MHz, CDCl_3) [overlapping signals] δ ppm: 144.83, 140.88, 140.18, 139.29, 129.51, 129.29 (q, $J = 32.3$ Hz), 129.14, 129.08, 129.04, 128.81, 128.46, 128.35, 127.44, 127.27, 127.24, 125.36 (q, $J = 3.6$ Hz), 124.41 (q, $J = 271.5$ Hz), 85.17 (d, $J = 171.9$ Hz), 69.90, 55.96, 52.86 (d, $J = 6.1$ Hz), 45.15 (d, $J = 18.4$ Hz); ^{19}F NMR (376 MHz, CDCl_3) δ ppm: -62.36 (s, 3F), -221.93 (td, $J = 48.0, 28.1$ Hz, 1F). **HRMS** (ESI⁺) m/z $\text{C}_{30}\text{H}_{28}\text{F}_4\text{N}^+$ [M+H]⁺: calculated 478.2152, found 478.2150. **IR** (thin layer film) ν (cm^{-1}) = 3062, 3028, 2952, 2834, 1619, 1600, 1493, 1452, 1422, 1326, 1165, 1123, 1069, 1017, 837, 764, 745, 700. $[\alpha]_{\text{D}}^{25}$ °C = + 4.0 ° (c = 0.4, CHCl_3 , e.r. = 95:5). **HPLC separation** DAICEL CHIRALPAK[®] IB-3, Heptane:ⁱPrOH = 99:1, 1 mL/min; $t_1 = 3.54$ min (minor), $t_2 = 4.35$ min (major).

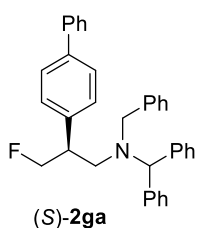
(S)-N-benzhydryl-N-ethyl-3-fluoro-2-(4-(trifluoromethyl)phenyl)propan-1-amine (2fb)



(S)-2fb was prepared from **1fb** (1 equiv., 0.1 mmol, 47.8 mg), according to the general procedure using 10 mol% of catalyst (S)-**D** (0.01 mmol, 8.4 mg) and stirring for 72 h.

Purification: FCC eluent = Pentane:Et₂O (100:0 to 90:10, gradient). White solid, 39.5 mg, 95% yield, e.r. = 95:5. ^1H NMR (400 MHz, CDCl_3) δ ppm: 7.54 (d, $J = 8.1$ Hz, 2H), 7.30 – 7.17 (m, 12H), 4.81 (s, 1H), 4.79 – 4.59 (m, 2H), 3.16 – 3.00 (m, 1H), 2.87 (dd, $J = 13.4, 8.3$ Hz, 1H), 2.74 – 2.54 (m, 3H), 0.97 (t, $J = 7.0$ Hz, 3H); ^{13}C NMR (101 MHz, CDCl_3) δ ppm: 144.95, 141.97, 141.90, 128.81 (q, $J = 32.3$ Hz), 128.73, 128.57, 128.53, 128.28, 128.27, 127.06, 127.00, 125.26 (q, $J = 3.8$ Hz), 124.25 (q, $J = 271.4$ Hz), 84.90 (d, $J = 172.0$ Hz), 70.89, 51.97 (d, $J = 6.5$ Hz), 45.32 (d, $J = 18.1$ Hz), 44.53, 10.70; ^{19}F NMR (376 MHz, CDCl_3) δ ppm: -62.42 (s, 3F), -223.56 (td, $J = 47.3, 24.1, 1.4$ Hz, 1F). **HRMS** (ESI⁺) m/z $\text{C}_{25}\text{H}_{26}\text{F}_4\text{N}^+$ [M+H]⁺: calculated 416.1996, found 416.1993. **IR** (thin layer film) ν (cm^{-1}) = 3027, 2966, 2833, 1619, 1492, 1452, 1421, 1326, 1165, 1124, 1070, 1018, 839, 706. **MP** 85 – 87 °C. $[\alpha]_{\text{D}}^{25}$ °C = – 2.6 ° (c = 0.4, CHCl_3 , e.r. = 95:5). **HPLC separation** DAICEL CHIRALPAK[®] IB-3, Heptane:ⁱPrOH = 99.75:0.25, 1 mL/min; $t_1 = 4.29$ min (minor), $t_2 = 4.85$ min (major).

(S)-2-([1,1'-biphenyl]-4-yl)-N-benzhydryl-N-benzyl-3-fluoropropan-1-amine (2ga)

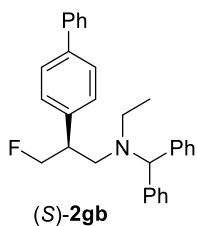


(S)-2ga

(S)-2ga was prepared from **1ga** (1 equiv., 0.1 mmol, 61.6 mg), according to the general procedure using 5 mol% of catalyst (S)-**D** (0.005 mmol, 4.2 mg) and stirring for 48 h.

Purification: FCC eluent = Pentane:Et₂O (100:0 to 90:10, gradient). Colorless oil, 39.7 mg, 82% yield, e.r. = 97:3. ¹H NMR (400 MHz, CDCl₃) δ ppm: 7.65 – 7.60 (m, 2H), 7.55 – 7.44 (m, 4H), 7.41 – 7.35 (m, 4H), 7.35 – 7.20 (m, 12H), 7.12 – 7.07 (m, 2H), 5.01 (s, 1H), 4.72 – 4.45 (m, 2H), 3.72 (d, *J* = 13.9 Hz, 1H), 3.67 (d, *J* = 13.9 Hz, 1H), 3.25 – 3.12 (m, 1H), 2.93 (dd, *J* = 13.2, 7.2 Hz, 1H), 2.82 (dddd, *J* = 13.2, 7.5, 1.8 Hz, 1H); ¹³C NMR (101 MHz, CDCl₃) [overlapping signals] δ ppm: 141.15, 140.87, 140.40, 139.96, 139.72 (d, *J* = 3.8 Hz), 139.56, 129.54, 129.24, 129.04, 128.92, 128.86, 128.42, 128.37, 128.27, 127.33, 127.31, 127.25, 127.19, 127.13, 85.68 (d, *J* = 171.7 Hz), 69.47, 55.65, 52.93 (d, *J* = 5.9 Hz), 44.83 (d, *J* = 17.9 Hz); ¹⁹F NMR (376 MHz, CDCl₃) δ ppm: -221.04 (td, *J* = 47.7, 20.9 Hz, 1F). HRMS (ESI⁺) *m/z* C₃₅H₃₃FN⁺ [M+H]⁺: calculated 486.2592, found 486.2587. IR (thin layer film) ν (cm⁻¹) = 3059, 3027, 2928, 2834, 1600, 1488, 1450, 1076, 1008, 835, 764, 743, 699. [α]_D²⁵ °C = + 25.5 ° (c = 0.4, CHCl₃, e.r. = 97:3). HPLC separation DAICEL CHIRALPAK[®] IB-3, Heptane:PrOH = 99:1, 1 mL/min; t₁ = 5.61 min (major), t₂ = 8.22 min (minor).

(S)-2-([1,1'-biphenyl]-4-yl)-N-benzhydryl-N-ethyl-3-fluoropropan-1-amine (2gb)

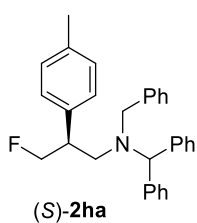


(S)-2gb

(S)-2gb was prepared from **1gb** (1 equiv., 0.1 mmol, 55.4 mg), according to the general procedure using 10 mol% of catalyst (S)-**D** (0.01 mmol, 8.4 mg) and stirring for 72 h.

Purification: FCC eluent = Pentane:Et₂O (100:0 to 90:10, gradient). Colorless oil, 36.4 mg, 86% yield, e.r. = 97:3. ¹H NMR (400 MHz, CDCl₃) δ ppm: 7.61 – 7.55 (m, 2H), 7.55 – 7.49 (m, 2H), 7.46 – 7.40 (m, 2H), 7.36 – 7.15 (m, 13H), 4.84 (s, 1H), 4.74 (dd, *J* = 47.6, 5.6 Hz, 2H), 3.18 – 3.03 (m, 1H), 2.89 (dd, *J* = 13.3, 8.5 Hz, 1H), 2.76 – 2.54 (m, 3H), 0.99 (t, *J* = 7.1 Hz, 3H); ¹³C NMR (101 MHz, CDCl₃) [overlapping signals] δ ppm: 142.38, 142.16, 141.12, 140.02 (d, *J* = 2.5 Hz), 139.89, 128.89, 128.87, 128.80, 128.72, 128.35, 127.30, 127.24, 127.19, 127.07, 127.04, 85.54 (d, *J* = 170.1 Hz), 70.96, 52.28 (d, *J* = 6.2 Hz), 45.10 (d, *J* = 18.4 Hz), 44.49, 10.92; ¹⁹F NMR (376 MHz, CDCl₃) δ ppm: -222.83 (td, *J* = 47.5, 23.2, 1.6 Hz, 1F). HRMS (ESI⁺) *m/z* C₃₀H₃₁FN⁺ [M+H]⁺: calculated 424.2435, found 424.2433. IR (thin layer film) ν (cm⁻¹) = 2980, 1487, 1451, 1382, 1252, 1147, 2079, 935, 833, 764, 732, 698. [α]_D²⁵ °C = + 9.7 ° (c = 0.3, CHCl₃, e.r. = 97:3). HPLC separation DAICEL CHIRALCEL[®] OJ-H, Heptane:EtOH = 60:40, 1 mL/min; t₁ = 22.06 min (major), t₂ = 34.84 min (minor).

(S)-N-benzhydryl-N-benzyl-3-fluoro-2-(*p*-tolyl)propan-1-amine (2ha)



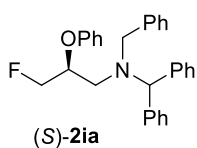
(S)-2ha

(S)-2ha was prepared from **1ha** (1 equiv., 0.1 mmol, 57.0 mg), according to the general procedure using 5 mol% of catalyst (S)-**D** (0.005 mmol, 4.2 mg) and stirring for 48 h.

Purification: FCC eluent = Pentane:Et₂O (100:0 to 90:10, gradient). Colorless oil, 35.6 mg, 84% yield, e.r. = 96.5:3.5. ¹H NMR (400 MHz, CDCl₃) δ ppm: 7.37 – 7.19 (m, 15H), 7.08 (d, *J* = 7.9 Hz, 2H), 7.90 (d, *J* = 7.9 Hz, 2H), 4.97 (s, 1H), 4.66 – 4.39 (m, 2H), 3.64

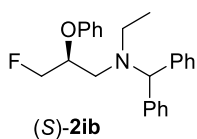
(s, 2H), 3.16 – 3.01 (m, 1H), 2.86 (dd, $J = 13.3, 7.5$ Hz, 1H), 2.73 (dddd, $J = 13.2, 7.3, 2.2$ Hz, 1H), 2.34 (s, 3H); ^{13}C NMR (101 MHz, CDCl_3) [overlapping signals] δ ppm: 140.75, 140.62, 139.62, 137.54 (d, $J = 3.8$ Hz), 136.55, 129.48, 129.31, 129.23, 128.39, 128.33, 128.27, 128.24, 127.24, 127.08, 85.79 (d, $J = 171.1$ Hz), 69.38, 55.58, 52.96 (d, $J = 6.0$ Hz), 44.70 (d, $J = 18.1$ Hz), 21.21; ^{19}F NMR (376 MHz, CDCl_3) δ ppm: -220.99 (tdd, $J = 48.0, 21.0, 1.5$ Hz, 1F). **HRMS** (ESI⁺) m/z $\text{C}_{30}\text{H}_{31}\text{FNO}^+$ [M+H]⁺: calculated 424.2435, found 424.2435. **IR** (thin layer film) ν (cm^{-1}) = 3059, 3026, 2951, 2838, 1600, 1515, 1493, 1451, 01133, 1077, 1028, 813, 763, 743, 700. $[\alpha]_{\text{D}}^{25}$ °C = + 14.8 ° (c = 0.5, CHCl_3 , e.r. = 96.5:3.5). **HPLC separation** DAICEL CHIRALCEL[®] OJ-H, Heptane:ⁱPrOH = 96:4, 1 mL/min; $t_1 = 7.77$ min (minor), $t_2 = 10.38$ min (major).

(S)-N-benzhydryl-N-benzyl-3-fluoro-2-phenoxypropan-1-amine (2ia)



(S)-**2ia** was prepared from **1ia** (1 equiv., 0.1 mmol, 55.6 mg), according to the general procedure using 5 mol% of catalyst (S)-**D** (0.005 mmol, 4.2 mg) and stirring for 48 h. **Purification**: FCC eluent = Pentane:Et₂O (100:0 to 90:10, gradient). Colorless oil, 42.0 mg, 99% yield, e.r. = 88:12. ^1H NMR (400 MHz, CDCl_3) δ ppm: 7.44 – 7.17 (m, 17H), 6.96 – 6.90 (m, 1H), 6.70 – 6.63 (m, 2H), 4.99 (s, 1H), 4.64 – 4.22 (m, 3H), 3.76 (d, $J = 13.8$ Hz, 1H), 3.70 (d, $J = 13.8$ Hz, 1H), 2.96 – 2.75 (m, 2H); ^{13}C NMR (101 MHz, CDCl_3) [overlapping signals] δ ppm: 157.95, 141.23, 140.84, 139.41, 129.61, 129.36, 129.14, 129.10, 128.57, 128.52, 127.44, 127.38, 127.33, 121.37, 116.02, 83.57 (d, $J = 173.7$ Hz), 75.86 (d, $J = 18.4$ Hz), 70.98, 56.86, 50.87 (d, $J = 6.7$ Hz); ^{19}F NMR (376 MHz, CDCl_3) δ ppm: -229.37 (td, $J = 47.6, 20.5$ Hz, 1F). **HRMS** (ESI⁺) m/z $\text{C}_{29}\text{H}_{29}\text{FNO}^+$ [M+H]⁺: calculated 426.2228, found 426.2225. **IR** (thin layer film) ν (cm^{-1}) = 3061, 3028, 2920, 2849, 1598, 1493, 1452, 1299, 1239, 1174, 1082, 1026, 925, 747, 700. $[\alpha]_{\text{D}}^{25}$ °C = + 21.2 ° (c = 0.6, CHCl_3 , e.r. = 88:12). **HPLC separation** DAICEL CHIRALCEL[®] OJ-3, Heptane:ⁱPrOH = 95:5, 1 mL/min; $t_1 = 12.51$ min (minor), $t_2 = 20.42$ min (major).

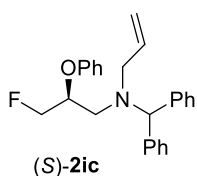
(S)-N-benzhydryl-N-ethyl-3-fluoro-2-phenoxypropan-1-amine (2ib)



(S)-**2ib** was prepared from **1ib** (1 equiv., 0.1 mmol, 49.4 mg), according to the general procedure using 10 mol% of catalyst (S)-**D** (0.01 mmol, 8.4 mg) and stirring for 72 h. **Purification**: FCC eluent = Pentane:Et₂O (100:0 to 90:10, gradient). Colorless oil, 30.5 mg, 84% yield, e.r. = 93.5:6.5. ^1H NMR (400 MHz, CDCl_3) δ ppm: 7.40 – 7.33 (m, 4H), 7.32 – 7.26 (m, 4H), 7.26 – 7.17 (m, 4H), 6.94 (tt, $J = 7.3, 0.9$ Hz, 1H), 6.74 – 6.68 (m, 2H), 4.86 (s, 1H), 4.80 – 4.53 (m, 2H), 4.41 – 4.30 (m, 1H), 2.92 – 2.77 (m, 2H), 2.75 – 2.59 (m, 2H), 1.01 (t, $J = 7.0$ Hz, 3H); ^{13}C NMR (101 MHz, CDCl_3) δ ppm: 158.10, 142.33, 142.30, 129.62, 128.94, 128.62, 128.55, 128.51, 127.32, 127.19, 121.40, 116.15, 82.57 (d, $J = 172.1$ Hz), 76.45 (d, $J = 18.2$ Hz), 71.71, 49.99 (d, $J = 6.7$ Hz), 46.03, 11.12; ^{19}F NMR (376 MHz, CDCl_3) δ ppm: -230.23 (td, $J = 47.5, 21.1, 2.0$ Hz, 1F). **HRMS** (ESI⁺) m/z $\text{C}_{24}\text{H}_{27}\text{FNO}^+$ [M+H]⁺: calculated 364.2071, found 364.2071. **IR** (thin layer film) ν (cm^{-1}) = 2969, 1598, 1493, 1453, 1240, 1174, 1082, 1025, 937, 793, 753, 707, 620. $[\alpha]_{\text{D}}^{25}$ °C = + 21.0 ° (c = 0.5, CHCl_3 , e.r. = 93.5:6.5).

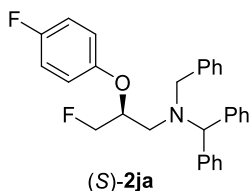
HPLC separation DAICEL CHIRALCEL® OJ-H, Heptane:EtOH = 96:4, 1 mL/min; t_1 = 13.57 min (minor), t_2 = 16.82 min (major).

(S)-N-benzhydryl-N-(3-fluoro-2-phenoxypropyl)prop-2-en-1-amine (2ic)



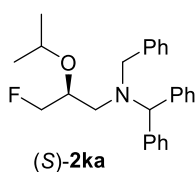
(S)-2ic was prepared from 1ic (1 equiv., 0.1 mmol, 50.6 mg), according to the general procedure using 10 mol% of catalyst (S)-D (0.01 mmol, 8.4 mg) and stirring for 36 h. **Purification:** FCC eluent = Pentane:Et₂O (100:0 to 90:10, gradient). Colorless oil, 34.2 mg, 91% yield, e.r. = 85:15. **¹H NMR** (400 MHz, CDCl₃) δ ppm: 7.38 – 7.19 (m, 12H), 6.94 (tt, J = 8.3, 1.0 Hz, 1H), 6.78 – 6.73 (m, 2H), 5.97 – 5.85 (m, 1H), 5.18 – 5.13 (m, 1H), 5.12 – 5.05 (m, 1H), 4.93 (s, 1H), 4.79 – 4.50 (m, 2H), 4.51 – 4.38 (m, 1H), 3.22 (d, J = 6.3 Hz, 2H), 2.93 – 2.81 (m, 2H); **¹³C NMR** (101 MHz, CDCl₃) [overlapping signals] δ ppm: 158.11, 141.86, 141.75, 135.28, 129.62, 129.00, 128.73, 128.57, 128.54, 127.39, 127.28, 121.43, 118.25, 116.19, 83.66 (d, J = 172.2 Hz), 76.32 (d, J = 18.5 Hz), 71.55, 55.41, 50.17 (d, J = 6.9 Hz); **¹⁹F NMR** (376 MHz, CDCl₃) δ ppm: -229.74 (tdd, J = 47.4, 27.2, 1.5 Hz, 1F). **HRMS** (ESI⁺) m/z C₂₅H₂₇FNO⁺ [M+H]⁺: calculated 376.2071, found 376.2067. **IR** (thin layer film) ν (cm⁻¹) = 3061, 3027, 2922, 2848, 1597, 1493, 1453, 1289, 1240, 1173, 1083, 1026, 928, 795, 753, 706. **$[\alpha]_D^{25}$** = + 18.9 ° (c = 0.4, CHCl₃, e.r. = 85:15). **HPLC separation** DAICEL CHIRALPAK® IB-3, Heptane:ⁱPrOH = 99.75:0.25, 1 mL/min; t_1 = 5.26 min (minor), t_2 = 5.70 min (major).

(S)-N-benzhydryl-N-benzyl-3-fluoro-2-(4-fluorophenoxy)propan-1-amine (2ja)



(S)-2ja was prepared from 1ja (1 equiv., 0.1 mmol, 57.4 mg), according to the general procedure using 10 mol% of catalyst (S)-D (0.01 mmol, 8.4 mg) and stirring for 48 h. **Purification:** FCC eluent = Pentane:Et₂O (100:0 to 90:10, gradient). Colorless oil, 27.5 mg, 62% yield, e.r. = 88:12. **¹H NMR** (400 MHz, CDCl₃) δ ppm: 7.42– 7.24 (m, 15H), 6.90 – 6.83 (m, 2H), 6.60 – 6.54 (m, 2H), 4.96 (s, 1H), 4.75 (ddd, J = 47.5, 10.1, 2.9 Hz, 1H), 4.36 (ddd, J = 47.6, 10.1, 5.5 Hz, 1H), 4.22 – 4.10 (m, 2H), 3.73 (d, J = 13.7 Hz, 1H), 3.68 (d, J = 13.7 Hz, 1H), 2.92 – 2.81 (m, 2H); **¹³C NMR** (101 MHz, CDCl₃) [overlapping signals] δ ppm: 157.42 (d, J = 239.2 Hz), 154.09 (d, J = 2.3 Hz), 141.20, 140.79, 139.31, 129.34, 129.15, 129.05, 128.60, 128.55, 127.49, 127.45, 127.38, 117.40 (d, J = 8.0 Hz), 115.90 (d, J = 23.0 Hz), 83.64 (d, J = 172.6 Hz), 77.16 (d, J = 18.4 Hz), 71.19, 57.02 50.87 (d, J = 7.1 Hz); **¹⁹F NMR** (376 MHz, CDCl₃) δ ppm: -123.00 – -123.09 (m, 1F), -223.31 (td, J = 47.5, 19.9 Hz, 1F). **HRMS** (ESI⁺) m/z C₂₉H₂₈F₂NO⁺ [M+H]⁺: calculated 444.2133, found 444.2126. **IR** (thin layer film) ν (cm⁻¹) = 2980, 1503, 1453, 1381, 1247, 1206, 1154, 1072, 1026, 953, 827, 744, 701. **$[\alpha]_D^{25}$** = + 15.7 ° (c = 0.9, CHCl₃, e.r. = 88:12). **HPLC separation** DAICEL CHIRALCEL® OJ-3, Heptane:ⁱPrOH = 80:20, 1 mL/min; t_1 = 6.80 min (minor), t_2 = 13.43 min (major).

(S)-N-benzhydryl-N-benzyl-3-fluoro-2-isopropoxypropan-1-amine (2ka)

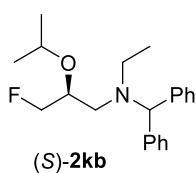


(S)-**2ka** was prepared from **1ka** (1 equiv., 0.1 mmol, 52.1 mg), according to the general procedure using 5 mol% of catalyst (S)-**D** (0.005 mmol, 4.2 mg) and stirring for 48 h.

Purification: FCC eluent = Pentane:Et₂O (100:0 to 90:10, gradient). Colorless oil, 34.0 mg, 87% yield, e.r. = 93:7. ¹H NMR (400 MHz, CDCl₃) δ ppm: 7.43 – 7.21 (m, 15H), 4.97 (s,

1H), 4.48 (ddd, *J* = 47.5, 9.7, 3.1 Hz, 1H), 4.36 (ddd, *J* = 48.1, 9.7, 6.3 Hz, 1H), 3.70 (d, *J* = 13.7 Hz, 1H), 3.65 (d, *J* = 13.7 Hz, 1H), 3.54 (sept, *J* = 6.1 Hz, 1H), 3.52 – 3.42 (m, 1H), 2.69 – 2.56 (m, 2H), 2.75 (dd, *J* = 6.1, 2.7 Hz, 6H); ¹³C NMR (101 MHz, CDCl₃) [overlapping signals] δ ppm: 140.99, 140.80, 139.54, 129.35, 129.30, 129.06, 128.50, 128.40, 128.35, 127.27, 85.28 (d, *J* = 170.6 Hz), 74.75 (d, *J* = 17.4 Hz), 71.32, 70.42, 56.73, 51.87 (d, *J* = 8.0 Hz), 22.82, 22.69; ¹⁹F NMR (376 MHz, CDCl₃) δ ppm: -227.86 (tdd, *J* = 48.3, 19.3, 2.3 Hz, 1F). HRMS (ESI⁺) *m/z* C₂₆H₃₁FNO⁺ [M+H]⁺: calculated 392.2384, found 392.2385. IR (thin layer film) ν (cm⁻¹) = 3061, 3028, 2967, 2926, 2848, 1600, 1494, 1452, 1368, 1330, 1180, 1123, 985, 763, 744, 700. [α]_D²⁵ °C = +10.5 ° (c = 0.5, CHCl₃, e.r. = 93:7). HPLC separation DAICEL CHIRALPAK[®] IC-3, Heptane:ⁱPrOH = 99:1, 1 mL/min; t₁ = 2.78 min (minor), t₂ = 3.09 min (major).

(S)-N-benzhydryl-N-ethyl-3-fluoro-2-isopropoxypropan-1-amine (2kb)

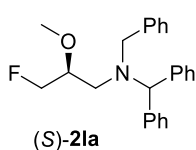


(S)-**2kb** was prepared from **1kb** (1 equiv., 0.1 mmol, 46.0 mg), according to the general procedure 10 mol% of catalyst (S)-**D** (0.01 mmol, 8.4 mg) and stirring for 72 h.

Purification: FCC eluent = Pentane:Et₂O (100:0 to 90:10, gradient). Colorless oil, 31.3 mg, 95% yield, e.r. = 95:5. ¹H NMR (400 MHz, CDCl₃) δ ppm: 7.39 – 7.33 (m,

4H), 7.33 – 7.24 (m, 4H), 7.25 – 7.17 (m, 2H), 4.83 (s, 1H), 4.60 (ddd, *J* = 47.8, 9.7, 3.0 Hz, 1H), 4.38 (ddd, *J* = 48.0, 9.6, 6.1 Hz, 1H), 3.57 (sept, *J* = 6.1 Hz, 1H), 3.54 – 3.42 (m, 1H), 2.69 – 2.52 (m, 4H), 1.08 (dd, *J* = 6.1, 3.7 Hz, 6H), 1.00 (t, *J* = 7.1 Hz, 3H); ¹³C NMR (101 MHz, CDCl₃) δ ppm: 142.34, 142.27, 128.96, 128.71, 128.42, 128.36, 127.15, 127.10, 85.23 (d, *J* = 170.3 Hz), 75.17 (d, *J* = 17.2 Hz), 71.55, 71.40, 51.20 (d, *J* = 7.9 Hz), 45.75, 22.82, 22.77, 11.24; ¹⁹F NMR (376 MHz, CDCl₃) δ ppm: -229.02 (td, *J* = 47.8, 20.3 Hz, 1F). HRMS (ESI⁺) *m/z* C₂₁H₂₉FNO⁺ [M+H]⁺: calculated 330.2228, found 330.2228. IR (thin layer film) ν (cm⁻¹) = 3027, 2970; 1492, 1453, 1379, 1333, 1122, 1021, 760, 746, 731, 706. [α]_D²⁵ °C = +12.5 ° (c = 0.5, CHCl₃, e.r. = 95:5). HPLC separation DAICEL CHIRALCEL[®] OJ-3, Heptane:ⁱPrOH = 99:1, 1 mL/min; t₁ = 4.93 min (major), t₂ = 6.63 min (minor).

(S)-N-benzhydryl-N-benzyl-3-fluoro-2-methoxypropan-1-amine (2la)



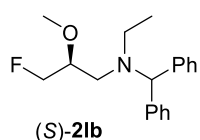
(S)-**2la** was prepared from **1la** (1 equiv., 0.1 mmol, 49.3 mg), according to the general procedure using 10 mol% of catalyst (S)-**D** (0.01 mmol, 8.4 mg) and stirring for 48 h.

Purification: FCC eluent = Pentane:Et₂O (100:0 to 90:10, gradient). Colorless oil, 30.9 mg, 85% yield, e.r. = 88:12. ¹H NMR (400 MHz, CDCl₃) δ ppm: 7.41 – 7.22 (m, 15H), 4.98 (s,

1H), 4.48 (ddd, *J* = 47.4, 10.0, 2.8 Hz, 1H), 4.23 (ddd, *J* = 48.1, 10.0, 6.2 Hz, 1H), 3.72 (d, *J* = 13.8 Hz, 1H), 3.64 (d, *J* = 13.8 Hz, 1H), 3.40 – 3.31 (m, 1H), 3.31 (s, 3H), 2.71 – 2.59 (m, 2H); ¹³C NMR (101 MHz, CDCl₃)

[overlapping signals] δ ppm: 141.05, 140.75, 139.55, 129.29, 129.03, 128.50, 128.42, 128.38, 127.30, 127.25, 84.71 (d, $J = 170.9$ Hz), 79.20 (d, $J = 17.3$ Hz), 71.35, 58.20, 56.46, 50.50 (d, $J = 8.2$ Hz); ^{19}F NMR (376 MHz, CDCl_3) δ ppm: -227.91 (tdd, $J = 48.2, 19.8, 2.0$ Hz, 1F). **HRMS** (ESI⁺) m/z $\text{C}_{24}\text{H}_{27}\text{FNO}^+$ [M+H]⁺: calculated 364.2071, found 364.2070. **IR** (thin layer film) ν (cm^{-1}) = 3027, 2931, 2832, 1493, 1453, 1099, 1028, 764, 744, 700. $[\alpha]_{\text{D}}^{25}$ °C = +11.6 ° (c = 0.5, CHCl_3 , e.r. = 88:12). **HPLC separation** DAICEL CHIRALPAK[®] IB-3, Heptane:^tPrOH = 99:1, 1 mL/min; $t_1 = 3.41$ min (minor), $t_2 = 4.24$ min (major).

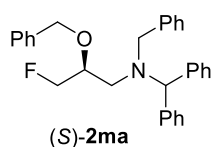
(S)-N-benzhydryl-N-ethyl-3-fluoro-2-methoxypropan-1-amine (2lb)



(S)-**2lb** was prepared from **1lb** (1 equiv., 0.1 mmol, 46.0 mg), according to the general procedure 10 mol% of catalyst (S)-**D** (0.01 mmol, 8.4 mg) and stirring for 72 h.

Purification: FCC eluent = Pentane:Et₂O (100:0 to 90:10, gradient). Colorless oil, 29.8 mg, 99% yield, e.r. = 91:9. ^1H NMR (400 MHz, CDCl_3) δ ppm: 7.38 – 7.17 (m, 10H), 4.85 (s, 1H), 4.63 (ddd, $J = 47.7, 9.9, 2.6$ Hz, 1H), 4.41 (ddd, $J = 48.9, 9.9, 5.9$ Hz, 1H), 3.42 – 3.29 (s + m overlapped, 4H), 2.71 – 2.52 (m, 4H), 1.00 (t, $J = 7.0$ Hz, 3H); ^{13}C NMR (101 MHz, CDCl_3) δ ppm: 142.22, 142.11, 128.90, 128.73, 128.43, 128.38, 127.16, 127.14, 84.57 (d, $J = 170.8$ Hz), 79.36 (d, $J = 17.2$ Hz), 71.43, 58.18, 49.81 (d, $J = 8.1$ Hz), 45.54, 11.31; ^{19}F NMR (376 MHz, CDCl_3) δ ppm: -229.07 (tdd, $J = 48.0, 21.0, 2.5$ Hz, 1F). **HRMS** (ESI⁺) m/z $\text{C}_{19}\text{H}_{25}\text{FNO}^+$ [M+H]⁺: calculated 302.1915, found 302.1916. **IR** (thin layer film) ν (cm^{-1}) = 2970, 1493, 1453, 1375, 1263, 1120, 1013, 760, 746, 731, 706, 620. $[\alpha]_{\text{D}}^{25}$ °C = +15.3 ° (c = 0.6, CHCl_3 , e.r. = 91:9). **HPLC separation** DAICEL CHIRALCEL[®] OJ-3, Heptane:^tPrOH = 98:2, 1 mL/min; $t_1 = 10.04$ min (major), $t_2 = 11.85$ min (minor).

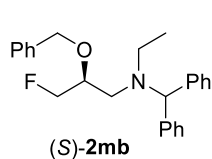
(S)-N-benzhydryl-N-benzyl-2-(benzyloxy)-3-fluoropropan-1-amine (2ma)



(S)-**2ma** was prepared from **1ma** (1 equiv., 0.1 mmol, 57.0 mg), according to the general procedure using 5 mol% of catalyst (S)-**D** (0.005 mmol, 4.2 mg) and stirring for 48 h.

Purification: FCC eluent = Pentane:Et₂O (100:0 to 90:10, gradient). Colorless oil, 42.1 mg, 96% yield, e.r. = 95:5. ^1H NMR (400 MHz, CDCl_3) δ ppm: 7.39 – 7.21 (m, 20H), 4.97 (s, 1H), 4.60 – 4.43 (m, 3H), 4.30 (ddd, $J = 48.2, 10.0, 6.3$ Hz, 1H), 3.72 – 3.56 (m, 3H), 2.76 – 2.61 (m, 2H); ^{13}C NMR (101 MHz, CDCl_3) [overlapping signals] δ ppm: 140.97, 140.76, 139.43, 138.48, 129.28, 129.03, 128.49, 128.41, 128.38, 127.98, 127.78, 127.29, 127.27, 127.23, 85.22 (d, $J = 171.2$ Hz), 76.80 (d, $J = 17.3$ Hz), 72.57, 70.24, 56.34, 51.03 (d, $J = 8.3$ Hz); ^{19}F NMR (376 MHz, CDCl_3) δ ppm: -227.18 (tdd, $J = 47.2, 19.5, 2.3$ Hz, 1F). **HRMS** (ESI⁺) m/z $\text{C}_{30}\text{H}_{31}\text{FNO}^+$ [M+H]⁺: calculated 440.2384, found 440.2383; **IR** (thin layer film) ν (cm^{-1}) = 3030, 2921, 1494, 1453, 1262, 1094, 1027, 765, 742, 699, 613. $[\alpha]_{\text{D}}^{25}$ °C = +4.7 ° (c = 0.2, CHCl_3 , e.r. = 95:5). **HPLC separation** DAICEL CHIRALCEL[®] OJ-H, Heptane:EtOH = 96:4, 1 mL/min; $t_1 = 17.70$ min (major), $t_2 = 23.32$ min (minor).

(S)-N-benzhydryl-2-(benzyloxy)-N-ethyl-3-fluoropropan-1-amine (2mb)

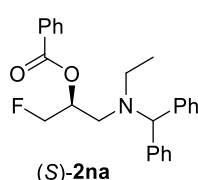


(S)-2mb was prepared from **1mb** (1 equiv., 0.1 mmol, 50.8 mg), according to the general procedure using 10 mol% of catalyst (S)-**D** (0.01 mmol, 8.4 mg) and stirring for 72 h.

Purification: FCC eluent = Pentane:Et₂O (100:0 to 90:10, gradient). Colorless oil, 37.4 mg, 99% yield, e.r. = 97:3. ¹H NMR (400 MHz, CDCl₃) δ ppm: 7.38 – 7.17 (m, 15H),

4.83 (s, 1H), 4.75 – 4.38 (m, 4H), 3.69 – 3.56 (m, 1H), 2.74 – 2.51 (m, 4H), 0.98 (t, *J* = 7.0 Hz, 3H); ¹³C NMR (101 MHz, CDCl₃) δ ppm: 142.20, 142.03, 138.60, 128.86, 128.76, 128.49, 128.41, 128.37, 127.91, 127.76, 127.14, 127.12, 85.07 (d, *J* = 170.3 Hz), 77.03 (d, *J* = 17.6 Hz), 72.51, 71.30, 50.36 (d, *J* = 8.0 Hz), 45.43, 11.24; ¹⁹F NMR (376 MHz, CDCl₃) δ ppm: -228.42 (td, *J* = 48.0, 20.1, 2.7 Hz, 1F). HRMS (ESI⁺) *m/z* C₂₅H₂₉FNO⁺ [M+H]⁺: calculated 378.2228, found 378.2227. IR (thin layer film) ν (cm⁻¹) = 3028, 2967, 1493, 1453, 1375, 1105, 1028, 734, 699. [α]_D²⁵ = +11.2° (c = 0.5, CHCl₃, e.r. = 97:3). HPLC separation DAICEL CHIRALCEL® OJ-3, Heptane:PrOH = 95:5, 1 mL/min; t₁ = 9.11 min (major), t₂ = 13.37 min (minor).

(S)-1-(benzhydryl(ethyl)amino)-3-fluoropropan-2-yl benzoate (2na)

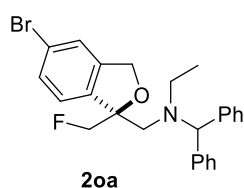


(S)-2na was prepared from **1na** (1 equiv., 0.1 mmol, 58.4 mg), according to the general procedure using 5 mol% of catalyst (S)-**D** (0.005 mmol, 4.2 mg) and stirring for 48 h.

Purification: FCC eluent = Pentane:Et₂O (100:0 to 90:10, gradient). Colorless oil, 34.0 mg, 87% yield, e.r. = 86.5:13.5. ¹H NMR (400 MHz, CDCl₃) δ ppm: 8.01 – 7.97 (m, 2H),

7.50 (t, *J* = 7.4 Hz, 1H), 7.37 (t, *J* = 7.6 Hz, 2H), 7.29 – 7.10 (m, 10H), 5.37 – 5.24 (m, 1H), 4.85 (s, 1H), 4.59 (ddd, *J* = 47.7, 10.2, 2.6 Hz, 1H), 4.79 (ddd, *J* = 47.2, 10.2, 4.6 Hz, 1H), 2.85 – 2.48 (m, 4H), 0.96 (t, *J* = 7.0 Hz, 3H); ¹³C NMR (101 MHz, CDCl₃) [overlapping signals] δ ppm: 166.07, 141.91, 141.66, 133.27, 129.96, 128.91, 128.75, 128.51, 128.44, 128.41, 127.19, 82.97 (d, *J* = 171.7 Hz), 71.71 (d, *J* = 18.4 Hz), 70.84, 49.18 (d, *J* = 6.9 Hz), 44.85, 11.41; ¹⁹F NMR (376 MHz, CDCl₃) δ ppm: -232.00 (td, *J* = 47.1, 23.3 Hz, 1F). HRMS (ESI⁺) *m/z* C₂₅H₂₇FNO₂⁺ [M+H]⁺: calculated 392.2020, found 392.2019. IR (thin layer film) ν (cm⁻¹) = 2980, 1720, 1492, 1452, 1270, 1113, 1070, 1026, 953, 762, 708. [α]_D²⁵ = +11.4° (c = 0.4, CHCl₃, e.r. = 86.5:13.5). HPLC separation DAICEL CHIRALPAK® IC-3, Heptane:PrOH = 99.55:0.45, 1 mL/min; t₁ = 5.22 min (minor), t₂ = 5.94 min (major).

N-benzyl-N-((5-bromo-1-(fluoromethyl)-1,3-dihydroisobenzofuran-1-yl)methyl)-1,1-diphenylmethanamine (2oa)



Absolute configuration not assigned

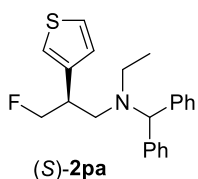
2oa was prepared from **1oa** (1 equiv., 0.1 mmol, 58.4 mg), according to the general procedure using 10 mol% of catalyst (S)-**D** (0.01 mmol, 8.4 mg) and stirring for 72 h.

Purification: FCC eluent = Pentane:Et₂O (100:0 to 90:10, gradient). White solid, 23.1 mg, 51% yield, e.r. = 83:17. ¹H NMR (400 MHz, CDCl₃) δ ppm: 7.43 – 7.13 (m,

12H), 6.91 (d, *J* = 8.1 Hz, 1H), 5.25 (s, 1H), 5.09 (s, 2H), 4.67 (dd, *J* = 47.1, 9.5 Hz, 1H), 4.60 (dd, *J* = 48.4, 9.5 Hz, 1H), 2.96 – 2.83 (m, 2H), 2.71 – 2.59 (m, 1H), 2.56 – 2.44 (m, 1H), 0.95 (t, *J* = 7.2 Hz, 3H); ¹³C NMR (101 MHz, CDCl₃) [overlapping signals] δ ppm: 142.60,

141.73, 140.89, 139.72 (d, $J = 2.4$ Hz), 130.58, 129.47, 129.01, 128.21, 128.19, 127.08, 126.94, 124.43, 123.91, 122.30, 90.65 (d, $J = 17.6$ Hz), 85.72 (d, $J = 175.1$ Hz), 72.45, 69.80, 54.19, 44.73, 12.03; ^{19}F NMR (376 MHz, CDCl_3) δ ppm: -229.02 (t, $J = 48.0$ Hz, 1F). **HRMS** (ESI⁺) m/z $\text{C}_{25}\text{H}_{26}\text{BrFNO}^+$ [M+H]⁺: calculated 454.1176, found 454.1175. **IR** (thin layer film) ν (cm^{-1}) = 2924, 2852, 1600, 1492, 1453, 1413, 1375, 1262, 1191, 1070, 1030, 818, 761, 731, 703. **MP** 95 – 97 °C. $[\alpha]_{\text{D}}^{25\text{ }^\circ\text{C}} = +11.7$ ° (c = 0.3, CHCl_3 , e.r. = 83:17). **HPLC separation** DAICEL CHIRALPAK[®] IC-3, Heptane:ⁱPrOH = 99.5:0.5, 1 mL/min; $t_1 = 3.35$ min (major), $t_2 = 3.92$ min (minor).

(S)-N-benzhydryl-N-ethyl-3-fluoro-2-(thiophen-3-yl)propan-1-amine (2pa)

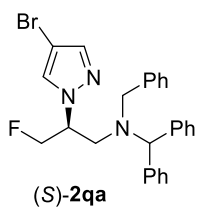


(S)-2pa was prepared from 1pa (1 equiv., 0.1 mmol, 48.3 mg), according to the general procedure using 10 mol% of catalyst (S)-D (0.01 mmol, 8.4 mg) and stirring for 72 h.

Purification: FCC eluent = Pentane:Et₂O (100:0 to 90:10, gradient). Colorless oil, 21.6 mg, 61% yield, e.r. = 93.5:6.5. ^1H NMR (400 MHz, CDCl_3) δ ppm: 7.34 – 7.17 (m, 11H), 6.97

(d br, $J = 2.2$ Hz, 1H), 6.87 (d br, $J = 4.9$ Hz, 1H), 4.83 (s, 1H), 4.73 (ddd, $J = 47.4, 8.8, 5.4$ Hz, 1H), 4.67 (ddd, $J = 47.8, 8.8, 4.5$ Hz, 1H), 3.22 – 3.06 (m, 1H), 2.84 (dd, $J = 13.5, 9.0$ Hz, 1H), 2.73 – 2.50 (m, 3H), 0.98 (t, $J = 7.0$ Hz, 3H); ^{13}C NMR (101 MHz, CDCl_3) [overlapping signals] δ ppm: 142.40, 142.16, 140.37 (d, $J = 2.6$ Hz), 128.87, 128.79, 128.36, 127.72, 127.05, 125.27, 121.43, 85.15 (d, $J = 173.0$ Hz), 71.01, 52.12 (d, $J = 6.2$ Hz), 44.66, 40.91 (d, $J = 18.6$ Hz), 11.01; ^{19}F NMR (376 MHz, CDCl_3) δ ppm: -223.77 (tdd, $J = 48.5, 25.9, 1.3$ Hz, 1F). **HRMS** (ESI⁺) m/z $\text{C}_{22}\text{H}_{25}\text{FNS}^+$ [M+H]⁺: calculated 354.1686, found 354.1687. **IR** (thin layer film) ν (cm^{-1}) = 3024, 2965, 1492, 1452, 1373, 1179, 1138, 1028, 914, 778, 760, 745, 732, 705. $[\alpha]_{\text{D}}^{25\text{ }^\circ\text{C}} = +3.7$ ° (c = 0.4, CHCl_3 , e.r. = 93.5:6.5). **SFC separation** DAICEL CHIRALCEL[®] OJ-3, CO₂:MeOH (95:5 to 40:60, gradient) + 0.3% isopropylamine, 3 mL/min; $t_1 = 2.13$ min (minor), $t_2 = 2.41$ min (major).

(S)-N-benzhydryl-N-benzyl-2-(4-bromo-1H-pyrazol-1-yl)-3-fluoropropan-1-amine (2qa)

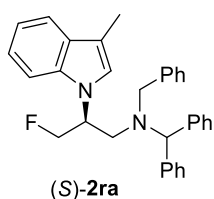


(S)-2qa was prepared from 1qa (1 equiv., 0.1 mmol, 60.8 mg), according to the general procedure using 5 mol% of catalyst (S)-D (0.005 mmol, 4.2 mg) and stirring for 48 h.

Purification: FCC eluent = Pentane:Et₂O (100:0 to 90:10, gradient). Colorless oil, 46.9 mg, 98% yield, e.r. = 87:13. ^1H NMR (400 MHz, CDCl_3) δ ppm: 7.44 (s, 1H), 7.37 – 7.20 (m,

15H), 7.11 (s, 1H), 4.89 (s, 1H), 4.47 (dd, $J = 47.0, 5.1$ Hz, 2H), 4.29 – 4.16 (m, 1H), 3.69 – 3.59 (m, 2H), 3.07 (ddd, $J = 14.0, 7.6, 2.0$ Hz, 1H), 2.95 (ddd, $J = 14.0, 5.9$ Hz, 1H); ^{13}C NMR (101 MHz, CDCl_3) [overlapping signals] δ ppm: 140.74, 140.34, 140.06, 138.93, 129.85, 129.30, 129.06, 128.94, 128.65, 128.61, 128.55, 127.57, 127.55, 127.43, 93.00, 83.10 (d, $J = 173.2$ Hz), 70.69, 61.80 (d, $J = 18.2$ Hz), 56.49, 51.69 (d, $J = 6.1$ Hz); ^{19}F NMR (376 MHz, CDCl_3) δ ppm: -226.12 (td, $J = 47.7, 20.1$ Hz, 1F). **HRMS** (ESI⁺) m/z $\text{C}_{26}\text{H}_{26}\text{BrFN}_3^+$ [M+H]⁺: calculated 478.1289, found 478.1286. **IR** (thin layer film) ν (cm^{-1}) = 3063, 3028, 2963, 2191, 2174, 2020, 1980, 1600, 1493, 1452, 1381, 1381, 1310, 1261, 1173, 1078, 1026, 953, 799, 765, 745, 701. $[\alpha]_{\text{D}}^{25\text{ }^\circ\text{C}} = -7.7$ ° (c = 0.4, CHCl_3 , e.r. = 87:13). **HPLC separation** DAICEL CHIRALPAK[®] IA-3, Heptane:ⁱPrOH = 99:1, 1 mL/min; $t_1 = 7.96$ min (minor), $t_2 = 9.68$ min (major).

(S)-N-benzhydryl-N-benzyl-3-fluoro-2-(3-methyl-1H-indol-1-yl)propan-1-amine (2ra)



(S)-2ra was prepared from 1ra (1 equiv., 0.1 mmol 59.2 mg), according to the general procedure using 5 mol% of catalyst (S)-D (0.005 mmol, 4.2 mg) and stirring for 48 h.

Purification: FCC eluent = Pentane:Et₂O (100:0 to 90:10, gradient). White solid, 46.0 mg, 99% yield, e.r. = 94:6. ¹H NMR (400 MHz, CDCl₃) δ ppm: 7.57 – 7.51 (m, 1H), 7.37 –

7.20 (m, 15H), 7.13 – 7.05 (m, 2H), 6.86 – 6.80 (m, 1H), 6.67 (s br, 1H), 4.92 (s, 1H),

4.64 (ddd, *J* = 47.1, 9.6, 5.3 Hz, 1H), 4.58 (ddd, *J* = 47.4, 9.6, 3.6 Hz, 1H), 4.44 – 4.30 (m, 1H), 3.75 (d, *J* =

13.8 Hz, 1H), 3.66 (d, *J* = 13.8 Hz, 1H), 3.18 (dd, *J* = 13.9, 7.5 Hz, 1H), 3.18 (ddd, *J* = 13.9, 6.8, 1.8 Hz, 1H),

2.27 (d, *J* = 0.9 Hz, 3H); ¹³C NMR (101 MHz, CDCl₃) δ ppm: 141.09, 140.62, 139.27, 136.54, 129.33, 129.11,

129.02, 128.69, 128.62, 128.59, 128.49, 127.49, 127.44, 127.30, 123.02 (d, *J* = 2.5 Hz), 121.49, 119.08,

118.94, 111.31, 109.18, 83.90 (d, *J* = 173.8 Hz), 70.85, 56.73, 54.38 (d, *J* = 18.8 Hz), 51.98 (d, *J* = 5.3 Hz),

9.80; ¹⁹F NMR (376 MHz, CDCl₃) δ ppm: -225.77 (td, *J* = 46.7, 23.8 Hz, 1F). **HRMS** (ESI⁺) *m/z* C₃₂H₃₂FN₂⁺

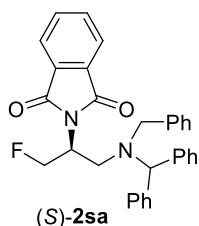
[M+H]⁺: calculated 463.2544, found 463.2547. **IR** (thin layer film) ν (cm⁻¹) = 3061, 3027, 2919, 2844, 1599,

1493, 1460, 1385, 1357, 1262, 1199, 1128, 1073, 0127, 797, 739, 700. **MP** 47 – 49 °C. [α]_D²⁵ °C = + 26.4 ° (c

= 0.5, CHCl₃, e.r. = 94:6). **HPLC separation** DAICEL CHIRALPAK[®] IB-3, Heptane:ⁱPrOH = 99:1, 1

mL/min; t₁ = 6.63 min (minor), t₂ = 8.47 min (major).

(S)-2-(1-(benzhydryl(benzyl)amino)-3-fluoropropan-2-yl)isoindoline-1,3-dione (2sa)



(S)-2sa was prepared from 1sa (1 equiv., 1 mmol, 608.6 mg), according to the general procedure using 5 mol% of catalyst (S)-D (0.05 mmol, 41.8 mg) and stirring for 36 h.

Purification: FCC eluent = Pentane:Et₂O (90:0 to 70:30, gradient). White solid, 440 mg, 92% yield, e.r. = 82.5:17.5. A single recrystallization in hexane/THF (reflux to r.t.)

afforded (S)-2sa as a single enantiomer, e.r. > 99.5:0.5 (320 mg, 0.67 mmol, 73%

recrystallization yield).* ¹H NMR (400 MHz, CDCl₃) δ ppm: 7.82 – 6.67 (m, 4H), 7.39 – 7.07 (m, 15H), 4.94

(s, 1H), 4.80 – 4.55 (m, 2H), 4.55 – 4.37 (m, 1H), 3.79 (d, *J* = 13.5 Hz, 1H), 3.55 (d, *J* = 13.5 Hz, 1H), 3.22 –

3.13 (m, 1H), 2.85 (dd, *J* = 14.0, 3.9 Hz, 1H); ¹³C NMR (101 MHz, CDCl₃) δ ppm: 168.13, 140.93, 140.06,

138.86, 134.00, 132.13, 129.39, 129.21, 129.08, 128.55, 128.40, 128.28, 127.46, 127.21, 127.16, 123.38, 81.01

(d, *J* = 174.1 Hz), 69.51, 55.74, 50.02 (d, *J* = 19.1 Hz), 48.27 (d, *J* = 5.9 Hz); ¹⁹F NMR (376 MHz, CDCl₃) δ

ppm: -223.10 (td, *J* = 46.5, 13.6 Hz, 1F). **HRMS** (ESI⁺) *m/z* C₃₁H₂₈FN₂O₂⁺ [M+H]⁺: calculated 479.2129,

found 479.2128. **IR** (thin layer film) ν (cm⁻¹) = 3028, 2843, 1775, 1711, 1494, 1467, 1453, 1387, 1193, 1056,

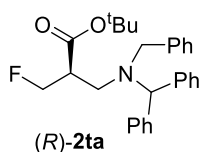
1016, 875, 746, 721, 700. **MP** 48 – 50 °C. [α]_D²⁵ °C = + 19.6 ° (c = 0.5, CHCl₃, e.r. > 99.5:0.5). **HPLC**

separation DAICEL CHIRALPAK[®] IC-3, Heptane:ⁱPrOH = 95:5, 1 mL/min; t₁ = 4.67 min (major), t₂ = 5.56

min (minor).

* N.B. The recrystallization affords the enantiopure product in the mother liquor.

tert-butyl (R)-3-(benzhydryl(benzyl)amino)-2-(fluoromethyl)propanoate (2ta)



(R)-2ta was prepared from **1ta** (1 equiv., 0.5 mmol, 281.8 mg), according to the general procedure using 10 mol% of catalyst (S)-**D** (0.05 mmol, 41.8 mg) and stirring for 24 h.

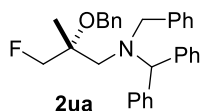
Purification: FCC eluent = Pentane:Et₂O (100:0 to 80:20, gradient). Colorless oil, 212 mg, 98% yield, e.r. = 92:8. After treatment with 2M HCl in Et₂O and removal of the volatiles

in vacuo, **2ta**·HCl was recrystallized in hexane/THF/EtOH (reflux to r.t.). After basification (NaHCO₃ sat.), (R)-**2ta** was obtained as a single enantiomer, e.r. = 99.5:0.5 (180 mg, 0.42 mmol, 85% recrystallization yield).*

¹H NMR (400 MHz, CDCl₃) δ ppm: 7.42 – 7.24 (m, 15H), 5.00 (s, 1H), 4.52 (d, *J* = 6.1 Hz, 1H), 4.40 (d, *J* = 6.1 Hz, 1H), 3.71 (d, *J* = 14.0 Hz, 1H), 3.60 (d, *J* = 14.0 Hz, 1H), 3.00 – 2.84 (m, 1H), 2.81 (ddd, *J* = 13.2, 6.4, 2.5 Hz, 1H), 2.61 (dd, *J* = 13.3, 7.7 Hz, 1H), 1.45 (s, 9H); **¹³C NMR** (101 MHz, CDCl₃) δ ppm: 171.72 (d, *J* = 3.6 Hz), 140.72, 140.10, 138.97, 129.42, 129.18, 129.06, 128.47, 128.40, 128.37, 127.36, 127.31, 127.26, 83.11 (d, *J* = 171.0 Hz), 81.31, 69.23, 55.09, 48.35 (d, *J* = 8.4 Hz), 46.39 (d, *J* = 19.1 Hz), 28.18; **¹⁹F NMR** (376 MHz, CDCl₃) δ ppm: -222.42 (tdd, *J* = 46.8, 18.1, 2.5 Hz). **HRMS** (ESI⁺) *m/z* C₂₈H₃₃FNO₂⁺ [M+H]⁺: calculated 434.2490, found 434.2487. **IR** (thin layer film) ν (cm⁻¹) = 3027, 2977, 1728, 1600, 1493, 1452, 1392, 1367, 1250, 1209, 1154, 1077, 1028, 1009, 916, 846, 763, 743, 699, 621, 602. [α]_D^{25 °C} = -2.9 ° (c = 1.1, CHCl₃, e.r. = 99.5:0.5). **HPLC separation** DAICEL CHIRALPAK[®] IB-3, Heptane:PrOH = 99.6:0.4, 1 mL/min; t₁ = 4.63 min (minor), t₂ = 4.97 min (major).

* N.B. The recrystallization affords the enantiopure product in the mother liquor.

N-benzhydryl-N-benzyl-2-(benzyloxy)-3-fluoro-2-methylpropan-1-amine (2ua)



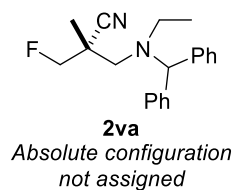
Absolute configuration
not assigned

(R)-**2ua** was prepared from **1ua** (1 equiv., 0.1 mmol, 58.3 mg), according to the general procedure using 20 mol% of catalyst (S)-**D** (0.02 mmol, 16.8 mg) and stirring for 72 h.

Purification: FCC eluent = Heptane:Et₂O (100:0 to 95:5, gradient). Colorless oil, 40.0 mg, 88% yield, e.r. = 87:13. **¹H NMR** (400 MHz, CDCl₃) δ ppm: 7.39 – 7.24 (m,

20H), 5.40 (s, 1H), 4.51 (s, 2H), 4.48 (dd, *J* = 48.4, 10.0 Hz, 1H), 4.25 (dd, *J* = 47.9, 10.0 Hz, 1H), 3.81 (d, *J* = 13.6 Hz, 1H), 3.65 (d, *J* = 13.6 Hz, 1H), 2.86 (dd, *J* = 14.3, 2.5 Hz, 1H), 2.75 (d, *J* = 14.2 Hz, 1H), 1.17 (d, *J* = 2.3 Hz, 3H); **¹³C NMR** (101 MHz, CDCl₃) [overlapping signals] δ ppm: 140.72, 140.03, 140.00, 139.38, 130.13, 129.82, 129.36, 128.43, 128.38, 128.15, 128.14, 127.41, 127.34, 127.12, 127.06, 87.69 (d, *J* = 175.1 Hz), 78.80 (d, *J* = 16.1 Hz), 68.39, 65.26 (d, *J* = 2.4 Hz), 56.06, 54.96 (d, *J* = 5.2 Hz), 18.19 (d, *J* = 5.3 Hz); **¹⁹F NMR** (376 MHz, CDCl₃) δ ppm: -226.99 (t, *J* = 48.1 Hz, 1F). **HRMS** (ESI⁺) *m/z* C₃₁H₃₃FNO⁺ [M+H]⁺: calculated 454.2541, found 454.2540. **IR** (thin layer film) ν (cm⁻¹) = 3028, 1494, 1453, 1371, 1093, 1067, 1028, 763, 740, 699, 535. [α]_D^{25 °C} = +3.3 ° (c = 0.6, CHCl₃, e.r. = 87:13). **SFC separation** DAICEL CHIRALCEL[®] OJ-3, CO₂:MeOH (85:15 to 50:50, gradient) + 0.2% isopropylamine, 2.5 mL/min; t₁ = 4.51 min (minor), t₂ = 4.88 min (major).

3-(benzhydryl(ethyl)amino)-2-(fluoromethyl)-2-methylpropanenitrile (2va)

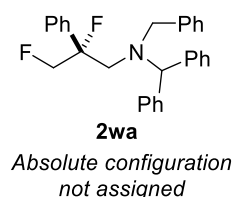


2va was prepared from **1va** (1 equiv., 0.1 mmol, 44.0 mg), according to the general procedure using 10 mol% of catalyst (*S*)-**D** (0.01 mmol, 8.4 mg) and stirring for 24 h.

Purification: FCC eluent = Heptane:Et₂O (100:0 to 95:5, gradient). Colorless oil, 28.0 mg, 90% yield, e.r. = 86:14. ¹H NMR (400 MHz, CDCl₃) δ ppm: 7.36 – 7.22 (m, 10H), 5.15 (s, 1H), 4.56 – 4.37 (m, 1H), 4.44 – 4.26 (m, 1H), 2.86 (s, 2H), 2.72 (q, *J* = 7.1 Hz, 2H), 1.34 (d, *J* = 1.6 Hz, 3H), 1.05 (t, *J* = 7.0 Hz, 3H); ¹³C NMR (101 MHz, CDCl₃) [overlapping signals] δ ppm: 140.87, 140.67, 129.31, 129.24, 128.45, 127.41, 127.38, 122.26 (d, *J* = 6.5 Hz), 85.03 (d, *J* = 181.3 Hz), 70.48, 53.98 (d, *J* = 3.6 Hz), 45.35, 39.09 (d, *J* = 19.6 Hz), 19.94 (d, *J* = 4.0 Hz), 12.34; ¹⁹F NMR (376 MHz, CDCl₃) δ ppm: -223.20 (t, *J* = 47.1 Hz).

HRMS (ESI⁺) *m/z* C₂₅H₂₃FN₂Na⁺ [M+Na]⁺: calculated 333.1737, found 333.1738. *IR* (thin layer film) ν (cm⁻¹) = 3328, 2973, 2883, 1485, 1452, 1420, 1380, 1088, 1046, 880, 605. $[\alpha]_D^{25}$ °C = -242.6 ° (c = 0.3, CHCl₃, e.r. = 99.5:0.5). *HPLC separation* DAICEL CHIRALCEL[®] OJ-3, Heptane:EtOH = 95:5, 1 mL/min; t₁ = 6.88 min (major), t₂ = 7.79 min (minor).

N-benzhydryl-*N*-benzyl-2,3-difluoro-2-phenylpropan-1-amine (2wa)

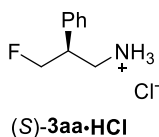


2wa was prepared from **1wa** (1 equiv., 0.75 mmol, 418.2 mg), according to the general procedure using 5 mol% of catalyst (*S*)-**D** (0.05 mmol, 31.4 mg) and stirring for 24 h.

Purification: FCC eluent = Pentane:Et₂O (100:0 to 90:10, gradient). Dense oil, 280 mg, 87% yield, e.r. = 84:16. For the recrystallization, the compound (0.43 mmol, 184 mg)

was treated with 2M HCl in Et₂O and volatiles were removed *in vacuo*. **2wa**·HCl was recrystallized in EtOH/H₂O (reflux to r.t.). After basification (NaHCO₃ sat.), **2wa** was obtained with an e.r. = 95:5 (92 mg, 0.21 mmol, 50% recrystallization yield). ¹H NMR (400 MHz, CDCl₃) δ ppm: 7.32 – 6.94 (m, 20H), 5.10 (s, 1H), 4.70 (ddd, *J* = 48.9, 17.6, 10.6 Hz, 1H), 4.29 (ddd, *J* = 46.9, 26.8, 10.6 Hz, 1H), 3.67 (d, *J* = 13.5 Hz, 1H), 3.47 (d, *J* = 13.5 Hz, 1H), 3.08 – 2.91 (m, 2H); ¹³C NMR (101 MHz, CDCl₃) [overlapping signals] δ ppm: 140.03, 139.48, 138.95, 138.46 (dd, *J* = 25.6, 3.8 Hz), 129.86, 129.77, 129.62, 128.44, 128.39 (d, *J* = 1.3 Hz), 128.36, 128.24, 128.04, 127.35, 127.27, 125.11 (d, *J* = 9.9 Hz); 100.09 (dd, *J* = 178.2, 15.9 Hz), 85.98 (dd, *J* = 178.3, 27.8 Hz), 68.42 (d, *J* = 3.6 Hz); 55.45 (d, *J* = 3.3 Hz); 54.91 (dd, *J* = 21.0, 4.0 Hz); ¹⁹F NMR (376 MHz, CDCl₃) δ ppm: -164.20 (qt, *J* = 24.8, 15.6 Hz, 1F), -230.90 (td, *J* = 47.9, 14.0 Hz, 1F). *HRMS* (ESI⁺) *m/z* C₂₉H₂₈F₂N⁺ [M+H]⁺: calculated 428.2184, found 428.2185. *IR* (thin layer film) ν (cm⁻¹) = 3028, 1794, 1453, 1371, 1093, 1067, 1028, $[\alpha]_D^{25}$ °C = +30.9 ° (c = 0.7, CHCl₃, e.r. = 95:5). *HPLC separation* DAICEL CHIRALPAK[®] AS-3, Heptane:PrOH = 98:2 + 0.2% BuNH₂, 1 mL/min; t₁ = 2.95 min (minor), t₂ = 3.35 min (major).

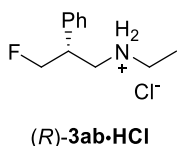
(*S*)-3-fluoro-2-phenylpropan-1-aminium chloride (3aa·HCl)



In a Schlenk flask, (*S*)-**2aa** (1 equiv., 1.70 mmol, 696 mg, e.r = 96:4) was dissolved in a 4:1 mixture of MeOH:CH₂Cl₂ (0.08 M, 21 mL) and Pd(OH)₂ 20 wt% loading (0.1 equiv., 0.17 mmol, 134 mg) was added. The flask was then purged with H₂ three times and the reaction

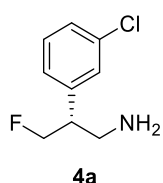
was stirred overnight at r.t. under an atmosphere of H₂ (balloon). The mixture was filtered on celite, the solvents were evaporated *in vacuo* and the free amine was stirred in a 1M HCl solution in methanol for 5 min. After evaporation of the volatiles, the corresponding chloride salt was obtained as a pale yellow solid in 79% yield (1.34 mmol, 254 mg) and e.r. = 96:4. A successive recrystallization on 1.05 mmol scale (200 mg) in hexane/EtOH (reflux to -20 °C) afforded (*S*)-**3aa** as a white solid with an e.r.= 99:1 (140 mg, 0.73 mmol, 70% recrystallization yield). ¹H NMR (400 MHz, CD₃OD) δ ppm: 7.34 – 7.21 (m, 5H), 4.76 (s br, 3H), 4.54 (dd, *J* = 47.1, 5.9 Hz, 2H), 3.40 – 3.18 (m, 3H); ¹³C NMR (101 MHz, CD₃OD) δ ppm: 137.27 (d, *J* = 6.5 Hz), 130.35, 129.42, 129.36, 86.02 (d, *J* = 172.8 Hz), 45.91 (d, *J* = 19.0 Hz), 42.33 (d, *J* = 4.6 Hz); ¹⁹F NMR (376 MHz, CD₃OD) δ ppm: -221.28 (td, *J* = 47.1, 17.9 Hz, 1F). HRMS (ESI⁺) *m/z*: calculated for C₉H₁₃FN⁺ [M-Cl]⁺ 154.1027, found 154.1029. IR (thin layer film) ν (cm⁻¹) = 3032, 2917, 1626, 1518, 1496, 1455, 1397, 1157, 1082, 934, 761, 702. MP 152 – 151 °C. [α]_D²⁵ °C = - 41.0 ° (c = 0.6, MeOH, e.r. = 99:1). HPLC separation (free amine) DAICEL CHIRALPAK® IF-3, Heptane:PrOH = 90:10 + 0.2% diethylamine, 1 mL/min; t₁ = 7.58 min (major), t₂ = 12.33 min (minor).

(*R*)-*N*-ethyl-3-fluoro-2-phenylpropan-1-aminium chloride (**3ab**·HCl)



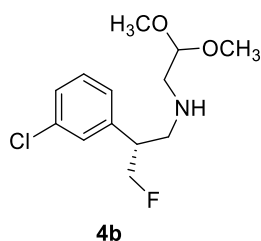
In a Schlenk flask, (*R*)-**2ab** (1 equiv., 1.73 mmol, 601 mg, e.r. = 96:4) was dissolved in a 2:1 mixture of MeOH:CH₂Cl₂ (0.15 M, 12 mL) and Pd/C 10 wt% loading (0.1 equiv., 0.173 mmol, 184 mg) was added. The flask was then purged with H₂ three times and the reaction was stirred overnight at r.t. under an atmosphere of H₂ (balloon). After filtration on celite and solvent evaporation *in vacuo*, the crude mixture was purified by FCC (eluent = Pentane:Et₂O:MeOH, 93:5:2 to 90:5:5 gradient). The purified amine was then stirred for 5 min in 1M HCl solution in methanol to afford the corresponding chloride salt as a colorless solid in 74% yield (1.28 mmol, 279 mg) and e.r. = 96:4. A successive recrystallization on 0.23 mmol scale (50 mg) in CH₂Cl₂/Et₂O (reflux to r.t.) afforded (*R*)-**3ab** with an e.r.= 98.5:1.5 (43.5 mg, 0.20 mmol, 87% recrystallization yield). ¹H NMR (500 MHz, CDCl₃) δ ppm: 9.61 (s br, 2H), 7.40 – 7.28 (m, 5H), 4.91 – 4.65 (m, 2H), 3.86 – 3.85 (m, 1H), 3.53 (dd, *J* = 13.0, 8.0 Hz, 1H), 3.53 (dd, *J* = 13.0, 6.7 Hz, 1H), 3.00 – 2.91 (m, 2H), 1.14 (t, *J* = 7.3 Hz, 3H); ¹³C NMR (126 MHz, CDCl₃) δ ppm: 137.07 (d, *J* = 4.5 Hz), 129.39, 128.40, 128.18, 84.71 (d, *J* = 175.0 Hz), 48.58 (d, *J* = 5.1 Hz), 43.79, 43.22 (d, *J* = 18.7 Hz), 11.21; ¹⁹F NMR (470 MHz, CDCl₃) δ ppm: -220.84 (td, *J* = 47.2, 22.0 Hz, 1F). HRMS (ESI⁺) *m/z*: calculated for C₁₁H₁₇FN⁺ [M-Cl]⁺ 182.1340, found 182.1340. IR (thin layer film) ν (cm⁻¹) = 2962, 2774, 2737, 2515, 2433, 2396, 2360, 2342, 1597, 1496, 1457, 1405, 1386, 1133, 1066, 1017, 986, 965, 889, 805, 762, 704, 668. MP 178 – 181 °C. [α]_D²⁵ °C = + 49.2 ° (c = 0.5, MeOH, e.r. = 98.5:1.5). HPLC separation (free amine) DAICEL CHIRALPAK® IF-3, Heptane:PrOH = 97:3 + 0.1% diethylamine, 1 mL/min; t₁ = 3.98 min (minor), t₂ = 4.69 min (minor).

(R)-2-(3-chlorophenyl)-3-fluoropropan-1-amine



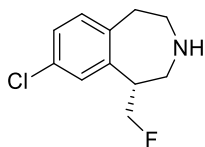
Adapted from a literature procedure.^{11b} In a round bottom flask, a solution of sodium bromate (3 equiv., 4.257 mmol, 642 mg) in water (14.2 mL) was added to a pre-stirred solution of (*R*)-**2da** (1 equiv., 1.419 mmol, 630 mg) in EtOAc (19.0 mL) and stirred at room temperature for 10 min. A solution of sodium dithionite (2.5 equiv., 3.55 mmol, 618 mg) in water (25.8 mL) was then added. The reaction was stirred at r.t. for 2 h. The organic solvent was evaporated *in vacuo* (bath temperature below 30 °C) and the water solution was freeze-dried overnight. The crude mixture was basified using ammonia in MeOH 7M, diluted in CH₂Cl₂, filtered and purified by flash column chromatography (eluent CH₂Cl₂:[CH₂Cl₂/NH₃ in MeOH 9/1] = 100:0 to 70:30, gradient) to afford **4a** as a colorless oil in 72% yield (1.02 mmol, 191.0 mg) and with an e.r. = 96:4 e.r. as colorless oil. ¹H NMR (400 MHz, CDCl₃) δ ppm: 7.32 – 7.21 (m, 3H), 7.13 (dt, *J* = 6.7, 1.9 Hz, 1H), 4.67 (qd, *J* = 9.4, 5.3 Hz, 1H), 4.56 (qd, *J* = 9.2, 5.7 Hz, 1H), 3.19 – 3.09 (m, 1H), 3.08 – 2.91 (m, 2H), 1.25 (s, 2H); ¹³C NMR (101 MHz, CDCl₃) δ ppm: 141.56 (d, *J* = 5.4 Hz), 134.76, 130.16, 128.45, 127.63, 126.55, 85.01 (d, *J* = 172.2 Hz), 49.72 (d, *J* = 18.7 Hz), 43.70 (d, *J* = 5.4 Hz); ¹⁹F NMR (376 MHz, CDCl₃) δ ppm: -222.20 (td, *J* = 47.2, 21.1 Hz, 1F). HRMS (ESI⁺) *m/z* calculated for C₉H₁₂ClFNO⁺ [M+H]⁺: 188.0637, found 188.0638. [α]_D²⁰ = + 12.7 (c = 0.05, DMF, e.r. = 96:4). SFC separation: DAICEL CHIRALPAK[®] ID-3, 40 °C, CO₂:EtOH (85:15 to 50:50, gradient) + 0.2% isopropylamine, t₁ = 1.48 min (minor), t₂ = 1.95 min (major).

(R)-2-(3-chlorophenyl)-N-(2,2-dimethoxyethyl)-3-fluoropropan-1-amine



A round bottom flask was charged with **4a** (0.74 mmol, 139.0 mg) and a solution of dimethoxyacetaldehyde (60 wt% in water, 1.2 equiv., 0.89 mmol, 154.2 mg) in 0.45 mL of MeOH was added. The reaction mixture was stirred at r.t. for 12 h. After that time, the mixture was diluted with additional 4.0 mL of MeOH and NaBH₃CN (2 equiv., 1.48 mmol, 93.1 mg) was added portionwise. The reaction mixture was stirred at r.t. for additional 12 h. The solvent was then evaporated (bath temperature below 30 °C) and the pH adjusted to 8–9. The crude mixture was then purified by flash column chromatography (eluent CH₂Cl₂:[CH₂Cl₂/NH₃ in MeOH 9/1] = 100:0 to 70:30, gradient) to afford **4b** as a yellow oil in 81% yield (0.60 mmol, 165.9 mg) and with an e.r. = 96:4. ¹H NMR (400 MHz, CDCl₃) δ ppm: 7.29 – 7.22 (m, 3H), 7.13 (dt, *J* = 6.5, 2.1 Hz, 1H), 4.66 (qd, *J* = 9.1, 5.7 Hz, 1H), 4.54 (qd, *J* = 9.1, 5.6 Hz, 1H), 4.41 (t, *J* = 5.4 Hz, 1H), 3.34 (s, 6H), 3.21 – 2.88 (m, 3H), 2.79 – 2.66 (m, 2H), 1.47 (s, 1H); ¹³C NMR (101 MHz, CDCl₃) δ ppm: 141.75 (d, *J* = 5.0 Hz), 134.73, 130.14, 128.35, 127.62, 126.47, 103.83, 85.30 (d, *J* = 172.6 Hz), 54.11 (d, *J* = 3.6 Hz), 51.31, 51.11 (d, *J* = 5.4 Hz), 46.68 (d, *J* = 18.7 Hz); ¹⁹F NMR (376 MHz, CDCl₃) δ ppm: -222.02 (td, *J* = 47.4, 20.6 Hz, 1F). HRMS (ESI⁺) *m/z* calculated for C₁₃H₂₀ClFNO₂⁺ [M+H]⁺: 276.1161, found 276.1161. [α]_D²⁰ = + 11.78 (c = 0.14, DMF, e.r. = 96:4). SFC separation DAICEL CHIRALPAK[®] IG, 40 °C, CO₂:MeOH (85:15 to 50:50, gradient) + 0.2% isopropylamine, t₁ = 1.32 min (minor), t₂ = 1.42 min (major).

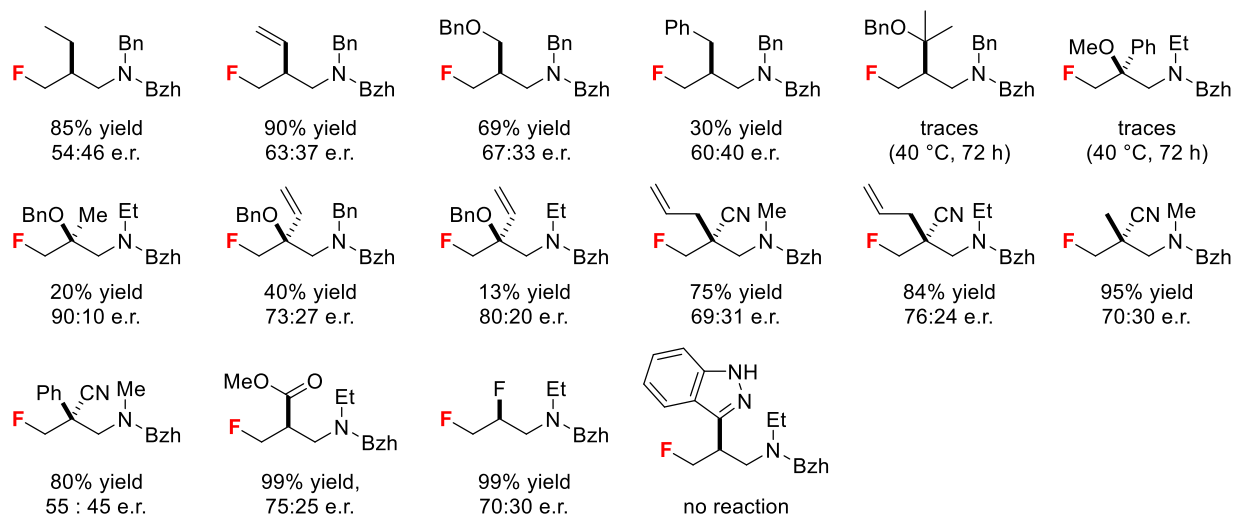
(R)-8-chloro-1-(fluoromethyl)-2,3,4,5-tetrahydro-1H-benzo[d]azepine (Fluorinated Lorcaserin)



Fluorinated Lorcaserin

In a round bottom flask, **4b** (1 equiv., 0.44 mmol, 120.3 mg) was dissolved in 1.85 mL of CH₂Cl₂ and trifluoromethanesulfonic acid (5 equiv., 2.18 mmol, 0.19 mL) was added dropwise at 0 °C. The reaction was stirred at r.t. for 30 min. The reaction mixture was then basified with NaHCO₃ sat. (30 mL) and extracted in CH₂Cl₂ (3 x 15 mL). The organic phase was evaporated, and the crude mixture was dissolved in THF (21.5 mL). Sodium phosphate monobasic (0.5 M water solution, 2.15 mL) was added, followed by portion-wise addition of sodium cyanoborohydride (9.9 equiv., 4.35 mmol, 273.2 mg). The mixture was stirred for 4 hours at r.t. after which the volatiles were evaporated *in vacuo* (bath temperature below 30 °C). After addition of NaHCO₃ sat. (30 mL) the crude product was extracted with CH₂Cl₂ (3 x 15 mL) and the solvent was evaporated *in vacuo*. The crude mixture was then purified by flash column chromatography (eluent CH₂Cl₂:[CH₂Cl₂/NH₃ in MeOH 9/1] = 100:0 to 70:30, gradient) to afford fluorinated Lorcaserin in 86% yield (0.37 mmol, 80.2 mg) and an e.r. = 96:4. **¹H NMR** (400 MHz, CDCl₃) δ ppm: 7.15 – 6.99 (m, 3H), 4.88 (ddd, *J* = 46.9, 9.1, 7.5 Hz, 1H), 4.69 (ddd, *J* = 46.9, 9.1, 6.0 Hz, 1H), 3.27 – 3.10 (m, 2H), 3.10 – 2.90 (m, 3H), 2.90 – 2.78 (m, 2H), 1.81 (s, 1H); **¹³C NMR** (101 MHz, CDCl₃) δ ppm: 142.08 (d, *J* = 6.2 Hz), 140.10, 132.08, 131.84, 129.19, 126.90, 83.39 (d, *J* = 170.8 Hz), 49.53 (d, *J* = 5.2 Hz), 48.99 (d, *J* = 18.9 Hz), 48.67, 39.21; **¹⁹F NMR** (376 MHz, CDCl₃) δ ppm: -220.86 (td, *J* = 46.6, 17.0 Hz). **HRMS** (ESI⁺) *m/z* calculated for C₁₁H₁₄ClFN⁺ [M+H]⁺: 214.0793, found 214.0795. [α]_D²⁰C = +1.4 (c = 0.14, DMF, e.r. = 96:4). **SFC separation** DAICEL CHIRALPAK[®] IG, 40 °C, CO₂:MeOH (85:15 to 50:50, gradient) + 0.2% isopropylamine, t₁ = 2.46 min (major), t₂ = 3.78 min (minor).

Additional Unsuccessful Substrates



Scheme S7: Additional substrates tested under optimized conditions: 10 mol% (*S*)-**D**, 2 equiv. CsF, 1,2-DCE (0.25 M), r.t., 24–72 h. Absolute configuration not assigned.

Determination of the Absolute Configuration (Single Crystal X-ray Diffraction Studies)

Low temperature¹² single crystal X-ray diffraction data were collected using a Rigaku Oxford Diffraction SuperNova diffractometer. Raw frame data were reduced using CrysAlisPro and the structures were solved using 'Superflip'¹³ before refinement with CRYSTALS¹⁴ as per the CIF. Full refinement details are given in the Supporting Information (CIF); Crystallographic data have been deposited with the Cambridge Crystallographic Data Centre (CCDC 1973306-07) and can be obtained via www.ccdc.cam.ac.uk/data_request/cif.

Data for (*S*)-**2ma**·HCl were collected at 150 K, whereas data for (*R*)-**3ab**·HCl were collected at 300 K. A variable temperature experiment using both Mo- and Cu radiation was performed for crystals of (*R*)-**3ab**·HCl, but all crystals split upon cooling to 150 K. Therefore only the 300 K data collected with Cu-radiation were used for refinement.

(S)-2ma·HCl

Empirical formula	C ₂₅ H ₂₉ Cl F N O	
Formula weight	413.96	
Temperature	150 K	
Wavelength	1.54184 Å	
Crystal system and Space group	Monoclinic <i>P</i> 2 ₁	
Unit cell dimensions	a = 9.98040(10) Å	α = 90°.
	b = 8.61600(10) Å	β = 102.1108(12)°.
	c = 12.82200(10) Å	γ = 90°.
Volume	1078.039(19) Å ³	
Z	2	
Density (calculated)	1.275 Mg/m ³	
Absorption coefficient	1.759 mm ⁻¹	
F(000)	439.997	
Crystal size	0.25 x 0.22 x 0.09 mm ³	
Theta range for data collection	3.526 to 76.232°.	
Index ranges	-12 ≤ h ≤ 12, -10 ≤ k ≤ 10, -16 ≤ l ≤ 10	
Reflections collected	10448	
Independent reflections	4454 [R(int) = 0.027]	
Completeness to theta = 74.707°	99.6%	
Absorption correction	Semi-empirical from equivalents	
Max. and min. transmission	0.85 and 0.74	
Refinement method	Full-matrix least-squares on F ²	
Data / restraints / parameters	4454 / 1 / 263	
Goodness-of-fit on F ²	0.9949	
Final R indices [I > 2σ(I)]	R1 = 0.0265, wR2 = 0.0700	
R indices (all data)	R1 = 0.0268, wR2 = 0.0706	
Absolute structure parameter	-0.010(5)	
Largest diff. peak and hole	0.05 and -0.06 e.Å ⁻³	

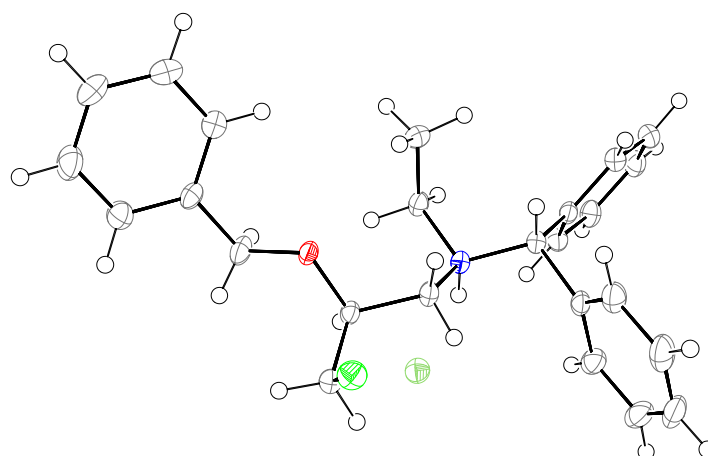


Figure S4. X-ray crystal structure (ellipsoid representation, probability level of 50%) for (S)-2ma·HCl.

(R)-3ab·HCl

Empirical formula	C11 H17 Cl F1 N
Formula weight	217.71
Temperature	300 K
Wavelength	1.54184 Å
Crystal system and Space group	Orthorhombic $P 2_1 2_1 2_1$
Unit cell dimensions	a = 9.95040(10) Å $\alpha = 90^\circ$. b = 10.52650(10) Å $\beta = 90^\circ$. c = 23.7547(4) Å $\gamma = 90^\circ$.
Volume	2488.14(5) Å ³
Z	8
Density (calculated)	1.162 Mg/m ³
Absorption coefficient	2.544 mm ⁻¹
F(000)	928.000
Crystal size	0.40 x 0.25 x 0.10 mm ³
Theta range for data collection	3.721 to 77.272°.
Index ranges	-11 ≤ h ≤ 12, -13 ≤ k ≤ 13, -30 ≤ l ≤ 29
Reflections collected	49083
Independent reflections	5262 [R(int) = 0.060]
Completeness to theta = 77.272°	99.8%
Absorption correction	Semi-empirical from equivalents
Max. and min. transmission	0.78 and 0.41
Refinement method	Full-matrix least-squares on F ²
Data / restraints / parameters	5262 / 48 / 307
Goodness-of-fit on F ²	1.0011
Final R indices [I > 2σ(I)]	R1 = 0.0343, wR2 = 0.0944
R indices (all data)	R1 = 0.0382, wR2 = 0.0997
Absolute structure parameter	0.001(6)
Largest diff. peak and hole	0.12 and -0.16 e.Å ⁻³

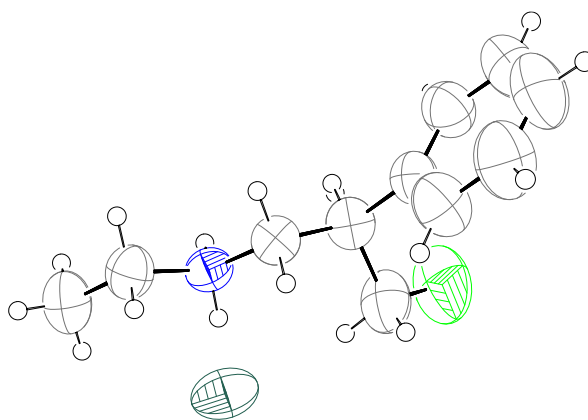


Figure S5. X-ray crystal structure (ellipsoid representation, probability level of 50%) for (R)-3ab·HCl.

Computational Studies

Level of Theory

Density Functional Theory (DFT)

Geometry optimization and frequency calculations were performed in Gaussian 16 Rev. A.03.¹⁵ The Minnesota M06-2X functional¹⁶ was used in combination with the def2-SVP(D) basis set, corresponding to def2-SVPD on electronegative atoms, and def2-SVP otherwise.^{17,18} Cs makes use of an effective core potential (ECP).¹⁹ The ultrafine integration grid was used.²⁰ Solvation in 1,2-dichloroethane (DCE) was modelled using the conductor-like polarizable continuum model (CPCM).²¹⁻²³

Single point energy corrections were implemented using the ORCA 4.2.0 software package^{24,25} with the ω B97X-D3 functional^{26,27}, incorporating the D3 dispersion correction by Grimme²⁸, in combination with the (ma)-def2-TZVPP basis set, consisting of ma-def2-TZVPP²⁹ on heteroatoms and def2-TZVPP otherwise. Integration utilized the Lebedev302 grid for SCF cycles and Lebedev590 grid for final energy evaluation. Solvation in DCE was accounted for using the CPCM solvation model, using relative permittivity of 10.5 and refractive index of 1.4448, with gaussian charge scheme and scaled van der Waals cavity. Thermochemistry was evaluated at 298.15 K, and a standard concentration of 1 M using *GoodVibes* python script.³⁰ The entropic contribution of low vibrational modes was corrected using a free-rotor description below a 100 cm⁻¹ cutoff.³¹

Conformational sampling of azetidinium ions and ion pairs was performed using the Conformer-Rotamer Ensemble Sampling Tool (CREST) version 2.7, based on the GFN-XTB method of Grimme and Pracht.³² Conformational sampling was run in CH₂Cl₂ with default parameters, however a larger energy window of 12.0 kcal/mol was used in combination with more stringent duplicate detection criteria (-rthr 0.0625, -ethr 0.05, -bthr 0.01) to preserve conformations of the 4-membered ring. Ion pairs were sampled using the built in nci mode, which applies an ellipsoid potential. Only the lowest energy conformers of highly flexible structures were optimized, guided by thorough sampling of the less flexible analogs.

Molecular Dynamics (MD)

Molecular dynamics simulations (MD) were performed in GROMACS 5.1.4. software package. The optimized potential for liquid simulations (OPLS-AA 2005) forcefield^{33,34} with restrained electrostatic potential charges^{35,36} was used, with compatible parameters generated in Schrödinger Maestro software (ffld_server utility, version 14),³⁷ and RESP charges generated by fitting the HF/6-31G(d) potential in Ambergtools.³⁸ All simulations were performed in the reaction solvent of 1,2-dichloroethane, with topology from virtualchemistry.org.^{39,40}

The system of interest was centered in a cubic box, with 3-dimensional periodic boundary conditions (PBC), and minimum molecule-boundary distance of 15 Å. System temperature and pressure were maintained with the velocity rescaling method (time constant = 100 fs),⁴¹ and the Parrinello-Rahman barostat (time constant = 2 ps, reference pressure = 1 bar, compressibility = 4.5 x 10⁻⁵ bar⁻¹)^{42,43} respectively. The particle mesh Ewald method and van der Waals interactions were implemented with 1 nm cutoff. The linear constraint solver algorithm (LINCS) was used.⁴⁴

Simulations were first minimized by steepest-descent method of 5000 steps. Equilibration was then performed, firstly by constant volume NVT simulation (200 ps, timestep = 1 fs, heavy atom position restraints, initial velocities derived from a 173 K Maxwell-Boltzmann distribution). Temperature was raised during the simulation to the required production temperature. Secondly, a constant pressure, NPT, equilibration was run (400 ps, timestep = 2 fs, production temperature) and the stability of the system volume verified. The production run results from a continuation of NPT simulation with data derived from 10 ps snapshots.

Transition states were sampled, using the same parameters as the ion pair, by constraining the length of the forming C-F bond and the breaking C-N bond, and restraining the F---C---N angle with a harmonic potential. Simulations were performed at elevated temperature of 423.15 K to enhance sampling. For the cis substrate, bonds were constrained to 2.2 Å and 1.98 Å respectively, and angle restrained to 180° with $k_{\theta} = 1.5$ kJ/mol/deg².

For the trans substrate, bonds were constrained to 2.0 Å and 1.98 Å respectively, with angle restraint of with $k_{\theta} = 3.0$ kJ/mol/deg². Constraint distances were based off distances from trial DFT computed TSs, with C–F bond elongated to enhance sampling and system stability. A stronger angle restraint was employed for the trans substrate due to persistence of unproductive conformations with large F---C---N angle.

Trajectories were clustered using the GROMOS algorithm,⁴⁵ with RMSD matrix accounting for molecular symmetry. Extraneous groups (e.g. CF₃) were excluded from RMSD calculation to ensure chemically relevant clustering.

Kinetics

The kinetics of the catalytic fluorination of azetidinium ions is interpreted within the framework of the energetic span model. For an overview of the model, its derivation and applicability, the reader is referred to the literature.⁴⁶⁻⁵⁰ The primary result is that the turnover frequency of a catalytic cycle can be described by the *energetic span* of the reaction – defined as the difference in energy between the *turnover determining intermediate* (TDI) and the *turnover determining transition state* (TDTS). The TDI and TDTS are the two states of the energetic profile identified such that the energetic span is maximized.

Azetidinium Substrate Reactivity

To investigate the difference in reactivity of the different azetidinium substrates under both HB PTC and homogeneous (TBAF) conditions, the barrier heights to fluorination with seven cis-substrates were computed. The seven substrates are given in Figure S6 and correspond to the ions in Scheme S4. Cis-azetidinium ions were computed for consistency and as this is the major diastereomer in most cases.



Figure S6: Structures of azetidinium ions used for computational reactivity study.

Structure of azetidinium ions

The smallest ion, Azet_{Me,Me}, forms three conformers, The four membered ring puckers to two different conformations, and the phenyl group can adopt two different conformations relative to the azetidinium ring (Figure S7). In ions with different N substitution, the azetidinium ring may take a planar conformation, rather than puckered.

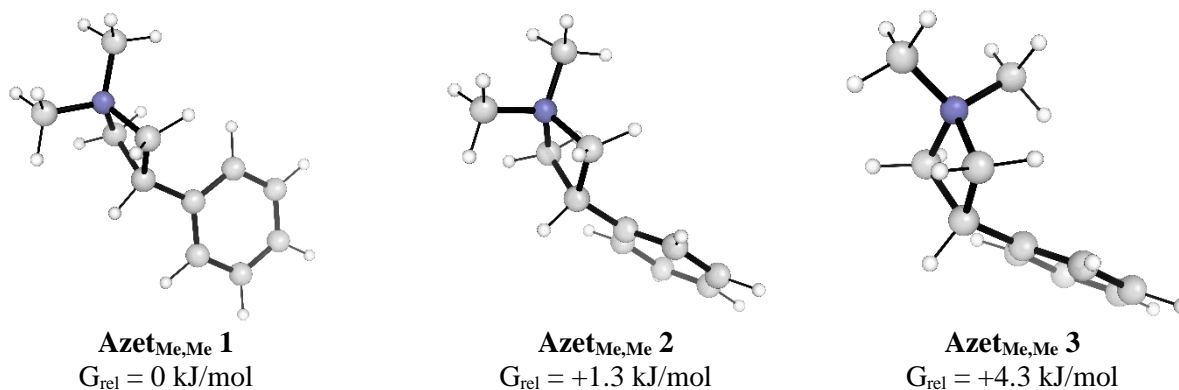
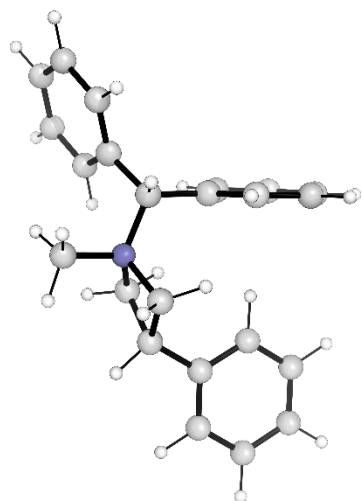
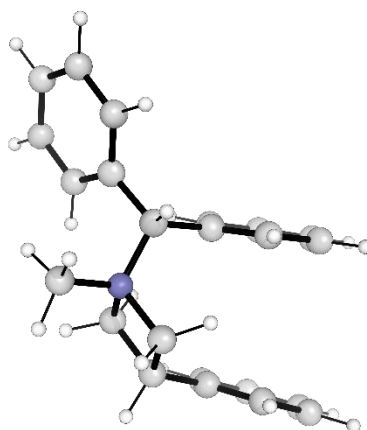


Figure S7: Conformations of Azet_{Me,Me}

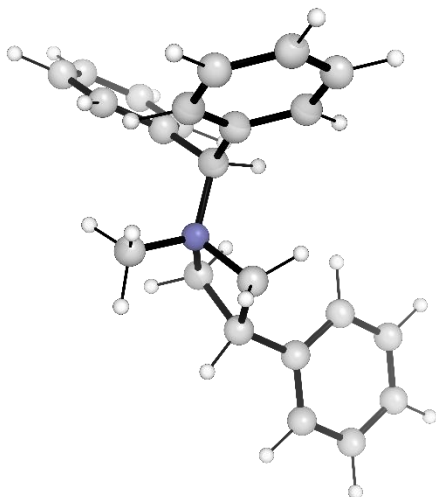
All other ions studied have a cis aromatic group, enabling π -interactions. This is exemplified by the lowest energy conformers of Azet_{Bzh,Me} in Figure S8 (mirror image conformers are not shown). The T-shape CH- π interaction is favored, facilitated in part by the pre-organization of the phenyl ring eclipsing the azetidinium ring.



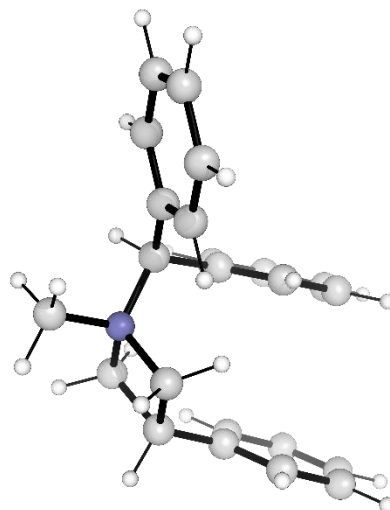
Azet_{Bzh,Me} 1 (T-Shape)
 $G_{\text{rel}} = 0 \text{ kJ/mol}$



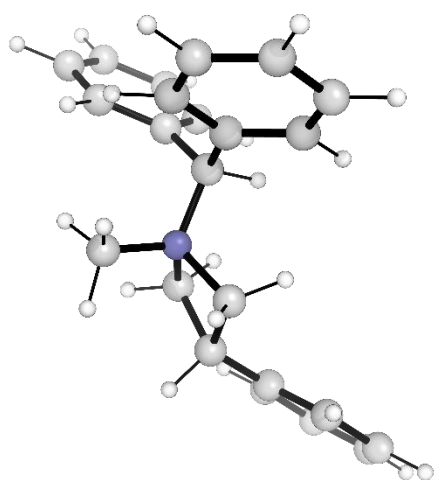
Azet_{Bzh,Me} 4 (Sandwich)
 $G_{\text{rel}} = +2.7 \text{ kJ/mol}$



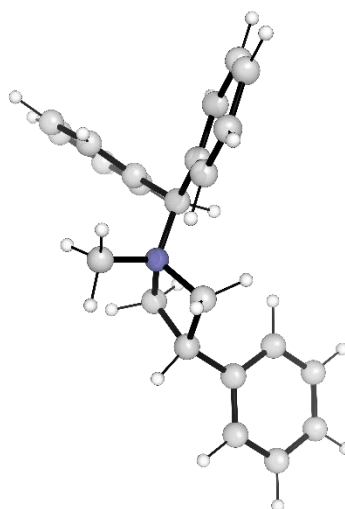
Azet_{Bzh,Me} 5 (None)
 $G_{\text{rel}} = +4.3 \text{ kJ/mol}$



Azet_{Bzh,Me} 7 (Sandwich)
 $G_{\text{rel}} = +5.5 \text{ kJ/mol}$



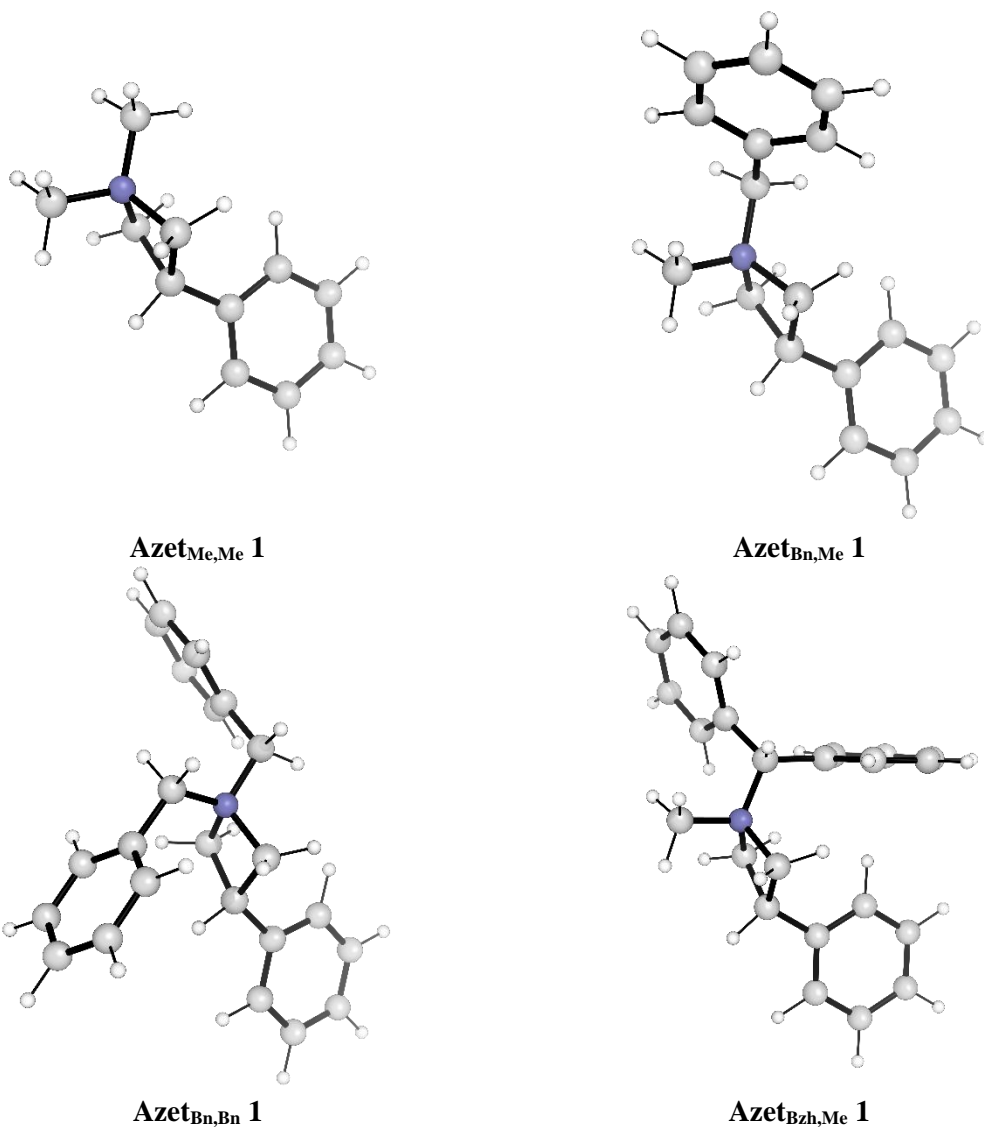
Azet_{Bzh,Me} 8 (None)
 $G_{\text{rel}} = +5.7 \text{ kJ/mol}$



Azet_{Bzh,Me} 9 (None)
 $G_{\text{rel}} = +6.2 \text{ kJ/mol}$

Figure S8: Conformations of Azet_{Bzh,Me} illustrating π -interactions

The lowest energy conformations of all of the ions studied are given in Figure S9. It should be noted that, with the exception of **Azet_{Bzh,Et}**, all ions have multiple low lying conformations, within computational error. With a benzhydryl substituent, formation of the CH- π interaction leads to additional conformational rigidity – the benzhydryl group in turn restricts the conformations available to the other nitrogen substituent, which chooses to eclipse the Bzh hydrogen rather than the bulkier Bzh phenyl ring (see **Azet_{Bzh,Et}**, **Azet_{Bzh,Allyl}**, and **Azet_{Bzh,Bn}** for orientation of ethyl, allyl and benzyl respectively).



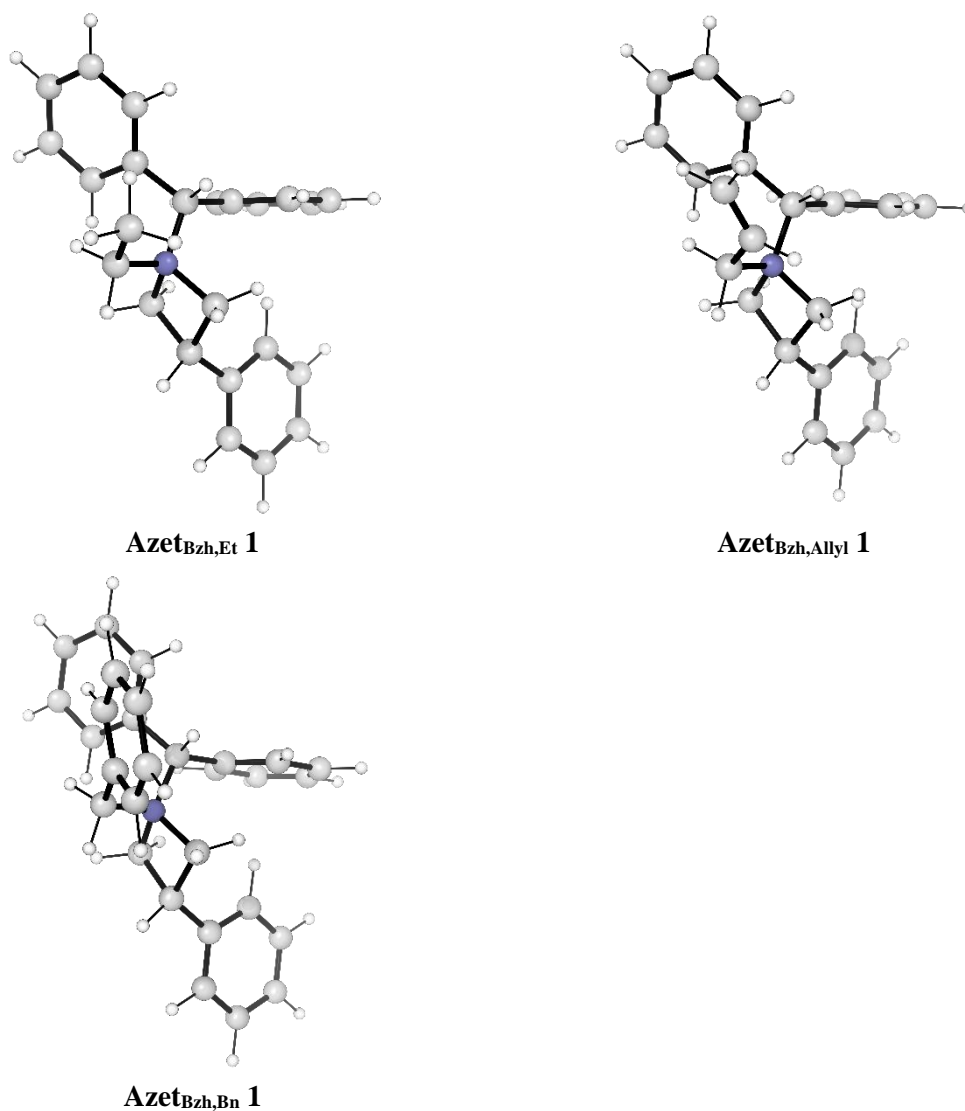
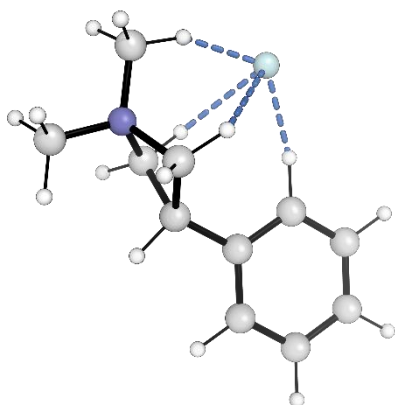


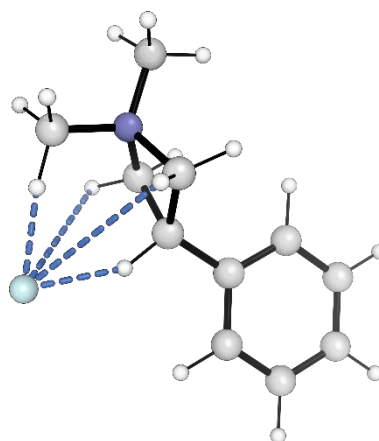
Figure S9: Lowest energy conformations of the studied azetidinium ions

Azetidinium-Fluoride Ion Pairs

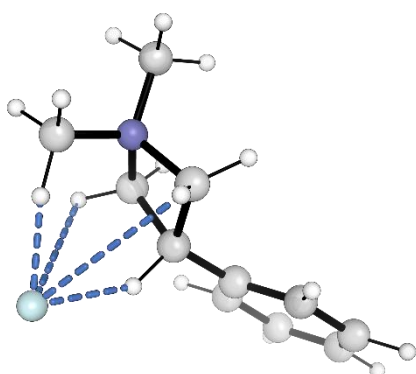
Ion pairs with fluoride favor proximity of the fluoride to the tetracoordinate nitrogen. Sampling with **Azet_{Me,Me}** shows the ion pair favors geometries with the fluoride either to the side, or against the face of, the four membered ring (Figure S10), with the azetidinium ion in its intrinsically favored conformations. Many geometries are located within computational error of the minimum energy geometry (illustrated). Selected higher energy geometries are also shown.



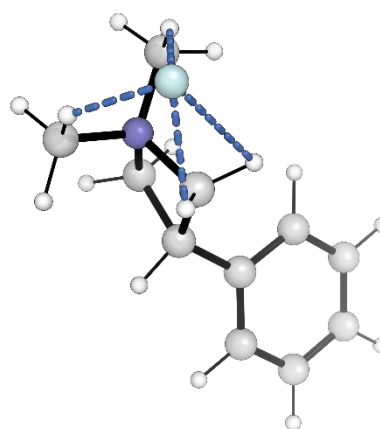
Azet_{Me,Me}-F 1
G_{rel} = 0.0 kJ/mol



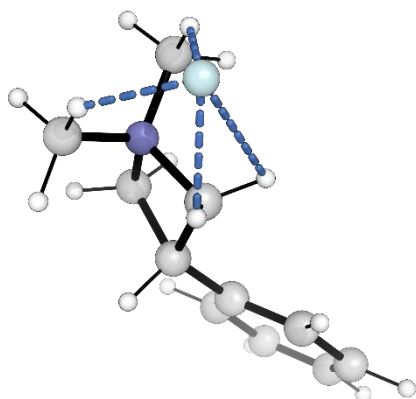
Azet_{Me,Me}-F 2
G_{rel} = +1.5 kJ/mol



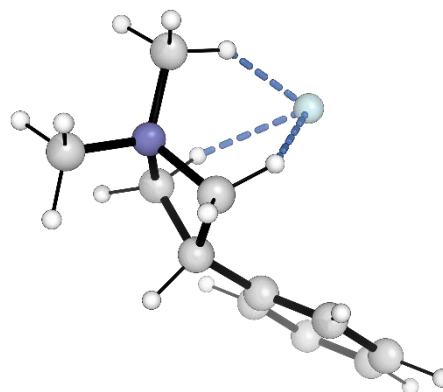
Azet_{Me,Me}-F 3
G_{rel} = +3.4 kJ/mol



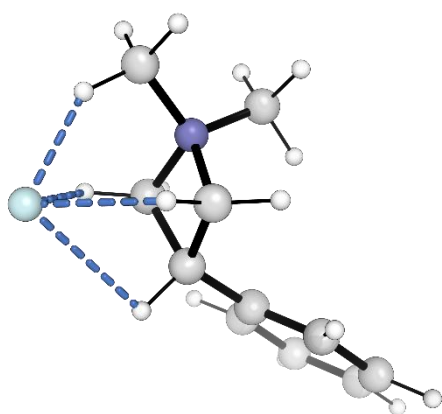
Azet_{Me,Me}-F 4
G_{rel} = +4.3 kJ/mol



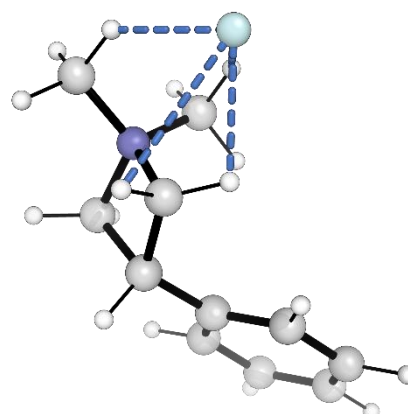
Azet_{Me,Me}-F 6
G_{rel} = +5.7 kJ/mol



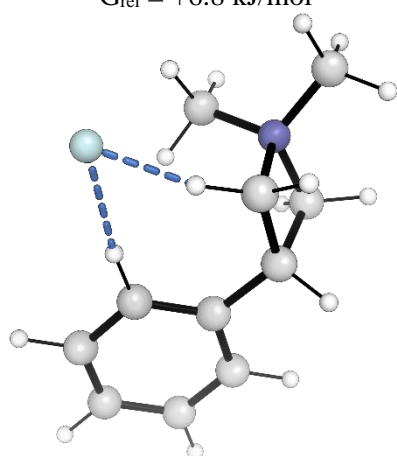
Azet_{Me,Me}-F 7
G_{rel} = +6.8 kJ/mol



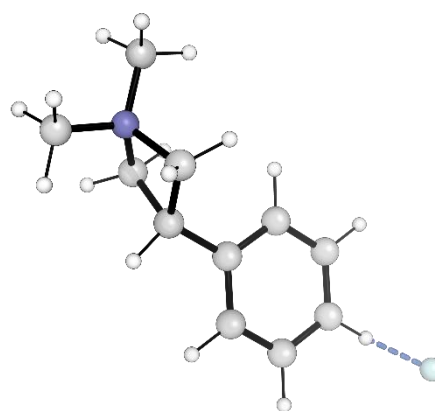
Azet_{Me,Me}-F 8
G_{rel} = +6.8 kJ/mol



Azet_{Me,Me}-F 9
G_{rel} = +8.9 kJ/mol



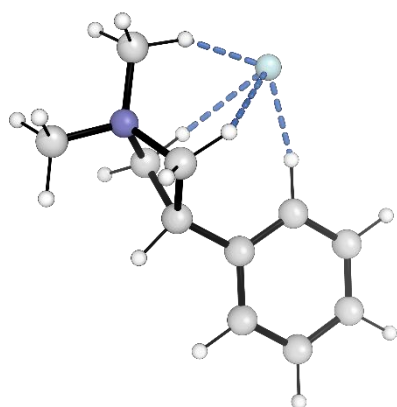
Azet_{Me,Me}-F 11
G_{rel} = +9.7 kJ/mol



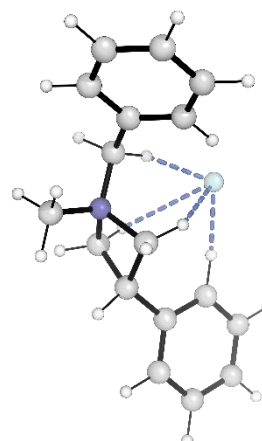
Azet_{Me,Me}-F 13
G_{rel} = +26.4 kJ/mol

Figure S10: Representative geometries of Azet_{Me,Me} ion pair with fluoride

In all fluoride ion pairs, except Azet_{Bzh,Bn}-F, the azetidinium adopts its favored conformer in the ion pair (Figure S11). The azetidinium ion that binds fluoride most weakly is Azet_{Bzh,Et} as the ethyl group prevents close approach of fluoride. For azetidinium ions without the benzhydryl group, fluoride interacts with azetidinium phenyl group in addition to being proximal to nitrogen. In ions with benzhydryl group, the intramolecular CH- π interaction is retained and fluoride positioned elsewhere.



Azet_{Me,Me}-F 1



Azet_{Bn,Me}-F 1

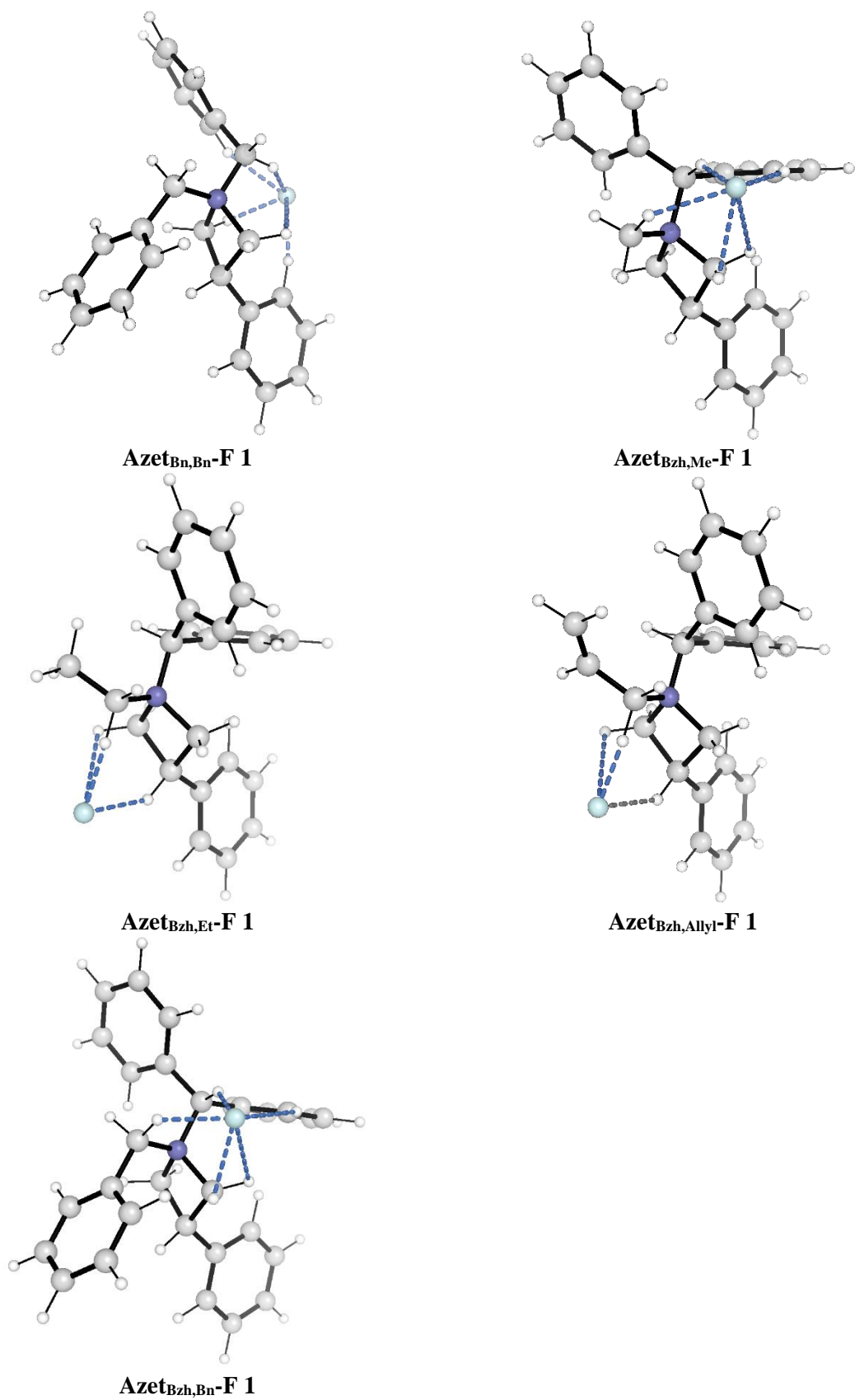
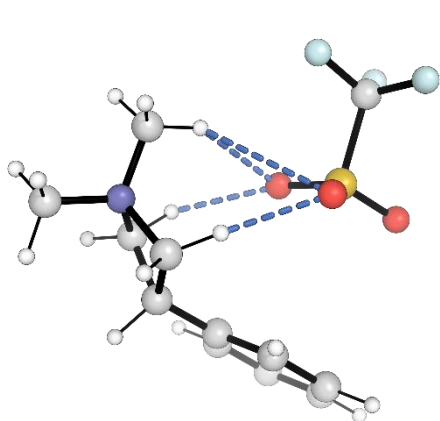


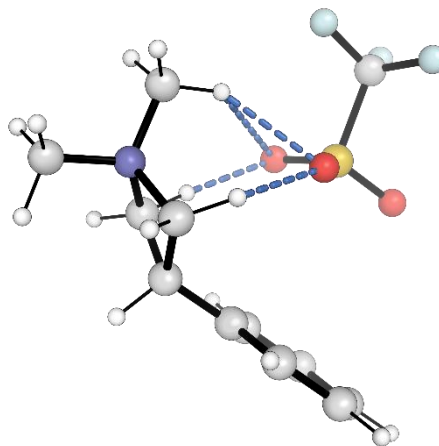
Figure S11: Geometries of lowest energy ion pairs with fluoride

Azetidinium-Triflate Ion Pairs

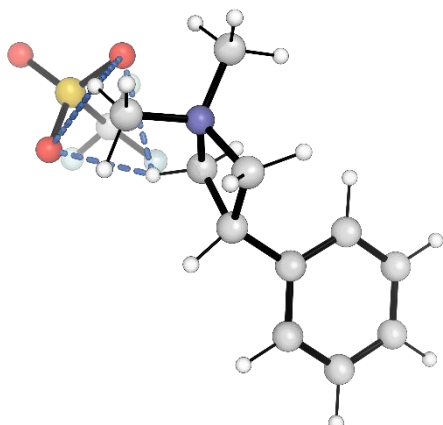
Ion pairs with triflate counterion have larger conformational space due to the rotation of the triflate ion. However, the ion pairs favor the negatively charged oxygen atoms in similar positions to the fluoride ion in the **Azet-F** ion pairs. The lowest energy ion pairs of **Azet_{Me,Me}-OTf** are given in Figure S12 – over 30 geometries were optimized within 5 kJ/mol.



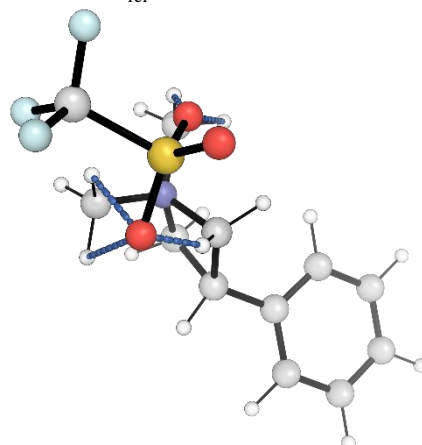
Azet_{Me,Me}-OTf 1
 $G_{\text{rel}} = 0.0$ kJ/mol



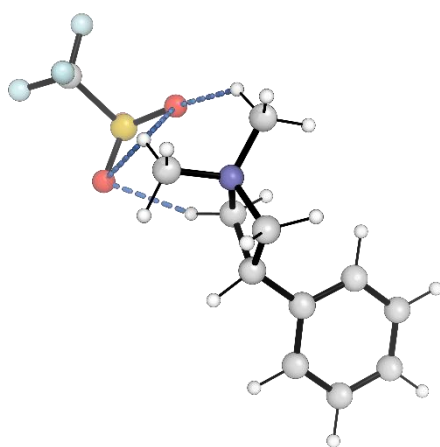
Azet_{Me,Me}-OTf 2
 $G_{\text{rel}} = +0.1$ kJ/mol



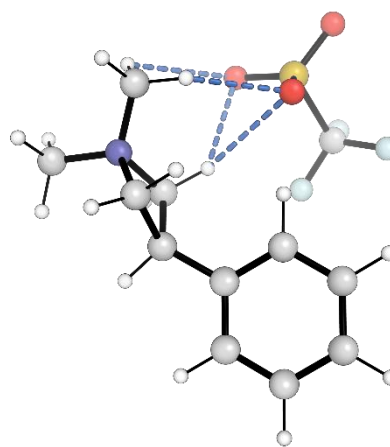
Azet_{Me,Me}-OTf 3
 $G_{\text{rel}} = +0.8$ kJ/mol



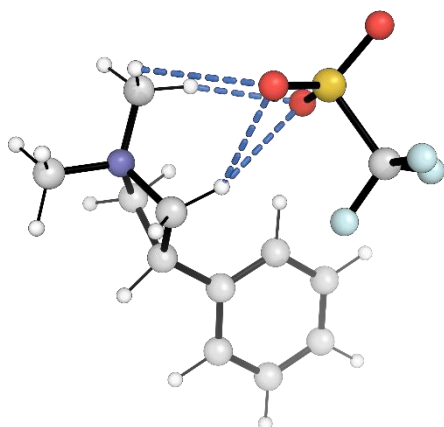
Azet_{Me,Me}-OTf 4
 $G_{\text{rel}} = +1.1$ kJ/mol



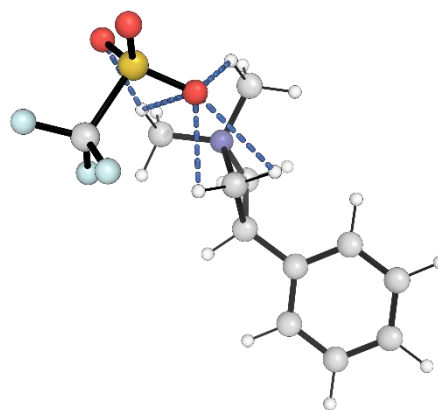
Azet_{Me,Me}-OTf 5
 $G_{\text{rel}} = +1.2$ kJ/mol



Azet_{Me,Me}-OTf 6
 $G_{\text{rel}} = +1.6$ kJ/mol



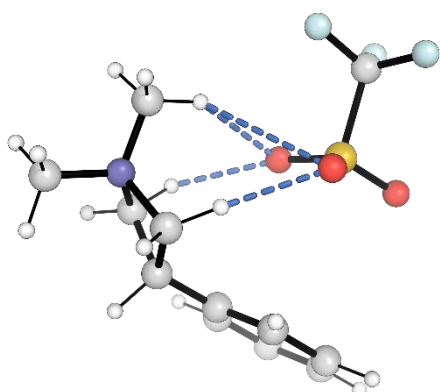
Azet_{Me,Me}-OTf 7
 $G_{\text{rel}} = +1.6 \text{ kJ/mol}$



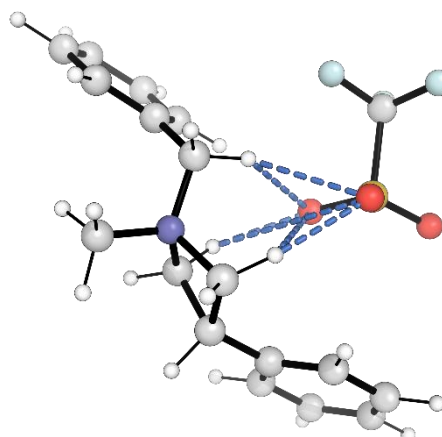
Azet_{Me,Me}-OTf 8
 $G_{\text{rel}} = +1.6 \text{ kJ/mol}$

Figure S12: Geometries of lowest energy **Azet_{Me,Me}** ion pairs with fluoride

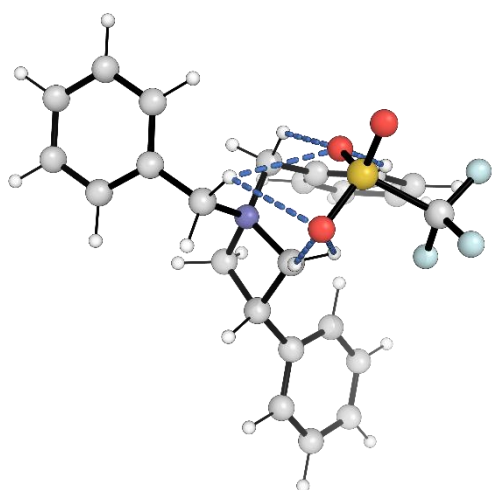
Ion pairs of the azetidinium ions with triflate counterion are given in Figure S13. In all cases, the triflate ion associates closely with the formally positive nitrogen, and surrounding C-H bonds, with many geometries within computational error. Sampling of larger, more flexible, azetidinium ions was guided by the lower energy structures of the less complex ions, as more exhaustive sampling was prohibitive.



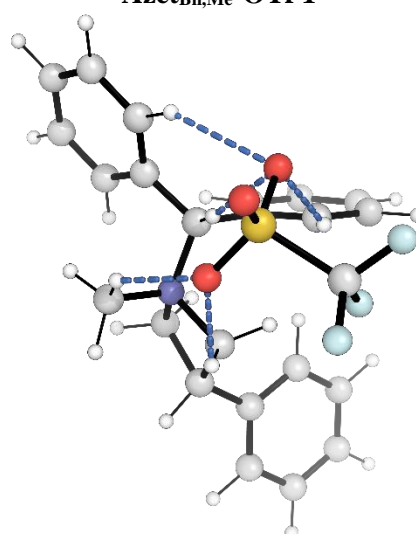
Azet_{Me,Me}-OTf 1



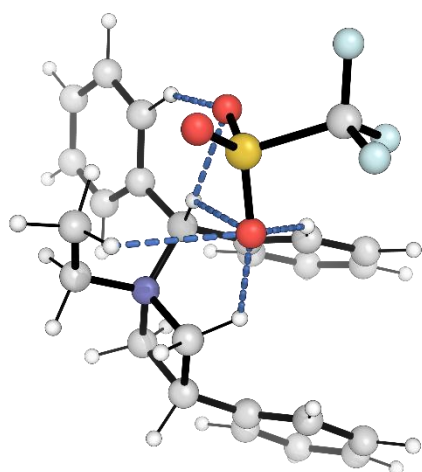
Azet_{Bn,Me}-OTf 1



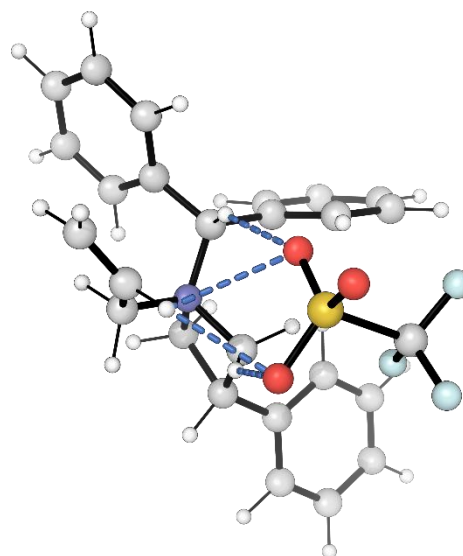
Azet_{Bn,Bn}-OTf 1



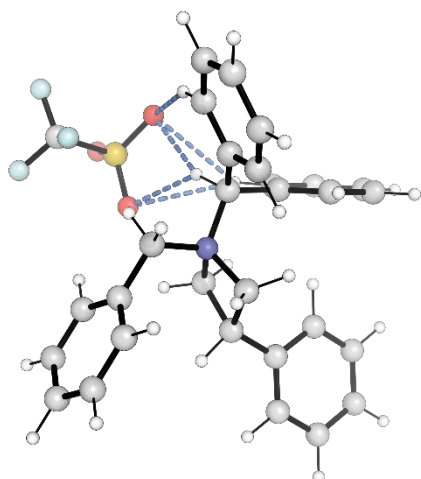
Azet_{Bzh,Me}-OTf 1



Azet_{Bzh,Et}-OTf 1



Azet_{Bzh,Allyl}-OTf 1

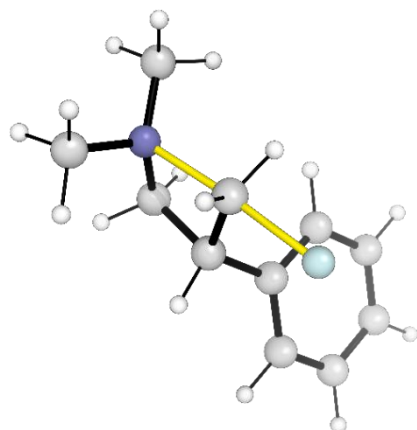


Azet_{Bzh,Bn}-OTf 1

Figure S13: Azet OTf ion pairs

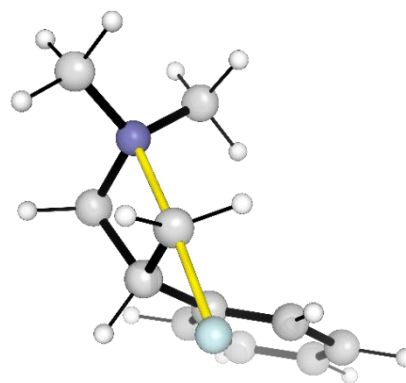
Azetidinium Fluorination Transition State Structures

In the fluoride delivery transition state structures conformational space is greatly reduced over the ion pair and the relative energies of the TS conformations mirror those in the ion. The conformations of the TS with **Azet_{Me,Me}** and the lowest energy conformations of the TS with **Azet_{Bzh,Me}** are given in Figure S14 and Figure S15 respectively.



TS-Azet_{Me,Me}-F 1

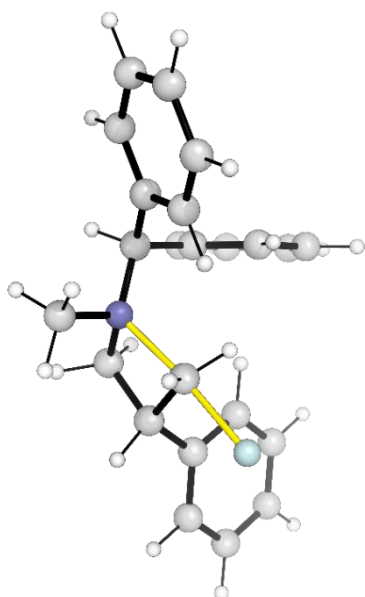
$G_{\text{rel}} = 0.0$ kJ/mol



TS-Azet_{Me,Me}-F 2

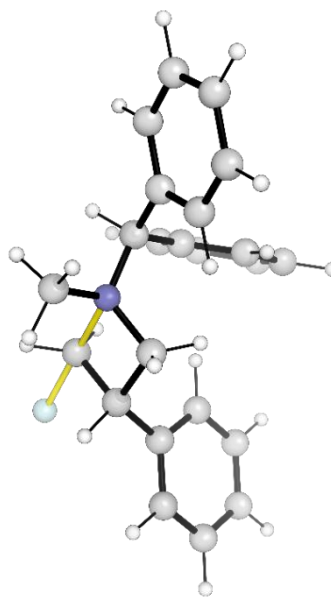
$G_{\text{rel}} = +3.6$ kJ/mol

Figure S14: TS conformations for delivery of fluoride to Azet_{Me,Me}



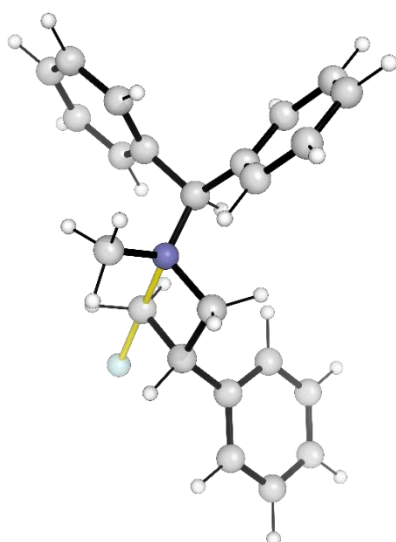
TS-Azet_{Bzh,Me}-F 1

$G_{\text{rel}} = 0.0$ kJ/mol



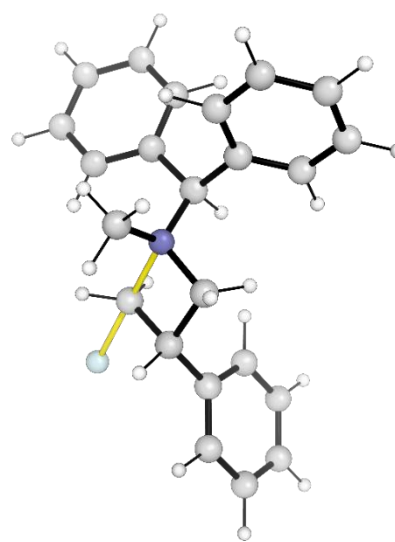
TS-Azet_{Bzh,Me}-F 2

$G_{\text{rel}} = +0.2$ kJ/mol



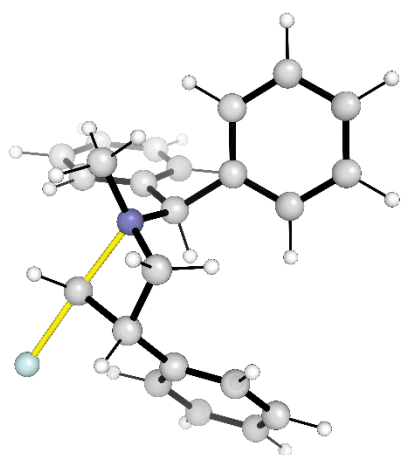
TS-Azet_{Bzh,Me}-F 3

$G_{\text{rel}} = +2.3$ kJ/mol

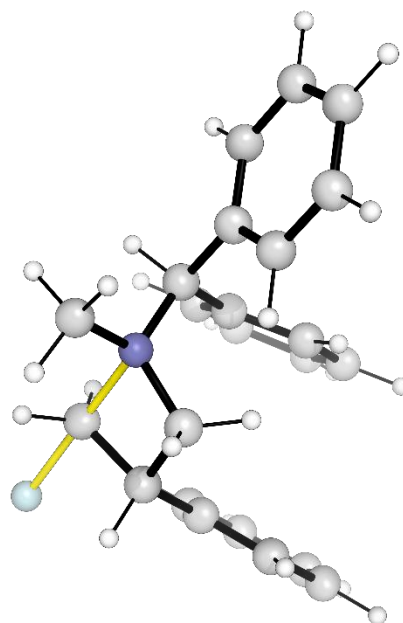


TS-Azet_{Bzh,Me}-F 4

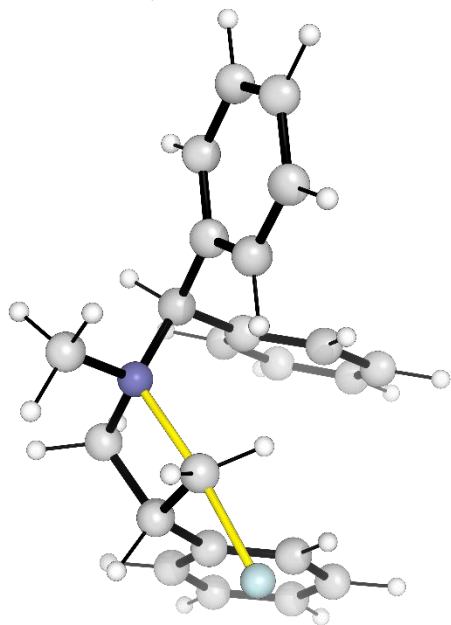
$G_{\text{rel}} = +3.5$ kJ/mol



TS-Azet_{Bzh,Me}-F 5
 $G_{\text{rel}} = +6.0 \text{ kJ/mol}$



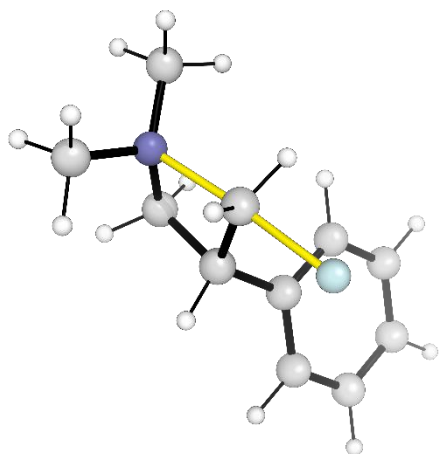
TS-Azet_{Bzh,Me}-F 6
 $G_{\text{rel}} = +8.2 \text{ kJ/mol}$



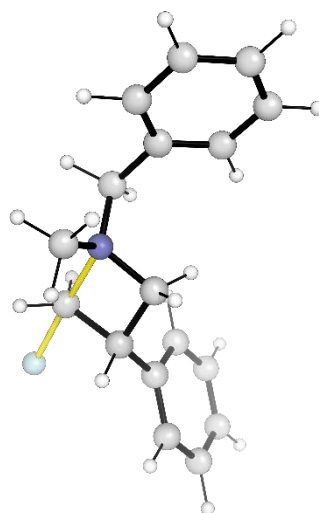
TS-Azet_{Bzh,Me}-F 7
 $G_{\text{rel}} = +8.3 \text{ kJ/mol}$

Figure S15: Geometries of TSs with **Azet_{Bzh,Me}**.

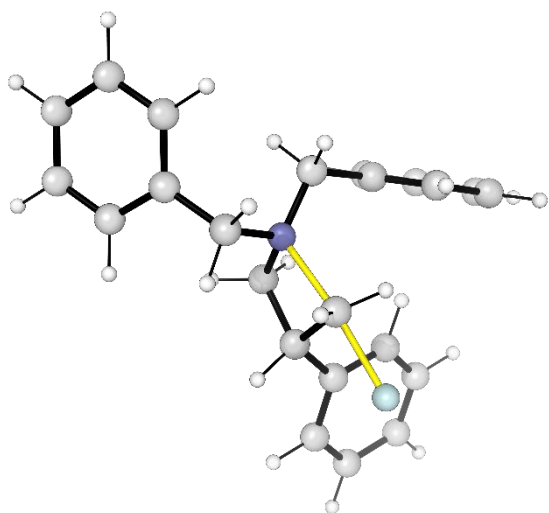
The lowest energy TSs with all azetidinium ions are given in Figure S16. All azetidinium ions, with the exception of **Azet_{Bn,Bn}**, adopt the same lowest energy conformation as in the free ion (the geometry adopted in the TS by **Azet_{Bn,Bn}** is within computational error of the lowest energy conformer in the free ion, so this is not significant).



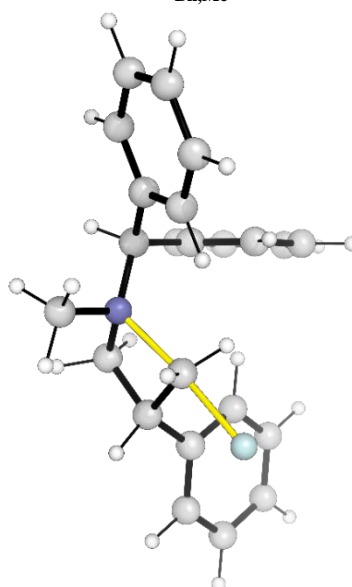
TS-Azet_{Me,Me}-F 1



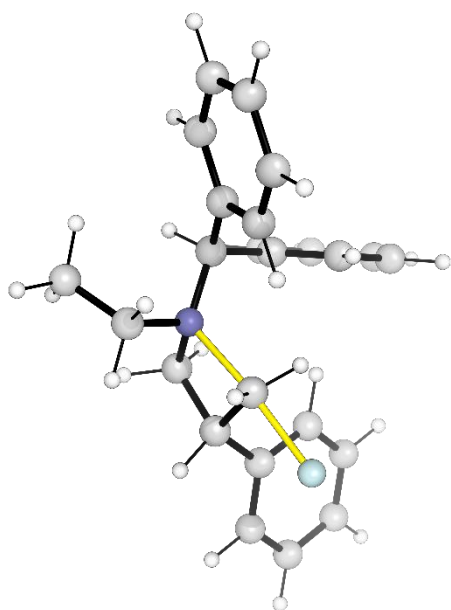
TS-Azet_{Bn,Me}-F 1



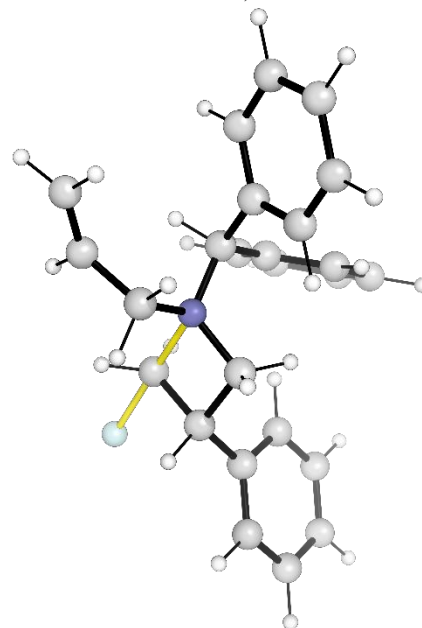
TS-Azet_{Bn,Bn}-F 1



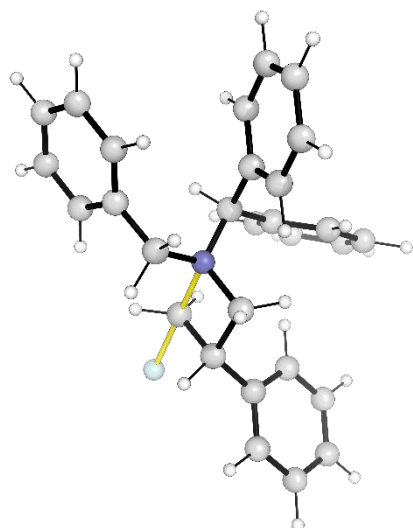
TS-Azet_{Bzh,Me}-F 1



TS-Azet_{Bzh,Et}-F 1



TS-Azet_{Bzh,Allyl}-F 1



TS-Azet_{Bzh,Bn}-F 1

Figure S16: Geometries of lowest energy TSs with fluoride

Azetidinium Fluorination Energetics

The computed energies of key states for fluorination of the azetidinium ions are given in Table S17. Species in curly braces, {}, indicate a tight ion pair. Lowest energy conformers are used.

Table S17: Gibbs free energies (298.15 K, 1 M) of key species for reactivity of cis-azetidinium ions with fluoride without urea catalyst.

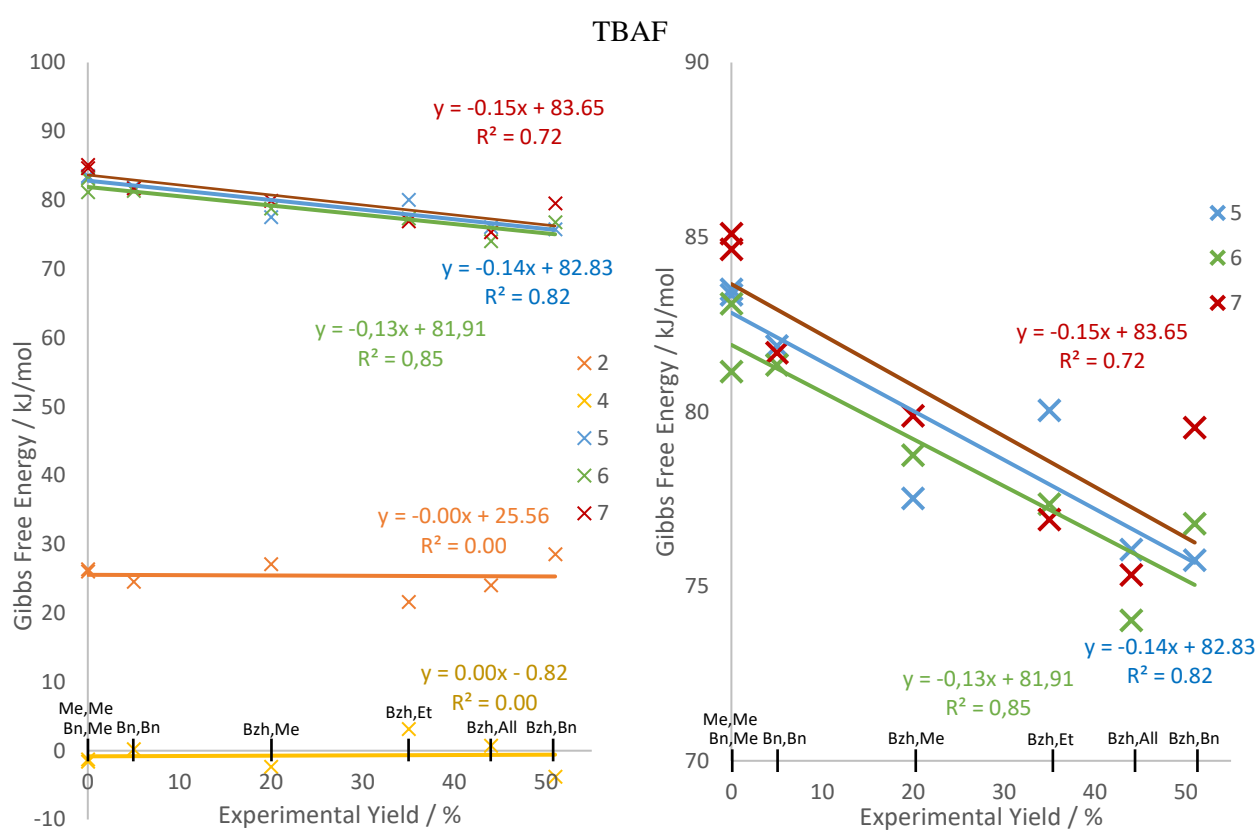
Species (Azet _{cis,trans})	Gibbs free energies / kJ/mol			
	I	II	III	IV [‡]
Azet _{Me,Me}	5.5	0.0	1.5	86.6
Azet _{Bn,Me}	3.4	0.0	1.8	86.5
Azet _{Bn,Bn}	3.7	0.0	3.3	85.0
Azet _{Bzh,Me}	1.9	0.0	0.8	80.7
Azet _{Bzh,Et}	5.8	0.0	6.3	83.2
Azet _{Bzh,Allyl}	5.2	0.0	3.9	79.2
Azet _{Bzh,Bn}	2.1	0.0	-0.6	78.9

Binding of the azetidinium triflate ion pair is relatively weak in all cases (**I-II**). Formation of the reactive ion pair from TBAF and the free azetidinium ion (**II-III**) is approximately neutral in Gibbs free energy, indicating similar affinity for fluoride of TBA⁺ and azetidinium ions. Fluoride delivery then proceeds with a barrier of approximately 75-85 kJ/mol.

The Gibbs free energy changes and activation barriers for various processes related to fluorination are tabulated in Table S18, with the appropriate kinetic barrier dependent on the reaction mechanism. Activation barriers are plotted against the yields of product obtained under HB PTC conditions (with catalyst) and with TBAF in Figure S17.

Table S18: Gibbs free energy changes and activation barriers for reactivity of azetidinium ions with fluoride without urea catalyst.

Barrier	Azetidinium Gibbs free energies / kJ/mol						
	Me,Me	Bn,Me	Bn,Bn	Bzh,Me	Bzh,Et	Bzh,All	Bzh,Bn
1 {Azet ⁺ OTf ⁻ } → Azet ⁺ + ⁻ OTf	-5.5	-3.4	-3.7	-1.9	-5.8	-5.2	-2.1
2 {Azet ⁺ F ⁻ } → Azet ⁺ + ⁻ F	26.3	26.0	24.5	27.1	21.6	24.0	28.5
3 {TBA ⁺ F ⁻ } + {Azet ⁺ OTf ⁻ } → {TBA ⁺ OTf ⁻ } + {Azet ⁺ F ⁻ }	-4.0	-1.6	-0.3	-1.1	0.4	-1.3	-2.7
4 {TBA ⁺ F ⁻ } + Azet ⁺ → TBA ⁺ + {Azet ⁺ F ⁻ }	-1.6	-1.3	0.2	-2.4	3.1	0.7	-3.8
5 {TBA ⁺ F ⁻ } + Azet ⁺ → TS + TBA ⁺	83.5	83.3	81.9	77.5	80.0	76.1	75.7
6 {TBA ⁺ F ⁻ } + {Azet ⁺ OTf ⁻ } → {TBA ⁺ OTf ⁻ } + TS	81.1	83.1	81.3	78.8	77.4	74.0	76.8
7 {Azet ⁺ F ⁻ } → TS	85.1	84.6	81.7	79.9	76.9	75.3	79.5



HB PTC

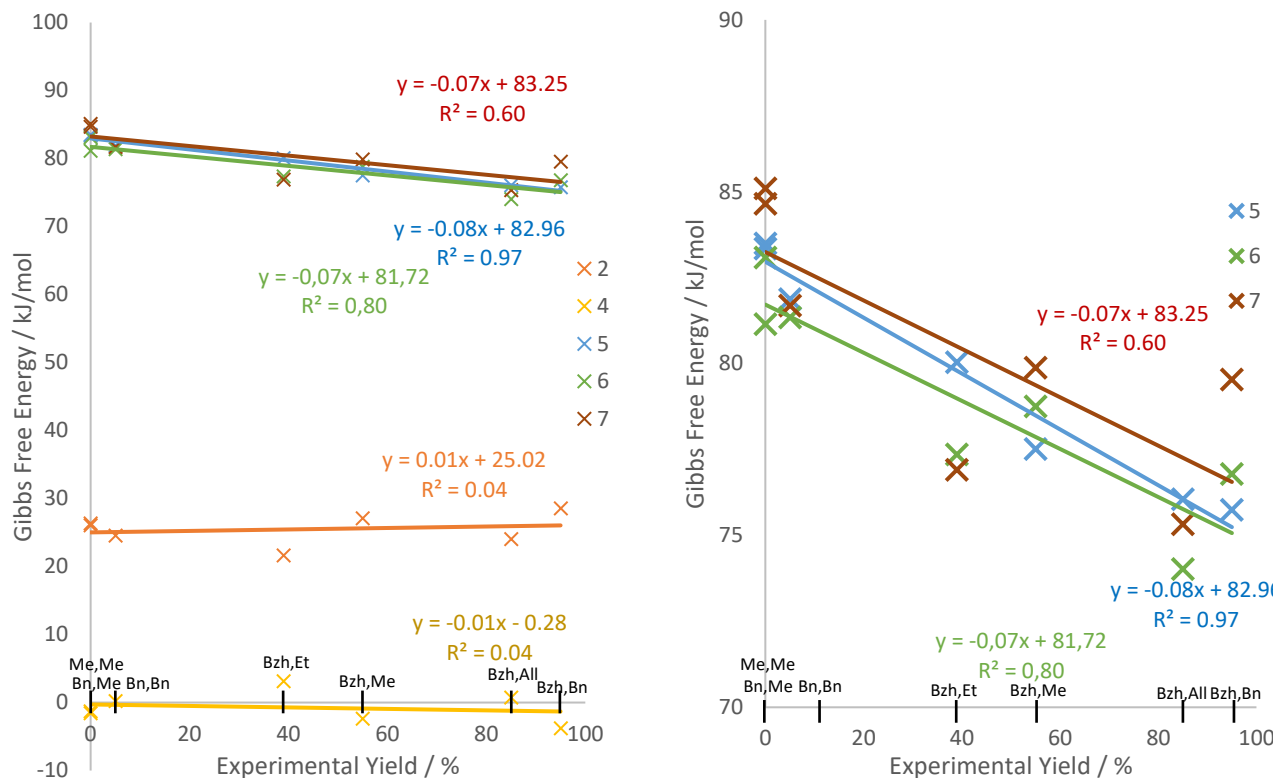


Figure S17: Plot of activation barriers/dissociation energies against experimental fluorination yields. Reactions yielding ‘traces’ are plotted as 5% yield. Linear trendlines are plotted to highlight general trends.

Both plots give qualitatively similar results. The uncertainty in computational results should be born in mind when interpreting the results, however, the correlation of several values reduces this. Activation barriers from free azetidinium ion (**5**), azetidinium triflate ion pair (**6**) and the reactive ion pair with fluoride (**7**) correlate negatively against reaction yield under both TBAF and HB PTC conditions, demonstrating consistency of computation and experiment. In contrast, there is no correlation (gradient ≤ 0.01 , $R^2 \leq 0.04$) between fluoride binding energy (**2**) and experimental yield with either fluoride source, suggesting that fluoride binding strength does not strongly influence reaction rate with either fluoride source.

HB PTC Mechanism

The lack of correlation of experimental yield (for a given reaction time) with the binding strength of azetidinium ion for fluoride suggests that the azetidinium-fluoride ion pair is not present in either of the turnover determining states in the catalyzed reaction (neither TDI nor TDTS). This supports that the azetidinium ion does not participate in a turnover determining phase-transfer process by binding fluoride. For example, **Azet**_{Bzh,Et} has the weakest complexation energy and therefore a low ability to bring fluoride into solution, but has a moderate yield. Note that the thermodynamics of phase-transfer may still contribute to the energetic span of the reaction, however the contribution is consistent for all of the azetidinium substrates.

In contrast, the good correlation of yield with the Gibbs free energy barrier to fluoride delivery relative to separated fluoride (**5**) supports that fluoride delivery by the catalyst in the catalyzed reaction is the TDTS, backed experimentally by the strong dependence of yield on substrate identity and similar reactivity profiles for TBAF and HB PTC conditions.

Additionally, as the intrinsic barrier to fluorination of the azetidinium ion is high, and approaching the maximum energetic span for a viable catalytic reaction at room temperature, the likelihood that one or the other of these states is turnover limiting is high (when coordinated by catalyst).

The Effect of the Benzhydryl *N*-Substituent

Experimental yields demonstrate that having a benzhydryl substituent on nitrogen is important for reactivity. This is reflected in computed activation barriers where these substrates have transition state structures lower in Gibbs free energy (relative to separated ion, with TBAF) than those without a benzhydryl group. The series **Azet**_{Me,Me} → **Azet**_{Bn,Me} → **Azet**_{Bzh,Me} (**Series**_{Me}) has activation barriers of 83.5, 83.3 and 77.5 kJ/mol, respectively, showing little change (< 1 kJ/mol) in barrier on conversion of methyl to benzyl, and a much larger change (6 kJ/mol) from benzyl to benzhydryl. A similar difference of 6 kJ/mol is seen between **Azet**_{Bn,Bn} and **Azet**_{Bzh,Bn} (**Series**_{Bn}) with barriers of 81.9 and 75.7 kJ/mol respectively, indicating a specific effect of the benzhydryl group worth a rate acceleration on the order of 10x over benzyl at room temperature. Critical bond distances are given in Table S19. Both minimum energy conformer and Boltzmann ensemble averaged distances are given.

As reaction yield increases (activation barrier decreases), the C-N distance in the ground state ion is increased. In **Series**_{Me}, the average C-N distance in the ground state ions are 1.517, 1.518 and 1.521 Å respectively. Likewise for **Series**_{Bn}, the distances are 1.518 and 1.523 Å. In both cases, the C-N distance in the benzhydryl substituted ions are significantly longer than those without. C-N distance correlates positively with experimental fluorination yield.

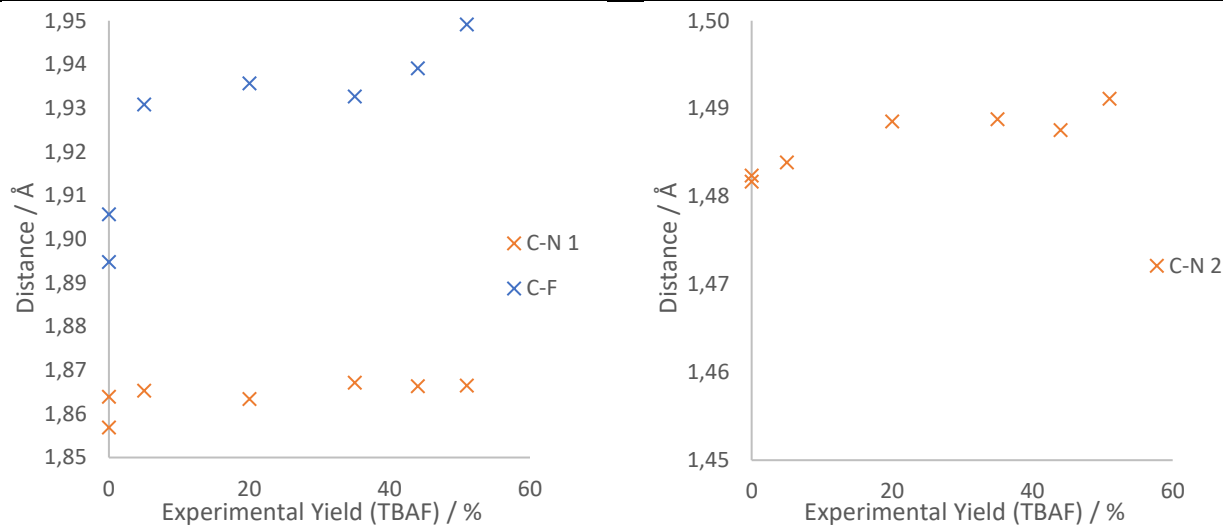
In the TSs, C-F separation increases as experimental yield increases, though without an orderly correlation. C-N separation of the breaking bond demonstrates no clear trend with experimental yield. This corresponds to a more ion pair like TS with increasing experimental yield. Increasing ground state C-N bond distances and more ion pair like TS positions are consistent with the Hammond postulate, where the TS more strongly resembles a more strained (closer in energy) ion. This is further supported by the increase in thermodynamic favorability of the ring opening reaction with fluoride in **Series**_{Me} of -85.5, -94.9 and -109.2 kJ/mol, where opening of the benzhydryl substituted ion is most exergonic.

Computation therefore supports that benzhydryl substituted azetidinium ions are intrinsically significantly more reactive than similarly substituted ions (such as benzyl) due to the ion being more strained.

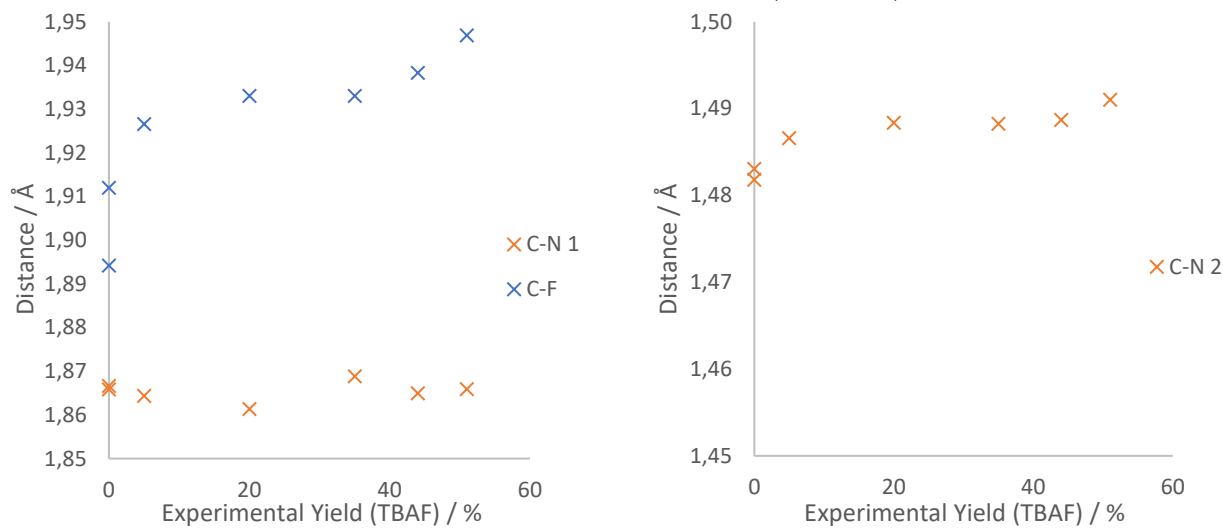
Table S19: Key bond distances with azetidinium ions

	Distance (Minimum Conformer) / Å			Distance (Ensemble) / Å		
	C-F	C-N 1*	C-N 2*	C-F	C-N 1*	C-N 2*
TS-Azet _{Me,Me} - F	1.895	1.864	1.482	1.894	1.867	1.482
TS-Azet _{Bn,Me} - F	1.906	1.857	1.482	1.912	1.866	1.483
TS-Azet _{Bn,Bn} - F	1.931	1.865	1.484	1.923	1.864	1.487
TS-Azet _{Bzh,Me} - F	1.936	1.863	1.489	1.933	1.861	1.488
TS-Azet _{Bzh,Et} - F	1.933	1.867	1.489	1.933	1.869	1.488
TS-Azet _{Bzh,Allyl} - F	1.939	1.866	1.488	1.938	1.865	1.489
TS-Azet _{Bzh,Bn} - F	1.949	1.867	1.491	1.947	1.866	1.491
Azet _{Me,Me}		1.517			1.517	
Azet _{Bn,Me}		1.518			1.518	
Azet _{Bn,Bn}		1.518			1.519	
Azet _{Bzh,Me}		1.521			1.522	
Azet _{Bzh,Et}		1.522			1.522	
Azet _{Bzh,Allyl}		1.522			1.522	
Azet _{Bzh,Bn}		1.523			1.523	

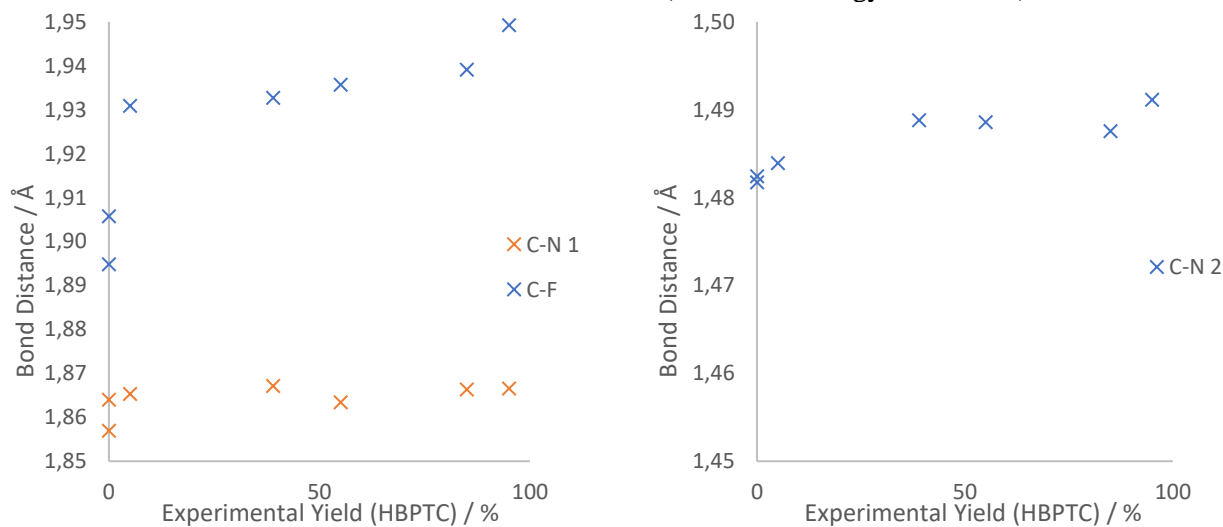
TS Bond Distances vs TBAF Yield (Minimum Energy Conformer)



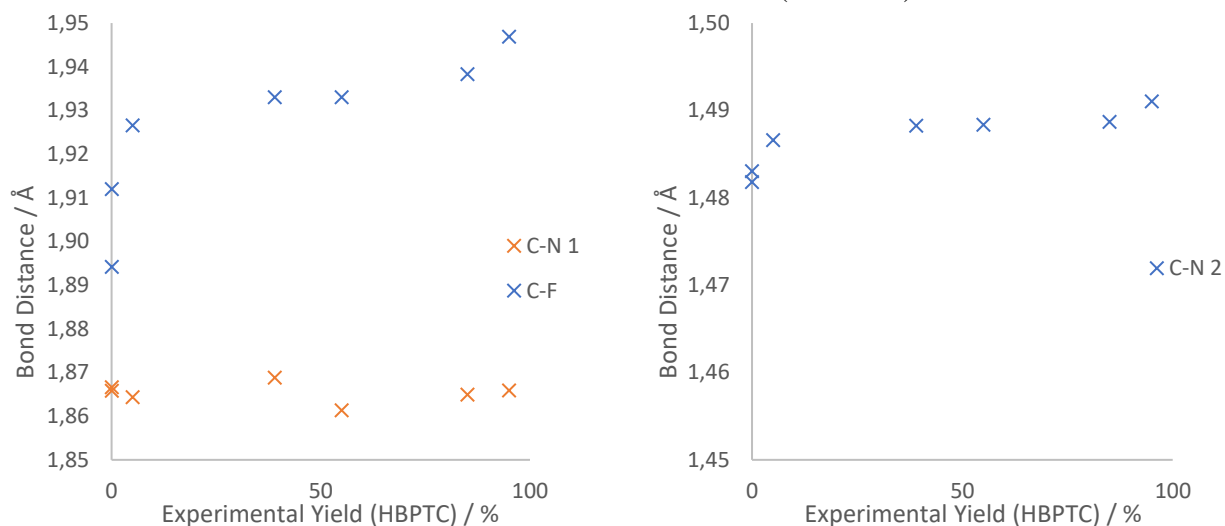
TS Bond Distances vs TBAF Yield (Ensemble)



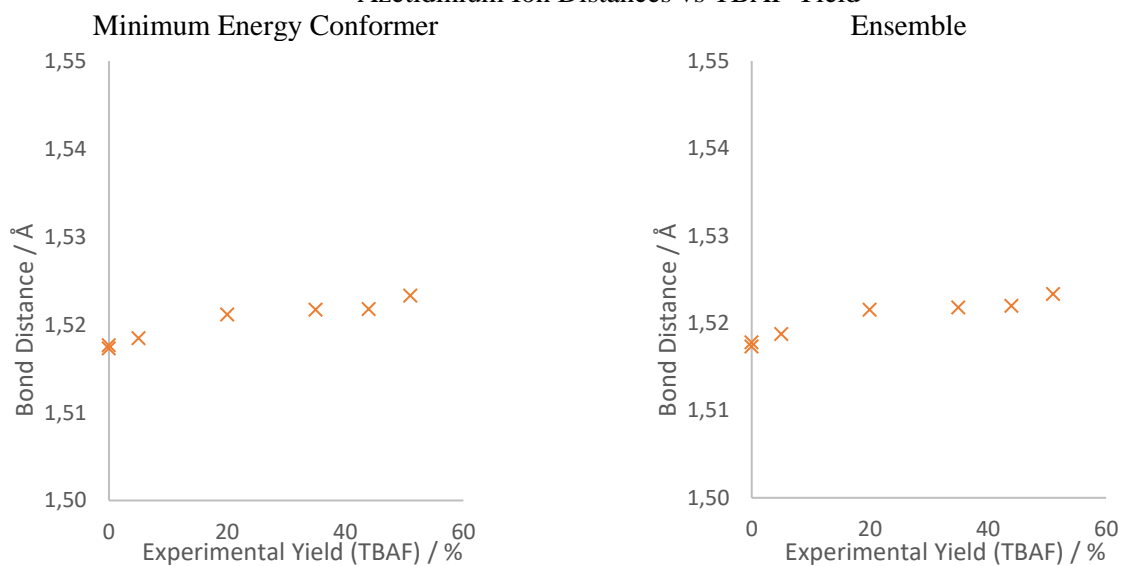
TS Bond Distances vs HBPTC Yield (Minimum Energy Conformer)



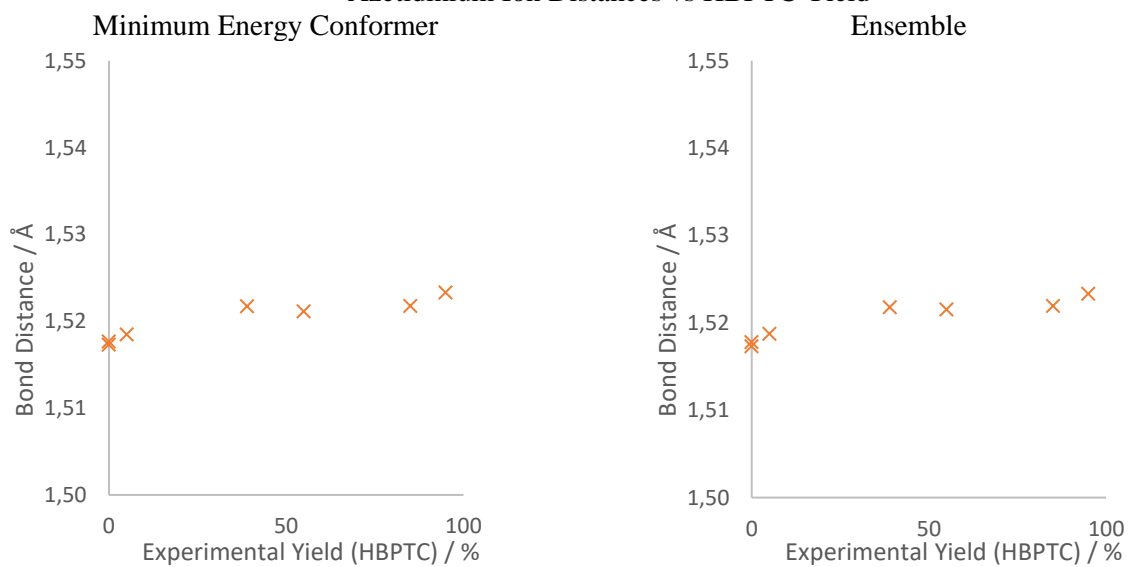
TS Bond Distances vs HBPTC Yield (Ensemble)



Azetidinium Ion Distances vs TBAF Yield



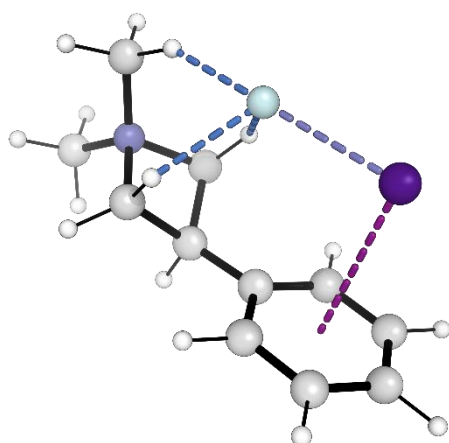
Azetidinium Ion Distances vs HBPTC Yield



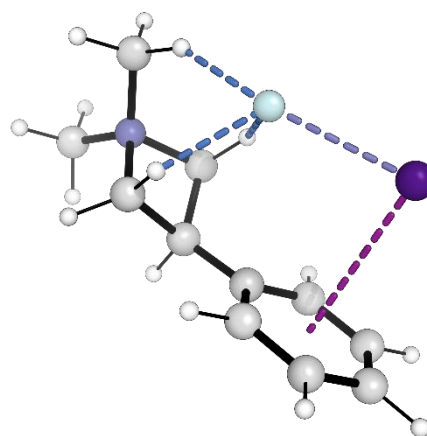
CsF Phase-Transfer

To further investigate the relative abilities of azetidinium ions and urea hydrogen bond donors to act as phase-transfer catalysts for CsF, the binding energies of **Azet**_{Me,Me} and catalyst **B** with a solvated CsF formula unit were evaluated (Figure S18).

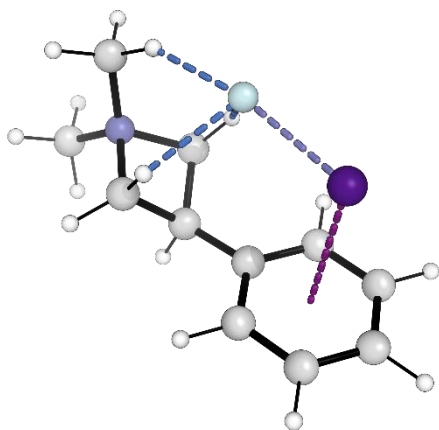
Azet_{Me,Me} binds a CsF ion pair weakly, with $\Delta G = -14.0$ kJ/mol, slightly overcoming the entropic penalty of coordination. Binding is weaker over the naked fluoride ion due to competition with the cesium ion and loss of rotational entropy of the CsF unit on coordination. Catalyst **B** on the other hand binds CsF much more strongly with $\Delta G = -69$ kJ/mol, originating from the three strong hydrogen bonds to fluoride. These results demonstrate that the neutral hydrogen bonding urea catalyst has a significantly higher potential to act as a CsF phase-transfer catalyst than the azetidinium ion.



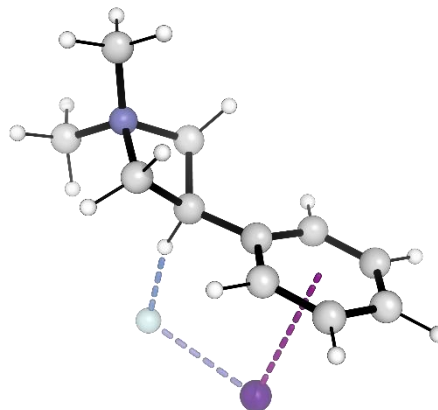
Azet_{Me,Me}-FCs 1
 $G_{\text{rel}} = 0.0$ kJ/mol



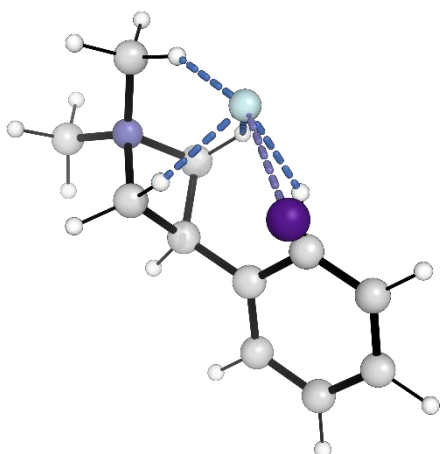
Azet_{Me,Me}-FCs 2
 $G_{\text{rel}} = +2.8$ kJ/mol



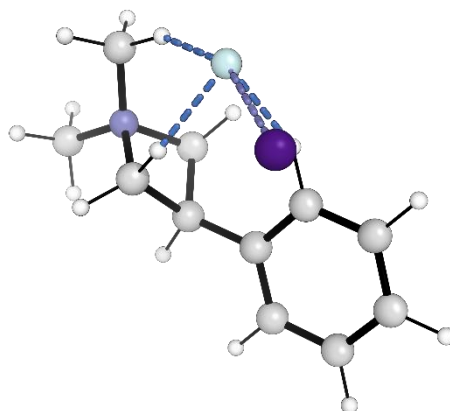
Azet_{Me,Me}-FCs 3
 $G_{\text{rel}} = +3.0$ kJ/mol



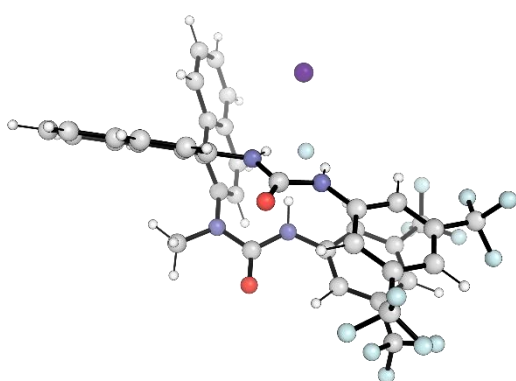
Azet_{Me,Me}-FCs 4
 $G_{\text{rel}} = +11.3$ kJ/mol



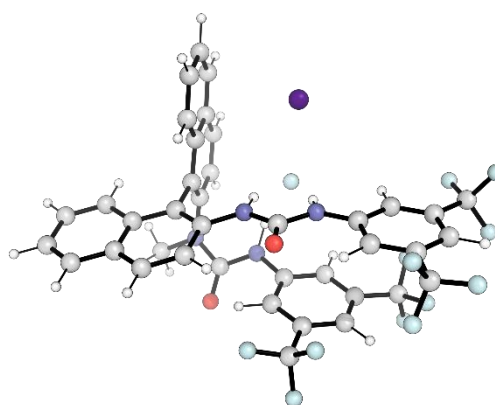
Azet_{Me,Me}-FCs 5
 $G_{\text{rel}} = +12.3$ kJ/mol



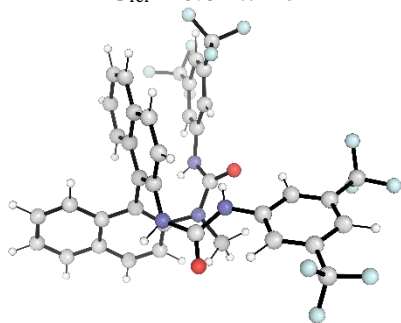
Azet_{Me,Me}-FCs 6
 $G_{\text{rel}} = +12.6$ kJ/mol



Cat B-FCs 1
 $G_{\text{rel}} = 0.0$ kJ/mol



Cat B-FCs 2
 $G_{\text{rel}} = +2.6$ kJ/mol

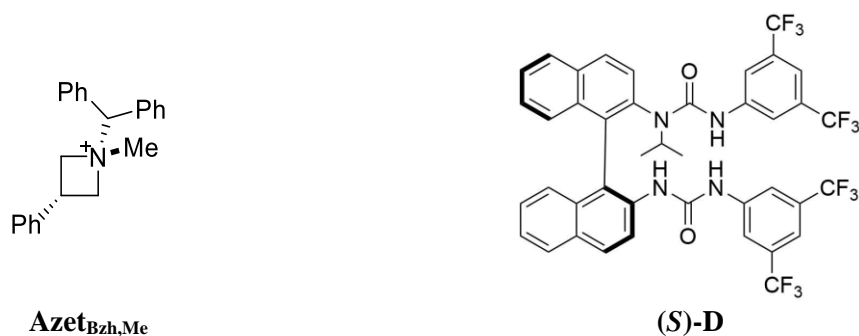


Cat B

Figure S18: Geometries of CsF complexes.

Enantioselective Fluorination of *cis*-Azet_{Bzh,Me}

Enantioselectivity was first evaluated on substrate **Azet_{Bzh,Me}** with (*S*)-**D** catalyst. Gibbs free energies are evaluated at 298.15 K and 1 M concentration unless otherwise stated.



Transition State Structures

The transition state structures to both enantiomers of product with *cis* substrate were simulated using classical molecular dynamics for 300 ns, leading to a total simulation time of 600 ns. All frames with $F\cdots C\cdots N > 150^\circ$ in each trajectory were used for clustering with RMSD cutoff of 1.0 Å. For attack at the carbon leading to (*R*) product, herein referred to as *R*-attack, 21796 frames were clustered, resulting in 10 clusters of greater than 1% weight. Lower weight clusters were manually inspected and verified that they contained no additional conformations of interest. The central frame from each cluster was then optimized using DFT, resulting in 10 unique TSs to (*R*) product. The same procedure was followed for *S*-attack, with 20495 frames clustered, resulting in 8 clusters of over 1% weighting, and 8 unique DFT optimized TSs to (*S*) product. The intramolecular T-shape CH- π interaction of the azetidinium was sampled manually. A total of 24 TSs were optimized – 14 to (*S*) product and 10 to (*R*) product – spanning an energy range of 41 kJ/mol. The ensemble indicates that (*S*) catalyst affords (*S*) product in 54:46 e.r. in 1,2-dichloroethane at 298.15 K. The experimental enantioinduction is 80.5:19.5 e.r., consistent within computational error (approximately 3.5 kJ/mol deviation).

The Gibbs free energy distribution of the low energy TSs is illustrated in Figure S19. Key geometric parameters are tabulated in Table S20. The highest contributing TSs to major and minor product are shown in more detail in Figure S20.

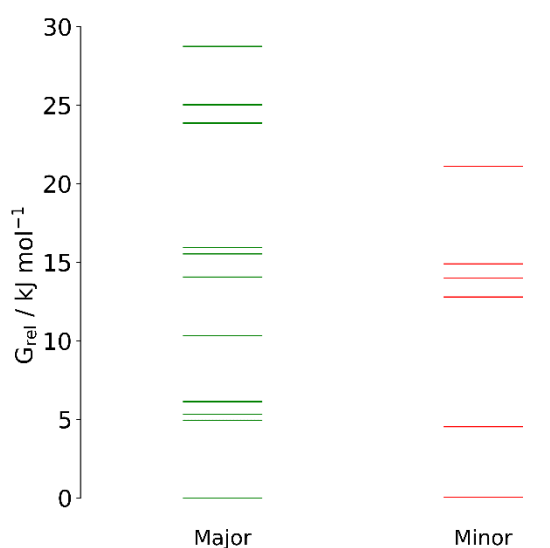
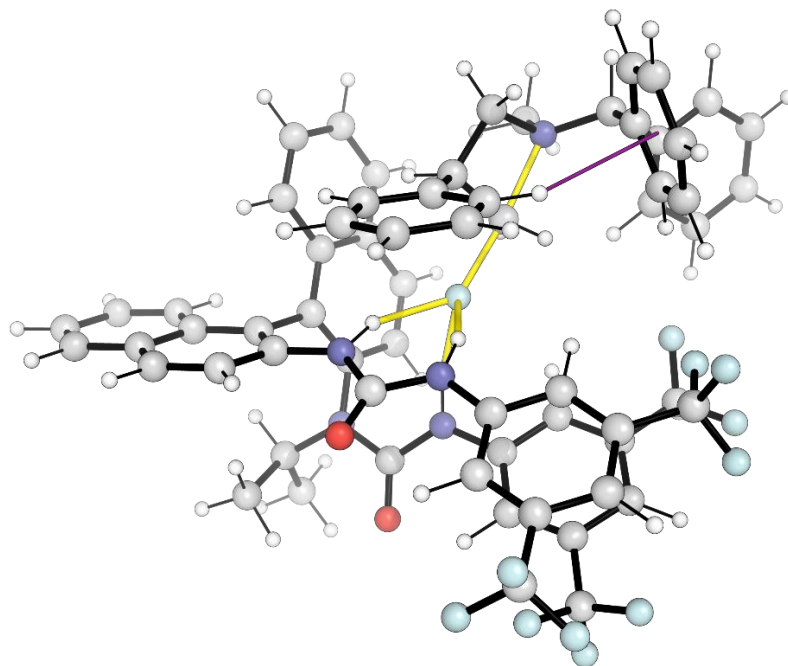


Figure S19: Gibbs free energy distribution of TSs in the ensemble.

Table S20: Key geometric parameters for the transition state structures

TS	Imag.	Key Distances/ Å					Key Angle/°			
		C-F	C-N	HB 1	HB 2	HB 3	Pucker	Benzhydryl	Backbone	
TS	Imag.	1.862	1.973	1.905	1.832	1.836	148.0	-12.0	-61.5	72.0
TS_Cis-Azet-major1	-649.8	1.844	1.957	1.828	1.906	1.824	148.8	-19.2	179.7	74.8
TS_Cis-Azet-major2	-645.7	1.842	1.968	1.840	1.865	1.859	149.2	-8.8	59.3	71.3
TS_Cis-Azet-major3	-648.6	1.841	1.956	1.852	1.905	1.832	148.7	-19.8	154.4	74.1
TS_Cis-Azet-major4	-647.6	1.866	1.975	1.915	1.836	1.848	144.4	-11.8	-61.3	68.3
TS_Cis-Azet-major5	-648.4	1.843	1.958	1.846	1.930	1.833	146.2	-19.1	154.1	69.8
TS_Cis-Azet-major6	-650.0	1.848	1.962	1.850	1.886	1.836	145.7	-15.4	-178.4	69.6
TS_Cis-Azet-major7	-644.3	1.850	1.970	1.919	1.814	1.861	143.0	-9.2	62.3	68.3
TS_Cis-Azet-major8	-648.7	1.831	1.954	1.868	1.778	1.884	146.6	-24.7	-159.3	95.2
TS_Cis-Azet-major9	-646.1	1.853	1.963	1.777	1.848	2.056	133.3	-17.5	-176.8	65.7
TS_Cis-Azet-major10	-637.0	1.853	1.963	1.777	1.848	2.056	133.3	-17.5	-176.8	65.7
TS_Cis-Azet-major11	-637.0	1.827	1.962	1.834	1.926	1.874	164.2	-9.8	-56.7	109.7
TS_Cis-Azet-major12	-648.8	1.844	1.957	1.931	1.776	1.930	139.3	-5.4	-176.1	103.5
TS_Cis-Azet-major13	-642.8	1.853	1.971	2.152	1.694	1.886	152.1	-25.3	152.9	107.6
TS_Cis-Azet-major14	-642.9	1.851	1.959	1.841	1.838	1.916	145.5	-18.2	-178.1	70.6
TS_Cis-Azet-minor1	-645.0	1.838	1.952	1.866	1.822	1.875	146.1	-21.7	-157.8	71.0
TS_Cis-Azet-minor2	-647.7	1.845	1.956	1.819	1.846	1.904	142.3	-20.7	-178.7	67.7
TS_Cis-Azet-minor3	-644.9	1.834	1.962	1.864	1.797	1.938	142.4	-14.6	166.2	76.6
TS_Cis-Azet-minor4	-641.8	1.819	1.942	1.746	1.969	1.886	147.8	-14.7	175.2	110.6
TS_Cis-Azet-minor5	-644.7	1.818	1.958	1.812	1.787	1.870	151.2	-21.2	-168.2	111.2
TS_Cis-Azet-minor6	-645.8	1.842	1.963	1.942	1.780	1.900	147.5	-24.2	153.0	74.9
TS_Cis-Azet-minor7	-645.5	1.858	1.983	1.890	1.880	2.096	159.1	1.1	66.2	104.5
TS_Cis-Azet-minor8	-650.0	1.864	1.959	2.050	1.707	2.006	135.5	-26.5	-156.0	102.8
TS_Cis-Azet-minor9	-646.4	1.864	1.980	1.854	1.766	1.960	145.0	-31.1	60.6	69.5

$TS_{Major-Cis}$



$TS_{Minor-Cis}$

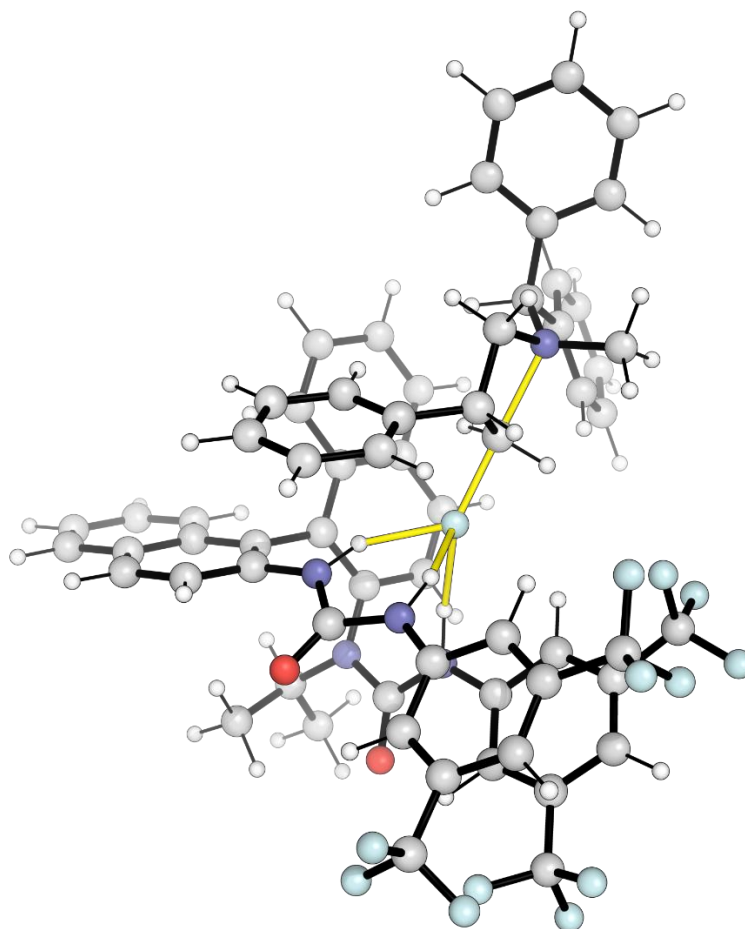


Figure S20: Lowest energy TSs to major and minor product. Azetidinium intramolecular T-shape CH- π interaction illustrated in purple in $TS_{Major-Cis}$.

Origins of Enantioselectivity

The two lowest energy TSs, with $\Delta\Delta G^\ddagger = 0.0$ kJ/mol, are superimposed in Figure S21. Catalyst geometry superimposes well. The phenyl group bonded to the azetidinium ring sits in the same place in both TSs, and results in a slight twist of the azetidinium ring. The benzhydryl group points in different directions in the two TSs.

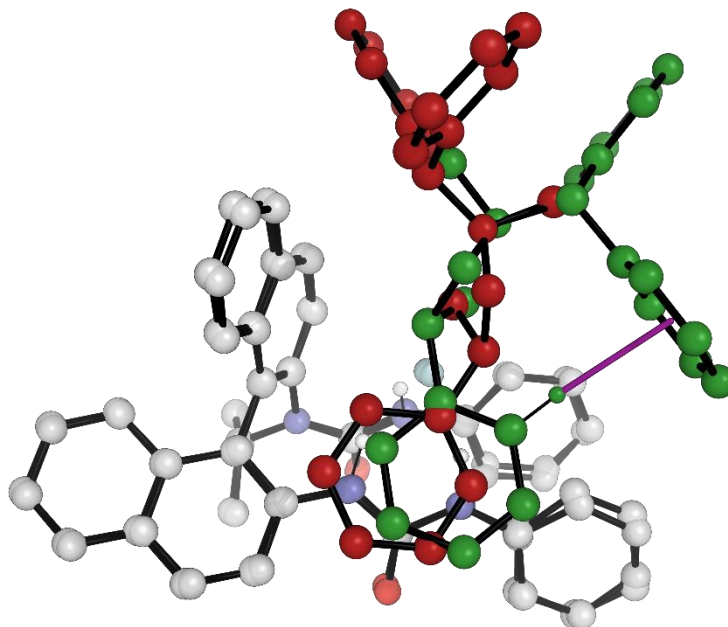


Figure S21: Superposition of $\text{TS}_{\text{Major-Cis}}$ (green) and $\text{TS}_{\text{Minor-Cis}}$ (red). Intramolecular T-shape CH- π interaction is shown in purple.

In $\text{TS}_{\text{Major-Cis}}$, the azetidinium ion can adopt the favored conformation seen with uncoordinated fluoride, forming an intramolecular T-shape CH- π interaction. The shape of the azetidinium ion, determined primarily by the phenyl group bonded to the azetidinium ring, fits neatly into the catalytic pocket, with phenyl group lying parallel to the bidentate urea. In contrast, the favored CH- π conformation cannot be adopted when delivering fluoride to the other carbon. In the lowest energy minor TS, the proximity of the binam backbone prevents formation of the CH- π interaction due to steric clash, however this must be compensated by stronger substrate-catalyst interactions. The difference in energy between the two azetidinium conformers in the absence of fluoride is 4.3 kJ/mol, reduced to 2.3 kJ/mol on uncoordinated fluoride delivery.

Distortion/Interaction-Activation Strain Analysis

Intrinsic reaction coordinate (IRC) calculations were run for $\text{TS}_{\text{Major-Cis}}$ and $\text{TS}_{\text{Minor-Cis}}$ and the distortion/interaction-activation strain analysis of Bickelhaupt and Houk applied.⁵¹ The system was partitioned into {catalyst-fluoride complex} + {azetidinium substrate}. The results of the analysis are given in Figure S22.

In both cases the total energy begins negative, as bringing the negatively charged fluoride complex and positively charged substrate together involves favorable coulombic interactions. In general, the profiles are very similar for both IRCs. $\text{IRC}_{\text{Minor}}$ consistently has stronger interaction than $\text{IRC}_{\text{Major}}$, however this is accompanied by higher distortion. Interestingly, towards the TS positions, there is little difference in distortion despite the substrate adopting a less favored conformer along $\text{IRC}_{\text{Minor}}$. The TS positions are very similar, so this is not a significant factor when comparing the distortions at the respective TS positions.

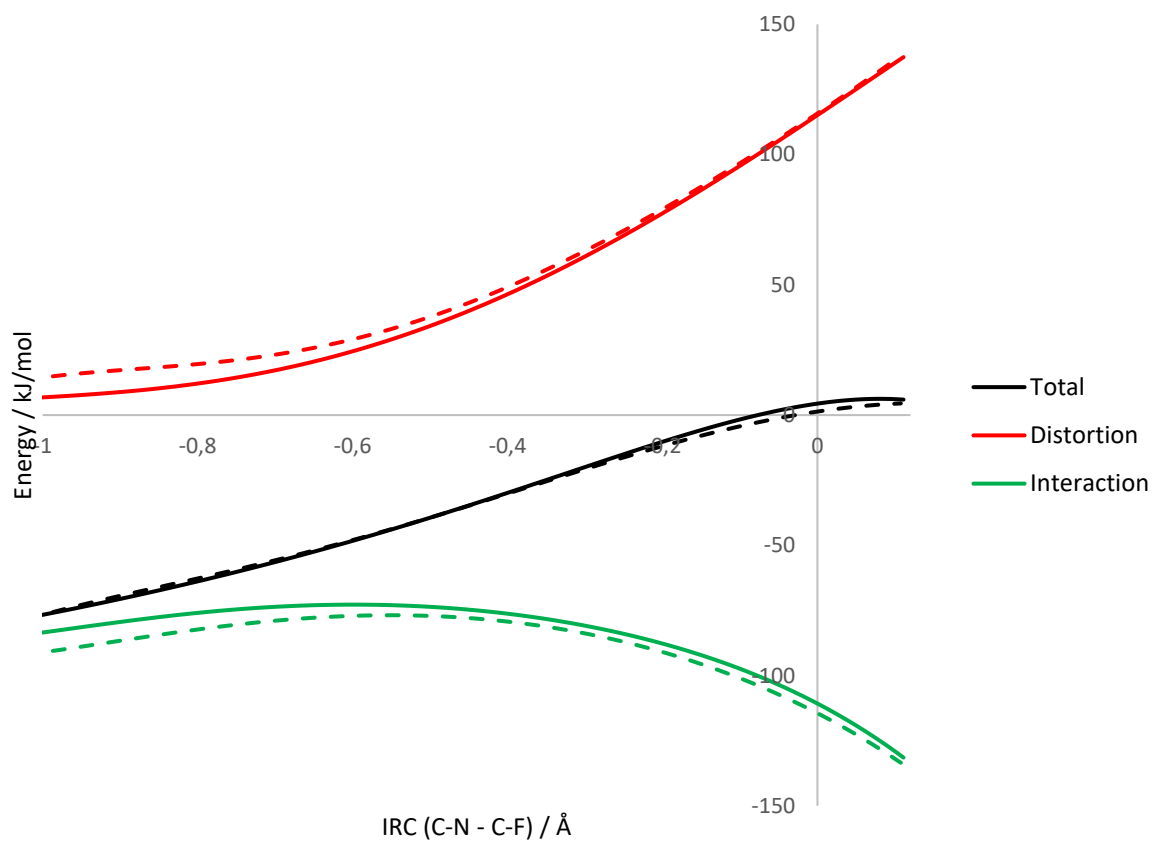


Figure S22: Distortion/interaction-activation strain analysis of fluoride delivery in $\text{TS}_{\text{Major-Cis}}$ and $\text{TS}_{\text{Minor-Cis}}$. The TS to major product has lower distortion and both pathways have similar interaction. The difference in TS position is minimal.

Truncated Models

To probe the contributions of different structural elements to enantioselectivity, the TSs were truncated in various ways, and the energy re-evaluated without optimization (Figure S23). Energies are tabulated in Table S21. Whilst the error in $\Delta\Delta G^\ddagger$ is significant compared to its magnitude, how $\Delta\Delta G^\ddagger$ changes on truncation of different groups can still yield qualitative insight.

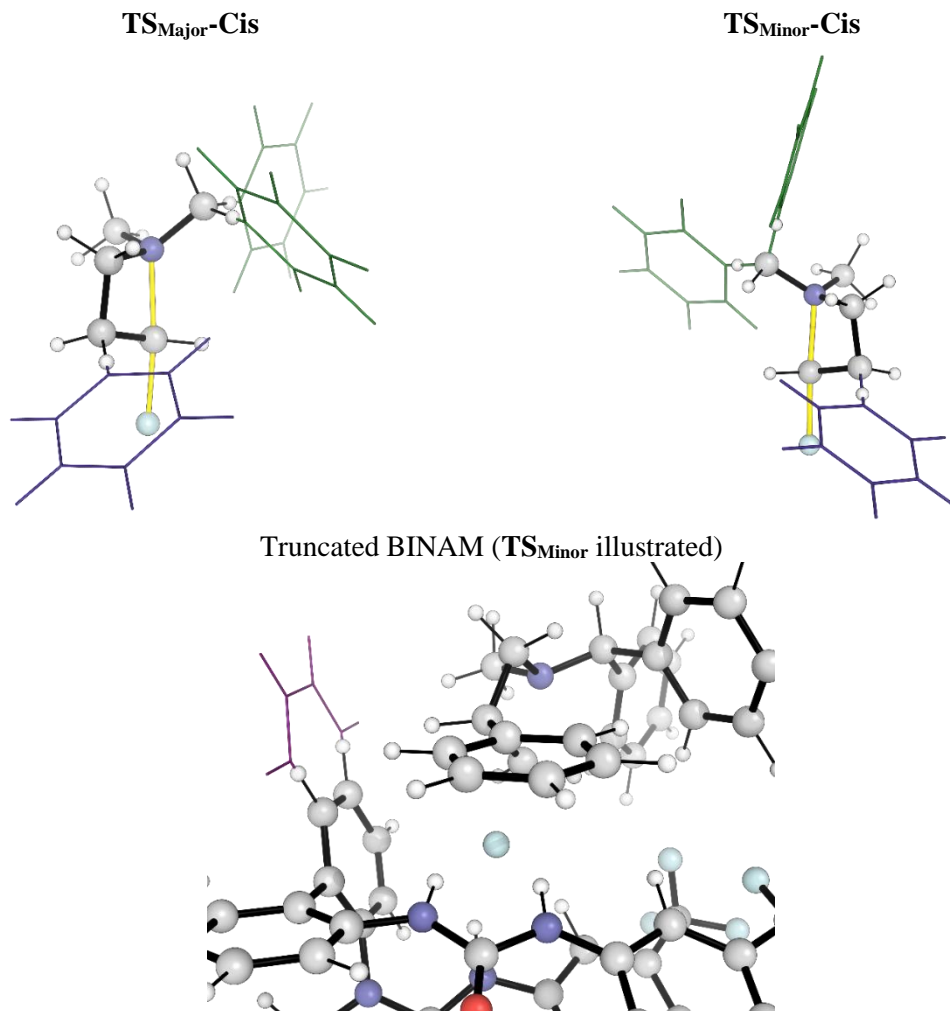


Figure S23: Illustration of the groups that are truncated to probe the origins of enantioselectivity. Green – benzhydryl, Blue – phenyl.

Table S21: $\Delta\Delta E^\ddagger$ selectivities with truncation of the system

Entry	Truncated Groups	$\Delta\Delta E^\ddagger$ / kJ/mol		
1	None	1.5*		
2	Ph	4.5		
3	Bzh	0.2		
4	Ph	Bzh	-2.7	
5	BINAM	-2.8		
6	Azet	1.1		
7	Cat	Fluoride	-1.6	
8	Cat	-4.7		
9	Cat	Ph	-0.2	
10	Cat	Bzh	0.0	
11	Cat	Ph	Bzh	-1.4

* $\Delta\Delta E^\ddagger$ favors the minor enantiomer due to exclusion of additional terms in $\Delta\Delta G^\ddagger$

Truncation of the azetidinium phenyl group (1→2) results in a $\Delta\Delta E^\ddagger$ of 4.5 kJ/mol indicating a shift towards minor product of 3 kJ/mol. This suggests that interactions of the Ph group are more favorable in **TS_{Major}** than **TS_{Minor}**. This change can be accounted for through loss of azetidinium intramolecular CH- π interaction, or catalyst-substrate interactions. If the same truncation is performed with the catalyst also removed (8→9), there is an energy change of 4.5 kJ/mol towards the minor, demonstrating that the major contributor is the loss of the intramolecular CH- π interaction in **TS_{Major}**.

Truncation of the benzhydryl group in the presence of catalyst (1→3) leads to a small change in $\Delta\Delta E^\ddagger$ of 1.3 kJ/mol, to 0.2 kJ/mol, suggesting the Bzh group has interactions of similar strength in both TSs. In the absence of catalyst, truncation of the Bzh group results in $\Delta\Delta E^\ddagger$ shifting towards minor product by 4.7 kJ/mol, highlighting significantly stronger interactions of the group in **TS_{Major}**. This is consistent with the intramolecular CH- π interaction only present in **TS_{Major}**. The large difference in behavior of truncating this group in the presence and absence of catalyst is consistent with stronger interactions of the Bzh group with the catalyst in **TS_{Minor}** – supported by NCI plots. In the absence of catalyst, truncation of the Ph group or the Bzh group have a similar effect on $\Delta\Delta E^\ddagger$, consistent with the dominant effect being loss of the intramolecular CH- π interaction.

If one of the aromatic rings of the binam backbone is truncated (1→5), selectivity increases by 4.3 kJ/mol, demonstrating a stronger interaction of the substrate with this group in the **TS_{Minor}**. This arises from interaction with the benzhydryl group of the substrate in **TS_{Minor}**, despite a shortened cation- π in **TS_{Major}**.

Non-covalent Interactions

Non-covalent interactions plays a key role in docking the substrate with the catalyst-fluoride complex. These non-covalent interactions are visualized in Figure S24 using the non-covalent interaction index. Both TSs have face-to-face π -interactions between azetidinium phenyl group and catalyst urea group, and a cation- π interaction between azetidinium and BINAM backbone. **TS_{Major}** benefits from an intramolecular T-shape CH- π interaction, which is not achieved in **TS_{Minor}**. However, **TS_{Minor}** can achieve an edge-to-face π -interaction between the catalyst BINAM backbone and one of the benzhydryl phenyl rings.

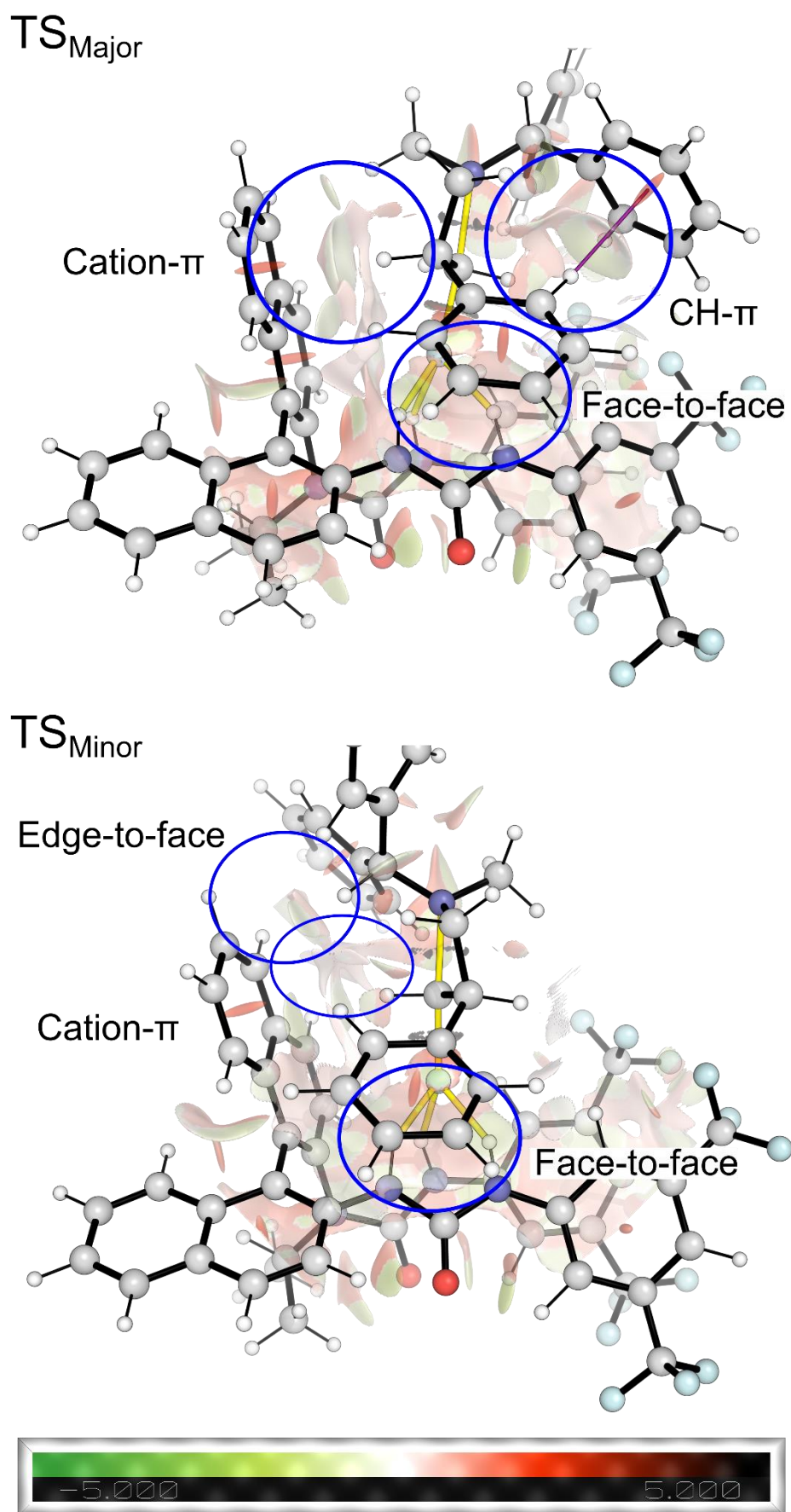


Figure S24: Non-covalent Interaction plots for $TS_{Major-Cis}$ and $TS_{Minor-Cis}$

Geometry Evolution over the Intrinsic Reaction Coordinate

Distances were monitored over the IRC pathway to major and minor products up to the TSs ($\text{IRC}_{\text{Major-Cis}}$ and $\text{IRC}_{\text{Minor-Cis}}$ respectively) and are plotted in Figure S25.

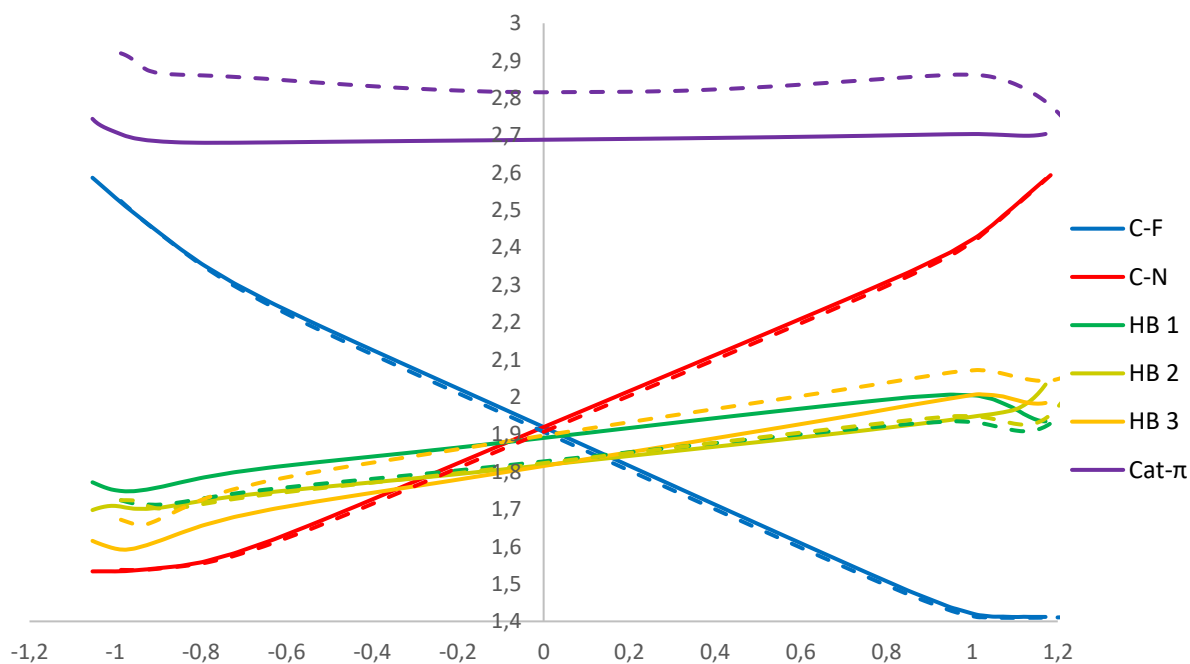


Figure S25: Plot of key geometric parameters over the IRC pathways to major and minor products.

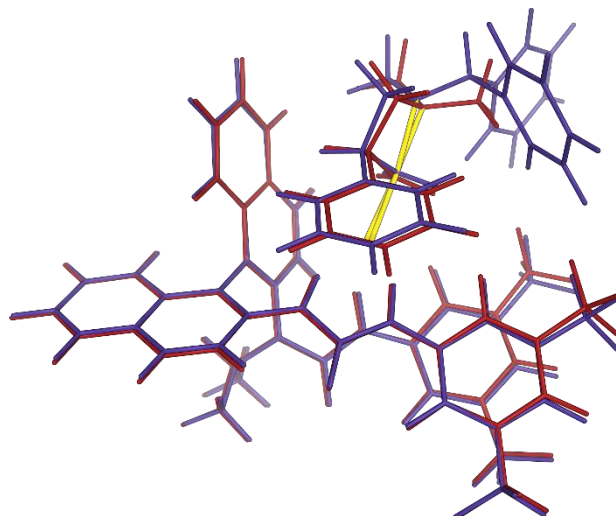
Distances on the pathway to major product

- Forming C-F and breaking C-N bonds are similar lengths along both IRC pathways, with $\text{IRC}_{\text{Major}}$ slightly looser.
- The azetidinium-binam cation- π interaction, measured from closest hydrogen atom, to the centroid of the ring is significantly longer along $\text{IRC}_{\text{Minor}}$, consistent with a weaker interaction.
- HB 2 is the same length and evolves at the same rate along both IRC pathways.
- HB 1 is longer in $\text{IRC}_{\text{Major}}$ and HB 3 is shorter, with the bonds increasing in length at a similar rate along both pathways. HB 3 elongates at the fastest rate along both pathways.

Points iii-iv indicate that fluoride is positioned further from the BINAM backbone along $\text{IRC}_{\text{Major}}$ and is positioned further towards the monodentate alkylated urea hydrogen bond donor.

Effect of the Bzh group

Superposition of $\text{TS}_{\text{Major-Cis}}$ and reoptimized TS with $\text{Azet}_{\text{Me,Me}}$



Superposition of $\text{TS}_{\text{Minor-Cis}}$ and reoptimized TS with $\text{Azet}_{\text{Me,Me}}$

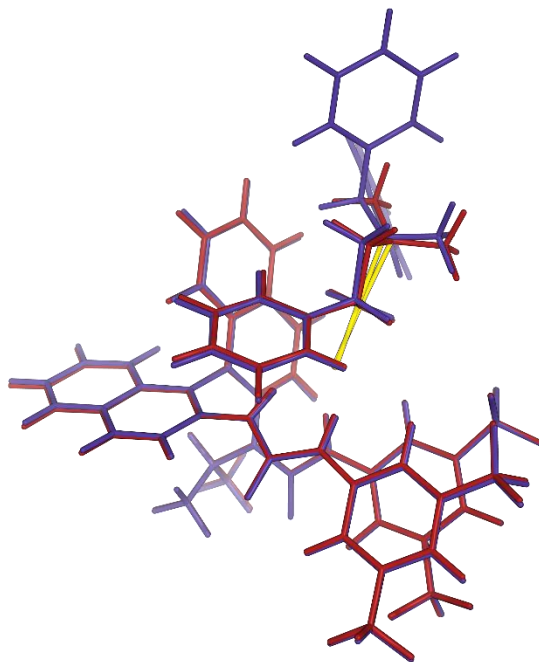


Figure S26: Reoptimization of $\text{TS}_{\text{Major-Cis}}$ and $\text{TS}_{\text{Minor-Cis}}$ without benzhydryl group demonstrates minimal change in TS geometries.

Replacement of the Bzh group in the two lowest energy TSs with a Me group (converting the substrate to $\text{Azet}_{\text{Me,Me}}$) followed by reoptimization yields TSs that superimpose well with the Bzh starting points, demonstrating that the Bzh group has minimal role in determining the substrate docking pose.

Enantioselectivity with $\text{Azet}_{\text{Bzh,Et}}$

To investigate the increased level of enantioselectivity with $\text{Azet}_{\text{Bzh,Et}}$ over $\text{Azet}_{\text{Bzh,Me}}$, $\text{TS}_{\text{Major-Cis}}$ and $\text{TS}_{\text{Minor-Cis}}$ were reoptimized after converting the *N*-Me group to *N*-Et. $\Delta\Delta G^\ddagger$ is increased from 0.0 to 6.4 kJ/mol. This is consistent in direction and qualitative magnitude with experimental results where e.r. is

increased from 81:19 to 96:4 corresponding to $\Delta\Delta G^\ddagger$ of approximately 3.6 and 7.9 kJ/mol. The TSs are superimposed in Figure S27.

In the **TS_{Major-Cis}**, the ethyl group slots cleanly into space, with the substrate as a whole adopting the lowest energy conformation seen in the TS with free fluoride. No change in catalyst or substrate geometry is seen, with perfect superposition of both (Figure S27, left). In contrast, in **TS_{Minor-Cis}**, the ethyl group cannot adopt a conformation without requiring distortion and movement of the substrate. The ethyl group adopts a less favored conformation, eclipsing the azetidinium ring. Figure S27, right, shows translation of the substrate and distortion of the azetidinium ring. As the ethyl group fits so perfectly into the lowest energy major TS, all other TSs are expected to be destabilized relative to this, consistent with the increase in enantioselectivity seen experimentally.

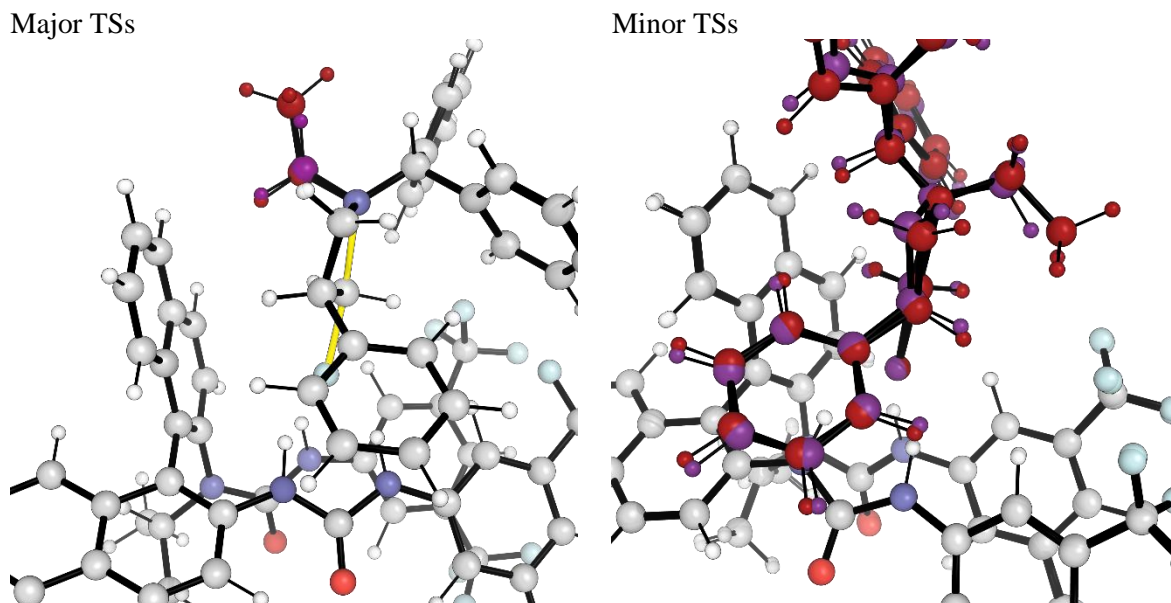


Figure S27: Superposition of lowest energy TSs with **Azet_{Bzh,Me}** (purple) and reoptimization with **Azet_{Bzh,Et}** (red) substrate. Left: Major, Right: Minor.

Summary

The catalyst adopts the same conformation in both the lowest energy TS to major and minor product, eliminating this as a major factor in enantioselectivity.

The docking pose of the substrate into the catalyst-fluoride complex in both cases is determined by face-to-face π -interactions between azetidinium phenyl ring and bidentate urea, in addition to the stereoelectronic requirements of the S_N2 mechanism.

The position of the large benzhydryl group has surprisingly little effect on TS geometries exemplified by completely different positioning in the lowest energy TSs to major and minor product.

In **TS_{Major-Cis}**, the benzhydryl groups forms a favorable intramolecular T-shape $CH-\pi$ interaction, exhibited in the TS with naked fluoride, and worth approximately 2-5 kJ/mol. In **TS_{Minor-Cis}**, however, the benzhydryl group can form an edge-to-face π -interaction with the BINAM backbone, compensating for this loss.

The cation- π distance in **TS_{Major-Cis}** is shorter, consistent with a stronger interaction.

Transition State Structures

The transition state structures to both enantiomers of product with trans substrate were simulated for 300 ns, leading to a total simulation time of 600 ns. All frames with F---C---N > 150° in each trajectory were used for clustering with RMSD cutoff of 1.0 Å. For R-attack, all frames were clustered, resulting in 10 clusters of greater than 1% weight. Lower weight clusters were manually inspected and verified that they contained no additional conformations of interest. The central frame from each cluster was then optimized using DFT, resulting in 9 unique TSs to (*R*) product. The same procedure was followed for S-attack, with all frames clustered, resulting in 9 clusters of over 1% weighting, and 9 unique DFT optimized TSs to (*S*) product. Manual sampling was used to augment the low energy conformers of the ensemble, resulting in a total of 37 TSs.

The TSs span an energy range of 46 kJ/mol. The ensemble indicates that (*S*) catalyst affords (*S*) product, however with greatly overestimated enantioselectivity of 98.6:1.4 e.r. in 1,2-dichloroethane at 298.15 K ($\Delta\Delta G^\ddagger = 12.6$ kJ/mol compared to experiment of approximately 3.5 kJ/mol). The major enantiomer is in agreement with crystallography, suggesting that a low energy TS to minor product is missing despite extensive effort to locate it. The structural similarity of the lowest energy TS to major product to the lowest energy TSs with cis substrate, and its low energy compared to all the located minor TSs with trans substrate gives confidence that the lowest energy TS to major product has indeed been located. The Gibbs free energy distribution of the low energy TSs is illustrated in Figure S28. Key geometric parameters for the lowest energy TSs are tabulated in Table S22. The lowest energy TS to major product, **TS_{Major}-Trans** is shown in Figure S29.

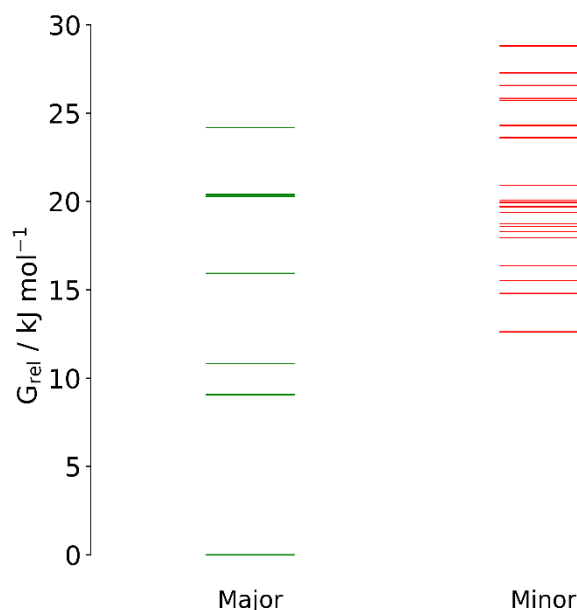


Figure S28: Gibbs free energy distribution of TSs in the ensemble. **TS_{Major}-Trans** is significantly lower in Gibbs free energy than all other TSs located.

Table S22: Key geometric parameters for the transition state structures

TS	Imag.	Key Distances/ Å				Key Angle ^o				
		C-F	C-N	HB 1	HB 2	HB 3	Pucker	Benzhydryl	Backbone	
TS_Trans-Azet-major1	-645.8	1.845	1.953	1.827	1.837	1.831	148.2	-15.8	172.8	74.5
TS_Trans-Azet-major2	-646.0	1.843	1.954	1.819	1.850	1.826	145.7	-15.0	172.2	70.1
TS_Trans-Azet-major3	-653.9	1.826	1.960	1.868	1.838	1.822	146.1	-1.8	-163.7	74.1
TS_Trans-Azet-major4	-640.5	1.859	1.993	1.812	1.761	2.005	143.9	-15.7	59.2	71.3
TS_Trans-Azet-major5	-639.2	1.849	1.972	1.925	1.775	1.820	161.2	-22.6	170.2	86.1
TS_Trans-Azet-major6	-639.2	1.849	1.972	1.925	1.774	1.820	161.2	-22.6	170.2	86.0
TS_Trans-Azet-major7	-646.0	1.861	1.958	2.033	1.822	1.873	142.0	-16.0	166.3	75.3
TS_Trans-Azet-major8	-640.7	1.844	1.986	1.868	1.747	1.943	144.0	-16.9	171.1	75.8
TS_Trans-Azet-major9	-646.7	1.846	1.960	1.914	1.748	2.022	131.9	-19.2	-173.6	106.7
TS_Trans-Azet-major10	-654.7	1.813	1.943	1.814	1.822	1.960	139.3	12.8	172.9	105.3
TS_Trans-Azet-minor1	-648.7	1.842	1.977	1.786	1.968	1.849	147.9	13.7	60.3	74.5
TS_Trans-Azet-minor2	-642.4	1.823	1.994	1.836	1.851	1.778	162.1	19.8	-58.7	88.0
TS_Trans-Azet-minor3	-643.5	1.855	1.962	1.769	1.892	1.916	142.4	-16.0	-60.5	69.1
TS_Trans-Azet-minor4	-653.7	1.829	1.970	1.798	1.928	1.874	147.7	6.9	-71.9	71.9
TS_Trans-Azet-minor5	-648.1	1.837	1.967	1.848	1.965	1.844	147.6	3.0	-72.3	74.3
TS_Trans-Azet-minor6	-652.0	1.840	1.974	1.820	1.878	1.923	145.4	-15.0	65.5	71.6
TS_Trans-Azet-minor7	-652.7	1.859	1.983	1.847	1.801	1.976	147.8	-12.1	-51.2	69.2
TS_Trans-Azet-minor8	-652.7	1.859	1.981	1.818	1.837	1.949	147.4	-13.0	-52.5	69.5
TS_Trans-Azet-minor9	-642.7	1.889	1.984	1.843	2.000	1.878	147.0	15.1	-67.5	74.1
TS_Trans-Azet-minor10	-648.8	1.837	1.974	1.874	1.853	1.819	149.9	16.2	168.5	82.3
TS_Trans-Azet-minor11	-653.6	1.833	1.971	1.802	1.922	1.899	147.4	7.4	-72.3	72.0
TS_Trans-Azet-minor12	-647.7	1.879	1.987	1.909	1.753	2.014	145.3	-20.2	-52.9	69.9
TS_Trans-Azet-minor13	-647.7	1.850	1.975	1.773	2.015	1.879	149.9	-14.8	-72.6	73.5
TS_Trans-Azet-minor14	-649.1	1.870	1.984	1.845	1.915	1.953	146.8	-2.4	-57.9	69.8
TS_Trans-Azet-minor15	-651.1	1.834	1.967	1.829	1.974	1.848	143.9	1.9	-71.6	70.7
TS_Trans-Azet-minor16	-649.0	1.835	1.974	1.864	1.863	1.825	147.8	16.3	169.3	78.4
TS_Trans-Azet-minor17	-654.5	1.848	1.974	1.899	1.780	1.981	146.7	-13.8	64.3	68.8
TS_Trans-Azet-minor18	-644.2	1.888	1.989	1.860	1.856	1.975	147.7	-18.4	-59.9	70.1
TS_Trans-Azet-minor19	-648.5	1.853	1.970	1.908	1.761	1.873	149.2	-18.9	-39.0	69.8
TS_Trans-Azet-minor20	-646.6	1.847	1.976	1.850	1.930	1.902	149.3	8.5	-45.0	74.0

TS_{Major}-Trans

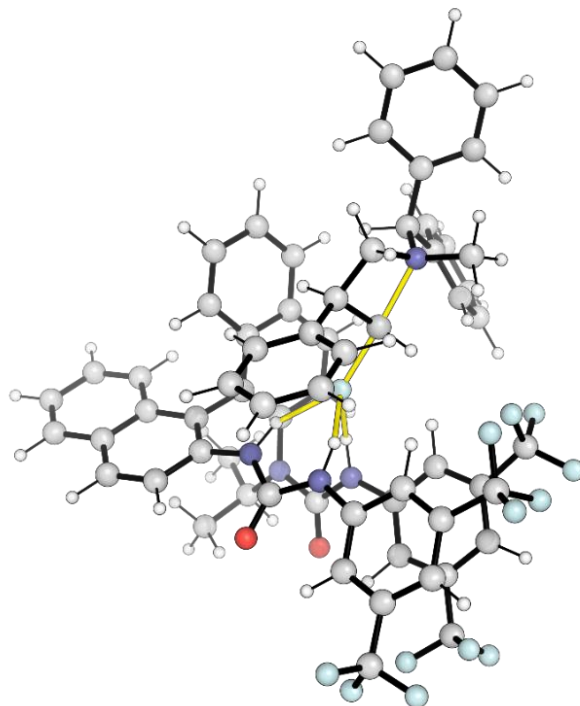


Figure S29: Lowest energy TS to major product

Non-covalent Interactions

Non-covalent interactions play a key role in docking the substrate with the catalyst-fluoride complex. These non-covalent interactions are visualized in Figure S30 using the non-covalent interaction index. **TS_{Major}-Trans** features similar NCIs to the TSs with cis substrate, with face-to-face π -interaction between azetidinium phenyl group and catalyst urea group, and a cation- π interaction between azetidinium and BINAM backbone.

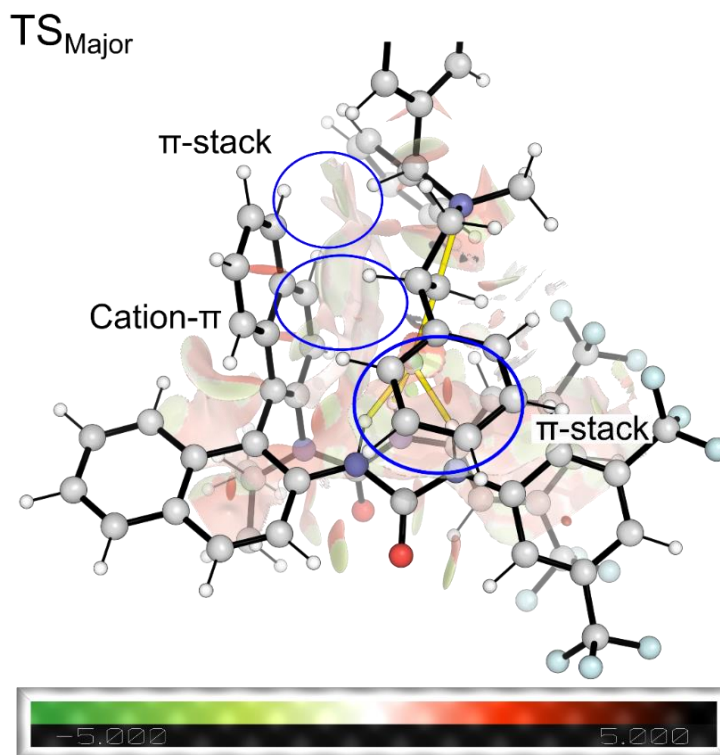


Figure S30: Non-covalent Interaction plots for **TS_{Major}-Trans**

Comparison of Cis and Trans TSs

Transition state structures with cis and trans substrate are superimposed in Figure S31.

TS_{Major} Superposition (TS_{Major}-Cis (red), TS_{Major}-Trans (blue))

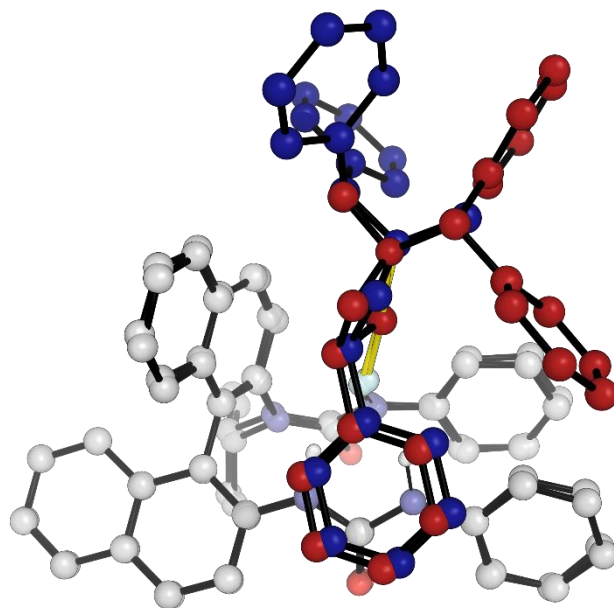


Figure S31: Superpositions of major and minor TSs with cis and trans substrates. Cis in green, trans in blue.

The major TSs with cis and trans substrate superimpose very well. Catalyst geometry is identical, and the substrates also superimpose very well, with the exception of the benzhydryl group pointing in opposite directions. The phenyl group directly bonded to the azetidinium aligns very well, forming a face-to-face interaction with the bidentate urea in both cases and dominating the docking pose of the substrate. The benzhydryl group, despite its steric bulk, projects away from the catalyst and into solvent, having a relatively minor effect on the TSs and enantioselectivity. In the TS with cis substrate, the benzhydryl group can form an intramolecular CH- π interaction whereas with the trans substrate, it can form an edge-to-face π -interaction with the BINAM backbone of the catalyst.

Origins of enantioconvergence of cis and trans azetidinium ions

The key reason for enantioconvergence is the importance of the azetidinium phenyl group in orienting the azetidinium ion in the catalytic pocket, and the lower importance of the orientation of the benzhydryl. The importance of the former is due to the shape complementarity of the ion and the catalyst, with phenyl group lying across the face of the bidentate urea. The lower importance of the latter is due to nitrogen substituents pointing out of the catalyst pocket and into solvent, despite the steric bulk of the group. The stereochemistry of the product is determined by the position of fluoride attack relative to the orientation of the azetidinium phenyl ring (the stereochemistry about nitrogen is lost in the product), and so fluoride favors attack at the same carbon regardless of whether the ion is cis or trans.

Generalization to Other Azetidinium Ions

A diverse range of azetidinium ions feature in the manuscript, not all of which have a phenyl group directly bonded to the azetidinium ring, nor Me/Et and Bzh nitrogen substituents. The TS model described above may be safely generalized to some substrates but can only give qualitative insight into others.

Substrates with different nitrogen substituents: The allyl group behaves similarly to the ethyl group in calculations with uncoordinated fluoride and so the TS model is expected to generalize well to *N*-allyl substrates. An *N*-Bn group is substantially larger and can form CH- π interactions, potentially having a large

effect. However, the overlay of the major TSs for cis and trans substrates shows an almost perfect overlay (Figure S31), demonstrating that the catalytic pocket is able to accommodate a Bzh group in both cis and trans positions simultaneously, ignoring intramolecular clash. Envisaging the substrate with *N*-Bn and Bzh (minus one phenyl group), suggests directly TSs for both the cis and trans substrates, avoiding significant reorganization of the TS, and avoiding further steric clash (Figure S32). It is therefore plausible that these remain the lowest energy TSs.

Plausible Major TS for **Azet**_{Bzh,Bn}, with Bzh group cis – Red and purple.

Plausible Major TS for **Azet**_{Bzh,Bn}, with Bzh group trans – Blue and purple.

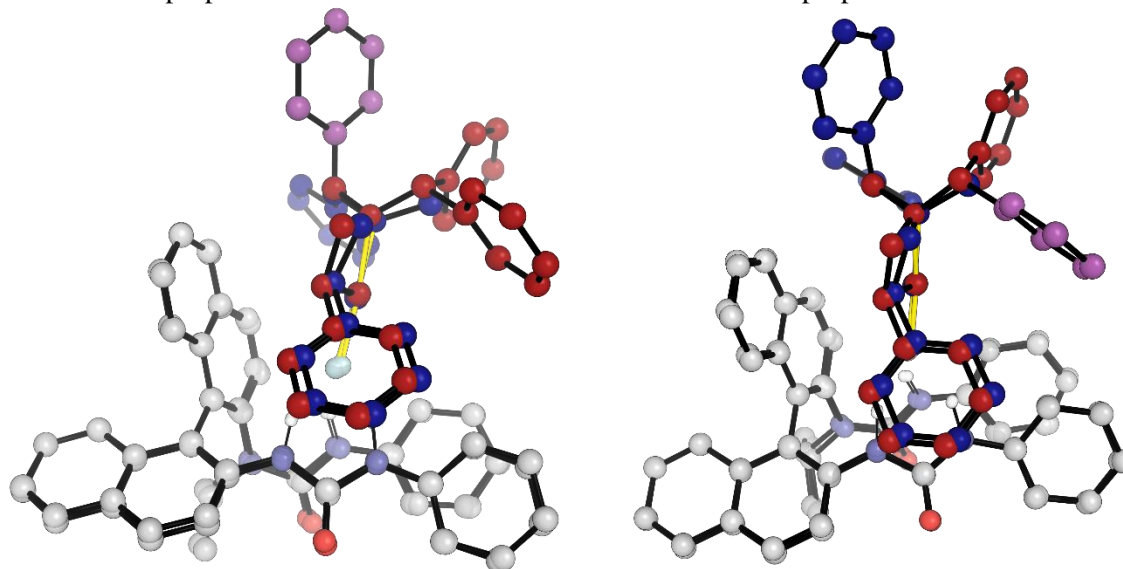


Figure S32: Plausible lowest energy TSs to major product with **Azet**_{Bzh,Bn}, both cis and trans isomers, as implied by the lowest energy TSs to major product with **Azet**_{Bzh,Me}. Cis substrate is given in red, and trans in blue. The perfect overlay of the substrates suggests plausible positions for the additional *N*-Bn group in place of methyl (purple).

Substrates with different substituents bonded to the azetidinium ring (in place of phenyl): When this substituent is a substituted aryl group it is unlikely that the TSs will change significantly as the substituents can point away from the catalyst. All are also capable of forming the same π interactions. With other substituents without a directly bonded aromatic, such as OBn and OMe, it is likely that the TSs will change significantly, due to different favored conformations and an inability to form an intramolecular CH- π interaction. The general factors that govern the TS geometries are, however, likely to be conserved i) the broad shape of the substrate is unchanged (the substituent projects from the azetidinium ion at the same angle), so similar docking poses will be favored ii) the lack of π -interactions with the catalyst for substituents such as OMe affects TSs to major and minor products in the same way iii) the π -interactions and the general positioning of the Bzh groups are unchanged iv) most TSs do not feature an intramolecular CH- π interaction, which this substrate cannot form.

Summary of Computational Work

- i) The difference in reactivity of different *N*-substituted azetidinium ions is explained by the relative energies of the transition state structures to fluoride delivery. Good correlation is seen between increasing experimental yield and decreasing reaction barrier.
- ii) Azetidinium ions with *N*-benzhydryl group have lower energy, and earlier fluoride delivery TSs. The ground state C-N bond length are also elongated, consistent with a less thermodynamically stable ion.
- iii) Much smaller differences are seen changing azetidinium *N*-substituents from Me to Bn, than converting Bn to Bzh, consistent with experimental observation.

- iv) Poor correlation is seen between azetidinium-fluoride ion pair binding energy and experimental yield under HB PTC. The *N*-substituents determine how closely, and the geometry in which, the fluoride can approach the quaternary nitrogen.
- v) Good correlation between fluoride delivery TS energies and yield supports that fluoride delivery in the catalyzed reaction is turnover determining (TDTS). Poor correlation of azetidinium fluoride binding energies with yield is inconsistent with a turnover determining azetidinium assisted phase-transfer process.
- vi) Relatively weak binding of the azetidinium ion to fluoride and a CsF ion pair – far inferior to the urea hydrogen bond donor – is not consistent with the azetidinium ion playing a significant role in CsF phase-transfer.
- vii) Enantioconvergence of *cis* and *trans* substrates occurs as the dominant factor in orienting the azetidinium ion in the catalyst pocket is the phenyl ring directly bonded to the azetidinium ring, whereas the benzhydryl substituent largely projects into solvent and has lower geometric preference. As the position of fluoride delivery relative to the former determines the configuration of the product, the major product is invariant to the configuration at nitrogen.

Tabulated Thermochemical Data

Conformers containing a single low imaginary frequency are identified by * next to the name. Only significant conformers were reoptimized to remove these frequencies.

Azetidinium ions

Table S23: Azet_{Me,Me}

	Energy (opt)	G (opt)	G-qh (opt)	E (sp)	G-qh (sp)
Azet_Me_Me_1	-482.790099	-482.570035	-482.569047	-483.425336	-483.204285
Azet_Me_Me_2	-482.789334	-482.570039	-482.568864	-483.424241	-483.203771
Azet_Me_Me_3	-482.789113	-482.569459	-482.568327	-483.423418	-483.202631

Table S24: Azet_{Bn,Me}

	Energy (opt)	G (opt)	G-qh (opt)	E (sp)	G-qh (sp)
Azet_Bn_Me_1	-713.579911	-713.285084	-713.282285	-714.492942	-714.195317
Azet_Bn_Me_2	-713.579911	-713.285070	-713.282279	-714.492943	-714.195312
Azet_Bn_Me_3	-713.582384	-713.286139	-713.284038	-714.493448	-714.195102
Azet_Bn_Me_4	-713.579912	-713.284325	-713.281781	-714.492821	-714.194690
Azet_Bn_Me_5	-713.579167	-713.285321	-713.282123	-714.491623	-714.194578
Azet_Bn_Me_6	-713.579276	-713.283691	-713.281285	-714.490948	-714.192956
Azet_Bn_Me_7	-713.579276	-713.283688	-713.281284	-714.490948	-714.192955
Azet_Bn_Me_8	-713.581435	-713.284250	-713.282685	-714.491593	-714.192843

Table S25: Azet_{Bn,Bn}

	Energy (opt)	G (opt)	G-qh (opt)	E (sp)	G-qh (sp)
Azet_Bn_Bn_1	-944.368987	-943.998373	-943.993976	-945.559212	-945.184201
Azet_Bn_Bn_2	-944.371126	-943.999223	-943.995352	-945.559951	-945.184177
Azet_Bn_Bn_3	-944.371126	-943.999216	-943.995347	-945.559949	-945.184170
Azet_Bn_Bn_4	-944.368192	-943.998609	-943.993911	-945.557888	-945.183606
Azet_Bn_Bn_5	-944.371771	-943.998686	-943.995264	-945.559695	-945.183188
Azet_Bn_Bn_6	-944.369345	-943.998408	-943.994220	-945.558219	-945.183093
Azet_Bn_Bn_7	-944.370320	-943.998548	-943.994997	-945.558203	-945.182880
Azet_Bn_Bn_8*	-944.369739	-943.997336	-943.993743	-945.558843	-945.182847
Azet_Bn_Bn_9	-944.370131	-943.997804	-943.994383	-945.558109	-945.182361
Azet_Bn_Bn_10	-944.366682	-943.996835	-943.992094	-945.556741	-945.182152
Azet_Bn_Bn_11	-944.365984	-943.995179	-943.990918	-945.556731	-945.181665
Azet_Bn_Bn_12	-944.365892	-943.996849	-943.991874	-945.555458	-945.181441
Azet_Bn_Bn_13	-944.367747	-943.996478	-943.992364	-945.556799	-945.181416

Azet_Bn_Bn_14	-944.365167	-943.994946	-943.990554	-945.555535	-945.180921
Azet_Bn_Bn_15	-944.366130	-943.995337	-943.991017	-945.555642	-945.180530
Azet_Bn_Bn_16	-944.366095	-943.994688	-943.990647	-945.555396	-945.179948
Azet_Bn_Bn_17	-944.366713	-943.995279	-943.991179	-945.555415	-945.179881
Azet_Bn_Bn_18	-944.366713	-943.995277	-943.991177	-945.555413	-945.179877
Azet_Bn_Bn_19	-944.365366	-943.995070	-943.990597	-945.554360	-945.179591
Azet_Bn_Bn_20	-944.364853	-943.993512	-943.989366	-945.554607	-945.179119
Azet_Bn_Bn_21	-944.364898	-943.993277	-943.989487	-945.554226	-945.178815
Azet_Bn_Bn_22	-944.364160	-943.993126	-943.989146	-945.553013	-945.178000
Azet_Bn_Bn_23	-944.363099	-943.992226	-943.988165	-945.552587	-945.177653
Azet_Bn_Bn_24	-944.364800	-943.992489	-943.988868	-945.552737	-945.176806
Azet_Bn_Bn_25	-944.362337	-943.991912	-943.987738	-945.551286	-945.176686
Azet_Bn_Bn_26	-944.362136	-943.990564	-943.986702	-945.550720	-945.175285

Table S26: Azet_{Bzh,Me}

	Energy (opt)	G (opt)	G-qh (opt)	E (sp)	G-qh (sp)
Azet_Bzh_Me_1	-944.367813	-943.995205	-943.991987	-945.555383	-945.179557
Azet_Bzh_Me_2	-944.367813	-943.995205	-943.991986	-945.555383	-945.179556
Azet_Bzh_Me_3	-944.366038	-943.993893	-943.990579	-945.553972	-945.178513
Azet_Bzh_Me_4	-944.366038	-943.993890	-943.990578	-945.553971	-945.178512
Azet_Bzh_Me_5	-944.362396	-943.991924	-943.987628	-945.552681	-945.177913
Azet_Bzh_Me_6	-944.362396	-943.991920	-943.987626	-945.552680	-945.177909
Azet_Bzh_Me_7	-944.366247	-943.993747	-943.990578	-945.553124	-945.177455
Azet_Bzh_Me_8	-944.361644	-943.992594	-943.987735	-945.551288	-945.177379
Azet_Bzh_Me_9	-944.363196	-943.992637	-943.988472	-945.551935	-945.177210
Azet_Bzh_Me_10	-944.361654	-943.991789	-943.987313	-945.551219	-945.176878
Azet_Bzh_Me_11	-944.361674	-943.991951	-943.987432	-945.550688	-945.176446
Azet_Bzh_Me_12	-944.362361	-943.991696	-943.987464	-945.550999	-945.176102
Azet_Bzh_Me_13	-944.362419	-943.992271	-943.988023	-945.550454	-945.176058
Azet_Bzh_Me_14	-944.362419	-943.992270	-943.988023	-945.550452	-945.176056
Azet_Bzh_Me_15	-944.362405	-943.990428	-943.986820	-945.549572	-945.173988
Azet_Bzh_Me_16	-944.362405	-943.990426	-943.986819	-945.549573	-945.173987

Table S27: Azet_{Bzh,Et}

	Energy (opt)	G (opt)	G-qh (opt)	E (sp)	G-qh (sp)
Azet_Bzh_Et_1	-983.634301	-983.234541	-983.231149	-984.876229	-984.473076
Azet_Bzh_Et_2	-983.633131	-983.233601	-983.230142	-984.874432	-984.471443
Azet_Bzh_Et_3	-983.629538	-983.232088	-983.227647	-984.872557	-984.470666
Azet_Bzh_Et_4	-983.629537	-983.232073	-983.227640	-984.872551	-984.470654
Azet_Bzh_Et_5	-983.631423	-983.231881	-983.228419	-984.873657	-984.470654
Azet_Bzh_Et_6	-983.625744	-983.228246	-983.223676	-984.870710	-984.468641
Azet_Bzh_Et_7	-983.627180	-983.229348	-983.224994	-984.870643	-984.468457
Azet_Bzh_Et_8	-983.624960	-983.228869	-983.223695	-984.869247	-984.467982
Azet_Bzh_Et_9	-983.628084	-983.228649	-983.225140	-984.870477	-984.467533
Azet_Bzh_Et_10	-983.626448	-983.229029	-983.224576	-984.869283	-984.467410
Azet_Bzh_Et_11	-983.626939	-983.227929	-983.224037	-984.868776	-984.465874
Azet_Bzh_Et_12	-983.626939	-983.227928	-983.224036	-984.868776	-984.465872
Azet_Bzh_Et_13	-983.627110	-983.226587	-983.223583	-984.868821	-984.465294
Azet_Bzh_Et_14	-983.624401	-983.226104	-983.221969	-984.867620	-984.465188
Azet_Bzh_Et_15	-983.624881	-983.225629	-983.221792	-984.868242	-984.465153
Azet_Bzh_Et_16	-983.624445	-983.226586	-983.222421	-984.866967	-984.464943
Azet_Bzh_Et_17*	-983.625266	-983.225268	-983.222119	-984.868057	-984.464910
Azet_Bzh_Et_18	-983.624682	-983.226170	-983.222267	-984.866452	-984.464036
Azet_Bzh_Et_19	-983.623107	-983.224651	-983.220555	-984.866506	-984.463954
Azet_Bzh_Et_20	-983.623107	-983.224647	-983.220553	-984.866506	-984.463952
Azet_Bzh_Et_21	-983.623655	-983.225371	-983.221231	-984.866216	-984.463792
Azet_Bzh_Et_22	-983.622222	-983.225061	-983.220516	-984.865165	-984.463459
Azet_Bzh_Et_23	-983.621959	-983.222202	-983.218684	-984.863978	-984.460703

Table S28: Azet_{Bzh,Allyl}

	Energy (opt)	G (opt)	G-qh (opt)	E (sp)	G-qh (sp)
Azet_Bzh_All_1	-1021.669513	-1021.266432	-1021.262689	-1022.954453	-1022.547630
Azet_Bzh_All_2	-1021.668952	-1021.265715	-1021.261847	-1022.954069	-1022.546964
Azet_Bzh_All_3	-1021.667432	-1021.266083	-1021.261336	-1022.952648	-1022.546552
Azet_Bzh_All_4	-1021.668367	-1021.265589	-1021.261678	-1022.952824	-1022.546136
Azet_Bzh_All_5	-1021.668367	-1021.265485	-1021.261628	-1022.952811	-1022.546072
Azet_Bzh_All_6	-1021.667438	-1021.265278	-1021.260962	-1022.952287	-1022.545810
Azet_Bzh_All_7	-1021.666874	-1021.264513	-1021.260509	-1022.952173	-1022.545808
Azet_Bzh_All_8	-1021.667048	-1021.264337	-1021.260393	-1022.952333	-1022.545678
Azet_Bzh_All_9	-1021.665329	-1021.263801	-1021.259262	-1022.951132	-1022.545065
Azet_Bzh_All_10	-1021.665329	-1021.263800	-1021.259261	-1022.951131	-1022.545063
Azet_Bzh_All_11	-1021.665293	-1021.263354	-1021.258896	-1022.950289	-1022.543892
Azet_Bzh_All_12	-1021.665293	-1021.263347	-1021.258893	-1022.950287	-1022.543887
Azet_Bzh_All_13	-1021.662626	-1021.261632	-1021.256792	-1022.949346	-1022.543511
Azet_Bzh_All_14	-1021.662626	-1021.261621	-1021.256786	-1022.949346	-1022.543506
Azet_Bzh_All_15	-1021.661259	-1021.259743	-1021.255026	-1022.949473	-1022.543241
Azet_Bzh_All_16	-1021.662724	-1021.261068	-1021.256334	-1022.949402	-1022.543012
Azet_Bzh_All_17	-1021.664677	-1021.261520	-1021.257602	-1022.949758	-1022.542682
Azet_Bzh_All_18	-1021.664591	-1021.261601	-1021.257736	-1022.949511	-1022.542655
Azet_Bzh_All_19	-1021.661995	-1021.261353	-1021.256275	-1022.947997	-1022.542276
Azet_Bzh_All_20	-1021.663834	-1021.260471	-1021.256965	-1022.949144	-1022.542275
Azet_Bzh_All_21	-1021.661977	-1021.261033	-1021.256163	-1022.947914	-1022.542100
Azet_Bzh_All_22	-1021.661342	-1021.260574	-1021.255873	-1022.947441	-1022.541972
Azet_Bzh_All_23	-1021.661191	-1021.260183	-1021.255264	-1022.947729	-1022.541802
Azet_Bzh_All_24	-1021.663626	-1021.260723	-1021.256901	-1022.948072	-1022.541348
Azet_Bzh_All_25	-1021.663626	-1021.260722	-1021.256901	-1022.948071	-1022.541346
Azet_Bzh_All_26	-1021.660556	-1021.260120	-1021.255306	-1022.946188	-1022.540939
Azet_Bzh_All_27	-1021.660344	-1021.258506	-1021.253921	-1022.947109	-1022.540685
Azet_Bzh_All_28	-1021.662009	-1021.260021	-1021.255543	-1022.947110	-1022.540645
Azet_Bzh_All_29	-1021.662008	-1021.260015	-1021.255541	-1022.947109	-1022.540642
Azet_Bzh_All_30	-1021.662662	-1021.259206	-1021.255897	-1022.947363	-1022.540598
Azet_Bzh_All_31	-1021.661729	-1021.259922	-1021.255309	-1022.946867	-1022.540446
Azet_Bzh_All_32	-1021.659624	-1021.258276	-1021.253515	-1022.946247	-1022.540138
Azet_Bzh_All_33	-1021.663135	-1021.259035	-1021.255543	-1022.947714	-1022.540122
Azet_Bzh_All_34	-1021.663135	-1021.259032	-1021.255542	-1022.947712	-1022.540118
Azet_Bzh_All_35	-1021.659987	-1021.257785	-1021.253336	-1022.946653	-1022.540002
Azet_Bzh_All_36	-1021.658996	-1021.257885	-1021.253598	-1022.945268	-1022.539870
Azet_Bzh_All_37	-1021.659455	-1021.257899	-1021.253346	-1022.945898	-1022.539790
Azet_Bzh_All_38	-1021.659455	-1021.257898	-1021.253346	-1022.945897	-1022.539788
Azet_Bzh_All_39	-1021.660452	-1021.259319	-1021.254590	-1022.945464	-1022.539602
Azet_Bzh_All_40	-1021.659222	-1021.258287	-1021.253224	-1022.945310	-1022.539312
Azet_Bzh_All_41	-1021.660221	-1021.258182	-1021.253604	-1022.945711	-1022.539094
Azet_Bzh_All_42	-1021.657300	-1021.257446	-1021.252287	-1022.944094	-1022.539080
Azet_Bzh_All_43	-1021.658108	-1021.257811	-1021.253173	-1022.944001	-1022.539065
Azet_Bzh_All_44	-1021.658530	-1021.256227	-1021.251924	-1022.945512	-1022.538906
Azet_Bzh_All_45	-1021.659586	-1021.257500	-1021.253253	-1022.945027	-1022.538693
Azet_Bzh_All_46	-1021.658580	-1021.257067	-1021.252572	-1022.944543	-1022.538535
Azet_Bzh_All_47	-1021.659290	-1021.256835	-1021.253046	-1022.944322	-1022.538078
Azet_Bzh_All_48	-1021.658779	-1021.257368	-1021.252841	-1022.943929	-1022.537991
Azet_Bzh_All_49	-1021.658874	-1021.256044	-1021.251998	-1022.944802	-1022.537926
Azet_Bzh_All_50	-1021.658413	-1021.254738	-1021.251171	-1022.943559	-1022.536317
Azet_Bzh_All_51	-1021.658413	-1021.254736	-1021.251172	-1022.943552	-1022.536312
Azet_Bzh_All_52	-1021.655555	-1021.252235	-1021.248250	-1022.943295	-1022.535989
Azet_Bzh_All_53	-1021.657153	-1021.254366	-1021.250285	-1022.942619	-1022.535751
Azet_Bzh_All_54	-1021.654302	-1021.253332	-1021.248303	-1022.940491	-1022.534492
Azet_Bzh_All_55	-1021.655652	-1021.253294	-1021.248989	-1022.940096	-1022.533433
Azet_Bzh_All_56	-1021.656226	-1021.253050	-1021.249393	-1022.939827	-1022.532993

Table S29: Azet_{Bzh,Bn}

	Energy (opt)	G (opt)	G-qh (opt)	E (sp)	G-qh (sp)
Azet_Bzh_Bn_1	-1175.156809	-1174.709106	-1174.703834	-1176.621556	-1176.168581
Azet_Bzh_Bn_2	-1175.156448	-1174.708435	-1174.703410	-1176.621277	-1176.168239
Azet_Bzh_Bn_3	-1175.156515	-1174.707931	-1174.703259	-1176.620081	-1176.166825
Azet_Bzh_Bn_4	-1175.156515	-1174.707925	-1174.703255	-1176.620080	-1176.166820
Azet_Bzh_Bn_5	-1175.152032	-1174.706731	-1174.700431	-1176.618411	-1176.166809
Azet_Bzh_Bn_6	-1175.152032	-1174.706687	-1174.700409	-1176.618411	-1176.166788
Azet_Bzh_Bn_7	-1175.154226	-1174.707105	-1174.701663	-1176.618903	-1176.166339
Azet_Bzh_Bn_8	-1175.151323	-1174.705157	-1174.699222	-1176.616910	-1176.164809
Azet_Bzh_Bn_9	-1175.151324	-1174.705015	-1174.699152	-1176.616915	-1176.164744
Azet_Bzh_Bn_10*	-1175.150684	-1174.701586	-1174.696897	-1176.618414	-1176.164627
Azet_Bzh_Bn_11	-1175.149918	-1174.703972	-1174.697845	-1176.616605	-1176.164532
Azet_Bzh_Bn_12	-1175.153734	-1174.704987	-1174.700500	-1176.617666	-1176.164433
Azet_Bzh_Bn_13*	-1175.149846	-1174.701752	-1174.696687	-1176.616912	-1176.163753
Azet_Bzh_Bn_14	-1175.149981	-1174.703267	-1174.697500	-1176.616198	-1176.163718
Azet_Bzh_Bn_15	-1175.149869	-1174.703039	-1174.697240	-1176.616018	-1176.163388
Azet_Bzh_Bn_16	-1175.149623	-1174.702937	-1174.697470	-1176.614989	-1176.162835
Azet_Bzh_Bn_17	-1175.150583	-1174.703600	-1174.697904	-1176.615162	-1176.162483
Azet_Bzh_Bn_18	-1175.152544	-1174.702858	-1174.698926	-1176.615723	-1176.162105
Azet_Bzh_Bn_19	-1175.147141	-1174.699977	-1174.694432	-1176.613926	-1176.161217
Azet_Bzh_Bn_20	-1175.148805	-1174.701643	-1174.696022	-1176.613888	-1176.161105
Azet_Bzh_Bn_21	-1175.148663	-1174.699907	-1174.695296	-1176.613882	-1176.160514
Azet_Bzh_Bn_22	-1175.148333	-1174.699865	-1174.695127	-1176.613014	-1176.159808
Azet_Bzh_Bn_23	-1175.146934	-1174.698457	-1174.693794	-1176.612543	-1176.159402
Azet_Bzh_Bn_24	-1175.146934	-1174.698440	-1174.693784	-1176.612540	-1176.159389
Azet_Bzh_Bn_25	-1175.147325	-1174.699867	-1174.694669	-1176.611572	-1176.158915
Azet_Bzh_Bn_26	-1175.148472	-1174.698747	-1174.694417	-1176.612604	-1176.158549
Azet_Bzh_Bn_27	-1175.148472	-1174.698749	-1174.694418	-1176.612602	-1176.158548
Azet_Bzh_Bn_28	-1175.146116	-1174.698070	-1174.693306	-1176.611063	-1176.158253
Azet_Bzh_Bn_29	-1175.148535	-1174.697963	-1174.693964	-1176.610848	-1176.156276

Azetidinium-Fluoride Ion Pairs**Table S30: Azet_{Me,Me}**

	Energy (opt)	G (opt)	G-qh (opt)	E (sp)	G-qh (sp)
Azet_Me_Me_F_1	-582.677639	-582.460844	-582.458859	-583.439845	-583.221065
Azet_Me_Me_F_2	-582.673553	-582.456974	-582.455031	-583.439000	-583.220478
Azet_Me_Me_F_3	-582.672790	-582.456562	-582.454584	-583.437988	-583.219782
Azet_Me_Me_F_4	-582.674890	-582.457172	-582.455733	-583.438576	-583.219418
Azet_Me_Me_F_5	-582.674890	-582.457167	-582.455730	-583.438574	-583.219415
Azet_Me_Me_F_6	-582.674159	-582.457594	-582.455722	-583.437323	-583.218885
Azet_Me_Me_F_7	-582.674710	-582.457174	-582.455690	-583.437505	-583.218485
Azet_Me_Me_F_8	-582.675630	-582.458535	-582.456846	-583.437266	-583.218482
Azet_Me_Me_F_9	-582.673867	-582.456746	-582.455008	-583.436531	-583.217672
Azet_Me_Me_F_10	-582.673868	-582.456723	-582.454995	-583.436522	-583.217649
Azet_Me_Me_F_11	-582.672584	-582.455852	-582.454026	-583.435937	-583.217379
Azet_Me_Me_F_12	-582.672584	-582.455783	-582.453989	-583.435942	-583.217347
Azet_Me_Me_F_13	-582.659366	-582.443906	-582.441487	-583.428883	-583.211004
Azet_Me_Me_F_14	-582.658450	-582.444154	-582.441198	-583.427697	-583.210445
Azet_Me_Me_F_15	-582.659493	-582.443072	-582.441224	-583.428357	-583.210087
Azet_Me_Me_F_16	-582.659682	-582.443009	-582.441092	-583.427670	-583.209080
Azet_Me_Me_F_17	-582.658670	-582.443162	-582.440636	-583.426981	-583.208948

Table S31: Azet_{Bn,Me}

	Energy (opt)	G (opt)	G-qh (opt)	E (sp)	G-qh (sp)
Azet_Bn_Me_F_1	-813.470129	-813.176288	-813.173393	-814.508720	-814.211984
Azet_Bn_Me_F_2	-813.470130	-813.176295	-813.173396	-814.508717	-814.211983
Azet_Bn_Me_F_3	-813.465220	-813.173055	-813.169316	-814.506990	-814.211087

Azet_Bn_Me_F_4	-813.463354	-813.172073	-813.168022	-814.506330	-814.210998
Azet_Bn_Me_F_5	-813.465038	-813.173390	-813.169671	-814.505656	-814.210289
Azet_Bn_Me_F_6	-813.466822	-813.174664	-813.171093	-814.505844	-814.210115
Azet_Bn_Me_F_7	-813.466822	-813.174647	-813.171087	-814.505838	-814.210103
Azet_Bn_Me_F_8	-813.462575	-813.171197	-813.167316	-814.505312	-814.210053
Azet_Bn_Me_F_9	-813.465445	-813.171673	-813.168773	-814.506683	-814.210011
Azet_Bn_Me_F_10	-813.469365	-813.174314	-813.172014	-814.506927	-814.209576
Azet_Bn_Me_F_11	-813.464877	-813.172602	-813.169052	-814.504892	-814.209066
Azet_Bn_Me_F_12	-813.464877	-813.172599	-813.169051	-814.504890	-814.209064
Azet_Bn_Me_F_13	-813.461444	-813.169364	-813.165877	-814.504608	-814.209041
Azet_Bn_Me_F_14	-813.461444	-813.169350	-813.165871	-814.504602	-814.209029
Azet_Bn_Me_F_15	-813.465758	-813.172394	-813.169392	-814.504837	-814.208471
Azet_Bn_Me_F_16	-813.465759	-813.172380	-813.169385	-814.504832	-814.208458
Azet_Bn_Me_F_17	-813.460921	-813.168671	-813.165207	-814.503616	-814.207903
Azet_Bn_Me_F_18	-813.468388	-813.172872	-813.171021	-814.505046	-814.207680
Azet_Bn_Me_F_19	-813.466638	-813.171397	-813.169401	-814.504230	-814.206993
Azet_Bn_Me_F_20	-813.466638	-813.171393	-813.169397	-814.504227	-814.206985
Azet_Bn_Me_F_21	-813.455903	-813.164287	-813.160580	-814.499197	-814.203874
Azet_Bn_Me_F_22	-813.453644	-813.162043	-813.158201	-814.498328	-814.202885
Azet_Bn_Me_F_23	-813.456697	-813.162916	-813.160019	-814.498425	-814.201746
Azet_Bn_Me_F_24	-813.456697	-813.162907	-813.160014	-814.498424	-814.201741

Table S32: Azet_{Bn,Bn}

	Energy (opt)	G (opt)	G-gh (opt)	E (sp)	G-gh (sp)
Azet_Bn_Bn_F_1	-1044.258298	-1043.888433	-1043.884060	-1045.574538	-1045.200300
Azet_Bn_Bn_F_2	-1044.258298	-1043.888431	-1043.884059	-1045.574537	-1045.200298
Azet_Bn_Bn_F_3	-1044.256859	-1043.888147	-1043.883205	-1045.573531	-1045.199876
Azet_Bn_Bn_F_4	-1044.259784	-1043.889429	-1043.885193	-1045.574247	-1045.199655
Azet_Bn_Bn_F_5	-1044.259034	-1043.888722	-1043.884569	-1045.573802	-1045.199338
Azet_Bn_Bn_F_6	-1044.256096	-1043.888205	-1043.883022	-1045.572236	-1045.199162
Azet_Bn_Bn_F_7	-1044.256048	-1043.887360	-1043.882385	-1045.572729	-1045.199065
Azet_Bn_Bn_F_8	-1044.256826	-1043.886532	-1043.882393	-1045.573377	-1045.198943
Azet_Bn_Bn_F_9	-1044.256728	-1043.887379	-1043.882696	-1045.572439	-1045.198407
Azet_Bn_Bn_F_10	-1044.258313	-1043.888057	-1043.884041	-1045.572610	-1045.198337
Azet_Bn_Bn_F_11	-1044.255213	-1043.885606	-1043.881249	-1045.572216	-1045.198252
Azet_Bn_Bn_F_12	-1044.257794	-1043.887009	-1043.883305	-1045.572255	-1045.197766
Azet_Bn_Bn_F_13	-1044.257794	-1043.887005	-1043.883303	-1045.572250	-1045.197759
Azet_Bn_Bn_F_14	-1044.254700	-1043.886484	-1043.881338	-1045.570764	-1045.197401
Azet_Bn_Bn_F_15	-1044.255838	-1043.885943	-1043.881552	-1045.571682	-1045.197395
Azet_Bn_Bn_F_16	-1044.257696	-1043.886991	-1043.883266	-1045.571634	-1045.197204
Azet_Bn_Bn_F_17	-1044.252393	-1043.883308	-1043.878833	-1045.570626	-1045.197067
Azet_Bn_Bn_F_18	-1044.257964	-1043.887083	-1043.883361	-1045.571598	-1045.196994
Azet_Bn_Bn_F_19	-1044.255587	-1043.886092	-1043.881601	-1045.570936	-1045.196950
Azet_Bn_Bn_F_20	-1044.254154	-1043.884733	-1043.880575	-1045.570521	-1045.196942
Azet_Bn_Bn_F_21	-1044.252944	-1043.884948	-1043.879792	-1045.570037	-1045.196886
Azet_Bn_Bn_F_22	-1044.255346	-1043.886223	-1043.881515	-1045.570702	-1045.196871
Azet_Bn_Bn_F_23	-1044.252781	-1043.884822	-1043.879641	-1045.569967	-1045.196827
Azet_Bn_Bn_F_24	-1044.253746	-1043.884104	-1043.879788	-1045.570229	-1045.196271
Azet_Bn_Bn_F_25	-1044.251027	-1043.883801	-1043.878512	-1045.568671	-1045.196156
Azet_Bn_Bn_F_26	-1044.251027	-1043.883801	-1043.878512	-1045.568671	-1045.196155
Azet_Bn_Bn_F_27	-1044.251563	-1043.882768	-1043.878093	-1045.569273	-1045.195803
Azet_Bn_Bn_F_28	-1044.253432	-1043.885131	-1043.879969	-1045.569009	-1045.195546
Azet_Bn_Bn_F_29	-1044.253383	-1043.885134	-1043.879977	-1045.568873	-1045.195466
Azet_Bn_Bn_F_30	-1044.253383	-1043.885131	-1043.879975	-1045.568873	-1045.195464

Table S33: Azet_{Bzh,Me}

	Energy (opt)	G (opt)	G-gh (opt)	E (sp)	G-gh (sp)
Azet_Bzh_Me_F_1	-1044.255741	-1043.885965	-1043.881860	-1045.570510	-1045.196628
Azet_Bzh_Me_F_2	-1044.254795	-1043.885884	-1043.881433	-1045.569762	-1045.196401

Azet_Bzh_Me_F_3	-1044.254773	-1043.885488	-1043.880962	-1045.569860	-1045.196050
Azet_Bzh_Me_F_4	-1044.253813	-1043.885075	-1043.880472	-1045.568841	-1045.195500
Azet_Bzh_Me_F_5	-1044.250705	-1043.881568	-1043.877207	-1045.568681	-1045.195183
Azet_Bzh_Me_F_6	-1044.253892	-1043.885215	-1043.880710	-1045.568064	-1045.194882
Azet_Bzh_Me_F_7	-1044.253892	-1043.885212	-1043.880708	-1045.568064	-1045.194880
Azet_Bzh_Me_F_8	-1044.251664	-1043.883560	-1043.878572	-1045.567240	-1045.194148
Azet_Bzh_Me_F_9	-1044.251168	-1043.882011	-1043.877885	-1045.567391	-1045.194108
Azet_Bzh_Me_F_10	-1044.249725	-1043.881576	-1043.876813	-1045.566664	-1045.193752
Azet_Bzh_Me_F_11	-1044.251369	-1043.883230	-1043.878574	-1045.566406	-1045.193611
Azet_Bzh_Me_F_12	-1044.252135	-1043.880591	-1043.877500	-1045.568231	-1045.193596
Azet_Bzh_Me_F_13	-1044.252135	-1043.880583	-1043.877494	-1045.568233	-1045.193592
Azet_Bzh_Me_F_14	-1044.245792	-1043.877773	-1043.872652	-1045.566253	-1045.193114
Azet_Bzh_Me_F_15	-1044.249030	-1043.881656	-1043.876626	-1045.565385	-1045.192981
Azet_Bzh_Me_F_16	-1044.249030	-1043.881550	-1043.876572	-1045.565394	-1045.192936
Azet_Bzh_Me_F_17	-1044.244994	-1043.878885	-1043.872980	-1045.564893	-1045.192880
Azet_Bzh_Me_F_18	-1044.244983	-1043.878274	-1043.872703	-1045.564883	-1045.192604
Azet_Bzh_Me_F_19	-1044.248734	-1043.881589	-1043.876129	-1045.565035	-1045.192429
Azet_Bzh_Me_F_20	-1044.251090	-1043.881728	-1043.877790	-1045.565489	-1045.192188
Azet_Bzh_Me_F_21	-1044.251090	-1043.881699	-1043.877774	-1045.565491	-1045.192175
Azet_Bzh_Me_F_22	-1044.247038	-1043.879920	-1043.874441	-1045.564740	-1045.192144
Azet_Bzh_Me_F_23	-1044.246481	-1043.877578	-1043.873049	-1045.565402	-1045.191970
Azet_Bzh_Me_F_24	-1044.248734	-1043.880683	-1043.875679	-1045.565022	-1045.191968
Azet_Bzh_Me_F_25	-1044.249783	-1043.879671	-1043.876106	-1045.564586	-1045.190909
Azet_Bzh_Me_F_26	-1044.248734	-1043.877977	-1043.874255	-1045.565025	-1045.190546
Azet_Bzh_Me_F_27	-1044.244939	-1043.876811	-1043.872167	-1045.563149	-1045.190376
Azet_Bzh_Me_F_28	-1044.246460	-1043.876436	-1043.872327	-1045.563853	-1045.189720
Azet_Bzh_Me_F_29	-1044.246460	-1043.876434	-1043.872325	-1045.563853	-1045.189718
Azet_Bzh_Me_F_30	-1044.249162	-1043.879508	-1043.875259	-1045.563595	-1045.189692
Azet_Bzh_Me_F_31	-1044.247077	-1043.876365	-1043.872780	-1045.563208	-1045.188911
Azet_Bzh_Me_F_32	-1044.247077	-1043.876355	-1043.872775	-1045.563204	-1045.188902
Azet_Bzh_Me_F_33	-1044.239415	-1043.871832	-1043.866727	-1045.560604	-1045.187917
Azet_Bzh_Me_F_34	-1044.239578	-1043.871057	-1043.866398	-1045.560892	-1045.187712
Azet_Bzh_Me_F_35	-1044.239578	-1043.871054	-1043.866394	-1045.560891	-1045.187707
Azet_Bzh_Me_F_36	-1044.239074	-1043.871006	-1043.866132	-1045.560154	-1045.187212
Azet_Bzh_Me_F_37	-1044.243063	-1043.874258	-1043.869876	-1045.560223	-1045.187036
Azet_Bzh_Me_F_38	-1044.238091	-1043.869907	-1043.865119	-1045.559585	-1045.186613
Azet_Bzh_Me_F_39	-1044.238572	-1043.869573	-1043.865178	-1045.560001	-1045.186607
Azet_Bzh_Me_F_40	-1044.237767	-1043.869782	-1043.864882	-1045.559285	-1045.186401
Azet_Bzh_Me_F_41	-1044.240532	-1043.870942	-1043.866855	-1045.560073	-1045.186396
Azet_Bzh_Me_F_42	-1044.237767	-1043.869763	-1043.864872	-1045.559284	-1045.186389
Azet_Bzh_Me_F_43	-1044.236856	-1043.868040	-1043.863489	-1045.559261	-1045.185894
Azet_Bzh_Me_F_44	-1044.237870	-1043.869939	-1043.865060	-1045.558572	-1045.185763
Azet_Bzh_Me_F_45	-1044.237870	-1043.869897	-1043.865042	-1045.558571	-1045.185744
Azet_Bzh_Me_F_46	-1044.236928	-1043.868330	-1043.863729	-1045.558704	-1045.185505
Azet_Bzh_Me_F_47	-1044.236828	-1043.868188	-1043.863708	-1045.557764	-1045.184644
Azet_Bzh_Me_F_48	-1044.237233	-1043.868387	-1043.863995	-1045.557698	-1045.184460
Azet_Bzh_Me_F_49	-1044.236388	-1043.867729	-1043.863301	-1045.557251	-1045.184163
Azet_Bzh_Me_F_50	-1044.235447	-1043.868057	-1043.863033	-1045.556379	-1045.183965

Table S34: Azet_{Bzh}Et

	Energy (opt)	G (opt)	G-qh (opt)	E (sp)	G-qh (sp)
Azet_Bzh_Et_F_1	-1083.516936	-1083.120077	-1083.115816	-1084.889173	-1084.488053
Azet_Bzh_Et_F_2	-1083.517995	-1083.120794	-1083.116805	-1084.889082	-1084.487892
Azet_Bzh_Et_F_3	-1083.519086	-1083.122576	-1083.118179	-1084.888760	-1084.487854
Azet_Bzh_Et_F_4	-1083.519050	-1083.124015	-1083.119091	-1084.887686	-1084.487728
Azet_Bzh_Et_F_5	-1083.520493	-1083.122445	-1083.118801	-1084.889189	-1084.487497
Azet_Bzh_Et_F_6	-1083.519057	-1083.122789	-1083.118462	-1084.888017	-1084.487422
Azet_Bzh_Et_F_7	-1083.517708	-1083.120376	-1083.116452	-1084.888613	-1084.487357
Azet_Bzh_Et_F_8	-1083.519085	-1083.121395	-1083.117591	-1084.888773	-1084.487280
Azet_Bzh_Et_F_9	-1083.517111	-1083.121436	-1083.116645	-1084.887504	-1084.487038

Azet_Bzh_Et_F_10	-1083.517111	-1083.121421	-1083.116638	-1084.887509	-1084.487035
Azet_Bzh_Et_F_11	-1083.519320	-1083.121717	-1083.117720	-1084.888604	-1084.487004
Azet_Bzh_Et_F_12	-1083.518160	-1083.119604	-1083.116376	-1084.888648	-1084.486865
Azet_Bzh_Et_F_13	-1083.515910	-1083.118796	-1083.114771	-1084.887226	-1084.486088
Azet_Bzh_Et_F_14	-1083.515909	-1083.118787	-1083.114767	-1084.887227	-1084.486085
Azet_Bzh_Et_F_15	-1083.517724	-1083.120321	-1083.116059	-1084.887617	-1084.485952
Azet_Bzh_Et_F_16	-1083.516638	-1083.118953	-1083.115374	-1084.886914	-1084.485651
Azet_Bzh_Et_F_17	-1083.517570	-1083.119697	-1083.116107	-1084.886521	-1084.485058
Azet_Bzh_Et_F_18	-1083.517570	-1083.119696	-1083.116105	-1084.886516	-1084.485051
Azet_Bzh_Et_F_19	-1083.510786	-1083.115543	-1083.110441	-1084.885109	-1084.484764
Azet_Bzh_Et_F_20	-1083.516933	-1083.119489	-1083.115409	-1084.886156	-1084.484633
Azet_Bzh_Et_F_21	-1083.515256	-1083.118054	-1083.114005	-1084.885726	-1084.484474
Azet_Bzh_Et_F_22	-1083.514536	-1083.118511	-1083.113775	-1084.885197	-1084.484436
Azet_Bzh_Et_F_23	-1083.513777	-1083.117058	-1083.112620	-1084.885183	-1084.484026
Azet_Bzh_Et_F_24	-1083.516079	-1083.118381	-1083.114499	-1084.885382	-1084.483802
Azet_Bzh_Et_F_25	-1083.513130	-1083.116474	-1083.112060	-1084.884017	-1084.482947
Azet_Bzh_Et_F_26	-1083.514332	-1083.116211	-1083.112643	-1084.884362	-1084.482674
Azet_Bzh_Et_F_27	-1083.514534	-1083.116840	-1083.113088	-1084.883678	-1084.482233
Azet_Bzh_Et_F_28	-1083.511334	-1083.114822	-1083.110289	-1084.879812	-1084.478767

Table S35: Azet_{Bzh,Allvl}

	Energy (opt)	G (opt)	G-qh (opt)	E (sp)	G-qh (sp)
Azet_Bzh_All_F_1	-1121.553328	-1121.153166	-1121.148583	-1122.968267	-1122.563522
Azet_Bzh_All_F_2	-1121.553527	-1121.153645	-1121.148725	-1122.967762	-1122.562960
Azet_Bzh_All_F_3	-1121.551635	-1121.152095	-1121.147051	-1122.967482	-1122.562899
Azet_Bzh_All_F_4	-1121.555663	-1121.155175	-1121.150546	-1122.967900	-1122.562783
Azet_Bzh_All_F_5	-1121.555501	-1121.155053	-1121.150477	-1122.967751	-1122.562726
Azet_Bzh_All_F_6	-1121.554111	-1121.154183	-1121.149530	-1122.967156	-1122.562575
Azet_Bzh_All_F_7	-1121.555786	-1121.154875	-1121.150603	-1122.967754	-1122.562571
Azet_Bzh_All_F_8	-1121.553694	-1121.154891	-1121.149473	-1122.966776	-1122.562555
Azet_Bzh_All_F_9	-1121.553427	-1121.152849	-1121.148426	-1122.967242	-1122.562242
Azet_Bzh_All_F_10	-1121.553622	-1121.154204	-1121.148997	-1122.966825	-1122.562200
Azet_Bzh_All_F_11	-1121.552786	-1121.152878	-1121.148014	-1122.966664	-1122.561891
Azet_Bzh_All_F_12	-1121.554188	-1121.154221	-1121.149609	-1122.965983	-1122.561404
Azet_Bzh_All_F_13	-1121.553616	-1121.152505	-1121.148088	-1122.966731	-1122.561203
Azet_Bzh_All_F_14	-1121.554167	-1121.153272	-1121.149107	-1122.966117	-1122.561056
Azet_Bzh_All_F_15	-1121.554167	-1121.153273	-1121.149107	-1122.966115	-1122.561055
Azet_Bzh_All_F_16	-1121.552069	-1121.151740	-1121.147140	-1122.965611	-1122.560683
Azet_Bzh_All_F_17	-1121.550730	-1121.151261	-1121.146147	-1122.965219	-1122.560636
Azet_Bzh_All_F_18	-1121.551697	-1121.151604	-1121.147004	-1122.964935	-1122.560242
Azet_Bzh_All_F_19	-1121.553208	-1121.152077	-1121.147753	-1122.965332	-1122.559878
Azet_Bzh_All_F_20	-1121.553202	-1121.152252	-1121.147683	-1122.965290	-1122.559771
Azet_Bzh_All_F_21	-1121.552305	-1121.151351	-1121.147158	-1122.964850	-1122.559702
Azet_Bzh_All_F_22	-1121.552358	-1121.151354	-1121.147177	-1122.964851	-1122.559669
Azet_Bzh_All_F_23	-1121.550752	-1121.150123	-1121.145803	-1122.963211	-1122.558262
Azet_Bzh_All_F_24	-1121.550752	-1121.150122	-1121.145800	-1122.963210	-1122.558259
Azet_Bzh_All_F_25	-1121.551236	-1121.150697	-1121.145945	-1122.963387	-1122.558097

Table S36: Azet_{Bzh,Bn}

	Energy (opt)	G (opt)	G-qh (opt)	E (sp)	G-qh (sp)
Azet_Bzh_Bn_F_1	-1275.045778	-1274.600736	-1274.594651	-1276.637323	-1276.186195
Azet_Bzh_Bn_F_2	-1275.042985	-1274.597830	-1274.591827	-1276.635679	-1276.184521
Azet_Bzh_Bn_F_3	-1275.042985	-1274.597820	-1274.591821	-1276.635682	-1276.184518
Azet_Bzh_Bn_F_4	-1275.043430	-1274.597931	-1274.592187	-1276.635001	-1276.183758
Azet_Bzh_Bn_F_5	-1275.043429	-1274.597925	-1274.592182	-1276.635002	-1276.183754
Azet_Bzh_Bn_F_6	-1275.041916	-1274.596424	-1274.590678	-1276.634742	-1276.183505
Azet_Bzh_Bn_F_7	-1275.041998	-1274.596518	-1274.590397	-1276.634946	-1276.183346
Azet_Bzh_Bn_F_8*	-1275.043421	-1274.596709	-1274.591444	-1276.635146	-1276.183170
Azet_Bzh_Bn_F_9	-1275.043041	-1274.597600	-1274.592030	-1276.634142	-1276.183132

Azet_Bzh_Bn_F_10	-1275.042301	-1274.595783	-1274.590588	-1276.634749	-1276.183036
Azet_Bzh_Bn_F_11	-1275.043394	-1274.597995	-1274.592098	-1276.634219	-1276.182922
Azet_Bzh_Bn_F_12	-1275.039765	-1274.595734	-1274.589350	-1276.633252	-1276.182836
Azet_Bzh_Bn_F_13	-1275.042375	-1274.596017	-1274.590571	-1276.634434	-1276.182631
Azet_Bzh_Bn_F_14	-1275.042375	-1274.596016	-1274.590571	-1276.634434	-1276.182631
Azet_Bzh_Bn_F_15	-1275.040178	-1274.595420	-1274.589270	-1276.633063	-1276.182154
Azet_Bzh_Bn_F_16	-1275.043486	-1274.596464	-1274.591477	-1276.634116	-1276.182107
Azet_Bzh_Bn_F_17	-1275.043486	-1274.596453	-1274.591470	-1276.634116	-1276.182100
Azet_Bzh_Bn_F_18	-1275.042732	-1274.596270	-1274.591127	-1276.633590	-1276.181985
Azet_Bzh_Bn_F_19	-1275.040928	-1274.594468	-1274.589317	-1276.633116	-1276.181505
Azet_Bzh_Bn_F_20	-1275.040584	-1274.593483	-1274.588573	-1276.633485	-1276.181475
Azet_Bzh_Bn_F_21	-1275.038186	-1274.594317	-1274.587763	-1276.631456	-1276.181032
Azet_Bzh_Bn_F_22	-1275.039839	-1274.593167	-1274.588044	-1276.632732	-1276.180937
Azet_Bzh_Bn_F_23	-1275.040956	-1274.594560	-1274.589390	-1276.632405	-1276.180840
Azet_Bzh_Bn_F_24	-1275.039839	-1274.593286	-1274.588091	-1276.632392	-1276.180644
Azet_Bzh_Bn_F_25	-1275.041920	-1274.594692	-1274.589906	-1276.632571	-1276.180557
Azet_Bzh_Bn_F_26	-1275.041920	-1274.594692	-1274.589907	-1276.632568	-1276.180555
Azet_Bzh_Bn_F_27	-1275.041301	-1274.594478	-1274.589701	-1276.631593	-1276.179993
Azet_Bzh_Bn_F_28	-1275.036808	-1274.591981	-1274.586000	-1276.630468	-1276.179659
Azet_Bzh_Bn_F_29	-1275.038785	-1274.593028	-1274.587554	-1276.630729	-1276.179498
Azet_Bzh_Bn_F_30	-1275.037959	-1274.592208	-1274.586597	-1276.630683	-1276.179321
Azet_Bzh_Bn_F_31	-1275.038536	-1274.592660	-1274.587295	-1276.630152	-1276.178911
Azet_Bzh_Bn_F_32	-1275.035376	-1274.590608	-1274.584297	-1276.628703	-1276.177624
Azet_Bzh_Bn_F_33	-1275.039469	-1274.592627	-1274.587712	-1276.629130	-1276.177372
Azet_Bzh_Bn_F_34	-1275.039469	-1274.592606	-1274.587701	-1276.629130	-1276.177362

Azetidinium-Triflate Ion Pairs

Table S37: Azet_{Me,Me}

	Energy (opt)	G (opt)	G-qh (opt)	E (sp)	G-qh (sp)
Azet_Me_Me_OTf_1	-1443.698994	-1443.465156	-1443.460315	-1445.227439	-1444.988760
Azet_Me_Me_OTf_2	-1443.698995	-1443.465082	-1443.460277	-1445.227434	-1444.988717
Azet_Me_Me_OTf_3	-1443.697351	-1443.464071	-1443.459021	-1445.226776	-1444.988446
Azet_Me_Me_OTf_4	-1443.697124	-1443.464116	-1443.458962	-1445.226488	-1444.988326
Azet_Me_Me_OTf_5	-1443.697125	-1443.464096	-1443.458952	-1445.226485	-1444.988312
Azet_Me_Me_OTf_6	-1443.697384	-1443.463708	-1443.458847	-1445.226707	-1444.988169
Azet_Me_Me_OTf_7	-1443.697384	-1443.463702	-1443.458844	-1445.226701	-1444.988161
Azet_Me_Me_OTf_8	-1443.696697	-1443.463804	-1443.458512	-1445.226338	-1444.988153
Azet_Me_Me_OTf_9	-1443.695979	-1443.464797	-1443.458813	-1445.225260	-1444.988093
Azet_Me_Me_OTf_10	-1443.697071	-1443.463874	-1443.458751	-1445.226379	-1444.988059
Azet_Me_Me_OTf_11	-1443.697596	-1443.464068	-1443.459133	-1445.226512	-1444.988049
Azet_Me_Me_OTf_12	-1443.697879	-1443.463161	-1443.458838	-1445.227075	-1444.988034
Azet_Me_Me_OTf_13	-1443.697317	-1443.464265	-1443.459006	-1445.226314	-1444.988003
Azet_Me_Me_OTf_14	-1443.697317	-1443.464271	-1443.459009	-1445.226306	-1444.987997
Azet_Me_Me_OTf_15	-1443.696869	-1443.464040	-1443.458920	-1445.225848	-1444.987899
Azet_Me_Me_OTf_16	-1443.697403	-1443.464460	-1443.459275	-1445.226024	-1444.987897
Azet_Me_Me_OTf_17	-1443.696869	-1443.464037	-1443.458918	-1445.225847	-1444.987896
Azet_Me_Me_OTf_18*	-1443.697543	-1443.462833	-1443.458445	-1445.226982	-1444.987884
Azet_Me_Me_OTf_19	-1443.696432	-1443.464302	-1443.458853	-1445.225442	-1444.987863
Azet_Me_Me_OTf_20	-1443.696432	-1443.464299	-1443.458852	-1445.225441	-1444.987861
Azet_Me_Me_OTf_21	-1443.695568	-1443.463337	-1443.457817	-1445.225597	-1444.987846
Azet_Me_Me_OTf_22	-1443.696218	-1443.462864	-1443.457812	-1445.226180	-1444.987774
Azet_Me_Me_OTf_23	-1443.697266	-1443.463176	-1443.458599	-1445.226435	-1444.987768
Azet_Me_Me_OTf_24	-1443.695909	-1443.463790	-1443.458351	-1445.225314	-1444.987756
Azet_Me_Me_OTf_25	-1443.695568	-1443.462866	-1443.457577	-1445.225595	-1444.987604
Azet_Me_Me_OTf_26	-1443.696479	-1443.463493	-1443.458325	-1445.225717	-1444.987562
Azet_Me_Me_OTf_27	-1443.697273	-1443.462797	-1443.458468	-1445.226326	-1444.987521
Azet_Me_Me_OTf_28	-1443.696655	-1443.463940	-1443.458562	-1445.225592	-1444.987500
Azet_Me_Me_OTf_29	-1443.695544	-1443.462630	-1443.457402	-1445.225588	-1444.987447
Azet_Me_Me_OTf_30	-1443.696017	-1443.462439	-1443.457486	-1445.225967	-1444.987437

Azet_Me_Me_OTf_31	-1443.695533	-1443.462652	-1443.457389	-1445.225572	-1444.987428
Azet_Me_Me_OTf_32	-1443.695568	-1443.462461	-1443.457362	-1445.225586	-1444.987380
Azet_Me_Me_OTf_33*	-1443.695903	-1443.462987	-1443.457596	-1445.225574	-1444.987268
Azet_Me_Me_OTf_34	-1443.696822	-1443.464509	-1443.459083	-1445.224975	-1444.987237
Azet_Me_Me_OTf_35	-1443.696822	-1443.464506	-1443.459082	-1445.224972	-1444.987231
Azet_Me_Me_OTf_36	-1443.696884	-1443.462725	-1443.458003	-1445.226007	-1444.987126
Azet_Me_Me_OTf_37	-1443.697232	-1443.464458	-1443.459173	-1445.225185	-1444.987125
Azet_Me_Me_OTf_38	-1443.697925	-1443.464147	-1443.459321	-1445.225577	-1444.986974
Azet_Me_Me_OTf_39	-1443.696788	-1443.462470	-1443.457847	-1445.225828	-1444.986887
Azet_Me_Me_OTf_40	-1443.696904	-1443.464291	-1443.458843	-1445.224923	-1444.986862
Azet_Me_Me_OTf_41	-1443.697490	-1443.463969	-1443.458964	-1445.225303	-1444.986778
Azet_Me_Me_OTf_42	-1443.695813	-1443.463857	-1443.458185	-1445.224400	-1444.986772
Azet_Me_Me_OTf_43	-1443.697490	-1443.463890	-1443.458920	-1445.225295	-1444.986726
Azet_Me_Me_OTf_44	-1443.697498	-1443.463594	-1443.458706	-1445.225440	-1444.986648
Azet_Me_Me_OTf_45	-1443.696203	-1443.462791	-1443.457825	-1445.224962	-1444.986584
Azet_Me_Me_OTf_46*	-1443.696863	-1443.461996	-1443.457656	-1445.225740	-1444.986532
Azet_Me_Me_OTf_47	-1443.697114	-1443.463844	-1443.458651	-1445.224961	-1444.986498
Azet_Me_Me_OTf_48	-1443.697114	-1443.463831	-1443.458645	-1445.224959	-1444.986489
Azet_Me_Me_OTf_49*	-1443.697109	-1443.461772	-1443.457718	-1445.225200	-1444.985810
Azet_Me_Me_OTf_50	-1443.696584	-1443.463346	-1443.458105	-1445.224221	-1444.985742
Azet_Me_Me_OTf_51	-1443.697800	-1443.462859	-1443.458655	-1445.224859	-1444.985714
Azet_Me_Me_OTf_52*	-1443.697112	-1443.461424	-1443.457362	-1445.224907	-1444.985156

Table S38:Azet_{Bn,Me}

	Energy (opt)	G (opt)	G-gh (opt)	E (sp)	G-gh (sp)
Azet_Bn_Me_OTf_1	-1674.491463	-1674.182673	-1674.175550	-1676.296505	-1675.980591
Azet_Bn_Me_OTf_2	-1674.492066	-1674.181088	-1674.175123	-1676.296734	-1675.979791
Azet_Bn_Me_OTf_3	-1674.492040	-1674.181250	-1674.175017	-1676.296439	-1675.979416
Azet_Bn_Me_OTf_4	-1674.488535	-1674.179304	-1674.172359	-1676.295558	-1675.979382
Azet_Bn_Me_OTf_5	-1674.492040	-1674.181182	-1674.174984	-1676.296433	-1675.979376
Azet_Bn_Me_OTf_6	-1674.488535	-1674.179273	-1674.172342	-1676.295556	-1675.979363
Azet_Bn_Me_OTf_7	-1674.490859	-1674.179959	-1674.173822	-1676.296085	-1675.979049
Azet_Bn_Me_OTf_8	-1674.490859	-1674.179952	-1674.173818	-1676.296081	-1675.979041
Azet_Bn_Me_OTf_9	-1674.489442	-1674.179735	-1674.173054	-1676.295379	-1675.978991
Azet_Bn_Me_OTf_10	-1674.488927	-1674.178852	-1674.172521	-1676.295354	-1675.978948
Azet_Bn_Me_OTf_11	-1674.491208	-1674.180901	-1674.174499	-1676.295473	-1675.978764
Azet_Bn_Me_OTf_12	-1674.491208	-1674.180900	-1674.174498	-1676.295474	-1675.978764
Azet_Bn_Me_OTf_13	-1674.491321	-1674.180686	-1674.174410	-1676.295598	-1675.978686
Azet_Bn_Me_OTf_14	-1674.487655	-1674.179078	-1674.171977	-1676.294348	-1675.978670
Azet_Bn_Me_OTf_15	-1674.490885	-1674.180228	-1674.174009	-1676.295529	-1675.978653
Azet_Bn_Me_OTf_16	-1674.486061	-1674.180014	-1674.171748	-1676.292934	-1675.978620
Azet_Bn_Me_OTf_17	-1674.487809	-1674.179718	-1674.172433	-1676.293977	-1675.978600
Azet_Bn_Me_OTf_18	-1674.490534	-1674.180227	-1674.173893	-1676.295201	-1675.978560
Azet_Bn_Me_OTf_19	-1674.491000	-1674.180205	-1674.174021	-1676.295519	-1675.978540
Azet_Bn_Me_OTf_20	-1674.491000	-1674.180199	-1674.174020	-1676.295514	-1675.978534
Azet_Bn_Me_OTf_21	-1674.491365	-1674.180195	-1674.174170	-1676.295717	-1675.978521
Azet_Bn_Me_OTf_22	-1674.489752	-1674.179303	-1674.172932	-1676.295325	-1675.978506
Azet_Bn_Me_OTf_23	-1674.489752	-1674.179295	-1674.172927	-1676.295321	-1675.978497
Azet_Bn_Me_OTf_24	-1674.491366	-1674.180150	-1674.174144	-1676.295715	-1675.978494
Azet_Bn_Me_OTf_25	-1674.488458	-1674.179121	-1674.172205	-1676.294677	-1675.978424
Azet_Bn_Me_OTf_26	-1674.487254	-1674.178641	-1674.171575	-1676.293819	-1675.978140
Azet_Bn_Me_OTf_27	-1674.487165	-1674.179872	-1674.172239	-1676.292964	-1675.978038
Azet_Bn_Me_OTf_28	-1674.491130	-1674.180244	-1674.174302	-1676.294832	-1675.978004
Azet_Bn_Me_OTf_29	-1674.490582	-1674.180843	-1674.174364	-1676.294082	-1675.977864
Azet_Bn_Me_OTf_30	-1674.487117	-1674.178618	-1674.171576	-1676.293335	-1675.977793
Azet_Bn_Me_OTf_31	-1674.491042	-1674.180031	-1674.174247	-1676.294483	-1675.977688
Azet_Bn_Me_OTf_32	-1674.491046	-1674.179960	-1674.174206	-1676.294477	-1675.977638
Azet_Bn_Me_OTf_33	-1674.491495	-1674.179406	-1674.174047	-1676.295064	-1675.977615
Azet_Bn_Me_OTf_34	-1674.491495	-1674.179396	-1674.174041	-1676.295063	-1675.977610
Azet_Bn_Me_OTf_35	-1674.487823	-1674.179023	-1674.171930	-1676.293464	-1675.977570

Azet_Bn_Me_OTf_36	-1674.491654	-1674.179510	-1674.174133	-1676.295023	-1675.977502
Azet_Bn_Me_OTf_37	-1674.491654	-1674.179488	-1674.174121	-1676.295021	-1675.977487
Azet_Bn_Me_OTf_38	-1674.490534	-1674.179896	-1674.173677	-1676.294292	-1675.977435
Azet_Bn_Me_OTf_39	-1674.490533	-1674.179884	-1674.173666	-1676.294282	-1675.977414
Azet_Bn_Me_OTf_40	-1674.491207	-1674.179773	-1674.174026	-1676.294260	-1675.977079
Azet_Bn_Me_OTf_41	-1674.487177	-1674.177733	-1674.170953	-1676.293047	-1675.976822
Azet_Bn_Me_OTf_42	-1674.490515	-1674.179042	-1674.173396	-1676.293777	-1675.976659
Azet_Bn_Me_OTf_43	-1674.490515	-1674.179034	-1674.173392	-1676.293767	-1675.976645
Azet_Bn_Me_OTf_44	-1674.487768	-1674.178178	-1674.171644	-1676.292304	-1675.976181

Table S39: Azet_{Bn,Bn}

	Energy (opt)	G (opt)	G-qh (opt)	E (sp)	G-qh (sp)
Azet_Bn_Bn_OTf_1	-1905.281263	-1904.895744	-1904.887165	-1907.363466	-1906.969369
Azet_Bn_Bn_OTf_2	-1905.282862	-1904.896229	-1904.888176	-1907.363383	-1906.968697
Azet_Bn_Bn_OTf_3	-1905.280321	-1904.894997	-1904.886465	-1907.362427	-1906.968571
Azet_Bn_Bn_OTf_4	-1905.280259	-1904.893874	-1904.885739	-1907.362937	-1906.968417
Azet_Bn_Bn_OTf_5	-1905.283691	-1904.894991	-1904.888004	-1907.364052	-1906.968365
Azet_Bn_Bn_OTf_6	-1905.282094	-1904.895140	-1904.887304	-1907.363151	-1906.968362
Azet_Bn_Bn_OTf_7	-1905.282094	-1904.895128	-1904.887300	-1907.363156	-1906.968362
Azet_Bn_Bn_OTf_8	-1905.280740	-1904.894403	-1904.886308	-1907.362568	-1906.968136
Azet_Bn_Bn_OTf_9	-1905.280889	-1904.894826	-1904.886869	-1907.362115	-1906.968095
Azet_Bn_Bn_OTf_10	-1905.282495	-1904.894669	-1904.887338	-1907.363197	-1906.968039
Azet_Bn_Bn_OTf_11	-1905.281002	-1904.894820	-1904.886825	-1907.362189	-1906.968012
Azet_Bn_Bn_OTf_12	-1905.277026	-1904.894155	-1904.884490	-1907.360406	-1906.967870
Azet_Bn_Bn_OTf_13	-1905.278728	-1904.893409	-1904.884764	-1907.361796	-1906.967832
Azet_Bn_Bn_OTf_14	-1905.281726	-1904.894533	-1904.887044	-1907.362458	-1906.967775
Azet_Bn_Bn_OTf_15	-1905.281726	-1904.894522	-1904.887038	-1907.362456	-1906.967768
Azet_Bn_Bn_OTf_16	-1905.282225	-1904.894822	-1904.887150	-1907.362670	-1906.967595
Azet_Bn_Bn_OTf_17	-1905.280606	-1904.895030	-1904.886705	-1907.361400	-1906.967500
Azet_Bn_Bn_OTf_18	-1905.282183	-1904.894172	-1904.887037	-1907.362603	-1906.967458
Azet_Bn_Bn_OTf_19	-1905.280652	-1904.894226	-1904.886012	-1907.362082	-1906.967442
Azet_Bn_Bn_OTf_20	-1905.280354	-1904.893836	-1904.886089	-1907.361648	-1906.967383
Azet_Bn_Bn_OTf_21	-1905.281933	-1904.894623	-1904.887215	-1907.361735	-1906.967018
Azet_Bn_Bn_OTf_22	-1905.281933	-1904.894596	-1904.887200	-1907.361729	-1906.966996
Azet_Bn_Bn_OTf_23	-1905.278074	-1904.892955	-1904.884325	-1907.360693	-1906.966945
Azet_Bn_Bn_OTf_24	-1905.282317	-1904.893758	-1904.886849	-1907.362146	-1906.966678
Azet_Bn_Bn_OTf_25	-1905.280964	-1904.891727	-1904.885225	-1907.362197	-1906.966458
Azet_Bn_Bn_OTf_26	-1905.282300	-1904.893187	-1904.886585	-1907.362159	-1906.966444
Azet_Bn_Bn_OTf_27	-1905.282300	-1904.893177	-1904.886582	-1907.362151	-1906.966432
Azet_Bn_Bn_OTf_28	-1905.281240	-1904.892636	-1904.885889	-1907.361651	-1906.966299
Azet_Bn_Bn_OTf_29	-1905.281241	-1904.892573	-1904.885862	-1907.361622	-1906.966244
Azet_Bn_Bn_OTf_30	-1905.279682	-1904.893142	-1904.885296	-1907.360563	-1906.966178
Azet_Bn_Bn_OTf_31	-1905.279682	-1904.893126	-1904.885288	-1907.360563	-1906.966169
Azet_Bn_Bn_OTf_32	-1905.281514	-1904.893082	-1904.886228	-1907.361233	-1906.965946
Azet_Bn_Bn_OTf_33	-1905.279455	-1904.892147	-1904.884680	-1907.360678	-1906.965903
Azet_Bn_Bn_OTf_34	-1905.279455	-1904.892148	-1904.884681	-1907.360676	-1906.965901
Azet_Bn_Bn_OTf_35	-1905.277105	-1904.892234	-1904.883455	-1907.359441	-1906.965791
Azet_Bn_Bn_OTf_36	-1905.280330	-1904.892510	-1904.885361	-1907.360464	-1906.965495
Azet_Bn_Bn_OTf_37	-1905.279370	-1904.891647	-1904.884281	-1907.360189	-1906.965101

Table S40: Azet_{Bzh,Me}

	Energy (opt)	G (opt)	G-qh (opt)	E (sp)	G-qh (sp)
Azet_Bzh_Me_OTf_1	-1905.277419	-1904.891864	-1904.883723	-1907.359096	-1906.965400
Azet_Bzh_Me_OTf_2	-1905.278552	-1904.890803	-1904.883712	-1907.359352	-1906.964512
Azet_Bzh_Me_OTf_3	-1905.277939	-1904.890957	-1904.883405	-1907.358768	-1906.964235
Azet_Bzh_Me_OTf_4	-1905.277939	-1904.890947	-1904.883401	-1907.358762	-1906.964225
Azet_Bzh_Me_OTf_5	-1905.278861	-1904.891035	-1904.883986	-1907.359052	-1906.964177
Azet_Bzh_Me_OTf_6	-1905.278861	-1904.891026	-1904.883983	-1907.359054	-1906.964175
Azet_Bzh_Me_OTf_7	-1905.278095	-1904.890608	-1904.883358	-1907.358729	-1906.963992

Azet_Bzh_Me_OTf_8	-1905.277302	-1904.891346	-1904.883271	-1907.357996	-1906.963965
Azet_Bzh_Me_OTf_9	-1905.276235	-1904.889919	-1904.882197	-1907.357834	-1906.963796
Azet_Bzh_Me_OTf_10	-1905.276236	-1904.889904	-1904.882191	-1907.357837	-1906.963792
Azet_Bzh_Me_OTf_11	-1905.276110	-1904.890898	-1904.882523	-1907.357232	-1906.963645
Azet_Bzh_Me_OTf_12	-1905.276502	-1904.889808	-1904.882260	-1907.357760	-1906.963519
Azet_Bzh_Me_OTf_13	-1905.276966	-1904.890469	-1904.882821	-1907.357659	-1906.963514
Azet_Bzh_Me_OTf_14	-1905.277602	-1904.890649	-1904.883096	-1907.358018	-1906.963511
Azet_Bzh_Me_OTf_15	-1905.277601	-1904.890654	-1904.883100	-1907.358013	-1906.963511
Azet_Bzh_Me_OTf_16	-1905.273710	-1904.890075	-1904.880906	-1907.356177	-1906.963373
Azet_Bzh_Me_OTf_17	-1905.277155	-1904.890284	-1904.882661	-1907.357663	-1906.963169
Azet_Bzh_Me_OTf_18	-1905.275893	-1904.890177	-1904.882014	-1907.356817	-1906.962937
Azet_Bzh_Me_OTf_19	-1905.274455	-1904.889194	-1904.880902	-1907.356410	-1906.962857
Azet_Bzh_Me_OTf_20	-1905.276548	-1904.890096	-1904.882327	-1907.356949	-1906.962729
Azet_Bzh_Me_OTf_21	-1905.274455	-1904.888955	-1904.880782	-1907.356401	-1906.962727
Azet_Bzh_Me_OTf_22	-1905.274399	-1904.888502	-1904.880451	-1907.356573	-1906.962624
Azet_Bzh_Me_OTf_23	-1905.274242	-1904.887899	-1904.880247	-1907.356495	-1906.962500
Azet_Bzh_Me_OTf_24	-1905.276089	-1904.889678	-1904.882135	-1907.356420	-1906.962466
Azet_Bzh_Me_OTf_25	-1905.276089	-1904.889683	-1904.882136	-1907.356417	-1906.962464
Azet_Bzh_Me_OTf_26	-1905.275226	-1904.889882	-1904.881718	-1907.355901	-1906.962394
Azet_Bzh_Me_OTf_27	-1905.275674	-1904.888644	-1904.881299	-1907.356560	-1906.962185
Azet_Bzh_Me_OTf_28	-1905.275674	-1904.888622	-1904.881290	-1907.356556	-1906.962172
Azet_Bzh_Me_OTf_29	-1905.276077	-1904.889701	-1904.881927	-1907.356289	-1906.962138
Azet_Bzh_Me_OTf_30	-1905.274465	-1904.889827	-1904.881054	-1907.355460	-1906.962048
Azet_Bzh_Me_OTf_31	-1905.276768	-1904.888647	-1904.881943	-1907.356705	-1906.961879
Azet_Bzh_Me_OTf_32	-1905.276769	-1904.888590	-1904.881909	-1907.356693	-1906.961832
Azet_Bzh_Me_OTf_33	-1905.274226	-1904.887634	-1904.879975	-1907.356056	-1906.961805
Azet_Bzh_Me_OTf_34*	-1905.274535	-1904.886298	-1904.879163	-1907.357161	-1906.961789
Azet_Bzh_Me_OTf_35*	-1905.275808	-1904.887882	-1904.880848	-1907.356645	-1906.961685
Azet_Bzh_Me_OTf_36	-1905.276767	-1904.889055	-1904.881804	-1907.356560	-1906.961597
Azet_Bzh_Me_OTf_37	-1905.274964	-1904.887330	-1904.880207	-1907.356256	-1906.961499
Azet_Bzh_Me_OTf_38	-1905.275830	-1904.888937	-1904.881481	-1907.355631	-1906.961282

Table S41: Azet_{Bzh,Et}

	Energy (opt)	G (opt)	G-qh (opt)	E (sp)	G-qh (sp)
Azet_Bzh_Et_OTf_1	-1944.543731	-1944.130145	-1944.122221	-1946.678935	-1946.257424
Azet_Bzh_Et_OTf_2	-1944.543731	-1944.129954	-1944.122126	-1946.678936	-1946.257330
Azet_Bzh_Et_OTf_3	-1944.545202	-1944.129845	-1944.122693	-1946.679704	-1946.257195
Azet_Bzh_Et_OTf_4	-1944.540849	-1944.129061	-1944.120357	-1946.677667	-1946.257175
Azet_Bzh_Et_OTf_5	-1944.544017	-1944.128834	-1944.121691	-1946.679370	-1946.257043
Azet_Bzh_Et_OTf_6	-1944.544019	-1944.128830	-1944.121684	-1946.679376	-1946.257041
Azet_Bzh_Et_OTf_7	-1944.543606	-1944.130213	-1944.122253	-1946.678285	-1946.256932
Azet_Bzh_Et_OTf_8	-1944.542924	-1944.130025	-1944.121875	-1946.677862	-1946.256814
Azet_Bzh_Et_OTf_9	-1944.544305	-1944.129230	-1944.121977	-1946.679119	-1946.256792
Azet_Bzh_Et_OTf_10	-1944.542006	-1944.128631	-1944.120592	-1946.678148	-1946.256734
Azet_Bzh_Et_OTf_11	-1944.543650	-1944.129354	-1944.121647	-1946.678674	-1946.256671
Azet_Bzh_Et_OTf_12	-1944.542547	-1944.128451	-1944.120947	-1946.678230	-1946.256629
Azet_Bzh_Et_OTf_13	-1944.543287	-1944.129345	-1944.121510	-1946.678086	-1946.256309
Azet_Bzh_Et_OTf_14	-1944.542831	-1944.128302	-1944.120831	-1946.678297	-1946.256297
Azet_Bzh_Et_OTf_15	-1944.543289	-1944.129314	-1944.121489	-1946.678086	-1946.256286
Azet_Bzh_Et_OTf_16	-1944.542646	-1944.127705	-1944.120430	-1946.678350	-1946.256133
Azet_Bzh_Et_OTf_17	-1944.542586	-1944.127850	-1944.120569	-1946.678110	-1946.256093
Azet_Bzh_Et_OTf_18	-1944.542142	-1944.127669	-1944.120194	-1946.677890	-1946.255941
Azet_Bzh_Et_OTf_19	-1944.540726	-1944.127209	-1944.119342	-1946.677013	-1946.255630
Azet_Bzh_Et_OTf_20	-1944.542188	-1944.128002	-1944.120387	-1946.677368	-1946.255566
Azet_Bzh_Et_OTf_21	-1944.540458	-1944.127768	-1944.119484	-1946.676422	-1946.255448
Azet_Bzh_Et_OTf_22	-1944.542691	-1944.126914	-1944.120263	-1946.677850	-1946.255422
Azet_Bzh_Et_OTf_23	-1944.540185	-1944.126876	-1944.118821	-1946.676722	-1946.255358
Azet_Bzh_Et_OTf_24	-1944.540915	-1944.127814	-1944.119559	-1946.676444	-1946.255088
Azet_Bzh_Et_OTf_25	-1944.541946	-1944.127757	-1944.120055	-1946.676630	-1946.254739
Azet_Bzh_Et_OTf_26	-1944.540491	-1944.126397	-1944.118730	-1946.675810	-1946.254050

Azet_Bzh_Et_OTf_27	-1944.540049	-1944.125384	-1944.117856	-1946.675961	-1946.253768
Azet_Bzh_Et_OTf_28	-1944.540416	-1944.127053	-1944.119061	-1946.674835	-1946.253480
Azet_Bzh_Et_OTf_29	-1944.540416	-1944.127061	-1944.119056	-1946.674812	-1946.253452
Azet_Bzh_Et_OTf_30	-1944.539514	-1944.127184	-1944.118595	-1946.674362	-1946.253444
Azet_Bzh_Et_OTf_31	-1944.539966	-1944.125798	-1944.118156	-1946.674860	-1946.253051
Azet_Bzh_Et_OTf_32	-1944.539966	-1944.125784	-1944.118148	-1946.674857	-1946.253040
Azet_Bzh_Et_OTf_33	-1944.540462	-1944.125382	-1944.118191	-1946.675290	-1946.253019
Azet_Bzh_Et_OTf_34	-1944.540462	-1944.125374	-1944.118186	-1946.675291	-1946.253015
Azet_Bzh_Et_OTf_35	-1944.540333	-1944.125930	-1944.118216	-1946.674987	-1946.252870
Azet_Bzh_Et_OTf_36	-1944.537381	-1944.124575	-1944.116078	-1946.673429	-1946.252125

Table S42: Azet_{Bzh,Allyl}

	Energy (opt)	G (opt)	G-qh (opt)	E (sp)	G-qh (sp)
Azet_Bzh_All_OTf_1	-1982.579455	-1982.161508	-1982.153719	-1984.757965	-1984.332229
Azet_Bzh_All_OTf_2	-1982.577067	-1982.162086	-1982.152819	-1984.756146	-1984.331898
Azet_Bzh_All_OTf_3	-1982.577067	-1982.162037	-1982.152794	-1984.756147	-1984.331874
Azet_Bzh_All_OTf_4	-1982.579471	-1982.161333	-1982.153678	-1984.757581	-1984.331788
Azet_Bzh_All_OTf_5	-1982.578507	-1982.160933	-1982.152913	-1984.757306	-1984.331712
Azet_Bzh_All_OTf_6	-1982.580886	-1982.161972	-1982.154491	-1984.758009	-1984.331614
Azet_Bzh_All_OTf_7	-1982.578023	-1982.160782	-1982.152682	-1984.756833	-1984.331492
Azet_Bzh_All_OTf_8	-1982.578164	-1982.161320	-1982.152808	-1984.756765	-1984.331409
Azet_Bzh_All_OTf_9	-1982.578998	-1982.160999	-1982.153178	-1984.757183	-1984.331362
Azet_Bzh_All_OTf_10	-1982.579397	-1982.161518	-1982.153778	-1984.756906	-1984.331287
Azet_Bzh_All_OTf_11	-1982.578085	-1982.160270	-1982.152396	-1984.756797	-1984.331108
Azet_Bzh_All_OTf_12	-1982.577262	-1982.161326	-1982.152358	-1984.755948	-1984.331044
Azet_Bzh_All_OTf_13	-1982.577495	-1982.160283	-1982.151945	-1984.756589	-1984.331039
Azet_Bzh_All_OTf_14	-1982.577033	-1982.159419	-1982.151586	-1984.756434	-1984.330987
Azet_Bzh_All_OTf_15	-1982.578643	-1982.161110	-1982.152979	-1984.756648	-1984.330984
Azet_Bzh_All_OTf_16	-1982.577505	-1982.160569	-1982.152109	-1984.756094	-1984.330698
Azet_Bzh_All_OTf_17	-1982.578021	-1982.160309	-1982.152316	-1984.756302	-1984.330597
Azet_Bzh_All_OTf_18	-1982.578021	-1982.160301	-1982.152312	-1984.756298	-1984.330588
Azet_Bzh_All_OTf_19	-1982.576527	-1982.160347	-1982.151557	-1984.755492	-1984.330522
Azet_Bzh_All_OTf_20	-1982.577728	-1982.160846	-1982.152331	-1984.755765	-1984.330369
Azet_Bzh_All_OTf_21	-1982.576105	-1982.160067	-1982.151192	-1984.755190	-1984.330276
Azet_Bzh_All_OTf_22	-1982.577926	-1982.159725	-1982.152160	-1984.756013	-1984.330247
Azet_Bzh_All_OTf_23	-1982.577926	-1982.159693	-1982.152147	-1984.755997	-1984.330218
Azet_Bzh_All_OTf_24	-1982.576553	-1982.160223	-1982.151472	-1984.755274	-1984.330193
Azet_Bzh_All_OTf_25	-1982.576634	-1982.159601	-1982.151204	-1984.755609	-1984.330179
Azet_Bzh_All_OTf_26	-1982.577109	-1982.159373	-1982.151181	-1984.756021	-1984.330093
Azet_Bzh_All_OTf_27	-1982.575867	-1982.159506	-1982.150723	-1984.755092	-1984.329948
Azet_Bzh_All_OTf_28	-1982.577748	-1982.159203	-1982.151476	-1984.756178	-1984.329906
Azet_Bzh_All_OTf_29	-1982.578061	-1982.160674	-1982.152431	-1984.755518	-1984.329887
Azet_Bzh_All_OTf_30	-1982.576851	-1982.159896	-1982.151419	-1984.755270	-1984.329839
Azet_Bzh_All_OTf_31	-1982.576513	-1982.159616	-1982.151076	-1984.755058	-1984.329621
Azet_Bzh_All_OTf_32	-1982.576033	-1982.160489	-1982.151443	-1984.754191	-1984.329601
Azet_Bzh_All_OTf_33	-1982.575832	-1982.158379	-1982.150144	-1984.755253	-1984.329565
Azet_Bzh_All_OTf_34	-1982.576033	-1982.160416	-1982.151405	-1984.754179	-1984.329552
Azet_Bzh_All_OTf_35*	-1982.576147	-1982.158429	-1982.150293	-1984.755325	-1984.329471
Azet_Bzh_All_OTf_36	-1982.576214	-1982.159180	-1982.150925	-1984.754565	-1984.329276
Azet_Bzh_All_OTf_37	-1982.576214	-1982.159162	-1982.150916	-1984.754563	-1984.329265
Azet_Bzh_All_OTf_38	-1982.576582	-1982.159223	-1982.150891	-1984.754740	-1984.329048
Azet_Bzh_All_OTf_39	-1982.576583	-1982.159206	-1982.150882	-1984.754737	-1984.329037

Table S43: Azet_{Bzh,Bn}

	Energy (opt)	G (opt)	G-qh (opt)	E (sp)	G-qh (sp)
Azet_Bzh_Bn_OTf_1	-2136.068799	-2135.605692	-2135.596489	-2138.426659	-2137.954349
Azet_Bzh_Bn_OTf_2	-2136.068799	-2135.605685	-2135.596486	-2138.426661	-2137.954348
Azet_Bzh_Bn_OTf_3	-2136.068857	-2135.605911	-2135.596687	-2138.426414	-2137.954244
Azet_Bzh_Bn_OTf_4	-2136.067984	-2135.605590	-2135.595977	-2138.425917	-2137.953910

Azet_Bzh_Bn_OTf_5	-2136.067766	-2135.606168	-2135.596211	-2138.425180	-2137.953625
Azet_Bzh_Bn_OTf_6	-2136.068544	-2135.604495	-2135.595714	-2138.426310	-2137.953480
Azet_Bzh_Bn_OTf_7	-2136.067561	-2135.605470	-2135.595654	-2138.425273	-2137.953366
Azet_Bzh_Bn_OTf_8	-2136.066197	-2135.605090	-2135.594984	-2138.424433	-2137.953221
Azet_Bzh_Bn_OTf_9	-2136.066663	-2135.605033	-2135.595073	-2138.424709	-2137.953119
Azet_Bzh_Bn_OTf_10	-2136.066663	-2135.605018	-2135.595065	-2138.424712	-2137.953113
Azet_Bzh_Bn_OTf_11	-2136.066779	-2135.604144	-2135.594802	-2138.424862	-2137.952885
Azet_Bzh_Bn_OTf_12	-2136.066748	-2135.603997	-2135.594621	-2138.424991	-2137.952864
Azet_Bzh_Bn_OTf_13*	-2136.067302	-2135.601881	-2135.593779	-2138.426341	-2137.952819
Azet_Bzh_Bn_OTf_14	-2136.065644	-2135.603092	-2135.593646	-2138.424594	-2137.952597
Azet_Bzh_Bn_OTf_15	-2136.065619	-2135.603861	-2135.594058	-2138.424029	-2137.952467
Azet_Bzh_Bn_OTf_16	-2136.066052	-2135.605201	-2135.595144	-2138.423361	-2137.952453
Azet_Bzh_Bn_OTf_17	-2136.066733	-2135.603959	-2135.594680	-2138.424242	-2137.952188
Azet_Bzh_Bn_OTf_18	-2136.065446	-2135.602838	-2135.593498	-2138.424011	-2137.952063
Azet_Bzh_Bn_OTf_19	-2136.064383	-2135.602717	-2135.592865	-2138.423554	-2137.952035
Azet_Bzh_Bn_OTf_20	-2136.065201	-2135.602379	-2135.593027	-2138.424042	-2137.951869
Azet_Bzh_Bn_OTf_21	-2136.065202	-2135.602353	-2135.593014	-2138.424043	-2137.951855
Azet_Bzh_Bn_OTf_22	-2136.066629	-2135.602918	-2135.594099	-2138.424272	-2137.951742
Azet_Bzh_Bn_OTf_23	-2136.066546	-2135.603812	-2135.594550	-2138.423528	-2137.951533
Azet_Bzh_Bn_OTf_24	-2136.067008	-2135.603017	-2135.594425	-2138.424043	-2137.951460
Azet_Bzh_Bn_OTf_25	-2136.066653	-2135.602481	-2135.593953	-2138.423980	-2137.951280
Azet_Bzh_Bn_OTf_26	-2136.066653	-2135.602438	-2135.593937	-2138.423970	-2137.951254
Azet_Bzh_Bn_OTf_27	-2136.067918	-2135.602968	-2135.594835	-2138.424264	-2137.951180
Azet_Bzh_Bn_OTf_28	-2136.065721	-2135.602214	-2135.593504	-2138.422500	-2137.950283
Azet_Bzh_Bn_OTf_29	-2136.064232	-2135.601271	-2135.592092	-2138.422260	-2137.950119
Azet_Bzh_Bn_OTf_30	-2136.065560	-2135.600870	-2135.592796	-2138.422835	-2137.950070
Azet_Bzh_Bn_OTf_31	-2136.065560	-2135.600871	-2135.592794	-2138.422834	-2137.950067
Azet_Bzh_Bn_OTf_32	-2136.066808	-2135.601630	-2135.593810	-2138.422965	-2137.949966
Azet_Bzh_Bn_OTf_33	-2136.065812	-2135.601078	-2135.592936	-2138.422328	-2137.949453
Azet_Bzh_Bn_OTf_34	-2136.064915	-2135.601020	-2135.592365	-2138.421431	-2137.948882
Azet_Bzh_Bn_OTf_35	-2136.064840	-2135.600541	-2135.592306	-2138.421044	-2137.948510
Azet_Bzh_Bn_OTf_36	-2136.063457	-2135.599965	-2135.591252	-2138.420408	-2137.948203
Azet_Bzh_Bn_OTf_37	-2136.063299	-2135.598857	-2135.590581	-2138.420775	-2137.948057
Azet_Bzh_Bn_OTf_38	-2136.063836	-2135.599653	-2135.591300	-2138.419610	-2137.947074

Azetidinium Fluorination Transition State Structures

Table S44: Azet_{Me,Me}

	Energy (opt)	G (opt)	G-qh (opt)	E (sp)	G-qh (sp)
TS_Me_Me_F_1	-582.644436	-582.428903	-582.427323	-583.405767	-583.188653
TS_Me_Me_F_2	-582.645614	-582.428995	-582.427974	-583.404913	-583.187272
TS_Me_Me_F_3	-582.645614	-582.428991	-582.427971	-583.404908	-583.187264

Table S45: Azet_{Bn,Me}

	Energy (opt)	G (opt)	G-qh (opt)	E (sp)	G-qh (sp)
TS_Bn_Me_F_1	-813.435421	-813.144173	-813.140916	-814.474250	-814.179744
TS_Bn_Me_F_2	-813.434691	-813.144325	-813.140638	-814.473635	-814.179582
TS_Bn_Me_F_3	-813.436899	-813.143884	-813.141469	-814.474775	-814.179345
TS_Bn_Me_F_4	-813.436899	-813.143882	-813.141468	-814.474769	-814.179338
TS_Bn_Me_F_5	-813.436899	-813.143879	-813.141466	-814.474770	-814.179337
TS_Bn_Me_F_6	-813.437395	-813.144843	-813.142228	-814.474045	-814.178878
TS_Bn_Me_F_7	-813.437395	-813.144842	-813.142228	-814.474043	-814.178876
TS_Bn_Me_F_8	-813.435712	-813.143502	-813.140737	-814.472622	-814.177647
TS_Bn_Me_F_9	-813.435712	-813.143499	-813.140735	-814.472619	-814.177641
TS_Bn_Me_F_10	-813.436557	-813.142480	-813.140660	-814.472194	-814.176297
TS_Bn_Me_F_11	-813.436557	-813.142480	-813.140660	-814.472194	-814.176297
TS_Bn_Me_F_12	-813.432898	-813.142201	-813.138815	-814.469521	-814.175438
TS_Bn_Me_F_13	-813.433285	-813.141334	-813.138401	-814.470115	-814.175231

Table S46: Azet_{Bn,Bn}

	Energy (opt)	G (opt)	G-qh (opt)	E (sp)	G-qh (sp)
TS_Bn_Bn_F_1	-1044.226744	-1043.857865	-1043.853752	-1045.542179	-1045.169187
TS_Bn_Bn_F_2	-1044.224829	-1043.857864	-1043.852778	-1045.540916	-1045.168865
TS_Bn_Bn_F_3	-1044.227483	-1043.858951	-1043.854579	-1045.541629	-1045.168725
TS_Bn_Bn_F_4	-1044.223862	-1043.857185	-1043.852043	-1045.540148	-1045.168329
TS_Bn_Bn_F_5	-1044.224122	-1043.857973	-1043.852476	-1045.539870	-1045.168224
TS_Bn_Bn_F_6	-1044.225211	-1043.856521	-1043.852388	-1045.541041	-1045.168218
TS_Bn_Bn_F_7	-1044.223366	-1043.856525	-1043.851454	-1045.539837	-1045.167925
TS_Bn_Bn_F_8	-1044.224254	-1043.857181	-1043.852189	-1045.539804	-1045.167739
TS_Bn_Bn_F_9	-1044.225800	-1043.857190	-1043.852845	-1045.540472	-1045.167517
TS_Bn_Bn_F_10	-1044.223745	-1043.856848	-1043.851816	-1045.539314	-1045.167385
TS_Bn_Bn_F_11	-1044.225124	-1043.856263	-1043.852162	-1045.540109	-1045.167147
TS_Bn_Bn_F_12	-1044.225124	-1043.856263	-1043.852162	-1045.540109	-1045.167147
TS_Bn_Bn_F_13	-1044.225362	-1043.857374	-1043.852749	-1045.539621	-1045.167009
TS_Bn_Bn_F_14	-1044.225380	-1043.857638	-1043.852877	-1045.539330	-1045.166826
TS_Bn_Bn_F_15	-1044.225412	-1043.857673	-1043.852791	-1045.539369	-1045.166748
TS_Bn_Bn_F_16	-1044.226500	-1043.857163	-1043.853467	-1045.539731	-1045.166698
TS_Bn_Bn_F_17	-1044.226500	-1043.857163	-1043.853466	-1045.539731	-1045.166697
TS_Bn_Bn_F_18	-1044.225763	-1043.856961	-1043.852960	-1045.539312	-1045.166509
TS_Bn_Bn_F_19	-1044.225763	-1043.856961	-1043.852960	-1045.539312	-1045.166509
TS_Bn_Bn_F_20	-1044.224217	-1043.855534	-1043.851190	-1045.539089	-1045.166063
TS_Bn_Bn_F_21	-1044.223963	-1043.855325	-1043.850960	-1045.538998	-1045.165994
TS_Bn_Bn_F_22	-1044.221989	-1043.855090	-1043.850118	-1045.537862	-1045.165991
TS_Bn_Bn_F_23	-1044.225470	-1043.856164	-1043.852199	-1045.538941	-1045.165671
TS_Bn_Bn_F_24	-1044.221493	-1043.854138	-1043.849479	-1045.537372	-1045.165358
TS_Bn_Bn_F_25	-1044.225834	-1043.855610	-1043.852127	-1045.538777	-1045.165070
TS_Bn_Bn_F_26	-1044.219786	-1043.852986	-1043.848004	-1045.536046	-1045.164265
TS_Bn_Bn_F_27	-1044.223383	-1043.855015	-1043.850819	-1045.536663	-1045.164099
TS_Bn_Bn_F_28	-1044.223701	-1043.854141	-1043.850384	-1045.537322	-1045.164005
TS_Bn_Bn_F_29	-1044.223628	-1043.854568	-1043.850690	-1045.536919	-1045.163980

Table S47: Azet_{Bzh,Me}

	Energy (opt)	G (opt)	G-qh (opt)	E (sp)	G-qh (sp)
TS_Bzh_Me_F_1	-1044.224371	-1043.855352	-1043.851688	-1045.538887	-1045.166204
TS_Bzh_Me_F_2	-1044.224412	-1043.855370	-1043.851700	-1045.538842	-1045.166130
TS_Bzh_Me_F_3	-1044.221393	-1043.854836	-1043.849986	-1045.536720	-1045.165313
TS_Bzh_Me_F_4	-1044.221932	-1043.854513	-1043.849970	-1045.536836	-1045.164873
TS_Bzh_Me_F_5	-1044.224260	-1043.855111	-1043.851244	-1045.536947	-1045.163931
TS_Bzh_Me_F_6	-1044.223795	-1043.854197	-1043.850953	-1045.535921	-1045.163079
TS_Bzh_Me_F_7	-1044.222760	-1043.852724	-1043.849596	-1045.536192	-1045.163027
TS_Bzh_Me_F_8	-1044.222769	-1043.852695	-1043.849633	-1045.535182	-1045.162046
TS_Bzh_Me_F_9	-1044.222020	-1043.853298	-1043.849350	-1045.534636	-1045.161966

Table S48: Azet_{Bzh,Et}

	Energy (opt)	G (opt)	G-qh (opt)	E (sp)	G-qh (sp)
TS_Bzh_Et_F_1	-1083.490333	-1083.093341	-1083.089800	-1084.859294	-1084.458761
TS_Bzh_Et_F_2	-1083.490148	-1083.093588	-1083.089832	-1084.858983	-1084.458666
TS_Bzh_Et_F_3	-1083.489687	-1083.092297	-1083.089010	-1084.856603	-1084.455925
TS_Bzh_Et_F_4	-1083.488428	-1083.091873	-1083.087960	-1084.856110	-1084.455642
TS_Bzh_Et_F_5	-1083.486271	-1083.089829	-1083.086104	-1084.855553	-1084.455385
TS_Bzh_Et_F_6	-1083.484842	-1083.089655	-1083.085140	-1084.855001	-1084.455299
TS_Bzh_Et_F_7	-1083.486301	-1083.089857	-1083.086054	-1084.855459	-1084.455211
TS_Bzh_Et_F_8	-1083.489195	-1083.091394	-1083.088387	-1084.855926	-1084.455117
TS_Bzh_Et_F_9	-1083.484283	-1083.090003	-1083.085053	-1084.854069	-1084.454839
TS_Bzh_Et_F_10	-1083.485359	-1083.089059	-1083.085187	-1084.854884	-1084.454712
TS_Bzh_Et_F_11	-1083.486526	-1083.090298	-1083.086389	-1084.854129	-1084.453992
TS_Bzh_Et_F_12	-1083.482936	-1083.088047	-1083.083433	-1084.852914	-1084.453410
TS_Bzh_Et_F_13	-1083.483152	-1083.087401	-1083.083158	-1084.852592	-1084.452598

TS_Bzh_Et_F_14	-1083.482972	-1083.086768	-1083.082808	-1084.852693	-1084.452529
TS_Bzh_Et_F_15	-1083.483922	-1083.088626	-1083.084183	-1084.852136	-1084.452397
TS_Bzh_Et_F_16	-1083.483147	-1083.087012	-1083.082776	-1084.852622	-1084.452250
TS_Bzh_Et_F_17	-1083.483751	-1083.088049	-1083.084019	-1084.851901	-1084.452169
TS_Bzh_Et_F_18	-1083.481776	-1083.086692	-1083.082301	-1084.851531	-1084.452056
TS_Bzh_Et_F_19	-1083.485114	-1083.088927	-1083.084802	-1084.852269	-1084.451957
TS_Bzh_Et_F_20	-1083.482132	-1083.086438	-1083.082076	-1084.851984	-1084.451928
TS_Bzh_Et_F_21	-1083.483617	-1083.087307	-1083.083312	-1084.852033	-1084.451728
TS_Bzh_Et_F_22	-1083.484602	-1083.087729	-1083.084242	-1084.852034	-1084.451673
TS_Bzh_Et_F_23	-1083.486026	-1083.088842	-1083.085436	-1084.852214	-1084.451624
TS_Bzh_Et_F_24	-1083.486026	-1083.088840	-1083.085435	-1084.852213	-1084.451623
TS_Bzh_Et_F_25	-1083.481898	-1083.086289	-1083.081922	-1084.851135	-1084.451160
TS_Bzh_Et_F_26	-1083.481222	-1083.086395	-1083.081605	-1084.850054	-1084.450437
TS_Bzh_Et_F_27	-1083.481088	-1083.084740	-1083.080937	-1084.850209	-1084.450058
TS_Bzh_Et_F_28	-1083.481545	-1083.085209	-1083.081073	-1084.850257	-1084.449785
TS_Bzh_Et_F_29	-1083.478935	-1083.083483	-1083.079046	-1084.848424	-1084.448535
TS_Bzh_Et_F_30	-1083.480468	-1083.084219	-1083.080061	-1084.848851	-1084.448443

Table S49: Azet_{Bzh,Allyl}

	Energy (opt)	G (opt)	G-qh (opt)	E (sp)	G-qh (sp)
TS_Bzh_All_F_1	-1121.526327	-1121.126787	-1121.122438	-1122.938723	-1122.534834
TS_Bzh_All_F_2	-1121.526411	-1121.126266	-1121.122155	-1122.938657	-1122.534401
TS_Bzh_All_F_3	-1121.525680	-1121.125495	-1121.121303	-1122.938076	-1122.533699
TS_Bzh_All_F_4	-1121.524757	-1121.124885	-1121.120553	-1122.937064	-1122.532860
TS_Bzh_All_F_5	-1121.526005	-1121.125300	-1121.121487	-1122.936425	-1122.531907
TS_Bzh_All_F_6	-1121.522829	-1121.123475	-1121.119013	-1122.935275	-1122.531459
TS_Bzh_All_F_7	-1121.522772	-1121.123112	-1121.118861	-1122.935332	-1122.531421
TS_Bzh_All_F_8	-1121.522511	-1121.123362	-1121.118826	-1122.934836	-1122.531151
TS_Bzh_All_F_9	-1121.522505	-1121.123011	-1121.118619	-1122.935029	-1122.531143
TS_Bzh_All_F_10	-1121.524148	-1121.124245	-1121.119739	-1122.935325	-1122.530917
TS_Bzh_All_F_11	-1121.520993	-1121.122711	-1121.117547	-1122.934354	-1122.530909
TS_Bzh_All_F_12	-1121.520109	-1121.123301	-1121.117507	-1122.933437	-1122.530835
TS_Bzh_All_F_13	-1121.521602	-1121.122238	-1121.117886	-1122.934540	-1122.530824
TS_Bzh_All_F_14	-1121.522177	-1121.122584	-1121.118096	-1122.934854	-1122.530772
TS_Bzh_All_F_15	-1121.525266	-1121.124004	-1121.120570	-1122.935412	-1122.530717
TS_Bzh_All_F_16	-1121.521105	-1121.122356	-1121.117456	-1122.934330	-1122.530680
TS_Bzh_All_F_17	-1121.523974	-1121.124223	-1121.119709	-1122.934896	-1122.530632
TS_Bzh_All_F_18	-1121.520679	-1121.122873	-1121.117451	-1122.933858	-1122.530630
TS_Bzh_All_F_19	-1121.523467	-1121.123851	-1121.119414	-1122.934327	-1122.530273
TS_Bzh_All_F_20	-1121.524408	-1121.123400	-1121.119730	-1122.934824	-1122.530146
TS_Bzh_All_F_21	-1121.519950	-1121.121628	-1121.116559	-1122.933149	-1122.529758
TS_Bzh_All_F_22	-1121.524105	-1121.123208	-1121.119293	-1122.934549	-1122.529737
TS_Bzh_All_F_23	-1121.518836	-1121.121561	-1121.116292	-1122.932198	-1122.529654
TS_Bzh_All_F_24	-1121.520204	-1121.121299	-1121.116631	-1122.933122	-1122.529549
TS_Bzh_All_F_25	-1121.519911	-1121.120460	-1121.116116	-1122.932964	-1122.529170
TS_Bzh_All_F_26	-1121.520694	-1121.121500	-1121.116947	-1122.932733	-1122.528985
TS_Bzh_All_F_27	-1121.518344	-1121.120676	-1121.115343	-1122.931931	-1122.528930
TS_Bzh_All_F_28	-1121.520652	-1121.121929	-1121.117128	-1122.932435	-1122.528911
TS_Bzh_All_F_29	-1121.520652	-1121.121868	-1121.117098	-1122.932430	-1122.528877
TS_Bzh_All_F_30	-1121.521158	-1121.122147	-1121.117745	-1122.932208	-1122.528795
TS_Bzh_All_F_31	-1121.521127	-1121.121832	-1121.117421	-1122.932489	-1122.528782
TS_Bzh_All_F_32	-1121.517775	-1121.120180	-1121.115323	-1122.931134	-1122.528682
TS_Bzh_All_F_33	-1121.518463	-1121.120107	-1121.115090	-1122.931884	-1122.528511
TS_Bzh_All_F_34	-1121.520553	-1121.121784	-1121.116979	-1122.931847	-1122.528272
TS_Bzh_All_F_35	-1121.519540	-1121.119789	-1121.115370	-1122.932193	-1122.528023
TS_Bzh_All_F_36	-1121.520149	-1121.120896	-1121.116626	-1122.931496	-1122.527973
TS_Bzh_All_F_37	-1121.520612	-1121.120679	-1121.116440	-1122.932108	-1122.527936
TS_Bzh_All_F_38	-1121.520852	-1121.120864	-1121.116875	-1122.931903	-1122.527926
TS_Bzh_All_F_39	-1121.521044	-1121.121928	-1121.117152	-1122.931785	-1122.527894
TS_Bzh_All_F_40	-1121.522294	-1121.121890	-1121.117999	-1122.932077	-1122.527781

TS_Bzh_All_F_41	-1121.519323	-1121.119576	-1121.114889	-1122.932082	-1122.527649
TS_Bzh_All_F_42	-1121.517465	-1121.119201	-1121.114481	-1122.930532	-1122.527548
TS_Bzh_All_F_43	-1121.521188	-1121.120690	-1121.116672	-1122.931819	-1122.527303
TS_Bzh_All_F_44	-1121.520429	-1121.120778	-1121.116146	-1122.931128	-1122.526844
TS_Bzh_All_F_45	-1121.520041	-1121.120100	-1121.116004	-1122.930513	-1122.526477
TS_Bzh_All_F_46	-1121.518071	-1121.117381	-1121.113701	-1122.929764	-1122.525394

Table S50: Azet_{Bzh,Bn}

	Energy (opt)	G (opt)	G-qh (opt)	E (sp)	G-qh (sp)
TS_Bzh_Bn_F_1	-1275.014246	-1274.569739	-1274.564087	-1276.606060	-1276.155901
TS_Bzh_Bn_F_2	-1275.014410	-1274.569500	-1274.563963	-1276.605929	-1276.155482
TS_Bzh_Bn_F_3	-1275.015001	-1274.569547	-1274.564416	-1276.604562	-1276.153977
TS_Bzh_Bn_F_4	-1275.012089	-1274.567064	-1274.561705	-1276.604157	-1276.153772
TS_Bzh_Bn_F_5	-1275.012080	-1274.567353	-1274.561816	-1276.603952	-1276.153688
TS_Bzh_Bn_F_6	-1275.010379	-1274.566507	-1274.560440	-1276.603355	-1276.153416
TS_Bzh_Bn_F_7	-1275.009693	-1274.567250	-1274.560575	-1276.602436	-1276.153317
TS_Bzh_Bn_F_8	-1275.012476	-1274.567097	-1274.562056	-1276.603688	-1276.153268
TS_Bzh_Bn_F_9	-1275.012633	-1274.567775	-1274.562121	-1276.603485	-1276.152974
TS_Bzh_Bn_F_10	-1275.013740	-1274.567690	-1274.562856	-1276.602895	-1276.152011
TS_Bzh_Bn_F_11	-1275.010036	-1274.566391	-1274.560048	-1276.601902	-1276.151914
TS_Bzh_Bn_F_12	-1275.009709	-1274.565461	-1274.559821	-1276.601392	-1276.151504
TS_Bzh_Bn_F_13	-1275.008377	-1274.564488	-1274.558460	-1276.601056	-1276.151139
TS_Bzh_Bn_F_14	-1275.008541	-1274.564380	-1274.558606	-1276.600735	-1276.150800
TS_Bzh_Bn_F_15	-1275.009538	-1274.564181	-1274.559183	-1276.600897	-1276.150542
TS_Bzh_Bn_F_16	-1275.011049	-1274.565666	-1274.560294	-1276.601152	-1276.150397
TS_Bzh_Bn_F_17	-1275.010522	-1274.566154	-1274.560504	-1276.600264	-1276.150246
TS_Bzh_Bn_F_18	-1275.011748	-1274.565545	-1274.561032	-1276.600847	-1276.150131
TS_Bzh_Bn_F_19	-1275.009271	-1274.565145	-1274.559162	-1276.599788	-1276.149680
TS_Bzh_Bn_F_20	-1275.006608	-1274.561289	-1274.556162	-1276.598737	-1276.148291
TS_Bzh_Bn_F_21	-1275.006434	-1274.561510	-1274.556112	-1276.598598	-1276.148276
TS_Bzh_Bn_F_22	-1275.011134	-1274.564005	-1274.559454	-1276.599943	-1276.148263
TS_Bzh_Bn_F_23	-1275.007642	-1274.562160	-1274.557310	-1276.598275	-1276.147943
TS_Bzh_Bn_F_24	-1275.009346	-1274.562289	-1274.557716	-1276.599475	-1276.147845
TS_Bzh_Bn_F_25	-1275.008435	-1274.562912	-1274.557743	-1276.598341	-1276.147648

Azetidinium Fluorination Products

Table S51: Azet_{Me,Me}

	Energy (opt)	G (opt)	G-qh (opt)	E (sp)	G-qh (sp)
Prod_Me_Me_1	-582.708649	-582.492942	-582.490973	-583.461258	-583.243582
Prod_Me_Me_2	-582.708489	-582.492633	-582.490690	-583.461308	-583.243509
Prod_Me_Me_3	-582.708375	-582.492466	-582.490536	-583.461300	-583.243461
Prod_Me_Me_4	-582.708933	-582.492694	-582.490879	-583.460845	-583.242791
Prod_Me_Me_5	-582.708704	-582.492630	-582.490682	-583.460549	-583.242528
Prod_Me_Me_6	-582.707018	-582.491058	-582.489134	-583.459804	-583.241920
Prod_Me_Me_7	-582.707167	-582.490762	-582.489146	-583.459361	-583.241339
Prod_Me_Me_8	-582.706151	-582.490525	-582.488433	-583.459015	-583.241297
Prod_Me_Me_9	-582.706093	-582.490345	-582.488560	-583.458489	-583.240956
Prod_Me_Me_10	-582.707046	-582.490220	-582.488733	-583.459111	-583.240799
Prod_Me_Me_11	-582.706825	-582.490873	-582.488924	-583.458389	-583.240489
Prod_Me_Me_12	-582.706351	-582.490133	-582.488218	-583.458491	-583.240358
Prod_Me_Me_13	-582.706054	-582.490507	-582.488352	-583.457865	-583.240164
Prod_Me_Me_14	-582.707221	-582.490332	-582.488840	-583.458393	-583.240012
Prod_Me_Me_15	-582.704668	-582.488806	-582.486760	-583.457782	-583.239874
Prod_Me_Me_16	-582.704530	-582.488352	-582.486502	-583.457569	-583.239542
Prod_Me_Me_17	-582.703981	-582.488009	-582.486071	-583.456137	-583.238226
Prod_Me_Me_18	-582.704105	-582.487730	-582.485982	-583.456167	-583.238044
Prod_Me_Me_19	-582.703397	-582.487382	-582.485367	-583.455251	-583.237221
Prod_Me_Me_20	-582.703356	-582.487107	-582.485586	-583.454930	-583.237160

Prod_Me_Me_21	-582.703034	-582.485967	-582.484438	-583.455006	-583.236410
Prod_Me_Me_22	-582.702512	-582.486705	-582.484754	-583.454000	-583.236242
Prod_Me_Me_23	-582.703387	-582.486031	-582.484660	-583.454566	-583.235839
Prod_Me_Me_24	-582.702799	-582.485538	-582.484164	-583.453825	-583.235190
Prod_Me_Me_25	-582.703258	-582.485801	-582.484421	-583.453662	-583.234825
Prod_Me_Me_26	-582.701842	-582.484796	-582.483284	-583.452360	-583.233802
Prod_Me_Me_27	-582.701838	-582.484066	-582.482725	-583.452817	-583.233705

Table S52: Azet_{Bn,Me}

	Energy (opt)	G (opt)	G-qh (opt)	E (sp)	G-qh (sp)
Prod_Bn_Me_1	-813.502216	-813.211663	-813.207690	-814.532734	-814.238208
Prod_Bn_Me_2	-813.502523	-813.210508	-813.207381	-814.532668	-814.237526
Prod_Bn_Me_3	-813.502442	-813.211223	-813.207604	-814.532283	-814.237444
Prod_Bn_Me_4	-813.501457	-813.211418	-813.207166	-814.531628	-814.237337
Prod_Bn_Me_5	-813.502589	-813.211801	-813.207831	-814.532049	-814.237291
Prod_Bn_Me_6	-813.500917	-813.210564	-813.206513	-814.531158	-814.236754
Prod_Bn_Me_7	-813.501971	-813.210465	-813.207072	-814.531463	-814.236564
Prod_Bn_Me_8	-813.500755	-813.210738	-813.206492	-814.530707	-814.236444
Prod_Bn_Me_9	-813.500462	-813.210408	-813.206201	-814.530508	-814.236247
Prod_Bn_Me_10	-813.501815	-813.210793	-813.206884	-814.530918	-814.235988
Prod_Bn_Me_11	-813.500322	-813.209634	-813.205564	-814.530704	-814.235945
Prod_Bn_Me_12	-813.500346	-813.208859	-813.205223	-814.530655	-814.235533
Prod_Bn_Me_13	-813.500314	-813.209519	-813.205542	-814.530189	-814.235417
Prod_Bn_Me_14	-813.499197	-813.208850	-813.204807	-814.529803	-814.235413
Prod_Bn_Me_15	-813.501524	-813.209494	-813.206314	-814.530540	-814.235330
Prod_Bn_Me_16	-813.502244	-813.209826	-813.206865	-814.530595	-814.235216
Prod_Bn_Me_17	-813.500156	-813.209614	-813.205673	-814.529678	-814.235195
Prod_Bn_Me_18	-813.500378	-813.208672	-813.205019	-814.530523	-814.235164
Prod_Bn_Me_19	-813.500919	-813.209609	-813.205803	-814.530161	-814.235045
Prod_Bn_Me_20	-813.500232	-813.209116	-813.205256	-814.529923	-814.234948
Prod_Bn_Me_21	-813.499464	-813.208947	-813.204952	-814.529439	-814.234928
Prod_Bn_Me_22	-813.500032	-813.209149	-813.205365	-814.529531	-814.234864
Prod_Bn_Me_23	-813.499644	-813.208837	-813.205040	-814.529146	-814.234542
Prod_Bn_Me_24	-813.500618	-813.208699	-813.205211	-814.529544	-814.234137
Prod_Bn_Me_25	-813.499446	-813.208245	-813.204590	-814.528892	-814.234037
Prod_Bn_Me_26	-813.500364	-813.208287	-813.204845	-814.529552	-814.234034
Prod_Bn_Me_27	-813.498446	-813.208839	-813.204279	-814.528094	-814.233926
Prod_Bn_Me_28	-813.500219	-813.209046	-813.205295	-814.528833	-814.233909
Prod_Bn_Me_29	-813.498692	-813.208329	-813.204200	-814.528124	-814.233632
Prod_Bn_Me_30	-813.498704	-813.207245	-813.203493	-814.528656	-814.233444
Prod_Bn_Me_31	-813.499657	-813.208195	-813.204627	-814.528242	-814.233212
Prod_Bn_Me_32	-813.500900	-813.208266	-813.205069	-814.529024	-814.233193
Prod_Bn_Me_33	-813.500579	-813.208422	-813.204956	-814.528793	-814.233170
Prod_Bn_Me_34	-813.498116	-813.206145	-813.202713	-814.528174	-814.232771
Prod_Bn_Me_35	-813.500135	-813.205824	-813.203599	-814.528391	-814.231855
Prod_Bn_Me_36	-813.499746	-813.205566	-813.203201	-814.528075	-814.231529
Prod_Bn_Me_37	-813.499776	-813.205683	-813.203322	-814.527201	-814.230747

Table S53: Azet_{Bzh,Me}

	Energy (opt)	G (opt)	G-qh (opt)	E (sp)	G-qh (sp)
Prod_Bzh_Me_1	-1044.293768	-1043.926966	-1043.921938	-1045.599729	-1045.227898
Prod_Bzh_Me_2	-1044.291928	-1043.926607	-1043.920787	-1045.598807	-1045.227665
Prod_Bzh_Me_3	-1044.292568	-1043.925762	-1043.920615	-1045.599618	-1045.227665
Prod_Bzh_Me_4	-1044.293776	-1043.926585	-1043.921766	-1045.599546	-1045.227536
Prod_Bzh_Me_5	-1044.293643	-1043.926221	-1043.921402	-1045.599457	-1045.227217
Prod_Bzh_Me_6	-1044.292969	-1043.926189	-1043.920936	-1045.598859	-1045.226825
Prod_Bzh_Me_7	-1044.291627	-1043.925416	-1043.920050	-1045.597598	-1045.226022
Prod_Bzh_Me_8	-1044.293808	-1043.925704	-1043.921314	-1045.598504	-1045.226011
Prod_Bzh_Me_9	-1044.293539	-1043.925043	-1043.920839	-1045.598547	-1045.225847

Prod_Bzh_Me_10	-1044.291513	-1043.925306	-1043.919821	-1045.597462	-1045.225770
Prod_Bzh_Me_11	-1044.292696	-1043.924765	-1043.920134	-1045.598072	-1045.225511
Prod_Bzh_Me_12	-1044.290150	-1043.923953	-1043.918459	-1045.597099	-1045.225408
Prod_Bzh_Me_13	-1044.290416	-1043.924075	-1043.918763	-1045.596973	-1045.225320
Prod_Bzh_Me_14	-1044.292313	-1043.924266	-1043.919739	-1045.597791	-1045.225217
Prod_Bzh_Me_15	-1044.292590	-1043.924150	-1043.919754	-1045.598030	-1045.225194
Prod_Bzh_Me_16	-1044.291997	-1043.923881	-1043.919285	-1045.597778	-1045.225065
Prod_Bzh_Me_17	-1044.291737	-1043.924434	-1043.919447	-1045.597328	-1045.225038
Prod_Bzh_Me_18	-1044.291201	-1043.924176	-1043.918995	-1045.597086	-1045.224880
Prod_Bzh_Me_19	-1044.289820	-1043.923228	-1043.917955	-1045.596700	-1045.224835
Prod_Bzh_Me_20	-1044.289619	-1043.923571	-1043.918221	-1045.596171	-1045.224773
Prod_Bzh_Me_21	-1044.292907	-1043.924711	-1043.920160	-1045.597427	-1045.224680
Prod_Bzh_Me_22	-1044.292612	-1043.924125	-1043.919845	-1045.597117	-1045.224350
Prod_Bzh_Me_23	-1044.291197	-1043.923423	-1043.918522	-1045.596791	-1045.224116
Prod_Bzh_Me_24	-1044.290997	-1043.924061	-1043.918908	-1045.596116	-1045.224028
Prod_Bzh_Me_25	-1044.290511	-1043.922670	-1043.917872	-1045.596565	-1045.223926
Prod_Bzh_Me_26	-1044.292119	-1043.924078	-1043.919280	-1045.596691	-1045.223852
Prod_Bzh_Me_27	-1044.291503	-1043.923654	-1043.918814	-1045.596428	-1045.223739
Prod_Bzh_Me_28	-1044.289632	-1043.922824	-1043.917621	-1045.595576	-1045.223564
Prod_Bzh_Me_29	-1044.290036	-1043.922529	-1043.917612	-1045.595739	-1045.223315
Prod_Bzh_Me_30	-1044.291393	-1043.922001	-1043.918094	-1045.595765	-1045.222467
Prod_Bzh_Me_31	-1044.290065	-1043.921388	-1043.916944	-1045.595511	-1045.222390
Prod_Bzh_Me_32	-1044.288578	-1043.921249	-1043.916241	-1045.593453	-1045.221116
Prod_Bzh_Me_33	-1044.287460	-1043.920568	-1043.915537	-1045.592898	-1045.220976
Prod_Bzh_Me_34	-1044.289761	-1043.920646	-1043.916346	-1045.594300	-1045.220885
Prod_Bzh_Me_35	-1044.288864	-1043.920578	-1043.916167	-1045.593293	-1045.220595

Asymmetric Fluorination Transition State Structures

Table S54: Azet_{Bzh,Me}

	Energy (opt)	G (opt)	G-qh (opt)	E (sp)	G-qh (sp)
TS _{Major} -Cis-1	-4187.904254	-4186.958416	-4186.940769	-4193.014743	-4192.051258
TS _{Major} -Cis-2	-4187.902588	-4186.957131	-4186.939106	-4193.012853	-4192.049371
TS _{Major} -Cis-3	-4187.903028	-4186.957249	-4186.939442	-4193.012822	-4192.049235
TS _{Major} -Cis-4	-4187.900377	-4186.956354	-4186.937643	-4193.011656	-4192.048923
TS _{Major} -Cis-5	-4187.903048	-4186.955345	-4186.938193	-4193.012178	-4192.047323
TS _{Major} -Cis-6	-4187.899365	-4186.954568	-4186.936071	-4193.009194	-4192.045900
TS _{Major} -Cis-7	-4187.901646	-4186.954038	-4186.936445	-4193.010540	-4192.045339
TS _{Major} -Cis-8	-4187.901408	-4186.953317	-4186.936213	-4193.010378	-4192.045183
TS _{Major} -Cis-9	-4187.893810	-4186.948599	-4186.929989	-4193.005990	-4192.042169
TS _{Major} -Cis-10	-4187.897339	-4186.950562	-4186.932517	-4193.006553	-4192.041731
TS _{Major} -Cis-11	-4187.897339	-4186.950560	-4186.932515	-4193.006549	-4192.041726
TS _{Major} -Cis-12	-4187.888635	-4186.946068	-4186.925600	-4193.003343	-4192.040309
TS _{Major} -Cis-13	-4187.895675	-4186.949604	-4186.931273	-4193.003238	-4192.038836
TS _{Major} -Cis-14	-4187.886415	-4186.944989	-4186.924476	-4193.000511	-4192.038572
TS _{Minor} -Cis-1	-4187.905521	-4186.958870	-4186.941462	-4193.015301	-4192.051242
TS _{Minor} -Cis-2	-4187.901322	-4186.956487	-4186.938179	-4193.012674	-4192.049531
TS _{Minor} -Cis-3	-4187.900990	-4186.955505	-4186.936718	-4193.010657	-4192.046384
TS _{Minor} -Cis-4	-4187.899292	-4186.952503	-4186.934907	-4193.010312	-4192.045926
TS _{Minor} -Cis-5	-4187.896368	-4186.952598	-4186.932663	-4193.009285	-4192.045580
TS _{Minor} -Cis-6	-4187.889391	-4186.948794	-4186.927601	-4193.005009	-4192.043219
TS _{Minor} -Cis-7	-4187.891753	-4186.945306	-4186.927335	-4193.003092	-4192.038675
TS _{Minor} -Cis-8	-4187.887141	-4186.944431	-4186.924367	-4193.001446	-4192.038672
TS _{Minor} -Cis-9	-4187.890274	-4186.945841	-4186.927181	-4193.001015	-4192.037921
TS _{Minor} -Cis-10	-4187.894899	-4186.942936	-4186.927355	-4193.003041	-4192.035498

Table S55: Azet_{Bzh,Et}

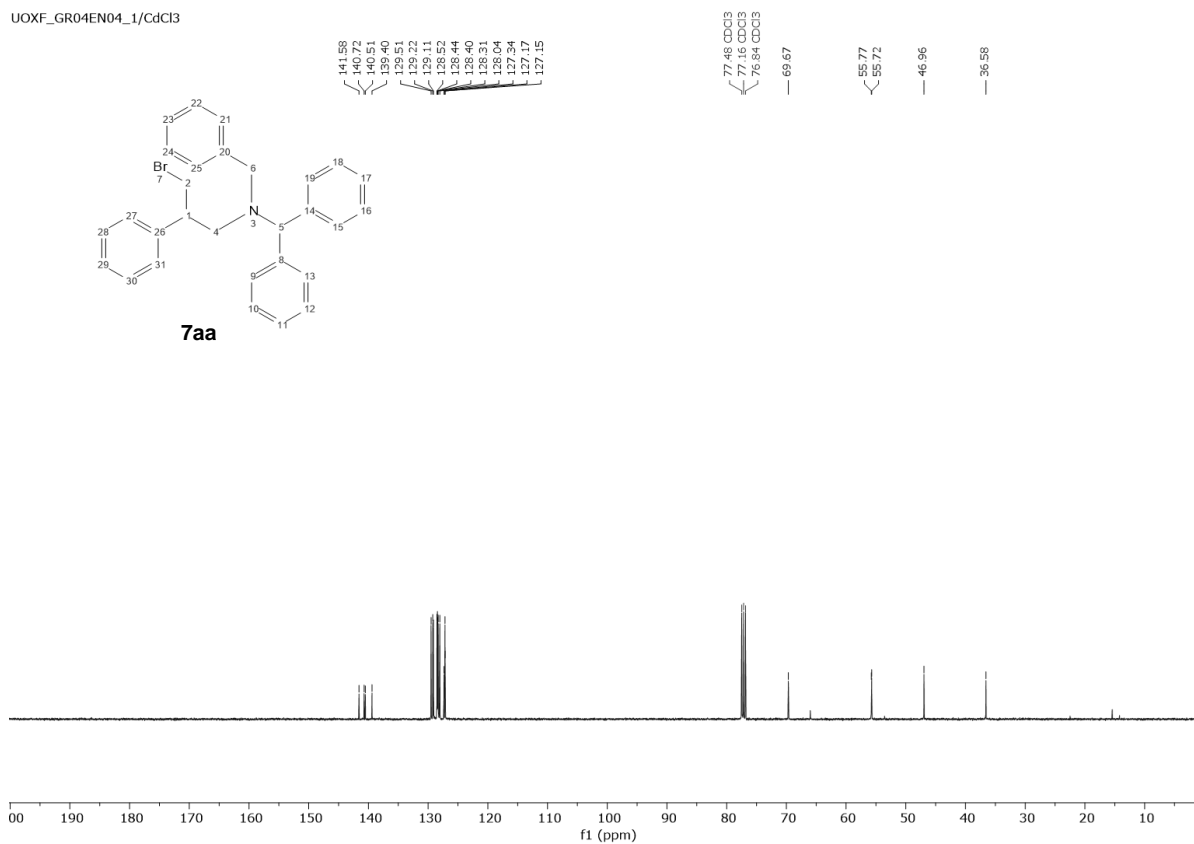
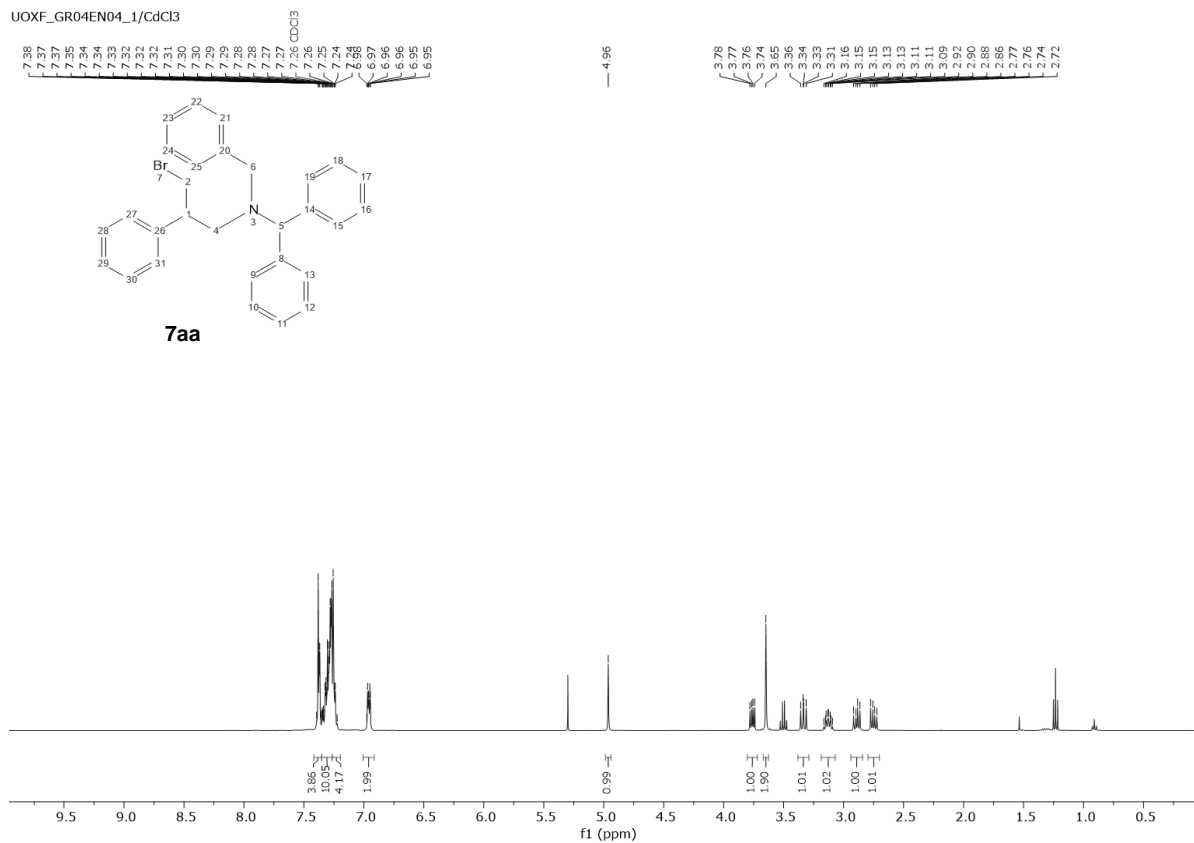
	Energy (opt)	G (opt)	G-qh (opt)	E (sp)	G-qh (sp)
TS _{Major} -Cis-1-Ethyl-1	-4227.170278	-4226.197188	-4226.179290	-4232.335611	-4231.344623

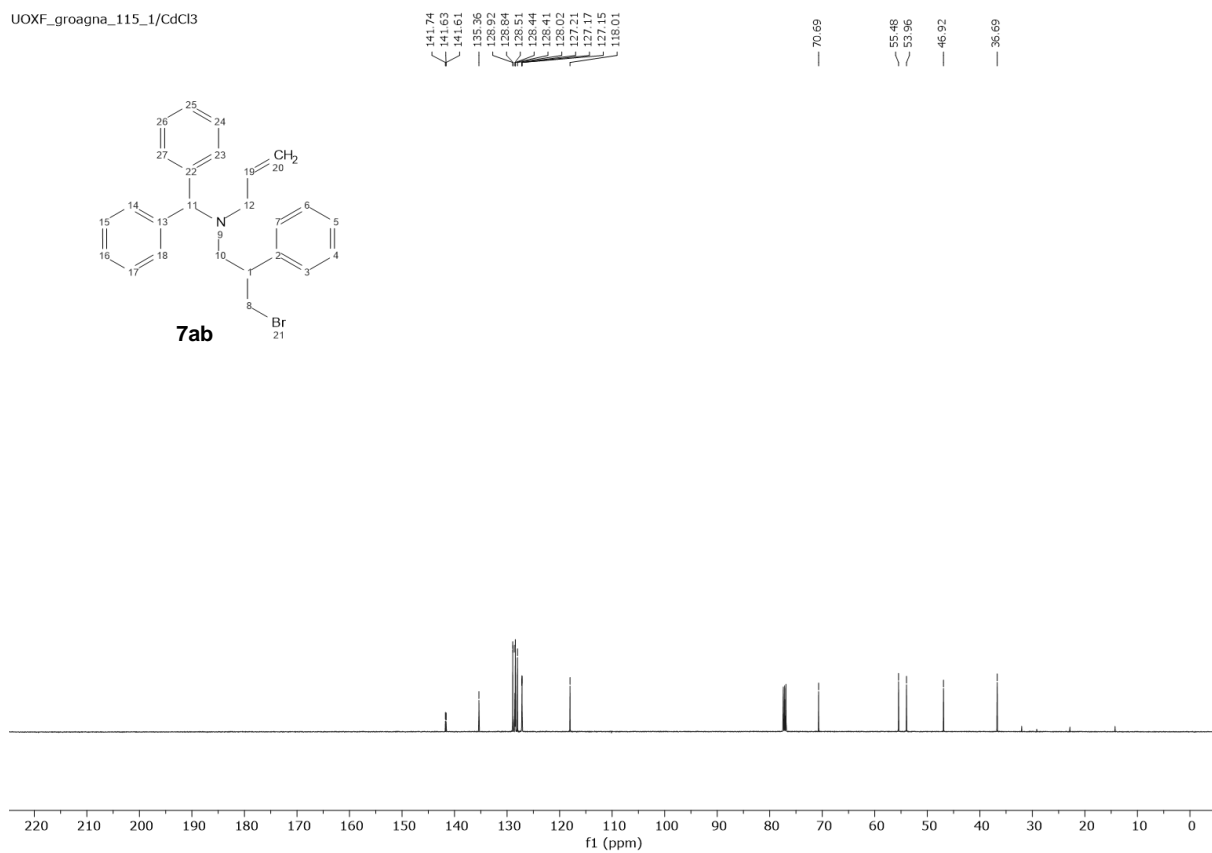
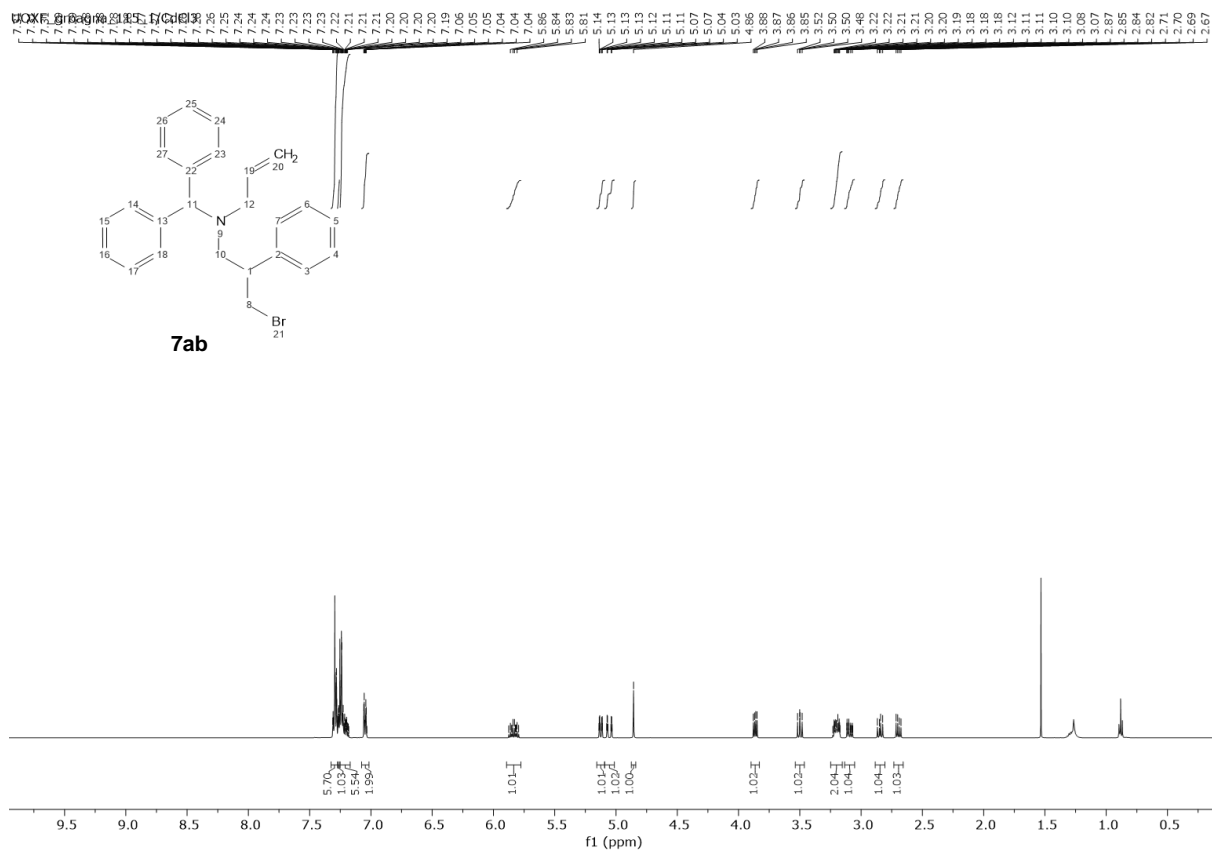
TS_{Major}-Cis-1-Ethyl-2	-4227.164451	-4226.190737	-4226.172949	-4232.330775	-4231.339274
TS_{Major}-Cis-1-Ethyl-3	-4227.164319	-4226.188732	-4226.171693	-4232.330099	-4231.337474
TS_{Minor}-Cis-1-Ethyl-1	-4227.168998	-4226.194329	-4226.177033	-4232.334152	-4231.342187
TS_{Minor}-Cis-1-Ethyl-2	-4227.166980	-4226.193250	-4226.175415	-4232.332037	-4231.340473
TS_{Minor}-Cis-1-Ethyl-3	-4227.164560	-4226.191401	-4226.173213	-4232.330216	-4231.338868
TS_{Minor}-Cis-2-Ethyl-1	-4227.163884	-4226.190944	-4226.172576	-4232.330271	-4231.338962
TS_{Minor}-Cis-2-Ethyl-2	-4227.160871	-4226.188861	-4226.170188	-4232.327466	-4231.336782
TS_{Minor}-Cis-2-Ethyl-3	-4227.163653	-4226.190470	-4226.172172	-4232.330386	-4231.338905

Table S56: Azet_{Bzh,Me}

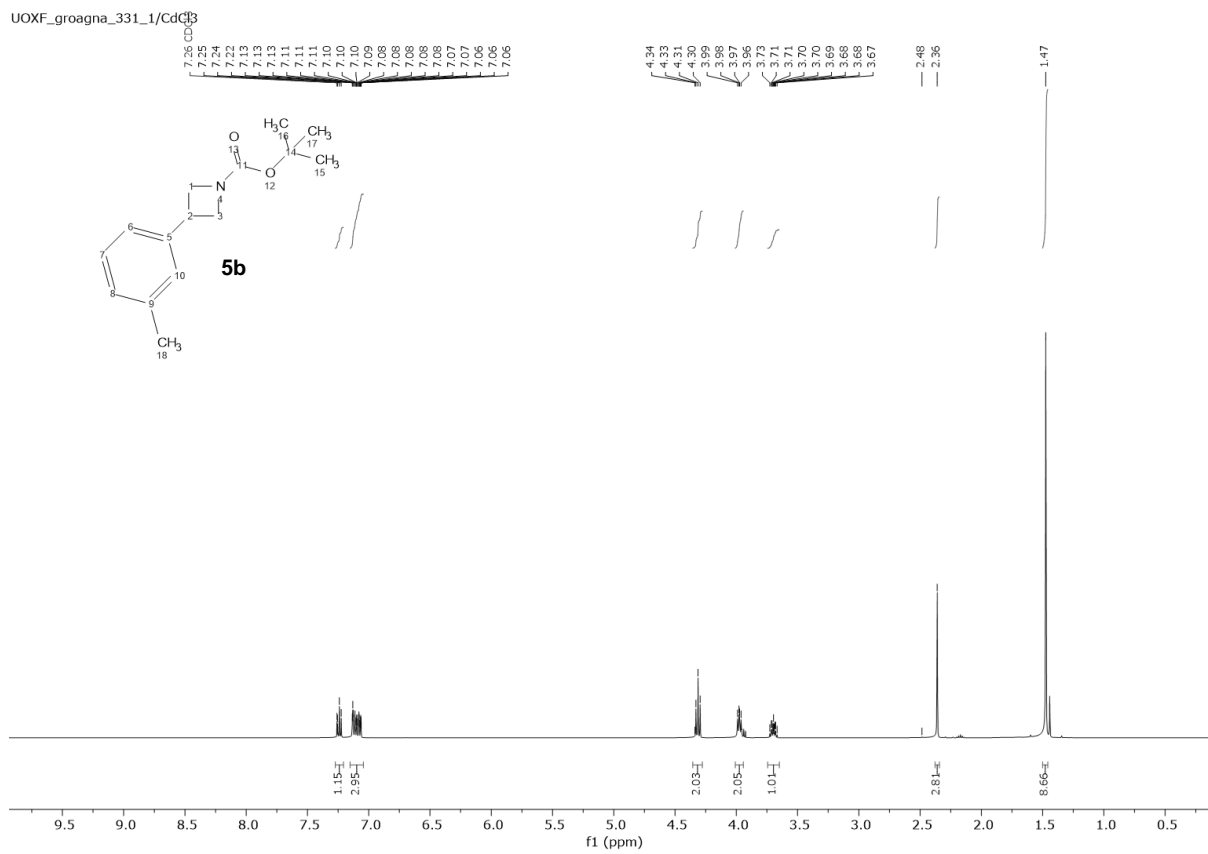
	Energy (opt)	G (opt)	G-gh (opt)	E (sp)	G-gh (sp)
TS_{Major}-Trans-1	-4187.906300	-4186.961432	-4186.942932	-4193.017984	-4192.054616
TS_{Major}-Trans-2	-4187.904980	-4186.958483	-4186.940490	-4193.015650	-4192.051160
TS_{Major}-Trans-3	-4187.901550	-4186.957388	-4186.938780	-4193.013264	-4192.050494
TS_{Major}-Trans-4	-4187.901172	-4186.956080	-4186.937598	-4193.012123	-4192.048549
TS_{Major}-Trans-5	-4187.893903	-4186.952134	-4186.931890	-4193.008899	-4192.046886
TS_{Major}-Trans-6	-4187.893903	-4186.952057	-4186.931851	-4193.008897	-4192.046846
TS_{Major}-Trans-7	-4187.896600	-4186.949868	-4186.932015	-4193.009991	-4192.045406
TS_{Major}-Trans-8	-4187.892564	-4186.947150	-4186.928749	-4193.006197	-4192.042382
TS_{Major}-Trans-9	-4187.887409	-4186.944195	-4186.924335	-4193.001313	-4192.038239
TS_{Major}-Trans-10	-4187.894851	-4186.948029	-4186.929774	-4193.002894	-4192.037817
TS_{Minor}-Trans-1	-4187.899930	-4186.957014	-4186.937528	-4193.012209	-4192.049807
TS_{Minor}-Trans-2	-4187.894128	-4186.953579	-4186.933096	-4193.010013	-4192.048981
TS_{Minor}-Trans-3	-4187.901958	-4186.956438	-4186.937731	-4193.012930	-4192.048704
TS_{Minor}-Trans-4	-4187.900386	-4186.956443	-4186.937532	-4193.011239	-4192.048385
TS_{Minor}-Trans-5	-4187.900206	-4186.956120	-4186.937371	-4193.010613	-4192.047779
TS_{Minor}-Trans-6	-4187.900019	-4186.955845	-4186.937368	-4193.010297	-4192.047646
TS_{Minor}-Trans-7	-4187.899421	-4186.954517	-4186.936254	-4193.010704	-4192.047536
TS_{Minor}-Trans-8	-4187.899686	-4186.953001	-4186.935626	-4193.011540	-4192.047479
TS_{Minor}-Trans-9	-4187.896802	-4186.953341	-4186.934371	-4193.009664	-4192.047233
TS_{Minor}-Trans-10	-4187.896587	-4186.953591	-4186.934528	-4193.009168	-4192.047109
TS_{Minor}-Trans-11	-4187.900309	-4186.954689	-4186.936676	-4193.010651	-4192.047017
TS_{Minor}-Trans-12	-4187.897677	-4186.953011	-4186.934666	-4193.009981	-4192.046969
TS_{Minor}-Trans-13	-4187.898909	-4186.953881	-4186.935226	-4193.010333	-4192.046651
TS_{Minor}-Trans-14	-4187.897524	-4186.951264	-4186.933777	-4193.009363	-4192.045616
TS_{Minor}-Trans-15	-4187.899780	-4186.954993	-4186.935997	-4193.009137	-4192.045354
TS_{Minor}-Trans-16	-4187.894892	-4186.951313	-4186.932382	-4193.007333	-4192.044823
TS_{Minor}-Trans-17	-4187.896789	-4186.952900	-4186.934439	-4193.007129	-4192.044778
TS_{Minor}-Trans-18	-4187.898485	-4186.950531	-4186.933677	-4193.009301	-4192.044494
TS_{Minor}-Trans-19	-4187.898350	-4186.951462	-4186.934183	-4193.008391	-4192.044224
TS_{Minor}-Trans-20	-4187.896470	-4186.951406	-4186.932998	-4193.007115	-4192.043643
TS_{Minor}-Trans-21	-4187.890583	-4186.945910	-4186.927264	-4193.006153	-4192.042834
TS_{Minor}-Trans-22	-4187.885516	-4186.945170	-4186.924292	-4193.003980	-4192.042756
TS_{Minor}-Trans-23	-4187.898829	-4186.951560	-4186.934242	-4193.006945	-4192.042359
TS_{Minor}-Trans-24	-4187.893252	-4186.947821	-4186.928800	-4193.004564	-4192.040112
TS_{Minor}-Trans-25	-4187.892450	-4186.948890	-4186.929381	-4193.003038	-4192.039970
TS_{Minor}-Trans-26	-4187.891363	-4186.947716	-4186.928204	-4193.002697	-4192.039538
TS_{Minor}-Trans-27	-4187.888556	-4186.944575	-4186.925201	-4193.000575	-4192.037221

Copies of NMR Spectra

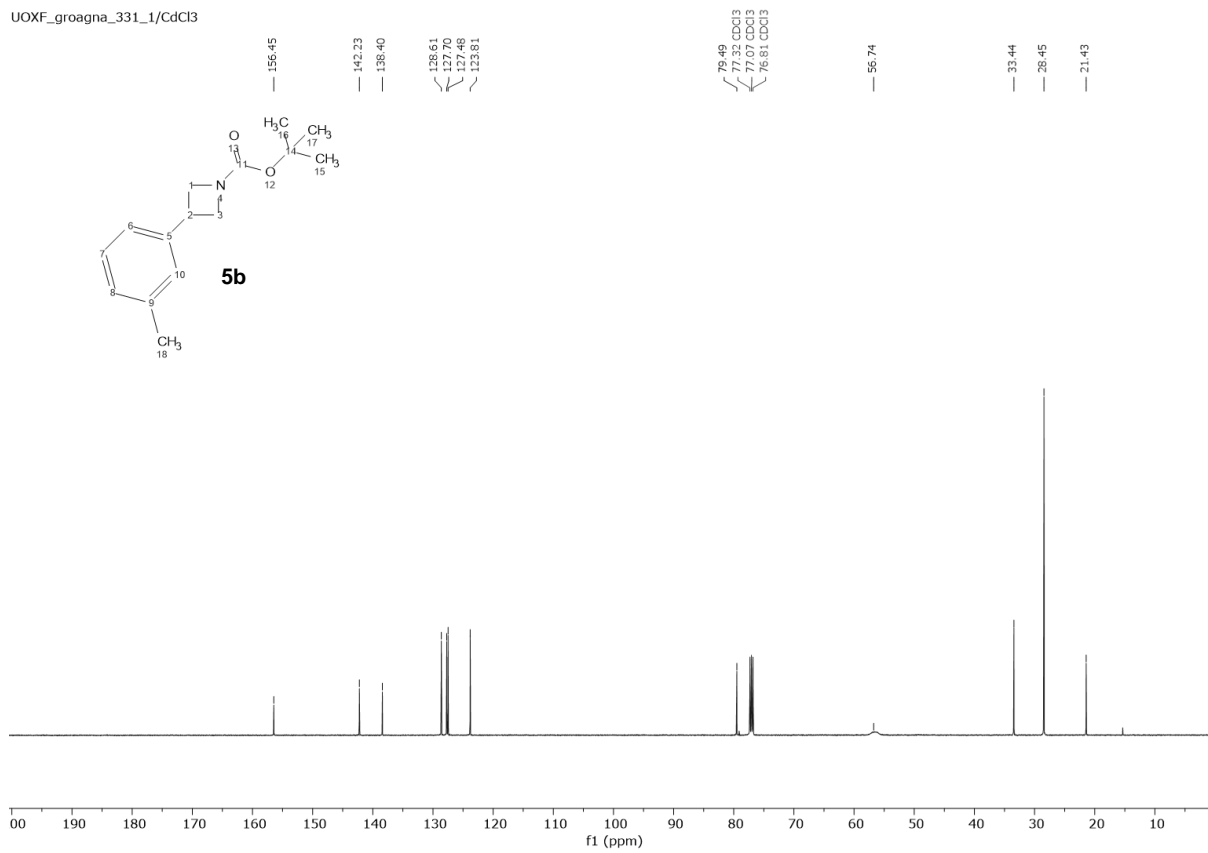




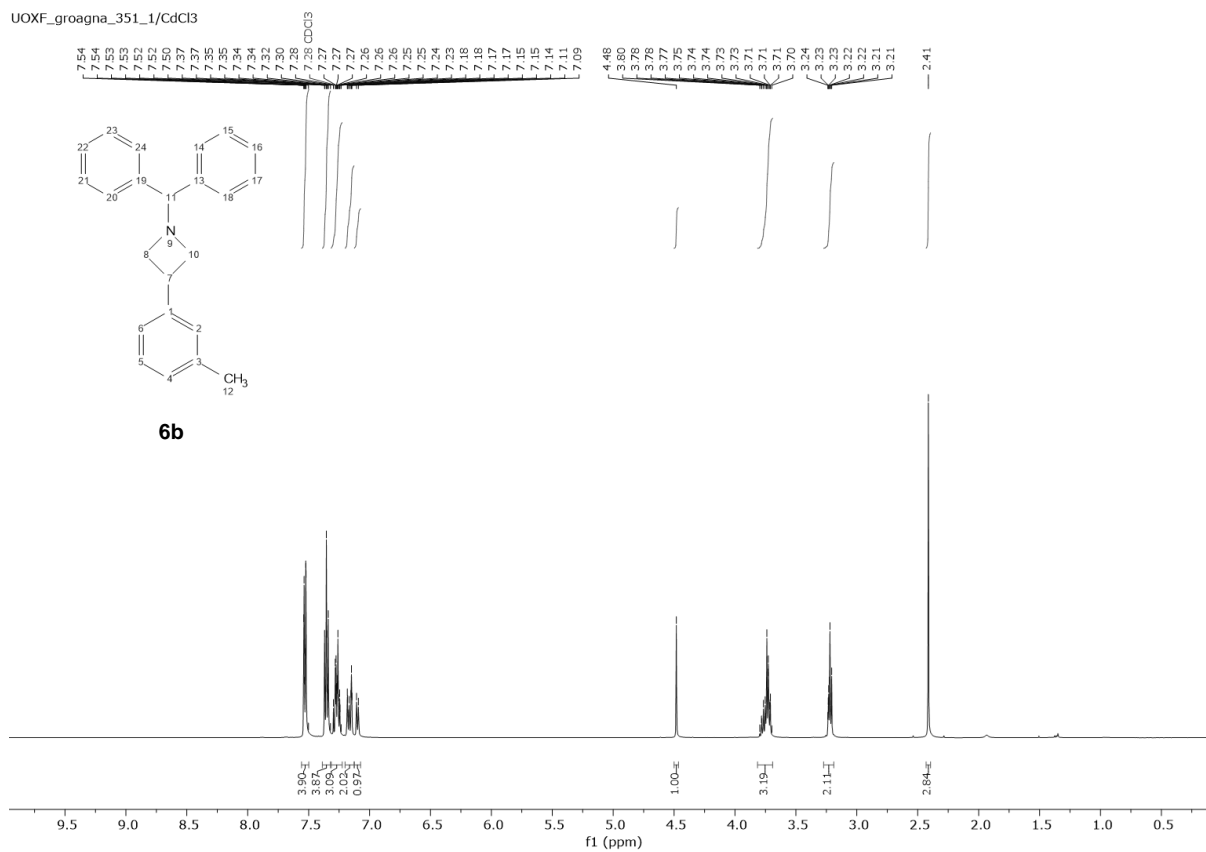
UOXF_groagna_331_1/CdCl3



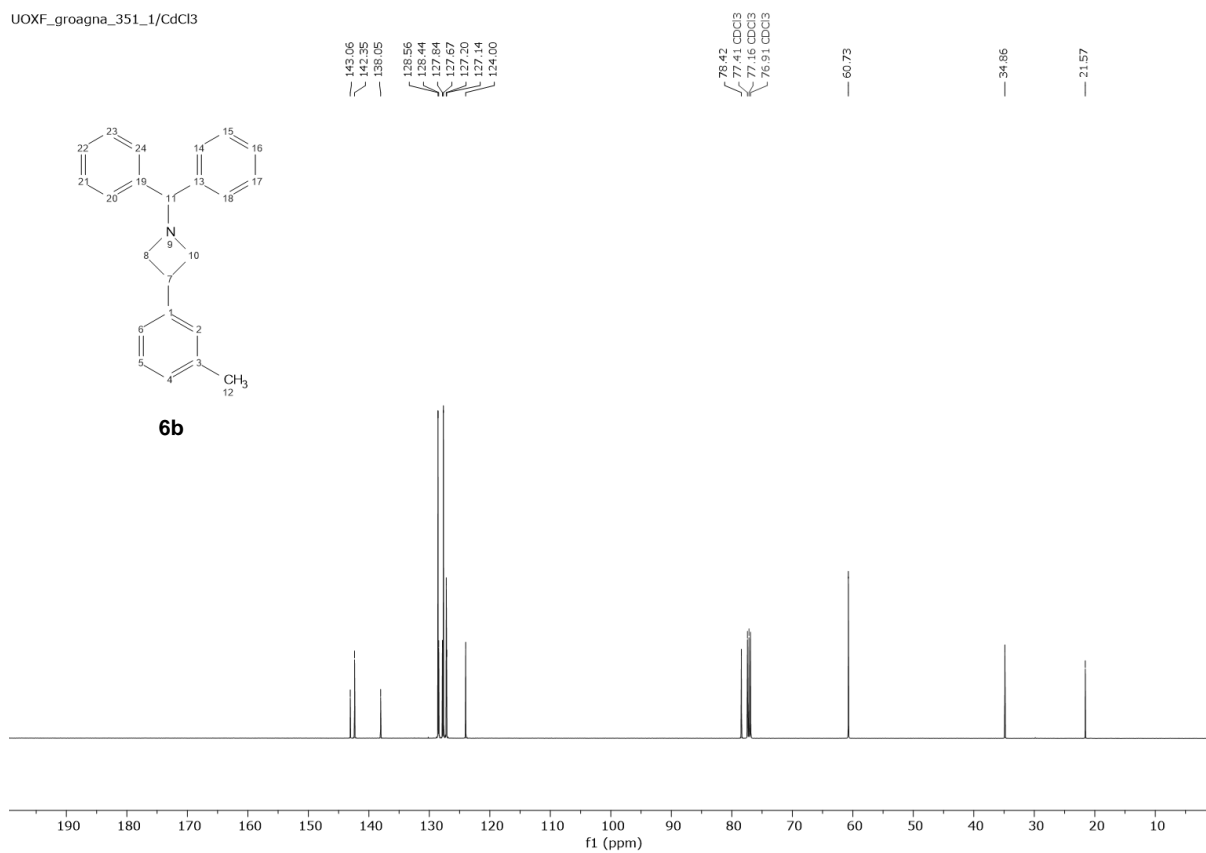
UOXF_groagna_331_1/CdCl3



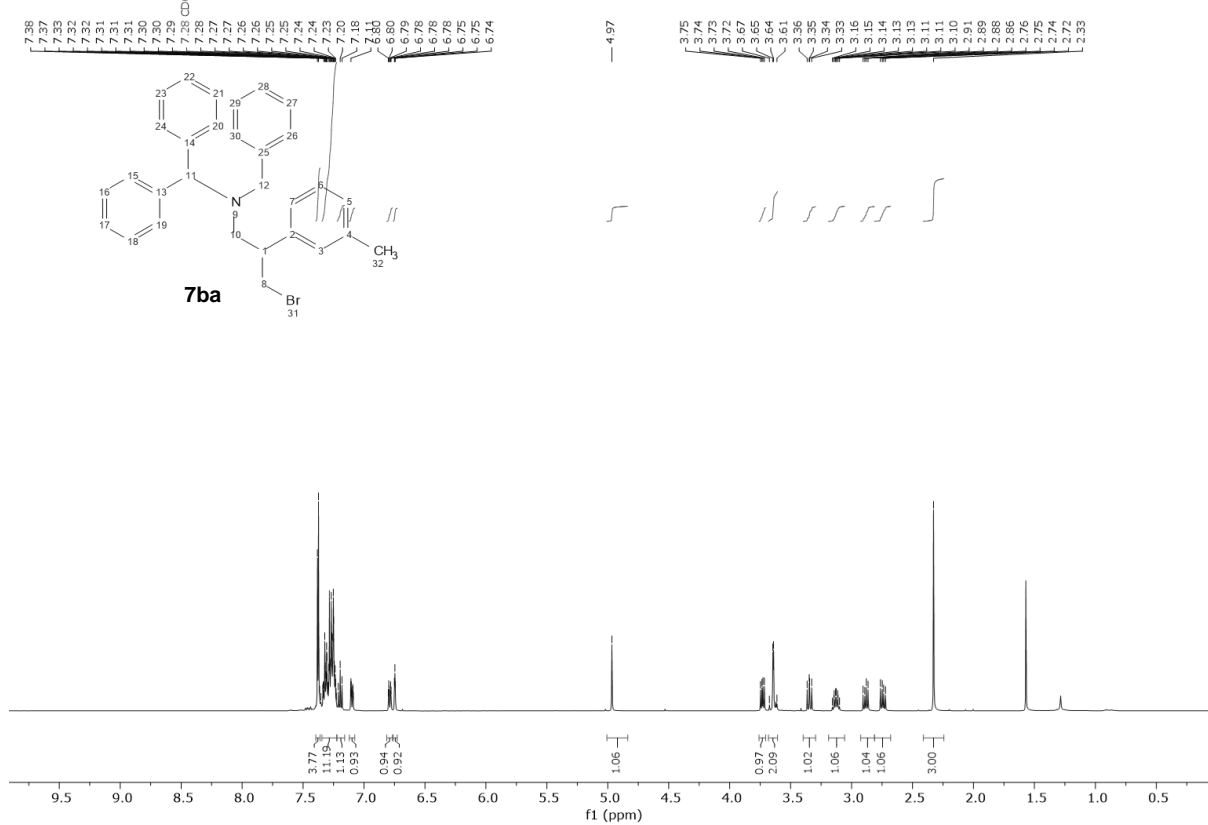
UOXF_groagna_351_1/CdCl3



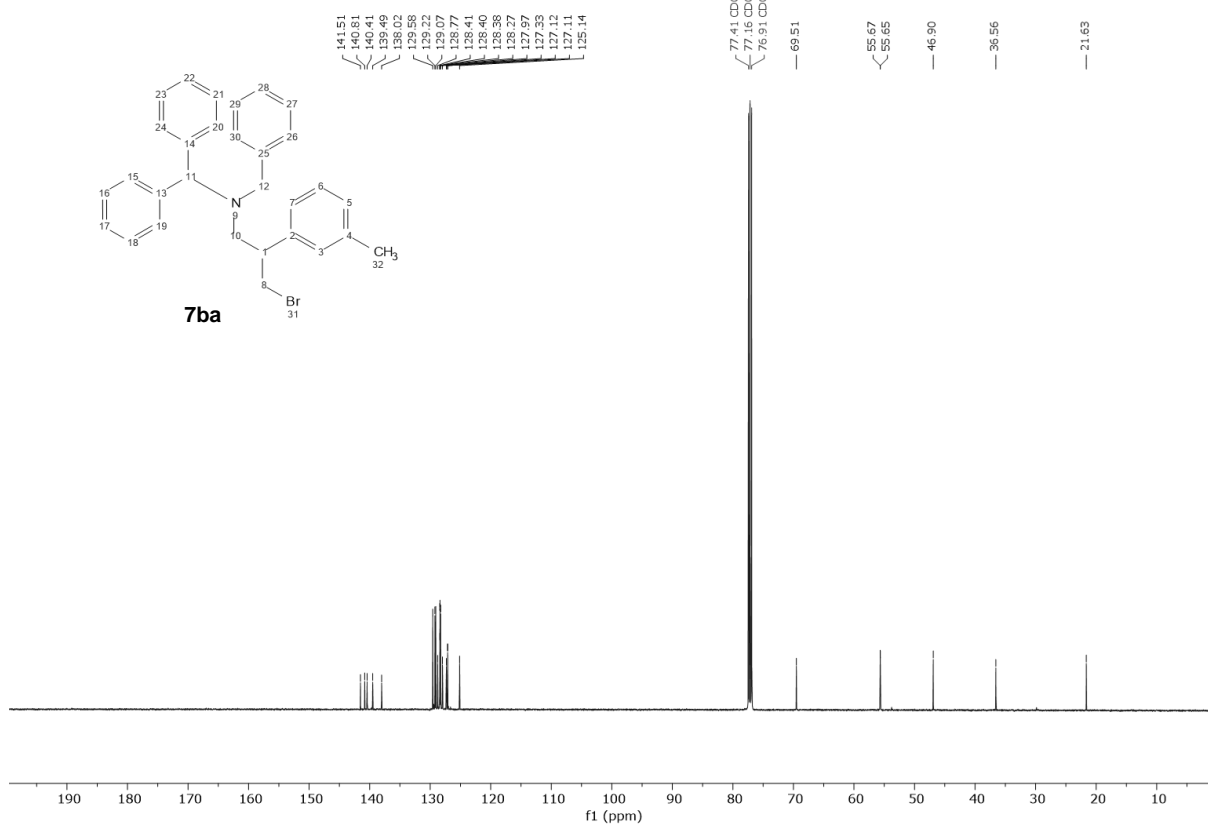
UOXF_groagna_351_1/CdCl3



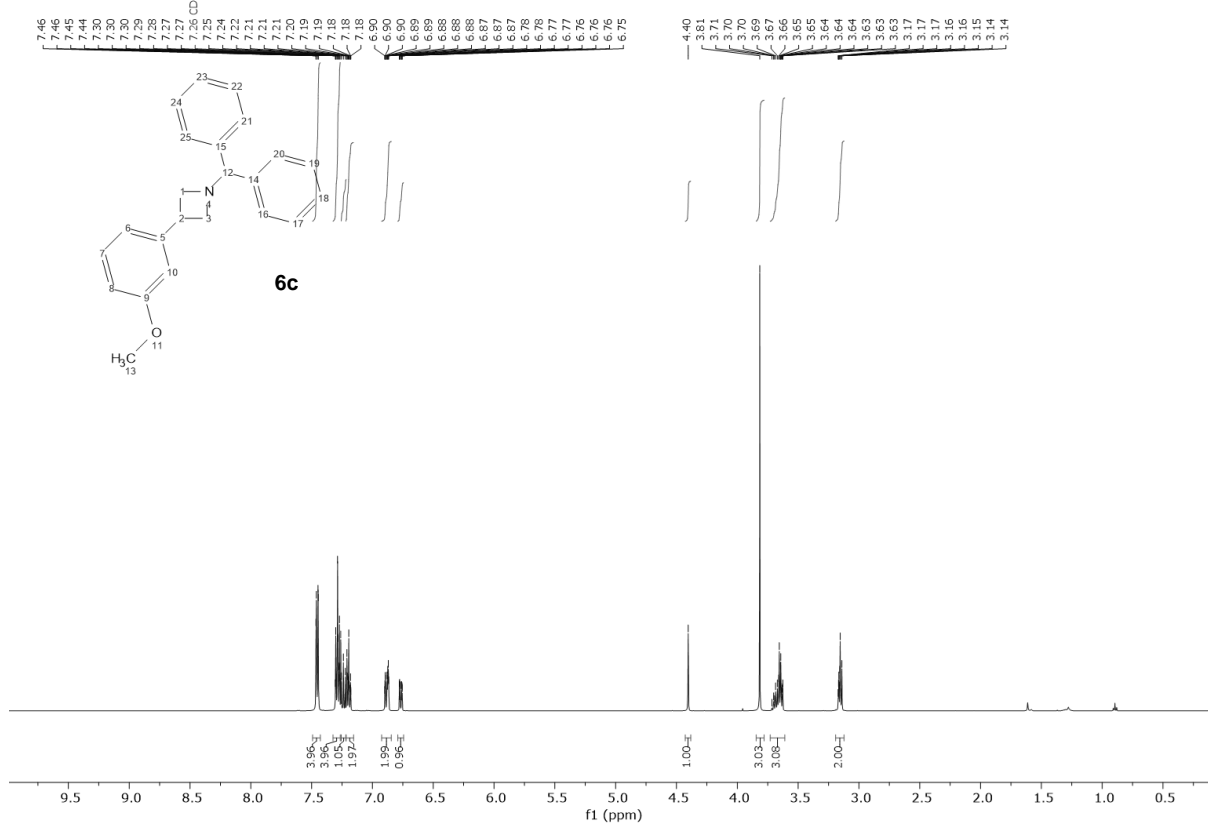
UOXF_groagna_362_1/CdCl3



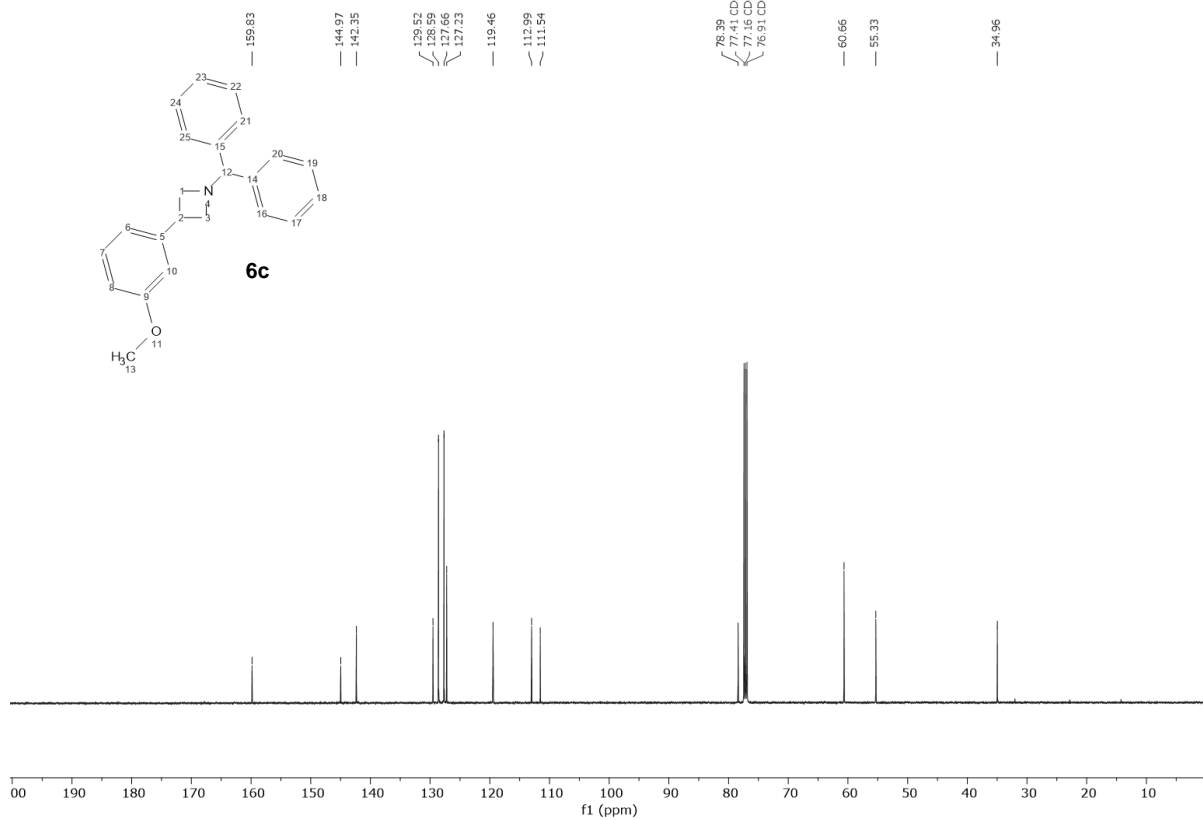
UOXF_groagna_362_1/CdCl3



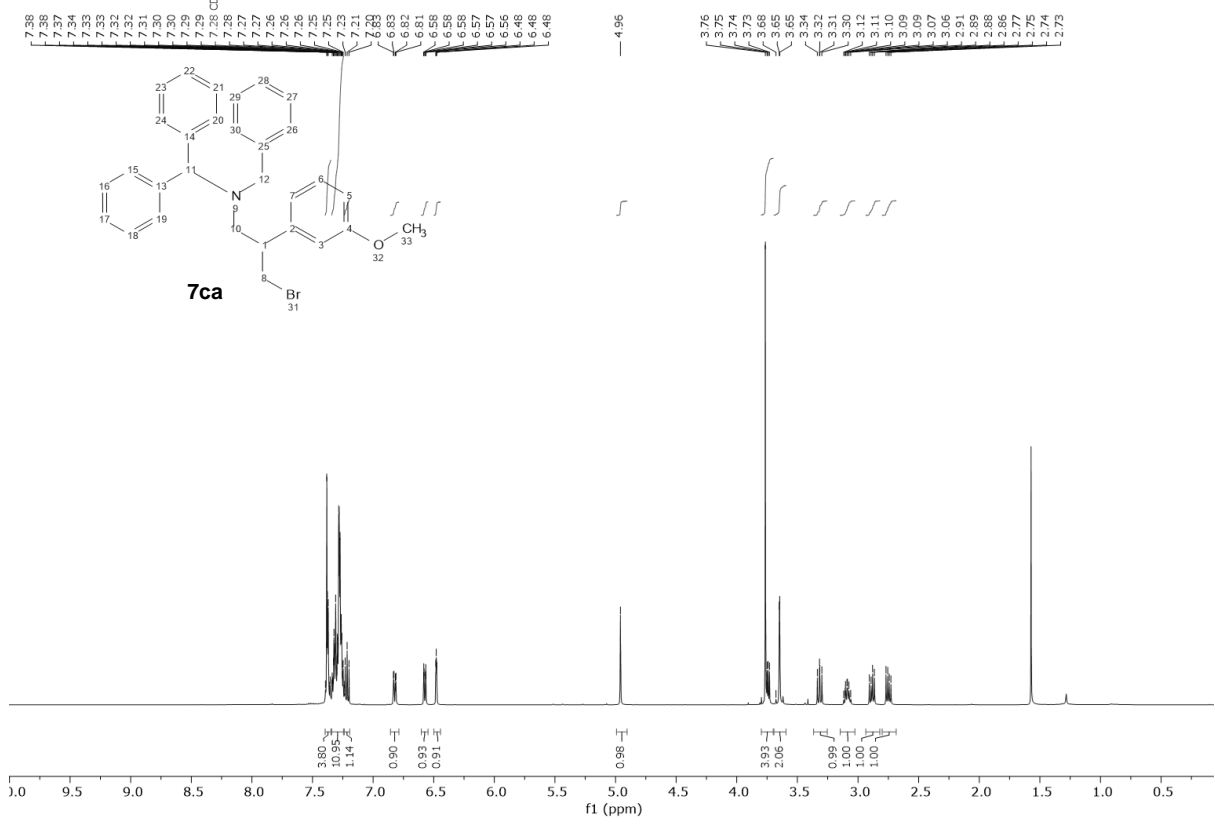
UOXF_groagna_352_A_1/CdCl3



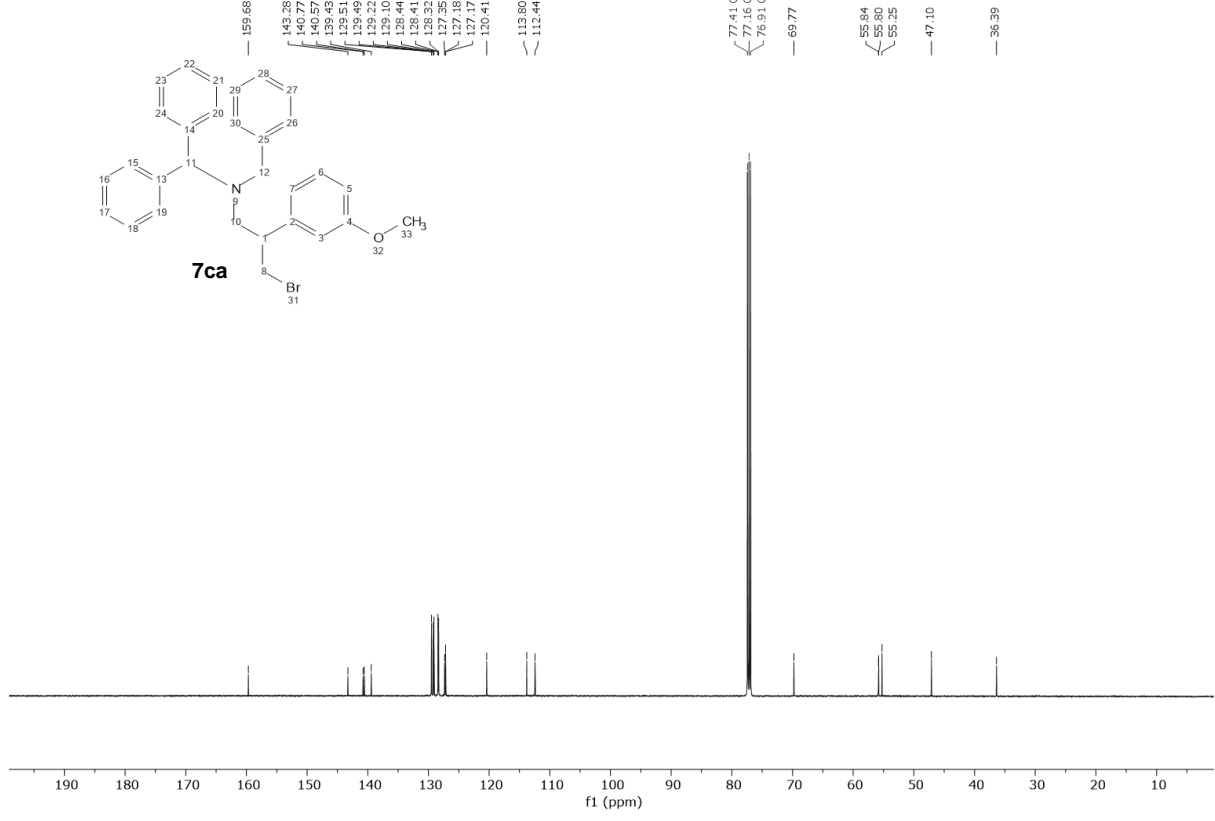
UOXF_groagna_352_A_1/CdCl3



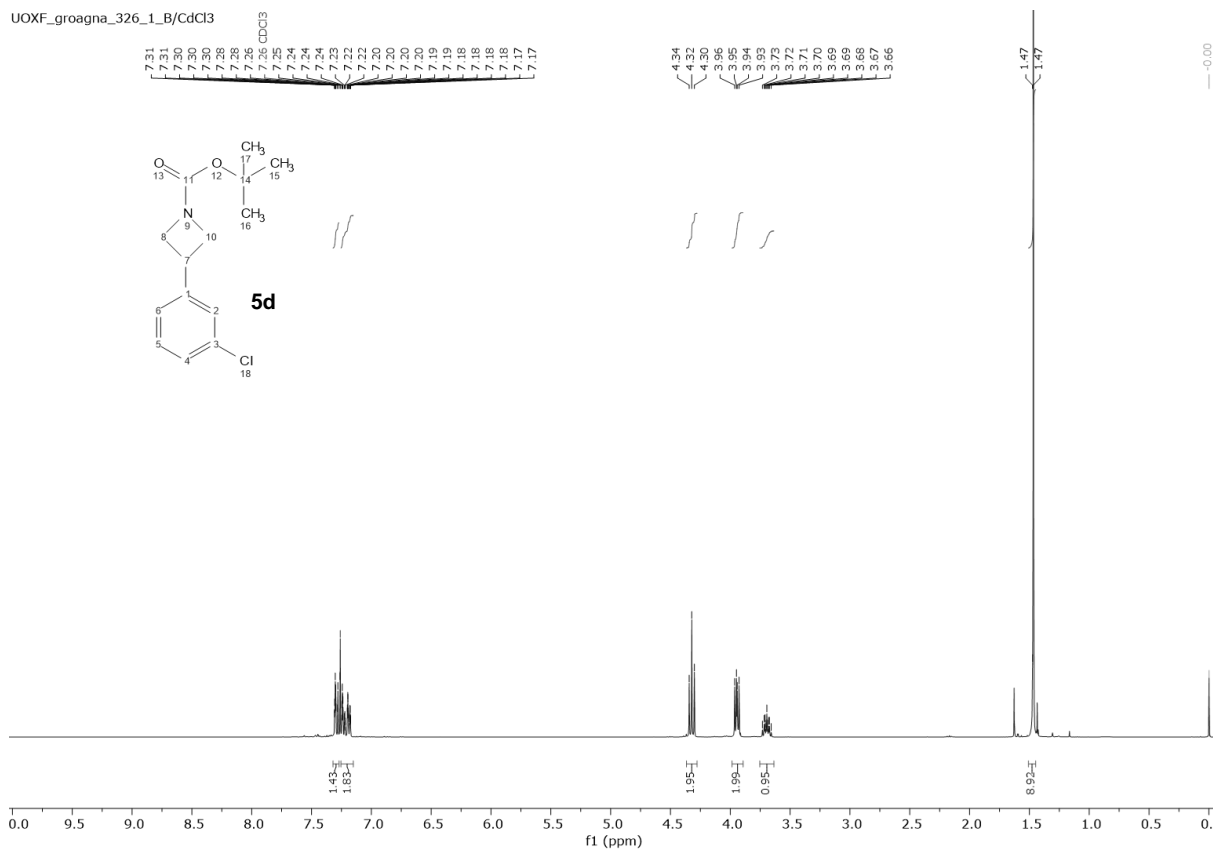
UOXF_groagna_364_1/CdCl3



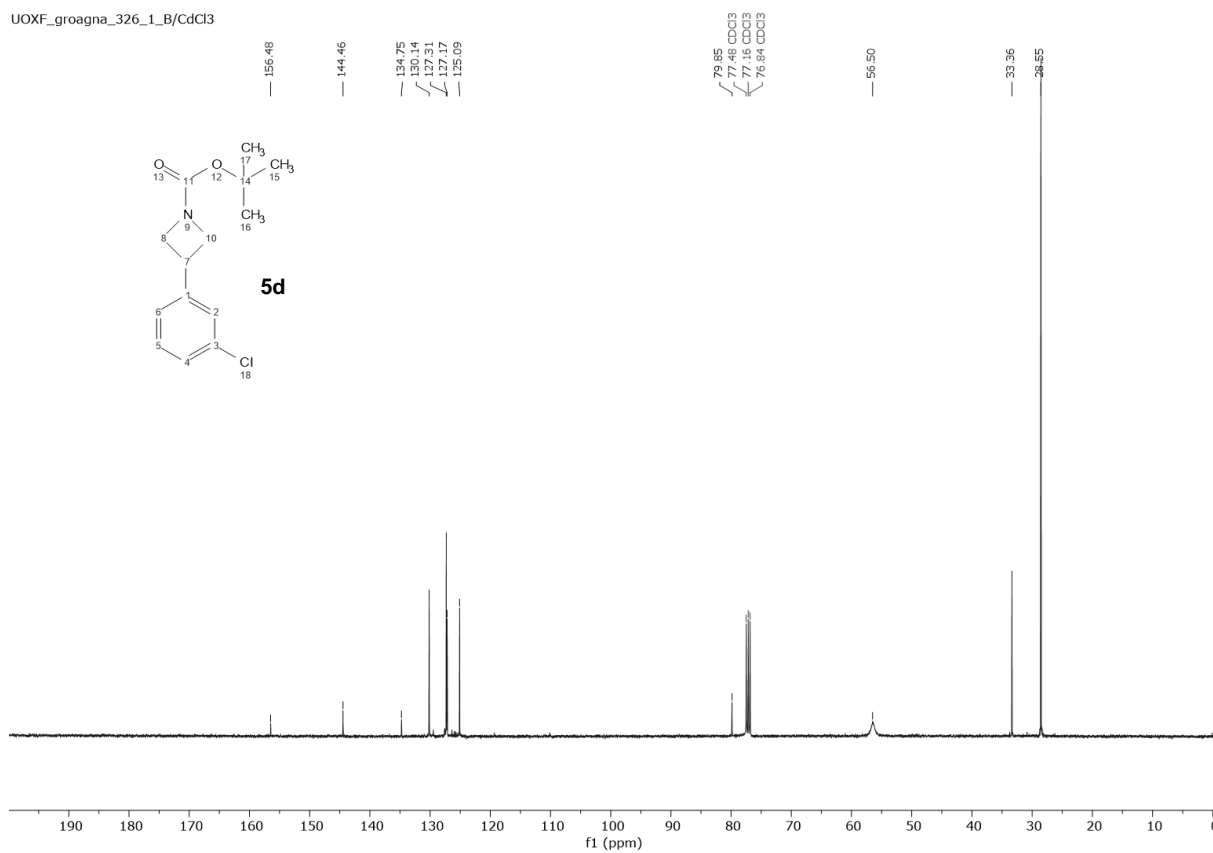
UOXF_groagna_364_1/CdCl3



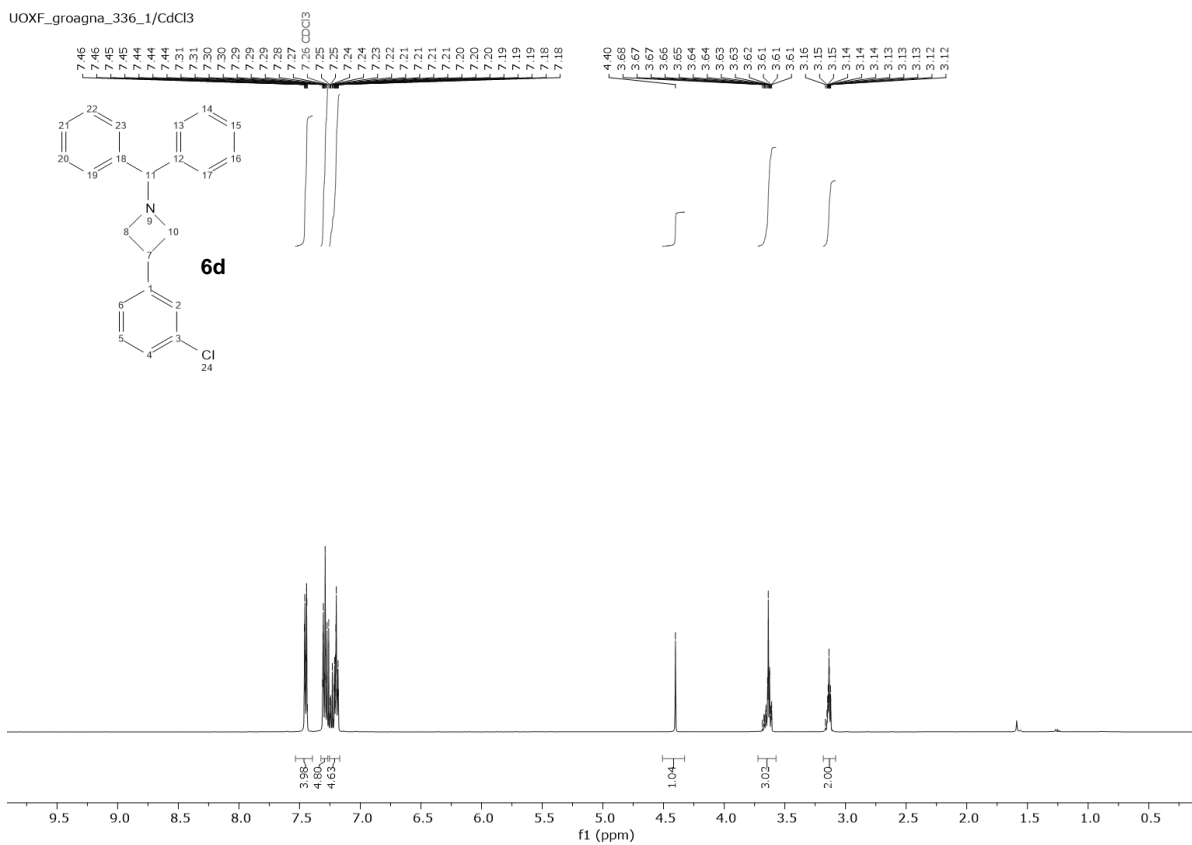
UOXF_groagna_326_1_B/CdCl3



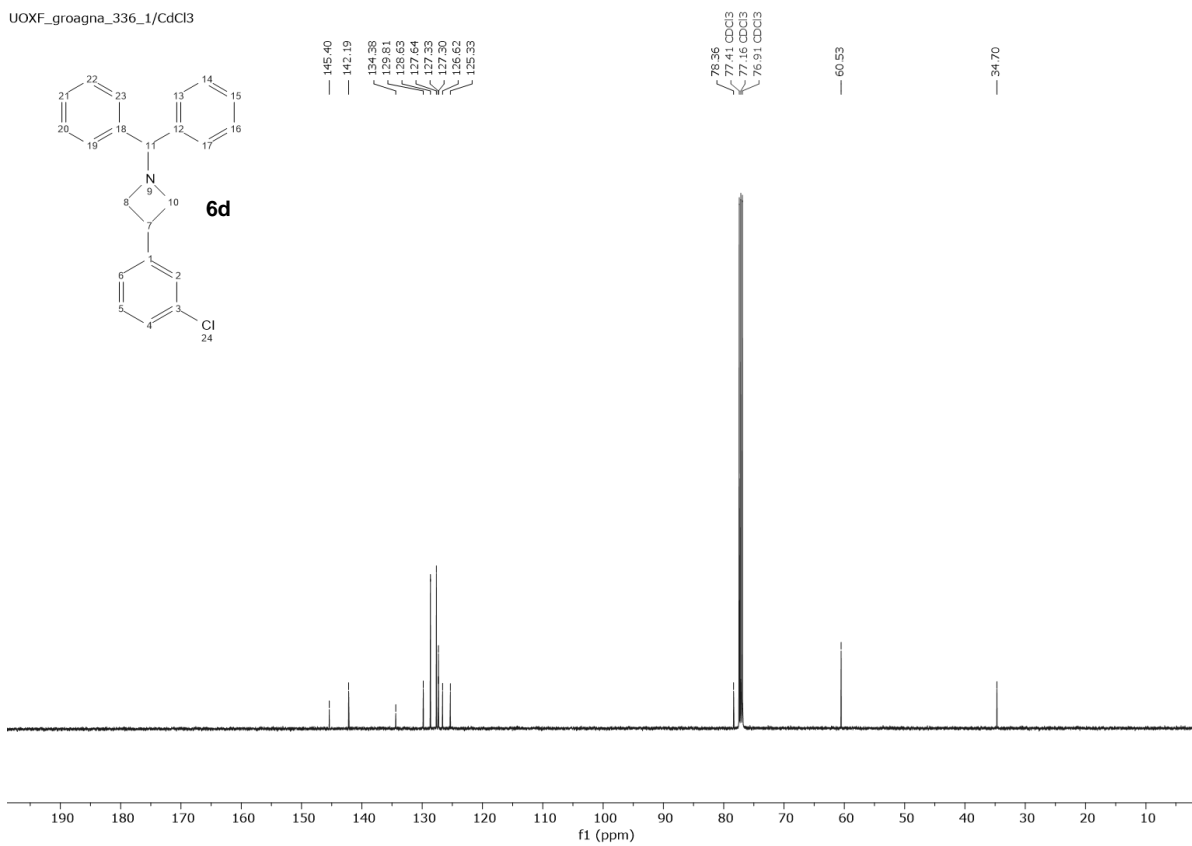
UOXF_groagna_326_1_B/CdCl3



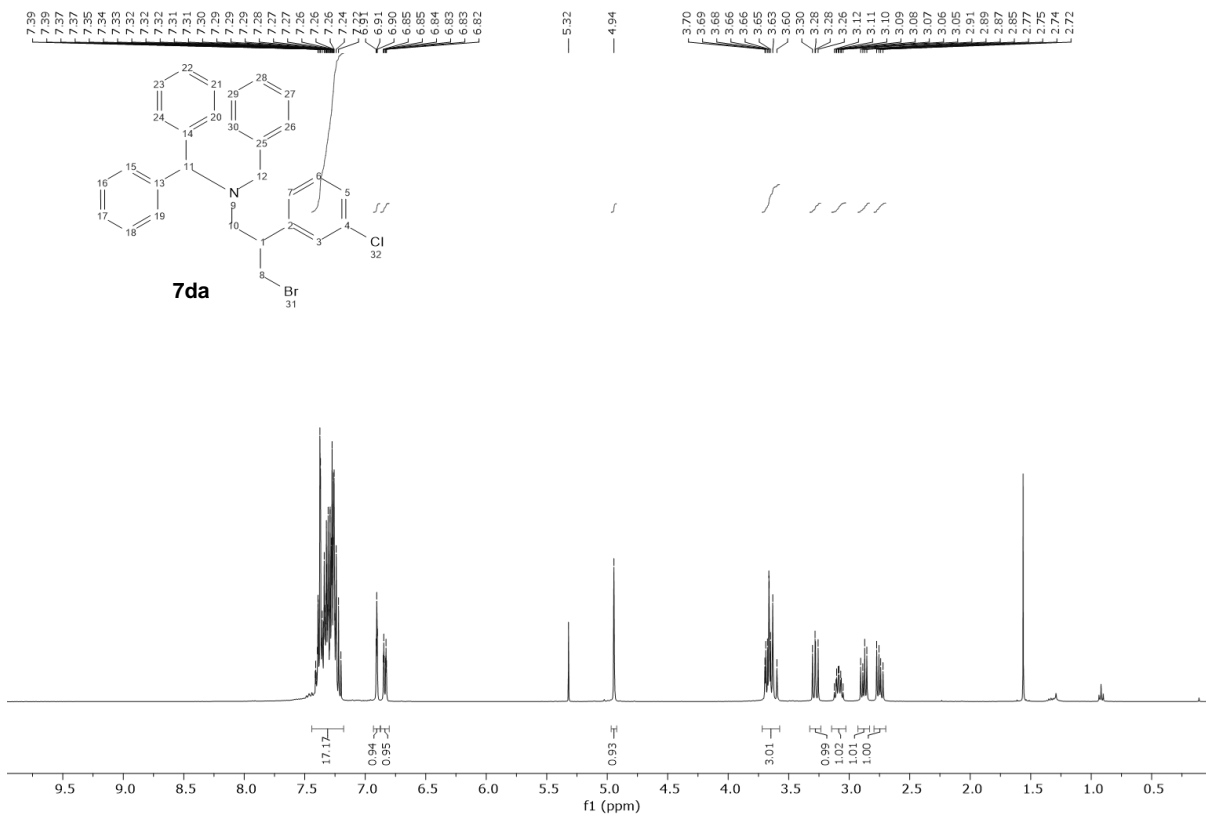
UOXF_groagna_336_1/CdCl3



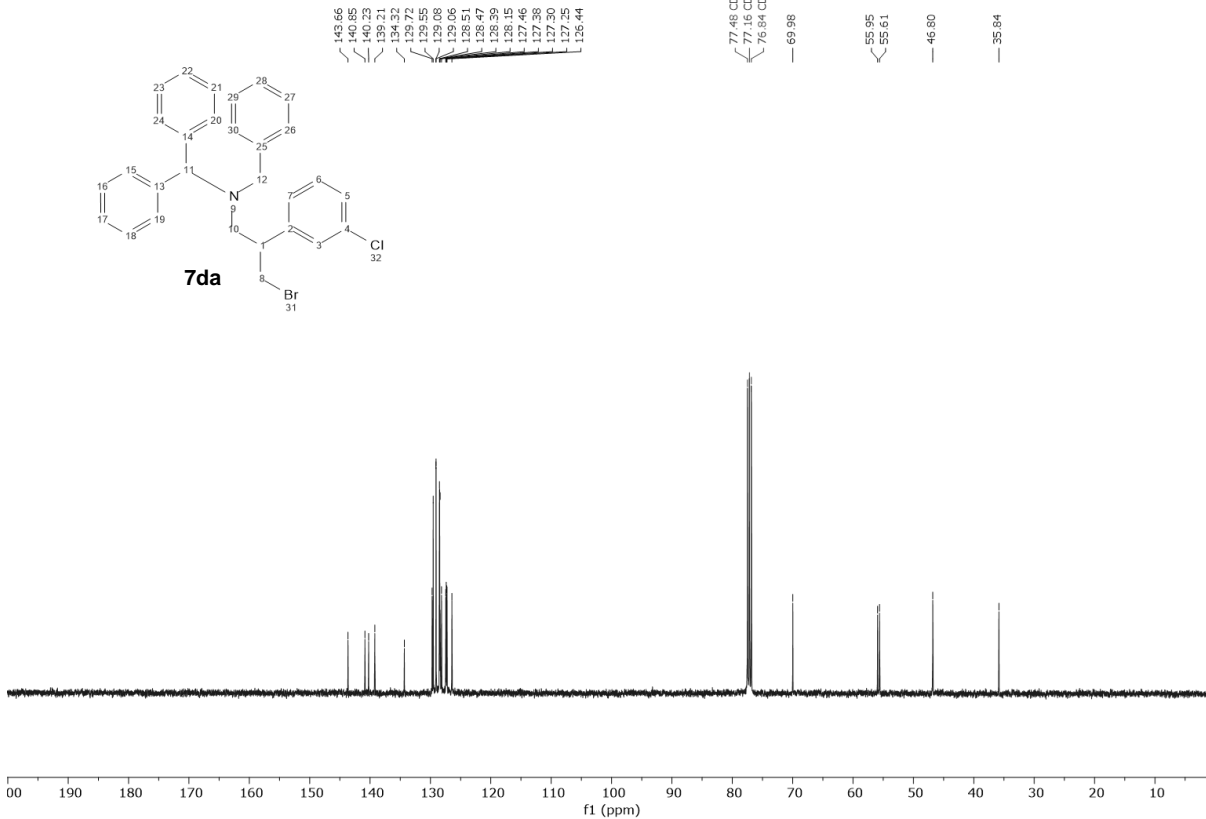
UOXF_groagna_336_1/CdCl3



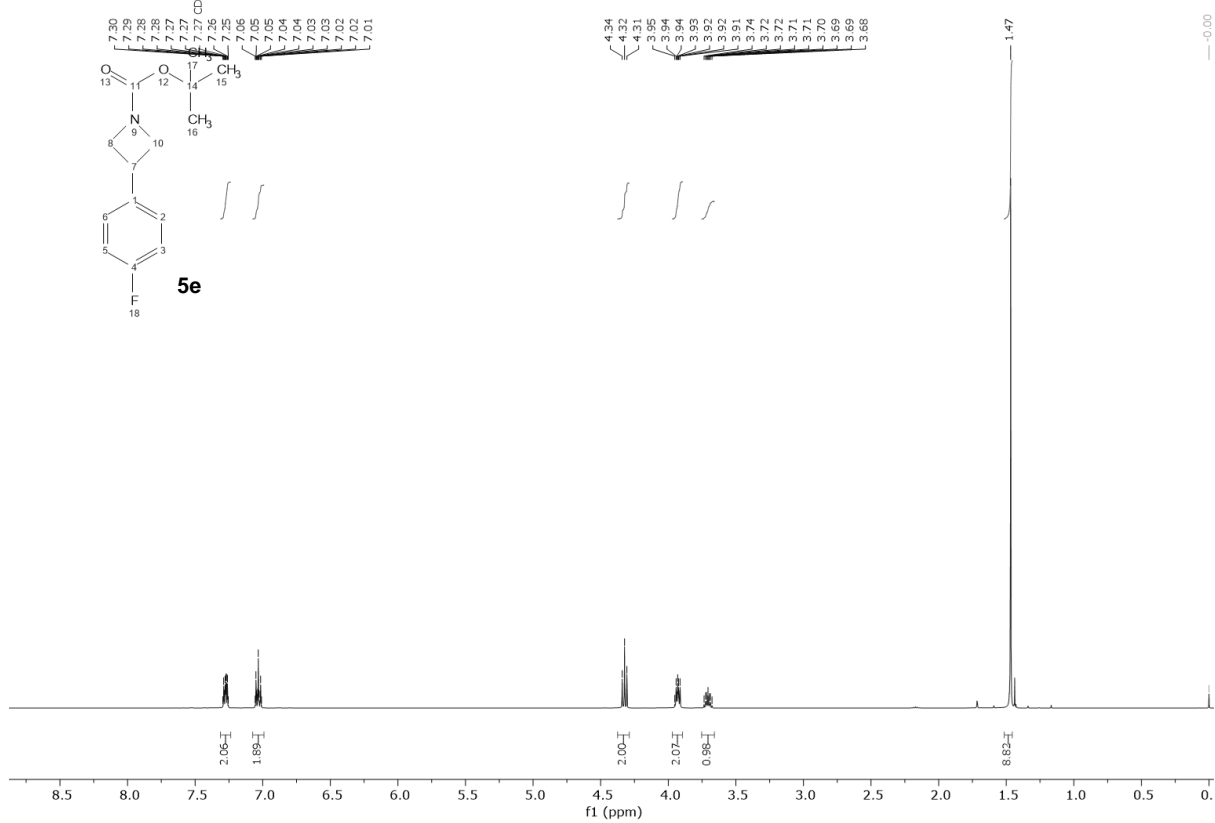
GR03EN55_1/CdCl3



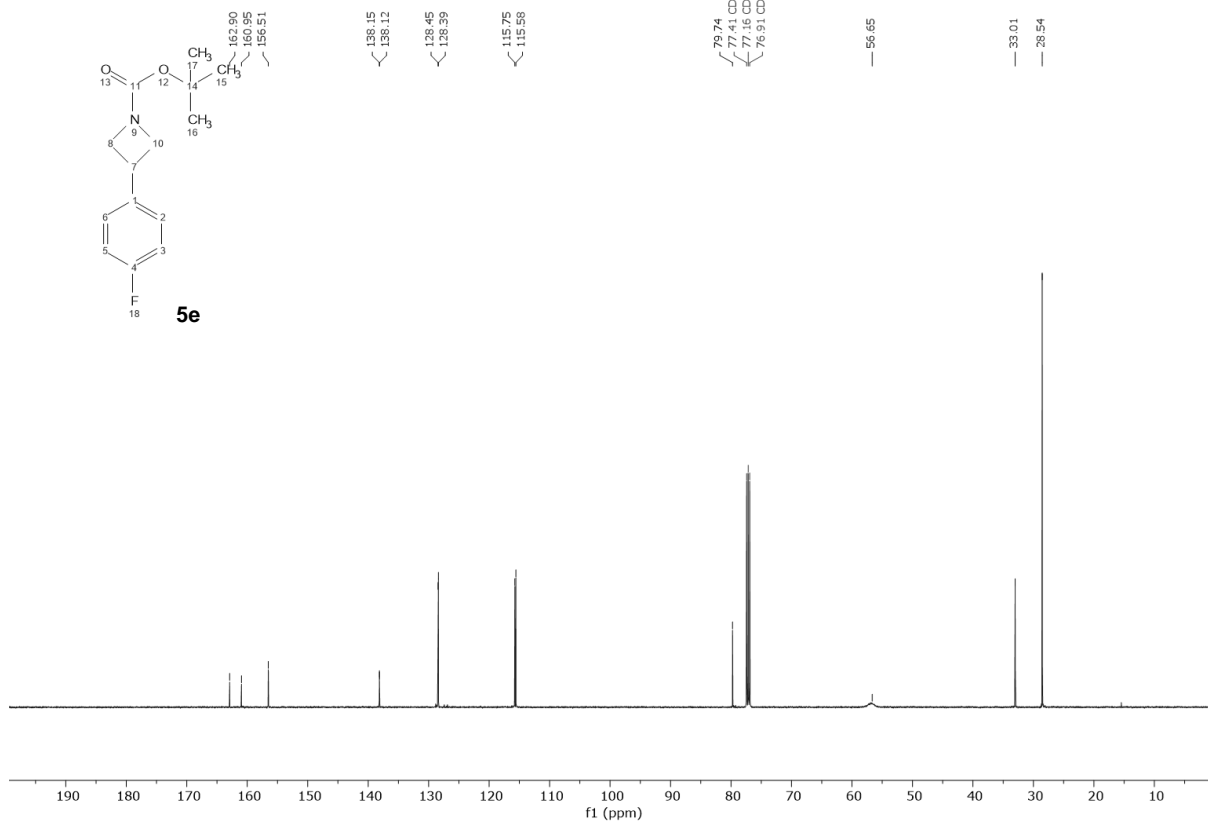
GR03EN55_1/CdCl3



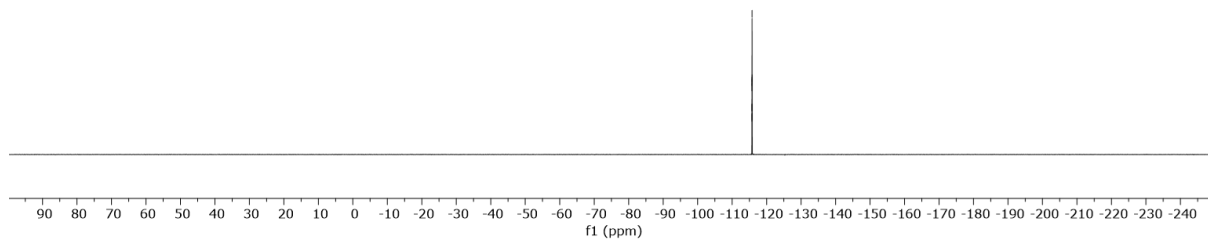
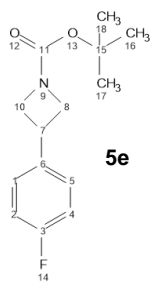
UOXF_groagna_430_1/CdCl3



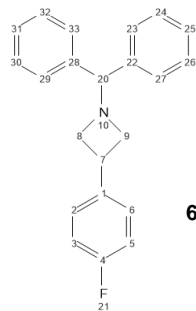
UOXF_groagna_430_1/CdCl3



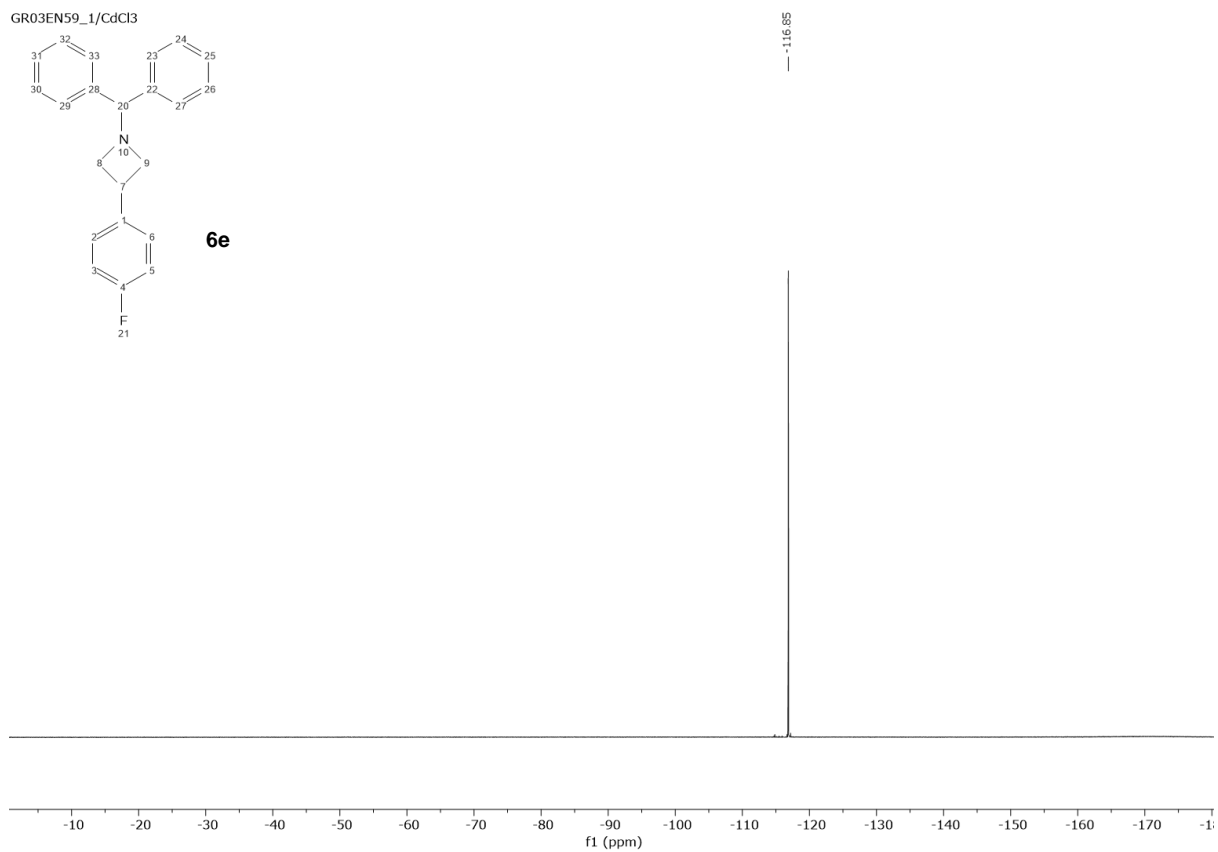
-115.74
-115.75
-115.76
-115.77
-115.78
-115.79
-115.80
-115.81



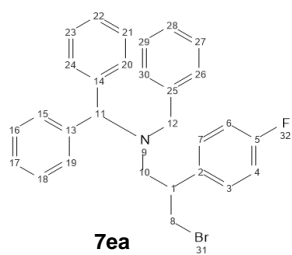
GR03EN59_1/CdCl3



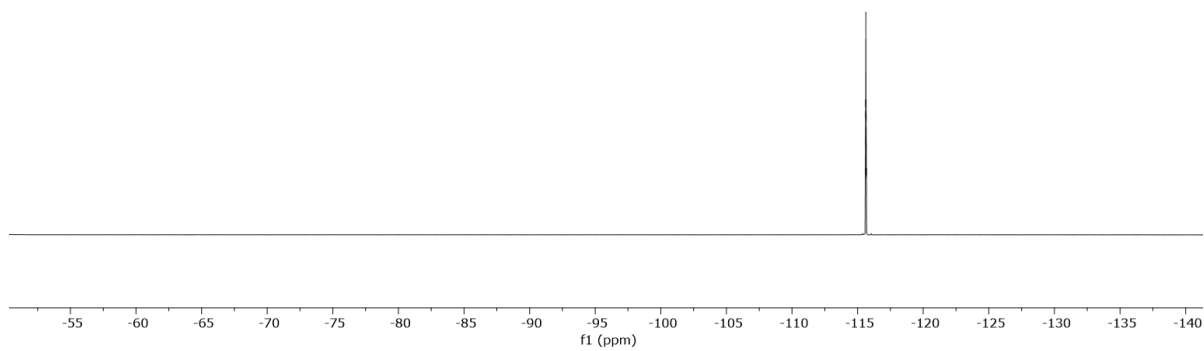
6e



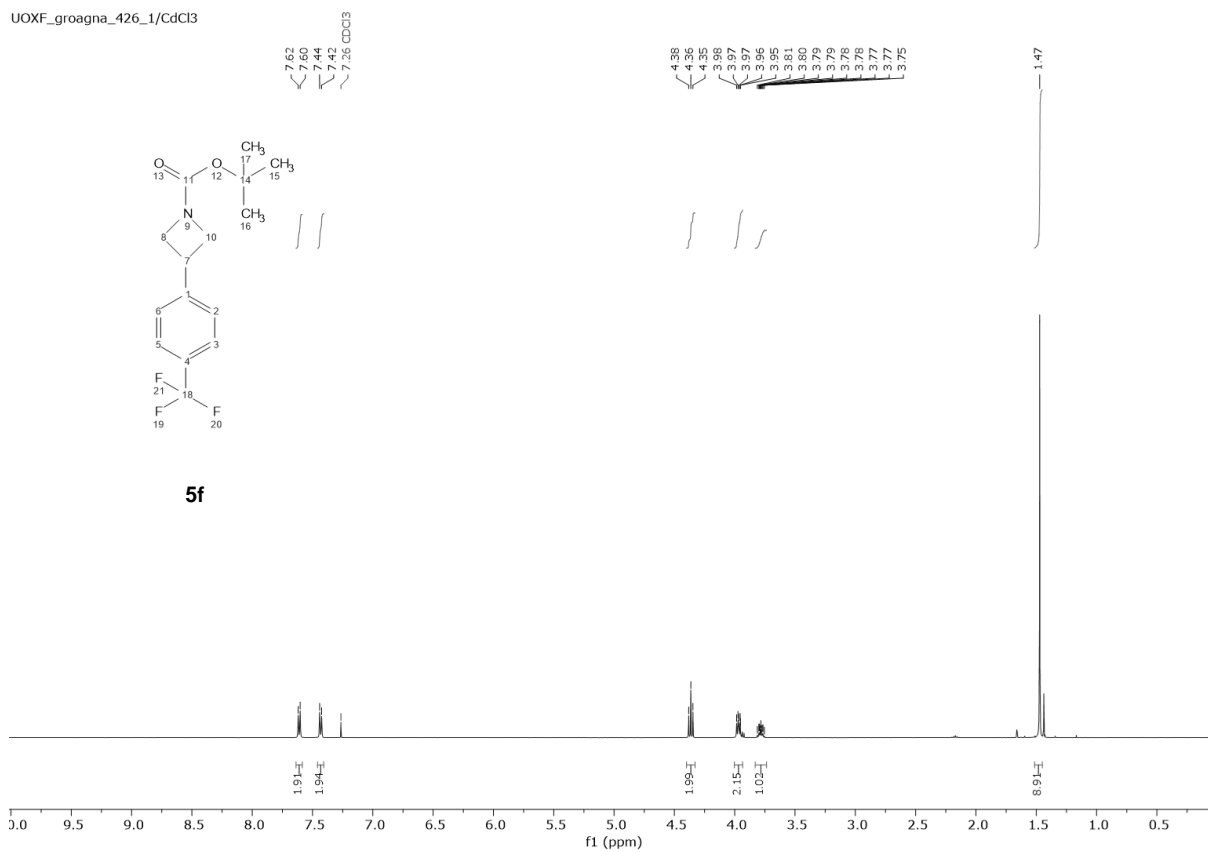
GR03EN79_1/CdCl3



115.59
115.61
115.61
115.62
115.61
115.61
115.65
115.66
115.69

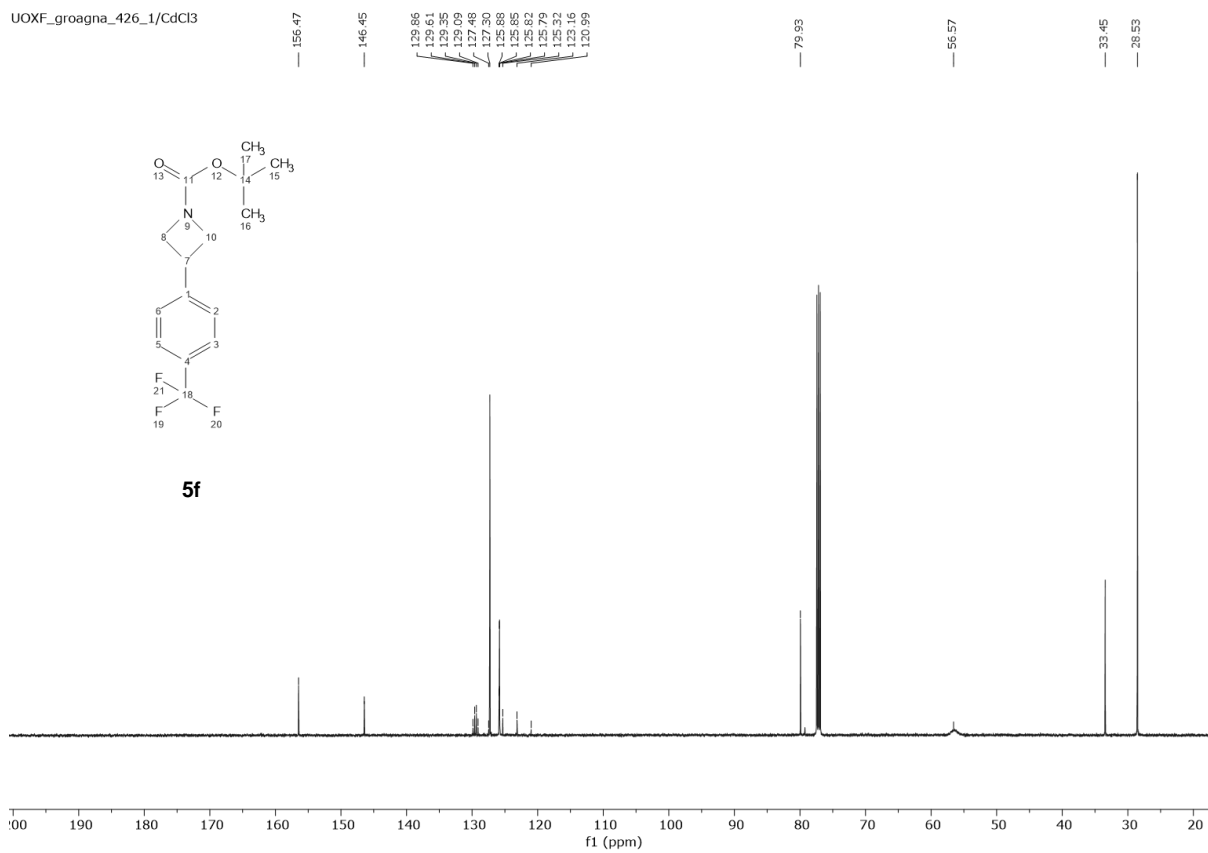


UOXF_groagna_426_1/CdCl3

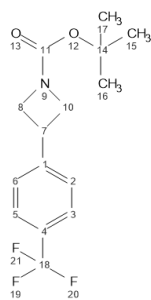


5f

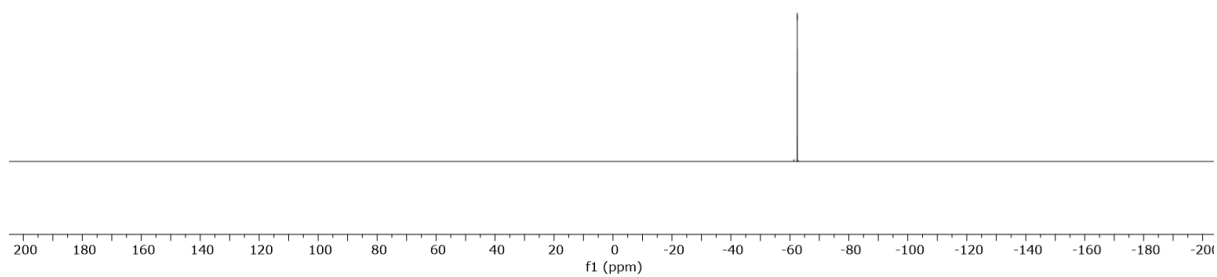
UOXF_groagna_426_1/CdCl3



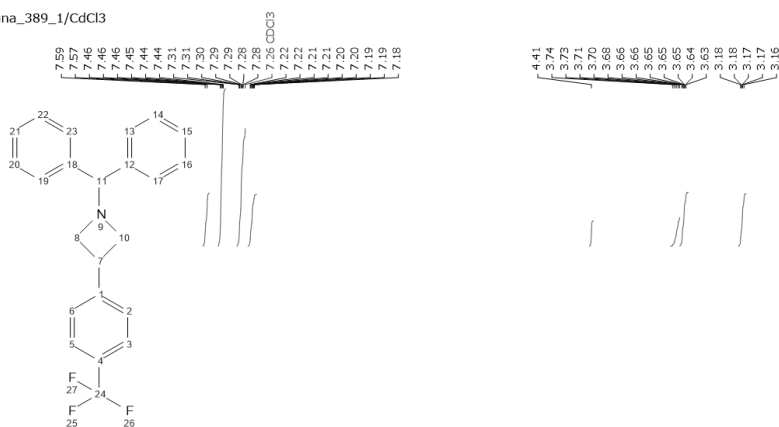
5f



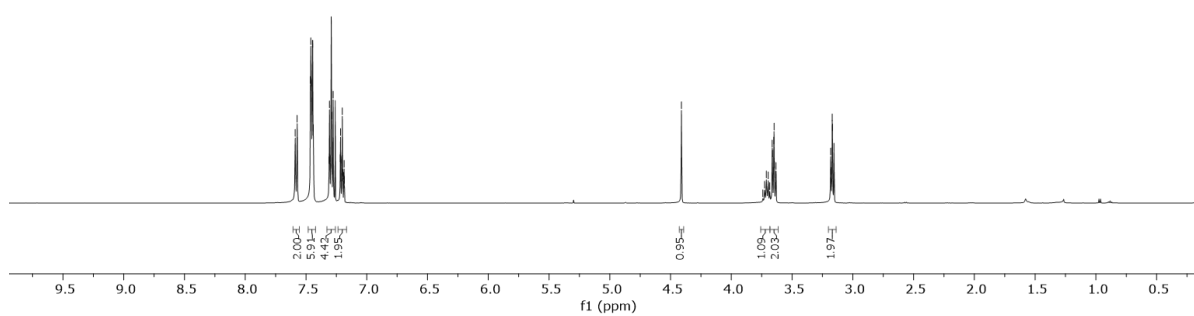
5f



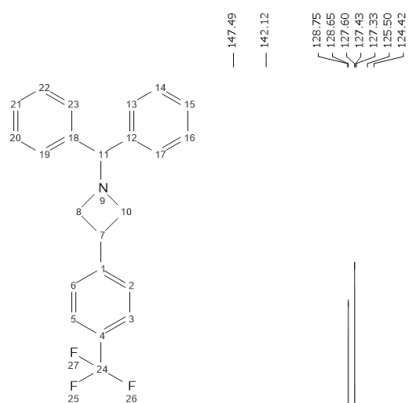
UOXF_groagna_389_1/CdCl3



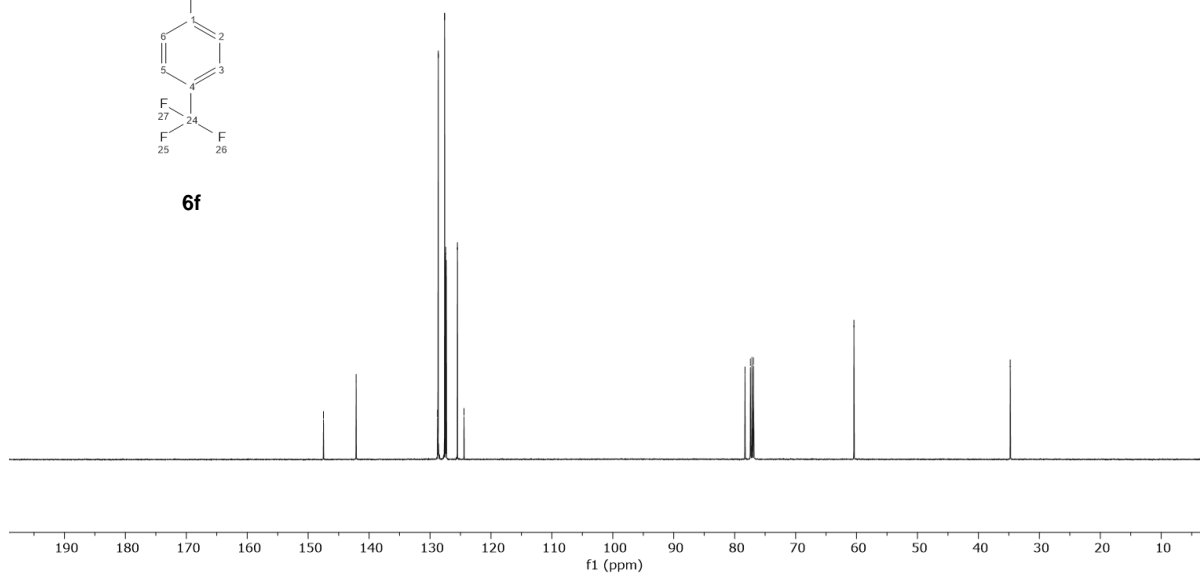
6f

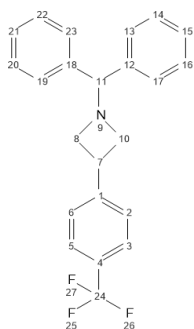


UOXF_groagna_389_1/CdCl3

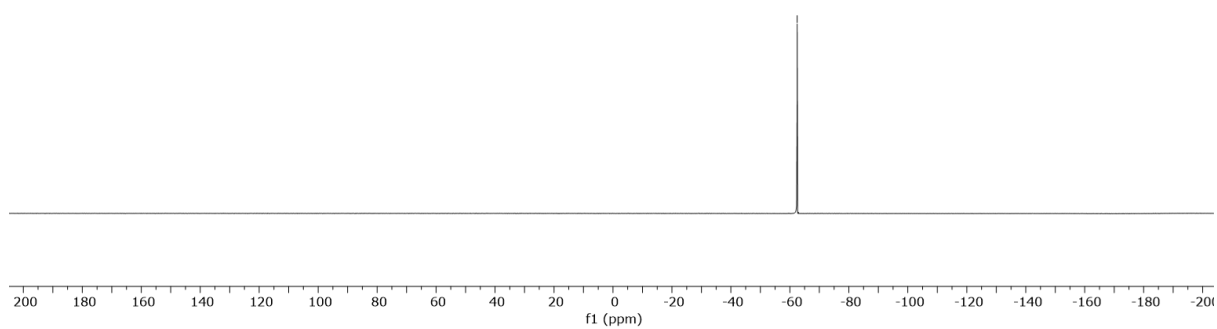


6f

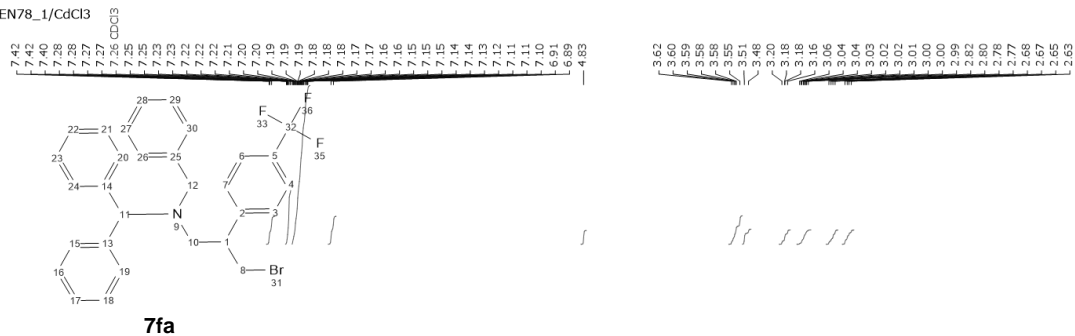




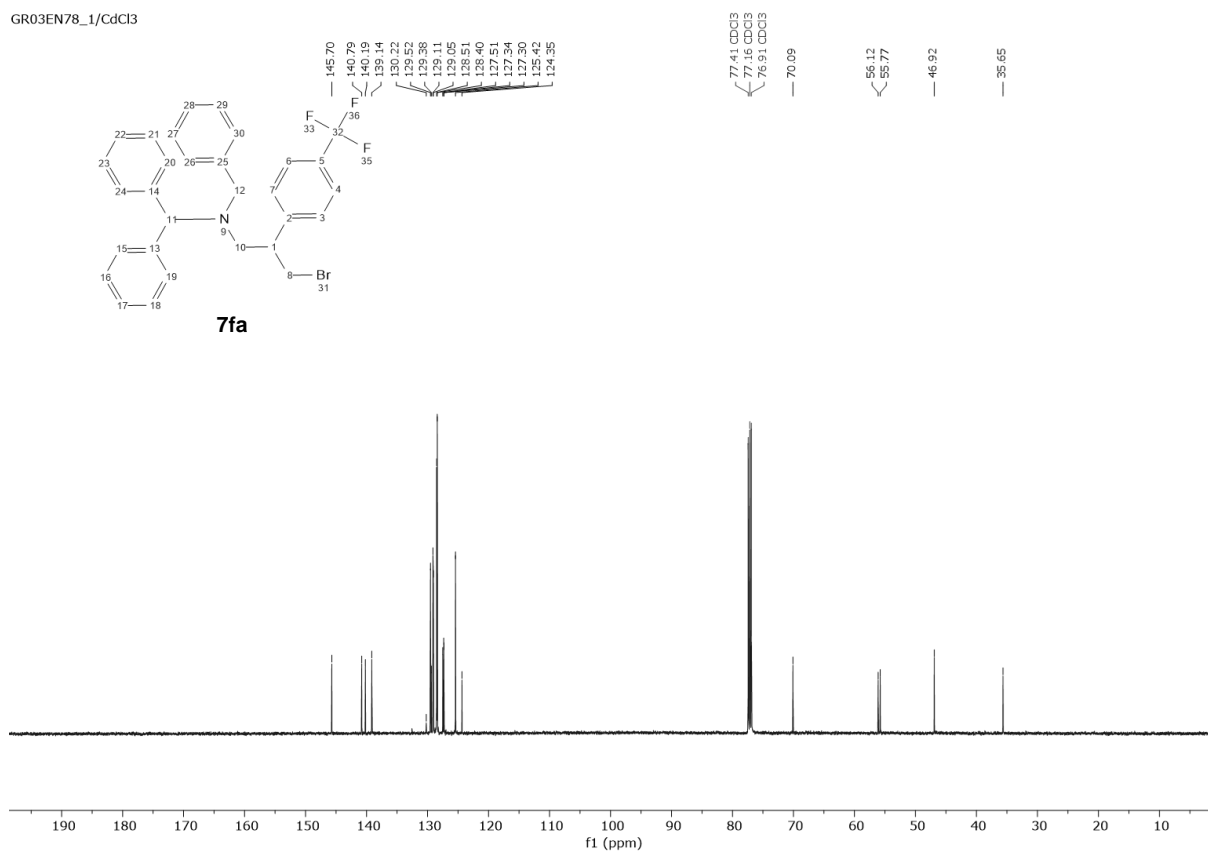
6f

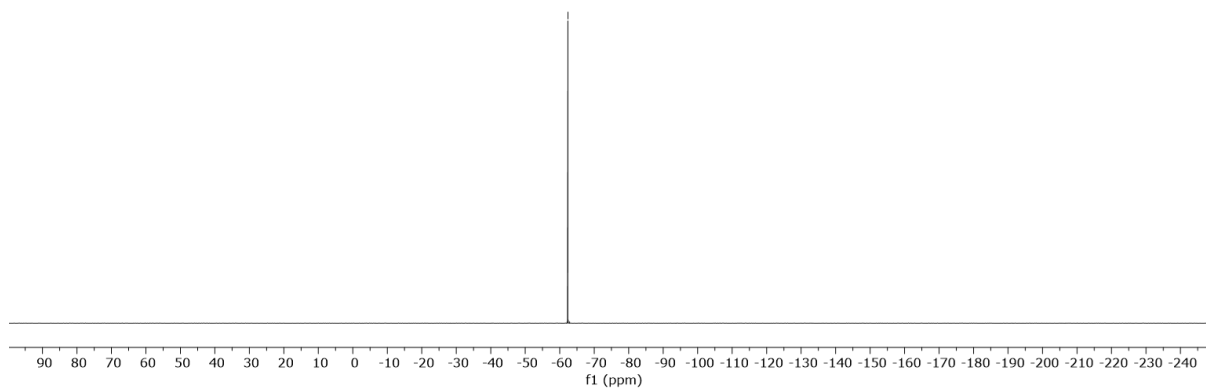
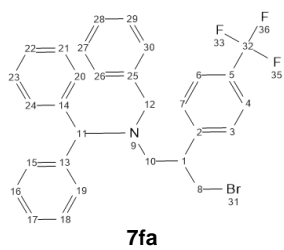


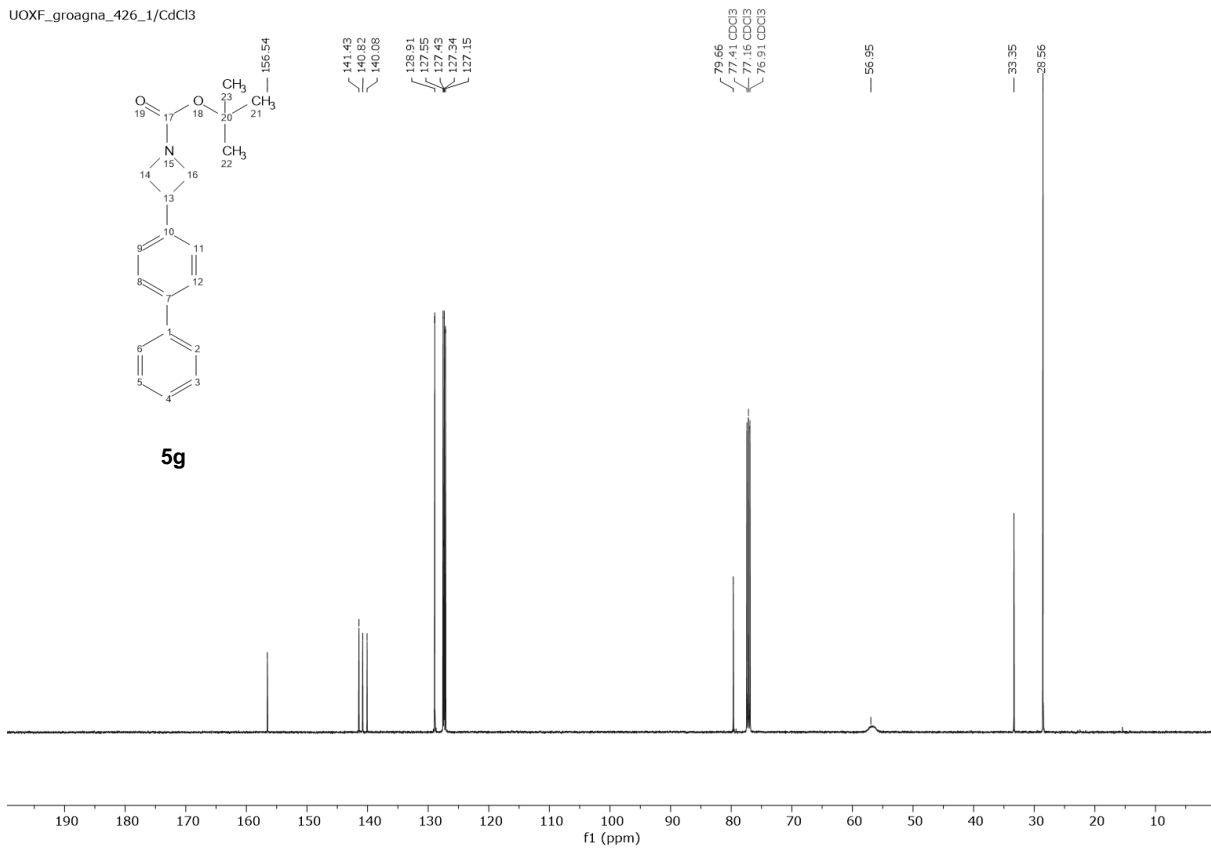
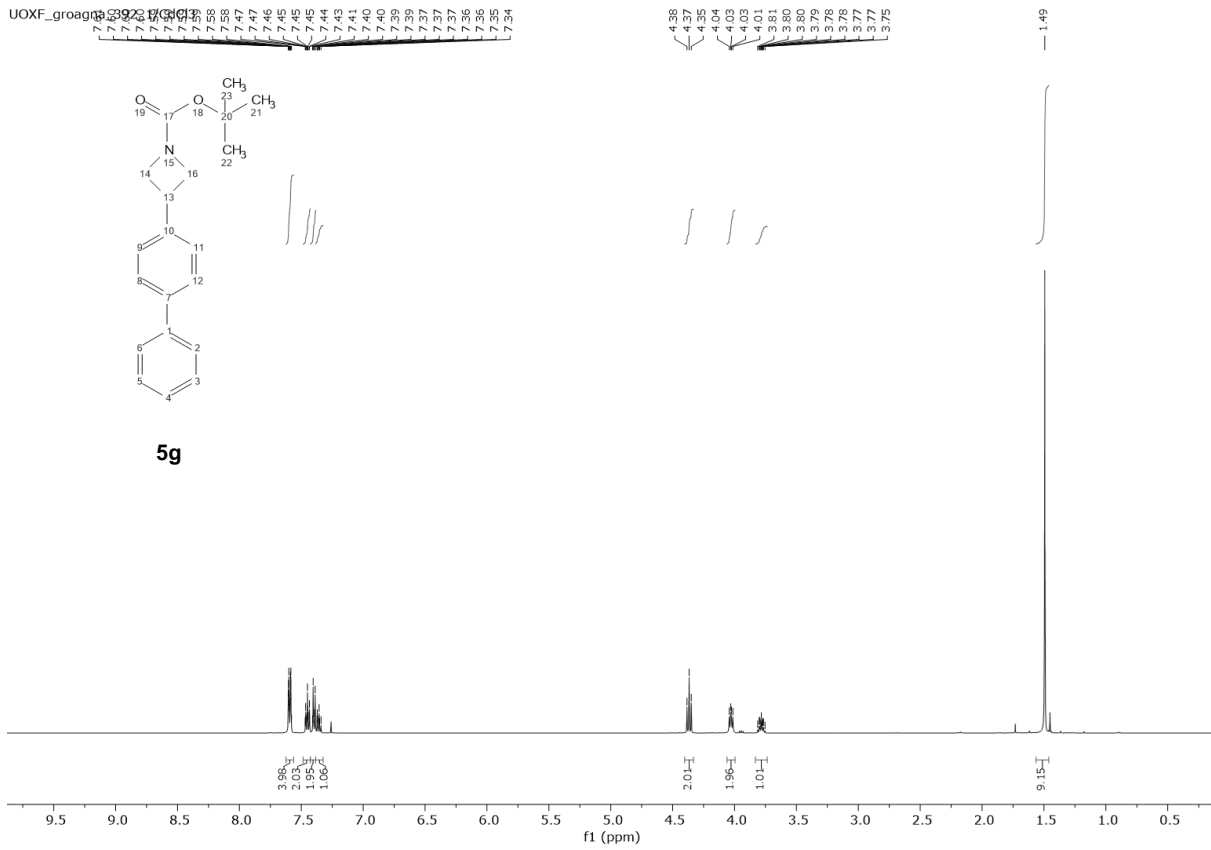
GR03EN78_1/CdCl3



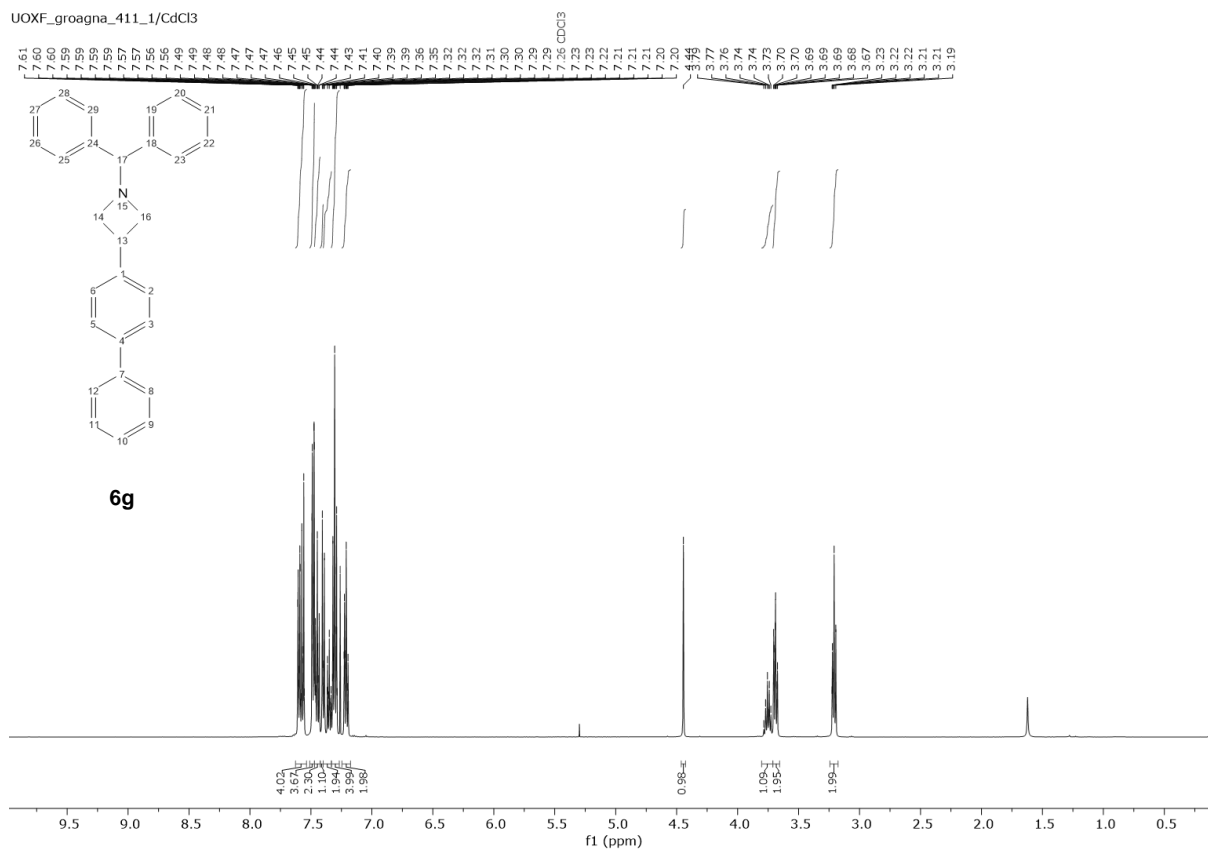
GR03EN78_1/CdCl3



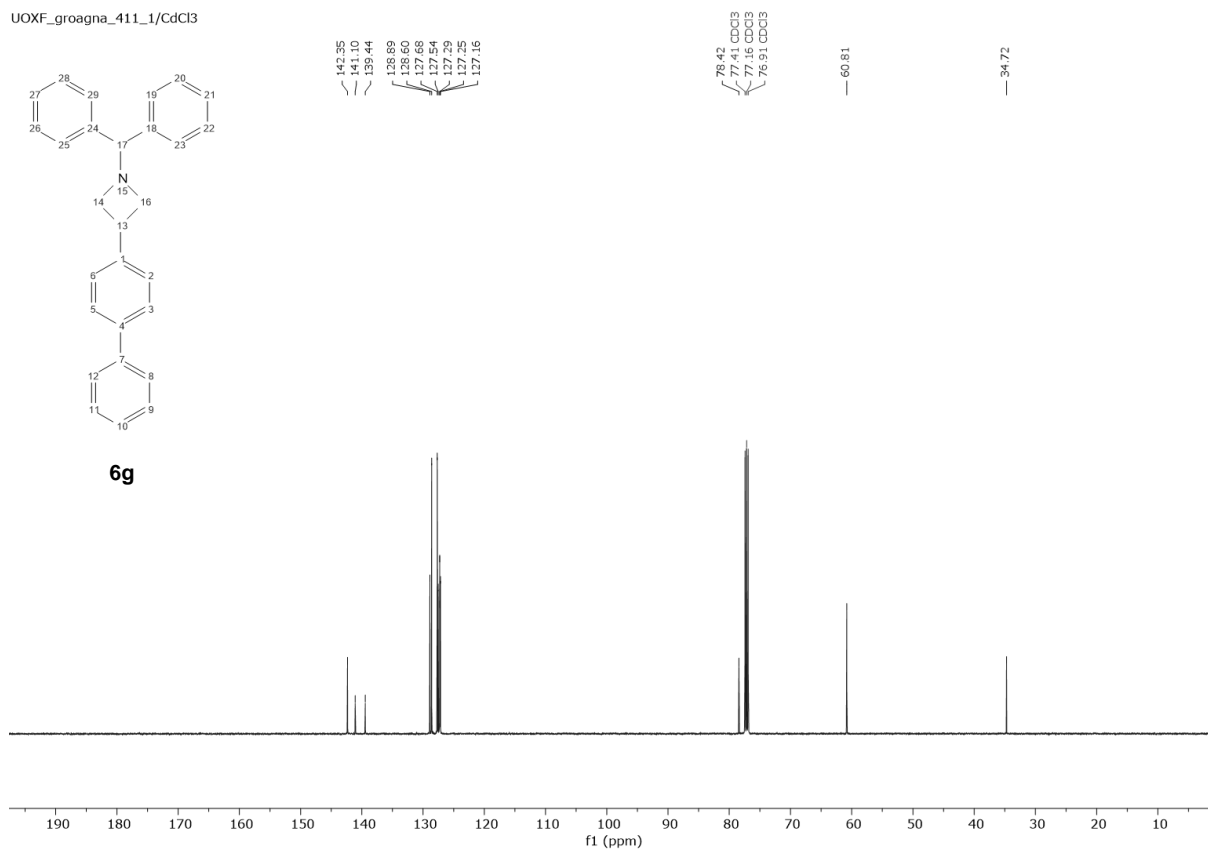


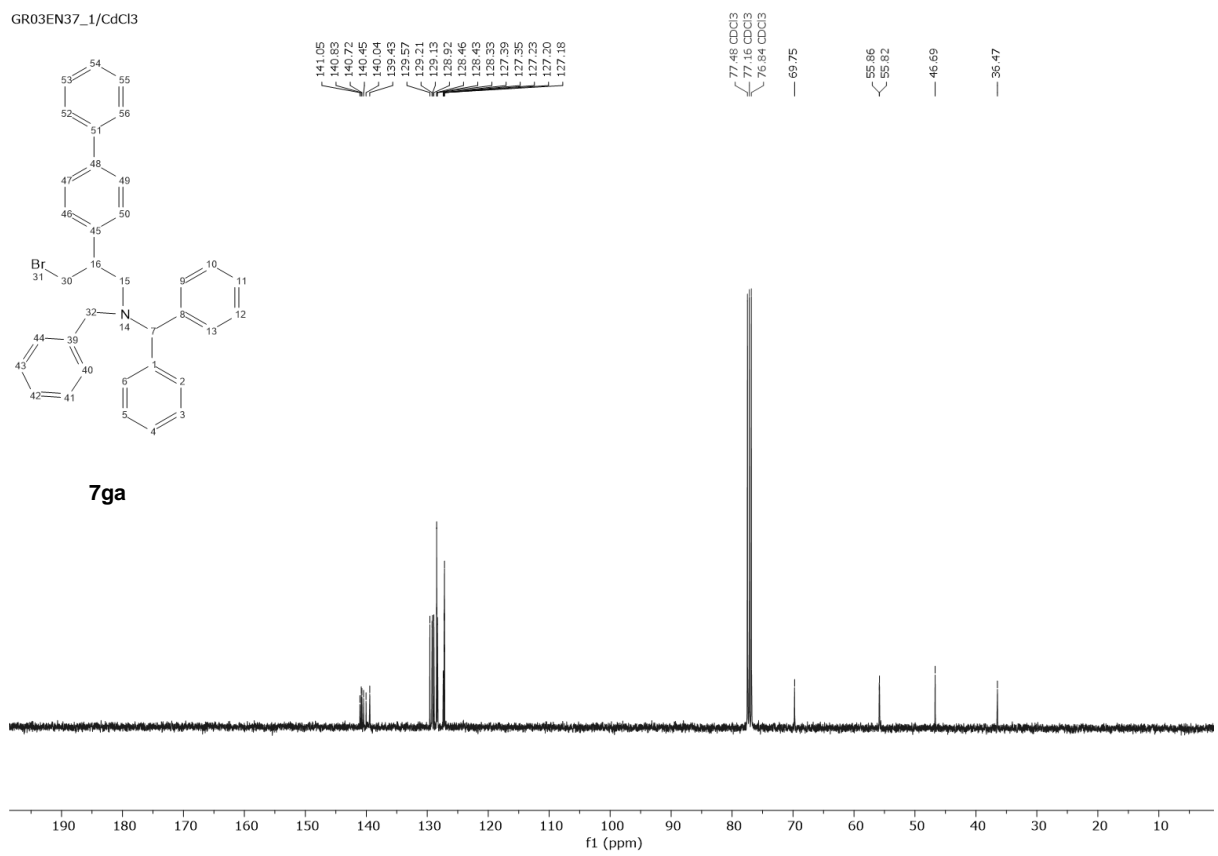
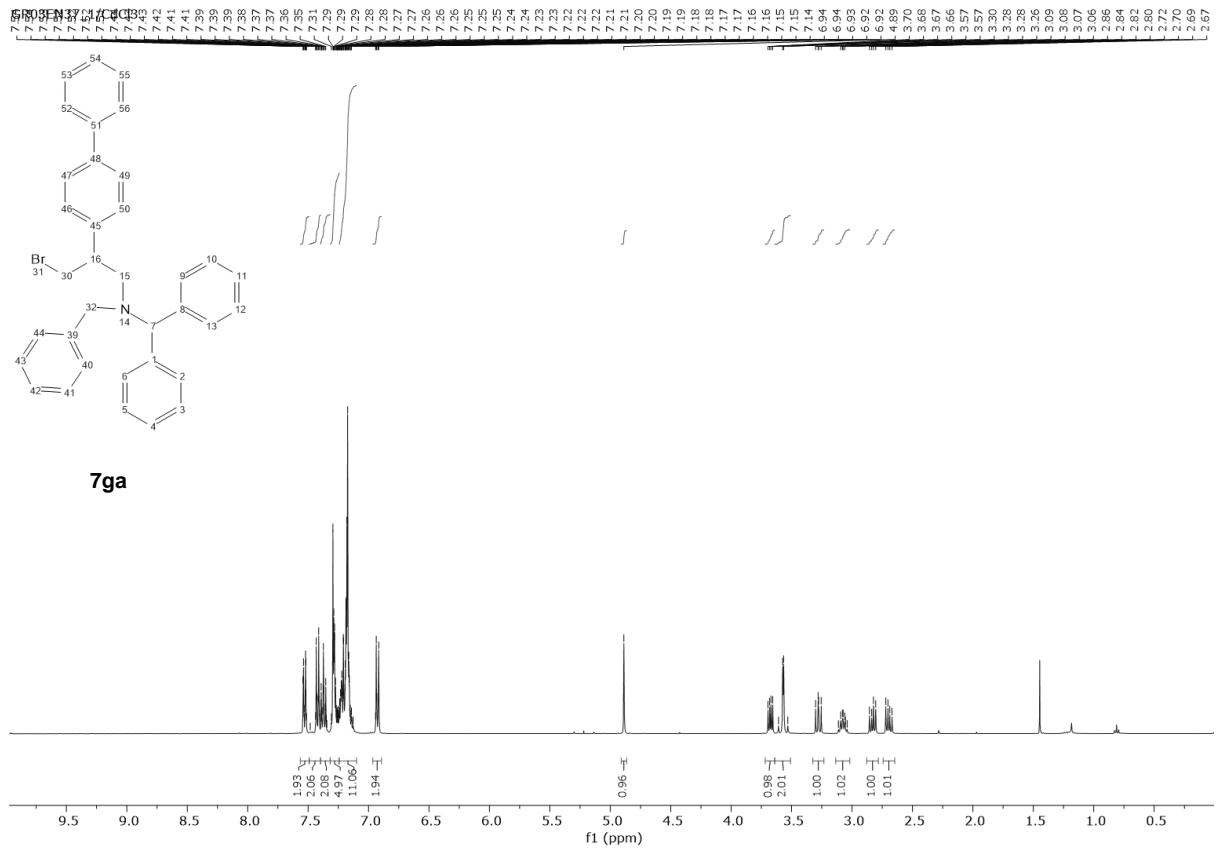


UOXF_groagna_411_1/CdCl3

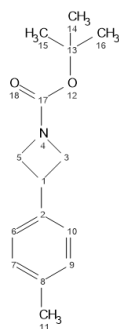


UOXF_groagna_411_1/CdCl3

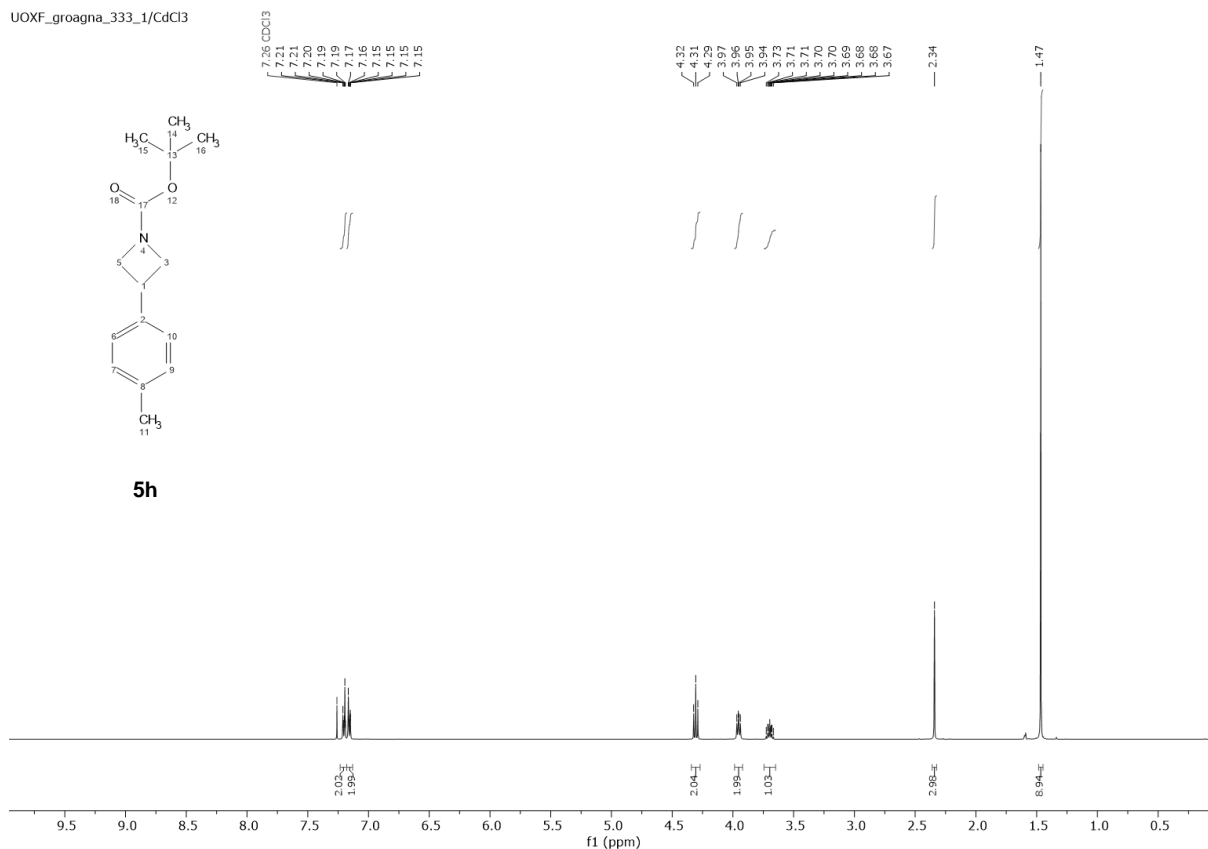




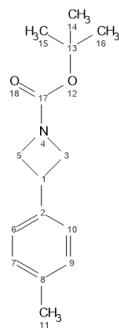
UOXF_groagna_333_1/CdCl3



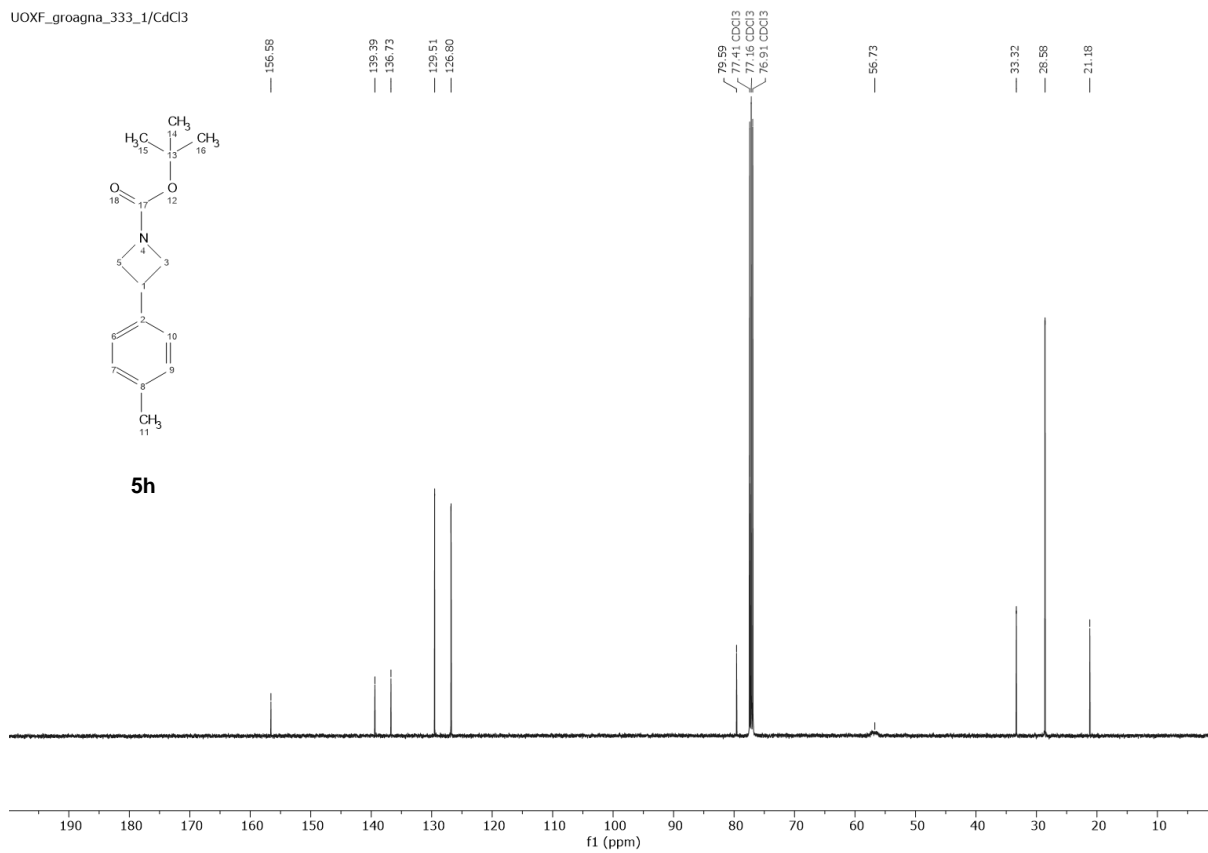
5h



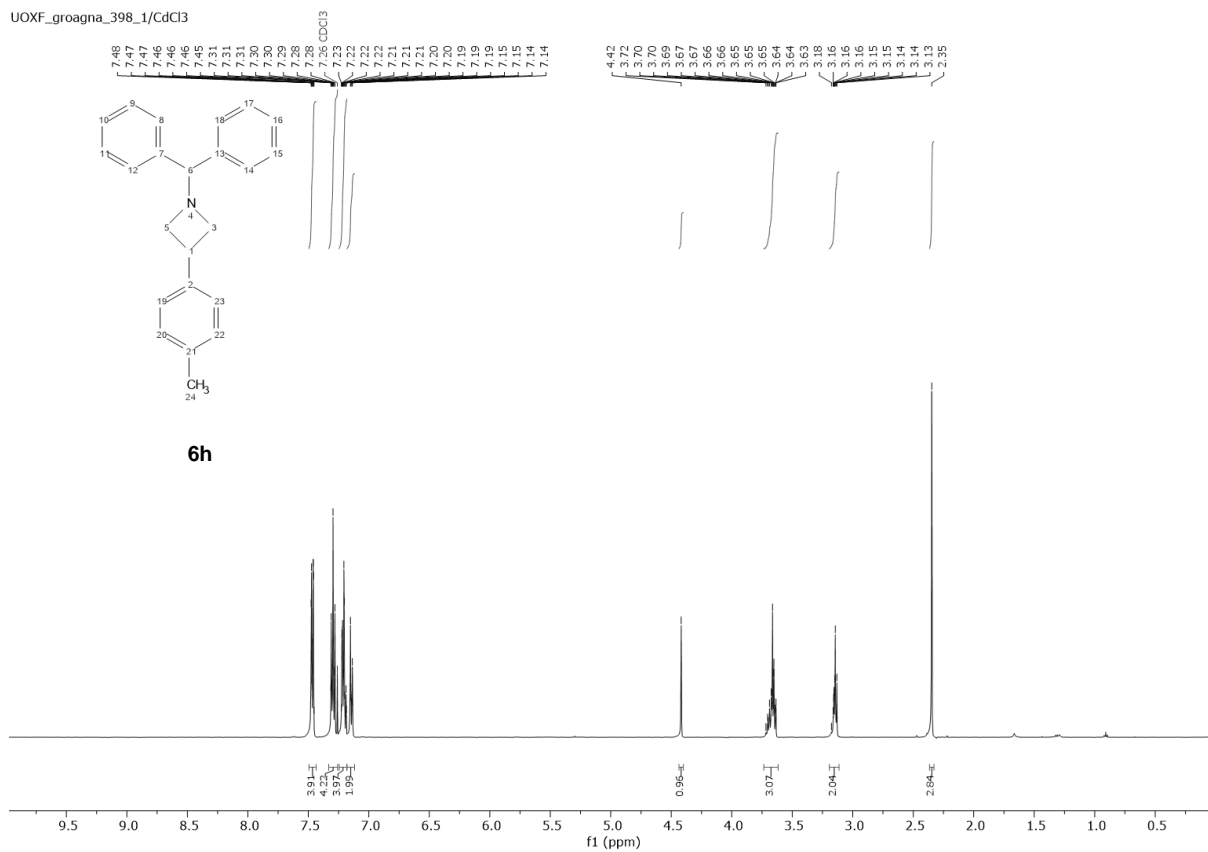
UOXF_groagna_333_1/CdCl3



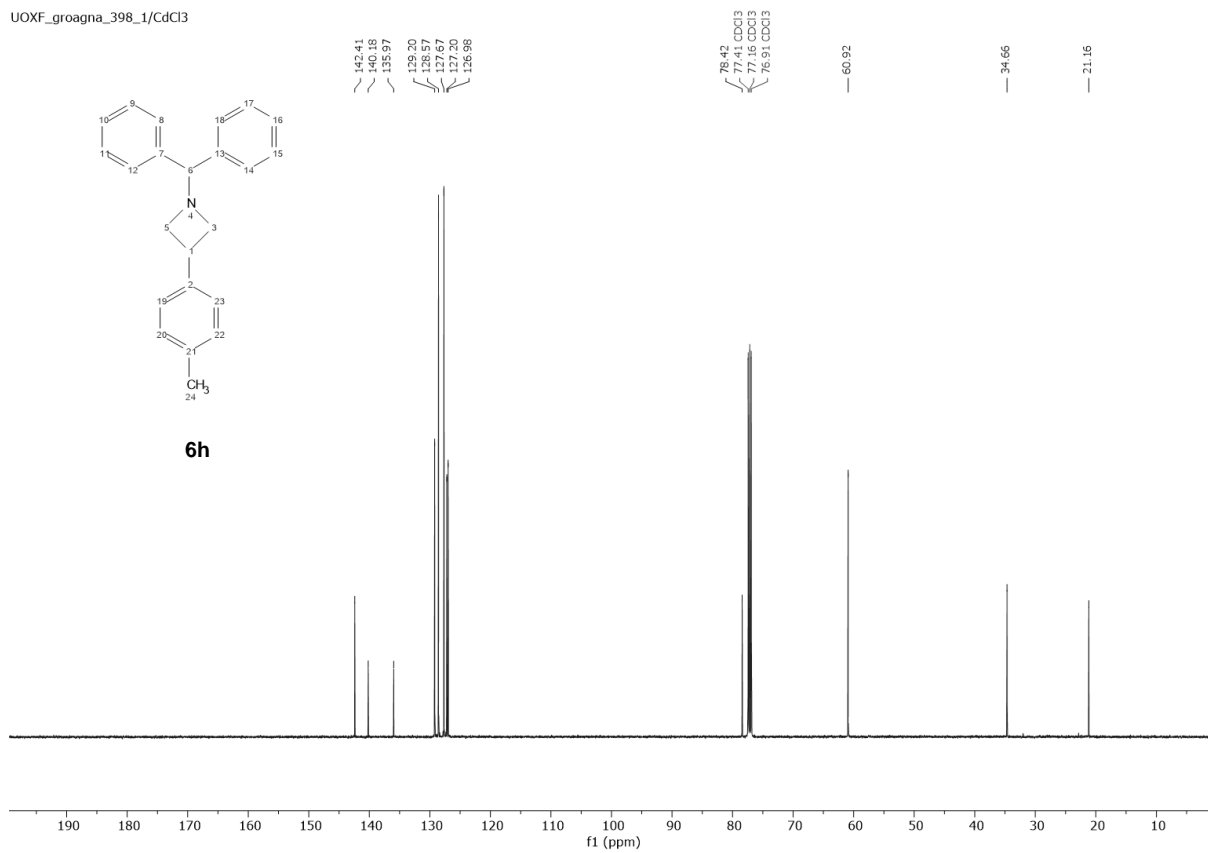
5h



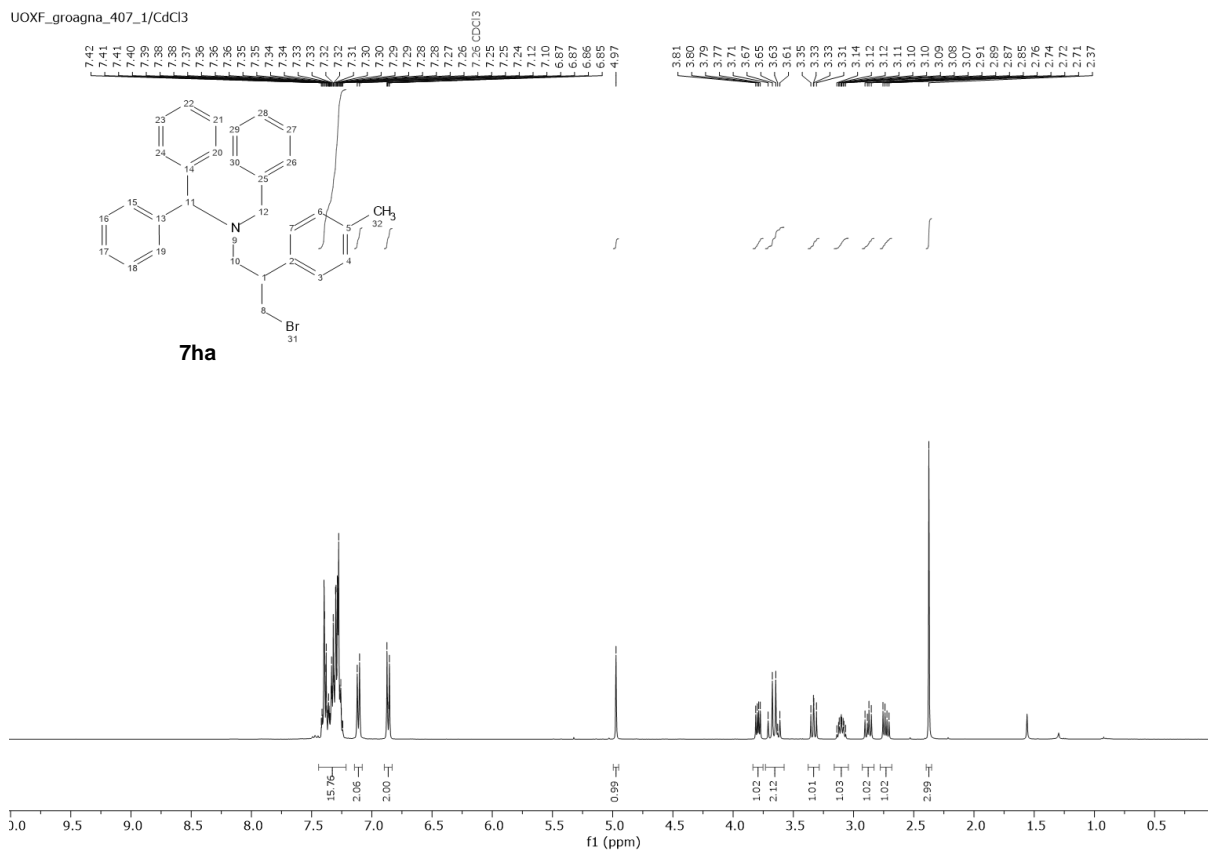
UOXF_groagna_398_1/CdCl3



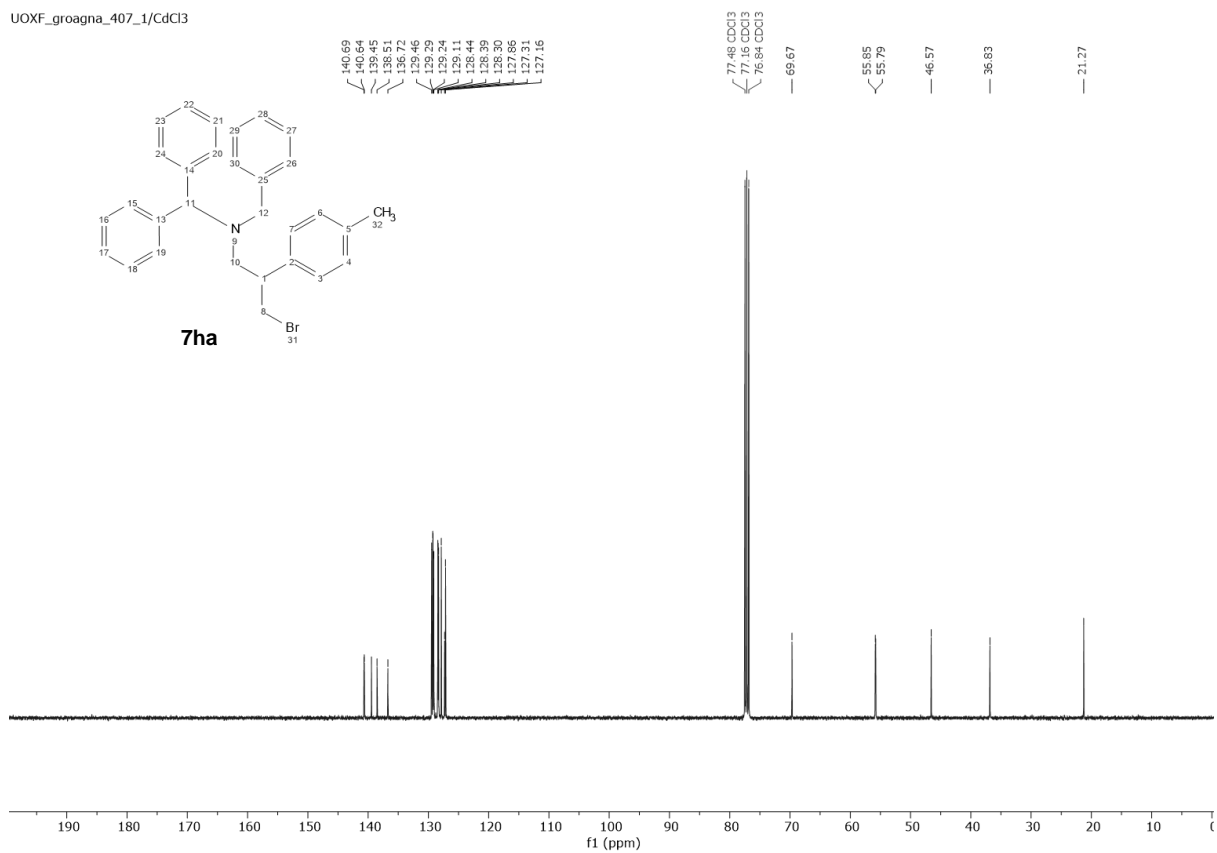
UOXF_groagna_398_1/CdCl3



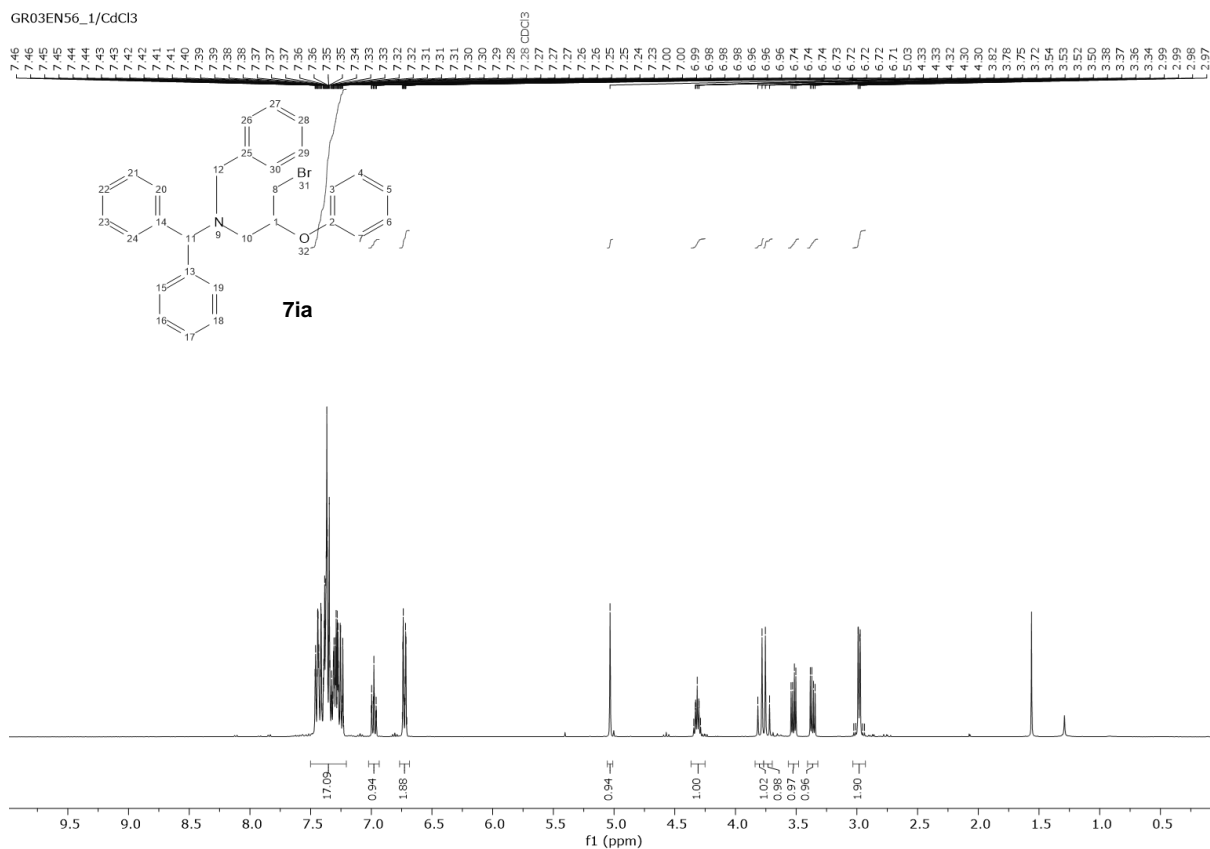
UOXF_groagna_407_1/CdCl3



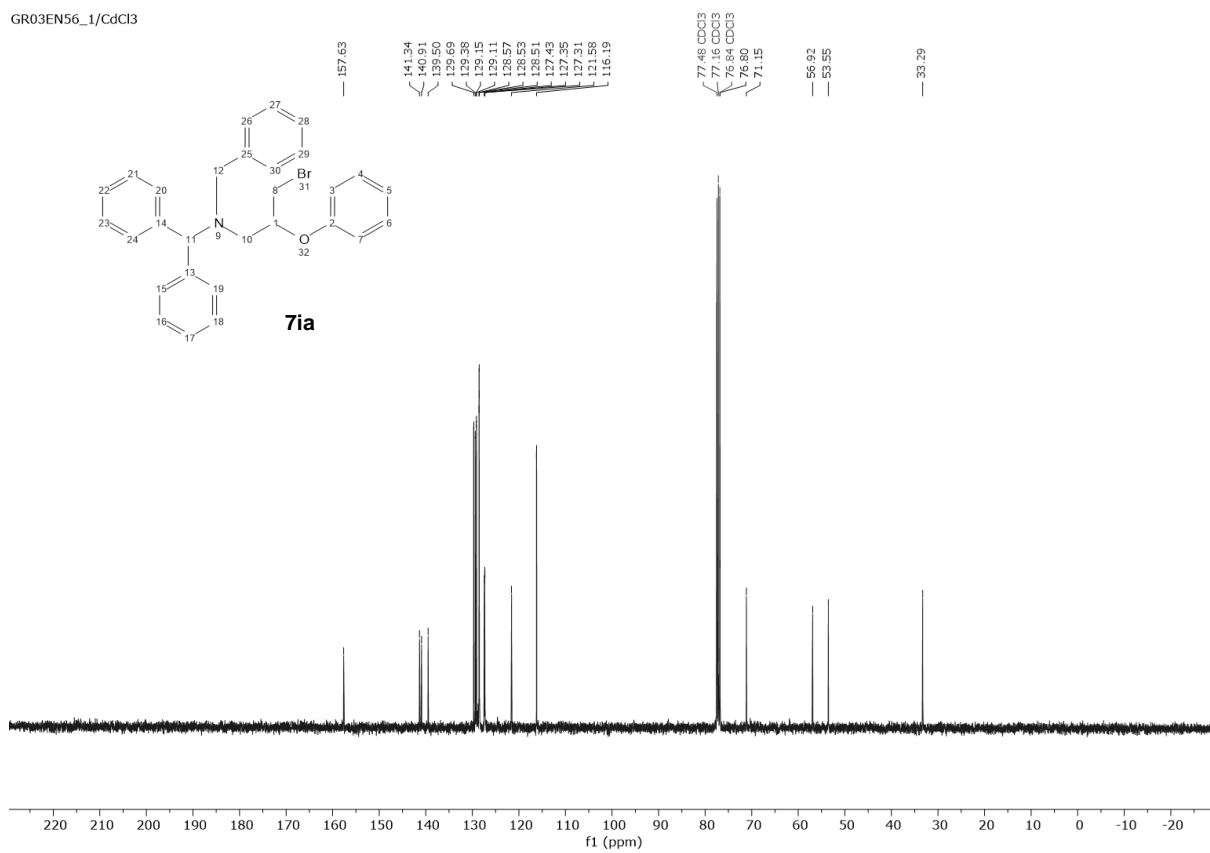
UOXF_groagna_407_1/CdCl3



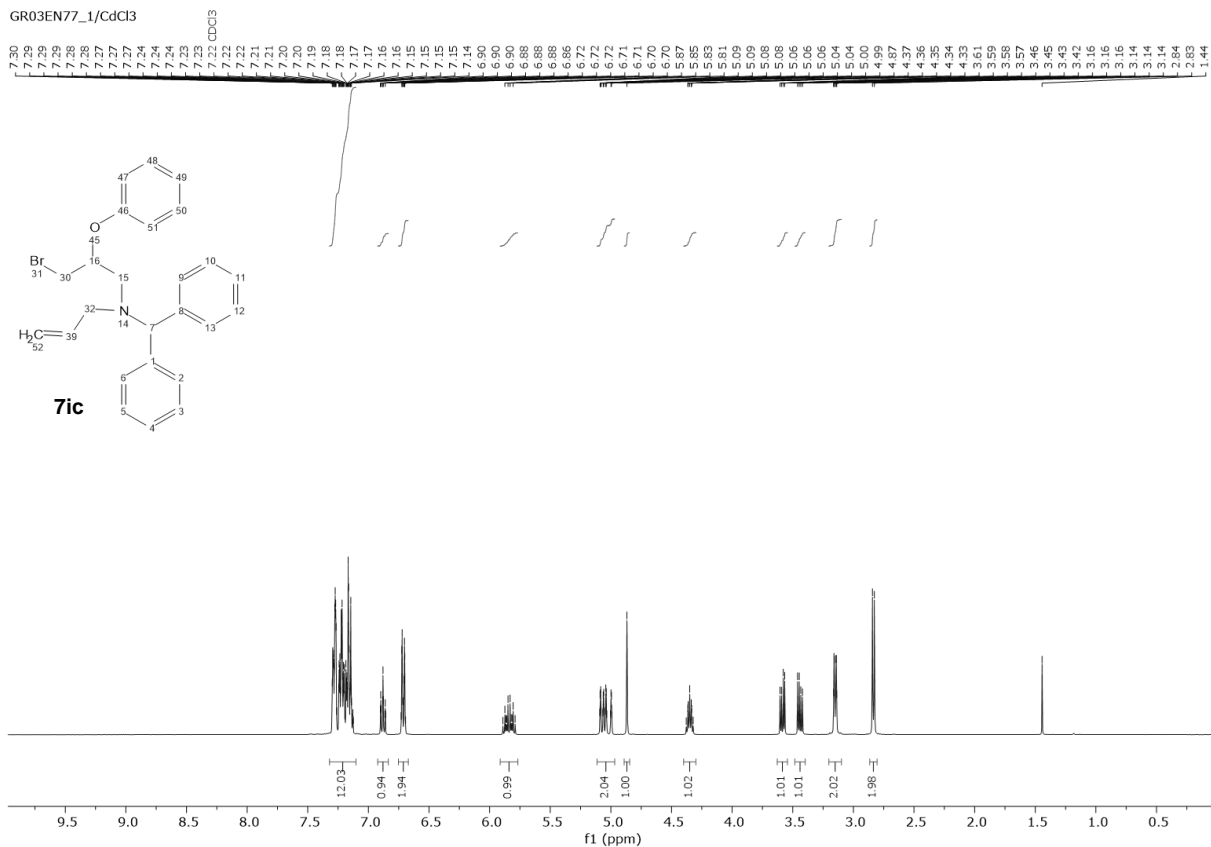
GR03EN56_1/CdCl3



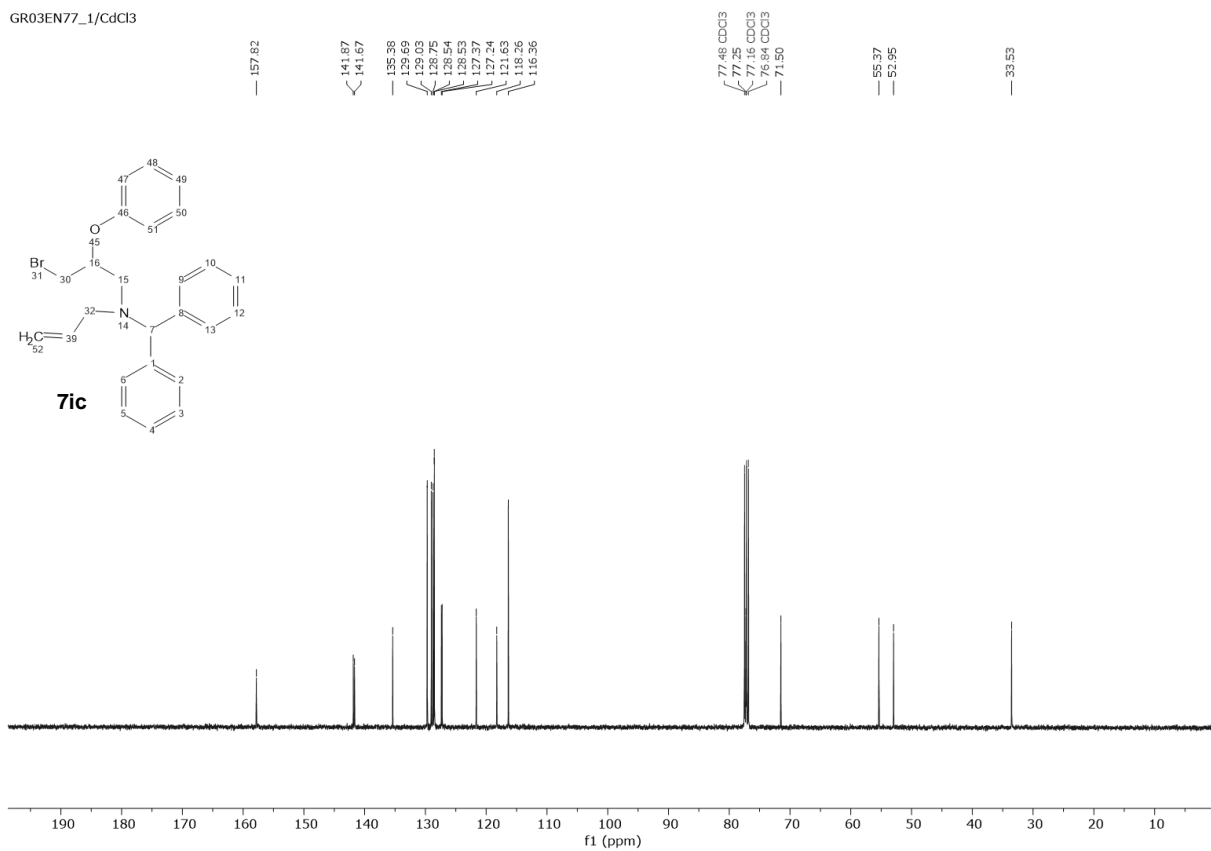
GR03EN56_1/CdCl3



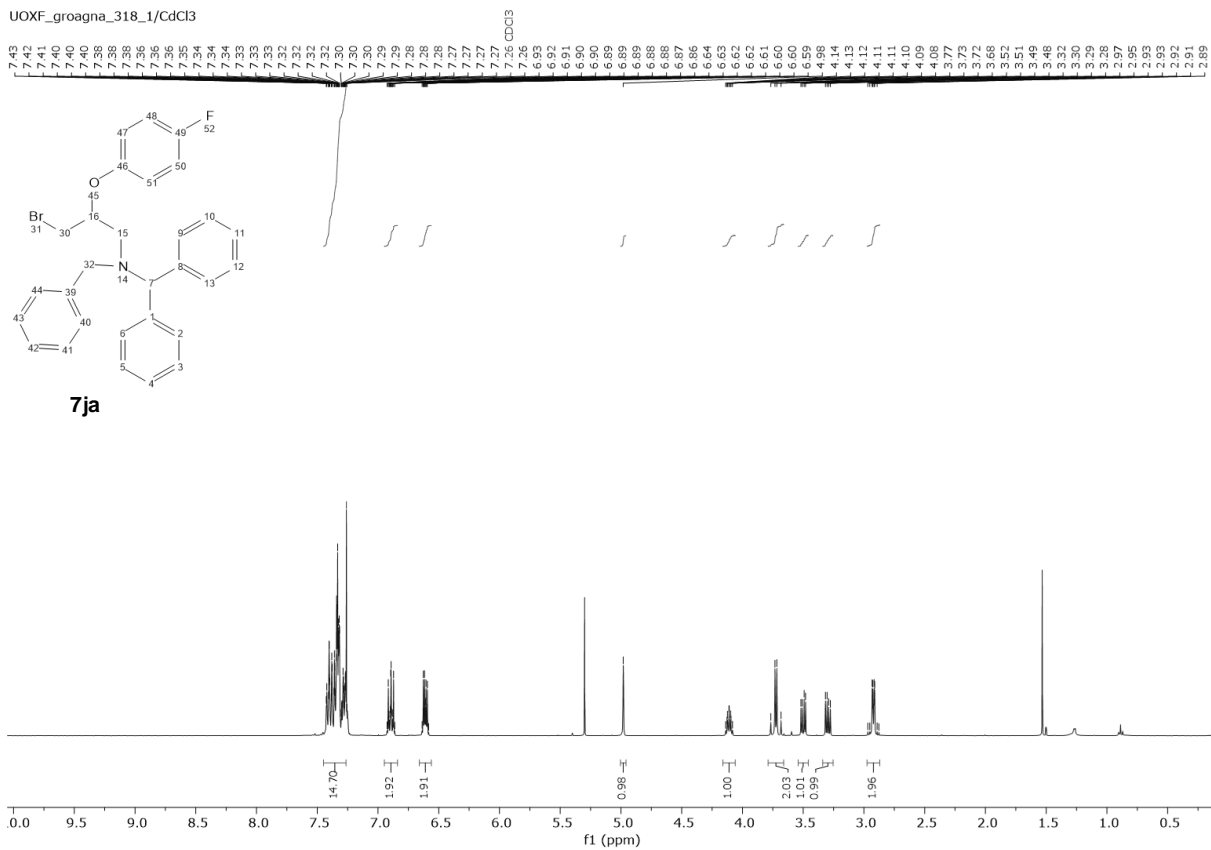
GR03EN77_1/CdCl3



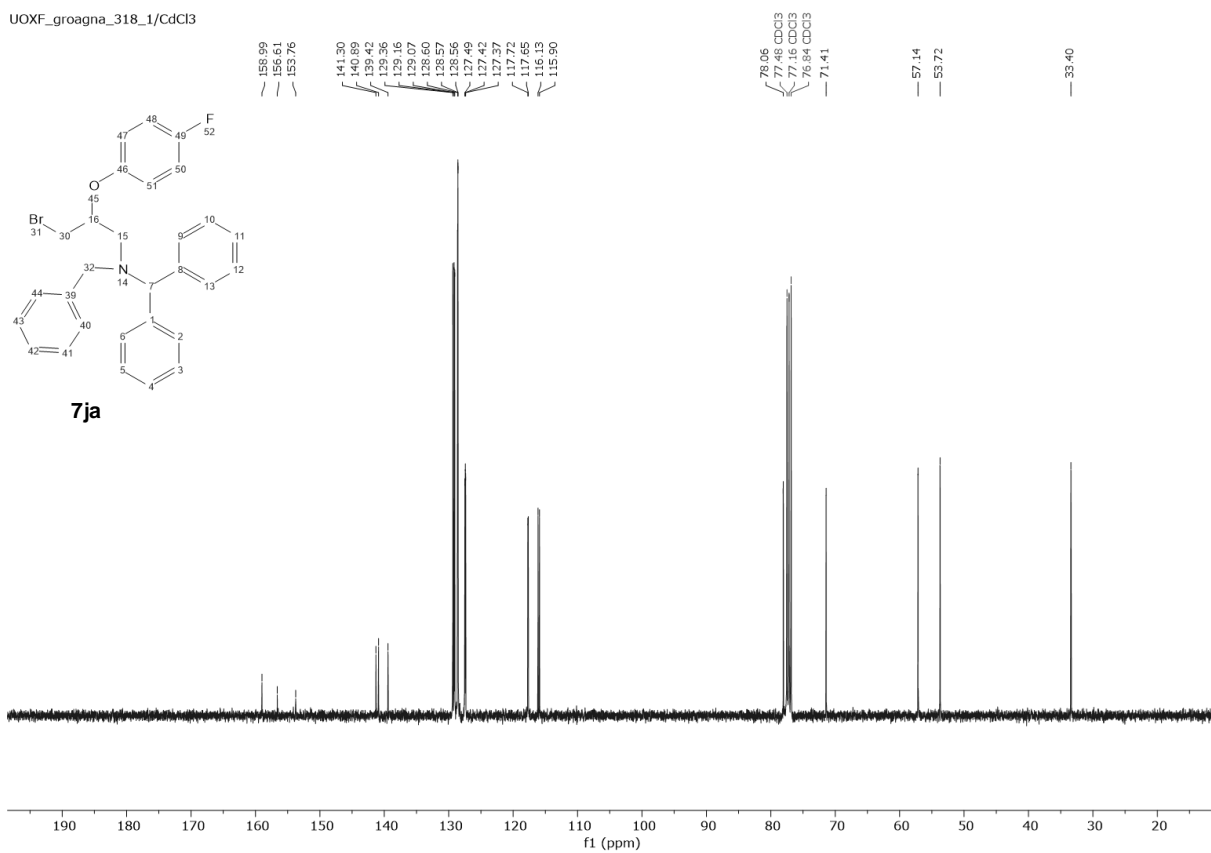
GR03EN77_1/CdCl3

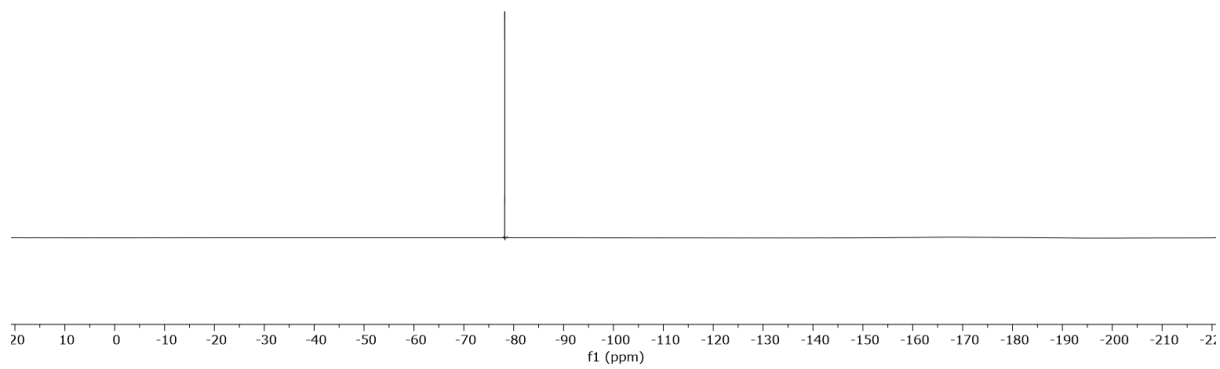
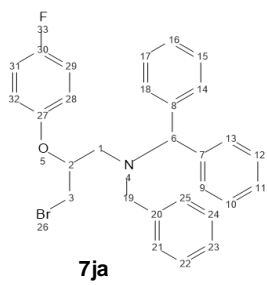


UOXF_groagna_318_1/CdCl3

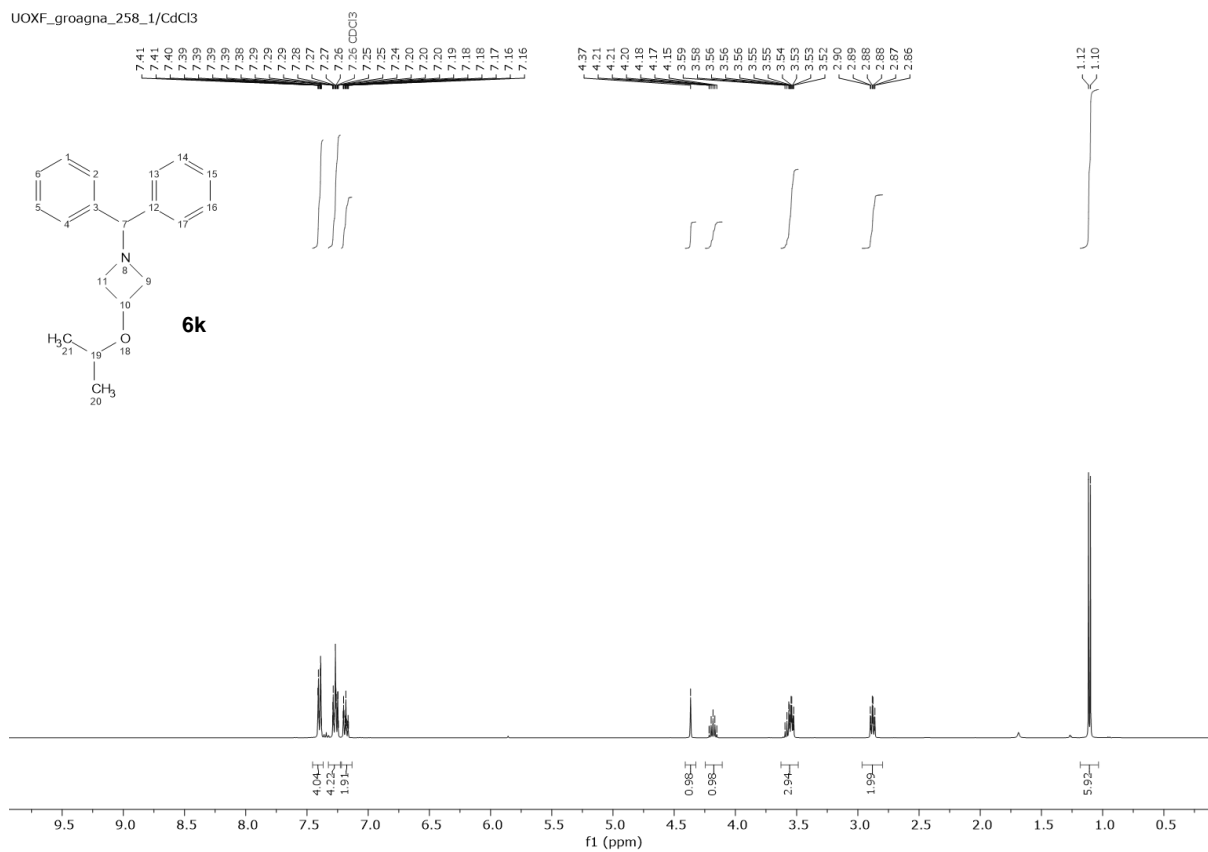


UOXF_groagna_318_1/CdCl3

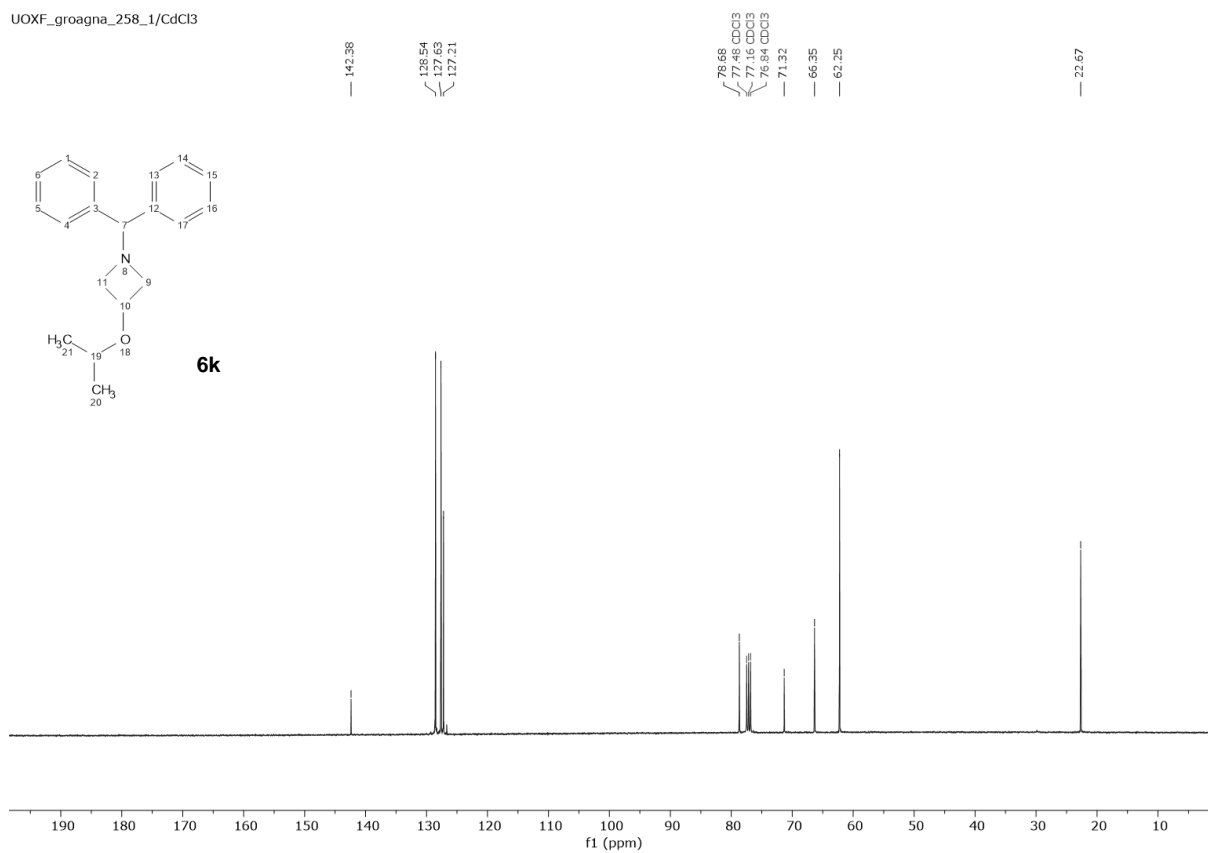


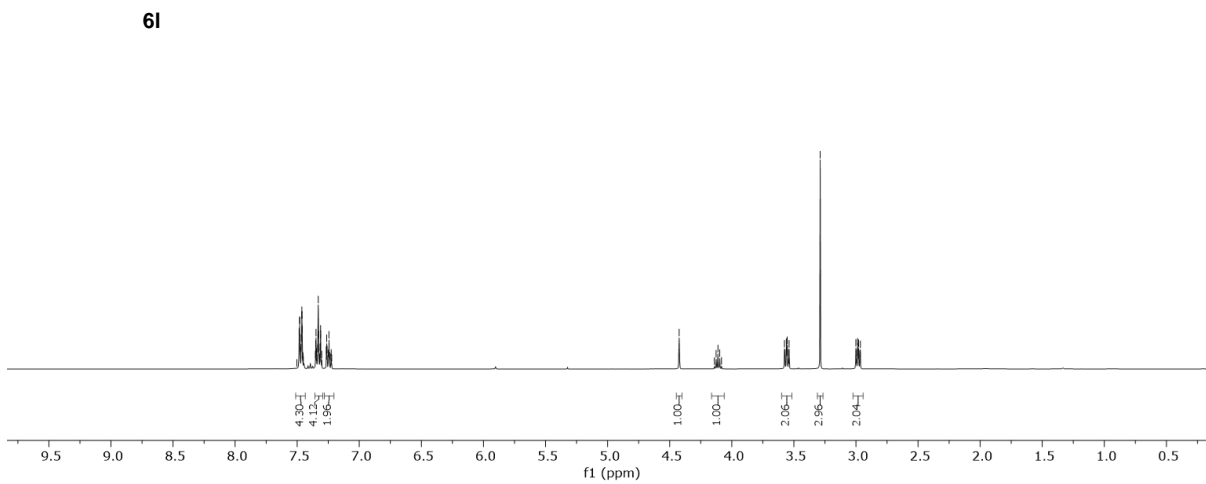
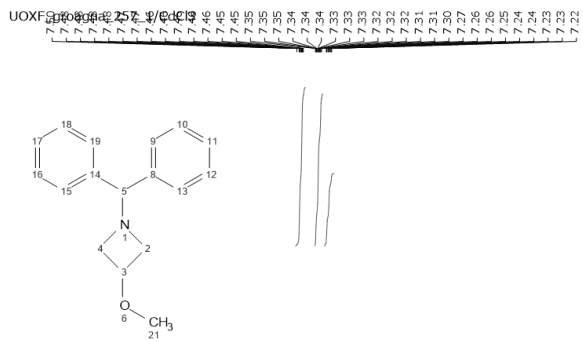


UOXF_groagna_258_1/CdCl3

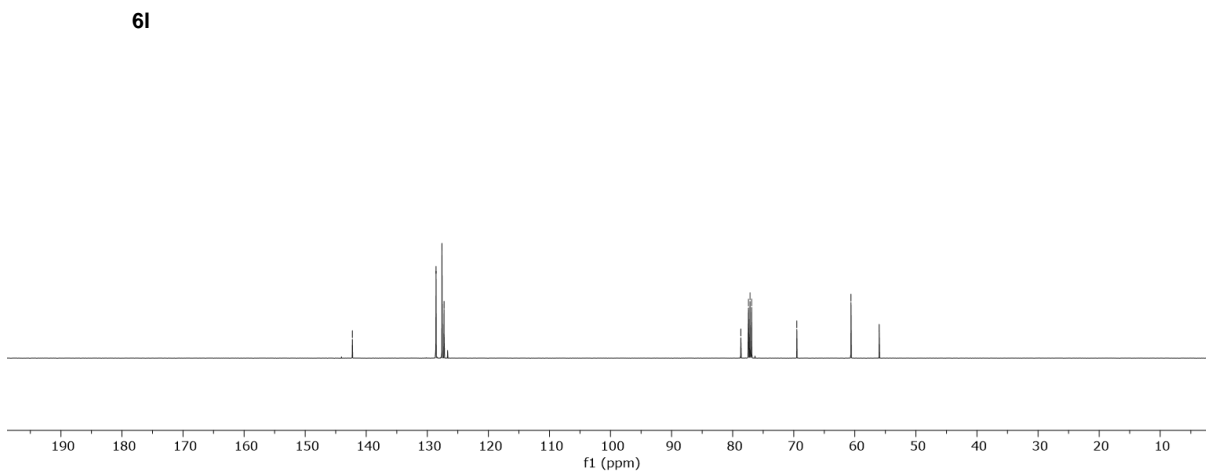


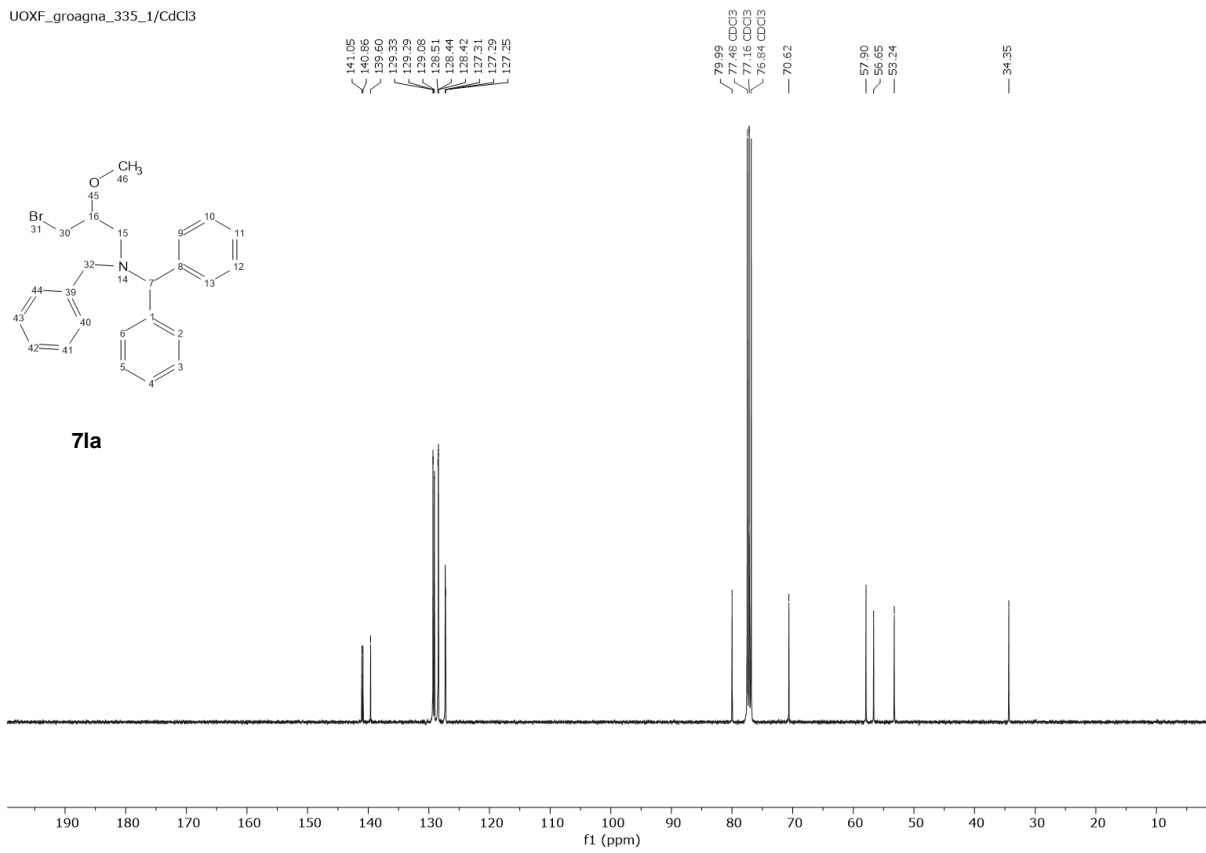
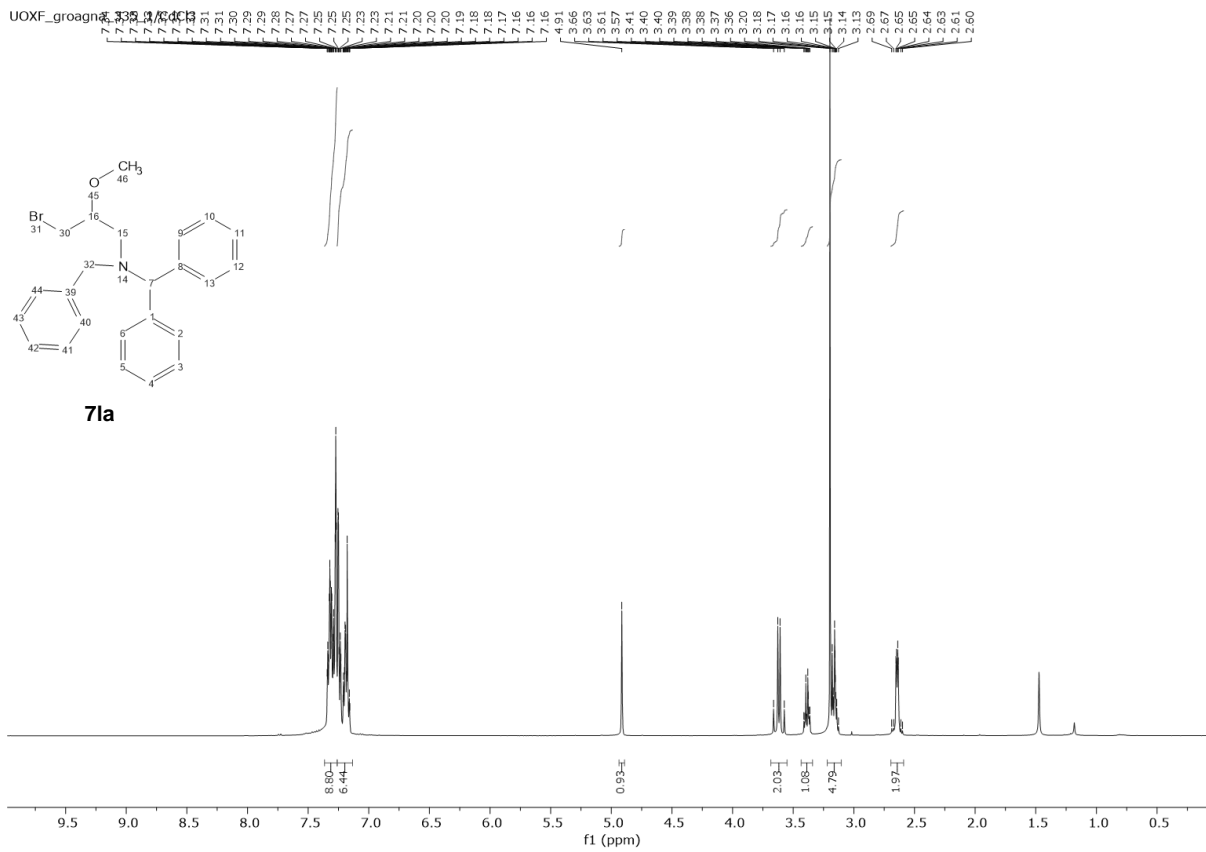
UOXF_groagna_258_1/CdCl3



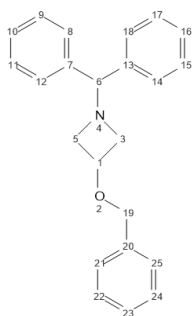


UOXF_groagna_257_1/CdCl3

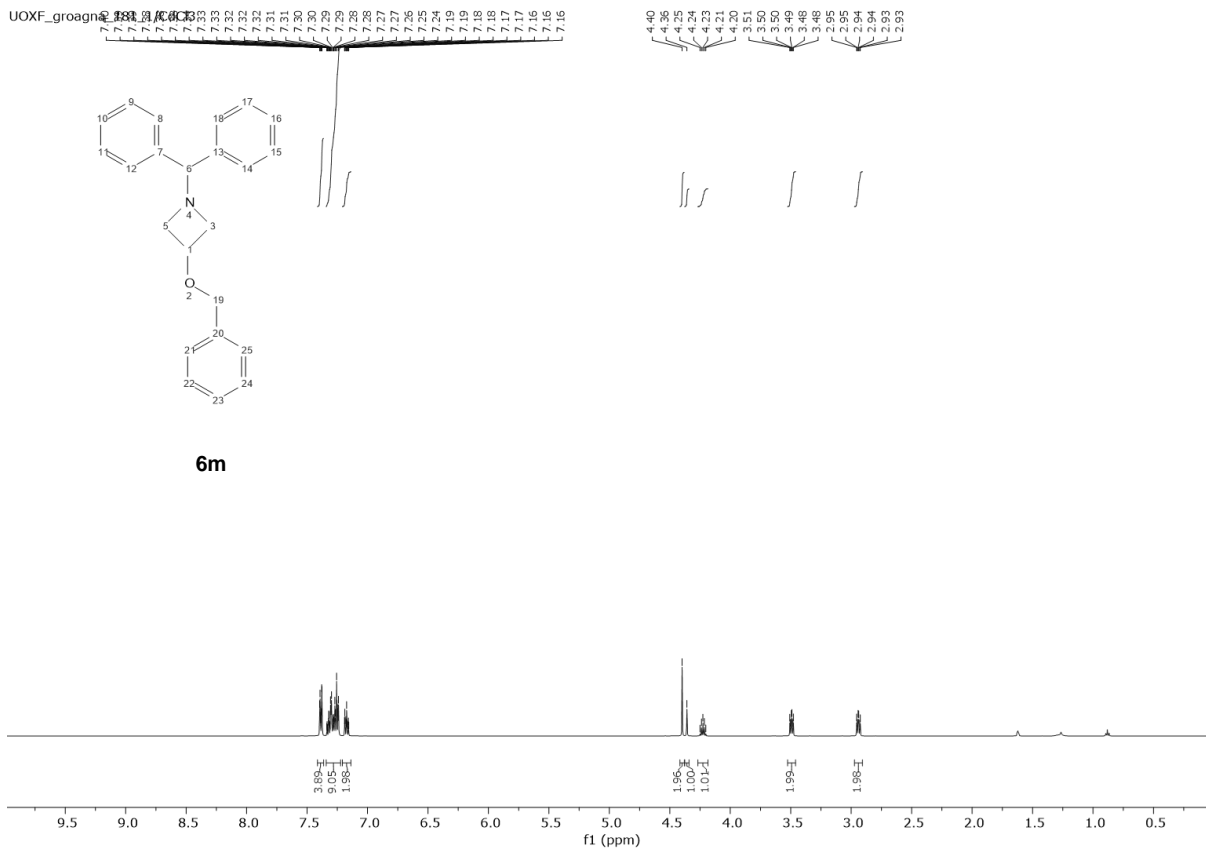




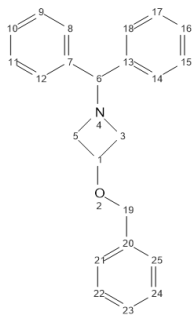
UOXF_groagna_181_1/CdCl3



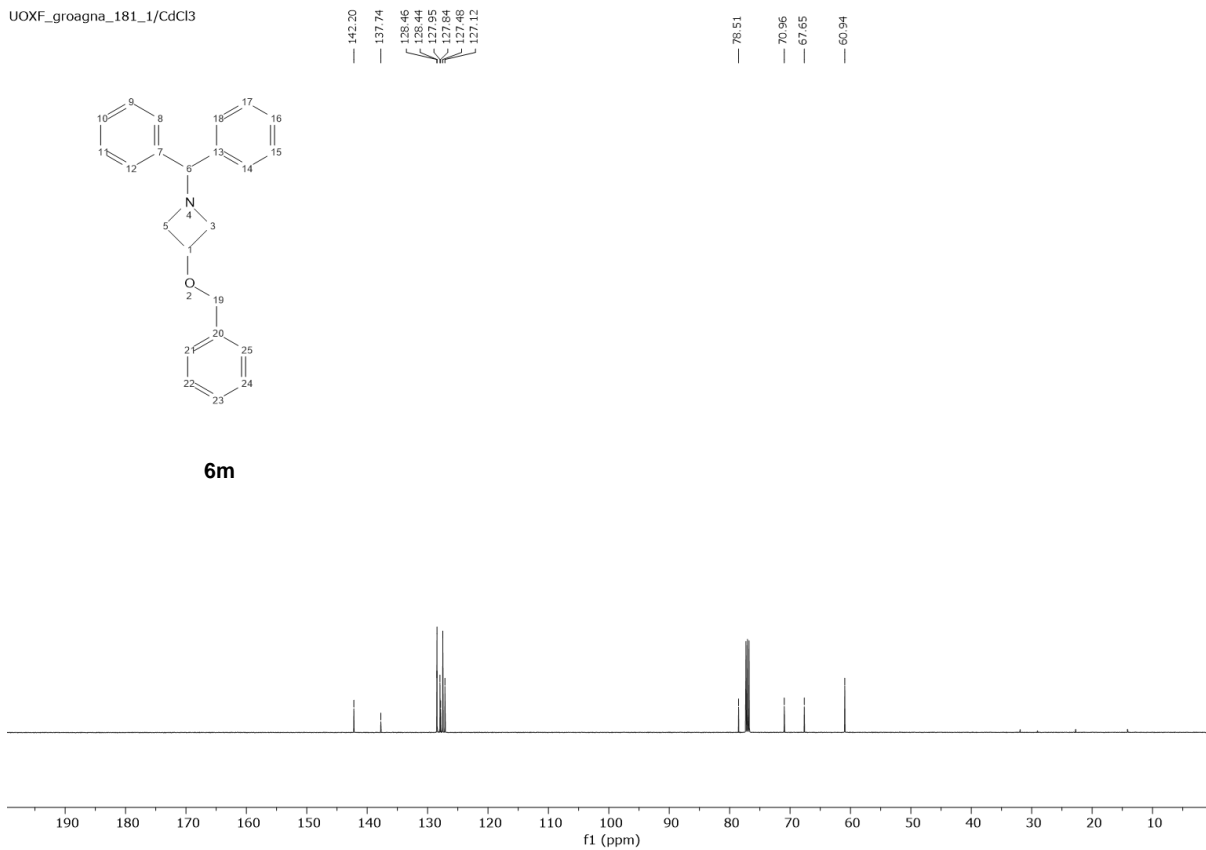
6m

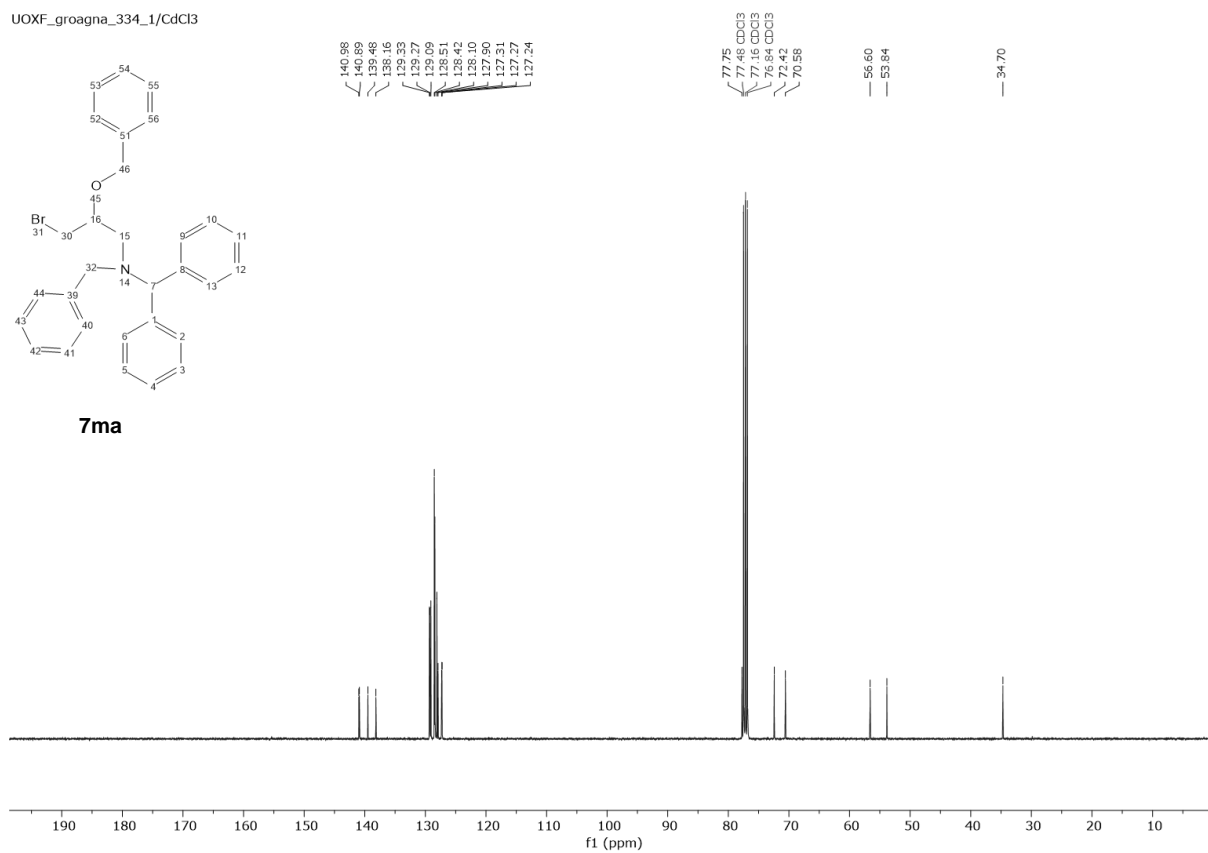
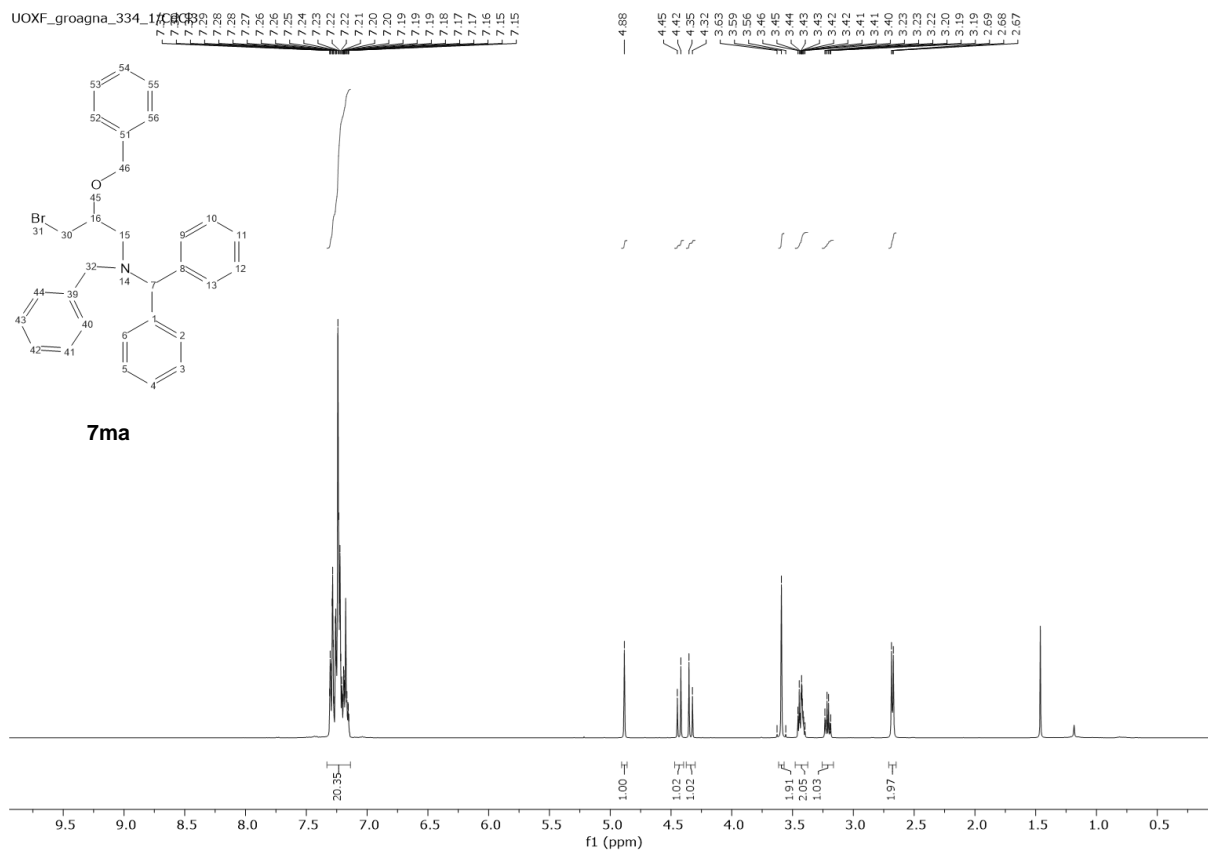


UOXF_groagna_181_1/CdCl3

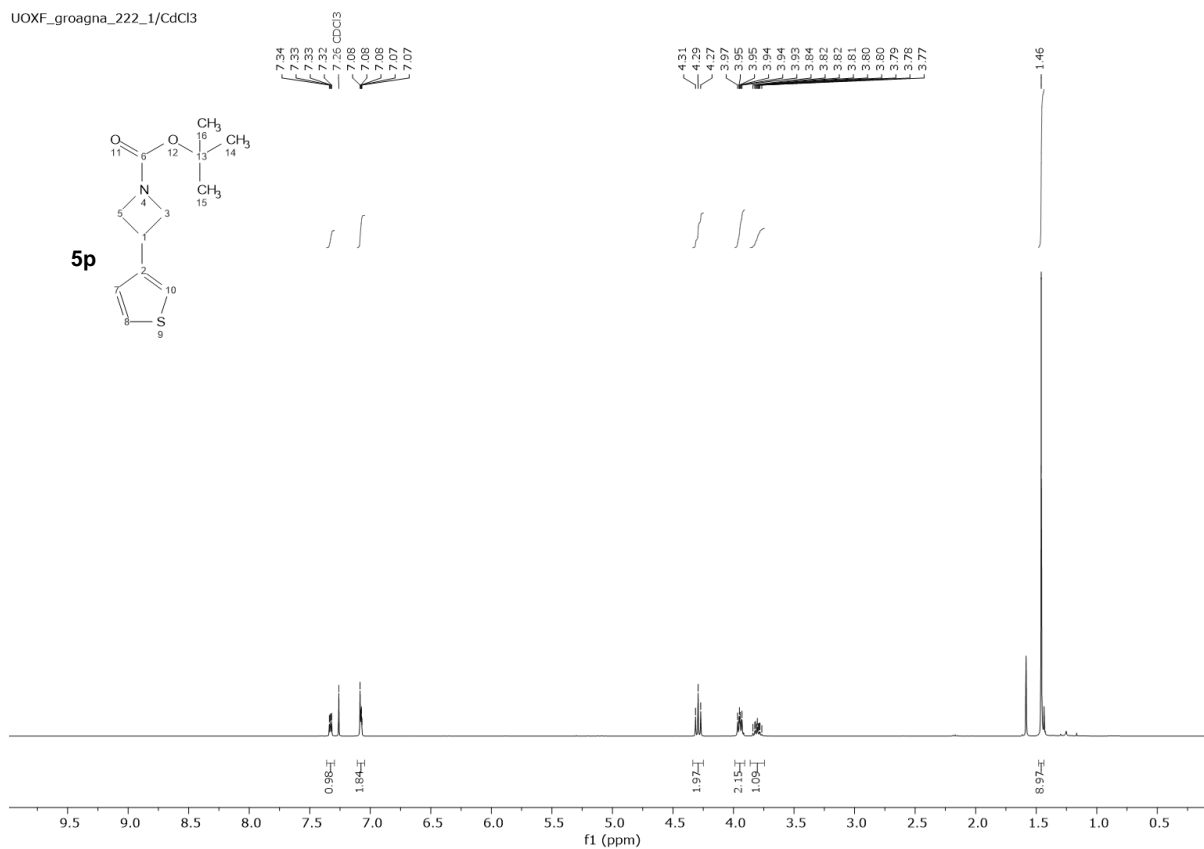


6m

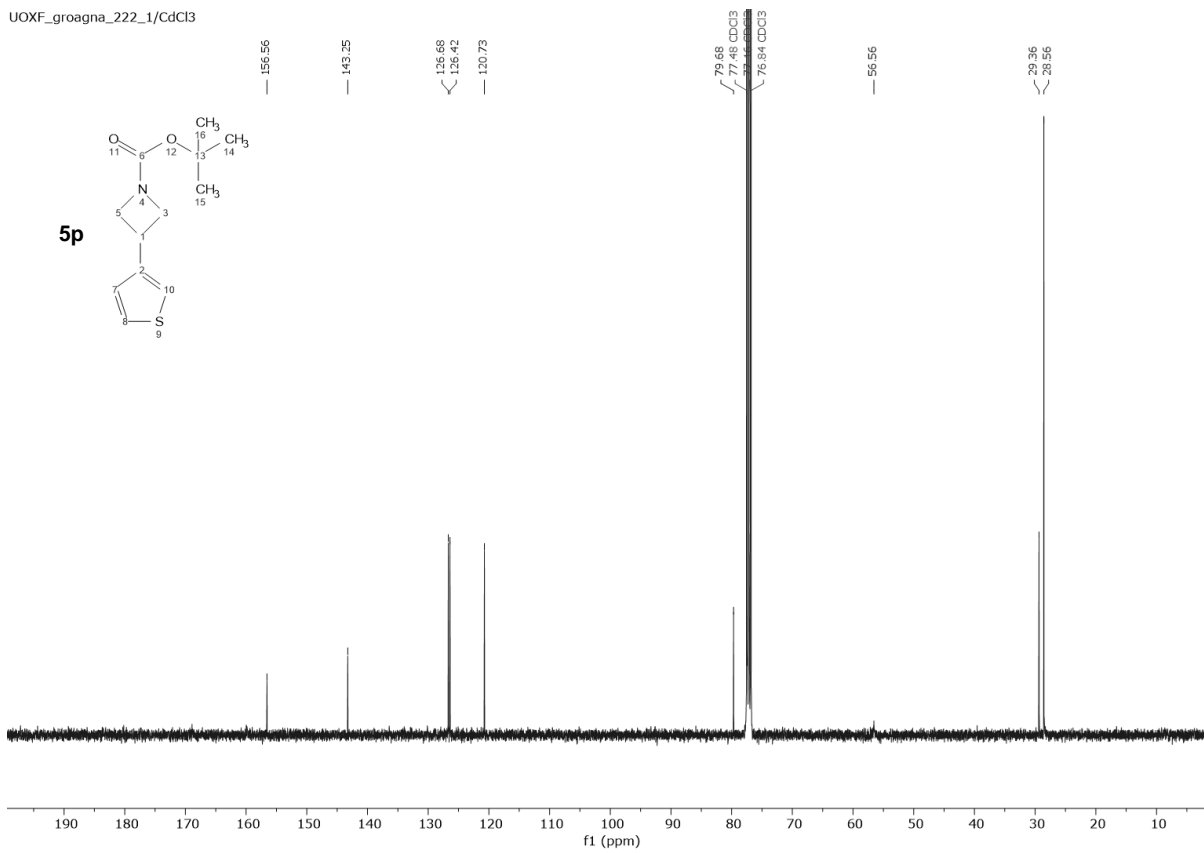




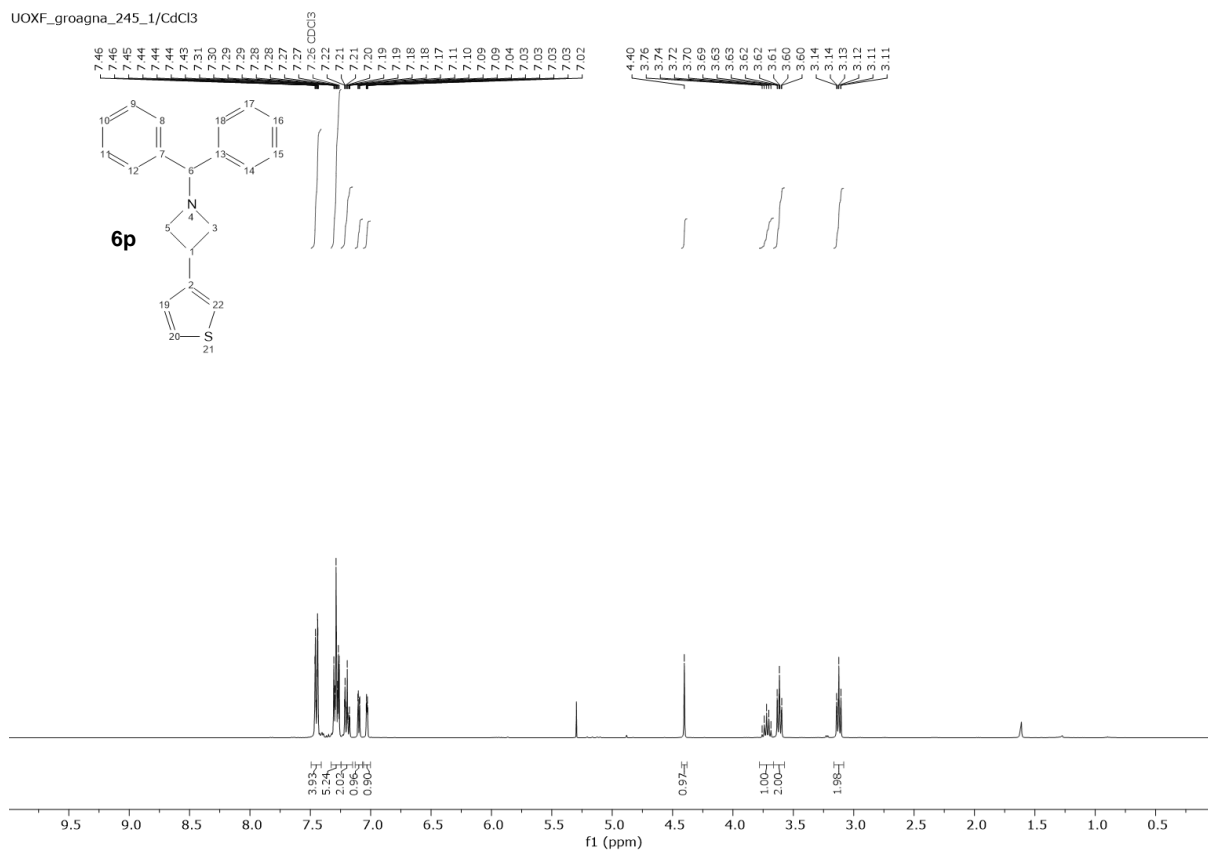
UOXF_groagna_222_1/CdCl3



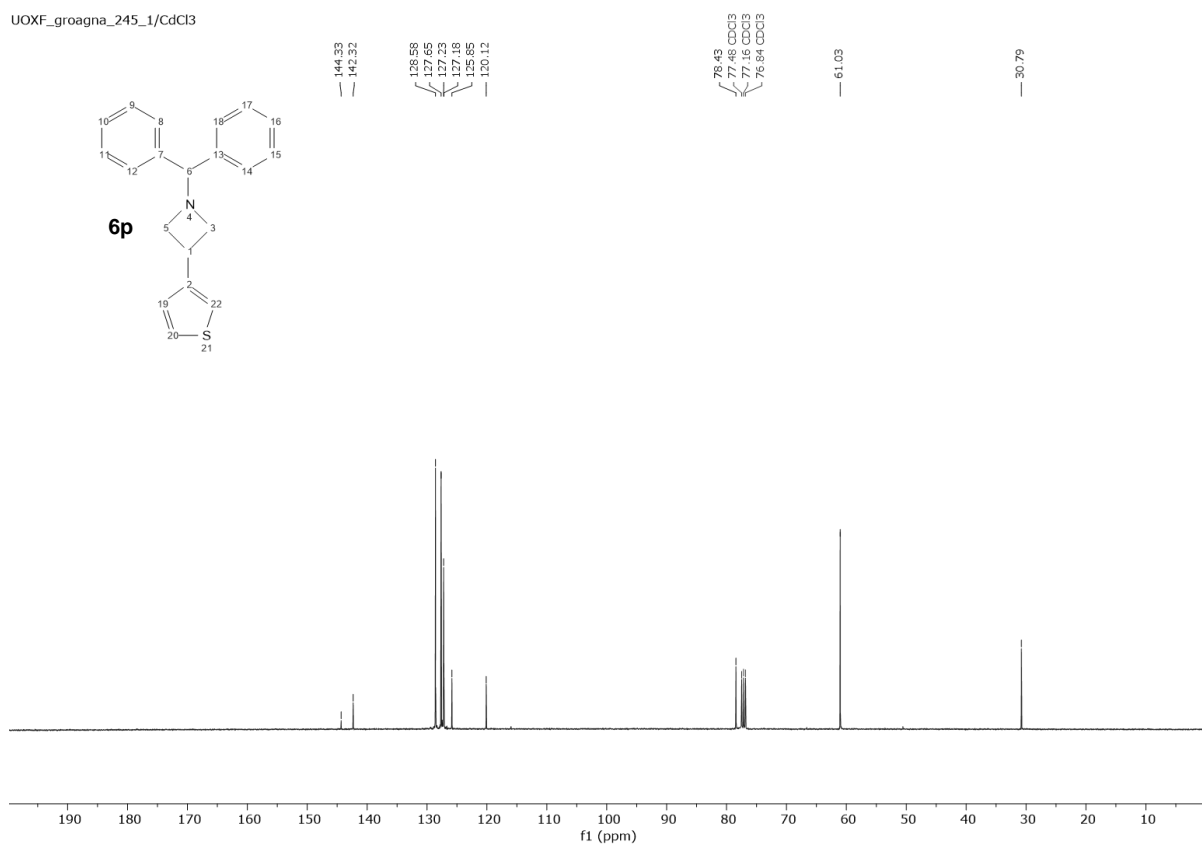
UOXF_groagna_222_1/CdCl3



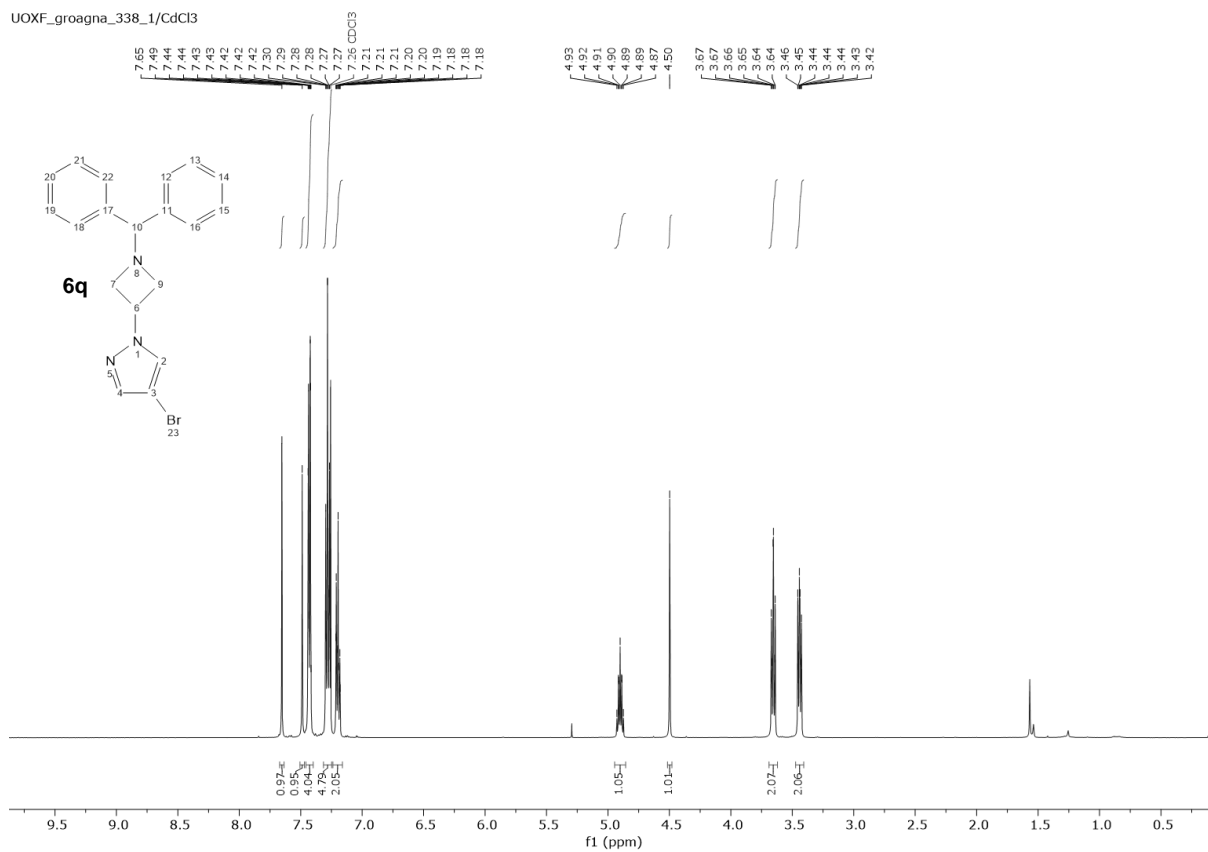
UOXF_groagna_245_1/CdCl3



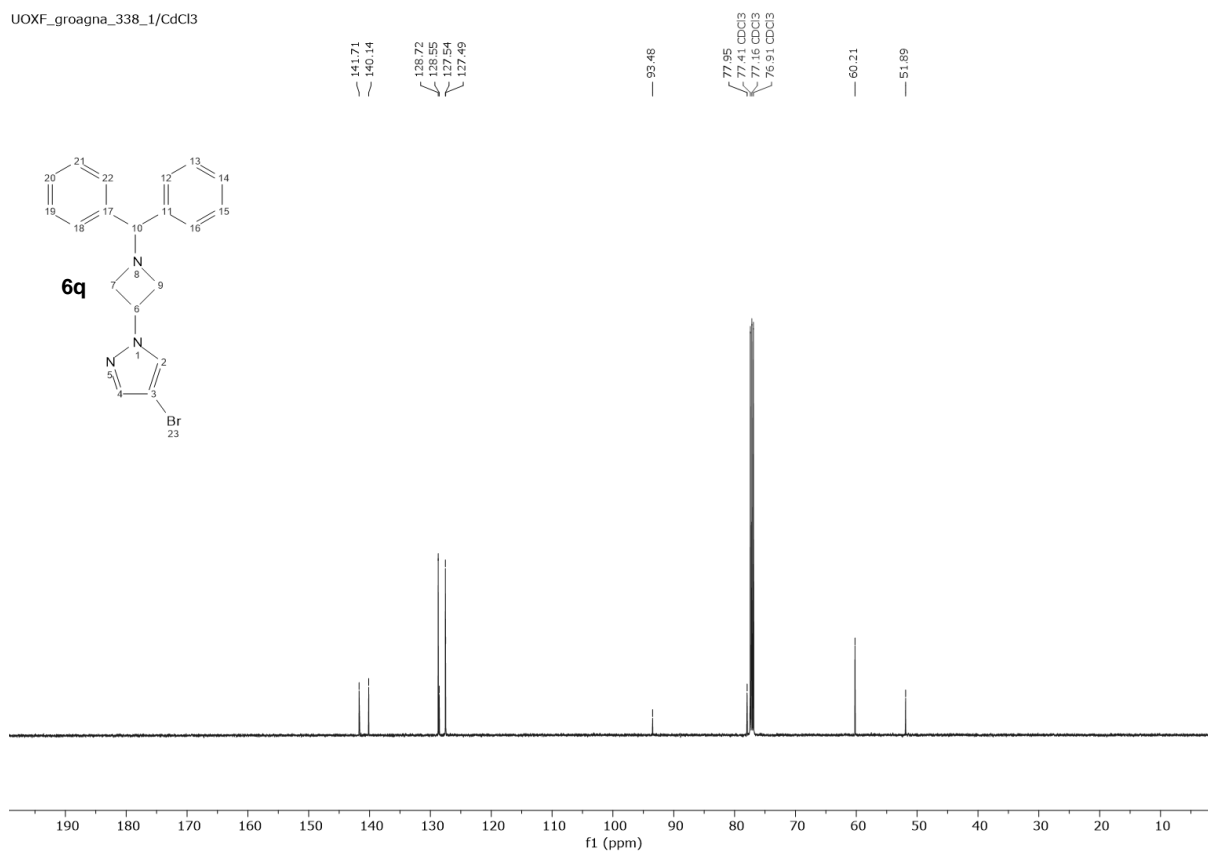
UOXF_groagna_245_1/CdCl3



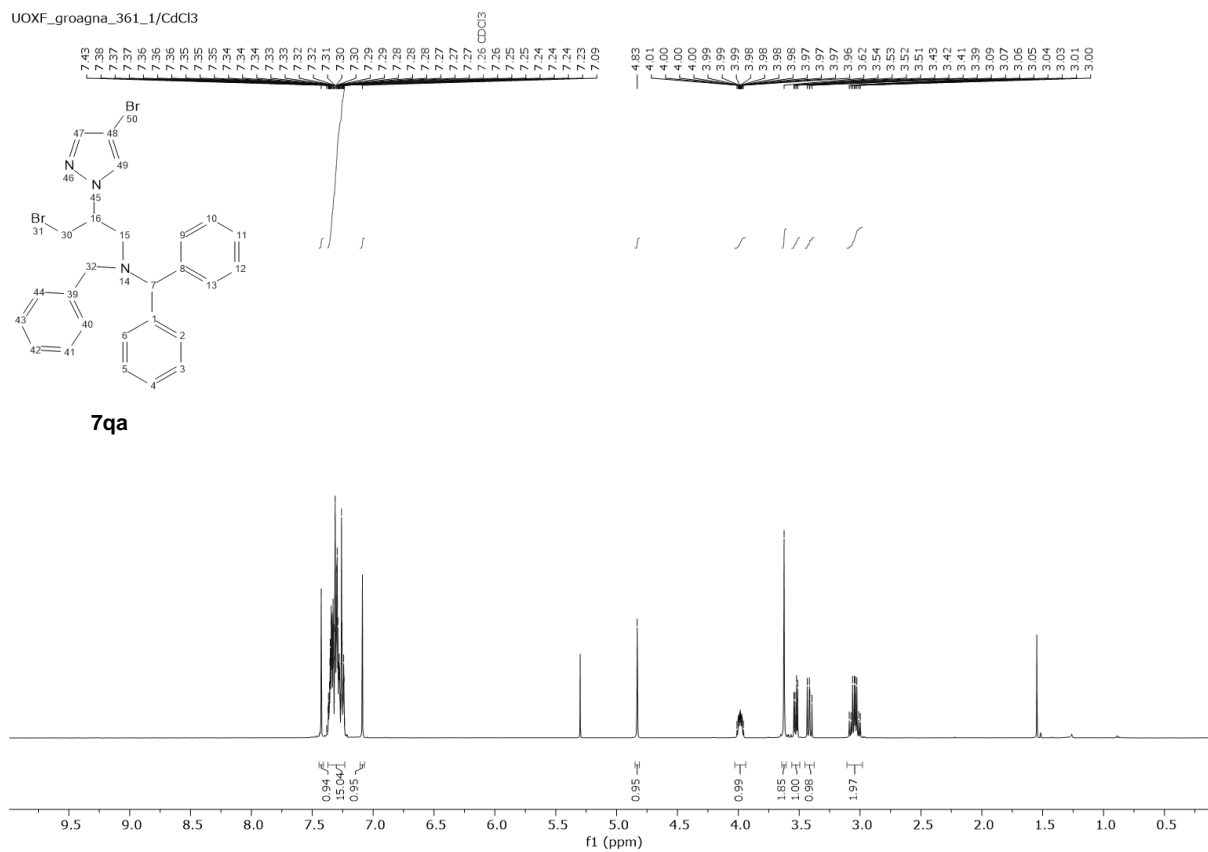
UOXF_groagna_338_1/CdCl3



UOXF_groagna_338_1/CdCl3

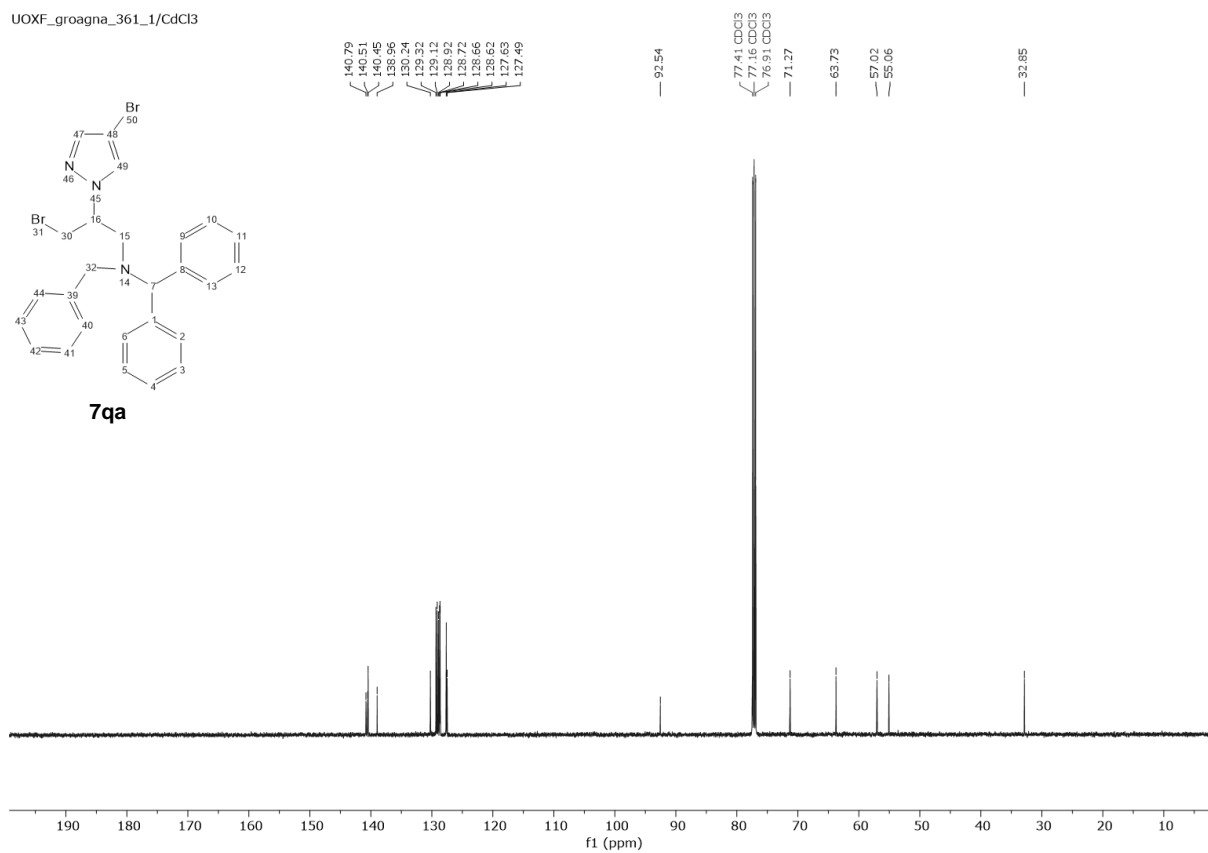


UOXF_groagna_361_1/CdCl3



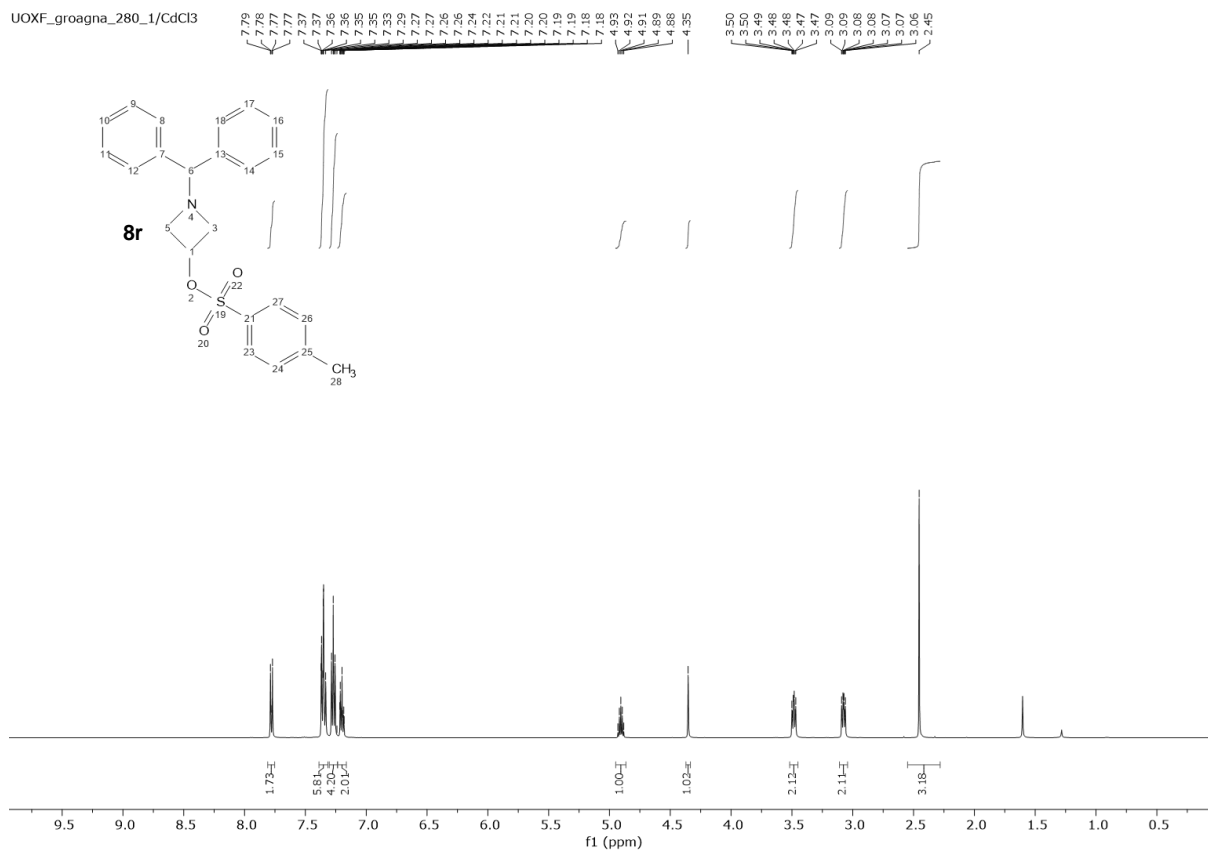
7qa

UOXF_groagna_361_1/CdCl3

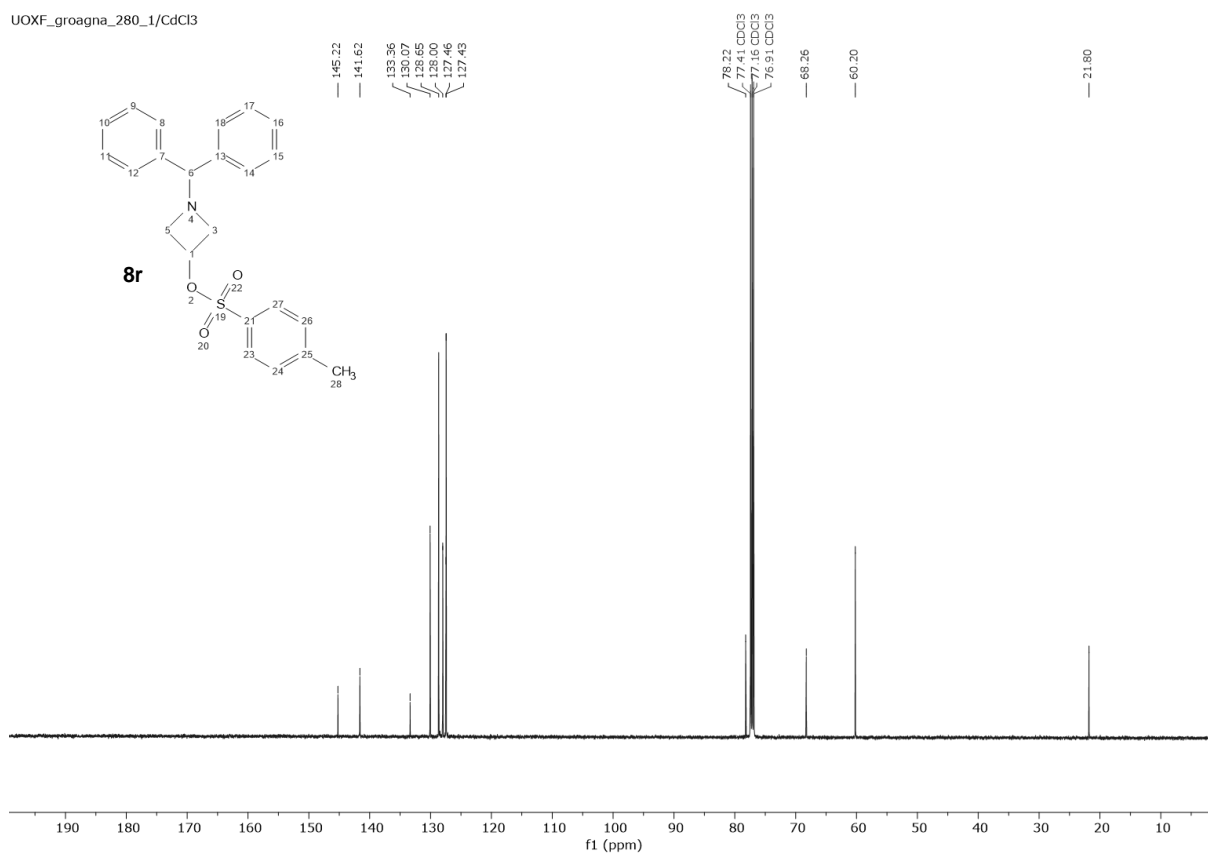


7qa

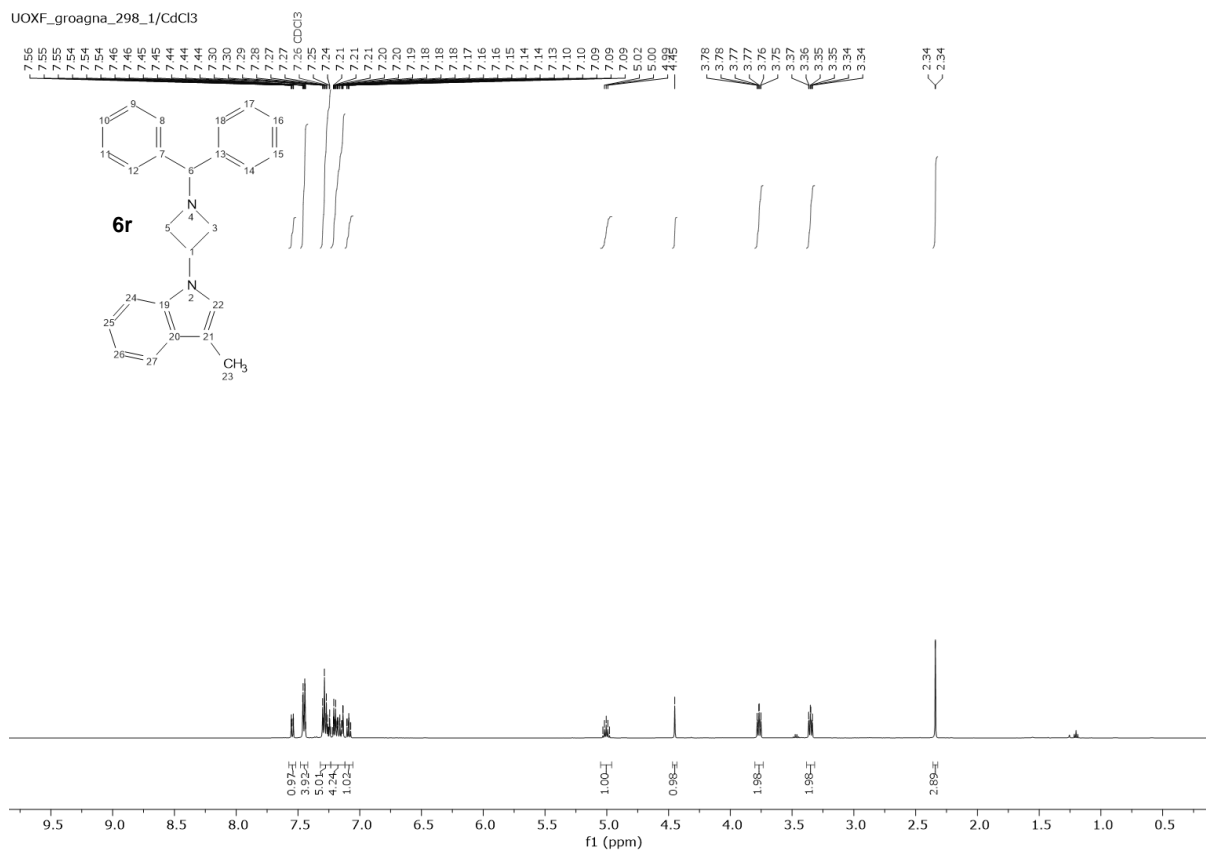
UOXF_groagna_280_1/CdCl3



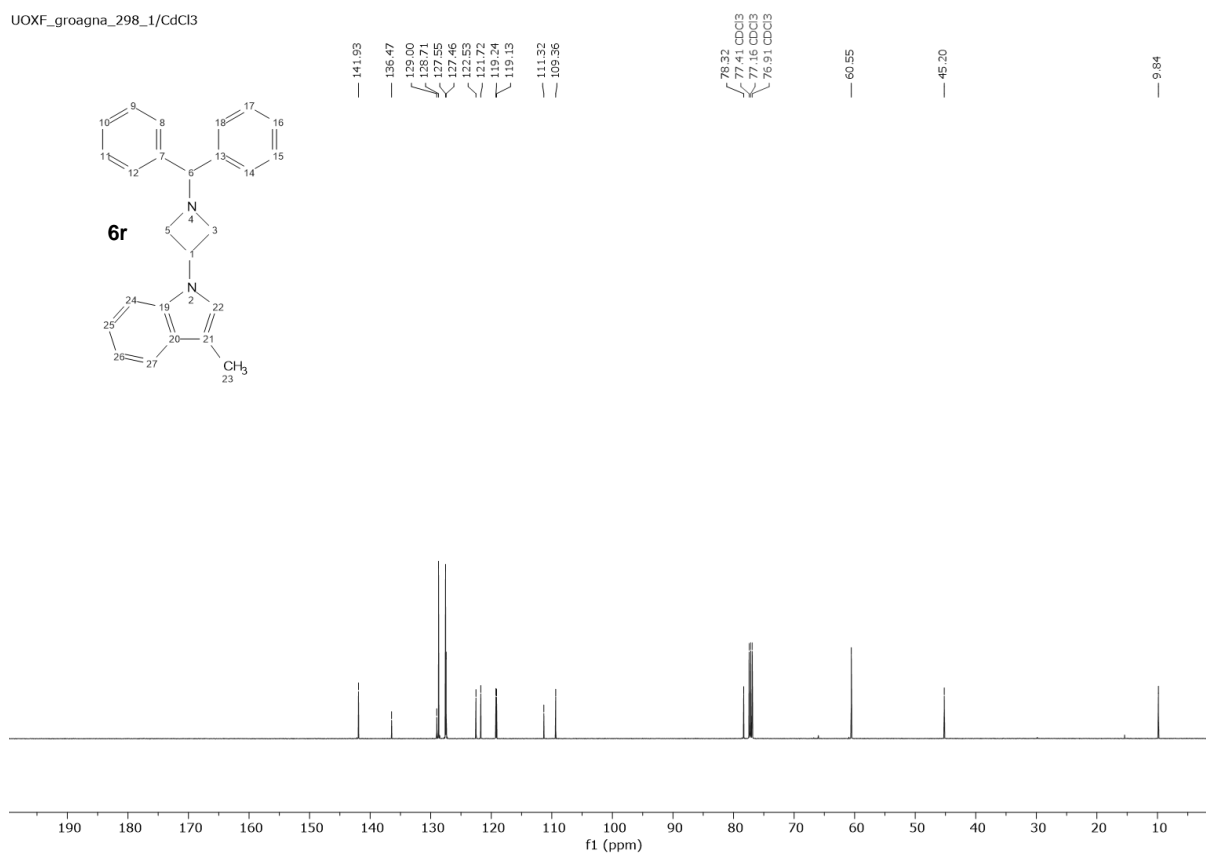
UOXF_groagna_280_1/CdCl3



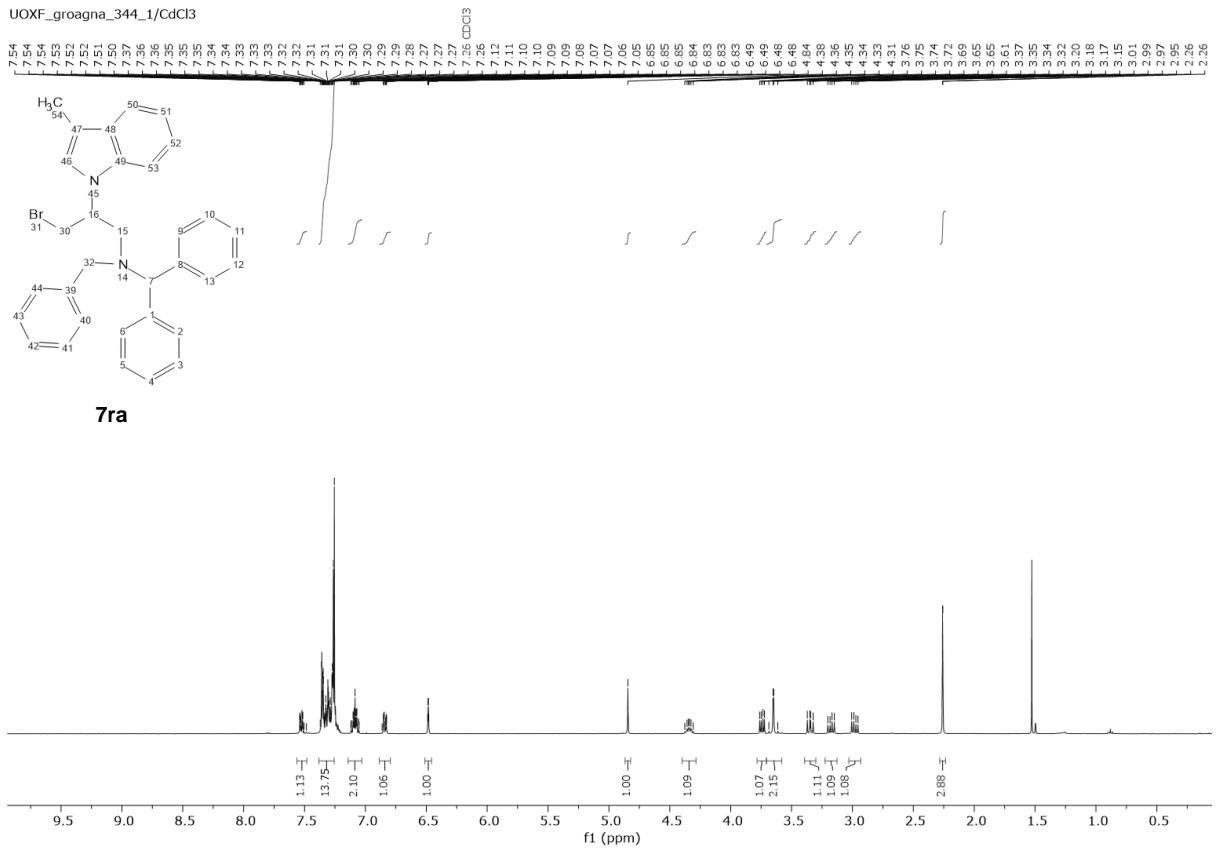
UOXF_groagna_298_1/CdCl3



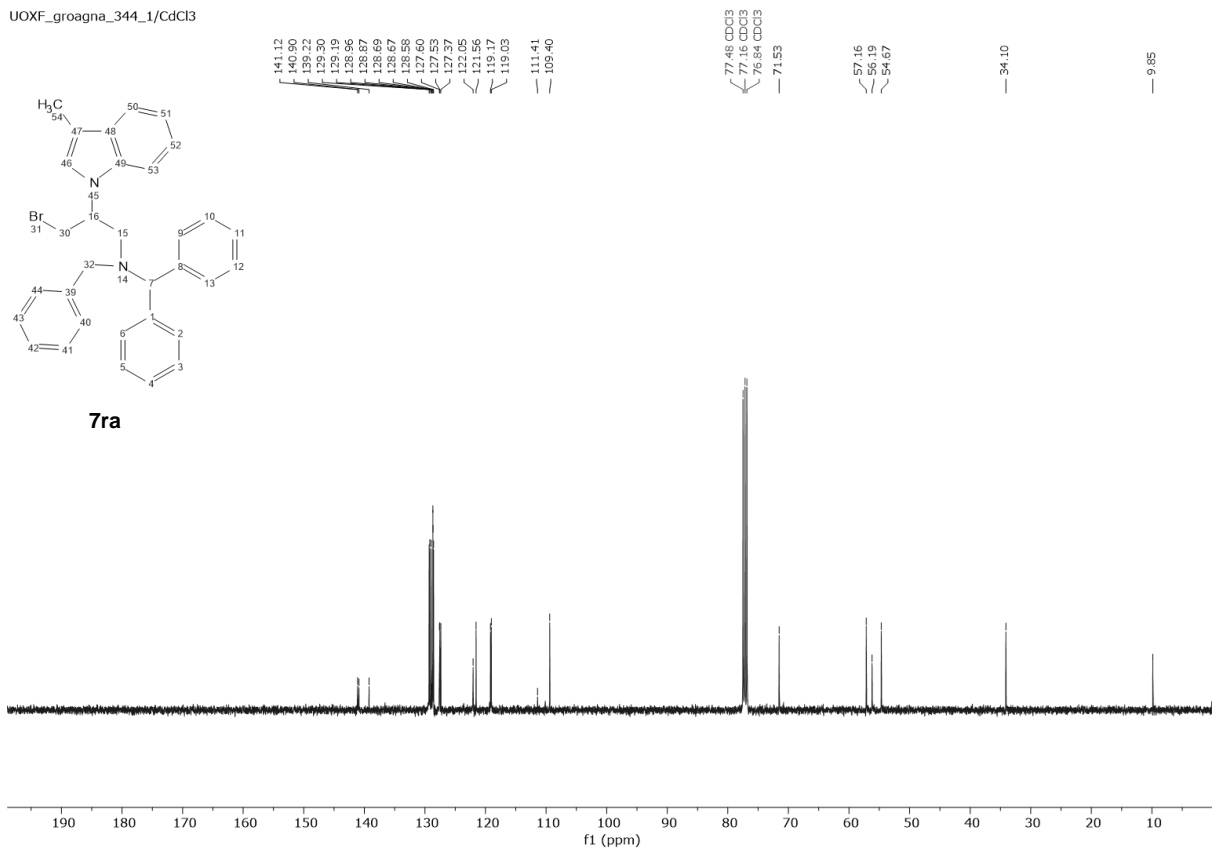
UOXF_groagna_298_1/CdCl3



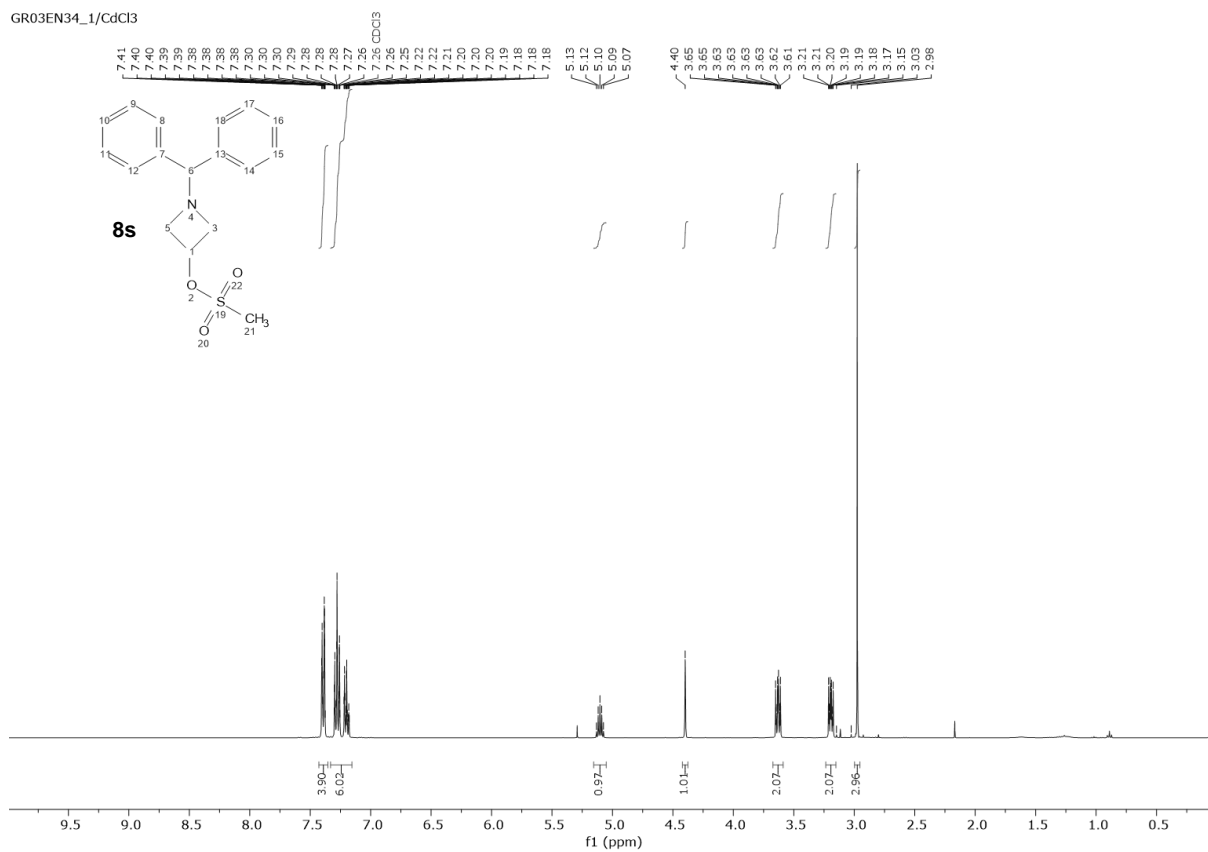
UOXF_groagna_344_1/CdCl3



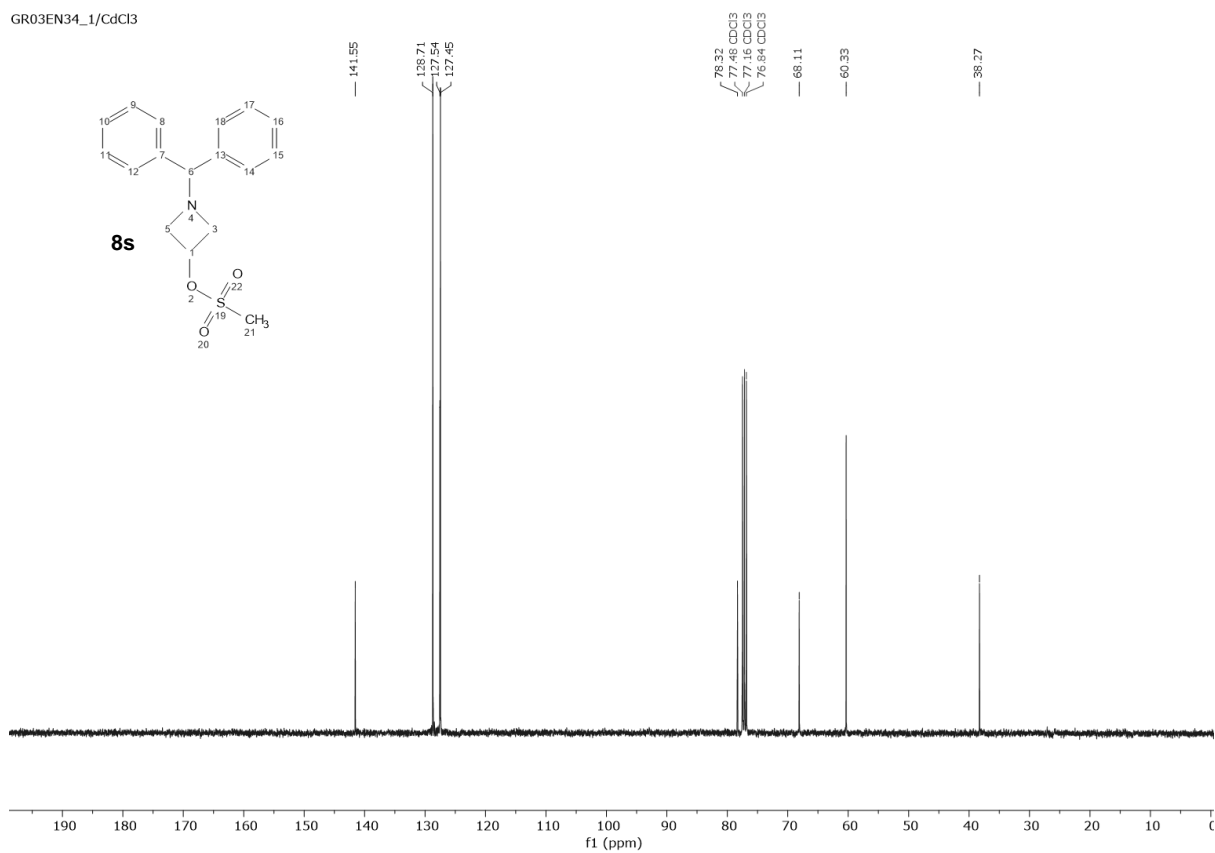
UOXF_groagna_344_1/CdCl3



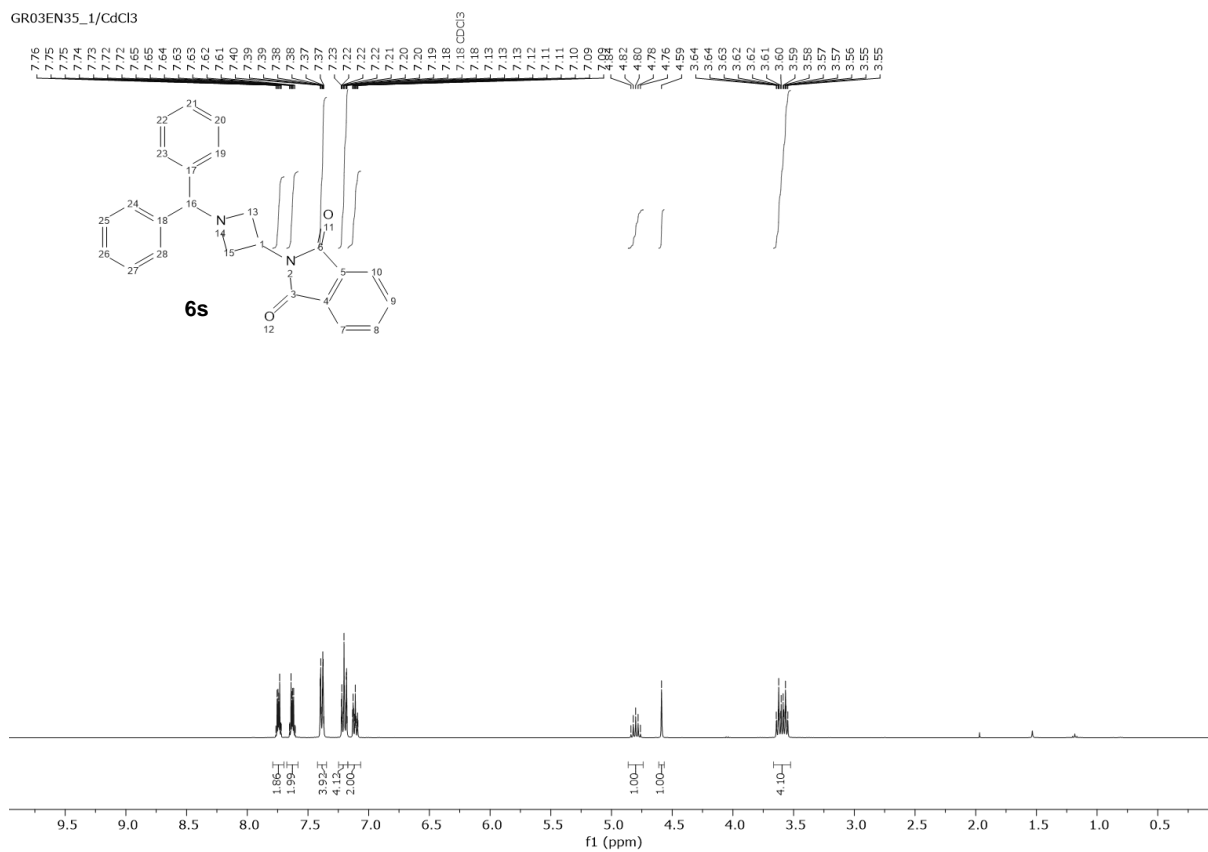
GR03EN34_1/CdCl3



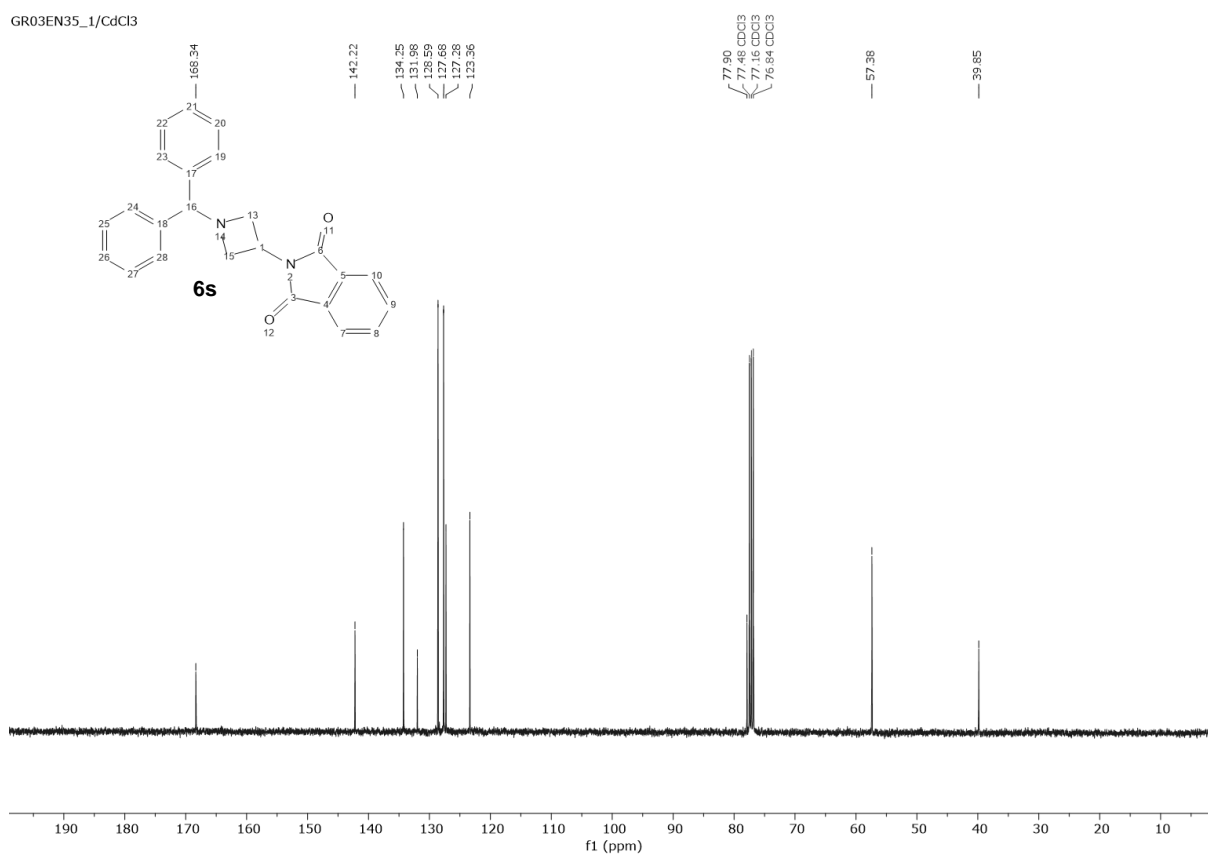
GR03EN34_1/CdCl3



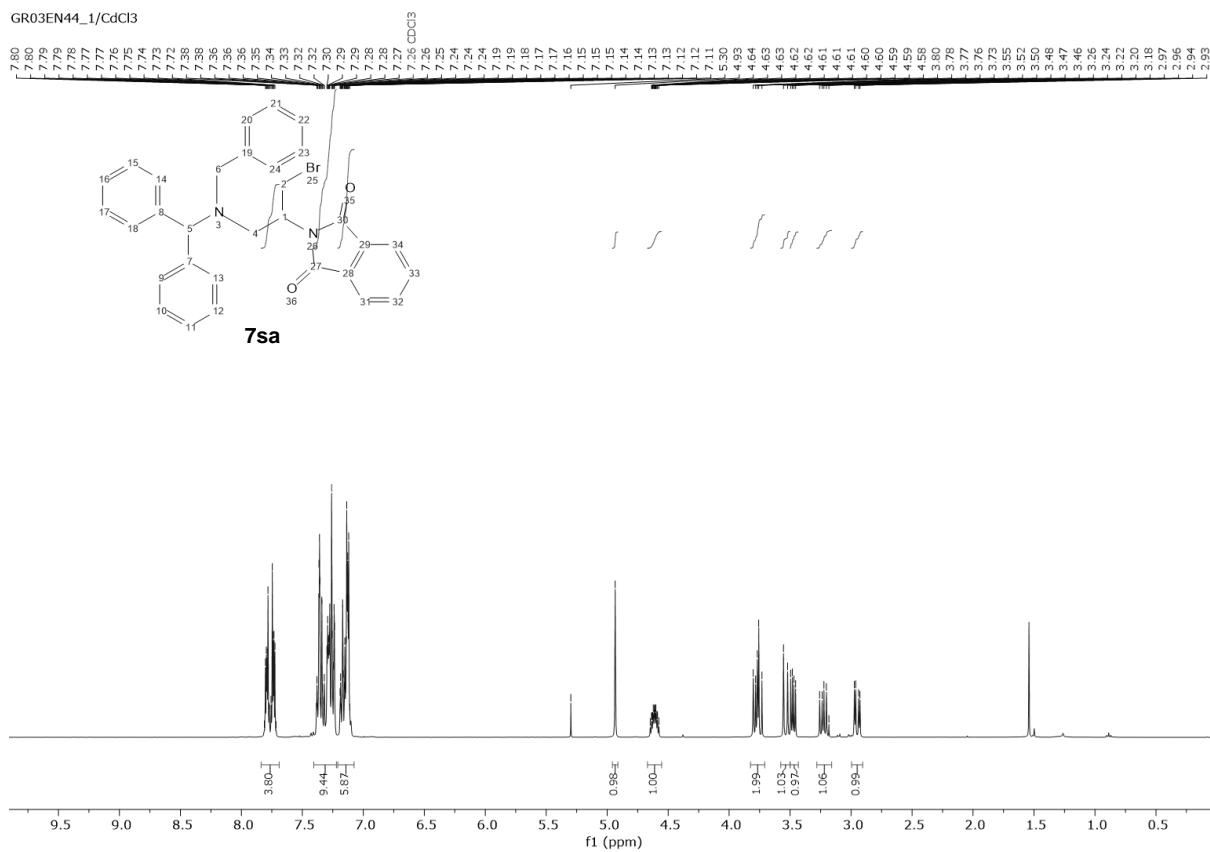
GR03EN35_1/CdCl3



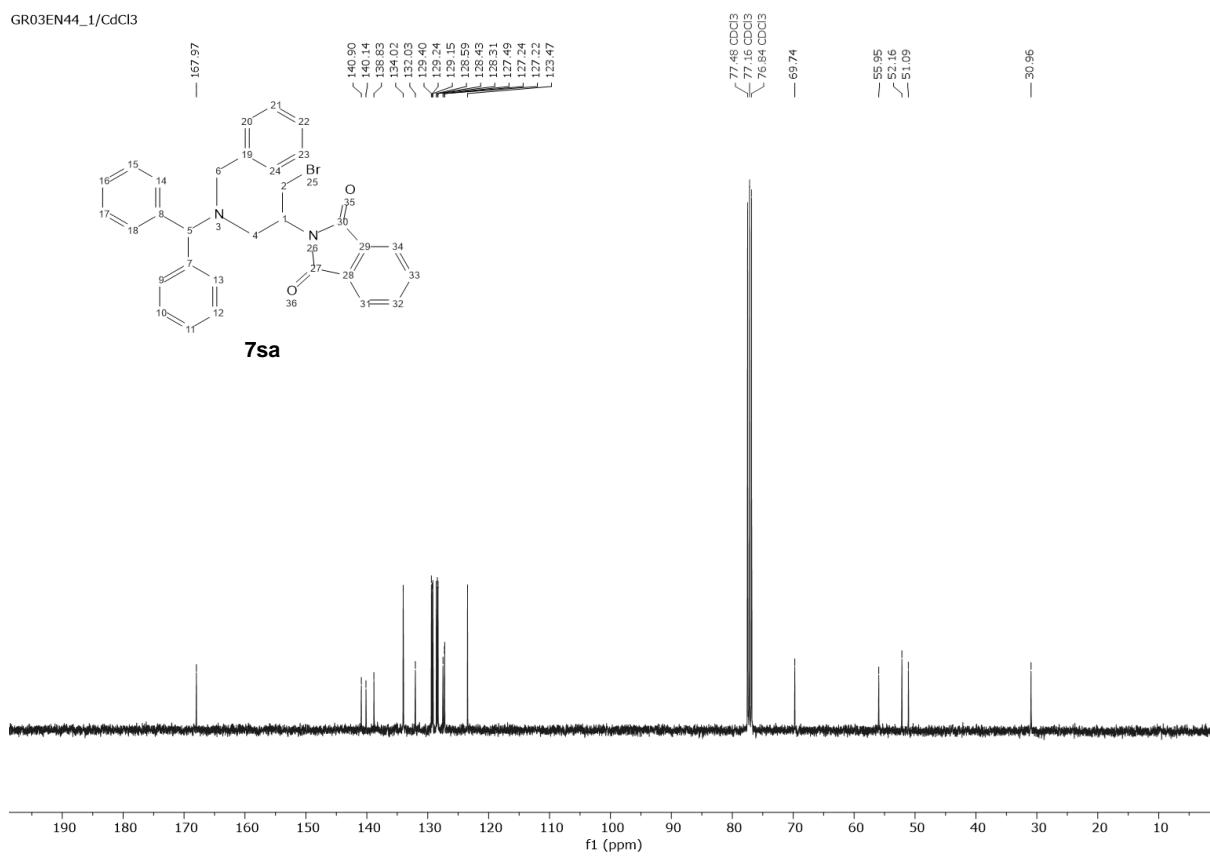
GR03EN35_1/CdCl3



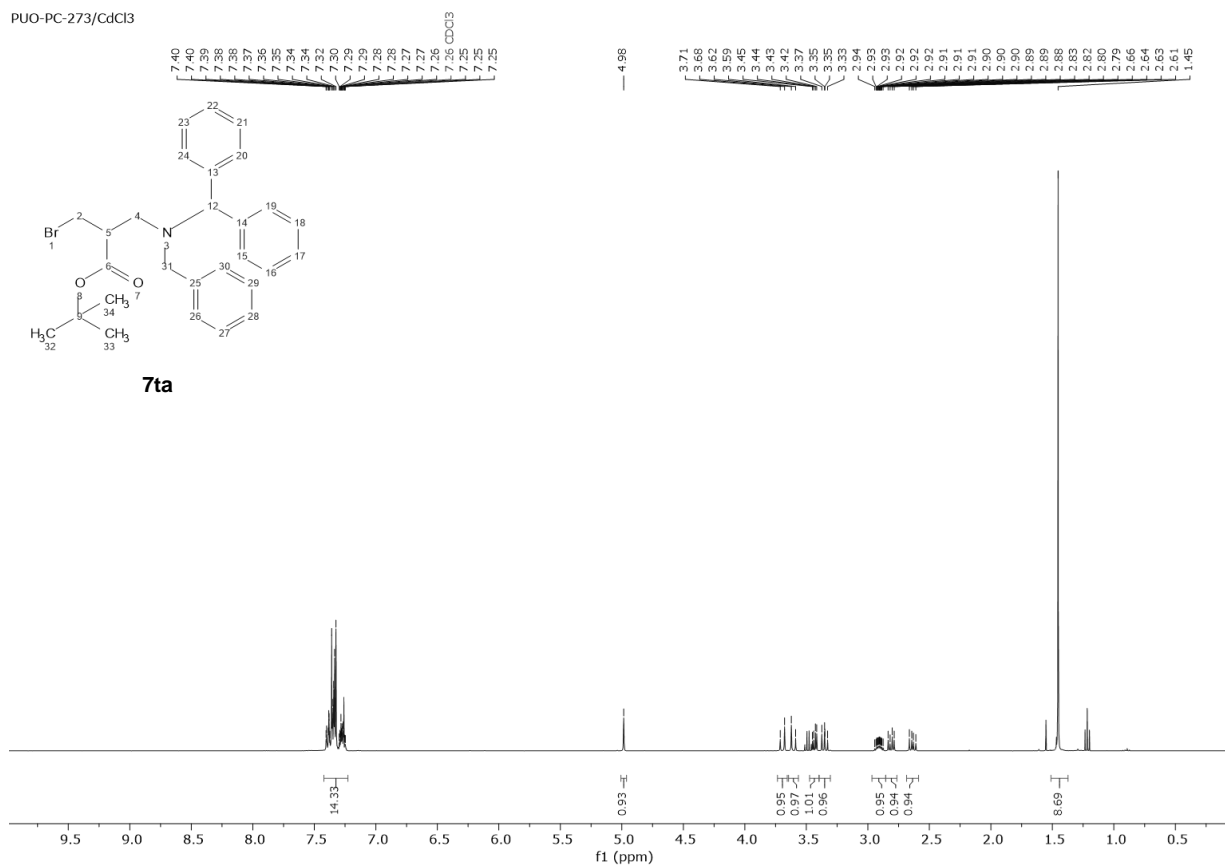
GR03EN44_1/CdCl3



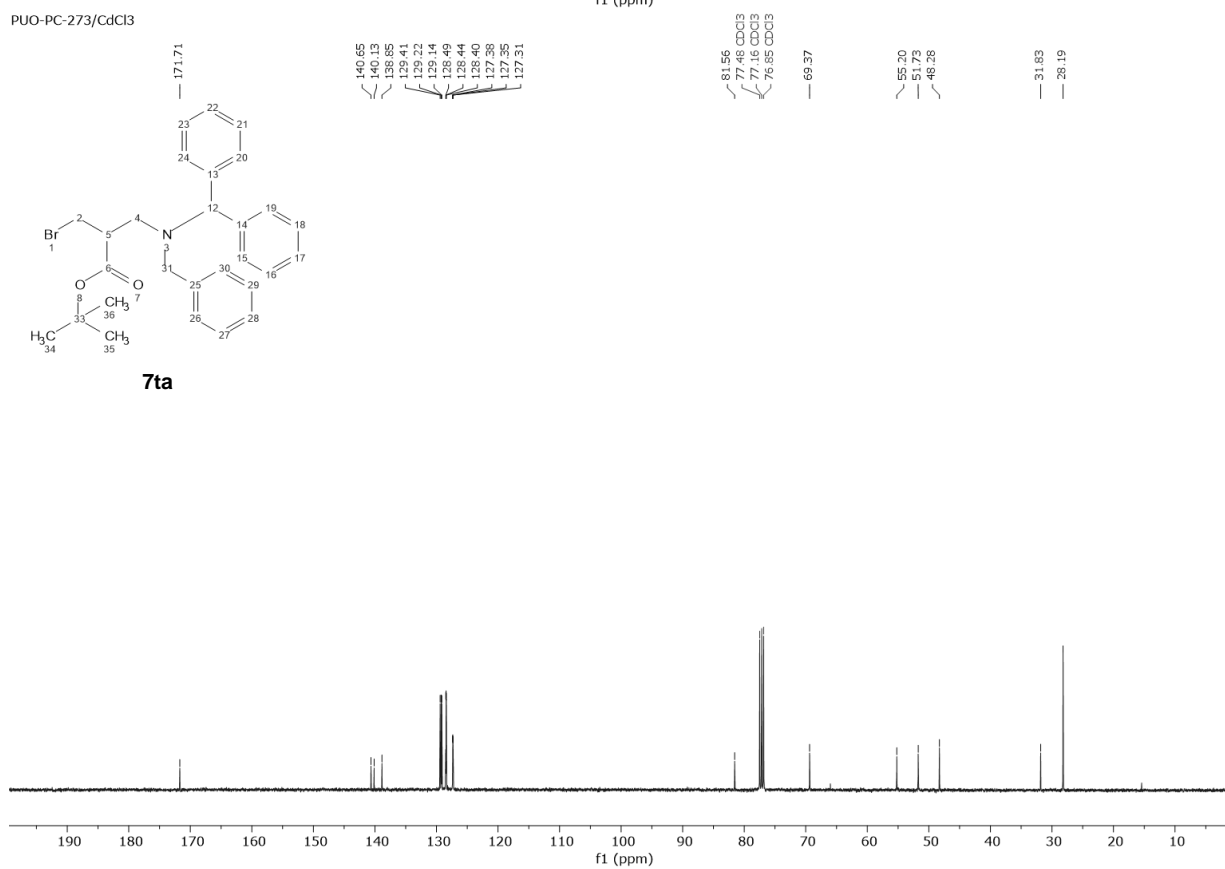
GR03EN44_1/CdCl3



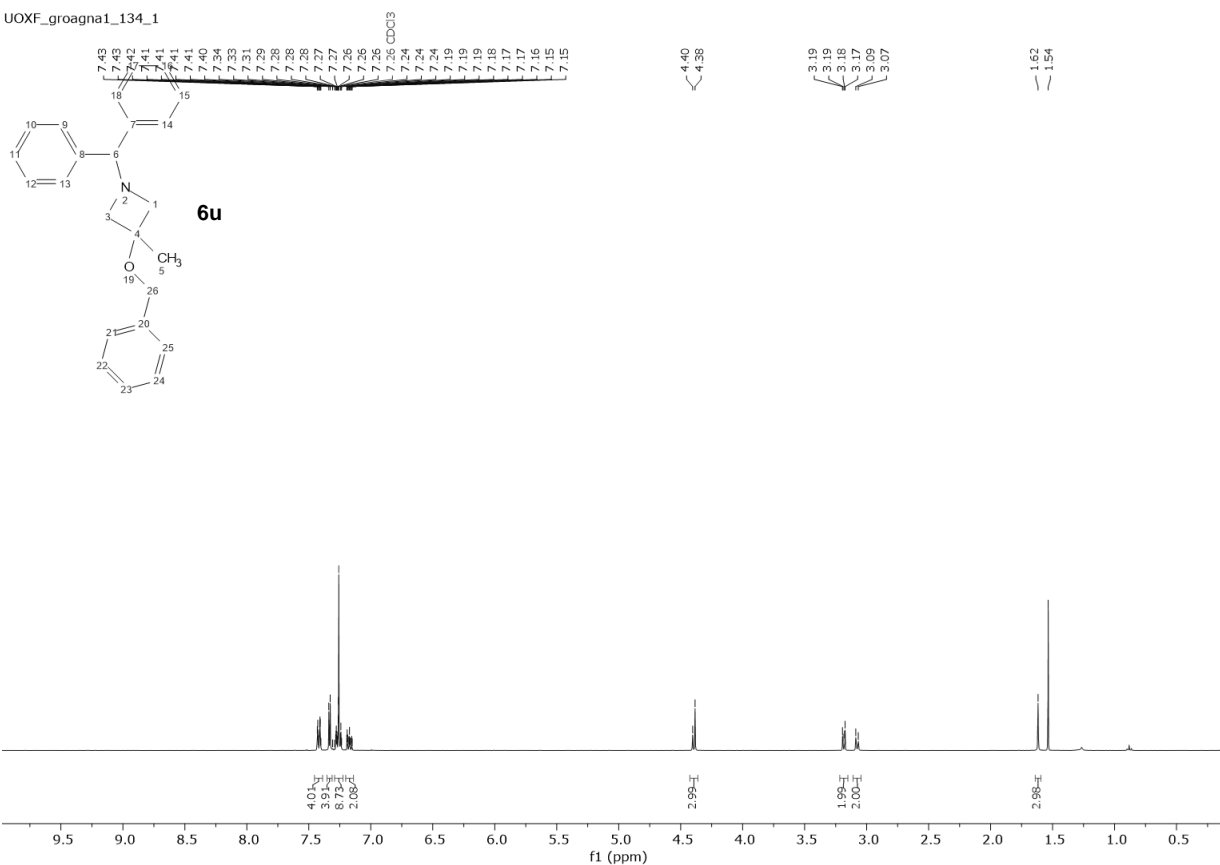
PUO-PC-273/CdCl3



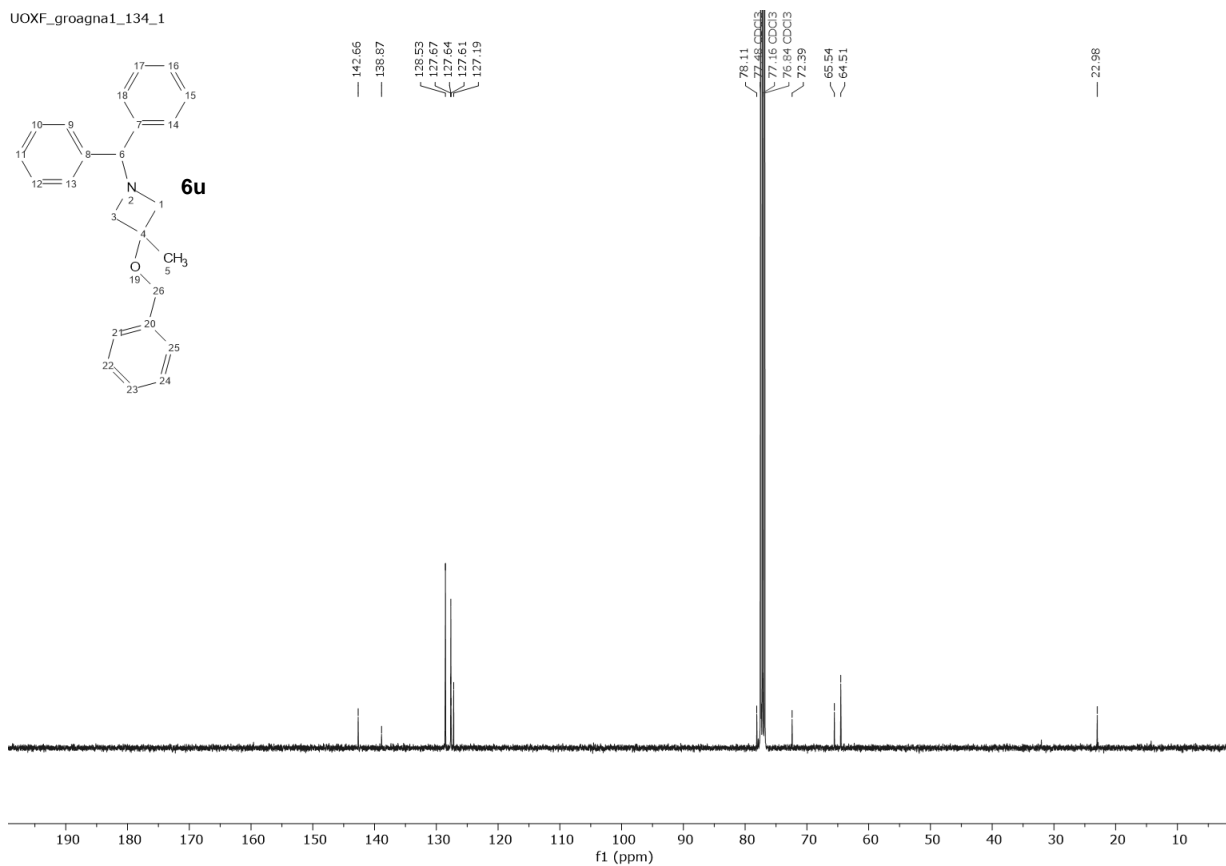
PUO-PC-273/CdCl3



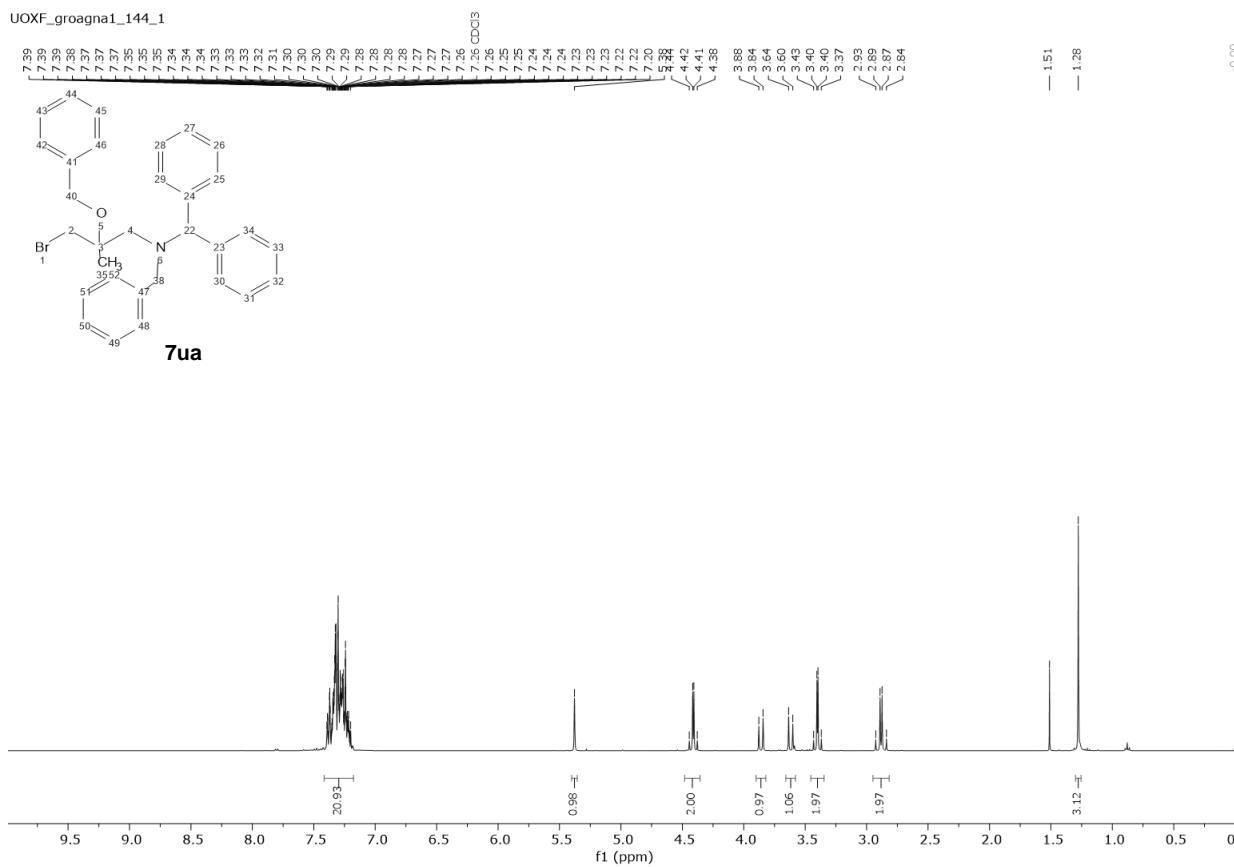
UOXF_groagna1_134_1



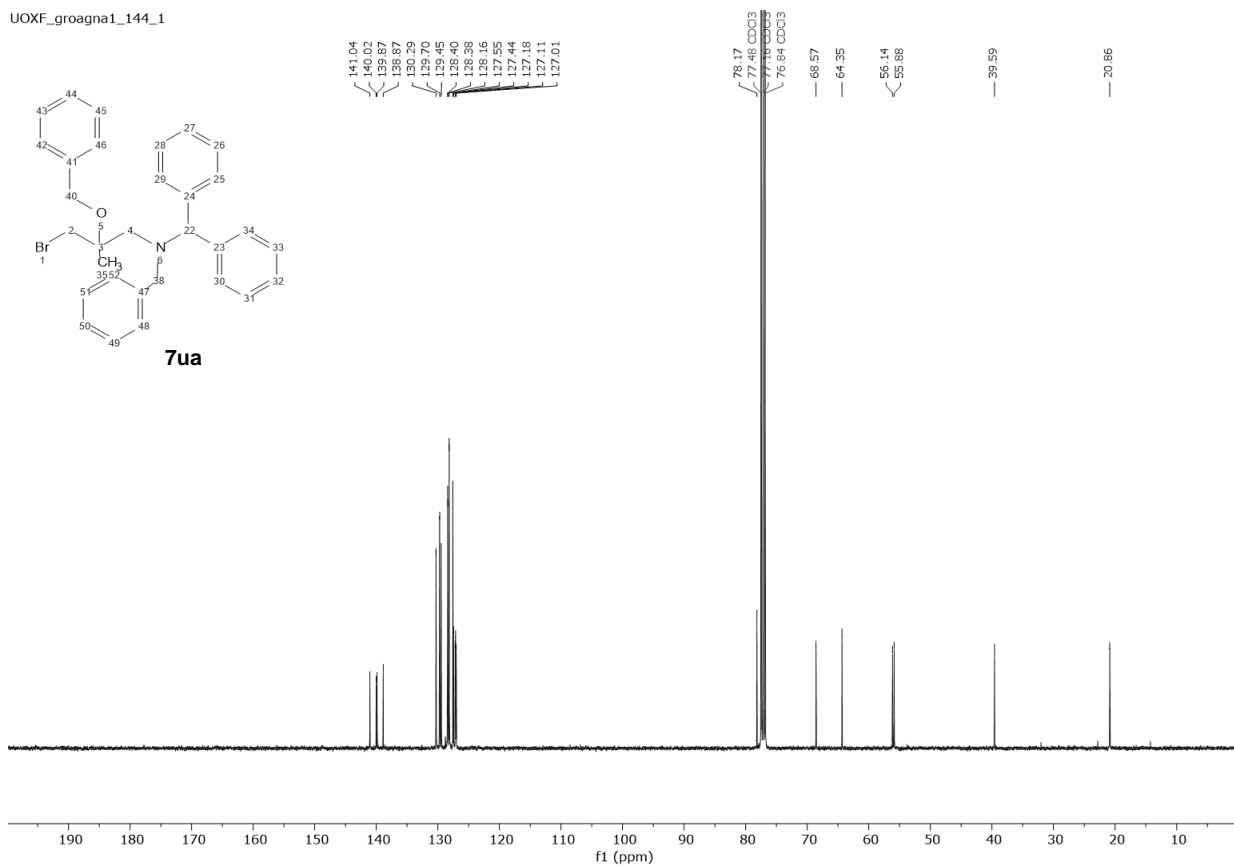
UOXF_groagna1_134_1



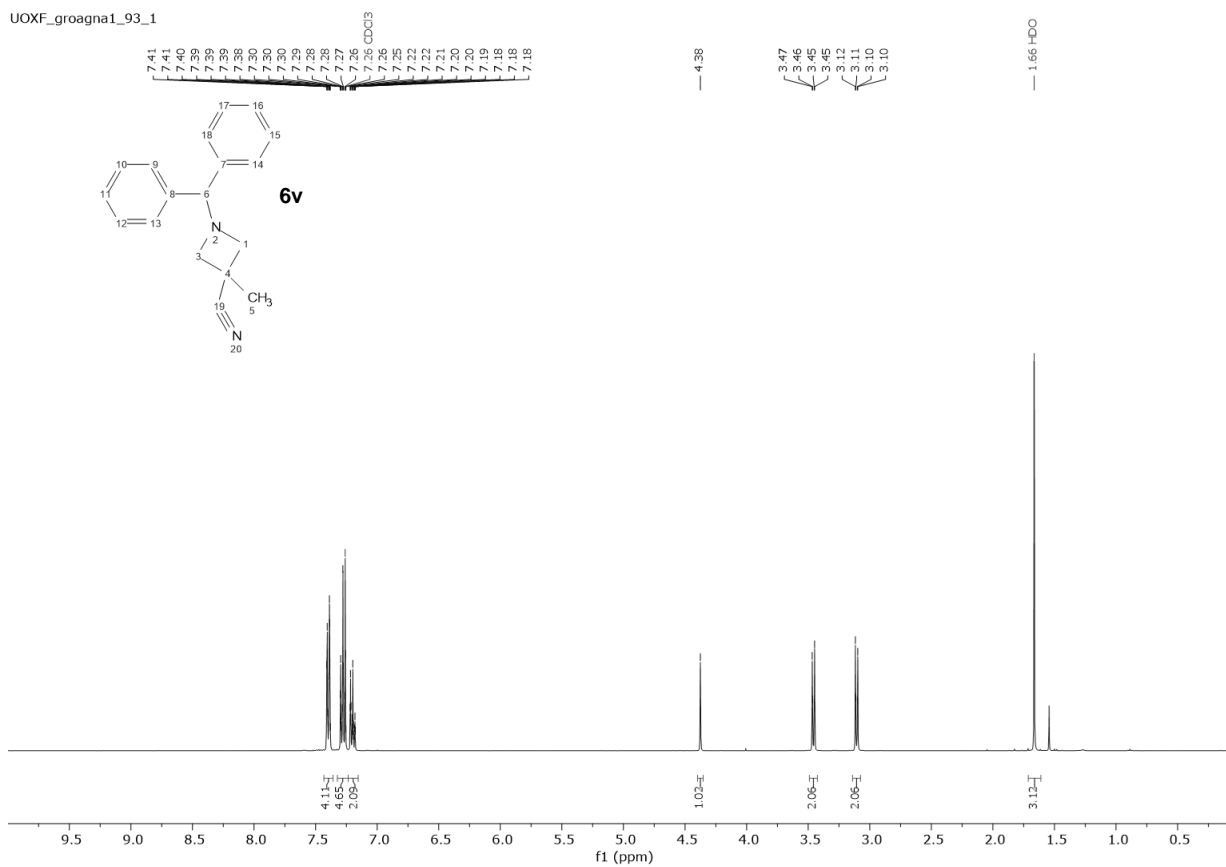
UOXF_groagna1_144_1



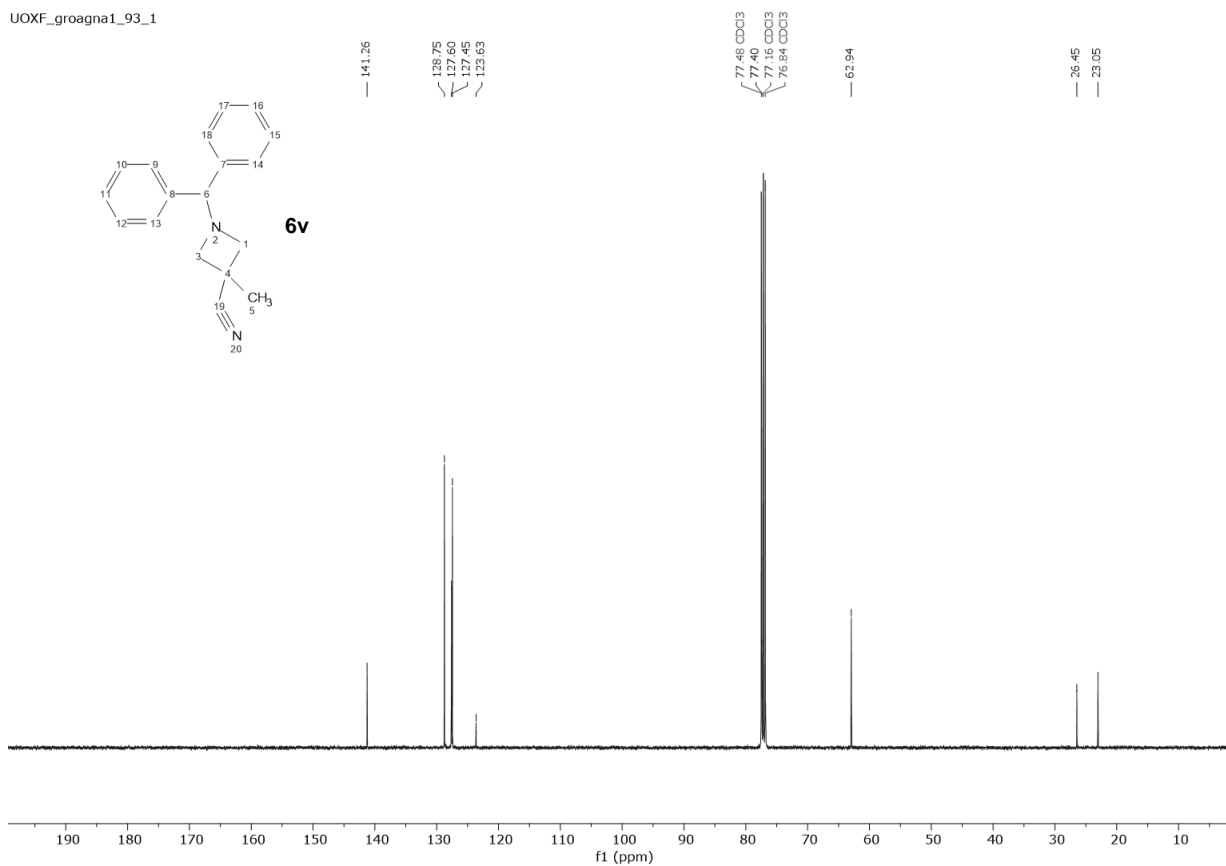
UOXF_groagna1_144_1



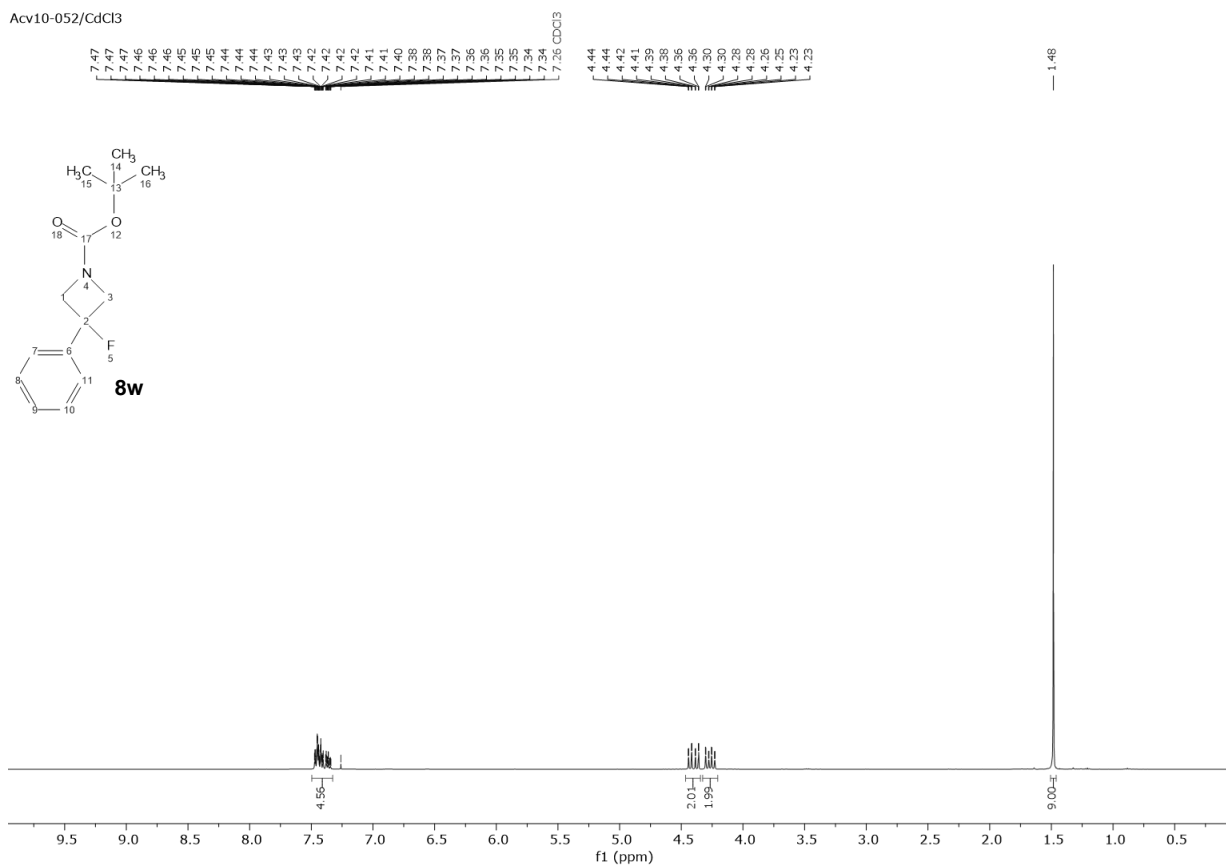
UOXF_groagna1_93_1



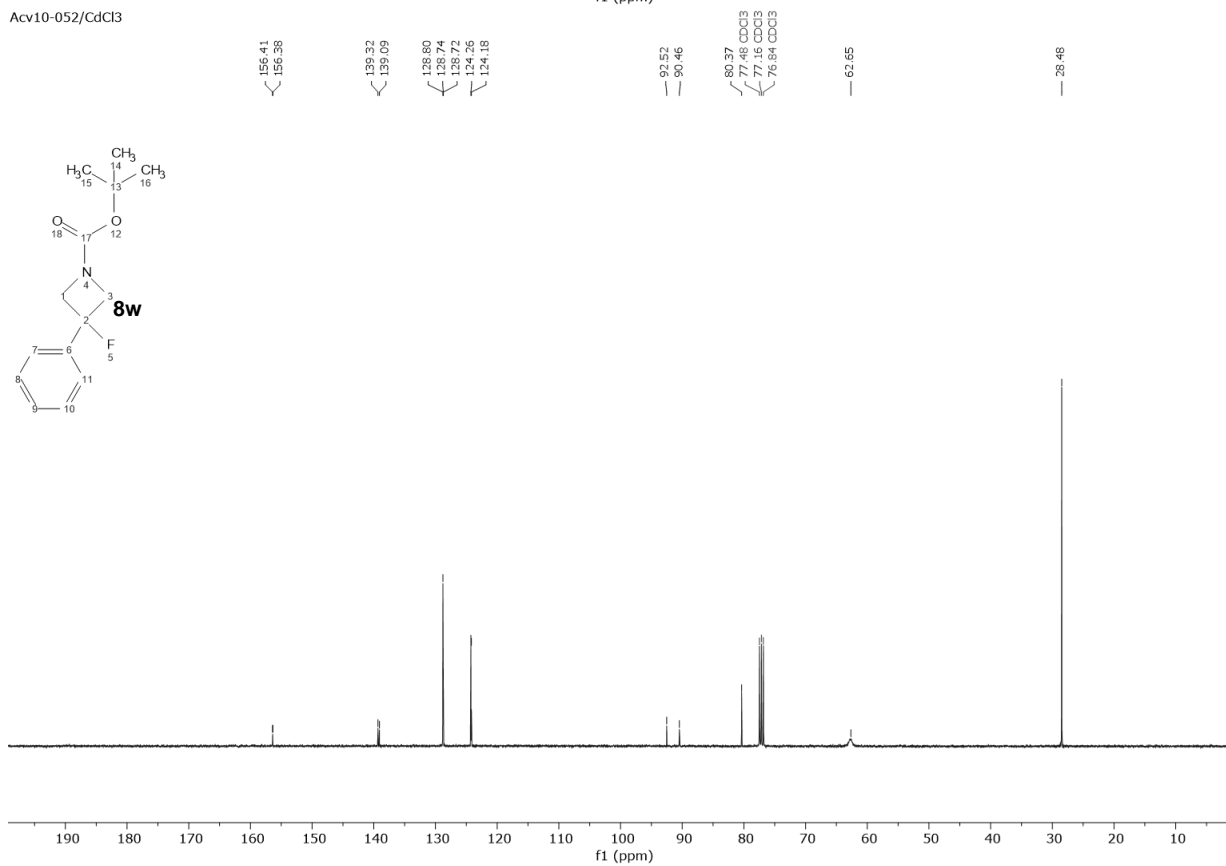
UOXF_groagna1_93_1



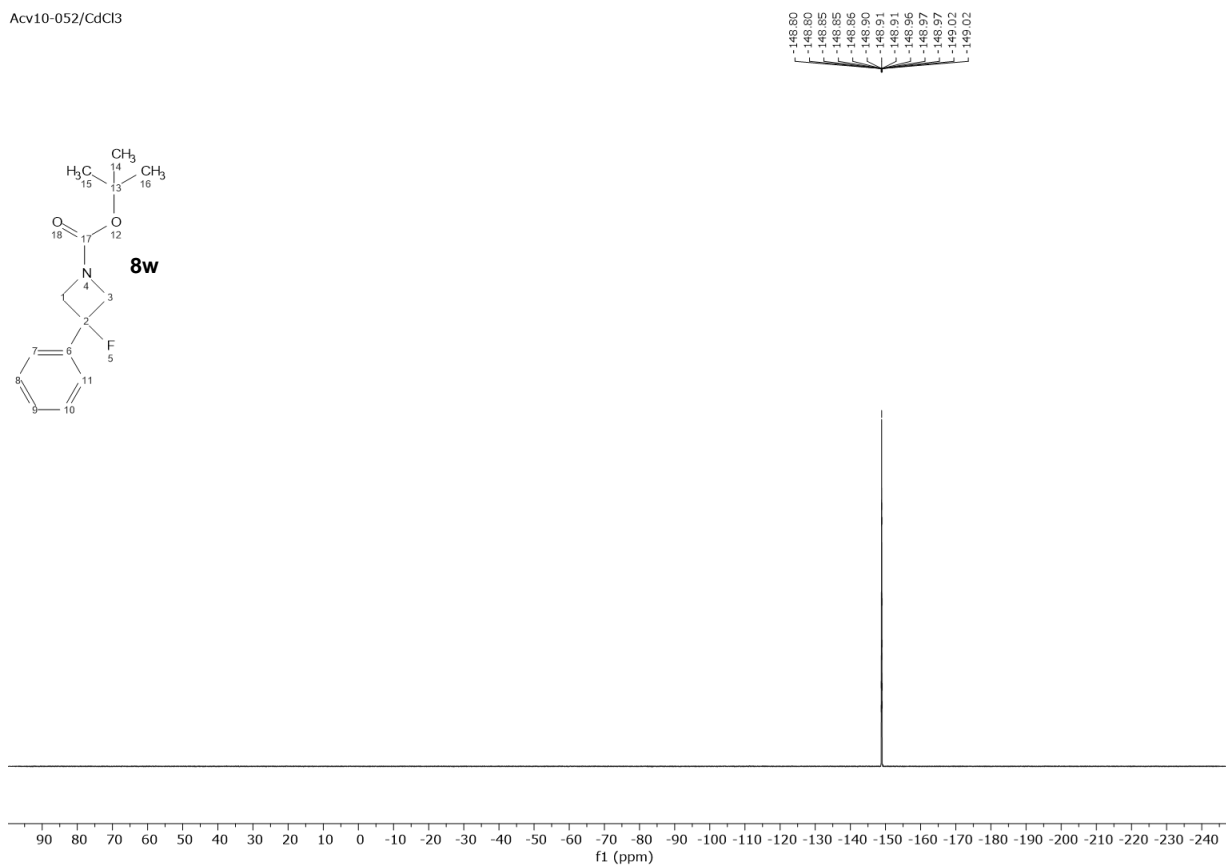
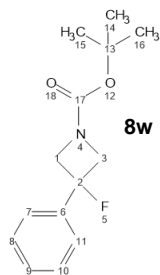
Acv10-052/CdCl3



Acv10-052/CdCl3

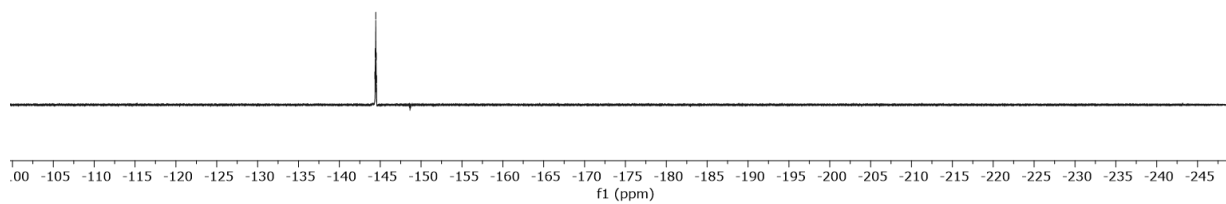
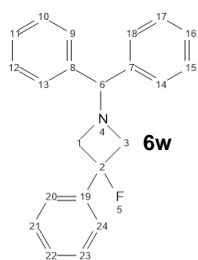


Acv10-052/CdCl3

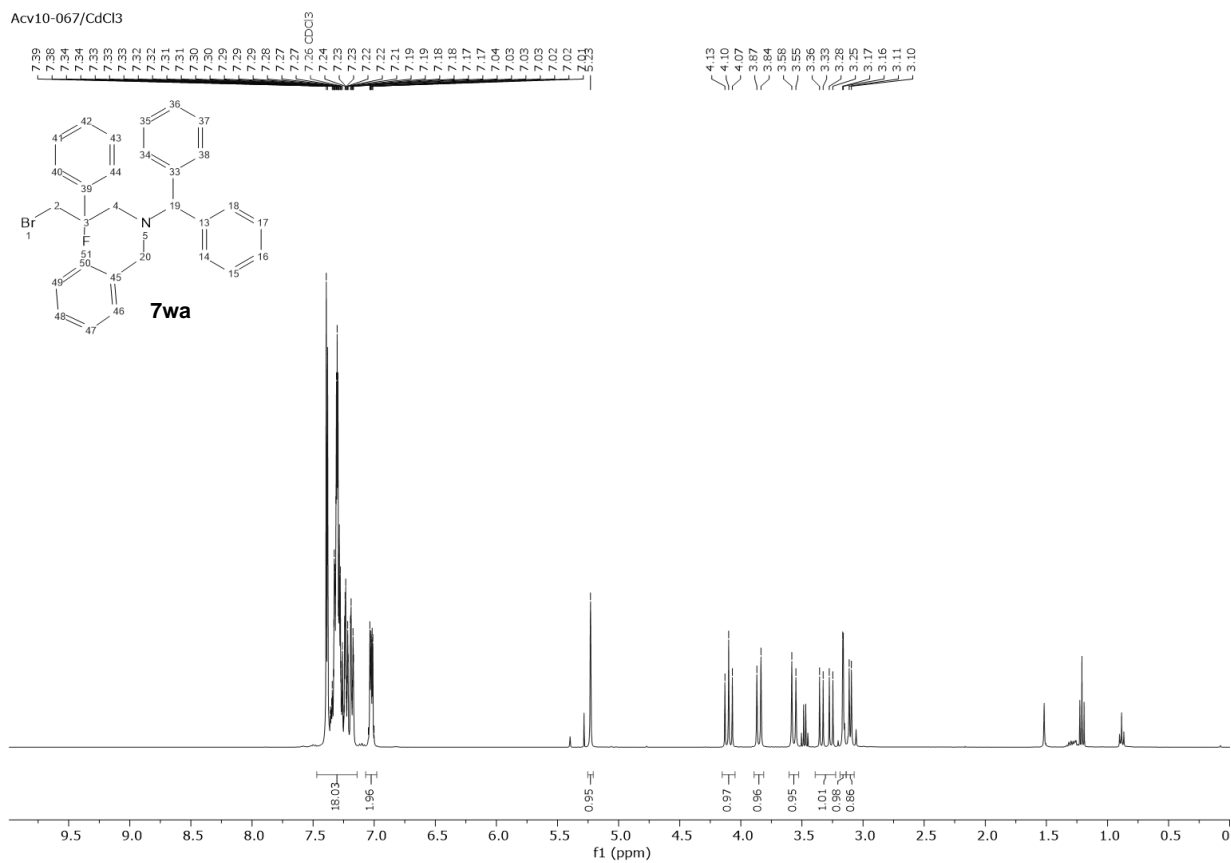


Acv-062/CdCl3

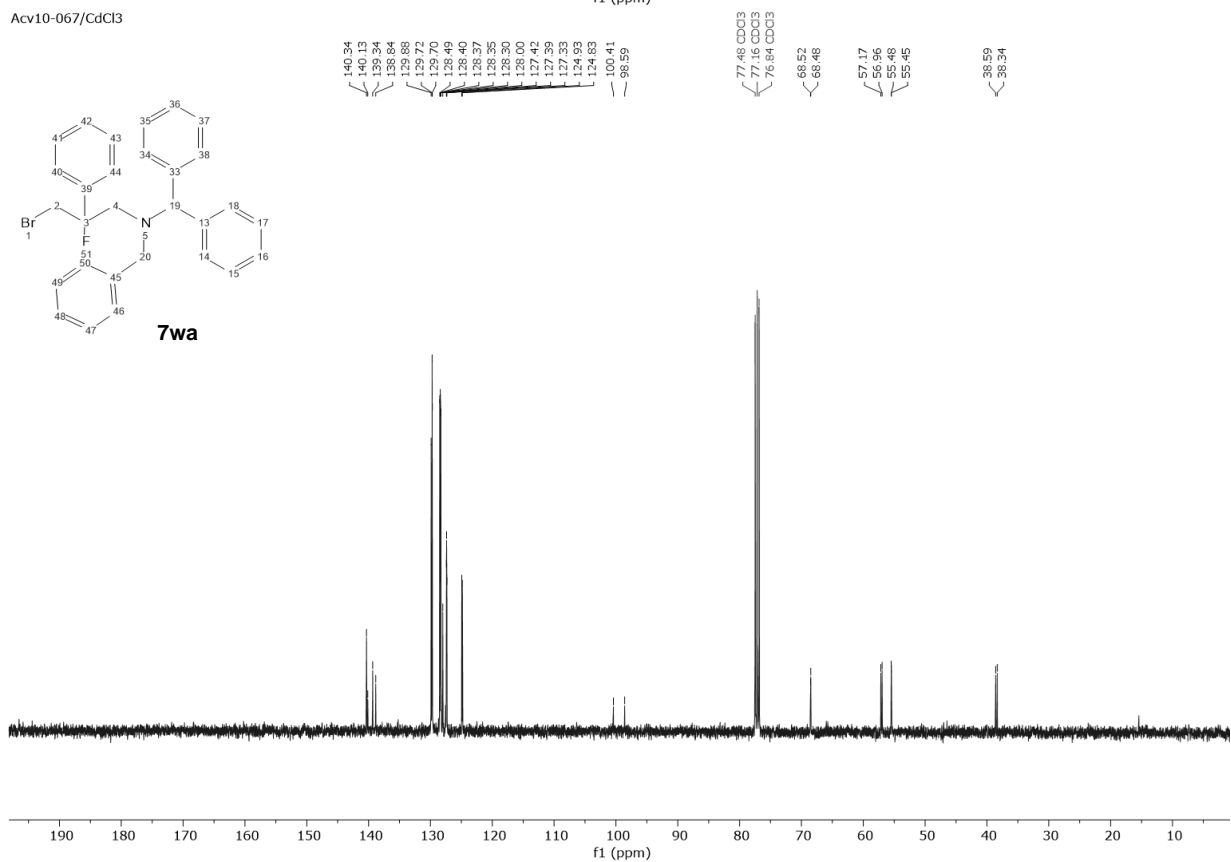
144.35
144.39
144.45
144.47
144.49
144.51
144.55



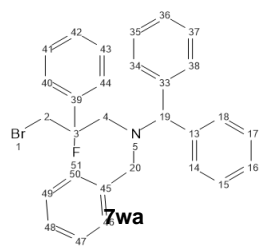
Acv10-067/CdCl3



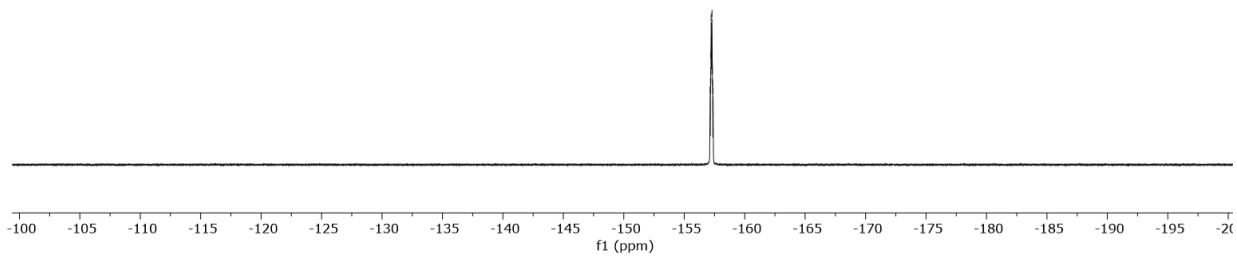
Acv10-067/CdCl3

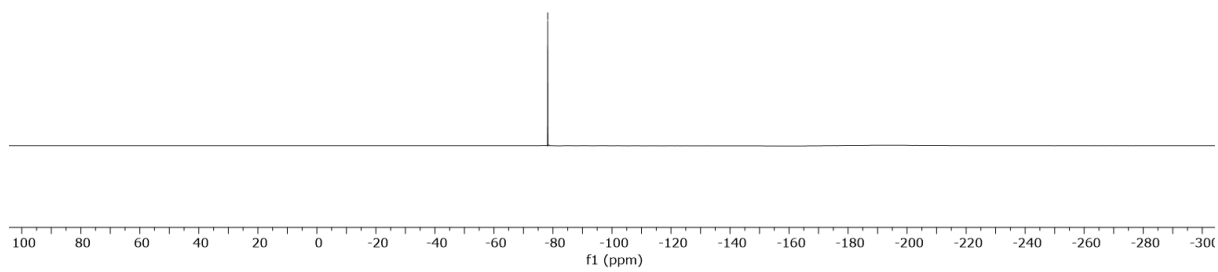
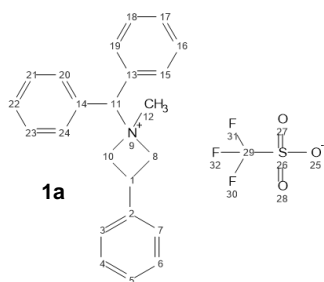


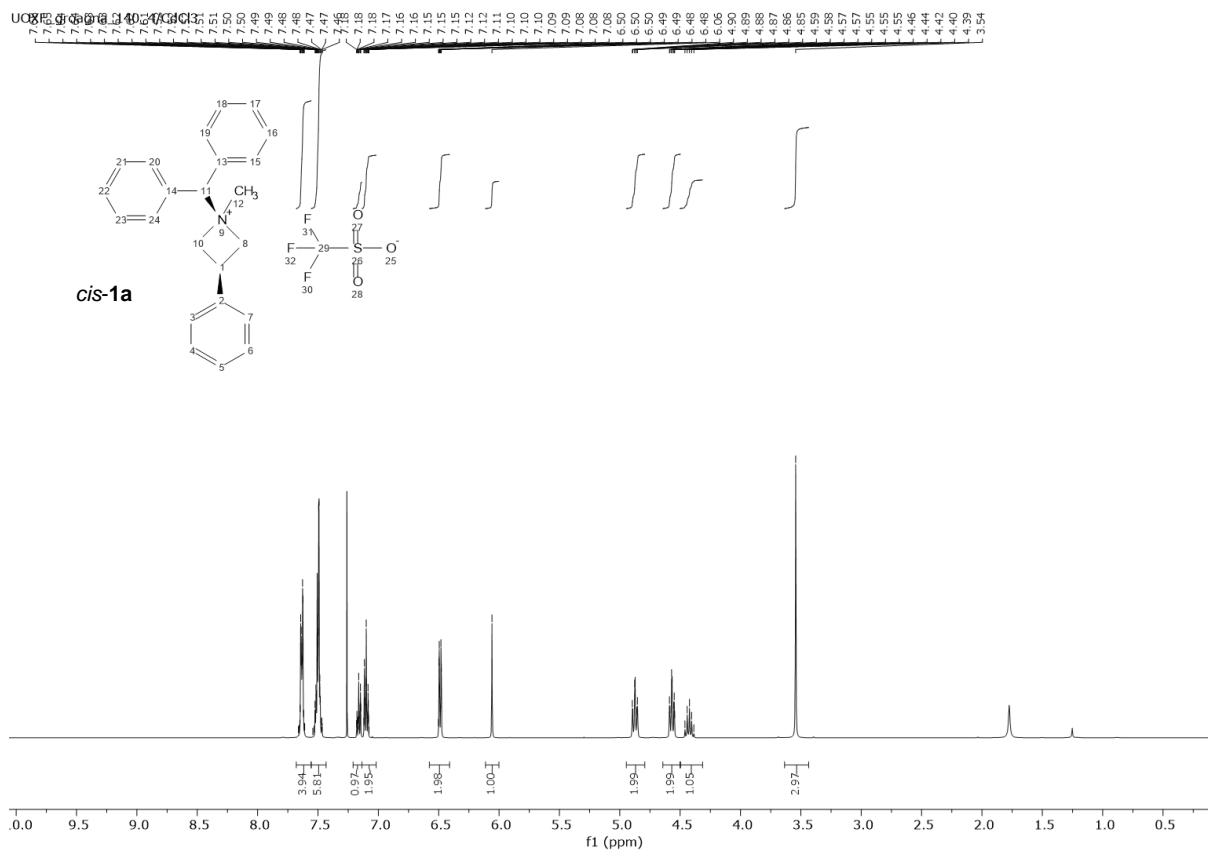
Acv10-067/CdCl3



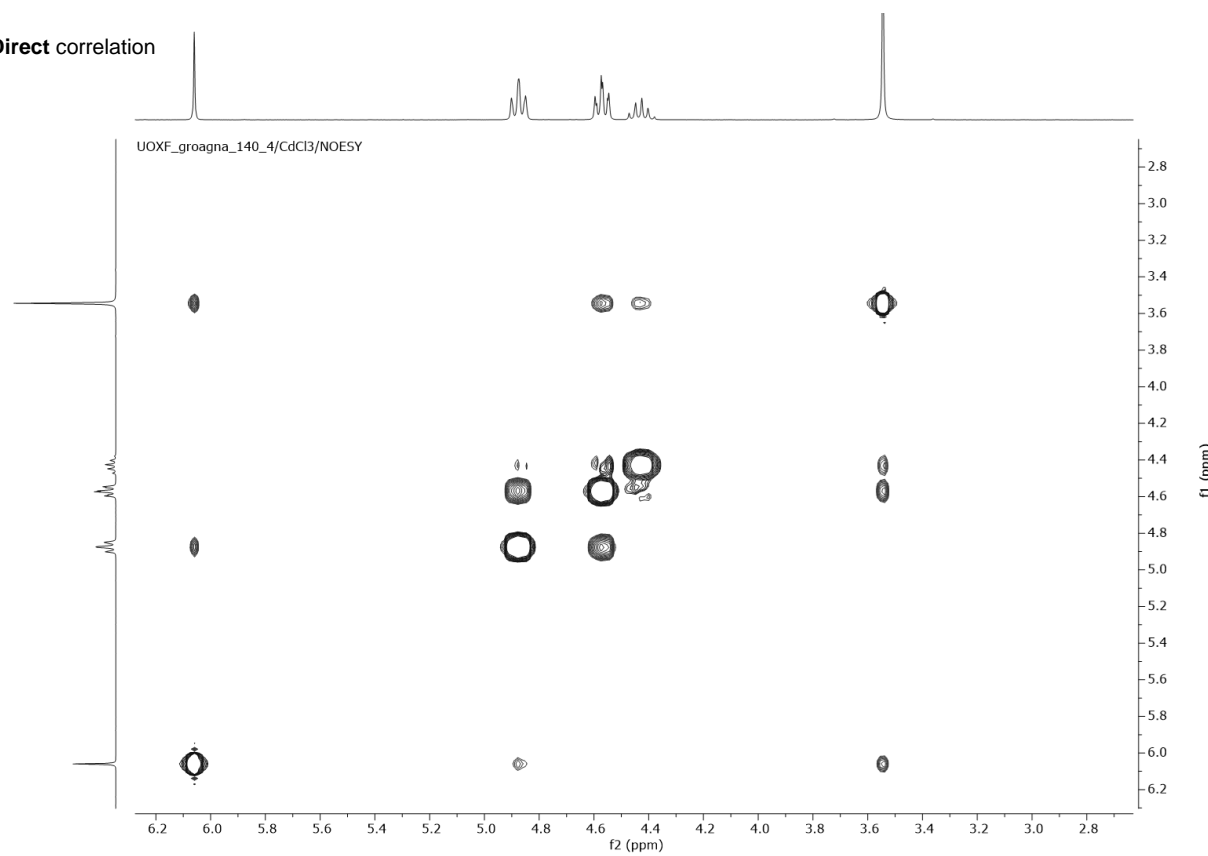
-157.14
-157.17
-157.19
-157.21
-157.22
-157.24
-157.26
-157.28
-157.29
-157.31
-157.32
-157.35
-157.38



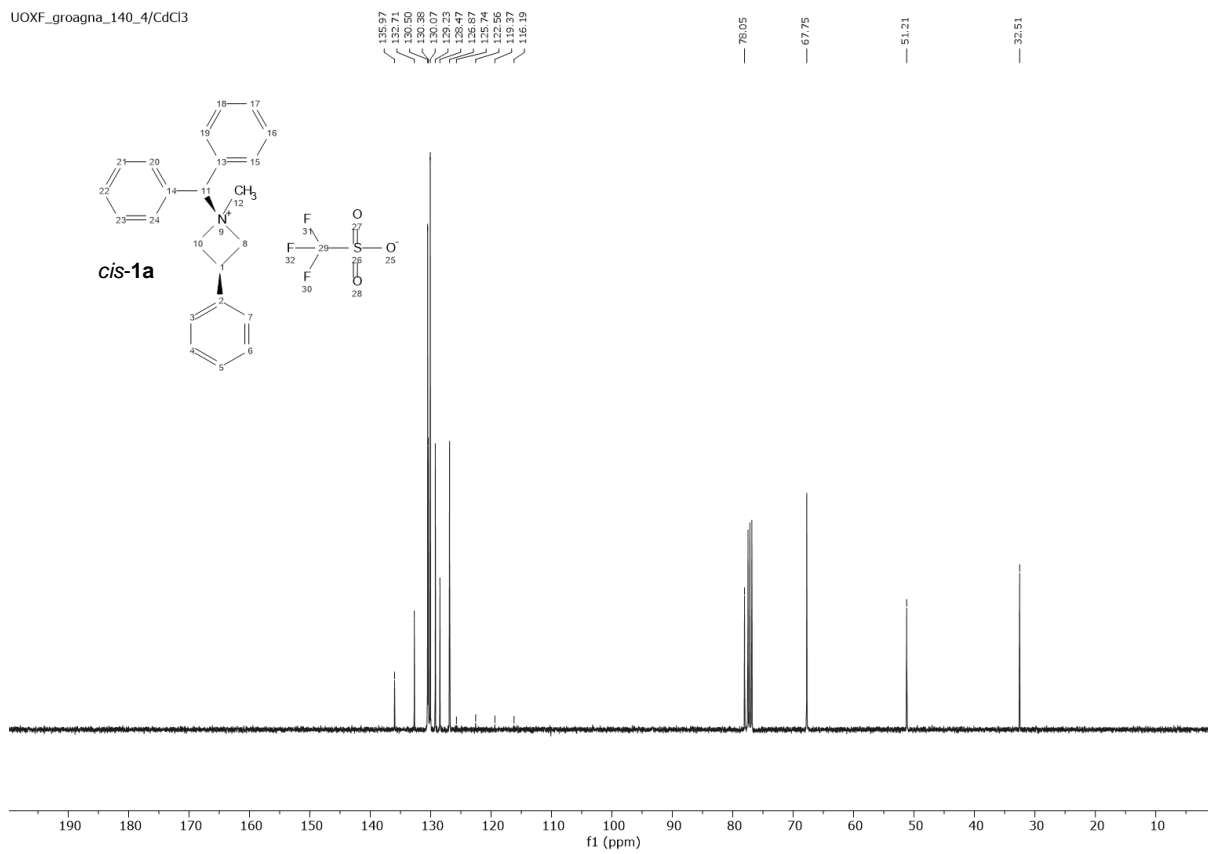




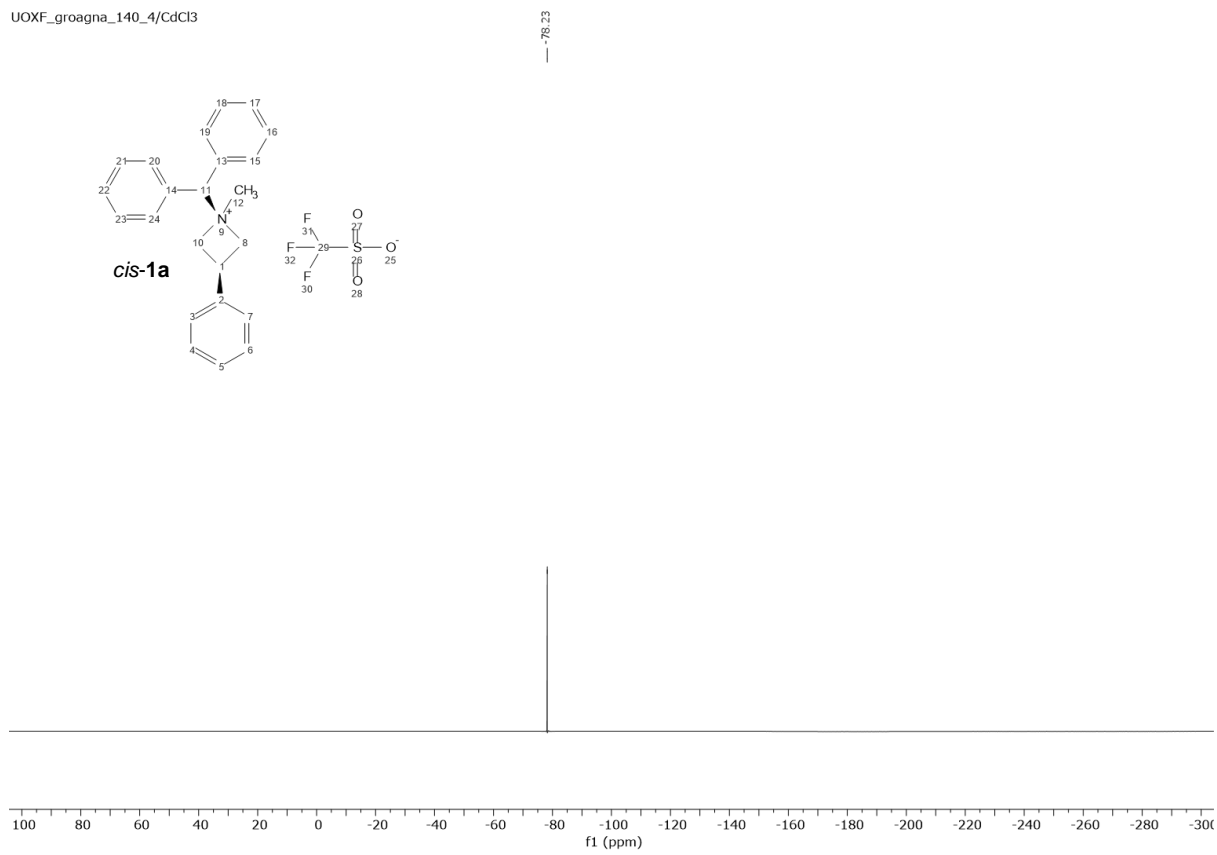
Direct correlation

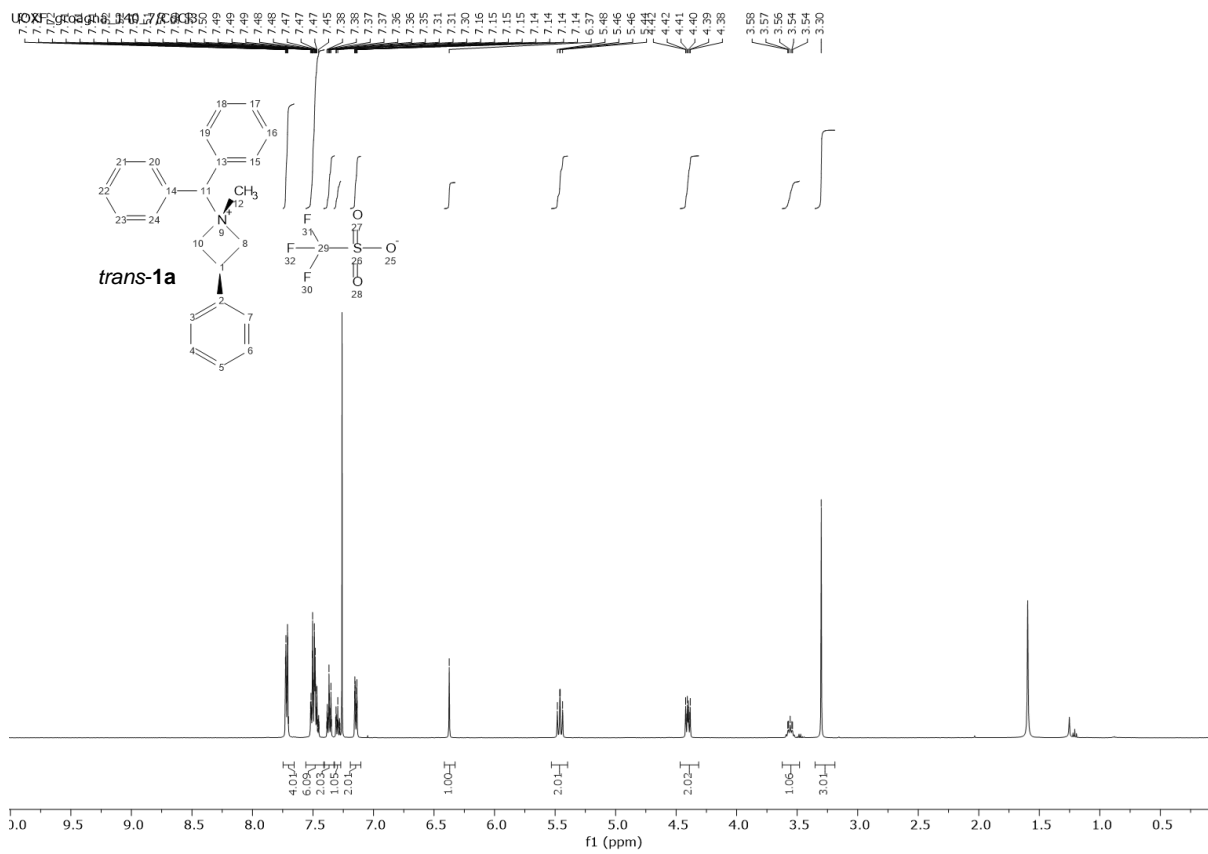


UOXF_groagna_140_4/CdCl3

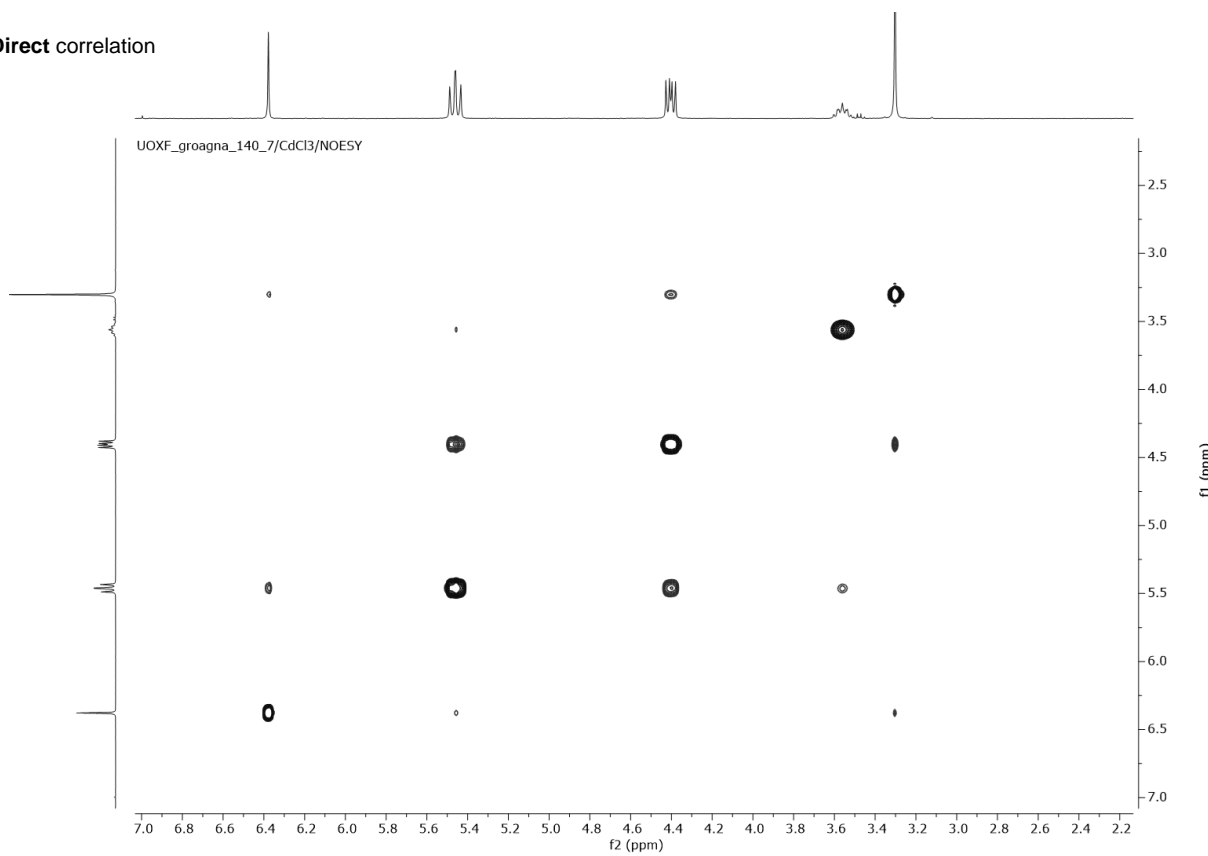


UOXF_groagna_140_4/CdCl3

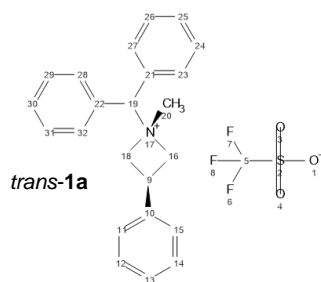




Direct correlation



UOXF_groagna_140_7



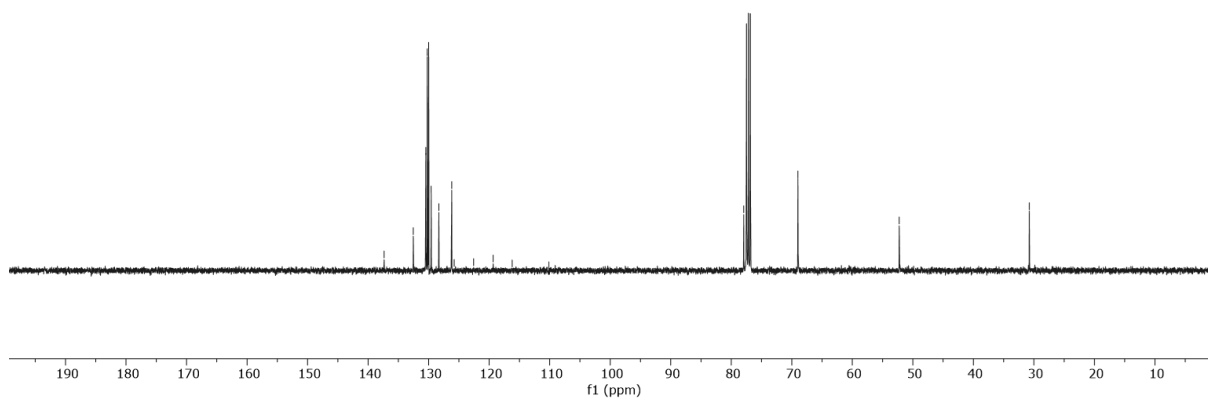
137.95
132.53
130.47
130.00
129.98
128.31
126.18
125.77
119.94
116.20

77.94

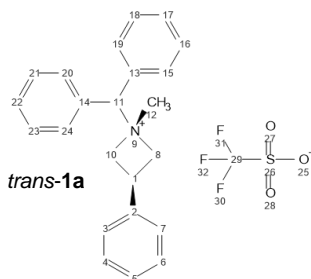
66.98

52.25

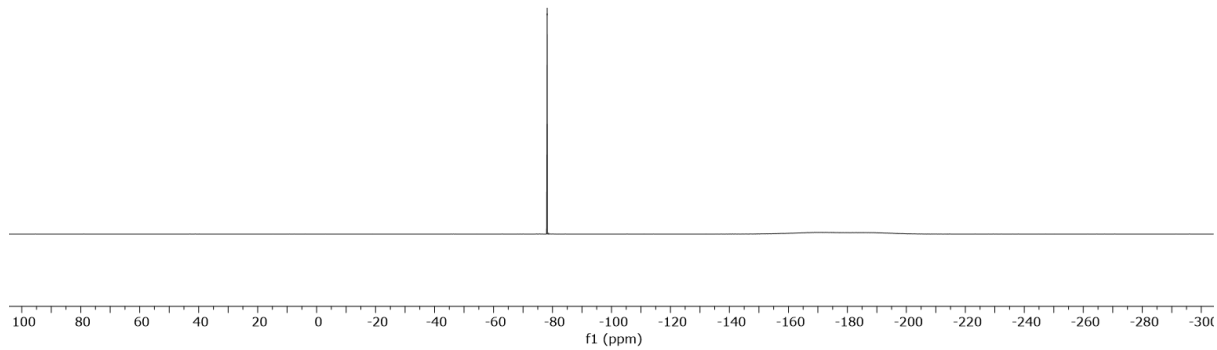
30.77



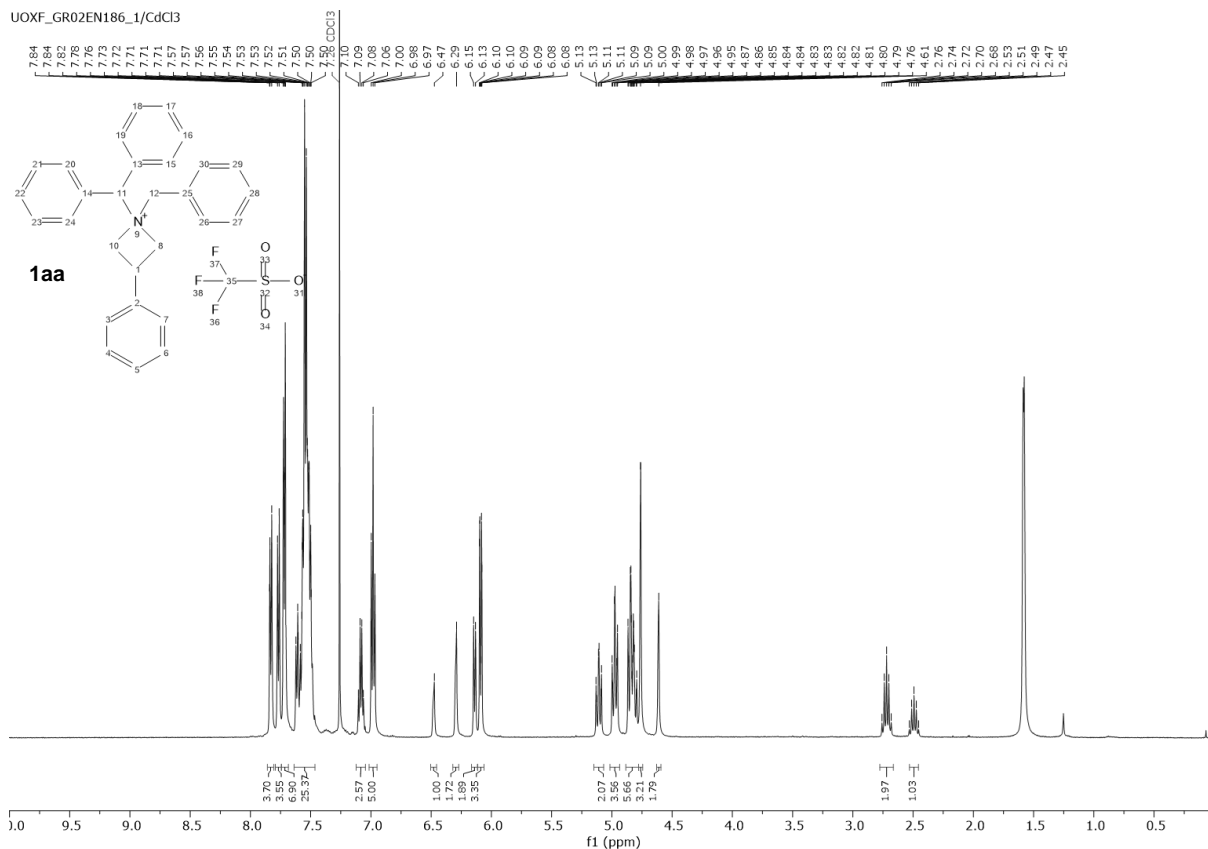
UOXF_groagna_140_7/CdCl3



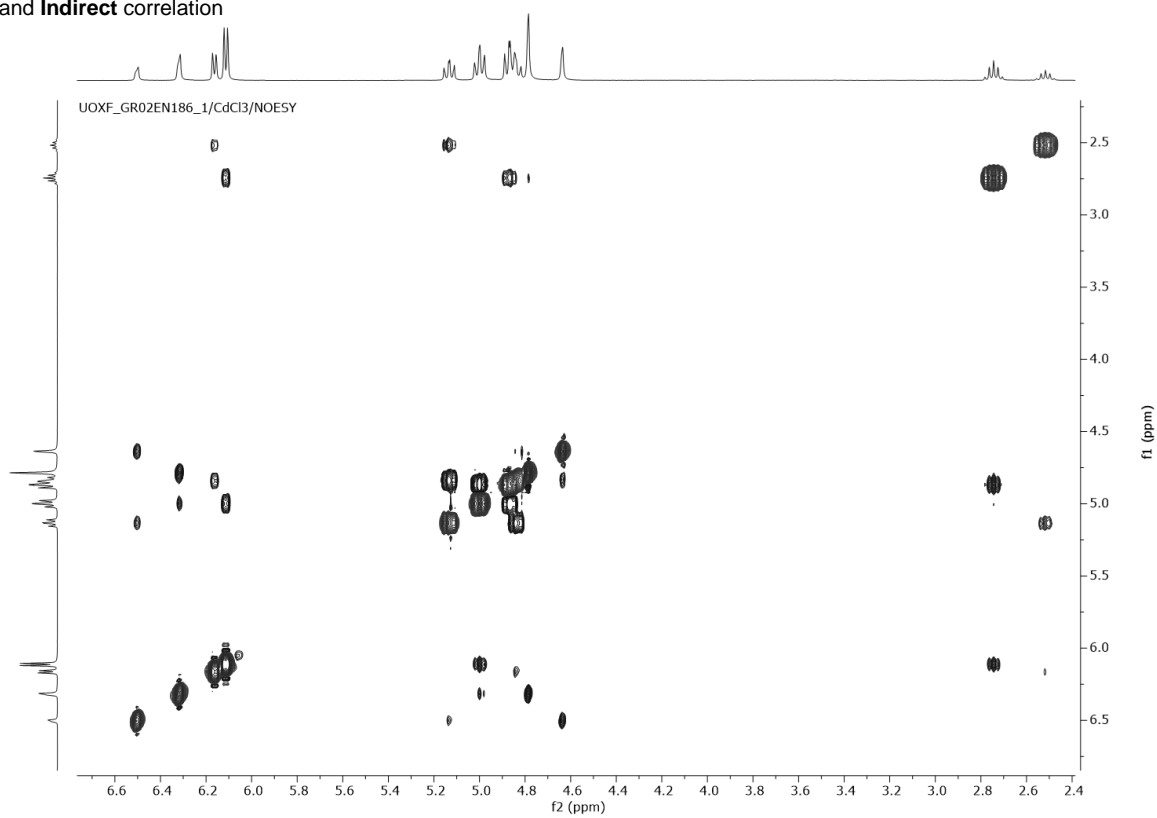
-78.20



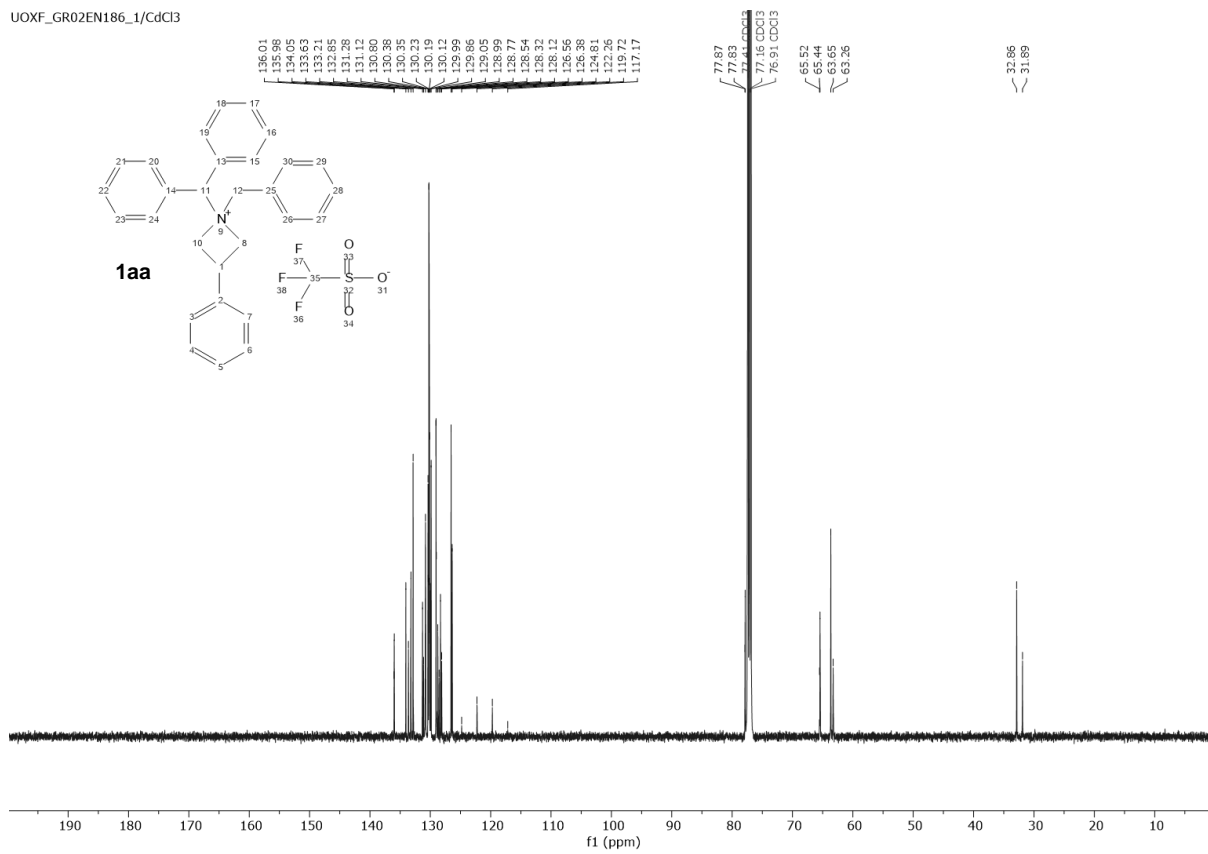
UOXF_GR02EN186_1/CdCl3



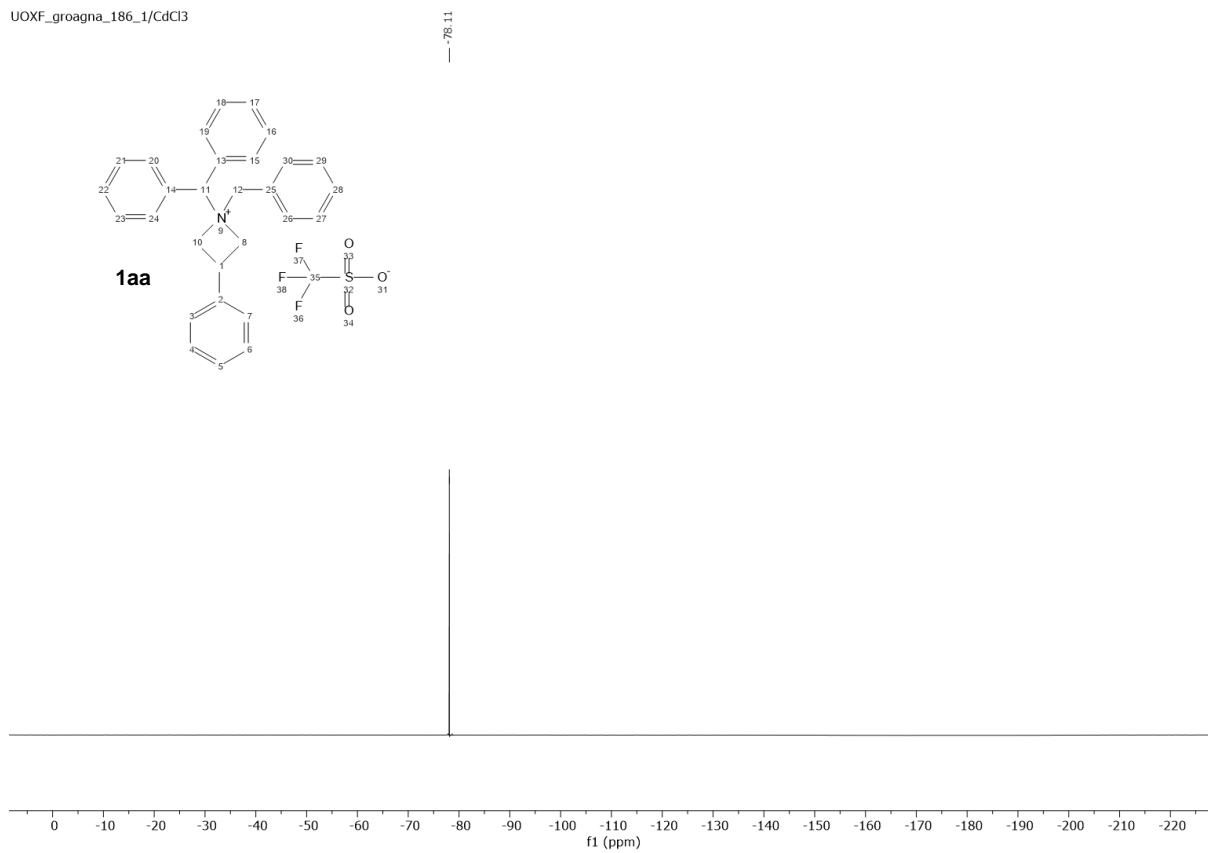
Direct and Indirect correlation

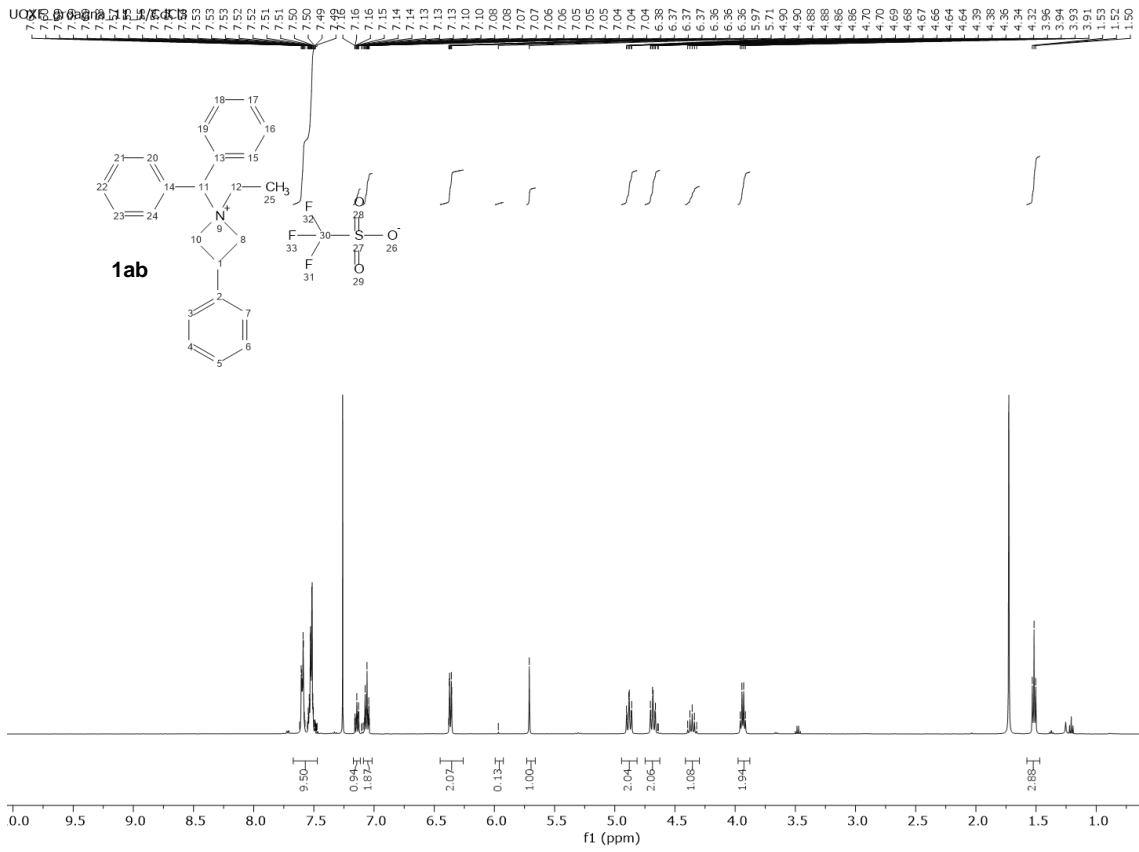


UOXF_GR02EN186_1/CdCl3

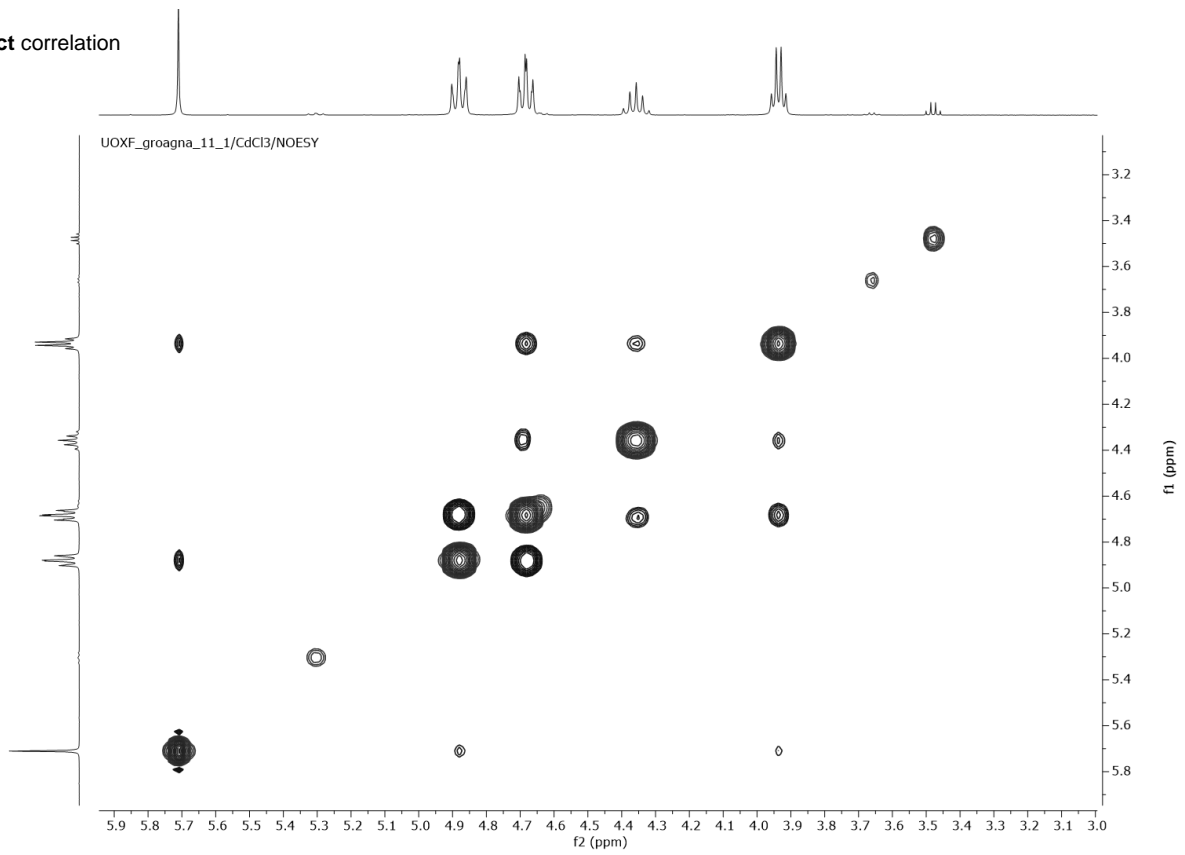


UOXF_groagna_186_1/CdCl3

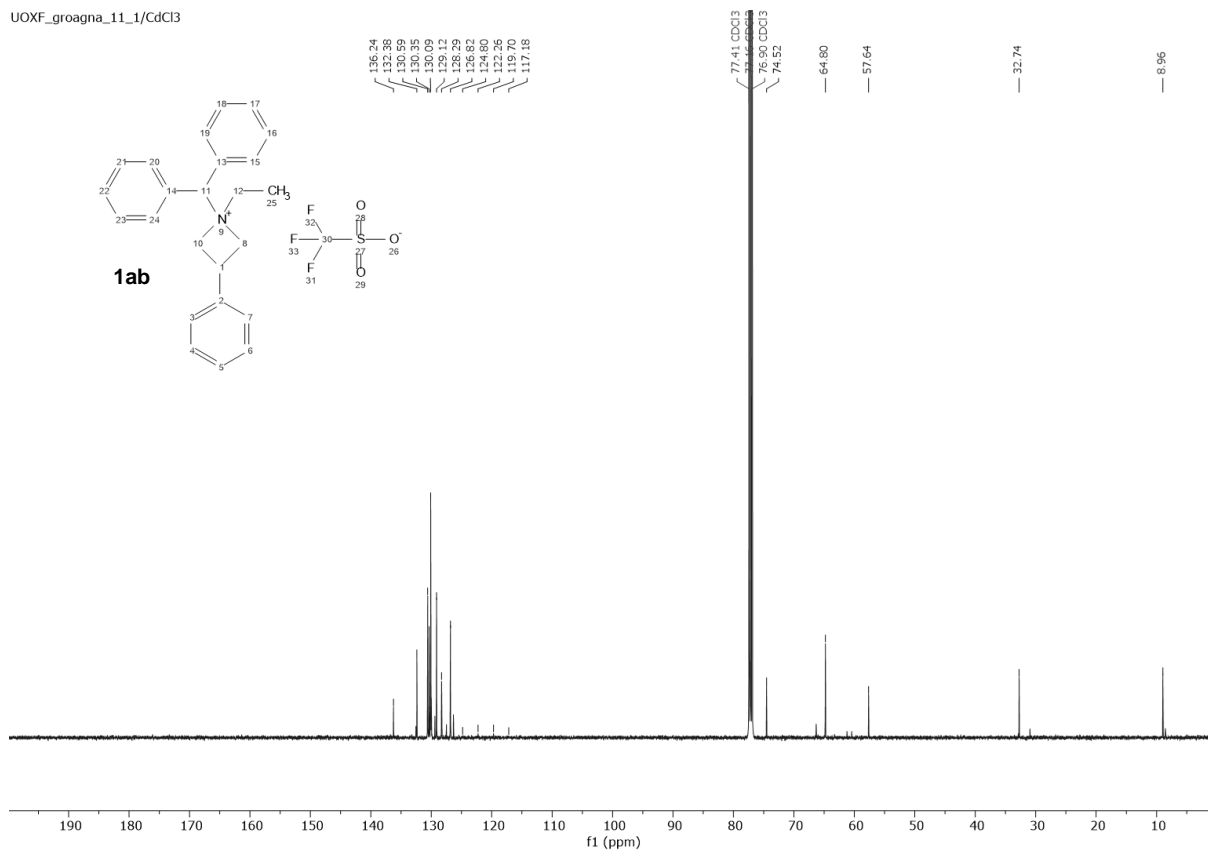




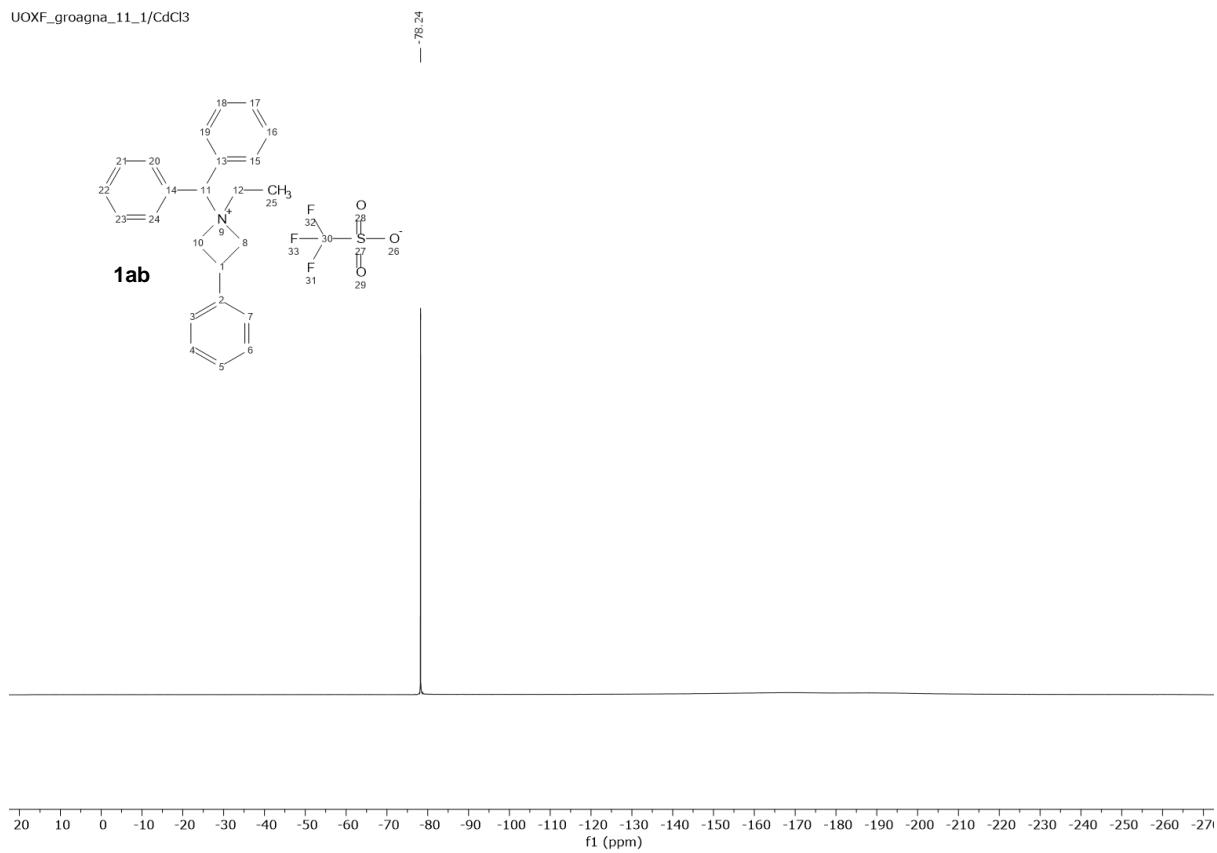
Direct correlation



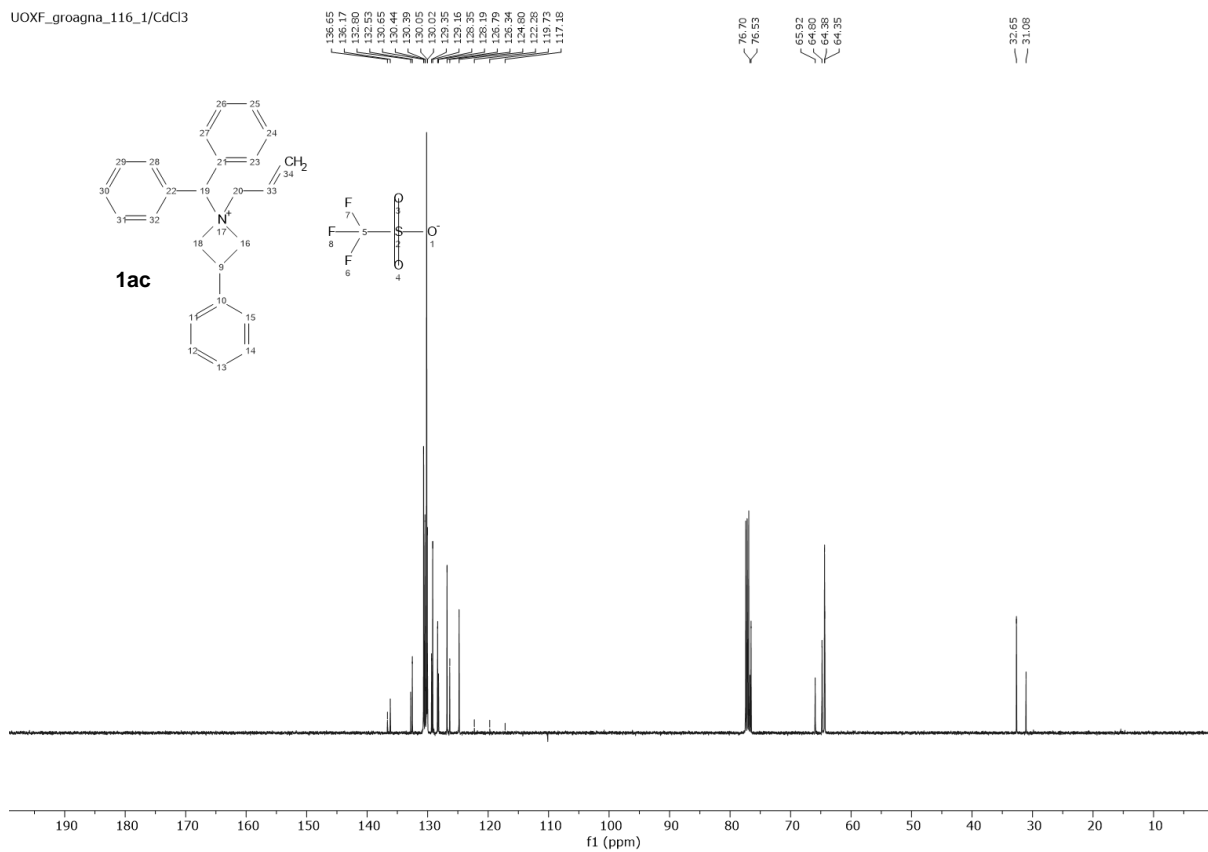
UOXF_groagna_11_1/CdCl3



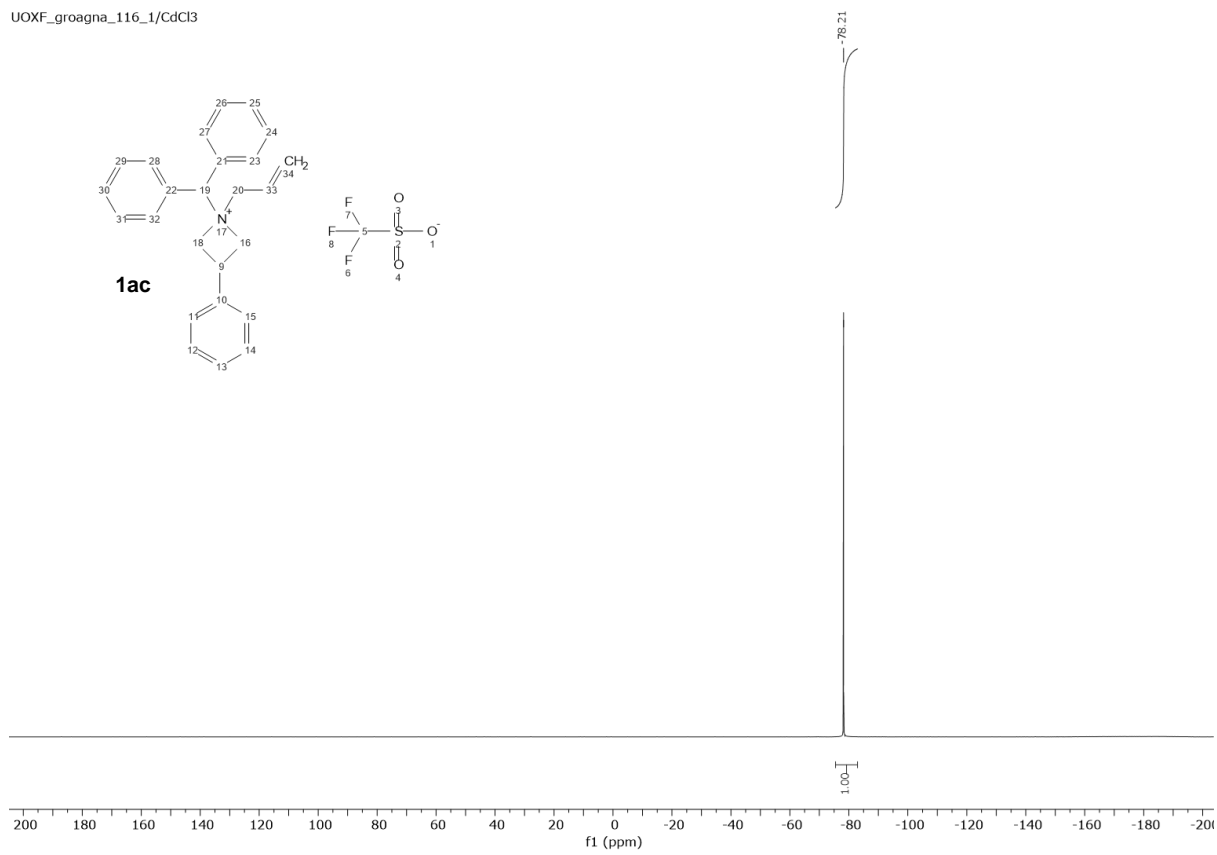
UOXF_groagna_11_1/CdCl3

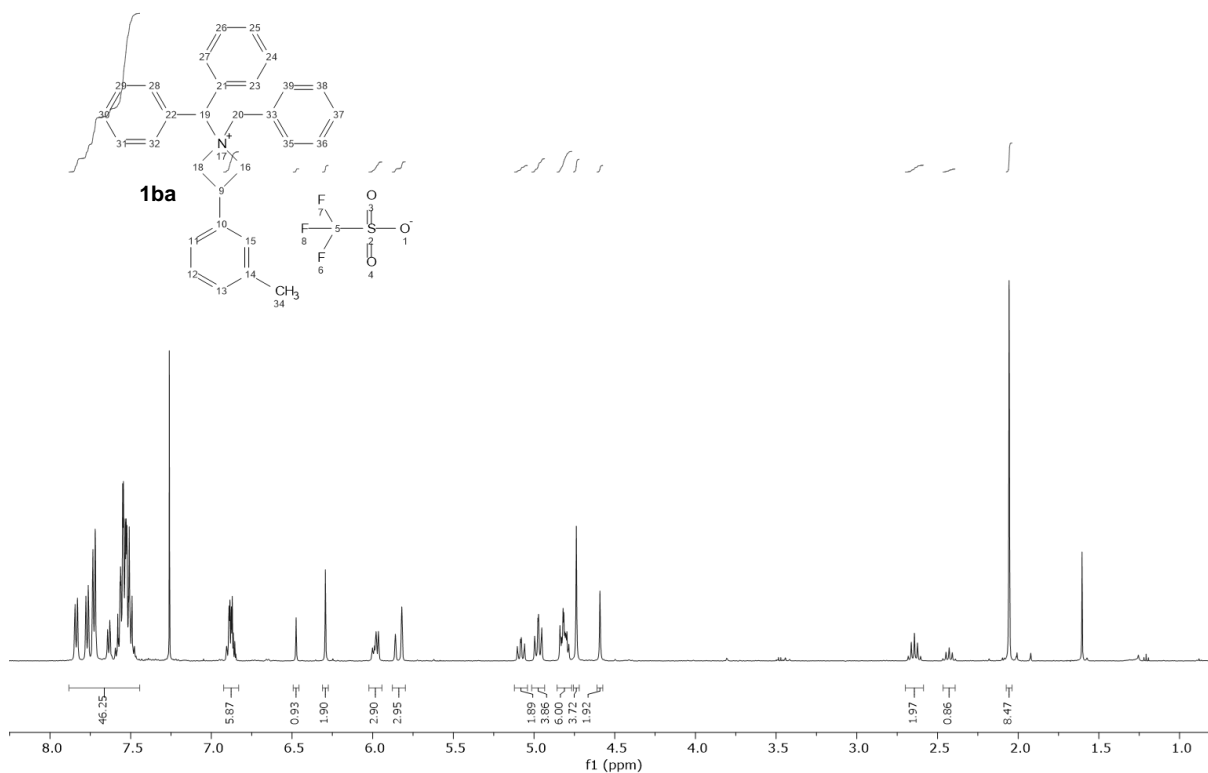


UOXF_groagna_116_1/CdCl3

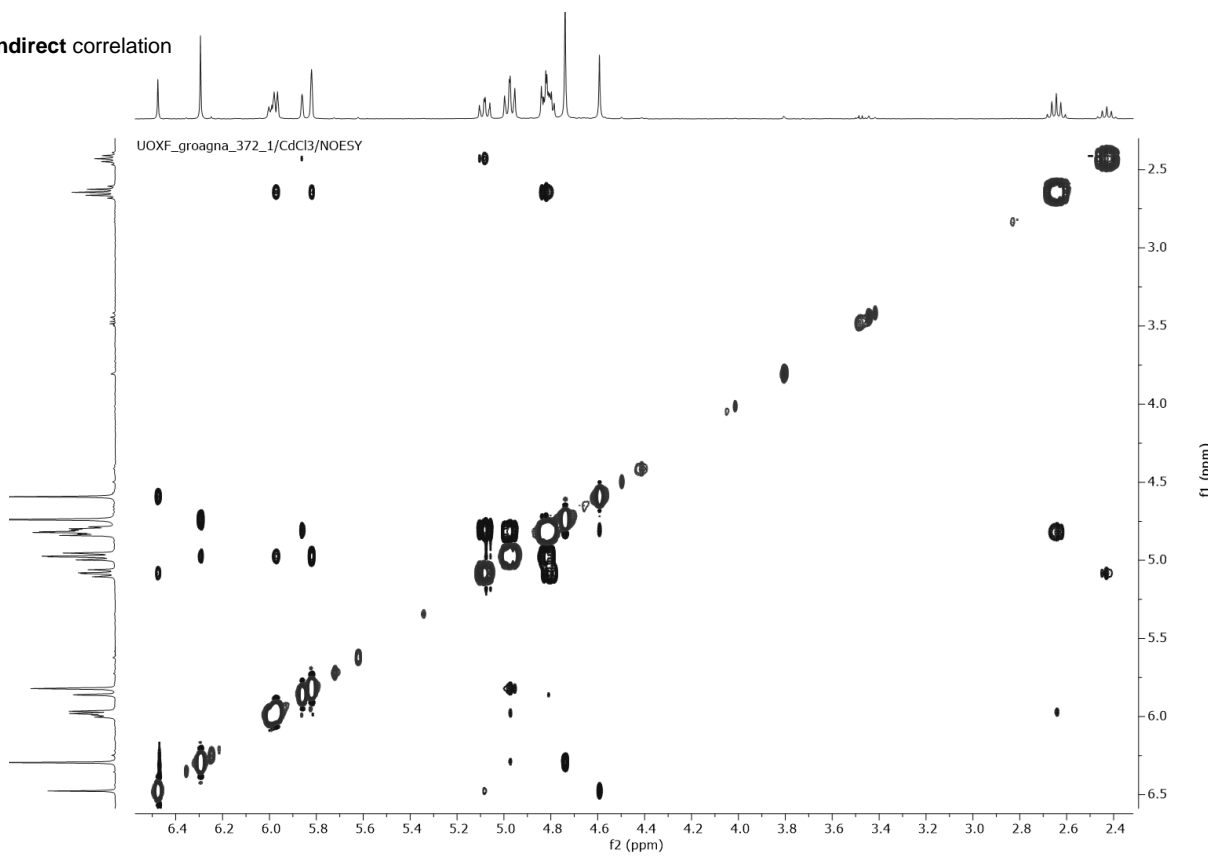


UOXF_groagna_116_1/CdCl3

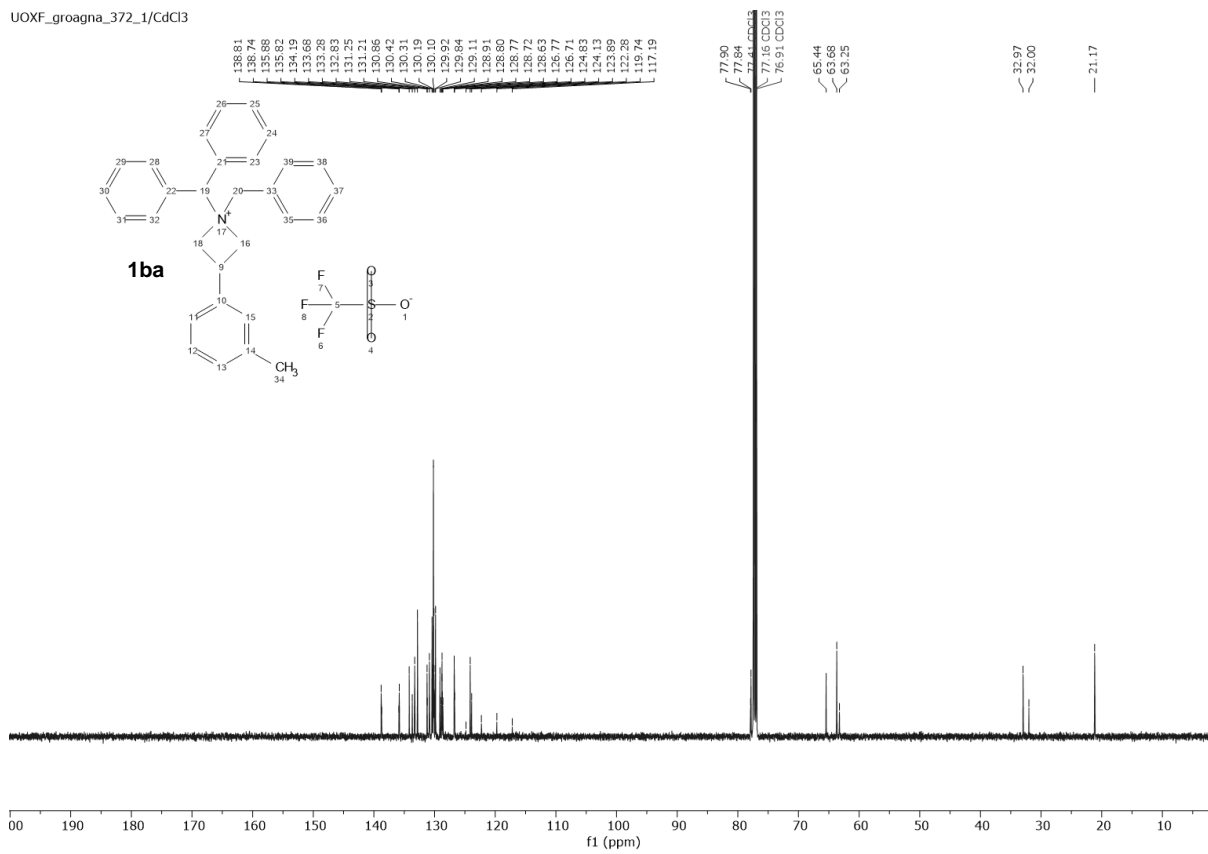




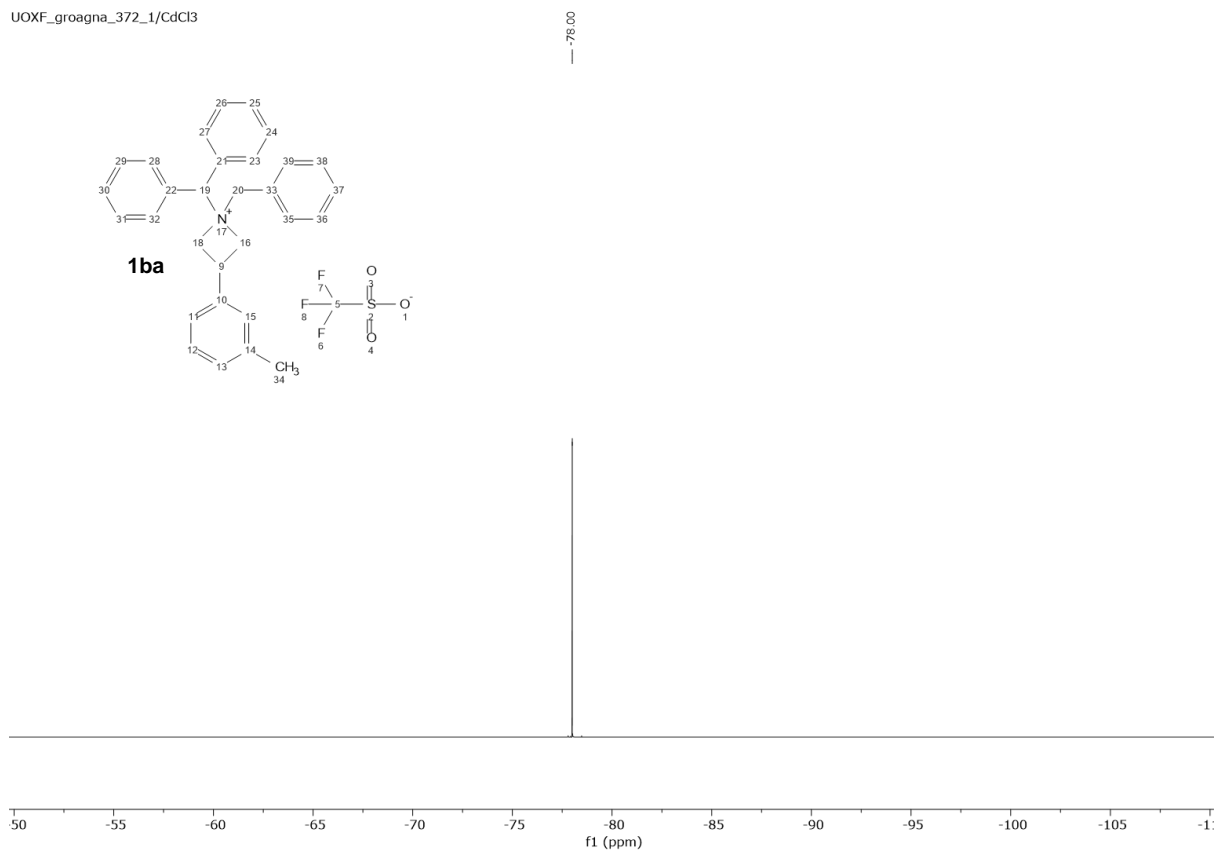
Indirect correlation



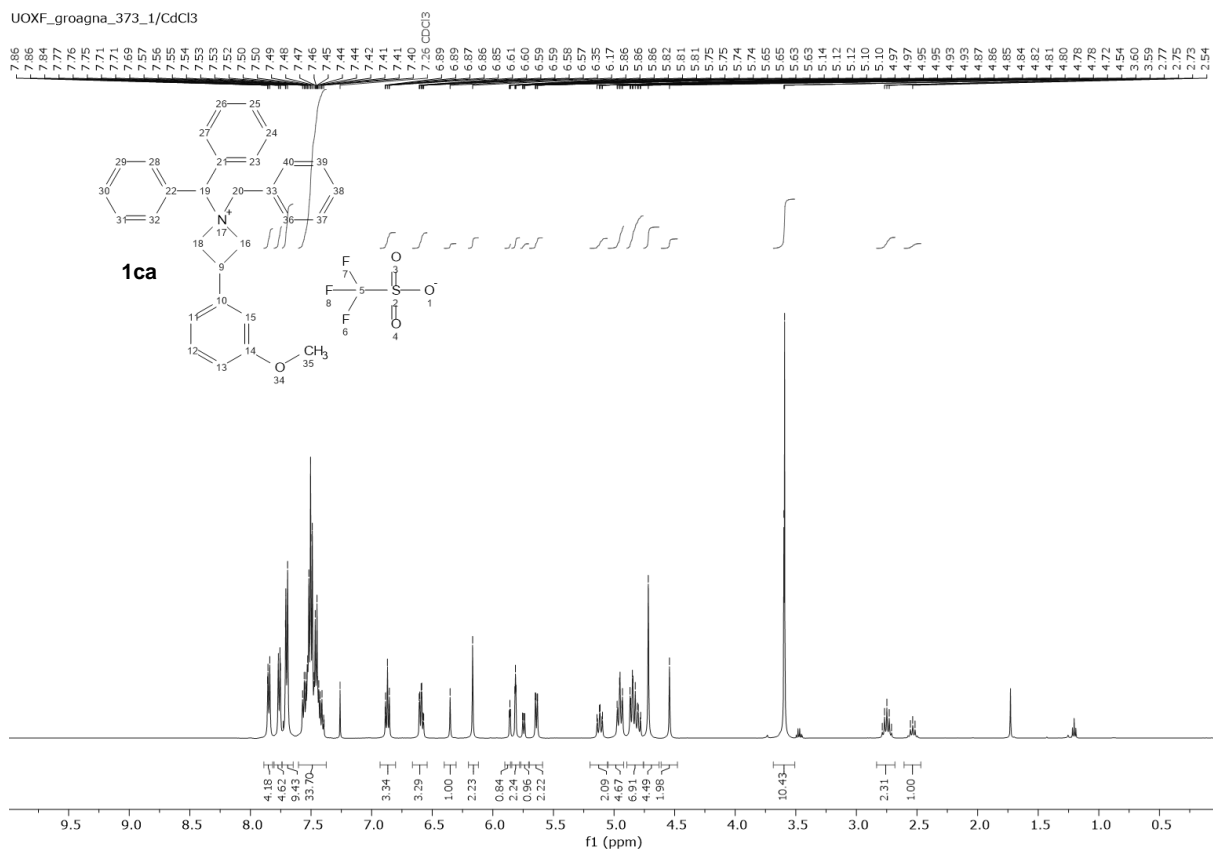
UOXF_groagna_372_1/CdCl3



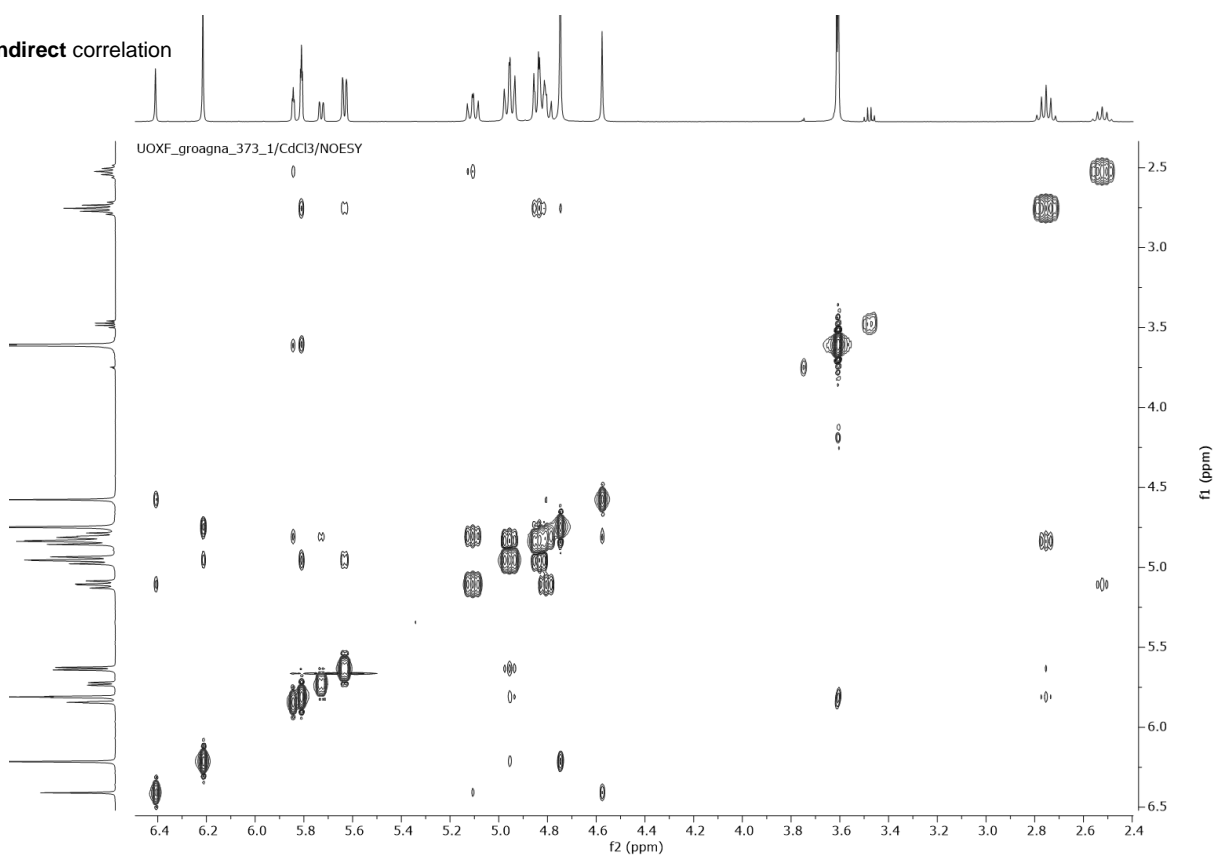
UOXF_groagna_372_1/CdCl3



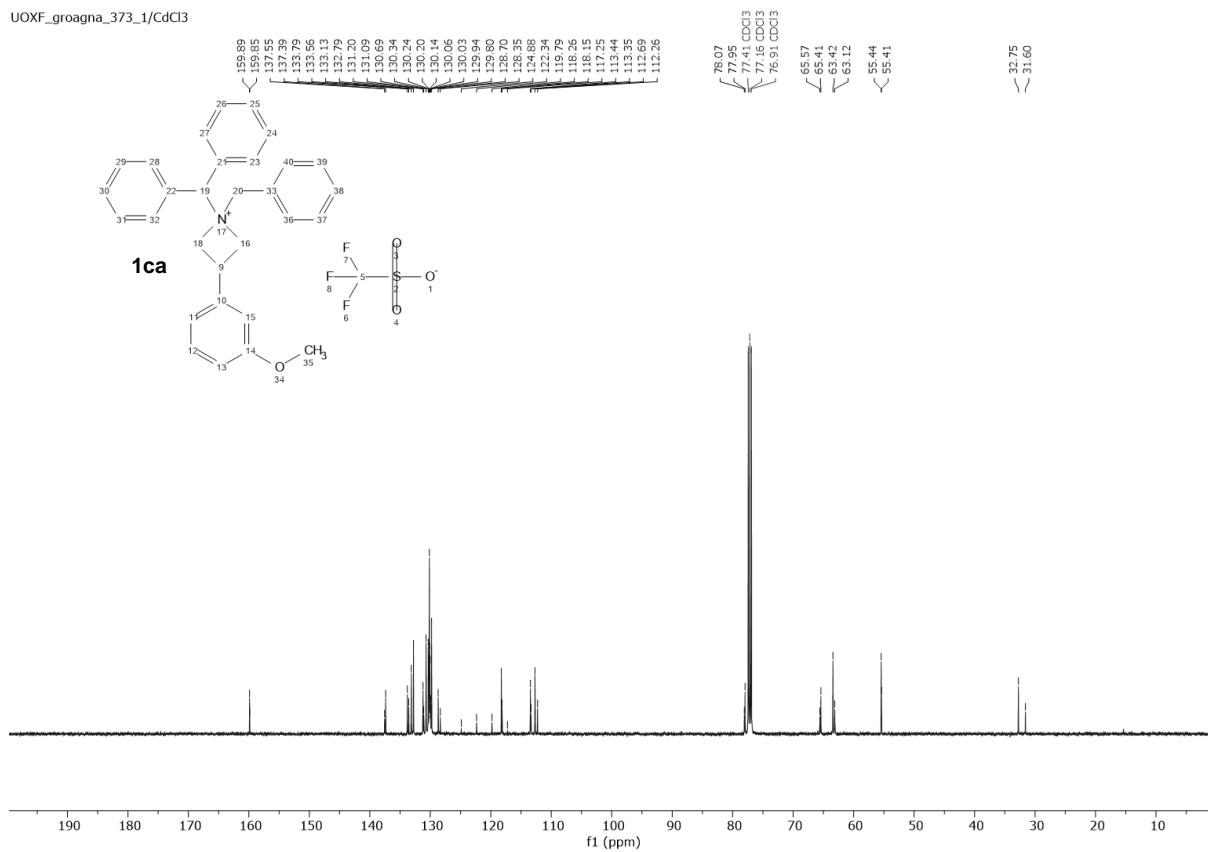
UOXF_groagna_373_1/CdCl3



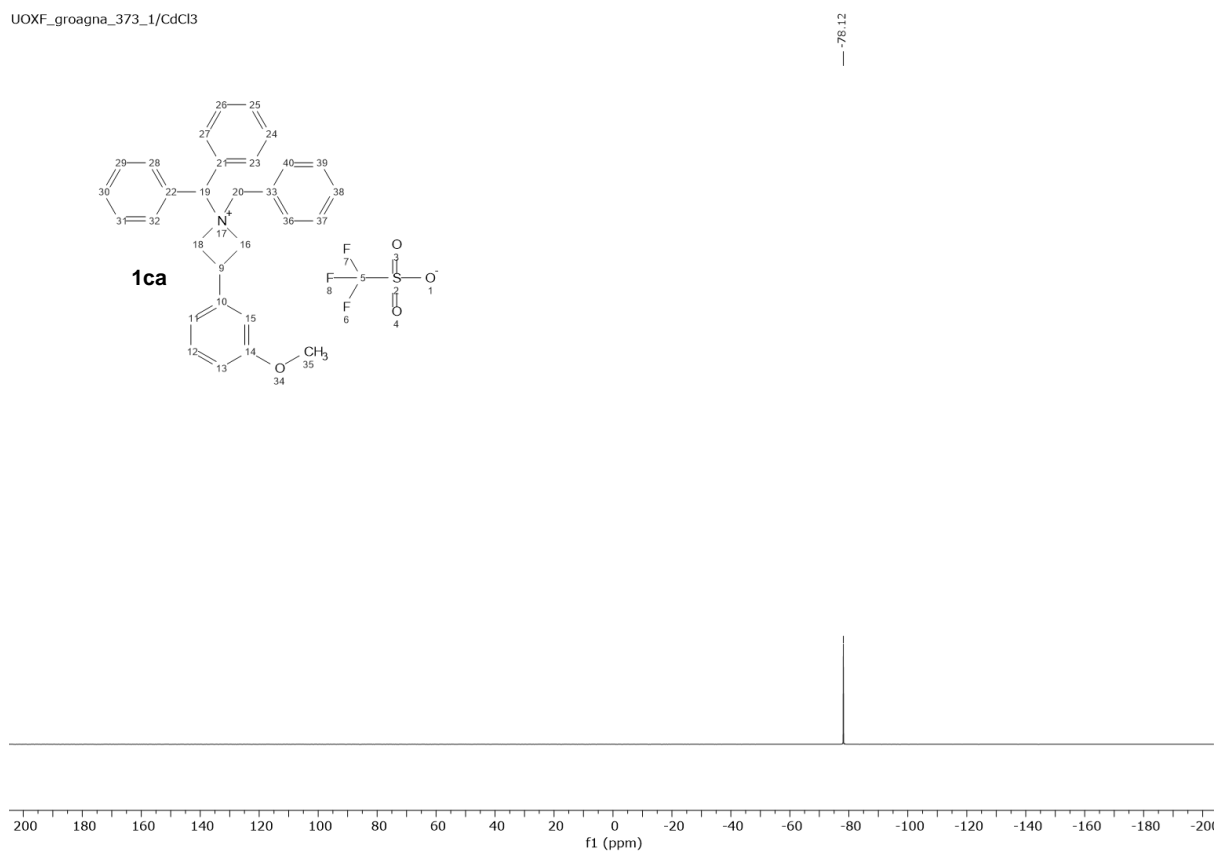
Indirect correlation



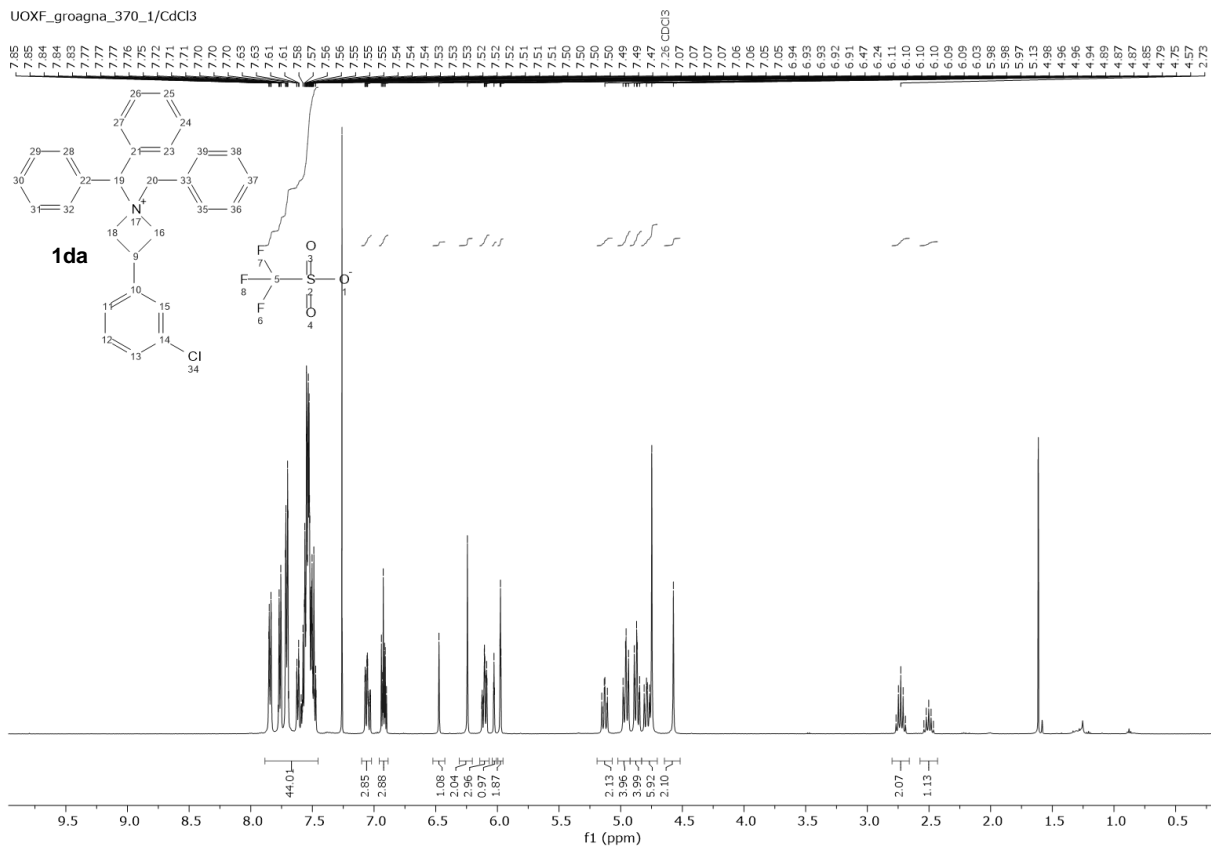
UOXF_groagna_373_1/CdCl3



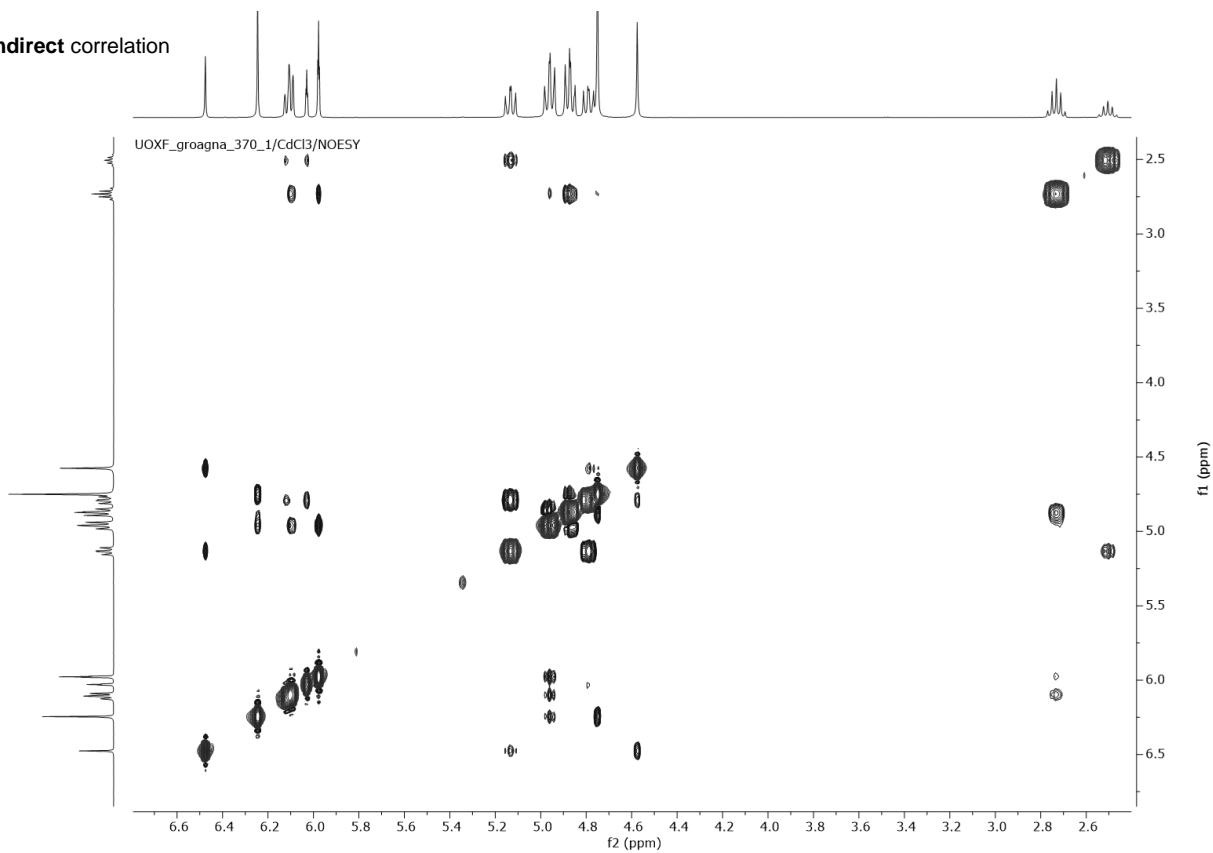
UOXF_groagna_373_1/CdCl3



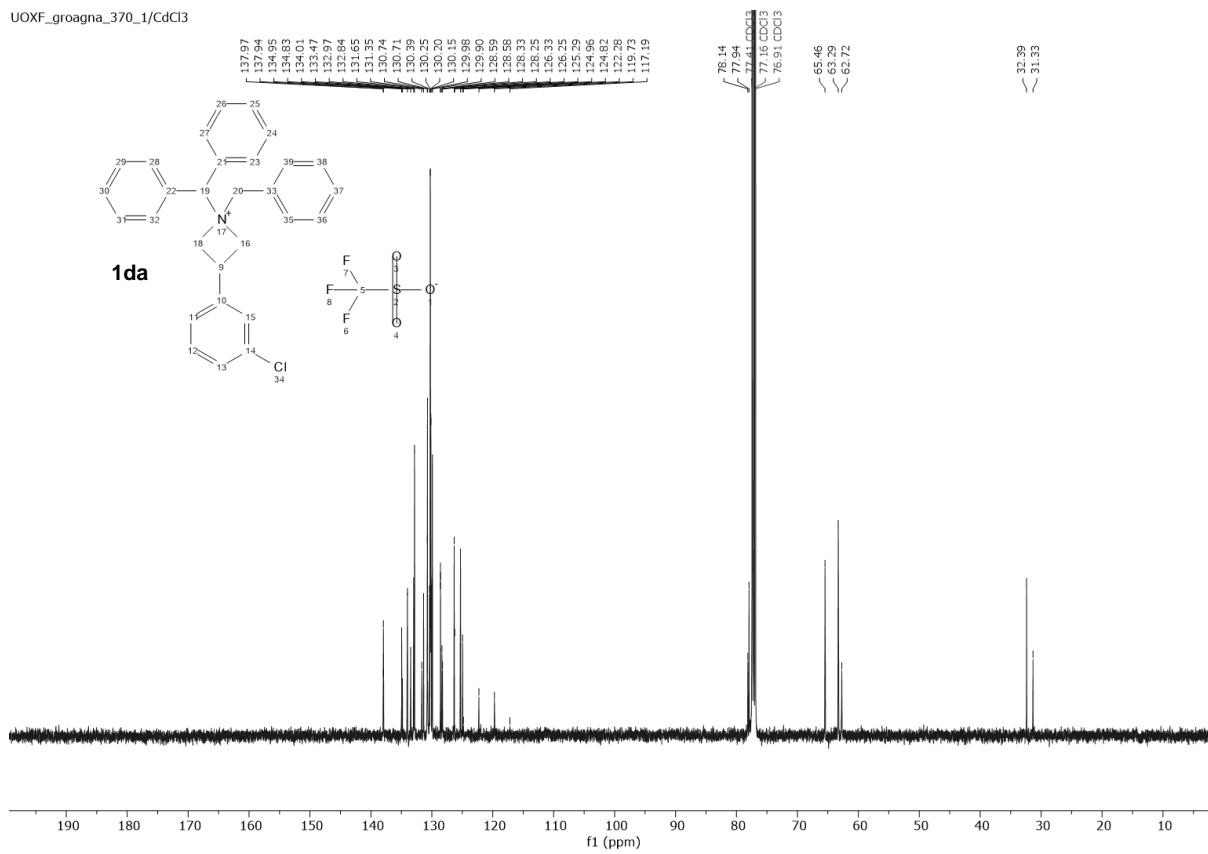
UOXF_groagna_370_1/CdCl3



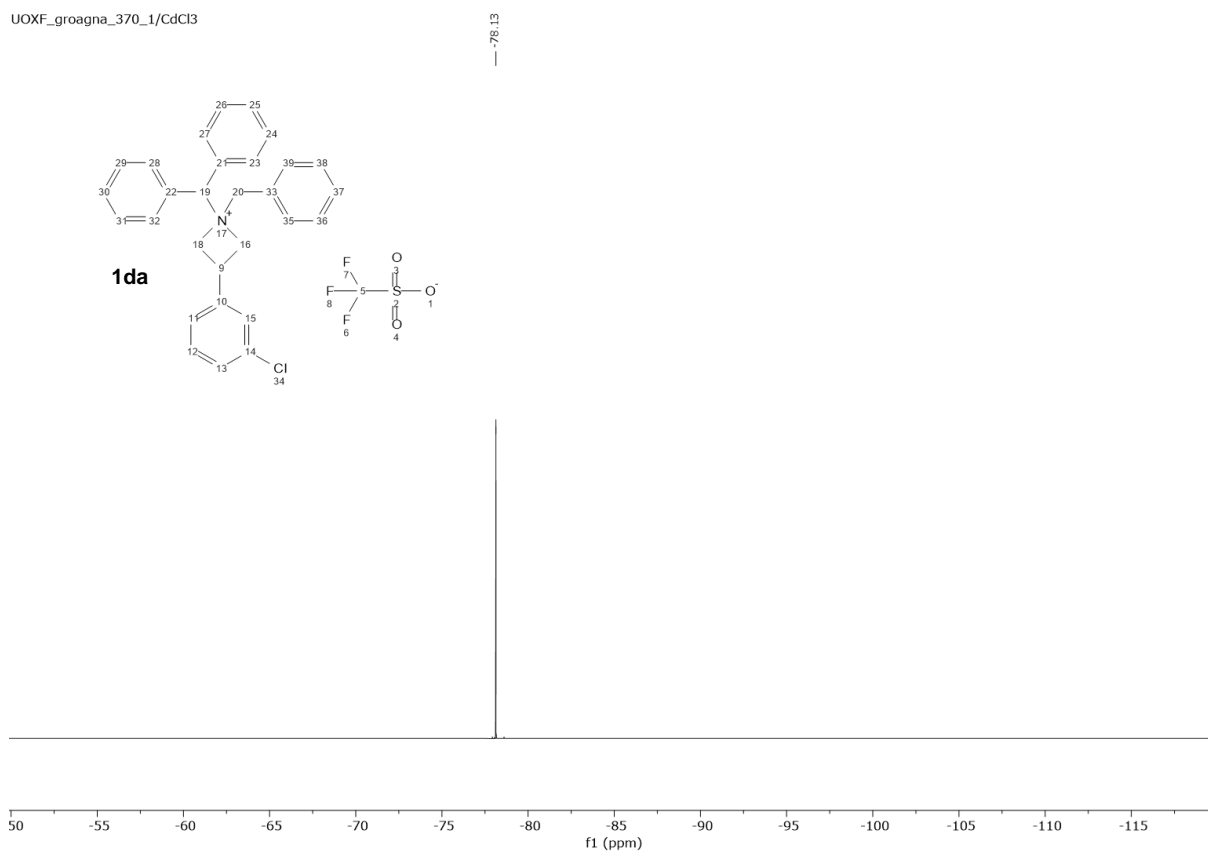
Indirect correlation

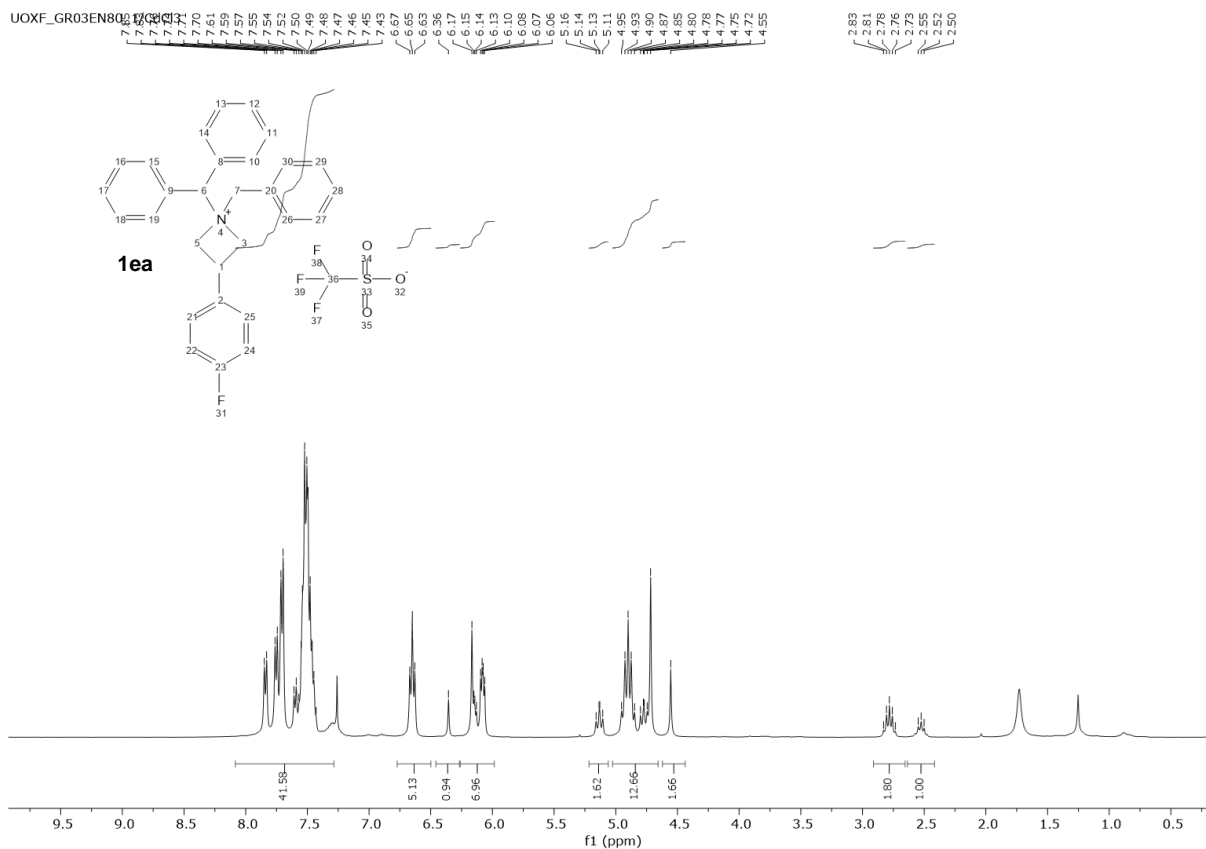


UOXF_groagna_370_1/CdCl3

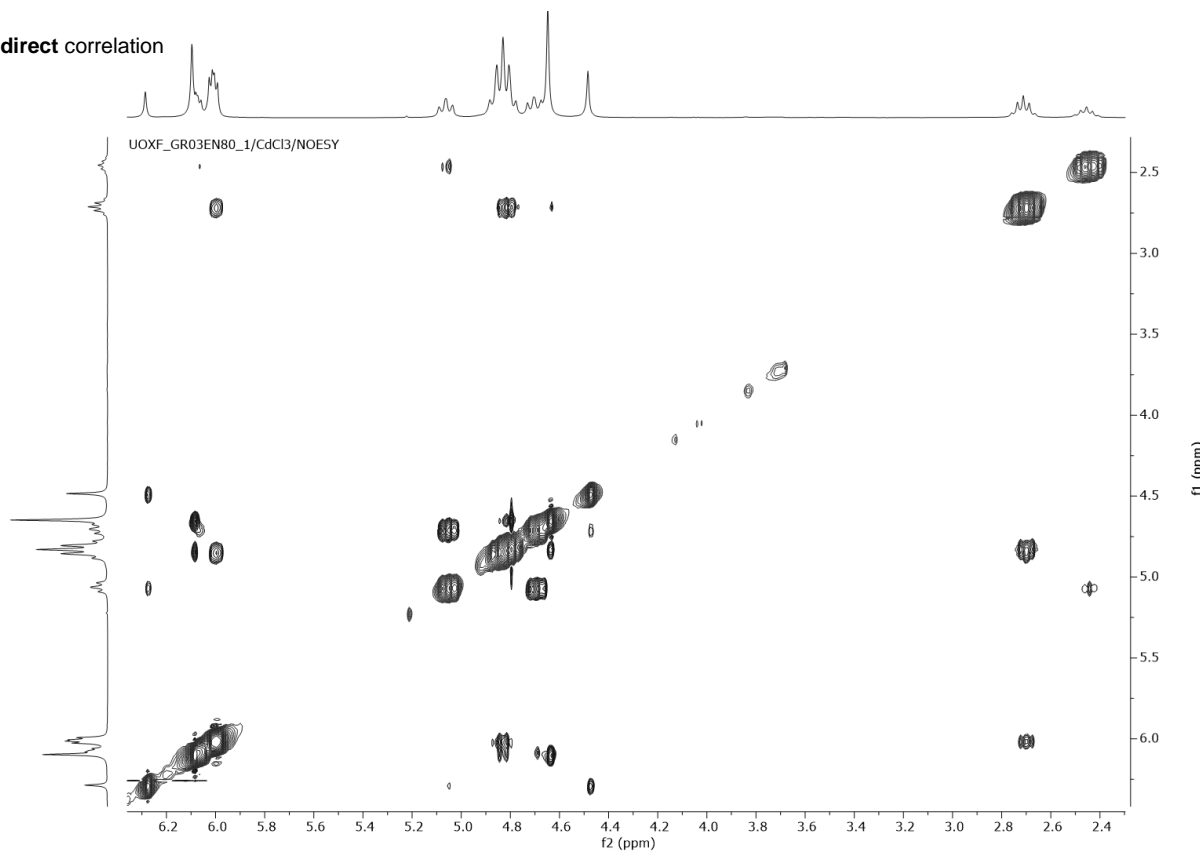


UOXF_groagna_370_1/CdCl3

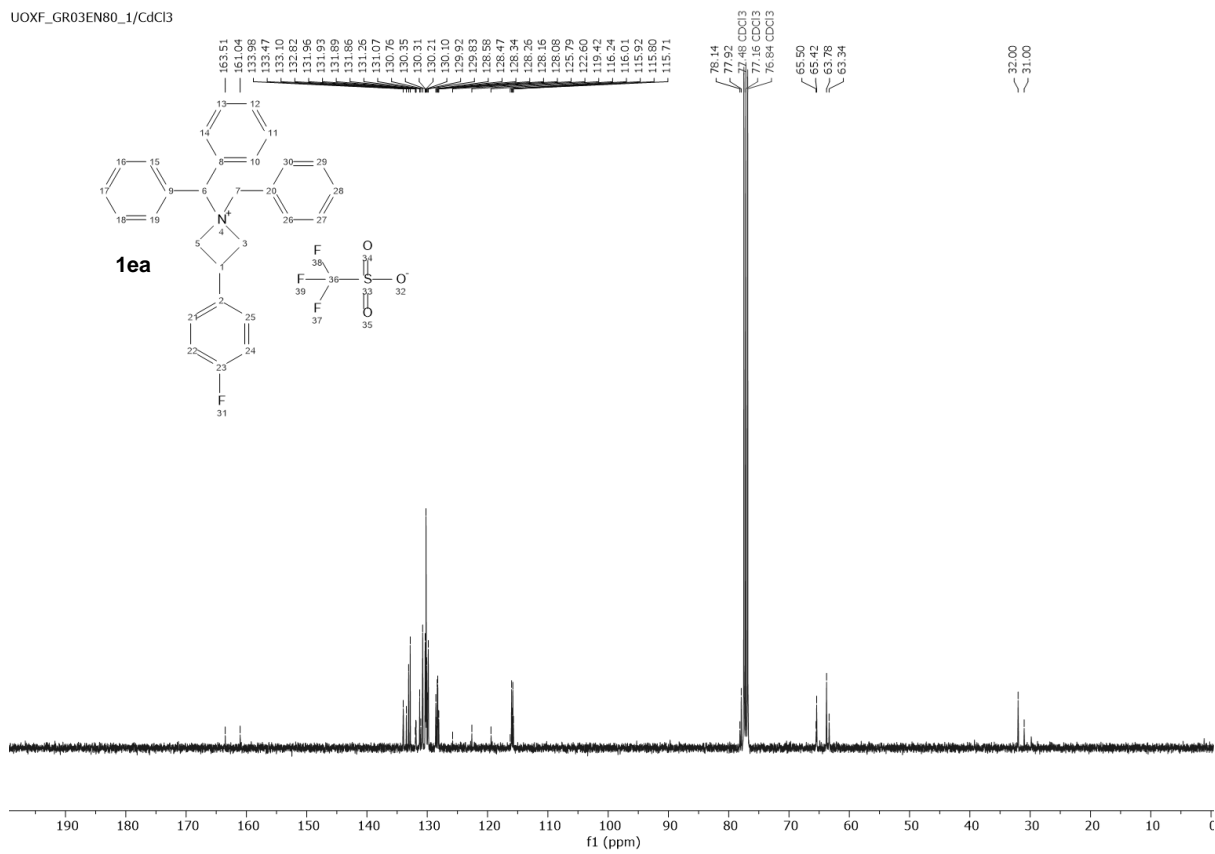




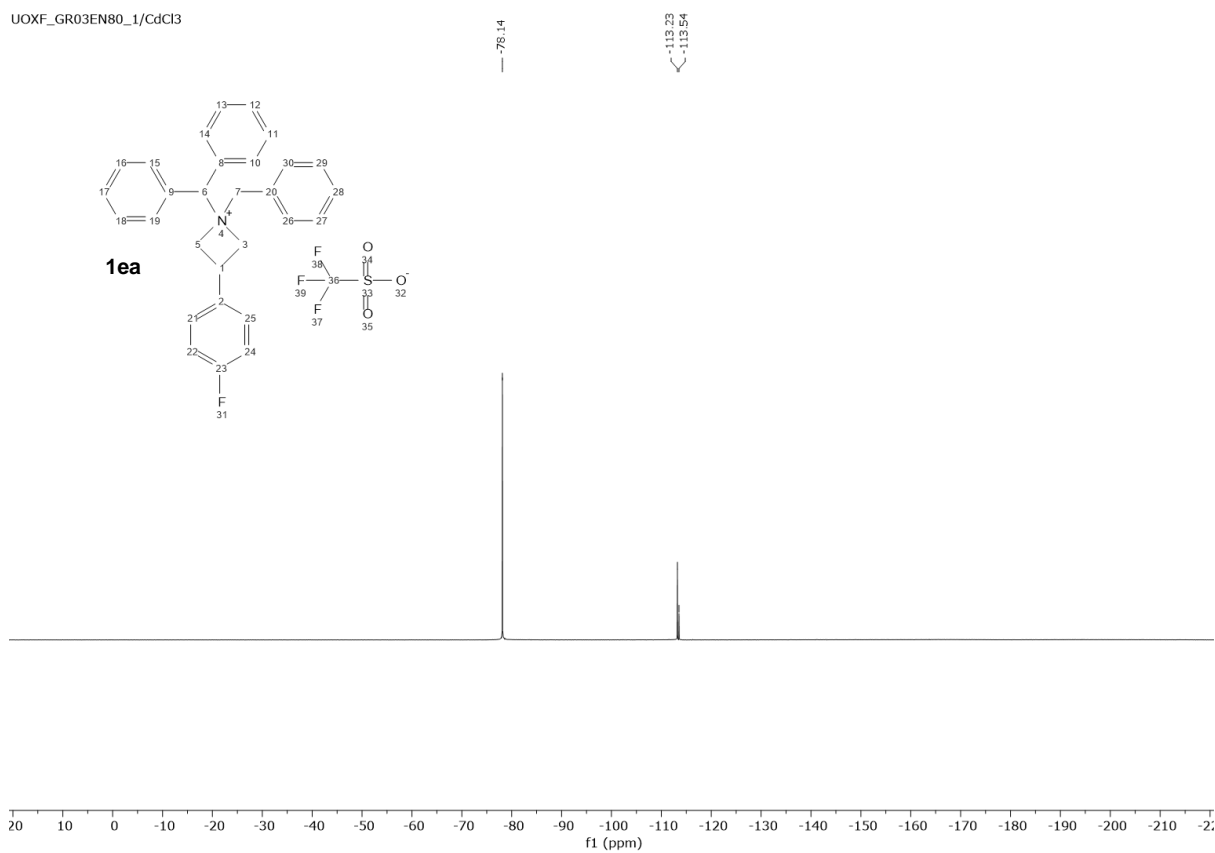
Indirect correlation



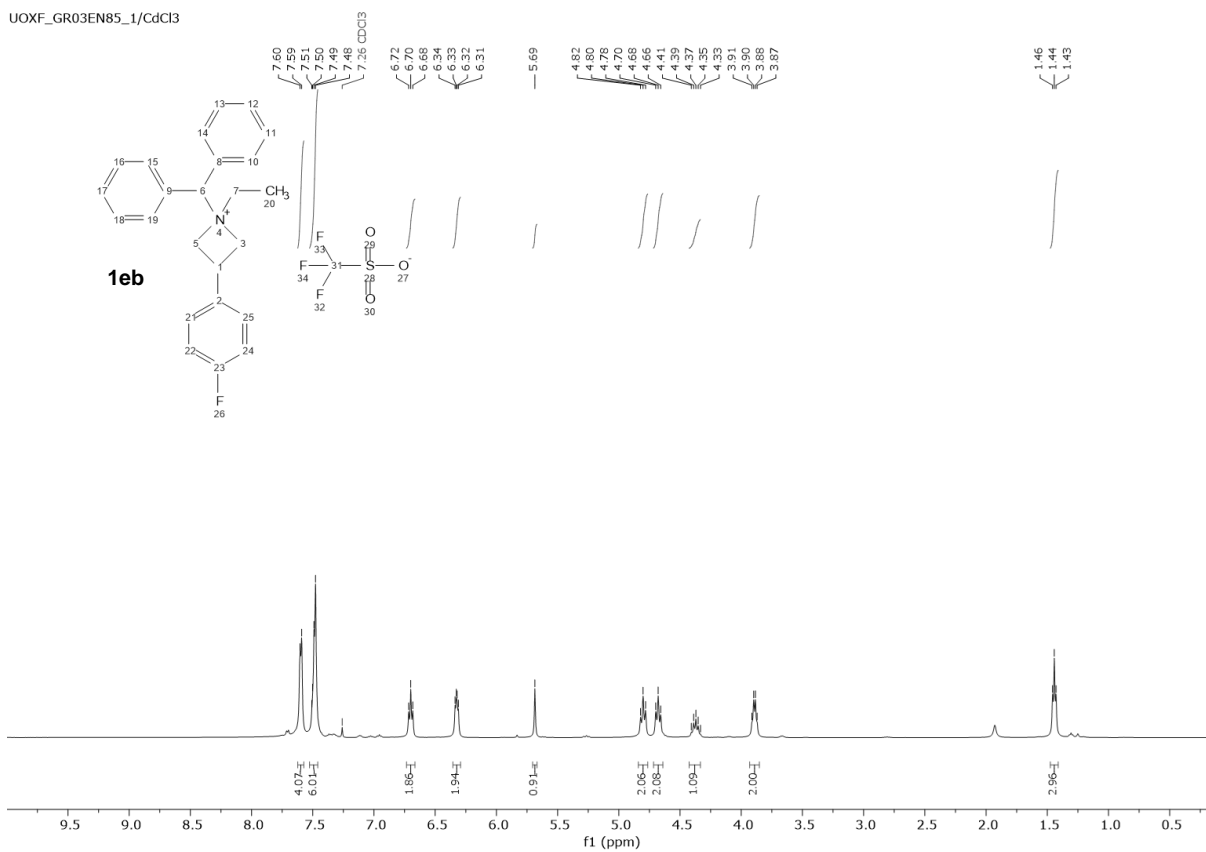
UOXF_GR03EN80_1/CdCl3



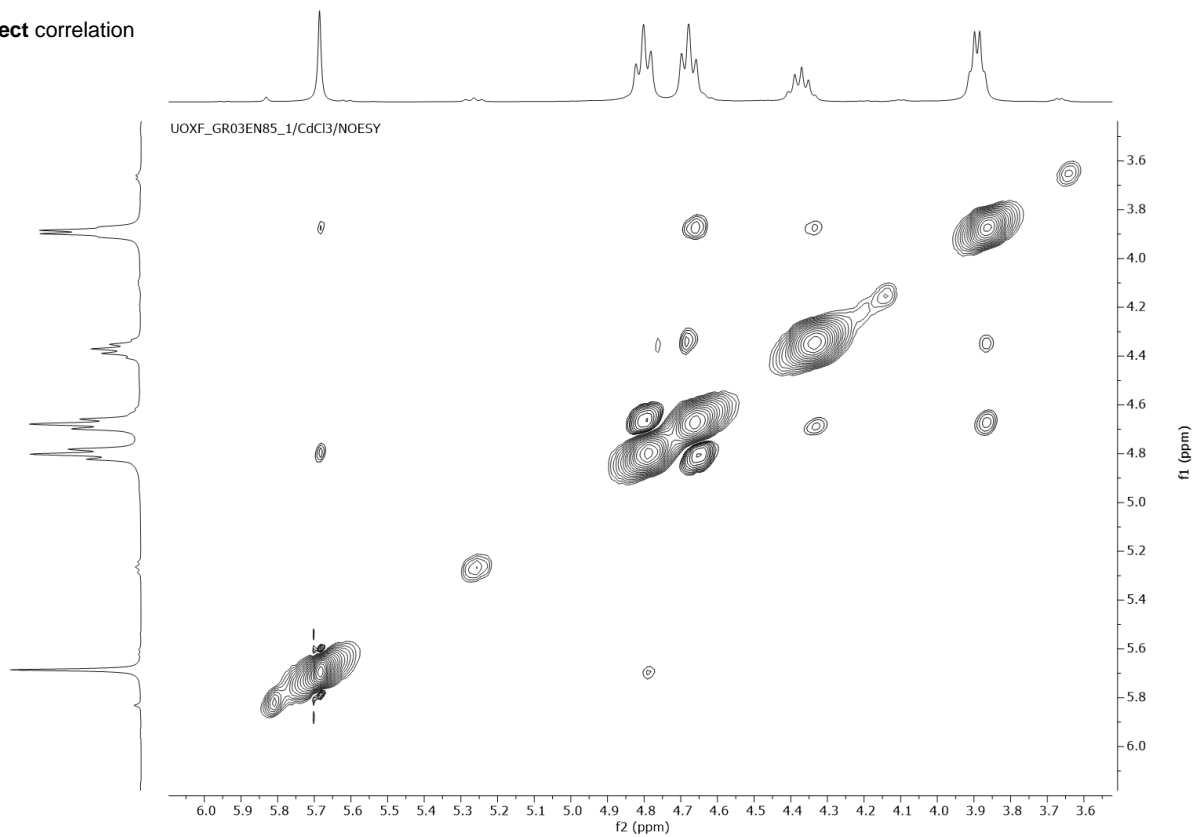
UOXF_GR03EN80_1/CdCl3



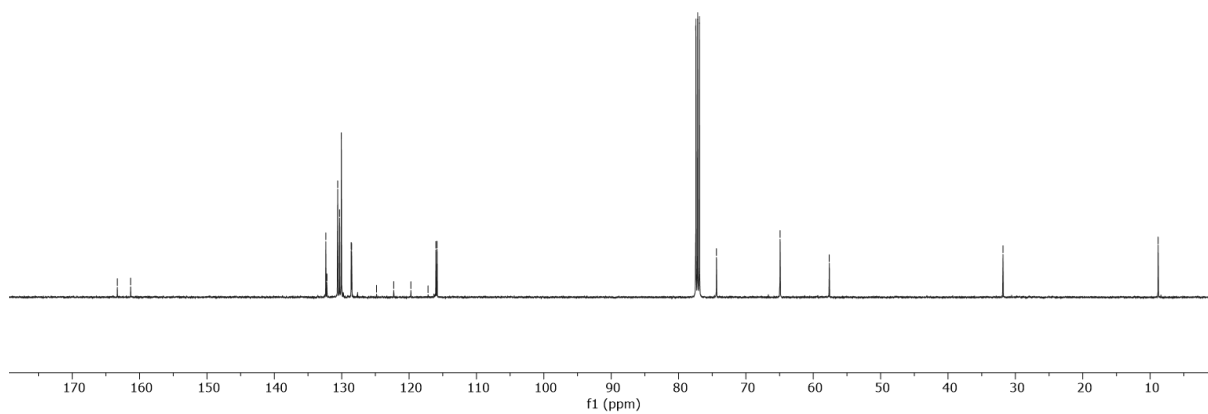
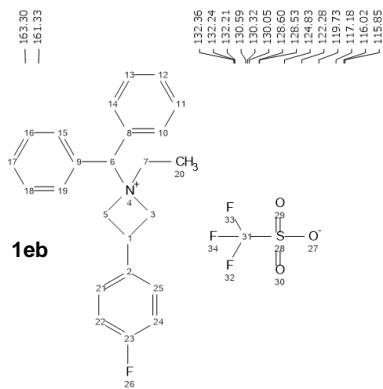
UOXF_GR03EN85_1/CdCl3



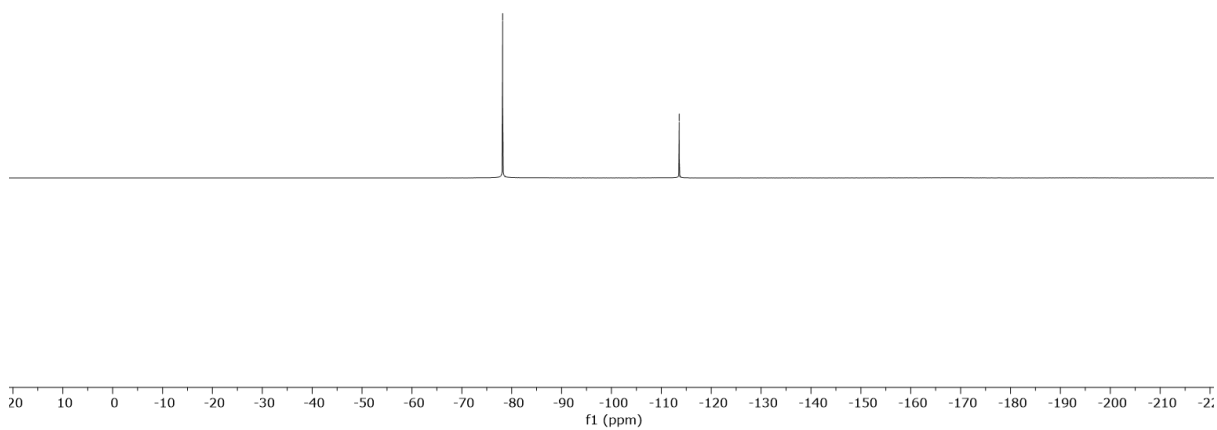
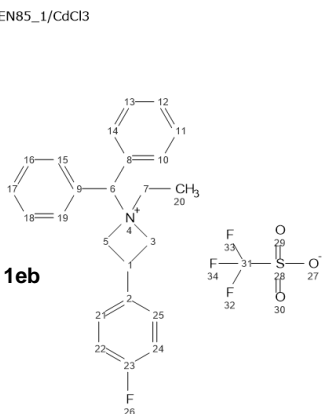
Direct correlation



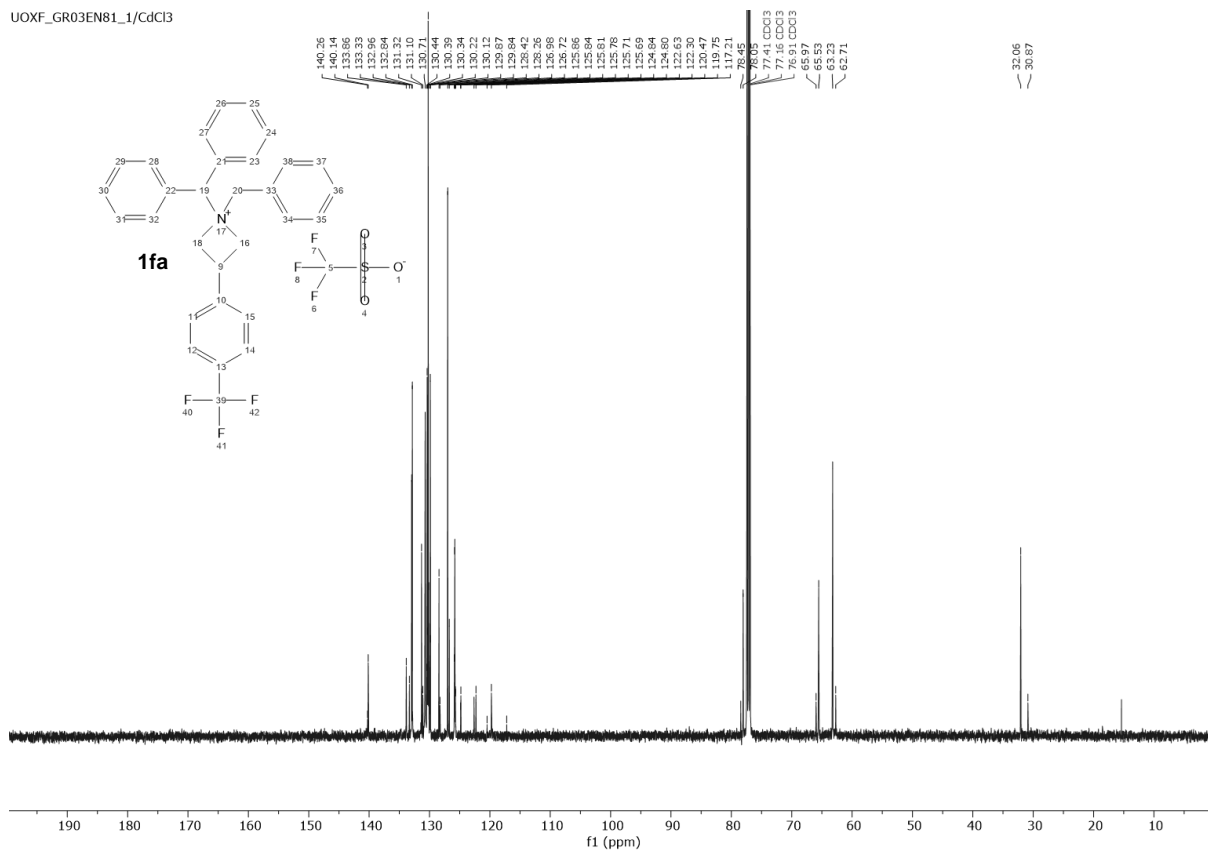
UOXF_GR03EN85_1/CdCl3



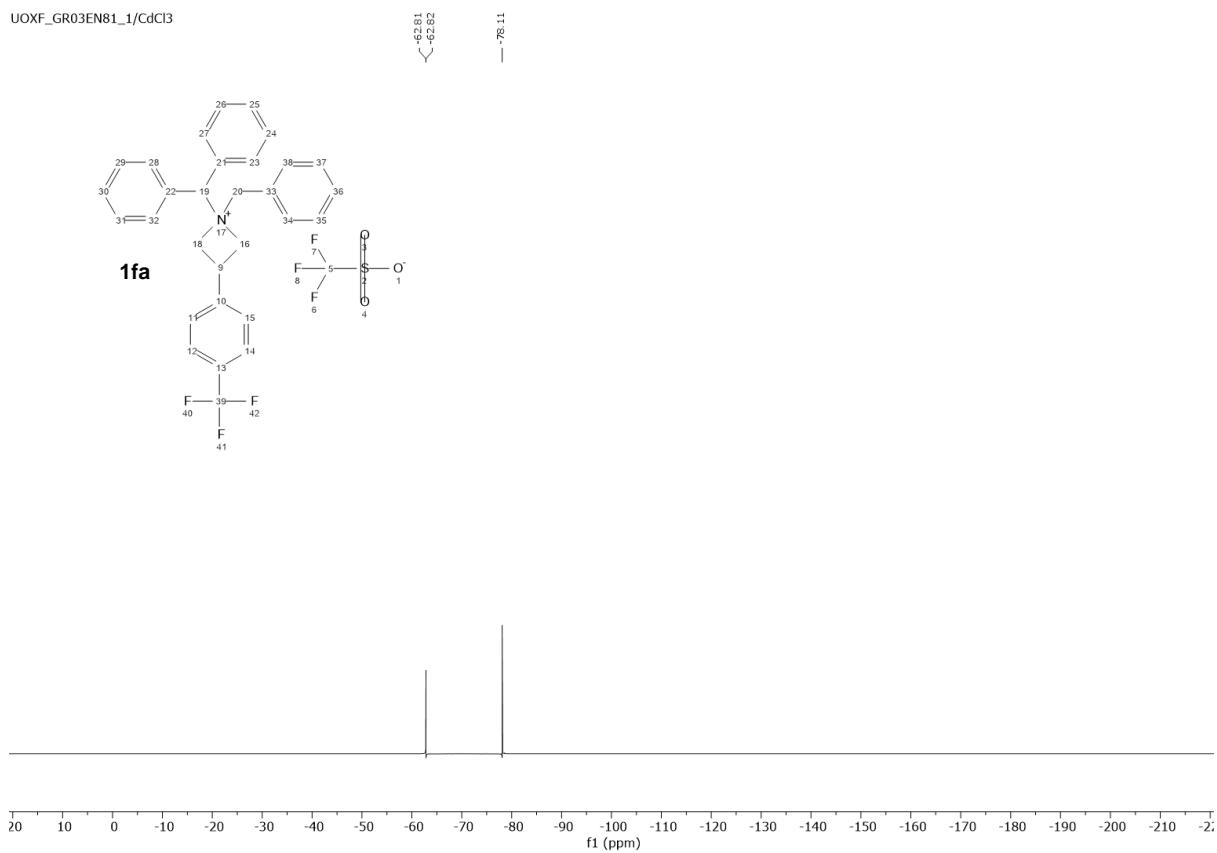
UOXF_GR03EN85_1/CdCl3



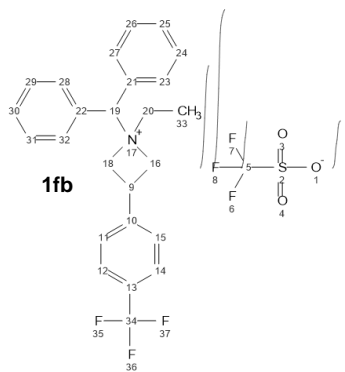
UOXF_GR03EN81_1/CdCl3



UOXF_GR03EN81_1/CdCl3



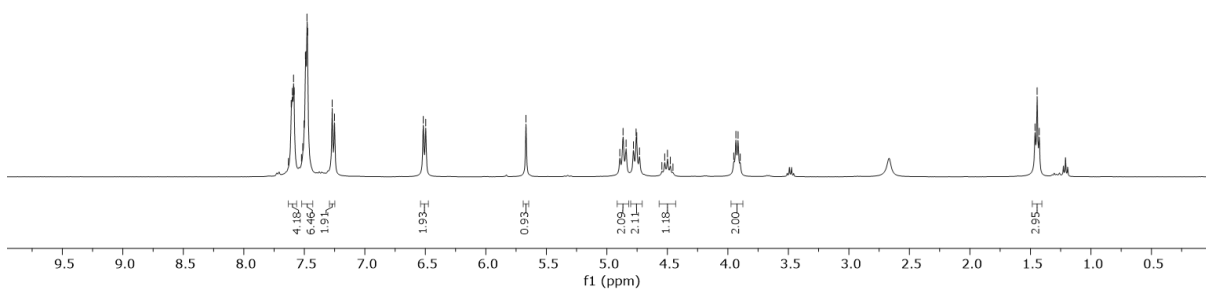
UOXF_GR03EN84_1/CdCl3



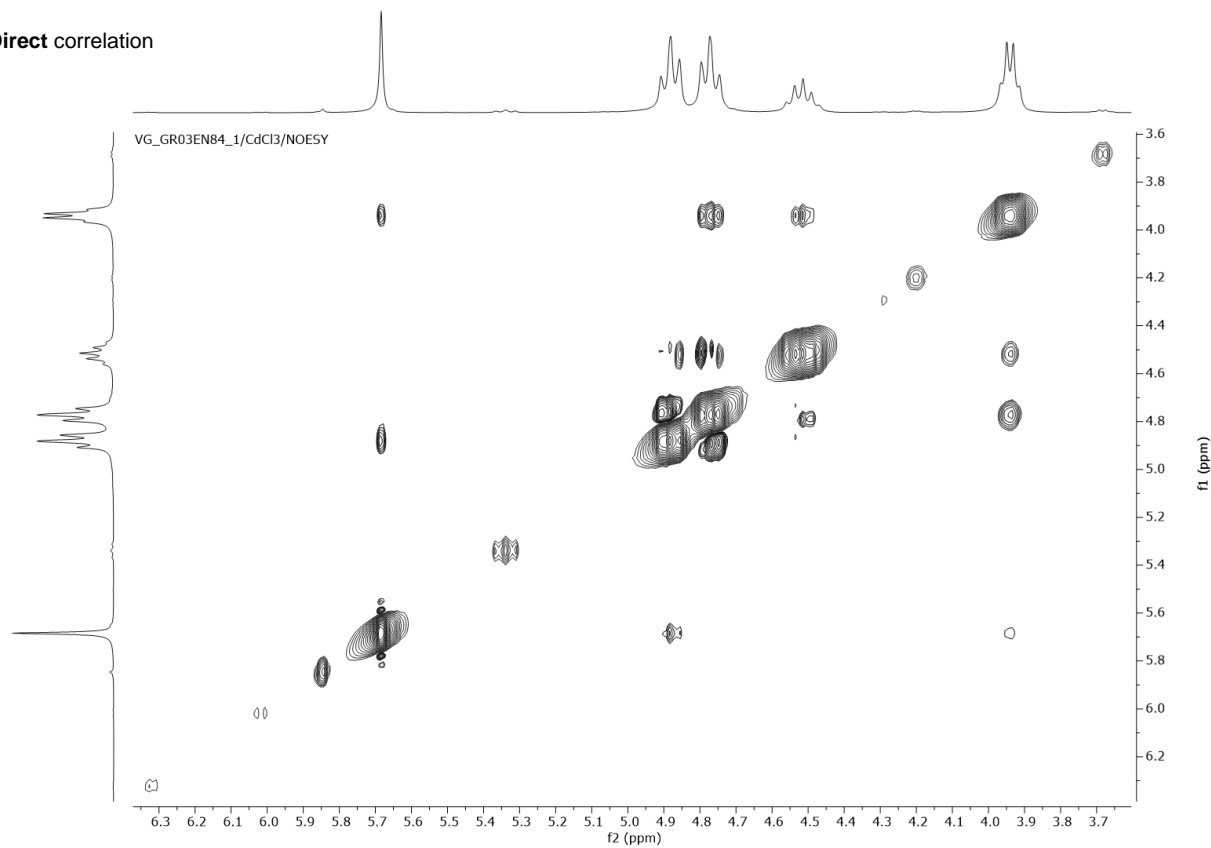
7.63
7.61
7.60
7.59
7.58
7.57
7.52
7.51
7.50
7.49
7.48
7.47
7.46
7.45
7.44
7.43
7.42
7.37
7.35
6.52
6.50

5.67
4.89
4.87
4.84
4.78
4.76
4.75
4.73
4.72
4.65
4.50
4.48
4.45
3.95
3.92
3.90

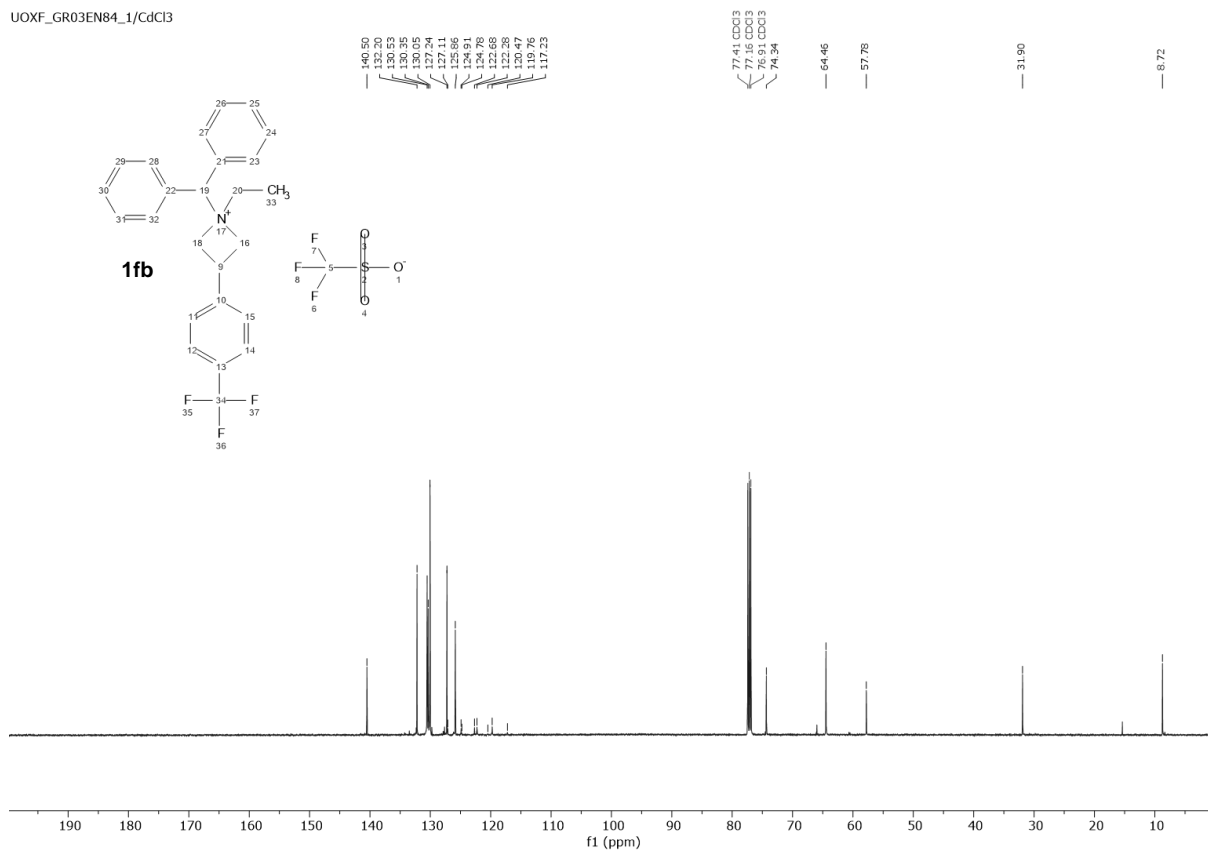
1.46
1.44
1.43



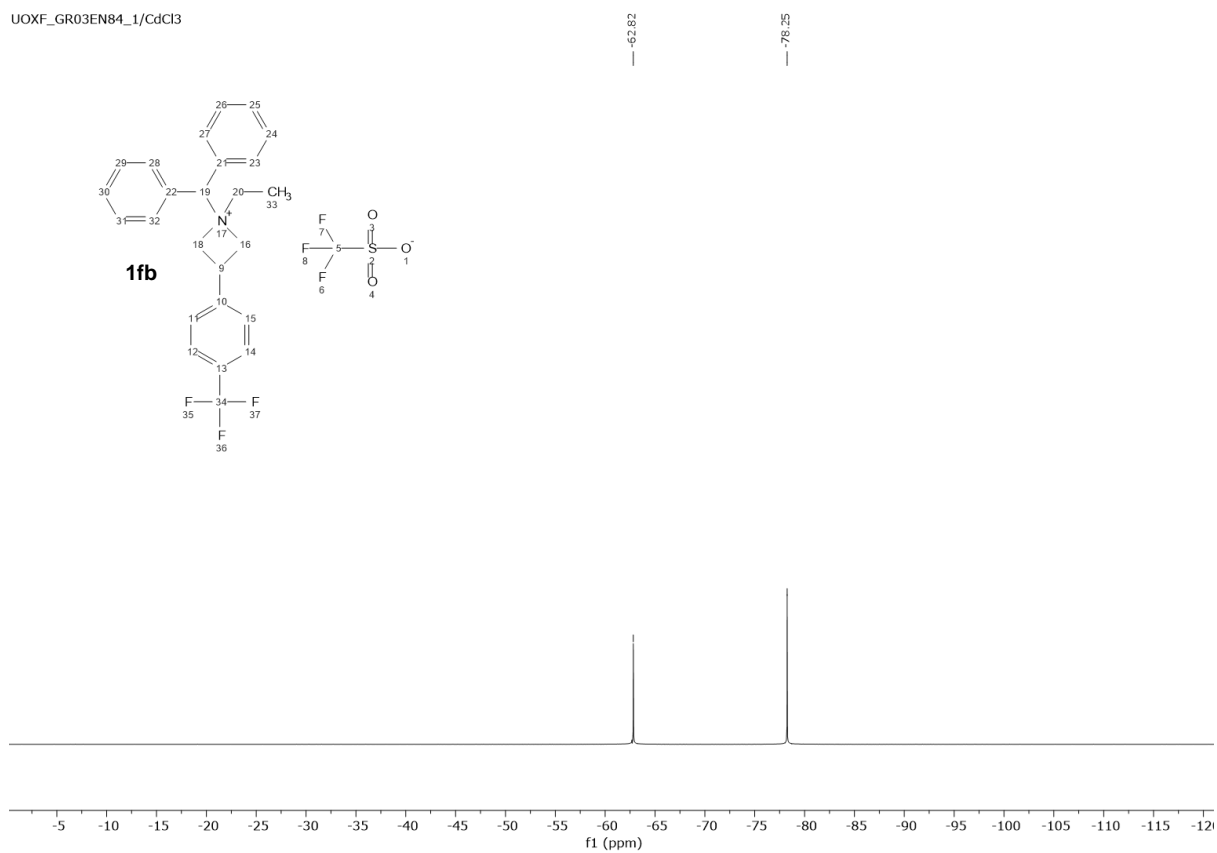
Direct correlation



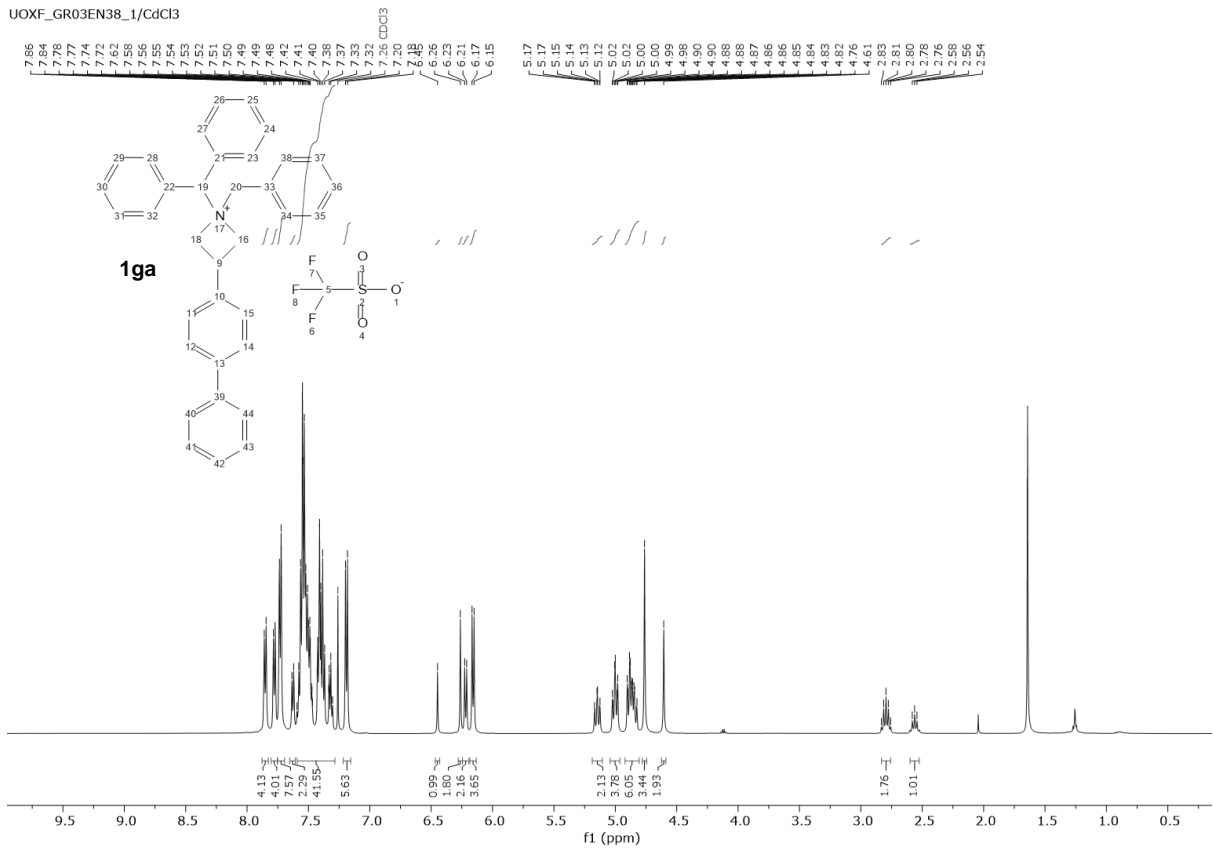
UOXF_GR03EN84_1/CdCl3



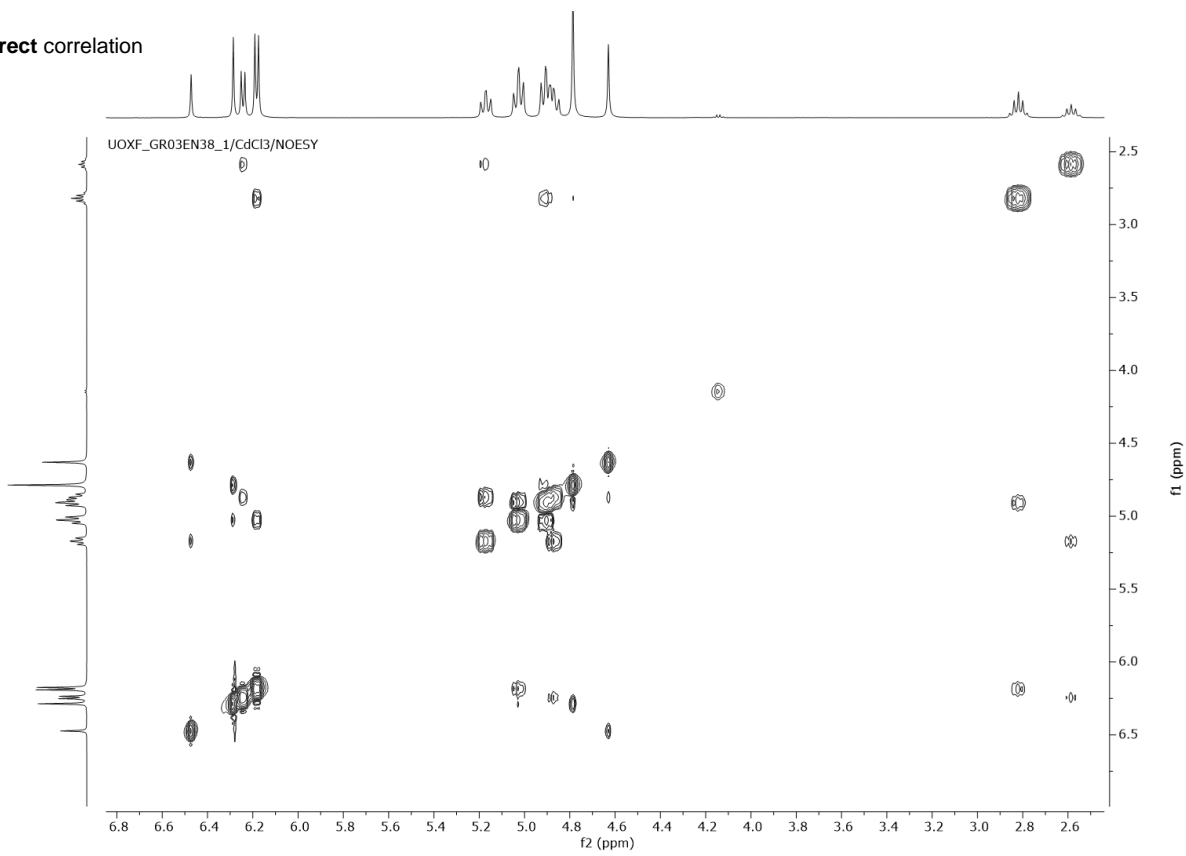
UOXF_GR03EN84_1/CdCl3



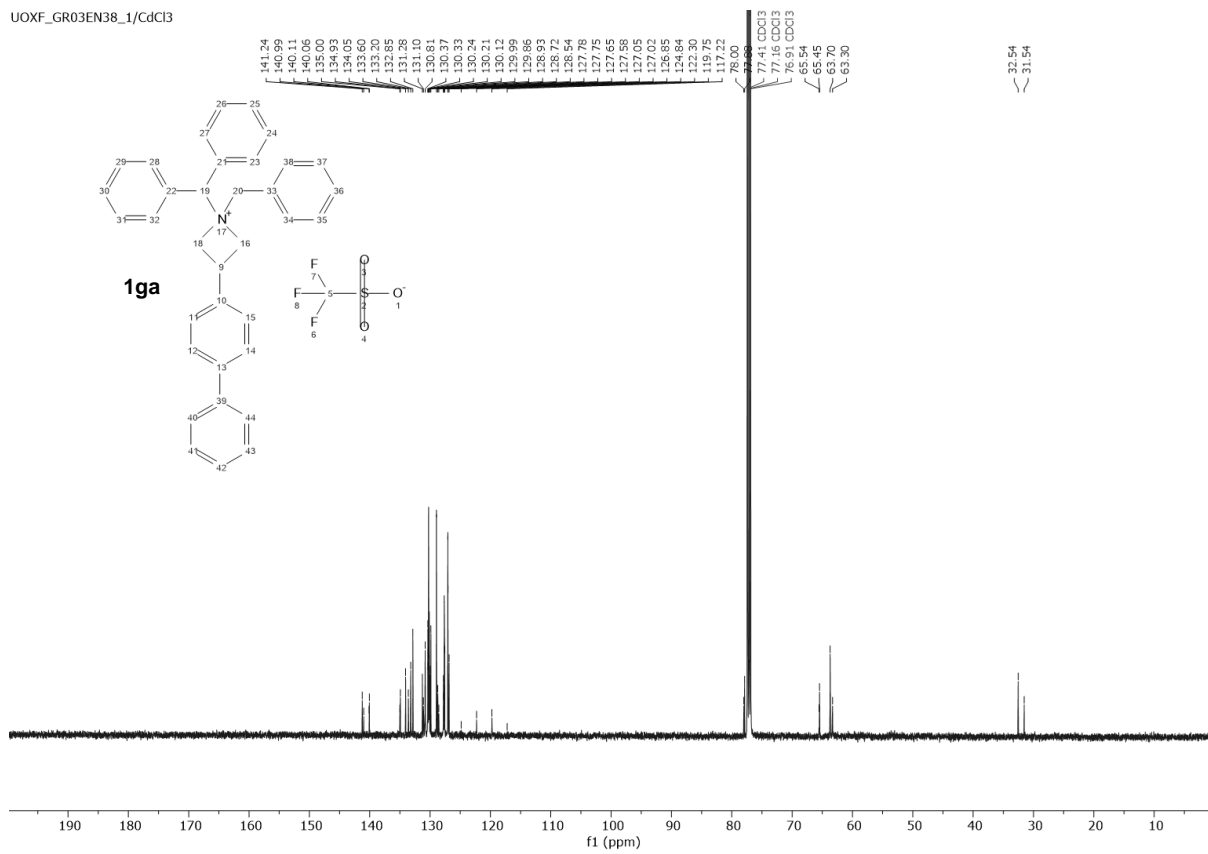
UOXF_GR03EN38_1/CdCl3



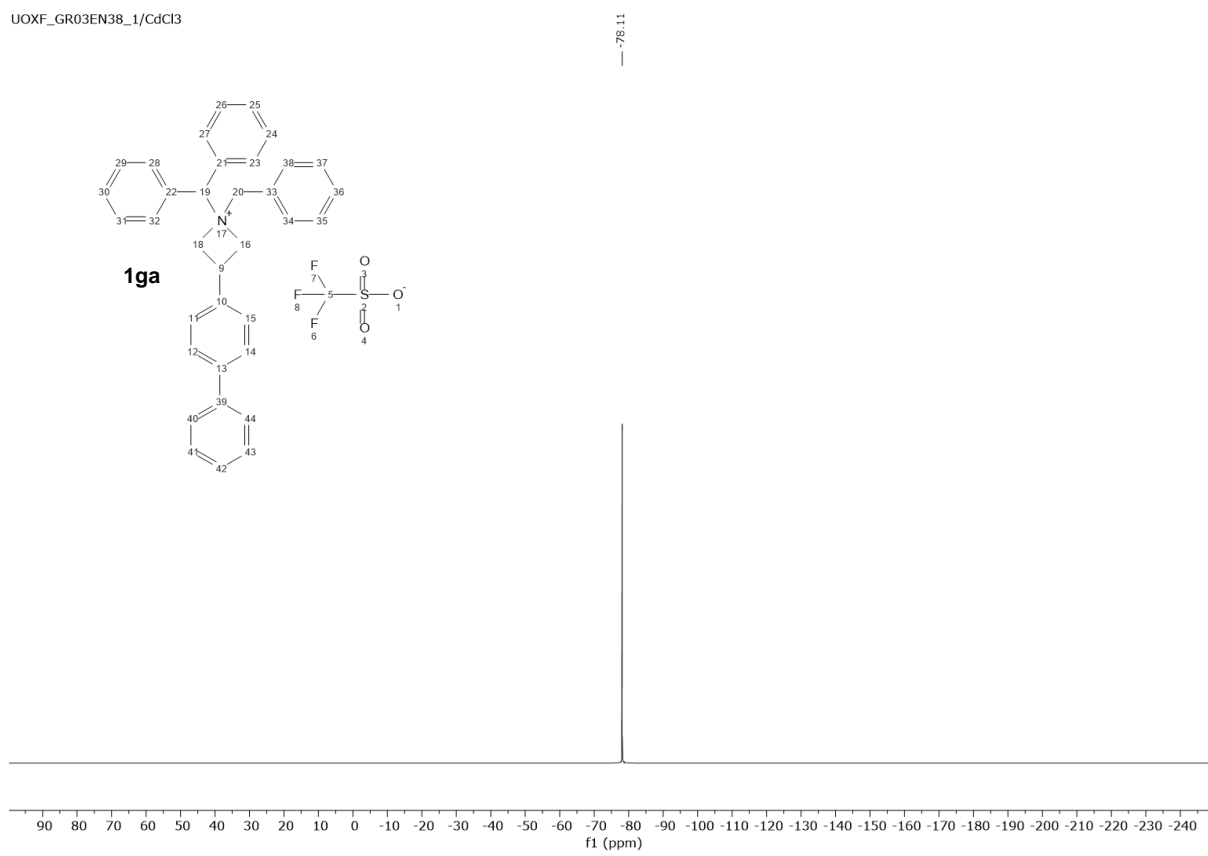
Indirect correlation



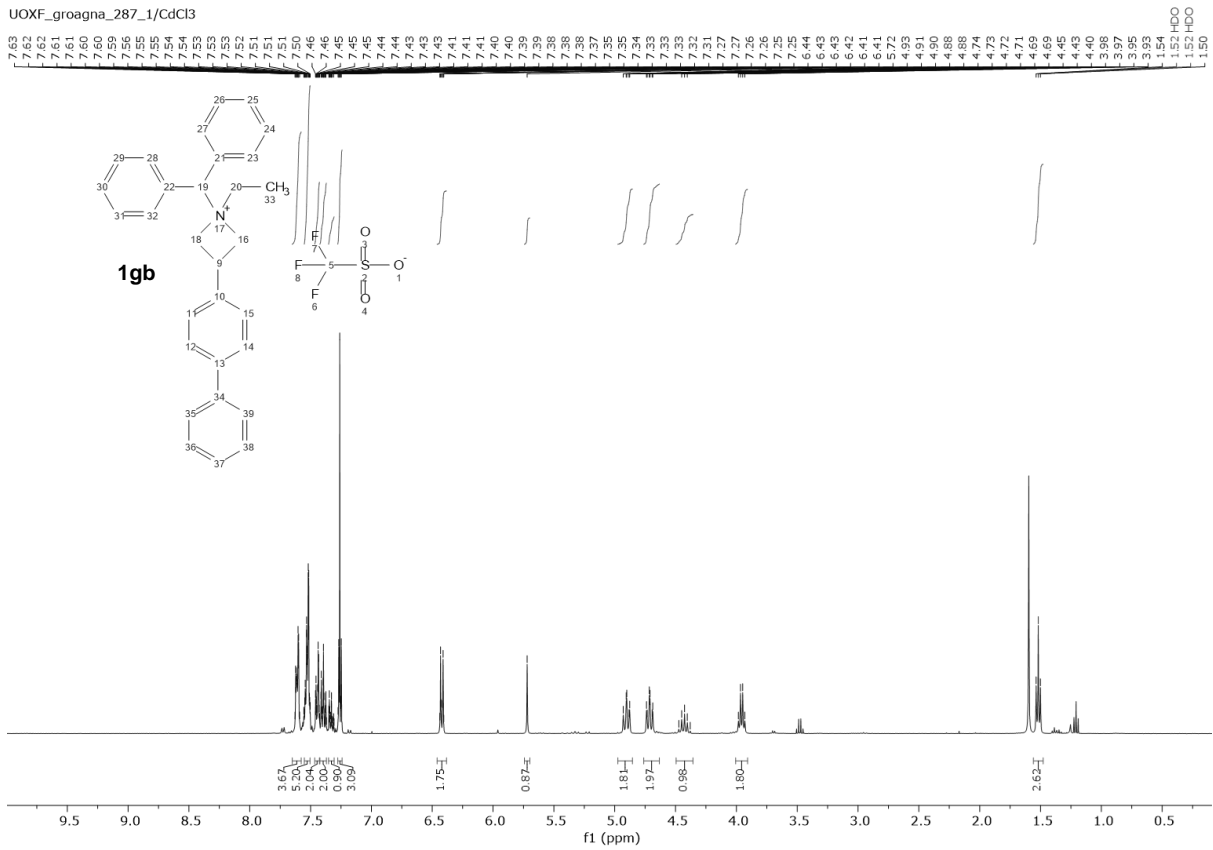
UOXF_GR03EN38_1/CdCl3



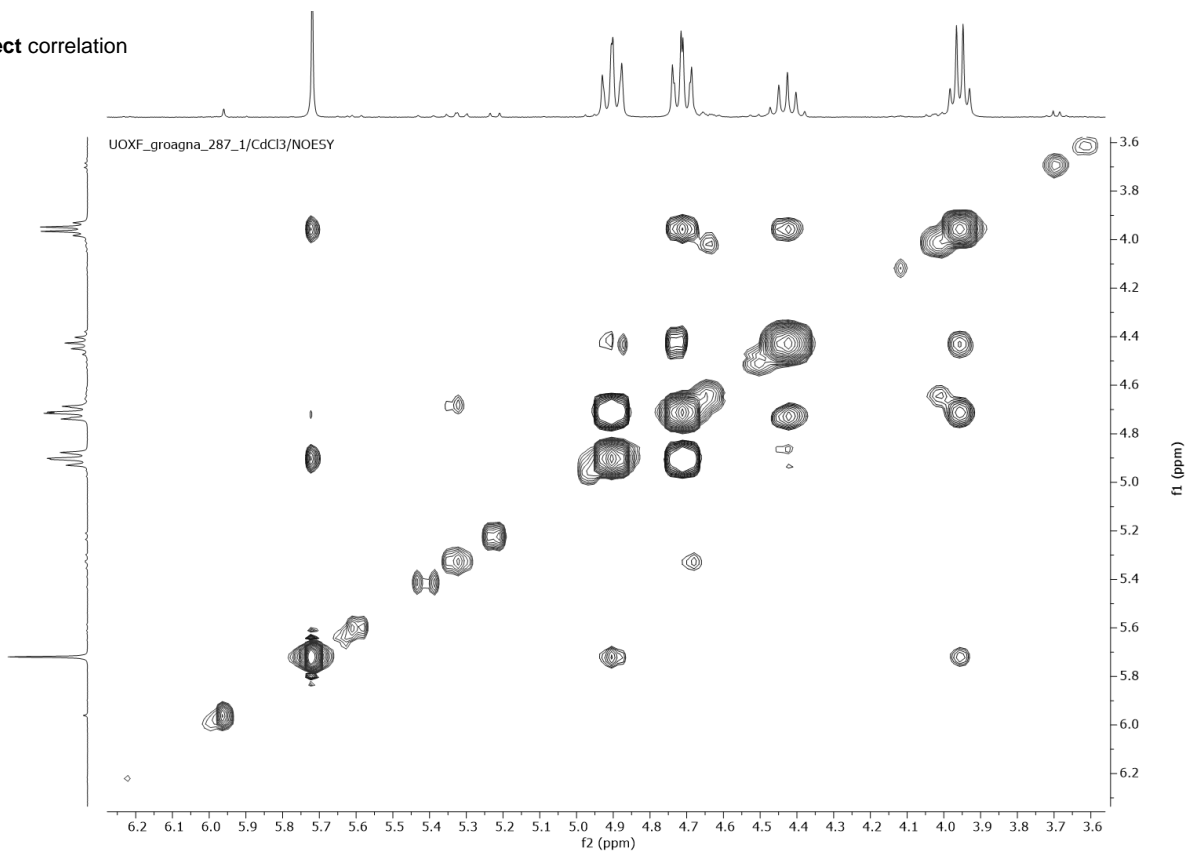
UOXF_GR03EN38_1/CdCl3



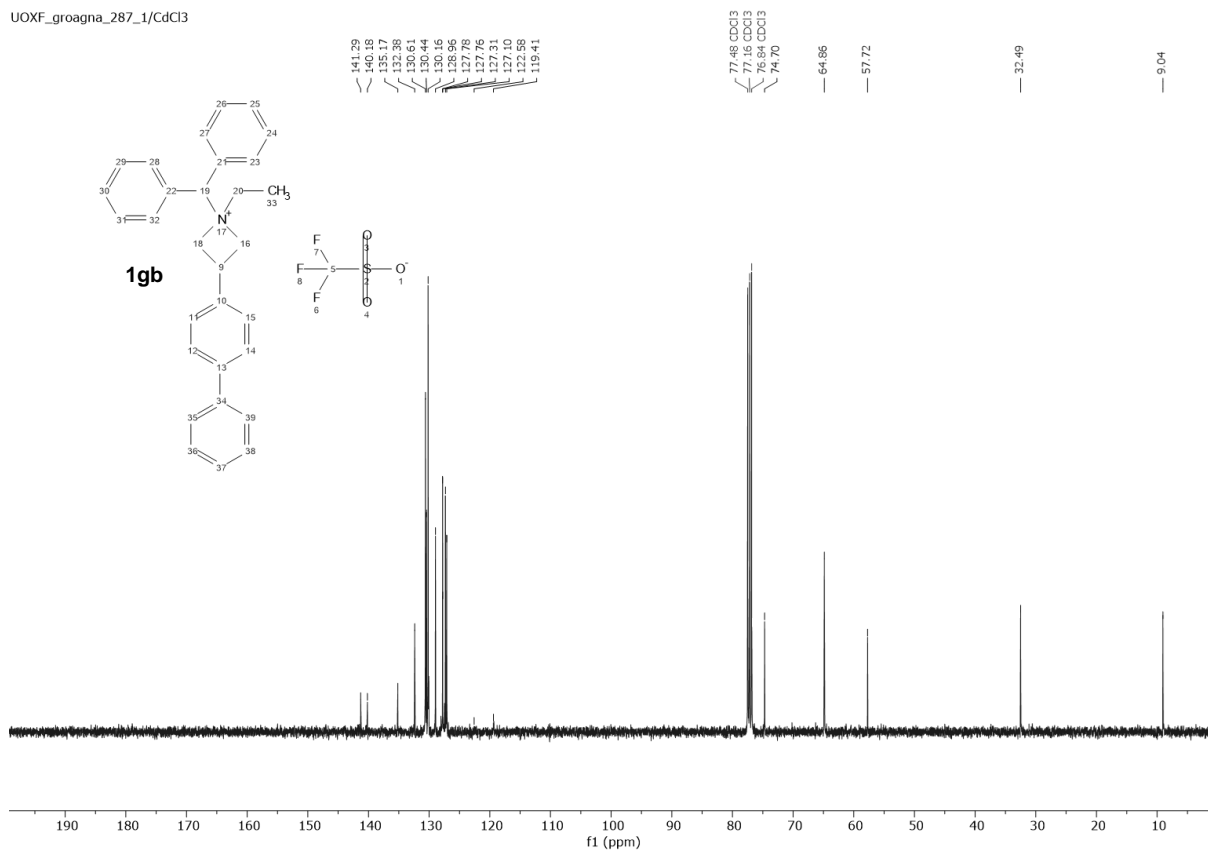
UOXF_groagna_287_1/CdCl3



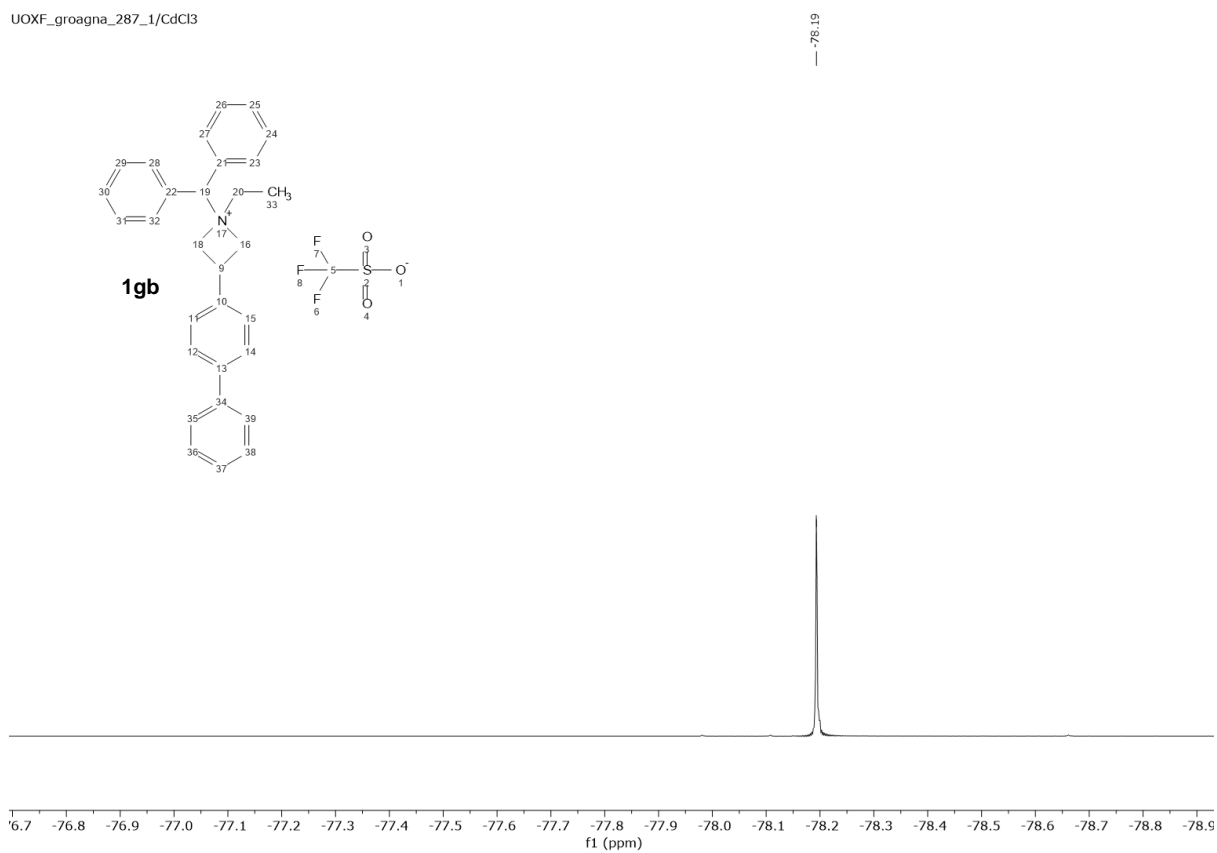
Direct correlation



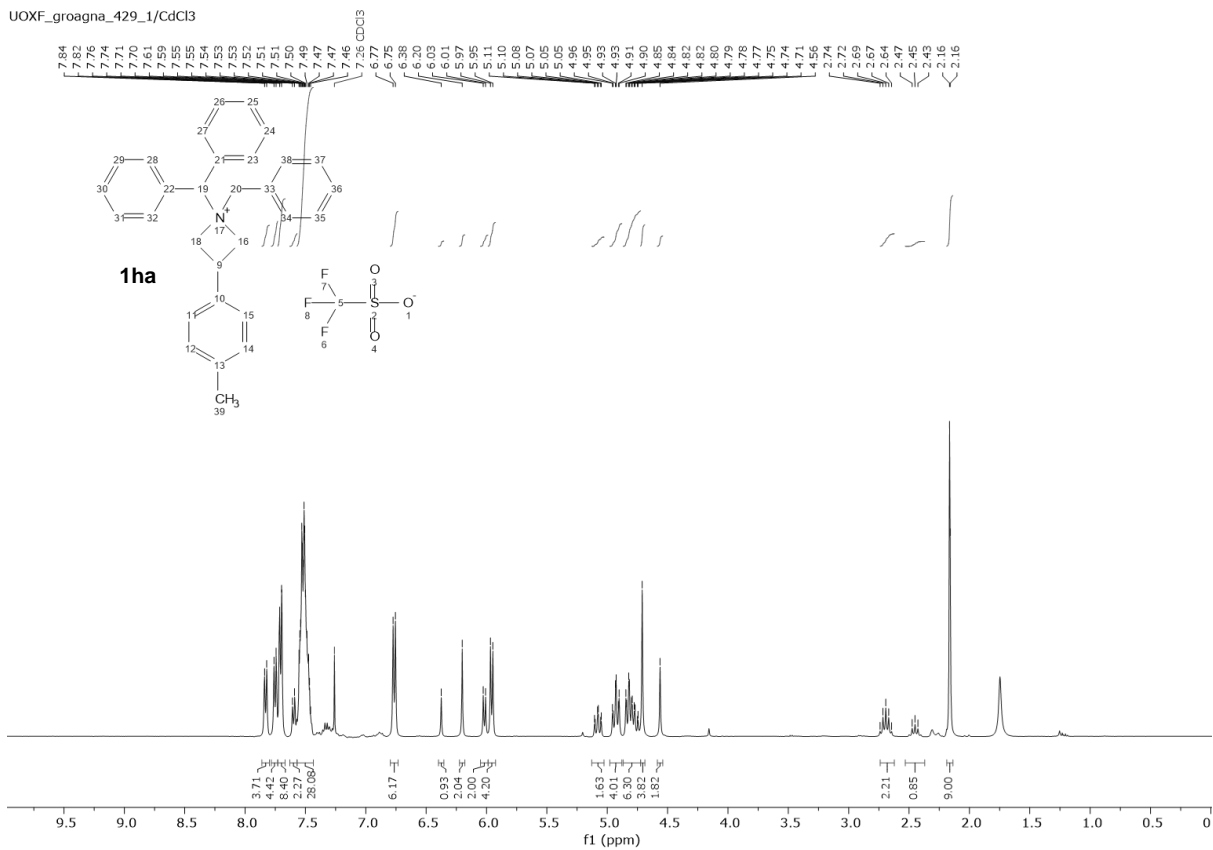
UOXF_groagna_287_1/CdCl3



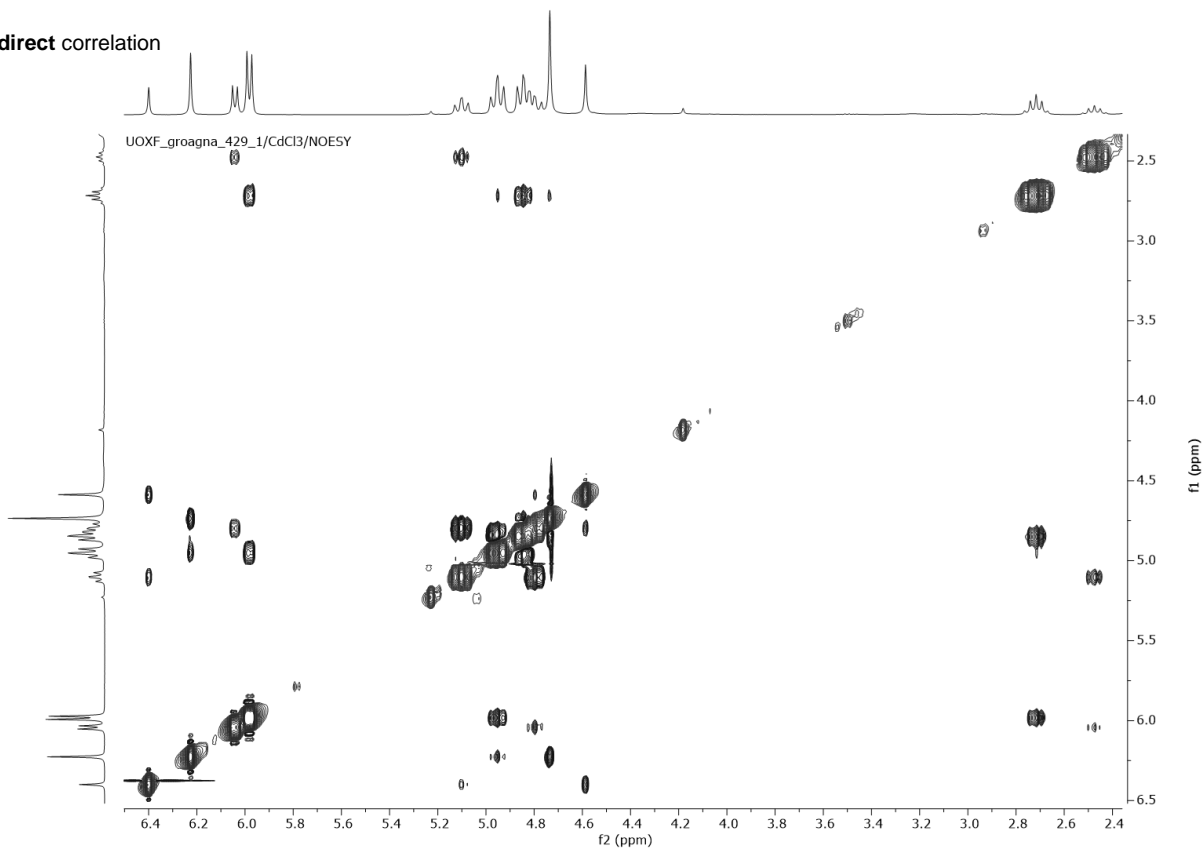
UOXF_groagna_287_1/CdCl3



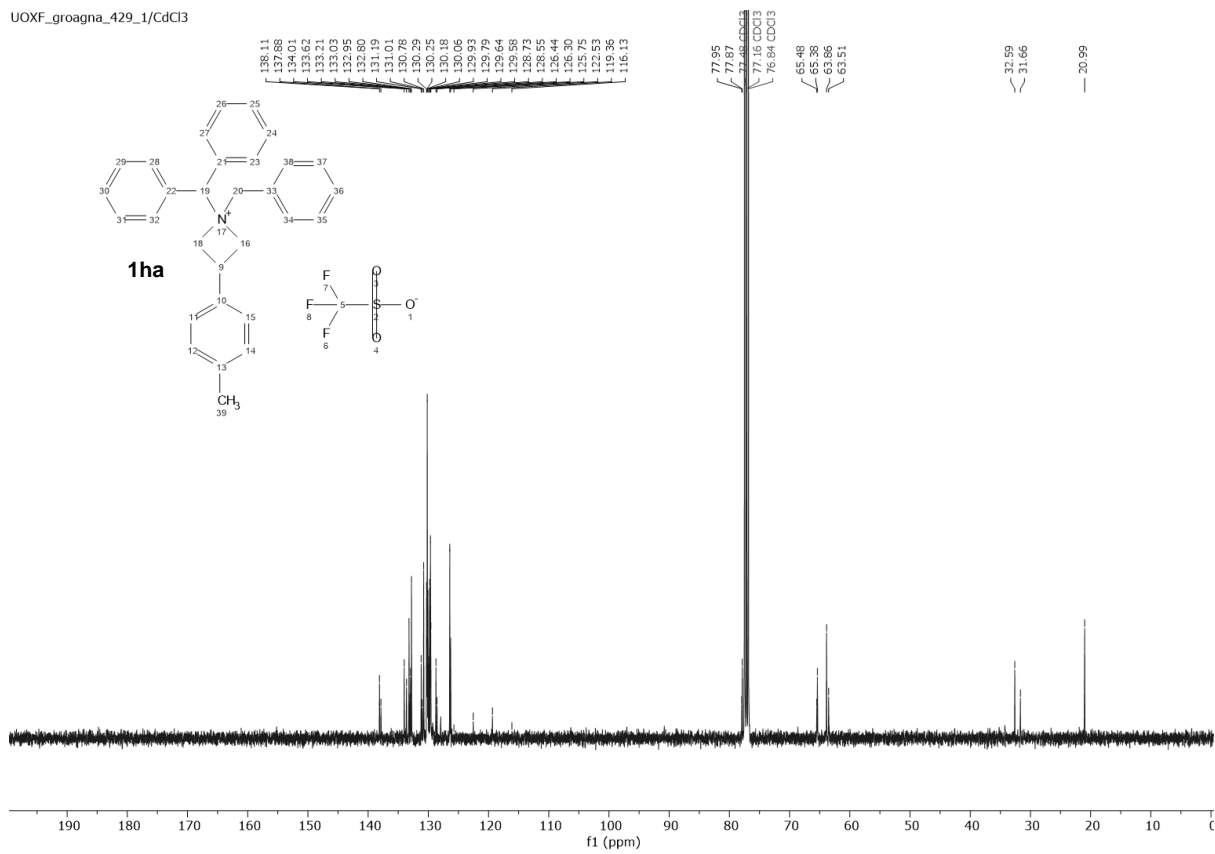
UOXF_groagna_429_1/CdCl3



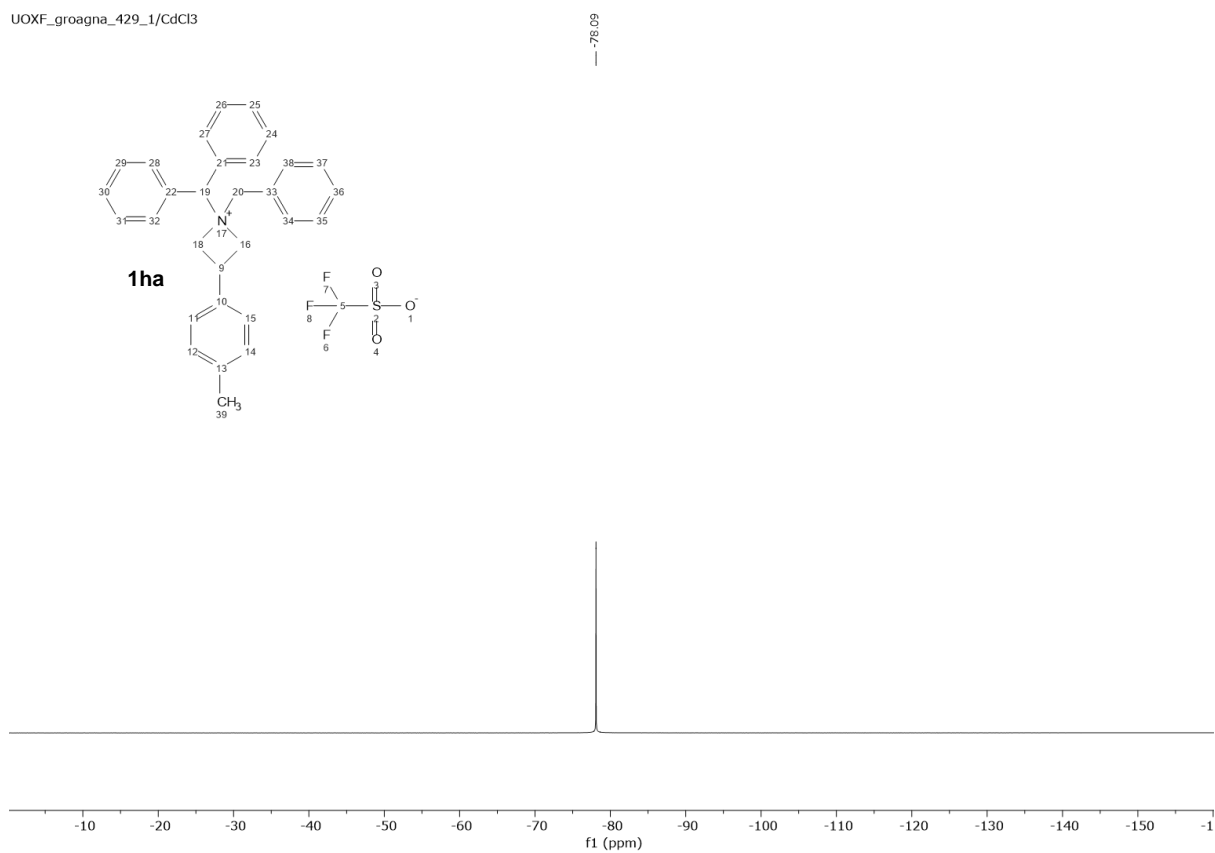
Indirect correlation



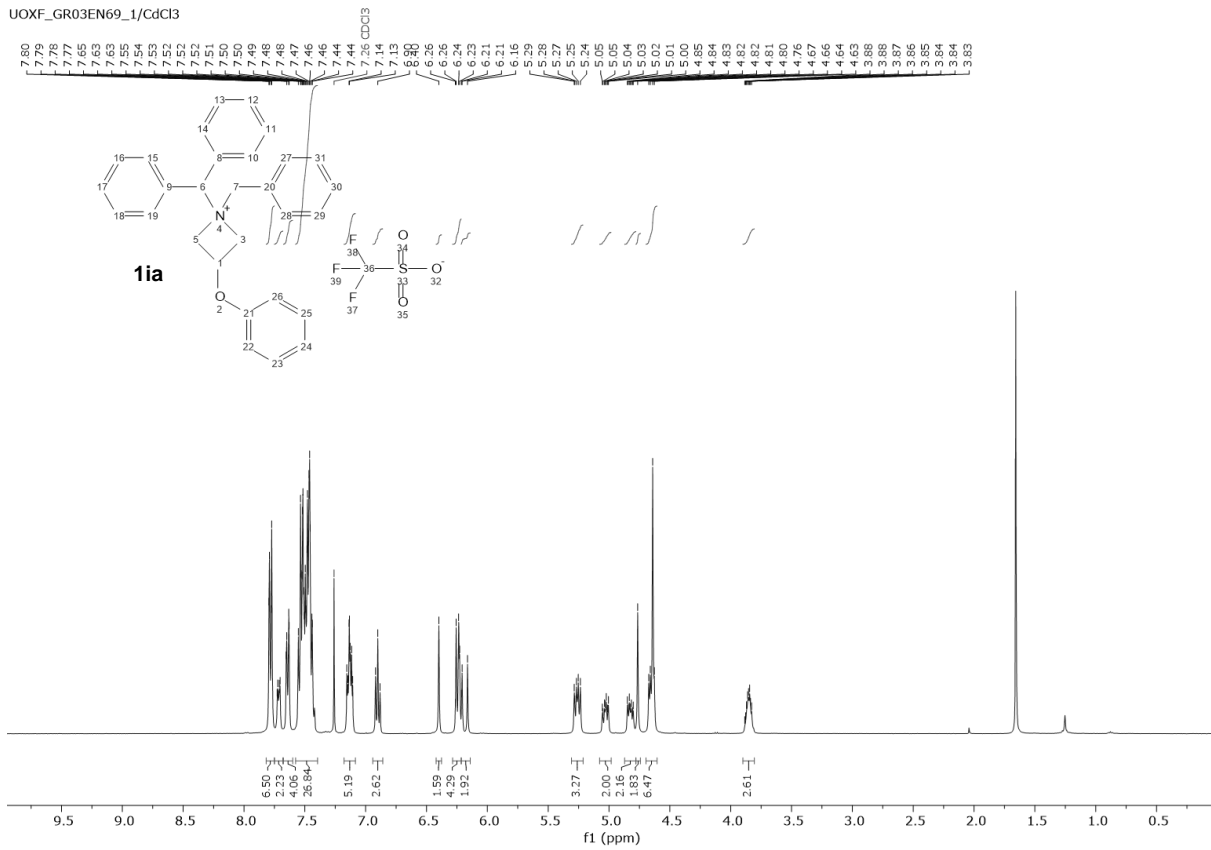
UOXF_groagna_429_1/CdCl3



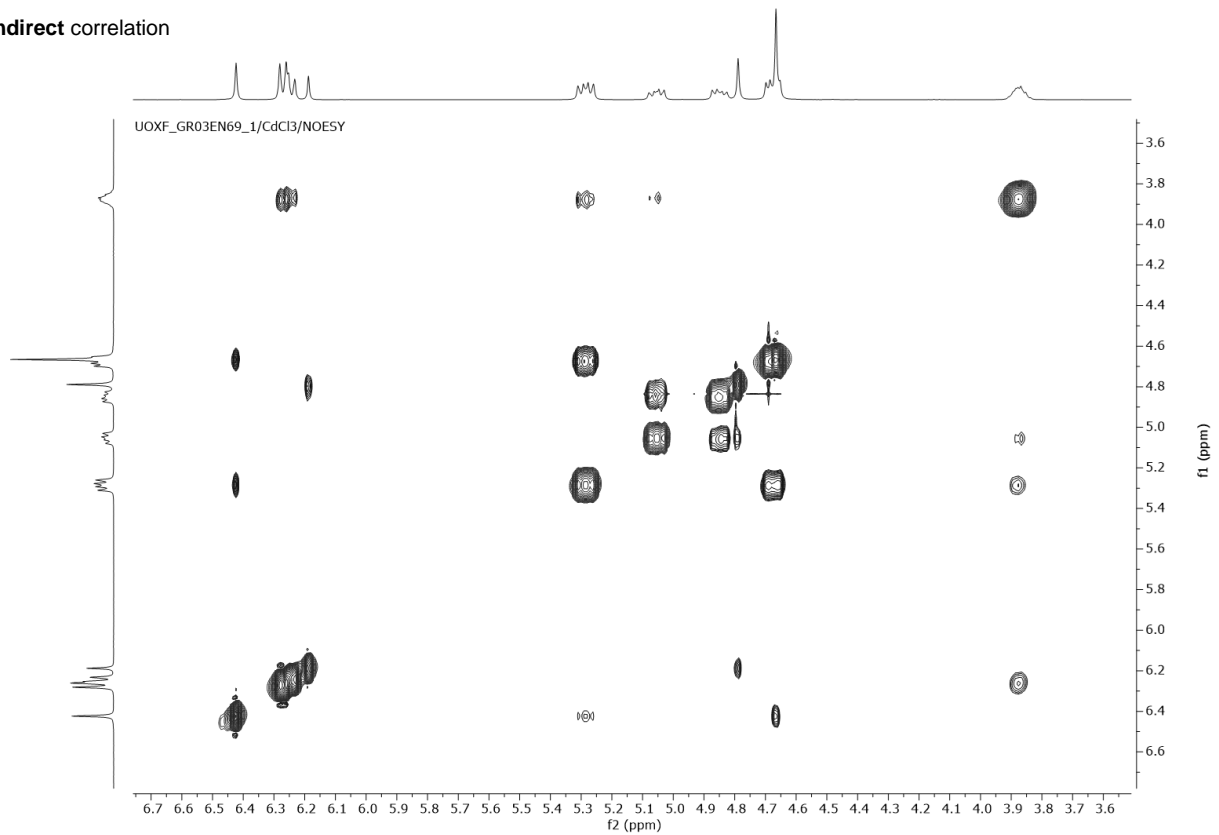
UOXF_groagna_429_1/CdCl3



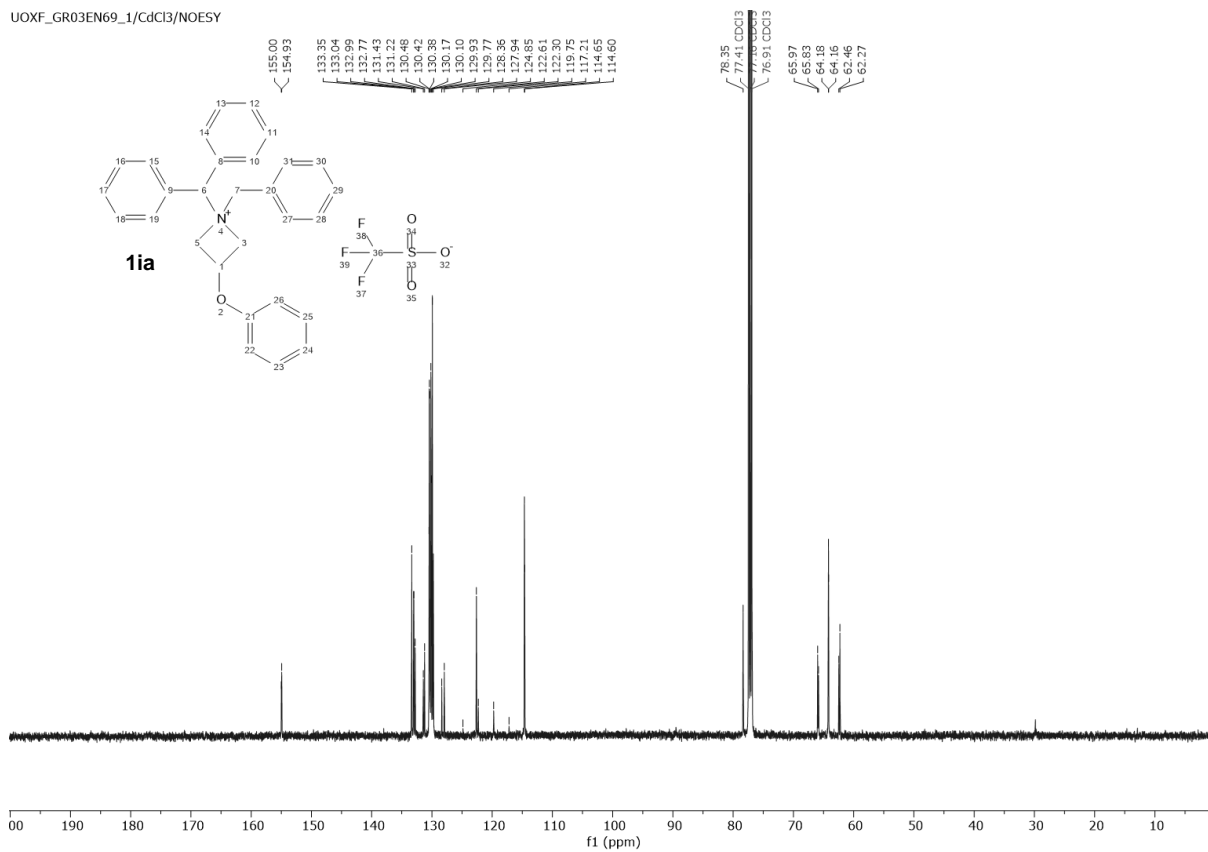
UOXF_GR03EN69_1/CdCl3



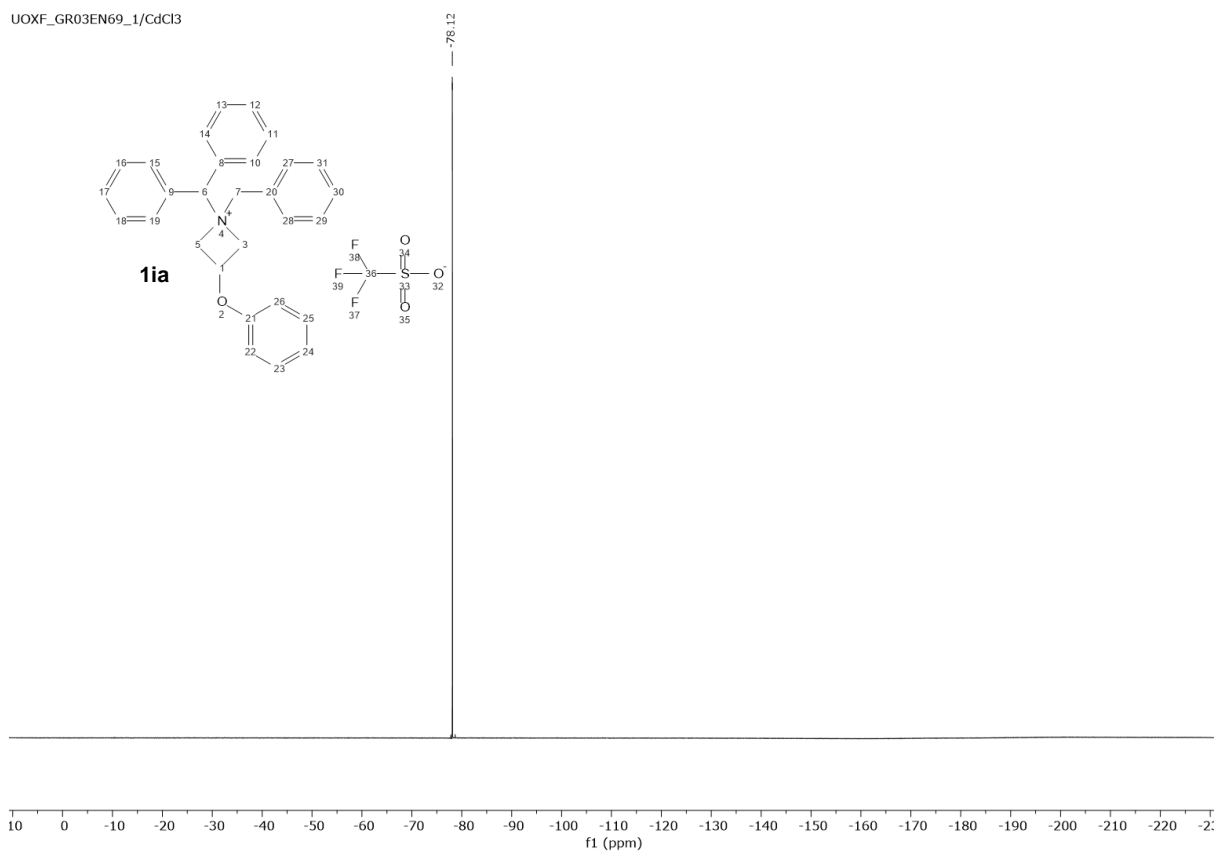
Indirect correlation

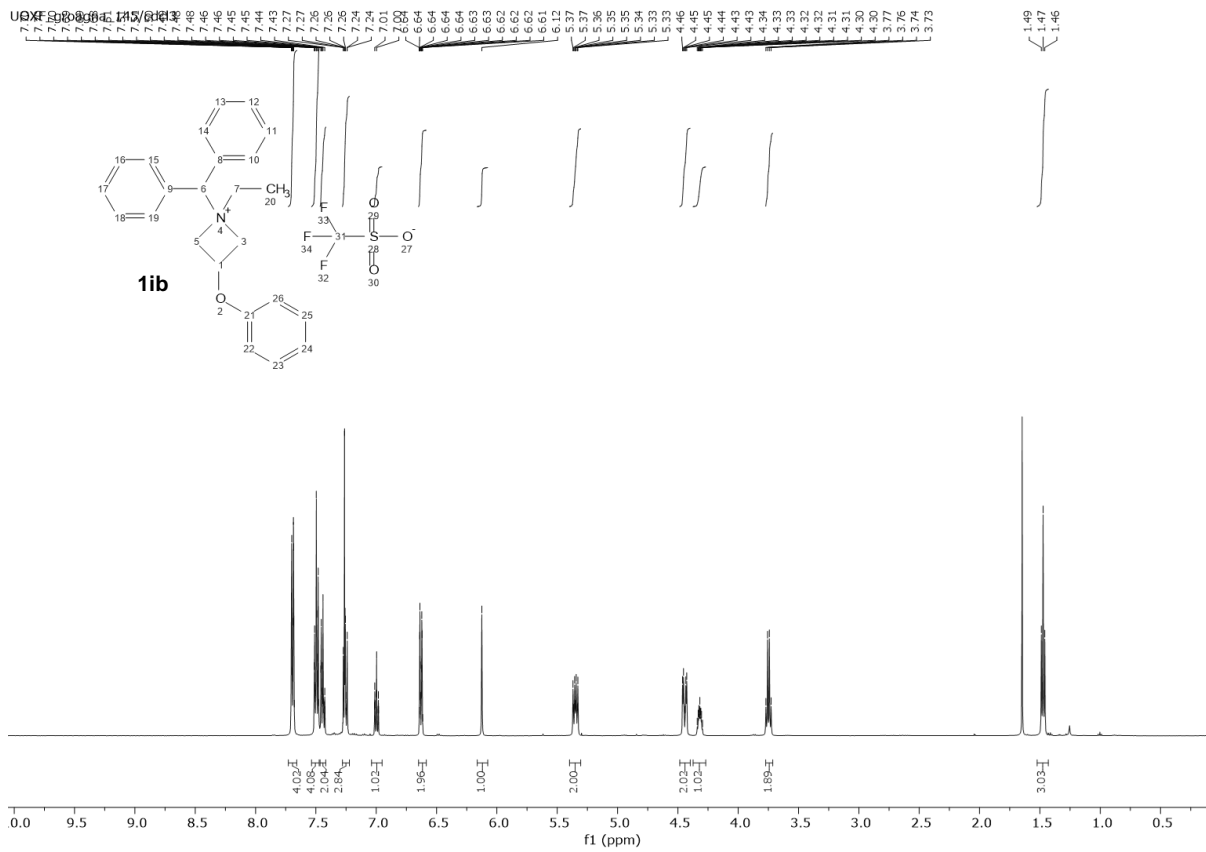


UOXF_GR03EN69_1/CdCl3/NOESY

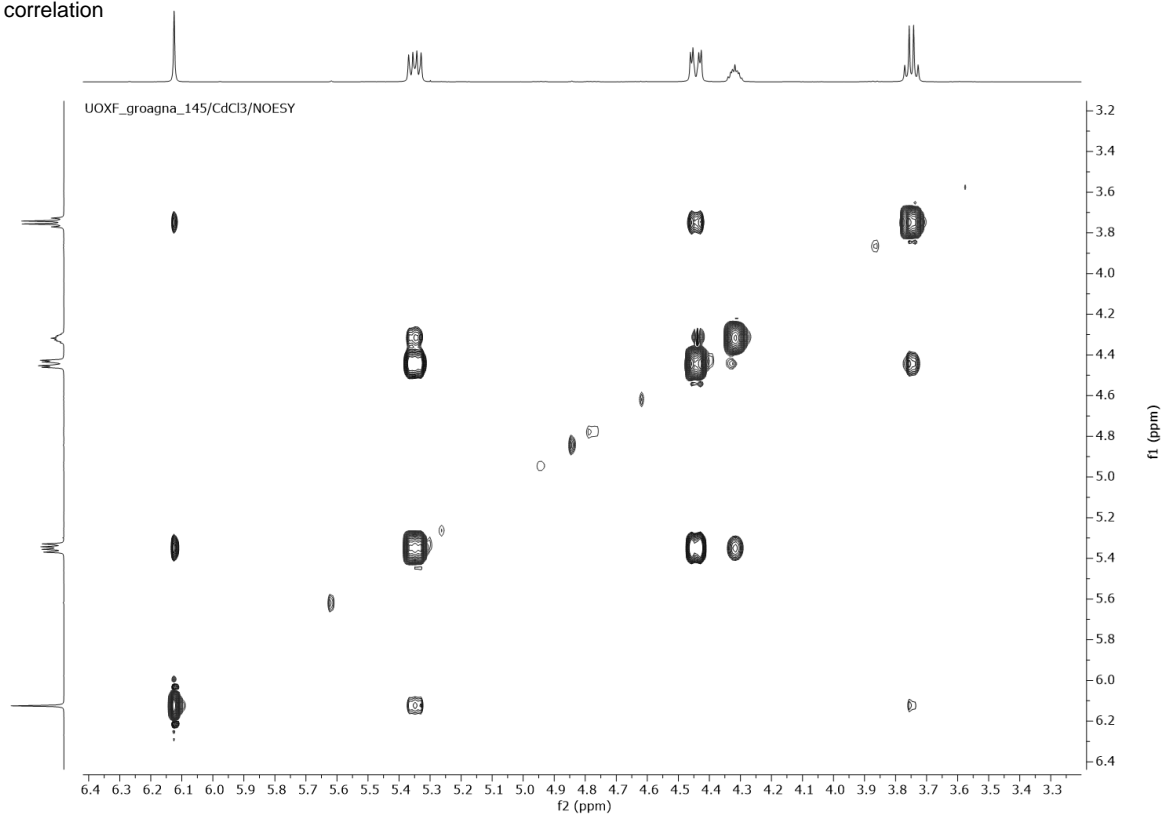


UOXF_GR03EN69_1/CdCl3

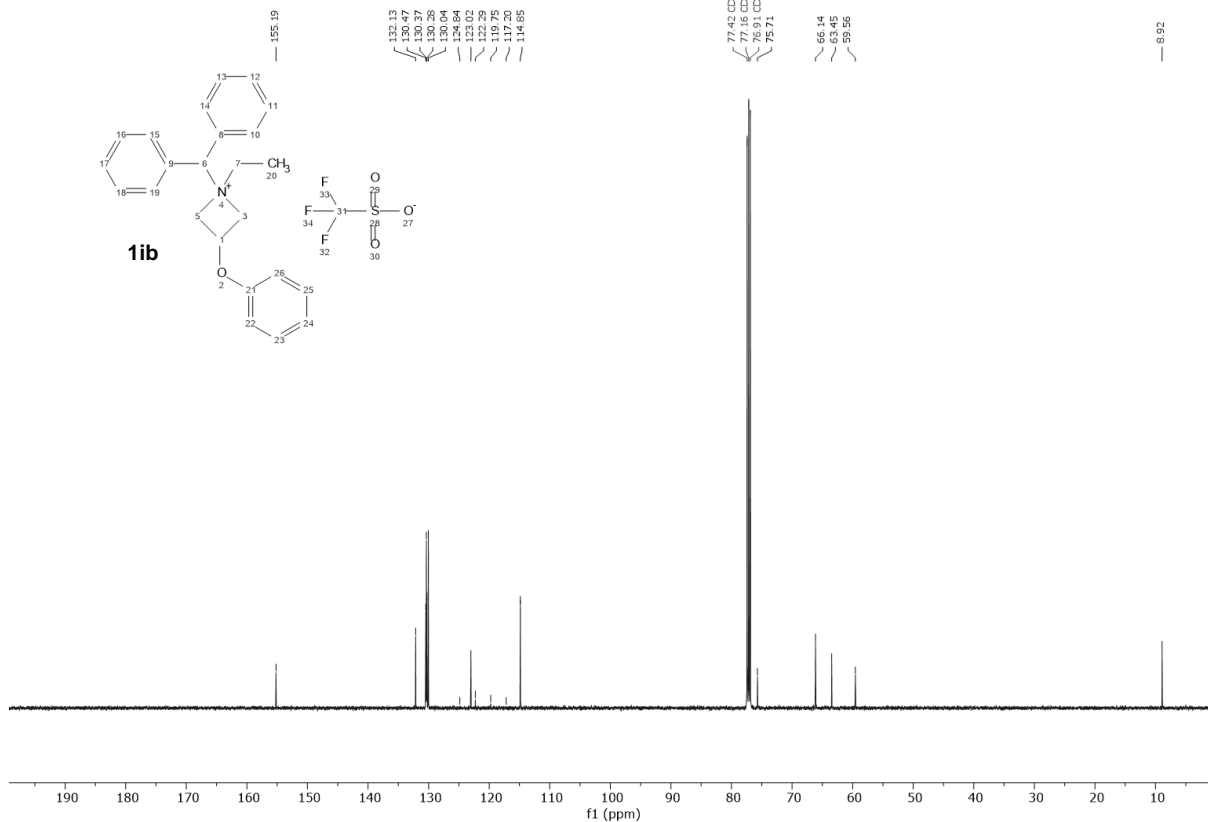




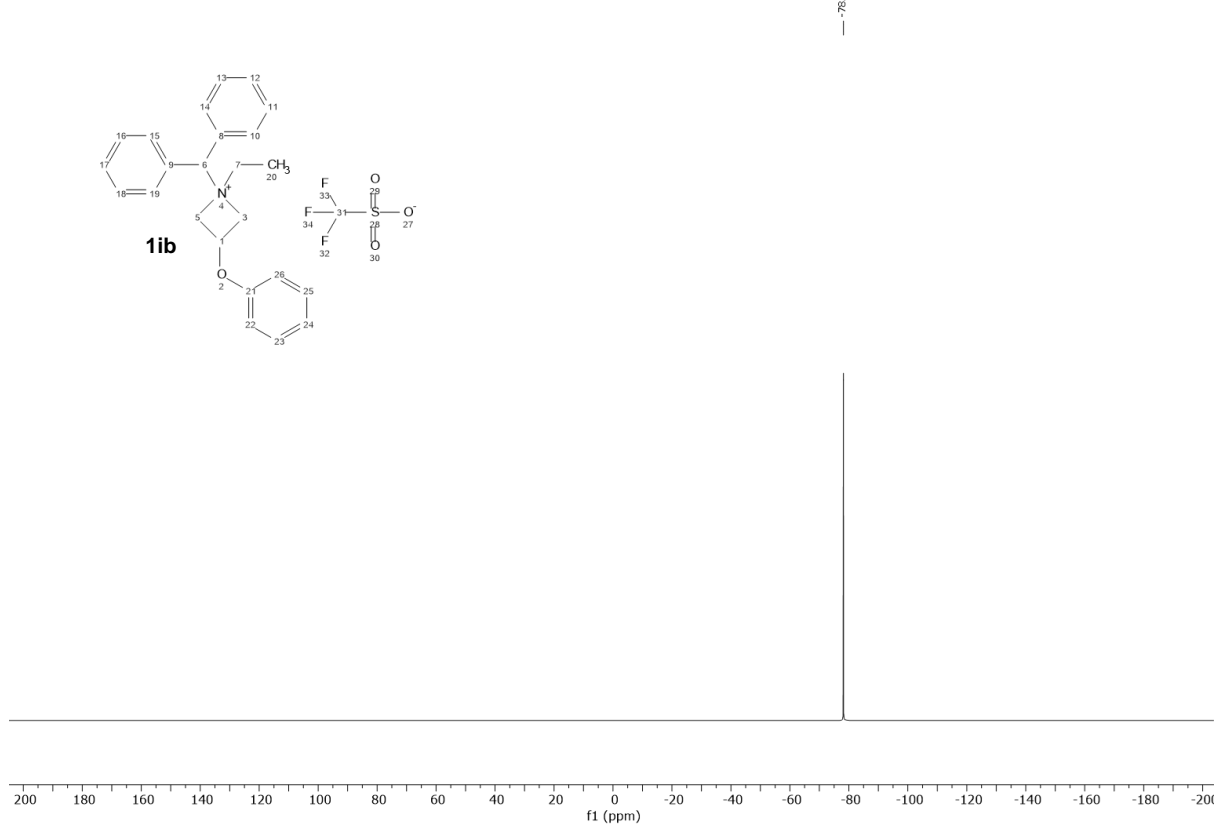
Direct correlation



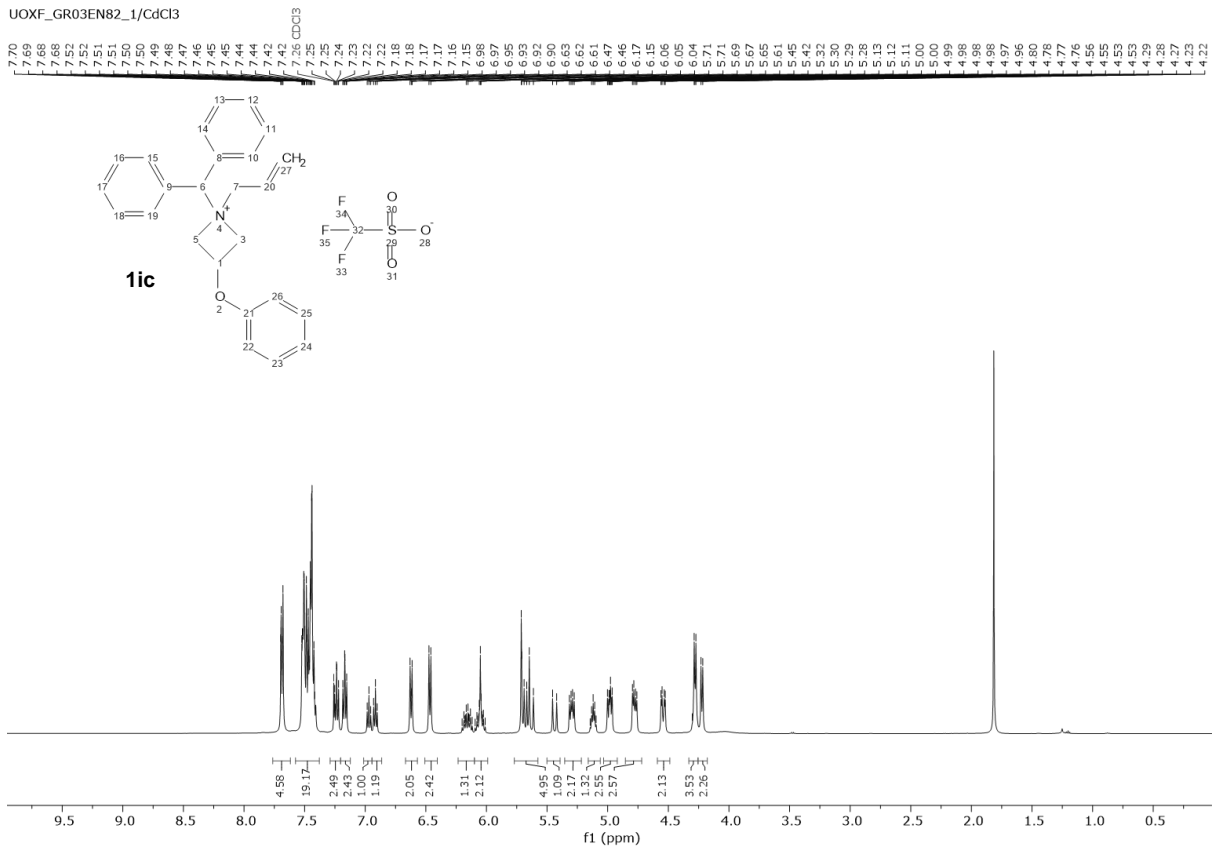
UOXF_groagna_145_1/CdCl3



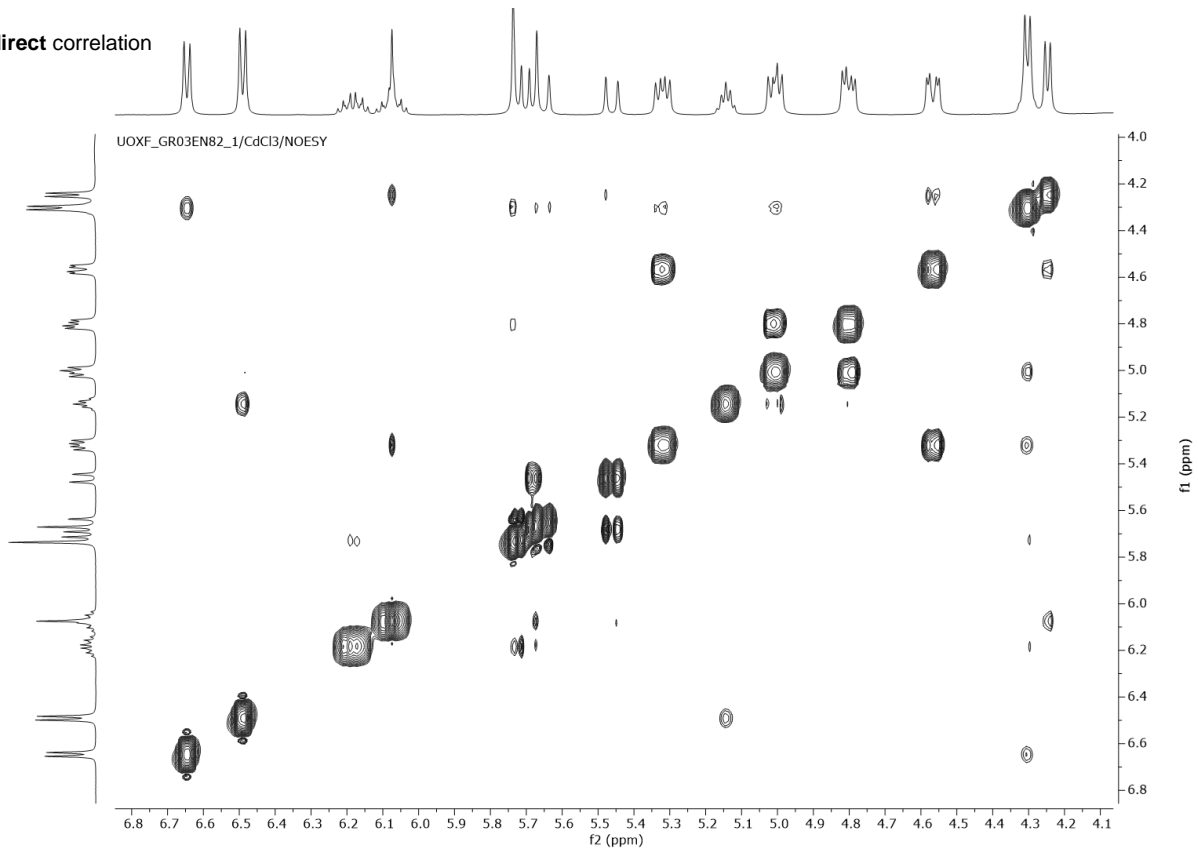
UOXF_groagna_145_1/CdCl3



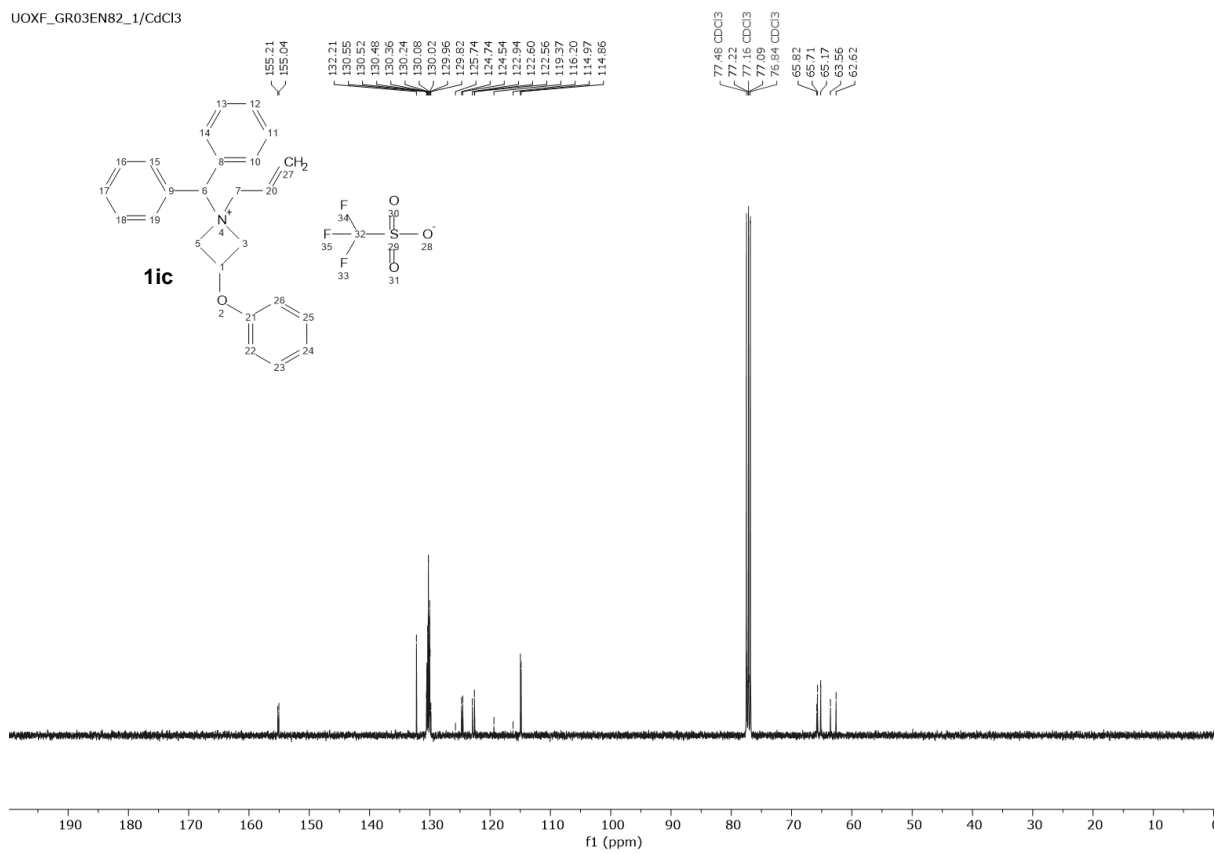
UOXF_GR03EN82_1/CdCl3



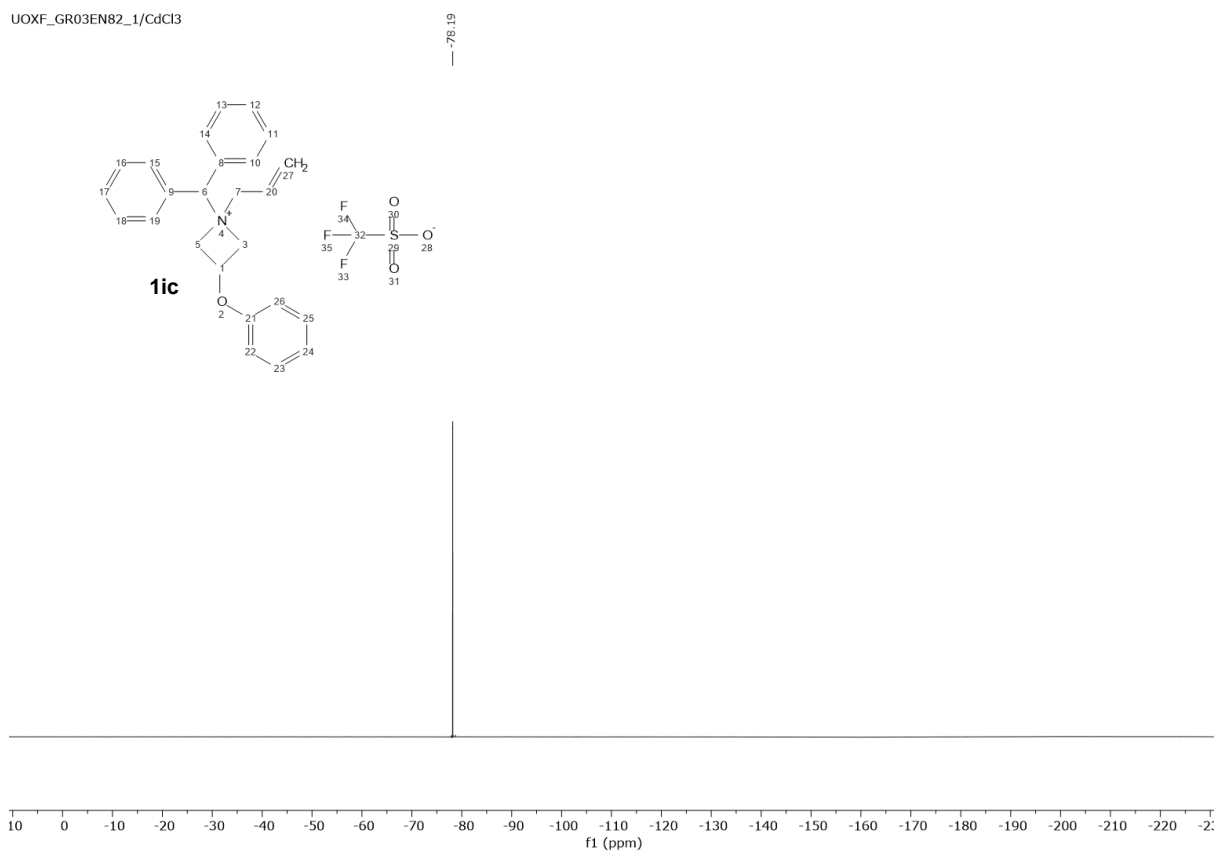
Indirect correlation



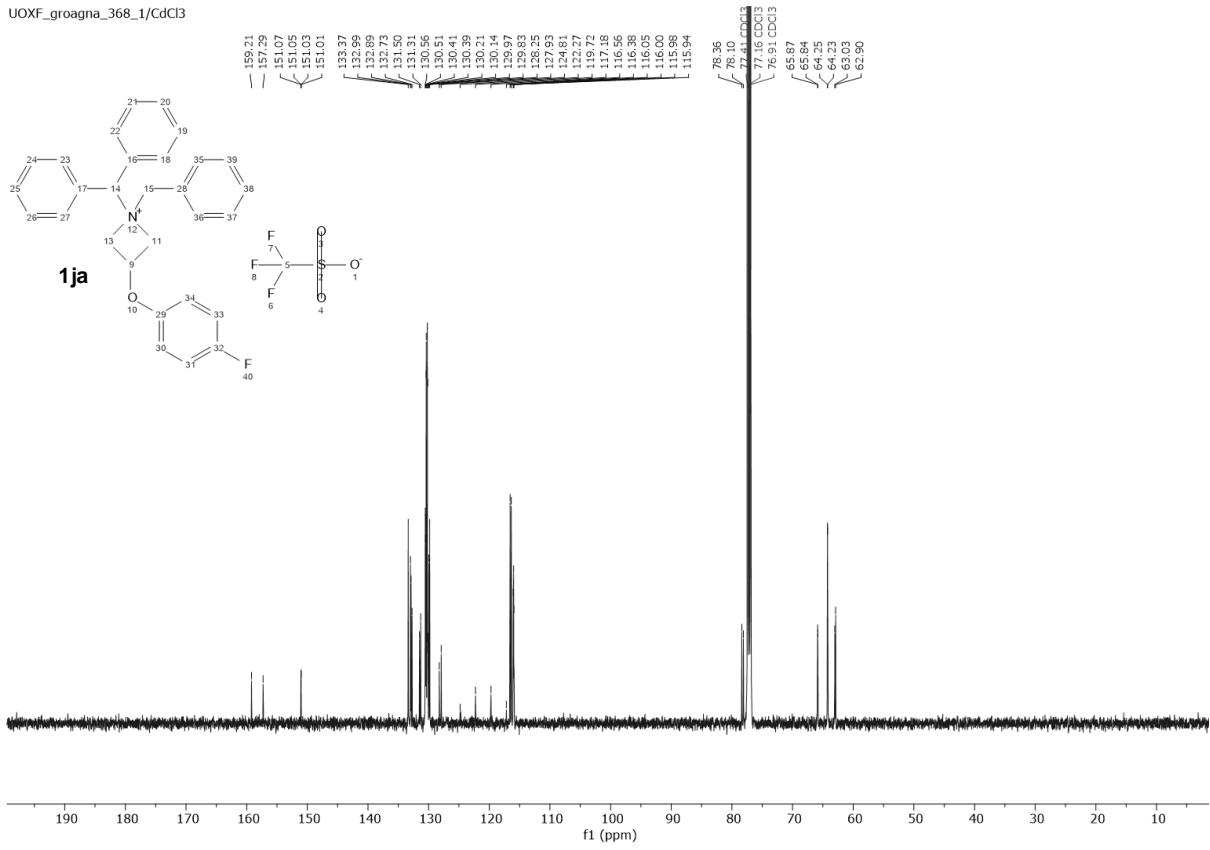
UOXF_GR03EN82_1/CdCl3



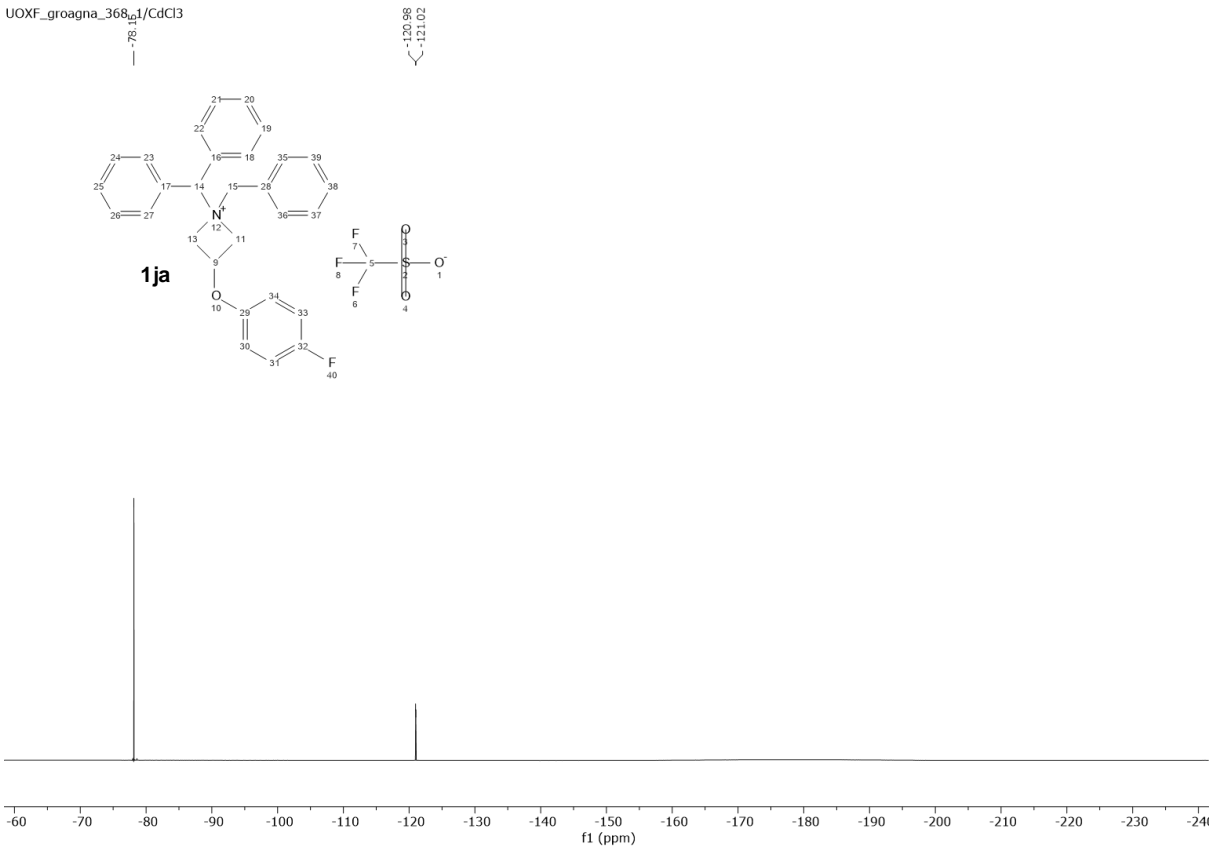
UOXF_GR03EN82_1/CdCl3



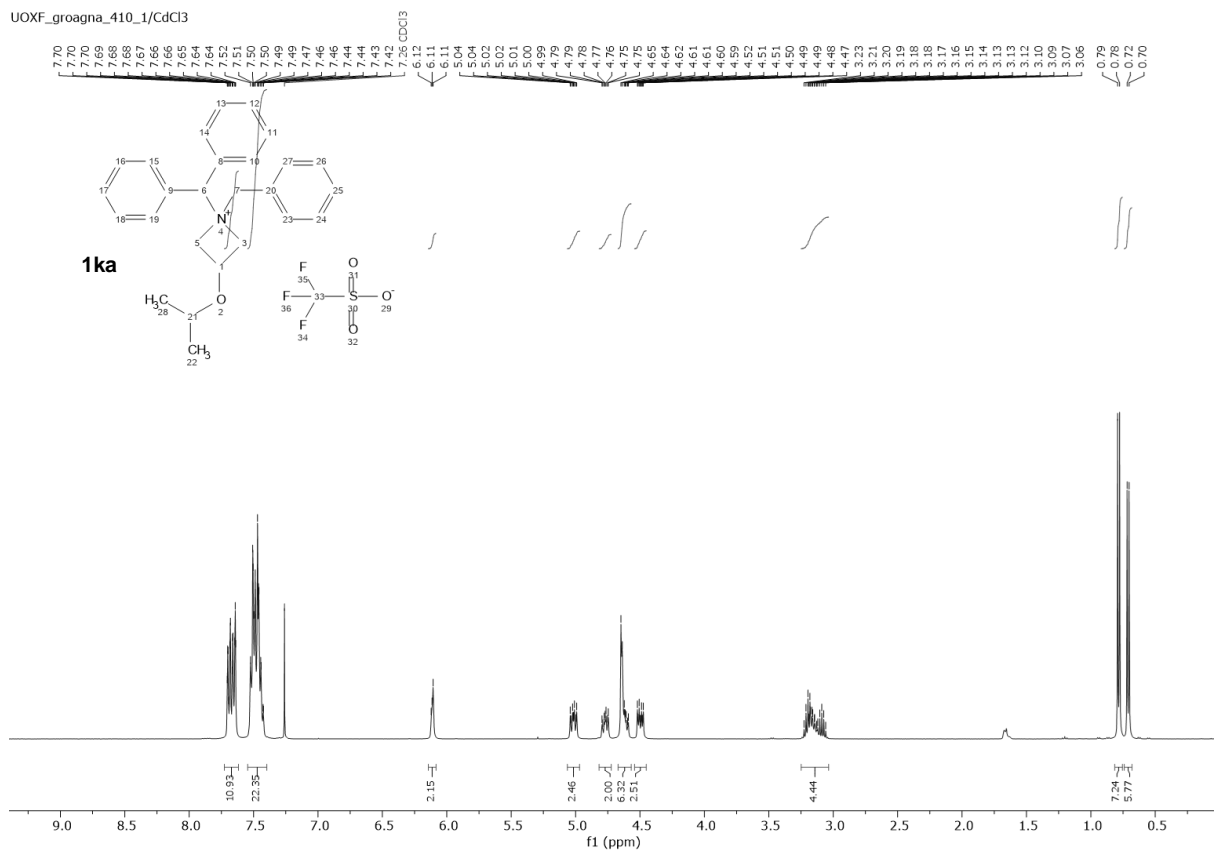
UOXF_groagna_368_1/CdCl3



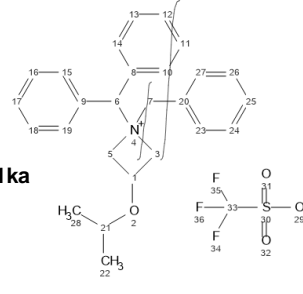
UOXF_groagna_368_1/CdCl3



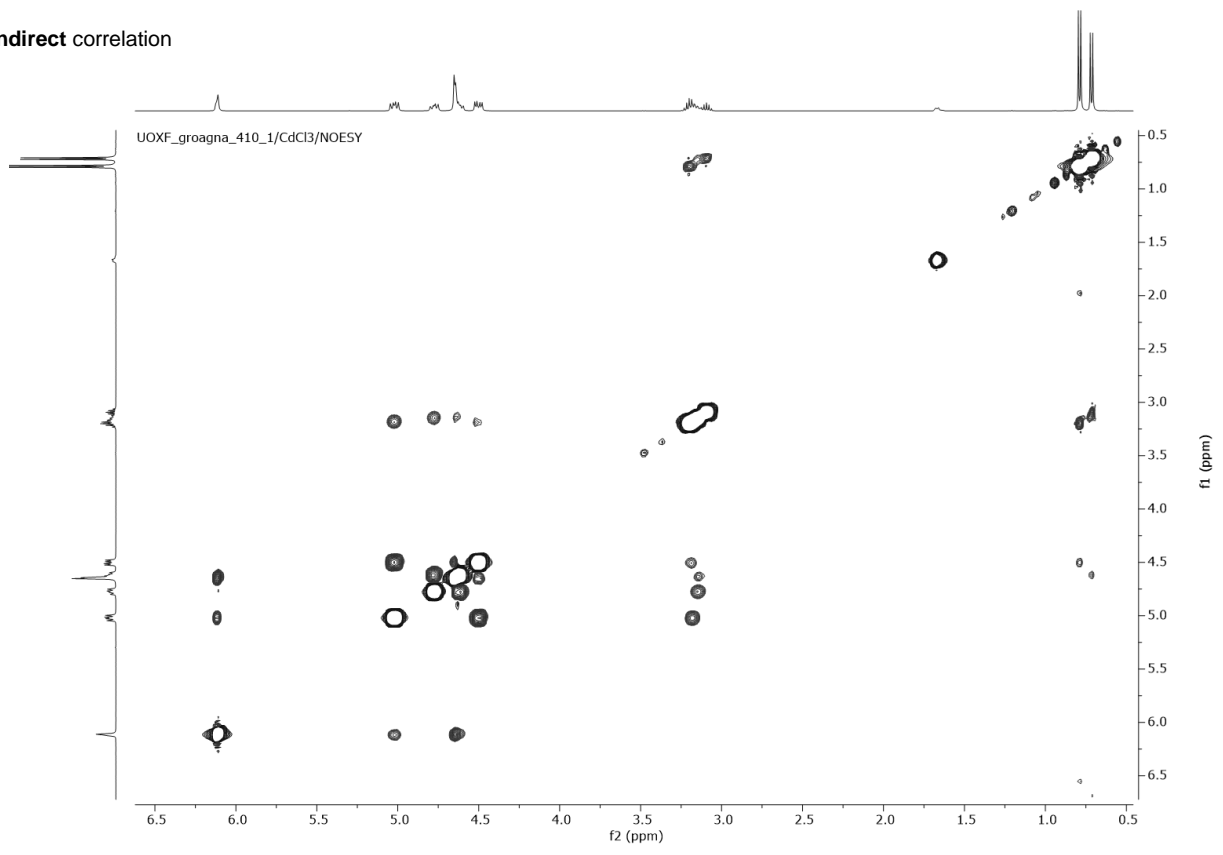
UOXF_groagna_410_1/CdCl3



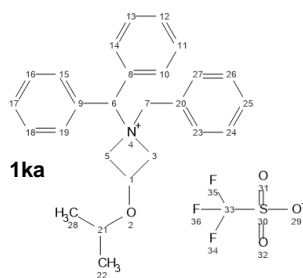
1ka



Indirect correlation



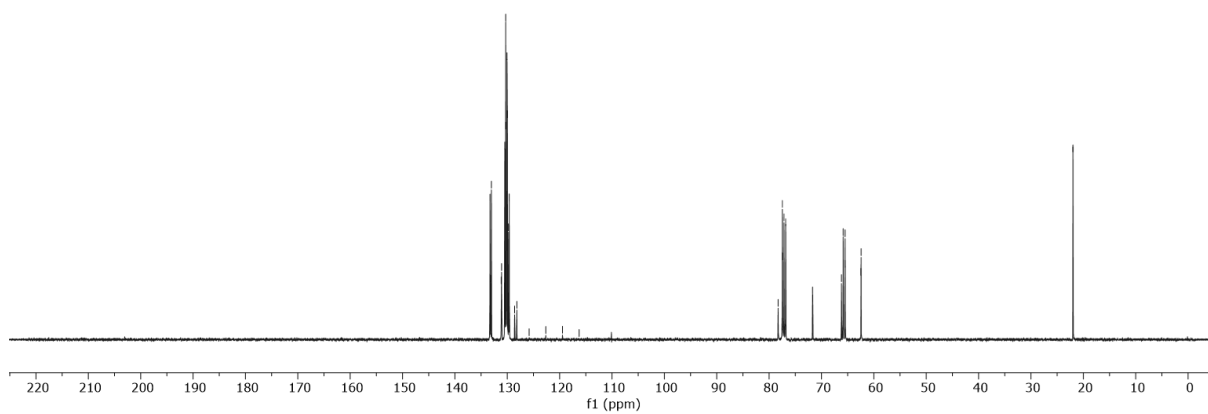
UOXF_groagna_410_1/CdCl3



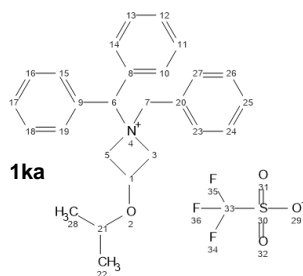
133.30
133.20
133.04
131.16
131.10
130.48
130.31
130.29
130.06
129.98
129.76
129.63
128.61
128.58
125.83
122.65
119.47
116.29

78.28
77.48 CDCl3
77.45
77.16 CDCl3
76.84 CDCl3
71.71
66.19
65.87
65.52
65.50
62.48
62.45

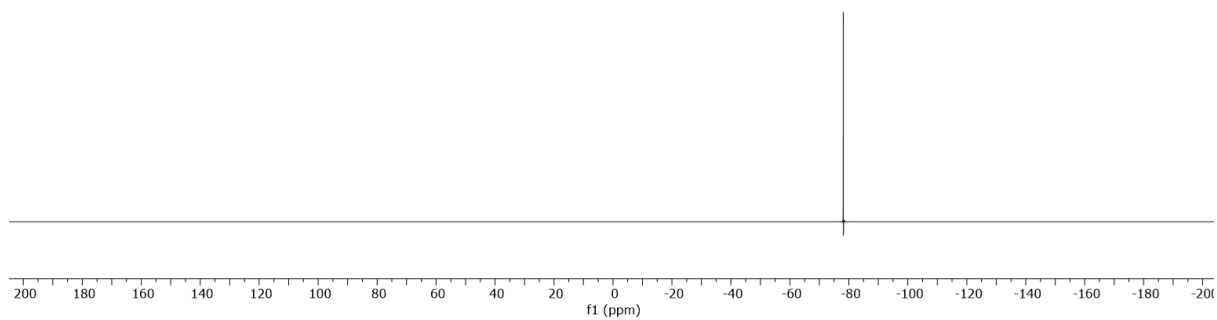
— 21.99

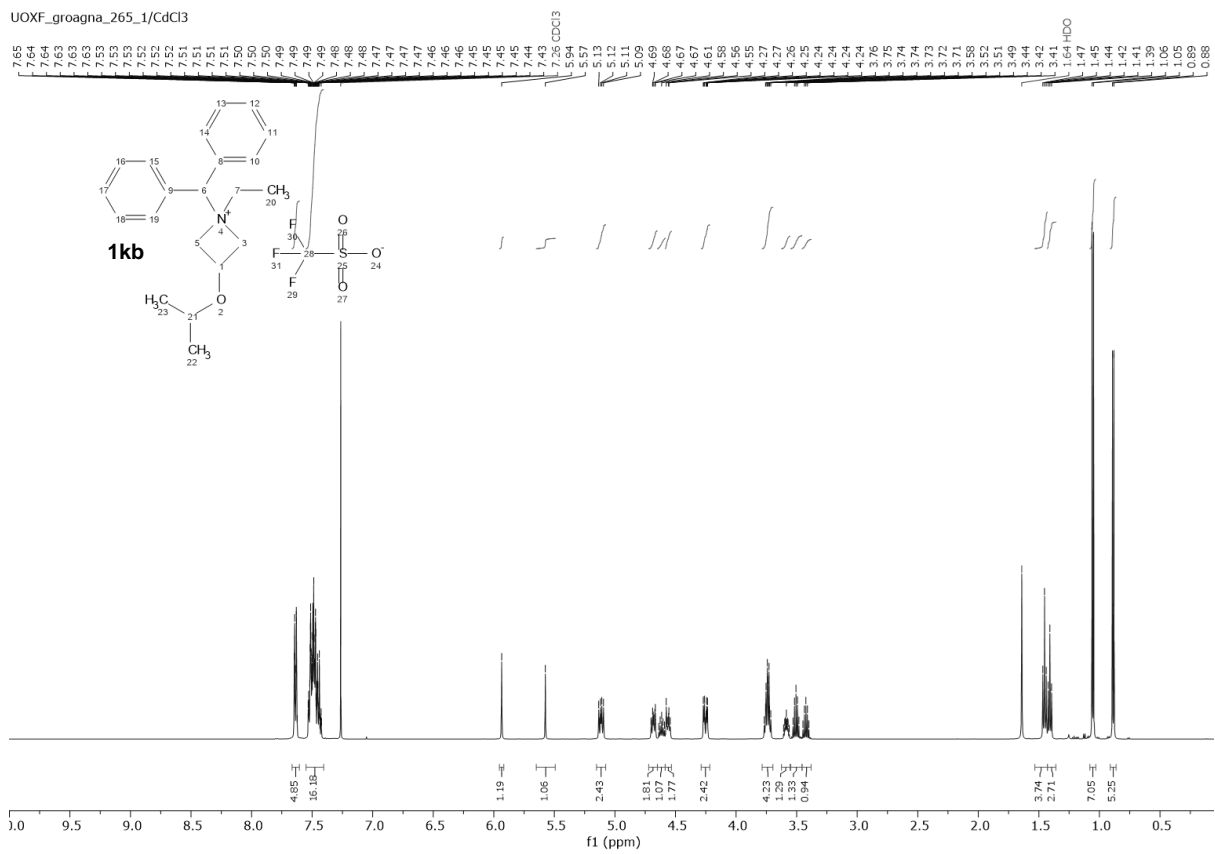


UOXF_groagna_410_1/CdCl3

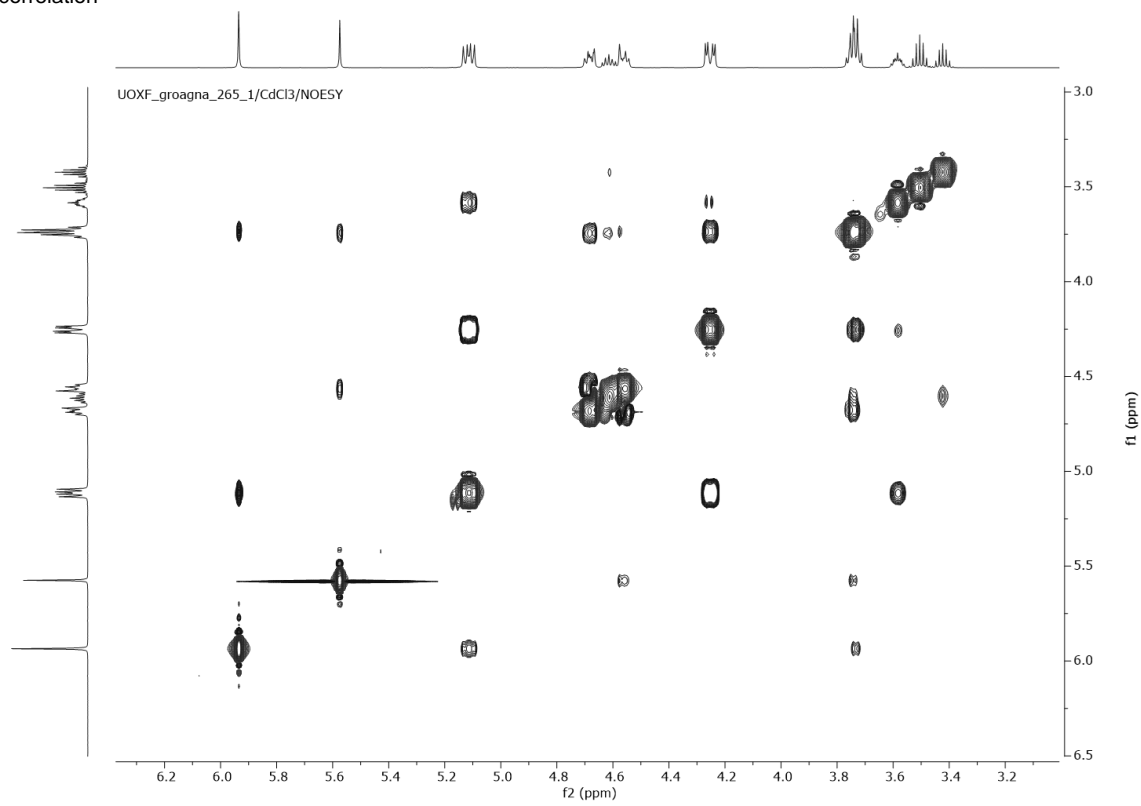


— 78.14

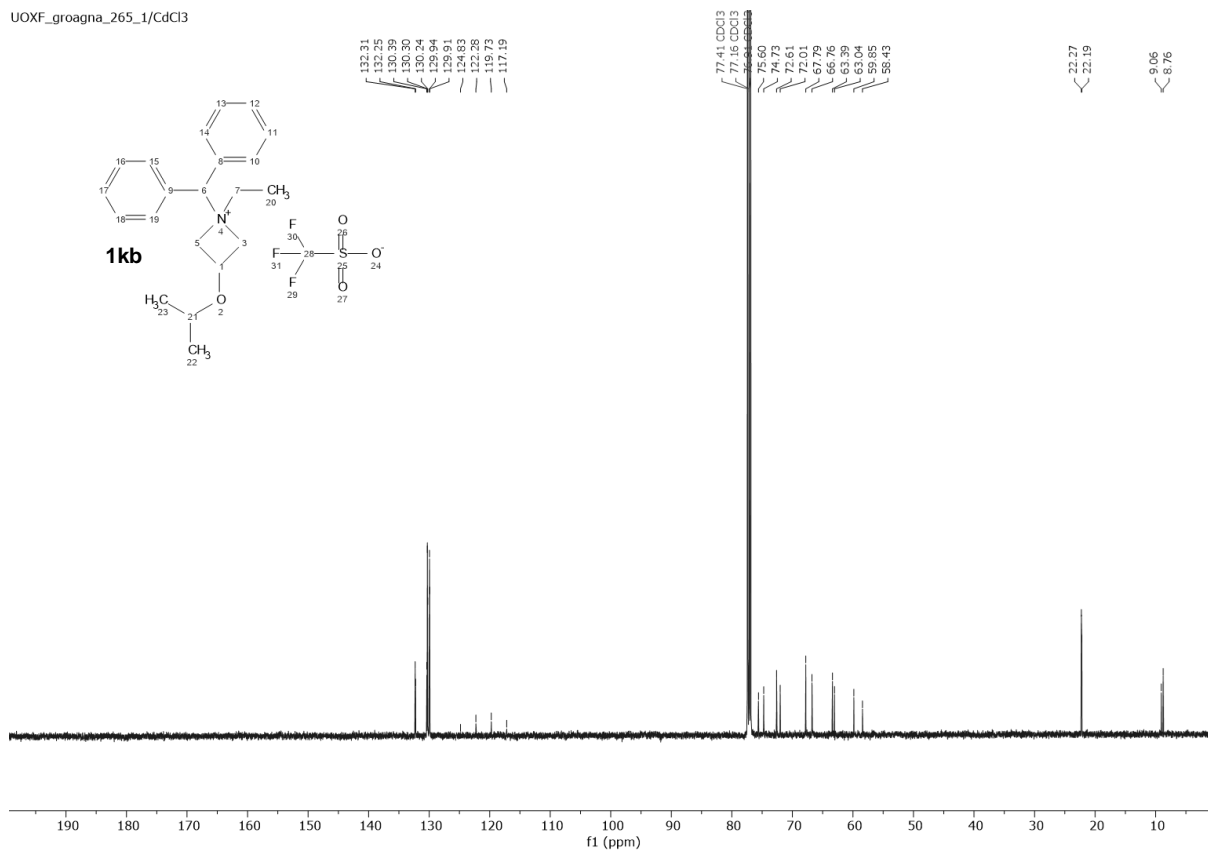




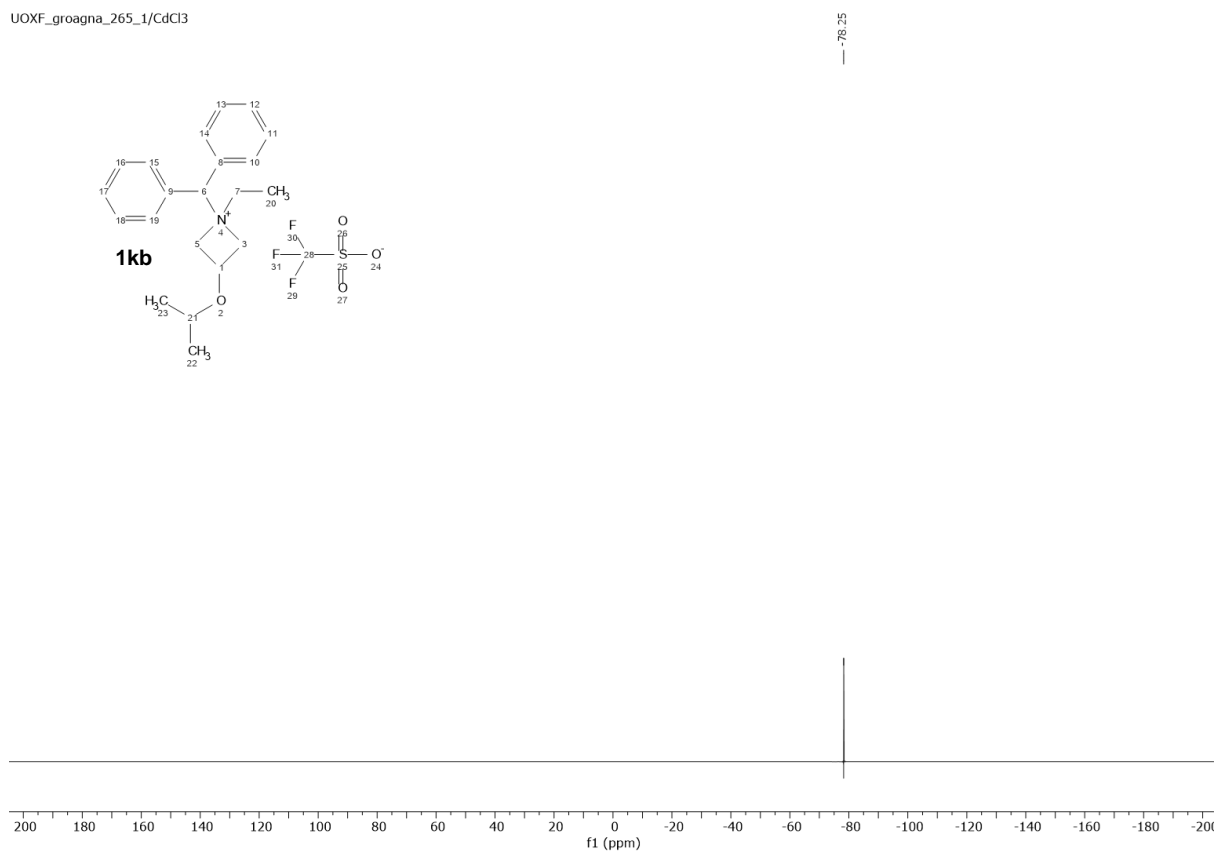
Indirect correlation

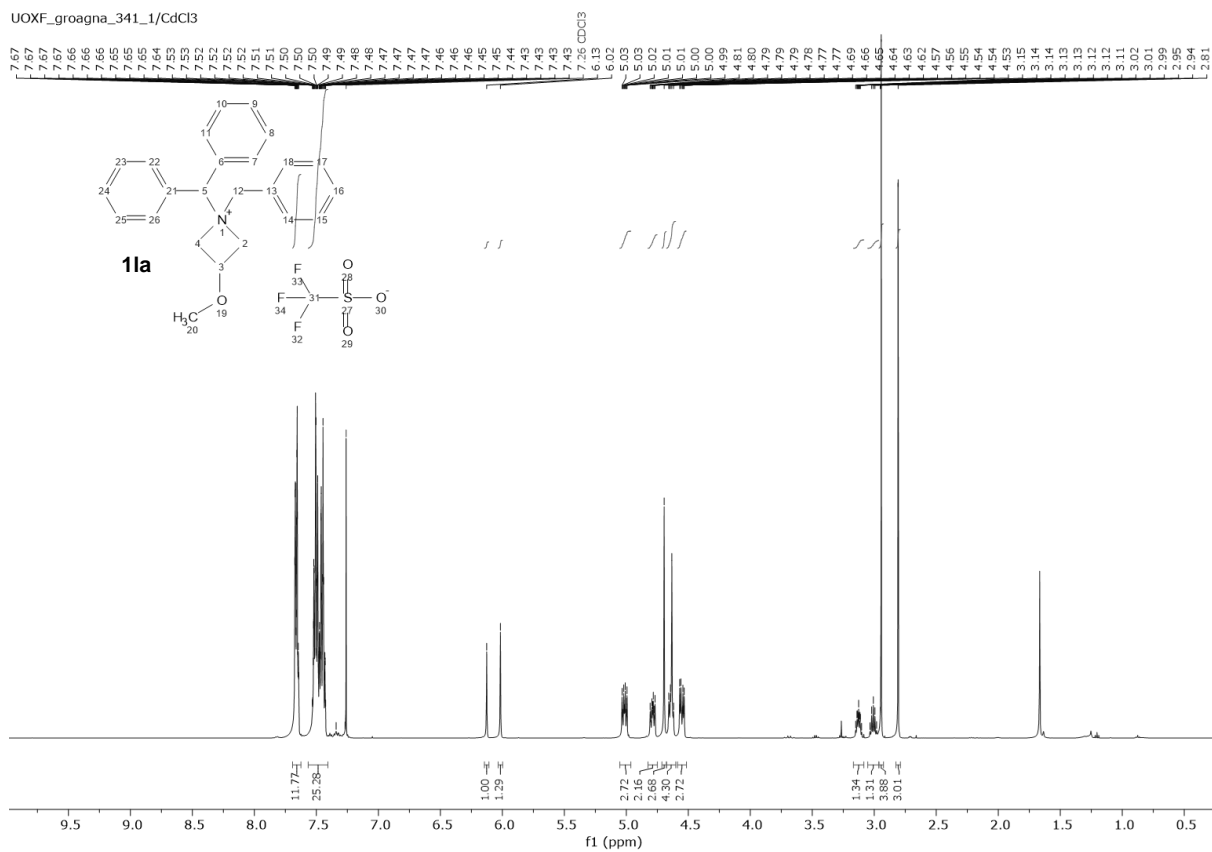


UOXF_groagna_265_1/CdCl3

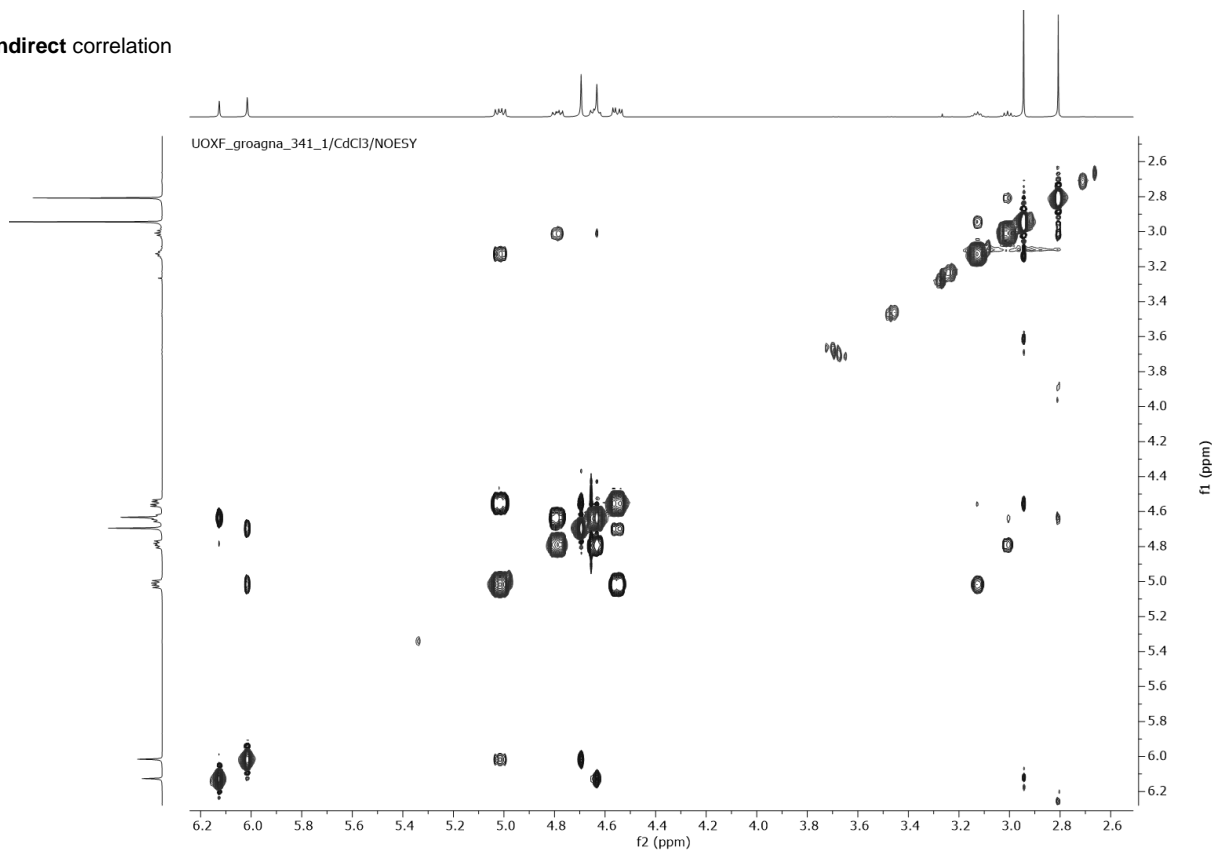


UOXF_groagna_265_1/CdCl3

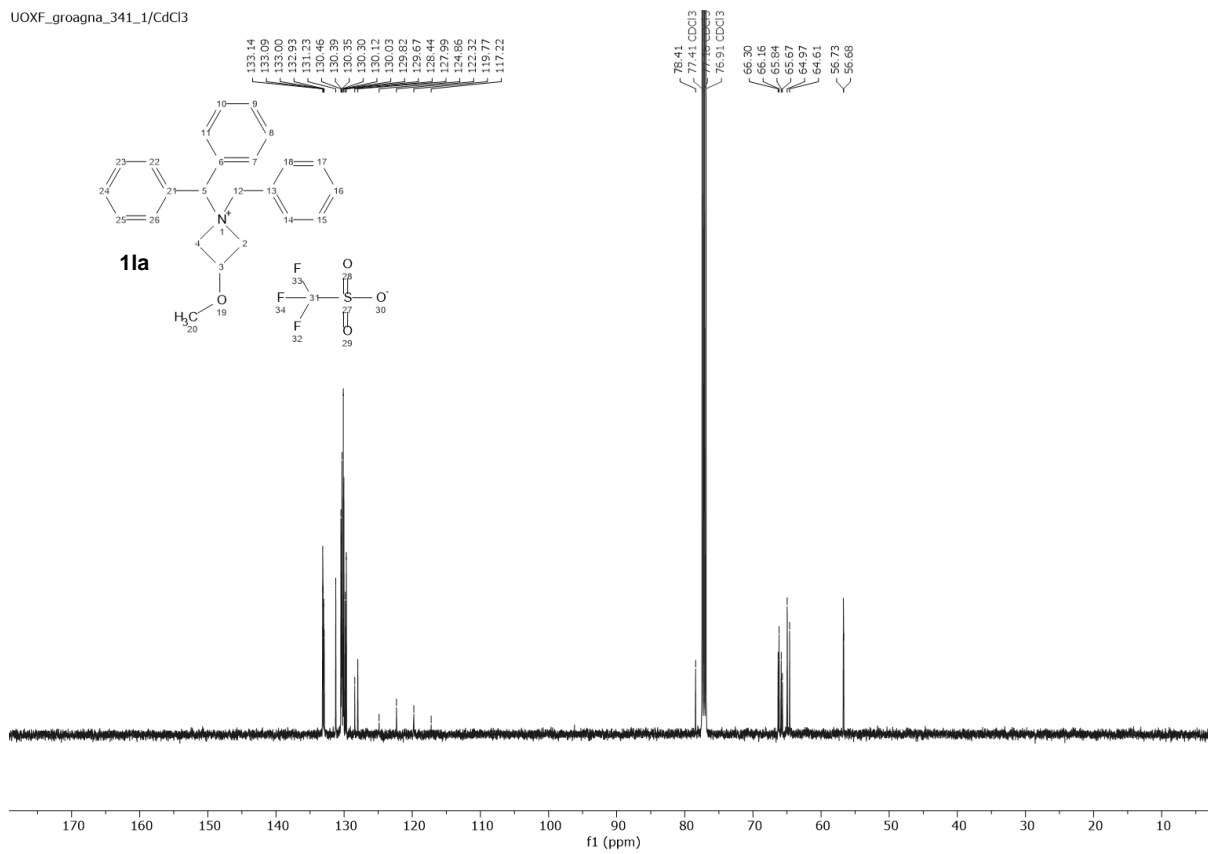




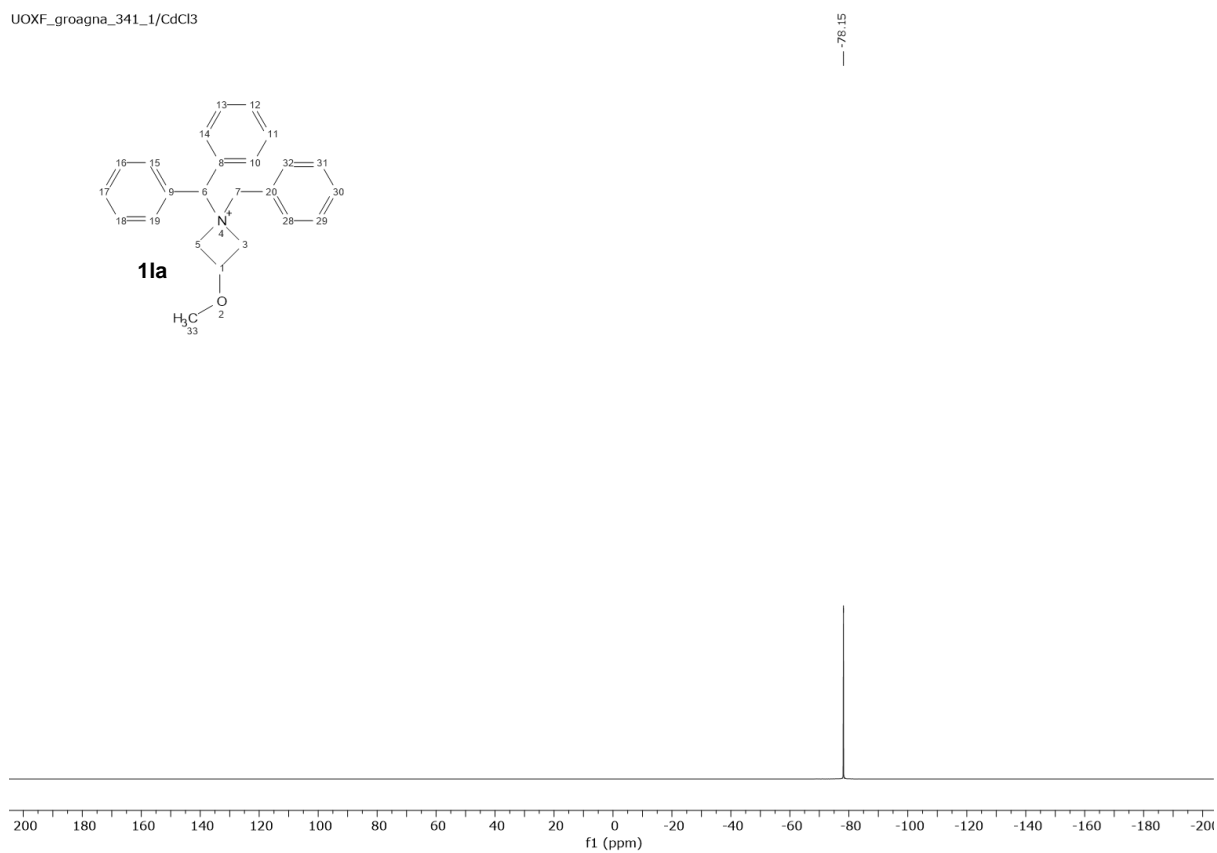
Indirect correlation

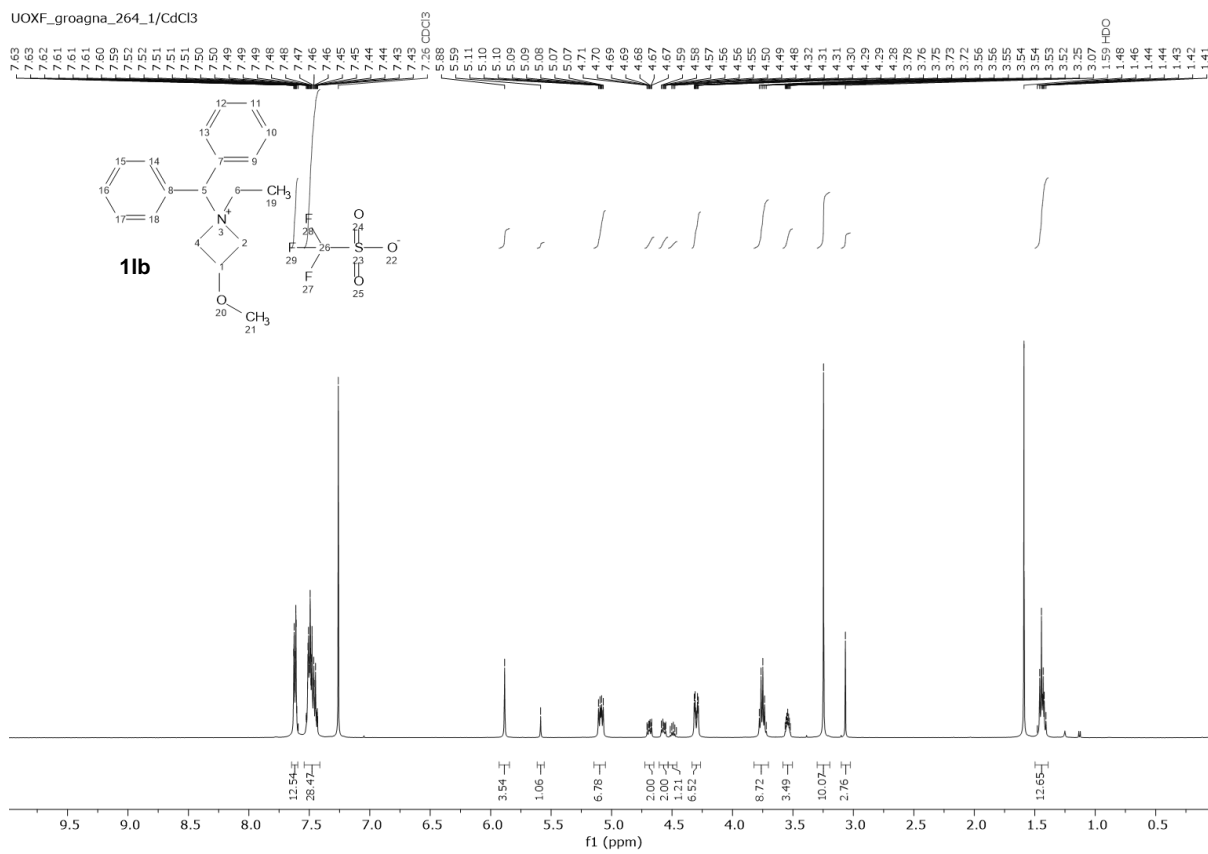


UOXF_groagna_341_1/CdCl3

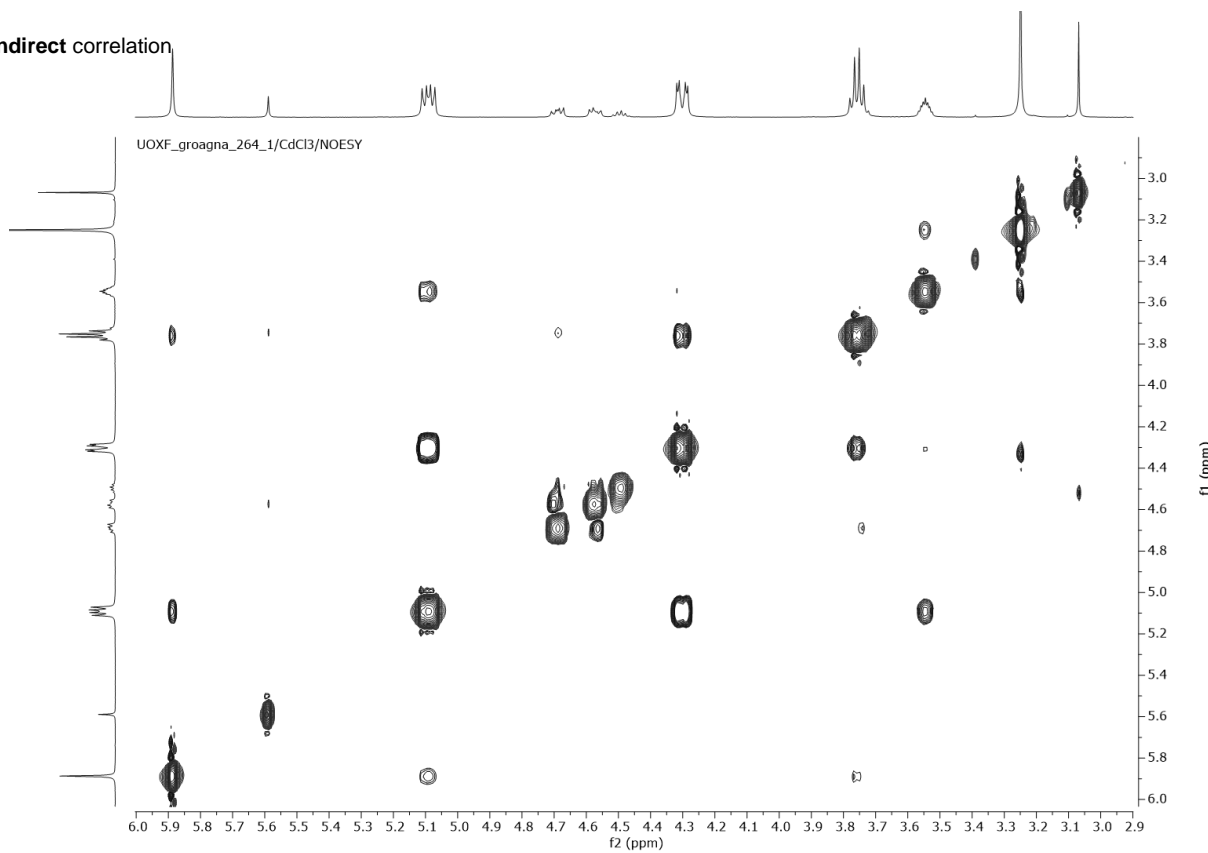


UOXF_groagna_341_1/CdCl3

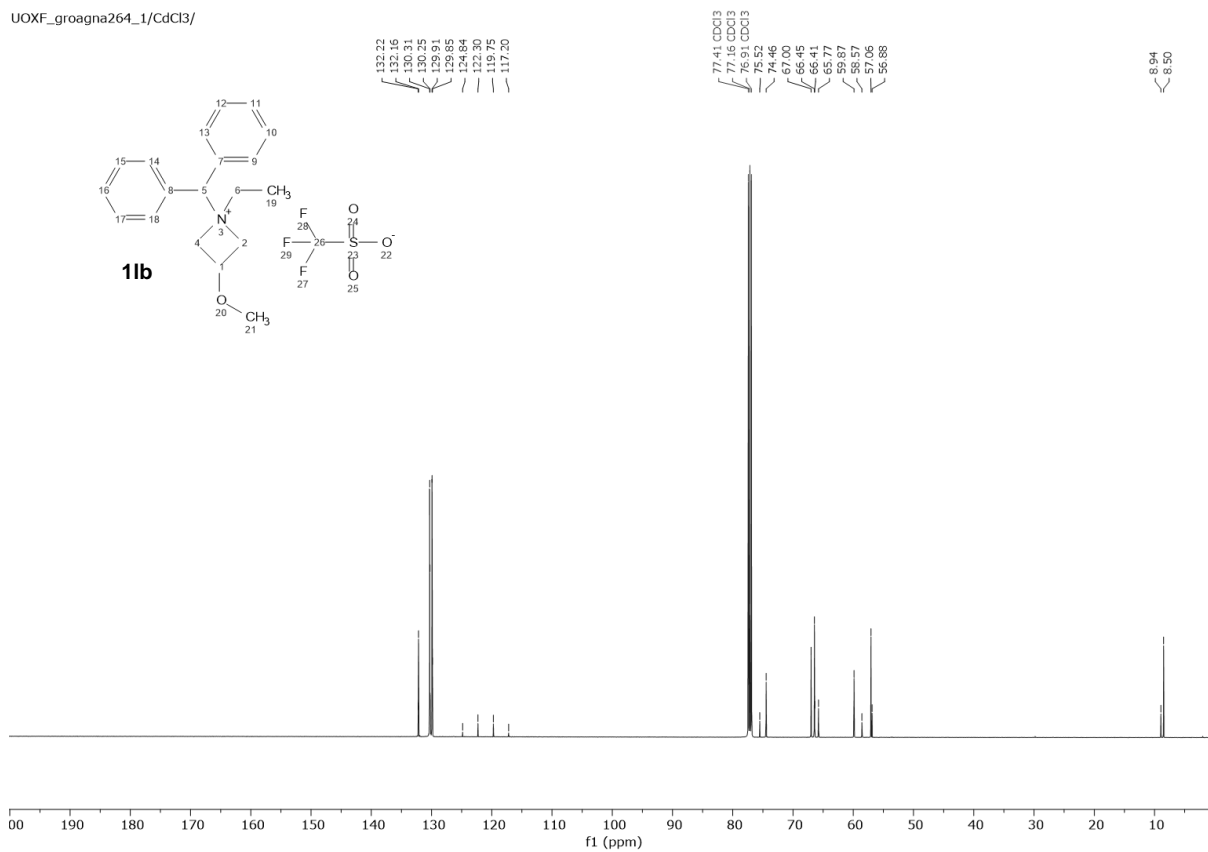




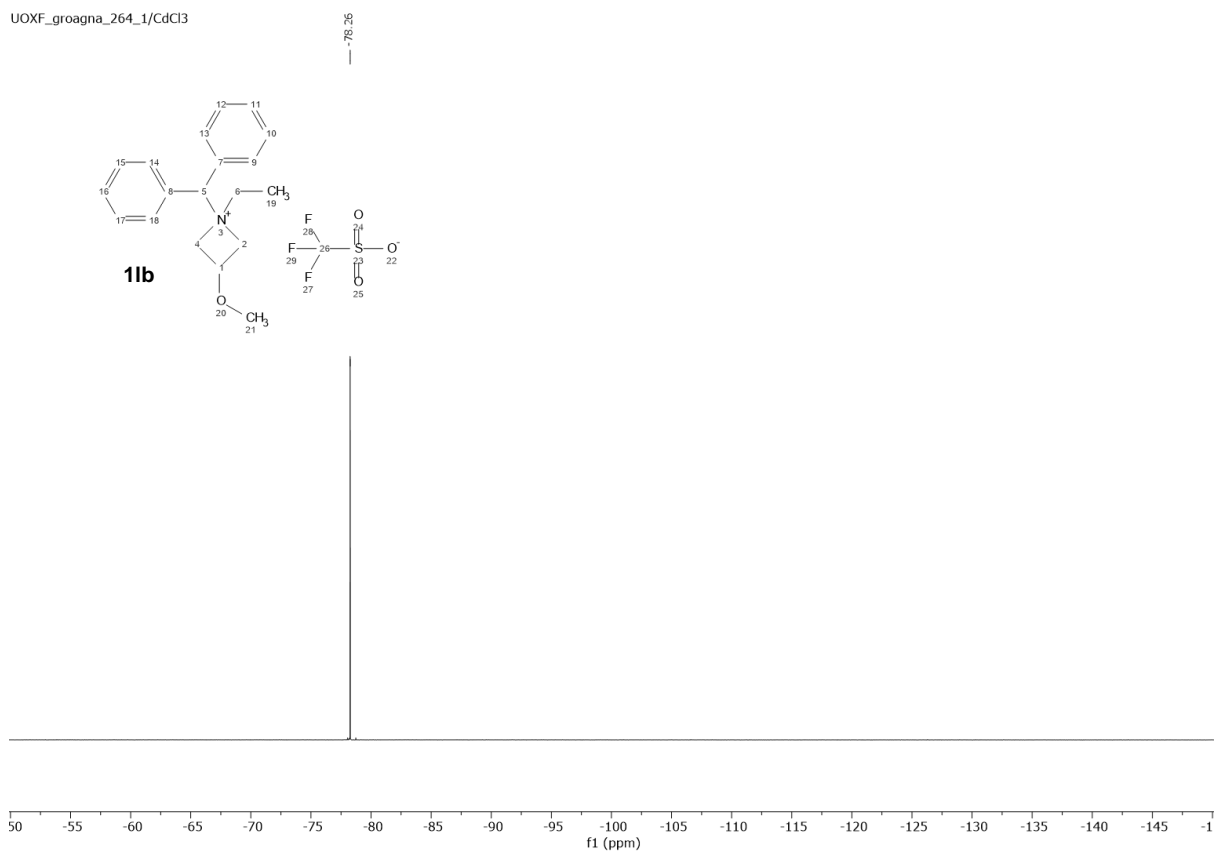
Indirect correlation



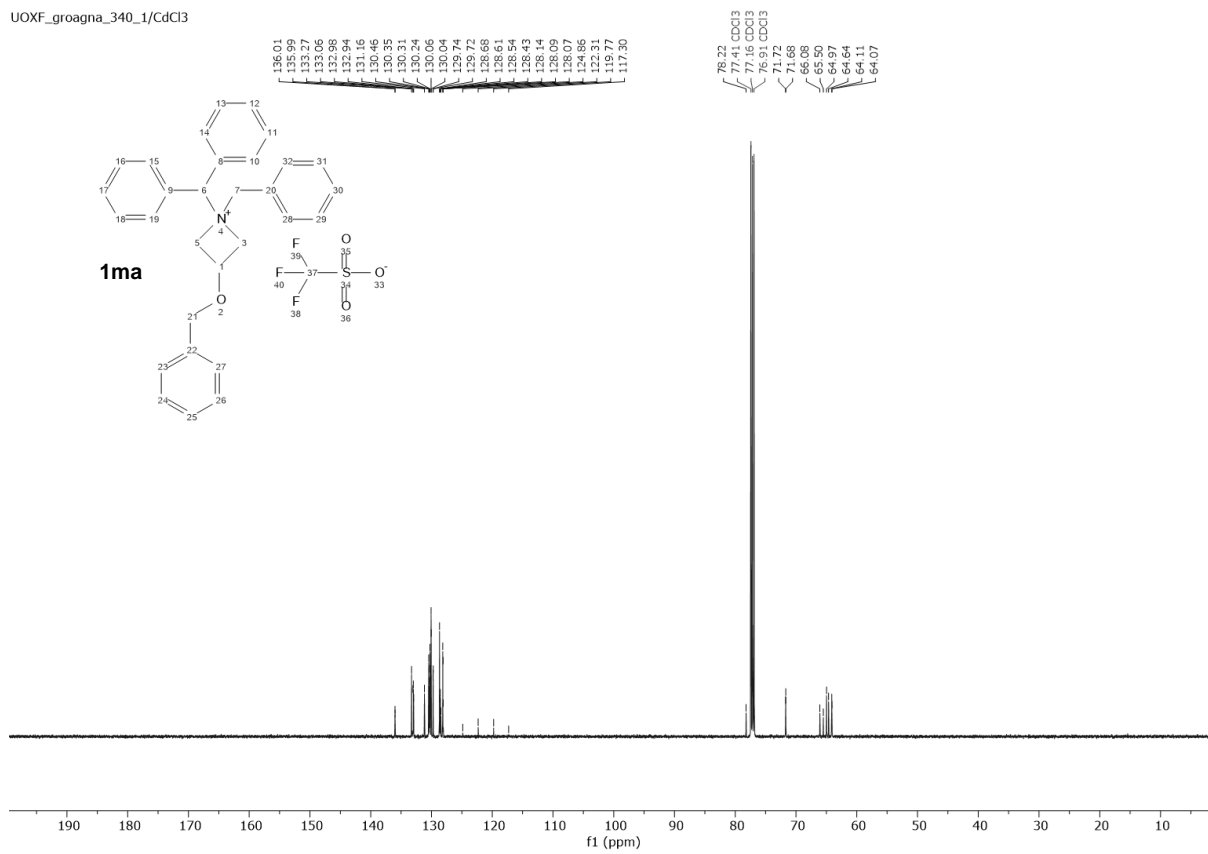
UOXF_groagna264_1/CdCl3/



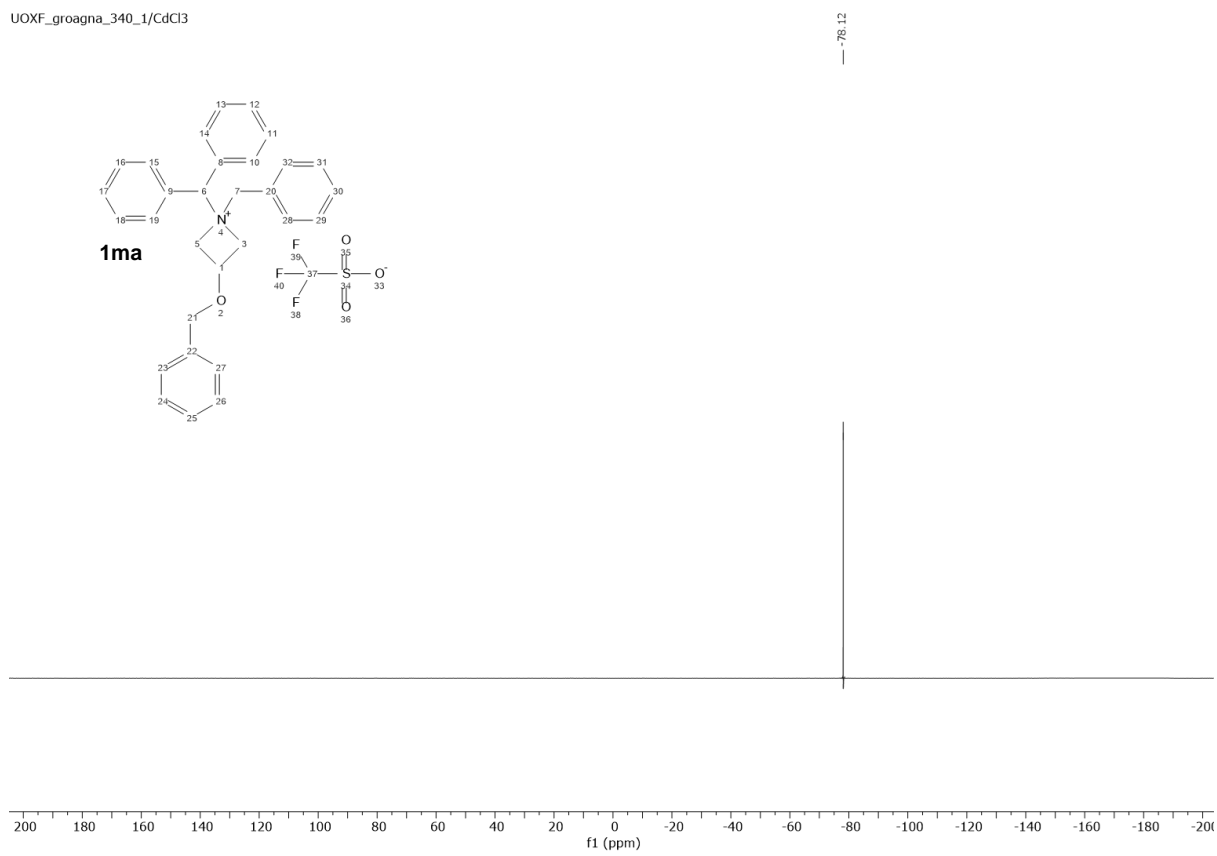
UOXF_groagna_264_1/CdCl3



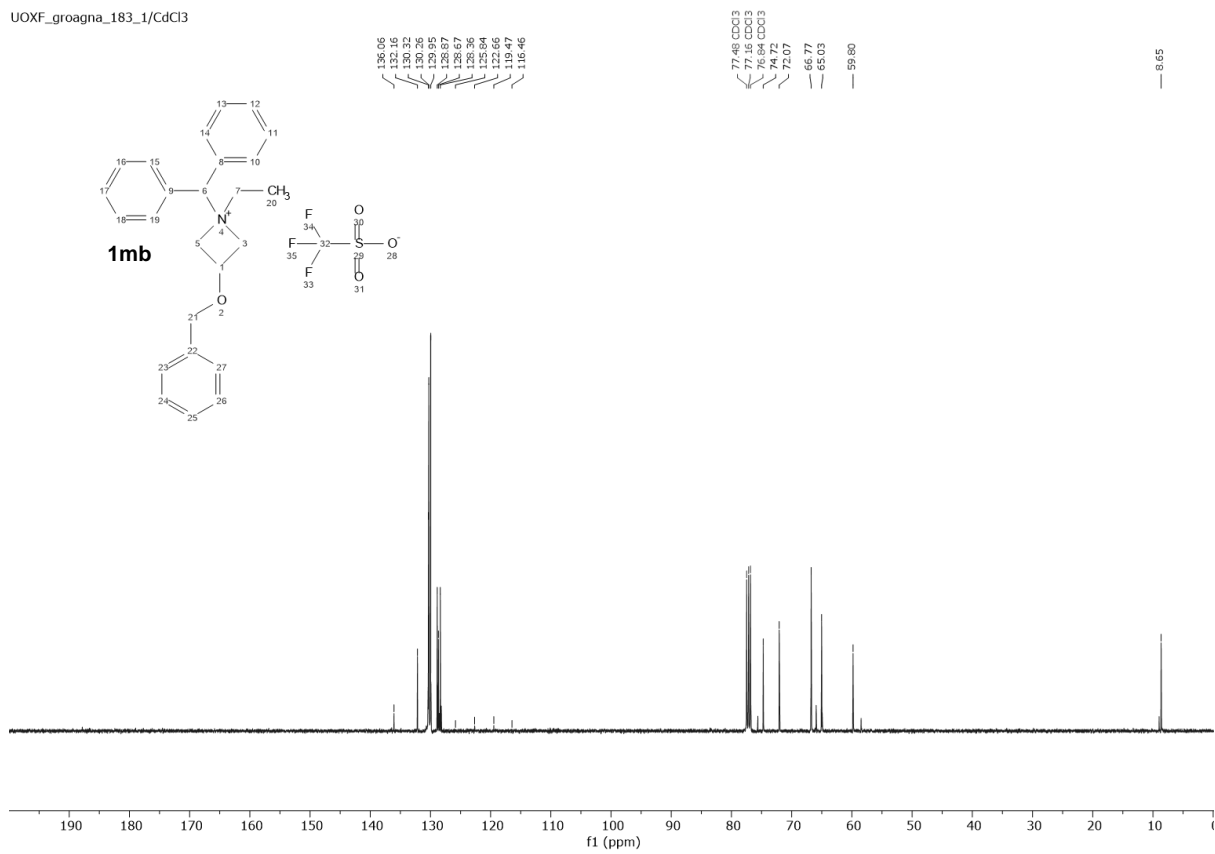
UOXF_groagna_340_1/CdCl3



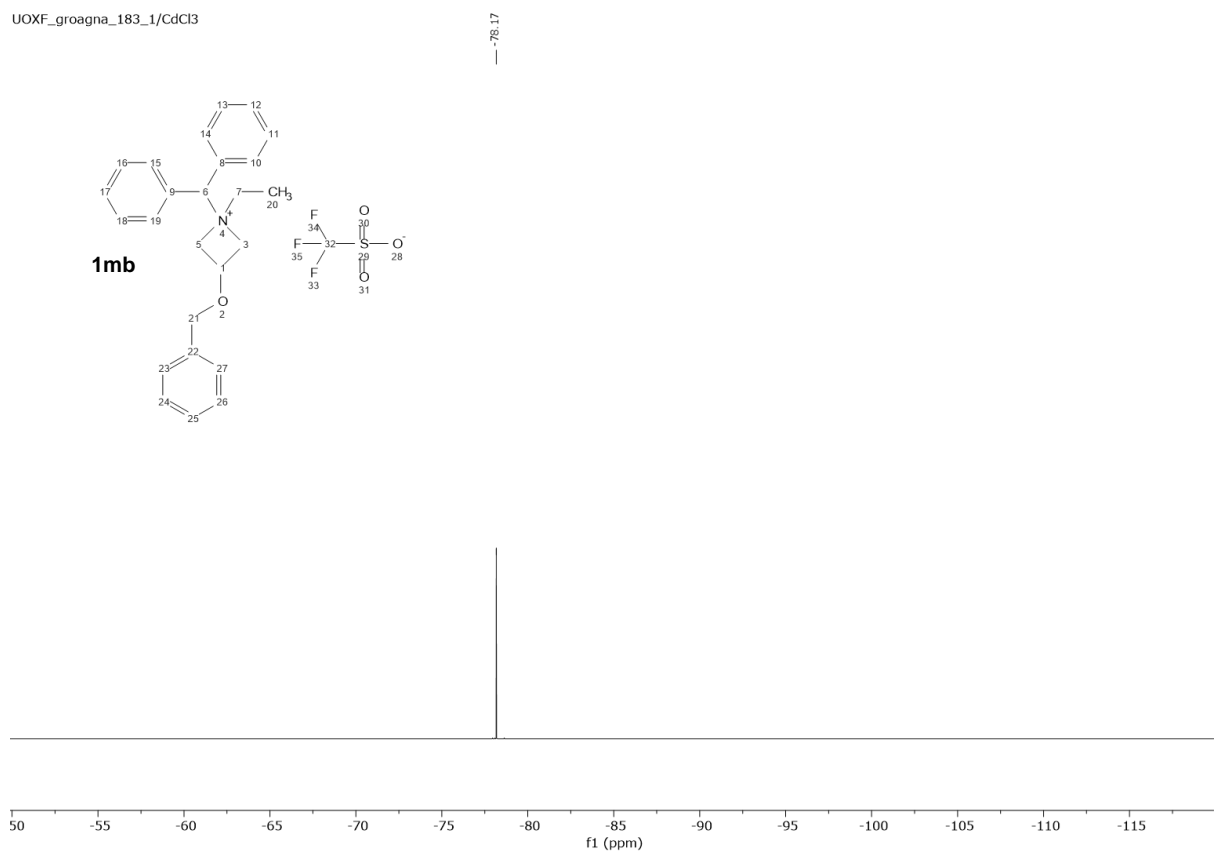
UOXF_groagna_340_1/CdCl3



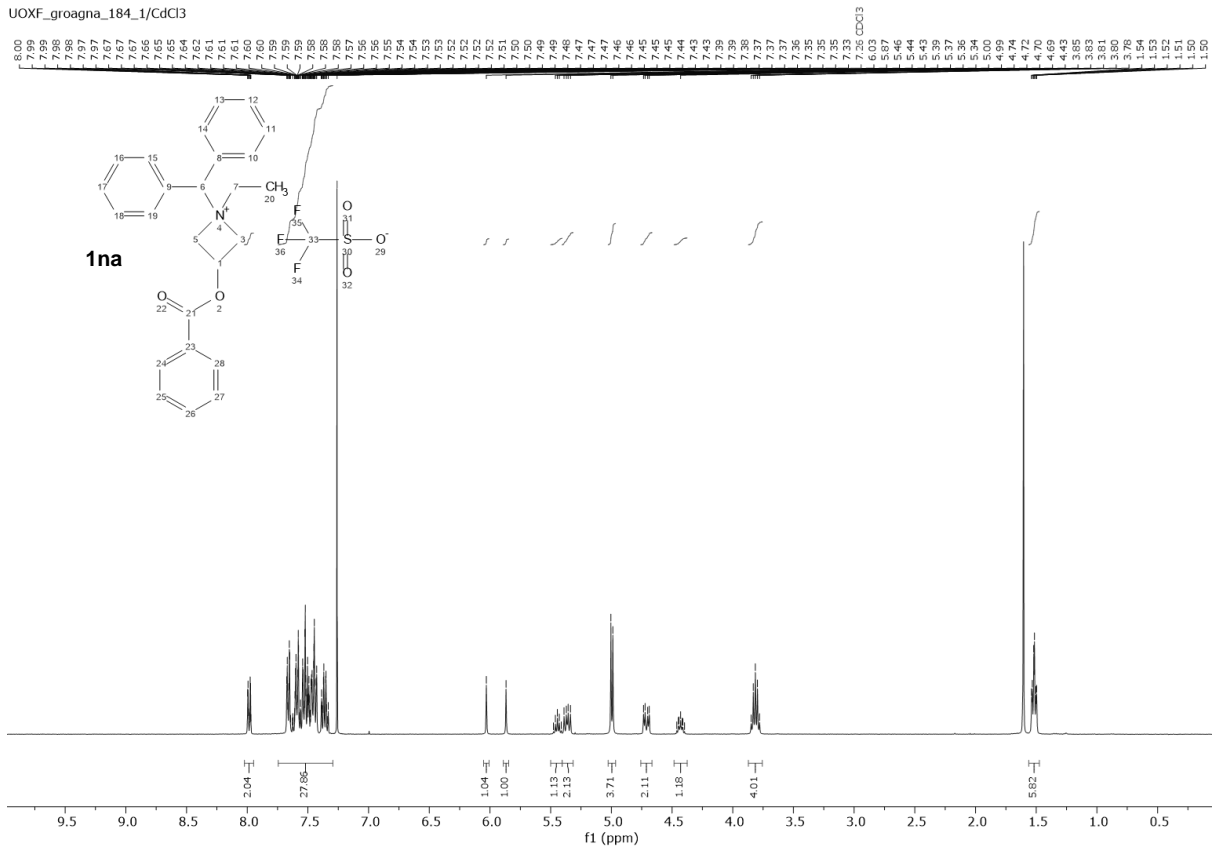
UOXF_groagna_183_1/CdCl3



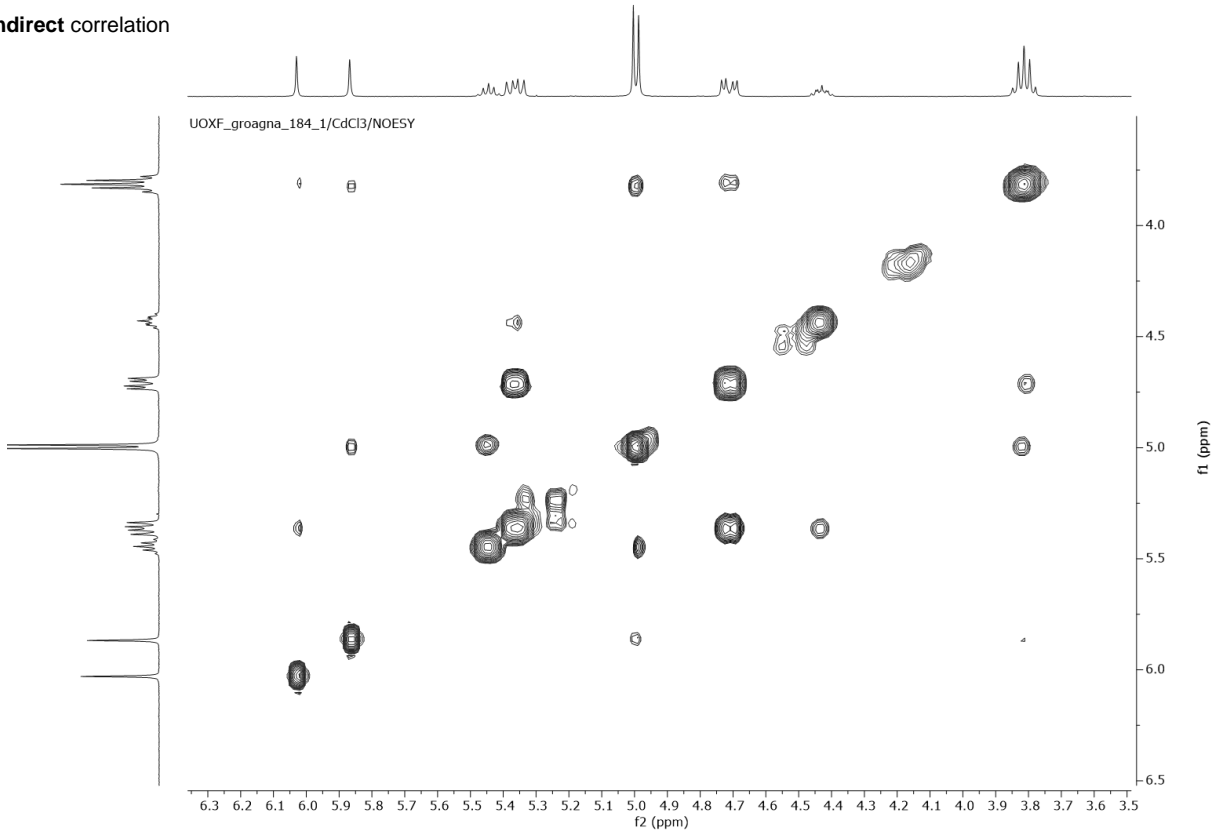
UOXF_groagna_183_1/CdCl3



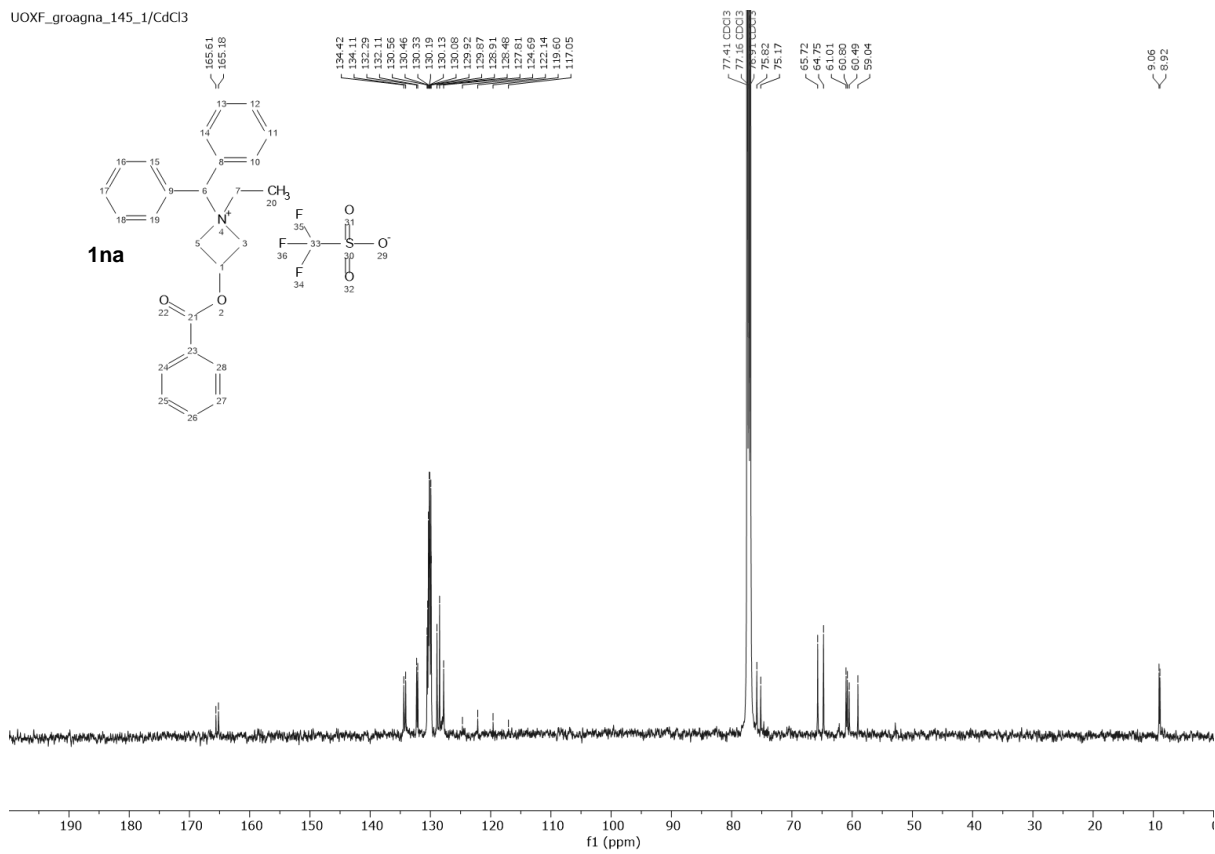
UOXF_groagna_184_1/CdCl3



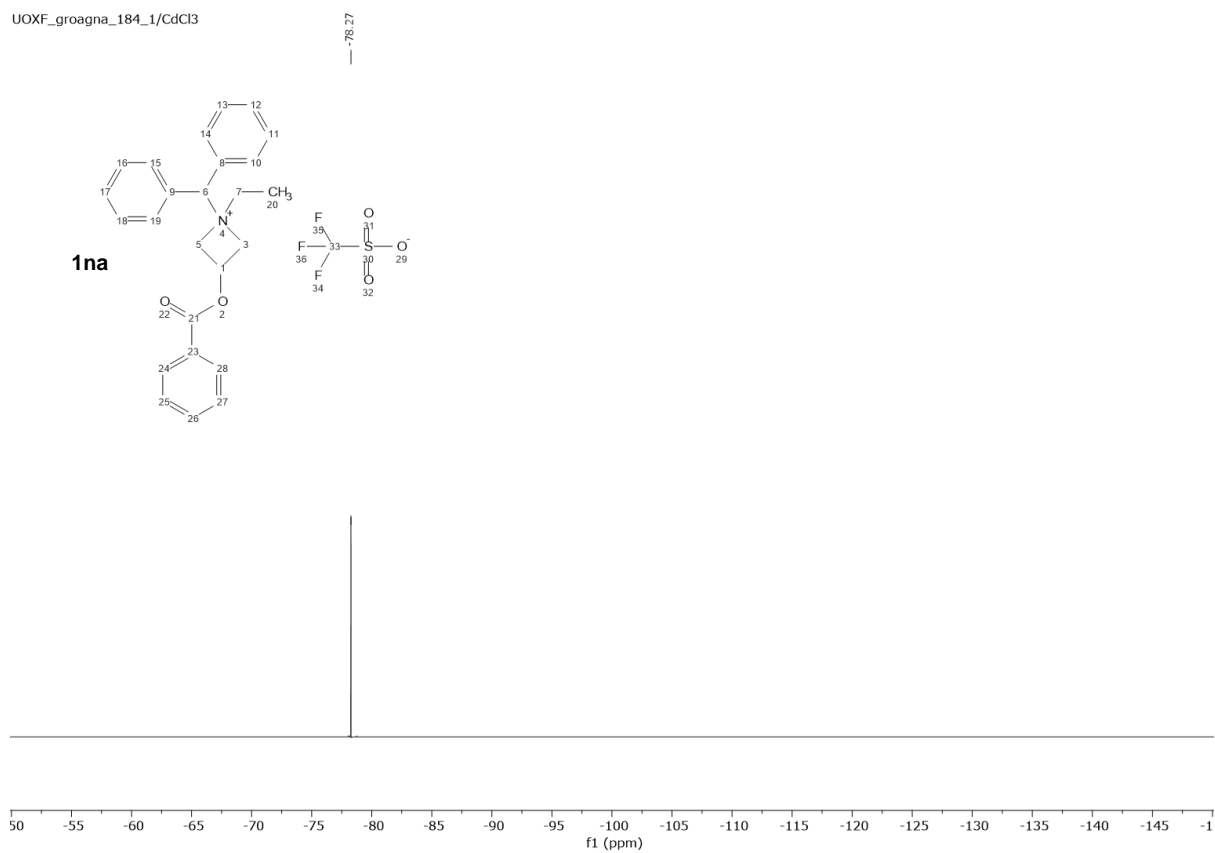
Indirect correlation



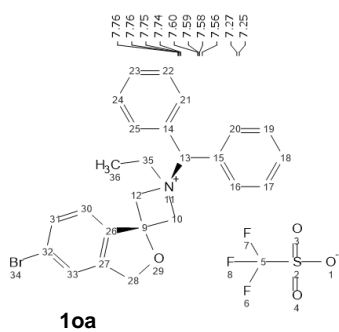
UOXF_groagna_145_1/CdCl3



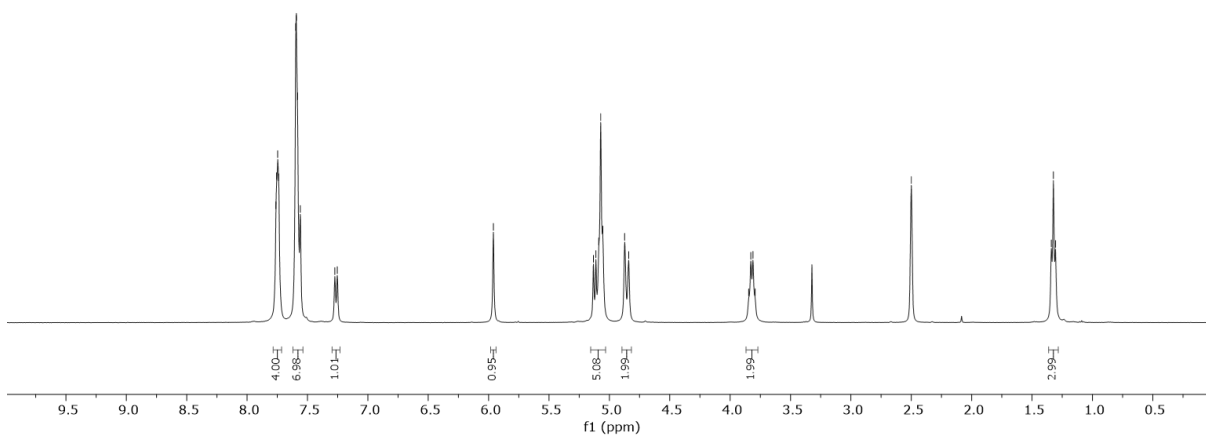
UOXF_groagna_184_1/CdCl3



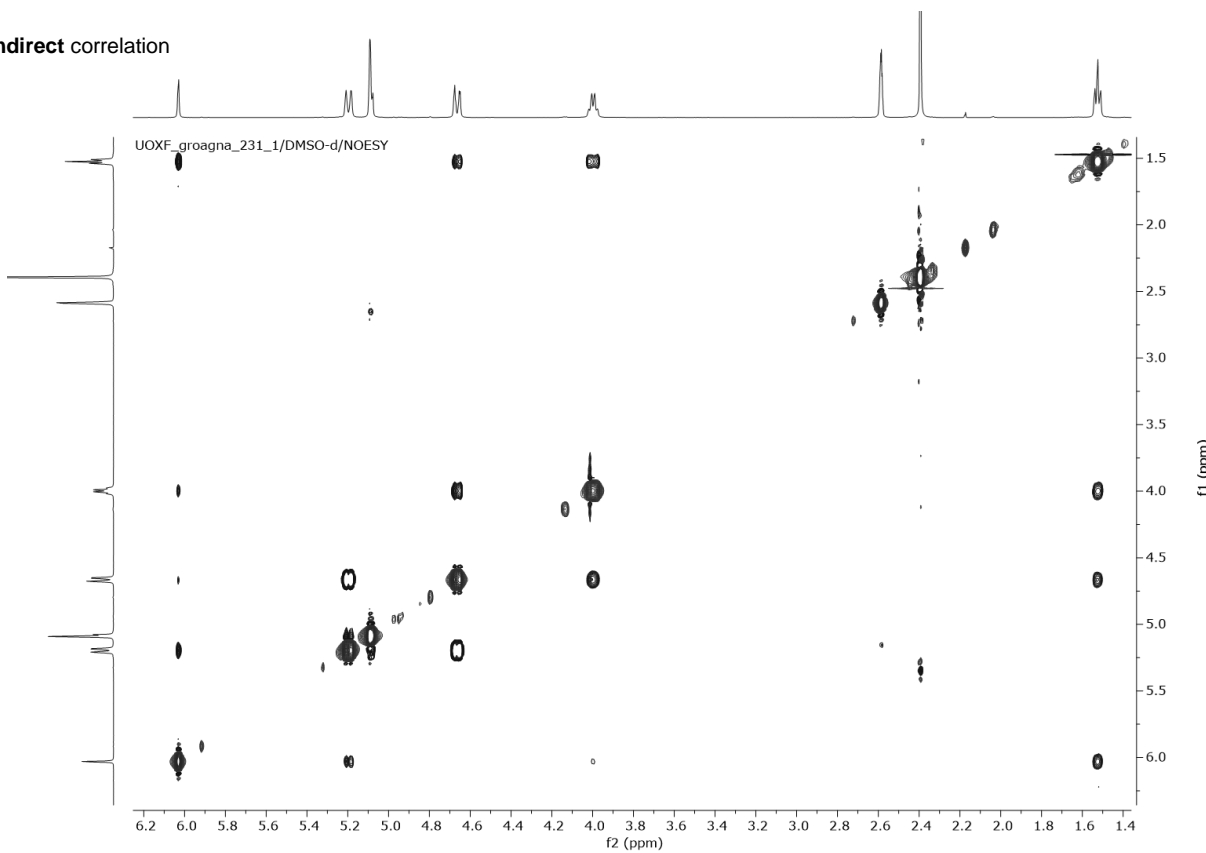
UOXF_groagna_231_1/DMSO-d



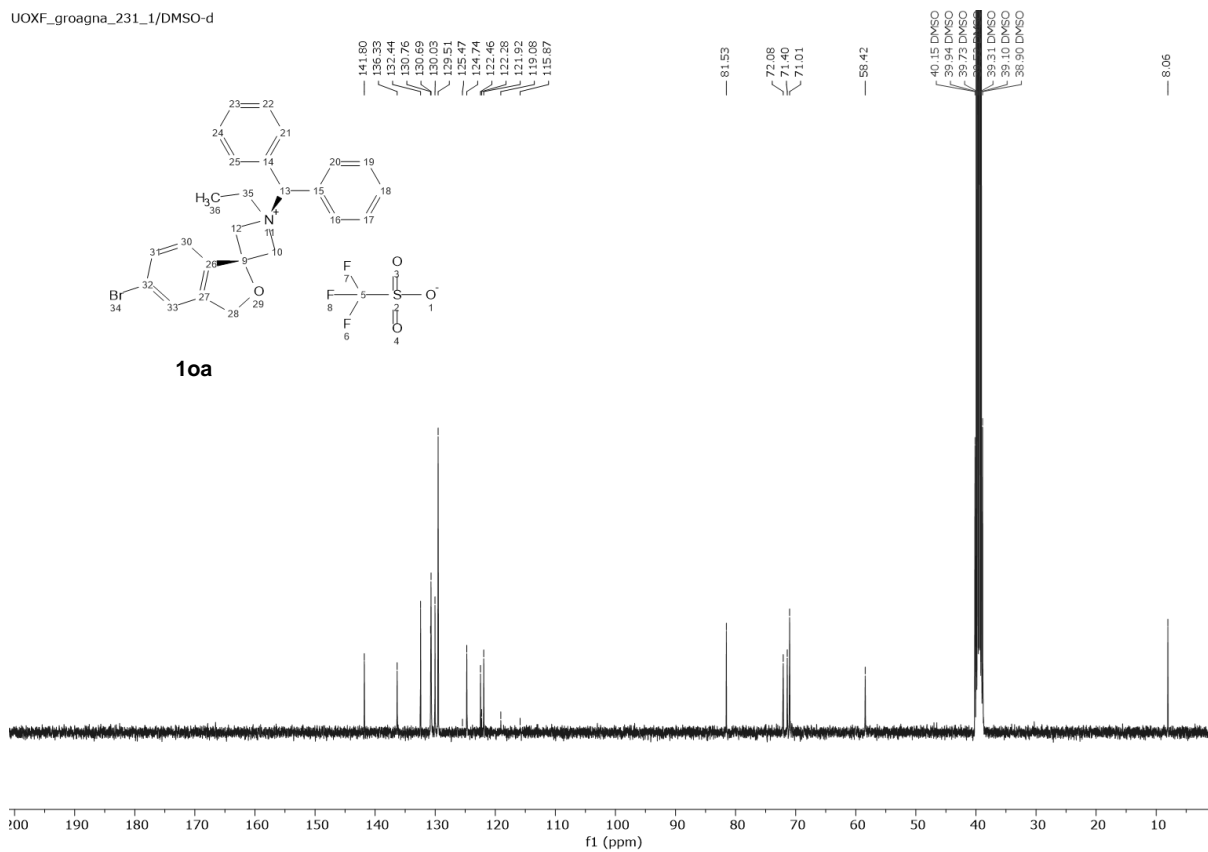
10a



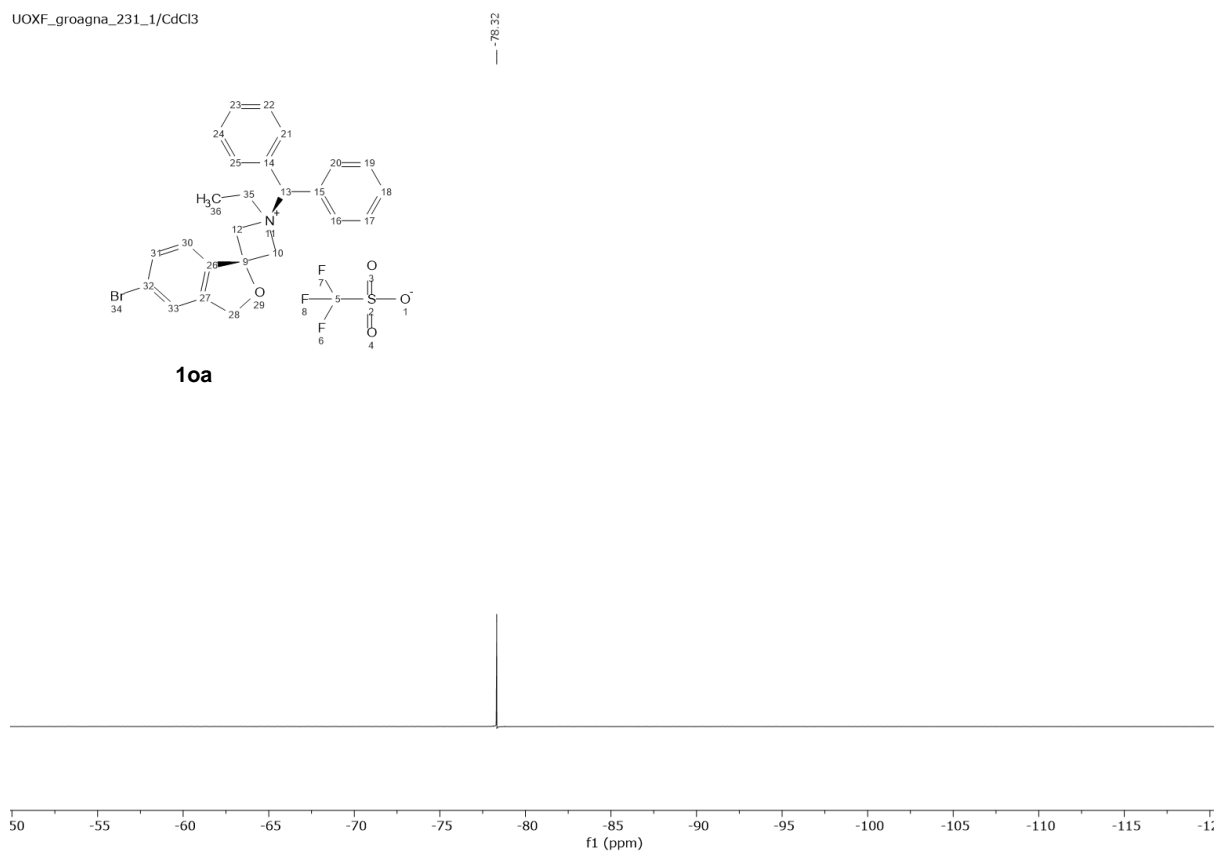
Indirect correlation

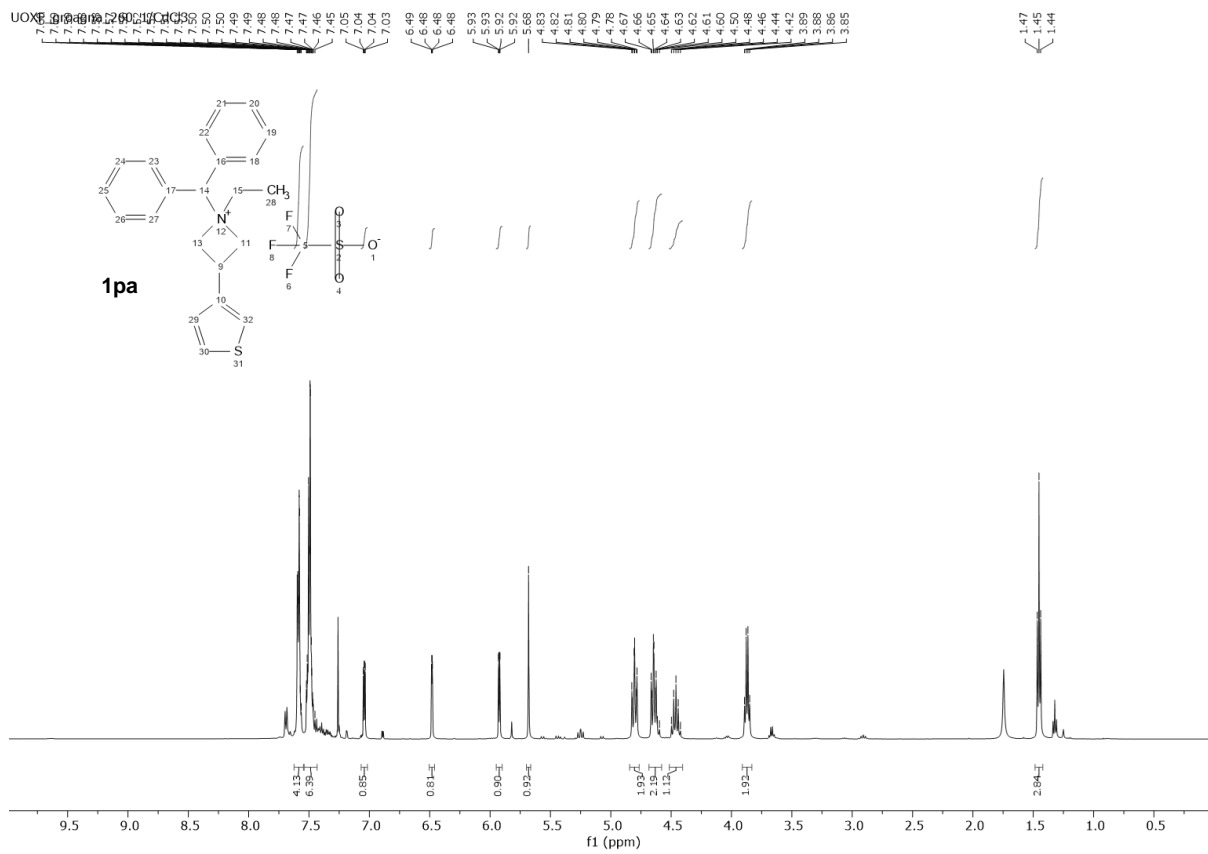


UOXF_groagna_231_1/DMSO-d

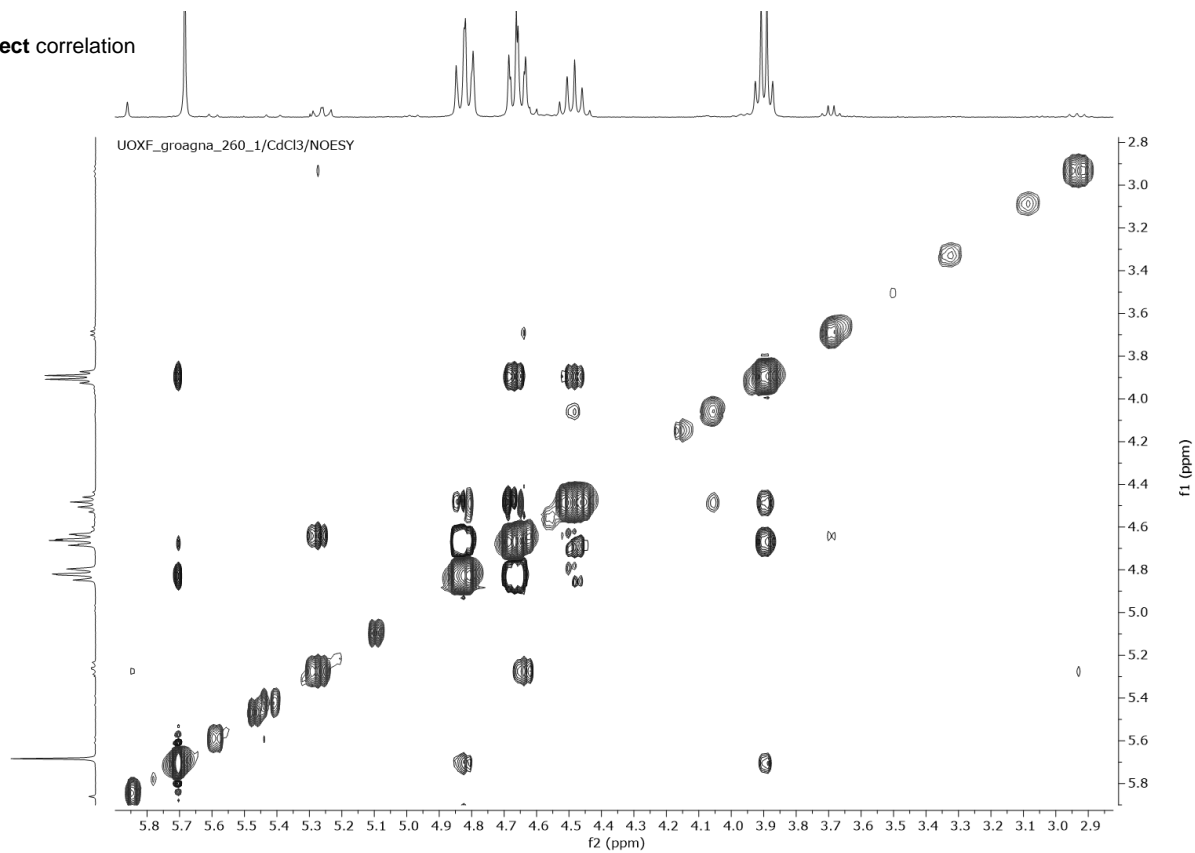


UOXF_groagna_231_1/CdCl3

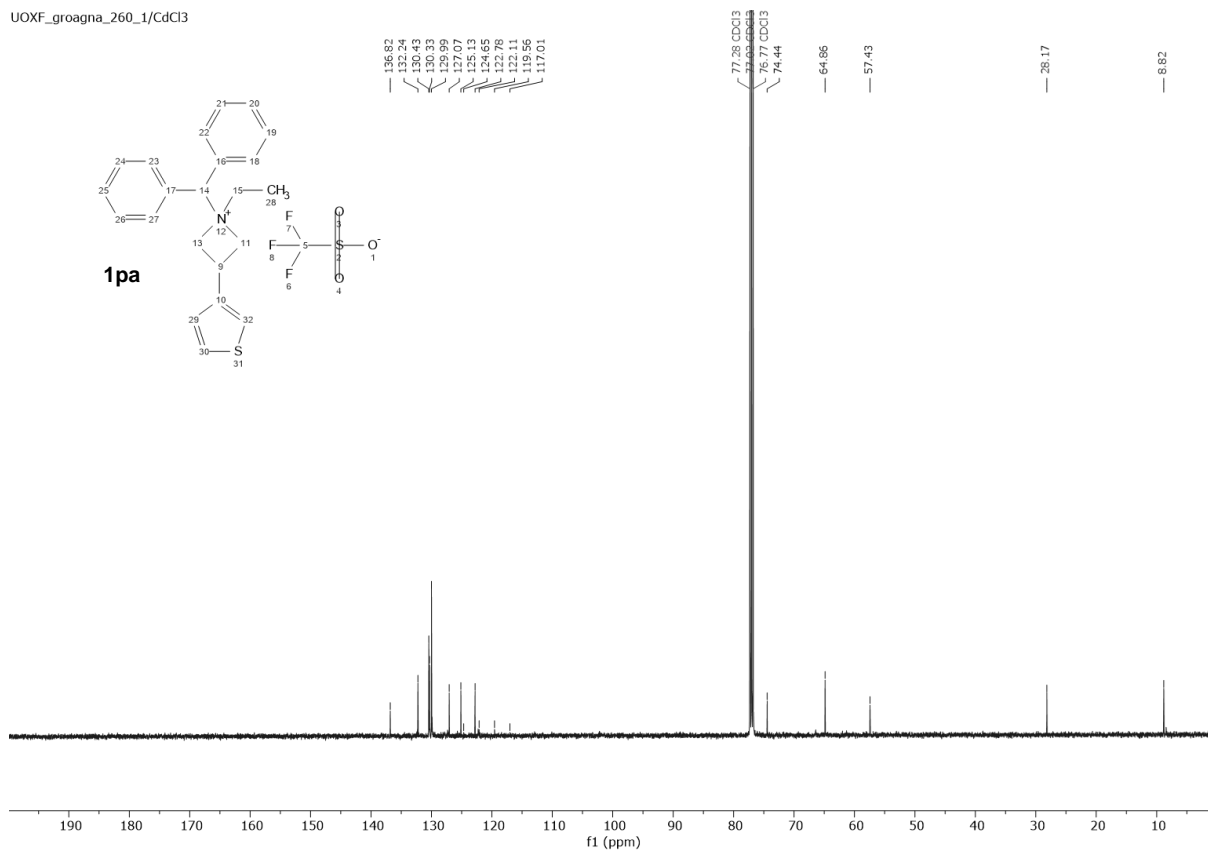




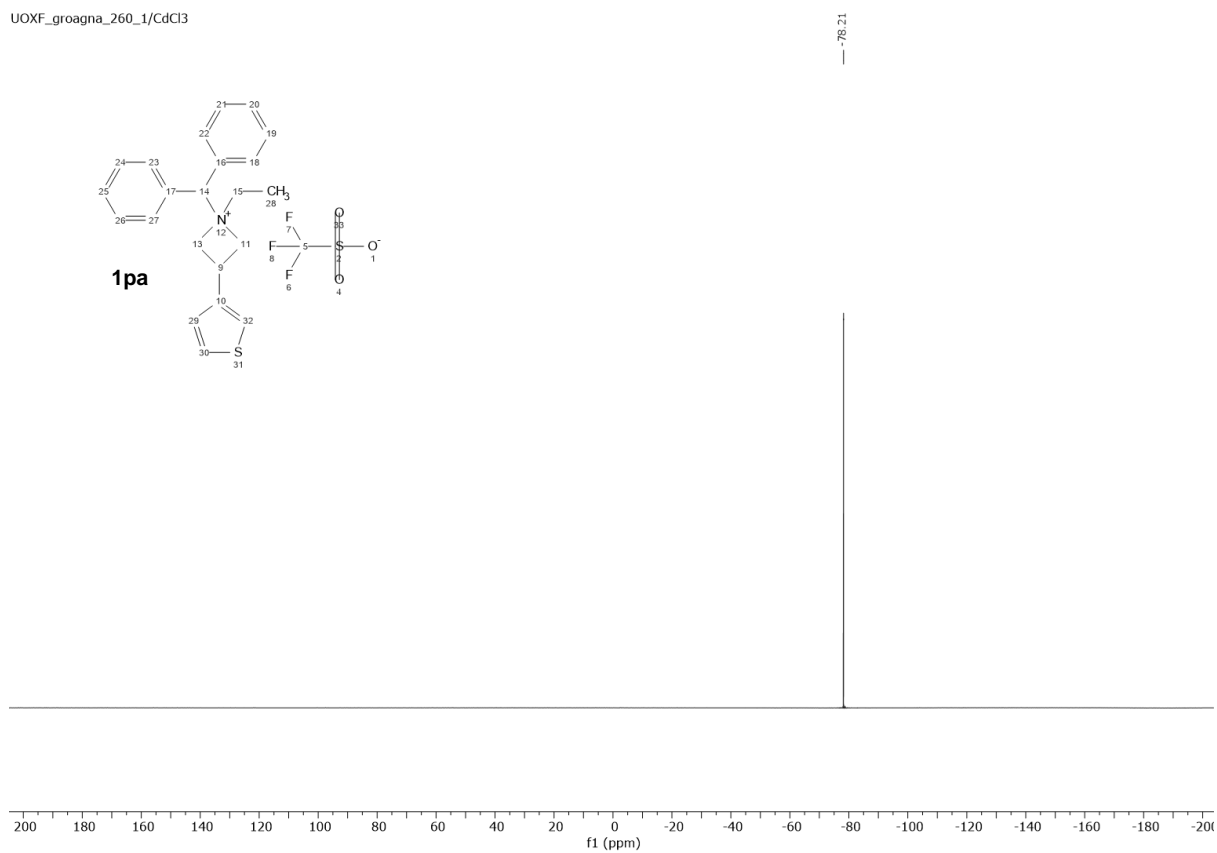
Direct correlation



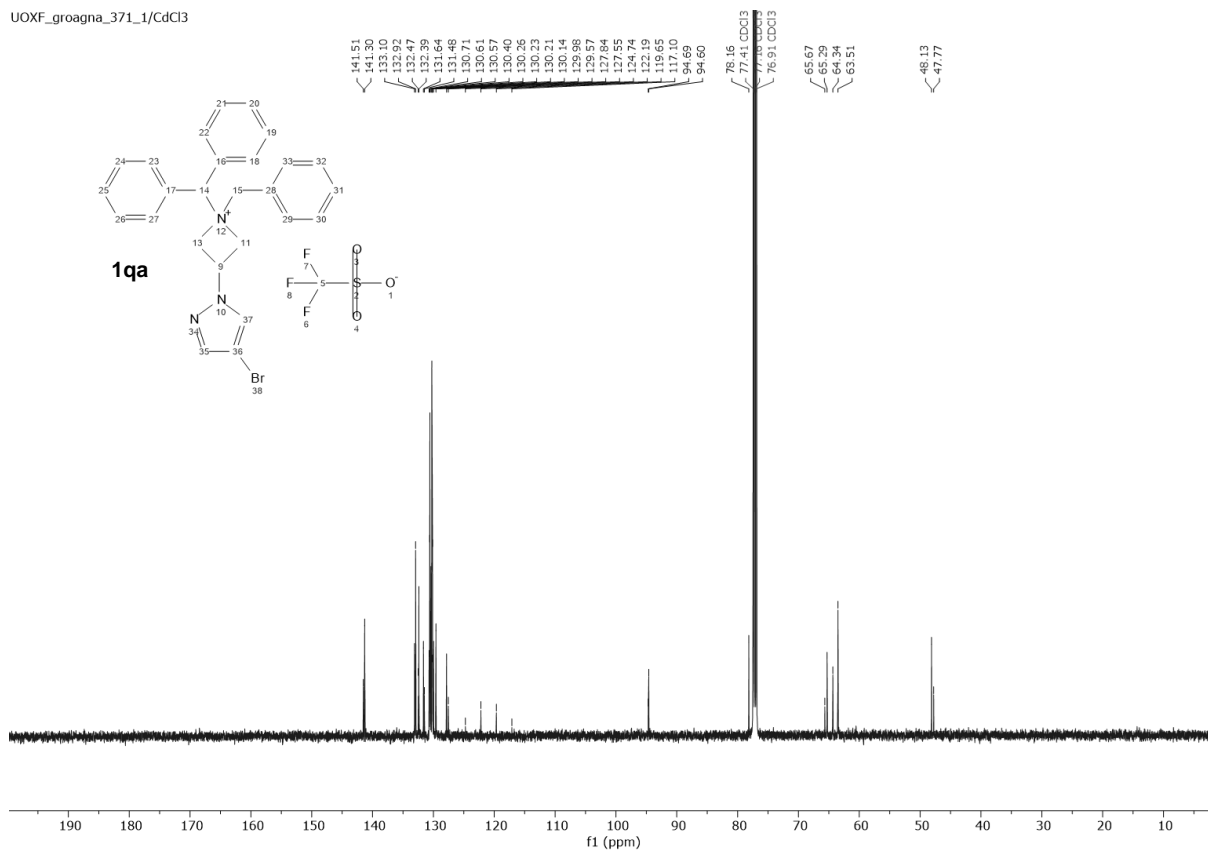
UOXF_groagna_260_1/CdCl3



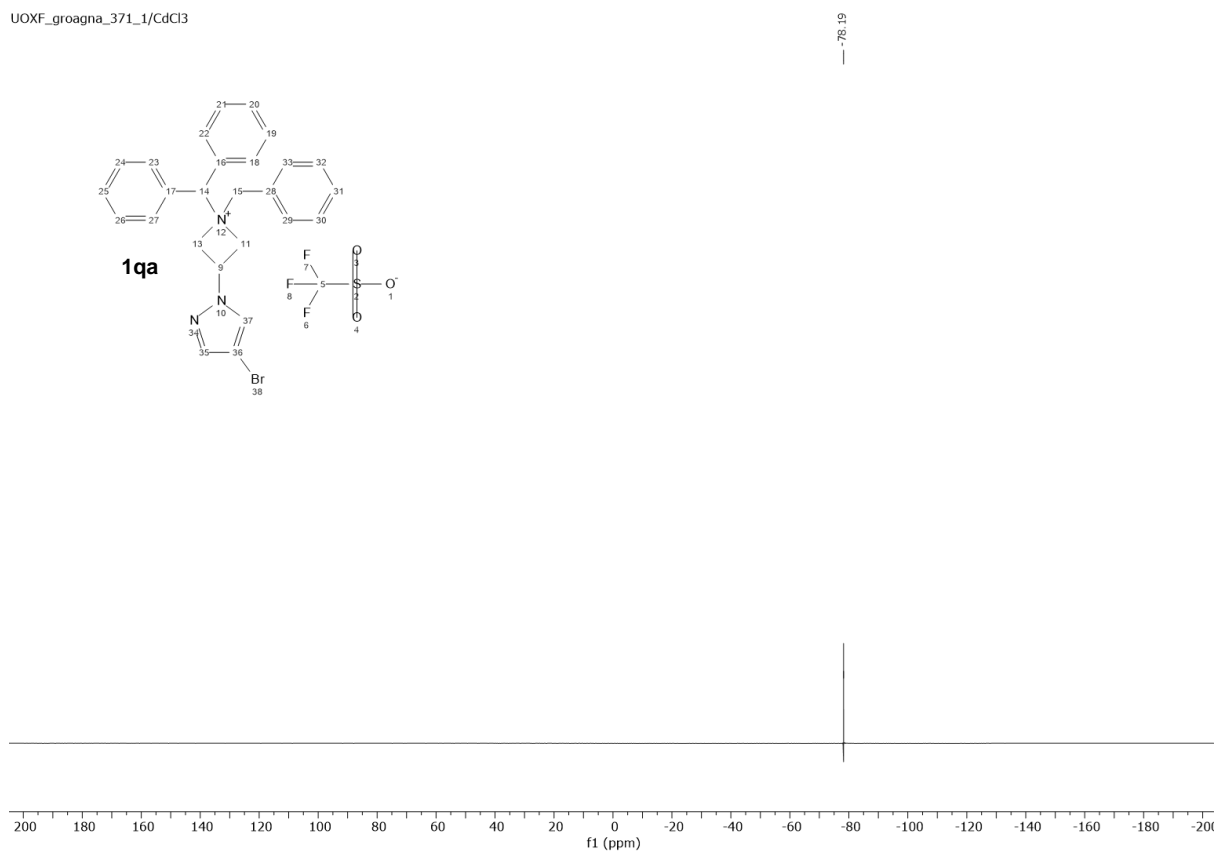
UOXF_groagna_260_1/CdCl3



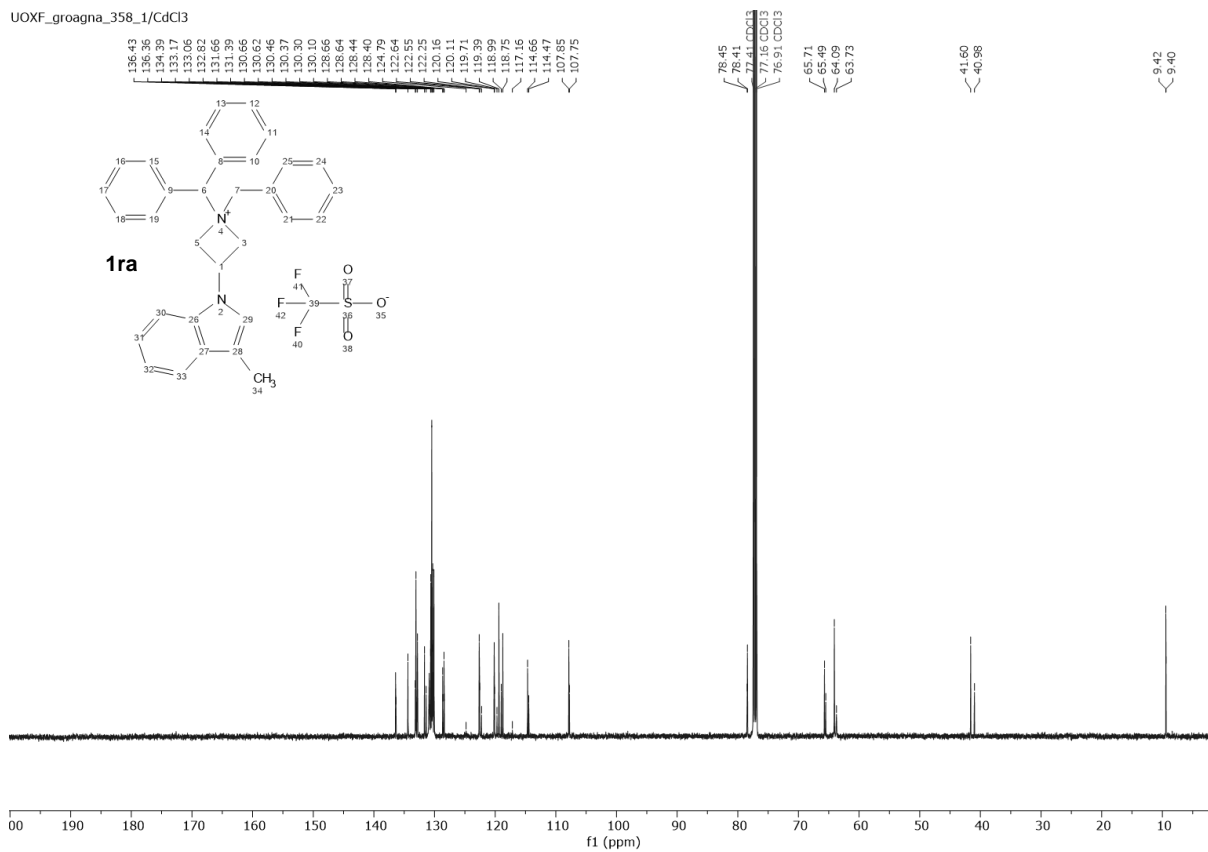
UOXF_groagna_371_1/CdCl3



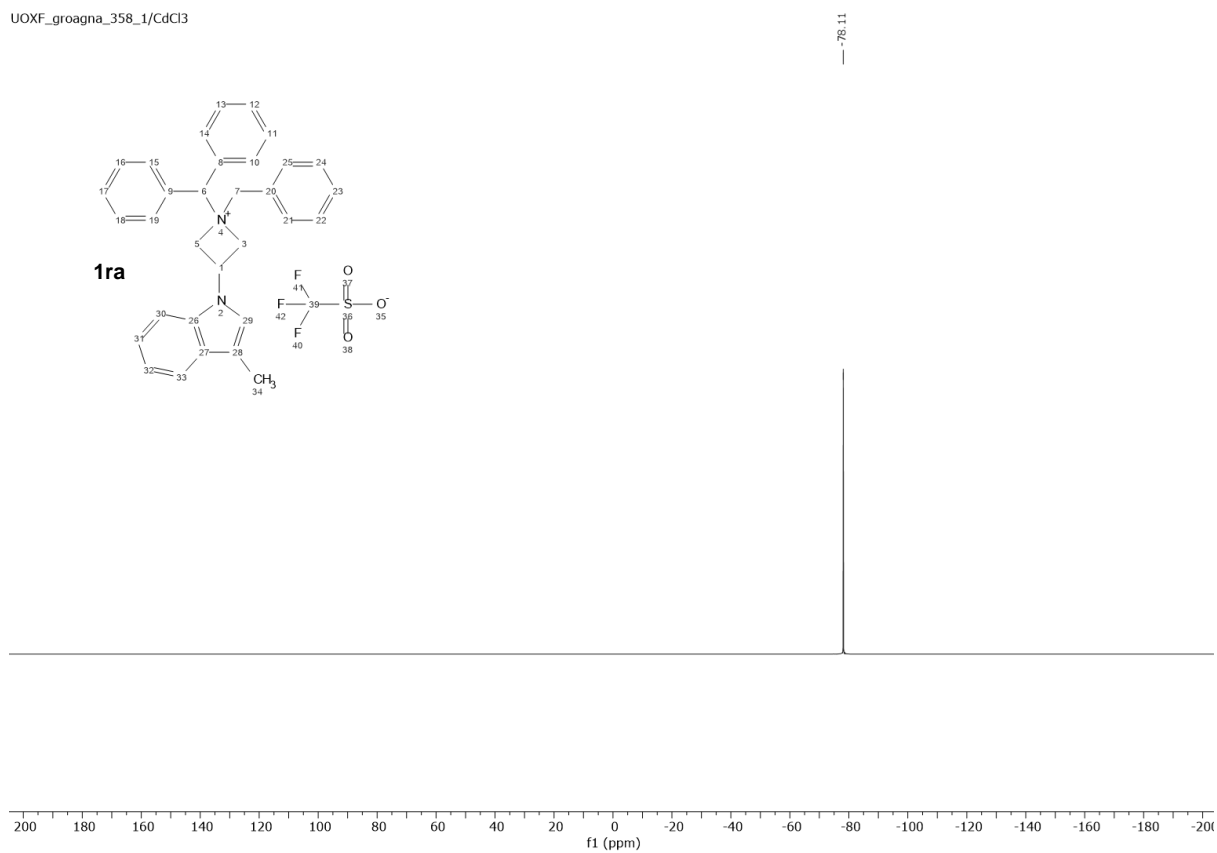
UOXF_groagna_371_1/CdCl3



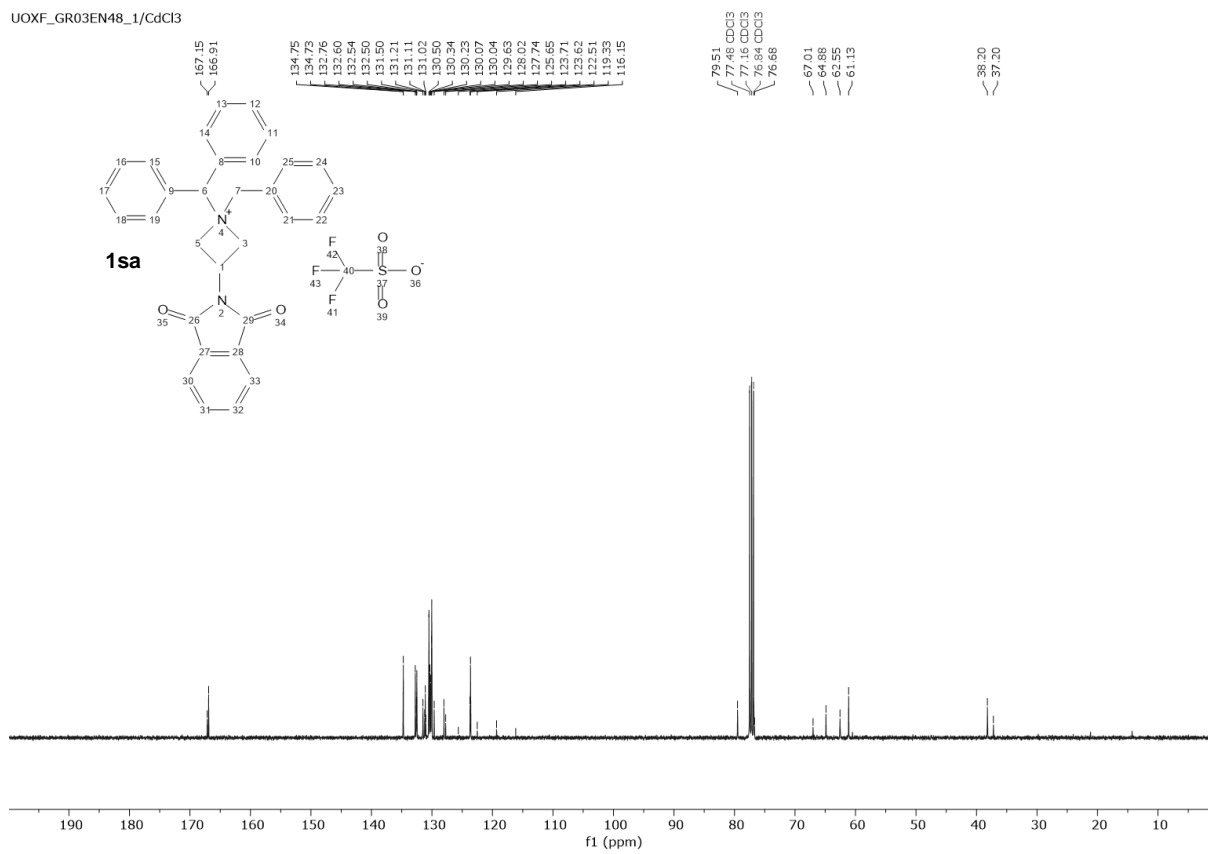
UOXF_groagna_358_1/CdCl3



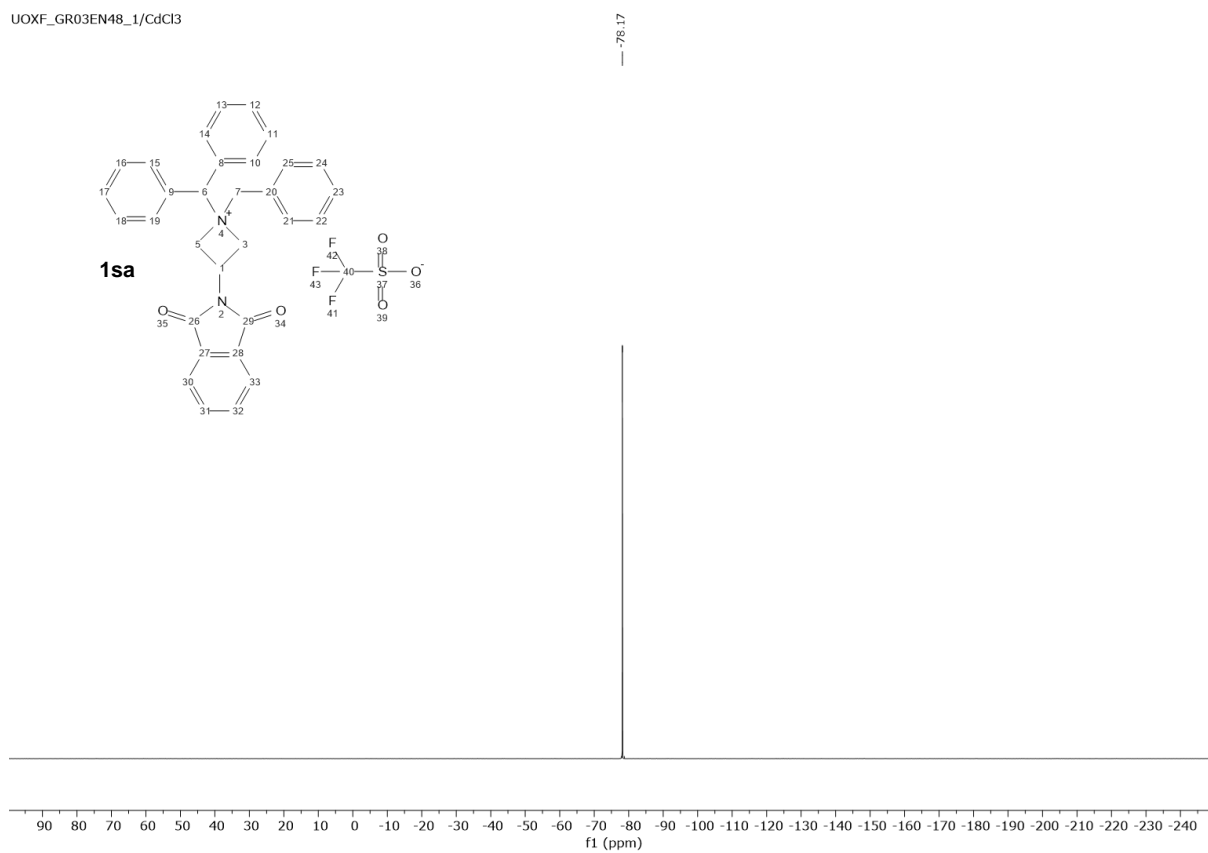
UOXF_groagna_358_1/CdCl3



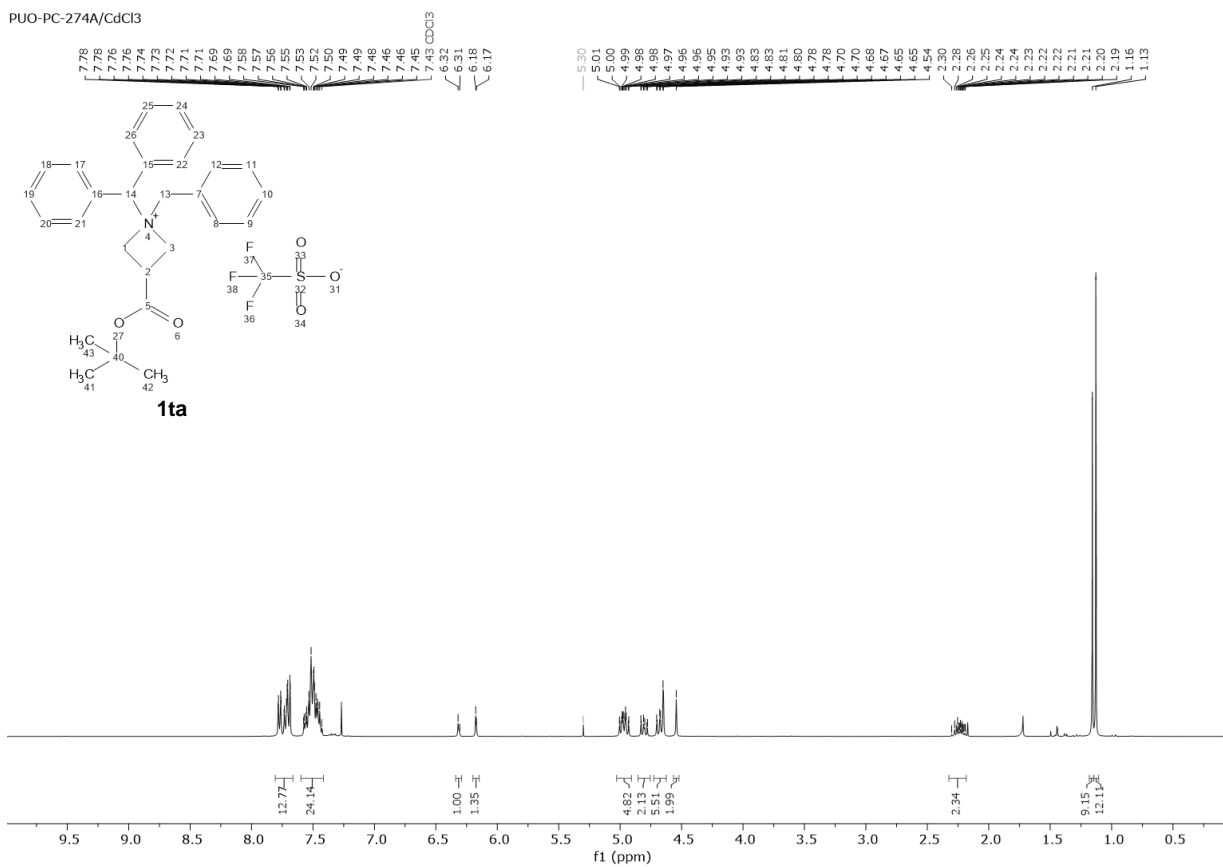
UOXF_GR03EN48_1/CdCl3



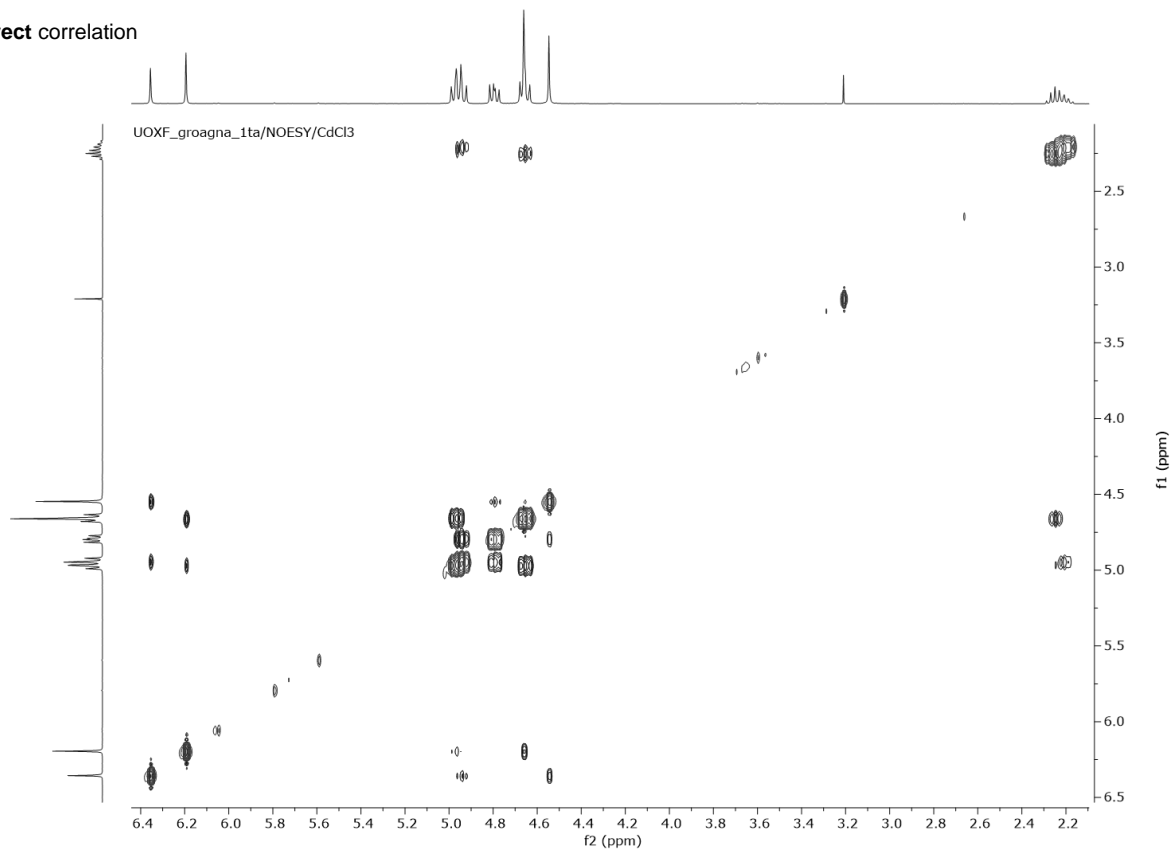
UOXF_GR03EN48_1/CdCl3



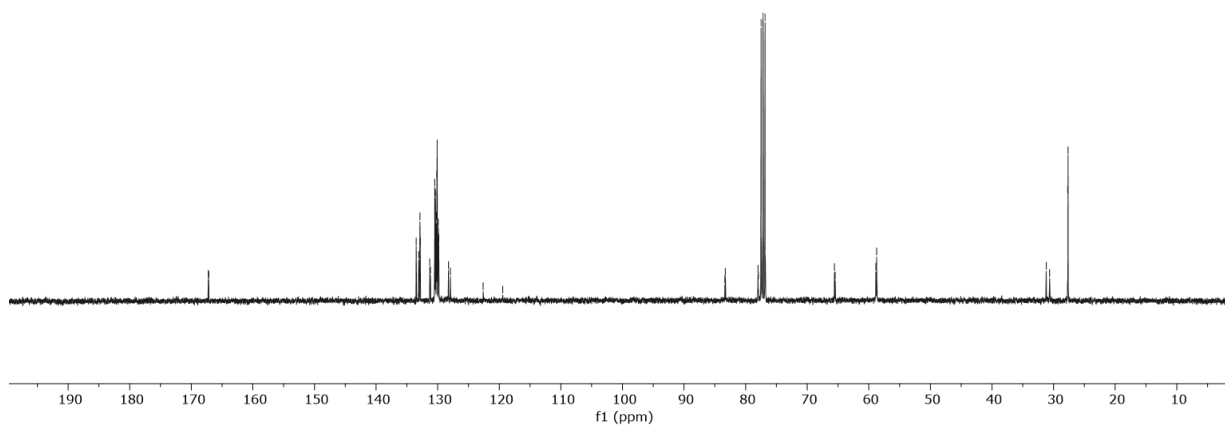
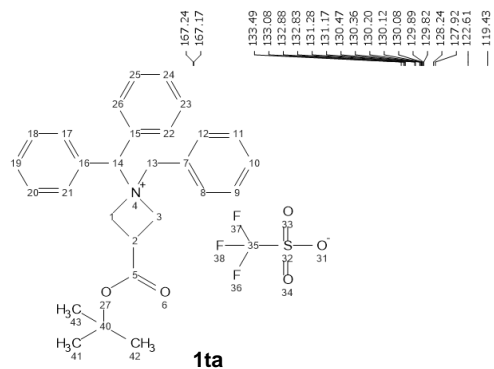
PUO-PC-274A/CdCl3



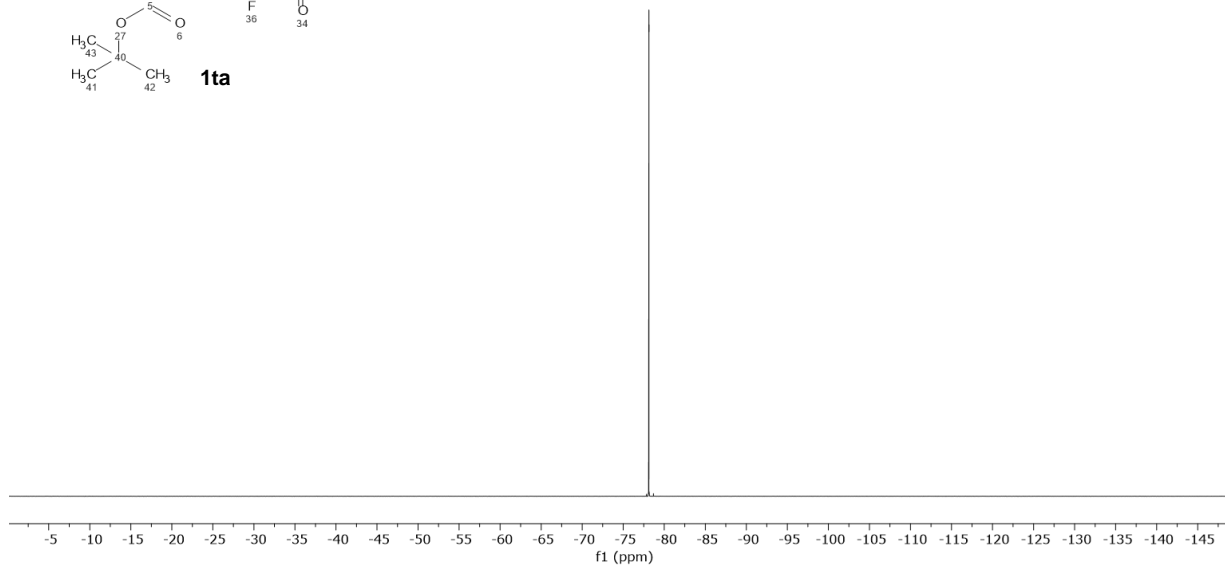
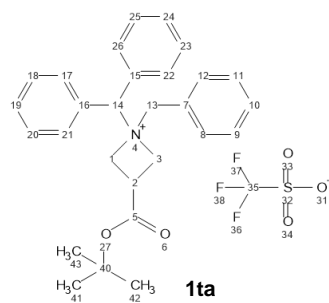
Indirect correlation



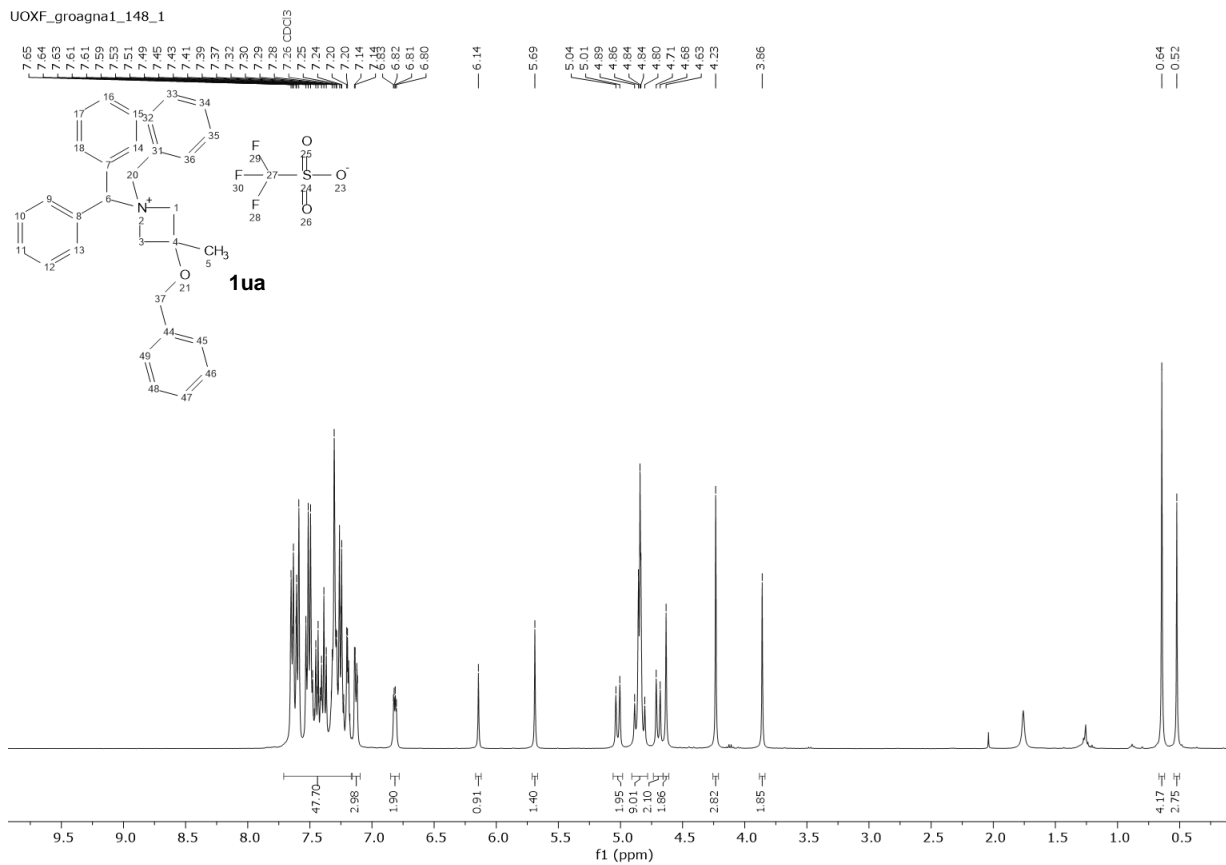
PUO-PC-274A/CdCl3



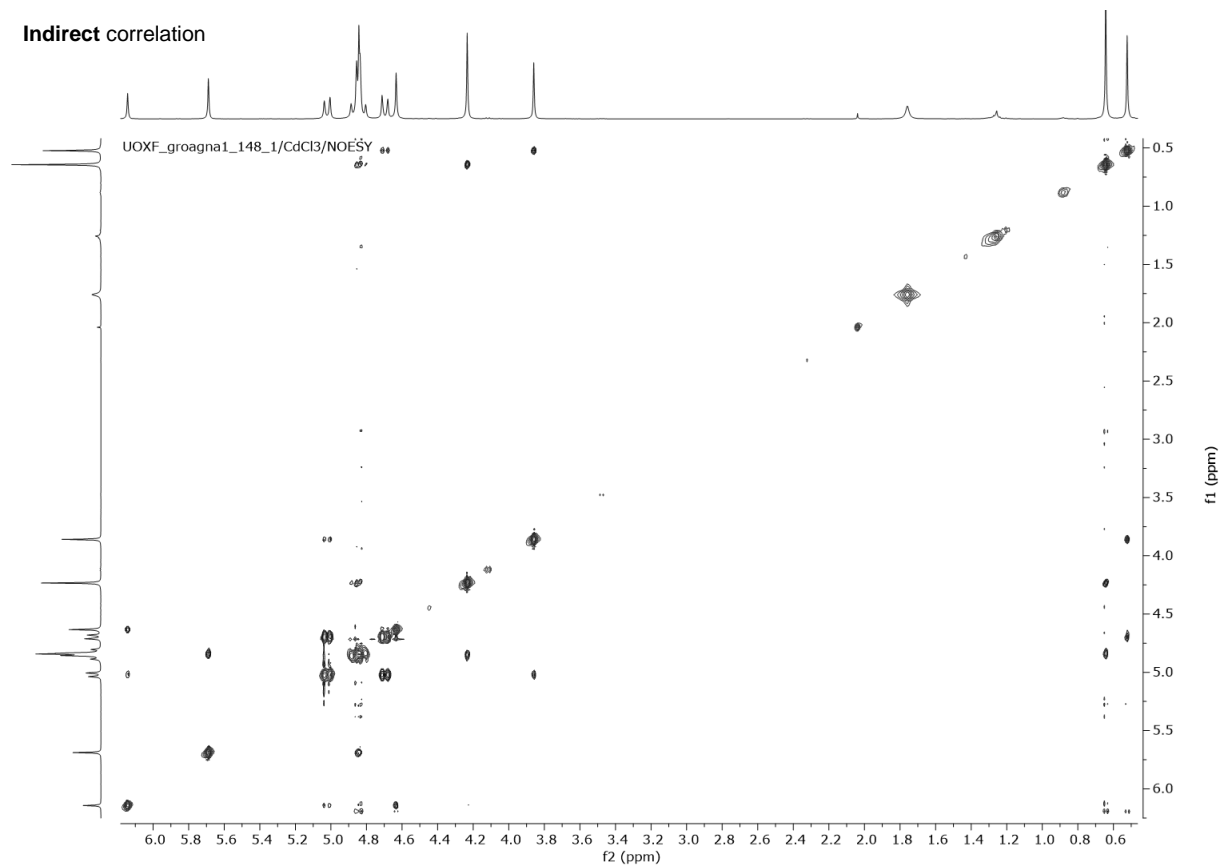
PUO-PC-274A/CdCl3



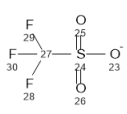
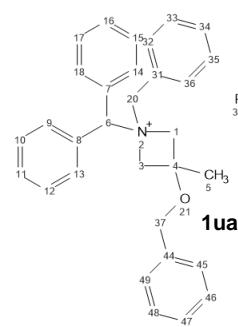
UOXF_groagna1_148_1



Indirect correlation



UOXF_groagna1_148_1

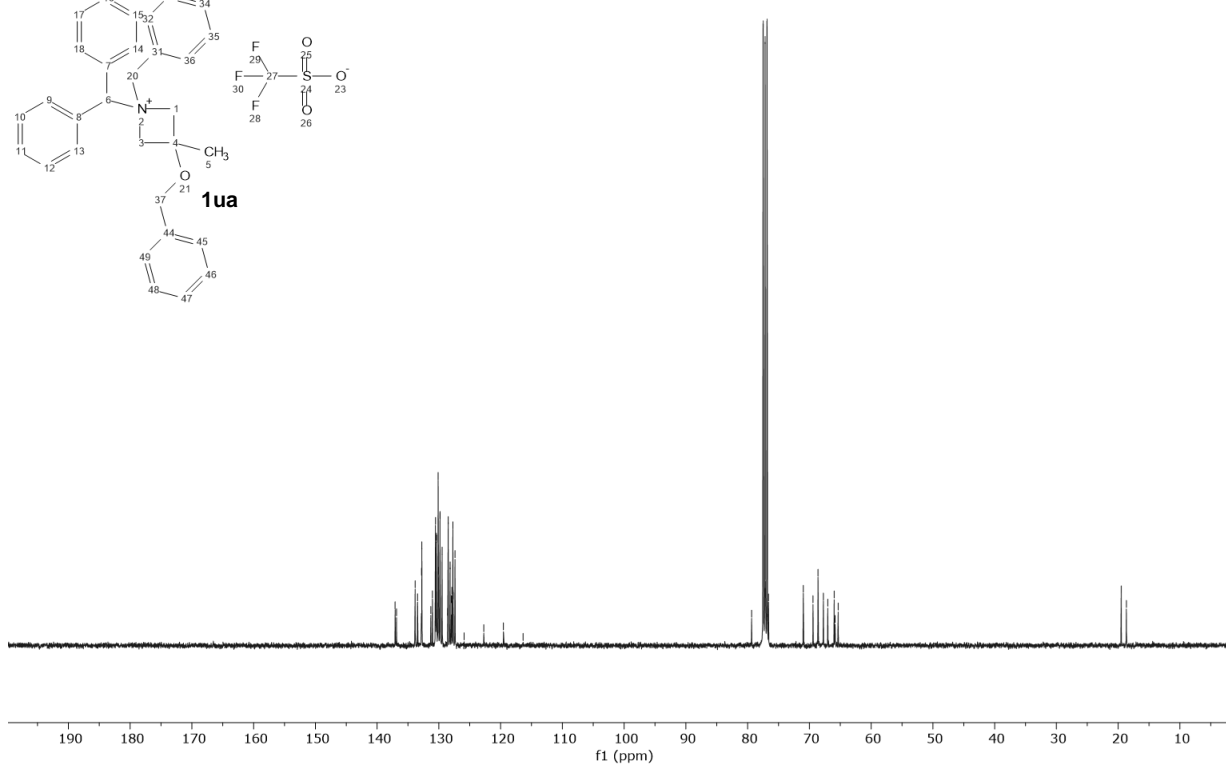


1ua

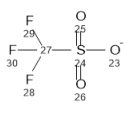
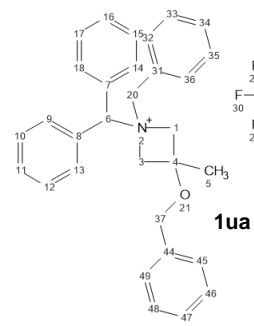
137.09
136.85
133.84
133.46
132.81
132.76
131.31
131.04
130.45
130.45
130.37
130.12
130.07
129.82
129.48
128.56
128.49
128.18
127.98
127.71
127.71
127.69
127.59
125.91
122.73
119.55
116.36

79.36
77.48 CDCl3
77.16 CDCl3
76.84 CDCl3
76.62
70.99
69.42
68.60
67.74
67.02
65.99
65.54
65.34

19.51
18.67

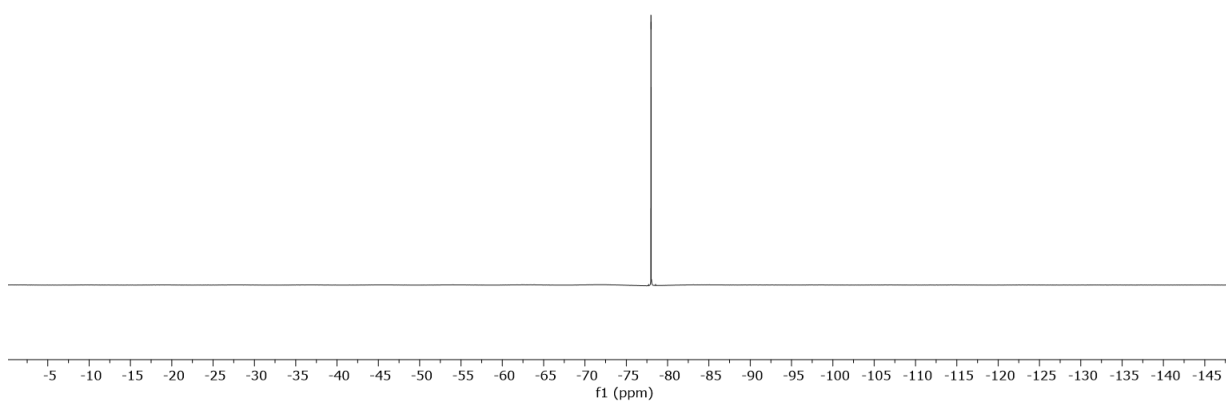


UOXF_groagna1_148_1

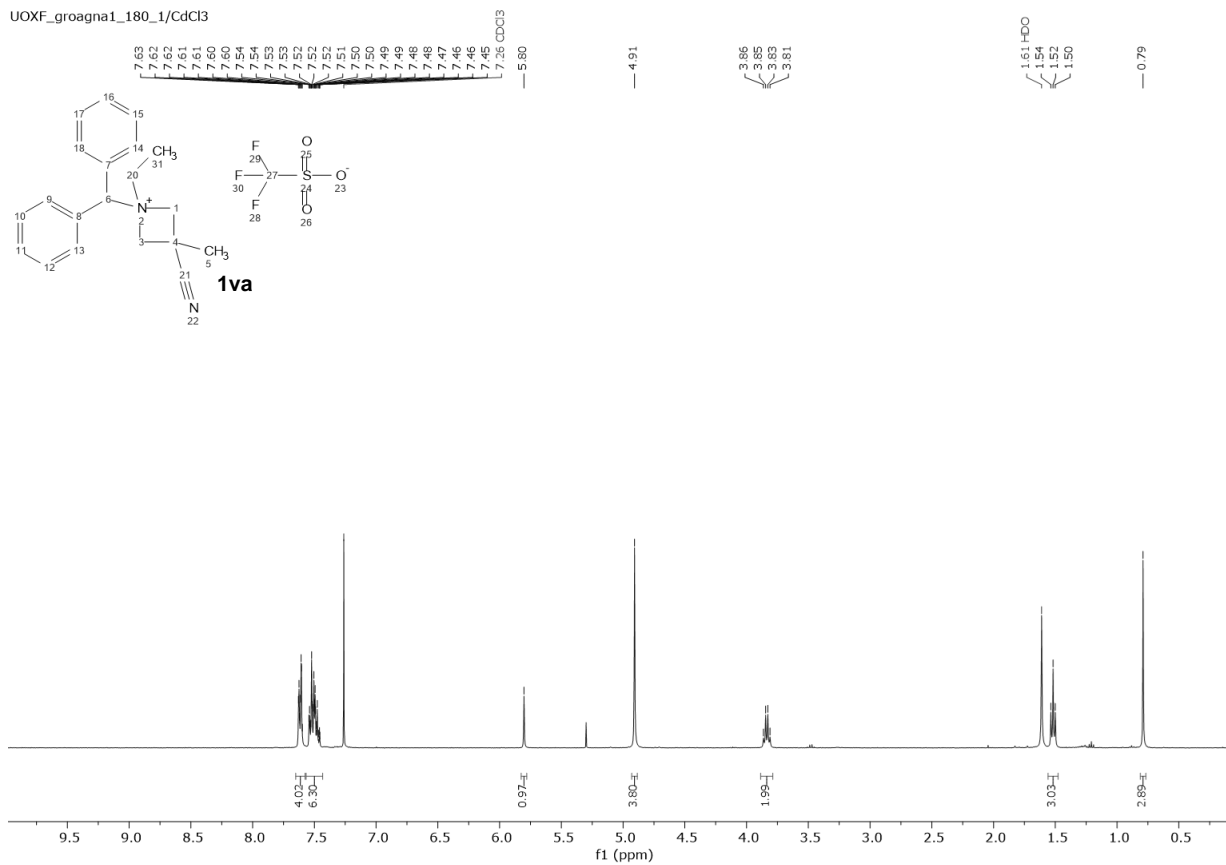


1ua

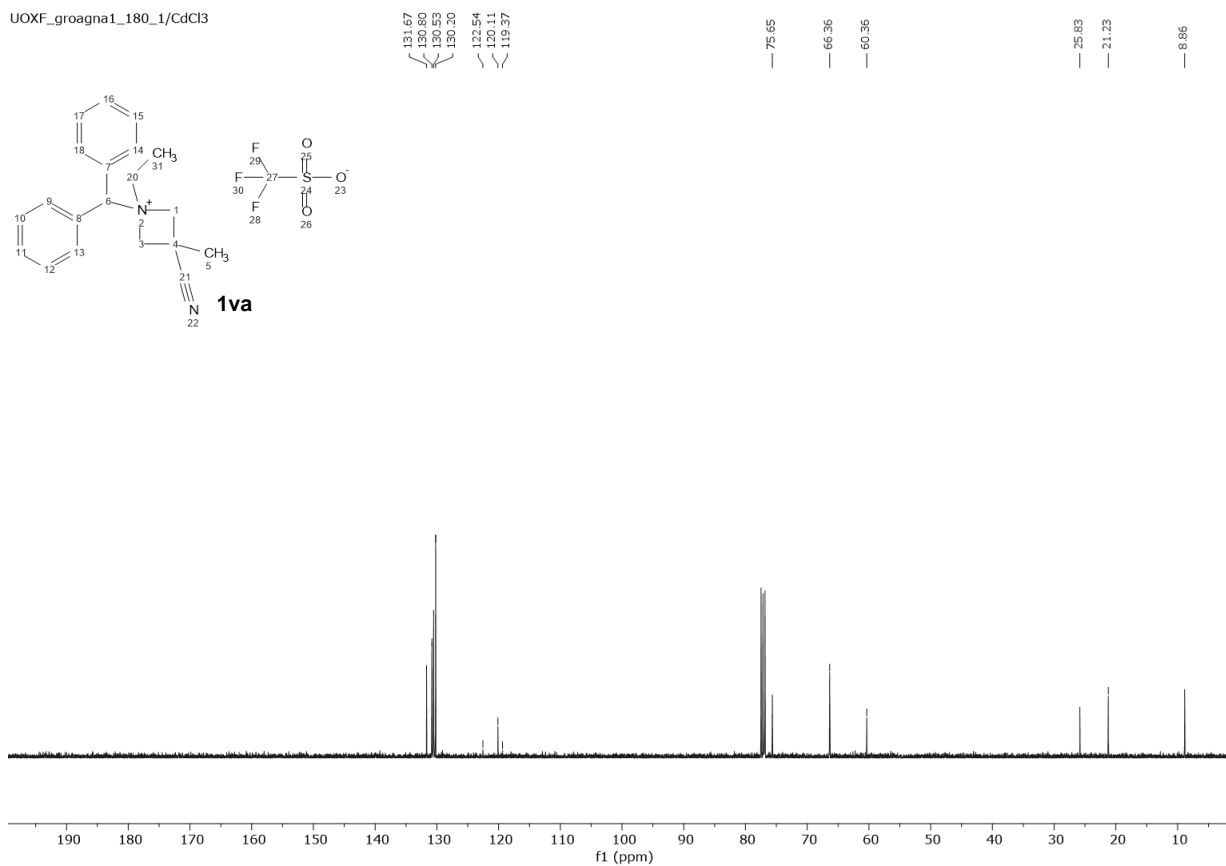
-78.00



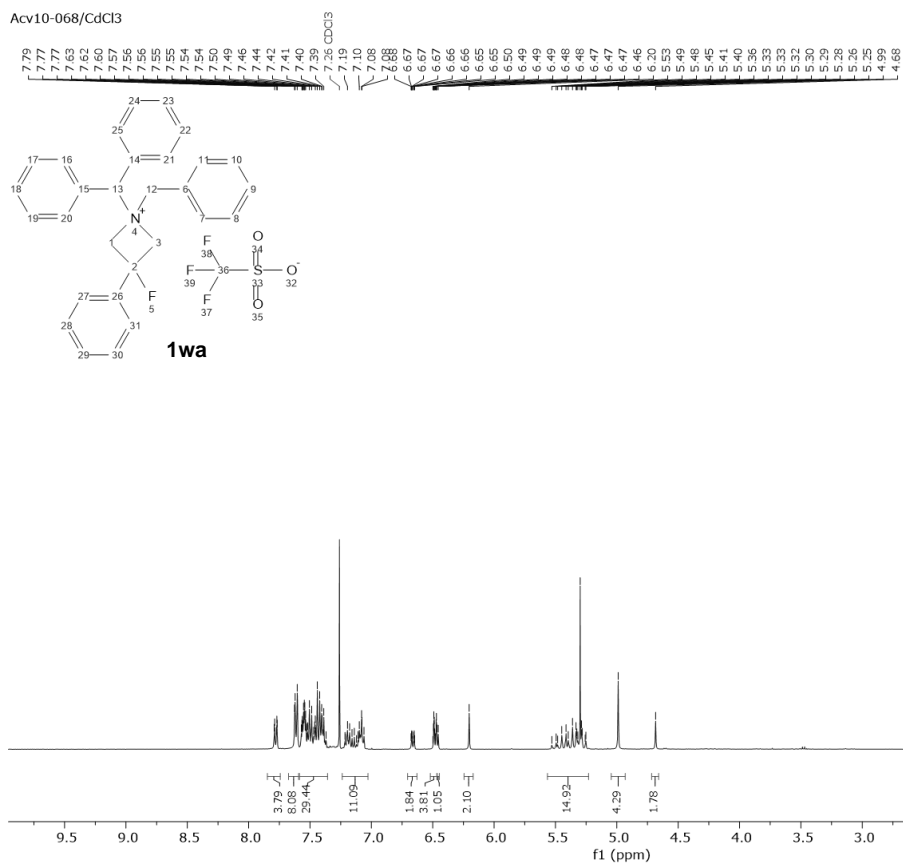
UOXF_groagna1_180_1/CdCl3



UOXF_groagna1_180_1/CdCl3

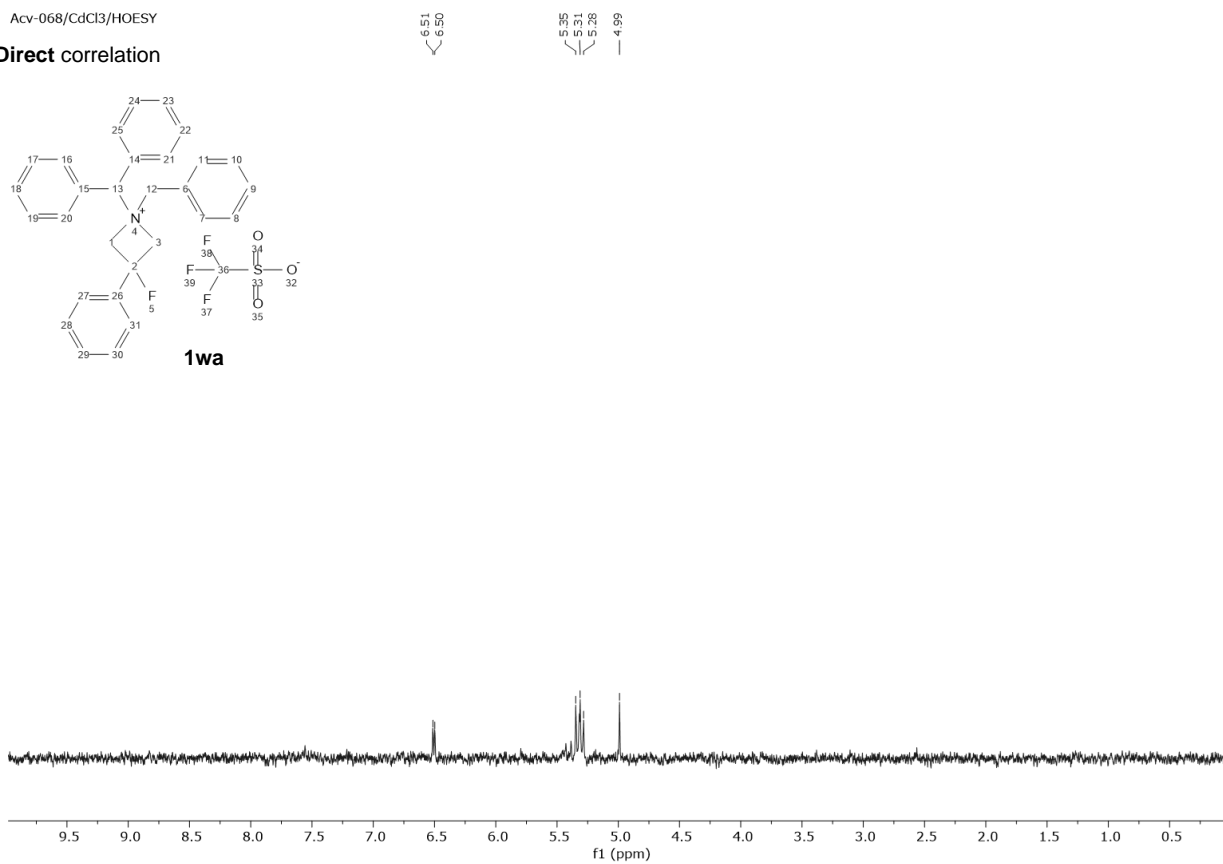


Acv10-068/CdCl3

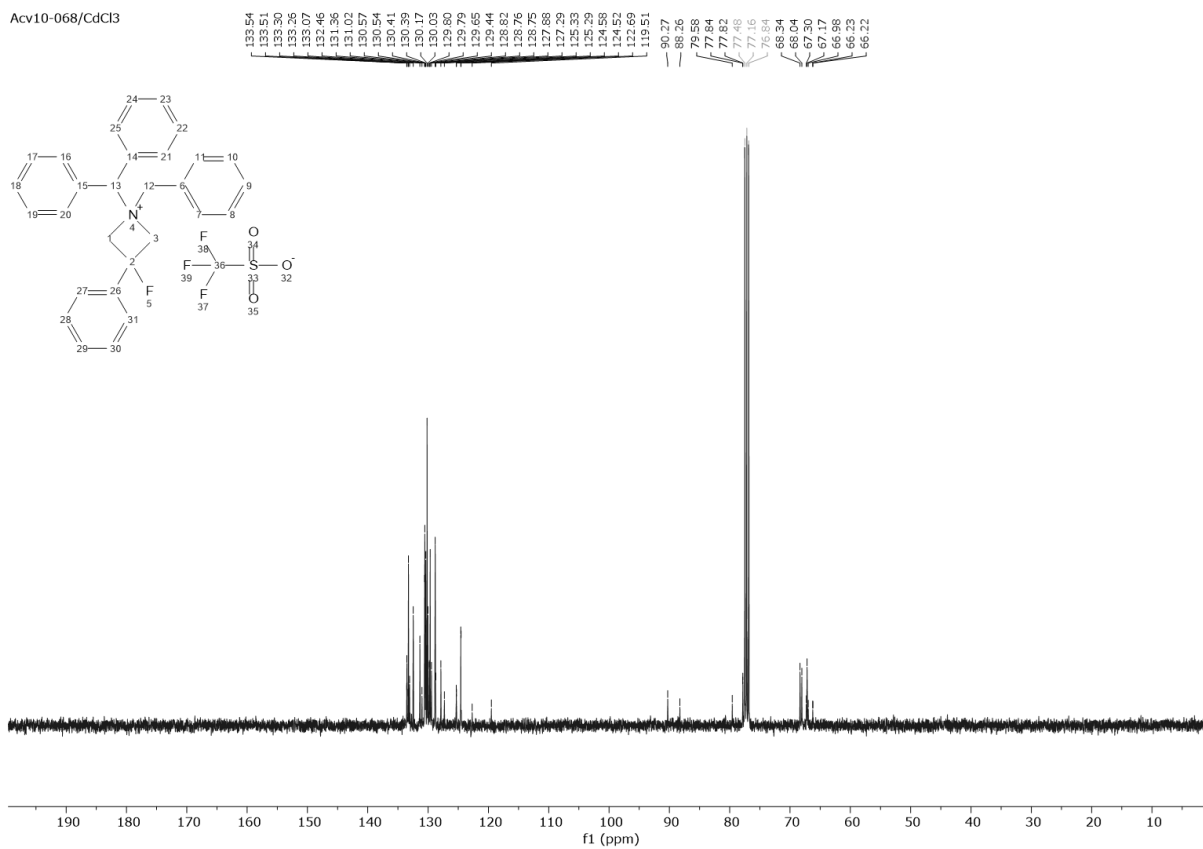


Acv-068/CdCl3/HOESY

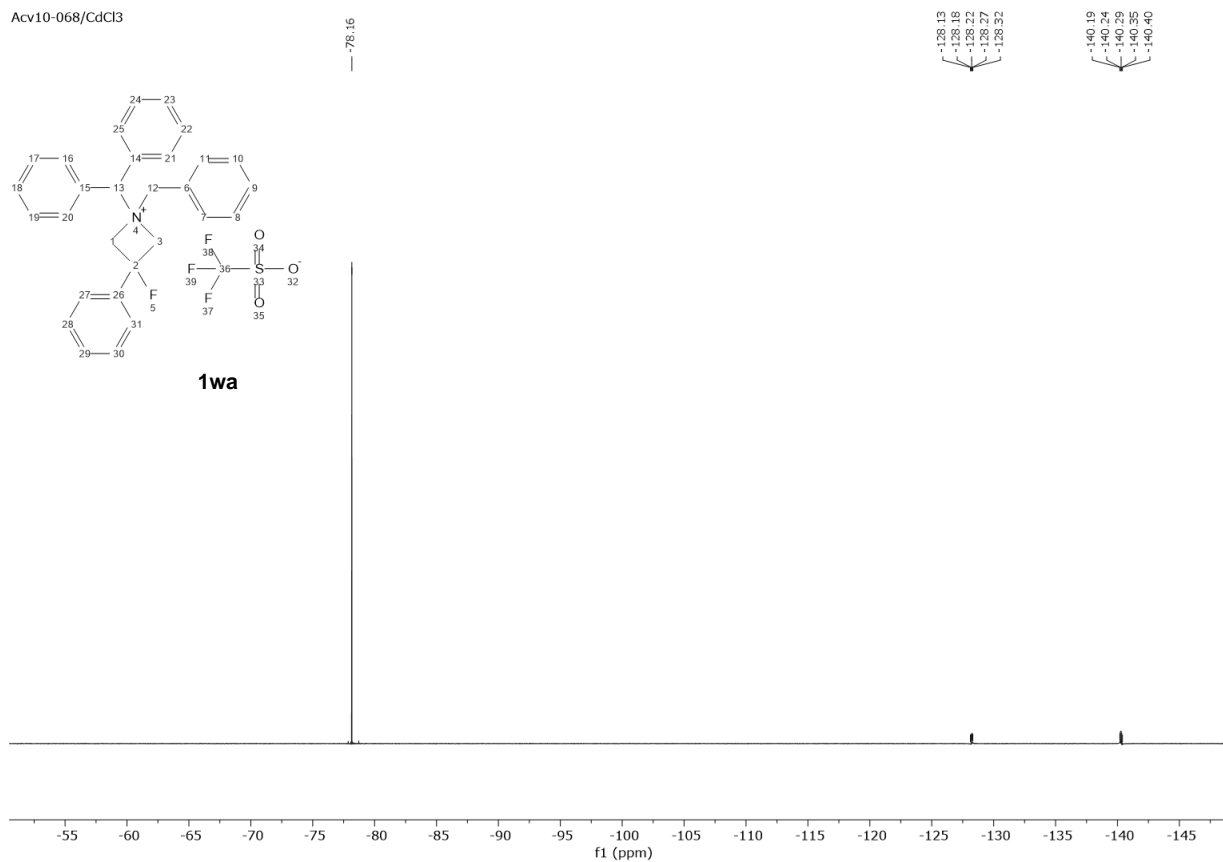
Direct correlation



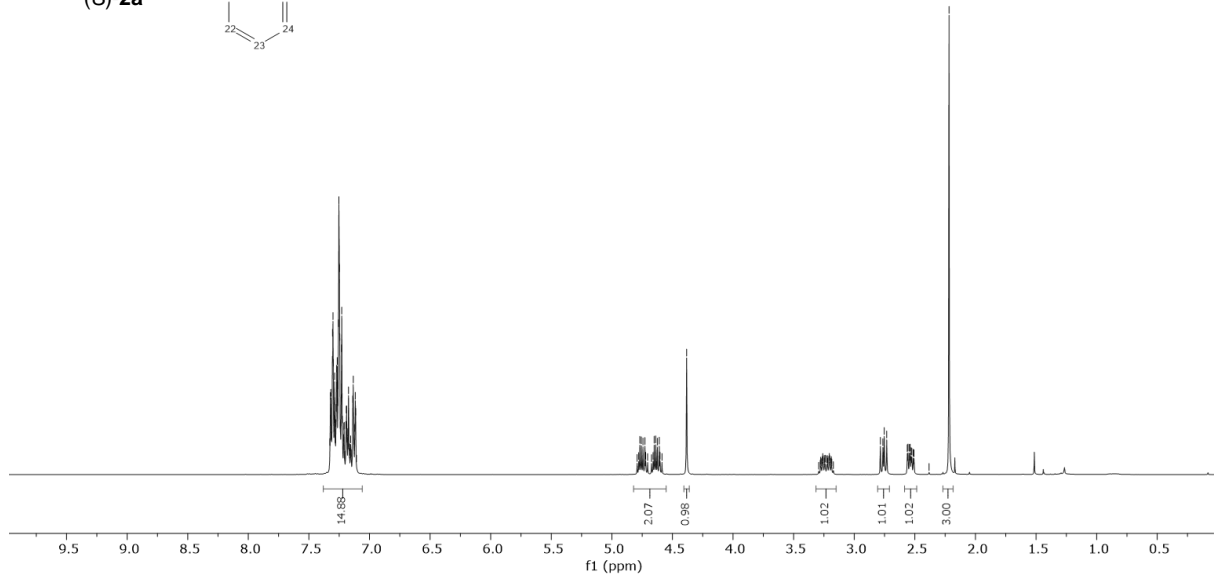
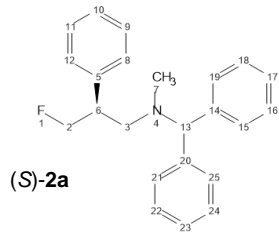
Acv10-068/CdCl3



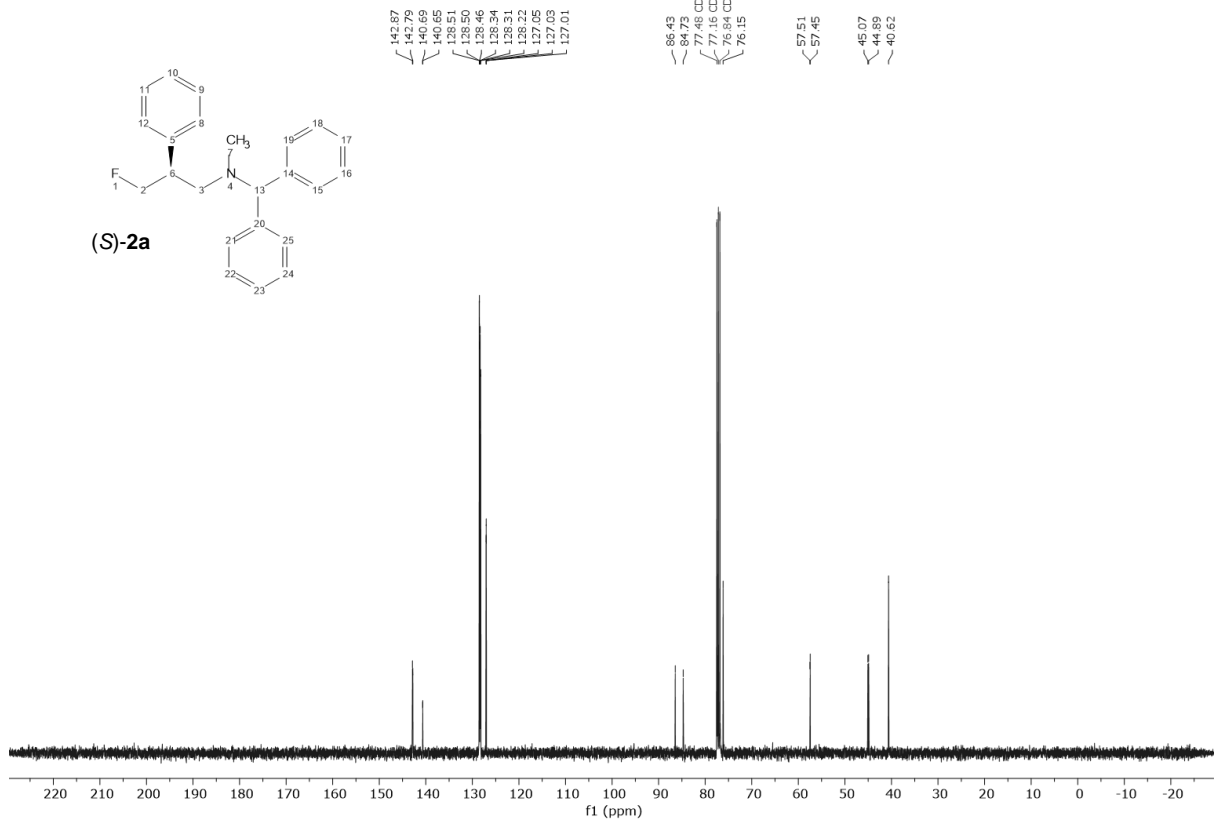
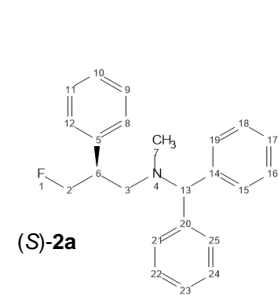
Acv10-068/CdCl3



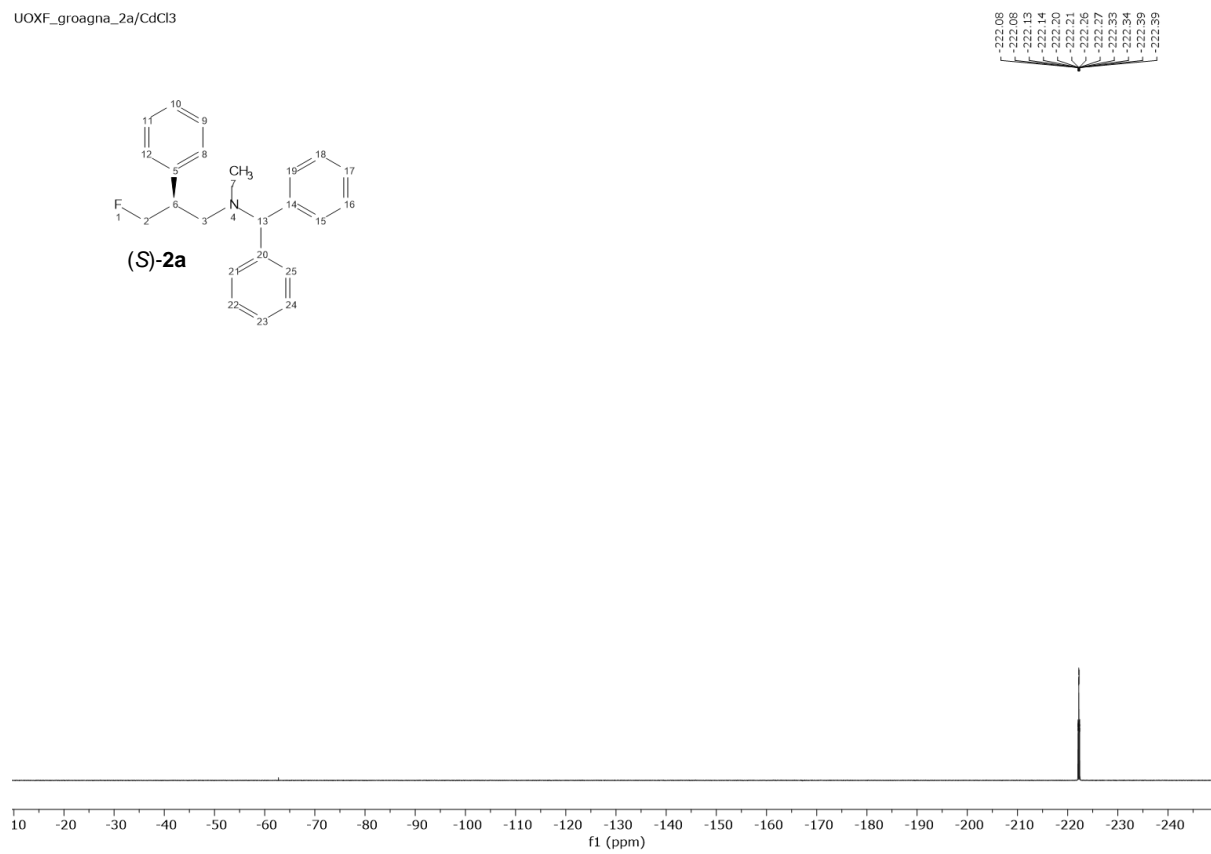
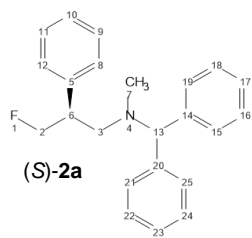
7.77, 7.76, 7.75, 7.74, 7.73, 7.72, 7.71, 7.70, 7.69, 7.68, 7.67, 7.66, 7.65, 7.64, 7.63, 7.62, 7.61, 7.60, 7.59, 7.58, 7.57, 7.56, 7.55, 7.54, 7.53, 7.52, 7.51, 7.50, 7.49, 7.48, 7.47, 7.46, 7.45, 7.44, 7.43, 7.42, 7.41, 7.40, 7.39, 7.38, 7.37, 7.36, 7.35, 7.34, 7.33, 7.32, 7.31, 7.30, 7.29, 7.28, 7.27, 7.26, 7.25, 7.24, 7.23, 7.22, 7.21, 7.20, 7.19, 7.18, 7.17, 7.16, 7.15, 7.14, 7.13, 7.12, 7.11, 7.10, 4.79, 4.78, 4.77, 4.76, 4.75, 4.74, 4.73, 4.72, 4.70, 4.67, 4.66, 4.65, 4.64, 4.63, 4.62, 4.61, 4.60, 4.59, 4.38, 3.26, 3.24, 3.23, 3.22, 3.21, 3.20, 3.19, 3.18, 3.17, 3.16, 3.15, 3.14, 3.13, 3.12, 3.11, 3.10, 3.09, 3.08, 3.07, 3.06, 3.05, 3.04, 3.03, 3.02, 3.01, 3.00, 2.99, 2.98, 2.97, 2.96, 2.95, 2.94, 2.93, 2.92, 2.91, 2.90, 2.89, 2.88, 2.87, 2.86, 2.85, 2.84, 2.83, 2.82, 2.81, 2.80, 2.79, 2.78, 2.77, 2.76, 2.75, 2.74, 2.73, 2.72, 2.71, 2.70, 2.69, 2.68, 2.67, 2.66, 2.65, 2.64, 2.63, 2.62, 2.61, 2.60, 2.59, 2.58, 2.57, 2.56, 2.55, 2.54, 2.53, 2.52, 2.51, 2.50, 2.49, 2.48, 2.47, 2.46, 2.45, 2.44, 2.43, 2.42, 2.41, 2.40, 2.39, 2.38, 2.37, 2.36, 2.35, 2.34, 2.33, 2.32, 2.31, 2.30, 2.29, 2.28, 2.27, 2.26, 2.25, 2.24, 2.23, 2.22

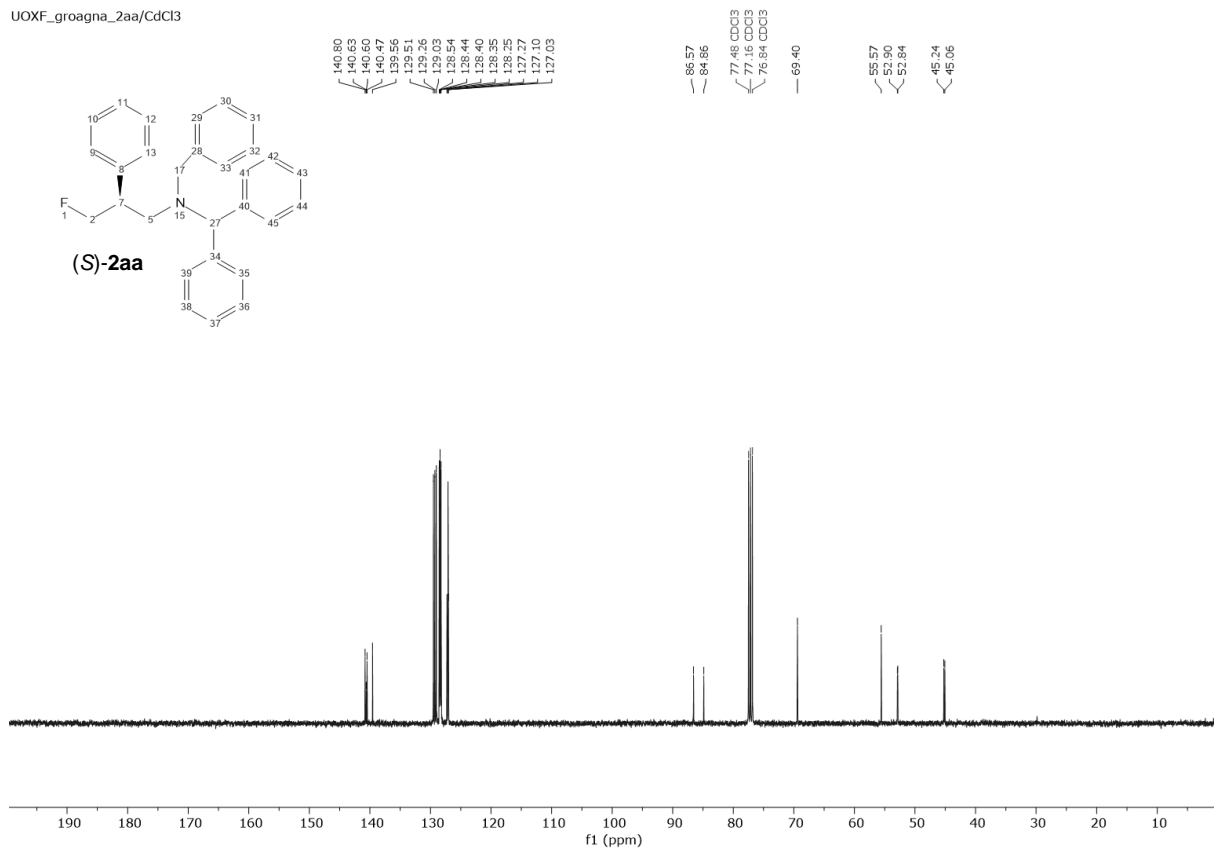
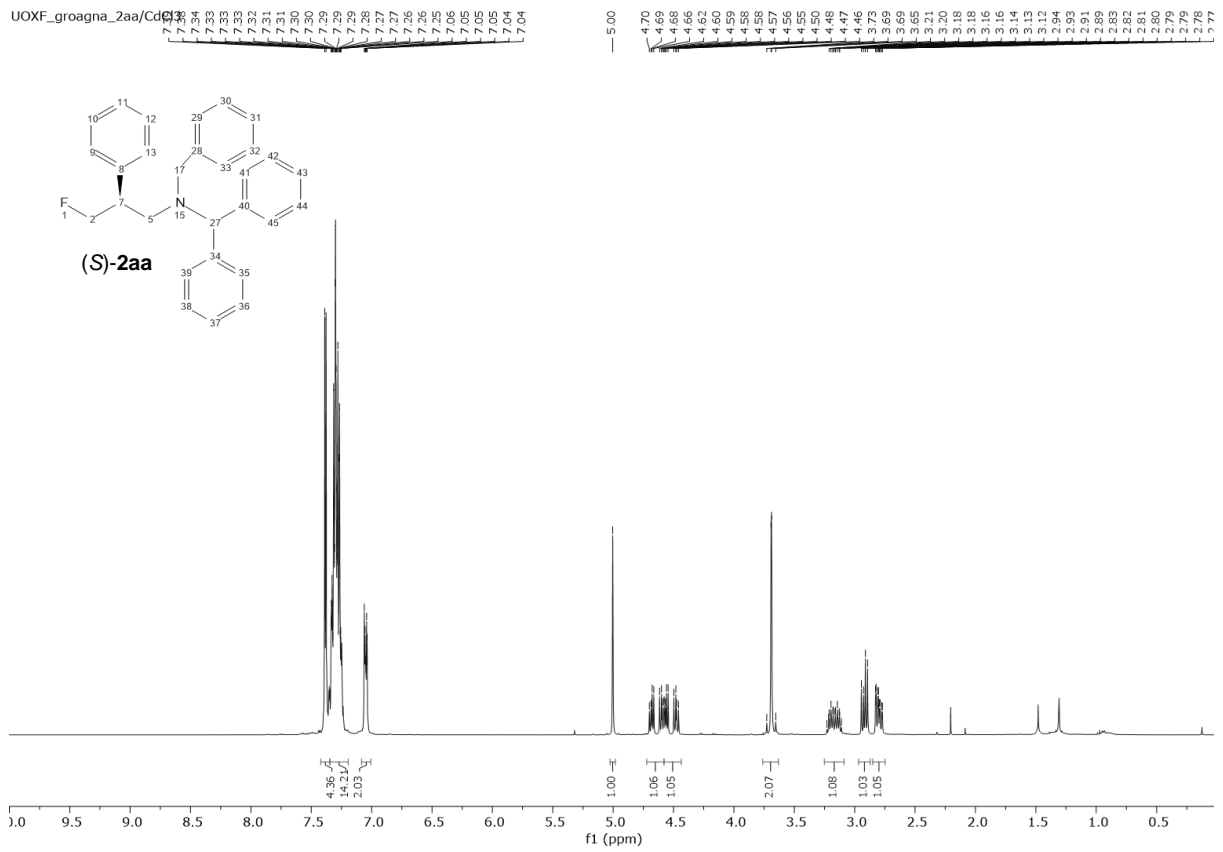


UOXF_groagna_2a/CdCl3

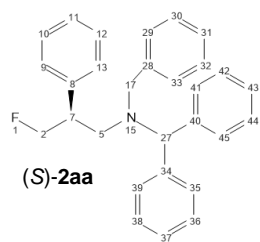


UOXF_groagna_2a/CdCl3



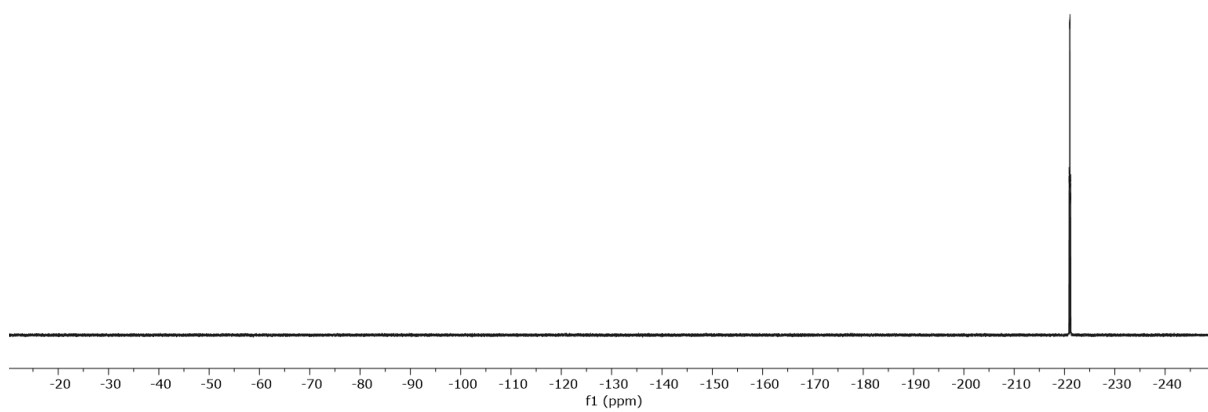


UOXF_groagna_2aa/CdCl3

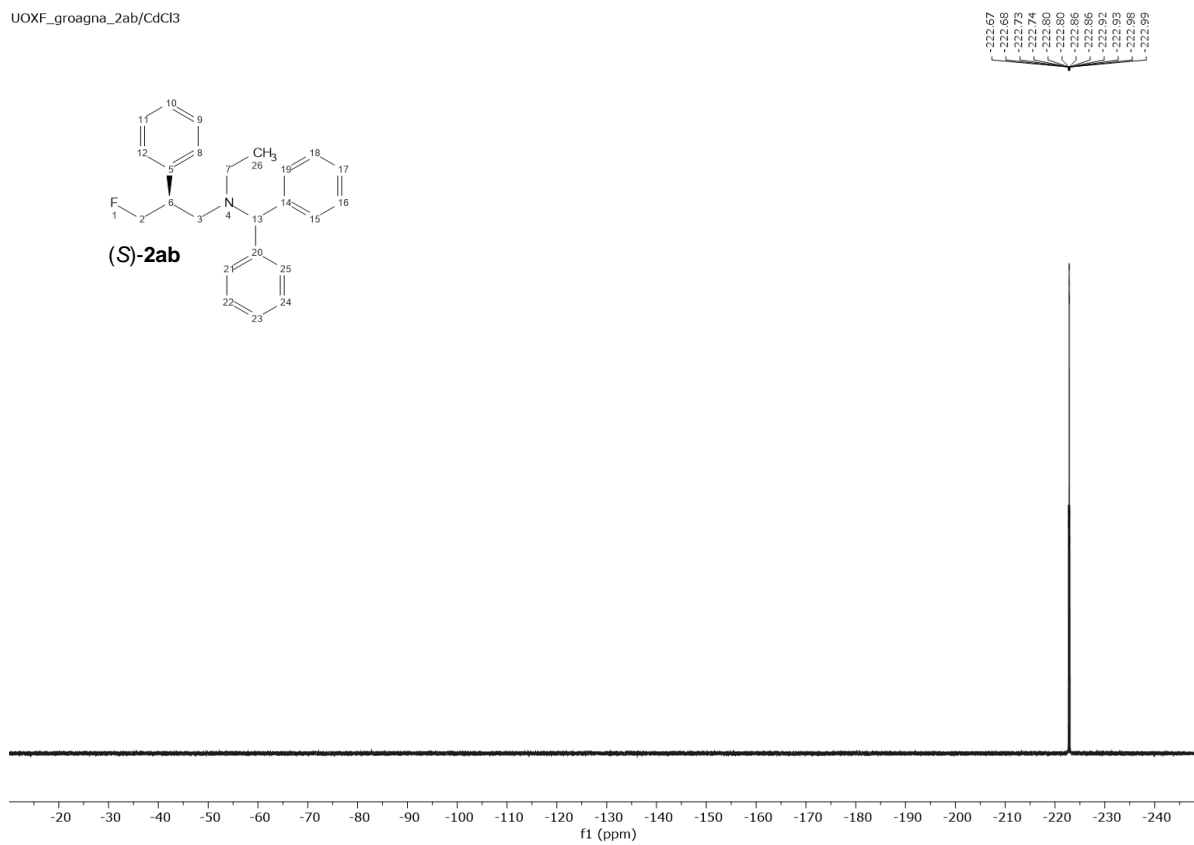
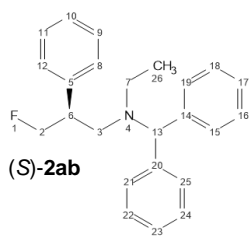


(S)-2aa

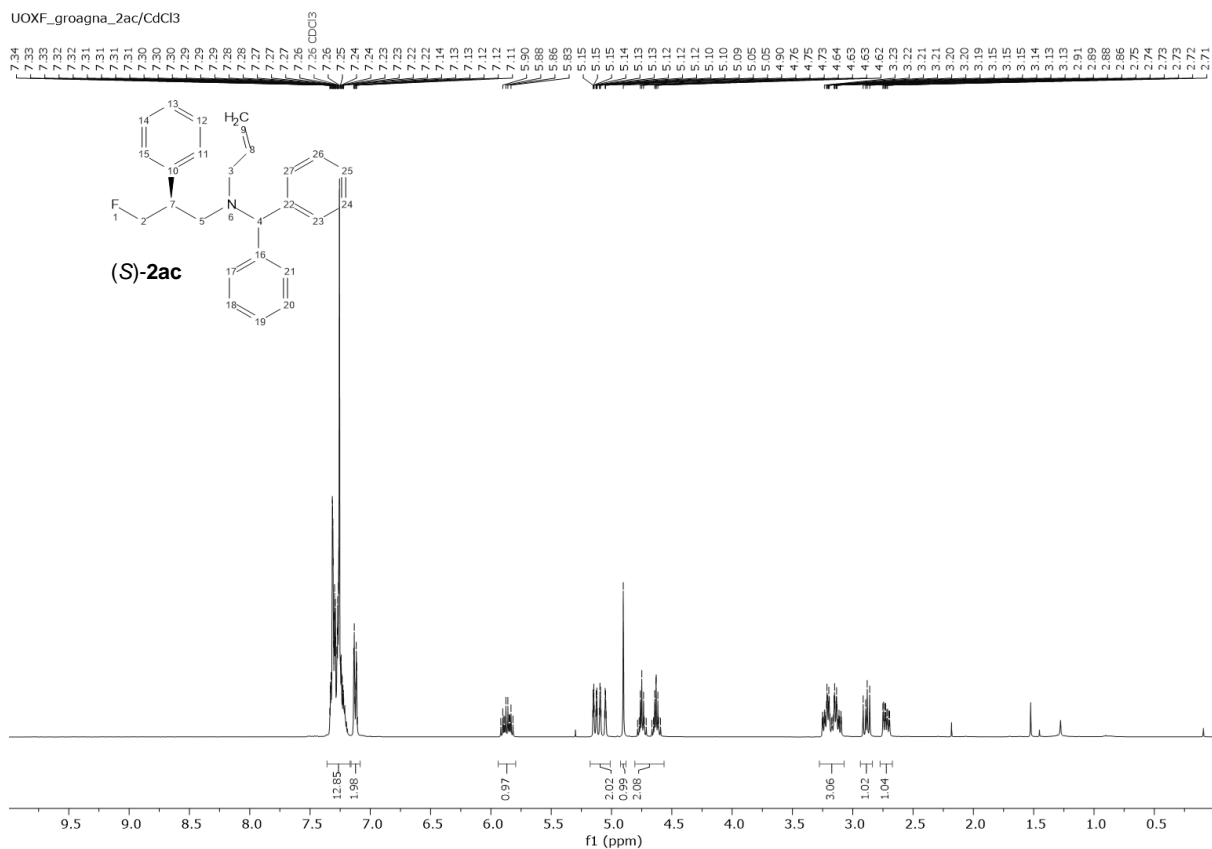
-220.91
-220.91
-220.97
-220.97
-221.04
-221.04
-221.09
-221.10
-221.13
-221.16
-221.17
-221.22
-221.22



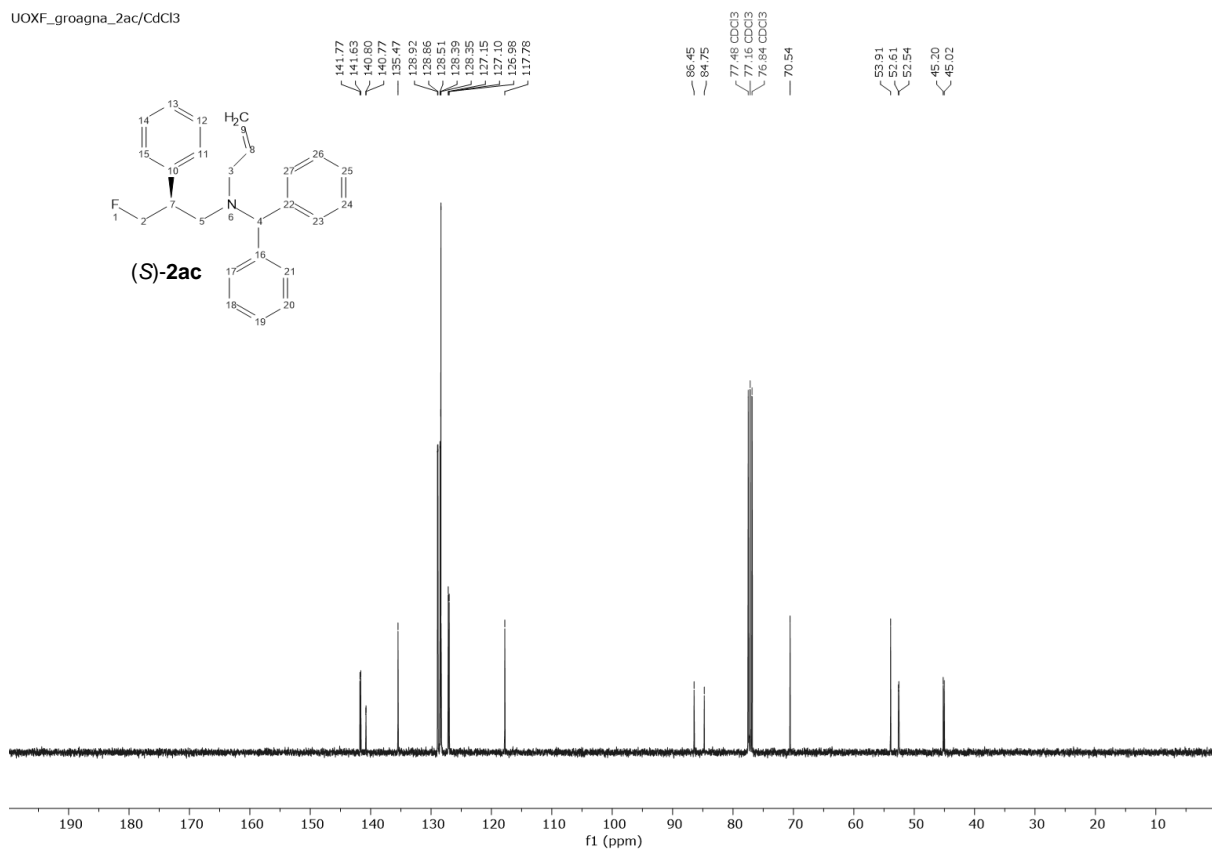
UOXF_groagna_2ab/CdCl3

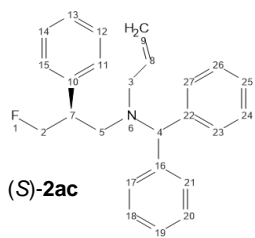


UOXF_groagna_2ac/CdCl3

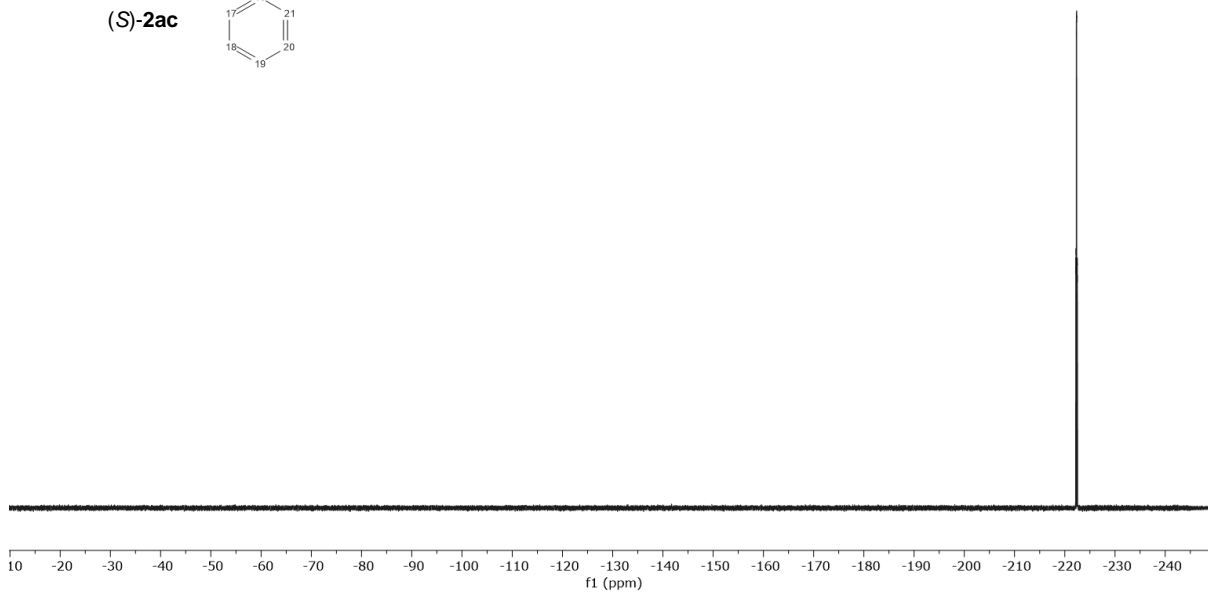


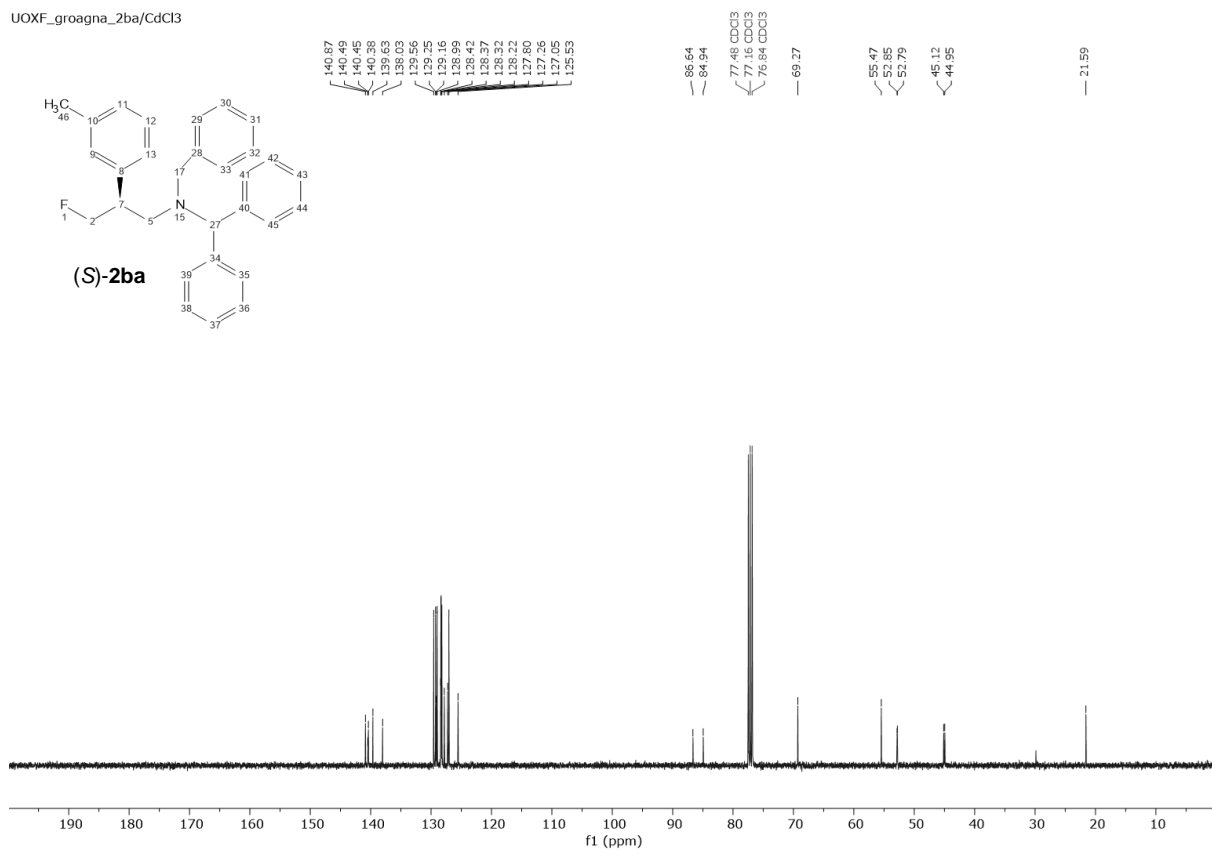
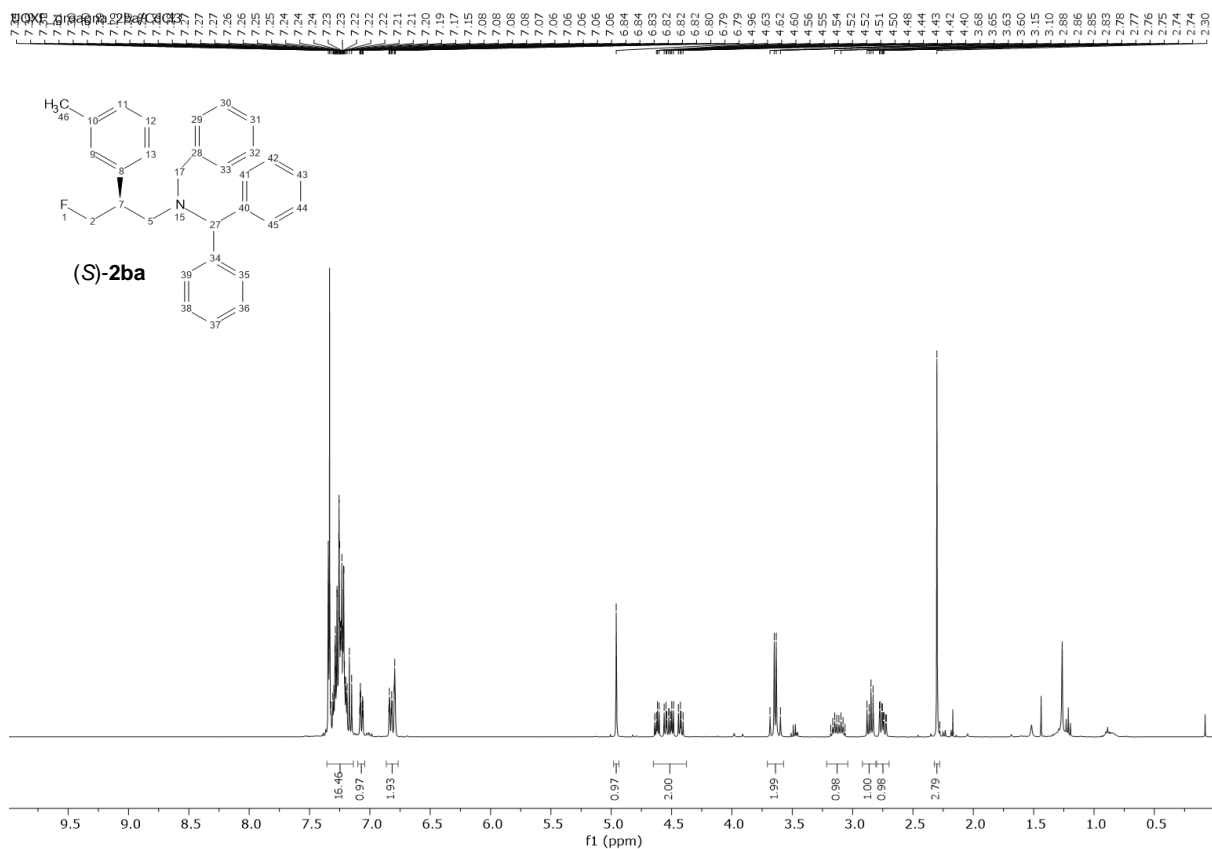
UOXF_groagna_2ac/CdCl3



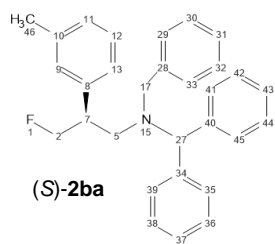


222.19
 222.19
 222.35
 222.31
 222.32
 222.37
 222.38
 222.44
 222.50
 222.50

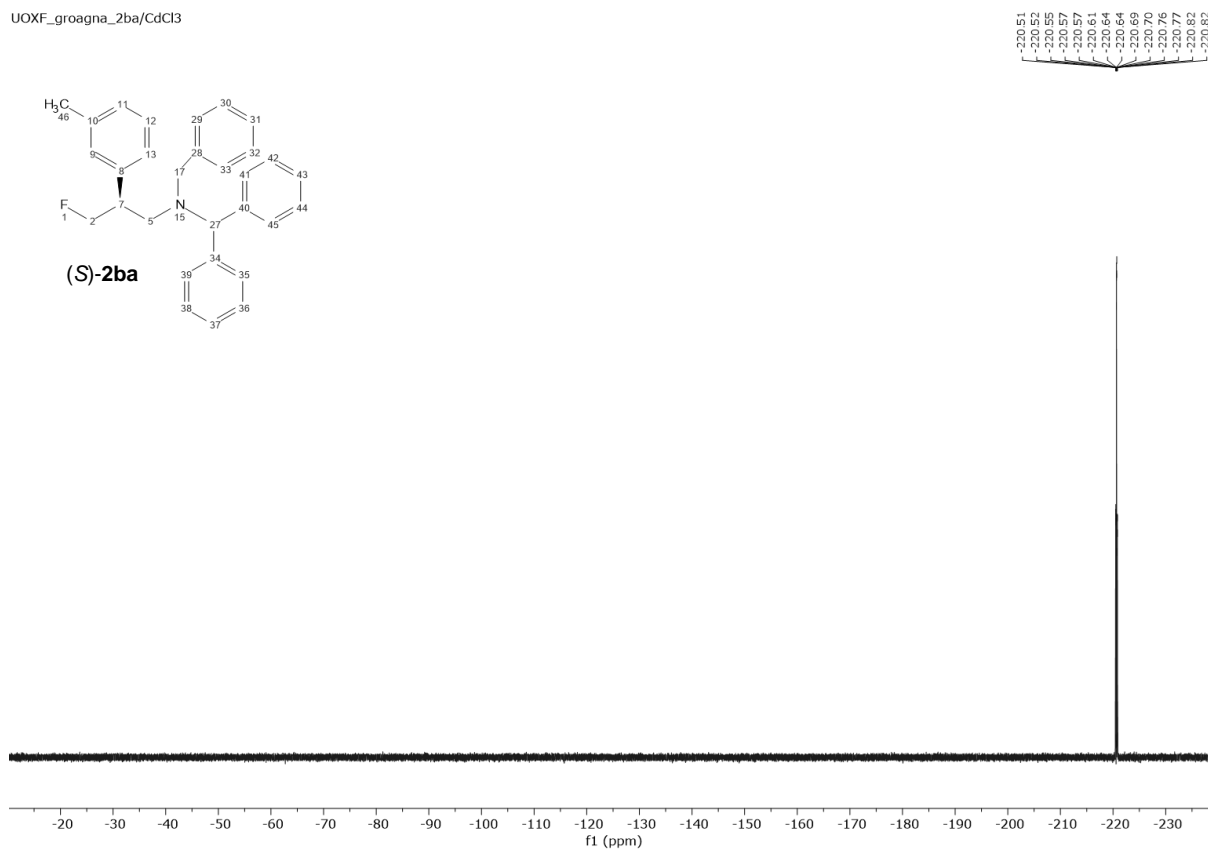




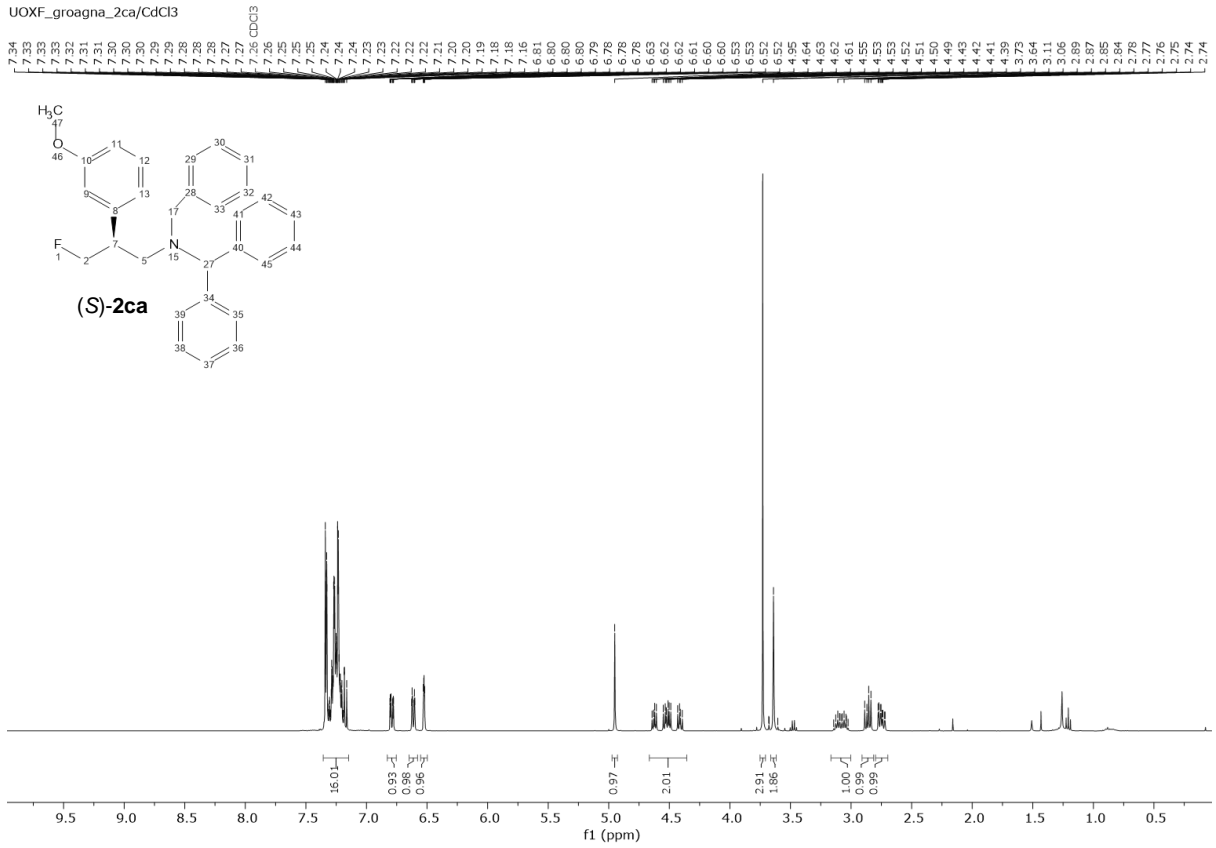
UOXF_groagna_2ba/CdCl3



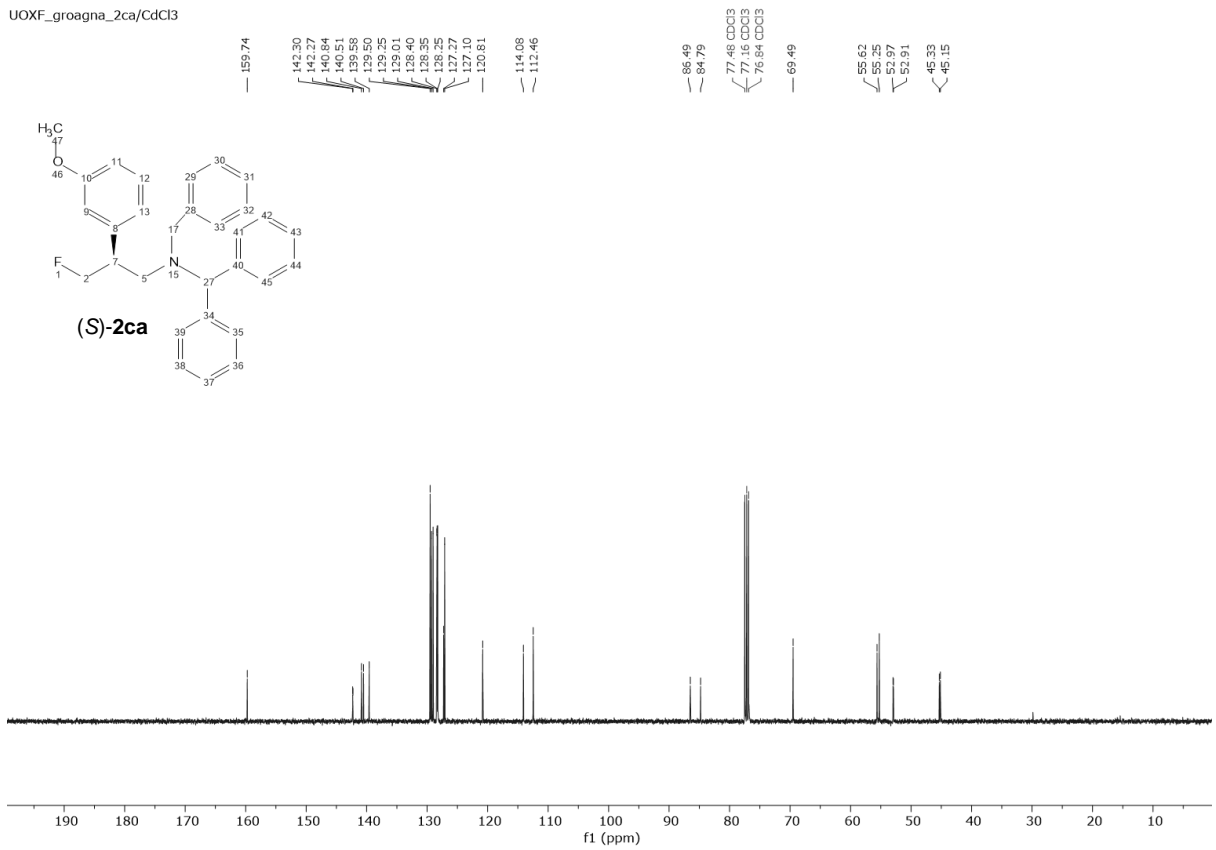
(S)-2ba

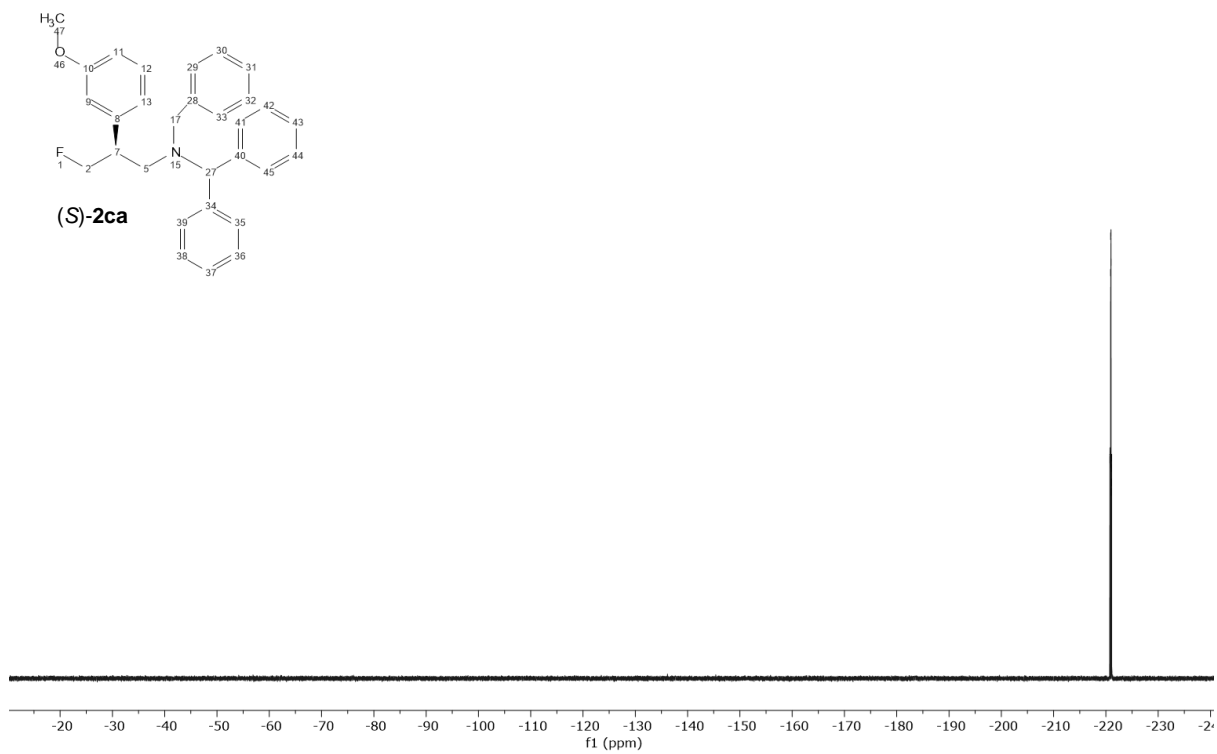


UOXF_groagna_2ca/CdCl3

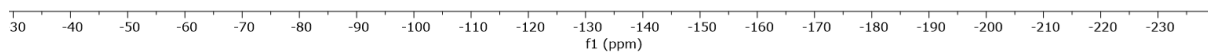
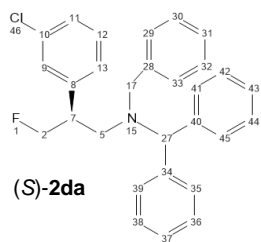


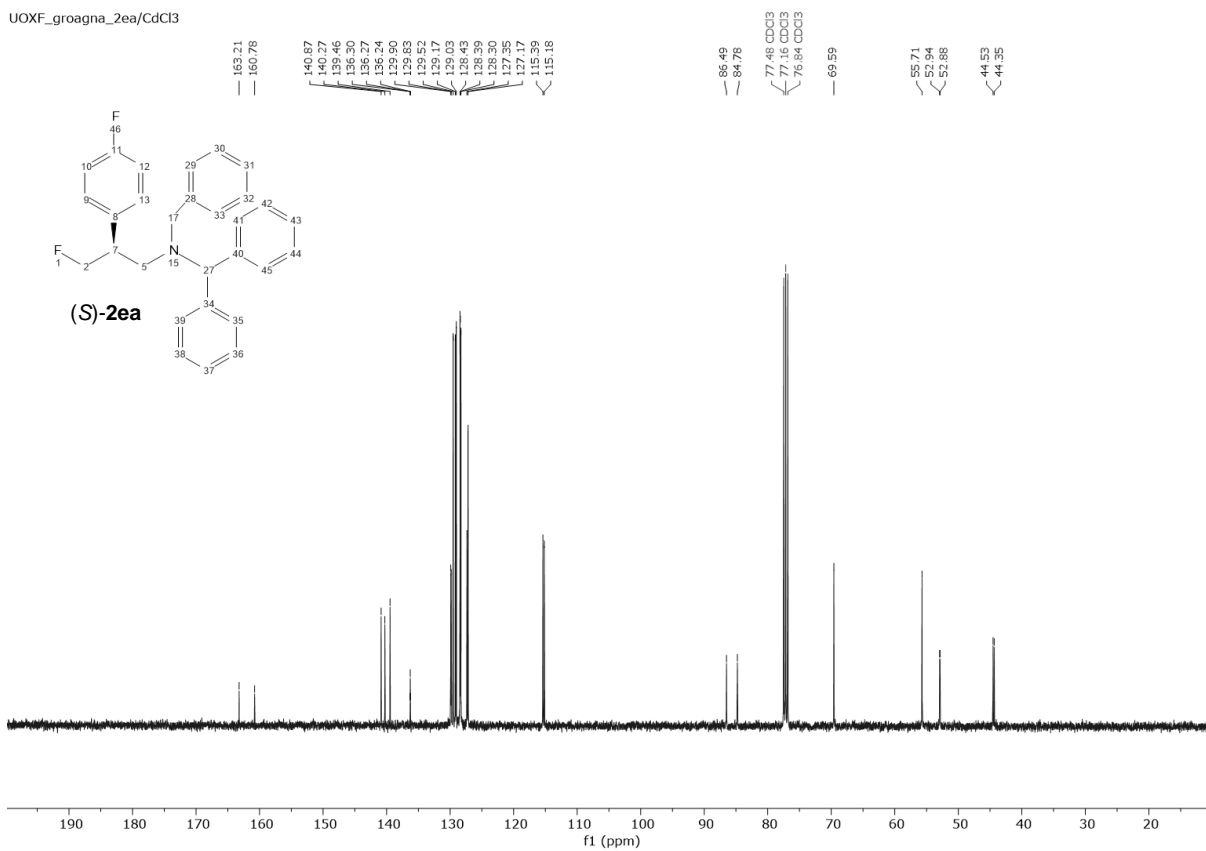
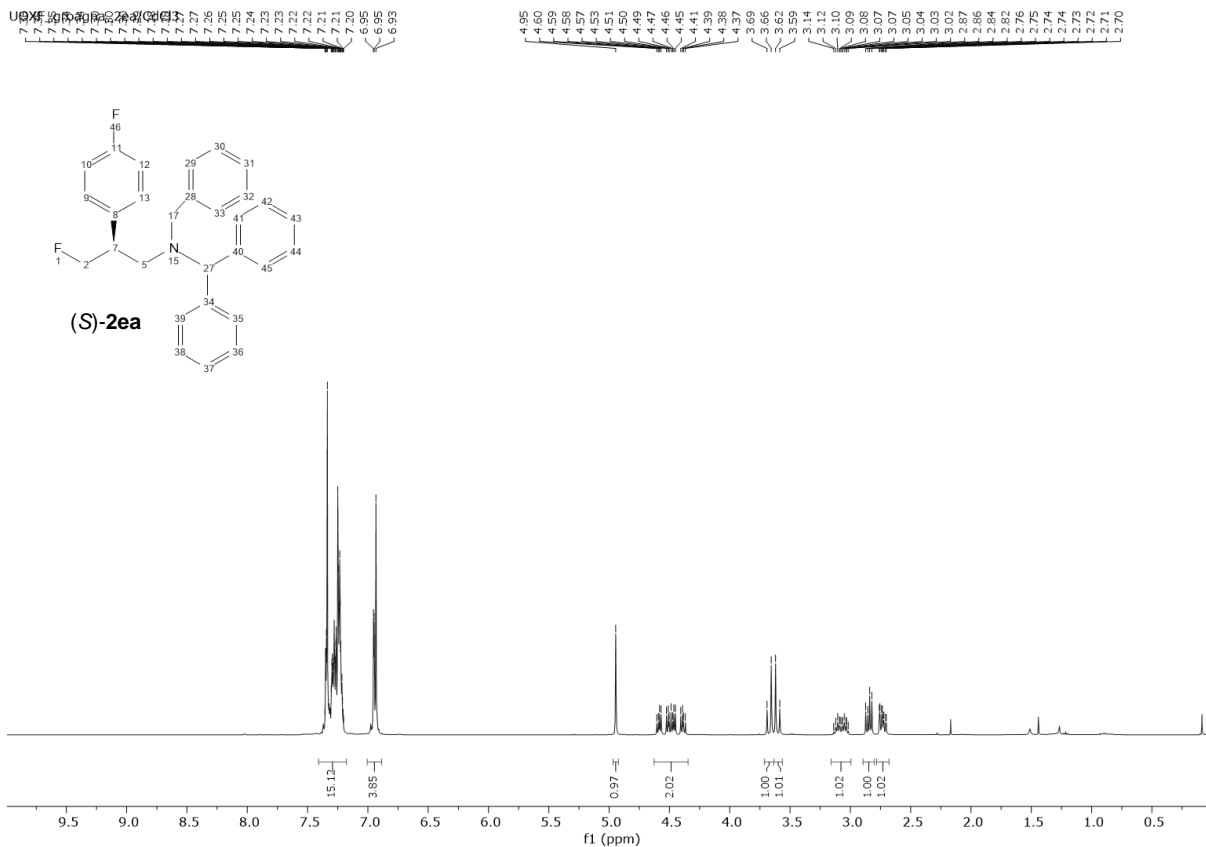
UOXF_groagna_2ca/CdCl3





-221.37
-221.43
-221.50
-221.55
-221.62
-221.68

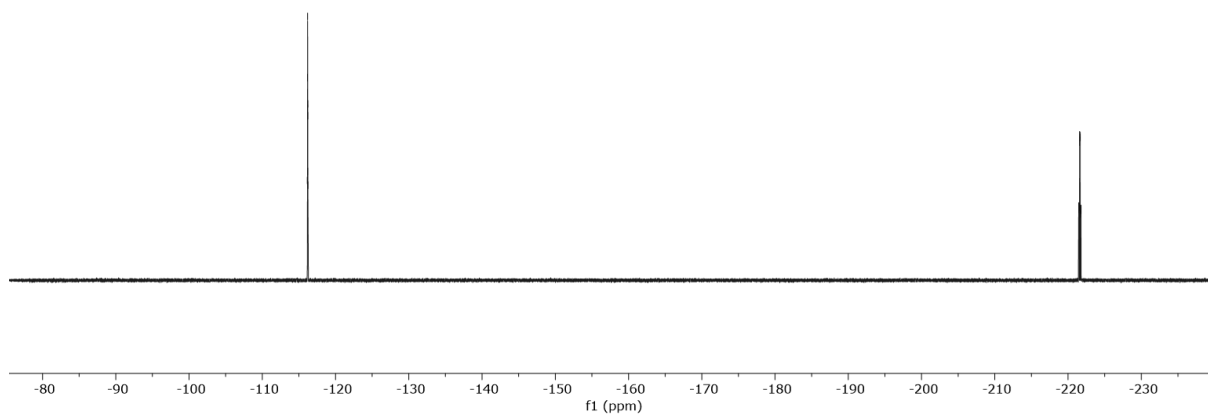
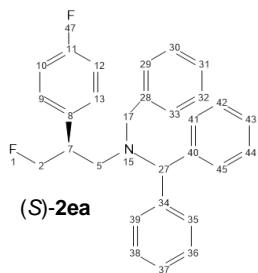




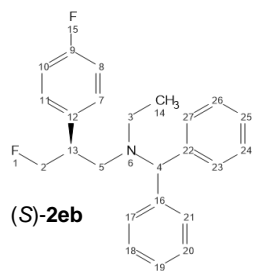
UOXF_groagna_2ea/CdCl3

-116.15
-116.17
-116.17
-116.18
-116.19
-116.21
-116.21
-116.23

-221.45
-221.46
-221.51
-221.51
-221.58
-221.58
-221.64
-221.64
-221.70
-221.71
-221.76
-221.77

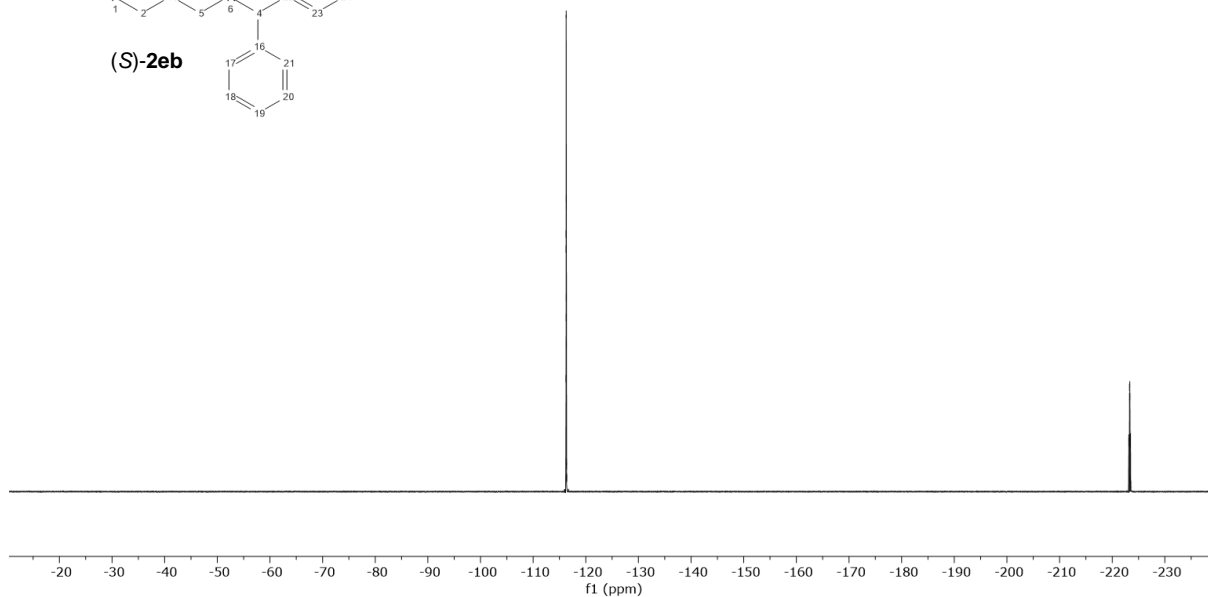


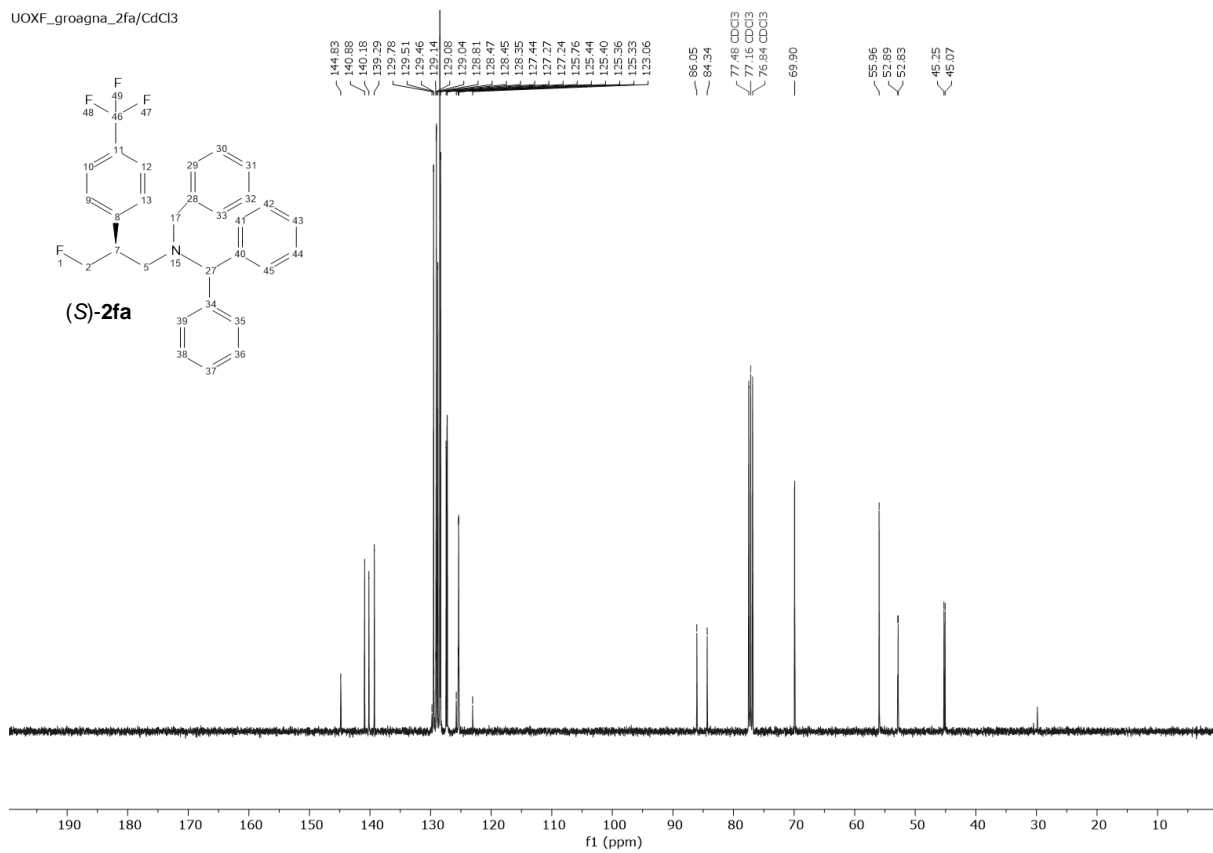
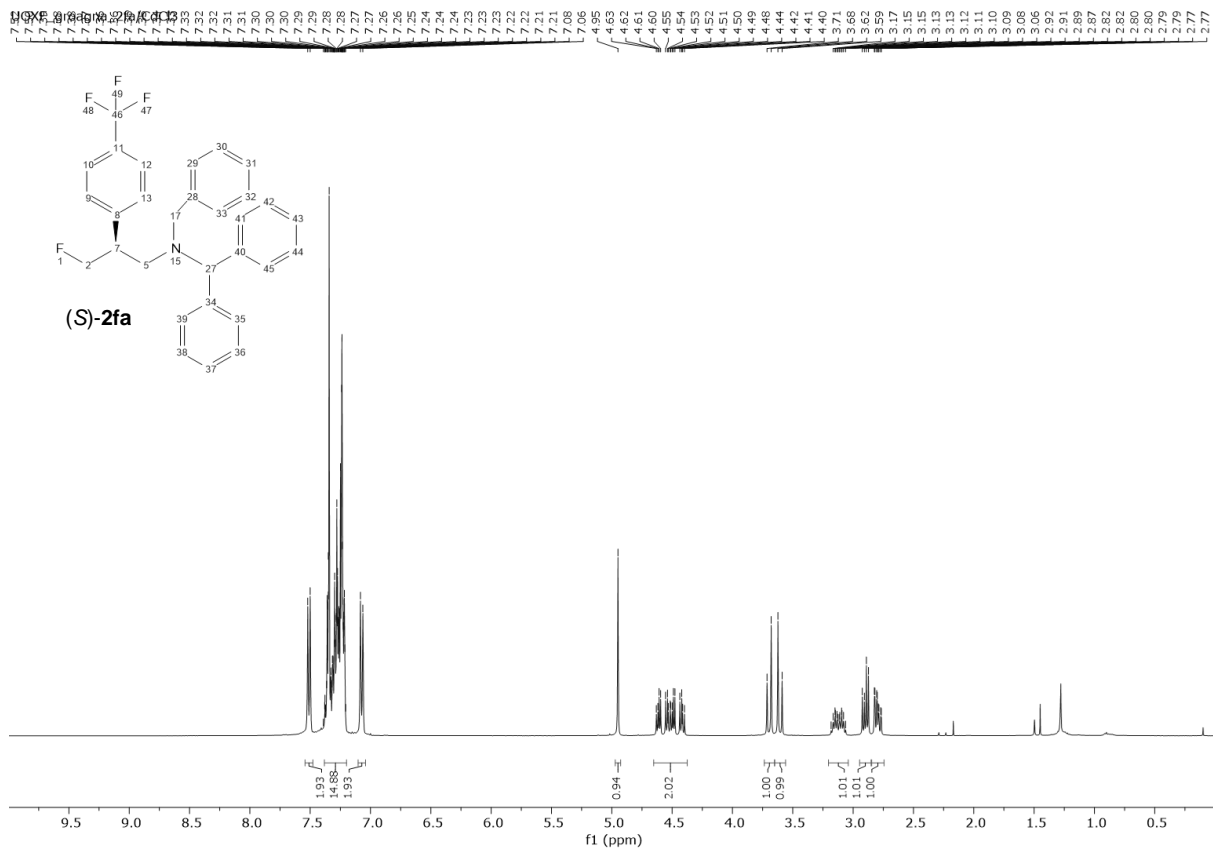
UOXF_groagna_2eb/CdCl3

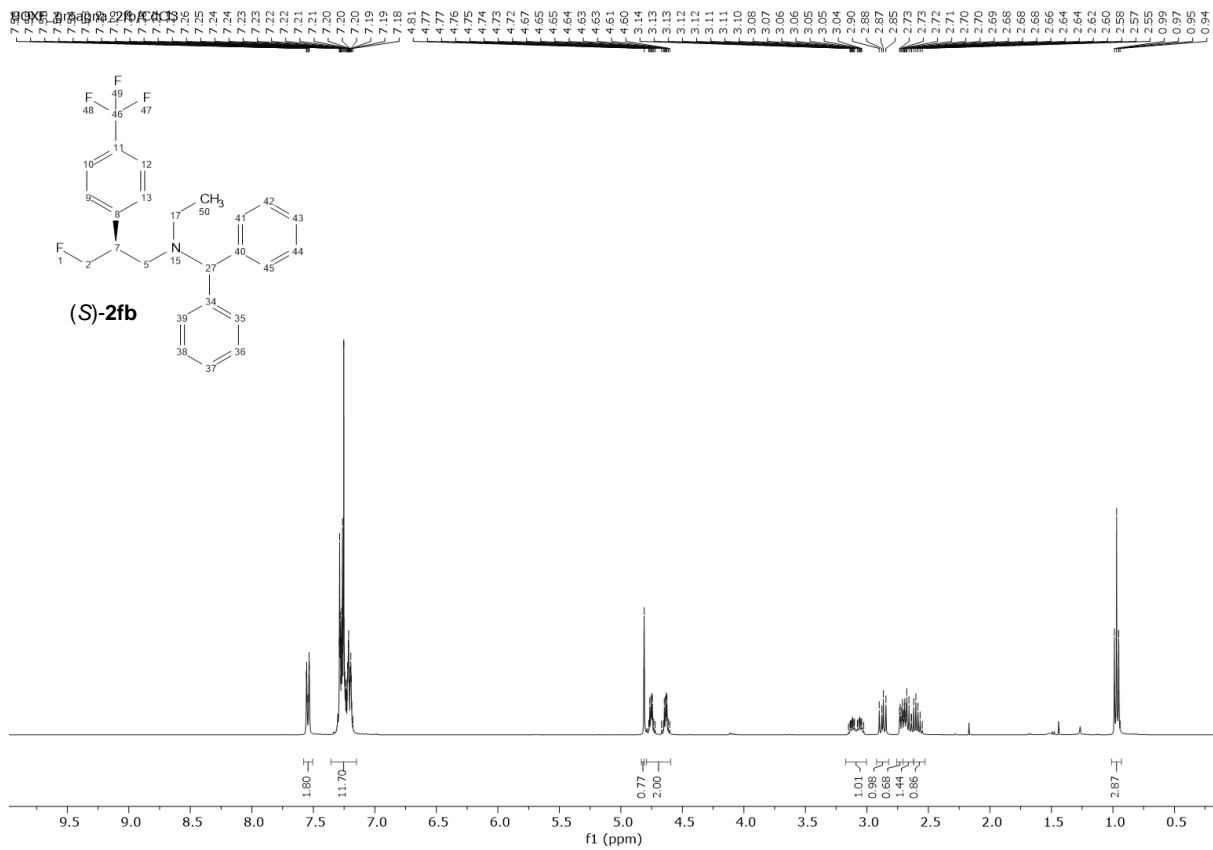


-116.25
-116.26
-116.27
-116.28
-116.29
-116.30
-116.31
-116.32
-116.33
-116.34
-116.35
-116.36

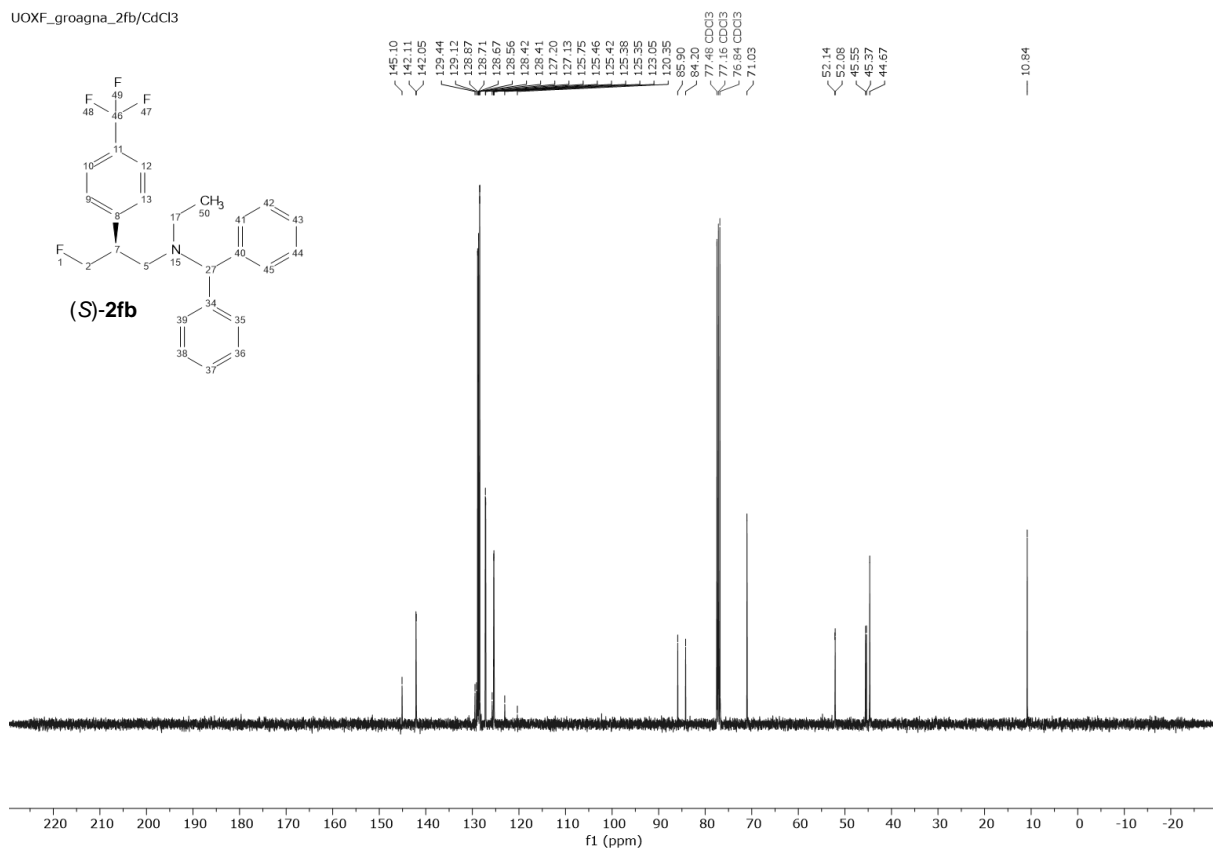
-223.15
-223.16
-223.22
-223.22
-223.22
-223.26
-223.29
-223.34
-223.35
-223.35
-223.41
-223.41
-223.43
-223.47
-223.48
-223.53



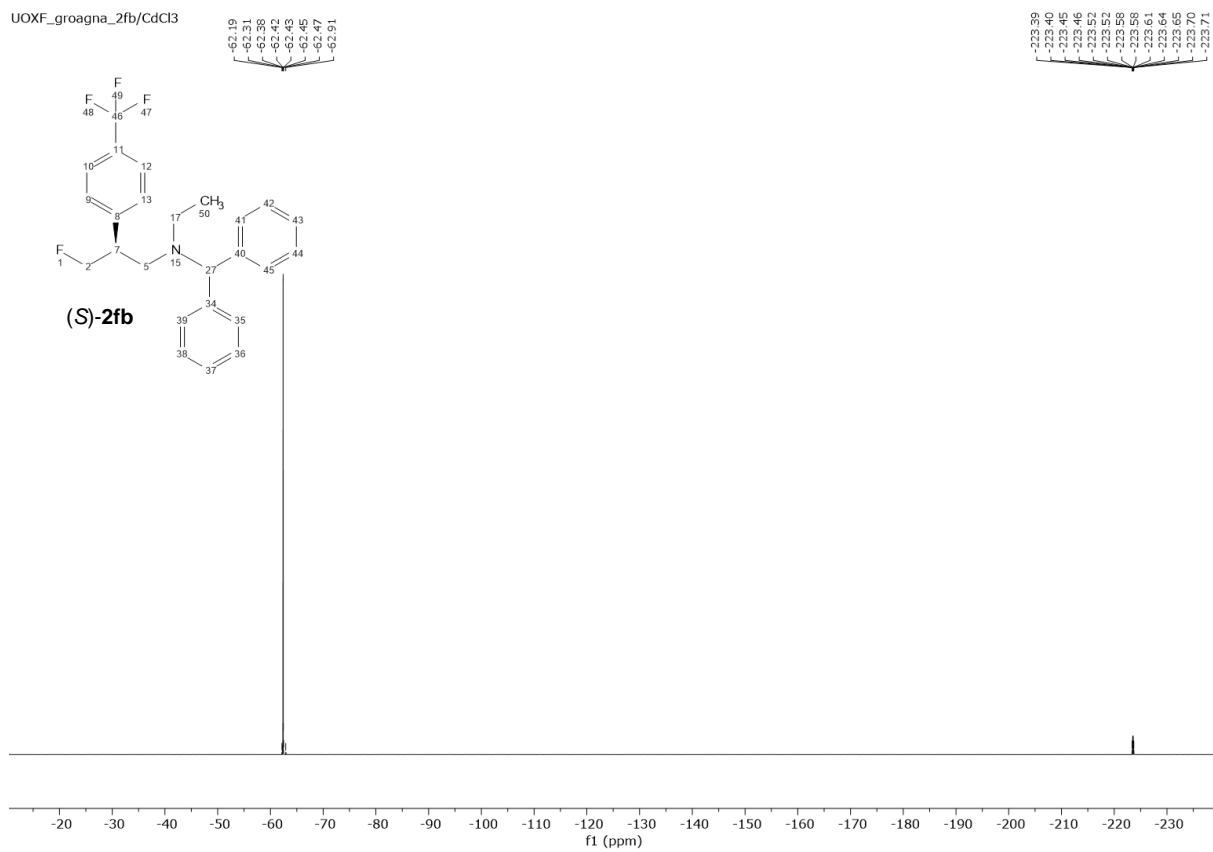




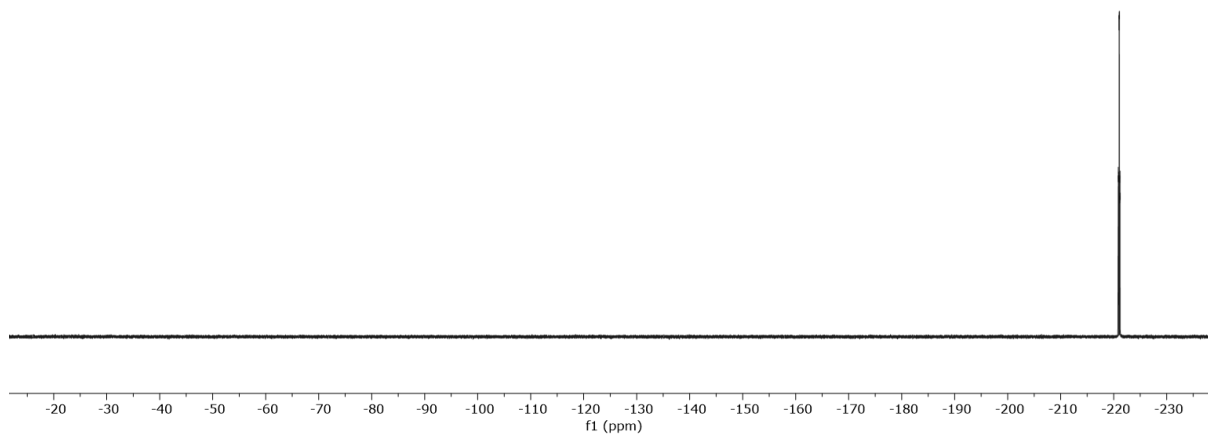
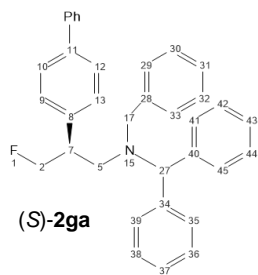
UOXF_groagna_2fb/CdCl3



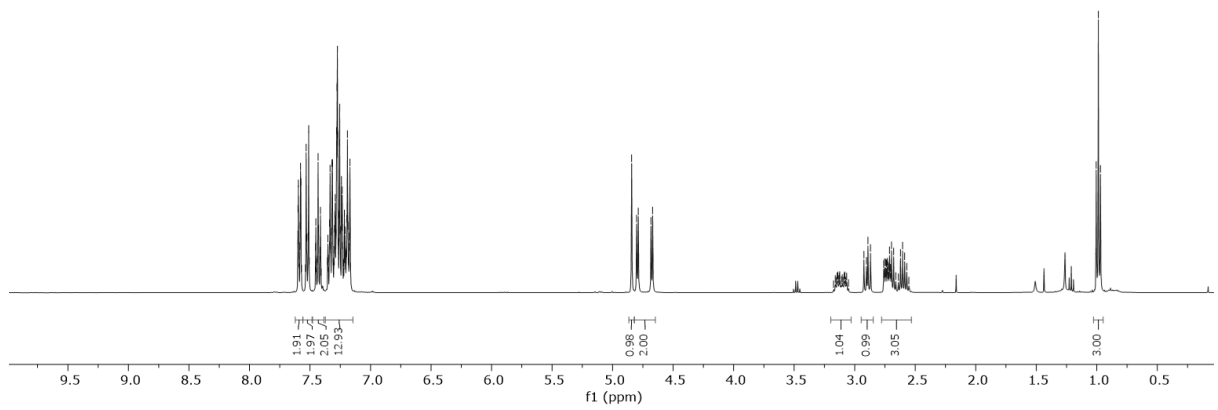
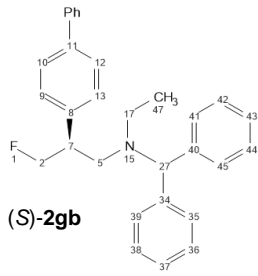
UOXF_groagna_2fb/CdCl3



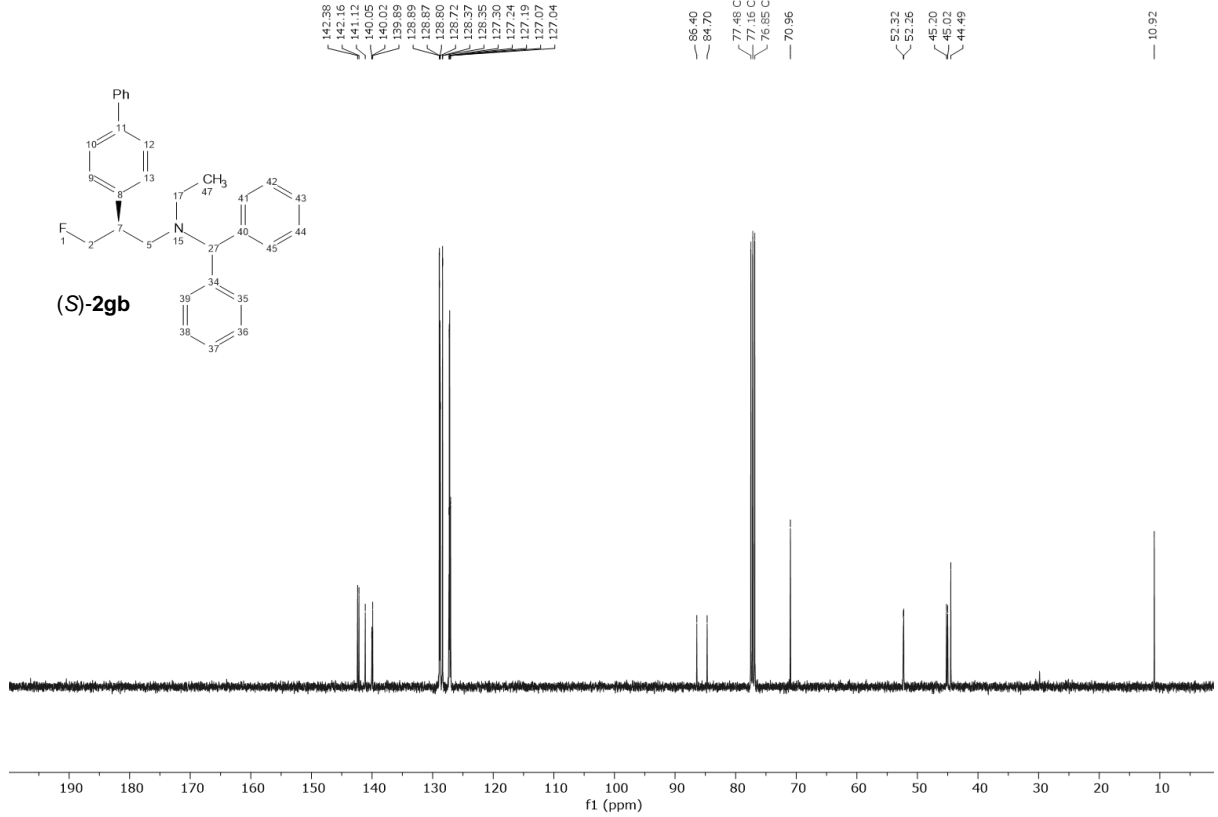
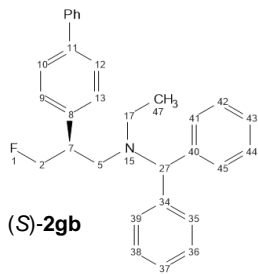
-220.88
-220.88
-220.93
-220.94
-221.00
-221.01
-221.07
-221.13
-221.13
-221.19
-221.19



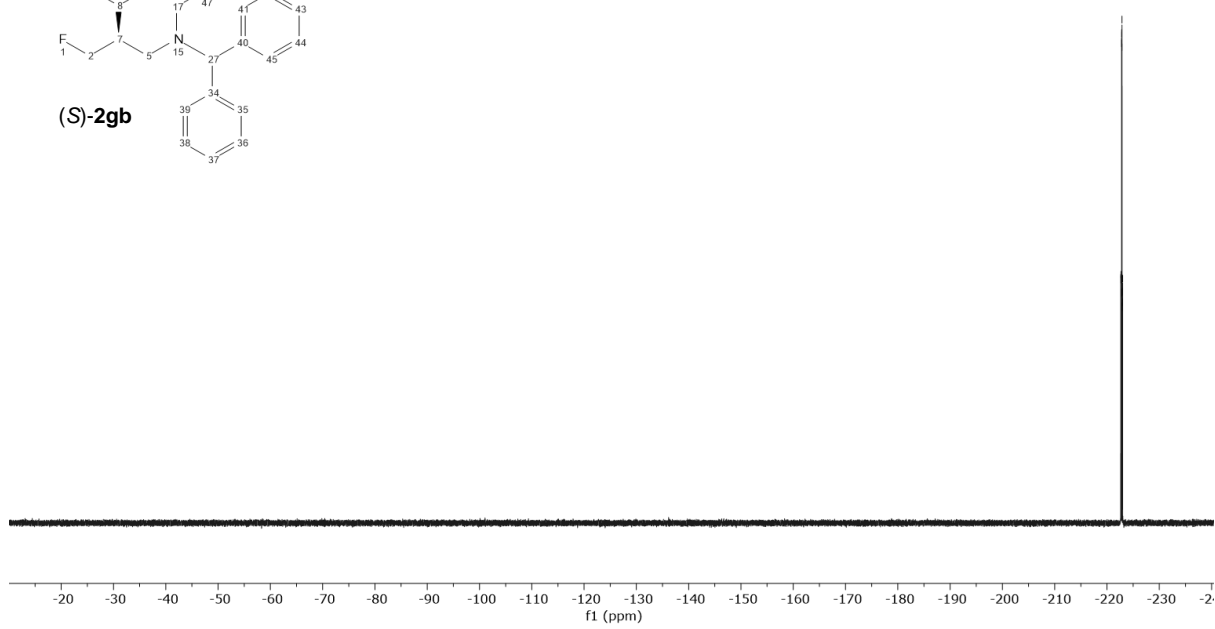
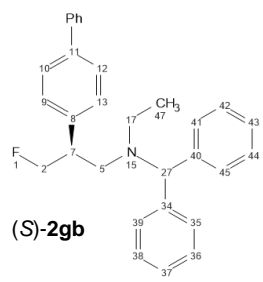
7.70
7.69
7.68
7.67
7.66
7.65
7.64
7.63
7.62
7.61
7.60
7.59
7.58
7.57
7.56
7.55
7.54
7.53
7.52
7.51
7.50
7.49
7.48
7.47
7.46
7.45
7.44
7.43
7.42
7.41
7.40
7.39
7.38
7.37
7.36
7.35
7.34
7.33
7.32
7.31
7.30
7.29
7.28
7.27
7.26
7.25
7.24
7.23
7.22
7.21
7.20
7.19
7.18
7.17
7.16
7.15
7.14
7.13
7.12
7.11
7.10
7.09
7.08
7.07
7.06
7.05
7.04
7.03
7.02
7.01
7.00
6.99
6.98
6.97



UOXF_groagna_2gb/CdCl3

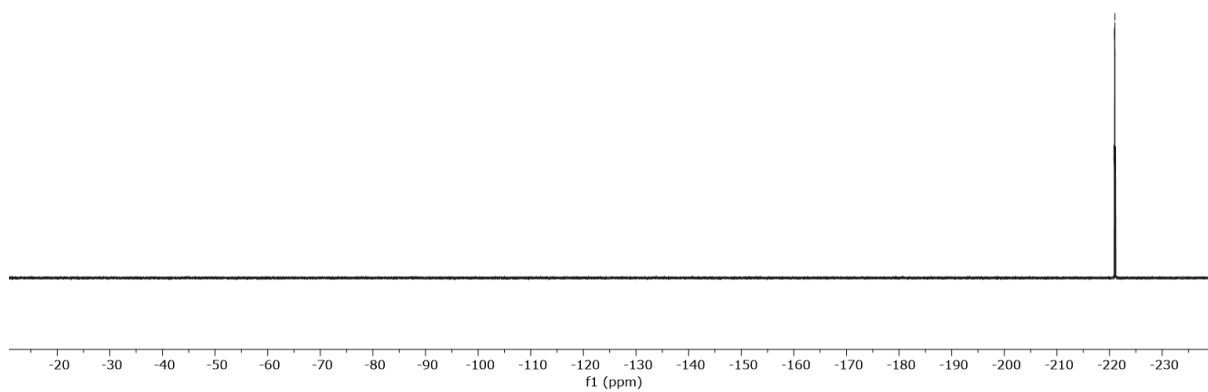
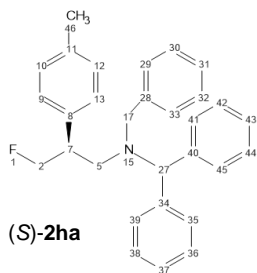


-222.68
 -222.68
 -222.74
 -222.74
 -222.80
 -222.81
 -222.86
 -222.87
 -222.95
 -222.96
 -222.98
 -223.00

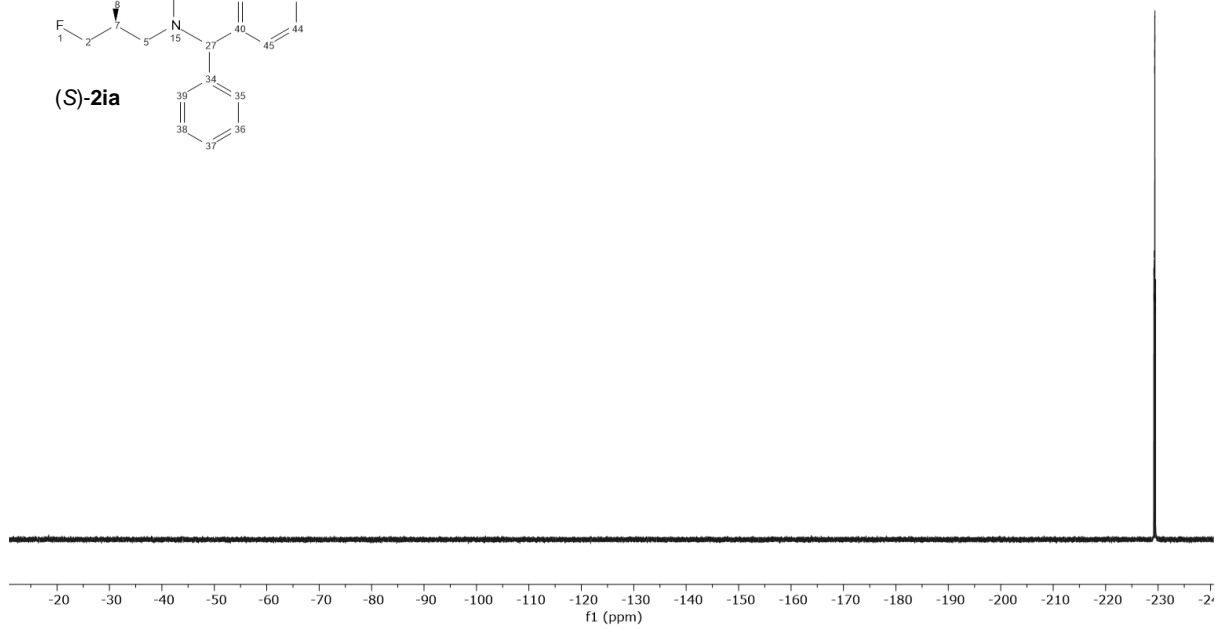
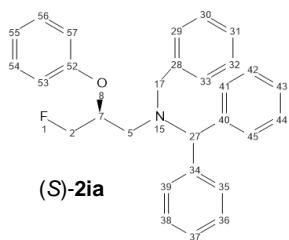


UOXF_groagna_2ha/CdCl3

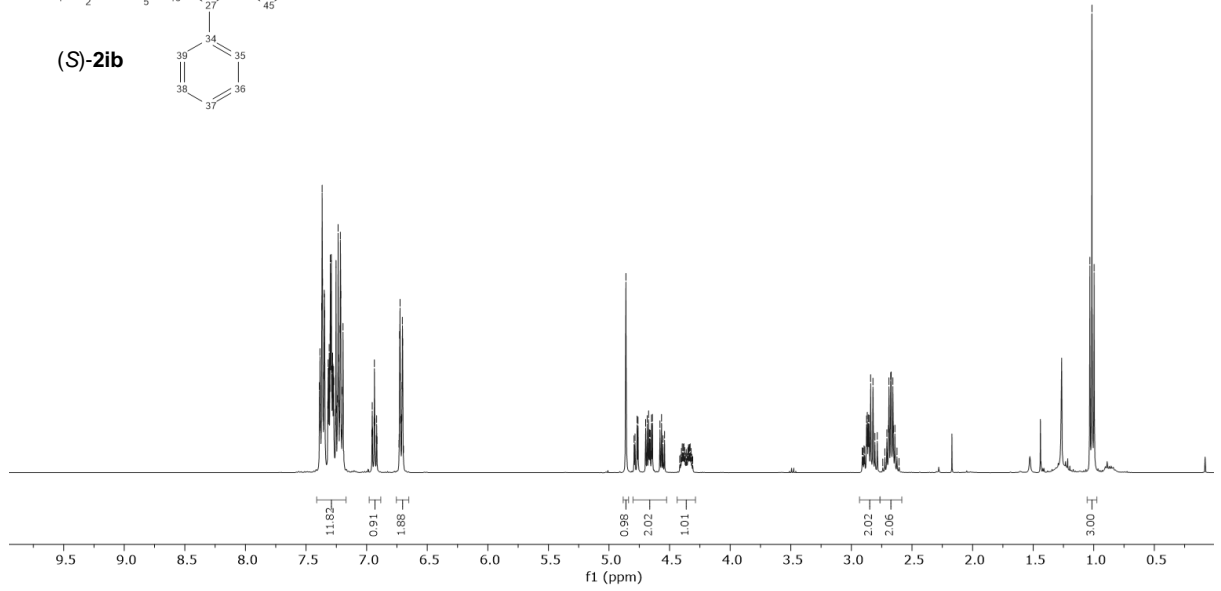
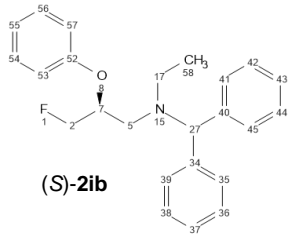
-220.83
-220.84
-220.89
-220.89
-220.96
-220.96
-221.02
-221.02
-221.08
-221.09
-221.14
-221.15



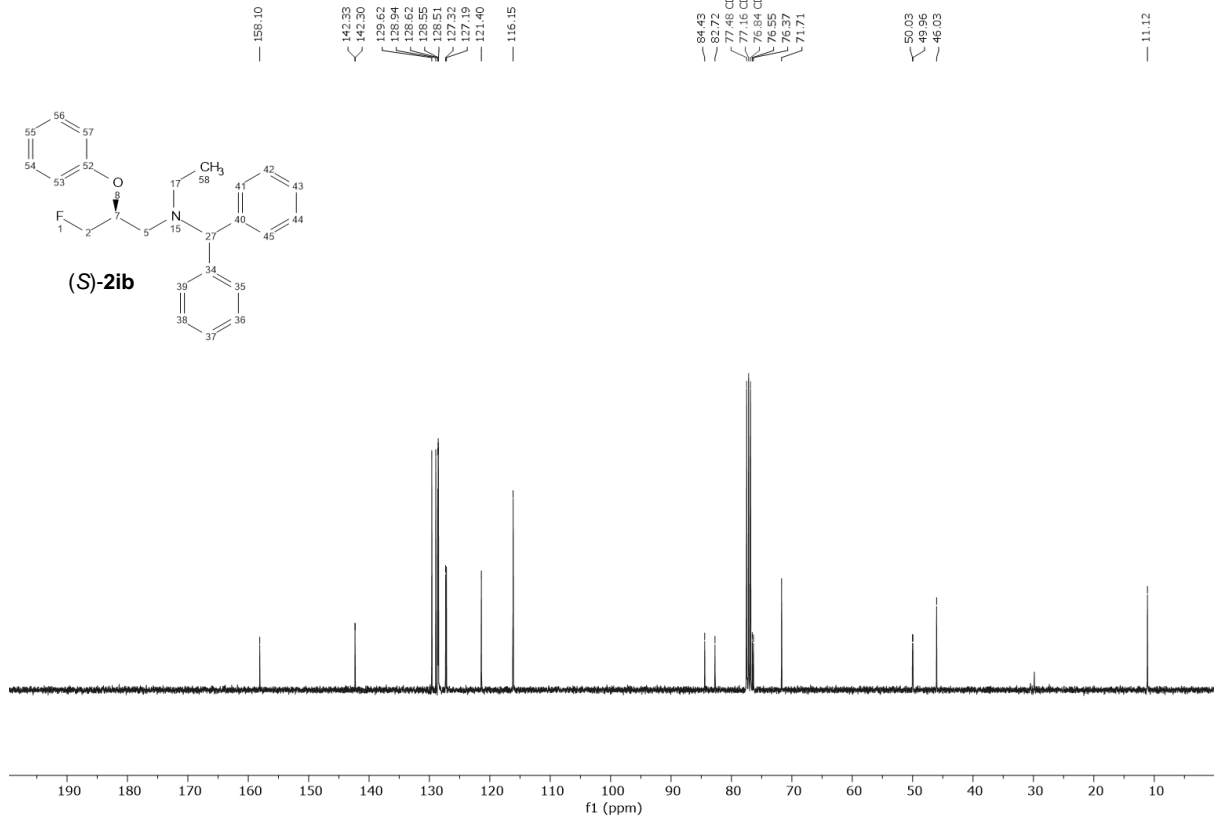
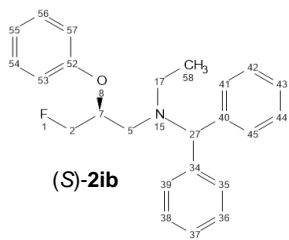
-229.21
-229.22
-229.25
-229.27
-229.27
-229.27
-229.34
-229.34
-229.39
-229.40
-229.47
-229.47
-229.52
-229.52



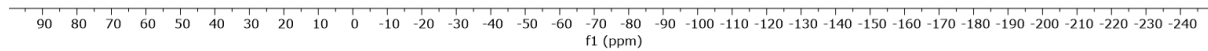
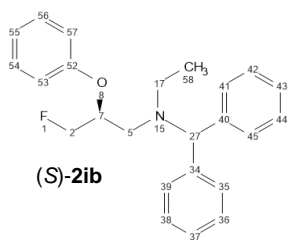
UOXF_groagna_2ib/CdCl3



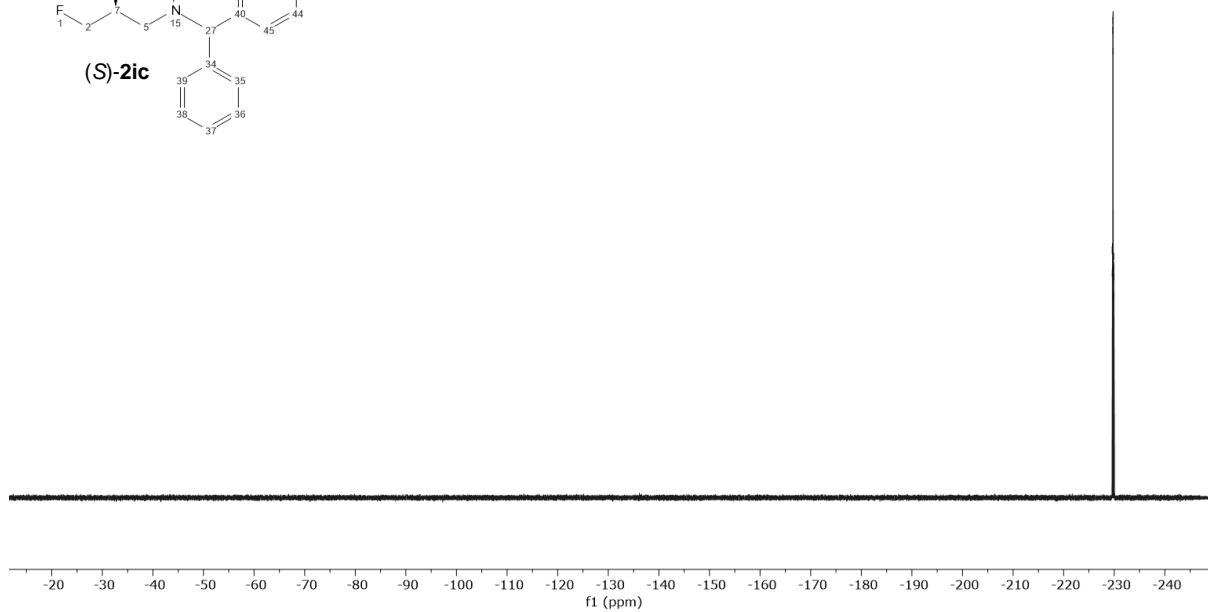
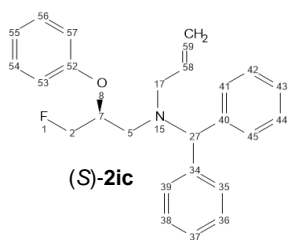
UOXF_groagna_2ib/CdCl3



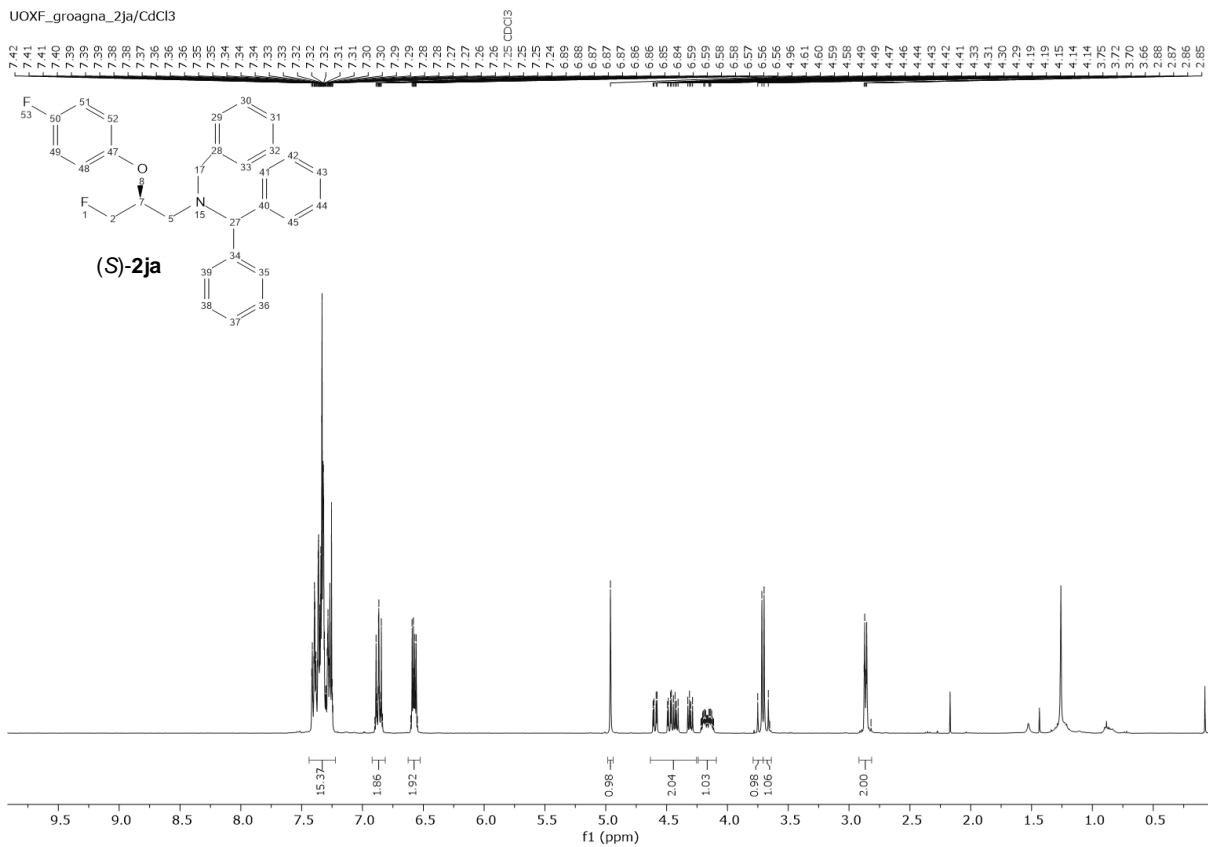
-230.07
 -230.08
 -230.13
 -230.14
 -230.20
 -230.21
 -230.26
 -230.26
 -230.33
 -230.33
 -230.38
 -230.39



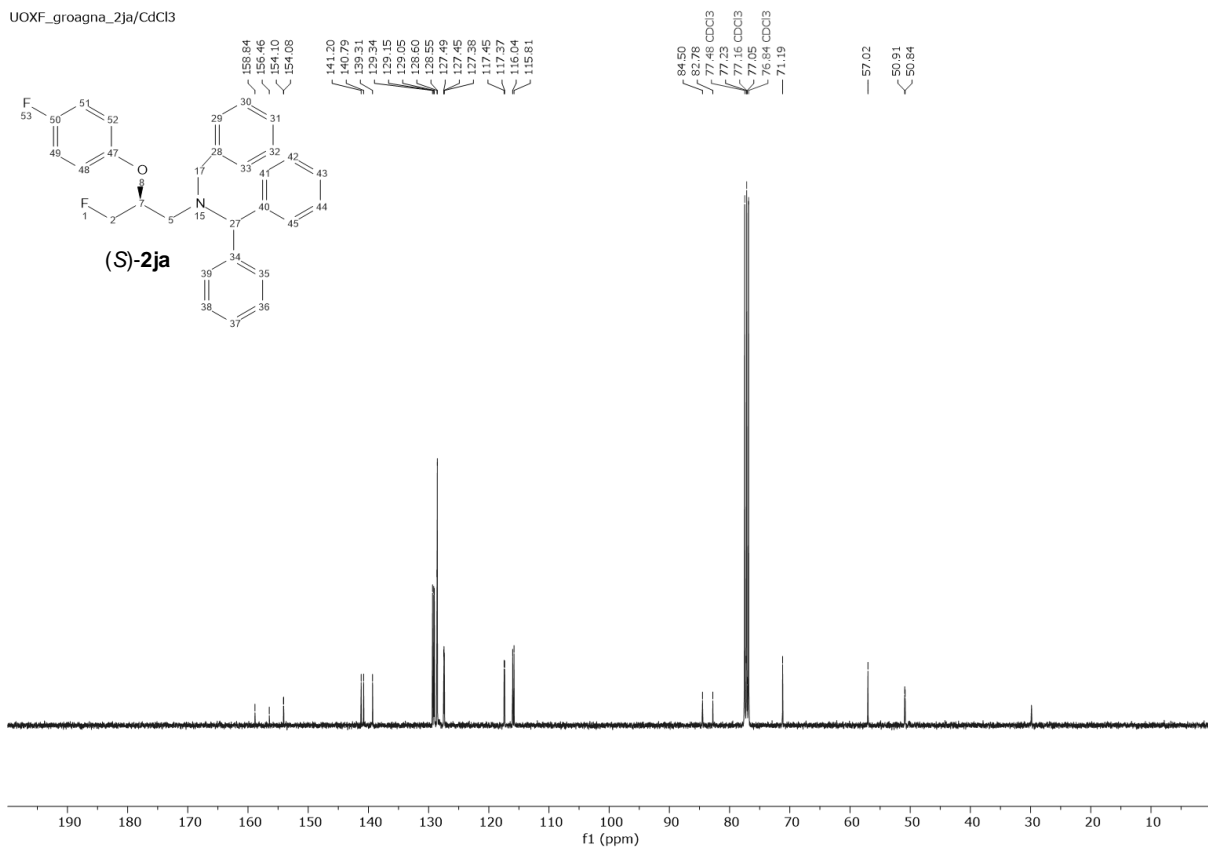
-229.59
 -229.60
 -229.64
 -229.65
 -229.72
 -229.77
 -229.78
 -229.84
 -229.85
 -229.90
 -229.90



UOXF_groagna_2ja/CdCl3



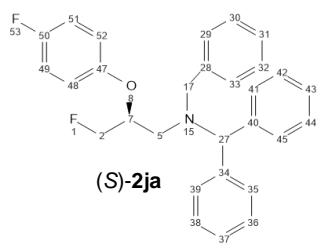
UOXF_groagna_2ja/CdCl3



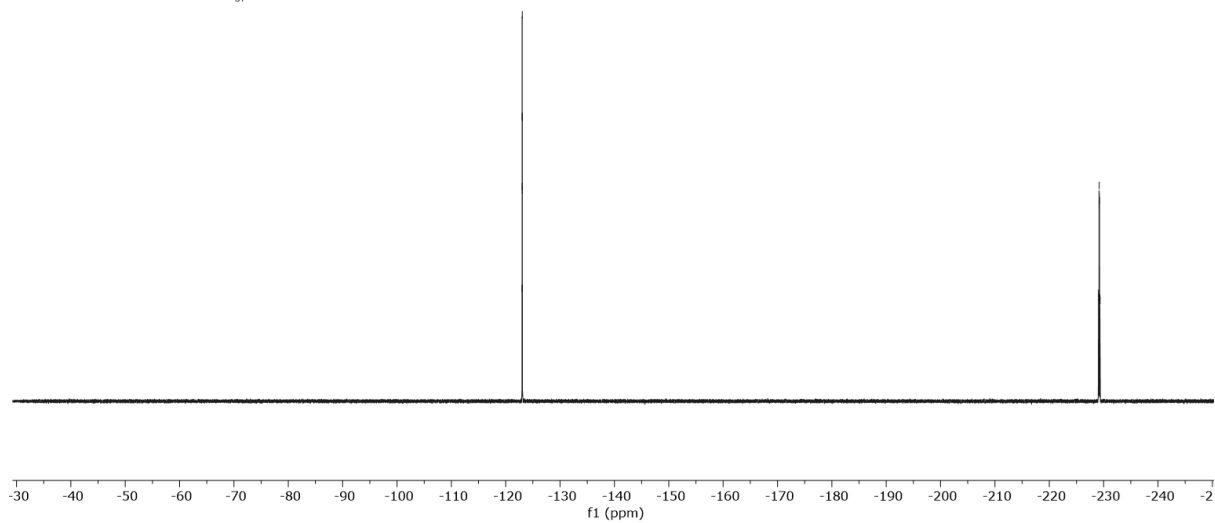
UOXF_groagna_2ja/CdCl3

-123.01
-123.02
-123.03
-123.04
-123.05
-123.06
-123.08

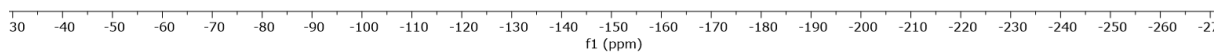
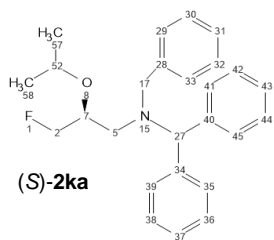
-229.05
-229.11
-229.18
-229.18
-229.23
-229.31
-229.36



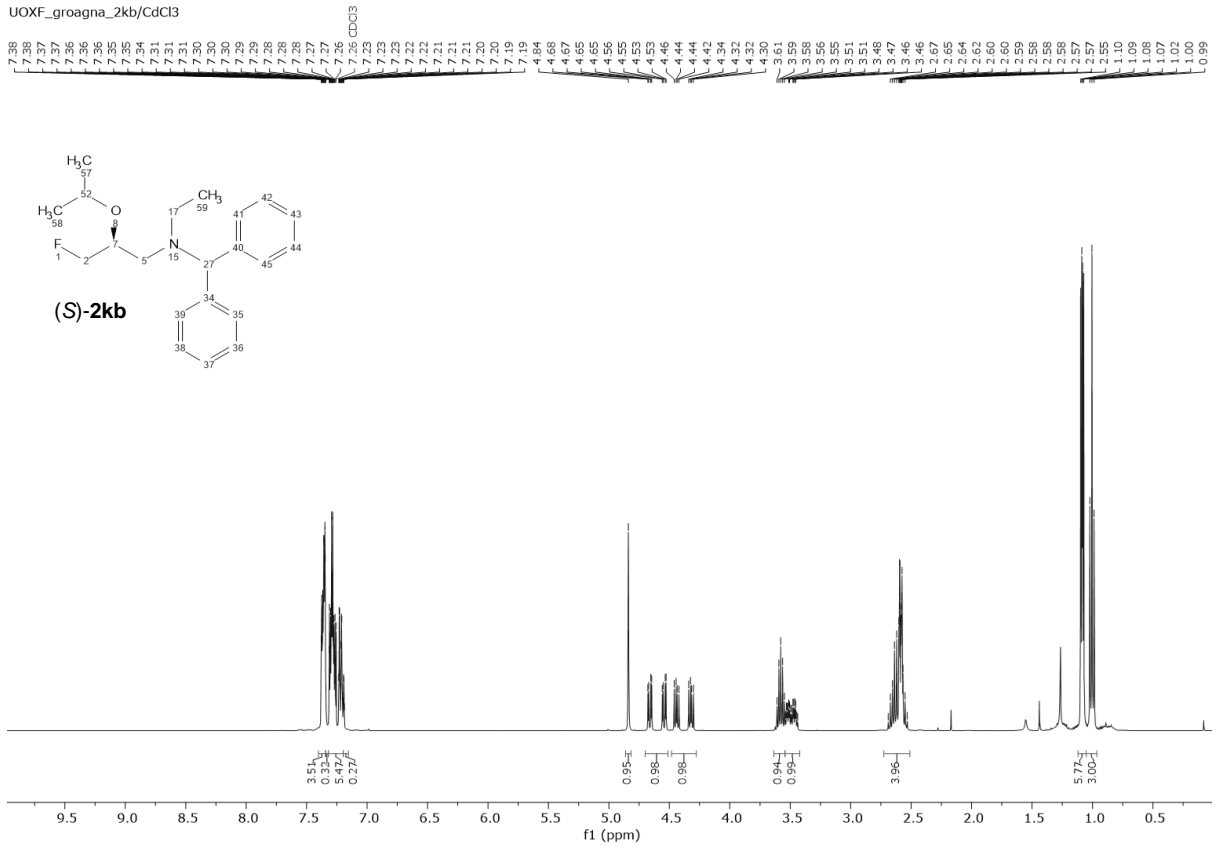
(S)-2ja



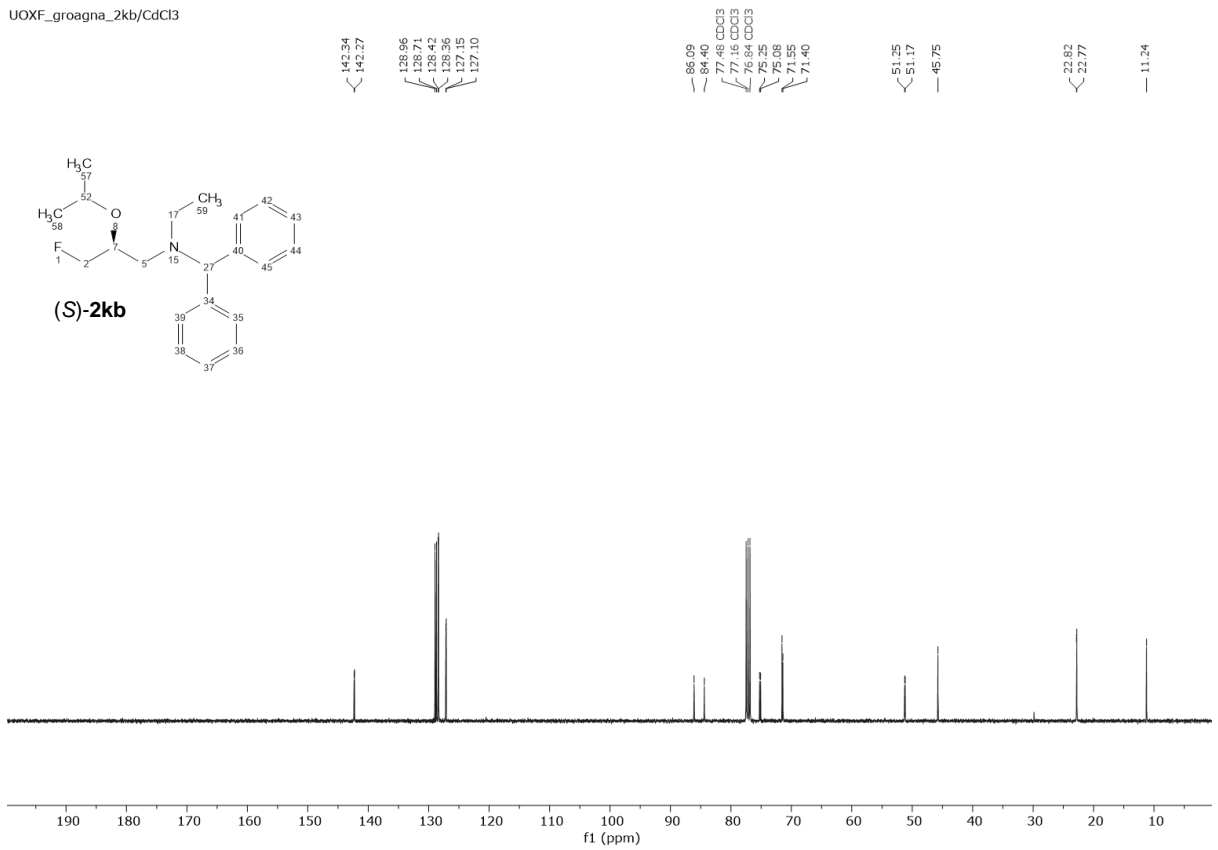
-227.70
-227.70
-227.75
-227.75
-227.83
-227.83
-227.87
-227.87
-227.95
-227.95
-228.00
-228.00
-228.01

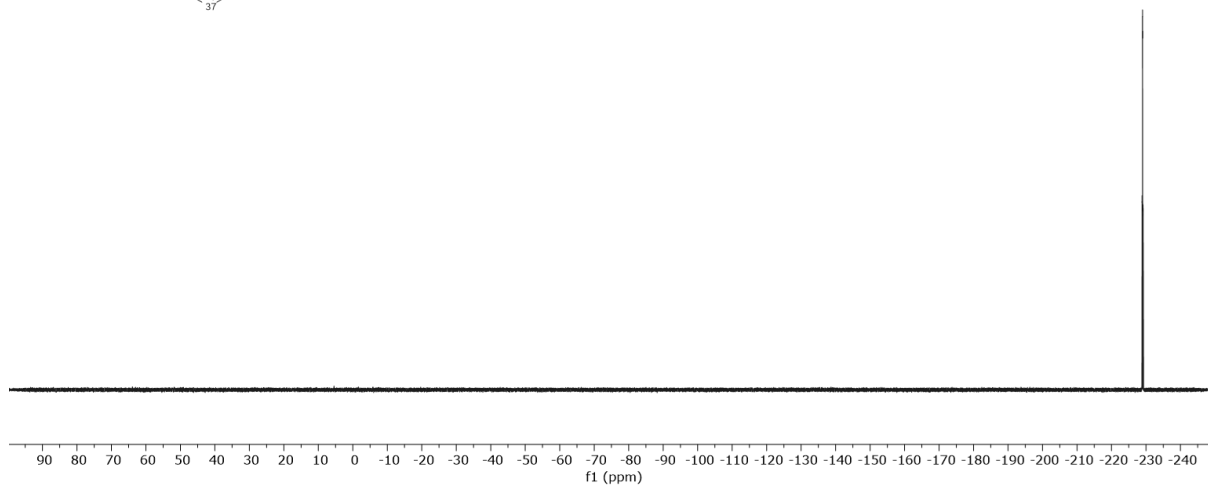
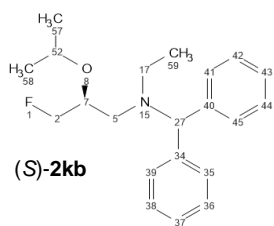


UOXF_groagna_2kb/CdCl3

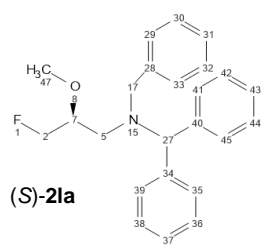


UOXF_groagna_2kb/CdCl3

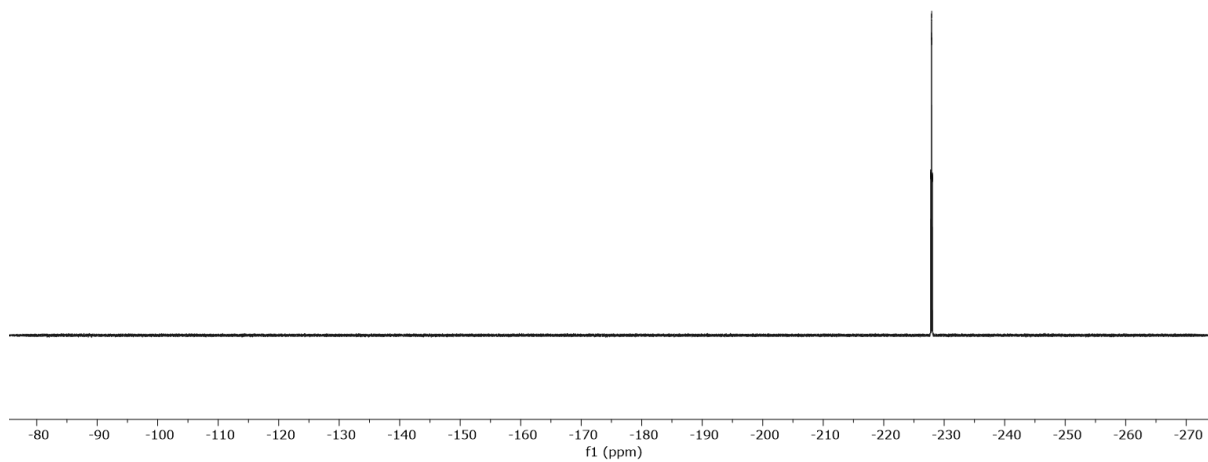




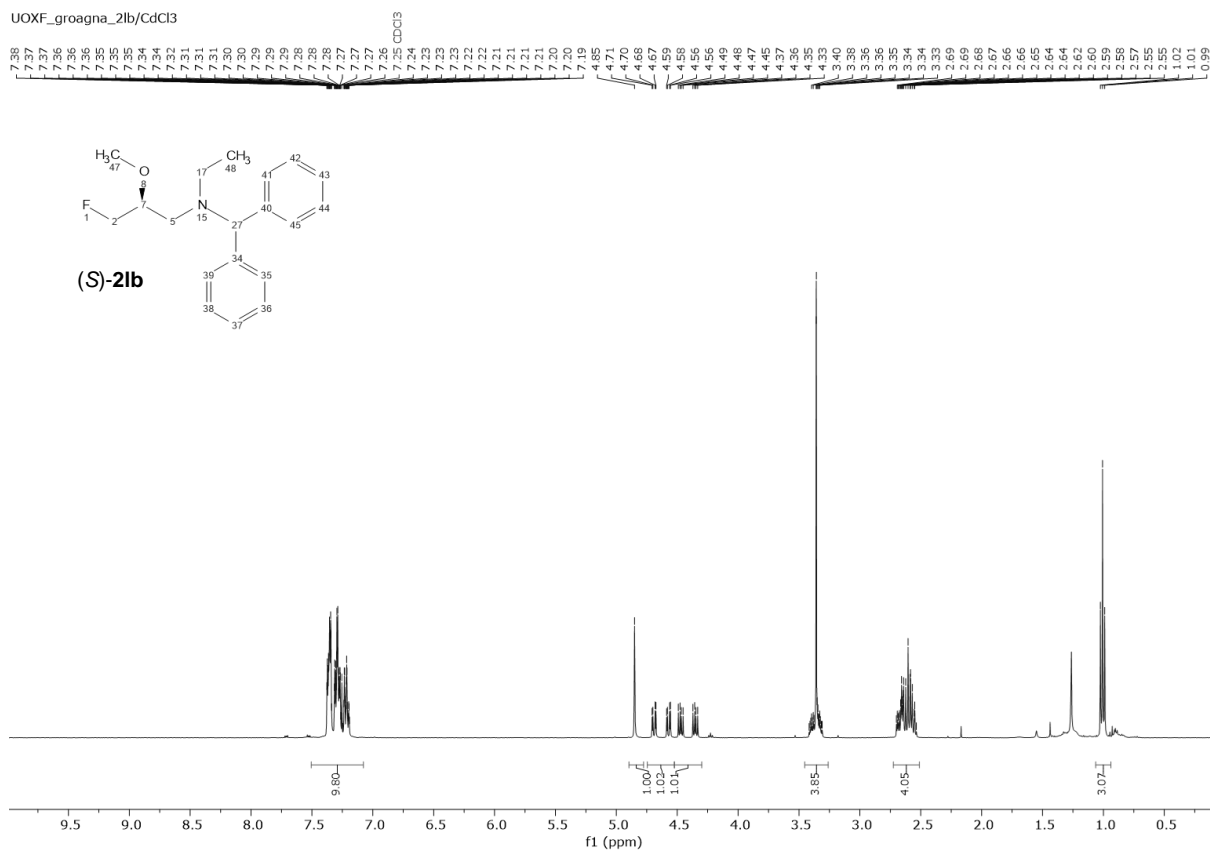
UOXF_groagna_2la/CdCl3



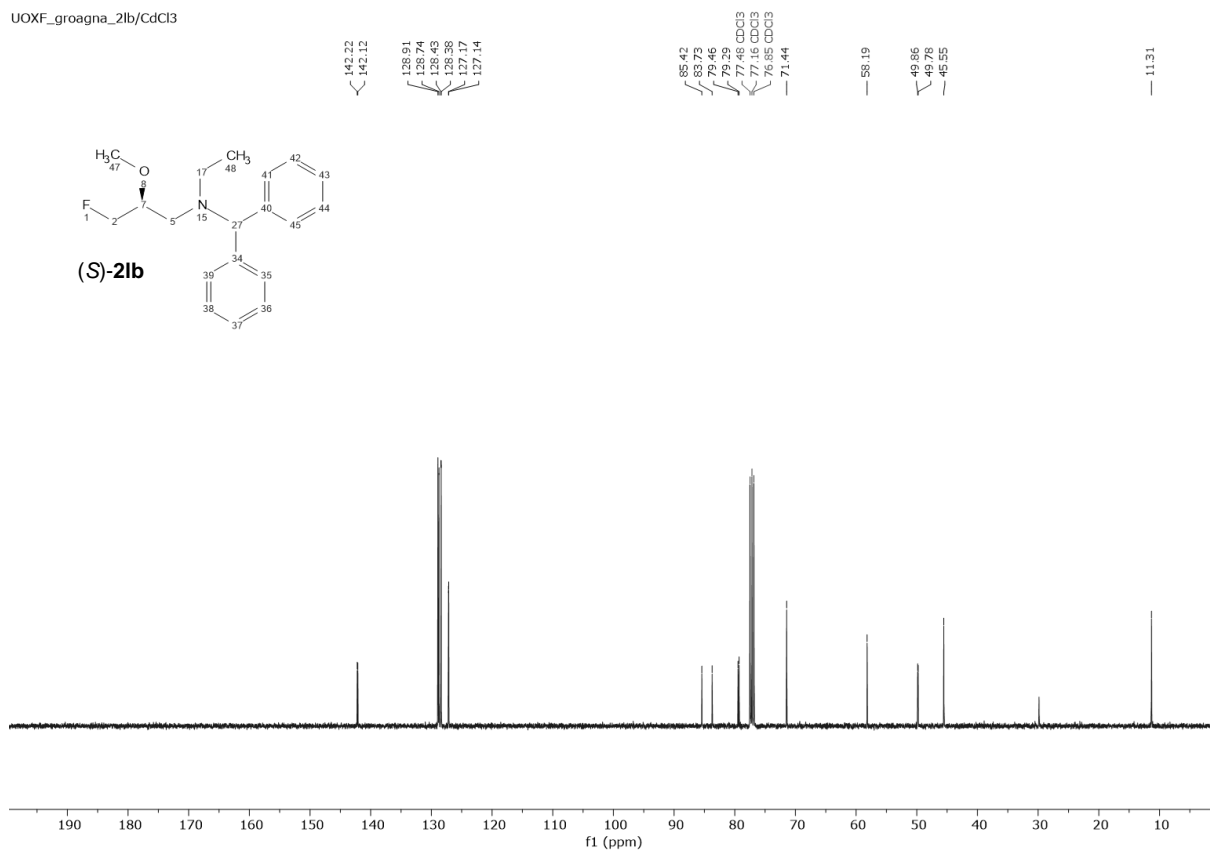
-227.75
-227.76
-227.80
-227.81
-227.88
-227.88
-227.93
-228.00
-228.01
-228.06
-228.06

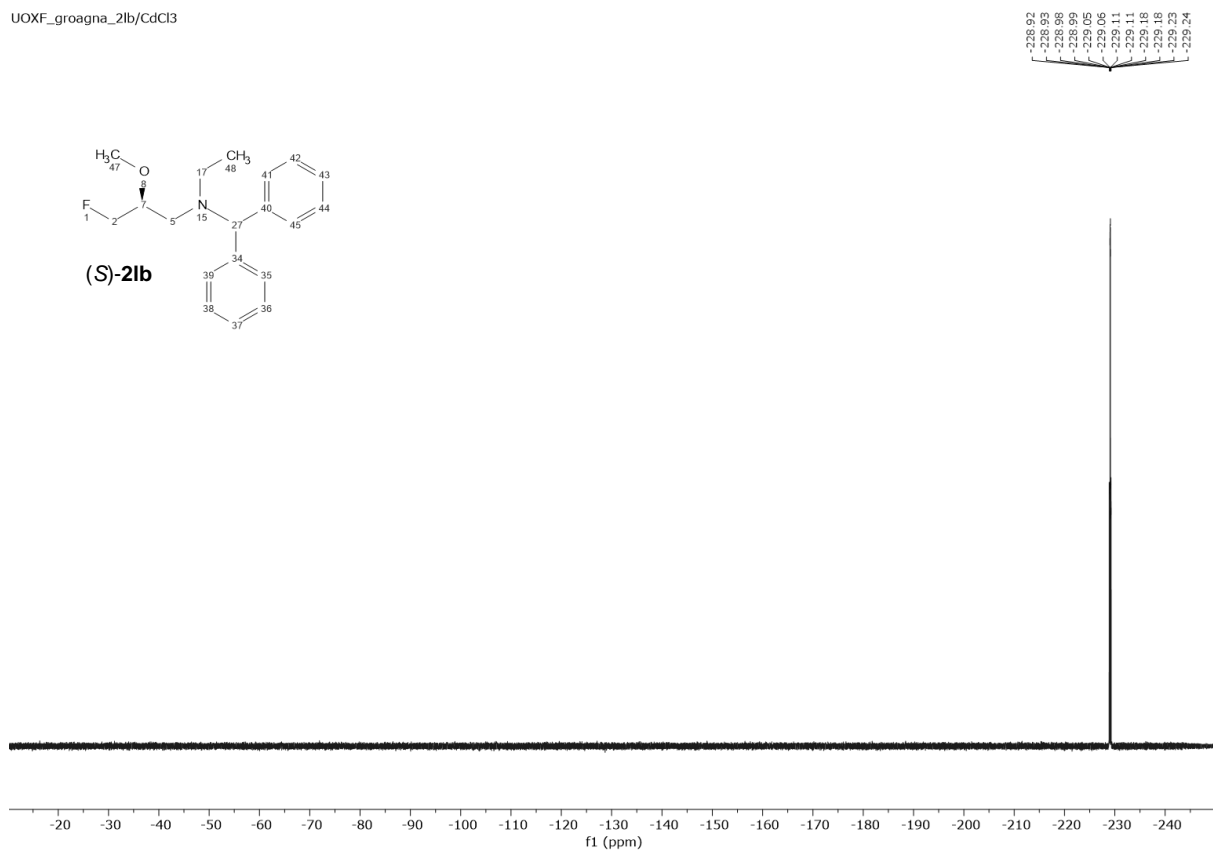


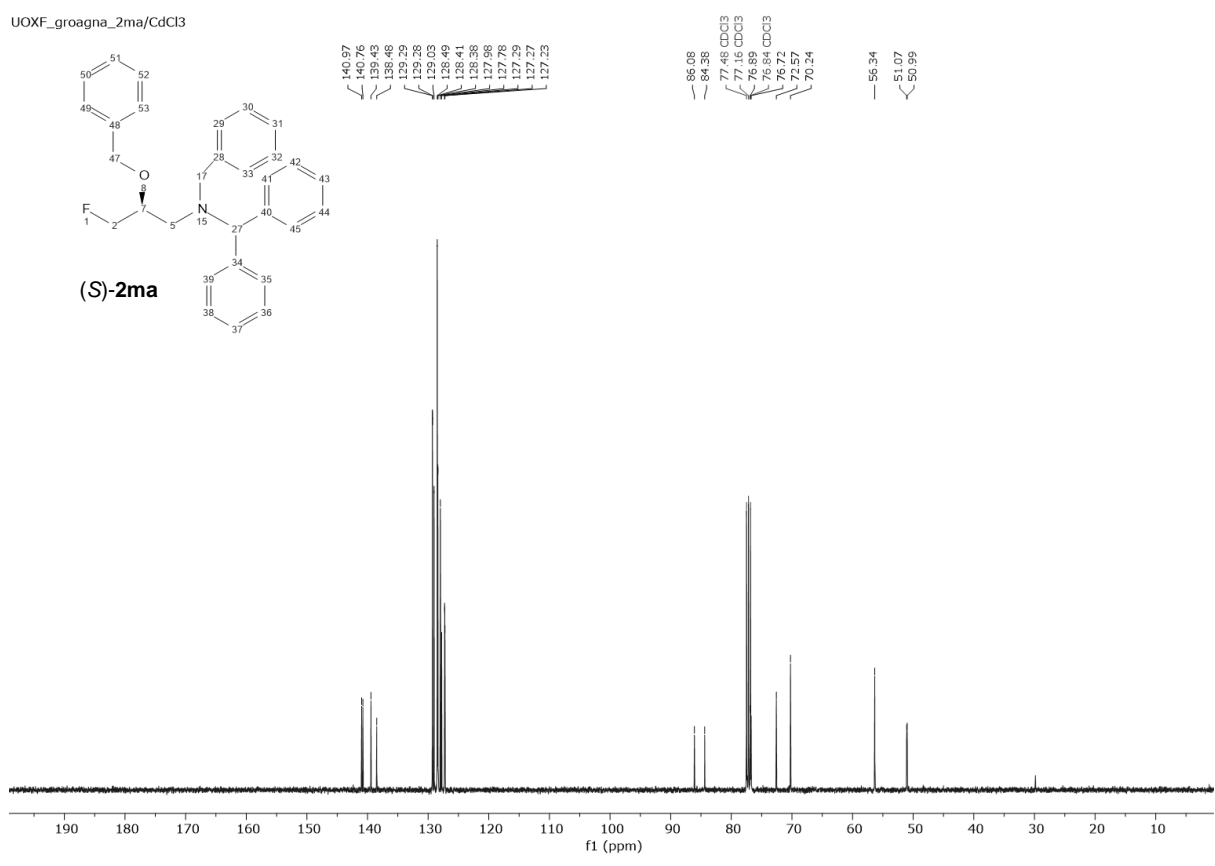
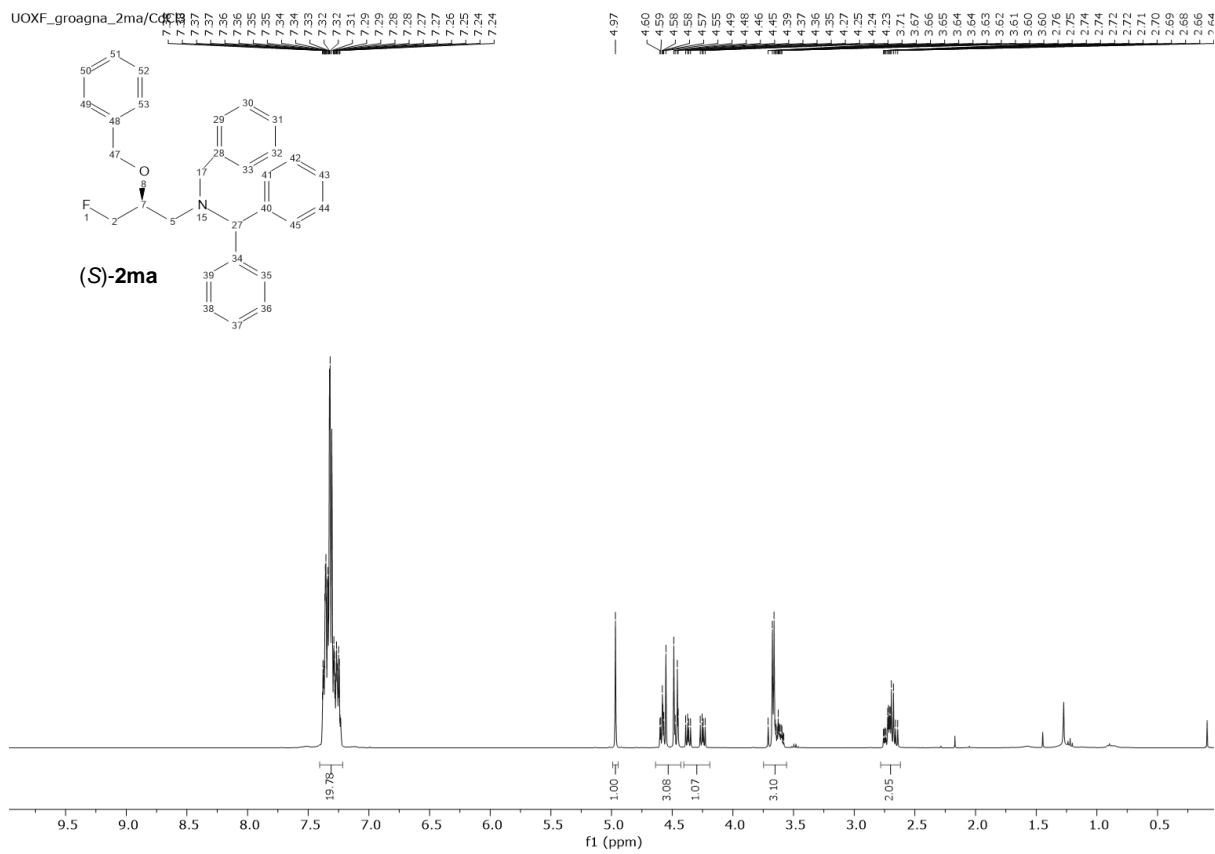
UOXF_groagna_2lb/CdCl3



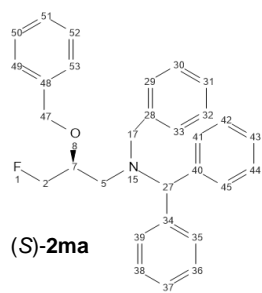
UOXF_groagna_2lb/CdCl3



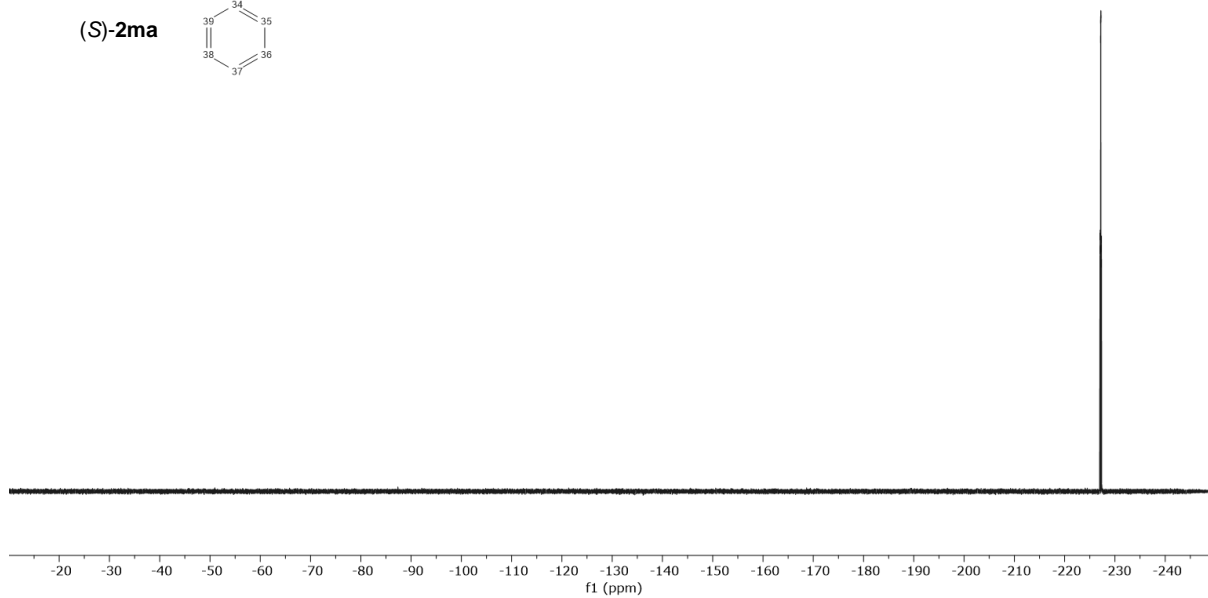




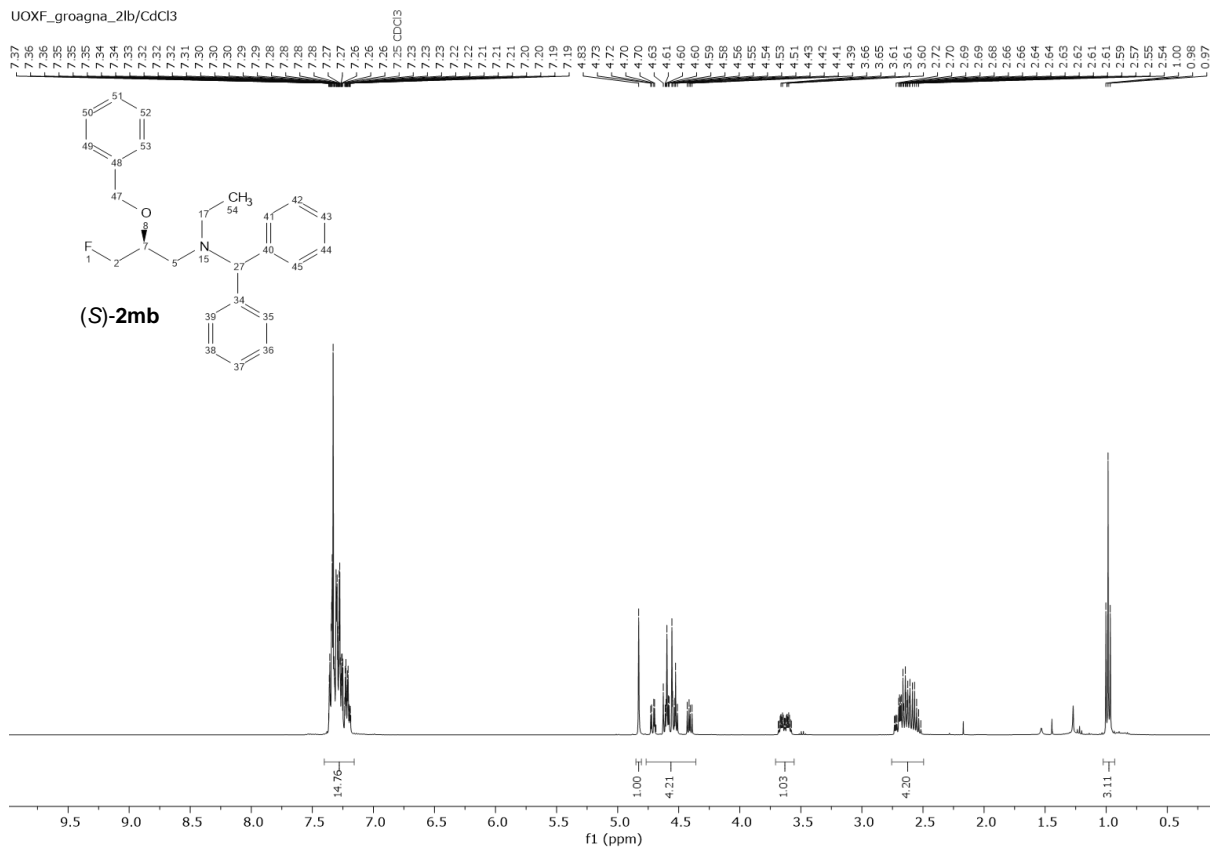
UOXF_groagna_2ma/CdCl3



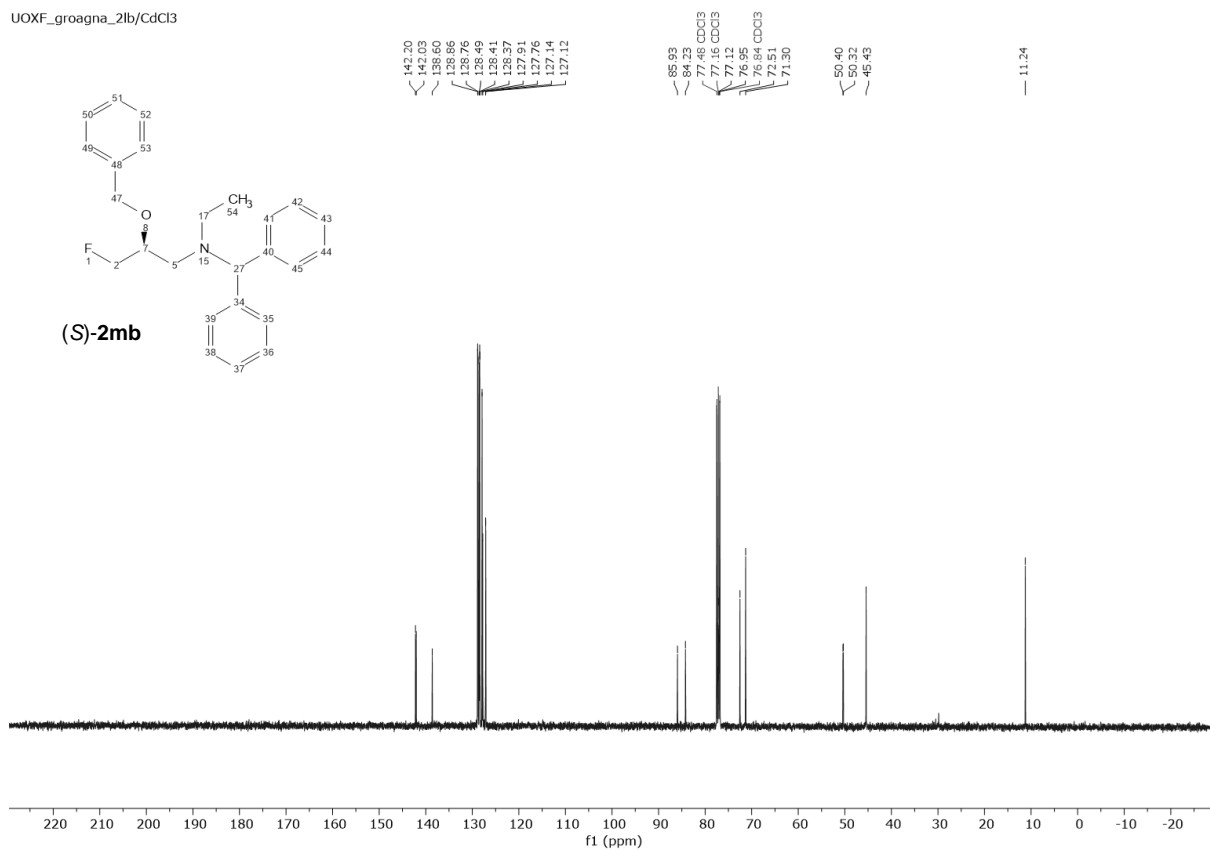
-227.03
-227.03
-227.08
-227.08
-227.15
-227.15
-227.20
-227.20
-227.26
-227.26
-227.29
-227.29
-227.33
-227.34



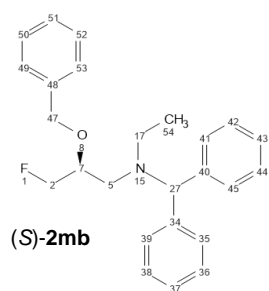
UOXF_groagna_2lb/CdCl3



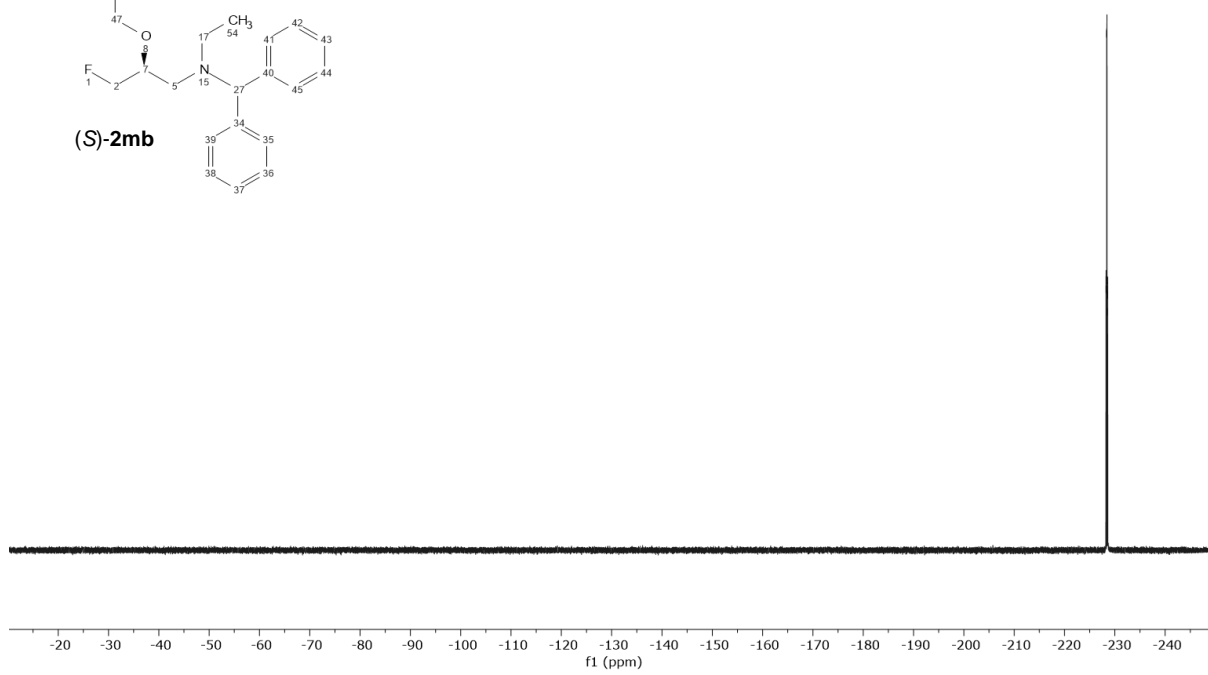
UOXF_groagna_2lb/CdCl3



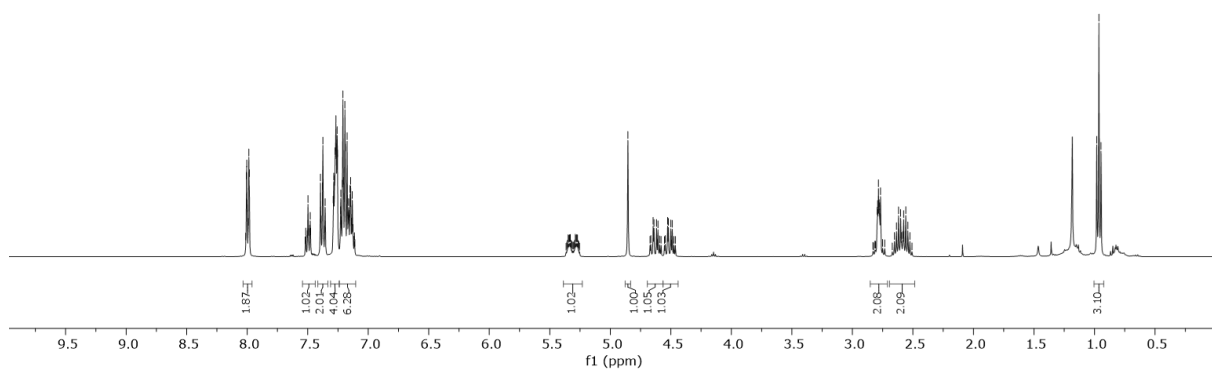
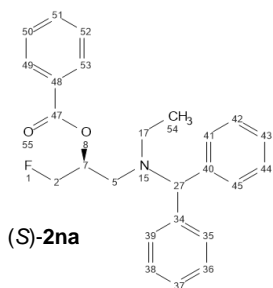
UOXF_groagna_2lb/CdCl3



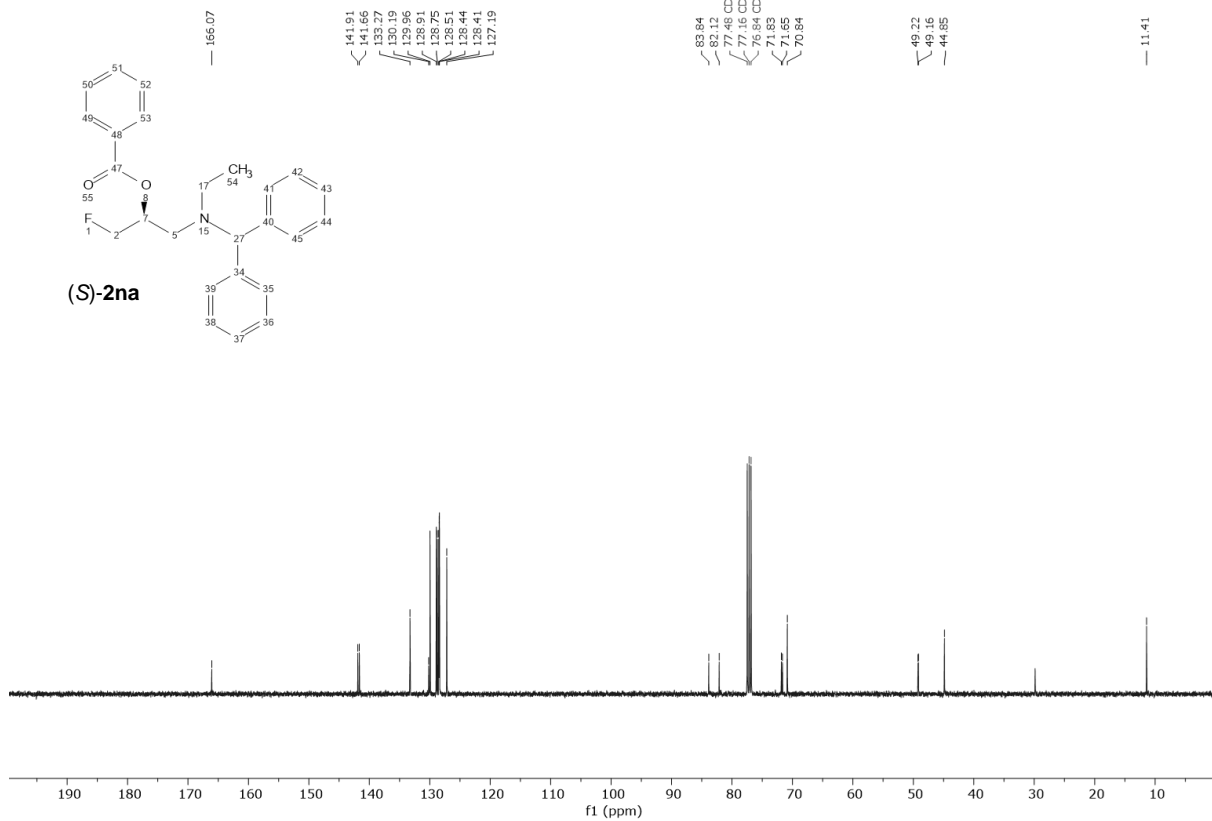
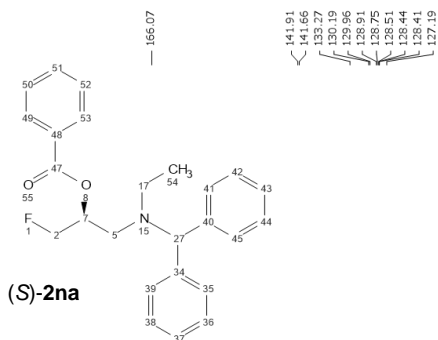
228.26
228.17
228.37
228.32
228.39
228.39
228.44
228.45
228.51
228.52
228.67
228.58



8.81 8.80 8.79 8.78 8.77 8.76 8.75 8.74 8.73 8.72 8.71 8.70 8.69 8.68 8.67 8.66 8.65 8.64 8.63 8.62 8.61 8.60 8.59 8.58 8.57 8.56 8.55 8.54 8.53 8.52 8.51 8.50 8.49 8.48 8.47 8.46 8.45 8.44 8.43 8.42 8.41 8.40 8.39 8.38 8.37 8.36 8.35 8.34 8.33 8.32 8.31 8.30 8.29 8.28 8.27 8.26 8.25 8.24 8.23 8.22 8.21 8.20 8.19 8.18 8.17 8.16 8.15 8.14 8.13 8.12 8.11 8.10 8.09 8.08 8.07 8.06 8.05 8.04 8.03 8.02 8.01 8.00 7.99 7.98 7.97 7.96 7.95 7.94 7.93 7.92 7.91 7.90 7.89 7.88 7.87 7.86 7.85 7.84 7.83 7.82 7.81 7.80 7.79 7.78 7.77 7.76 7.75 7.74 7.73 7.72 7.71 7.70 7.69 7.68 7.67 7.66 7.65 7.64 7.63 7.62 7.61 7.60 7.59 7.58 7.57 7.56 7.55 7.54 7.53 7.52 7.51 7.50 7.49 7.48 7.47 7.46 7.45 7.44 7.43 7.42 7.41 7.40 7.39 7.38 7.37 7.36 7.35 7.34 7.33 7.32 7.31 7.30 7.29 7.28 7.27 7.26 7.25 7.24 7.23 7.22 7.21 7.20 7.19 7.18 7.17 7.16 7.15 7.14 7.13 7.12 7.11 7.10 7.09 7.08 7.07 7.06 7.05 7.04 7.03 7.02 7.01 7.00 6.99 6.98 6.97 6.96 6.95 6.94 6.93 6.92 6.91 6.90 6.89 6.88 6.87 6.86 6.85 6.84 6.83 6.82 6.81 6.80 6.79 6.78 6.77 6.76 6.75 6.74 6.73 6.72 6.71 6.70 6.69 6.68 6.67 6.66 6.65 6.64 6.63 6.62 6.61 6.60 6.59 6.58 6.57 6.56 6.55 6.54 6.53 6.52 6.51 6.50 6.49 6.48 6.47 6.46 6.45 6.44 6.43 6.42 6.41 6.40 6.39 6.38 6.37 6.36 6.35 6.34 6.33 6.32 6.31 6.30 6.29 6.28 6.27 6.26 6.25 6.24 6.23 6.22 6.21 6.20 6.19 6.18 6.17 6.16 6.15 6.14 6.13 6.12 6.11 6.10 6.09 6.08 6.07 6.06 6.05 6.04 6.03 6.02 6.01 6.00 5.99 5.98 5.97 5.96 5.95 5.94 5.93 5.92 5.91 5.90 5.89 5.88 5.87 5.86 5.85 5.84 5.83 5.82 5.81 5.80 5.79 5.78 5.77 5.76 5.75 5.74 5.73 5.72 5.71 5.70 5.69 5.68 5.67 5.66 5.65 5.64 5.63 5.62 5.61 5.60 5.59 5.58 5.57 5.56 5.55 5.54 5.53 5.52 5.51 5.50 5.49 5.48 5.47 5.46 5.45 5.44 5.43 5.42 5.41 5.40 5.39 5.38 5.37 5.36 5.35 5.34 5.33 5.32 5.31 5.30 5.29 5.28 5.27 5.26 5.25 5.24 5.23 5.22 5.21 5.20 5.19 5.18 5.17 5.16 5.15 5.14 5.13 5.12 5.11 5.10 5.09 5.08 5.07 5.06 5.05 5.04 5.03 5.02 5.01 5.00 4.99 4.98 4.97 4.96 4.95 4.94 4.93 4.92 4.91 4.90 4.89 4.88 4.87 4.86 4.85 4.84 4.83 4.82 4.81 4.80 4.79 4.78 4.77 4.76 4.75 4.74 4.73 4.72 4.71 4.70 4.69 4.68 4.67 4.66 4.65 4.64 4.63 4.62 4.61 4.60 4.59 4.58 4.57 4.56 4.55 4.54 4.53 4.52 4.51 4.50 4.49 4.48 4.47 4.46 4.45 4.44 4.43 4.42 4.41 4.40 4.39 4.38 4.37 4.36 4.35 4.34 4.33 4.32 4.31 4.30 4.29 4.28 4.27 4.26 4.25 4.24 4.23 4.22 4.21 4.20 4.19 4.18 4.17 4.16 4.15 4.14 4.13 4.12 4.11 4.10 4.09 4.08 4.07 4.06 4.05 4.04 4.03 4.02 4.01 4.00 3.99 3.98 3.97 3.96 3.95 3.94 3.93 3.92 3.91 3.90 3.89 3.88 3.87 3.86 3.85 3.84 3.83 3.82 3.81 3.80 3.79 3.78 3.77 3.76 3.75 3.74 3.73 3.72 3.71 3.70 3.69 3.68 3.67 3.66 3.65 3.64 3.63 3.62 3.61 3.60 3.59 3.58 3.57 3.56 3.55 3.54 3.53 3.52 3.51 3.50 3.49 3.48 3.47 3.46 3.45 3.44 3.43 3.42 3.41 3.40 3.39 3.38 3.37 3.36 3.35 3.34 3.33 3.32 3.31 3.30 3.29 3.28 3.27 3.26 3.25 3.24 3.23 3.22 3.21 3.20 3.19 3.18 3.17 3.16 3.15 3.14 3.13 3.12 3.11 3.10 3.09 3.08 3.07 3.06 3.05 3.04 3.03 3.02 3.01 3.00 2.99 2.98 2.97 2.96 2.95 2.94 2.93 2.92 2.91 2.90 2.89 2.88 2.87 2.86 2.85 2.84 2.83 2.82 2.81 2.80 2.79 2.78 2.77 2.76 2.75 2.74 2.73 2.72 2.71 2.70 2.69 2.68 2.67 2.66 2.65 2.64 2.63 2.62 2.61 2.60 2.59 2.58 2.57 2.56 2.55 2.54 2.53 2.52 2.51 2.50 2.49 2.48 2.47 2.46 2.45 2.44 2.43 2.42 2.41 2.40 2.39 2.38 2.37 2.36 2.35 2.34 2.33 2.32 2.31 2.30 2.29 2.28 2.27 2.26 2.25 2.24 2.23 2.22 2.21 2.20 2.19 2.18 2.17 2.16 2.15 2.14 2.13 2.12 2.11 2.10 2.09 2.08 2.07 2.06 2.05 2.04 2.03 2.02 2.01 2.00 1.99 1.98 1.97 1.96 1.95 1.94 1.93 1.92 1.91 1.90 1.89 1.88 1.87 1.86 1.85 1.84 1.83 1.82 1.81 1.80 1.79 1.78 1.77 1.76 1.75 1.74 1.73 1.72 1.71 1.70 1.69 1.68 1.67 1.66 1.65 1.64 1.63 1.62 1.61 1.60 1.59 1.58 1.57 1.56 1.55 1.54 1.53 1.52 1.51 1.50 1.49 1.48 1.47 1.46 1.45 1.44 1.43 1.42 1.41 1.40 1.39 1.38 1.37 1.36 1.35 1.34 1.33 1.32 1.31 1.30 1.29 1.28 1.27 1.26 1.25 1.24 1.23 1.22 1.21 1.20 1.19 1.18 1.17 1.16 1.15 1.14 1.13 1.12 1.11 1.10 1.09 1.08 1.07 1.06 1.05 1.04 1.03 1.02 1.01 1.00 0.99 0.98 0.97 0.96 0.95

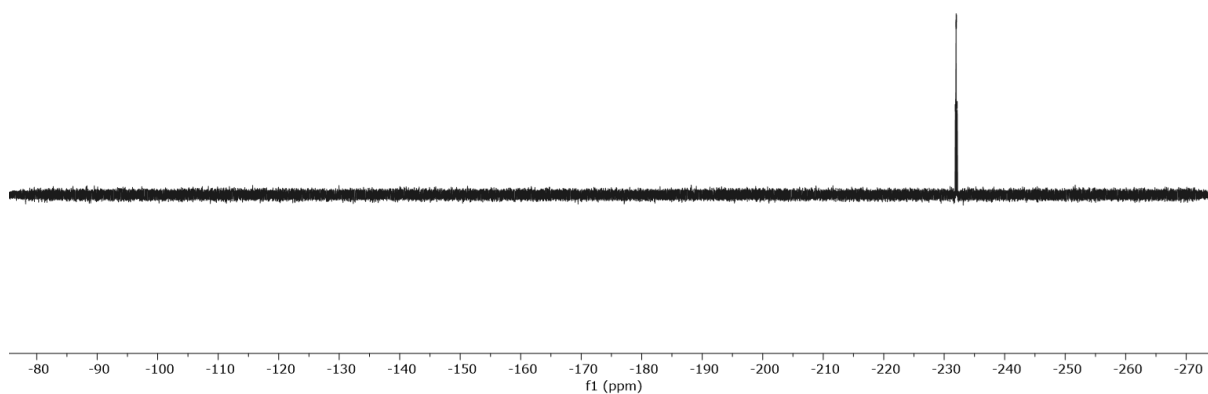
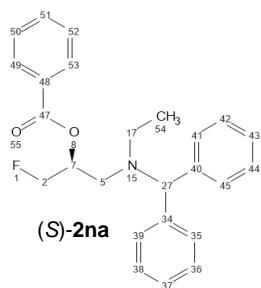


UOXF_groagna_2na/CdCl3

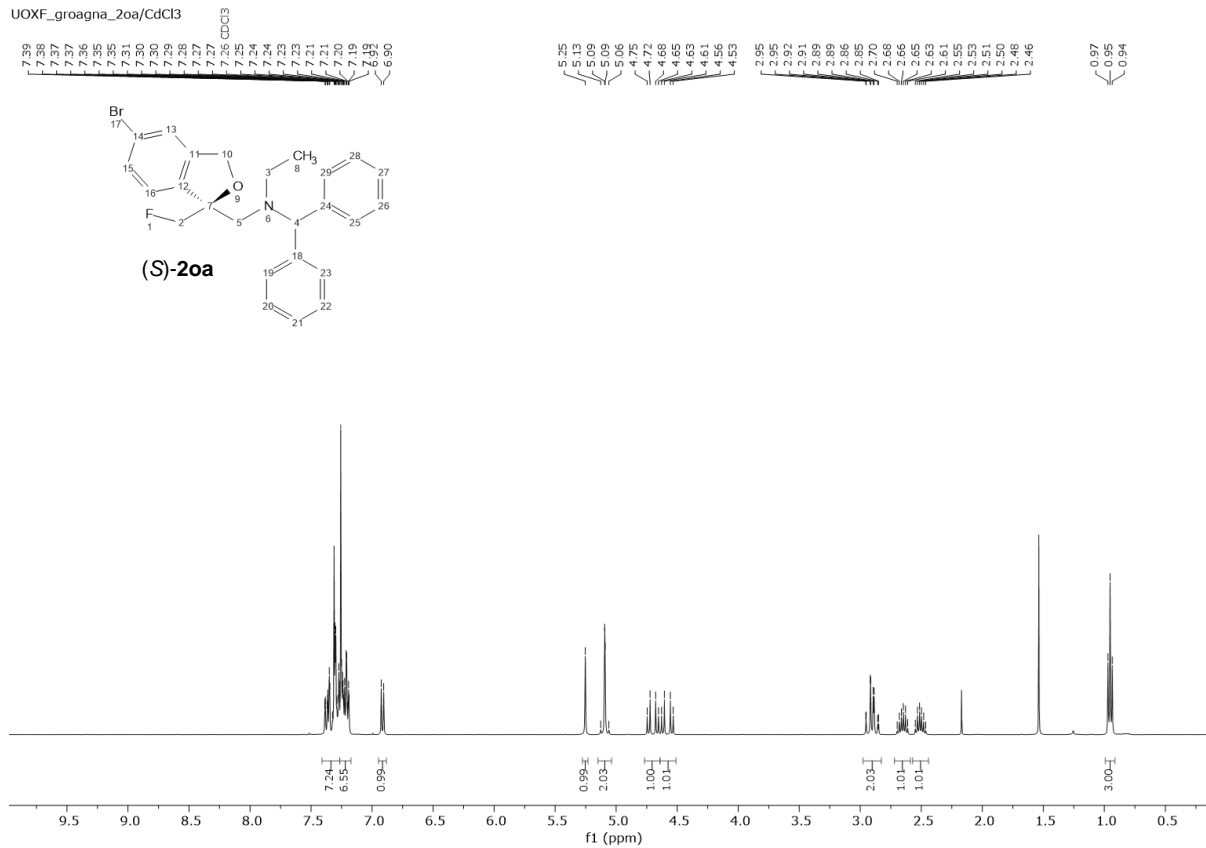


UOXF_groagna_2na/CdCl3

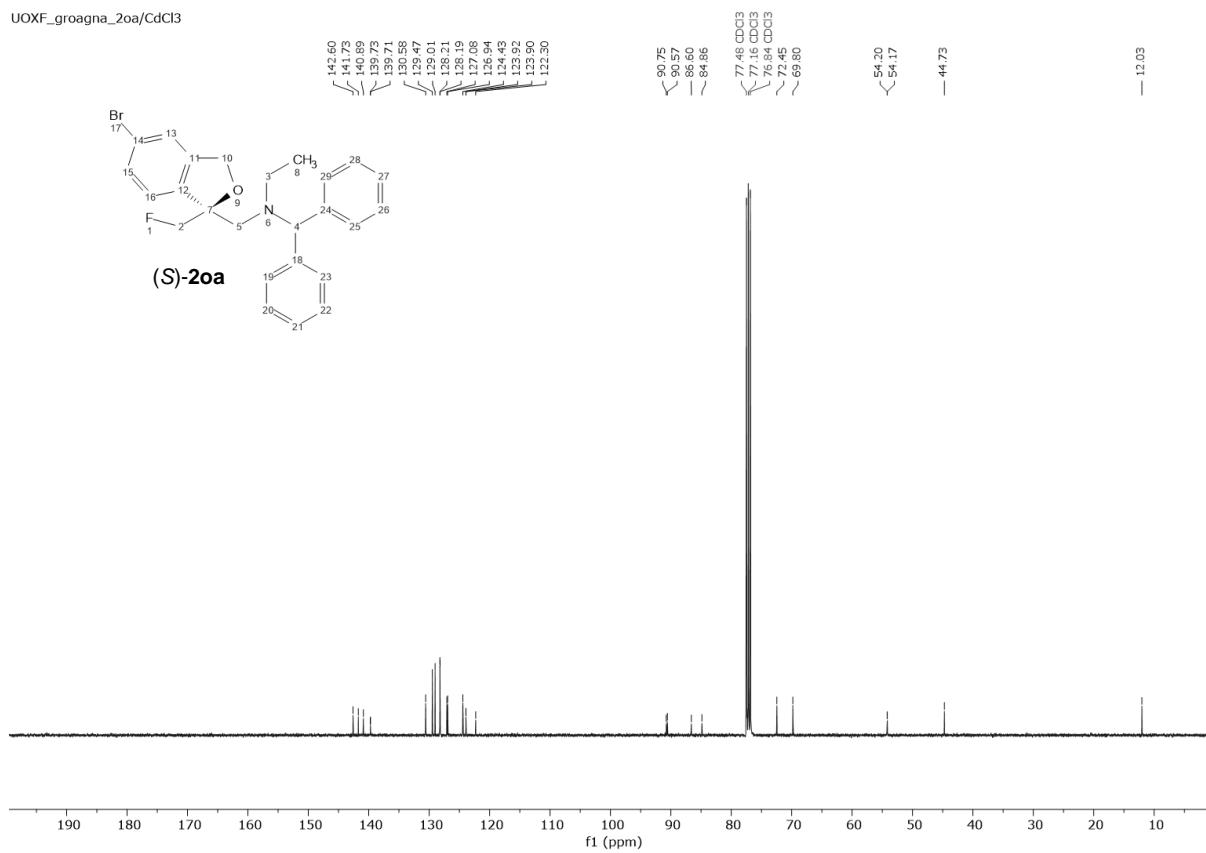
-231.84
-231.84
-231.90
-231.96
-231.97
-232.03
-232.09
-232.15



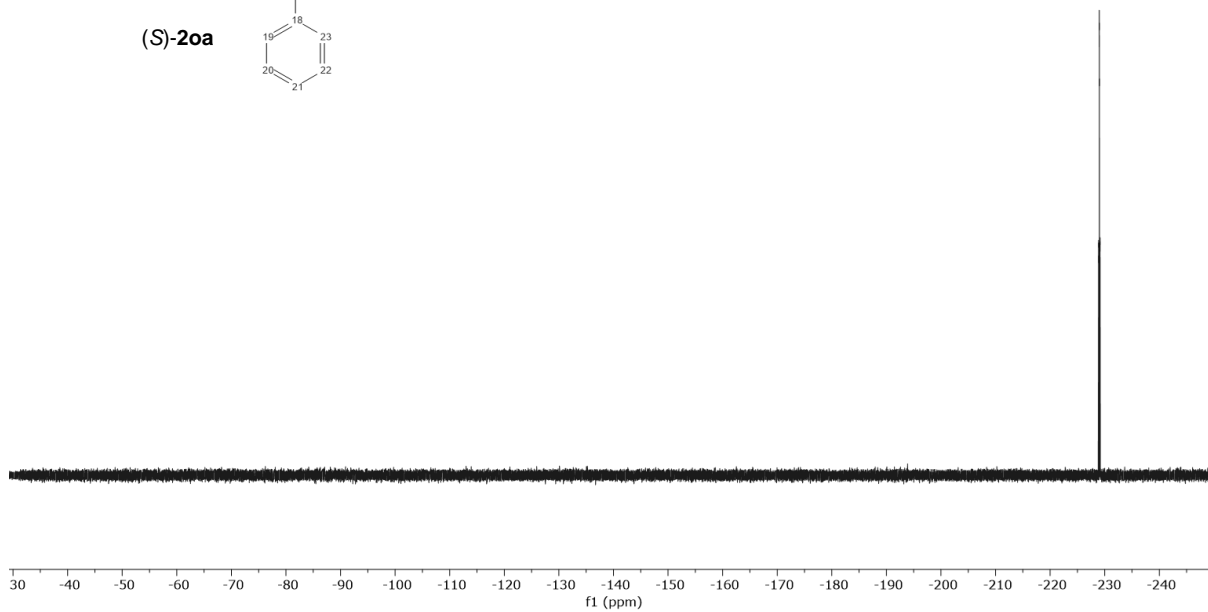
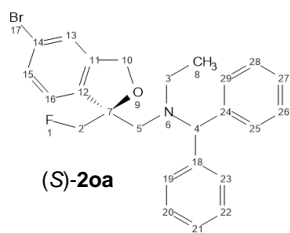
UOXF_groagna_2oa/CdCl3



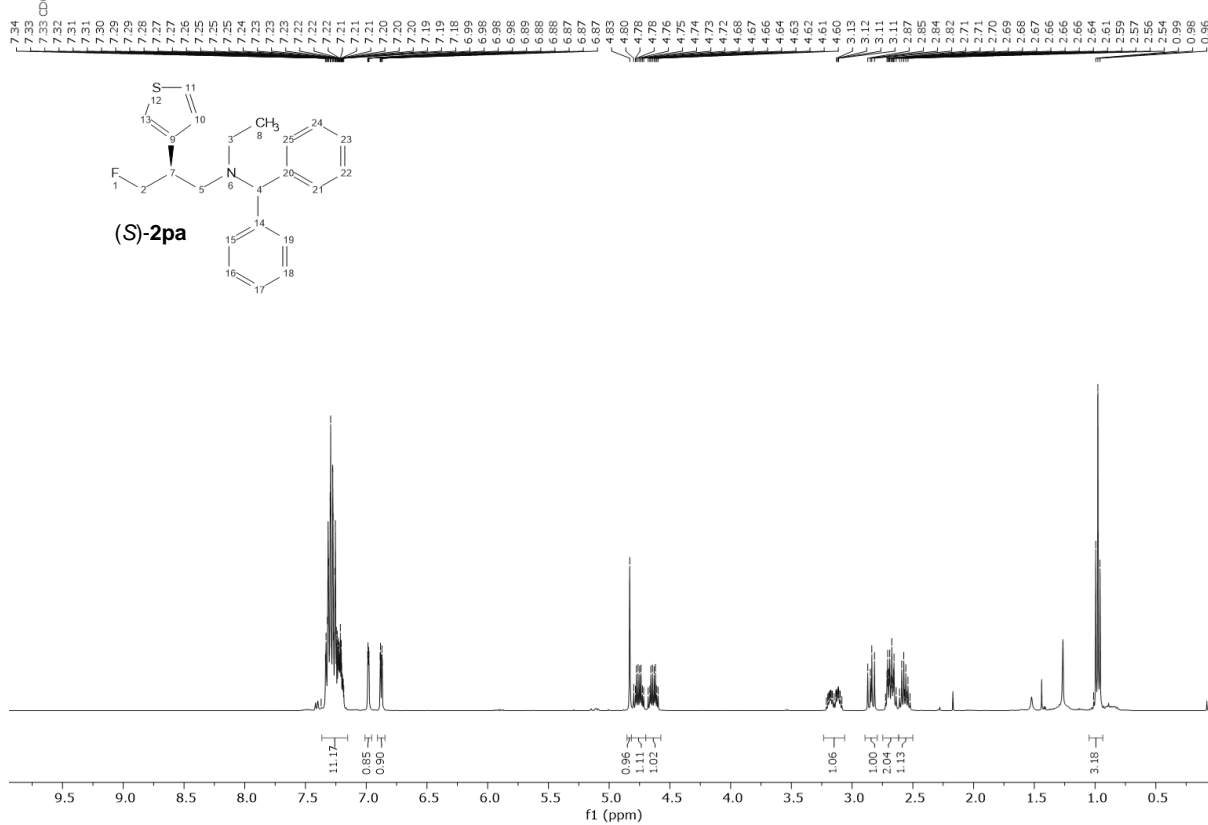
UOXF_groagna_2oa/CdCl3



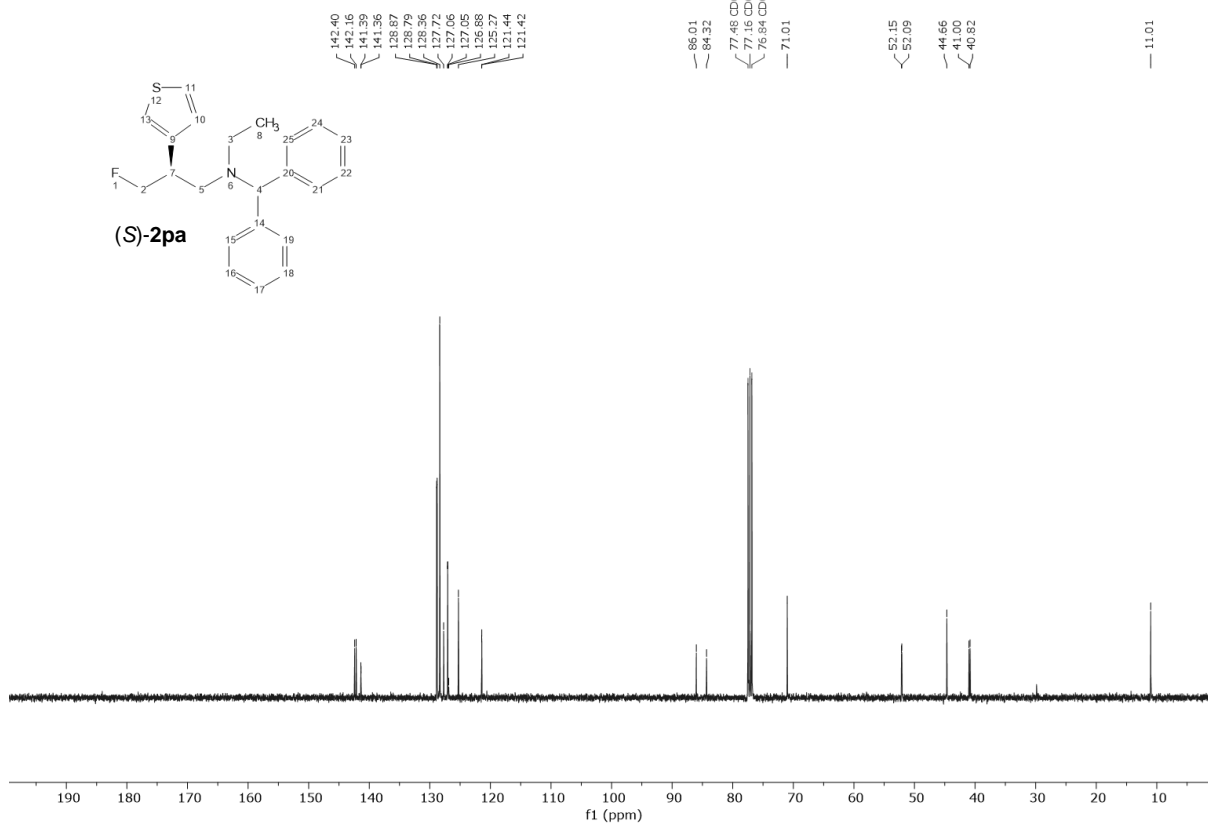
-228.686
 -228.689
 -229.01
 -229.14
 -229.15



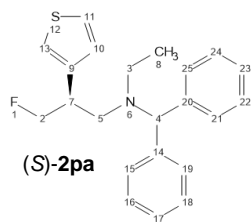
UOXF_groagna_2pa/CdCl3



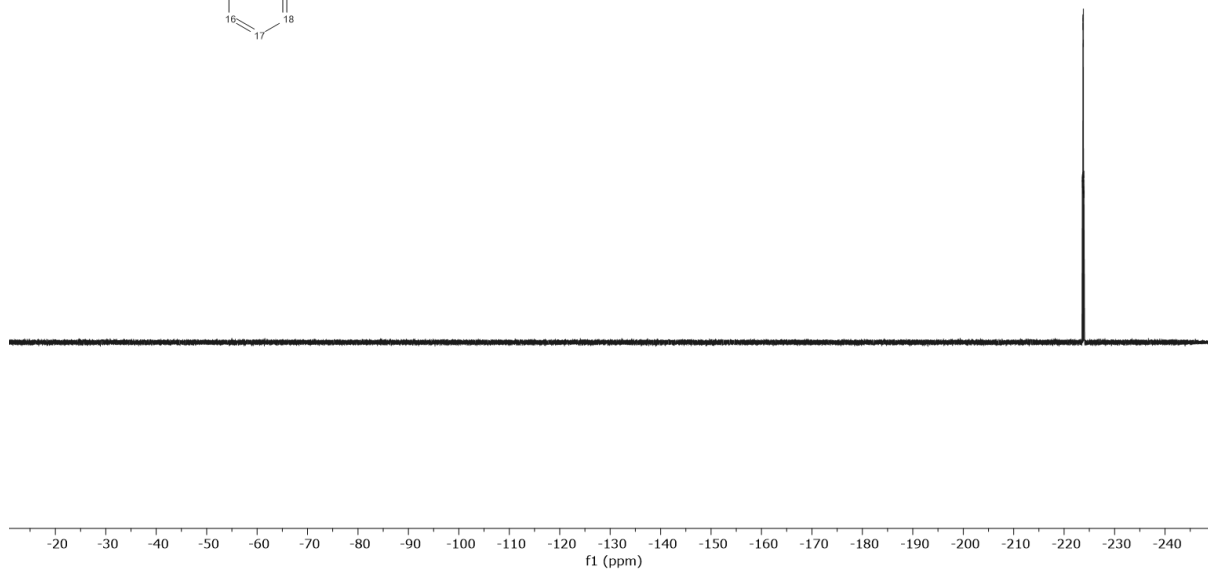
UOXF_groagna_2pa/CdCl3



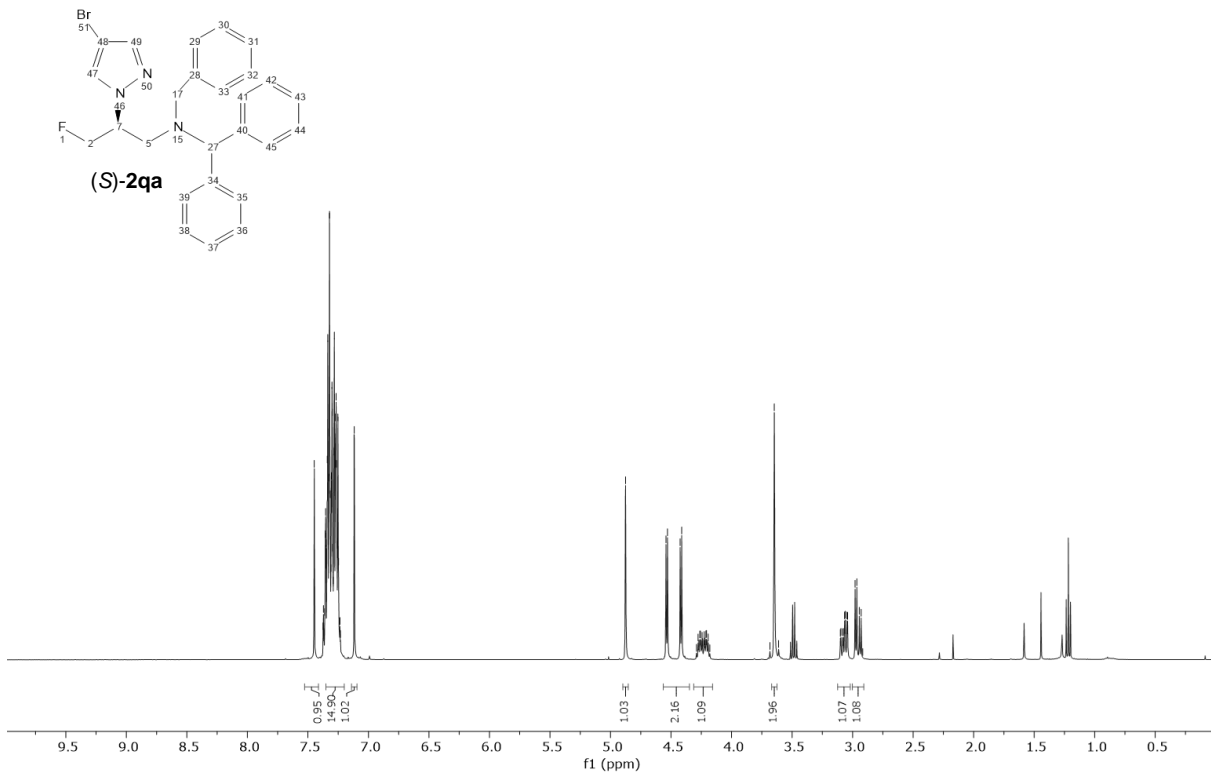
UOXF_groagna_2pa/CdCl3



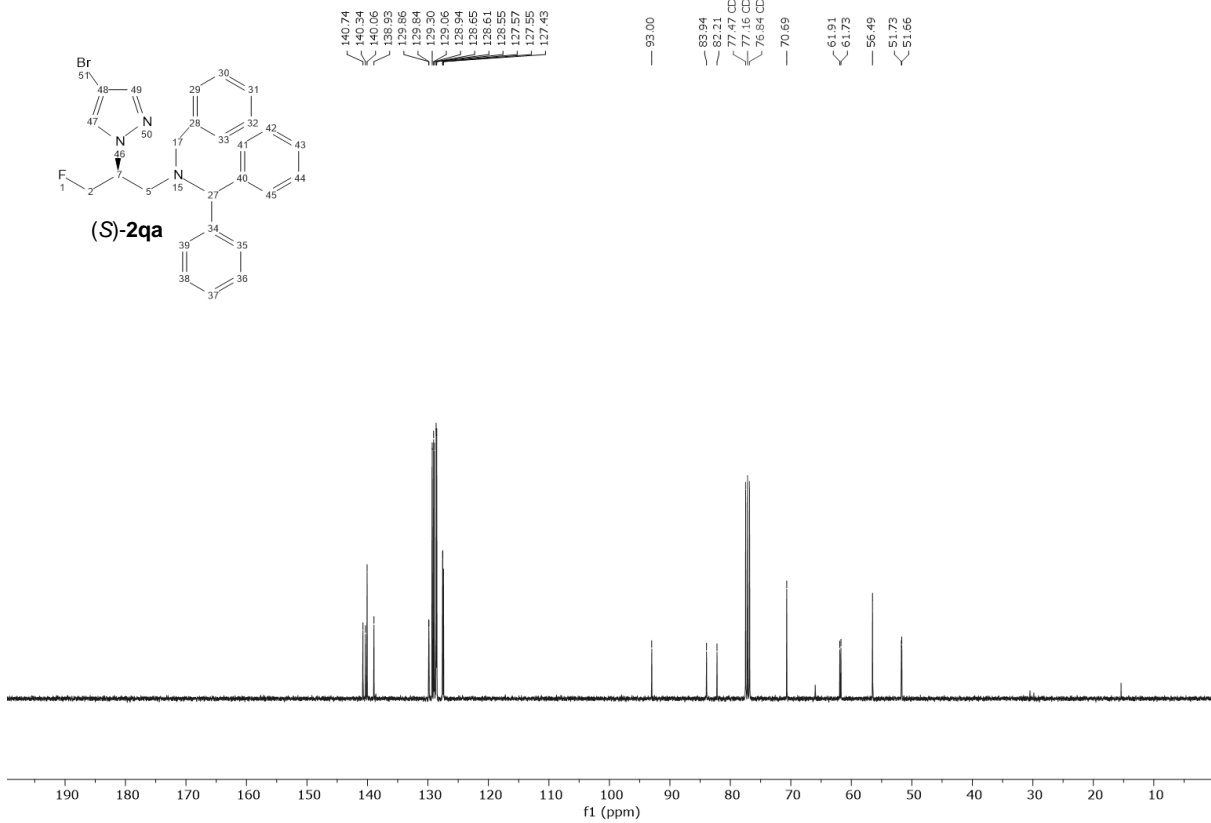
-223.60
-223.61
-223.67
-223.68
-223.73
-223.74
-223.80
-223.81
-223.86
-223.86
-223.93
-223.93



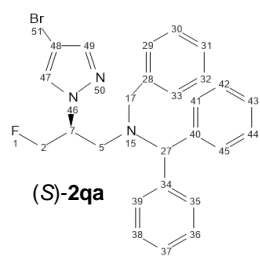
UOXF_groagna_2qa/CdCl3



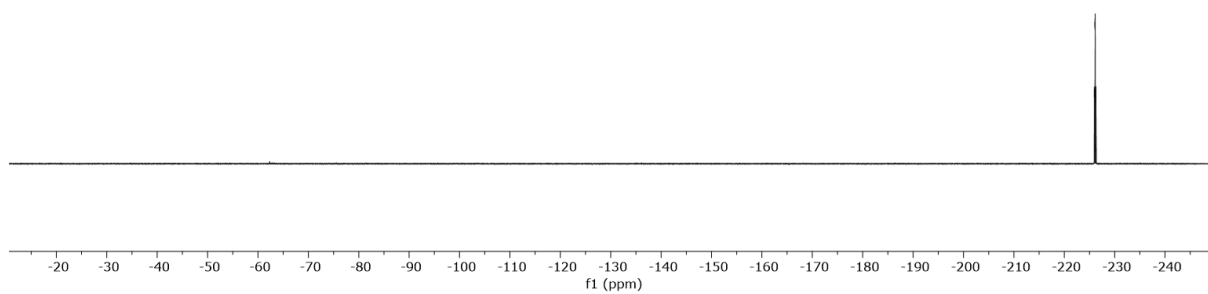
UOXF_groagna_2qa/CdCl3



UOXF_groagna_2qa/CdCl3

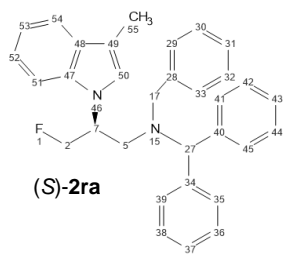


235.06
235.07
235.01
235.02
235.09
235.09
235.10
235.14
235.14
235.21
235.21
235.26
235.27

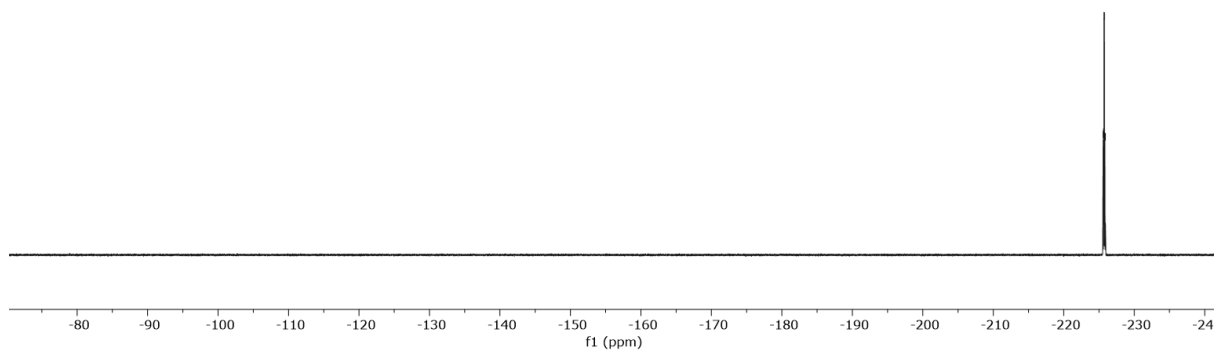


UOXF_groagna_2ra/CdCl3

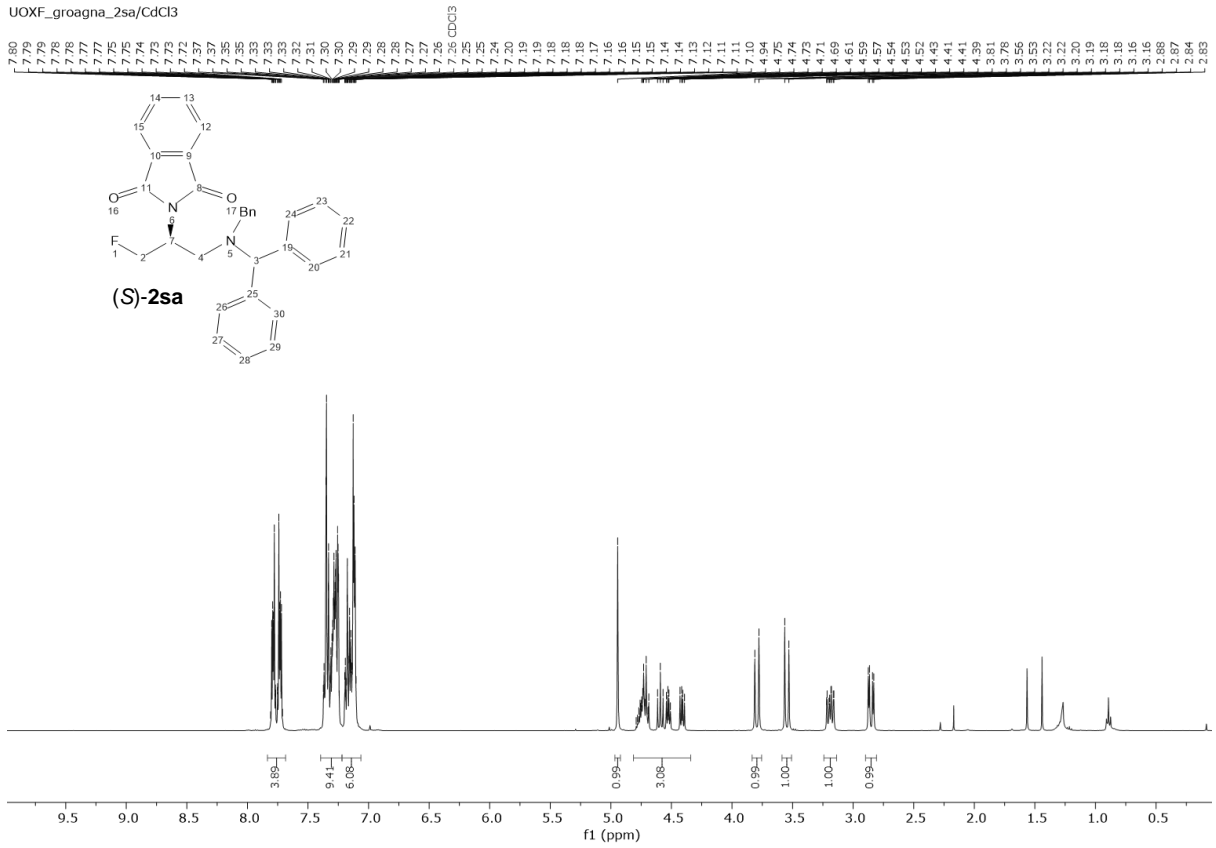
-235.98
-235.95
-235.77
-235.83
-235.87
-235.90



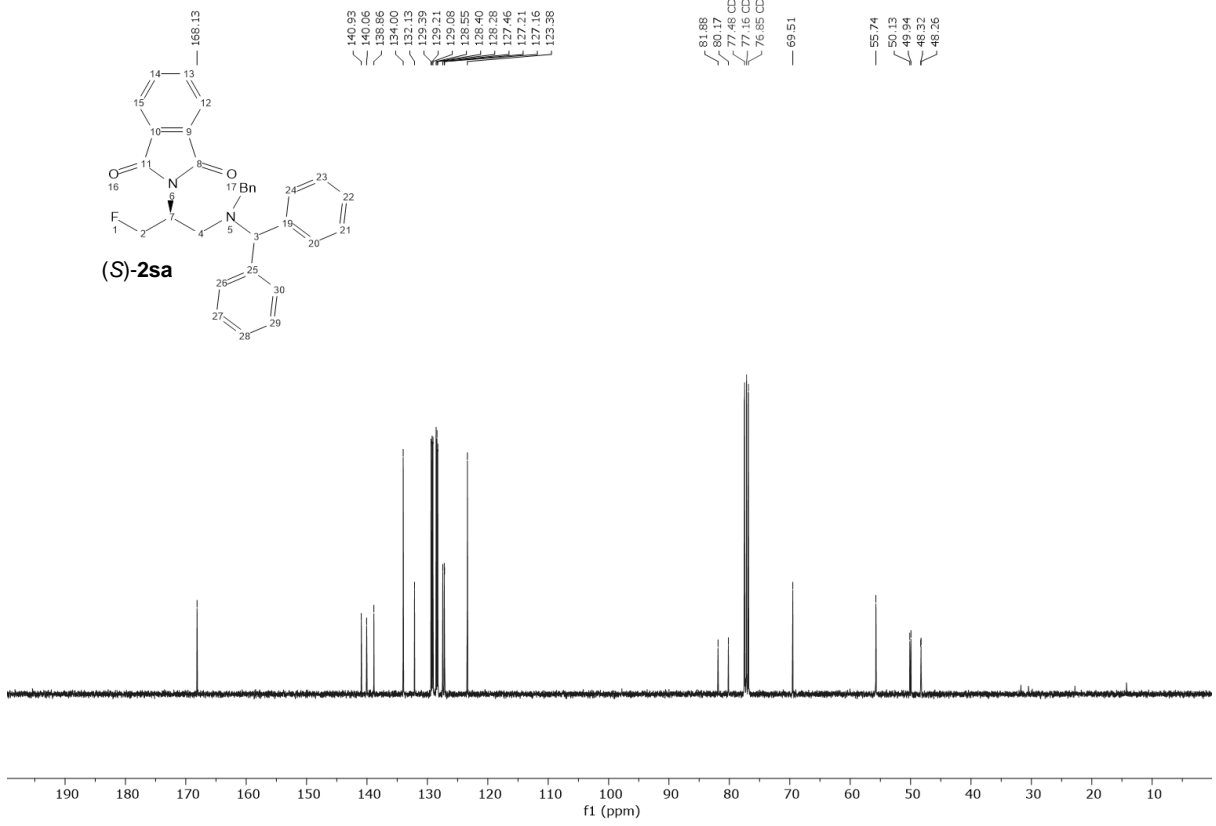
(S)-2ra



UOXF_groagna_2sa/CdCl3

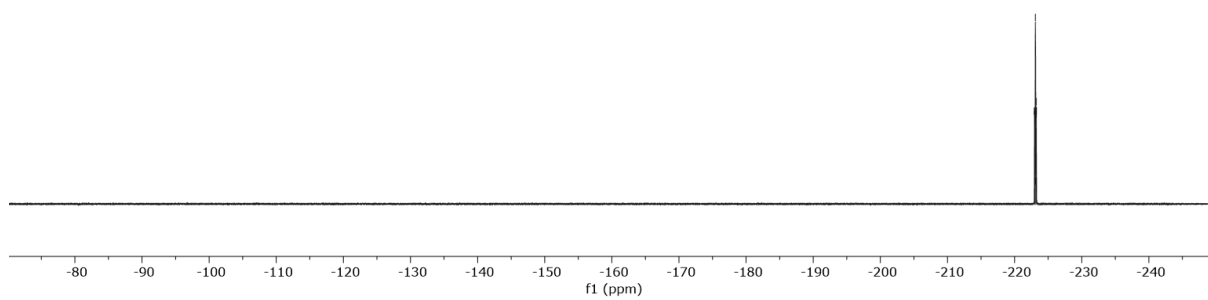
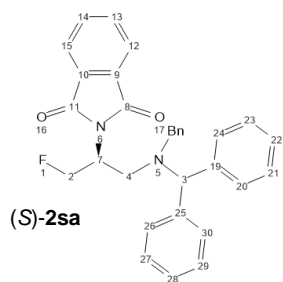


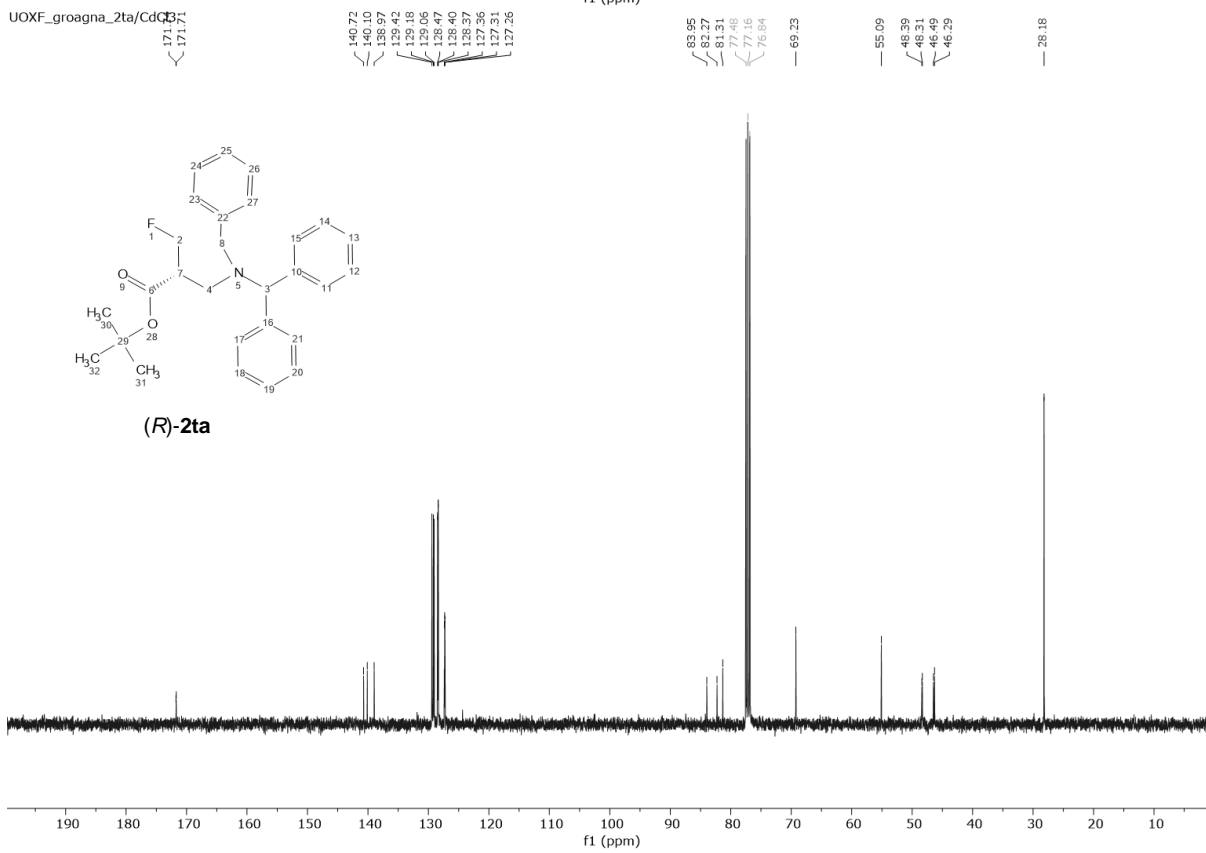
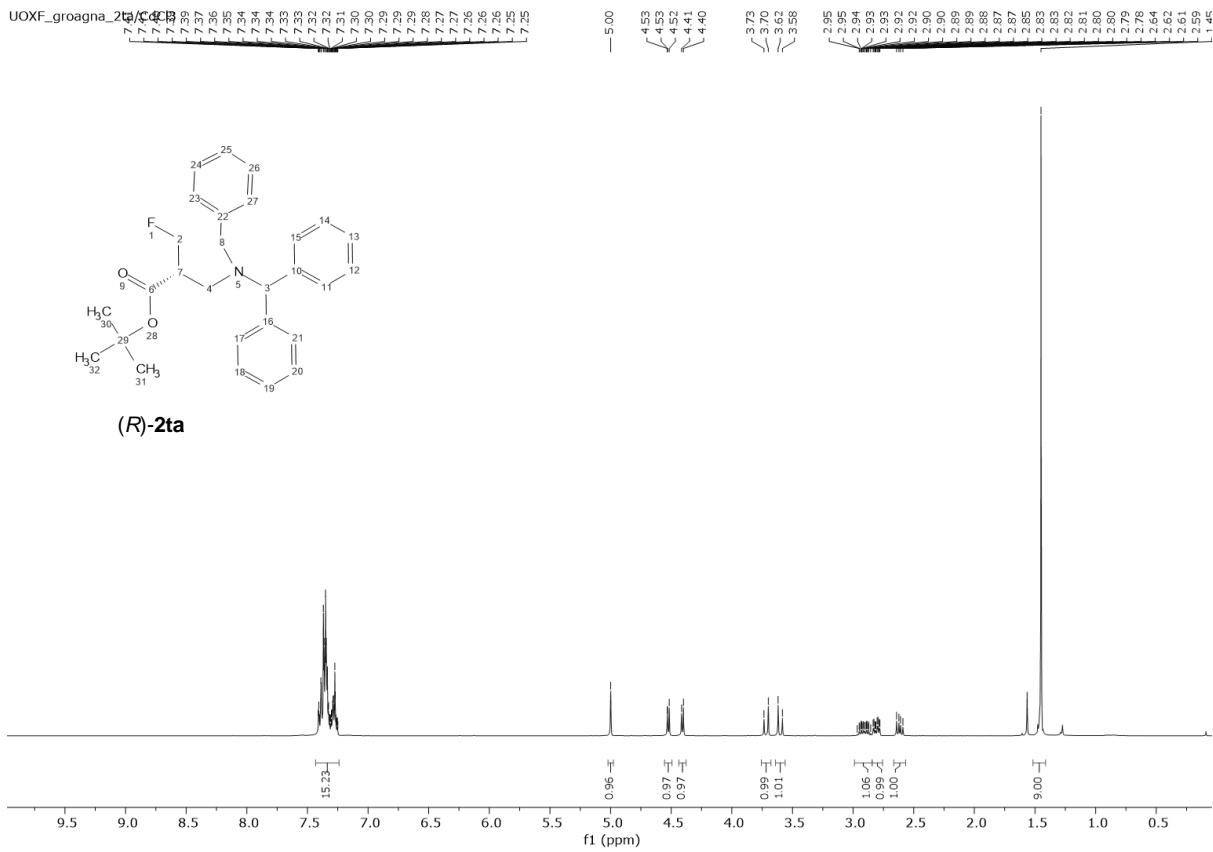
UOXF_groagna_2sa/CdCl3



UOXF_groagna_2sa/CdCl3

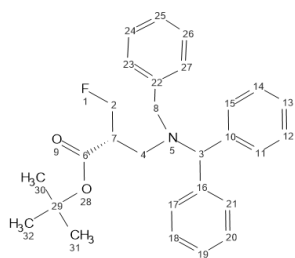
-222.96
-222.97
-223.00
-223.01
-223.09
-223.11
-223.12
-223.13
-223.21
-223.24
-223.25



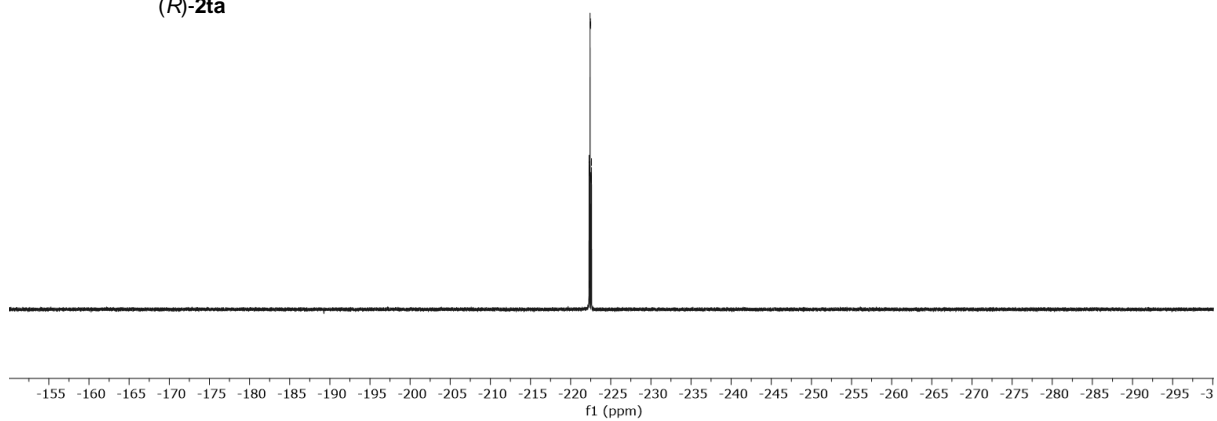


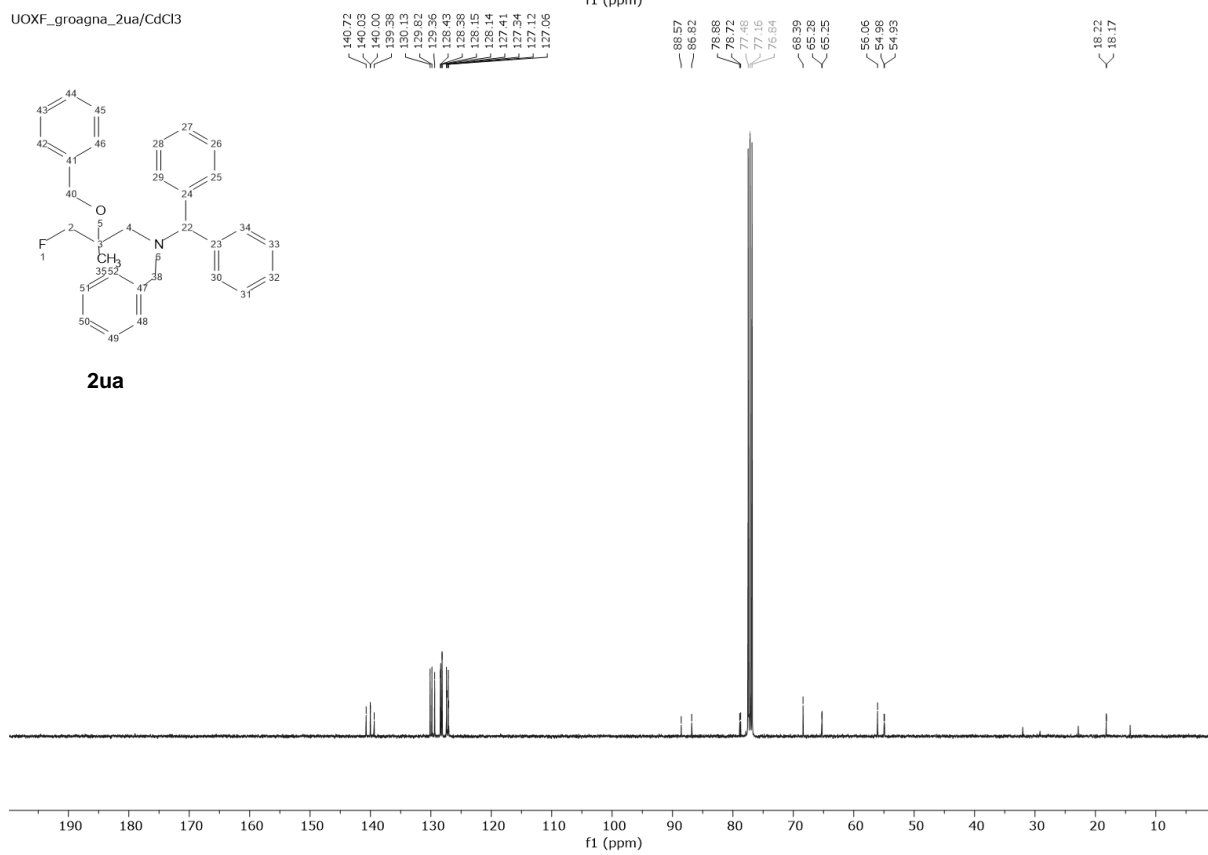
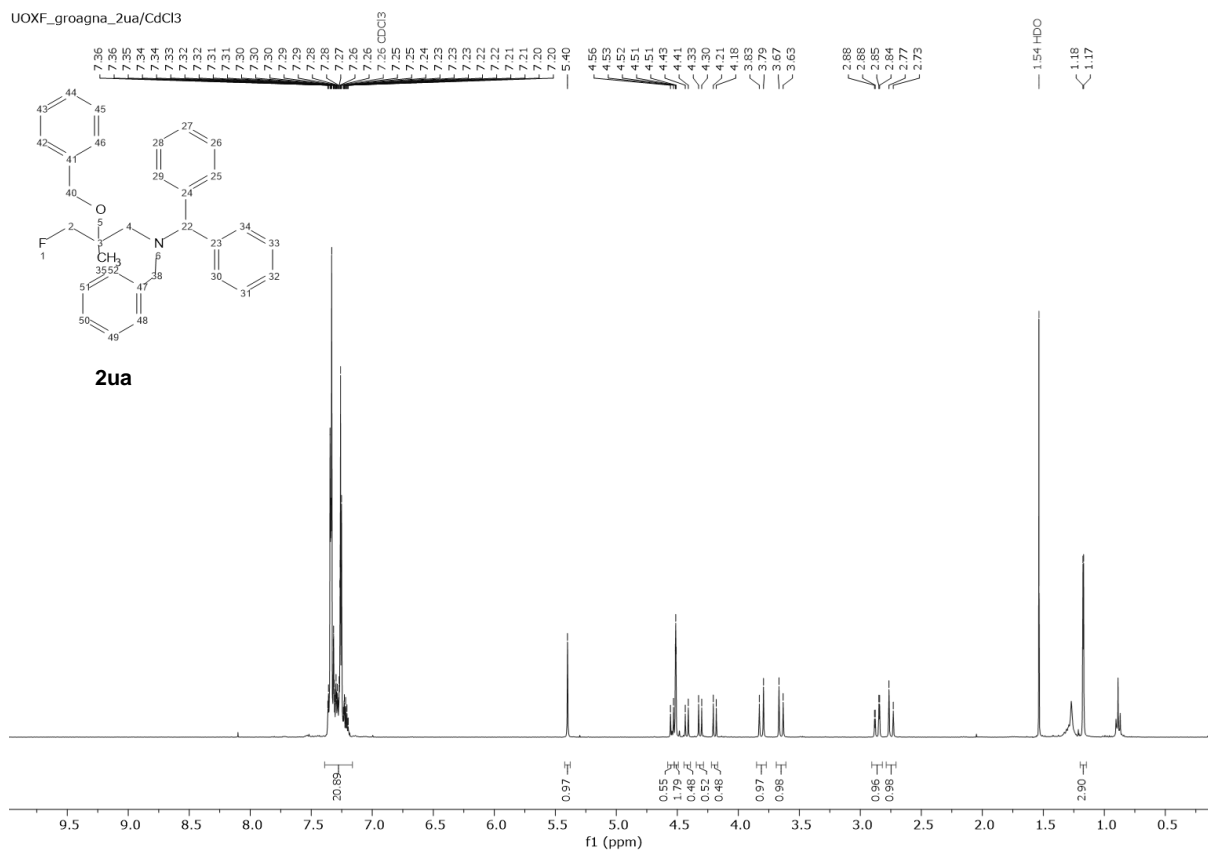
UOXF_groagna_2ta/CdCl3

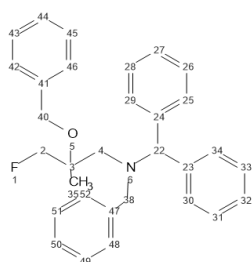
-222.30
-222.34
-222.34
-222.36
-222.36
-222.42
-222.42
-222.43
-222.47
-222.48
-222.55
-222.55
-222.56
-222.60



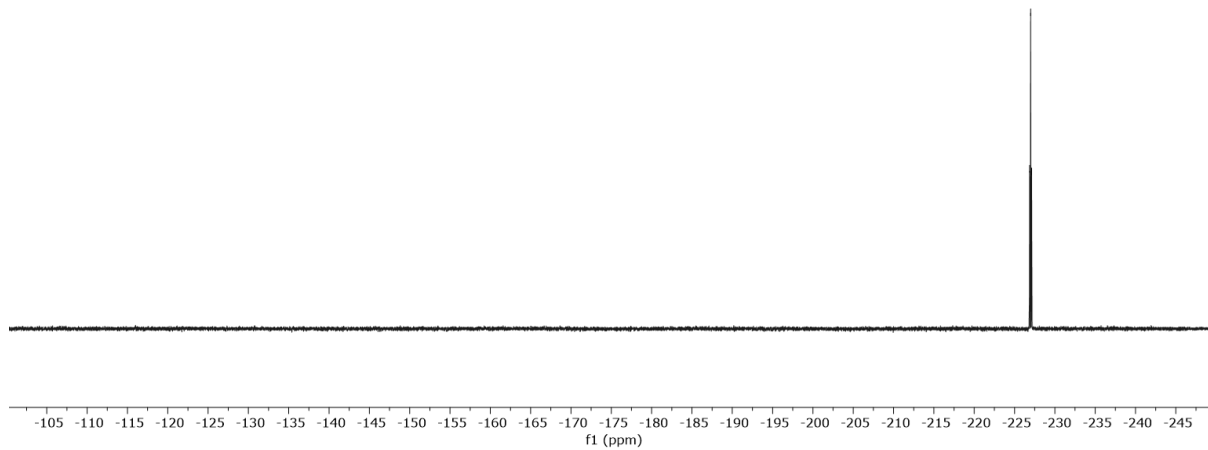
(*R*)-2ta

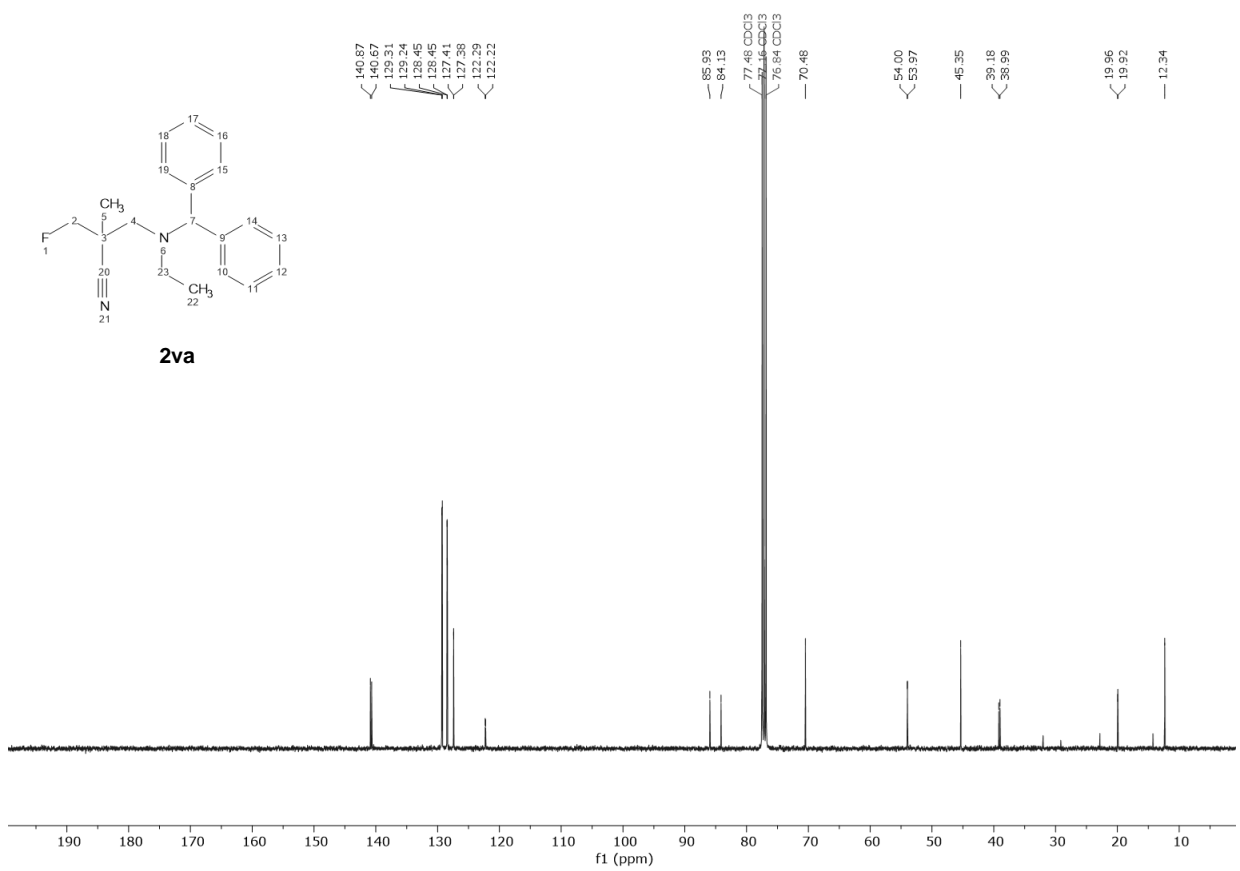
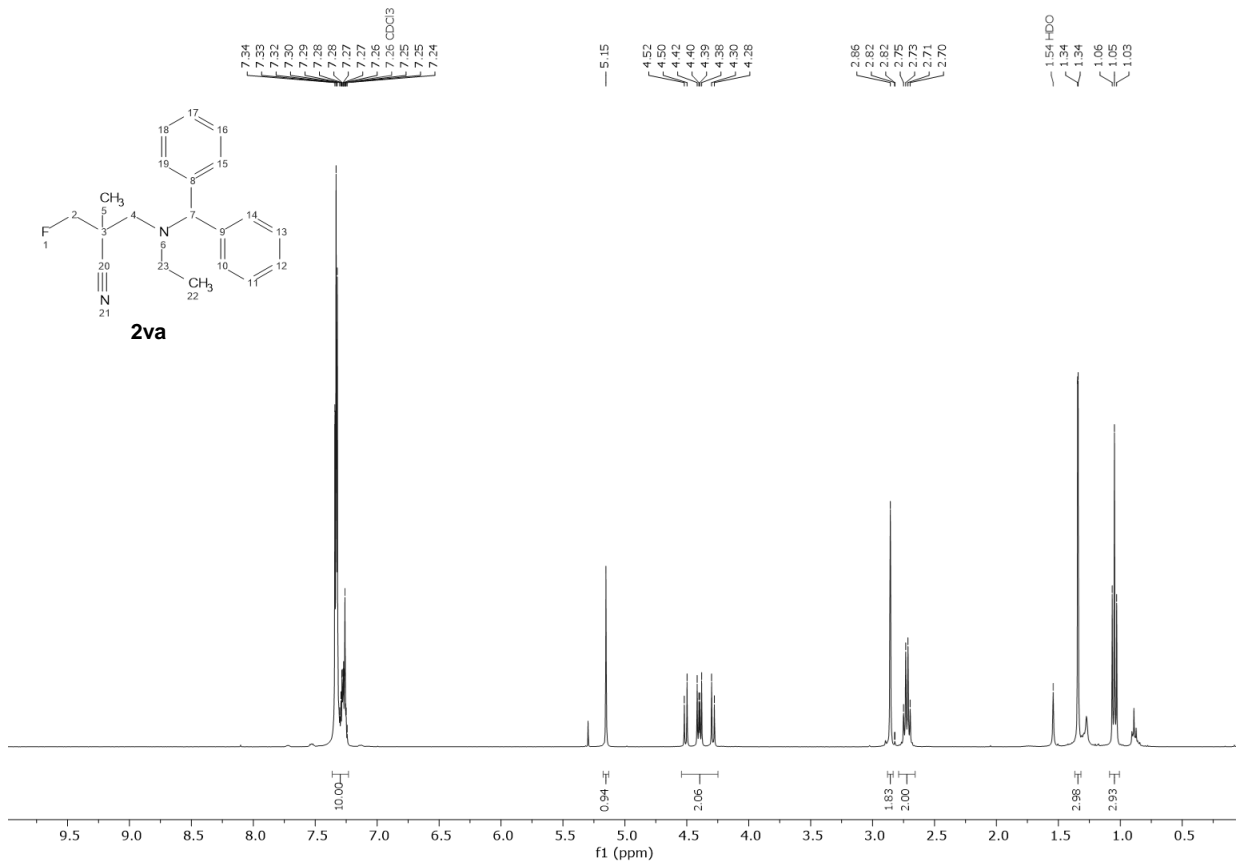


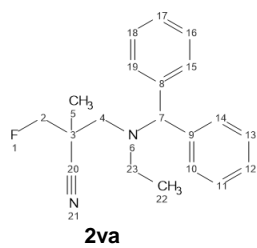




2ua



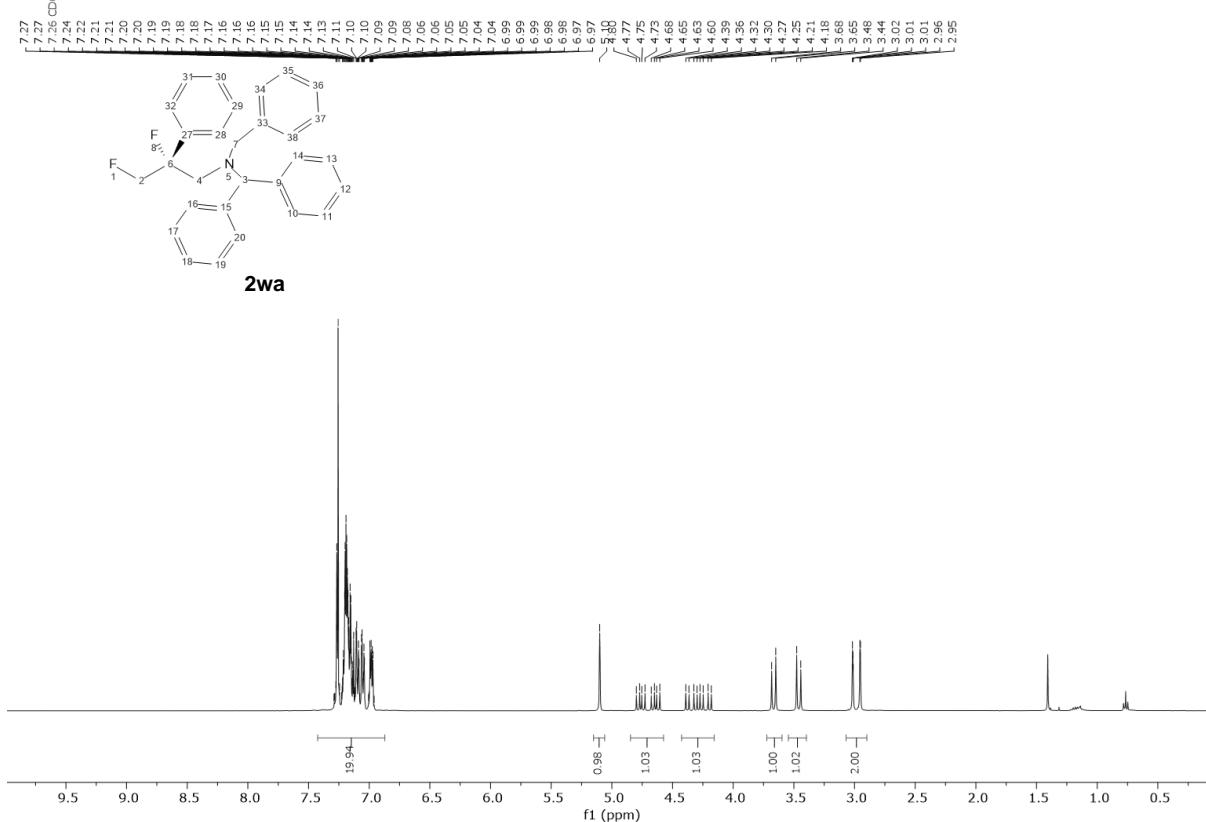




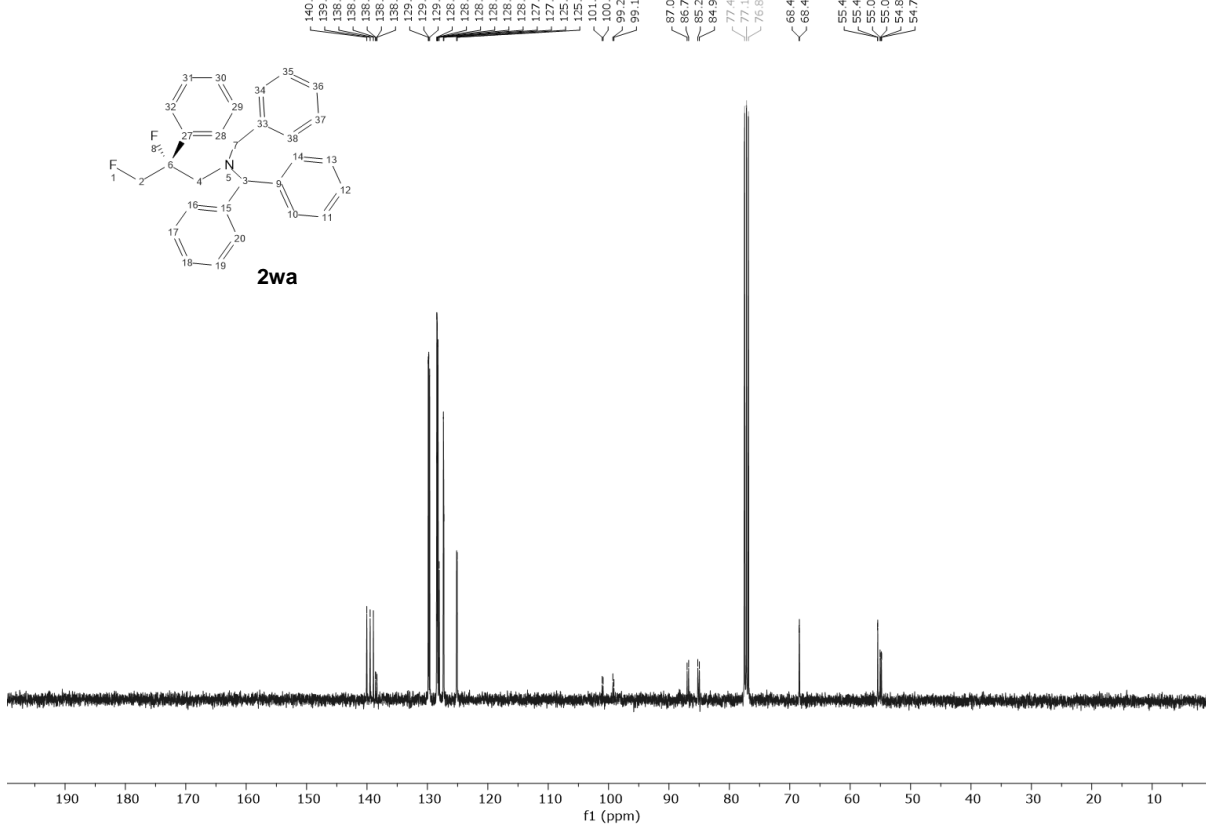
2va



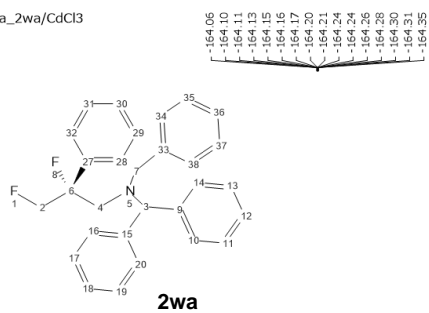
UOXF_groagna_2wa/CdCl3



UOXF_groagna_2wa/CdCl3

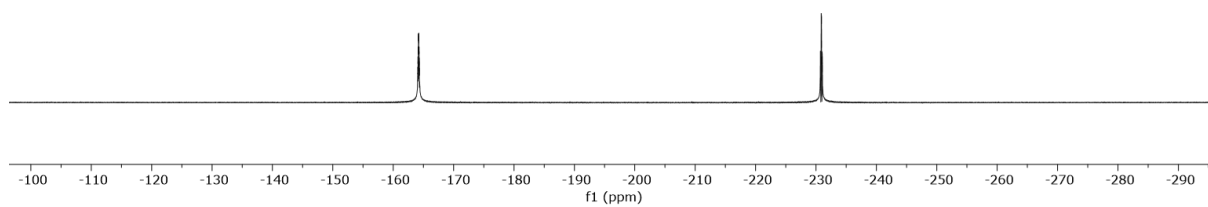


UOXF_groagna_2wa/CdCl3

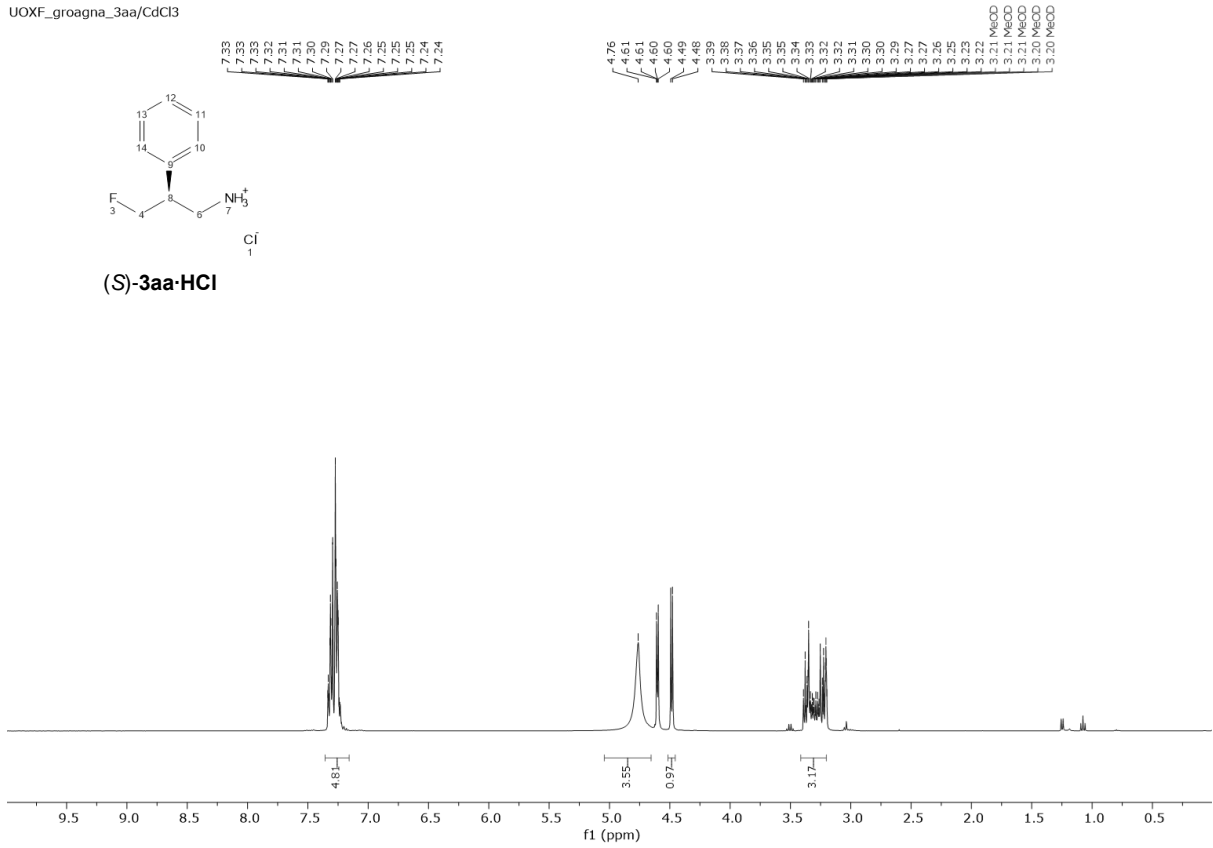
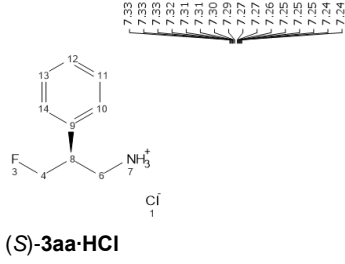


-164.06
-164.10
-164.11
-164.13
-164.15
-164.16
-164.17
-164.20
-164.21
-164.24
-164.26
-164.28
-164.30
-164.31
-164.35

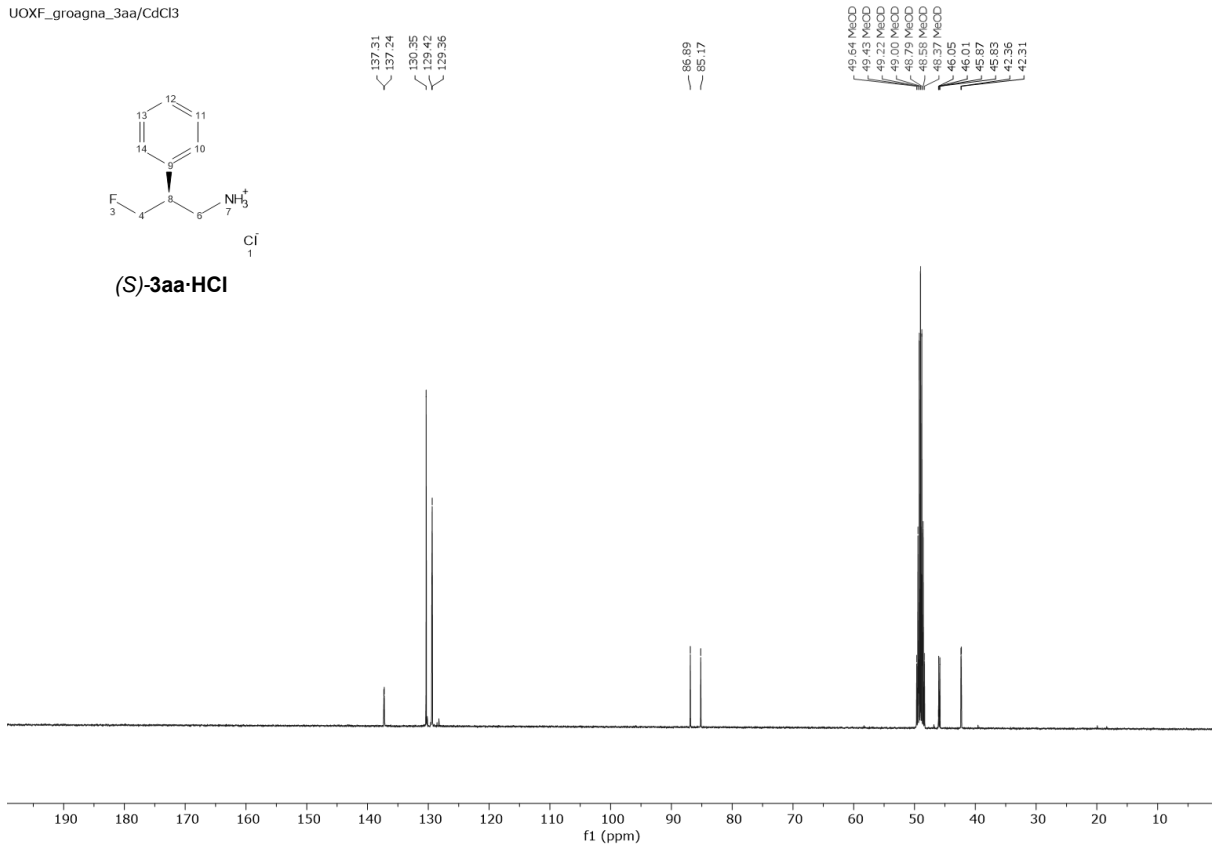
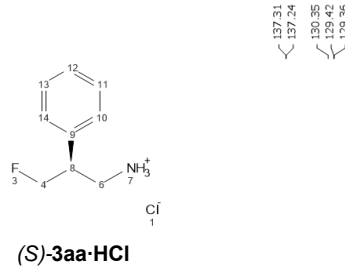
-230.75
-230.79
-230.88
-230.91
-230.92
-231.00
-231.04
-231.05



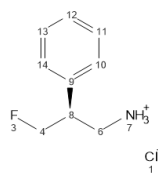
UOXF_groagna_3aa/CdCl3



UOXF_groagna_3aa/CdCl3

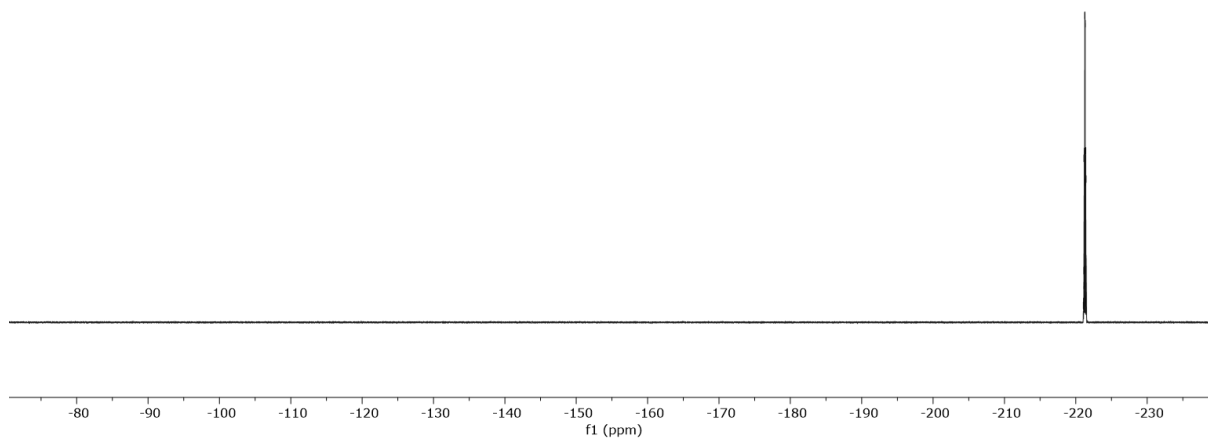


UOXF_groagna_3aa/CdCl3

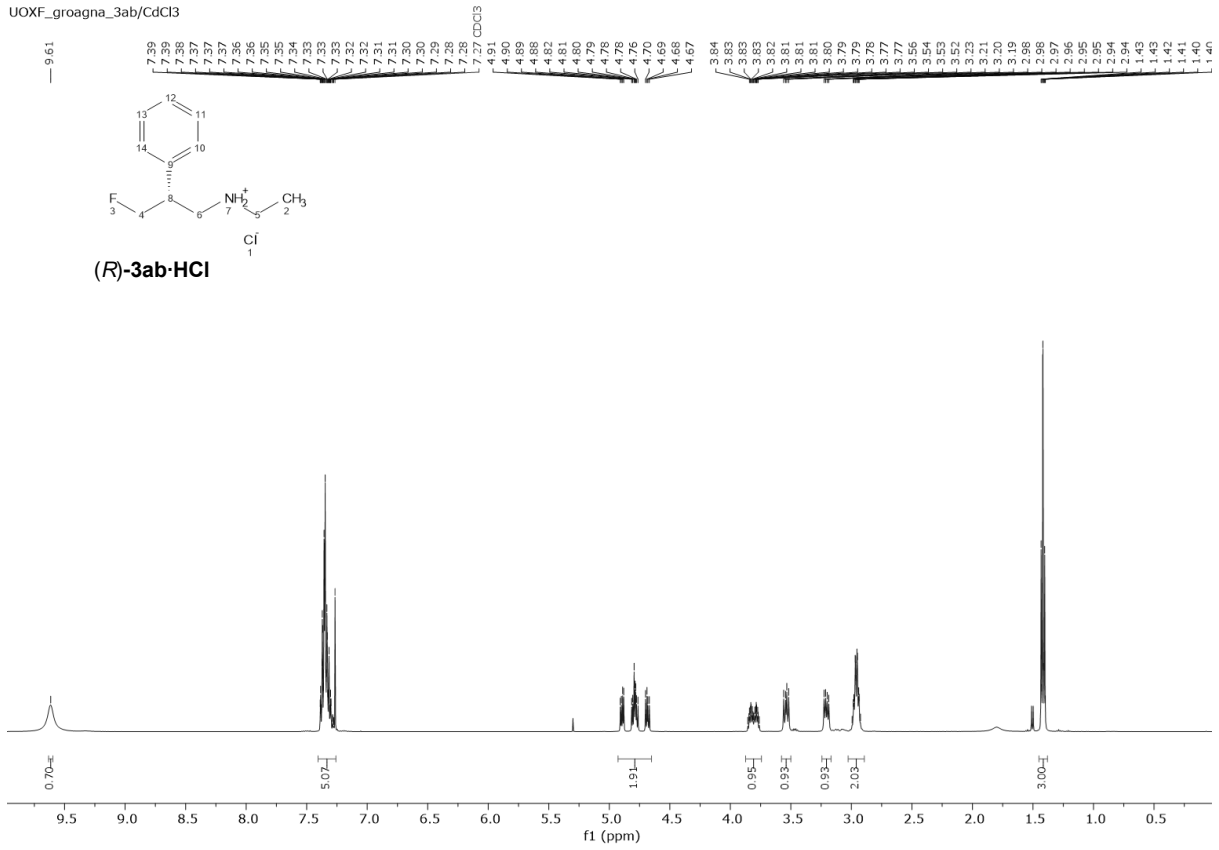


(S)-3aa·HCl

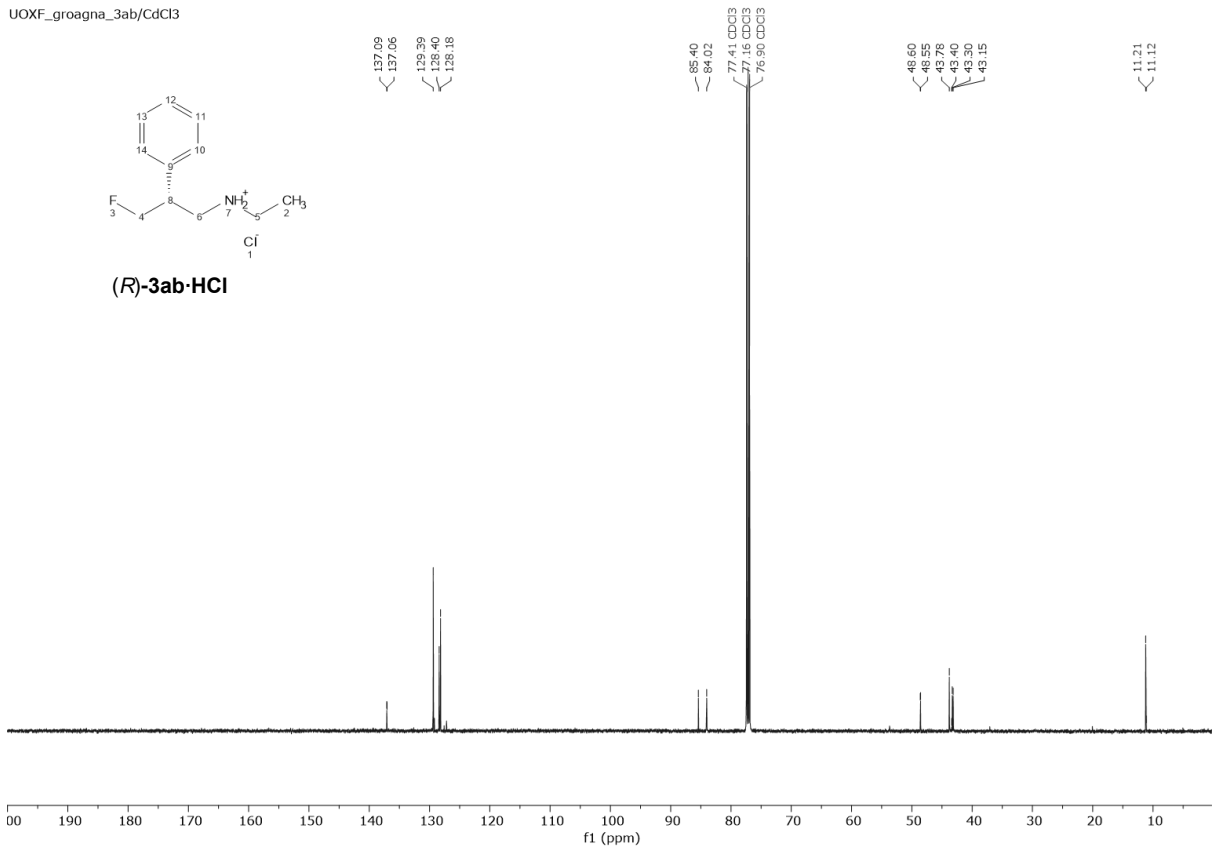
-221.05
-221.10
-221.12
-221.13
-221.14
-221.16
-221.17
-221.18
-221.19
-221.20
-221.22
-221.24
-221.25
-221.27
-221.31
-221.35
-221.37
-221.39
-221.44



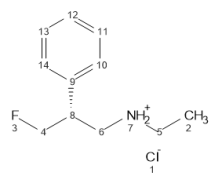
UOXF_groagna_3ab/CdCl3



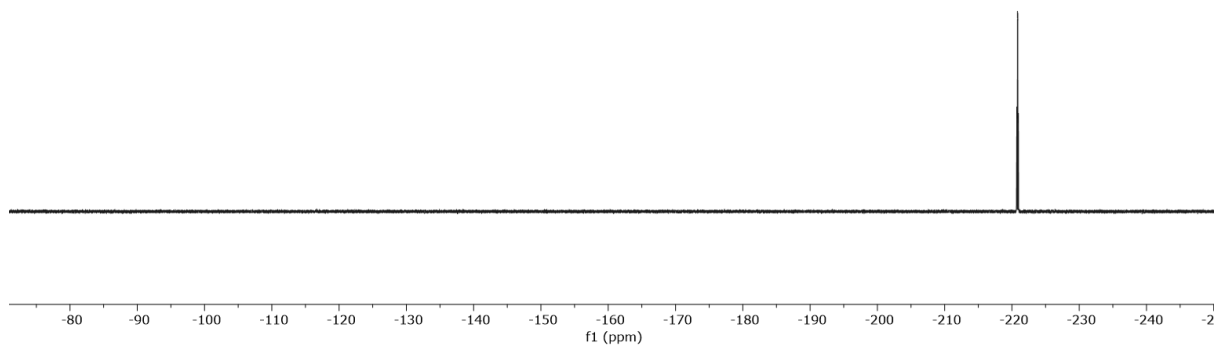
UOXF_groagna_3ab/CdCl3



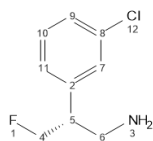
-220.72
-220.67
-220.67
-220.87
-220.92
-220.97



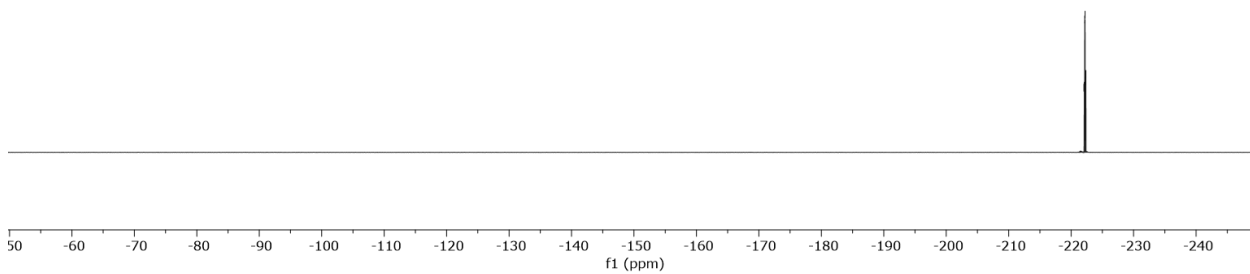
(R)-3ab-HCl



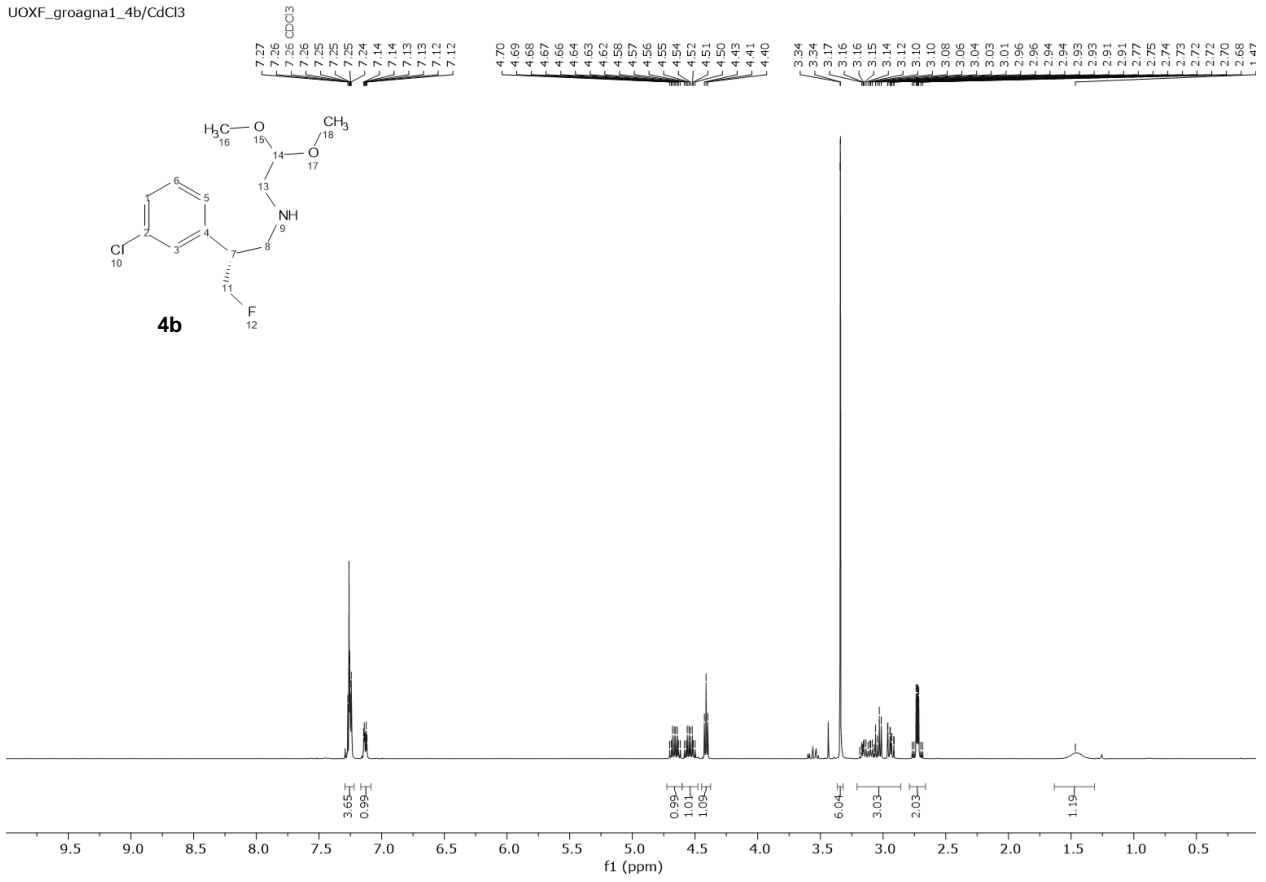
-222.05
-222.10
-222.17
-222.23
-222.30
-222.35



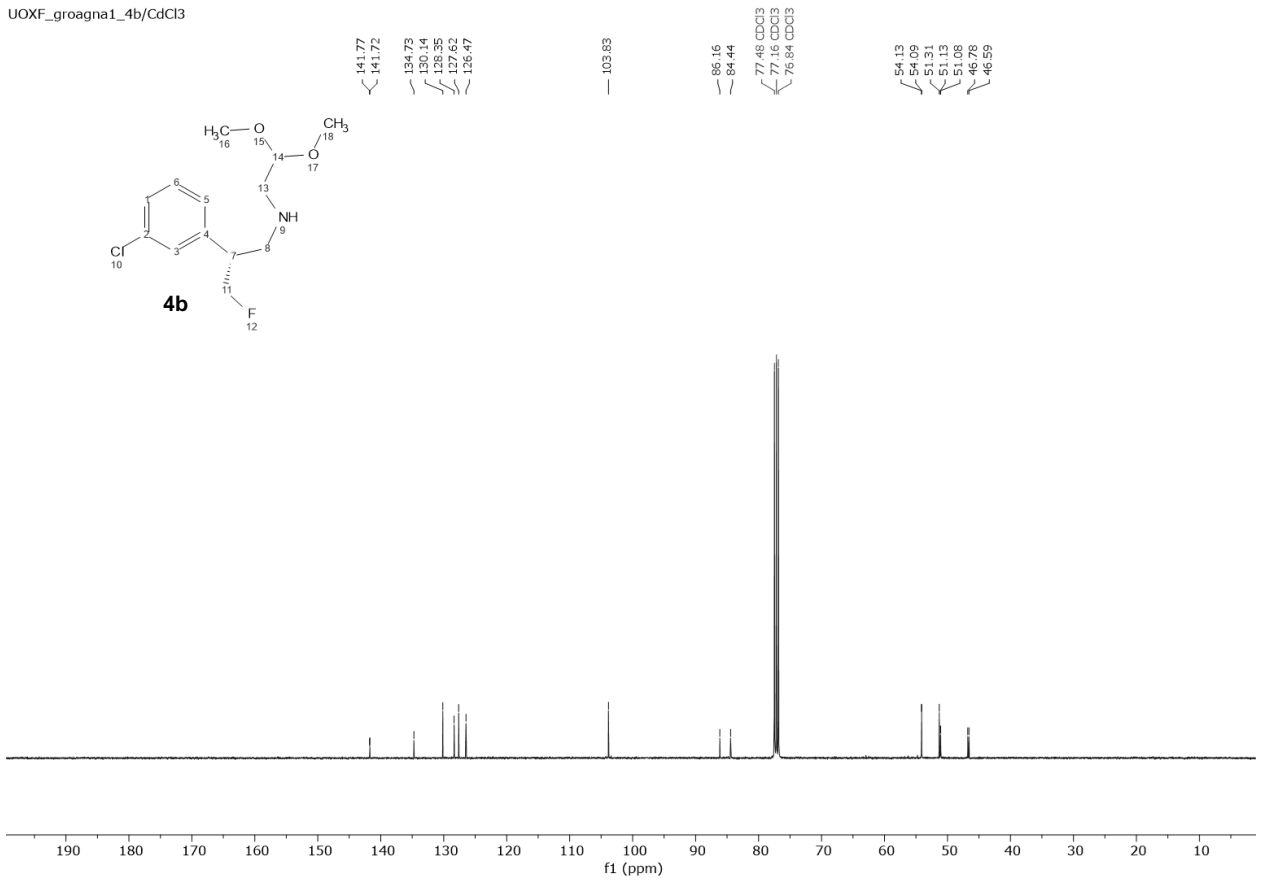
4a



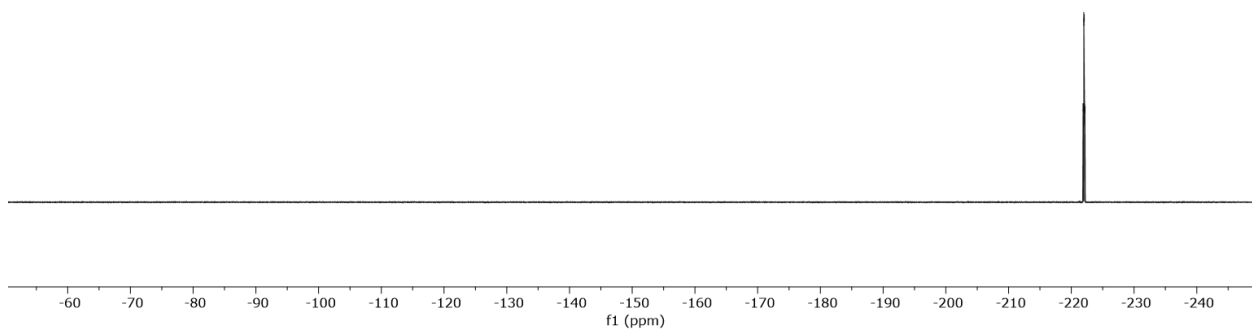
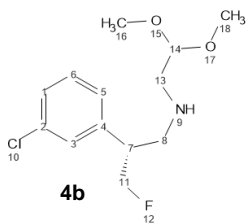
UOXF_groagna1_4b/CdCl3



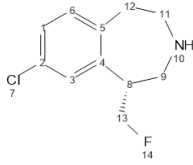
UOXF_groagna1_4b/CdCl3



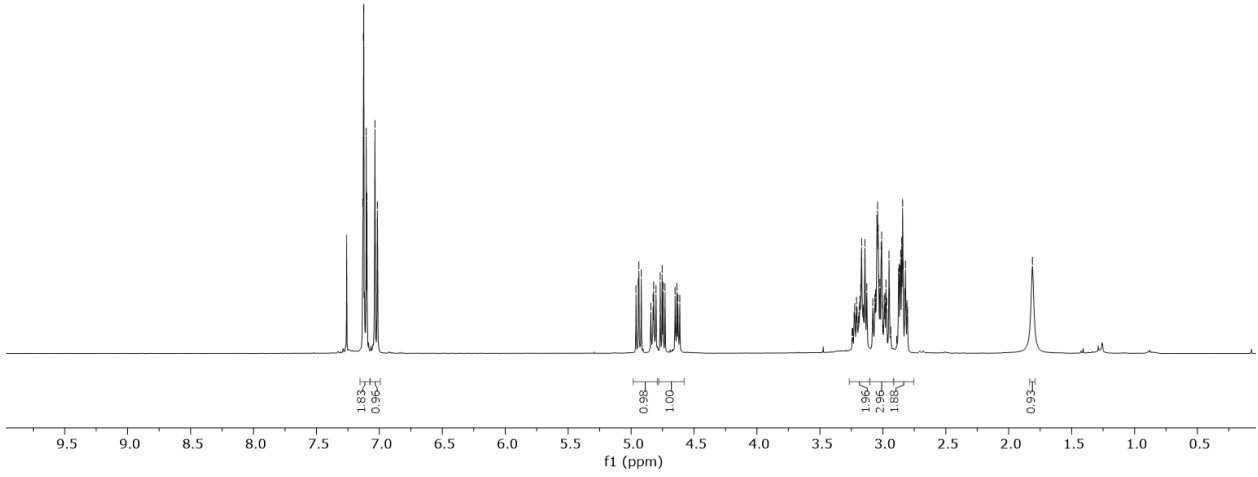
-221.87
-221.92
-221.99
-222.05
-222.12
-222.17



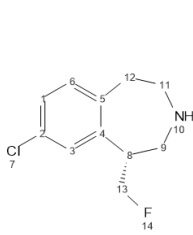
UOXF_groagna1_4c/CdCl3



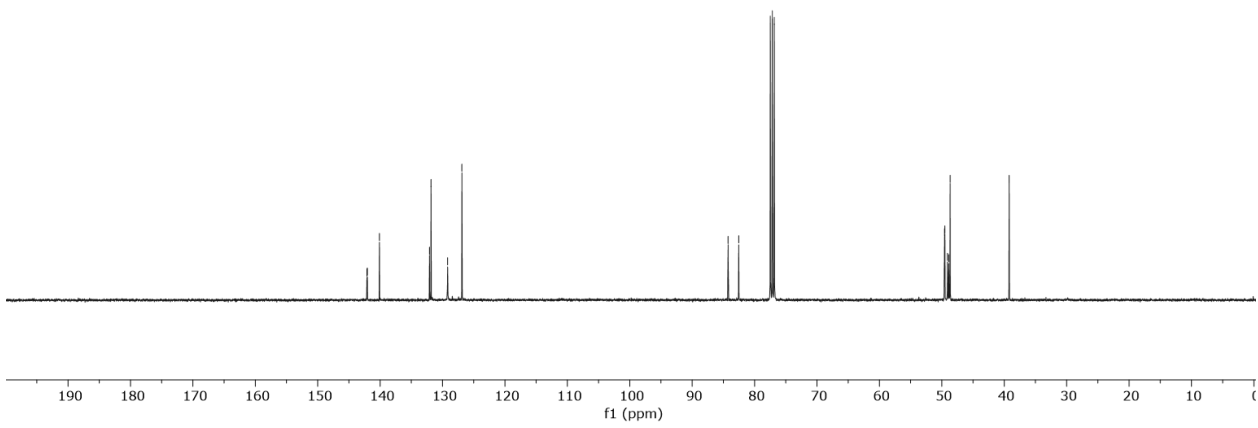
Fluorinated Lorcaserin



UOXF_groagna1_4c/CdCl3

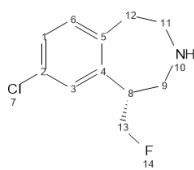


Fluorinated Lorcaserin

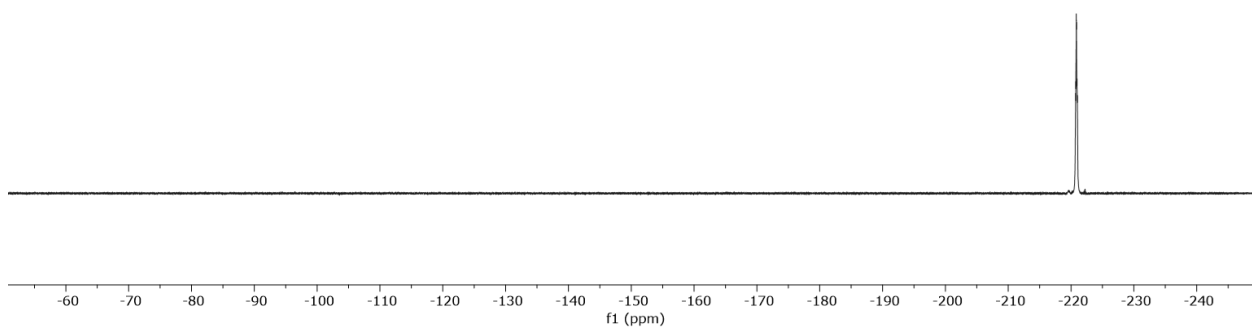


UOXF_groagna1_4c/CdCl3

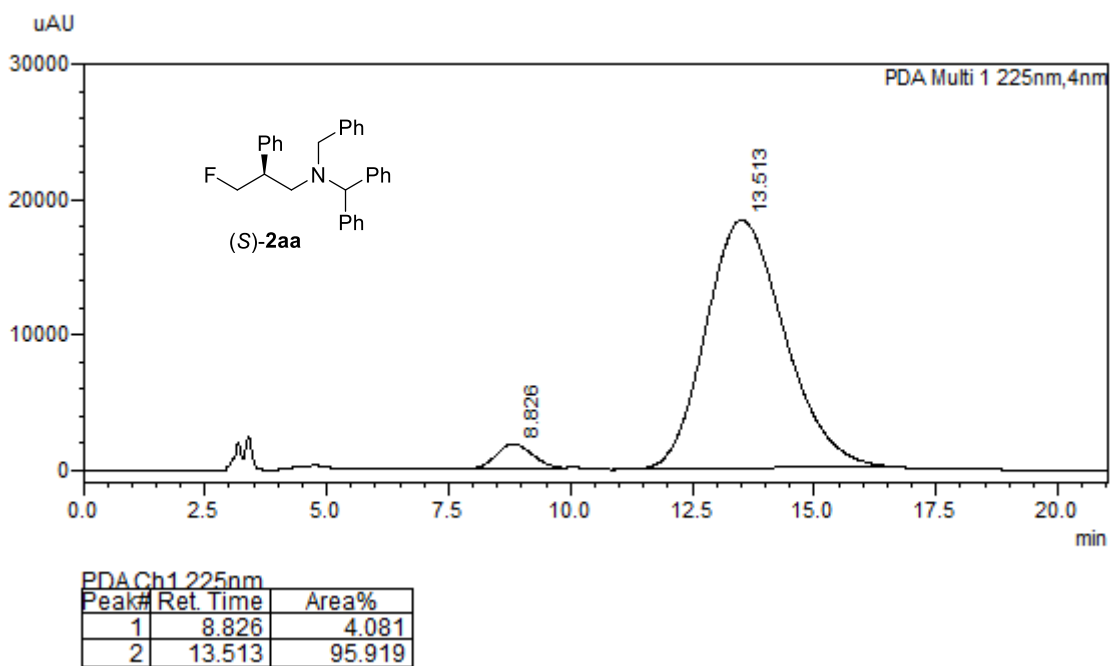
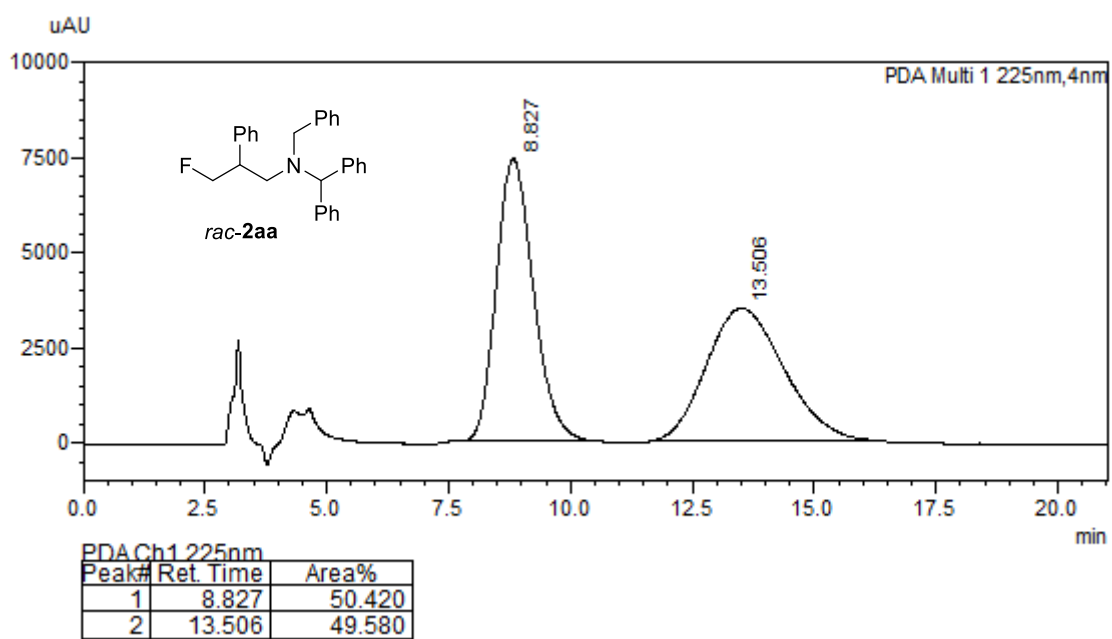
-220.71
-220.76
-220.84
-220.88
-220.96
-221.01

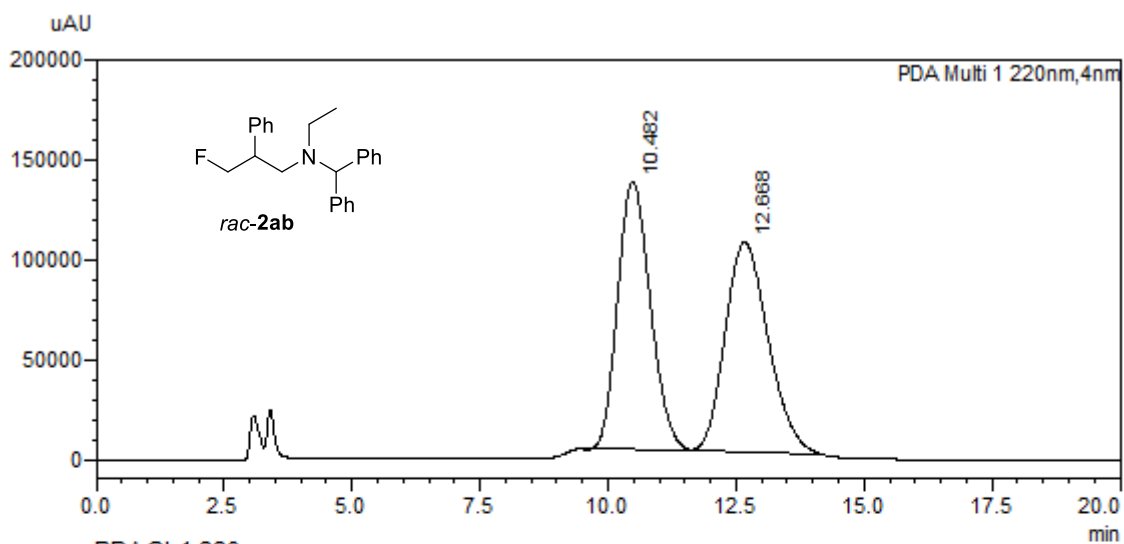


Fluorinated Lorcasein



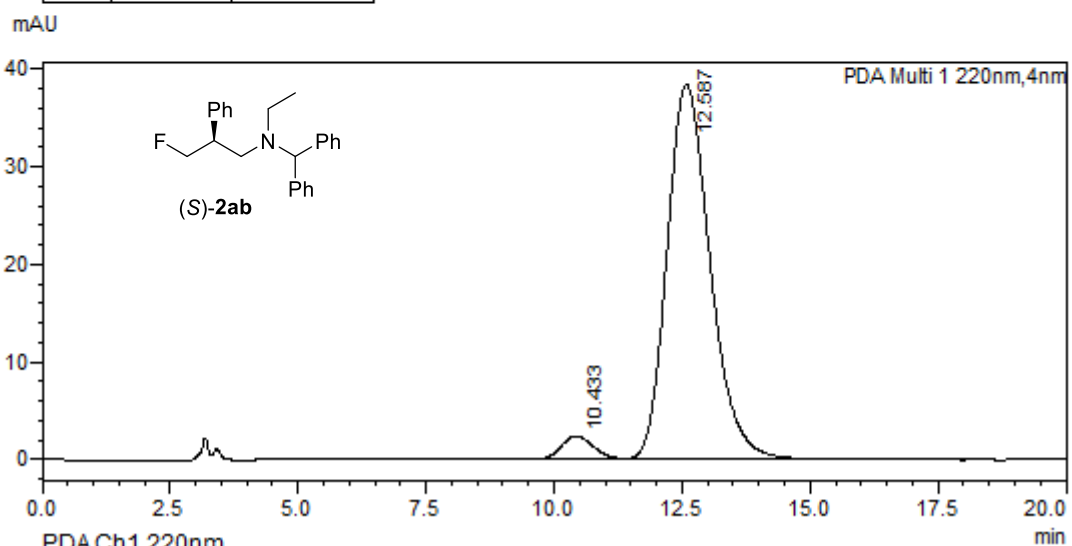
Copies of HPLC traces





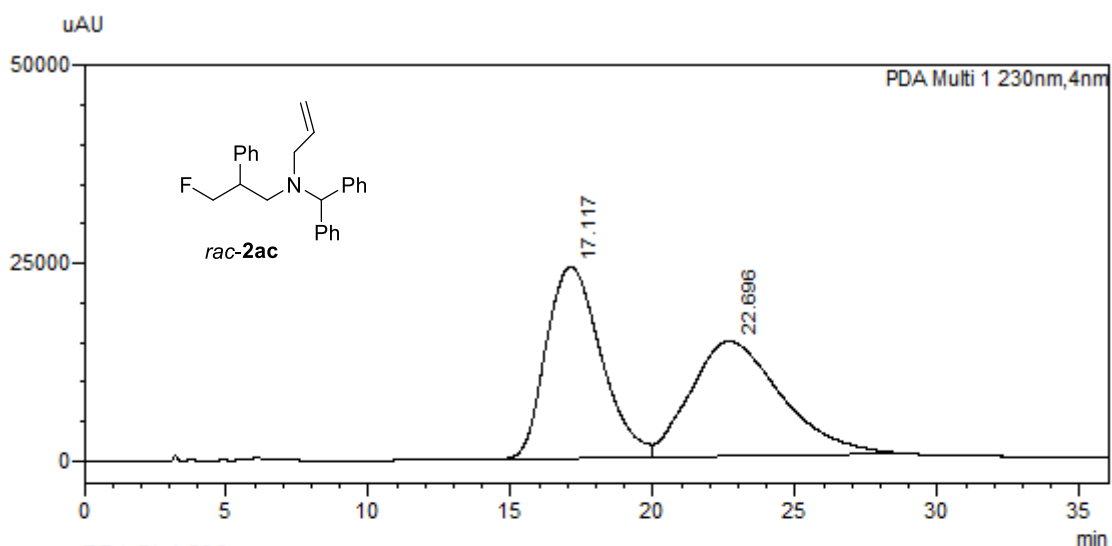
PDA Ch1 220nm

Peak#	Ret. Time	Area%
1	10.482	49.263
2	12.668	50.737



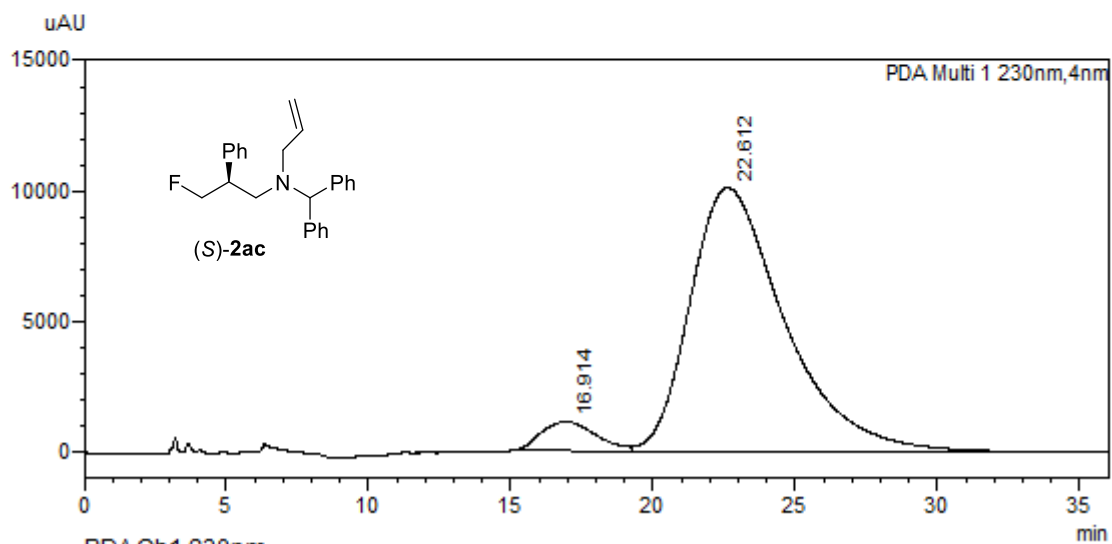
PDA Ch1 220nm

Peak#	Ret. Time	Area%
1	10.433	4.078
2	12.587	95.922



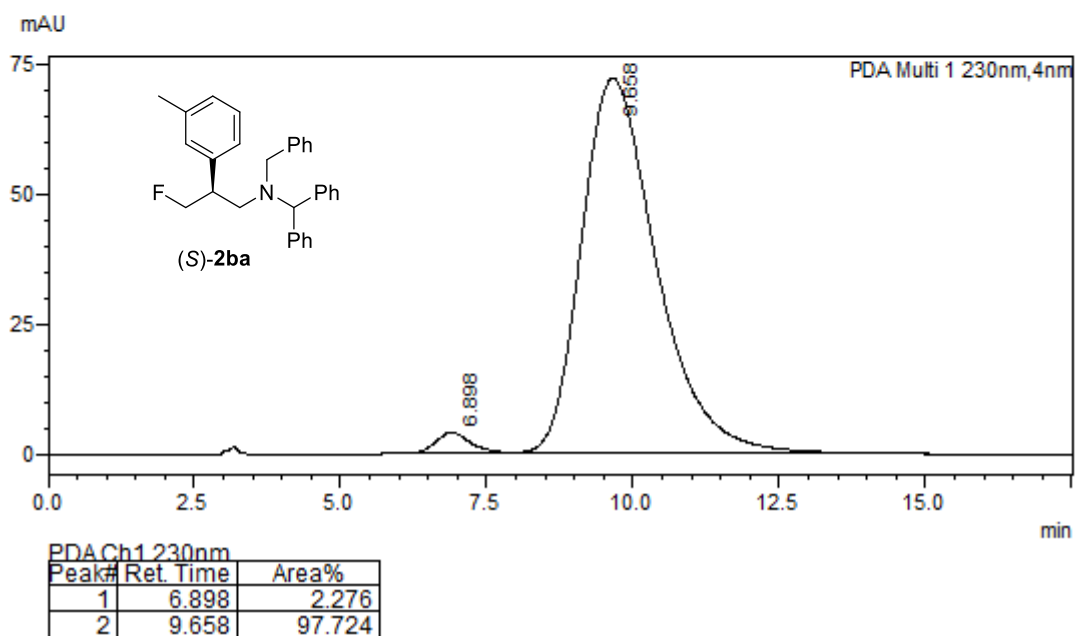
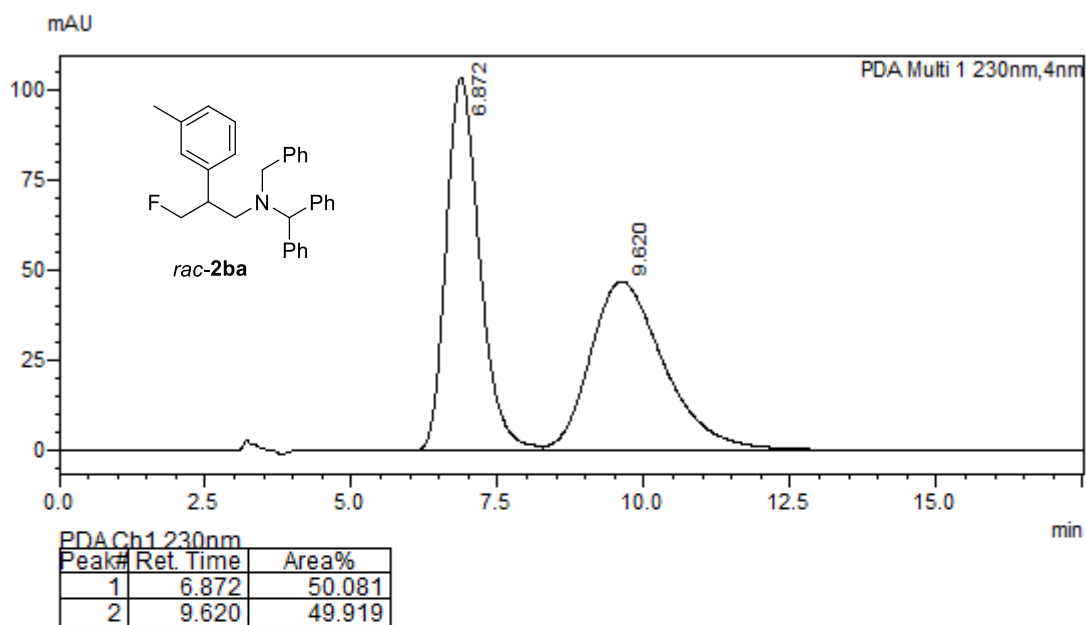
PDACh1 230nm

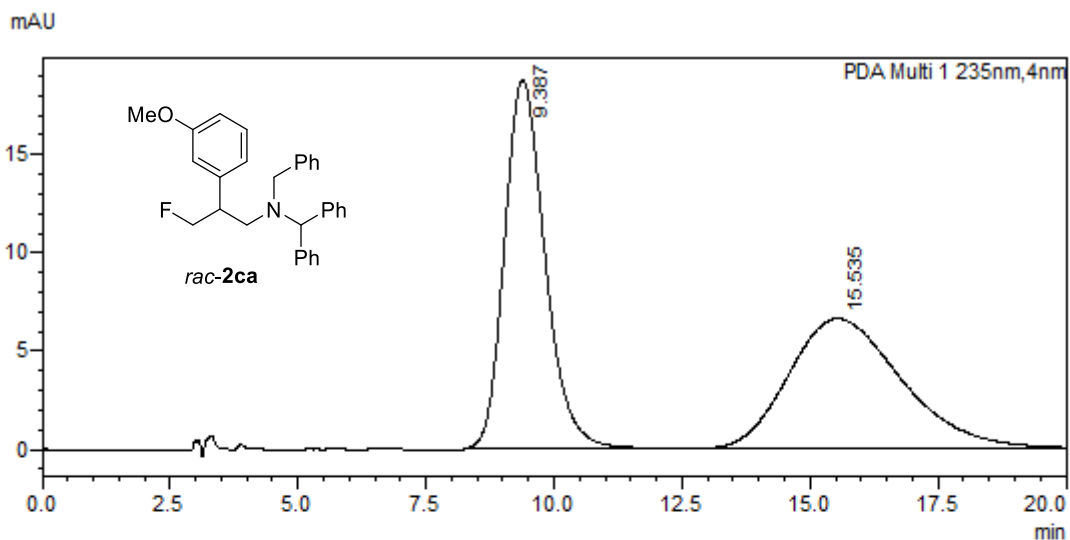
Peak#	Ret. Time	Area%
1	17.117	49.884
2	22.696	50.116



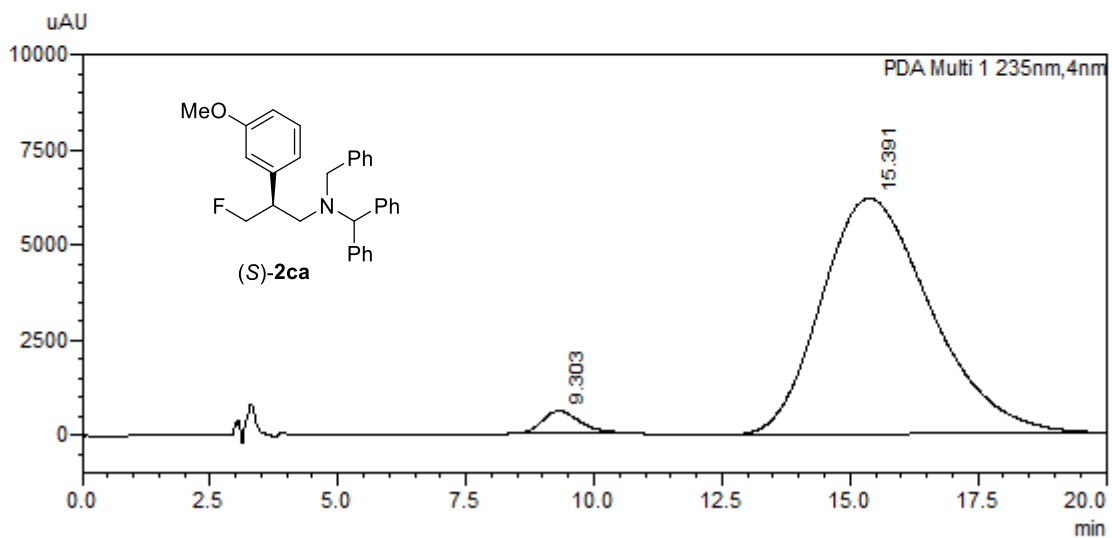
PDACh1 230nm

Peak#	Ret. Time	Area%
1	16.914	5.998
2	22.612	94.002

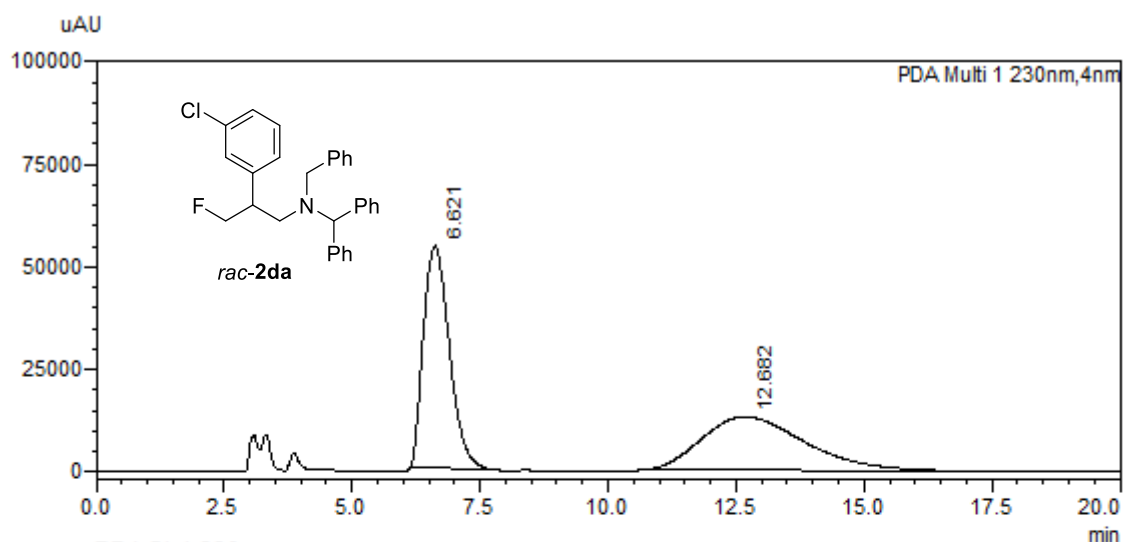




Peak#	Ret. Time	Area%
1	9.387	50.641
2	15.535	49.359

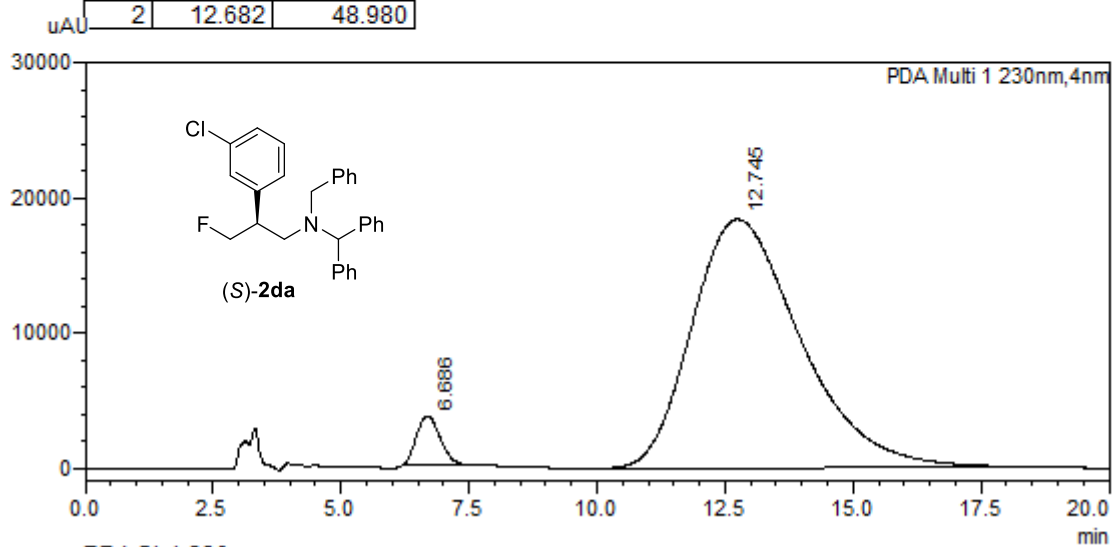


Peak#	Ret. Time	Area%
1	9.303	2.842
2	15.391	97.158



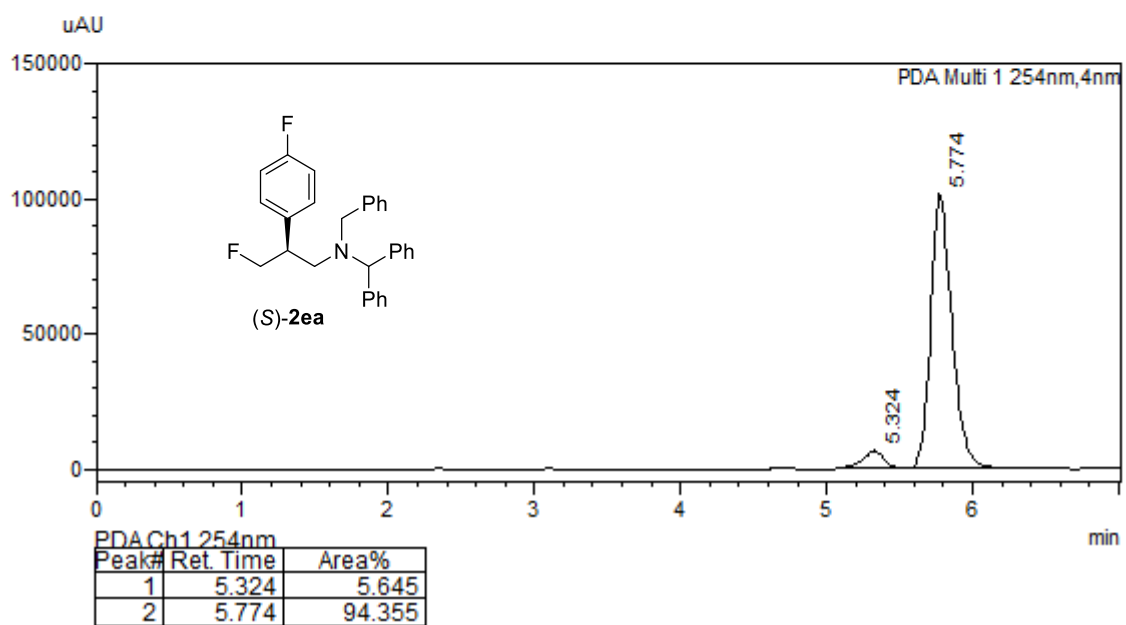
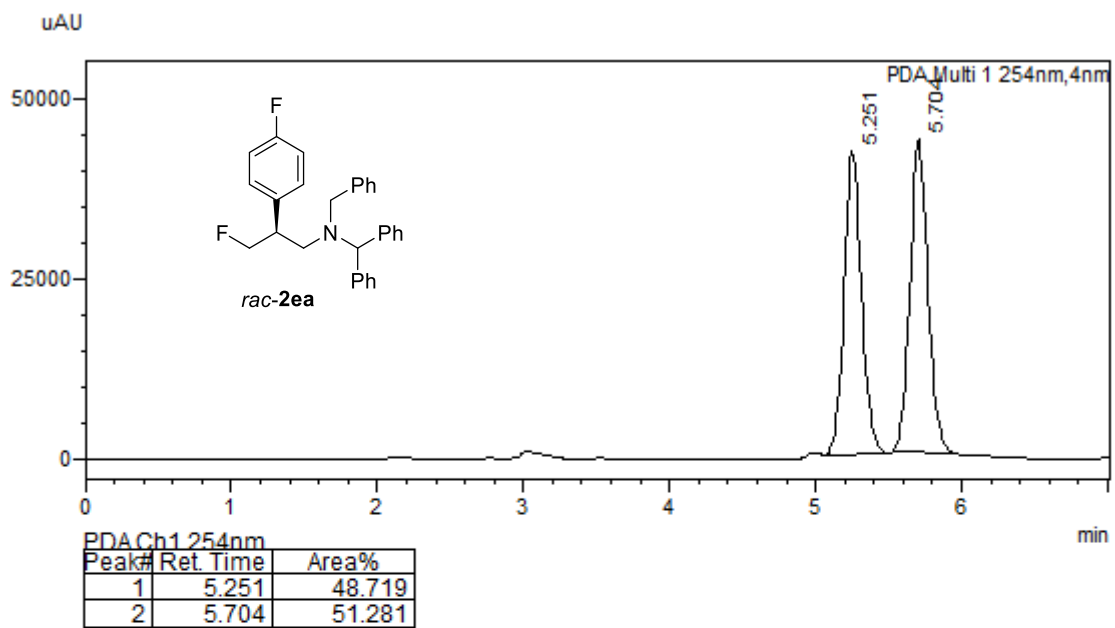
PDA Ch1 230nm

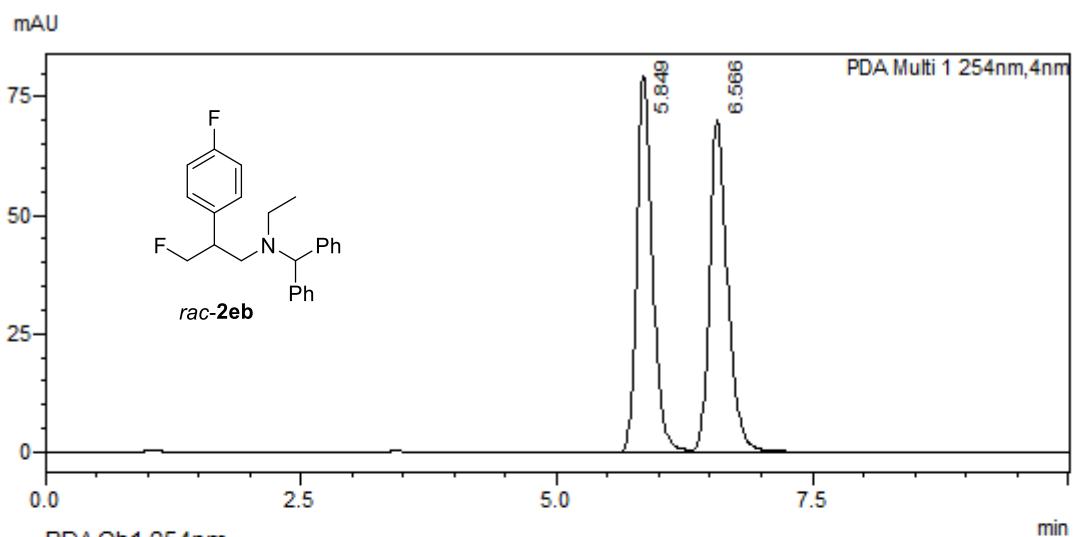
Peak#	Ret. Time	Area%
1	6.621	51.020
2	12.682	48.980



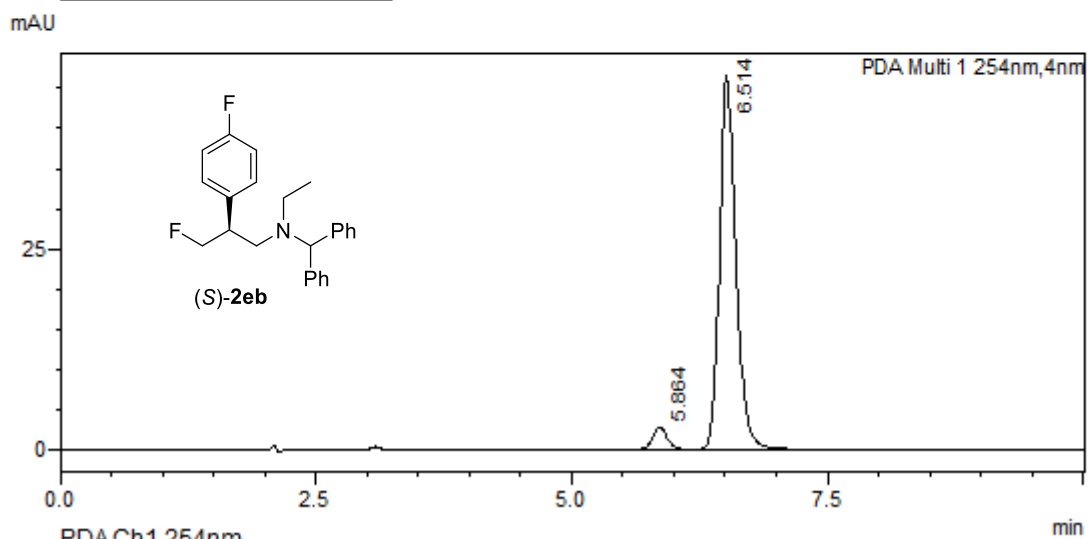
PDA Ch1 230nm

Peak#	Ret. Time	Area%
1	6.686	4.135
2	12.745	95.865

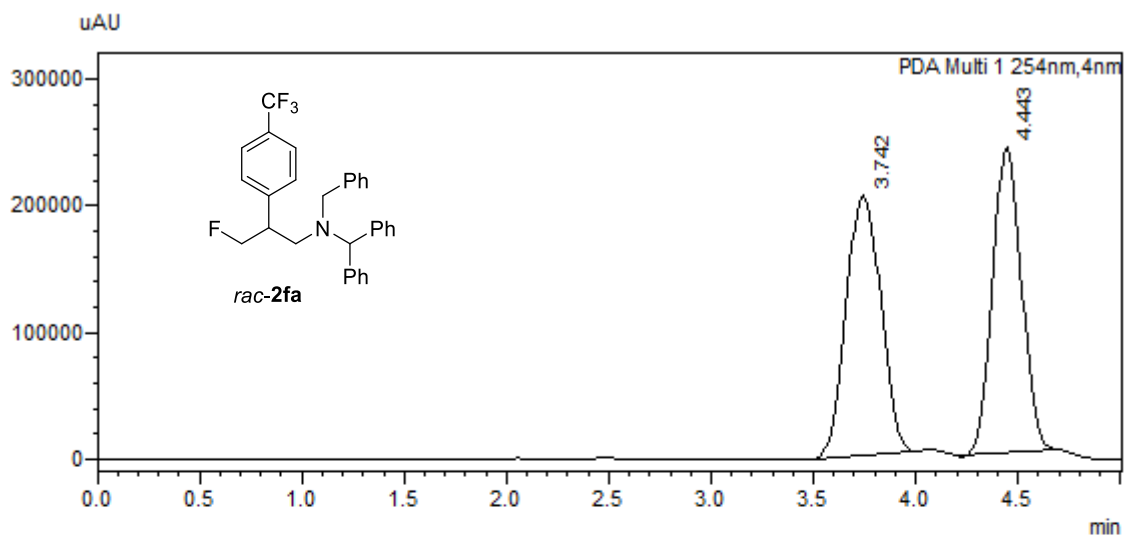




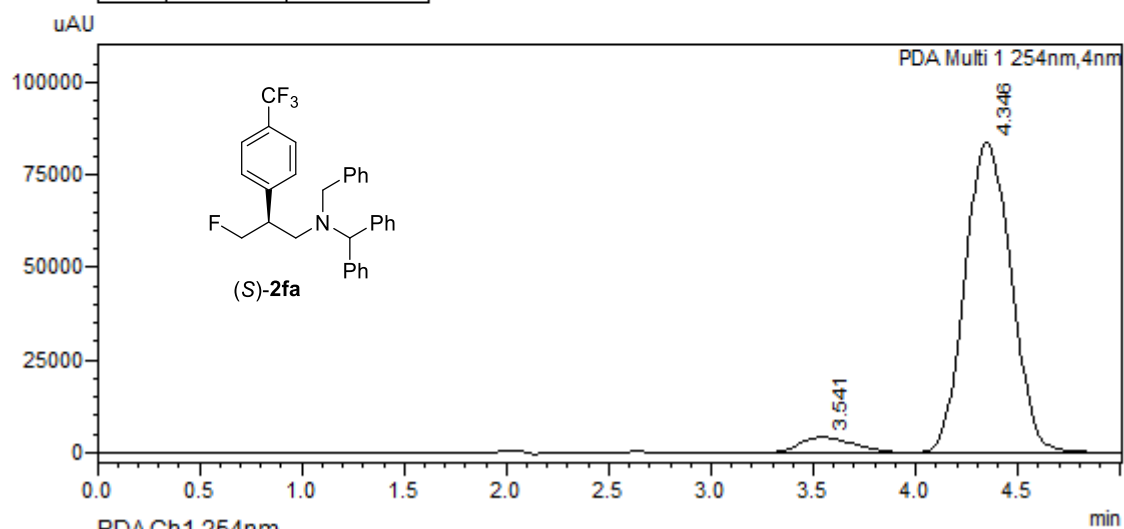
PDA Ch1 254nm		
Peak#	Ret. Time	Area%
1	5.849	49.763
2	6.566	50.237



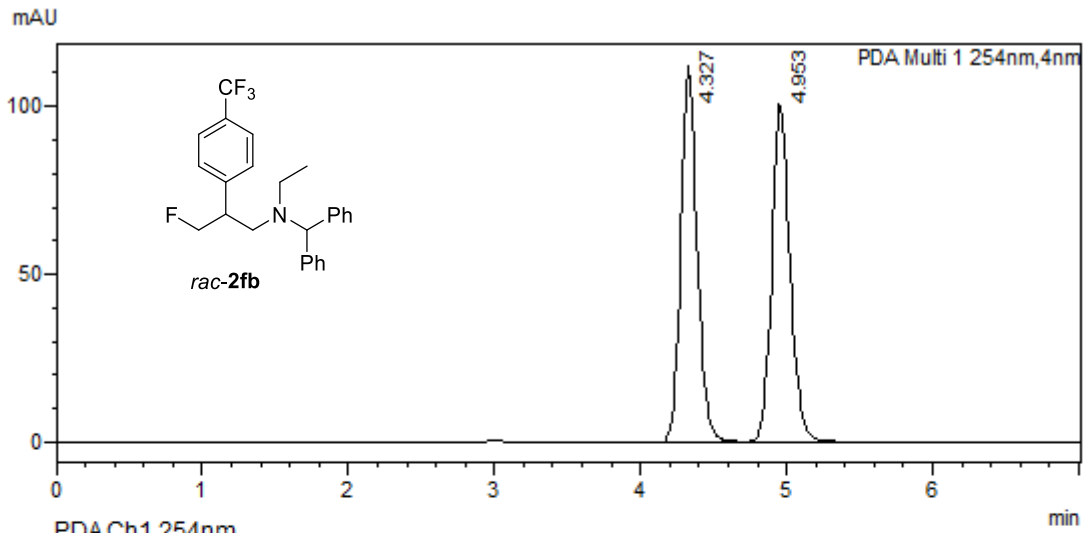
PDA Ch1 254nm		
Peak#	Ret. Time	Area%
1	5.864	4.817
2	6.514	95.183



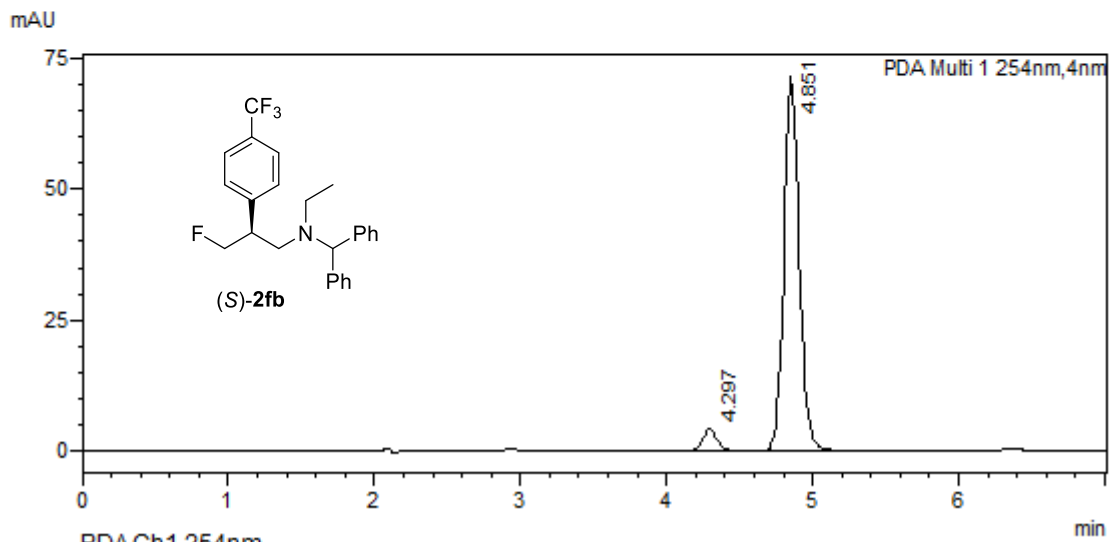
Peak#	Ret. Time	Area%
1	3.742	50.579
2	4.443	49.421



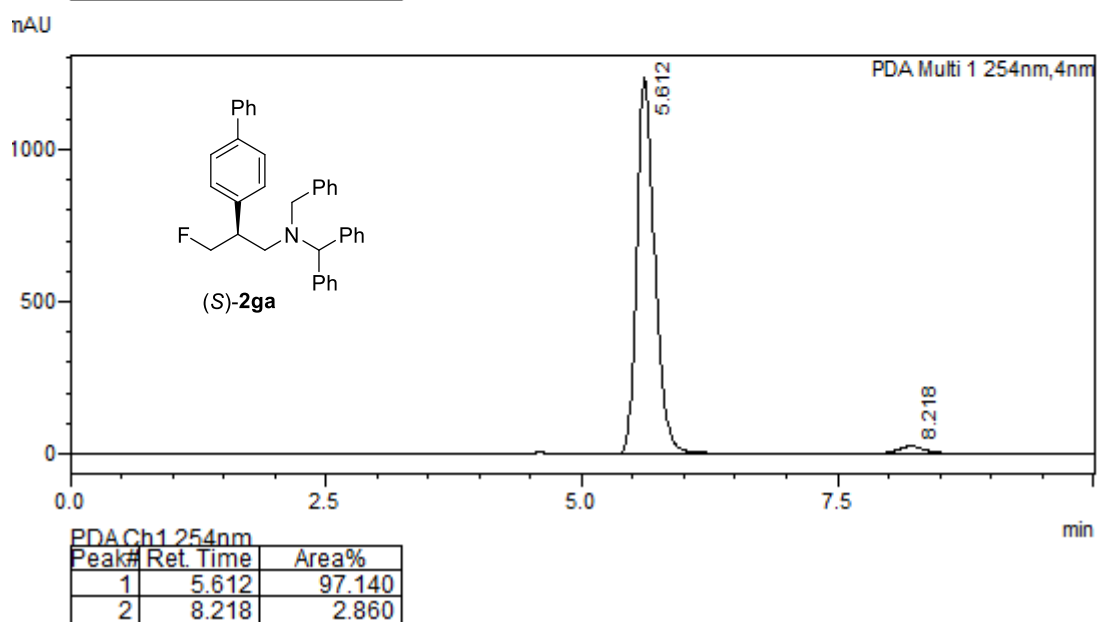
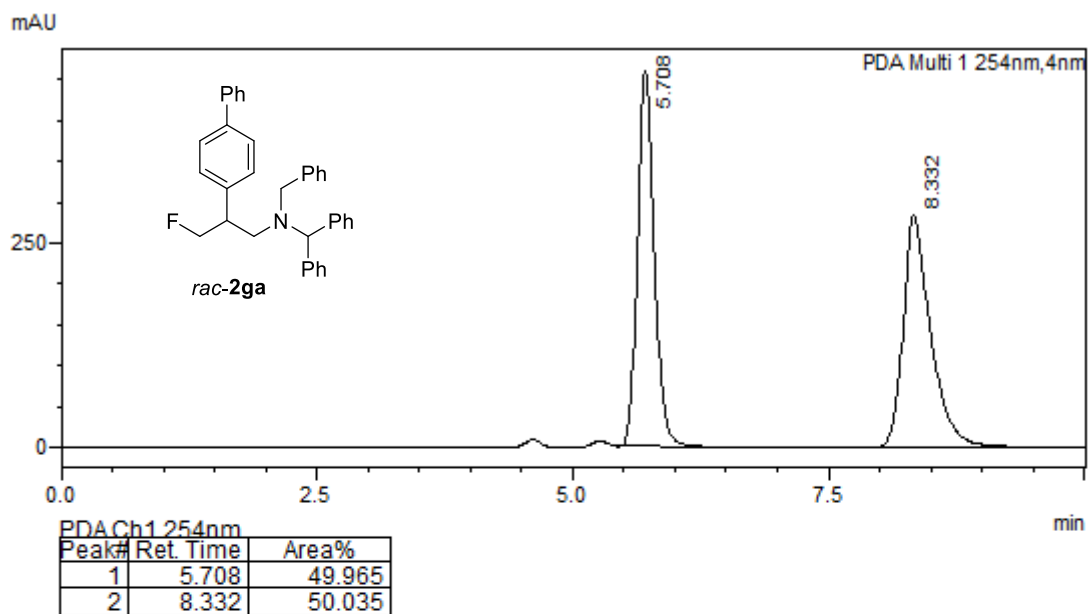
Peak#	Ret. Time	Area%
1	3.541	5.085
2	4.346	94.915

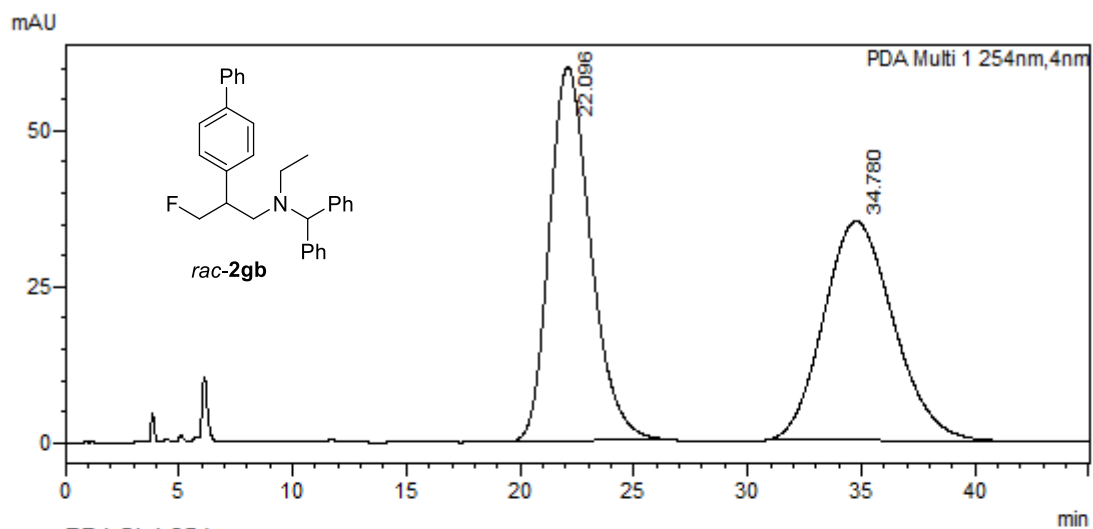


PDA Ch1 254nm		
Peak#	Ret. Time	Area%
1	4.327	49.868
2	4.953	50.132



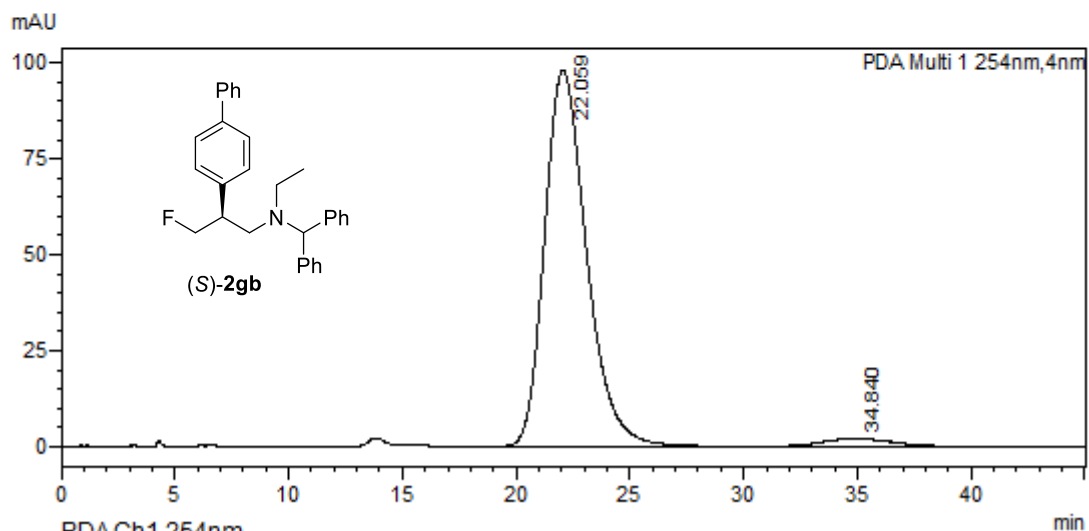
PDA Ch1 254nm		
Peak#	Ret. Time	Area%
1	4.297	4.953
2	4.851	95.047





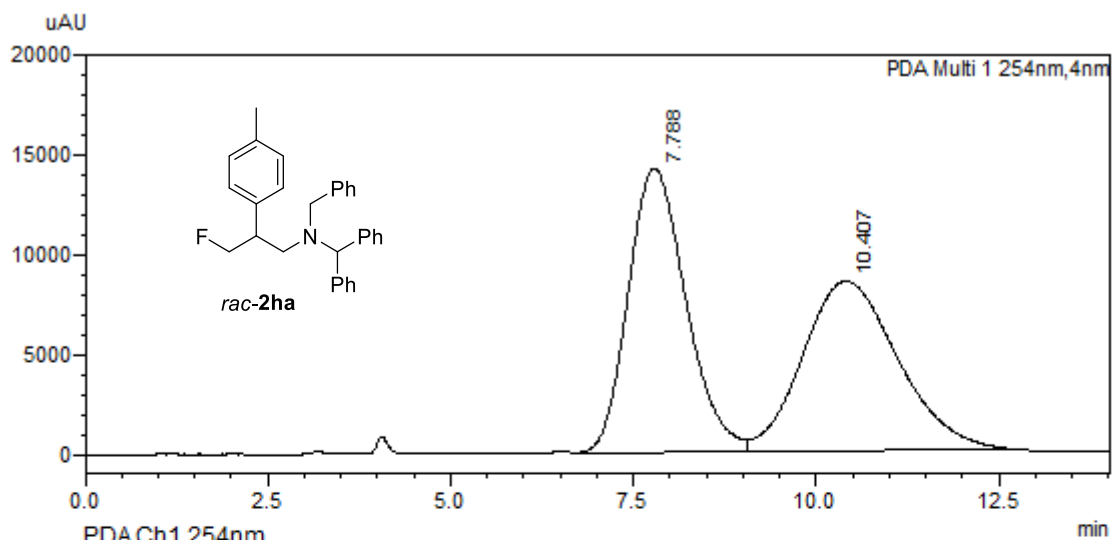
PDA Ch1 254nm

Peak#	Ret. Time	Area%
1	22.096	50.197
2	34.780	49.803



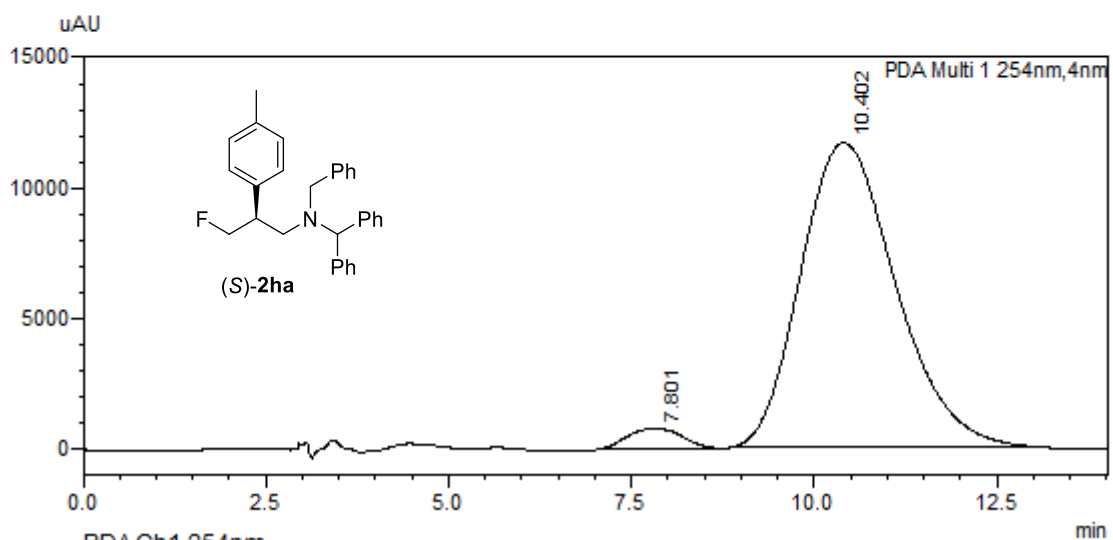
PDA Ch1 254nm

Peak#	Ret. Time	Area%
1	22.059	96.772
2	34.840	3.228



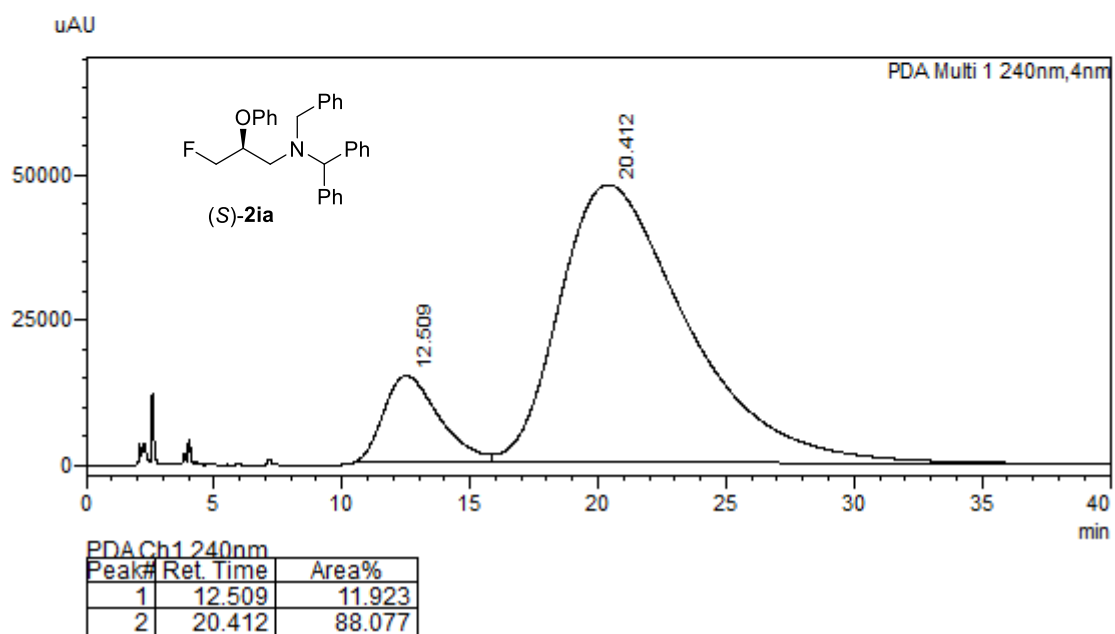
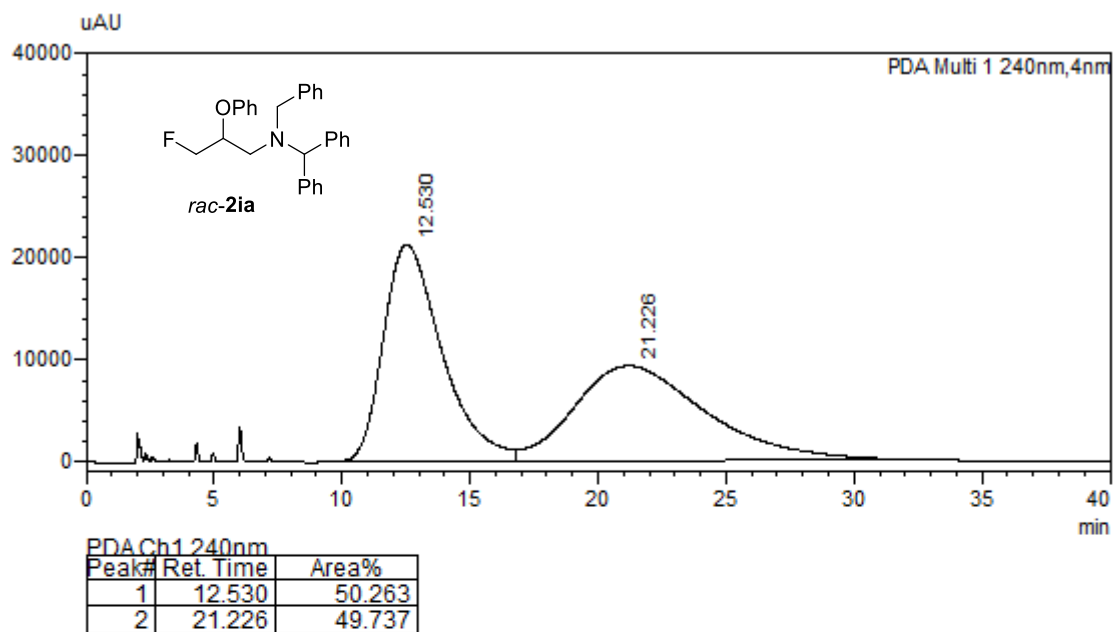
PDA Ch1 254nm

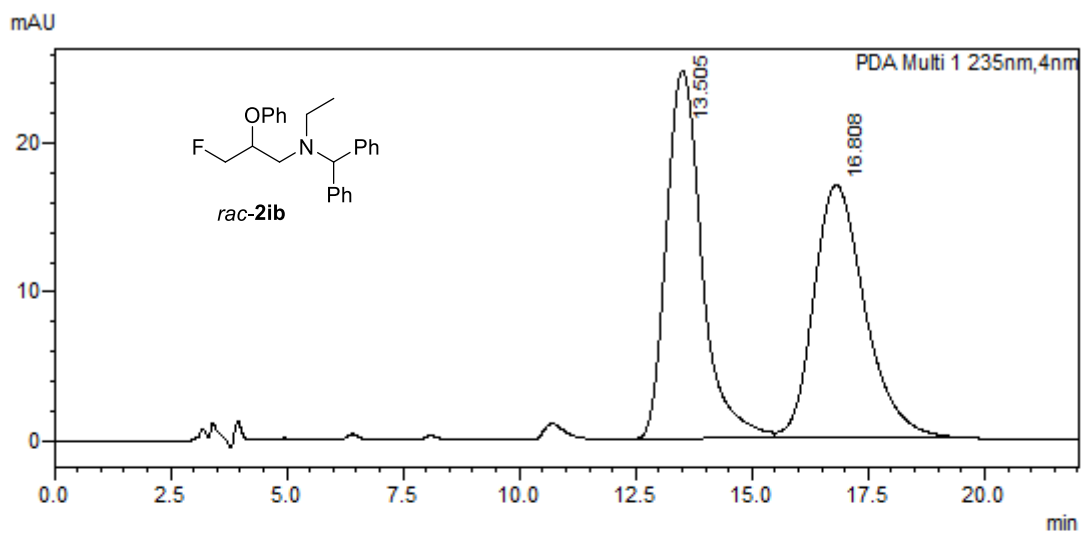
Peak#	Ret. Time	Area%
1	7.788	50.163
2	10.407	49.837



PDA Ch1 254nm

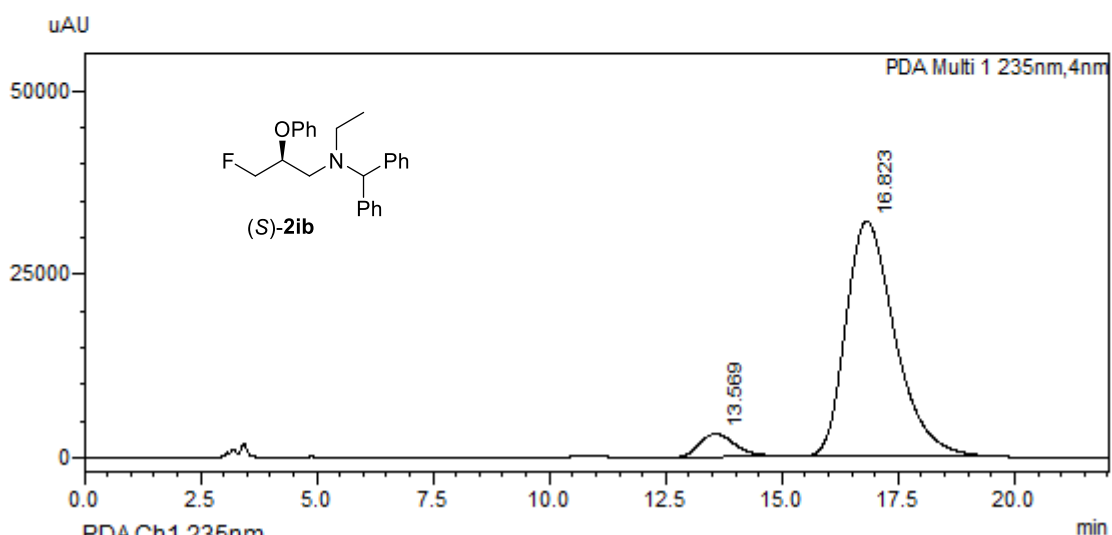
Peak#	Ret. Time	Area%
1	7.801	3.499
2	10.402	96.501





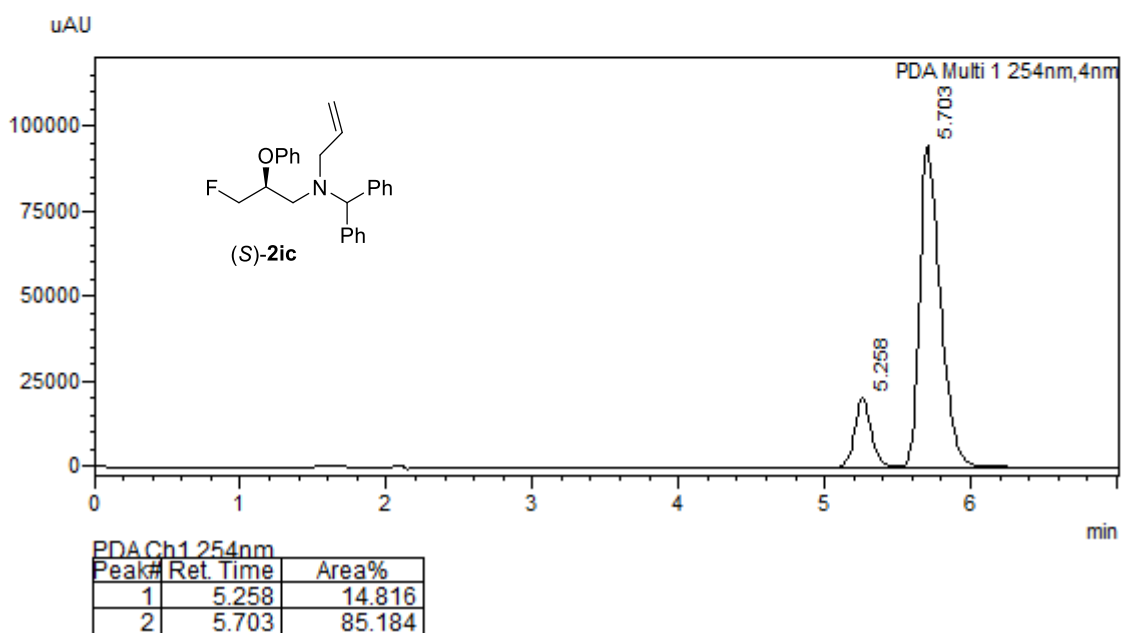
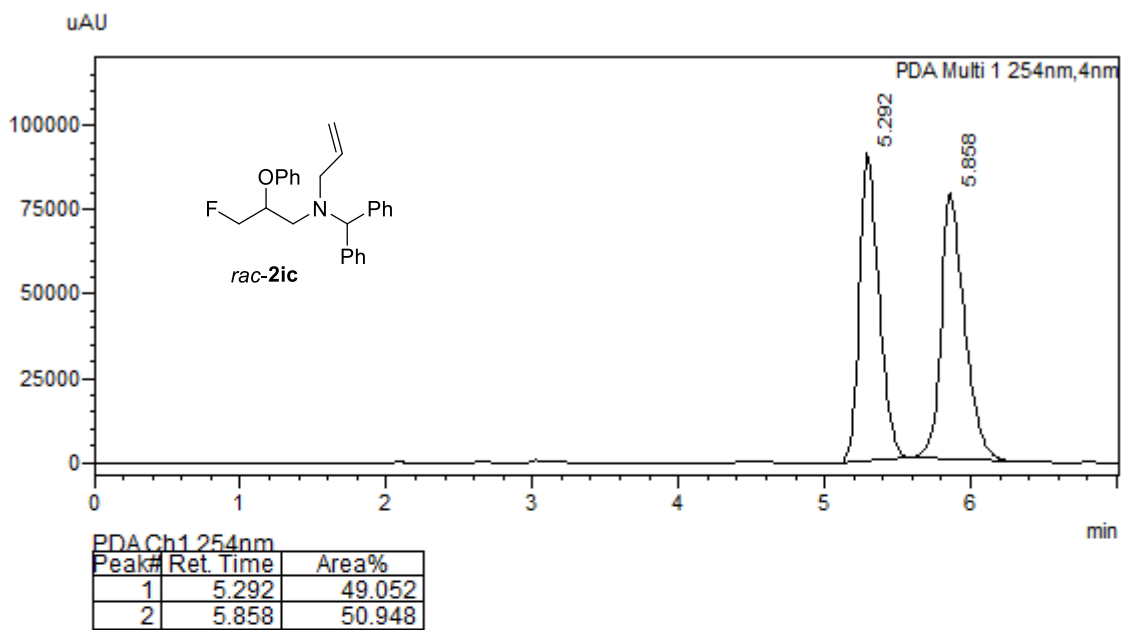
PDA Ch1 235nm

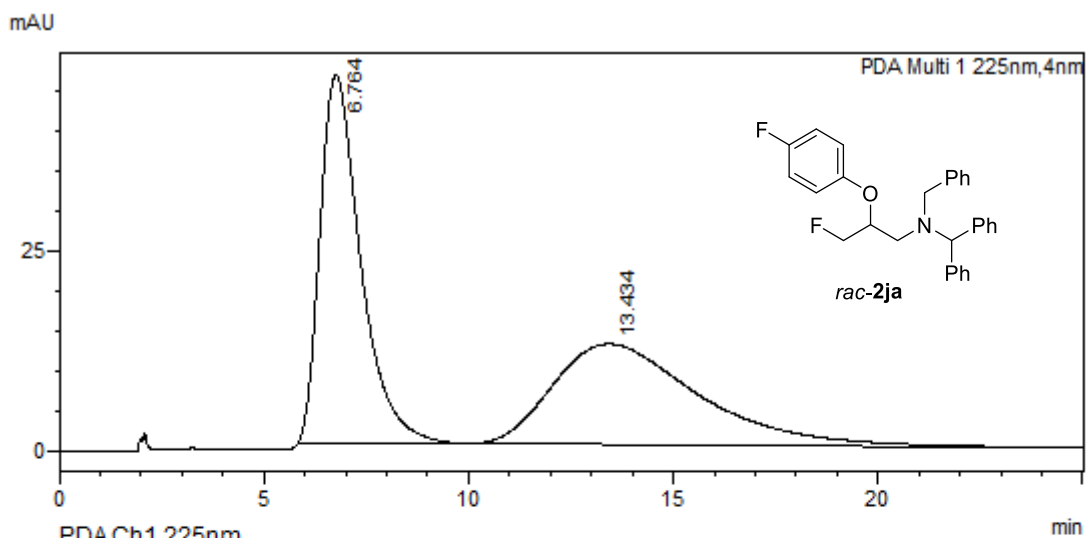
Peak#	Ret. Time	Area%
1	13.505	50.242
2	16.808	49.758



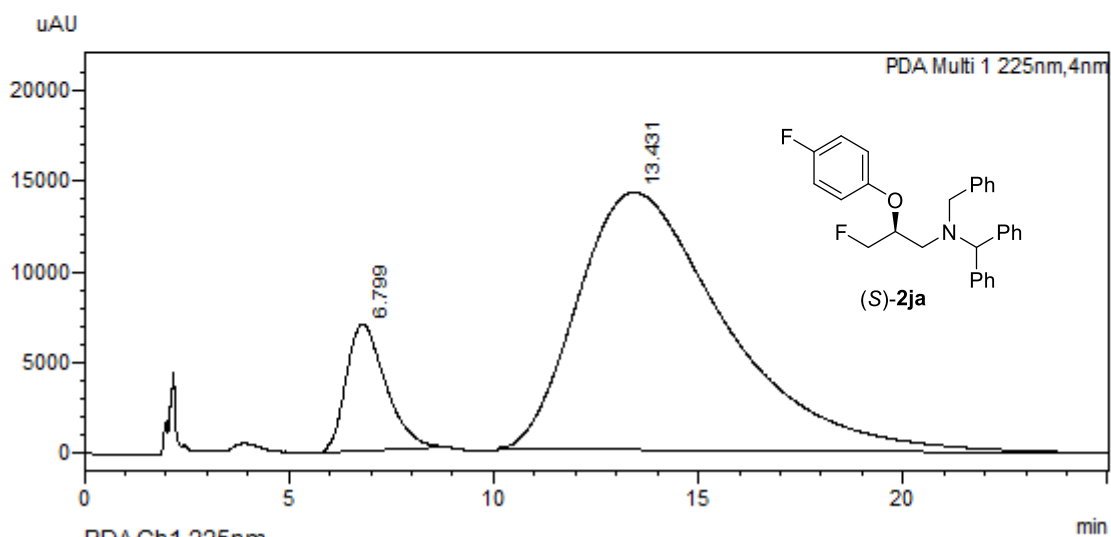
PDA Ch1 235nm

Peak#	Ret. Time	Area%
1	13.569	6.534
2	16.823	93.466

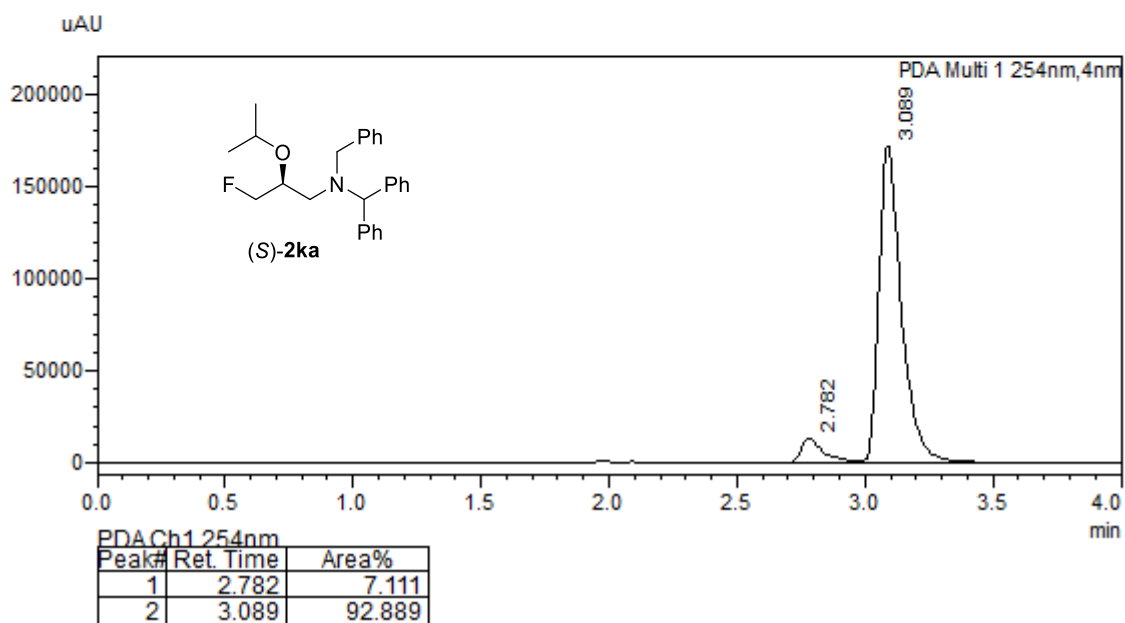
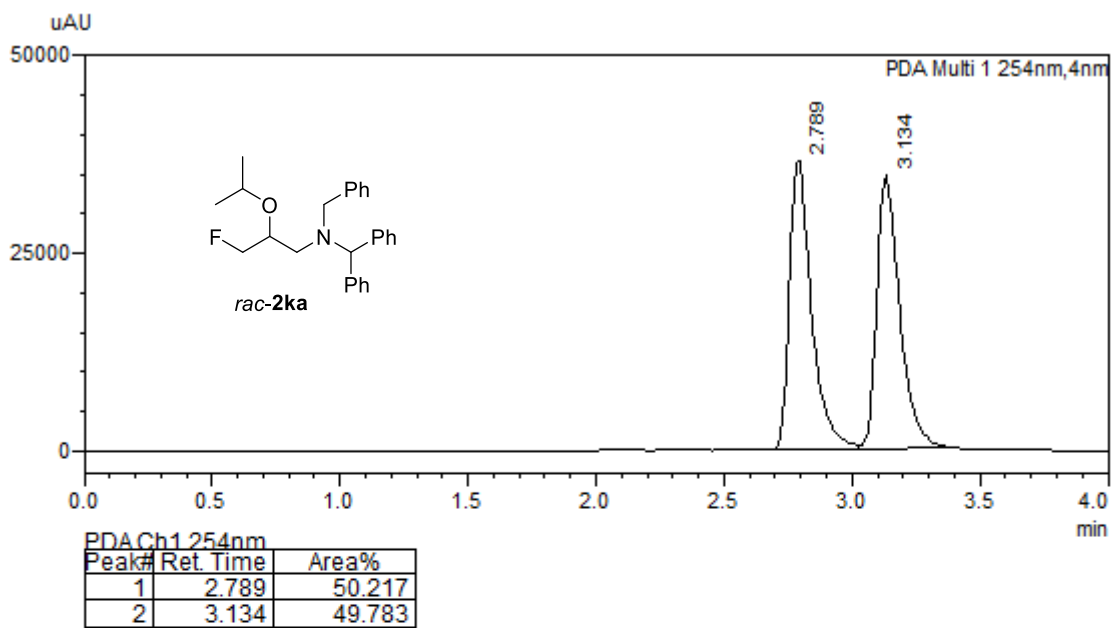


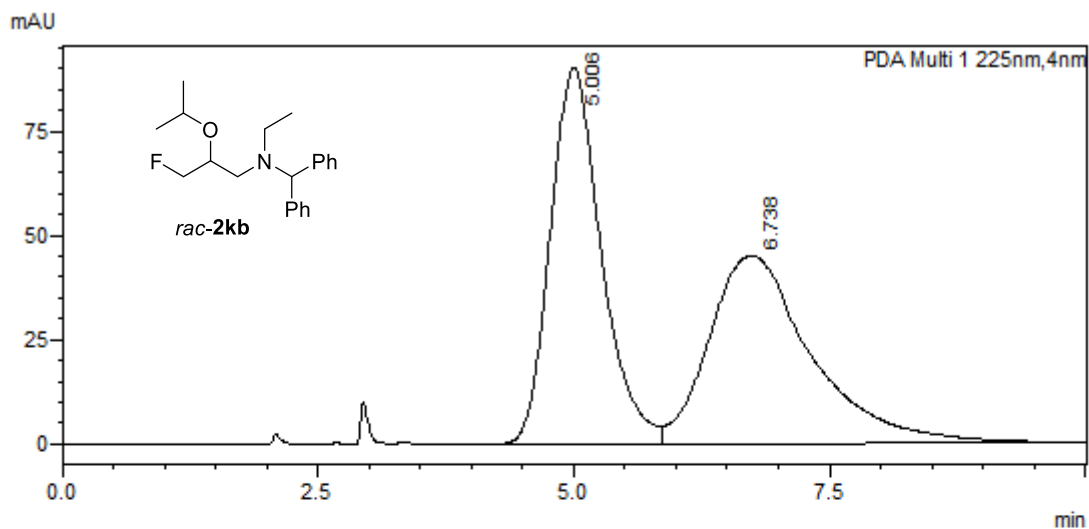


PDA Ch1 225nm		
Peak#	Ret. Time	Area%
1	6.764	50.810
2	13.434	49.190

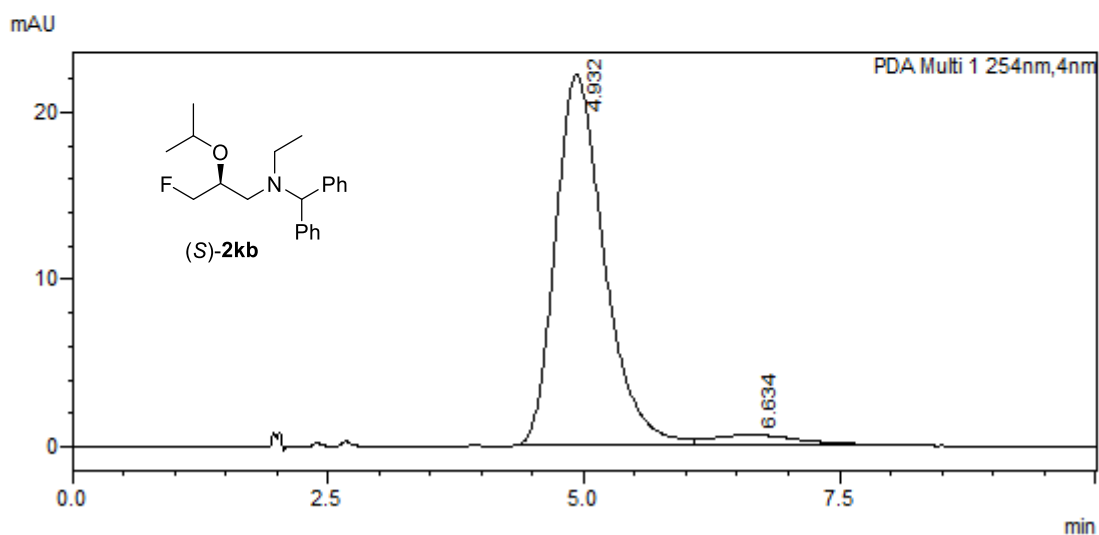


PDA Ch1 225nm		
Peak#	Ret. Time	Area%
1	6.799	11.836
2	13.431	88.164

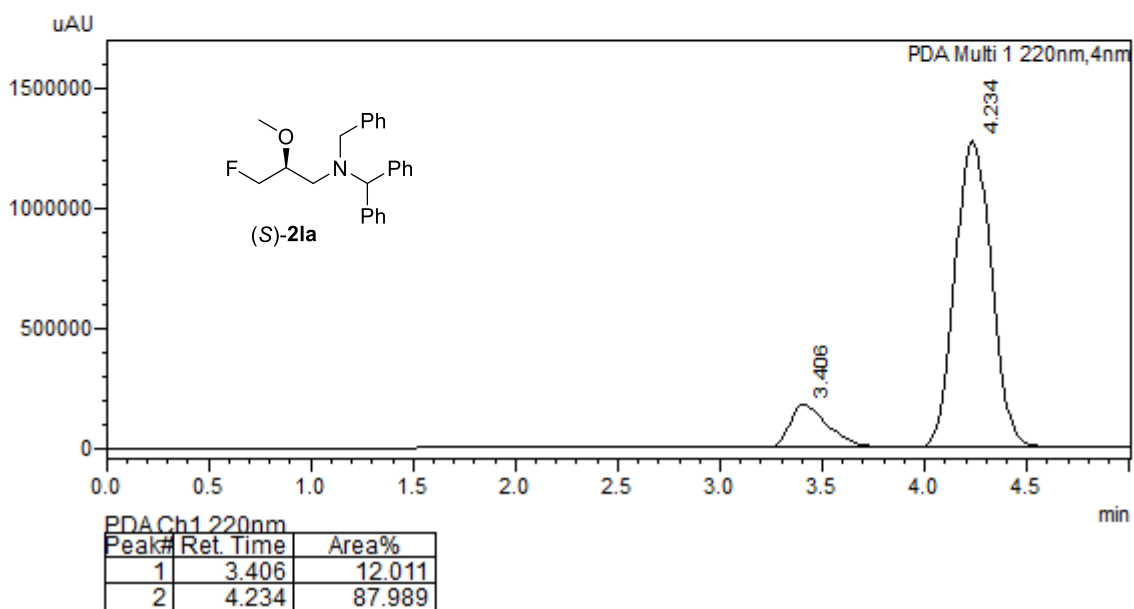
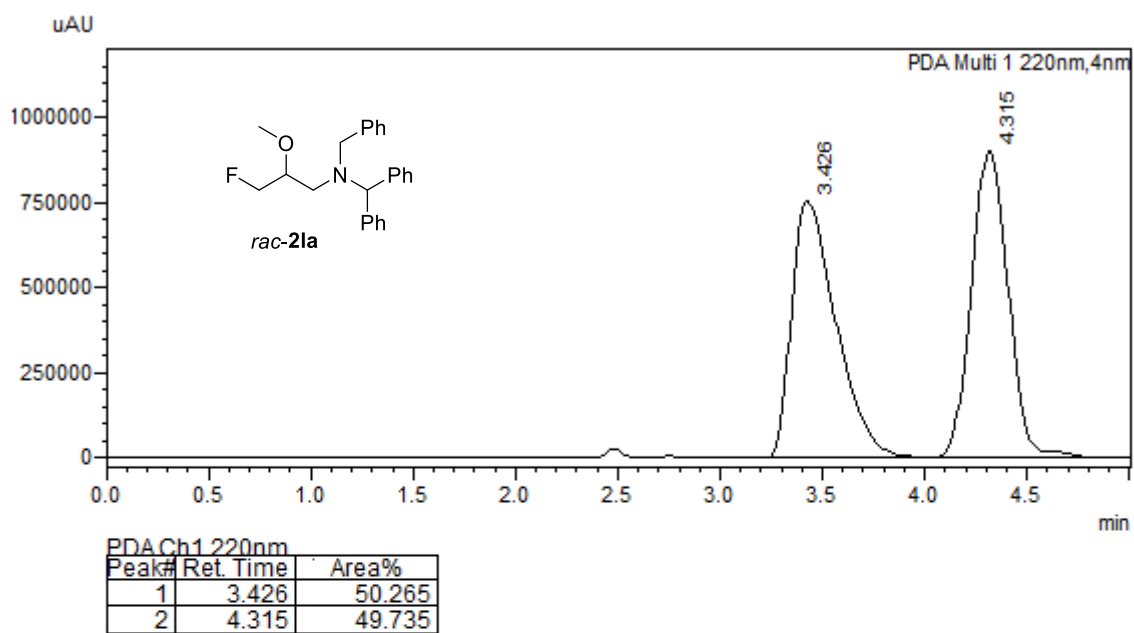


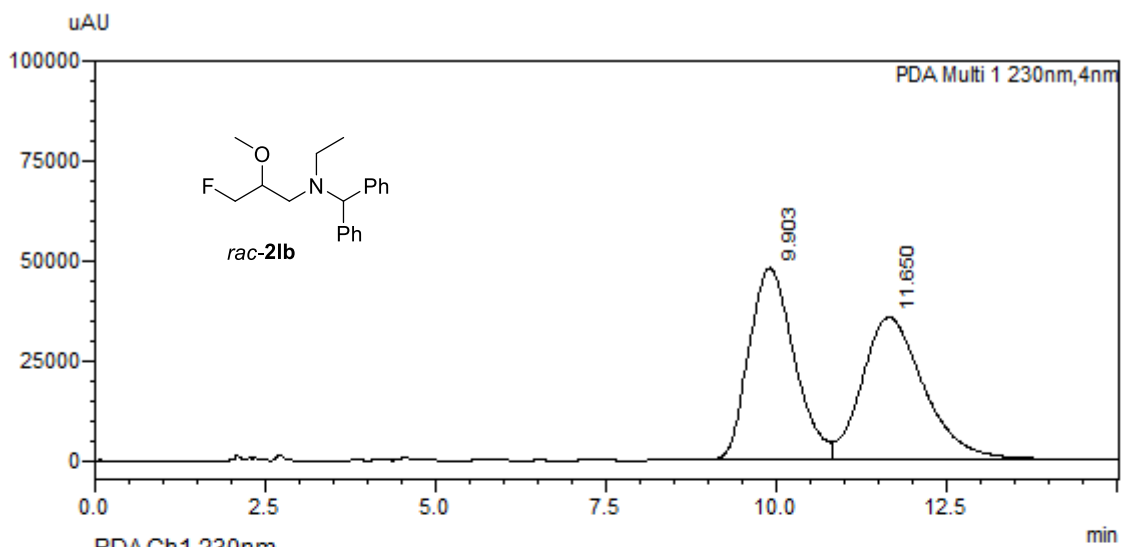


PDA Ch1 225nm		
Peak#	Ret. Time	Area%
1	5.006	49.962
2	6.738	50.038



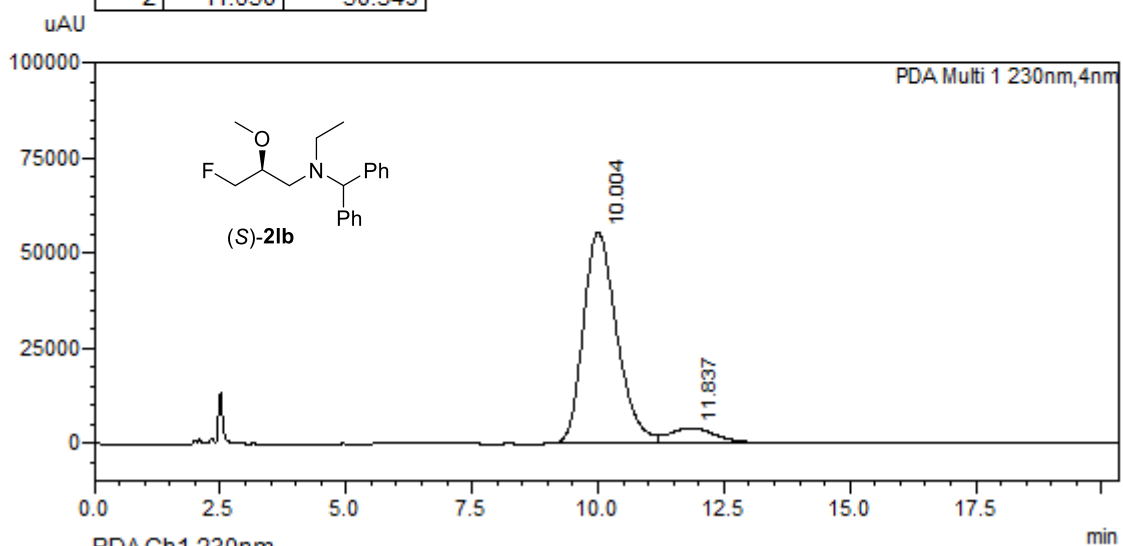
PDA Ch1 254nm		
Peak#	Ret. Time	Area%
1	4.932	94.796
2	6.634	5.204





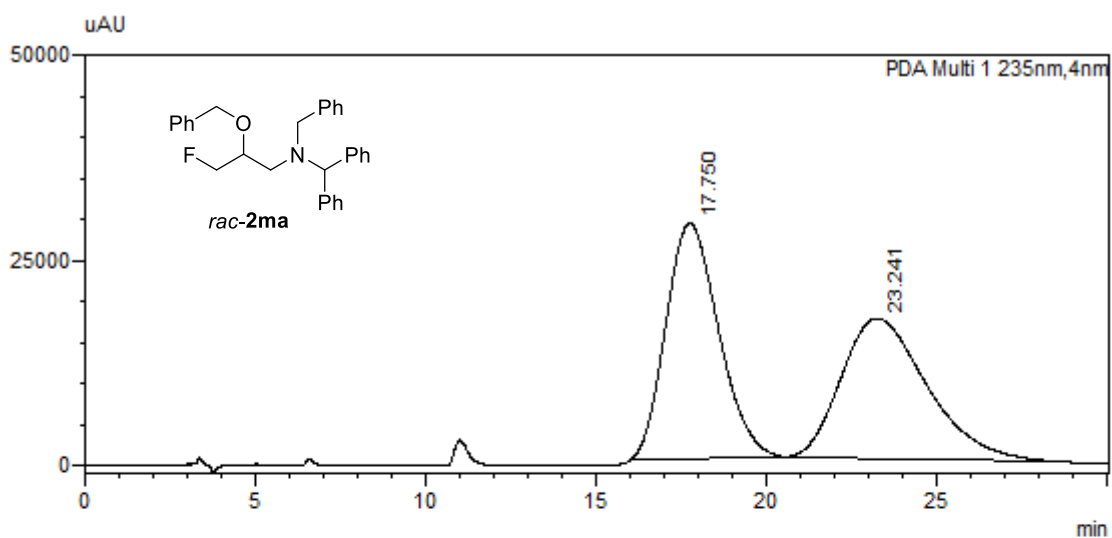
PDA Ch1 230nm

Peak#	Ret. Time	Area%
1	9.903	49.651
2	11.650	50.349



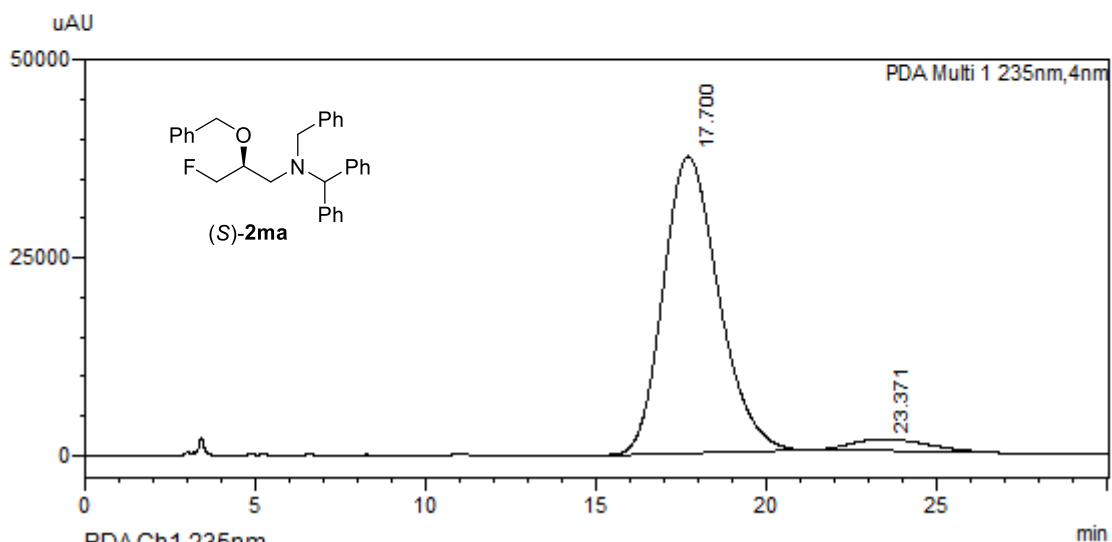
PDA Ch1 230nm

Peak#	Ret. Time	Area%
1	10.004	90.756
2	11.837	9.244



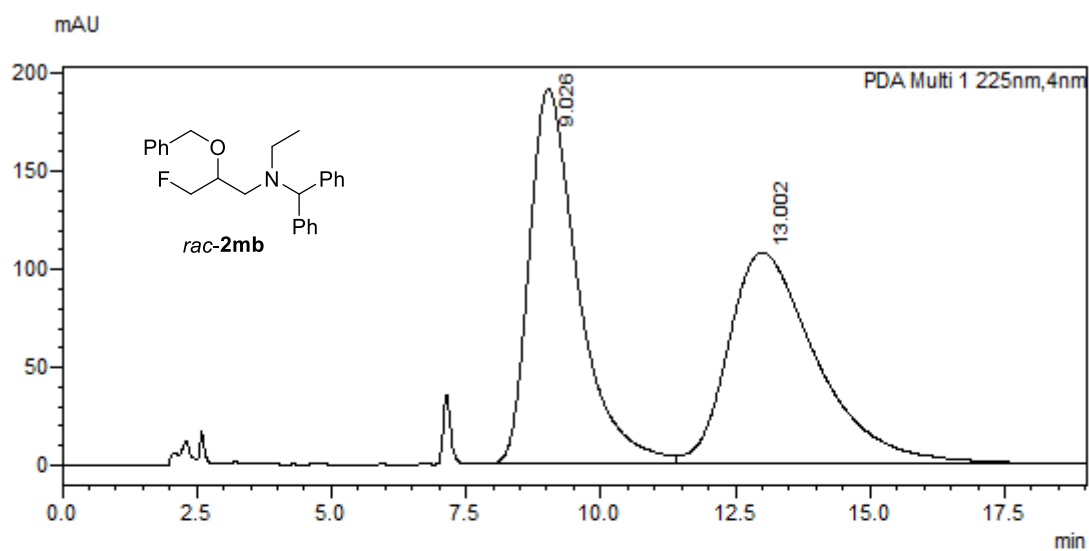
PDA Ch1 235nm

Peak#	Ret. Time	Area%
1	17.750	50.853
2	23.241	49.147

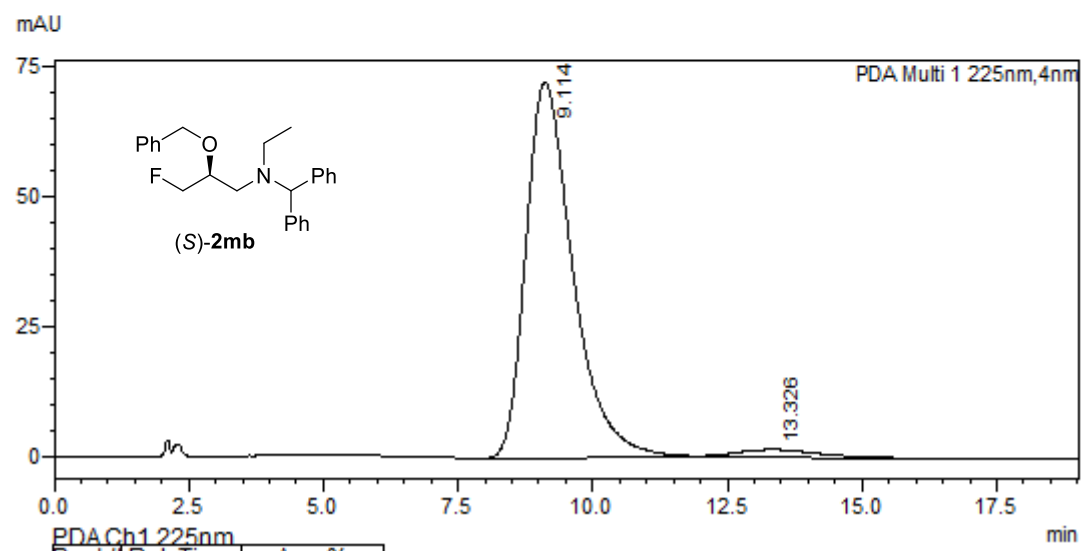


PDA Ch1 235nm

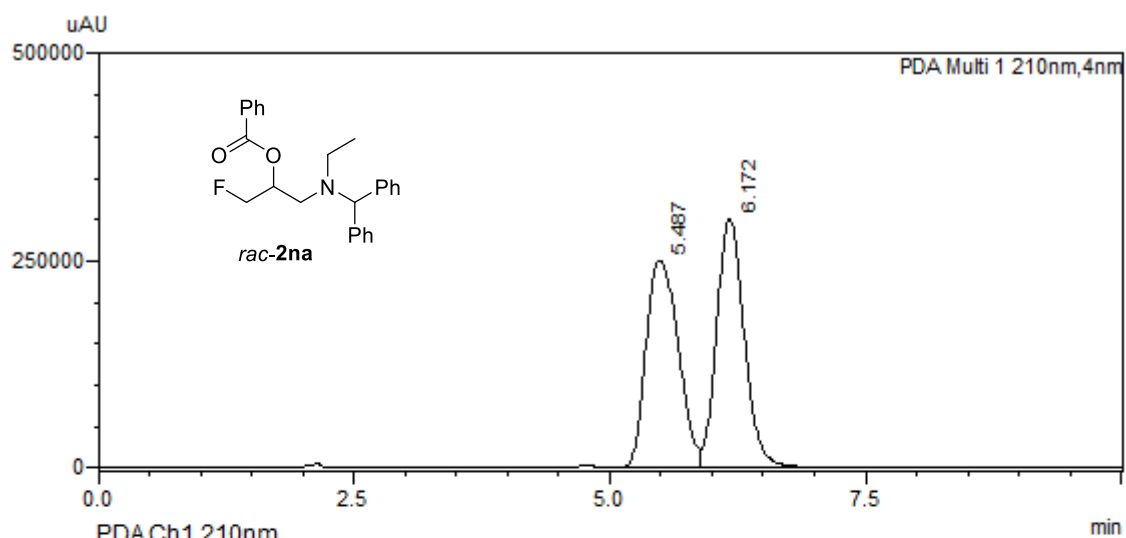
Peak#	Ret. Time	Area%
1	17.700	95.271
2	23.371	4.729



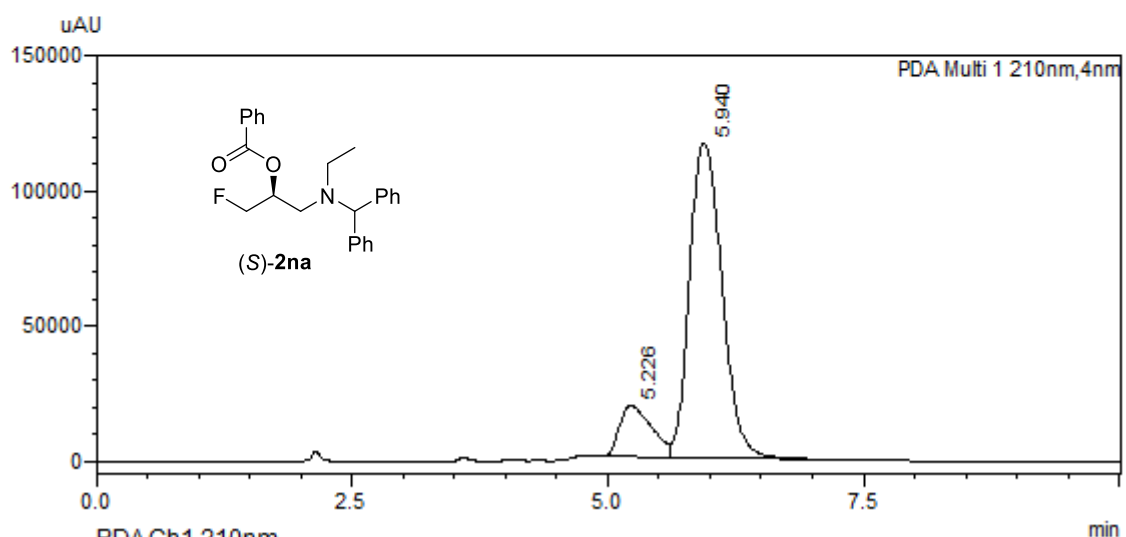
PDA Ch1 225nm		
Peak#	Ret. Time	Area%
1	9.026	49.371
2	13.002	50.629



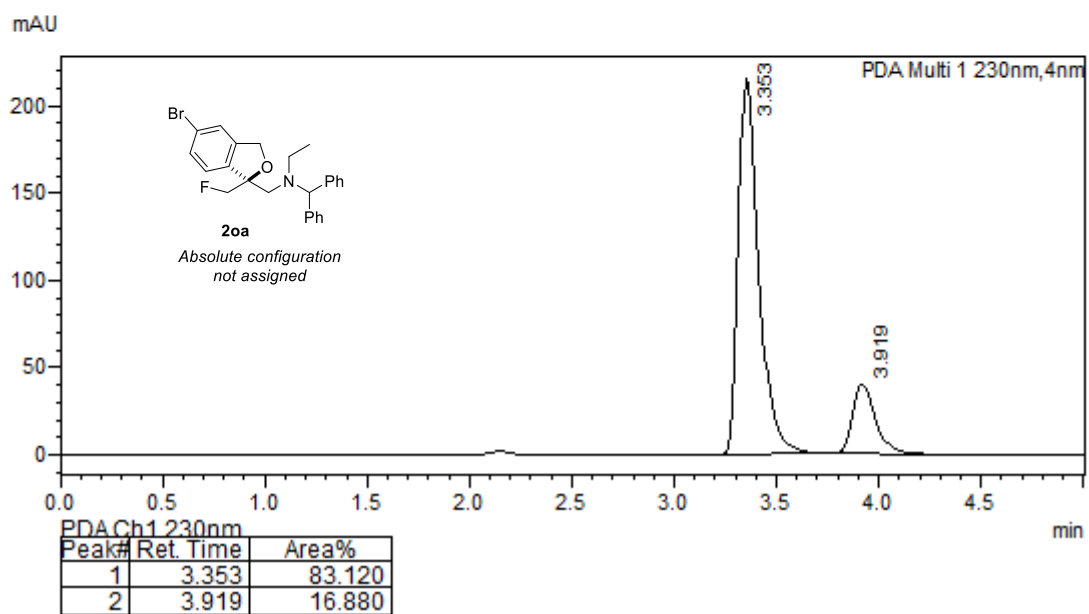
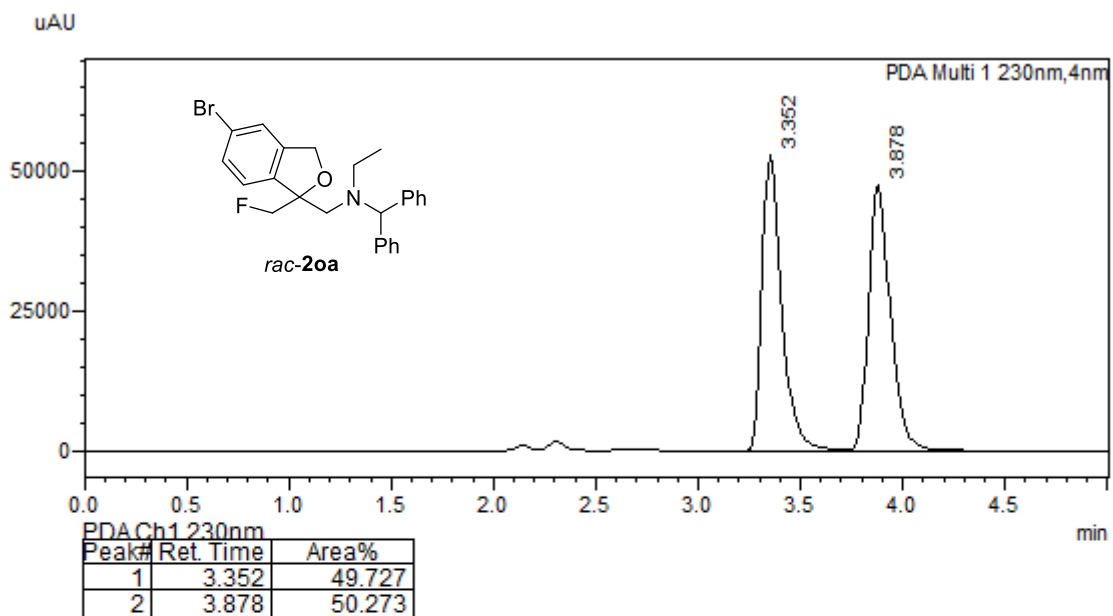
PDA Ch1 225nm		
Peak#	Ret. Time	Area%
1	9.114	96.998
2	13.326	3.002

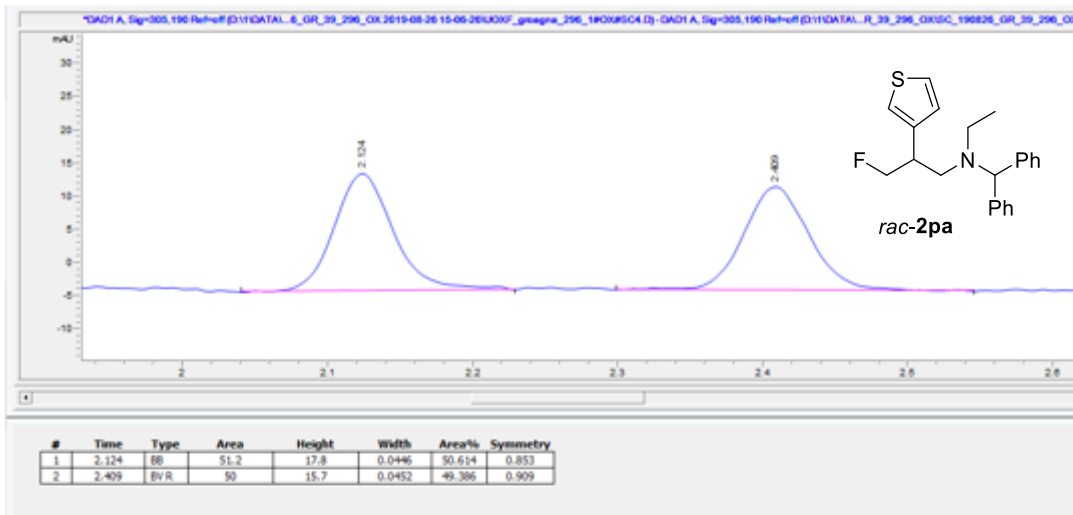


Peak#	Ret. Time	Area%
1	5.487	49.268
2	6.172	50.732



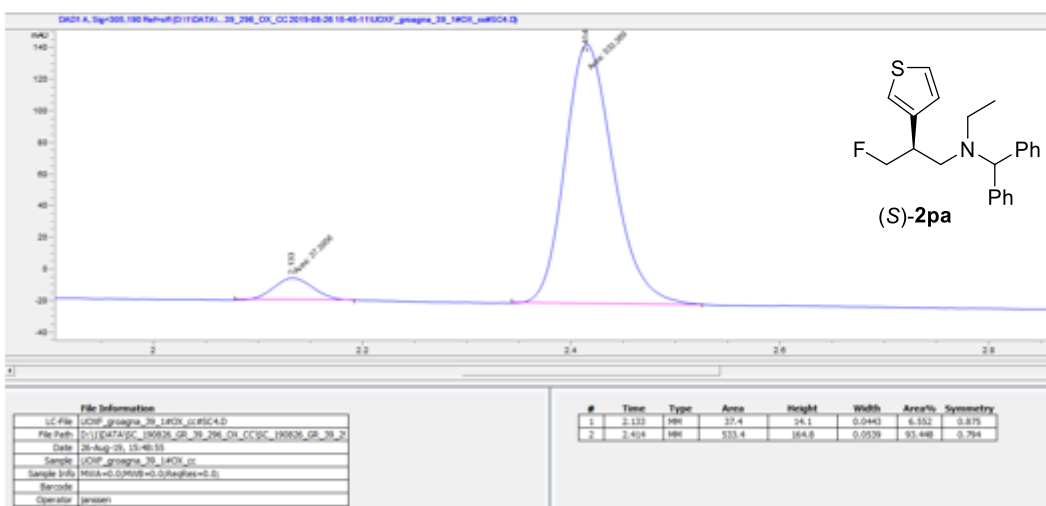
Peak#	Ret. Time	Area%
1	5.226	13.723
2	5.940	86.277





Peak #	RetTime [min]	Type	Width [min]	Area [mAU*s]	Height [mAU]	Area %
1	2.124	BB	0.0446	51.24637	17.79112	50.6135
2	2.409	BV R	0.0452	50.00393	15.66250	49.3865

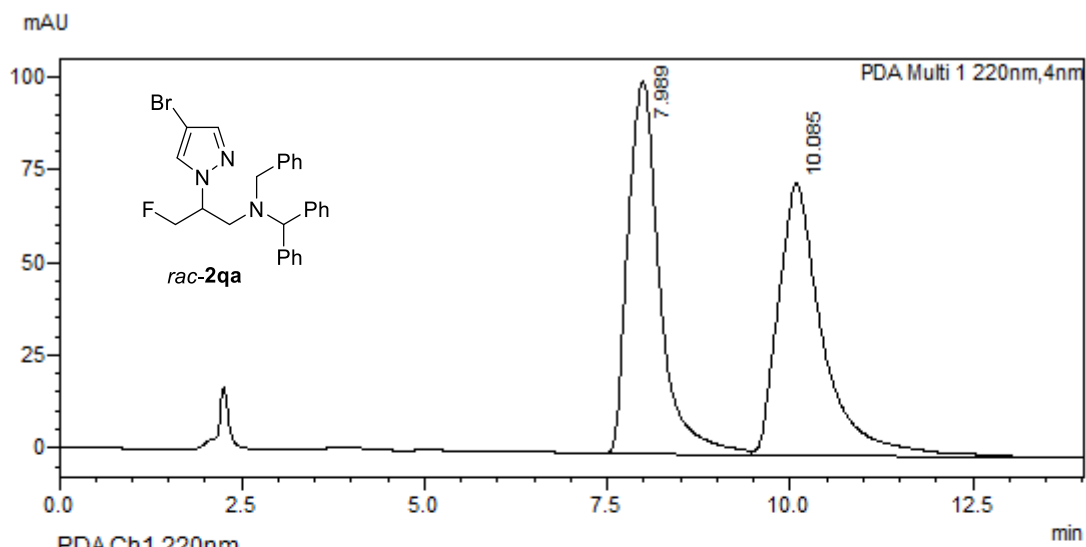
Totals : 101.25030 33.45362



Signal 1: DAD1 A, Sig=305,190 Ref=off

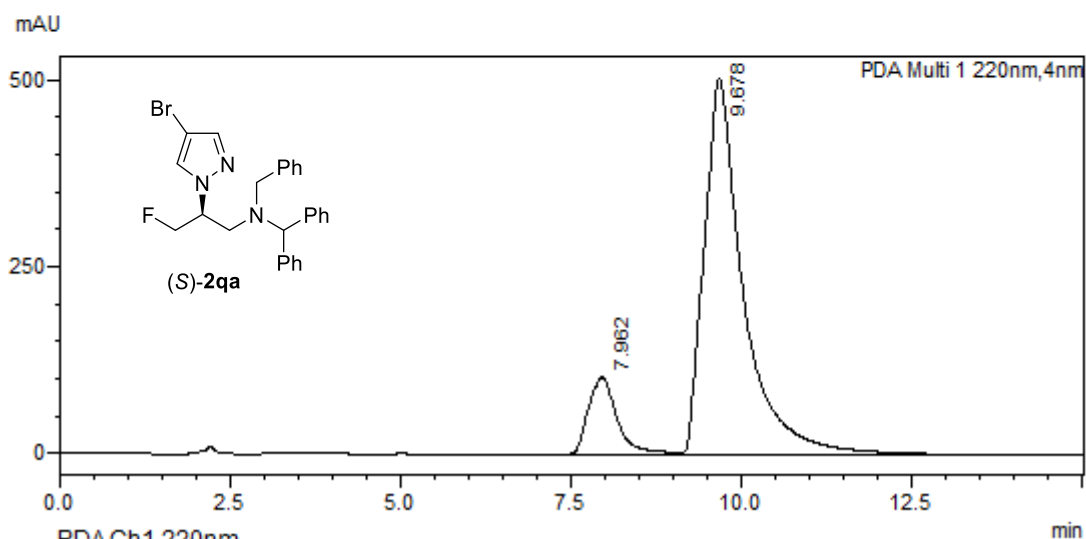
Peak #	RetTime [min]	Type	Width [min]	Area [mAU*s]	Height [mAU]	Area %
1	2.133	MM	0.0443	37.39555	14.07308	6.5516
2	2.414	MM	0.0539	533.38910	164.82869	93.4484

Totals : 570.78465 178.90177



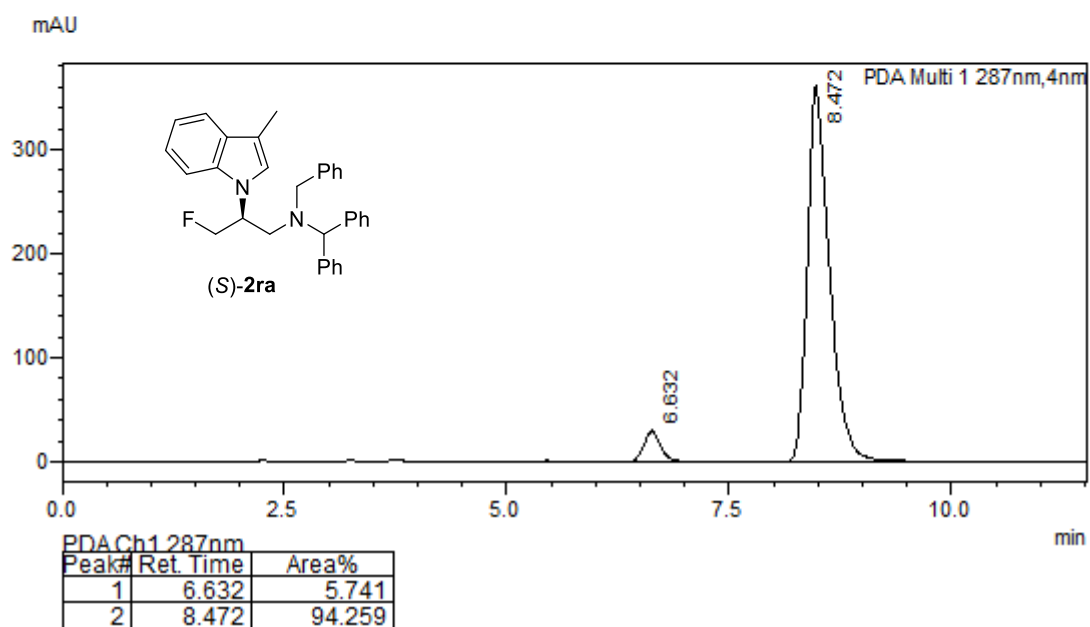
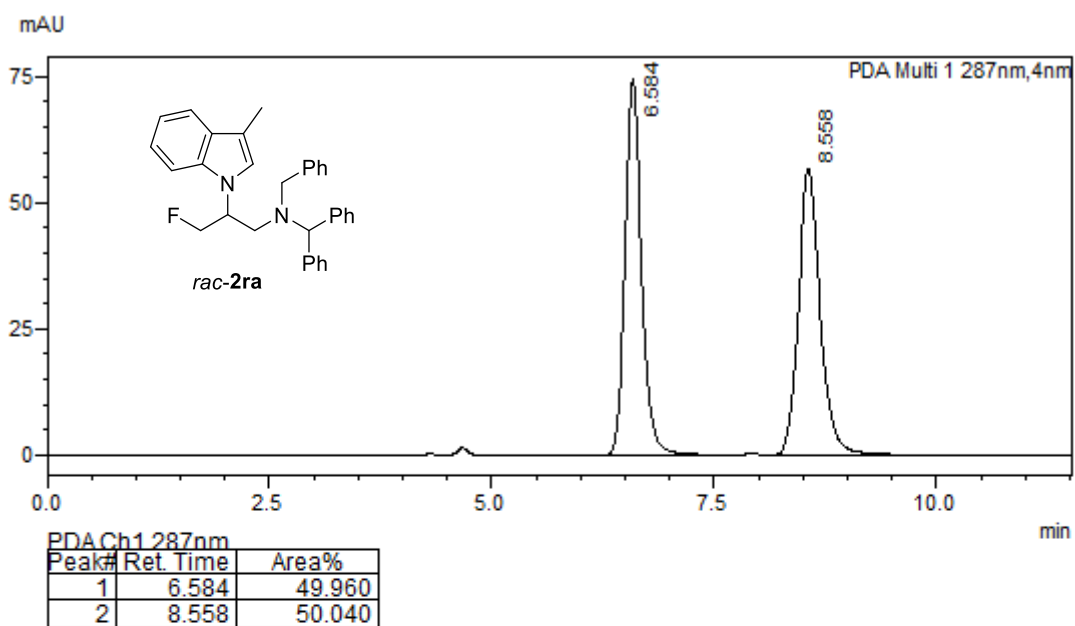
PDA Ch1 220nm

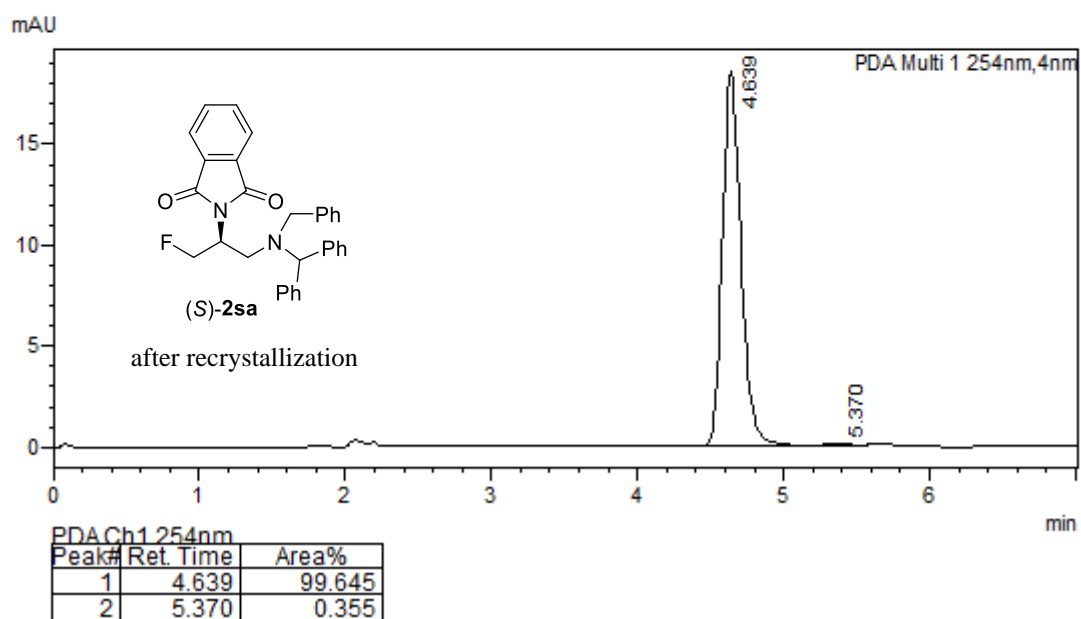
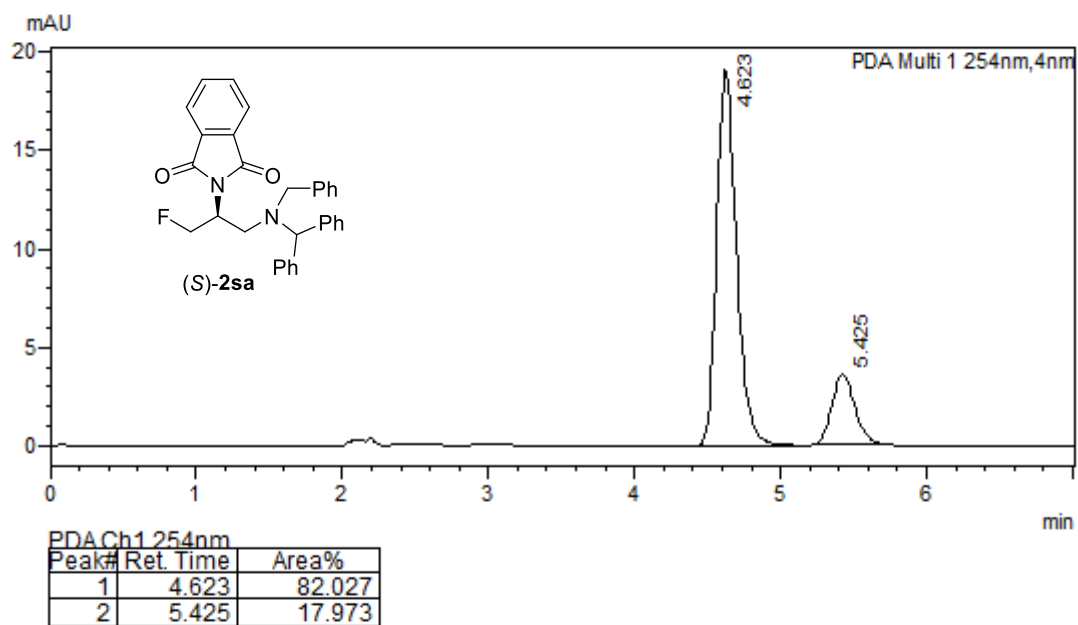
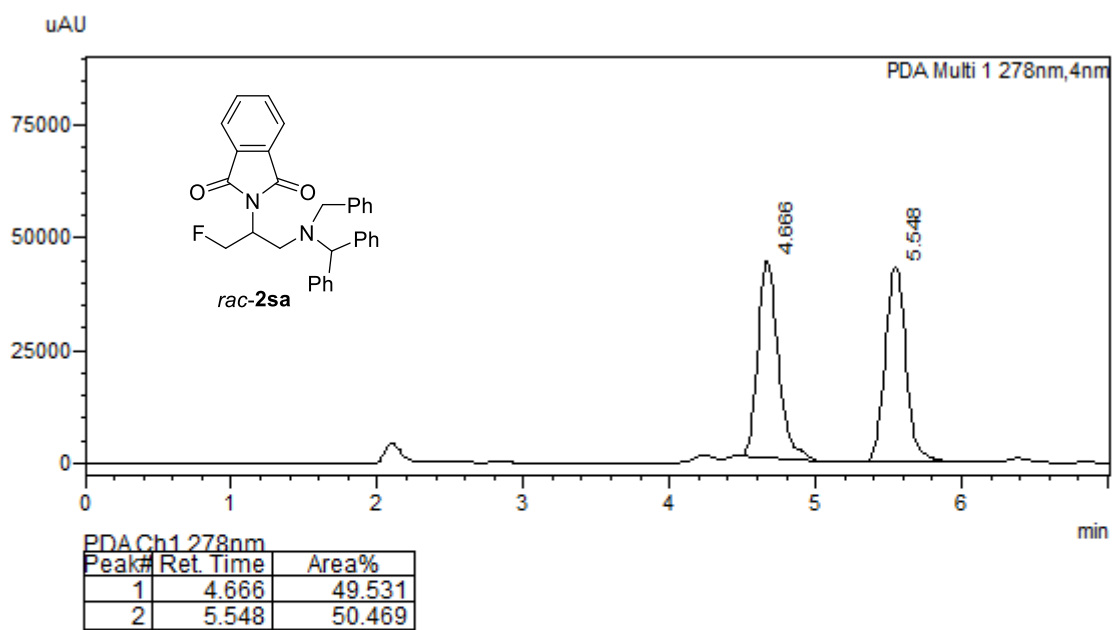
Peak#	Ret. Time	Area%
1	7.989	49.595
2	10.085	50.405

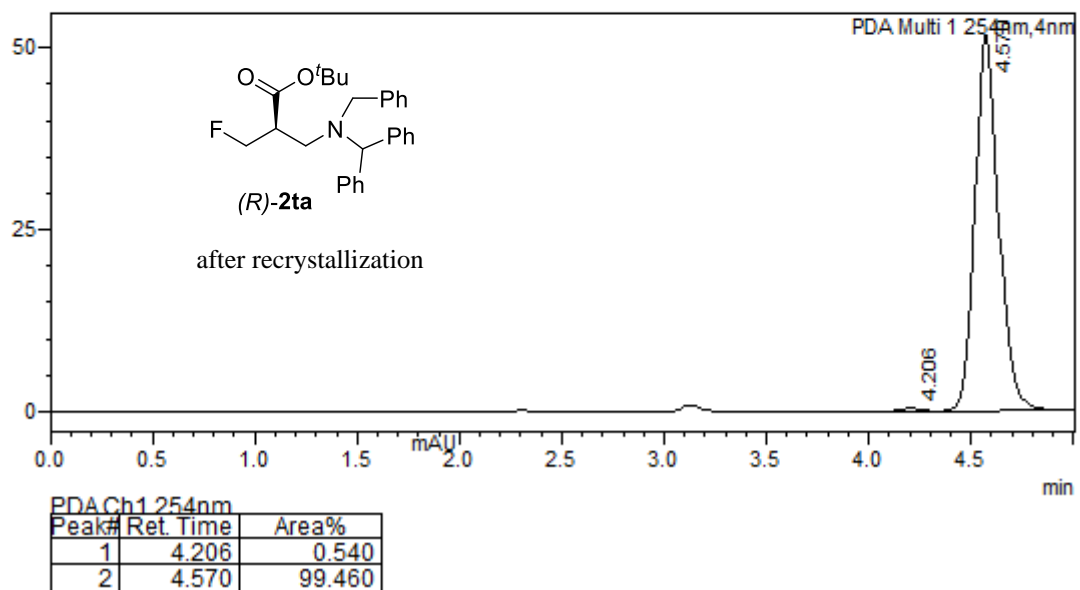
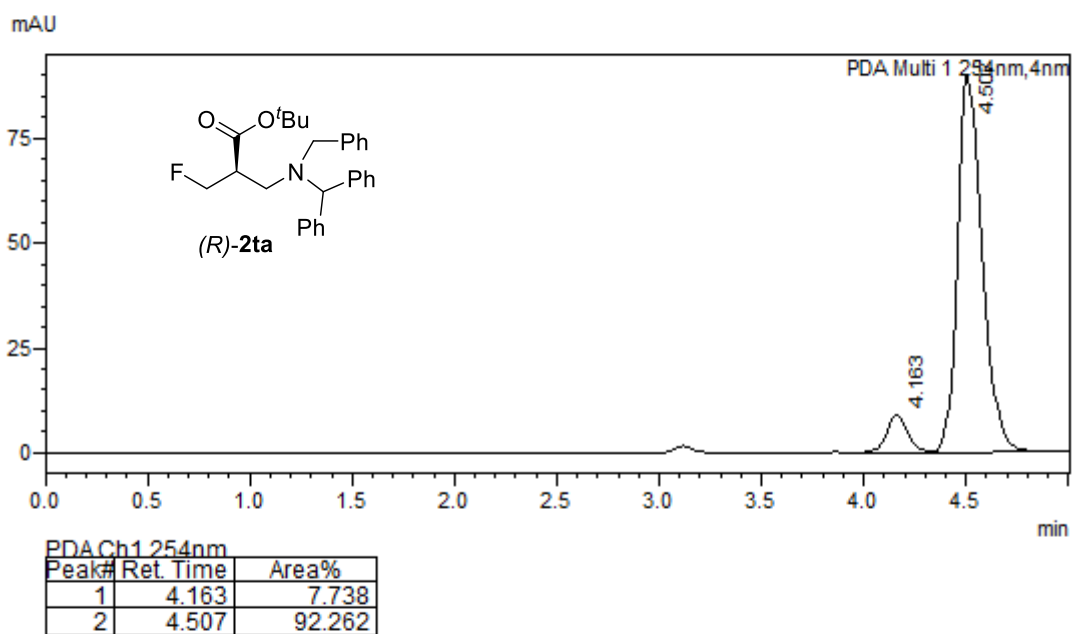
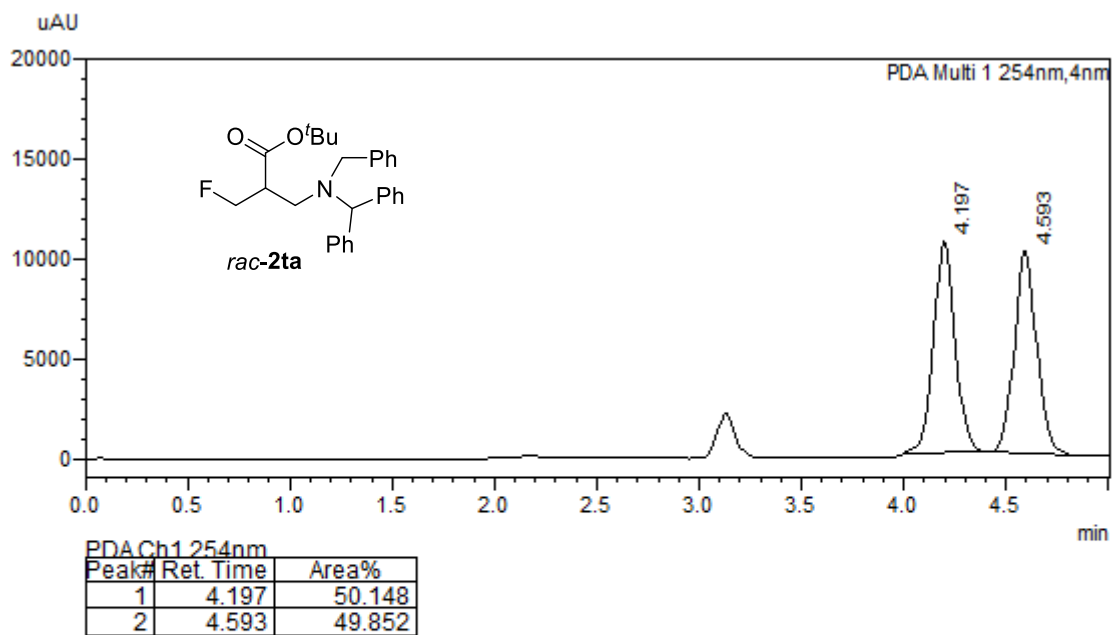


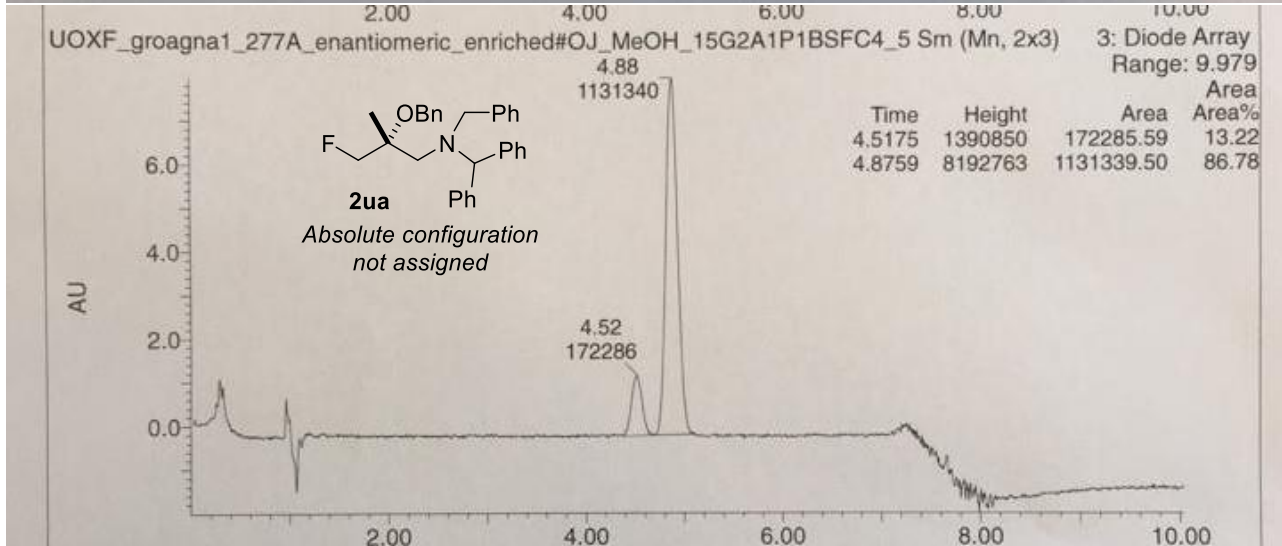
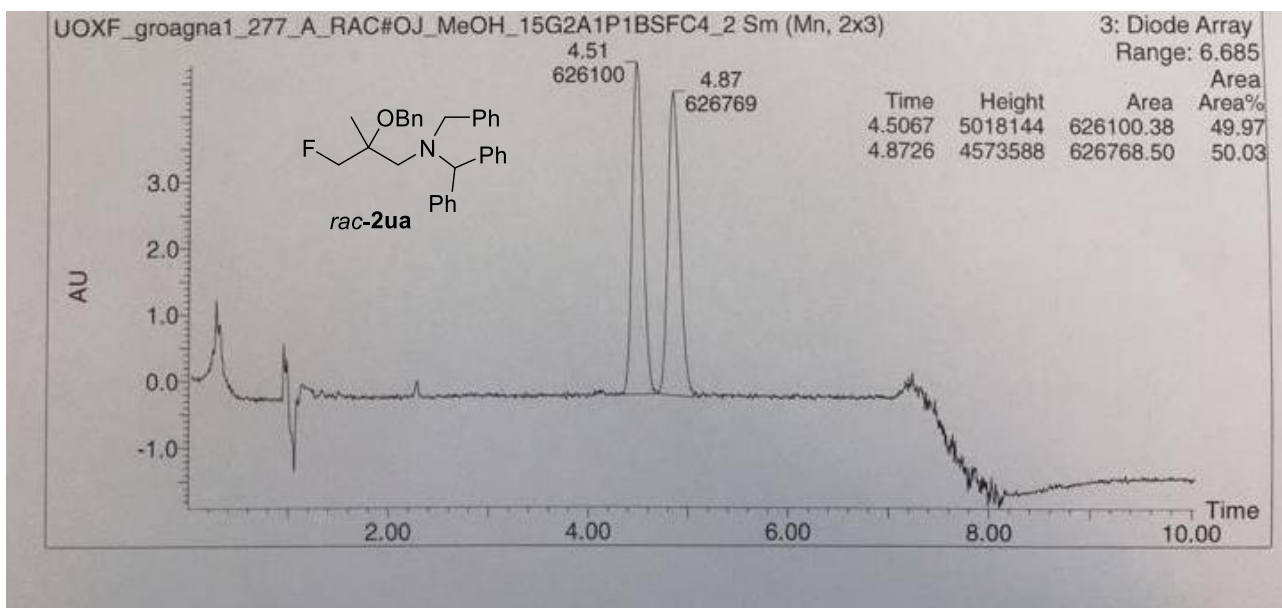
PDA Ch1 220nm

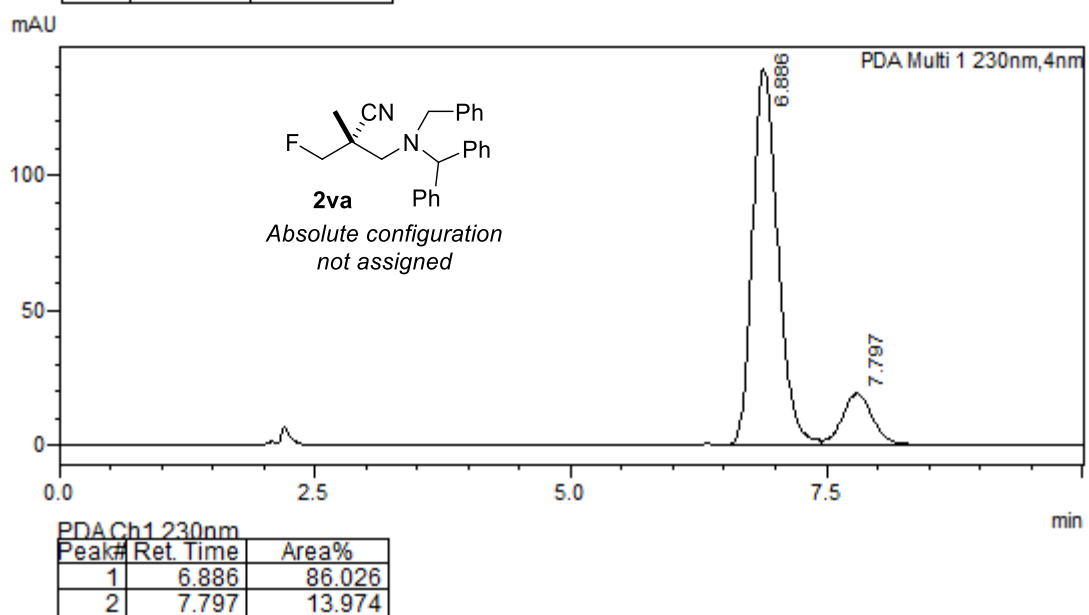
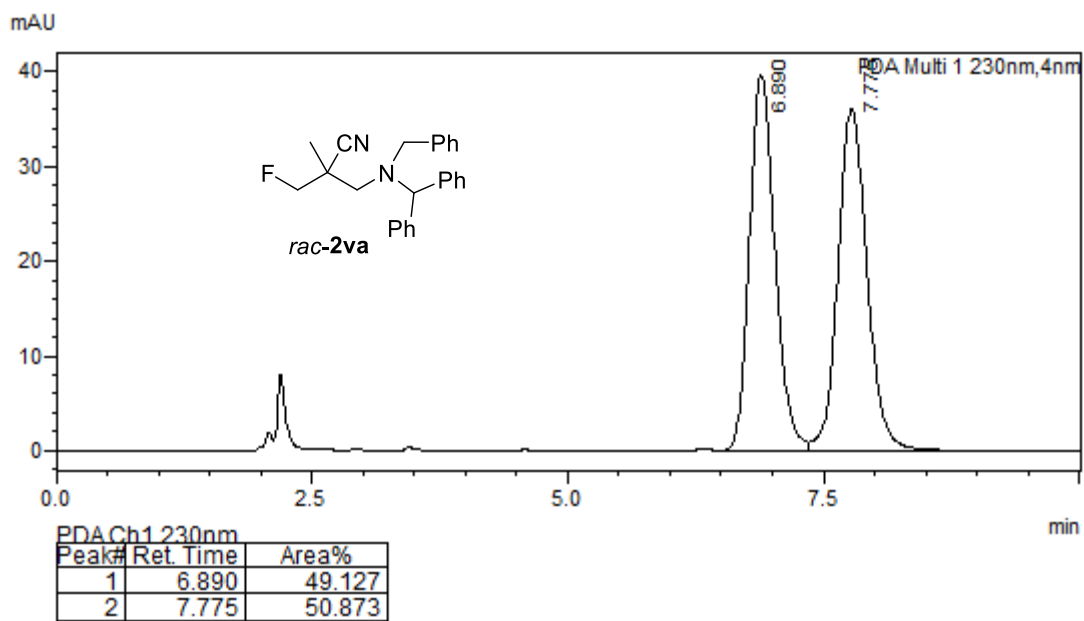
Peak#	Ret. Time	Area%
1	7.962	13.106
2	9.678	86.894

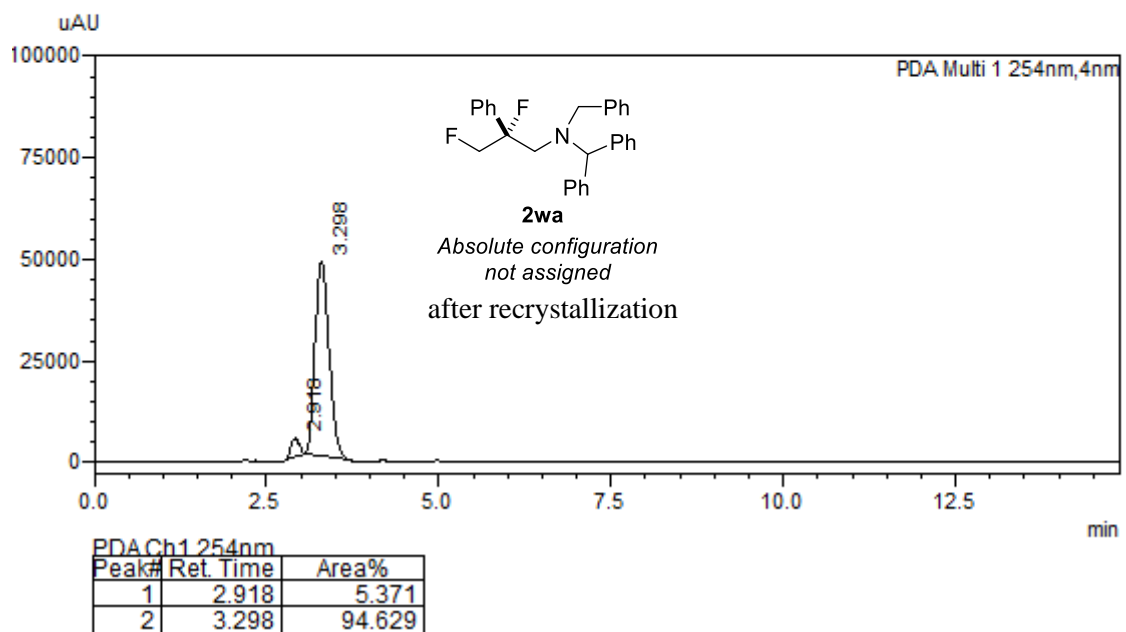
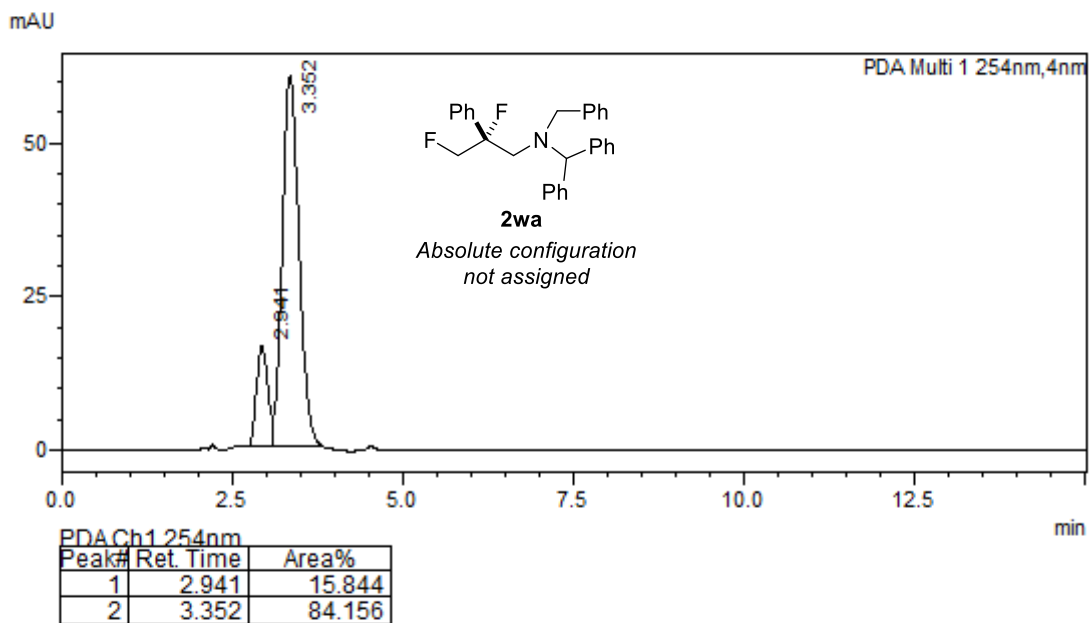
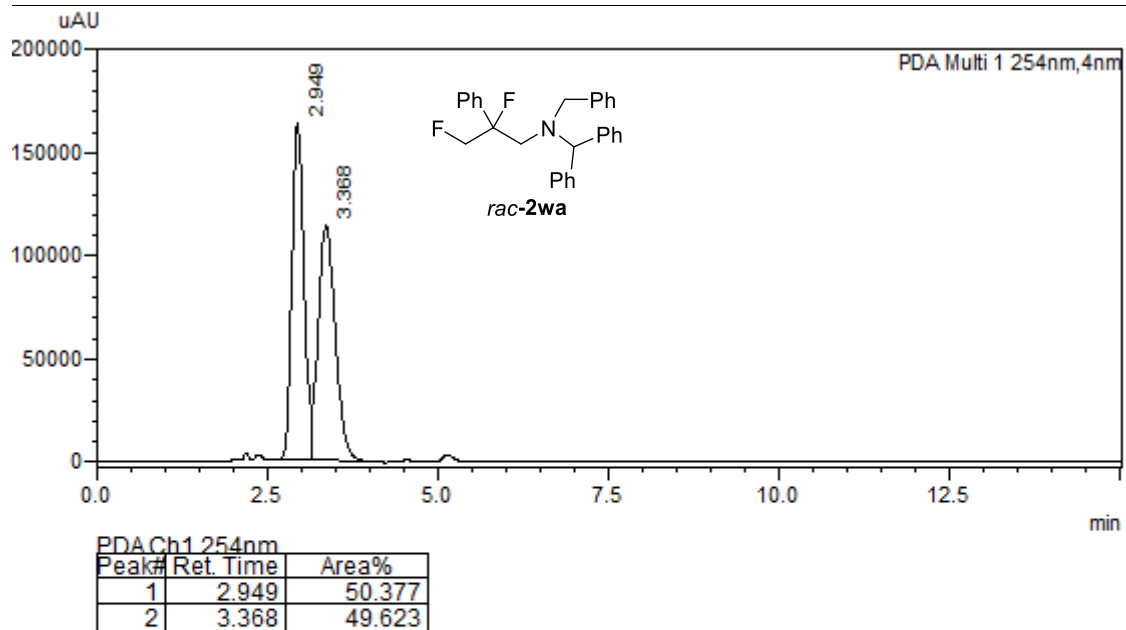


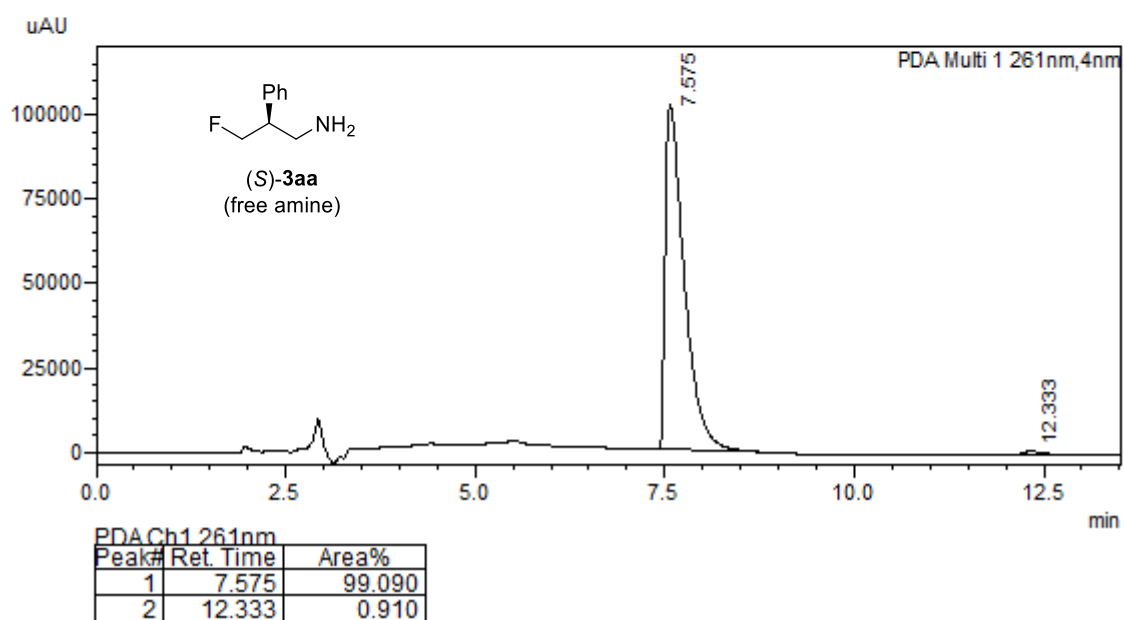
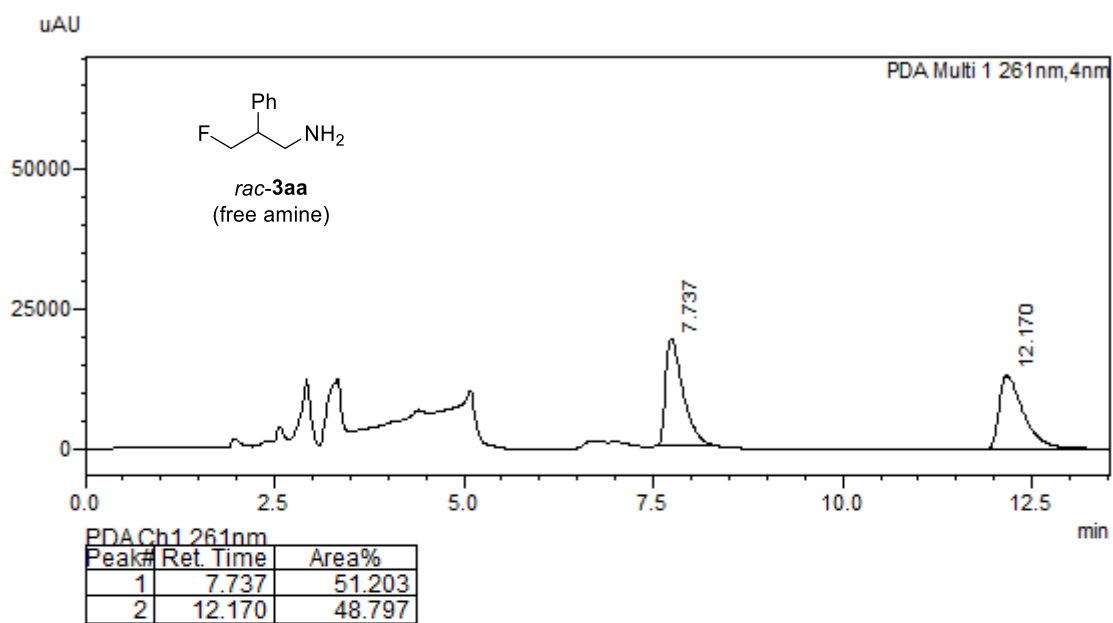


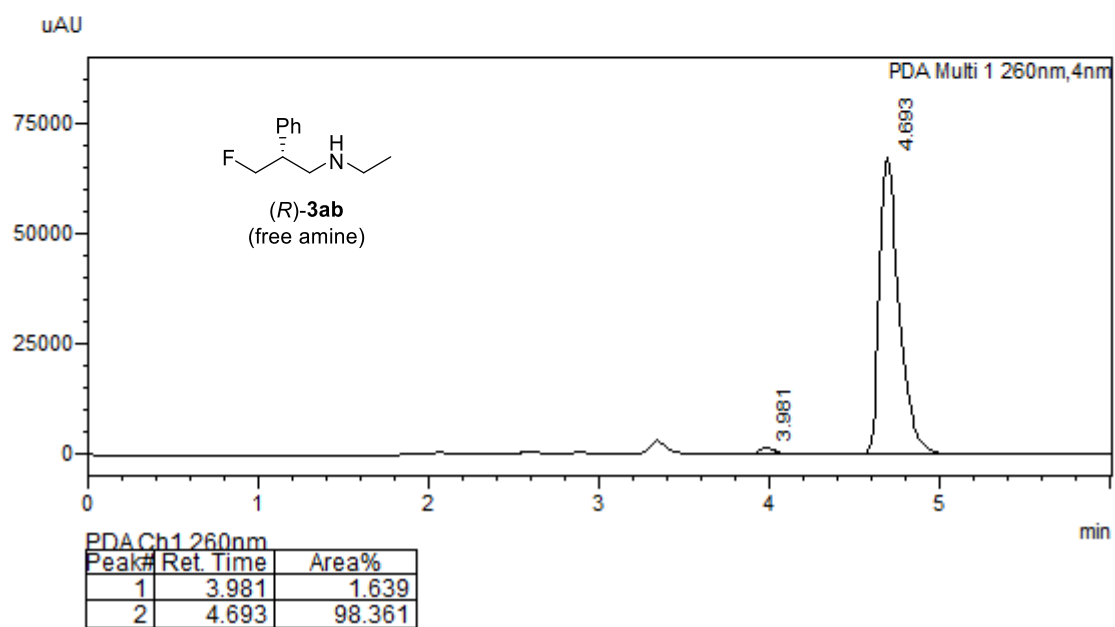
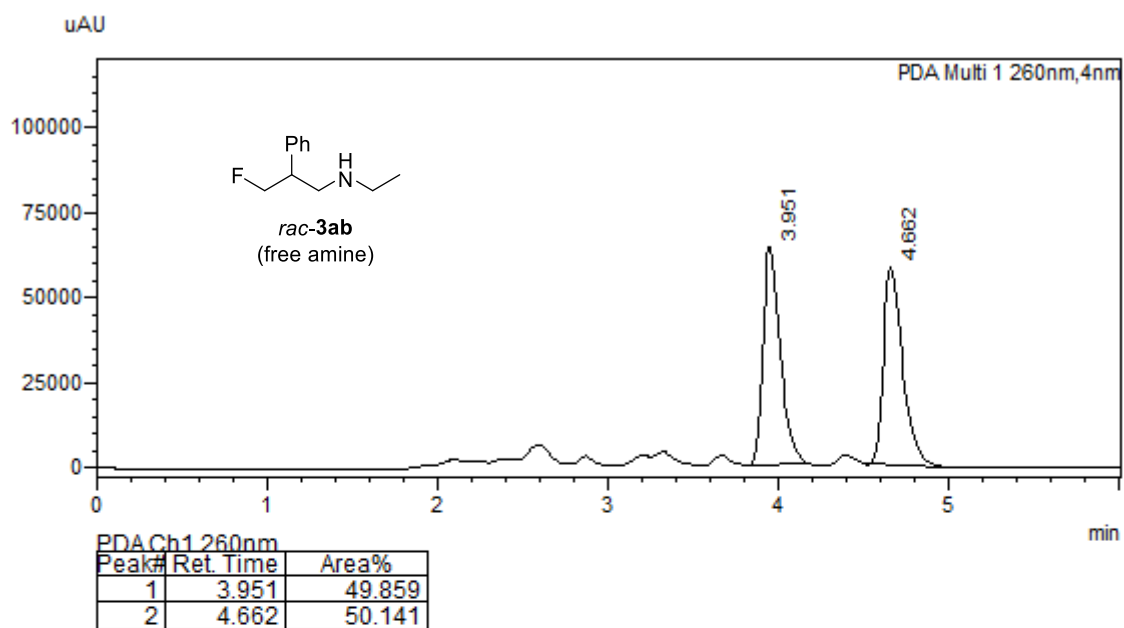




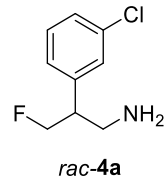
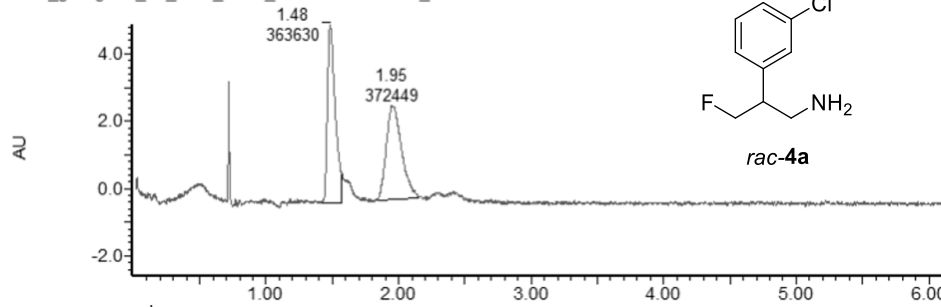








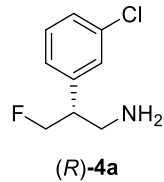
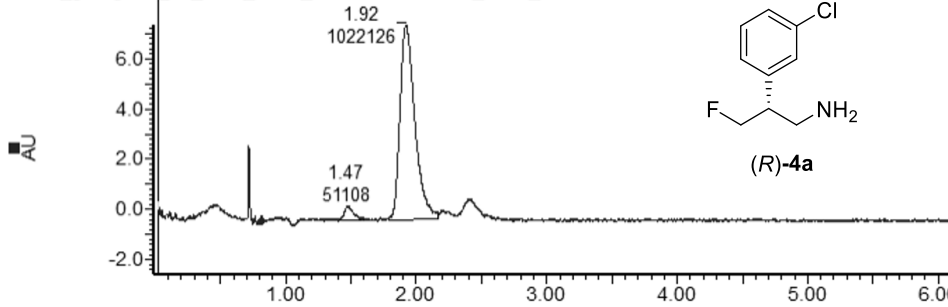
UOXF_groagna1_72_1#ID_EtOH_15G1A1P1BSFC2_1



3: Diode Array
Range: 7.384

Time	Height	Area	Area%
1.4834	5287908	363630.44	49.40
1.9484	2797522	372448.69	50.60

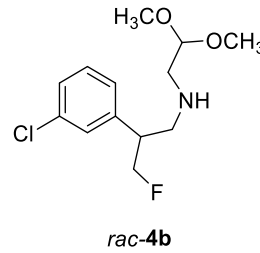
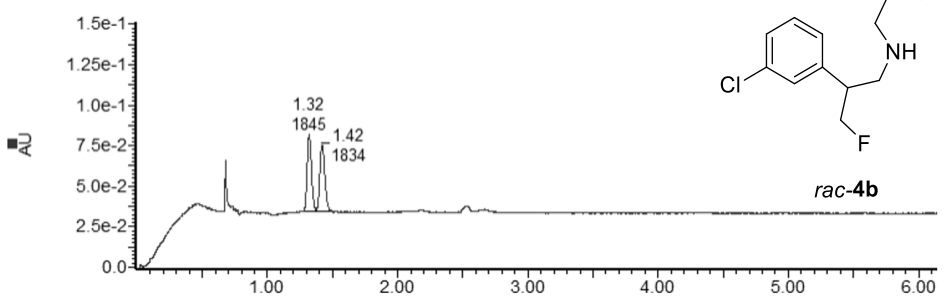
UOXF_groagna1_88_1#ID_EtOH_15G1A1P1BSFC2_1912_2



3: Diode Array
Range: 9.813

Time	Height	Area	Area%
1.4700	585238	51107.98	4.76
1.9226	7720270	1022125.81	95.24

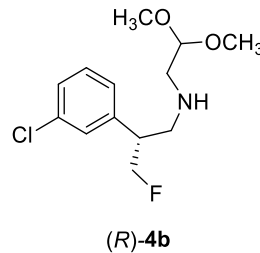
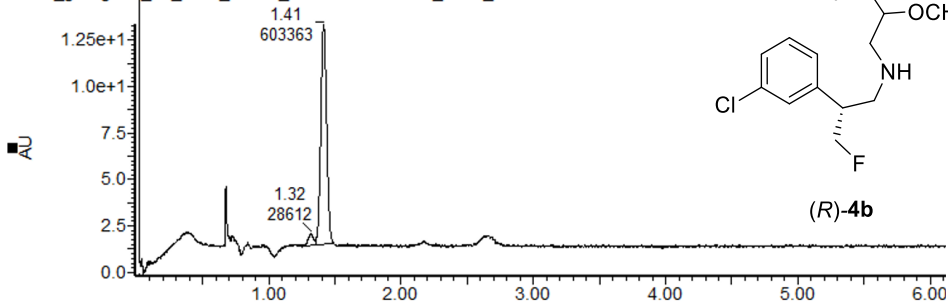
UOXF_groagna1_82_1#G_MeOH_15G1A1P1BSFC2



3: Diode Array
Range: 1.51e-1

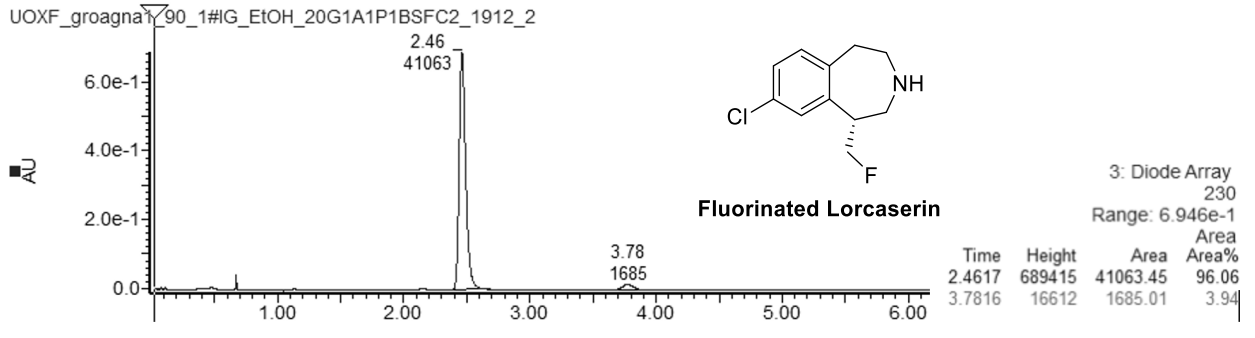
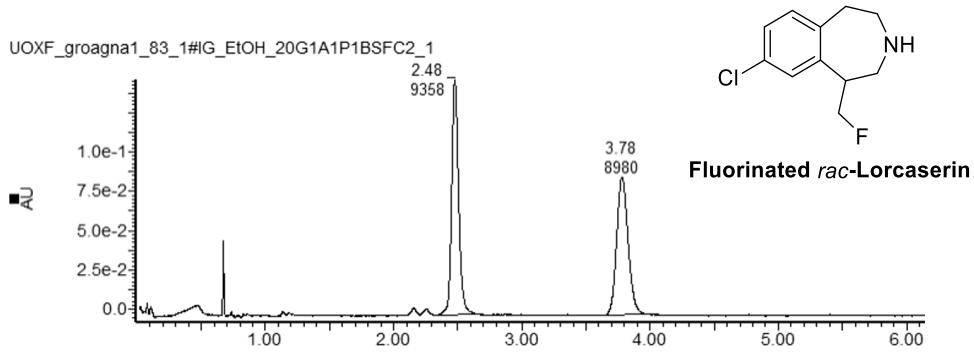
Time	Height	Area	Area%
1.3200	47423	1844.87	50.14
1.4192	40944	1834.45	49.86

UOXF_groagna1_89_1#G_MeOH_15G1A1P1BSFC2_1912_4



3: Diode Array
Range: 1.342e+1

Time	Height	Area	Area%
1.3175	624373	28612.35	4.53
1.4142	11812460	603363.31	95.47



References

- 1) Pupo, G.; Ibba, F.; Ascough, D. M. H.; Vicini, A. C.; Ricci, P.; Christensen, K.; Pfifer, L.; Morphy, J. R.; Brown, J. M.; Paton, R.; Gouverneur, V. Asymmetric Nucleophilic Fluorination under Hydrogen Bonding Phase-transfer Catalysis. *Science* **2018**, *360*, 638.
- 2) Adams, R. W.; Holroyd, C. M.; Aguilar, J. A.; Nilsson, M.; Morris, G. A. "Perfecting" WATERGATE: Clean Proton NMR Spectra from Aqueous Solution. *Chem. Commun.* **2013**, *49*, 358
- 3) a) Brynn Hibbert, D.; Thordarson, P. The Death of the Job Plot, Transparency, Open Science and Online Tools, Uncertainty Estimation Methods and Other Developments in Supramolecular Chemistry Data Analysis. *Chem. Commun.* **2016**, *52*, 12792; b) Thordarson, P. Determining Association Constants from Titration Experiments in Supramolecular Chemistry. *Chem. Soc. Rev.* **2011**, *40*, 1305.
- 4) Brak, K.; Jacobsen, E. N. Asymmetric Ion-Pairing Catalysis. *Angew. Chem. Int. Ed.* **2013**, *52*, 534.
- 5) Qian, D.; Chen, M.; Bissember, A. C.; Sun, J. Counterion-Induced Asymmetric Control in Ring-Opening of Azetidiniums: Facile Access to Chiral Amines. *Angew. Chem. Int. Ed.* **2018**, *57*, 3763.
- 6) Parmar, D.; Henkel, L. Dib, J.; Rueping, M. Iron Catalysed Cross-couplings of Azetidines – Application to the Formal Synthesis of a Pharmacologically Active Molecule. *Chem. Comm.* **2015**, *51*, 2111.
- 7) Barré, B.; Gonnard, L.; Campagne, R.; Reymond, S.; Marin, J.; Ciapetti, P.; Brellier, M.; Guérinot A.; Cossy, J. Iron- and Cobalt-Catalyzed Arylation of Azetidines, Pyrrolidines, and Piperidines with Grignard Reagents. *Org. Lett.* **2014**, *16*, 6160.
- 8) Dequirez, G.; Bourotte, M.; Porrás de Francisco, E.; Remuiñan, M. J.; Déprez, B.; Willand Microwave-Assisted Suzuki-Miyaura Cross Coupling using Nickel as Catalyst to Rapidly Access to 3-Arylazetidines. *ChemistrySelect* **2017**, *2*, 8841.
- 9) Hillier, M. C.; Chen, C. –Y. A One-Pot Preparation of 1,3-Disubstituted Azetidines. *J. Org. Chem.* **2006**, *71*, 7885.
- 10) Berton, M.; Huck, L.; Alcazar, J. On-demand synthesis of organozinc halides under continuous flow conditions. *Nature Protoc.* **2018**, *13*, 324.
- 11) a) Nisato, D.; Frigerio, M. Synthèse de 1-amino-3 azétidine. *J. Heterocycl. Chem.* **1985**, *22*, 961; b) Davies, S. G.; Fletcher, A. M.; Frost, A. B.; Roberts, P. M.; Thomson, J. E. Asymmetric Synthesis of Substituted *anti*- β -Fluorophenylalanines. *Org. Lett.* **2015**, *17*, 2254.
- 12) Cosier, J.; Glazer, A. M. A nitrogen-gas-stream cryostat for general X-ray diffraction studies. *J. Appl. Cryst.* **1986**, *19*, 105.
- 13) Palatinus, L.; Chapuis, G. "SUPERFLIP - a computer program for the solution of crystal structures by charge flipping in arbitrary dimensions. *J. Appl. Cryst.* **2007**, *40*, 786.
- 14) a) Parois, P.; Cooper, R. I.; Thompson, A. L. Crystal structures of increasingly large molecules: meeting the challenges with CRYSTALS software. *Chem. Cent. J.* **2015**, *9*, 30; b) Cooper, R. I.; Thompson, A. L.; Watkin, D. J. CRYSTALS Enhancements: Dealing with Hydrogen Atoms in Refinement. *J. Appl. Cryst.* **2010**, *43*, 1100.

- 15) Frisch, M. J.; Trucks, G. W.; Schlegel, H. B.; Scuseria, G. E.; Robb, M. A.; Cheeseman, J. R.; Scalmani, G.; Barone, V.; Petersson, G. A.; Nakatsuji, H.; Li, X.; Caricato, M.; Marenich, A.; Bloino, J.; Janesko, B. G.; Gomperts, R.; Mennucci, B.; Hratchian, H. P.; Ortiz, J. V.; Izmaylov, A. F.; Sonnenberg, J. L.; Williams-Young, D.; Ding, F.; Lipparini, F.; Egidi, F.; Goings, J.; Peng, B.; Petrone, A.; Henderson, T.; Ranasinghe, D.; Zakrzewski, V. G.; Gao, J.; Rega, N.; Zheng, G.; Liang, W.; Hada, M.; Ehara, M.; Toyota, K.; Fukuda, R.; Hasegawa, J.; Ishida, M.; Nakajima, T.; Honda, Y.; Kitao, O.; Nakai, H.; Vreven, T.; Throssell, K.; Montgomery Jr., J. A.; Peralta, J. E.; Ogliaro, F.; Bearpark, M.; Heyd, J. J.; Brothers, E.; Kudin, K. N.; Staroverov, V. N.; Keith, T.; Kobayashi, R.; Normand, J.; Raghavachari, K.; Rendell, A.; Burant, J. C.; Iyengar, S. S.; Tomasi, J.; Cossi, M.; Millam, J. M.; Klene, M.; Adamo, C.; Cammi, R.; Ochterski, J. W.; Martin, R. L.; Morokuma, K.; Farkas, O.; Foresman, J. B.; Fox, D. J. *Gaussian 16*. Gaussian Inc: Wallingford, CT **2016**.
- 16) Zhao, Y.; Truhlar, D. G. The M06 Suite of Density Functionals for Main Group Thermochemistry, Thermochemical Kinetics, Noncovalent Interactions, Excited States, and Transition Elements: Two New Functionals and Systematic Testing of Four M06-Class Functionals and 12 Other Functionals. *Theor. Chem. Acc.* **2008**, *120*, 215.
- 17) Weigend, F.; Ahlrichs, R. Balanced Basis Sets of Split Valence, Triple Zeta Valence and Quadruple Zeta Valence Quality for H to Rn: Design and Assessment of Accuracy. *Phys. Chem. Chem. Phys.* **2005**, *7*, 3297.
- 18) Rappoport, D.; Furche, F. Property-Optimized Gaussian Basis Sets for Molecular Response Calculations. *J. Chem. Phys.* **2010**, *133*, 134105.
- 19) Leininger, T.; Nicklass, A.; Küchle, W.; Stoll, H.; Dolg, M.; Bergner, A. The Accuracy of the Pseudopotential Approximation: Non-Frozen-Core Effects for Spectroscopic Constants of Alkali Fluorides XF (X = K, Rb, Cs). *Chem. Phys. Lett.* **1996**, *255*, 274.
- 20) Wheeler, S. E.; Houk, K. N. Integration Grid Errors for Meta-GGA-Predicted Reaction Energies: Origin of Grid Errors for the M06 Suite of Functionals. *J. Chem. Theory Comput.* **2010**, *6*, 395.
- 21) Barone, V.; Cossi, M. Quantum Calculation of Molecular Energies and Energy Gradients in Solution by a Conductor Solvent Model. *J. Phys. Chem. A* **1998**, *102*, 1995.
- 22) Cossi, M.; Rega, N.; Scalmani, G.; Barone, V. Energies, Structures, and Electronic Properties of Molecules in Solution with the C-PCM Solvation Model. *J. Comput. Chem.* **2003**, *24*, 669.
- 23) Takano, Y.; Houk, K. N. Benchmarking the Conductor-like Polarizable Continuum Model (CPCM) for Aqueous Solvation Free Energies of Neutral and Ionic Organic Molecules. *J. Chem. Theory Comput.* **2005**, *1*, 70.
- 24) Neese, F. The ORCA Program System. *Wiley Interdiscip. Rev. Comput. Mol. Sci.* **2012**, *2*, 73.
- 25) Neese, F. Software Update: The ORCA Program System, Version 4.0. *Wiley Interdiscip. Rev. Comput. Mol. Sci.* **2018**, *8*, e1237.
- 26) Chai, J.-D.; Head-Gordon, M. Long-Range Corrected Hybrid Density Functionals with Damped Atom-Atom Dispersion Corrections. *Phys. Chem. Chem. Phys.* **2008**, *10*, 6615.

- 27) Lin, Y.-S.; Li, G.-D.; Mao, S.-P.; Chai, J.-D. Long-Range Corrected Hybrid Density Functionals with Improved Dispersion Corrections. *J. Chem. Theory Comput.* **2013**, *9*, 263.
- 28) Grimme, S.; Antony, J.; Ehrlich, S.; Krieg, H. A Consistent and Accurate Ab Initio Parametrization of Density Functional Dispersion Correction (DFT-D) for the 94 Elements H-Pu. *J. Chem. Phys.* **2010**, *132*, 154104.
- 29) Zheng, J.; Xu, X.; Truhlar, D. G. Minimally Augmented Karlsruhe Basis Sets. *Theor. Chem. Acc.* **2011**, *128*, 295.
- 30) Paton Lab; Rodriguez-Guerra, J.; Chen, J. T.; Paton, R. S. Goodvibes 2019 DOI: 10.5281/zenodo.595246.
- 31) Grimme, S. Supramolecular Binding Thermodynamics by Dispersion-Corrected Density Functional Theory. *Chem. Eur. J.* **2012**, *18*, 9955.
- 32) Grimme, S.; Bannwarth, C.; Dohm, S.; Hansen, A.; Pisarek, J.; Pracht, P.; Seibert, J.; Neese, F. Fully Automated Quantum-Chemistry-Based Computation of Spin-Spin-Coupled Nuclear Magnetic Resonance Spectra. *Angew. Chem. Int. Ed.* **2017**, *56*, 14763.
- 33) Jorgensen, W. L.; Tirado-Rives, J. The OPLS Potential Functions for Proteins. Energy Minimizations for Crystals of Cyclic Peptides and Crambin. *J. Am. Chem. Soc.* **1988**, *110*, 1657.
- 34) Jorgensen, W. L.; Maxwell, D. S.; Tirado-Rives, J. Development and Testing of the OPLS All-Atom Force Field on Conformational Energetics and Properties of Organic Liquids. *J. Am. Chem. Soc.* **1996**, *118*, 11225.
- 35) Bayly, C. I.; Cieplak, P.; Cornell, W. D.; Kollman, P. A. A Well-Behaved Electrostatic Potential Based Method Using Charge Restraints for Deriving Atomic Charges: The RESP Model. *J. Phys. Chem.* **1993**, *97*, 10269.
- 36) Comell, W. D.; Cieplak, P.; Bayly, C. I.; Kollman, P. A. Application of RESP Charges To Calculate Conformational Energies, Hydrogen Bond Energies, and Free Energies of Solvation. *J. Am. Chem. Soc.* **1993**, *115*, 9620.
- 37) Schrodinger LLC. Schrodinger Release 2017-2. MS Jaguar: New York, NY **2017**.
- 38) Case, D. A.; Cerutti, D. S.; Cheatham III, T. E.; Darden, T.A.; Duke, R. E.; Giese, T. J.; Gohlke, H.; Goetz, A. W.; Greene, D.; Homeyer, N.; Izadi, S.; Kovalenko, A.; Lee, T.S.; LeGrand, S.; Li, P.; Lin, C.; Liu, J.; Luchko, T.; Luo, R.; Mermelstein, D.; Merz, K.M.; Monard, G. Nguyen, H.; Omelyan, I.; Onufriev, A.; Pan, F.; Qi, R.; Roe, D. R.; Roitberg, A.; Sagui, C.; Simmerling, C. L.; Botello-Smith W. M.; Swails, J. Walker, R. C.; Wang, J.; Wolf, R. M.; Wu, X.; Xiao, L.; York, D. M.; Kollman, P. A.; AMBER 2017. University of California: San Francisco **2017**.
- 39) van der Spoel, D.; van Maaren, P. J.; Caleman, C. GROMACS Molecule & Liquid Database. *Bioinformatics* **2012**, *28*, 752.
- 40) Chen, S.; Yi, S.; Gao, W.; Zuo, C.; Hu, Z. Force Field Development for Organic Molecules: Modifying Dihedral and 1-n Pair Interaction Parameters. *J. Comput. Chem.* **2015**, *36*, 376.

- 41) Bussi, G.; Donadio, D.; Parrinello, M. Canonical Sampling through Velocity Rescaling. *J. Chem. Phys.* **2007**, *126*, 014101.
- 42) Parrinello, M.; Rahman, A. Crystal Structure and Pair Potentials: A Molecular Dynamics Study. *Phys. Rev. Lett.* **1980**, *45*, 1196.
- 43) Parrinello, M.; Rahman, A. Polymorphic Transitions in Single Crystals: A New Molecular Dynamics Method. *J. Appl. Phys.* **1981**, *52*, 7182.
- 44) Hess, B.; Bekker, H.; Berendsen, H. J. C.; Fraaije, J. G. E. M. LINCS: A Linear Constraint Solver for Molecular Simulations. *J. Comput. Chem.* **1997**, *18*, 1463.
- 45) Daura, X.; Gademann, K.; Jaun, B.; Seebach, D.; van Gunsteren, W. F.; Mark, A. E. Peptide Folding: When Simulation Meets Experiment. *Angew. Chem. Int. Ed.* **1999**, *38*, 236.
- 46) Kozuch, S.; Shaik, S. A Combined Kinetic-Quantum Mechanical Model for Assessment of Catalytic Cycles: Application to Cross-Coupling and Heck Reactions. *J. Am. Chem. Soc.* **2006**, *128*, 3355.
- 47) Kozuch, S.; Shaik, S. Kinetic-Quantum Chemical Model for Catalytic Cycles: The Haber-Bosch Process and the Effect of Reagent Concentration. *J. Phys. Chem. A* **2008**, *112*, 6032.
- 48) Kozuch, S.; Lee, S. E.; Shaik, S. Theoretical Analysis of the Catalytic Cycle of a Nickel Cross-Coupling Process: Application of the Energetic Span Model. *Organometallics* **2009**, *28*, 1303.
- 49) Kozuch, S.; Shaik, S. How to Conceptualize Catalytic Cycles? The Energetic Span Model. *Acc. Chem. Res.* **2011**, *44*, 101.
- 50) Kozuch, S. A Refinement of Everyday Thinking: The Energetic Span Model for Kinetic Assessment of Catalytic Cycles. *WIREs Comput. Mol. Sci.* **2012**, *2*, 795.
- 51) Bickelhaupt, F. M.; Houk, K. N. Analyzing Reaction Rates with the Distortion/Interaction-Activation Strain Model. *Angew. Chem. Int. Ed.* **2017**, *56*, 10070.